AD-A154 338

AIR FORCE OFFICE OF SCIENTIFIC RESEARCH

UNITED STATES AIR FORCE

SUMMER FACULTY
RESEARCH PROGRAM

conducted by the

SOUTHEASTERN CENTER

FOR ELECTRICAL ENGINEERING EDUCATION

(SCEEE)

1984

TECHNICAL REPORT

VOLUME I OF III

WARREN D. PEELE   EARL L. STEELE

PROGRAM DIRECTORS SCEEE

ELECTE
MAY 30 1985

D

THE SCEE

AD-A154 338

REPORT DOCUMENTATION PAGE

1a. REPORT SECURITY CLASSIFICATION UNCLASSIFIED	1b. RESTRICTIVE MARKINGS
2a. SECURITY CLASSIFICATION AUTHORITY	3. DISTRIBUTION/AVAILABILITY OF REPORT
2b. DECLASSIFICATION/DOWNGRADING SCHEDULE	APPROVED FOR PUBLIC RELEASE; DISTRIBUTION UNLIMITED
4. PERFORMING ORGANIZATION REPORT NUMBER(S)	5. MONITORING ORGANIZATION REPORT NUMBER(S) AFOSR-TR- 85-0481

6a. NAME OF PERFORMING ORGANIZATION Southeastern Center for Electrical Engineering Education	6b. OFFICE SYMBOL (If applicable) XOT	7a. NAME OF MONITORING ORGANIZATION Air Force Office of Scientific Research/XOT
6c. ADDRESS (City, State and ZIP Code) 11th & Massachusetts Ave. St. Cloud, FL 32769		7b. ADDRESS (City, State and ZIP Code) Building 410 Bolling AFB, DC 20332-6448

8a. NAME OF FUNDING/SPONSORING ORGANIZATION AFOSR	8b. OFFICE SYMBOL (If applicable) XOT	9. PROCUREMENT INSTRUMENT IDENTIFICATION NUMBER F49620-82-C-0035

8c. ADDRESS (City, State and ZIP Code) Building 410 Bolling AFB, DC 20332	10. SOURCE OF FUNDING NOS.			
	PROGRAM ELEMENT NO. 61102F	PROJECT NO. 2301	TASK NO. D5	WORK UNIT NO.

11. TITLE (Include Security Classification)
United States Air Force Summer Faculty Research Program (1984) Volume 3

12. PERSONAL AUTHOR(S)
Warren D. Peele, Earl L. Steele, Major Amos L. Otis

13a. TYPE OF REPORT Final	13b. TIME COVERED FROM _____ TO _____	14. DATE OF REPORT (Yr., Mo., Day) December 1984	15. PAGE COUNT

16. SUPPLEMENTARY NOTATION

17. COSATI CODES			18. SUBJECT TERMS (Continue on reverse if necessary and identify by block number)
FIELD	GROUP	SUB. GR.	

19. ABSTRACT (Continue on reverse if necessary and identify by block number)

20. DISTRIBUTION/AVAILABILITY OF ABSTRACT	21. ABSTRACT SECURITY CLASSIFICATION
UNCLASSIFIED/UNLIMITED ☒ SAME AS RPT. ☐ DTIC USERS ☐	UNCLASSIFIED

22a. NAME OF RESPONSIBLE INDIVIDUAL MAJOR AMOS L. OTIS	22b. TELEPHONE NUMBER (Include Area Code) (202) 767-4971	22c. OFFICE SYMBOL XOT

DD FORM 1473, 83 APR   EDITION OF 1 JAN 73 IS OBSOLETE.

20030116016

PREFACE

The United States Air Force Summer Faculty Research Program (USAF-SFRP) is a program designed to introduce university, college, and technical institute faculty members to Air Force research. This is accomplished by the faculty members being selected on a nationally advertised competitive basis for a ten-week assignment during the summer intersession period to perform research at Air Force laboratories/centers. Each assignment is in a subject area and at an Air Force facility mutually agreed upon by the faculty members and the Air Force. In addition to compensation, travel and cost of living allowances are also paid. The USAF-SFRP is sponsored by the Air Force Office of Scientific Research, Air Force Systems Command, United States Air Force, and is conducted by the Southeastern Center for Electrical Engineering.
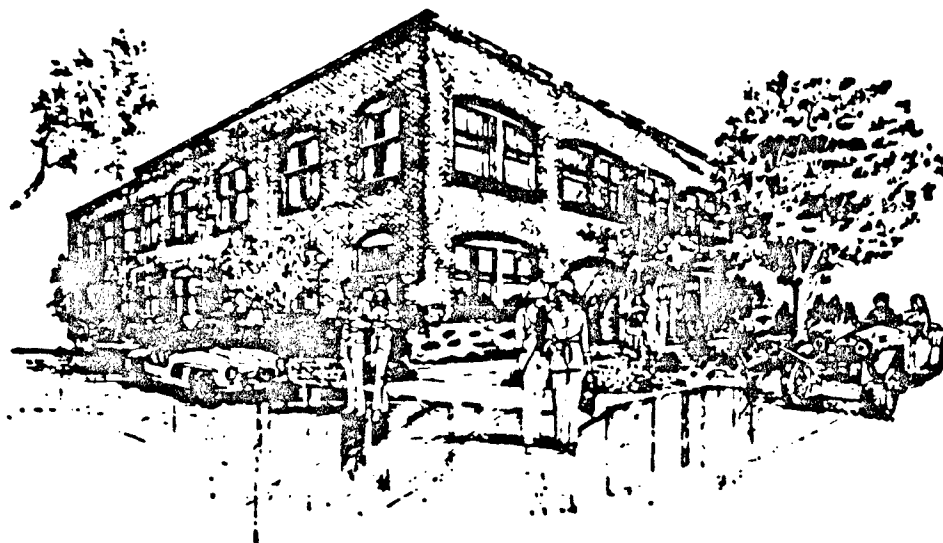
The specific objectives of the 1984 USAF-SFRP are:

(1) To provide a productive means for Scientists and Engineers holding Ph.D. degrees to participate in research at the Air Force Weapons Laboratory;

(2) To stimulate continuing professional association among the Scholars and their professional peers in the Air Force;

(3) To further the research objectives of the United States Air Force;

(4) To enhance the research productivity and capabilities of Scientists and Engineers especially as these relate to Air Force technical interests.

During the summer of 1984, 152 faculty members participated. These researchers were assigned to 25 USAF laboratories/centers across the country. This three volume document is a compilation of the final reports written by the assigned faculty members about their summer research efforts.

AFOSR-TR. 86-0481

AFOSR-TR. 86-0481

SCEEE
©
1984

UNITED STATES AIR FORCE

SUMMER FACULTY RESEARCH PROGRAM

1984

PROGRAM MANAGEMENT REPORT

SOUTHEASTERN CENTER FOR ELECTRICAL ENGINEERING EDUCATION

Volume III of III

Program Directors, SCEEE   Program Manager, AFOSR
    Warren D. Peele   Major Amos L. Otis
    Earl L. Steele

Submitted to

Air Force Office of Scientific Research

Bolling Air Force Base

Washington, DC

December 1984

The United States Air Force Summer Faculty Research Program (USAF-SFRP) is a program designed to introduce university, college, and technical institute faculty members to Air Force research. This is accomplished by the faculty members being selected on a nationally advertised competitive basis for a ten-week assignment during the summer intersession period to perform research at Air Force laboratories/centers. Each assignment is in a subject area and at an Air Force facility mutually agreed upon by the faculty members and the Air Force. In addition to compensation, travel and cost of living allowances are also paid. The USAF-SFRP is sponsored by the Air Force Office of Scientific Research, Air Force Systems Command, United States Air Force, and is conducted by the Southeastern Center for Electrical Engineering.

The specific objectives of the 1984 USAF-SFRP are:

(1) To provide a productive means for Scientists and Engineers holding Ph.D. degrees to participate in research at the Air Force Weapons Laboratory;

(2) To stimulate continuing professional association among the Scholars and their professional peers in the Air Force;

(3) To further the research objectives of the United States Air Force;

(4) To enhance the research productivity and capabilities of Scientists and Engineers especially as these relate to Air Force technical interests.

During the summer of 1984, 152 faculty members participated. These researchers were assigned to 25 USAF laboratories/centers across the country. This three volume document is a compilation of the final reports written by the assigned faculty members about their summer research efforts.

NAME/ADDRESS	DEGREE, SPECIALTY, LABORATORY ASSIGNED

Dr. Annalingam Anandarajah
Assistant Professor
S.D. School of Mines & Tech.
Civil Engineering Dept.
Rapid City, SD 57701
(605) 394-2443

Degree: Ph.D., Civil Engineering
1982
Specialty: Geotechnical Engineering
Assigned: ESC

Dr. Gloria Anderson
Chairman
Morris Brown College
Chemistry Dept.
Atlanta, GA 30314
(404) 525-7831

Degree: Ph.D., Chemistry, 1968
Specialty: Organic Chemistry
Assigned: RPL

Dr. Richard Anderson
Professor
University of Missouri
Physics Department
Rolla, MO 65401
(314) 341-4341

Degree: Ph.D., Physics, 1959
Specialty: Optics, Atomic and Molecular
Physics
Assigned: APL

Dr. Deborah Armstrong
Assistant Professor
University of Texas
Life Sciences
San Antonio, TX 78285
(512) 691-4458

Degree: Ph.D., Biopsychology, 1982
Specialty: Neurophysiology
Assigned: SAM

Dr. Francesco Bacchialoni
Associate Professor
University of Lowell
Dept. of Electrical Eng.
Lowell, MA 01854
(617) 452-5000

Degree: Ph. D., Engineering, 1946
Specialty: Control Systems, Digital
Signal Processing,
Microprocessors
Assigned: GL

Dr. John Bahng
Associate Professor
Northwestern University
Dept. of Physics & Astronomy
Evanston, IL 60201
(312) 492-7527

Degree: Ph.D., Astronomy, 1957
Specialty: Astronomical Instrumentation,
Computer Programming
Assigned: GL

Dr. James Baird
Professor
Brown University
Chemistry & Physics Dept.
Providence, RI 02912
(401) 863-3325

Degree: Ph.D., Physics, 1959
Specialty: Spectroscopy-laser,
Microwave
Assigned: GL

Dr. Mukul Banerjee
Professor
Meharry Medical College
Dept. of Physiology
Nashville, TN 37208
(615) 327-6288

Degree: Ph.D., Animal Physiology,
1964
Specialty: Respiratory Physiology,
Environmental Physiology
Assigned: SAM

Dr. Alan Bentley
Assistant Professor
Eastern Montana College
Dept. of Physics
Billings, MT 59101
(406) 657-2026

Degree: Ph.D., Infrared
Astrophysics, 1980
Specialty: Infrared Physics and
Astrophysics
Assigned: GL

Dr. Richard Bernhard
Professor
North Carolina State Univ.
Industrial Engr. Dept.
Raleigh, NC 27695
(919) 737-2362

Degree: Ph.D., Operations Research,
1961
Specialty: Engineering and Managerial
Economics; Decision Anal.
Assigned: BRMC

Dr. Albert Biggs
Professor
University of Kansas
Electrical Engr. Dept.
Lawrence, KS 66045
(913) 864-4836

Degree: Ph.D., Electrical Engr.,
1968
Specialty: Microwaves and Antennas
Assigned: AL

Dr. Louis Buckalew
Associate Professor
Alabama A&M University
Dept. of Psychology
Normal, AL 35762
(205) 859-7451

Degree: Ph.D., Phys. Psychology,
1984
Specialty: Physiological Psychology
Assigned: LMDC

Mr. Mike Burlakoff
Assistant Professor
Southwest Mo. State Univ.
Computer Science Dept.
Springfield, MO 65804
(417) 836-5930

Degree: M.S., Math/Computer Science,
1965
Specialty: Languages and Environments
Assigned: AL

Dr. Myron Calhoun
Associate Professor
Kansas State University
Computer Science Dept.
Manhattan, KS 66506
(913) 532-6350

Degree: Ph. D., Electrical Engr., 1967
Specialty: Digital Hardware and Software
Assigned: AD

Dr. Jeya Chandra
Assistant Professor
Pennsylvania State Univ.
Dept. of Ind. & Mgmt. Engr.
University Park, PA 16802
(814) 863-2358

Degree: Ph. D., Ind. Eng. and Operations Rsch., 1980
Specialty: Stochastic Processes
Assigned: SAM

Dr. Do Chang
Associate Professor
Averett College
Chemistry Department
Danville, VA 24541
(804) 793-7811

Degree: Ph. D., Chemistry, 1968
Specialty: Chemical Kinetics, Phase Transitions
Assigned: AD

Dr. Huei-huang Chiu
Professor
University of Illinois
Dept. of Mechanical Engr.
Chicago, IL 60680
(312) 996-3426

Degree: Ph. D., Aeronautical Eng., 1962
Specialty: Combustion, Fluid Mechanics, and Propulsion
Assigned: APL

Dr. Philip Chong
Assistant Professor
Dept. of Industrial Engr.
North Dakota State Univ.
Fargo, ND 58105
(701) 237-7223

Degree: Ph. D., Ind. Eng. and Operations Rsch., 1977
Specialty: Computerized Resource Planning and Scheduling
Assigned: LMC

Dr. Louis Chow
Assistant Professor
Washington State University
Mechanical Engr. Dept.
Pullman, WA 99164
(509) 335-1327

Degree: Ph. D., Mechanical Engr., 1978
Specialty: Heat Transfer, Fluid Dynamics
Assigned: APL

Dr. David Chung
Professor
Howard University
Department of Physics
Washington, DC 20059
(202) 636-7903

Degree: Ph. D., Solid State Physics, 1966
Specialty: Fiber Optics Sensors Ultra-sound, Solid State Elect.
Assigned: FJSRL

Dr. David Cohoon
Professor
Temple University
Dept. of Mathematics
Philadelphia, PA 19122
(215) 787-7284

Degree: Ph. D., Mathematics, 1969
Specialty: Partial Differential Equations
Assigned: SAM

Dr. Frank Colby, Jr.
Assistant Professor
University of Lowell
Dept. of Earth Sciences
Lowell, MA 01854
. (617) 452-2551

Degree: Ph. D., Meterology, 1983
Specialty: Boundary-layer Meteorology
Assigned: GL

Dr. Robert Colclaser, Jr.
Professor & Chairman
University of Pittsburgh
Electrical Engineer
Pittsburgh, PA 15261
(412) 624-5391

Degree: Ph. D., Sci., Elec. Engr., 1968
Specialty: High Power Arcs, Circuit Breaker Design and Test, Electrical Transients
Assigned: WL

Dr. Gregory Corso
Assistant Professor
Georgia Inst. of Tech.
School of Psychology
Atlanta, GA 30332
(404) 894-2680

Degree: Ph. D., Engr. Psychology, 1978
Specialty: Human Factors, Human Performance
Assigned: AEDC

Dr. Robert Courter
Associate Professor
Louisiana State University
Mechanical Engr. Dept.
Baton Rouge, LA 70803
(504) 388-5792

Degree: Ph. D., Aerospace Engr., 1965
Specialty: Aerodynamics, Gasdynamics, Blast Waves
Assigned: AD

Dr. John Cyranski
Assistant Professor
Clark College
Physics Department
Atlanta, GA 30314
(404) 681-3080

Degree: Ph. D., Physics, 1974
Specialty: Math. Physics and Information Theory
Assigned: GL

Dr. Subramaniam Deivanayagam
Associate Professor
University of Texas
Dept. of Industrial Engr.
Arlington, TX 76109
(817) 273-3092

Degree: Ph. D., Industrial Engr., 1973
Specialty: Ergonomics/Human Factors
Assigned: HRL/Wright-Patterson

Dr. Hermann Donnert
Professor
Kansas State University
Dept. of Nuclear Engr.
Manhattan, KS 66506
(913) 532-5960

<u>Degree:</u> Ph. D., Mathematics and
Physics, 1951
<u>Specialty:</u> Plasma Physics, Radiation
Physics
<u>Assigned:</u> FJSRL

Dr. Robert Dorman
Assistant Professor
Kent State University
Dept. of Biological Sci.
Kent, OH 44242
(216) 672-3613

<u>Degree:</u> Ph. D., Physiological
Chemistry, 1976
<u>Specialty:</u> Neurochemistry
<u>Assigned:</u> SAM

Dr. George Doyle, Jr.
Associate Professor
University of Dayton
Mechanical Engr. Dept.
Dayton, OH 45469
(513) 229-2835

<u>Degree:</u> Ph. D., Mechanical Engr.,
1973
<u>Specialty:</u> Dynamics
<u>Assigned:</u> FDL

Dr. Eric Drumm
Assistant Professor
University of Tennessee
Dept. of Civil Engr.
Knoxville, TN 37996
(615) 974-7715

<u>Degree:</u> Ph. D., Civil Engineering,
1983
<u>Specialty:</u> Geotechnical Engineering
<u>Assigned:</u> ESC

Dr. Charles Drummond, III
Associate Professor
Ohio State University
Dept. of Ceramic Engr.
Columbus, OH 43210
(614) 422-2960

<u>Degree:</u> Ph. D., Applied Physics,
1974
<u>Specialty:</u> Glass Structure and
Properties
<u>Assigned:</u> ML

Dr. Delcie Durham
Assistant Professor
University of Vermont
Civil & Mech. Engr. Dept.
Burlington, VT 05405
(802) 656-3320

<u>Degree:</u> Ph. D., Mechanical Engr.,
1981
<u>Specialty:</u> Metal Behavior at High
Strains and Strain Rates
<u>Assigned:</u> ML

Dr. Terrence Dwan
Associate Professor
The Citadel
Dept. of Elect. Engr.
Charleston, SC 29409
(803) 792-5057

<u>Degree:</u> Ph. D., Elecrical Engr.
1975
<u>Specialty:</u> Large Scale Systems,
Modelling, Controls
<u>Assigned:</u> AD

Dr. Franklin Eastep
Professor
University of Dayton
Dept. of Aerospace Engr.
Dayton, OH 45469
(513) 229-2241

Degree: Ph. D., Aeronautics, 1968
Specialty: Aeroelasticity
Assigned: FDL

Dr. James Eberhart
Professor
University of Colorado
Chemistry Department
Colorado Springs, CO 80933
(303) 593-3284

Degree: Ph. D., Chemistry, 1963
Specialty: Physical and Surface
          Chemistry
Assigned: FJSRL

Dr. Frederick Eisler
Associate Professor
College of Staten Island
Dept. of Applied Science
Staten Island, NY 10301
(212) 390-7973

Degree: Ph. D., Physics, 1970
Specialty: Particle Physics,
          Holography, Accelerators
Assigned: WL

Dr. Emory Enscore, Jr.
Associate Professor
Penn. State University
Dept. of Ind. & Mgmt. Syst. Eng.
University Park, PA 16802
(814) 863-2353

Degree: Ph. D., Ind. Engr., 1972
Specialty: Industrial Engineering
Assigned: HRL/Wright-Patterson

Dr. John Erdei
Assistant Professor
University of Dayton
Dept. of Physics
Dayton, OH 45469
(513) 229-2727

Degree: Ph. D., Physics, 1983
Specialty: Many Body Theory, Critical
          Phenomena
Assigned: APL

Dr. Adly Fam
Associate Professor
State University of New York
Dept. of Electrical & Comp. Eng.
Buffalo, NY 14260
(716) 636-2422

Degree: Ph. D., Electrical Engr.,
          1977
Specialty: Digital Signal Processing
          and System Theory
Assigned: RADC

Dr. Bruce R. Feiring
Assistant Professor
University of Minnesota
Dept. of Mgmt. Sciences
Minneapolis, MN 55455
(612) 376-1376

Degree: Ph. D., Industrial Engr.,
          1979
Specialty: Optimization
Assigned: HRL/Brooks

Dr. William Feld
Associate Professor
Wright State University
Dept. of Chemistry
Dayton, OH 45435
(513) 873-2511

Degree: Ph. D., Chemistry, 1971
Specialty: Organic Chemistry
Assigned: ML

Dr. Dennis Flentge
Assistant Professor
Cedarville College
Dept. of Math/Sci.
Cedarville, OH 45314
(513) 766-2211

Degree: Ph. D., Physical Chemistry,
           1974
Specialty: Catalysis, IR Spectroscopy
Assigned: APL

Dr. Cynthia Ford
Assistant Professor
Jackson State University
Psychology Department
Jackson, MS 39217
(601) 968-2371

Degree: Ph. D., Educ. Psychology,
           1979
Specialty: General Psychology,
           Statistics
Assigned: HRL/Brooks

Dr. Eddie Fowler
Associate Professor
Kansas State University
Electrical Engr. Dept.
Manhattan, KS 66056
(913) 532-5600

Degree: Ph. D., Elec. Eng., 1969
Specialty: C^3I Modeling and Sim-
           ulation Nuclear Degrad-
           ation of Comm. Networks
Assigned: WL

Dr. Basil Gala
Professor
California State University
Division of Engineering
Chico, CA 95929
(916) 895-5374

Degree: Ph. D., Electrical Engr.,
           1973
Specialty: Computers-Pattern
           Recognition
Assigned: RADC

Dr. Barry Ganapol
Associate Professor
University of Arizona
Dept. of Nuclear & Energy Engr.
Tucson, AZ 85721
(602) 621-4728

Degree: Ph. D., Nuclear Science,
           1971
Specialty: Particle Transport Theory
Assigned: RADC

Dr. David Gilliam
Assistant Professor
Texas Tech. University
Dept. of Mathematics
Lubbock, TX 79409
(806) 742-2566

Degree: Ph. D., Mathematics, 1977
Specialty: Applied Partial
           Differential Equations
Assigned: RADC

Dr. Larry Glasgow
Assistant Professor
Kansas State University
Chemical Engr. Dept.
Manhattan, KS 66506
(913) 532-5585

Degree: Ph. D., Chemical Engr., 1977
Specialty: Fluid Mechanics, Transport Phenomena, Laser-Doppler Velocity
Assigned: FJSRL

Dr. Sallie Gordon
Assistant Professor
Wright State University
Dept. of Psychology
Dayton, OH 45435
(513) 873-2391

Degree: Ph. D., Psychology, 1982
Specialty: Social/Cognitive Psychology
Assigned: HRL/Wright-Patterson

Dr. Thomas Graham
Professor
University of Dayton
Physics Dept.
Dayton, OH 45469
(513) 229-2329

Degree: Ph. D., Physics, 1967
Specialty: Solid State/Surface Physics/ Magnetic Resonance
Assigned: ML

Dr. Edward Greco, Jr.
Assistant Professor
University of Miami
Biomedical Engr. Dept.
Coral Gables, FL 33124
(305) 284-2442

Degree: Ph. D., Elec./Bioengr., 1976
Specialty: Digital Signal Processing, Biosystem Analysis and Ventilatory Control
Assigned: SAM

Dr. Ronald Greene
Associate Professor
University of New Orleans
Physics Deptartment
New Orleans, LA 70148
(504) 286-6714

Degree: Ph. D., Physics, 1974
Specialty: Plasma Spectroscopy
Assigned: AL

Dr. Paul Griesacker
Associate Professor
Gannon University
Deptartment of Physics
Erie, PA 16541
(814) 871-7649

Degree: Ph. D., Physics, 1963
Specialty: Physical Optics, Coherent Radiation
Assigned: AL

Dr. Thomas Gulledge, Jr.
Assistant Professor
Louisiana State University
Dept. of Quantitative Bus. Anal.
Baton Rouge, LA 70803
(504) 388-2126

Degree: Ph. D., Eng. Mgmt., 1981
Specialty: Management Science
Assigned: BRMC

Dr. Vijay Gupta
Associate Professor
Central State University
Chemistry Department
Wilberforce, OH 45384
(513) 376-6423

Degree: Ph. D., Chemistry, 1969
Specialty: Physical Chemistry
Assigned: ML

Dr. Hendrik Hameka
Professor
University of Pennsylvania
Chemistry Dept.
Philadelphia, PA 19104
(215) 898-8303

Degree: Ph. D., Theoretical Chem.,
          1956
Specialty: Quantum Chemistry,
          Theoretical Chemistry
Assigned: FJSRL

Dr. Arthur Harriman
Professor
Oklahoma State University
Dept. of Psychology
Stillwater, OK 74078
(405) 624-6561

Degree: Ph. D., Exp. Psychology,
          1952
Specialty: Physiological Psychology
Assigned: HRL/Williams

Dr. Doyle Hasty
Assistant Professor
Motlow State Community College
Dept. of Engineering
Tullahoma, TN 37388
(615) 455-8511

Degree: M.S., Engineering Admn.,
          1974
Specialty: Electronics, Physics,
          Instrumentation, Computers,
          High-altitude Engine Test.
Assigned: AEDC

Dr. Albert Havener
Assistant Professor
University of Dayton
Dept. of Mechanical Engr.
Dayton, OH 45469
(513) 229-2835

Degree: Ph. D., Aerospace Engr.,
          1983
Specialty: Applied Aero Optical
          Measuring Techniques
Assigned: FDL

Dr. Peter Hierl
Professor
Kansas University
Chemistry Department
Lawrence, KS 66045
(913) 864-3019

Degree: Ph. D., Physical Chemistry
          1964
Specialty: Gas-phase Kinetics
Assigned: GL

Dr. Paul Hoffman
Assistant Professor
Villanova University
Dept. of Civil Engineering
Villanova, PA 19085
(215) 645-4960

Degree: Ph. D., Civil Engineering
          1982
Specialty: Structural Eng. and Solid
          Mechanics
Assigned: ESC

Dr. Brian Holmes	Degree:	Ph. D., Physics, 1980
Assistant Professor	Specialty:	Solid State/Low
San Jose State University		Temperature; Magnetic
Dept. of Physics		Resonance
San Jose, CA 95912	Assigned:	RADC
(408) 277-2361		

Dr. Gwendolyn Howze	Degree:	Ph. D., Molecular Biology,
Associate Professor		1974
Texas Southern University	Specialty:	Cell Biology/Chromatin,
Dept. of Biology		Electron Microscopy,
Houston, TX 77004		Tissue Cult
(713) 527-7005	Assigned:	AMRL

Dr. Chen-Chi Hsu	Degree:	Ph. D., Eng. Mech., 1965
Professor	Specialty:	Applied Mechanics,
University of Florida		Computational Aerodynamics
Dept. of Engineering Sci.	Assigned:	AD
Gainesville, FL 32611		
(904) 392-0961		

Dr. Mario Innocenti	Degree:	Ph. D., Aeronautics
Assistant Professor		Astronautics, 1983
Auburn University	Specialty:	Flight Dynamics Handling
Aerospace Engr. Dept.		Qualities Optimal Control
Auburn, AL 36849	Assigned:	FDL
(205) 826-4874		

Dr. Kakkattukuzhy Isaac	Degree:	Ph. D., Aerospace Eng.,
Assistant Professor		1982
University of Missouri	Specialty:	Fluid Mechanics
Dept. of Mech. & Aero. Engr.	Assigned:	APL
Rolla, MO 65401		
(314) 341-4626		

Dr. Robert Jackson, Jr.	Degree:	Ph. D., Elec. Eng., 1982
Assistant Professor	Specialty:	Electromagnetics, Active
University of Massachusetts		Devices for Microwave and
Dept. of Elec. & Comp. Engr.		Millimeter Wave Integrated
Amherst, MA 01003		Circuits
(413) 545-1386	Assigned:	RADC

Dr. Vinod Jain	Degree:	Ph. D., Mech. Eng., 1980
Assistant Professor	Specialty:	Materials and Manufactor-
University of Dayton		ing, Design, and Tri-
Dept. of Mechanical Engr.		biology
Dayton, OH 45469	Assigned:	ML
(513) 229-2835		

Dr. Bruce Janson
Assistant Professor
Carnegie Mellon University
Dept. of Civil Engr.
Pittsburgh, PA 15213
(412) 578-3866

Degree: Ph. D., Civil Eng., 1981
Specialty: Engineering Planning and
Management
Assigned: LMC

Dr. Charles Jones
Associate Professor
North Carolina Central
Dept. of Physics
Durham, NC 27707
(919) 684-6452

Degree: Ph. D., Physics, 1977
Specialty: Lasers and their
Applications, Optics,
Electro-Optics
Assigned: AD

Dr. Walter Jones
Assistant Professor
University of Tennessee
Dept. of Engr. Sci. Mech.
Knoxville, TN 37996
(615) 974-7684

Degree: Ph. D., Engr. Mechanics,
1982
Specialty: Mechanical Behavior of
Composite Materials
Assigned: FDL

Dr. Robert Kallman
Professor
North Texas State University
Dept. of Mathematics
Denton, TX 76203
(817) 565-2155

Degree: Ph. D., Mathematics, 1968
Specialty: Analysis
Assigned: AD

Dr. William Kane, Jr.
Associate Professor
Western Carolina University
Management Dept.
Cullowhee, NC 28723
(704) 227-7401

Degree: Ph. D., Organ. Behavior,
1977
Specialty: Organizational Behavior-
Strategic Management
Assigned: HRL/Wright-Patterson

Dr. Yong Kim
Instructor
McNeese State University
Civil & Mechanical Engr. Dept.
Lake Charles, LA 70609
(318) 477-2520

Degree: Ph. D., Civil Engineering
1984
Specialty: Geotechnical Engineering
Assigned: ESC

Dr. Ronald Kline
Assistant Professor
University of Oklahoma
School of Aero. Mech., & Nuc. Eng.
Norman, OK 73019
(405) 325-5011

Degree: Ph. D., Mech, and Material
Sci., 1978
Specialty: Nondestructive Testing,
Mechanics of Composite
Materials
Assigned: ML

Dr. Kent Knaebel
Assistant Professor
Ohio State University
Chemical Engineering Dept.
Columbus, OH 43210
(614) 422-2508

Degree: Ph. D., Chemical Engr., 1980
Specialty: Adsorption, Ion-exchange, Separations
Assigned: SAM

Dr. David Kohfeld
Professor
Southern Illinois University
Dept. of Psychology
Edwardsville, IL 62006
(618) 692-2582

Degree: Ph. D., Exper. Psychology, 1966
Specialty: Methods of Psychological Inquiry
Assigned: HRL/Williams

Dr. Gabriel Kojoian
Associate Professor
University of Wisconsin
Dept. of Physics/Astronomy
Eau Claire, WI 54701
(715) 836-3148

Degree: Ph. D., Physics, 1966
Specialty: Radio Astronomy
Assigned: GL

Dr. Arthur Kovitz
Professor
Northwestern University
Mechanical Engr. Dept.
Evanston, IL 60201
(312) 492-7066

Degree: Ph. D., Aero Eng., 1957
Specialty: Fluid Mechanics
Assigned: WL

Dr. Madakasira Krishna
Associate Professor
South Carolina State College
Dept. of Math. & Comp. Sci.
Orangeburg, SC 29117
(803) 536-7121

Degree: Ph. D., Applied Math., 1974
Specialty: Computational Fluid Dynamics
Assigned: AEDC

Dr. Raj Krishnan
Associate Professor
North Texas State University
Physics Dept.
Denton, TX 76203
(817) 565-3284

Degree: Ph. D., Physics, 1966
Specialty: Nuclear Physics, Solid State Physics
Assigned: SAM

Dr. William Kyros
Associate Professor
University of Lowell
Mechanical Eng. Dept.
Lowell, MA 01854
(617) 452-5000

Degree: Ph. D., Education, 1980
Specialty: Mechanical Behavior of Materials
Assigned: ML

Dr. David Lai
Professor
University of Vermont
Electrical Engr. & Comp. Sci.
Burlington, VT 05405
(802) 656-3330

Degree: Ph. D., Elec. Eng., 1960
Specialty: Signal Processing, Radar Signal Processing, Image Processing
Assigned: RADC

Dr. Charles Lardent, Jr.
Associate Professor
Auburn University
Dept. of Management
Montgomery, AL 36117
(205) 271-9478

Degree: Ph. D., Organ. Behavior, 1979
Specialty: Leadership, Motivation, and Psychometric Assessment
Assigned: LMDC

Dr. Nabil Lawandy
Assistant Professor
Brown University
Engineering Dept.
Providence, RI 02912
(401) 863-2755

Degree: Ph. D., Chem. Physics, 1980
Specialty: Lasers, Spectroscopy, Lasers Atom Interactions
Assigned: GL

Dr. E. Miller Layton, Jr.
Assoc. Professor
Sterling College
Dept. of Chemistry & Applied Math.
Sterling, KS 67579
(316) 278-2173

Degree: Ph. D., Chem. Physics, 1962
Specialty: Molecular Spectroscopy, Theoretical Molecular Calculations
Assigned: RPL

Dr. Evelyn Leggette
Associate Professor
Jackson State University
Dept. of Elem./Early Child/Reading
Jackson, MS 39217
(601) 968-2186

Degree: Ph. D., Curriculum and Inst., 1976
Specialty: Reading Ed., Dev. Ed., Prog. Dev. and Implementation Curriculum
Assigned: LMC

Dr. Meng Liou
Associate Professor
University of Michigan
Aerospace Engr. Dept.
Ann Arbor, MI 48104
(313) 764-3310

Degree: Ph. D., Aerospace Eng., 1977
Specialty: Computational Fluid Dynamics, Gas Dynamics, Unsteady Flow
Assigned: FDL

Dr. David Lohman
Assistant Professor
University of Iowa
College of Education
Iowa City, IA
(319) 353-5961

Degree: Ph. D., Educ. Psychology, 1979
Specialty: Information Processing Theories of Aptitude for Learning
Assigned: HRL/Brooks

Dr. Lonnie Ludeman
Professor
New Mexico State University
Dept. of Elect. & Comp. Engr.
Las Cruces, NM 88003
(505) 646-1321

Degree: Ph. D., Elec. Eng., 1968
Specialty: Digital Signal Processing, Statistical Communication Theory
Assigned: RADC

Dr. Larry Ludwick
Professor
Tuskegee Institute
Dept. of Chemistry
Tuskegee Institute, AL 36088
(205) 727-8836

Degree: Ph. D., Inorganic Chem., 1969
Specialty: Transition Metal Chem., Siloxane Polymers
Assigned: ML

Dr. Robert MacCallum
Associate Professor
Onio State University
Psychology Dept.
Columbus, OH 43210
(614) 422-1030

Degree: Ph. D., Psychology, 1974
Specialty: Quantitive Psychology
Assigned: AMRL

Dr. William McCormick
Associate Professor
Wright State University
Dept. of Electrical Engr.
Dayton, OH 45435
(513) 873-2849

Degree: Ph. D., Electrical Engr. 1967
Specialty: Radar, Communications and Electromagnetics
Assigned: AL

Dr. Odis McDuff
Professor
University of Alabama
Dept. of Electrical Engr.
University, AL 35486
(205) 348-6351

Degree: Ph. D., Electrical Engr., 1966
Specialty: Lasers and Optics, Electromagnetics
Assigned: SAM

Dr. Bernard McIntyre
Associate Professor
University of Houston
Electronics Dept.
Houston, TX 77004
(713) 749-4753

Degree: Ph. D., Solid State Physics, 1970
Specialty: Diamagnetism in Metals
Assigned: GL

Dr. Richard Miers
Associate Professor
Indiana University
Department of Physics
Fort Wayne, IN 46805
(219) 482-5693

Degree: Ph. D., Atomic Physics, 1970
Specialty: Atom Physics
Assigned: APL

Dr. John Minor
Assistant Professor
University of Oklahoma
Elect. Engr. & Comp. Sci. Dept.
Norman, OK 73069
(405) 325-4721

Degree: Ph. D., Computer Science, 1979
Specialty: Artifical Intelligence
Assigned: RADC

Dr. Charles Mitchell
Professor
Colorado State University
Dept. of Mechanical Engr.
Fort Collins, CO 80523
(303) 491-6558

Degree: Ph. D., Aerospace and Mechanical Science, 1967
Specialty: Combustion Instability, Combustion, Gas Dynamics
Assigned: RPL

Dr. Don Mittleman
Professor
Oberlin College
Dept. of Mathematics
Oberlin, OH 44074
(216) 775-8385

Degree: Ph. D., Mathematics, 1951
Specialty: Geometry, Analysis, Mech.
Assigned: FDL

Dr. Dale Moses
Associate Professor
San Diego State University
Aerospace & Mechan. Engr. Dept.
San Diego, CA 92182
(619) 265-5764

Degree: Ph. D., Aerospace Engr., 1981
Specialty: Wind Tunnel Testing, Aerodynamics
Assigned: FDL

Dr. Kevin Mossholder
Associate Professor
Auburn University
Management Department
Auburn, AL 36849
(205) 826-4071

Degree: Ph. D., Ind./Organ. Psychology, 1978
Specialty: I/O Topics: Organizational Behavior, Human Resources Mgmt.
Assigned: LMDC

Dr. James Mrotek
Associate Professor
Meharry Medical College
Dept. of Physiology
Nashville, TN 37208
(615) 327-6979

Degree: Ph. D., Biology, 1973
Specialty: Endocrine Cell Intracellular Exchanges
Assigned: SAM

Dr. Richard Murphy
Professor
University of Missouri
Department of Physics
Kansas City, MO 64110
(816) 276-1604

Degree: Ph. D., Physics, 1968
Specialty: Statistical Mechanics; Theory of Liquids and Solids
Assigned: FJSRL

Dr. Lena Myers
Professor
Jackson State University
Department of Sociology
Jackson, MS 39217
(601) 968-2591

Degree: Ph. D., Sociology, 1973
Specialty: Social Psychology
Assigned: SAM

Dr. Datta Naik
Chairman & Assoc. Professor
Monmouth College
Dept. of Chemistry
West Long Branch, NJ 07764
(201) 222-6600

Degree: Ph. D., Chemistry, 1972
Specialty: Analytical/Inorganic
Chemistry
Assigned: ESC

Dr. Stephan Nix
Assistant Professor
Syracuse University
Dept. of Civil Engr.
Syracuse, NY 13210
(315) 423-2311

Degree: Ph. D., Environmental Eng.,
1982
Specialty: Environmental Resources
Mgmt., Operations Rsch.,
Economics, Hydrology
Assigned: OEHL

Dr. William Norton
Associate Professor
Southeastern La. University
Biology Department
Hammond, LA 70402
(504) 549-2173

Degree: Ph. D., Cell Biology, 1975
Specialty: Cytopathology, Cellular
Ultrastructure
Assigned: AMRL

Dr. Kendall Nygard
Associate Professor
North Dakota State University
Dept. of Mathematical Sci.
Fargo, ND 58103
(701) 237-8178

Degree: Ph. D., Oper. Rsch., 1978
Specialty: Optimization, Simulation
Modeling, Computer
Graphics
Assigned: LC

Dr. Robert O'Connell
Assistant Professor
University of Missouri
Dept. of Electrical & Comp. Eng.
Columbia, MO 65211
(314) 882-8373

Degree: Ph. D., Elec. Eng., 1975
Specialty: Physical and Quantum
Electronics, and Applied
Optics
Assigned: FJSRL

Dr. William Pardo
Associate Professor
University of Miami
Physics Department
Coral Gables, FL 33124
(305) 284-2323

Degree: Ph. D., Physics, 1957
Specialty: Experimental Plasma
Physics
Assigned: AD

Dr. Martin Patt
Associate Professor
University of Lowell
Department of Elect. Engr.
Lowell, MS 01854
(617) 452-5000

Degree: M.S., Electrical Engr., 1964
Specialty: Computer Science
Assigned: GL

Dr. James Patterson
Professor
S.D. School of Mines/Tech.
Physics Dept.
Rapid City, SD 57701
(605) 394-2361

Degree: Ph. D., Physics, 1962
Specialty: Theoretical Solid State Physics
Assigned: AL

Dr. M. Carr Payne, Jr.
Professor
Georgia Inst. of Tech.
Dept. of Psychology
Atlanta, GA 30332
(404) 894-2681

Degree: Ph. D., Psychology, 1951
Specialty: Experimental Psychology, Psychoacoustics, Eng. Psy.
Assigned: AEDC

Dr. William Perrizo
Associate Professor
North Dakota State University
Dept. of Computer Science
Fargo, ND 58105
(701) 237-7248

Degree: Ph. D., Dynamical Systems, 1972
Specialty: Distributed Database Systems
Assigned: ESD

Dr. Boake Plessy
Professor
Dillard University
Chemistry Department
New Orleans, LA 70122
(504) 283-8822

Degree: Ph. D., Physical Chem., 1974
Specialty: Polymers and Biopolymers, Analytical Chemistry
Assigned: SAM

Dr. Kuldip Rattan
Associate Professor
Wright State University
Dept. of Systems Eng.
Dayton, OH 45435
(513) 873-2403

Degree: Ph. D., Electrical Engr., 1975
Specialty: Digital Control Systems
Assigned: FDL

Dr. Hemen Ray
Assistant Professor
N. C. Argic. & Tech. St. Univ.
Dept. of Mechanical Engr.
Greensboro, NC 27411
(919) 379-7621

Degree: Ph. D., Eng. Mech., 1979
Specialty: Advanced Composites
Assigned: FDL

Dr. Larry Reeker
Professor
Tulane University
Computer Science Dept.
New Orleans, L. 70118
(504) 865-5840

Degree: Ph. D., Comp. Sci., 1974
Specialty: Computational Linguistics,
           Programming Languages,
           Computer-aided
Assigned: HRL/Lowry

Dr. David Reynolds
Assistant Professor
Wright State University
Dept. of Engineering
Dayton, OH 45435
(513) 873-2403

Degree: Ph. D., Biomedical Eng.,
           1978
Specialty: Pulmonary Mechanics,
           Biofluid Mechanics
Assigned: AMRL

Dr. Joseph Saliba
Assistant Professor
University of Dayton
Civil Engr. Dept.
Dayton, OH 45469
(513) 299-3847

Degree: Ph. D., Solid Mechanics,
           1983
Specialty: Structures
Assigned: AMRL

Dr. Walter Salters
Associate Professor
South Carolina State College
Dept. of Natural Science
Orangeburg, SC 29115
(803) 536-7114

Degree: Ph. D., Cell Biology, 1976
Specialty: Cell and Molecular Biology
Assigned: SAM

Dr. Lowell Schipper
Professor
Bowling Green State University
Dept. of Psychology
Bowling Green, OH 43403
(419) 372-2556

Degree: Ph. D., Psychology, 1953
Specialty: Statistics, Measurement
Assigned: HRL/Williams

Dr. Robert Schlegel
Assistant Professor
University of Oklahoma
Dept. of Industrial Engr.
Norman, OK 73019
(405) 325-3721

Degree: Ph. D., Ind. Eng., 1980
Specialty: Human Factors Engineering/
           Ergonomics
Assigned: AMRL

Dr. Howard Schleier
Department Chairman
Norwalk State Tech. College
Department of Chemistry
Norwalk, CT 06854
(203) 838-0601

Degree: M.S., Chem. Eng., 1962
Specialty: Fluid Mechanics, Heat and
           Mass Transfer,
           Thermodynamics
Assigned: RPL

Dr. James Schneider
Professor
University of Dayton
Physics Department
Dayton, OH 45469
(513) 229-2727

Degree: Ph. D., Physics, 1965
Specialty: Solid State Physics
Assigned: ML

Dr. Gordon Schrank
Associate Professor
St. Cloud State University
Dept. of Biological Sciences
St. Cloud, MN 56301
(612) 255-2036

Degree: Ph. D., Med. Microbiology, 1974
Specialty: Electron Microscopy
Assigned: SAM

Dr. Keith Seitter
Assistant Professor
University of Lowell
Dept. of Earth Sciences
Lowell, MA 01854
(617) 452-5000

Degree: Ph. D., Geophysical Sci., 1982
Specialty: Dynamic Meteorology
Assigned: GL

Dr. Paavo Sepri
Associate Professor
University of Oklahoma
Nuclear Engr. Dept.
Norman, OK 73019
(405) 325-5011

Degree: Ph. D., Engr. Science 1971
Specialty: Fluid Mechanics and Heat Transfer
Assigned: APL

Dr. Robert Shaw
Professor
University of Connecticut
Dept. of Psychology
Storrs, CT 06268
(203) 486-4107

Degree: Ph. D., Psychology, 1965
Specialty: Perception/Cognition/Math. Models/Growth Simulation Models
Assigned: AMRL

Dr. John Sheldon
Professor
Florida International Univ.
Dept. of Physical Sci.
Miami, FL 33199
(305) 554-2608

Degree: Ph. D., Engineering, 1964
Specialty: Chemical Kinetics
Assigned: AD

Dr. Harold Sorensen
Associate Professor
Washington State University
Dept. of Civil & Env. Engr.
Pullman, WA 99164
(509) 335-5183

Degree: Ph. D., Engineering Mech., 1966
Specialty: Structural Mechanics
Assigned: WL

Dr. Charles Spiteri
Assistant Professor
Queensborough Community College
Dept. of Elect. & Comp. Tech.
Bayside, NY 11364
(212) 631-6207

Degree: M.E.E., Elec. Eng., 1980
Specialty: Computer Communications,
Local Networks
Assigned: ESD

Dr. William Squires
Associate Professor
Texas Lutheran College
Dept. of Biology
Seguin, TY 78155
(512) 379-4161

Degree: Ph. D., Exercise
Physiology, 1979
Specialty: Biology, Physiology
Assigned: SAM

Dr. Arthur Sterling
Professor
Louisiana State University
Dept. of Chemical Engr.
Baton Rouge, LA 70803
(504) 388-1426

Degree: Ph. D., Chemical Engr.,
1969
Specialty: Fluid Mechanics, Heat
Transfer
Assigned: ESC

Dr. Alexander Stone
Professor
University of New Mexico
Mathematics Dept.
Albuquerque, NM 87131
(505) 277-1613

Degree: Ph. D., Mathematics, 1965
Specialty: Differential Geometry,
Differential Equations,
Electromagnetism
Assigned: SAM

Dr. William Stone
Assistant Professor
Meharry Medical College
Division of Biomedical Sci.
Nashville, TN 37208
(615) 327-6506

Degree: Ph. D., Molecular and
Cellular Biology, 1972
Specialty: Retinal Biochemistry and
Lipid Peroxidation
Assigned: WL

Dr. Jimmy Street
Associate Professor
University of Florida
Soil Science Dept.
Gainesville, FL 32611
(904) 392-1951

Degree: Ph. D., Soil Chem., 1976
Specialty: Soil Pollution
Assigned: ESC

Dr. John Swetits
Professor
Old Dominion University
Mathematics Department
Norfolk, VA 23508
(804) 440-3911

Degree: Ph. D., Mathematics, 1968
Specialty: Approximation Theory and
Numerical Analysis
Assigned: AL

Dr. Richard Tankin
Professor
Northwestern University
Mech. & Nuclear Engr. Dept.
Evanston, IL 60201
(312) 492-3532

Degree: Ph. D., Mech. Engineering, 1960
Specialty: Fluid Mechanics, Heat Transfer
Assigned: APL

Dr. William Thomas
Assistant Professor
Meharry Medical College
Physiology Dept.
Nashville, TN 37208
(615) 327-6979

Degree: Ph. D., Biochemistry, 1980
Specialty: Neurochemistry
Specialty: SAM

Dr. Ken Tomiyama
Assistant Professor
Pennsylvania State University
Dept. of Electrical Eng.
University Park, PA 16802
(814) 865-7667

Degree: Ph. D., System Science, 1977
Specialty: Appl. of System Science in various Fields
Assigned: GL

Dr. Albert Tong
Assistant Professor
University of Texas
Dept. of Mechanical Engr.
Arlington, TX 76019
(817) 273-2297

Degree: Ph. D., Mechanical Engr., 1983
Specialty: Thermoscience
Assigned: APL

Dr. Robert Vance
Assistant Professor
Ohio State University
Psychology Department
Columbus, OH 43210
(614) 422-0685

Degree: Ph. D., Ind./Organ. Psy., 1981
Specialty: Personnel Psychology, Organizational Behavior
Assigned: HRL/Brooks

Dr. Brian Vick
Assistant Professor
Va. Polytechnic Inst. & St. Univ.
Mech. Engr. Dept.
Blacksburg, VA 24061
(703) 961-7596

Degree: Ph. D., Mechanical Engr., 1981
Specialty: Heat Transfer
Assigned: RPL

Dr. Stephen Wallace
Assistant Professor
University of Colorado
Inst. of Cognitive Science
Boulder, CO 80309
(303) 492-8086

Degree: Ph. D., Human Motor Behavior, 1976
Specialty: Human Motor Behavior
Assigned: HRL/Lowry

Dr. Yin-min Wei
Professor
Ohio State University
Computer Science Dept.
Athen, OH 45701
(614) 594-6574

Degree: Ph. D., Electrical Engr.,
1966
Specialty: Signal Processing
Assigned: AMRL

Dr. Isaac Weiss
Assistant Professor
Wright State University
Deptartment of Engineering
Dayton, OH 45435
(513) 873-3021

Degree: Ph. D., Metallurgy, 1978
Specialty: Thermomechanical
Processing, Deformation
Processing
Assigned: ML

Martin Werner
Assistant Professor
University of Texas
School of Public Health
San Antonio, TX 78284
(512) 691-6845

Degree: Ph. D., Environmental
Engr., 1982
Specialty: Hazardous Waste Mgmt.
Engineering TmT
Assigned: ESC

Dr. John Wilson
Associate Professor
South Carolina State College
Habilitative Science Dept.
Orangeburg, SC 29117
(803) 536-8179

Degree: Ph. D., Speech Science/
Communications, 1979
Specialty: Acoustic and Experimental
Phonetics
Assigned: RADC

Dr. Krystine Yaworsky
Associate Professor
Le Moyne College
Psychology Department
Syracuse, NY 13214
(315) 446-2882

Degree: Ph. D., Cognitive
Psychology, 1977
Specialty: Cognitive Processes in
Perception, Human Learning
and Memory
Assigned: HRL/Wright-Patterson

Dr. Chyang Yu
Assistant Professor
Wilkes College
Dept. of Materials Engr.
Wilkes-Barre, PA 18766
(717) 824-4651

Degree: Ph. D., Ceramic Eng., 1977
Specialty: Structural Ceramic
Materials, Electronic
Ceramics, Microanalysis
Assigned: ML

<u>PARTICIPANT LABORATORY ASSIGNMENT (Page 1)</u>

1984 USAF/SCEEE SUMMER FACULTY RESEARCH PROGRAM

AERO PROPULSION LABORATORY
   (Wright-Patterson Air Force Base)
1.	Richard Anderson	6.	Kakkattukuzhy Isaac
2.	Huei-huang Chiu	7.	Richard Miers
3.	Louis Chow	8.	Paavo Sepri
4.	John Erdei	9.	Richard Tankin
5.	Dennis Flentge	10.	Albert Tong

AEROSPACE MEDICAL RESEARCH LABORATORY
   (Wright-Patterson Air Force Base)
1.	Gwendolyn Howze	5.	Joseph Saliba
2.	Robert MacCallum	6.	Robert Schlegel
3.	William Norton	7.	Robert Shaw
4.	David Reynolds	8.	Yin-Min Wei

ARMAMENT DIVISION
   (Eglin Air Force Base)
1.	Myron Calhoun	6.	Charles Jones
2.	Do Chang	7.	Robert Kallman
3.	Robert Courter	8.	William Pardo
4.	Terrence Dwan	9.	John Sheldon
5.	Chen-Chi Hsu		

ARNOLD ENGINEERING DEVELOPMENT CENTER
   (Arnold Air Force Station)
1. Gregory Corso
2. Doyle Hasty
3. Madakasira Krishna
4. M. Carr Payne, Jr.

AVIONICS LABORATORY
   (Wright-Patterson Air Force Base)
1. Albert Biggs
2. Mike Burlakoff
3. Ronald Greene
4. Paul Griesacker
5. William McCormick
6. James Patterson
7. John Swetits

BUSINESS RESEARCH MANAGEMENT CENTER
   (Wright-Patterson Air Force Base)
1. Richard Bernhard
2. Thomas Gulledge, Jr.

ELECTRONICS SYSTEMS DIVISION
   (Hanscom Air Force Base)
      1. William Perrizo
      2. Charles Spiteri

ENGINEERING & SERVICES CENTER
   (Tyndall Air Force Base)
      1. Annalingam Anandarajah   5. Datta Naik
      2. Eric Drumm   6. Arthur Sterling
      3. Paul Hoffman   7. Jimmy Street
      4. Yong Kim   8. Martin Werner

FLIGHT DYNAMICS LABORATORY
   (Wright-Patterson Air Force Base)
      1. George Doyle   6. Meng Liou
      2. Franklin Eastep   7. Don Mittleman
      3. Albert Havener   8. Dale Moses
      4. Mario Innocenti   9. Kuldip Rattan
      5. Walter Jones   10. Hemen Ray

FRANK J. SEILER RESEARCH LABORATORY
   (USAF Academy)
      1. David Chung   5. Hendrik Hameka
      2. Hermann Donnert   6. Richard Murphy
      3. James Eberhart   7. Robert O'Connell
      4. Larry Glasgow

GEOPHYSICS LABORATORY
   (Hanscom Air Force Base)
      1. Francesco Bacchialoni   8. Gabriel Kojoian
      2. John Bahng   9. Nabil Lawandy
      3. James Baird   10. Bernard McIntyre
      4. Alan Bentley   11. Martin Patt
      5. Frank Colby   12. Keith Seitter
      6. John Cyranski   13. Ken Tomiyama
      7. Peter Hierl

HUMAN RESOURCES LABORATORY/LRL
   (Wright-Patterson Air Force Base)
      1. Subramaniam Deivanayagam
      2. Emory Enscore, Jr.
      3. Sallie Gordon
      4. William Kane, Jr.
      5. Krystine Yaworsky

HUMAN RESOURCES LABORATORY/OTR
   (Williams Air Force Base)
      1. Arthur Harriman
      2. David Kohfeld
      3. Lowell Schipper

HUMAN RESOURCES LABORATORY/MO
(Brooks Air Force Base)
1. Bruce Feiring
2. Cynthia Ford
3. David Lohman
4. Robert Vance

HUMAN RESOURCES LABORATORY/ID
(Lowry Air Force Base)
1. Larry Reeker
2. Stephen Wallace

LEADERSHIP & MANAGEMENT DEVELOPMENT CENTER
(Maxwell Air Force Base)
1. Louis Buckalew
2. Charles Lardent
3. Kevin Mossholder

LOGISTICS COMMAND
(Wright-Patterson Air Force Base)
1. Kendall Nygard

LOGISTICS MANAGEMENT CENTER
(Gunter Air Force Base)
1. Philip Chong
2. Bruce Janson
3. Evelyn Leggette

MATERIALS LABORATORY
(Wright-Patterson Air Force Base)
1. Charles Drummond, III
2. Delcie Durham
3. William Feld
4. Thomas Graham
5. Vijay Gupta
6. Vinod Jain
7. Ronald Kline
8. William Kyros
9. Larry Ludwick
10. James Schneider
11. Isaac Weiss
12. Chyang Yu

OCCUPATIONAL & ENVIRONMENTAL HEALTH LABORATORY
(Brooks Air Force Base)
1. Stephan Nix

ROCKET PROPULSION LABORATORY
(Edwards Air Force Base)
1. Gloria Anderson
2. E. Miller Layton, Jr.
3. Charles Mitchell
4. Howard Schleier
5. Brian Vick

ROME AIR DEVELOPMENT CENTER
(Griffiss Air Force Base)
1. Adly Fam
2. Basil Gala
3. Barry Ganapol
4. David Gilliam
5. Brian Holmes
6. Robert Jackson, Jr.
7. David Lai
8. Lonnie Ludeman
9. John Minor
10. Johnny Wilson

SCHOOL OF AEROSPACE MEDICINE
(Brooks Air Force Base)
1. Deborah Armstrong
2. Mukul Banerjee
3. Jeya Chandra
4. David Cohoon
5. Robert Dorman
6. Edward Greco, Jr.
7. Kent Knaebel
8. Raj Krishnan
9. Odis McDuff
10. James Mrotek
11. Lena Myers
12. Boake Plessy
13. Walter Salters
14. Gordon Schrank
15. William Squires
16. William Stone
17. William Thomas

WEAPONS LABORATORY
(Kirtland Air Force Base)
1. Robert Colclaser, Jr.
2. Frederick Eisler
3. Eddie Fowler
4. Arthur Kovitz
5. Harold Sorensen
6. Alexander Stone

RESEARCH REPORTS
1984 USAF-SCEEE SUMMER FACULTY RESEARCH PROGRAM

xxviii

Report Number	Title	Research Associate
12	USAF Spouse Survey: Theoretical Model, Critique, and Revision	Dr. L.W. Buckalew
13	Ada Compiler Evaluation and Validation (E&V) Taxonomy	Mike Burlakoff
14	Software Drivers for the Z-204 Multiport Interface Card	Dr. Myron A. Calhoun
15	The Analysis of a Single Base in an Airlift Operation	Dr. M. Jeya Chandra
16	The Roles of PEI as an Additive in EAK	Dr. Do Ren Chang
17	The Uniqueness of Phase Retrieval from Intensity Measurements	Dr. Huei-huang Chiu
18	Investigating the Potential Application of an "Integrated" Resource Management System to Various Air Force Environments	Dr. Philip S. Chong
19	Low Temperature Expandable Mega-Watt Pulse Power Radiator	Dr. Louis C. Chow
20	Experimental Evaluation and Development of Components for an Infrared Passive Laser Gyro	Dr. David Y. Chung
21	The Electromagnetic Pulse Response of Structures with Frequency Dependent Electrical Properties	Dr. David K. Cohoon
22	Comparison Between Two Atmospheric Boundary Layer Models: Second-Order Turbulence Closure Versus Highly Parameterized, Simplified Physics	Dr. Frank P. Colby, Jr.
23	A Study of the Shiva Star-Type Inductive Pulse Compression System	Dr. R. Gerald Colclaser
24	An Identification of the Human Limitations in the Control Room of Wind Tunnel 4T	Dr. Gregory M. Corso
25	Internal Flow Studies of a Class of Ballistic Launchers	Dr. Robert W. Courter

Report Number	Title	Research Associate
26	Dynamical Spectral Analysis for Nonstationary processes	Dr. John F. Cyranski
27	An Experimental Investigation of Human Torque Strength	Dr. S. Deivanayagam
28	Effects of Nuclear Radiation on the Optical Characteristics of Laser Components	Dr. Hermann J. Donnert
29	Phospholipid Metabolism in a Synaptic Membrane Preparation Isolated from Cerebellar Cortex	Dr. Robert V. Dorman
30	A Review of Computer Simulations for Aircraft-Surface Dynamics	Dr. George R. Doyle, Jr.
31	Constitutive Modelling for Blast Induced Wave Propagation	Dr. E. C. Drumm
32	SiC Reinforced Glass-Ceramic Composites	Dr. Charles H. Drummond
33	Computer Simulation of TI-6AL-4V and Rene' 95 Disks for the T-700 Engine	Dr. Delcie R. Durham
34	Graphics Generation and Image Enhancement and Restoration Techniques	Dr. Terrence E. Dwan
35	Structural Modifications to Enhance the Active Vibration Control of Large Flexible Structures	Dr. Franklin E. Eastep
36	Wetting Behavior of Imidazolium-Containing Room-Temperature Molten Salts	Dr. James G. Eberhart
37	The Emittance of Particle and Laser Beams and Measurement of the Angle Between Crossed Laser and Particle Beams to High Precision	Dr. Frederick R. Eisler
38	A Generic Logistics Model for Evaluating Operational Readiness of a Weapon System	Dr. E. Emory Enscore, Jr.

xxx

Report Number	Title	Research Associate
39	Characterization of Turbulence Through Methods of Field Theory	Dr. John E. Erdei
40	Issues in High Throughput Signal Processing	Dr. Adly T. Fam
41	Upgrade of Policy Specifying	Dr. Bruce Feiring
42	New Phenoxy Substituted Dianhydrides	Dr. William A. Feld
43	Cyclic Voltammetric and Cobra Analysis of Synthetic Lubricant Degradation	Dr. Dennis R. Flentge
44	Gender Differences on Subtests of the ASVAB and the Relationship Between ASVAB Subtest Scores and Psychological/Social Variables for Males and Females	Dr. Cynthia A. Ford
45	Communications Network Simulation Topics	Dr. Eddie R. Fowler
46	Nonparametric CFAR Detection of MTI Radar Signals in Heavy Clutter	Dr. Basil E. Gala
47	Benchmark Solutions for the Spencer-Lewis Equation Describing Electron Transport in an Infinite Medium	Dr. Barry D. Ganapol
48	Electromagnetic Waves in a Disturbed Atmosphere Environment	Dr. David S. Gilliam
49	Alternative Computational Methods for Separated Flows on Pitched Airfoils	Dr. Larry A. Glasgow

Volume II

50	Manual and Computer-Aided Sequential Diagnostic Inference	Dr. Sallie E. Gordon
51	Angle Resolved Ion-Scattering Spectroscopy-a Feasibility Study	Dr. Thomas P. Graham
52	Electrogastrogram and its Effectiveness in Evaluation of Motion Sickness	Dr. Edward C. Greco, Jr.

Report Number	Title	Research Associate
53	Far-Infrared Absorption Profiles for Shallow Donors in GaAs-GaAlAs Quantum Well Structures	Dr. Ronald L. Greene
54	Digital Signal Processing Approaches for Analysis and Evaluation of Communication Systems	Dr. Paul B. Griesacker
55	Production Rate Variations Cost Models	Dr. Thomas R. Gulledge, Jr.
56	Thermal Stability Characteristics of Silahydrocarbons	Dr. Vijay K. Gupta
57	Calculations of Electron Spin Resonance Coupling Constants	Dr. Hendrik F. Hameka
58	Effects of Pyridostigmine on Performance of Mission-ready Pilots in the OT Simulation Facility	Dr. Arthur E. Harriman
59	Propulsion Facility Planning for Test Information Productivity Improvement with Emphasis on Data Measurement Uncertainty in the Engine Test Facility	Dr. Doyle E. Hasty
60	A Study on Point Diffraction Interferometry Plus Holographic Measurements of a Turbulent Boundary Layer on a Roughened Wind Tunnel Wall	Dr. A. George Havener
61	Effects of Temperature and Reactant Solvation Upon the Rates of Gas-Phase Ion-Molecule Reactions	Dr. Peter M. Hierl
62	A Monte Carlo Sampling of BDR Times	Dr. Paul C. Hoffman
63	Bismuth Silicon Oxide: Sample Variability Investigated with Thermally Stimulated Conductivity and Thermoluminescence	Dr. Brian W. Holmes

Report Number	Title	Research Associate
64	Comparison of Periosteums from Femur and Vertebral Bone	Dr. Gwendolyn B. Howze
65	On a Thin-Layer Navier-Stokes Code and Transonic Projectile Aerodynamics	Dr. Chen-Chi Hsu
66	Effect of Display Dynamics in Manual Control Tasks	Dr. Mario Innocenti
67	Computational Study of Ramjet Compustor Flowfields	Dr. Kakkattukuzhy M. Isaac
68	Numerical Characterization of Microstrip Discontinuities on Thick Substrates	Dr. Robert W. Jackson, Jr.
69	Advanced Physical Modeling/ Wedge Test Development	Dr. Vinod K. Jain
70	Development of a Vehicle Fleet Analysis System	Dr. Bruce N. Janson
71	Photographic Emulsions for Preparation of Holographic Filters	Dr. Charles R. Jones
72	Fracture Behavior of Cross-Ply Graphite/Epoxy Composite Laminates	Dr. Walter F. Jones
73	The Optimal Construction of Synthetic Discriminant Functions for Optical Matched Filters	Robert R. Kallman
74	Stress and Aircraft Maintenance Performance in a Combat Environment	Dr. William D. Kane, Jr.
75	Finite Element Analysis of Certrifuged Concrete Culverts	Dr. Yong S. Kim
76	Acoustic Emission in Composites	Dr. Ronald A. Kline
77	Process Configuration Alternatives for Separation of Gas Mixtures by Pressure Swing Adsorption	Dr. Kent S. Knaebel
78	The Distributional Analysis of Contrast Sensitivity Measures	Dr. David L. Kohfeld

Report Number	Title	Research Associate
79	The Relation Between Hard X-Ray Bursts and Type II Radio Emission	Dr. Gabriel Kojoian
80	Thermal Layer Development with Energy Flux at the Ground/Air Interface	Dr. Arthur A. Kovitz
81	Computational Fluid Dynamics Grids-Flow Properties Interpretation Algorithm	Dr. Madakasira G. Krishna
82	Development of an Optical Multichannel Analyzer System	Dr. Raj. M. Krishnan
83	Interlaminar Shear Testing of Carbon/Carbon Composites	Dr. William Kyros
84	Two-Dimensional Median for Image Preprocessing in Machine Recognition	Dr. David C. Lai
85	Psychological Correlates of Physiological Indicators of Stress-Related Disorders: A Search for Structure and Relatedness	Dr. Charles L. Lardent, Jr.
86	Optical Bistability with Liquid Media: Experimental Studies and Theoretical Predictions	Dr. N.M. Lawandy
87	Survey of High-Energy Molecular Systems	Dr. E. Miller Layton, Jr.
88	Rewrite of AFM 28-345	Dr. Evelyn J. Leggette
89	Numerical Simulation of a Supersonic Inlet Flow	Dr. Meng-Sing Liou
90	Information Processing Analysis of Spatial Synthesis and of the Relationship Between Learning and Intelligence	Dr. David F. Lohman
91	Suboptimum Extrapolation for Spectral Estimation	Dr. Lonnie C. Ludeman

Report Number	Title	Research Associate
92	Silane-Treated Silica Fillers for Elastomer Reinforcement	Dr. Larry M. Ludwick
93	The Application of Structural Equation Modeling to Experimental Data	Dr. Robert MacCallum
94	The use of the Instantaneous Frequency Transient in the Design and Optimization of the Channelized Receiver and Instantaneous Frequency Measurement (IFM) Versions of the Passive EW Receiver	Dr. William S. McCormick
95	Techniques for Ultra-Short Pulses in Nd:YAG Lasers	Dr. Odis P. McDuff
96	Plasma Generation and Diagnostics for Ionospheric Plasma Simulation	Dr. Bernard McIntyre
97	Spectroscopic Studies of Thyratron Discharges	Dr. Richard E. Miers
98	On Interfacing Logic Programming Systems and Relational Databases	Dr. John T. Minor

Volume contains 51 papers developed during the summer '84 program.

Volume III

99	Evaluation of Models for Liquid Propellant Rocket Combustion Instability	Dr. Charles E. Mitchell
100	Large Space Structure Dynamic Testing	Dr. Don Mittleman
101	Acquisition of Wind Tunnel Wall Pressure Distributions for use in Developing a 3-D Transonic Wall Correction Code	Dr. Dale F. Moses
102	Leadership Effects as Measured by the Organizational Assessment Package: A Multi-level Perspective	Dr. Kevin W. Mossholder
103	Raman Spectroscopy of Unstimulated and Stimulated Cultured Normal and Neoplastic Human or Mammalian Cells	Dr. James J. Mrotek

Report Number	Title	Research Associate
104	Preliminary Monte Carlo Studies of the Structure of Molten Salts	Dr. R. D. Murphy
105	Military Family Stress	Dr. Lena Wright Myers
106	Air Oxidation of Hydrazine -- A Kinetic Study	Dr. Datta V. Naik
107	Conceptual Design of the USAF Installation Restoration Program Information Management System	Dr. Stephan J. Nix
108	The Cytotoxic Effects of Trimethylpentane on Rat Renal Tissue	Dr. William N. Norton
109	Computer-Based Optimization Algorithms for LOGAIR Cargo Allocation	Dr. Kendall E. Nygard
110	Laser Damage Studies in Purified and Plasticized Polyakylmethacrylates	Dr. Robert M. O'Connell
111	Experimental Physics Aspects of the AFATL Railgun Effort	Dr. William B. Pardo
112	Analysis of the Validity of Barnes Transmissometer Data	Dr. Martin A. Patt
113	Permanent Periodic Magnets and the Reproducibility of Traveling Wave Tubes	Dr. James D. Patterson
114	Operator Activities in Wind Tunnel 4T	Dr. M. Carr Payne, Jr.
115	Future Tactical Air Control System Database Design	Dr. William Perrizo
116	Raman Spectroscopy of Glycosaminoglycans from Bovine Cornea	Dr. Boake L. Plessy
117	Study of Control Mixer Concept for Reconfigurable Flight Control System	Dr. Kuldip S. Rattan

Report Number	Title	Research Associate
118	Analyslis of Armor Bracketry	Dr. Hemen Ray
119	Artificial Intelligence and Computational Linguistics Research	Dr. Larry H. Reeker
120	Mathematical Modeling of the Human Cardiopulmonary System	Dr. David B. Reynolds
121	Nonlinear Modeling of Seat Cushions	Dr. Joseph E. Saliba
122	The Relationship of Fibrinogen and Plasma Lipids to Bubble Formation at the Air Interface During Decompression Sickness	Dr. Walter L. Salters
123	N/A	Dr. Lowell Schipper
124	Evaluation of Training Performance for the USAF Criterion Task Set	Dr. Robert E. Schiegel
125	Regenerative Heat Transfer in an LSSCDS Engine	Dr. Howard Schleier
126	Raman Spectroscopy Studies of Extrinsic P-Type Silicon	Dr. James Schneider
127	Bacteriologic Techniques for the Isolation and Identification of Legionellae	Dr. Gordon D. Schrank
128	A Three-Dimensional Radiation Boundary Condition for Mesoscale Numerical Models	Dr. Keith L. Seitter
129	Calculation of Enhanced Heating in Turbulent Boundary Layers Influenced by Free Stream Turbulence	Dr. Paavo Sepri
130	An Adjoint Systems Approach to Learning and Transfer of Training	Dr. Robert E. Shaw
131	The Theory of Self-Heating Phenomena in Explosives with Applications to EAK	Dr. John W. Sheldon

Report Number	Title	Research Associate
132	The Development of Computational Efficiencies in Continuum Finite Element Codes using Matrix Difference Equations	Dr. Harold Sorensen
133	Base Communications Architecture Security Issues	Dr. Charles J. Spiteri
134	Cardiovascular Responses of High- and Low-Fit Men to Head-Down Rest Followed by Ortho-stasis and Exercise	Dr. William Squires
135	Recommendations on Combustion Research at Tyndall Air Force Base, Florida	Dr. Arthur M. Sterling
136	Electromagnetic Lens Design Techniques	Dr. Alexander P. Stone
137	The Role of Antioxidant Nutrients in Preventing Hyperbaric Oxygen Damage to the Retina	Dr. William L. Stone
138	Naphthalene Adsorption by Florida Soils	Dr. Jimmy J. Street
139	An Optimal Trajectory Problem	Dr. John J. Swetits
140	The Role of Vortex Shedding in a Bluff-Body Combustor	Dr. Richard S. Tankin
141	An Investigation of Acetylcholine as a Neurotransmitter of Cerebellar Mossy Fibers	Dr. William E. Thomas
142	Unified Real Part of Susceptibility over Millimeter through Infrared Region	Dr. Ken Tomiyama
143	Numerical Modeling of Multi-phase Turbulent Recirculating Flows in Sudden-Expansion Ramjet Geometry	Dr. Albert Y. Tong

Report Number	Title	Research Associate
144	Development of Three Covariance Structure Models for Analysis of Performance Measurement Project Data	Dr. Robert J. Vance
145	Laminarization in Highly Accelerated Flow	Dr. Brian Vick
146	Development of Computer Assisted Instruction in Basic Electronic Trouble Shooting	Dr. Stephen A. Wallace
147	The Development of a Computerized System for Management Information and Inter-Office Communication	Dr. Yin-min Wei
148	The Processing Window for the Near Beta Ti-10V-2Fe-3A1 Alloy	Dr. Isaac Weiss
149	Effects of Humidity on Gaseous Phase Adsorption of Trichloroethylene by Activated Carbon	Dr. Martin D. Werner
150	A Comparative Analysis of Whispered and Normally Phonated Speech using an LPC-10 Vocoder	Dr. Johnny R. Wilson
151	Cognitive Factors in Computer-Aided Fault Diagnosis	Dr. Krystine B. Yaworsky
152	Characterization of Ceramic-Ceramic Composites	Dr. Chyang John Yu

1984 USAF-SCEEE SUMMER FACULTY RESEARCH PROGRAM

Sponsored by the

AIR FORCE OFFICE OF SCIENTIFIC RESEARCH

Conducted by the

SOUTHEASTERN CENTER FOR ELECTRICAL ENGINEERING EDUCATION

FINAL REPORT

EVALUATION OF MODELS FOR LIQUID PROPELLANT ROCKET
COMBUSTION INSTABILITY

Prepared by: Dr. Charles E. Mitchell

Academic Rank: Professor

Department and   Department of Mechanical Engineering
    University: Colorado State University

Research Location: Air Force Rocket Propulsion Laboratory, Propulsion
                   Analysis Division, Aerothermochemistry Branch

USAF Research: Mr. Wayne E. Roe

Date: August 28, 1984

Contract No.:   F49620-82-C-0035

EVALUATION OF MODELS FOR LIQUID PROPELLANT

ROCKET COMBUSTION INSTABILITY

by

Charles E. Mitchell

ABSTRACT

Models for the determination of the stability characteristics of liquid
propellant rocket engine combustors are evaluated. Recommendations
concerning the use of the four most widely used models; the Priem Model,
the Crocco-Reardon Model, the Beidmann-Feiler Model, and the Dykema
Model are made. Each of these models is found to be incomplete,
inaccurate and/or approximate as far as predictive capability is
concerned. The continuing need for fundamental understanding and
modeling of the (open-loop) response of the combustion process is
discussed, and research aimed at gaining this understanding is
suggested. The need for an overall (closed-loop) combustion instability
model which includes the major combustor features which may interact and
affect stability is pointed out, and such a model, developed at Colorado
State University, is presented and proposed for further development.

I. <u>INTRODUCTION</u>

The problem of combustion instability has plagued the development and
application of liquid propellant rocket engines from the earliest days
of their use. A tremendous amount of effort and resources has been
expended over the last three decades in controlling this problem. The
major period of activity in this country extended from the early 1950's
to the early 1970's. During this time, some considerable progress in
understanding the nature of the instabilities was made, and analytical,
numerical, empirical and semi-empirical models were developed in order
to aid in the production of stable engines. No complete, universal
solution to the problem was found, however, and no single widely
acceptable predictive model emerged. Rather, a fragmented situation
resulted in which design engineers from different engine manufacturers
used different techniques and models to work toward stable
configurations. Much of this, in the end, depended on the practical
experience and skill of the particular engineers involved for success:
more art than science was required. On the theoretical side, all the
models were limited to some extent, and controversy as to the physical
and mathematical correctness of the several theories was rife, and never
resolved satisfactorily.

With the decline in interest in the development of new liquid
propellant motors which occurred in the 1970's, their stability problems
became less important and the number of investigators working on the

problem, as well as the resources dedicated to its solution, dropped

essentially to zero. Recently, however, a new range of potential

applications for liquid propellant engines, associated with orbital

transfers, and satellite repair, modification, managment and

destruction, has been identified. Stability problems are to be

anticipated with the new engines required, and in fact have already

occurred in one development program. At this time, however, the people

who developed the earlier models and cultivated a hard won skill in

their use are, by and large, gone from the scene. The body of available

information which remains is plentiful, complex, diffuse and confusing

to new engineers involved in the design process. A need both for a

critical review of the older work as well as a renewed efffort in the

fundamental solution of the liquid rocket stability problem has been

identified by the Air Force Rocket Propulsion Laboratory. It is the

purpose of the research described here to contribute to the satisfaction

of this need.

The SCEEE Faculty Fellow involved (C. E. Mitchell) performed liquid

rocket stability research (funded by NASA and NSF) continuously from

1968 to 1978. During this ten year period a closed loop stability theory

for liquid rocket combustors was pursued by the Fellow and his graduate

students at Colorado State University The development of this theory was

never finished due to the lack of interest (and funding) which occurred

at the end of the 1970's, though several partial or approximate analyses

evaluating the effects of injector face baffles, acoustic cavities, and

both linear and nonlinear waveforms on overall combustor stability were

completed. A computer code based on a simplified, linearized version of

the theory was also written, documented and distributed.

Though recently involved in other research areas, Professor Mitchell has retained a strong interest in liquid rocket stability and welcomed the opportunity afforded by the SCEEE program and the renewed interest of the Air Force in liquid rockets to return to the field, assess the state of the art, and resurrect the stability theory mentioned above.

II. OBJECTIVES OF THE RESEARCH EFFORT

The general goal of this research was to initiate a comprehensive review and critical evaluation of the state of the art in liquid rocket combustion instability analysis and modeling. The intent was primarily to help provide a knowledge base from which future research in stability modeling might proceed. One element of this knowledge base was to be the stability code developed by the SCEEE Fellow and discussed briefly in the Introduction.

Concisely, the specific objectives were:

(1) To critically review and evaluate the stability models which have been used most widely in the past, particularly in liquid rocket development programs, and to determine and define their strengths, weaknesses, and limitations.

(2) To identify essential areas for additional research, based primarily on this review of the existing models, but including reference

to the general body of theoretical and experimental literature on combustion instability as time permitted.

(3) To install and make operational the Fellow's integral, closed loop stability model on the AFRPL computer system and to familiarize a staff member with its use.

III. <u>EVALUATION OF EXISTING STABILITY MODELS</u>

As mentioned in the Introduction, the bulk of the liquid rocket instability work performed in this country was completed by the early 1970's. A reference book[2] on liquid rocket combustion instability which was published in 1972 therefore served as an excellent starting point for this review. Both the summaries given there and the extensive reference list provided were extremely useful. In addition the proceedings of the JANNAF Combustion Meetings (1964-1983) were used extensively. Other papers and reports both from the Fellow's personal library and from the AFRPL library were also employed.

Though considerable background and general review was done to reacquaint the Fellow with the field, attention was focused primarily on the four stability models which have been used most often in the past in designing stable liquid rocket combustors. These are: the Priem Model;[3,4,5] the Crocco-Reardon (sensitive time lag) Model;[6,7,8] the Dykema Model;[9,10] and the Heidmann-Feiler (response factor)

11,12,13

Model. Particularly in the case of the Priem Model and the Crocco-Reardon Model, no single computer code or reference exists, but rather a body of experimental, analytical and numerical work all following generally the same approach and modeling philosophy. This is, an organization will say that, for example, the Priem Model was used to evaluate the stability of a certain engine. In reality that organization's version of the Priem Model, often extended and/or modified in several ways was used. With this in mind each of the four modeling approaches was studied and evaluated to determine its generic strengths and weaknesses. Both mathematical and physical features of the several models were considered and conclusions as far as the correctness, applicability, accuracy, and future potential of each of them were drawn. Recommendations based on these conclusions are given later in this report. Space limitations permit neither a presentation of the analytical approach used in these models, nor a critical discussion of their features here. However, a report containing this information for each of the four models considered is currently being completed and will be submitted to the Air Force Rocket Propulsion Laboratory separately.

IV. INSTALLATION OF THE CSU STABILITY MODEL

A simplified computer code [1] based on a general stability theory developed by the Fellow and his gradute students at Colorado State

University was transmitted to AFRPL and made operational on its CDC computer system during the appointment period.

Several distinct analyses all based in a general way on an integral Green's function approach to the evaluation of overall liquid rocket engine stability were performed by the CSU group from 1969-1979, and included treatment of slot absorbers, acoustic liners, conical nozzles, nonlinear waveforms, wave distortion effects on vaporization response, axial combustion distribution, and injector face baffles. In general these formed thesis topics for the graduate students involved, most were published in the literature in one form or another (A complete list of these is given in Reference 1.)

The code MODULE, as it exists, contains a simplified form of the anlysis. The intent in writing it was to produce a somewhat user friendly program which could be used and understood by someone with only a modest background in liquid rocket stability. The code can be used either to produce stability maps, or to determine frequency and decay rates for a given configuration. The simplified form considers three dimensional linear oscillations in a cylindrical combustor with a nozzle of arbitrary acoustic admittance, a slot acoustic absorber or partial length acoustic liner, a combustion zone response of abritrary frequency dependence, concentrated at the injector and an arbitrary mean flow Mach number. Injector face baffles, axial combustion distribution and finite amplitude wave effects are not included in this simplified form because the original analyses of these features were cumbersome, time consuming numerically, or incomplete. Reworking and improvement of these aspects of the model so that they could be added to MODULE in order to increase

99-8

its comprehensiveness is suggested as a goal of follow-on work.

An APRPL cooperative student, Steve Wall, was given some
introductory tutoring in the use and interpretation of the code. By the
end of the summer appointment period he had gained some facility in its
use and had run several test cases.

V. RECOMMENDATIONS

(1) Use of the Four Stability Models Reviewed

Each of the models reviewed, the Priem Model, the Crocco-Reardon
Model, the Heidmann-Feiler Model, and the Dykema Model, was found to be
flawed and wanting as far as the ability to predict stability behavior
quantitatively is concerned.

It is recommended that no one-dimensional (standard form) of the
Priem Model be used in making stability predictions. It is worthwhile
to study this model in order to gain familiarity with the numerical
approach involved, and to serve as a knowledge base from which
multi-dimensional forms of this type of model can be developed (See
Recommendation (5)). However, the one dimensional collapsed geometry
assumed, and the frequency independent vaporization model used are
sufficiently unrealistic that predictions must be rated unreliable.

The Crocco-Reardon Model depends upon empirical correlations for
its predictions. The model parameters (interaction index and time lag)
determined through these correlations can only be taken as quite

99-9

approximate for any injector-propellant combination. Moreover, in
order to use these correlations it is necessary that an accurate
stability map (in terms of interaction index and time lag required)
which correctly includes all other chamber features be available. The
capability for this is only now being developed (See Recommendation
(3)). Consequently, it is recommended that this type of prediction be
used only qualitatively, and with great caution.

The open-loop models reviewed (Heidmann-Feiler, Dykema) are
specific to an assumed combustion mechanism in each case. It is not
known a priori which of these, if any, is the critical stability
mechanism in a given liquid rocket engine. In addition the models have
not been validated experimentally. (See Recommendations (4) and (2)).
Finally, these models are open-loop in form and at best can only give
directions for stability improvement, not the magnitude of the changes
required. Therefore, it is recommended that this type of model not be
used directly for stability prediction, but rather that each be
evaluated experimentally and, if verified, then be used as input
elements of an overall stability model.

(2) Combustion Response Characterization and Modeling

The review conducted indicated that the mechanisms by which the
combustion process in liquid rocket engines responds to high frequency
pressure and velocity oscillations is not yet well understood. Indeed,
the response models available are almost entirely quasi-steady
extensions of steady state models and correlations. Diagnostic

techniques developed in related combustion fields during the past decade (CARS, LDV, etc.) appear to make detailed experimental studies of the unsteady injection, atomization, vaporization and diffusion processes feasible at the present time. Consequently it is recommended that an experimental program with the goal of describing and characterizing the mechanisms present in the several phases of the unsteady combustion response process be carried out. Specifically, these experiments should be designed so that the effects of imposed oscillations (pressure and velocity) of varying amplitude, waveform and frequency can be observed and measured. Results of these experiments should be used as inputs to, and in conjunction with, modeling efforts directed at the characterization of individual mechanisms as well as the overall response process in open-loop form.

(3) Development and Improvement of the CSU Stability Model

The Colorado State University stability model is probably the most comprehensive analytical technique for the evaluation and prediction of the overall stability of liquid propellant rocket engines currently available. The model's present form is incomplete as discussed above. It is recommended that the existing model be extended and modified to predict the effect of arbitrary combustion distribution, nonlinear and distorted waveforms, and injector face baffles. That these features can, in principle, be treated by the integral Green's function approach employed has been established in several limited and/or approximate analyses of these effects, already perfomred by the author and his

students. The code should also be generalized so that it can accept as inputs the results of the open-loop combustion response models generated as a result of the experimental and analytical efforts of Recommendation (2). Part of this effort could be completed under the RISE follow-on research program.

(4) Liquid Rocket Instability Research Engine

It is recommended that an experimental liquid propellant rocket research engine dedicated solely to the evaluation and validation of both open-loop combustion response models (Recommendation (2)) and the overall combustor stability model (Recommendation (3)) be designed and constructed. In the past the great majority of data on liquid rocket stability has been gleaned as a by-product in development or stability improvement programs associated with production engines. This has led to incomplete, sparse and fragmented data on instability being the frequent result. A single research test bed developed in coordination with the open-loop and overall stability modeling efforts should avoid this and lead to a synergistic solution to the problem. Certainly the research engine should be of an extremely flexible design and reconfigurable as far as the major engine elements critical to stability (injector, baffles, acoustic absorber, nozzle) are concerned. In addition, a system for controlled pulsing of the engine would be a necessity.

(5) Numerical Analysis of Wave Develoment

The overall stability model of Recommendation (3) evaluates and
predicts the stability of a periodic or almost periodic oscillation. It
cannot predict the temporal development of such a wave or oscillation,
nor, directly, the size or shape of combustor disturbance necessary to
initiate it. A numerical integration of the governing conservation
equations, given a combustion response model and geometrical
configuration could provide such information. This type of analysis
(which would be in the spirit of, and an extension to, the Priem
approach) would have to be at least two dimensional (see the discussion
of the Priem Model given above) and flexible enough to accept arbitrary
open-loop combustion response models. Results from calculations should
be useful i. predicting triggering behavior and in evaluating
numerically the relative potential of open loop response mechanisms for
initiating oscillations. Preliminary work in the development of this
analysis is suggested as an appropriate part of a RISE program.

ACKNOWLEDGEMENTS

REFERENCES

1. Mitchell, C.E., and Eckert, K., "A Simplified Compu'er Program for the Prediction of the Linear Stability Behavior of Liquid Propellant Combustors", NASA Contractor Report 3169, 1979.

2. Harjje, D.T., (Editor) Liquid Propellant Rocket Combustion Instability, NASA SP-194, 1972.

3. Priem, R.J., Liquid Propellant Rocket Combustion Instability, pp.194-208.

4. Priem, R.J., "Combustion Process Influence on Stability", Chemical Engineering Progress Symposium Series, Vol. 62, No. 61, 1966, pp.103-112.

5. Priem, R.J. and Guentert, D.C., "Combustion Instability Limits Determined by a Nonlinear Theory and a One dimensional Model", NASA TN D-1409, Oct. 1962.

6. Crocco, L., "Research on Combustion Instability in Liquid Propellant Rockets", Twelfth Symposium (International) on Combustion, The Combustion Institute, 1969, p.958.

7. Crocco, L., "Theoretical Studies on Liquid Propellant Rocket Instability", Tenth Symposium (International) on Combustion, The Combustion Institute, 1965, pp.1101-1128.

8. Reardon, F.H., Liquid Propellant Rocket Combustion Instability, pp.277-286.

9. Dykema, O.W., Liquid Propellant Rocket Combustion Instability, pp.214-217.

10. Dykema, O.W., "An Engineering Approach to Combustion Instability", Second ICRPG Combustion Conference, CPIA Pub. No. 105, May 1966, pp.205-223.

11. Heidmann, M.F., and Weiber, P.R., "Analysis of n-Heptane Vaporization in Unstable Combustors with Traveling Transverse Oscillation:, NASA TN D-3424, 1966.

12. Feiler, C.E., and Heidmann, M.F., "Dynamic Response of Gaseous Hydrogen Flow System and Its Application to High Frequency Combustion Instability", NASA TN D-4040, June 1967.

13. Heidmann, M.F., and Groenweg, J.F., "Analysis of the Dynamic Response of Liquid Jet Atomization to Acoustic Oscillations", NASA TN D-5339, July 1969.

1984 USAF-SCEEE SUMMER FACULTY RESEARCH PROGRAM

Sponsored by the

AIR FORCE OFFICE OF SCIENTIFIC RESEARCH

Conducted by the

SOUTHEASTERN CENTER FOR ELECTRICAL ENGINEERING EDUCATION

FINAL REPORT

LARGE SPACE STRUCTURE DYNAMIC TESTING

Prepared by: Dr. Don Mittleman

Academic Rank: Professor

Department and   Department of Mathematics
  University: Oberlin College

Research Location: Air Force Wright Aeronautical Laboratories
                     Structures & Dynamics Division
                     Structural Vibration Branch (AFWAL/FIBG)
                     Wright-Patterson AFB OH 45433

USAF Research: Jerome Pearson

Date: July 20, 1984

Contract No: F49620-82-C-0035

LARGE SPACE STRUCTURE DYNAMIC TESTING

by

Don Mittleman

ABSTRACT

The focus of this work is to describe theoretically the behavior of a flexible body subject to vibrations in a zero- gravity environment and to be able to simulate this behavior in a 1-g environment. Thus, if we have a flexible body suspended at n-points by fine wires that pass over friction-less pulleys and these wires then extend over a second set of pulleys and drop down to a second flexible body that is an identical copy of the first and is similarly attached to the wires, then the net forces, at least at the points of suspension, acting on either body, are zero. While we are far from solving the vibrational characteristics of such complex systems, these characteristics have been analyzed for two simple cases. These consist of a single and two masses rigidly connected. The theory and the apparatus for both cases are presented. The results of several numerical experiments as well as those of some physical experiments are described.

Acknowledgement

The author would like to thank the Air Force Systems Command, the Air Force Office of Scientific Research and the Southeastern Center for Electrical Engineering Education for providing the opportunity for him to spend a very worthwhile and stimulating summer at the Air Force Wright Aeronautical Laboratories, Wright-Patterson Air Force Base, Ohio. In particular, he would like to acknowledge the hospitality and the excellent working conditions provided by the Flight Dynamics Laboratory, and its Structures and Dynamics Division. The work carried out was done in the Structural Vibration Branch which deserves unstinting praise for its cooperation and interest.

There are many people who deserve not only thanks but recognition for their assistance. It would be remiss not to mention James Janik, who helped with the computer programs, Lieutenant Michael Zeigler, USAF, for writing the main computer programs and for his day-to-day supervision of construction and operation of the equipment, and Michael Hart, for assembling the apparatus and helping run the experiments. Mr. Otto Maurer and Major H. C. Briggs, USAF, reviewed the mathematical theory and were constant in their support and encouragement.

Finally, Jerome Pearson. Jerome discussed the overall problem with me, and pointed out the possibilities for a mechanical solution. Without his support and guidance, this work would not have been possible. It is with great pleasure that I express my thanks to him.

I. Introduction

The purpose of this work is to be able to describe theoretically the behavior of a flexible body subject to vibrations in a zero-gravity environment and to be able to simulate this behavior in a laboratory in a 1-g environment. Thus, if we have a flexible body suspended at n-points by fine wires that pass over frictionless pulleys and these wires then extend over a second set of pulleys and drop down to a second flexible body that is an identical copy of the first and is similarly attached to the wires, then the net forces, at least at the points of suspension, acting on either body, are zero. While we are far from solving the vibrational characteristics of such complex systems, these characteristics have been analyzed for two simple cases. These two cases consist of (1): a single mass, and (2): two masses rigidly connected. While it was hoped to describe the behavior of two masses, flexibly connected, time did not permit. The description of the theory, the apparatus, the results of several numerical experiments as well as those of some physical experiments are described in the succeeding sections.

II. A Single Mass - Mathematical Statement

The experiment to be analyzed is depicted in Figure 1. Two frictionless pulleys, each of radius R and lying in the plane $y = 0$, are attached to a framework so that their line of centers is h meters above the $z = 0$ plane. The total length of the fine wire (.010" diameter) is constant and equals $\ell_1 + \ell_2 + \pi R + d$. When the mass m_2 is displaced through an angle θ, the distance from m_2 to the point of contact (tangency) on the pulley is called ρ. If the coordinates of m_1 are (x_1, y_1, z_1), we may assume $x_1 = -R$ (as measured from the center of pulley 1), $y_1 = 0$ (i.e. the only allowable motion is in the vertical direction) and $z_1 = h - \ell_1$. If the coordinates of m_2 are (x_2, y_2, z_2), then, when measured from the center of pulley 2, $x_2 = R\cos\theta + \rho\sin\theta$, $y_2 = 0$, and $z_2 = h + R\sin\theta - \rho\cos\theta$. Since $\ell_1 + \frac{1}{2}\pi R + d + (\frac{1}{2}\pi - \theta)R + \rho = \ell_1 + \frac{1}{2}\pi R + d + \frac{1}{2}\pi R + \ell_2$, we have that $\rho = \ell_2 + \theta R$. From the geometry, it is clear that

$$\ell_1 + \ell_2 = L, \text{ a constant, and therefore}$$

$$\rho = L - \ell_1 + \theta R = L - (h - z_1) + \theta R$$
$$= (L - h) + \theta R + z_1$$

where L-h is a constant we shall refer to as ρ_0.

Thus: $\rho = \rho_0 + \theta R + z_1$

The quantity ρ_0 is easily measured. With the apparatus in the unperturbed state, $\theta = 0$, and $\rho = \rho_0 + z_1$. In this position $\rho = h - z_2$ and thus $\rho_0 = h - z_1 - z_2$.

The kinetic energy of the system is given by

$$T = \tfrac{1}{2}m_1 (\dot{x}_1^2 + \dot{y}_1^2 + \dot{z}_1^2) + \tfrac{1}{2}m_2 (\dot{x}_2^2 + \dot{y}_2^2 + \dot{z}_2^2)$$

and, in terms of z_1 and θ,

$$T = \tfrac{1}{2}(m_1 + m_2)\, \dot{z}_1^2 + \tfrac{1}{2} m_2 \rho^2 \dot{\theta}^2$$

(The kinetic energy of the pulleys was ignored in defining T.) The potential energy $V = m_1 g z_1 + m_2 g z_2 = m_1 g z_1 + m_2 g\,(h + R \sin\theta - \rho\cos\theta)$. Using the lagrangian $L = T - V$, Newton's equations of motion are found to be:

$$\rho\ddot{\theta} + 2\dot{z}_1\dot{\theta} + R\dot{\theta}^2 + g\sin\theta = 0 \qquad (1)$$

$$(m_1 + m_2)\,\ddot{z}_1 - m_2\,\rho\,\dot{\theta}^2 + m_1 g - m_2 g \cos\theta = 0 \qquad (2)$$

III. Numerical Results

These equations were programmed for a digital computer using a Range-Kutta-Fehlberg-(4) routine and run on a Xerox-Sigma-9 at Oberlin College. The program was subsequently rewritten for a VAX-780 at AFWAL/FIBG and run in double precision. The results from these two sets of computer runs were identical. Before discussing the results themselves, some observations on the parameters used in the calculations are in order.

At first, the two masses m_1 and m_2 were assumed equal and the common radius of the pulleys was measured to be 1.238 cm. In all cases, for initial values, we used $z_1 = \dot{z}_1 = \dot{\theta} = 0$. The initial angular displacement of m_2, θ_0, was taken to be successively .01, .1, .2, .5 radians. In all four cases, z_1 went slightly negative but then began to increase. Numerically, the simulation ran for 120 seconds. In an effort to see if this rise in z_1 would continue over longer periods, some cases were run for as long as 6000 seconds; the rise continued. The rise was greater for larger initial amplitudes, θ_0. Figures 2, 3, 4, 5.

This behavior may be understood by examining equation (2). The net gravitational effect is determined by $m_1 g - m_2 g \cos\theta$; the motion of m_1, i.e. the height z_1, is also influenced by the centrifugal term, $m_2\rho\dot{\theta}^2$.

For larger initial 0_0, this term has a greater influence on z_1 than does
$m_1g - m_2g\cos\theta$.

A second set of numerical experiments were run to determine the effect
of the size of the radius of the pulleys; in particular, if we let $R \rightarrow 0$,
would there be a discernable change in the results? It was found that
using an $R = 0$ had no discernable effect on the results obtained. Based on
thi evidence, it was decided to ignore the size of the pulleys in analyzing
the systems to be described in Section VI.

While numerical values were obtained, we chose to present all results
in graphical form and the eye could detect no change.

IV. Experimental Results

While the qualitative behavior observed in the laboratory was in
agreement with the numerically obtained results, the friction of the pulleys
caused some problems. Whereas the theory predicted a specific rise in m_1 in
a certain period of time, the time observed in the laboratory for that rise
was about twice as long. We attribute this difference to friction in the
pulleys. Our rationale is based on the following.

In an effort to compensate for the friction, the apparatus was modified
slightly. The two masses were weighed and found to be 1.005 lbs each. When
suspended for any z_1, they remained at rest, i.e. whatever difference there
might be in their weights was not sufficient to overcome the inertial
resistance of the pulleys. However, if either mass, initially at rest, was
given a slight impulse, the two masses began to move but quickly came to
rest. This indicated that, within the distances over which we were
measuring z_1, about 5 feet, the resistance of the pulleys was too great to
be neglected. Accordingly, we modified the equipment to the following

extent. We added a mass of about 3.9 grams (.00858 oz.) to m_2 and then, with both masses restricted to move in the z- direction, gave a slight impulse to the system, allowing m_1 to rise 5 feet, m_2 to fall the corresponding distance. When measured in this way, z_1 seemed to be moving in a gravitational field of about .0049 ft/sec^2.

Using these unbalanced weights, the experiment was rerun and the results agreed well with the theoretically predicted values.

While it would be desirable to present the numerical results of the laboratory experiment, time, and the crudeness of the apparatus and our measuring procedures, precludes our reporting finer details.

V. Additional Numerical Experiments

Since the theory predicted that for equal masses, m_1 and m_2, the mass m_1 would rise indefinitely when m_2 is swung as a pendulum, we speculated as to how much additional mass should be added to m_1 so as to produce an oscillatory motion. With an increase in mass of .26%, the mass m_1 oscillated between -15cm and .5cm as viewed for the first 300 seconds. With an increase of .25%, the mass m_1 exhibited a total oscillation of about .8cm, and a total change of about 2cm in 300 seconds. In both cases, the initial θ_0 = .1rad and the maximum amplitude of the pendulum motion remained at .1rad. Figures 6, 7.

This numerical experiment was repeated for different initial θ_0. It was found that the functional relationship between the needed additional weight and the initial θ_0 to sustain the oscillatory behavior is quadratic:

$$m_1 = 1.000 + 7.451 \times 10^{-8}\theta_0 + 0.250 \theta_0^2.$$

This formula was obtained using a least squares fit to data points corresponding to θ_0 = .1, .2, .3, .4, and .5.

VI. The Two Masses - Mathematical Statement

Figure 8 is intended to illustrate the following. Four pulleys, each of radius R, are placed so that the centers of p_1 and p_2 are d_2 meters apart and the centers of p_3 and p_4 are d'_2 meters apart. The two lines joining p_1, p_2 and p_3, p_4 are parallel and d_1 meters apart. These four centers lie in a plane normal to the direction of gravity, g, and at a distance h above a reference plane $z = 0$. A fine wired (.010 in. dia.) is strung over pulleys p_1 and p_3 and the masses m_1 and m_3 are attached at the ends. Similarly, a fine wire is strung over pulleys p_2, p_4 and the masses m_2 and m_4 are attached at the ends. A rigid weightless rod of length R_1 connects the masses m_1 and m_2; a rigid weightless rod of length R_3 connects the masses m_3 and m_4.

The masses m_3 and m_4 are pictured in their unperturbed positions, hanging freely under gravity. The distance of m_3 above the ground plane is called z_3; the distance of m_4 above the ground plane is called z_4.

The masses m_1 and m_2 are shown in two positions; one, by dashed lines, as they might hang in their unperturbed position and two, by solid lines as they might be positioned when moved from their unperturbed positions.

In what follows, we shall assume that the radius of the pulleys, R, is small compared to the lengths $\ell_1, \ell_2, \ell_3, \ell_4$, and will be neglected. This simplifies the geometry considerably and is justified in light of the numerical results of the experiment described in Section III.

Whatever the motion of $m_1 R_1 m_2$, the lengths $\ell_1 + \ell_3$ and $\ell_2 + \ell_4$ remain constant. We therefore write $\ell_1 = L_1 - \ell_3$ and $\ell_2 = L_2 - \ell_4$.

In its unperturbed position, the quadralateral $\ell_1 R_1 \ell_2 d_2$ lies in a vertical plane as depicted in the figure. The line ℓ_1 makes an angle φ_1 with the z direction and the projection of ℓ_1 on this direction is $\ell_1 \cos\varphi_1$. The projection of ℓ_1 on the (x,y) plane is $\ell_1 \sin\varphi_1$. If we call the angle between the projection and the x axis θ_1, then the projection of ℓ_1 on the x axis is $\ell_1 \sin\varphi_1 \cos\theta_1$, its projection on the y axis is $\ell_1 \sin\varphi_1 \sin\theta_1$. (In the unperturbed position, $\theta_1 = \tfrac{1}{2}\pi$.)

The coordinates of m_1 are:

$$x_1 = \tfrac{1}{2}d_1 + \ell_1 \sin\varphi_1 \cos\theta_1 \tag{1}$$

$$y_1 = -\tfrac{1}{2}d_2 + \ell_1 \sin\varphi_1 \sin\theta_1$$

$$z_1 = h - \ell_1 \cos\varphi_1$$

The coordinates of m_2 are

$$x_2 = \tfrac{1}{2}d_1 + \ell_2 \sin\varphi_2 \cos\theta_2 \tag{2}$$

$$y_2 = \tfrac{1}{2}d_2 + \ell_2 \sin\varphi_2 \sin\theta_2$$

$$z_2 = h - \ell_2 \cos\varphi_2$$

Since the distance between m_1 and m_2 is to be fixed, we have the constraining condition that

$$(x_1-x_2)^2 + (y_1-y_2)^2 + (z_1-z_2)^2 = R_1^2. \tag{3}$$

Similar formula can be written for the coordinate of the masses m_3 and m_4.

$$x_3 = -\tfrac{1}{2}d_1 + \ell_3 \sin\varphi_3 \cos\theta_3 \tag{4}$$

$$y_3 = -\tfrac{1}{2}d'_2 + \ell_3 \sin\varphi_3 \sin\theta_3$$

$$z_3 = h - \ell_3 \cos{}_3$$

and

$$x_4 = -\tfrac{1}{2}d_1 + \ell_4 \sin\varphi_4 \cos\theta_4 \tag{5}$$

$$y_4 = \tfrac{1}{2}d'_2 + \ell_4 \sin\varphi_4 \sin\theta_4$$

$$z_4 = h - \ell_4 \cos\phi_4$$

Again, the two masses m_3 and m_4 are rigidly connected and the distance between them is R_3.

$$(x_3 - x_4)^2 + (y_3 - y_4)^2 \quad (z_3 - z_4)^2 = R_3{}^2. \tag{6}$$

In the system of equations that specify x_1, y_1, ..., z_4, we may think of $\phi_1,...,\phi_4$, $\theta_1,...,\theta_4$, and ℓ_1,ℓ_2 as independent of one another except for the two constraining equations (3) and (6). Thus, there are at most 8 dependent variables plus the one independent variable, time. The kinetic energy KE of the four masses is

$$KE = \sum_{i=1}^{4} \tfrac{1}{2}m_i \; (x_i + y_i + z_i) \tag{7}$$

The potential energy PE of the four mass with respect to the $z = 0$ plane, is

$$PE = \sum_{i=1}^{4} m_i g z_i$$

The kinetic energy of m_i ($i = 1, 2, 3, 4$) is

$$\tfrac{1}{2}m_i(\dot{x}_i{}^2 + \dot{y}_i{}^2 + \dot{z}_i{}^2) = \tfrac{1}{2}m_i(\ell_i{}^2\sin^2\phi_i\dot{\theta}_i{}^2 + \ell_i{}^2\dot{\phi}_i{}^2 + \dot{\ell}_i{}^2) \tag{8}$$

The constraint equation (3) becomes

$$\ell_1{}^2 - 2B_1\,\ell_1\ell_2 + \ell_2{}^2 - 2D_1\ell_1 + 2E_1\ell_2 = R_1{}^2 - d_2{}^2 \tag{9}$$

where

$$B_1 = \sin\phi_1 \cos\theta_1 \sin\phi_2 \cos\theta_2 + \sin\phi_1 \sin\theta_1 \sin\phi_2 \sin\theta_2 + \cos\phi_1 \cos\phi_2$$

$$D_1 = d_2 \sin\phi_1 \sin\theta_1$$
$$E_1 = d_2 \sin\phi_2 \sin\theta_2.$$

Similarly, the constraint equation (6) becomes

$$\ell_3{}^2 - 2B_3\ell_3\ell_4 + \ell_4{}^2 - 2D_3\ell_3 + 2E_3\ell_4 = R_2{}^2 - d_2'{}^2 \tag{10}$$

and

$$B_3 = \sin\phi_3 \cos\theta_3 \sin\phi_4 \cos\theta_4 + \sin\phi_3 \sin\theta_3 \sin\phi_4 \sin\theta_4 + \cos\phi_3 \cos\phi_4$$

$$D_3 = d'_2 \sin\phi_3 \sin\theta_3$$

$$E_3 = d'_2 \sin\phi_4 \sin\theta_4$$

To equations (9) and (10) we adjoin

$$\ell_1 + \ell_3 = L_1 \tag{11}$$

$$\ell_2 + \ell_4 = L_2 \tag{12}$$

This system of four (4) equations define ℓ_1, ℓ_2, ℓ_3, ℓ_4, in terms of the variables $\phi_1, \ldots, \phi_4, \theta_1, \ldots, \theta_4$, which we take as our generalized coordinates.

The potential energy PE is given by

$$PE = \sum_{i=1}^{4} m_i g z_i = \sum_{i=1}^{4} m_i g (h - \ell_i \cos\phi_i).$$

From these definitions, we form the Lagrangian function L = T-V and derive the Newton equations of motion.

VII. Recommendations

1) The mathematical equations for the case of the single mass are clearly enough understood and may be verified to any degree of accuracy if the friction of the pulleys can be reduced. If that should prove unattainable within the limits of the laboratory equipment available, the equations would then have to be modified to account for friction. This should be done only if necessary.

2) The laboratory experiments to substantiate the theory for the single mass requires more sophisticated equipment than was used. This is being done and the results should be forthcoming within a reasonable time.

3) While this report indicates how the Newton equations of motion can be obtained for the two masses connected by a rigid rod, the details of that computation still have to be carried out. This should be done and the equations programed for a computer and run.

4) Experimental verification of the numerical results expected from recommendation 3) should be obtained. Again, if friction plays too great a role, these equations will have to be modified.

5) The most important recommendation is to continue the theoretical investigation into the case of two point masses connected by a flexible rod. For this, the constraint equations, (3) and (6), would have to be modified to account for the flexibility of the rod and the energy, when the rod is flexed, introduced into the system. Concomitant with this would be the derivation of the Newton equations of motion, the writing of the computer program and the experimental verification. Recommendation 5) is clearly the most challenging.

Figure 1

Figure 2(a)

100-15

INITIAL CONDITIONS:

M1 = M2	=	1.000000
M3	=	0.000000 X10^{-101}
THETA	=	0.010000
THETA-DOT	=	0.000000 X10^{-101}
Z	=	0.000000 X10^{-101}
Z-DOT	=	0.000000 X10^{-101}
RADIUS OF PULLEY	=	0.012380
LENGTH OF WIRE	=	3.000000
INITIAL TIME	=	0.000000 X10^{-101}
FINAL TIME	=	120.000000

Z (meters)

TIME (sec)

THETA (radians) *10^{-1}

100—15

Figure 2(b)-16

INITIAL CONDITIONS:

M1 = M2	=	1.000000
M3	=	0.000000 $\times 10^{-01}$
THETA	=	0.010000
THETA-DOT	=	0.000000 $\times 10^{-01}$
Z	=	0.000000 $\times 10^{-01}$
Z-DOT	=	0.000000 $\times 10^{-01}$
RADIUS OF PULLEY =		0.012380
LENGTH OF WIRE =		3.000000
INITIAL TIME =		0.000000 $\times 10^{-01}$
FINAL TIME =		120.000000

Figure 3(a)

Z (meters)

40.   32.   24.   16.   8.   0.0

INITIAL CONDITIONS:

M1 = M2	=	1.000000
M3	=	0.000000 X10^{-18}
THETA	=	0.10000
THETA-DOT	=	0.000000 X10^{-18}
Z	=	0.000000 X10^{-18}
Z-DOT	=	0.012380
RADIUS OF PULLEY	=	0.000000
LENGTH OF WIRE	=	3.000000
INITIAL TIME	=	0.000000 X10^{-18}
FINAL TIME	=	120.000000

THETA (radians)

0.10   0.06   0.02   -0.02   -0.06   -0.10

0.0   15   30   45   60   75   90

TIME (sec)

Figure 3(b)

100-18

Z-DOT (meters/sec)

0.39   0.31   0.23   0.15   0.07   -0.01

INITIAL CONDITIONS:

M1 = M2   =   1.000000
M3   =   0.000000   X10⁻¹⁸¹
THETA   =   0.100000
THETA-DOT   =   0.000000   X10⁻¹⁸¹
Z   =   0.000000   X10⁻¹⁸¹
Z-DOT   =   0.000000   X10⁻¹⁸¹
RADIUS OF PULLEY = 0.012380
LENGTH OF WIRE   = 3.000000
INITIAL TIME   = 0.000000 X10⁻¹⁸¹
FINAL TIME   = 120.000000

TIME (sec)

THETA-DOT (rad/sec)

0.22   0.14   0.06   -0.02   -0.10   -0.18

Figure 4(a)

100-19

Z (meters)

INITIAL CONDITIONS:

M1 = M2   =   1.000000
M3   =   0.000000   X10⁻¹⁰¹
THETA   =   0.200000
THETA-DOT   =   0.000000   X10⁻¹⁰¹
Z   =   0.000000   X10⁻¹⁰¹
Z-DOT   =   0.000000   X10⁻¹⁰¹
RADIUS OF PULLEY = 0.012380
LENGTH OF WIRE   = 3.000000
INITIAL TIME =   0.000000   X10⁻¹⁰¹
FINAL TIME   = 120.000000
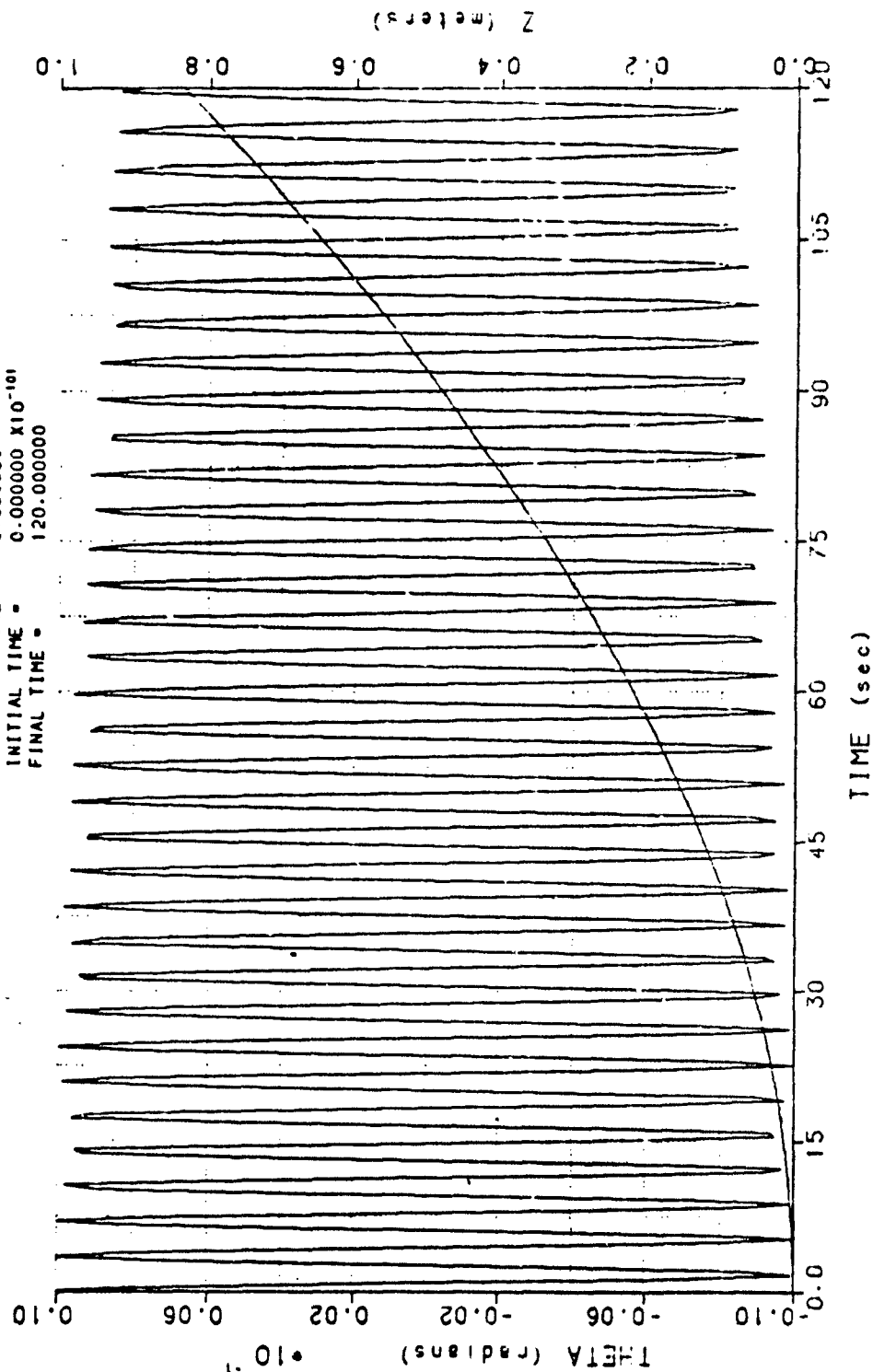
THETA (radians)

TIME (sec)

Figure 4 (b)

100-20

Z-DOT (meters/sec)

THETA-DOT (rad/sec)

TIME (sec)

INITIAL CONDITIONS:

M1 = M2	=	1.000000
M3	=	0.000000 X10⁻¹⁰¹
THETA	=	0.200000
THETA-DOT	=	0.000000 X10⁻¹⁰¹
Z	=	0.000000 X10⁻¹⁰¹
Z-DOT	=	0.000000 X10⁻¹⁰¹
RADIUS OF PULLEY	=	0.012380
LENGTH OF WIRE	=	3.000000
INITIAL TIME	=	0.000000 X10⁻¹⁰¹
FINAL TIME	=	120.000000

Figure 5(a) 100-21

Z (meters)

200   160   120   80   70   0.0

INITIAL CONDITIONS:

M1 = M2   =   1.000000
M3   =   0.000000 X10⁻¹⁸
THETA   =   0.500000
THETA-DOT   =   0.000000 X10⁻¹⁸
Z   =   0.000000 X10⁻¹⁸
Z-DOT   =   0.000000 X10⁻¹⁸
RADIUS OF PULLEY =   0.012380
LENGTH OF WIRE =   3.000000
INITIAL TIME   =   0.000000 X10⁻¹⁸
FINAL TIME   =   120.000000

TIME (sec)

0.5   0.3   0.1   -0.1   -0.3   -0.5

THETA (radian)

Figure 5(b)

100-22

Figure 64a)
100-23

Z (meters)

INITIAL CONDITIONS:

M1	=	1.002600
M2	=	1.000000
M3	=	0.003000 x10^-01
THETA	=	0.100000
THETA-DOT	=	0.000000 x10^-01
Z	=	0.000000 x10^-01
Z-DOT	=	0.000000 x10^-01
RADIUS OF PULLEY	=	0.012380
LENGTH OF WIRE	=	3.000000
INITIAL TIME	=	0.000000 x10^-01
FINAL TIME	=	300.000000

TIME (sec)

THETA (radians)

Figure 6(b)

100-24

Z-DOT (meters/sec) •10⁻¹

INITIAL CONDITIONS.

M1	=	1.002600
M2	=	1.000000
M3	=	0.000000 X10⁻⁰¹
THETA	=	0.100000
THETA-DOT	=	0.000000 X10⁻⁰¹
Z	=	0.000000 X10⁻⁰¹
Z-DOT	=	0.000000 X10⁻⁰¹
RADIUS OF PULLEY	=	0.012380
LENGTH OF WIRE	=	3.000000
INITIAL TIME	=	0.000000 X10⁻⁰¹
FINAL TIME	=	300.000000

TIME (sec)

THETA-DOT (rad/sec)

Figure 7(a)

100-25

Z (meters) $\times 10^{-1}$

0.19 0.14 0.09 0.04 0.0 -0.01 -0.06

INITIAL CONDITIONS:

M1	=	1.002500
M2	=	1.000000
M3	=	0.000000 $\times 10^{-101}$
THETA	=	0.100000
THETA-DOT	=	0.000000 $\times 10^{-101}$
Z	=	0.000000 $\times 10^{-101}$
Z-DOT	=	0.000000 $\times 10^{-101}$
RADIUS OF PULLEY	=	0.012380
LENGTH OF WIRE	=	3.000000
INITIAL TIME	=	0.000000 $\times 10^{-101}$
FINAL TIME	=	300.000000

TIME (sec)

300 263 225 188 150 113 75 38 0.0

THETA (radians)

0.10 0.06 0.02 -0.02 -0.06 -0.10

Figure 7(b)

100-26

INITIAL CONDITIONS:

M1	=	1.002500
M2	=	1.000000
M3	=	0.000000 X10^{-101}
THETA	=	0.100000
THETA-DOT	=	0.000000 X10^{-101}
Z	=	0.000000 X10^{-101}
Z-DOT	=	0.000000 X10^{-101}
RADIUS OF PULLEY	=	0.012380
LENGTH OF WIRE	=	3.000000
INITIAL TIME	=	0.000000 X10^{-101}
FINAL TIME	=	300.000000

Figure 8
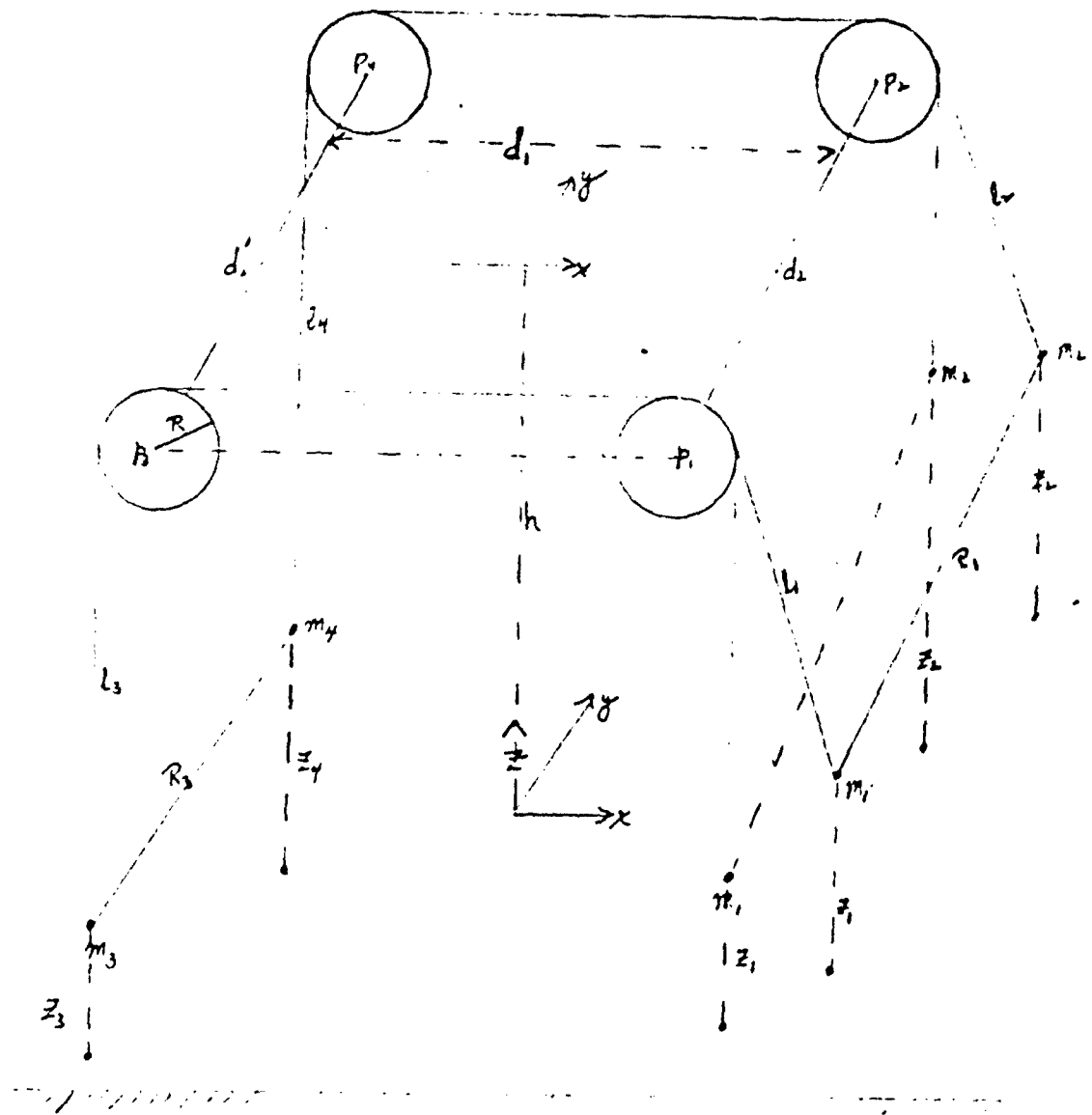
100-27

FINAL REPORT

ACQUISITION OF WIND TUNNEL WALL PRESSURE DISTRIBUTIONS FOR USE IN DEVELOPING A 3-D TRANSONIC WALL CORRECTION CODE

Prepared by: Dr. Dale Moses

Academic Rank: Associate Professor

Department and   Department of Aerospace Engineering &
University   Engineering Mechanics
                          San Diego State University

Research Location: Air Force Wright Aeronautical Laboratory,
                          Aeromechanics Division, Aerodynamics &
                          Airframe Branch

USAF Research   Robert Guyton

Date: August 24, 1984

Contract No: F49620-82-C-0035

ACQUISITION OF WIND TUNNEL WALL PRESSURE DISTRIBUTIONS FOR

USE IN DEVELOPING A 3-D TRANSONIC WALL CORRECTION CODE

by

Dale F. Moses

ABSTRACT

The case for low subsonic Mach numbers is discussed and results
of wall pressure signatures at M=.3 are given. Runs were made at
transonic Mach numbers of M=.6, .7, and .75 for odd angles of attack
from α =3° to α =19°. The results are discussed. The interference
from the model support sting and angle of attack adjustment crescent
was evaluated and the model wall pressures were corrected for this
interference.

Transonic wall pressure signatures were obtained at a model
position 14" forward of the test section window $\mathcal{C}$.

Acknowledgement

I. INTRODUCTION

As part of my doctoral work with Professor William R. Sears I developed a computer program which computes the wind tunnel wall interference on model measurements for low speed, solid wall tunnels.[1] Most of the testing done in the Trisonic Gasdynamics Facility wind tunnel of AFWAL is at compressible Mach numbers which usually go up to M=.75. In addition, a large part of these tests in the TGF are conducted with solid walls. I recently applied for and received a RISE contract to develop a code to calculate three dimensional wall corrections for transonic, solid wall wind tunnels. This code will use the same methodology described in ref.1 but will include the effect of compressibility. This code will be an intermediate stage in any future effort to produce a code for slotted or perforated wall, 3-D transonic wind tunnels which will require only a change in the nature of the inner flow boundary conditions.

A natural feature of the solid wall code development is proving it out with actual data from such a wind tunnel. The acquisition of this data formed the bulk of the work done under this Summer Faculty Research Program effort.

II. OBJECTIVES OF THE RESEARCH EFFORT

Originally the research objectives dealt with refining the low speed wall corrections code and developing it into a production version that could be used in routine testing. These objectives were:

1. Determine the minimum number of wall static pressures needed for an improved wall correction in the low speed regime and their optimum distribution. This will be done by investigating subsets of test data.

2. Develop a production version of the Sears method code for routine use. Investigate methods of accelerating convergence to unconfined flow such as step-varying relaxing factor.

3. Compare the lift corrections from the Sears method with those produced by the Hackett method.

After delays caused by extending the previous test and problems with the pressure instrumentation, wall pressure data was obtained at M=.3.

As discussed in the next section, the quality of these pressure differentials was too poor to be able to accomplish the first two objectives. The effort of implementing the Hackett method for lift correction, which was not a part of this SFRP work, was not successful so that the comparison in objective 3 could not be made. Instead, the following was substituted as the objective for this 1984 SFRP:

    4. Obtain wall pressure coefficients on all four boundaries in the presence of the model for the Mach number range .6-.75. Account for sting and crescent interference. Cp is measured on test section floor and ceiling. In order to obtain equivalent sidewall Cp's, the model is rolled 90° and the pressures are measured again (test section is square). Since the flow near the wall is linear, the effect of sting and crescent can be superimposed. Runs will be made successively removing the sting, the crescent and measuring the resulting Cp's on the floor and ceiling.

III. WIND TUNNEL WALL PRESSURE DISTRIBUTIONS AT LOW MACH NUMBERS

The code described in ref.1 applies only to incompressible flow-fields. Also, in order to enable it to be used efficiently in a day-to-day production mode we need to reduce the number of perturbation pressures that are required to be measured and reduce the number of iterations required for convergence. In order to do this wall static pressure measurements were made at 60 points on both the bottom and top boundaries of the test section, see Fig 1. The importance of side wall pressures was to be investigated by rolling the model 90° and taking bottom and top boundary measurements again. These sidewall pressures were to be checked against pressures on the centerline of the test section vertical boundaries, see Fig 2. In order to determine the Mach number limits in accuracy of the low speed wall correction code runs were planed at M=.5 and M=.6; however the first run was made at M=.3. Figures 3 and 4 contain the perturbation pressures measured on the bottom and top boundaries respectfully. Here the model nose is located 11.75 in. ahead of the test section window center-line. These distri-
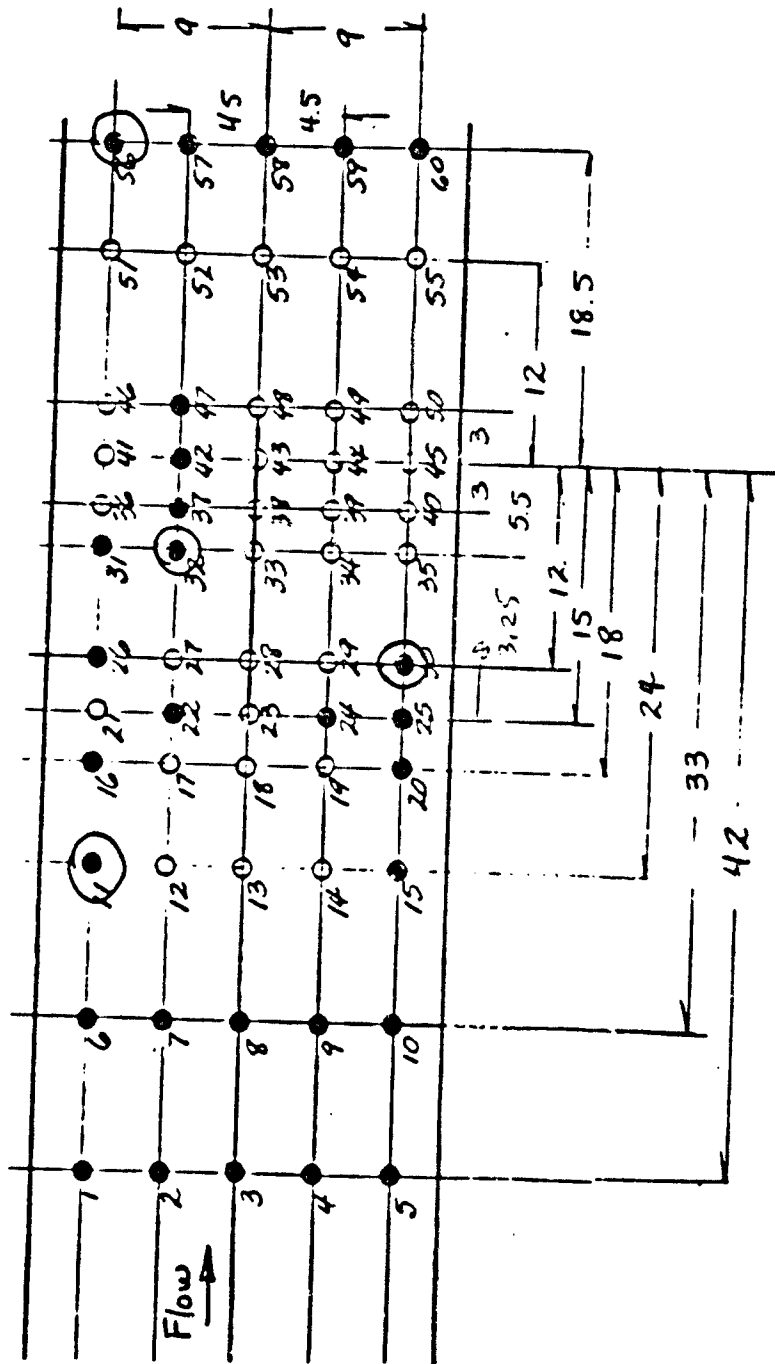
Figure 1a: Floor static pressure taps

Figure 1b: Ceiling static pressure taps

Tubing Schedule - Both Sidewalls

NOTE: This tap (south side) shall be used for PS of tunnel.

south side #3

north side #3

139 140 141 121 122 123 124 125 126 127 128

130 131 132 133 134 135 136 137 138

21 27 30 36 42 48 54 60 66 72 78 84
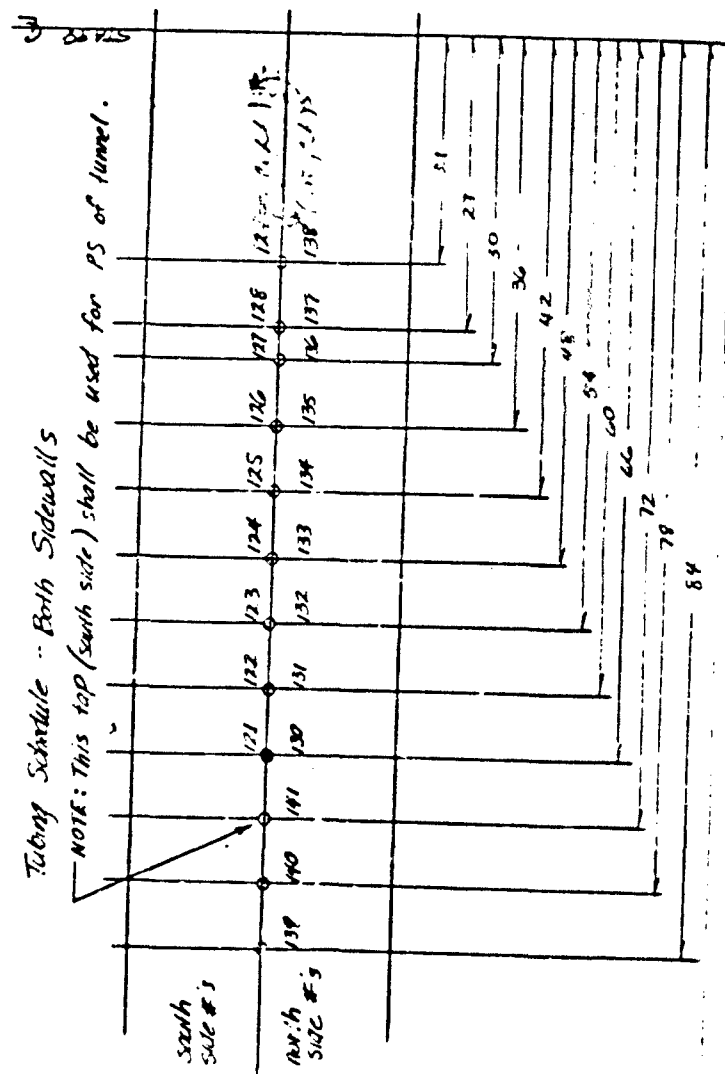
Figure 2: Side-wall static pressure taps

Figure 3: Test section bottom boundary perturbation pressures. $\alpha = 3.94°$, $M = .3$
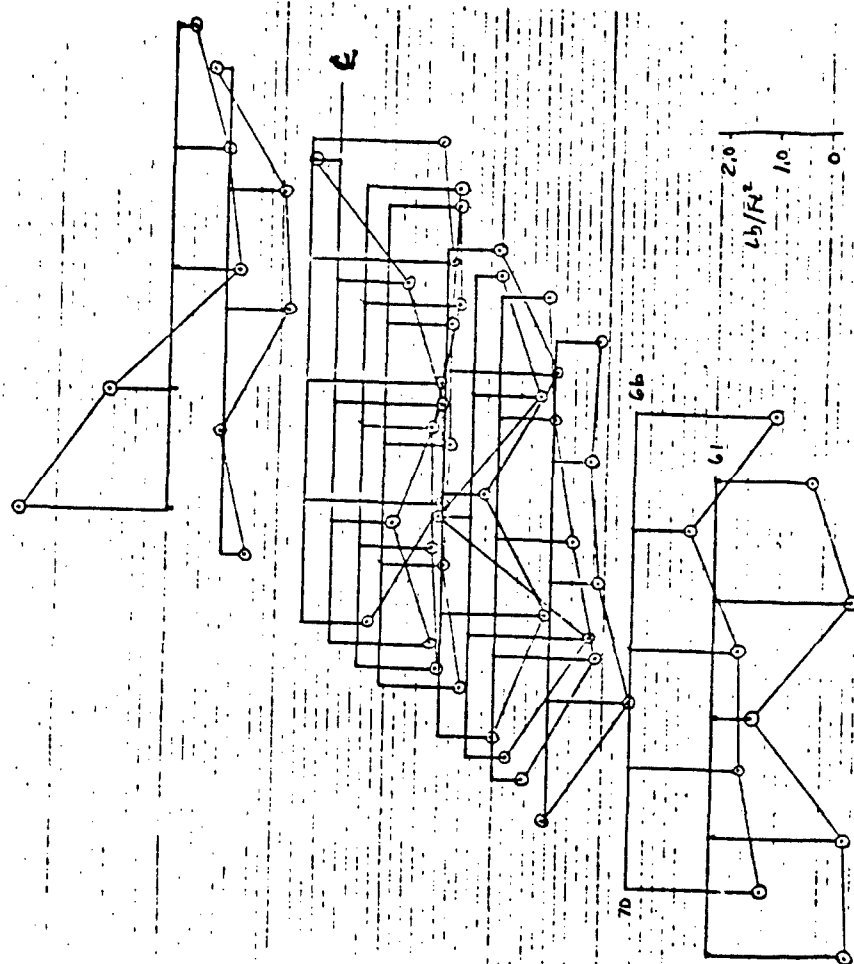
Figure 4: Top boundary perturbation pressures. $\alpha = 3.94°$, $M = .3$

butions are very erratic and do not show a clear model effect even near the model location. The perturbations should diminish to zero at the two upstream-most rows but instead they remain high and the point-to-point variations are large. Since the wall correction code smooths the data before generating its boundary conditions it is clear that this measured data is too much in error to get meaningful results from the wall correction. Pressure tubing was checked for leaks, blown out and reconnected in an effort to fix the problem but with little effect. In the course of the search for the cause of the bad data it was discovered that the wall pressures were oscillating together as much as 2 lb/ft^2 on a frequency of $\frac{1}{2}$ - 1 cycles per second. Further investigations revealed a 3 in., rearward-facing step in the diffuser. The wall static pressure just ahead of this step was fluctuating in phase with the wall pressures, suggesting the step as the cause of the test section unsteadiness. Since the problems with the pressures could not be solved in the time allowed this summer the objectives associated with the low speed wall corrections code were abandoned, as mentioned above. The program then shifted to obtaining wall pressure distributions at transonic Mach numbers which could be used in proving out the transonic wall correction code being developed separately. The first runs to check data quality were made at M=.80. Perturbation pressures for an angle of attack of 5.54 degrees on bottom and top boundaries are plotted in Figures 5 and 6 respectively. In general the point-to-point pattern remains similiar to that of the low Mach number runs; however, the magnitudes of the variations are smaller fraction of the absolute measurements so that the distribution is much smoother. If one eliminates certain points that are obviously bad, such as tap #16, then the pressure variation doesn't look too bad. Since the repeatability of the individual perturbation pressures was good and the distributions displayed the right trends it was judged that the data was probably usable

As seen in Figures 5 and 6 there is a large support interference at the downstream most rows of taps. The flowfield in this region is still linear so that perturbation pressures produced by the sting and angle of attack adjustment crescent can be superimposed. To evaluate this interference runs were made successively with sting and crescent only, with crescent only, and finally no crescent. Figure 7 shows

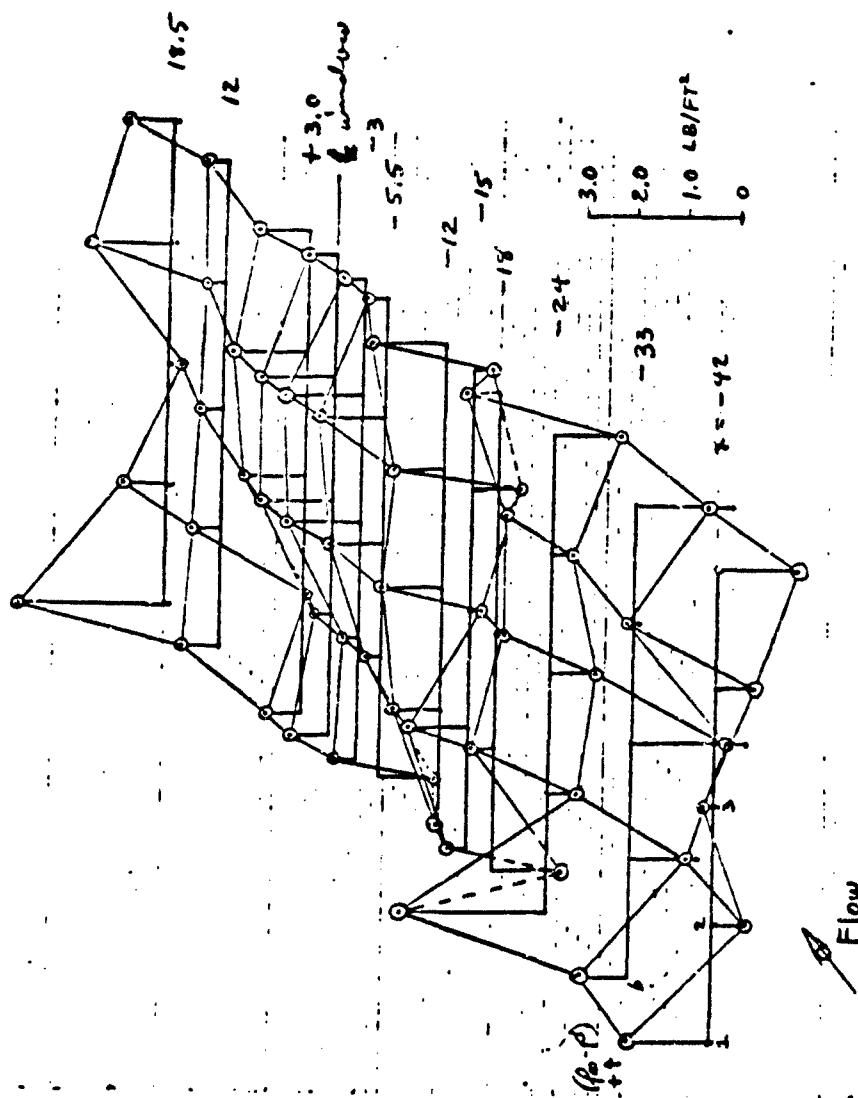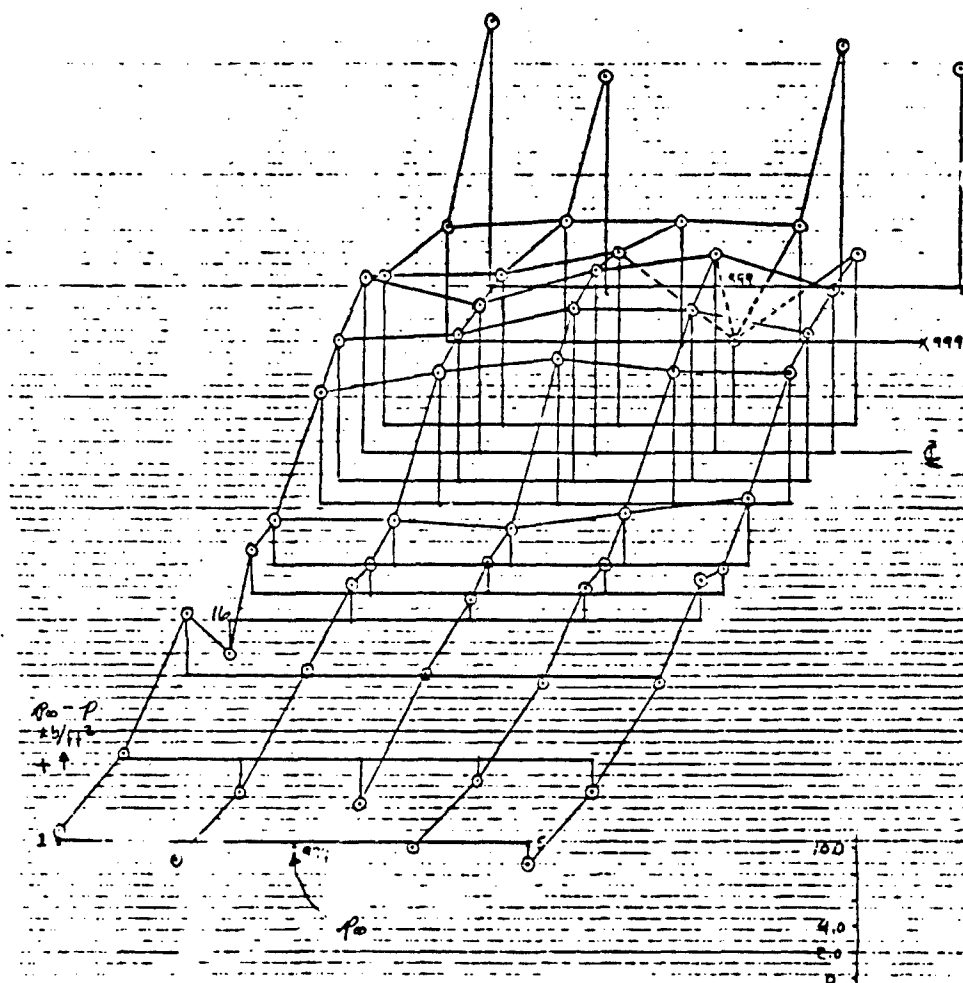Figure 5: Bottom boundary perturbation pressures. $\alpha = 5.54°$, $M = .80$
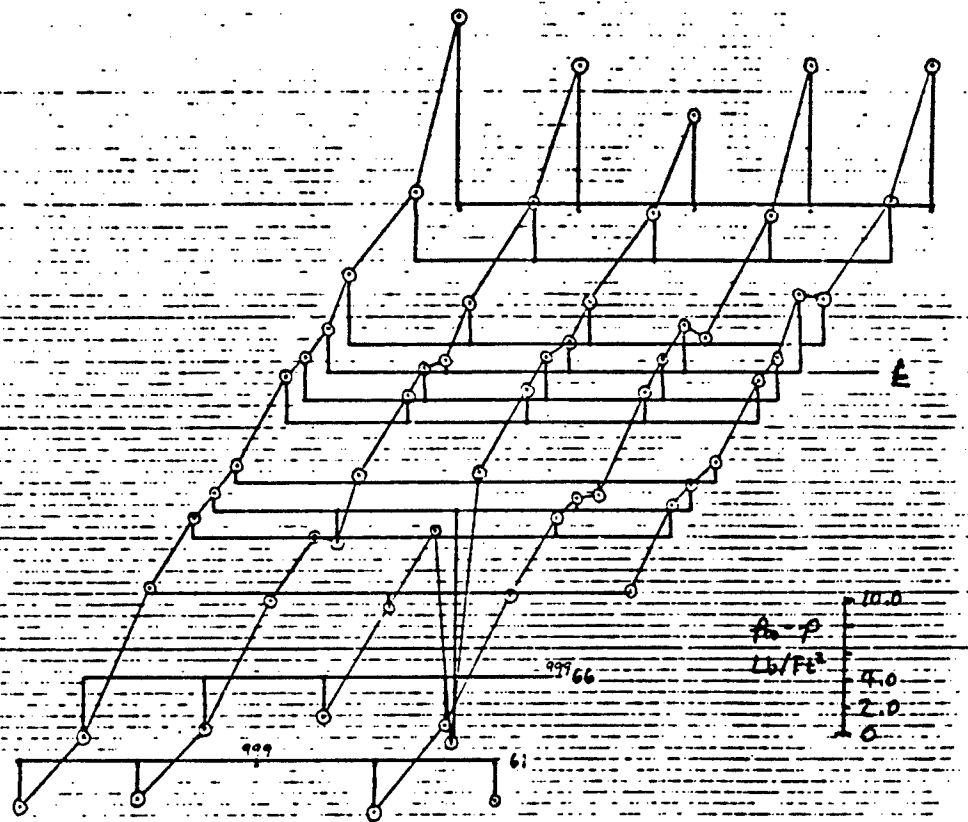
Figure 6: Top boundary perturbation pressures. $\alpha = 5.54°$, $M = .80$

□ TPN = 299   — $M = .60$ Empty tunnel
△ TPN = 295   — $M = .60$ Crescent only
○ TPN = 278 $\alpha = 7.07$ deg $M = .61$ Crescent + sting

$$(p_o - p) + 1 \quad \frac{1}{8} \quad 2 \frac{Lb}{Ft^2}$$
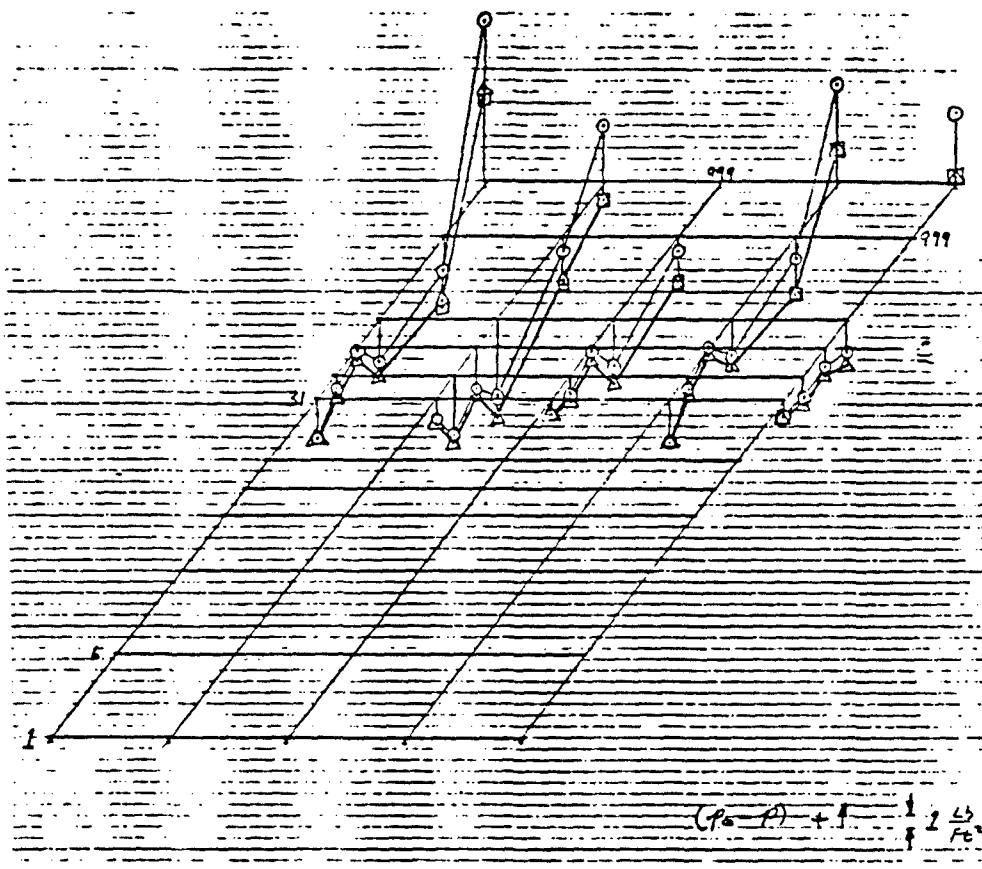
Figure 7: Effect of sting and crescent on wall
pressures. $M = .6$, $\alpha = 7.07°$

that the crescent by itself has virtually no effect on the wall pressures but the sting has a considerable effect and extends to at least 5.5 inches ahead of the window center-line. Figure 8 shows a longitudinal plot of model ι _surements corrected for sting interference at M=.76.

The 11" wingspan close-coupled canard model, see Figure 9, which had up to this point only been tested at the window center-line position was moved upstream 14 inches on a sting extension. The window center-line angles of $\alpha = 3^\circ$, 5°, 7°, 9°, 11°, 13°, 15°, & 17° were repeated in the forward position. Also, in order to get equivalent side-wall pressures, the model was rolled 90° at each α and wall pressures were taken again. In the rolled configuration the model C_L was matched with the un-rolled configuration because sting deflection due to weight caused significant differences we were not able to make a direct comparison with the window center-line runs. Sting interference was again evaluated and subtracted from the model data.

IV. RECOMMENDATIONS:

Because the Sears method deals directly with boundary conditions of the governing equations it is inherently exact and it has been shown that the process converge to the unique case of unconfined flow. The largest source of error is the accuracy of the perturbation pressure measurements. Since the method will produce a more accurate wall correction for large models it is recommended that the low Mach number instrumentation be studied and fixed so that the wall distributions are smooth, vanish upstream and show the correct form elsewhere.

In order for the wall correction code to be efficient in day-to-day use the number of data points should be reduced and ways or accelerating the convergence should be tried.

It is also recommended that when the transonic wall correction code is finished that it be run at M=.2 or M=.3 and the results compared with those from the low speed code.

o Uncorrected
△ Corrected for sting interference
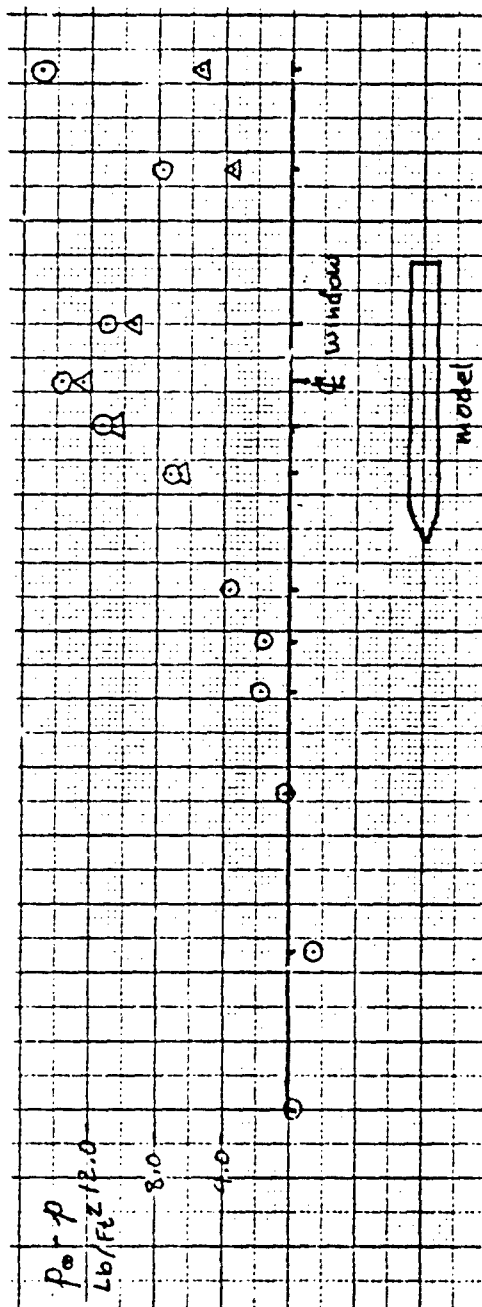
Figure 8: Wall pressures corrected for sting interference, α = 7.79°, M = .76, y = -4.5 in.
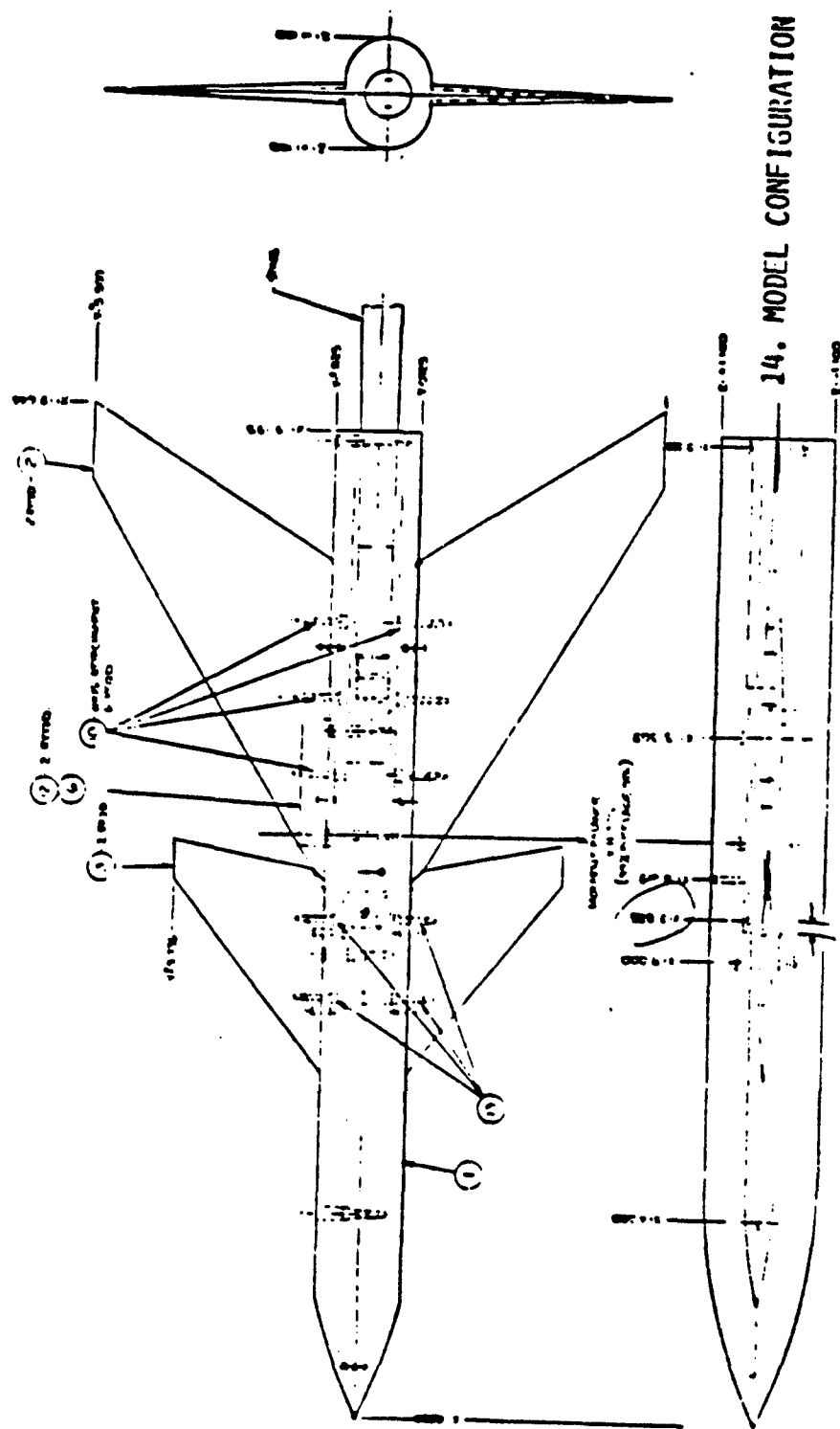
Figure 9 : Close - coupled canard model

REFERENCES

1. Moses, D.F., "Wind Tunnel Wall Corrections Deduced by Iterating From Measured Wall Static Pressure", *AIAA Journal*, Vol. 21, No. 12, Dec, 1983

1984   USAF-SCEEE SUMMER FACULTY RESEARCH PROGRAM

Sponsored by

AIR FORCE OFFICE OF SCIENTIFIC RESEARCH

Conducted by the

SOUTHEASTERN CENTER FOR ELECTRICAL ENGINEERING EDUCATION

<u>FINAL REPORT</u>

<u>LEADERSHIP EFFECTS AS MEASURED BY THE ORGANIZATIONAL</u>

<u>ASSESSMENT PACKAGE: A MULTILEVEL PERSPECTIVE</u>

Prepared by: Dr. Kevin W. Mossholder

Academic Rank: Associate Professor

Department and   Department of Management
   University: Auburn University

Research Location: Leadership and Management Development Center,
                      Directorate of Research and Analysis,
                      Maxwell Air Force Base, Alabama

USAF Research: Maj. Mickey Dansby and
                      Capt. Michael Cox

Date: August 18, 1984

Contract No: F49620-82-C-CC35

LEADERSHIP EFECTS AS MEASURED BY THE ORGANIZATIONAL

ASSESSMENT PACKAGE: A MULTILEVEL PERSPECTIVE

Kevin W. Mossholder

ABSTRACT

The purpose of the present research was to conduct an exploratory
analysis of leadership effects on selected factors measured by the
Organizational Assessment Package (OAP). A multilevel perspective
examining individual and group leadership effects on attitudinal
factors served as the basis for the model used. In accordance with
the contextual approach to multilevel analysis, hierarchical regres-
sion analysis was performed using as subjects workgroup members
from selected functional areas. Results suggested that additional
understanding of leadership effects may possibly be gained by utiliz-
ing a multilevel framework. Recommendations were made regarding
the conceptualization of leadership as measured by the OAP and sugges-
tions were offered concerning the consulting process as well as
future research.

I. INTRODUCTION

The Leadership and Management Development Center (LMDC) is
a multifaceted organization whose broad goal is to enhance leadership
and management processes of the Air Force personnel worldwide.
The impetus for establishing the LMDC can be traced back to 1973
and the proposal for a volunteer force. Faced with the recognition
that it would have to compete for available human resources, the
Air Force established a task force (Air Force Management Improvement
Group--AFMIG) to consider enhancing the nontechnical aspects of
Air Force life. A first step in fulfilling this goal was the design
and administration of a survey assessing active duty personnel's
perceptions of nonjob factors (e.g. leisure time and health) and
job-related factors (e.g. the work itself and leadership/supervision).
The sample, consisting of more than 38,000 military members, spouses
and civilian employees, represented 11% of the Air Force's personnel
strength. A key finding of the survey was that while 81% of those
surveyed felt leadership and management were important, 71% also
felt the quality of Air Force leadership and management was "average"
to "poor."[32]

In response to these findings, the LMDC was established as
part of Air University of Maxwell Air Force Base. The LMDC was
charged with leadership and management education for the Air Force.
It also offered leadership and management consultation to Air Force
commanders providing them with data on leadership and organizational
trends. The consulting process used by the LMDC may be described

briefly in the following fashion:

1. _Invitation and initial contact_. A written request from
an Air Force Commander must be made before the consultation process
can ensue. Given this condition, an LMDC consultant explores interven-
tion possibilities with the client group. A contract for services
is agreed upon by the LMDC and client which outlines consulting
processes and goals.

2. _Data collection and analysis_. Data relevant to the client
organization's leadership and management processes and work environs
are obtained through a variety of sources (e.g., mission statements,
interviews with supervisors, open-ended questionnaires). A principal
source of information derives from the Organizational Assessment
Package (OAP), administered to client personnel. The OAP was devel-
oped jointly by LMDC and the Air Force Human Resources Laboratory
at Brooks Air Force Base.[21] The OAP is a 109-item self-report ques-
tionnaire which taps areas like job satisfaction, supervision and
management, and organizational climate, among others. (Additional
information concerning studies of the OAP's reliability and validity
may be found in Short, Hightower, & Snow.[39]) OAP data is analyzed
in such a way as to permit the consultant to determine weaknesses
and strengths of the client organization as perceived by the respon-
dents. Norm-based feedback materials are developed for work groups
having four or more members completing the survey.

3. The tailored visit. The client organization's commander is briefed on the general condition of the organization. Feedback is carried down to the work group supervisor level to give supervisors information about their work groups. Where OAP analysis has identified problems, suitable invention techniques are employed to induce desired changes.

4. Follow-up. After sixteen weeks, post-engagement surveys are mailed to the client organization to gather information about the intervention from the commander and supervisors. At approximately six months, LMDC consultants collect post-intervention OAP data which is compared to the pre-intervention visit in order to determine if changes have occurred. Comparative information is given to the client organization in the form of a final report, marking the termination of the formal consultation process. Commanders may, of course, request additional consulting visits at future dates.

A primary purpose of the consulting process is to provide information to the client organization so it may rectify deficiencies in its organizational and management processes. For such information to be maximally useful, two conditions should hold. First, the means by which data are collected should exhibit the traditional measurement requisites of reliability and validity. The key instrument used in the consulting process, the OAP, has been examined for these characteristics and appears to demonstrate adequate levels of both.[39] Second, an acceptable theoretical framework should exist to guide

the organizational interventions to bring about intended changes. With respect to the use of OAP information, it seems that less work has been directed toward this condition.

Additional theoretical delineation of the OAP's use in consulting could lead to better integration among measures and greater continuity between the consultative and evaluative efforts within LMDC.[19] Such constructive theory building could be pursued along the lines of both process and content perspectives. With respect to the LMDC's consultative mission, a process perspective would refer to the theoretical model guiding interventions into client organizations. The model utilized by LMDC in this regard stems from Mann's[33] survey feedback approach. Little theoretical work is required of this model since its utility has been documented in the organization development literature.[3]

From a content perspective, which is one referring to relationships among variables of interest, there is room for additional theoretical development. The LMDC has employed two general frameworks in considering relationships among OAP components. A contingency approach served as the foundation for development of the OAP[20] while a systems model (input, throughput, output) is presently followed. These frameworks are recognized as serving largely descriptive functions. That is, though providing a means of understanding broad organizational phenomena, they possess less power in explaining relationships among components within more narrow substantive areas like those appearing in the OAP.[1,5] For this reason, a look at

particular OAP variables and factors using more specific theoretical
models could have utility.

Some background on theory building (modeling) in applied areas
is now provided to better convey the thrust of the current research
project. The data collection, intervention, and consulting activities
of the LMDC underscore the applied nature of its mission. With
respect to building models germane to organizational application,
it is important that those who will use outcomes of the theory play
a role in defining the content of the model. It is difficult to
say meaningful things about the real world without starting in the
real world. Sound observation and description of target behavior
is one step down the road to useful theoretical models. The key
instrument used in the consulting process is illustrative of these
notions. OAP content has been built through an interaction of (a)
consultants having experience in confronting work/nonwork facets
of Air Force life and (b) analysts/specialists having a more conceptual
comprehension of the same facets. And yet, few attempts appear
to have been made concerning how such facets interact. In that
a major point of congruence between consultants and analysts is
their goal to improve undesirable situations in the field, building
more focused models of the processes encountered is a natural out-
growth of LMDC's prime function.

Although the problem-solving orientation of applied research
may shift somewhat the emphasis among facets of theory building,
the overall process is the same whether intended for immediate applica-

tion or further scientific rumination. This process, described
by Dubin,[10] is seen as involving the following conditions.

(1) Things, variables, or units whose interactions constitute
the subject matter of attention.

(2) Laws of interaction among units etc. of the model specify-
ing how these units interact.

(3) Boundaries which are set forth to describe the limits
within which the theory operates.

(4) System states reflecting conditions under which units
etc. interact differently and mirror the complexity of
the system in which the model operates.

Addressing these basic conditions, those expecting to use the
model may develop propositions for empirical testing. After suffi-
cient cycles of testing (and usually revision), the resultant model
is ready for application. Certainly, the development of and subse-
quent validation work with the OAP measure[22,40] has followed Dubin's[10]
description. It seems consistent to continue research to suggest
improvements in using OAP information.

II. OBJECTIVES

The objective of this report is to begin addressing some substan-
tive concerns involving components measured by the OAP instrument.
In essence, this research represents an effort at theory building
in an applied area since the variables examined are employed by
LMDC in its consulting mission. Because the OAP contains factors

that have been configured in the organizational literature into various theoretical models, it was necessary to limit the substantive scope of this report to factors of greater interest to the Air Force overall. Since a key stimulus for establishing the LMDC was a concern about Air Force leadership and management capabilities, this area was chosen for study. The research model developed includes OAP factors that are relevant to understanding management and supervisory influences impacting on subordinates.

The model will examine management and supervisory influences as potentially affecting subordinates as individuals and as members of intact work groups. Any modeling approach considering effects across conceptually different units of analysis (i.e. the individual and the work group) can be viewed as falling within a so-called multilevel perspective of organizational behavior. This perspective is especially relevant to leadership and related phenomena like management and supervisory behavior. Given the applied theoretical bent of the project, it is anticipated that a clearer understanding of management and supervisory influences will have import for intervention and data collection activities relating to such influences.

III. LEADERSHIP CONSIDERATIONS AND A MULTILEVEL APPROACH

Leadership concepts and the OAP

The focused nature of this report militates against in-depth consideration of the leadership concept. Suffice it to say that leadership has been defined in many ways.[2] A common thread among

definitions is that of interpersonal influence, occurring when a person is moved because of something another person does (as opposed to responding because of some impersonal organizational policy). Leadership is both a process and a property.[25] The use of noncoercive influence to direct activities of subordinates toward accomplishment represents the process component of leadership. As a property, it may be considered as the set of characteristics attributed to persons who are perceived to successfully use such influence. For organizational contexts, it is useful to consider another point about leadership. In the form of interpersonal influence, leadership can occur in both formal and informal guises. Formal leadership exists when an individual operates from an authority position. Informal leadership occurs when a person exerts influence on others without having been designated as an authority figure.

Item loadings on the OAP "leadership" factor -- Management and Supervision -- suggest it is measuring largely formal leadership activities. Without belaboring the issue, this focus indicates the OAP is probably addressing management and supervisory processes more than leadership.[23] In behavioral terms, supervision is interpreted as involving the use of position-based power (reward, coercive, and legitimate -- see reference 14) while leadership involves more personal-oriented power bases (expert and referent). Of course, it is difficult to distinguish leadership and supervision when these processes occur in applied settings.[24]

The above comments serve to introduce the phenomenon examined in this report. Although the content of the OAP Management and Supervision (M&S hereafter) factor seems to favor formal leadership processes, the model introduced below applies to either formal or informal leadership. In reviewing relevant literature, the terms "leadership" and "supervision" are used interchangeably to maintain consistency with studies examined.

Individual and group level perspectives on leadership

In hierarchically structured organizations like those commonly found in the military, leadership influence processes unfold within group contexts. Units tend to have well-defined functions and clear delineations of authority. Subordinates have designated reporting relationships with supervisors responsible for controlling their direction and effort. In such a leadership environment, one can envision two ways in which subordinates are affected by supervisory influence. The supervisor may influence subordinates as a group and/or as individuals. In the case of the former effect, subordinates could be expected to react in basically the same way to the supervisor's leadership efforts while with the latter effect they would be expected to show more variation in their responses. The perspective holding that subordinates tend to respond similarly to the leader has been labeled the Average Leadership Style (ALS) approach while the perspective allowing for meaningful variation in subordinate responses has been labeled the Vertical Dyad Linkage (VDL) approach.

Since both perspectives will be considered in the model proposed by this report, each is briefly reviewed.

Average Leadership Style Perspective

Most traditional approaches to leadership focus on the formally des'gnated leader, seeking to determine the behavioral patterns that result in the maximal effectiveness for the leader's unit.[2] This search has led most approaches to propose dimensions thought to best describe leadership behaviors crucial to influencing the unit. For example, the Ohio State studies of leadership dimensions -- initiating structure and consideration -- resulted from research of this vein.[30] Given basic dimensions, the task then becomes discovering the mix of the dimensions that influences the unit to contribute to organizational effectiveness. The leader is assumed to be responsible for the summative output of the unit. At the extreme, the leader is viewed as influencing persons comprising the unit much as one would operate a machine, and set procedures are established for maintaining maximal influence.

Finding the best mix of leadership dimensions or best average leadership style involves two assumptions. First, it is assumed that the leader's behavior toward subordinates is consistent over time and homogeneous across group members such that his/her behavior needs only to be averaged to represent total leader behavior. The variance in behavior around the averaged style is assumed to be random as the leader's behavior is not viewed as depending on particu-

lar relationships he/she may have with various subordinates. A second assumption of the approach is that subordinates' perceptions of leader behavior are homogeneous. That is, subordinates react to the leader's influence attempts in essentially similar manners. Figure 1 depicts these assumptions and the ALS approach.

A typical way of assessing leadership style within the ALS approach is to use the subordinate group as the unit of analysis. With each group, the behavior of the leader is described by subordinates, who should be in a position to observe the leader across time and situations. Operationally, the ALS approach stipulates that an aggregate score, usually an arithemetic mean, be calculated to represent the true style of the leader. In allowing a mean to represent the leader's style, the homogeneity assumptions concerning leader behavior and subordinate reaction are accepted as fact. Averaging over descriptions of group members thus reduces measurement error: positive biases of one member tend to cancel the negative biases of another member.[38]

For this operationalization to be valid, leader behavior cannot be contingent upon personality (needs or abilities) or the situation of particular group members. Although not extensive, research supports some implications of the ALS position, showing there is a moderate amount of agreement in the way subordinates describe their leaders. Interrater correlations group around .6.[12,13] More recently, Schriesheim[37] found a high similarity between individual-oriented and group-oriented leadership descriptions by subordinates. Thus, there may be general behavioral patterns that subordinates recognize

and respond to.

Given moderate subordinate agreement in describing leader behavior, some researchers have been disposed to postulate group level relationships between leader behavior and other organizational variables. For example, Bell[4] hypothesized that the degree of perceived looseness of supervision would be negatively correlated with the degree of task structure. Differences were anticipated in "looseness" among supervisors, in structure among work groups, and these differences were held to be correlated. Aggregate scores in perceived supervisory looseness were used to represent collective group responses.

It is worth noting that the manner in which the OAP's M&S factor is treated in the consultation process would suggest that the ALS approach has been adopted as the approach of choice. Mean score information is fed back to supervisors to apprise them of how their groups stand in regard to similar groups and Air Force groups as a whole. The implication is that differences between supervisors (between group differences) are of greatest importance and that interventions offered by the consultants will operate from this perspective. Of course, rarely would persons working in applied settings consciously deny the existence of subordinate perceptual or response differences within target groups. However, considering theoretical implications of the ALS approach serves to stimulate consideration of an equally likely leadership perspective that is quite different.

Vertical Dyad Linkage perspective

One alternative to the ALS approach is the Vertical Dyad Linkage
(VDL) approach.[9,15] The VDL approach makes the following assumptions
about the leadership context. First, leader behavior is dependent
upon relationships with particular group members. This suggests
that leader behavior will be more homogeneous toward individual
members than members on the average. That is, variation in leader
behavior will be less around the average for each particular member
than around the averaged style as computed in the ALS approach.
Within the ALS perspective, when leader behavior is described by
subordinates, deviations of their observations from the averaged
style are considered as error. The VDL perspective holds that individ-
ual member's observations may vary meaningfully and this variance
should be examined. A second assumption of the VDL perspective
is that a group may be heterogeneous with respect to members' percep-
tions and reactions to leader behavior. In sum, the unit of analysis
in studying leadership should be the dyadic relationship between
the leader and subordinate. This position is in opposition to the
ALS perspective and is depicted in Figure 2.

Holding that leader behavior is conditioned by relationships
between the leader and individual members, the VDL perspective accepts
the possibility that certain members may have higher (or lower)
interdependence with the leader than other members. In other words,
key members (or unimportant members) may exist within the group,

something not possible from a strict ALS framework. The emergence
of differing relationships between a supervisor and group members
can be explained using social exchange notions to describe influence
processes used by the supervisor.[9] Briefly, vertical exchanges
between the superior and subordinate may involve formal and informal
influence processes (as noted in an earlier section of this report).
In using formal influence, the superior relies mostly on the employment
contract, which usually specifies that the subordinate will submit
to legitimate authority regarding certain supervisory requests.
Minimal social exchange is needed.

In contrast, when a superior uses informal influence processes,
the power of the employment contract is diminished and he/she must
rely on more interpersonally-oriented influence bases. The superior
may show greater (or lesser) confidence in and consideration for
the subordinate, and offer more (or less) influence in decision
making and job latitude. The subordinate can reciprocate accordingly.
Overall, variation in superior-subordinate interdependence and rela-
tionship quality is expected to occur and maximal social exchange
is required.

There is a fairly substantial body of research indicating that
the VDL perspective is tenable. For example, both Evans[11] and
Graham[18] found the agreement between superior and averaged subordinate
descriptions of leader behavior to be close to zero, indicating
a wide variance in perceptions of the supposed same behavior. The
idea that superiors form relationships with subordinates varying
in level of interdependency or quality (e.g., subordinates classified

102-16

as having in- or out-group status) has been documented and shown
to determine various leadership outcomes such as subordinate satisfac-
tion, job problems, etc. [9,17,31,41,42] It appears that the VDL approach
does present an alternative view of leadership processes than that
advanced by the ALS perspective.

Combining individual and group perspectives: The multilevel approach

The existence of two seemingly opposed perspectives presents
problems for those both studying and exercising leadership. [8] Most
individuals, whether first-line supervisors, CEO's, or military
personnel, realize the ALS approach may be inadequate: leaders
cannot treat all subordinates similarly. Likewise, practitioners
find the VDL approach of multiple unique individual relationships
is not a totally acceptable description of real life: subordinate
feelings of inequity as well as drains on the leader's time would
occur. There must be some core of consistency if leaders are to
be successful. It is because of such theoretical predicaments that
hybrid or multilevel models of leadership have been developed.

The multilevel perspective supports the notion that leadership
influences function at both the individual and group/aggregate level.
Proponents suggest that level of analysis issues created by ALS
vs. VDL models should not be addressed in either-or terms. [7] Generally,
multilevel analysis refers to analytical procedures that partition
effects at one or more levels of analysis among variables belonging
to separate levels of analysis, such as to individuals and to groups
they comprise. [35] In the case of the ALS and VDL leadership models,

multilevel analysis may be of value in determining if both models simultaneously explain leadership effects. Recent multilevel research examining leadership influences has tended to support the notion that leadership influences can be detected using both individuals and groups as the unit of analysis.[28,41]

With reference to the M&S factor on the OAP, it was noted that items measuring formal, group-oriented leadership processes predominate. Formal leadership influences are identified with conditions that tend to result in similar responses on the part of subordinates.[9] As such, one might expect that the group as a unit of analysis perspective (ALS) would be appropriate in treating OAP data. However, in a multilevel study involving Army National Guard members, within-group effects (VDL) were found even though the items used to gauge leadership processes asked respondents to describe the leader's behavior toward the group.[28] Thus, multilevel tests with the M&S factor may be useful. Additionally, Green[19] noted that LMDC consultants are instructed to evaluate within-group score distributions on the OAP even though they probably pay more attention to the comparative distribution of group means. It would seem LMDC consultants are faced with evaluative tasks that implicitly involve multilevel ways of thinking about leadership.

The model to be examined allows for the possibility of both individual (within-group) and group (between-group) level effects of leadership. This multilevel model is depicted in Figure 3. In keeping with most leadership research, the direction of the arrows indicates the model portrays leadership processes as resulting in

various work-related outcomes (see reference 30). These outcome variables are ones available from the OAP, are likely reactions to leadership influences, and commonly appear in ALS and VDL studies.[31,37] It should be noted that as an exploratory study, this report will not attempt to establish the proposed model as the optimal one: this is a matter for confirmatory analysis. At the same time though, variants of this model are found throughout recent leadership literature and thus it does have sufficient theoretical underpinnings to warrant examination.

IV. METHODOLOGY

Sample

The sample consisted of individuals selected using work group codes employed by LMDC to classify units into functional areas. The four-digit work group codes of groups selected and the number of groups within each code are listed in Table 1. LMDC personnel familiar with the data base inspected work group code, base, and batch information to insure that those identified were from the same groups (i.e. individuals reporting to the same supervisor). It should be noted that because data are collected only from personnel who are available and volunteer to respond to the OAP, responses of entire work groups are not captured intact. Assuming there are no systematic explanations for "no shows" in the data collection process, partial group responses should not cause problems for the study. Work groups for the study consisted of at least four but no more than ten respondents. Unit size was constrained to be rather

homogeneous to guard against unit size effects that could influence worker affective reactions independently of leader behavior.[28,41]

Measures

Measures used had been developed through a series of OAP factor analyses. A description of the OAP and information concerning psychometric characteristics of derived factors may be found in Short et al.[39] The factors appeared to be adequate in a measurement sense for use in an exploratory effort. Specific factors were: Management and Supervision -- M&S (V818), perceived degree to which the leader provides guidance, support, and establishes standards/good work procedures; Work Group Effectiveness (V821), one's perception of the quantity, quality, and efficiency of the work group; Job Performance Goals (V810), one's perception of how clear, difficult, and realistic performance goals are; and Supervisory Communications Climate (V819), perceived degree of supervisory rapport, encouragement, and feedback. Job Satisfaction (V723) a one-item global indicator, measured satisfaction with the job as a whole. The use of such a satisfaction measure has been supported elsewhere.[36] The wording of items tapping reactions to leader behavior revealed they were perceptually-based. Thus, the factors they comprised were considered as individual level operationalizations. A group level operationalization of M&S was formed by calculating aggregated scores (means). Though aggregation using means is not the only way of representing group level phenomena, it is the most common technique found in the organizational literature.[35]

Analysis

A hierarchical regression approach to multilevel analysis, contextual analysis, was employed.[6] Basically, this study followed variance partitioning procedures employed by Katerberg and Hom,[28] and Vecchio,[41,42] among others, to test for within- and between-group leadership effects. Mean M&S scores were assigned by group to each group's respondents and outcome variables were regressed on these M&S scores. The resultant squared multiple correlation (R^2) generated for each outcome variable represented the proportion of variance in respondents' outcomes that could be explained by supervisor differences across work groups. In other words, this R^2 indicates how well the ALS model fit the data. Respondents' raw M&S scores were included next in the regression equations in addition to the M&S group mean scores. Resultant increases in R^2 have been argued to represent incremental explanatory effects of within-supervisor differences (VDL model) on the outcome variables. It should be noted that other approaches to examining within- and between-group effects have been offered as alternatives to contextual analysis.[34] Though currently most popular, it is not clear that contextual analysis is the best way (or that there is any best way) to examine multilevel phenomena. However, this issue is beyond the scope of the present study.

V. RESULTS AND DISCUSSION

Descriptive statistics for the study variables are shown in
Table 2. All variables were positively intercorrelated with most
in the low to moderate range. Though the individual/aggregate M&S
score correlation was higher, common variance between these factors
was only moderate. Supervisory Communications Climate correlated
highly with individual level M&S, indicating these factors may be
measuring aspects of the same thing. (These factors have been com-
bined in latest revision of the OAP).

Since some amount of homogeneity in subordinate perceptions
of leader behavior is required before aggregate M&S responses can
represent a group level response, a check on within-group homogeneity
was performed. Following techniques developed by James,[26] eta coeffi-
cients were computed and indicated that 29% of the total variation
in M&S scores was associated with between-group differences. Though
no formal guidelines exist for minimal agreement levels,[27] it was
felt this level was sufficient for exploratory purposes.

Table 3 lists the results of contextual analyses for all groups
involved in the study. The first two columns of Table 3 contain
the R^2s generated by regressing the criteria on group mean M&S scores
only and on group mean and individual M&S scores together. The
increment in R^2 obtained by considering the individual level M&S
variable in addition to the group level M&S variable is shown in
column 3. Group level M&S accounted for generally small but signifi-
cant amounts of variance in all criterion variables. Importantly,

individual level M&S accounted for significant amounts of criterion variance beyond that explained by group level M&S alone. In other words, within-group variation in M&S responses explained criterion variance even after the effects of between-group variation had been controlled. These results suggest that both the ALS and VDL perspectives are supported by the data.

With respect to particular criterion variables, the supervisor's feedback and encouragement behavior (Supervisory Communications Climate--SCC) provided the strongest evidence of VDL effects. Undoubtedly, some of this effect was due to common method variance. Items of the M&S and SCC factors contain some content overlap since both refer specifically to supervision. Conceptually, however, it is not surprising that VDL effects would appear more strongly with SCC as this factor captures VDL social exchange notions better than any of the other criterion variables. That is, rapport and reward conditions measured by SCC would likely reflect the varying quality of the social (rather than formal) exchanges that occur between superiors and subordinates. Analyses with Job Performance Goals and Work Group Effectiveness variables revealed about the same level of support for VDL effects. Support for VDL effects was weakest (though still significant) in connection with the Job Satisfaction measure.

Some additional analyses were conducted to explore the influence that the social context of the work group might exert in connection with individual and group M&S effects. An informal criterion used in sampling work groups for study involved the degree that coordina-

tive effort or "teamwork" was part of the work group function. (Note that this criterion did not measure actual teamwork but was based only on a work group code expert's knowledge of members' task duties). Twenty-nine groups (N=171) whose jobs required more teamwork were identified along with 69 groups (N=388) whose jobs required less teamwork. Higher teamwork groups included firemen, weapons loading/handling, and tactical combat support personnel: lower teamwork classifications included base personnel office, security police, fuel distribution, and shipping personnel.

Contextual analyses were run for both high and low teamwork samples. Multilevel effects similar to those occurring in analyses with the total sample were found. One interesting exception resulted, however. For high teamwork groups, no significant VDL effects were found with Job Performance Goals as the criterion variable. Speculatively, this may be due to the nature of team-oriented tasks as much as ALS effects per se. Though supervisors of such groups are responsible for establishing goal clarity, etc., the interdependency of team members would necessitate that members know their task goals as members of a team. Individual perceptions would tend to be more homogeneous in team-oriented groups since members would reinforce each other's goal awareness to increase the probability of task success. Moreover, this perceptual homogeneity might correspond with group perceptions of the supervisor's management/supervision skills since a supervisor is more likely to be viewed as part of the group under team vs. nonteamwork conditions. In a sense, teamwork dynamics may have effectively served as a "substitute for the formal

102-24

(ALS) goal structuring leadership function.[29]

Overall, the present study concurs with previous research[28,41] in finding that leadership influence as measured by the M&S factor operates at both individual and group levels. In terms of the ALS perspective, moderate agreement was found among subordinate perceptions of leader behavior. Moreover, a group level indicator of leader behavior (i.e., aggregate M&S scores) correlated with individual responses on factors potentially affected by leader behavior. From the VDL perspective, it was found that an individual level indicator of leader behavior (i.e., individual M&S scores) accounted for significant additional variance in criterion variables. In sum, leader influence was found to operate in multilevel fashion.

Some caveats to this study should be noted before general implications and specific recommendations are offered. First, this study was exploratory in the sense that a conceptually and empirically supported model was applied for the first time within an Air Force context. The sampling procedure, though guided by work group size and function considerations, was one of convenience. Complete intact work groups were probably not sampled. Future research along the lines of this study should consider more representative sampling procedures. Second, the measures employed were from the OAP rather than its replacement, the OAS. Though caution in generalizing results across measures is advised, results found with OAP factors should extend to the OAS as multilevel effects have been documented using a variety of leadership-related instruments.[41] A third and final caveat concerns the use of contextual analysis in multilevel research.

Though variable intercorrelations suggest minimal common method variance problems, multicollinearity can undermine regression-based techniques like contextual analysis. As noted, previously, there are alternative means of examining multilevel phenomena although contextual analysis is currently the most used technique. Future tests concerning multilevel leadership effects might profitably employ other techniques to insure robustness of the current findings.

VI. RECOMMENDATIONS

Recommendations deriving from this research effort follow. Ones relating more to model building are covered first followed by recommendations pertaining to leadership and work group topics.

1. With the intent of producing a useful product, a theoretical multilevel leadership model was tested and supported. Further efforts to discover meaningful relationships among other factors contained in LMDC survey instruments will yield a better understanding of how these content areas interrelate. Such understanding could in turn provide consultants with information concerning intervention techniques to correct problems in specific areas (e.g., see recommendation 4 below). Knowing if (and which) factors have primacy in a network of causal relationships would permit consultants to intervene earlier in the causal chain, rectifying more primary than secondary problems. The construction and testing of applied theoretical models should be continued with revised versions of the OAP (i.e., the OAS). Relevant connections between the OAS and the other survey instruments (e.g., Family and Spouse Survey) should also be pursued.

2. Just as multilevel supervisory effects were discovered,
so too may multilevel effects be uncovered in other content areas
(combat readiness, organizational climate, and stress) assessed
by the OAP (and OAS). While it is not suggested that only multilevel
models are worthy of investigation, given the hierarchical structuring
of most Air Force organizations, it would seem prudent where appro-
priate to consider unit of analysis, measurement, and effect issues
in testing future models. When relevant, multilevel issues should
be considered in building applied theoretical models.

3. The exploratory tenor of this study necessitated some design
limitations. Future multilevel research with OAP (and OAS) factors
should consider the following design options: (a) For any N individ-
uals, design strategy should maximize the number of aggregate units
sampled; (b) When possible use independently measured global variables
in addition to aggregate ones; and (c) Use varying analytical ap-
proaches, e.g., contextual analysis, analysis of covariance, and
within-and-between analysis.[8] Option (a) guards against insufficient
variability in aggregate characteristics, option (b) provides for
a check against the natural collinearity between individual responses
and aggregates formed from the same responses, and option (c) guards
against findings being "method-bound."

4. The current focus of consultants is on differences between
work groups rather than differences in within-group perceptions
of the same supervisor.[19] Given the results of the current study,
equal attention should be paid the latter. Within-group as well
as between-group differences in perceptions of supervisory behavior

should be addressed by consultants. Intervention training techniques that address supervisor-member exchanges may be usefully applied where there is wide within-group variation in members' perceptions of the supervisor. This holds for groups registering lower and higher mean M&S scores. A particular mode of training, called LMX training,[16] has been shown to be beneficial in this regard.

5. With-in group standard deviations (SD) of the M&S factor are computed as a tool to help consultants spot work groups where leader-member exchanges need attention. If a reference sample were identifiable for different types of functional work groups, distributions of work group SD's could be used as yardsticks to gauge when work groups are exhibiting high within-group SD's. Appropriate distributions of within-group SD's should be generated. This also applies for other factors. For example, a comparatively high within-group SD (regardless of mean level) on the Job Performance Goals factors might indicate goal ambiguity problems.

6. The results regarding teamwork/nonteamwork influences on perceived supervisory behaviors were tentative. But, it would be worthwhile to further investigate this topic because of team structuring of many Air Force jobs. Consultant interventions involving supervisory behavior may need to be conditioned on the amount of teamwork required by the nature of processes operating in the functional area.[29] Teamwork influences on the perception of leader behavior should be further investigated.

7. In drawing a sample for the study, it was difficult to identify unique work groups because of code limitations. This problem

will hopefully be corrected by coding inprovements in the OAS.

Nevertheless, because many of the factors measured by the OAP (and

OAS) have meaning at the work group level, care should be taken

in inputing and sampling data so unique groups can be identified

at that level of analysis. Information used to classify and identify

work groups should include work group code, base, batch, and Julian

date (of cite visit). Likewise, if other levels of analysis and

variables are to be studied, say, the squadron level and organizational

climate, LMDC should collect information allowing unique identification

of the appropriate focal units.

8. It was noted that in this study, complete work group re-
sponses were not collected. Given that participation in surveys

is voluntary, it is not practical to expect responses from the whole

work group. For this reason, response rate percentages should be

calculated down to the work group level. This information will

help consultants determine representativeness of responses at the

level of the work group rather than some higher level.

9. Current OAP datafiles aggregate by work group code. This

provides useful information to consultants as they know base, batch,

and data collection dates. When such information is stored in a

permanent aggregate datafile, however, the workgroup code delineation

represents information aggreg ted across bases and batches. One

interested in unique work group data must create new files (as was

done in the current study) using work group code, base, and batch

information. Though SPSS[x] facilitates this, it would be easier

for researchers to be able to call such information up directly

from the permanent aggregate file. The aggregate file should be
built at the lowest possible level (i.e., unique work groups).
Such files should include information identifying larger aggregates
to which unique work groups belong (e.g., squadrons) so information
at higher levels cf analysis could be retrieved.

Table 1

Functional Areas -- Aggregate Code Descriptions

CODE	N	DESCRIPTION
2D85	7	CBPO Customer Assistance Branch--Records & Personal Affairs
2D86	10	CBPO Manning Control--Assignments
2D87	4	CBPO Quality Force, Special Actions, Separations
2E36	28	Security Police--Law Enforcement
2G33	6	Fire Station Personnel
2G35 2G36	10	Other Fire Specialties
2G39	1	Geographically Separated Units (Fire Stations)
3585	1	Fuel Storage
3587	9	Fuel Distribution
3622	8	Household Goods/Personal Property Shipping
3624	2	Air Freight Shipping
464A 464B 4735 4736	5	Weapons Loaders/Handlers
9A8B	3	Radio Maintenance Technicians
9A8D	4	Tactical Air Combat Support

Note: N signifies the number of work groups within each area.

Table 2

Descriptive Statistics and Intercorrelations Among Study Variables

Variables	M	SD	2	3	4	5	6
1. M&S (individual)	5.17	1.75	.54	.21	.27	.67	.31
2. M&S (group)	5.17	.95		.22	.20	.38	.23
3. Job satisfaction	4.53	1.99			.24	.23	.30
4. Job Performance goals	4.80	1.33				.28	.32
5. Supervisory communications climate	4.81	1.90					.26
6. Work group effectiveness	5.41	1.48					

Note: All correlations are significant, p. < .001, N = 559.

Table 3

Effects of Within- and Between-Group Leadership Variation

Criterion Variables	R^2		ΔR^2
	Agg.	Agg.+Ind.	
Job satisfaction	.05	.06	.01
Job performance goals	.04	.08	.04
Supervisory communications climate	.15	.45	.30
Work group effectiveness	.05	.10	.05

Note: All R^2s and R^2 increments are significant (p<.001).

Agg. = Aggregate M&S scores, Ind. = Individual M&S scores.

102-33

References

1. Baron, R. A. <u>Behavior in organizations</u>. Boston: Allyn and
    Bacon, 1983.

2. Bass, B. M. <u>Stogdill's handbook of leadership: A survey of</u>
    <u>theory and research</u>. New York: The Free Press, 1981.

3. Beer, M. Technology of organizational development. In M. D.
    Dunnette (Ed.), <u>Handbook of industrial and organizational psy-</u>
    <u>chology</u>. New York: Wiley & Sons, 1983, pp. 937-993.

4. Bell, G. The influence of technological components of work
    upon management control. <u>Academy of Management Journal</u>, 1965,
    <u>8</u>, 127-132.

5. Berrien, F. K. <u>A general systems approach to organizations</u>.
    In M. D. Dunnette (Ed.), <u>Handbook of industrial and organization-</u>
    <u>al psychology</u>. New York: Wiley & Sons, 1983, pp. 41-62.

6. Burstein, L. The analysis of multilevel data in educational
    research and evaluation. In L. Schulman (Ed.), <u>Review of re-</u>
    <u>search in education</u>. Itasca, IL: Peacock, 1980, pp. 158-233.

7. Cummings, L. L. Assessing the Graen/Cashman model and comparing
    it with other approaches. In J. Hunt & L. Larson (Eds.), <u>Leader-</u>
    <u>ship frontiers</u>. Kent, OH: Kent State University Press, 1975,
    pp. 181-185.

8. Dansereau, F., Alutto, J. A., Markham, S. E., & Dumas, M.
    Multiplexed supervision and leadership: An application of
    within and between analysis. In J. Hunt, U. Sekaran, & C.
    Schriesheim (Eds.), <u>Leadership: Beyond establishment views</u>.

Carbondale, IL: Southern Illinois University Press, 1982, pp. 81-103.

9. Dansereau, F., Graen, G., & Haga, W. J. A vertical dyad linkage approach to leadership within formal organizations: A longitudinal investigation of the role making process. _Organizational Behavior and Human Performance_, 1975, _13_, 46-78.

10. Dubin, R. Theory building in applied areas. In M. D. Dunnette (Ed.), _Handbook of industrial and organizational psychology_. New York: Wiley & Sons, 1983, pp. 17-39.

11. Evans, M. G. The effects of supervisory behavior on the path goal relationship. _Organizational Behavior and Human Performance_, 1970, _5_, 277-298.

12. Fleishman, E. A. A leader behavior description for industry. In R. M. Stogdill & A. E. Coons (Eds.), _Leader behavior: Its description and measurement_. Columbus: Bureau of Business Research, Ohio State University, 1957, pp. 103-119.

13. Fleishman, E. A., Harris, E. F. & Burtt, H. E. _Leadership and supervision in industry_. Columbus: Bureau of Educational Research, Ohio State University, 1955.

14. French, J. R. P., & Raven, B. The bases of social power. In D. Cartwright (Ed.), _Group dynamics: Research and theory_. Evanston, IL: Row, Peterson, 1962, pp. 259-269.

15. Graen, G., & Cashman, J. A role-making model of leadership in formal organizations: A developmental approach. In J. Hunt & L. Larson (Eds.), _Leadership frontiers_. Kent, OH: Kent State University Press, 1975, pp. 143-166.

16. Graen, G., Novak, M. A., & Sommerkamp, P. The effects of leader-
    member exchange and job design on productivity and satisfaction:
    Testing a dual attachment model. Organizational Behavior and
    Human Performance, 1982, 30, 109-131.

17. Graen, G., & Schiemann, W. Leader-member agreement: A vertical
    dyad linkage approach. Journal of Applied Psychology, 1978,
    63, 206-212.

18. Graham, W. A. Perceptions of leader behavior and evaluation
    of leaders across organizational levels. Experimental publica-
    tion system (APA), 1970, 4, 144A.

19. Green, S. B. An evaluation of the measurement system used
    by LMDC for the assessment of its consulting efforts. (USAF-SCEEE
    Summer Faculty Research Program). Maxwell AFB, AL: Leadership
    and Management Development Center, 1983.

20. Hendrix, W. H. Contingency approaches to leadership: A review
    and synthesis. (AFHRL-TR-76-17, AD-A028485). Lackland AFB,
    TX: Occupational and Manpower Research Division, Air Force
    Human Resources Laboratory, 1976.

21. Hendrix, W. H., & Halverson, V. B. Organizational survey assess-
    ment package for Air Force organizations (AFHRL-TR-78-93).
    Brooks AFB, TX: Air Force Human Resources Laboratory, 1979.

22. Hightower, J. M., & Short, L. O. Factor stability of the Organi-
    zational Assessment Package. (LMDC-TR-82-1). Maxwell AFB,
    AL: Leadership and Management Development Center, 1982.

23. Hunt, J. G. Leadership and managerial behavior. In F. E.
    Kast and J. E. Rosenzweig (Eds.), Modules in Management.

Chicago: SRA, 1984.

24. Jacobs, T. Leadership and exchange in formal organizations.
    Alexandria, VA: Human Resources Research Organization, 1971.

25. Jago, A. G. Leadership: Perspectives in theory and research.
    Management Science, 1982, 28, 315-336.

26. James, L. R. Aggregation bias in estimates of perceptual agree-
    ment. Journal of Applied Psychology, 1982, 67, 219-229.

27. Jones, A. P., & James, L. R. Psychological climate: Dimensions
    and relationships of individual and aggregated work environment
    perceptions. Organizational Behavior and Human Performance,
    1979, 23, 201-250.

28. Katerberg, R., & Hom, P. W. The effects of within-group and
    between-group variation in leadership. Journal of Applied
    Psychology, 1981, 66, 218-223.

29. Kerr, S., & Jermier, J. M. Substitutes for leadership: Their
    meaning and measurement. Organizational Behavior and Human
    Performance, 1978, 22. 375-403.

30. Kerr, S., & Schriesheim, C. A. Consideration, initiating struc-
    ture, and organizational criteria: An update of Korman's 1966
    review. Personnel Psychology, 1974, 27, 555-568.

31. Liden, R. C., & Graen, G. Generalizability of the Vertical
    Dyad Linkage model of leadership. Academy of Management Journal,
    1980, 23, 451-465.

32. Mahr, T. A. Manual for the Organizational Assessment Package
    Survey. (LMDC-TR-82-1560). Maxwell AFB, AL: Leadership and
    Management Development Center, 1982.

33. Mann, F. C. Studying and creating change: A means to understand-
ing social organization. In Research in industrial human rela-
tions. Industrial Relations Research Association, Publication
No. 17, 1957, 146-167.

34. Markham, S. E., Dansereau, F., Alutto, J. A., & Dumas, M.
Leadership convergence: An application of within and between
analysis to validity. Applied Psychological Measurement, 1983,
7, 63-72.

35. Mossholder, K. W., & Bedeian, A. G. Cross-level inference
and organizational research: Perspectives on interpretation
and application. Academy of Management Review, 1983, 8, 547-558.

36. Scarpello, V., & Campbell, J. P. Job satisfaction: Are all
the parts there? Personnel Psychology, 1983, 36, 577-600.

37. Schriesheim, C. A. The similarity of individual directed and
group directed leader behavior descriptions. Academy of Manage-
ment Journal, 1979, 22, 345-355.

38. Schriesheim, C. A., House, R., & Kerr, S. Leader initiating
structure: A reconciliation of discrepant research results
and some empirical tests. Organizational Behavior and Human
Performance, 1976, 15, 297-321.

39. Short, L. O., Hightower, J. M., & Snow, J ". Management consul-
tation in the Air Force: A description a d case study of survey
feedback in a complex system. Paper presented at the 44th
Annual Meeting of the Academy of Management, Boston, MA, 1984.

40. Short, L. O., & Wilkerson, D. A. An examination of the group
differences aspect of the construct validity of the Organization-

al Assessment Package. Paper presented at the 23rd Annual Conference of the Military Training Association, Arlington, VA, 1981.

41. Vecchio, R. P. A further test of leadership effects due to between-group variation and within-group variation. *Journal of Applied Psychology*, 1982, *67*, 200-208.

42. Vecchio, R. P., & Gobdel, B. C. The Vertical Dyad Linkage model of leadership: Problems and prospects. *Organizational Behavior and Human Performance*, 1984, in press.

Figure 1

The Average Leadership Style Approach
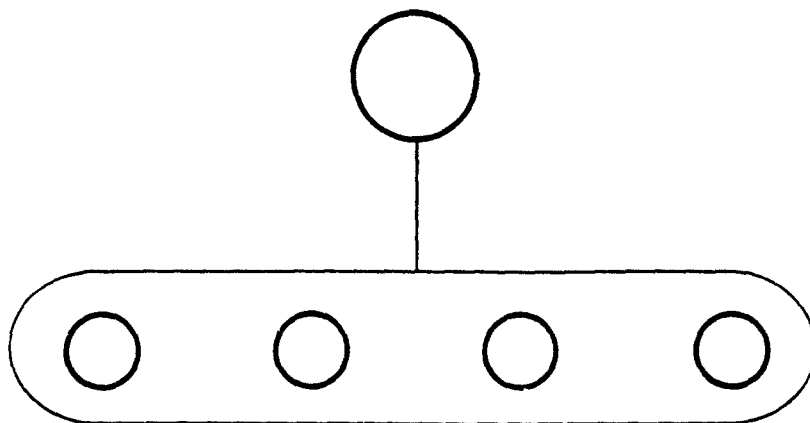
Figure 2

The Vertical Dyad Linkage Approach

102-40
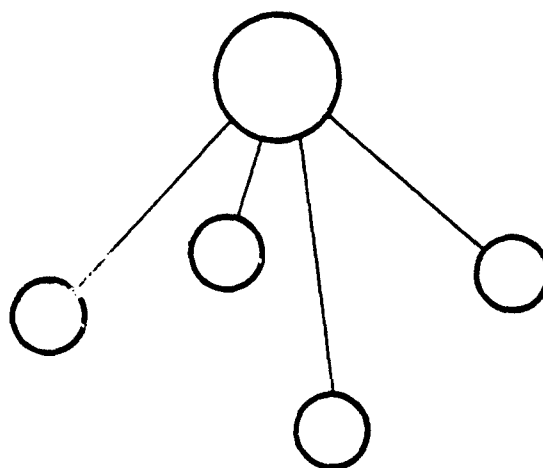
Figure 3

Proposed Multilevel Model of Leadership Effects

102-41

/ 4

ACKNOWLEDGEMENTS

1984 USAF-SCEEE SUMMER FACULTY RESEARCH PROGRAM

Sponsored by the

AIR FORCE OFFICE OF SCIENTIFIC RESEARCH

Conducted by the

SOUTHEASTERN CENTER FOR ELECTRICAL ENGINEERING EDUCATION

FINAL REPORT

RAMAN SPECTROSCOPY OF
UNSTIMULATED AND STIMULATED, CULTURED
NORMAL AND NEOPLASTIC HUMAN OR MAMMALIAN CELLS

Prepared by: Dr. James J. Mrotek

Academic Rank: Associate Professor

Department,   Department of Physiology
 School and   School of Medicine
University: Meharry Medical College

Research Location: School of Aerospace Medicine
                            Clinical Sciences Division
                            Neurosciences Branch
                            Brooks Air Force Base, Texas

USAF Research: Dr. John Taboada

Date: October 10, 1984

Contract No: F49620-82-C-0035

RAMAN SPECTROSCOPY OF UNSTIMULATED AND STIMULATED, CULTURED NORMAL AND NEOPLASTIC HUMAN OR MAMMALIAN CELLS

by

James J. Mrotek

ABSTRACT

Y-1 mouse adrenal tumor cells, and a human neoplastic, respiratory tract, fibroblast cell line, HEp-2, were examined using laser Raman spectroscopy. Methods were designed, and their efficacy tested, to produce cell suspensions for use in the Raman spectrometer. Because differentiated cellular function depends on large concentrations of certain unique intracellular molecules, attempts were made to determine whether characteristic Raman spectra would be produced by intracellular HEp-2 or Y-1 molecules irradiated with a laser beam tuned to one of several wavelengths. Using 514 and 488 nm data obtained from both cell lines was encouraging but inconclusive because of insufficient replication. Y-1 experiments using 476.5 nm involved runs repeated on the same sample, runs on different samples, and a run on a pool of three different cell generations. This wavelength produced what appeared to be several characteristic Y-1 emissions; some of these were analogous to emissions others previously obtained from carotenoids and heme-containing proteins. The Y-1 cells also seemed to respond to cAMP stimulation by producing emissions that differed from those of control cells. Detection of 476.5 nm-stimulated emissions appeared to improve if a parallel polarizer was inserted between sample and detector.

Acknowledgement

The objectives proposed for the RISE grant were based on problems encountered during the 1983 SCEEE summer research fellowship. The RISE proposal was designed to optimize methods for preparing and examining cell samples in the Raman spectrometer. The Utah consortium contract was intended to provide funds for equipment to be used to rapidly and accurately determine cell numbers, to determine division times of the cultured cells being examined by spectrometry and to develop methods for examining purified molecules that are characteristic of cultured adrenal cells. The 1984 AFOSR/SCEEE summer research fellowship which is the subject of this report provided the time and living expenses to use newly developed methods and the equipment.

In attempt to present a complete and integrated description of the accomplishments on this project, this report combines the results obtained using funds from each individual source. To avoid the appearance of funding duplication for the same effort, care is taken to distinguish which result was obtained using funds from a particular source.

I. INTRODUCTION

Through the use of USAF School of Aerospace Medicine lab director's funds and support, Dr. John Taboada, working in the Clinical Sciences Division of the School of Aerospace Medicine, developed a research program and experimental facility to investigate the laser-Raman spectroscopy of molecules in living systems. This approach to clinical testing is directed toward improving non-invasive clinical diagnosis of Air Force personnel.

The object of my 1983 collaboration with Dr. Taboada was to determine whether cultured normal and neoplastic

mammalian and human cell types produced Raman spectra
and whether these spectra were modified by exogenous
stimulants. Since I was familiar with properties of the
Y-1 mouse adrenal tumor cell line and its special cul-
ture conditions, we began the studies with these cells.
Cultured steroid producing cells can be used for study-
ing the internal and external conditions affecting ster-
oid production, and Raman spectra, because the intra-
cellular molecules and steps involved in steroidogenesis
are relatively well defined.

THEORETICAL BACKGROUND FOR RAMAN SPECTROSCOPICAL STUDIES:

Because a molecule interacts with the incident pho-
tons with which it is irradiated, a small number of
photons of shorter (anti-Stokes) or longer (Stokes)
wavelengths than those of the original incident light
will be scattered by the molecule during the irradia-
tion. Laser-Raman spectroscopy is performed by scanning
a range of wavelengths immediately preceeding, and suc-
ceeding, the wavelength of the incident photons to de-
tect photons scattered by the irradiated molecules. In
theory, a given molecule will produce only a limited
number of specific spectra.

II. OBJECTIVES

The study of molecules and cells using laser Raman
spectrocscopy is intended to provide semi- or non-inva-
sive diagnostic techniques to monitor the suitability of

Air Force personel to perform their tasks. The promise of laser Raman spectrometry in carrying out this intent is evident from existing literature (1-4) and from preliminary published and unpublished experiments conducted by Dr. Taboada and me (5). However, much basic data regarding the technique remains to be obtained. Frequently data acquisition must be deferred while solving logistical and procedural problems impeding progress. During the past year this report author was funded by three different sources: an AFOSR/SCEEE RISE grant, a contract from the AFOSR/Utah Consortium for Biotechnology Research and a second SCEEE summer research fellowship. Each of these grants and fellowships contributed to the development of procedures designed to provide information on the experimental system to insure that laser Raman data acquisition would be valid.

The objectives proposed for the RISE grant were based on problems encountered during the 1983 SCEEE summer research fellowship. The RISE proposal was designed to optimize methods for preparing and examining cell samples in the Raman spectrometer. The Utah consortium contract was intended to provide funds for equipment to be used to rapidly and accurately determine cell numbers, to determine division times of the cultured cells being examined by spectrometry and to develop methods for examining purified molecules that are characteristic of cultured adrenal cells. The 1984 AFOSR/SCEEE summer

research fellowship which is the subject of this report provided the time and living expenses to use newly developed methods and the equipment.

III. RESULTS

METHODS DEVELOPED TO PROVIDE CELLS FOR RAMAN SPECTROSCOPY

In the summer of 1983 we adapted the handling of cultured cells to the system existing for Raman spectroscopy of bacterial cell suspensions (see 1983 SCEEE Summer Research Fellowship Report). Using funds from the 1983 RISE grant, the preliminary procedures used to produce suspensions in summer 1983 were confirmed during trips to Brooks AFB in 1983-84 and this summer during my summer research fellowship. In the discussion which follows the rationale and difficulties associated with the use of these procedures, and the solution to these difficulties are described.

In each of these procedures sterility was maintained to avoid introduction of contaminant microorganisms which would produce confounding Raman spectra (1). Human and mammalian cells were washed thoroughly in a nutrient medium we found experimentally to be non-fluorescent, Hank's buffered salt solution (HBSS). Washing removed the standard cell culture medium, Eagle's minimum essential medium with Earle's salts that contains fluorescent serums, vitamins, amino acids and the pH indicator, phenol red. Since drastic changes in envirnment caused by changes in incubation media might affect

physiological functions, comparisons were made between the published compositions of HBSS and standard media to determine how compositions of each differed (Gibco catalog, Palo Alto, CA). We found that they did not differ markedly (Table I).

The maximum incubation period without serums, vitamins and amino acids for the cells was never greater than nine hours. Y-1 cells incubated in buffered salts for 24 hours still produced steroids under these conditions (6), suggesting that a major physiological function of these cells was not compromised by lack of serums, vitamins and amino acids. In our present work, HEp-2 cells maintained 24 hours in HBSS before being mixed with the live/dead stain, trypan blue (7), contained no more dead cells than samples evaluated the previous day (data not shown).

To produce cell suspensions, HEp-2 and Y-1 cells were then incubated, with occasional gentle rocking, for 5-15 minutes in 1-4 ml (depending on culture flask size) of 0.05% trypsin. As small sheets of adrenal cells began to float loose from the flask surface, a volume of 1 mM EGTA, a calcium chelator, equal to that of trypsin was used to inhibit trypsin by removing the calcium necessary for its activity, to produce single cells by causing internalization of desmosomal junctions holding adjacent cells together and to prevent cells from subsequent reclumping. Since trypsin released individual

TABLE I*

	NaCl**	KCl	Anhy. MgSO4	MgSO4 *7H2O	Anhy. CaCl2	CaCl2 *2H2O	HEPES Buffer	Glucose
HBSS	8.0	0.4		0.2	0.14			1.0
MEM+	7.2	0.4	0.1			0.26	5.86	1.0

	Na2HPO4*12H2O	KH2PO4	NaH2PO4*H2O
HBSS		0.12	0.06
MEM	0.14		

* HBSS   total monovalent cation (Sodium/Potassium) equivalents: 0.36.
  MEM   total monovalent cation (Sodium/Potassium) equivalents: 0.31.
** grams/liter
+ Eagle's Minimum Essential Medium with Earle's Salts

TABLE II*

	LIVE	DEAD	FRAGMENTS	CLUMPS
FLASK 1	55.9±10.3	20.9±7.8	20.4±7.8	2.9±0.8
FLASK 2	32.3±6.3	13.3±3.8	15.4±5.3	3.4±1.0

* Mean ± S.E.M for four determinations;

HEp-2 cells without the need for EGTA and EGTA did not prevent HEp-2 cells from reclumping; 0.5 mg/ml trypsin inhibitor/HBSS, added to the cells in a volume equal to that of trypsin, prevented clumping. Following suspension, and whenever cells were transferred from one container to another, they were rapidly pipetted up and down to ensure homogeneous suspensions and to dislodge any cells which might have clumped. We were initially concerned that this procedure might fragment cells, but data presented in Table II suggests this is not a concern. We were also concerned that EGTA treatment was traumatic to the physiology of the cell because any excess EGTA might cause intracellular calcium to diffuse to the extracellular fluid and alter intracellular activity. I initially proposed in the 1983 RISE application that the use of cell suspensions for Raman spectroscopy could be avoided if cells grown on coverslips were inverted over a welled microscope slide containing HBSS. In a trip to Brooks AFB in November 1983 we found this proposal to be impractical because it necessitated focusing the incident laser beam within a single cell. Another method suggested by Dr. Taboada involved "tunneling" the laser beam into the edge of a microscope slide to which cells are attached, the beam caroms from surface to surface down the slide and stokes and anti-stokes wavelengths emitted from contacted cells on the slide surface are scanned by the photon detector. While discussing this and other geometric arrangements, we

realized that most samples which would be used in Air Force tests would be suspended from epithelial cell scrapings or from biopsies. We, therefore, reluctantly returned to the trypsin, EGTA and trypsin inhibitor methods developed in the summer of 1983. Dr. Taboada's "tunneling" procedure remains to be tried.

In using cell suspensions the effects of trypsin, EGTA and trypsin inhibitor on the viability and physiology of suspended cells could be questioned. While we conducted no direct experiments to measure physiology and viability, other investigators had. Steroid production and adrenal cell viability was recently shown by Voorhees and Mrotek (8) to be unaffected by trypsin and trypsin inhibitor; while Brown, Mrotek and Hall (1975, unpublished data) showed that adrenal cells suspended in EGTA were able to respond to ACTH and produce steroids. These findings suggest that at least one adrenal cell physiological parameter was unaffected by our suspension procedures. Since HEp-2 cells have no readily measurable physiological parameters, we have no information regarding the effects of any of the suspending agents on their physiology. Live/dead cells, cell fragments, bacterial and fungal particulates and cell clumps were counted in HEp-2 cell samples suspended with trypsin and EGTA (Table II). Although suspended at the same time, flask two was counted five hours later than flask one. Thus it is apparant that prolonged suspension of the

cells does not harm viability.   Suspended cells counted
24 hours later did not exhibit any increased mortality
(data   not   shown).   Fragments, including crystalline
serum   proteins,   stain particles and rounded objects
1/25th the size of cells, seemed to be non-cellular
material.   Clumps, defined as two or more attached cells
or cell parts, represented only a small percentage of
the total counted material. Maximum clump size consisted
of no more than four, but usually two, cells.   In the
last two 1984 SCEEE summer fellowship weeks, attempts
were made using the Coulter counter purchased with Utah
consortium funds to verify fragmentation and clumping
results for HEp-2 cells, then extend this data to Y-1
cells. As understanding of counter operation improved,
we also attempted to establish approximate cell diame-
ters.   By resetting the count discriminators to detect
larger and larger particles after each count, fragment
and clump counts, and cell size, was infered (Table
III).   Data for run 1 with HEp-2 cells suggested that
there were relatively few particles between 0-15 microns
or of 20 or greater microns; two to ten times as many
particles ranged between 15-20 microns.   Run 2 data
suggested that the majority of the particles range in
size between 10-15 microns, with nine times fewer parti-
cles averaging 20 microns or greater.   Most particles in
run 3 also ranged between 10-15 microns in diameter;
very few were greater than 20 microns in diameter.
Collectively, the data was consistent with the view that

TABLE III

HEp-2

RUN	10-13*	10-15	13-15	15-20	20-25
1		0.66**		1.18	0.13
2		18.29		12.10	1.80
3	16.22		9.24		0.11

Y-1

	7-10	10-11	11-13	11-15	13-15	15-20	20-25
1		6.35		13.88		4.60	0.35
2	4.04	2.54		3.90			
3	0.06	3.82	9.36		7.17		

* Counts for particles whose diameters (in microns) fall within this range. Space limitations precluded including standard error of the mean; all counts were statistically valid.
** X 10-5 particles.

HEp-2 cells ranged from 10 to 20 microns in diameter and that few clumps larger than 20 microns in diameter existed in suspensions; data regarding 0-10 micron fragments was inconclusive. **Further experiments are required to determine fragment counts and refine cell diameter ranges.** The majority of the particles in Y-1 cell suspensions ranged between 7 and 15 microns with the largest numbers being in the 11-15 micron range. With the exception of run 2 in which there was relatively little change in particulate numbers between 7-15 microns, few particulates were found in 7-10 and greater than 20 micron ranges. Collectively, these data may suggest a probable cell size in the 11-15 micron range and little fragmentation and clumping. **Lack of clear results in these counting experiments resulted from inconsistent experimental designs, and lack of time and experience with the Coulter counter. Additional work is suggested.**

We were also concerned about long-term laser irradiation of a suspended cell. Dr. Taboada had previously circumvented this difficulty by horizontally moving the sample-containing cuvette through the laser beam. Because cells suspended in buffer are continuously settling through the fluid, there is a possibility of too few cells at the spectrophotometer photon detector site if the detector is scanning the upper regions of the cuvette, or too many if lower regions are scanned. This

difficulty was overcome by raising the cuvette so that the midpoint of its vertical axis was adjacent to the spectrophotometer photon detector. Thus, as cells settled out of the detection point, other cells settled into this point. Total scan time was short enough to insure a continuous supply of cells falling from the upper cuvette half into the detection point. This geometry also insured short-time cell exposure to the laser (elimina...g the need to laterally translate the cuvette). Nevertheless, beam effects on cell mortality were determined by counting live/dead cells before and after Raman spectrometry (data not shown). Within the experimental error of the method (5%), there was no measurable increase in cell mortality. Laser effects on physiological parameters remain to be determined. We were aware that as cells accumulated on the cuvette bottom, the mass of material might occlude the laser beam. Using the Coulter counter purchased with Utah consortium funds to accurately and rapidly count cells, we could always dilute our samples to maintain a concentration of 1.2 million cells. As determined in successive laser runs using fewer HEp-2 cells, 1.2 million cells seemed to optimize Raman spectra detection while minimizing beam occlusion due to cell accumulation (spectral data not shown).

To explain high levels of Raman spectral activity obtained from HEp-2 and Y-1 cells during my 1983 summer research fellowship, I suggested metabolic and cell

103-15

surface activities as sources of these spectra and Dr. Taboada felt that mitosis might also be a source of this activity; these suggestions were based on my experience with cell surfaces and cytoskeleton (8-14), and Dr. Taboada's with bacterial fission. In addition, we wished to monitor viability, fragmentation, cell clumping and contamination of cell suspensions to assure applicability of Raman data to only the cells being examined. To conduct these evaluations, an inverted Nikon microscope with photographic and time-lapse videotaping capabilities was purchased using funds from a contract with the Utah consortium. Time-lapse videomicroscopy can establish the cycle time between mitoses and also the cell surface activity. Live/dead counts, fragments, contaminants and clumping may also be determined with this microscope. Several factors prevented us from obtaining data related to the above goals. First, the microscope did not arrive until three weeks before the end of the fellowship; second, a useable videotape recorder capable of time-lapse operation could not be found on base; third, the "real-time" videotape of microscope images was not be enlarged enough and illumination was of insufficient intensity for adequate contrast. While evaluation of cell suspensions might have been conducted with the inverted microscope, a microscope Dr. Taboada obtained from surplus property was used to complete most of this work before it ar-

rived. Future experiments to clarify the involvement of cell surface activity and mitosis in Raman activity are planned when funds become available for purchase of a time-lapse video recorder and a microscope objective more powerful than the existing 40X. The problem of insufficient illumination can be corrected by purchasing a video camera having a more sensitive detection system.

Since Dr. Taboada has detected Raman signals associated with fission in synchronized bacterial cells, he is interested in similar phenomena in mitotic mammalian cells. It is his working hypothesis that Raman signals we have detected from rapidly proliferating mammalian cancer cells may derive from the random mitotic activity of the cancer cells. Synchronization of these cells would then intensify the signals and improve reproducibility. Several lines of evidence suggest to me that Raman signals detected in these experiments are independent of mitosis: (a) bacterial fission is different than eukaryotic mitosis, (b) neoplastic cell division rates need not be different from normal cell counterparts (even the most malignant tumors possess an average 18- to 24-hour cell cycle); the analogs only differ in their ability to cease division when all available growth space is lost and adjacent cells are in complete contact with each other (15), (c) most cell division cycles are between 10 - 24 hours long, however, the length of mitosis is seldom longer than two hours. At any given time, therefore, from 8 - 20% of a randomly dividing

cell population will be dividing. It seems unlikely that the entire Raman activity detected in our cells can be ascribed to such a relatively small division percentage. However, metabolic and cell surface activity is continuous during non-dividing cell phases, and differentiated function occupies at least four, if not more, non-dividing hours. Thus, molecules associated with these cellular activities would seem to be more probable causes of Raman activity following laser irradiation.

LASER DATA

Using a laser tuned to one of several different wavelengths, preliminary Raman spectral data were obtained from HEp-2 and Y-1 cells before and after stimulation with ATP or cAMP (Tables IV, V, VI and VII). Before a summary of the data in the tables is presented, several points should be made regarding methods and definitions used for data interpretation. An experimental group was defined as a specific cell type irradiated at a given laser wavelength. A treatment component was either the biochemical stimulant, cAMP or ATP, or the spectrometer modification, presence or absence of a polarizing filter between the sample and detection system. A replicate was the repeated laser scans of a cell type receiving a specific treatment component; except in scans conducted at 476.5 nm, no attempt was made to distinguish between repeated scans of a single sample and a scan of different, but similarly treated, sample,

103-18

because of the enormity of the data. An event was
defined as a single graphic excursion measuring one cm
or more from lowest to highest point; as defined in (b)
below an event was also a collection of events never
differing from each other by no more than four wave
numbers. The event wave number was the photon wavelength
emitted following laser irradiation of a cell. The
summary for each experimental group following shortly
will be organized to present Raman events associated
with a single treatment component within an experiment,
with two treatment components having elements in common
or with events occurring in the majority of the treat-
ment components in that experimental group. To inter-
pret this data these criteria were established: (a) two
wave numbers differing by five or more were considered
to be different (our reasons for this were: in most
instances two different individuals read the laser-Raman
graphs within four wave numbers of each other; during my
readings I accidentally reread wave numbers from several
different portions of the graphs, these readings dif-
fered by no more than four wave numbers; and, the reso-
lution of the detector is 5/cm), (b) since a range of
five wave numbers from replicate runs would not be
different, for reporting they were combined into a range
(a given range was often large because each successive
excursion that was 0 - 4 higher than the preceeding
excursion was included in that range until an excursion

103-19

differing from the last range excursion differed from the next wave number by five; the exception occurred if an excursion added to the given range caused two excursions from the same run to be included (c) in summarizing this data only excursions replicated three or more times in a given experimental treatment or between treatments appear, (d) in multi-treatment experiments, only excursions replicated in all three treatment components, or in three out of a four component experiment, were recorded as events commonly exhibited by those cells when irradiated at that laser wavelength, (e) for each wavelength, events from each treatment component coinciding with water and HBSS solution events were eliminated if they occurred within four of a given wave number; thus, events reported in the tables are those remaining after removal of background events; the sole exception to this was Y-1 adrenal cells irradiated at 488 nm, which had no background runs due to lack of time during the last days of my summer fellowship.

The repeated emissions by intracellular molecules in the six control, HEp-2 replications irradiated at 514 nm (Table IV), were at 418-20, 450-54, 1120-25, and 1670-74 twice, at 970-75 three times, at 878-80 and 1056-60 four times, and 1010-15 five times. Events occurring in two, or three, out of three treatments (nine possible replicates for three treatments) were repeated three times at 144, 150, 298-300, 626-30, 980-85, 1720, and 1778-85, four times at 560-64, 808-10, 900-05, 1000-04, 1218-24,

TABLE IV

WAVELENGTH OF HEp-2 CELL RAMAN LINES PRODUCED AFTER IRRADIATION AT 514 nm

WAVE NUMBER	CONTROL*	cAMP**	ATP+
144	2++	1	-
150	2	-	1
220	1	-	-
240-44	1	1	-
260-64	1	1	-
290	-	1	1
298-300	2	1	-
320	1	-	-
346	1	-	-
397-402	1	1	-
418-20	2	-	-
450-54	2	-	-
470-72	2	2	1
517-20	-	1	1
560-64	2	1	1
576-80	1	-	-
626-30	1	2	-
700	1	-	1
720-24	1	-	-
730	-	1	1
748	1	-	-
780	1	1	-
808-10	2	2	-
830	1	1	-
838-40	1	1	-
860-64	1	-	-
878-80	4	-	-
900-05	3	1	-
910	-	-	1
920	1	1	-
938-40	1	-	1
945-50	1	1	-
958	-	-	1
970-75	3	-	-
980-85	2	1	-
1000-04	2	1	1
1010-15	5	-	-
1040-44	1	1	-
1050	1	-	1
1056-60	4	-	-
1067	-	-	1
1090	-	1	-
1098	1	-	-
1120-25	2	-	-
1148-52	3	1	1
1178	1	-	-
1190	-	1	-

103-21

WAVE NUMBER	CONTROL*	cAMP**	ATP+
1210	1	1	-
1218-24	2	1	1
1230	1	-	-
1240	-	1	-
1268-70	1	1	-
1318-24	2	2	1
1390	1	-	-
1396	1	-	-
1460	-	-	1
1520-24	3	1	-
1540-44	3	1	1
1588-90	1	1	-
1597	1	-	-
1615-20	3	1	-
1630	-	-	1
1670-74	2	-	-
1710	1	-	-
1720	2	1	-
1738	-	1	-
1768-70	1	1	-
1778-85	2	1	-
1800	1	1	-
1810	-	1	-
1850	-	1	-
1860	-	1	-
1890	-	1	-
1920	1	1	-
1930	-	1	-
1944	1	-	-
1950	-	1	-
1980	-	1	1
2000	1	-	-

* Six replicates (two different samples were each scanned three times; one of those repeat scans was performed on 0.6 million cells - it contained many events found in scans using 1.2 million cells and a large number of events associated with buffer scans).

** Two replicates (successive repeats on the same sample).

\+ Single scan.

Bold type was used to emphasize that an event was recorded two or more times at that wave number.

and 1615-20, and five times at 470-72, 1148-52 and 1540-44. Out of two replications, no repeats were associated exclusively with cAMP. Since ATP was only used once as a HEp-2 treatment, results were inconclusive. It must be noted that undetected events for any treatment component could indicate that the events have not occurred, or that events are missed when they occur during scanning-time for another event because the spectrophotometer cannot detect all events simultaneously. In addition, there are numerous situations where attempts to economize by recording more than one run on the same graph sheet resulted in overlapping and obscured results. We also had several instances of pen skipping which caused event loss. While we always tried to scan through 2000/cm, frequently the run would either terminate prematurely, or, the pen would not be lifted from the paper as the machine reset itself. Therefore, results from 1870/cm onward were incomplete. The sum of these technical difficulties suggests that events occurring in other treatments may not have been detected. For all these reasons, the events recorded from control cells are probably not exclusive, although the five repetitions of the event at 1010-15 must be considered interesting. Similarly, molecule(s) causing emissions at 470-72, 1148-52 and 1540-44 regardless of treatment may reflect characteristic "signature" molecules within the HEp-2 cell. Which molecules these might be, are

TABLE V

WAVELENGTH OF Y-1 CELL RAMAN LINES PRODUCED
AFTER IRRADIATION AT 514 nm

WAVE NUMBER	CONTROL*	cAMP**	WAVE NUMBER	CONTROL	cAMP
100	–	1	140	–	1
150	1	–	164	–	1
210	–	1	270	1	1
280	–	1	290	1	–
398	1	–	420	1	1
430	–	1	570	–	1
628	1	1	664	–	1
670	1	1	700	–	2
717	1	–	778-80	1	1
800	1	1	806	1	1
860	–	1	868-70	1	1
970	–	1	998-1000	1	1
1050	–	1	1066	–	1
1090	–	1	1100	–	1
1118	1	–	**1124**	–	2
1130	1	–	1130	1	–
1150	1	1	1180	–	1
1190	–	1	1210	1	–
1230	–	2	1250	1	1
1258	–	1	1264	–	1
1290-93	–	2	1318-20	–	2
1330	1	–	1340	–	1
1370	–	1	1388	–	1
1410	1	2	1460	1	1
1476	1	–	1510	1	–
1520-24	1	1	1540	–	1
1587-90	1	1	1610	1	1
1624	–	1	1644	–	1
1668-70	1	1	1708	–	1
1718-24	1	2	1740	–	1
1764	–	1	1780	–	1
1798	1	1	1860	–	2
1870	1	–	1900	–	1
1950	–	1	1978	–	1

* Single replicate.
** Two replicates (successive repeats on the same sample).

Bold type was used to emphasize that an event was recorded two or more times at that wave number.

presently unknown. We used ATP as one of the HEp-2 stimulants because of the interesting effects it caused when used in the summer of 1983 (5). Why we were unable to repeat these results is unclear. Our use of cAMP as a stimulant resulted from information obtained during a literature search conducted as part of the Utah consortium contract. Dibutyryl cAMP was used to decrease the yield of Herpes-Simplex 1 virus particles released from inoculated HEp-2 cells (16). Although our cells were uninoculated, we used the precedence of this work to guide ours. Too few replicates were conducted to sustain any conclusions about this work. We had also intended to investigate cytochrome response to irradiation at 476.5 and 488 nm because literature studies indicated that HEp-2 cells irradiated with 6.5 mm radiowaves of 1 mW/cm2 flux density reduced cytochrome oxidase and NAD- and NADP-diaphorase activities (17). After effort focal point vacations, spectrometer redesigns and usage by two other SCEEE fellows, little time remained to include all intended experiments. It is expected that funds from a 1984 AFOSR/SCEEE RISE grant will permit continuation of these investigations under more ideal circumstances.

Two repeated emissions by intracellular molecules in the two cAMP-treated Y-1 replicates irradiated with 514 nm (Table V), were found at 700, 1124, 1230, 1290-93, 1318-20, and 1860. Whether these events result from cAMP treatment, or characteristic emmisions of the Y-1

adrenal cell, was uncertain for reasons described above. Events detected in all three runs of control and cAMP-treated cells were at 1410 and 1718-24. Since control cells were only scanned once, results were inconclusive. There were too few replicates in this experiments to draw conclusions about "signature" molecules.

Repeated emissions by intracellular molecules in the three control, Y-1 replications irradiated at 488 nm (Table VI), were twice found at 140-54, 320, 598, 610, 644-5-50, 710, 920, 960, 970, 984-95, 1030, 1142-44, 1158-60-2, 1190, 1210-14, 1344-6-50, 1390-94, 1437, 1468-70-3, 1560, 1564-8, 1590, 1628-30, 1670, 1680-84, 1720-24, 1778-80, 1818-20, 1824, 1908-10, and 1920-24. Similarly, events were observed at the following wave numbers in all three control replicates: 200-04, 300-04, 668-70-4, 690, 1080-4-90, 1108-10, 1600, and 1800-4-8. For the events occurring in both treatment components, there are four replicates. Events repeated three times were found at 170, 270-8-80, 328-30, 340-44, 400, 430-38, 450, 496-500, 574-78, 658-60-2, 764-8-72, 1038-40-4, 1057-60, 1122-4-30-2, 1178-80-4, 1200-04, 1300, 1525-30, 1548-50-4-60, and 1860-4-8, while events repeated in all four replicates occurred at the following wave numbers: 790-8-800, 890-4-8, 1310-8-20-2, 1458-60-4-5, and 1508-10-14. Lack of repetition of the cAMP run prevents conclusions from being drawn. As discussed previously, events occurring only in controls may also occur in

TABLE VI

WAVELENGTH OF Y-1 CELL RAMAN LINES PRODUCED AFTER IRRADIATION AT 488 nm+

WAVE NUMBER	CONTROL*	cAMP**	WAVE NUMBER	CONTROL	cAMP
130	-	1	135	1	-
240-54	2	-	160	1	-
170	2	1	178	1	-
190	1	-	200-04	3	-
215	1	-	225	1	-
240	1	-	260	1	-
264-75	1	-	270-8-80	2	1
300-04	3	-	d/310	-	1
320	2	-	328-30	2	1
340-44	2	1	362	1	-
370	1	-	375	-	1
384	-	1	392	1	-
400	2	1	408	1	-
415	1	-	420	1	1
430-38	2	1	d/440	1	-
450	2	1	462-64	1	1
480	1	-	488	-	1
490	1	-	496-500	2	-
515	1	-	520	-	1
530	1	1	540	1	-
560	-	1	568-70	1	1
574-78	2	-	580	1	-
590	-	1	598	2	-
610	2	-	620	-	1
624	1	1	630	1	-
644-5-50	2	-	668-70-4	3	-
690	3	-	700	1	-
710	2	-	724	1	-
738	-	1	743	-	1
748	1	-	758-60-2	2	1
764-8-72	2	1	778	1	1
784	1	-	796-8-800-4	3	1
810	1	1	820-24	1	1
820	1	1	846-48	1	1
854	1	-	870	1	1
890-4-8	3	1	900-04	1	-
910	1	-	920	2	-
930	1	-	940	1	1
950	1	-	950	2	-
970	2	-	984-95	2	-
1000	1	-	1010	-	1
1020	1	-	1025	-	1
1030	2	-	1038-40+-44	2	1
1050	1	-	1057-60	2	1
1068-70	1	1	1080-4-90	3	-
1094	1	-	1100	1	-

WAVE NUMBER	CONTROL	cAMP	WAVE NUMBER	CONTROL	cAMP
1108-10	3	-	112?-4-30-2	3	1
1142-44	2	-	1150	1	1
1158-60-2	2	-	1165-68	1	1
1178-80-4	2	1	1190	2	-
1200-04	2	1	1210-14	2	-
1224	1	-	1230	1	1
d/1240	1	-	1250	1	-
1257-60	1	1	1264	1	-
1270	1	-	1287	1	-
1300	2	1	1310-8-20-2	3	1
d/1330	1	-	1344-6-50	2	-
1355	1	-	1364	1	-
1370	-	1	1380-85	1	1
1390-94	2	-	1400	1	1
1396-1408	1	-	1410	1	-
1418-0-2-4-6	2	1	1430	-	1
1437	2	-	1450	1	1
1458-60-4-5	3	1	1468-70-3	2	-
1485	1	-	d/1490	1	-
1498-1500	1	1	1508-10-14	3	1
1520	1	-	1525-30	2	1
1542	1	-	1548-50-4-60	2	1
1560	2	-	1564-68	2	-
1580	1	-	1590	2	-
1600	3	-	1608-10-8	1	1
1620	-	1	1628-30	3	-
1640-44	1	1	1658	1	1
1660-64	1	1	1670	2	-
1680-84	2	-	1684-94	1	-
1690	-	1	1700	1	-
1710	1	1	1720-24	2	-
1740	1	-	1750	1	-
1764-5	1	1	1778-80	2	-
1790	1	-	1800-4-8	3	-
1818-20	2	-	1824	2	-
1830	-	1	1855	1	-
1860-4-8	2	1	1880	1	-
1890	1	-	1900	1	-
1908-10	2	-	1920-24	3	-
1930	1	-	1944	1	1
1954	1	-	1964	1	-
1984	1	-	2000	1	-

* Single replicate.

** Two replicates (successive repeats on the same sample).

+ A doublet (d/) begins at that wave number.

Bold type was used to emphasize that an event was recorded two or more times at that wave number.

Underlined numbers represent wavelengths at which carotenoids and heme-containing proteins emit.

cAMP-treated cells but be missed during the scanning procedure. In addition, three replications do not seem sufficient to draw conclusions about control events. It is interesting that there are a limited number of events common to both treatments; particularly those events with ranges encompassing only 6, 7 and 8 wave numbers may represent emissions by characteristic Y-1 cell molecules responding to light at 488 nm. We note that events within the ranges centering on 1040 and 1300 were repeated in three out of four replicates, while the range including 1460 appeared in all four replications. More replication is required to verify these possibilities.

In attempting to understand the significance of replication of responses to irradiation at 488 nm, we found that this wavelength caused carotinoids and cytochromes to emit at wave numbers of 1040, 1300, and 1460 (18). Most mammalian cells in vivo and in vitro are unable to synthesize carotenoids and their derivatives; they are, however, able to absorb them from their nutrients (19). Vitamin A, a carotenoid, is stored in intracellular adrenocortical lipid droplets (20, 21). Rats deficient in vitamin A show reduced rates of glucocorticoid production, probably due to failure of deoxycorticosterone to be hydroxylated to the gucocorticoid, corticosterone (22, 23). The Eagle's minimum essential medium with Earle's salts used in culturing Y-1 adrenal cells did not contain carotenoids (Gibco catalog, Palo Alto, CA).

103-29

Whether these molecules could be absorbed from the serums used in their maintenance was unknown until recently. Now information regarding the major constituents of serums is available; HyClone Laboratories (Logan, Utah) indicates that their fetal bovine and horse serums contain, respectively, a total of $\geq$ 209 and 233 ng/100 g serum of these carotenoids: retinoic acid, retinyl palmitate, retinyl acetate, retinol and carotene. While we used fetal bovine and horse serum from KC Biological (Lexina, Kansas), serums from different commercial sources should not differ. Particularly because most cattle and horses are genetically inbred, and, serums from many animals are pooled to produce the marketed product. With regard to iron-containing proteins, adrenal cells contain large concentrations of various cytochromes, flavo- and heme proteins, including cytochromes a, a3, b, b5, c, c1, side-chain cleavage, 11 beta and 21 beta P-450s, P-420, adrenodoxin, flavoprotein and non-heme iron (24, 25). These iron-containing proteins are used in the synthesis of steroid hormones, or to provide energy-containing compounds for viability and steroid synthesis (26). Besides being useful as models for studying carotenoids, steroid synthesizing cells are also ideal for examining laser Raman spectra associated with iron-containing compounds. Concentrations recorded for a few bovine adrenal mitochondrion and microsome heme proteins are summarized in Table VIII. To convert

TABLE VIII

HEMOPROTEINS IN BOVINE ADRENAL
MITOCHONDRIA AND MICROSOMES +

	Mitochondria*	Microsomes**
a	3.5 ± 0.7	-
a3	1.2 ± 0.4	-
b	2.0 ± 0.4	-
b5	-	0.06
c	2.4 ± 0.6	-
c1	1.8 ± 0.4	-
Fp	4.5 ± 1.9	-
P-420	-	0.16
P-450	8.3 ± 2.8	0.23

+ nanomoles/mg nitrogen
* (C♦)
** (♦♦)

these figures from mg nitrogen to mg protein a multipli-
cation factor of 6.25 must be used (27).   Thus, a total
of 151 nanomoles heme protein/ mg protein may exist in a
bovine adrenal cell. While similar figures do not exist
for Y-1 adrenal cells, the bovine concentrations may be
extrapolated using the conversion factor: 0.6 nanograms
protein/mouse adrenal cell (10).   In our experiments we
routinely used 1.2 million cells; our sample, therefore,
had approximately 108.7 total nanomoles heme protein.

Control Y-1 intracellular molecules irradiated at
476.5 nm emitted photons which were scanned without a
polarizer in five essentially complete, and one partial,
replicate runs (Table VII).   Control events were re-
peated twice at wave numbers 120-40 and 910, three times
at numbers 590, 1320-22, and 1408. To reduce fluores-
cence causing progressive upward displacement of the
events being recorded, scanning was conducted using a
filter which polarized parallel; out of four replicates,
wave numbers 125-28, 816-18, 1244-45, 1780 and 1904 were
repeated twice; numbers 200-04 and 1268-70 were repeated
three times.   Out of nine replicates, events occurring
simultaneously in polarized and non-polarized controls
were repeated three times at 260-64, 368-70, 604-8-13,
735-7-40, 1277-80, 1760, 1775, and 1820 or four times at
240-2-4, 1020 and 1874-8-90.   Pooling replicates from
the non-polarized components, six controls and two cAMP
treatments, events repeating three times appeared at
270, 850, 1224-25, and 1368-70, with 1930 being the wave

103-32

TABLE VII

WAVELENGTH OF Y-1 CELL RAMAN LINES PRODUCED
AFTER IRRADIATION AT 476.5 nm

WAVE NUMBER	CONTROL*	PARALLEL POLARIZ. CONTROL+	cAMP**	PARALLEL POLARIZ. cAMP++
102	-	-	-	1
125-28 ‡‡	-	2	-	-
120-40	2	-	-	-
134-6-8-42	-	2	-	1
150	1	1	-	-
d/164 ‡	-	1	-	-
186-83	1	-	-	1
194	1	-	-	-
200-04	-	3	-	-
210	1	1	-	-
218-20	1	-	-	1
223	-	-	-	1
228-30	2	-	1	1
240-2-4	1	3	-	-
250-53	-	1	-	1
260-64	1	2	-	-
270	2	-	1	-
278-82-3	-	1	1	1
296-300	1	2	-	1
306-7-8	-	2	-	1
318-20-5	1	2	1	1
328	-	-	-	1
336-8-40-2-3	-	1	1	1
358-60	1	1	1	2
368-70	1	2	-	-
390-1-5-400	2	1	-	1
405-6-8-10	4	3	-	1
428-30	1	-	2	1
440-3-4	2	2	1	-
450-53	2	2	-	1
458-60-4	1	3	1	-
d/466	-	-	1	-
472-5-6-8-80°	3	1	-	1
476-7-8-90	2	2	-	1
504-8-10-1-2	2	2	-	1
520-22	3	2	1	-
528-30	1	2	-	1
538-40-2-4	1	1	1	1
546	-	-	-	1
555-6-8-60	1	3	-	2
573	1	-	-	1
580-83	1	1	-	-
584-602	-	-	-	1
590	3	-	-	-
596-7-8-600	1	3	1	-
604-8-13	2	1	-	-

103-33

WAVE NUMBER	CONTROL	PARALLEL POLARIZ. CONTROL	cAMP	PARALLEL POLARIZ. cAMP
626-8-30-5	3	1	1	2
638-40-2	2	3	1	1
648	-	-	1	1
658-60	1	1	1	-
664	1	1	-	-
670-5-8-80	3	2	1	2
690	2	2	1	-
710	1	-	-	-
715	-	1	-	-
720-1-3-4-8-30	5	3	1	2
735-7-40	2	1	-	-
745	-	-	-	1
750	-	1	1	-
755-8-60-4-5	3	1	-	1
770	1	-	-	-
790-2-4	1	2	1	-
798-800-4-5	2	1	-	1
808-10	-	1	2	1
816-18	-	2	-	-
850	1	-	2	-
858	-	-	-	2
868-70	2	1	1	-
872-78	-	1	-	-
875-8-82	1	1	1	-
890	-	1	-	-
894-900	-	-	-	1
898-900-4	-	2	2	1
d/910	2	-	-	-
918-20-2-5-8	2	3	1	2
938-40-2	2	2	2	1
950-3-5-6-8-60	3	3	2	1
968-70	-	2	-	2
968-74	-	-	1	-
978	-	1	-	-
985	-	1	-	-
986-98	-	1	-	-
990-92	-	1	-	1
1000	-	1	1	-
1005-8-10	2	1	2	2
1020	1	3	-	-
1020-40	1	-	-	-
1022-3-5	1	1	-	1
1030-2-6-8	1	1	-	2
1042-44	-	3	-	1
1050-52	-	3	-	1
1060-2-6-8	2	2	1	2
1070-73	1	2	-	1
1078-80-2-3	2	1	2	2
1188-90-2	2	2	-	1
1200-2-5-8-10	2	3	1	1
1218-20-2	3	1	1	-

WAVE NUMBER	CONTROL	PARALLEL POLARIZ. CONTROL	CAMP	PARALLEL POLARIZ. CAMP
1224-25	2	-	1	-
1228-30-3-6-8	1	3	2	1
1244-45	-	2	-	-
1242-50	-	1	-	-
1250-54	1	2	2	-
1260	-	2	1	-
1260-70	1	-	-	-
1268-70	-	3	-	1
1277-80	2	1	-	-
1288-90-2	2	-	-	1
1308-10	1	2	-	2
1320-22	3	-	-	-
1300				
1338-40-2	1	2	1	-
1347-50-2	1	2	1	1
1358-60-2-4-6	1	2	1	2
1368-70	2	-	1	-
1370-80	1	-	-	-
1375-6-8-80	-	3	-	1
1385	-	1	-	-
1390	1	1	-	1
1385-1400	1	-	-	-
1395-8-400-3-5	2	3	2	1
1408-10	3	-	-	-
1425-6	-	1	2	-
1430				
1448-50	2	2	-	1
1458-60	2	3	-	1
1468-70	1	1	1	-
1478-80-3	1	1	-	2
1486-8-90	2	1	1	1
1495	-	1	-	-
1498-1500	1	1	-	-
1525	-	1	1	-
1530	1	1	-	-
1536-8-40	1	1	1	2
1570	1	1	2	-
1570-78	1	-	-	-
1570-90	1	-	-	-
1575	1	-	-	-
1578-82-3-4	-	2	1	1
1588-90	2	-	1	1
1608-10	3	3	1	1
1612	-	-	-	1
1626-7-30	1	1	1	1
1648-50-3	1	-	2	1
1658-60	2	2	-	2
1664-8-72	1	-	2	1
1680	-	1	-	-
1688-90	1	2	1	1
1694-6-8-1700	3	1	1	-

WAVE NUMBER	CONTROL	PARALLEL POLARIZ. CONTROL	cAMP	PARALLEL POLARIZ. cAMP
1704-6-7-8-10	2	2	1	1
1716-20-2	1	2	1	-
1724-6-8-30	3	2	-	2
1740-44	2	-	-	-
1745-58	-	1	-	-
<u>1750-2-5</u>	-	1	<u>2</u>**	2
1760	1	2	-	-
1765-8-70	-	2	-	2
1775	2	1	-	-
1780	-	2	-	-
1787-8-90	1	-	1	2
1796-8-1800	1	2	1	2
1818	1	1	-	1
1820	1	2	-	-
1830	-	1	-	-
1836-8-40	1	2	1	1
1844-8-50	-	2	1	2
1860-2-4-5-6	2	2	1	1
1868	-	1	-	1
1874-8-90	1	3	-	-
1895-98	2	1	-	1
1900-02	-	1	-	1
1904	-	2	-	-
1915-16	1	-	-	1
1930	2	-	2	-
1938	-	1	-	-
1946	-	-	-	1
1958-60	-	2	1	-
1966-70	-	1	2	1
1980	1	-	-	-
1996	-	-	-	1

* Five essentially complete (some skipping and duplicate graphing overlap) and one partial replicate (these six represent three separate scanning experiments: one a single incomplete experiment, another scan repeated twice and a third repeated three times).
** Two replicates (repeats on the same sample).
+ Four replicates (repeats on the same sample).
++ Two replicates (repeats on the same sample).
# A doublet (d/) begins at that wave number.
Bold type emphasizes that an event was recorded two or more times at that wave number.
• Underlined wave numbers represent wavelengths emitted by carotenoids and heme-containing proteins.
•• The underlined 2 at 1750 represents 2 graphic excursions of large magnitude.

number of an event repeated four times. Using these same treatments, but polarizing emissions parallel, the six replicates produced events repeated three times at 134-6-8-42 and 306-7-8 or four times at 1042-44, 1050-52, 1375-6-8-80 and 1765-8-70. Summarizing repetitions when all treatment components were examined for common events presented numerical logistical problems. To minimize numbers from the 14 replicates, only repeats appearing five or more times were recorded. In addition, these repeats were subdivided into two categories: repeats appearing in any three out of four treatment components, and repeats appearing in all four components. In the first category 440-3-4, 450-53, 458-60-4, 472-5-6-8-80, 476-7-8-90, 504-8-10-1-2, 596-7-8-600, 690, 755-8-60-4-5, 898-900-4, 968-70/968-74, 1188-90-2, 1218-20-2, 1250-54, 1308-10, 1347-50-2, 1448-50, 1486-8-90, 1536-8-40, 1688-90, 1694-6-8-1700, 1750-2-5, 1836-8-40, 1844-8-50 were all repeated five times, while 520-22, 555-6-8-60, 1358-60-2-4-6, 1458-60, 1658-60, 1704-6-7-8-10, 1796-8-1800, and 1860-2-4-5-6 appeared six times, 1078-80-2-3 and 1228-30-3-6-8 repeated seven times, and 1608-10 was common to eight pooled runs. Those having at least five out of a possible fourteen repeats and appearing in all four treatment components, were found at 318-20-5 and 358-60, seven repeats at 626-8-30-5, 638-40-2, 938-40-2, 1005-8-10, 1060-2-6-8, 1200-2-5-8-10 and 1724-6-8-30, eight at 405-6-8-10, 670-5-8-80, 918-20-2-5-8, 1395-8-400-3-5, nine and eleven repeats at

950-3-5-6-8-60 and 720-1-3-4-8-30, respectively.

The occurance of only a few events per component category, the repetition of an event in at least 50% of the replicates, a relatively narrow range of wave numbers in an event, and the appearance of a given event in $\geq$ 3 treatment components, were criteria used in suggesting that an event may be characteristic to Y-1 cells irradiated at 476.5 nm. Thus, non-polarized emissions from controls appeared in a narrow event range in 50% of the replicates at three different wave numbers, $\geq$50% of the polarized control cell emissions were associated with seven narrow range events, and only three events were narrow range in 44% of the control replicates regardless of polarity. Because of the number of runs on different Y-1 samples, one of which was pooled from cultures of three different doubling numbers, these emissions may be considered characteristic of the various control Y-1 cell treatment components at 476.5 nm. Only a single non-polarized relatively narrow range emission from the control/cAMP treatment component was replicated in 50% of the runs. Polarization permitted detection of six relatively narrow range events in 50% or more of the replicates. The relatively large number of replications available by pooling all treatment components revealed that sixteen relatively narrow range emissions occurred $\geq$50% in three, or four, of the components; one of these (720-1-3-4-8-30) was replicated eleven out of fourteen times.

103-38

Events at 480, 600, 900, 970, 1010, 1060, 1650, and 1750 are associated with 476.5 nm irradiated carotenoid and heme protein emissions (18). Although two other wave numbers also associated with these molecules (1330 and 1430), events were cancelled by water scan background events. If water events at 1335 were disregarded, six out of fourteen events would be recorded. Similarly, 1418 and 1438 ±5 water events cancelled three events centering around 1430.

Using 476.5 nm irradiated Y-1 adrenal cells encouraging data suggest that relatively large concentrations of unique intracellular molecules can produce characteristic Raman signatures for a particular cell type. In addition, event detection appears improved using a polarizer. This implies that laser Raman spectrometry may provide a semi-non-invasive technique to develop procedures to improve nightvision, study age-related pilot vision deterioration, to diagnosis cancer early in Air Force personnel (4), and to determine dietary and exercise regime effects on physiological and chronological age as it applies to individual performance. Y-1 adrenal cell use as study models is particularly important to Air Force missions because adrenals protect personnel against stress (28). Recent Seattle, Washington, reports about microwave irradition effects and human adrenal enlargement amplify these concerns (29).

VI. RECOMMENDATIONS:

As noted previously we experienced numerous instances

where events were undetected due to mechanical logistics. Such malfunctions cc red us to question whether events had occurred, or whether events were missed during scanning-time for another event because the spectrophotometer cannot detect all events simultaneously. Some of these mechanical situations resulted from attempts to economize by recording more than one run on the same graph sheet causing overlapping and obscured results. We also had several instances of pen skipping causing event loss. For future experiments I strongly recommend administrative support for Dr. Taboada's plans to upgrade the spectrophotometer by linking it to photon detectors which simultaneously scan broad wave bands. In addition, the data collected by the detector should be fed to a computer and programs for its analysis, manipulation and comparison should be implimented according to Dr. Taboada's proposed designs. This report was delayed by the necessity of two individuals manually reading 47 graphs and recording, compiling, asimilating and analysing the resulting data. The undertaking required approximately 300 man-hours. A requirement which discourages the dedicated assult which the problem requires. Note that a number of our investigations are inconclusive because of a lack of replication. One is reluctant to do this replication because of the logistical problems. Since most of the preceeding recommendations have been initiated, all that is required is

concentrated financial, technical and administrative support for their completion.

Until the spectrometer is updated concerned effort must be made to avoid economization by recording more than one run on the same graph sheet. To avoid pen skipping which caused event loss, Dr. Taboada must obtain reliable chart recorders from the equipment pool. To scan all events through 2000/cm, care must be exercised to avoid premature run termination and pen remaining on the paper as the machine resets itself.

Specific problems which require further investigation include the following.

1. Determining practicality of the scanning method suggested by Dr. Taboada ("tunneling" the laser beam into the edge of a microscope slide to which cells are attached, caromming the beam from surface to surface down the slide and scanning the stokes and anti-stokes wavelengths emitted from contacted cells on the slide surface with the photon detector).

2. Using the Coulter counter, further experiments are required to confirm existing data on Y-1 and HEp-2 cell fragment counts and refine cell diameter ranges. Lack of clear results in the Coulter counting experiments resulted from inconsistent experimental designs, and lack of time and experience with the counter.

3. Although short exposure beam effects on cell mortality were negligible as determined by counting live/dead cells, laser effects of short-time cell exposure on

physiological parameters, such as steroidogenesis, remain to be determined.

*. Future experiments are required to clarify the involvement of cell surface activity and mitosis in Raman activity. There depend on funds becoming available for purchase of a time-lapse video recorder and for a microscope objective more powerful than the existing 40X to increase cellular details. The problem of insufficient illumination experienced during our summer studies can be corrected by purchasing a video camera having a more sensitive detection system.

5. Emissions by intracellular molecules in HEp-2 cAMP- and ATP-treated cells irradiated at 514 nm need to be repeated. In the two replications reported above, no repeats were associated exclusively with cAMP. In addition, ATP was only used once as a HEp-2 treatment; results were, therefore, inconclusive. As noted, all events associated with a single treatment component will continue to be inconclusive if they occur during scanning-time for another event because the present spectrophotometer cannot detect all events simultaneously. The cytochrome response to irradiation at 476.5 and 488 nm should also be investigated because literature studies indicated that HEp-2 cells irradiated with 6.5 mm radiowaves of 1 mW/cm2 flux density reduced cytochrome oxidase and NAD- and NADP-diaphorase activities (17). Funds from a 1984 AFOSR/SCEEE RISE grant could permit continuation of these investigations.

6. Two repeated emissions by intracellular molecules were obtained from the two cAMP-treated Y-1 replicates irradiated with 514 nm (Table V). Whether these events result from cAMP treatment, or characteristic emmisions of the Y-1 adrenal cell, was uncertain for reasons described above. Since control cells were only scanned once, results were inconclusive. There were too few replicates in this experiments to draw conclusions about "signature" molecules in Y-1 cells irradiated at 514 nm.

7. There were no repeated emissions by intracellular molecules in the cAMP-treated Y-1 cells irradiated at 488 nm. Lack of repetition of this cAMP run prevents conclusions from being drawn. As discussed previously, events presently noted only in controls may also occur but be missed during scanning. In addition, the three replications of the experiment do not seem sufficient to draw conclusions about common cellular events, although it was interesting that there were a limited number of events common to both treatments. In particular, those events encompassing a range of 6 - 8 wave numbers might represent characteristic Y-1 cell molecular emissions after irradiation at 488 nm. More replication is required to verify these possibilities.

8. Techniques for enriching cellular carotenoids in Y-1 and HEp-2 cells should be used to examine effects on signature spectra. In addition, inhibitors which bind or poison cytochromes should be added to cell suspensions to determine effects on characteristic emissions.

REFERENCES

1. Webb, S.J., and Stoneham, M.E., "Resonances Between Ten To The Eleventh Power And Ten To The Twelfth Power Hz In Active Bacterial Cells As Seen By Laser Raman Spectroscopy," *Physics Letters*, Vol. 60A, pp. 267-268 (1977).

2. Davydov, A.S., "The Migration Of Energy And Electrons In Biological Systems. *Biology And Quantum Mechanics*, (Pergamon Press, Oxford, U.K., 1982), pp. 185-207.

3. Bilz, H., Buttner, H., and Froelich, H., "Electret Model For The Collective Behavior Of Biological Systems," *Z. Naturforsch.*, Vol. 36B, pp. 208-212 (1981).

4. Webb, S.J., Lee, R., and Stoneham, M.E., "Possible Viral Involvement In Human Mammary Carcinoma: A Microwave and Laser-Raman Study," *International Journal of Quantum Chemistry, Quantum Biology Symposium 4*, (John Wiley and Sons, Inc., New York, 1977), pp. 277-284.

5. Taboada, J., and Mrotek, J., "Evidence for Davydov Solitons in the Anti-stokes Raman Spectra of Living HEp-2 and Y-1 Cancer Cells," Abstract presented to the annual American Physical Society meetings, San Antonio, Texas (1984).

6. Sato, G.H., Rossman, T., Edelstein, L., Holmes, S., and Buonassisi, V., "Continued Steroid Production by Murine Adrenal Cells Incubated in Krebs-Ringer Buffer," *Science*, Vol. 148, pp. 1733-1737 (1965).

7. Phillips, H., "Dye Exclusion Tests for Cell Viability, *Tissue Culture Methods and Applications*, (Academic Press, N.Y.), pp. 406-407 (1973).

8. Voorhees, H.L., and Mrotek, J.J., "Rounding and Steroidogenesis of Enzyme- and ACTH-treated Y-1 Mouse Adrenal Tumor Cells," *Cell Biology International Reports*, Vol. 8, pp. 483-509 (1984).

9. Mrotek, J.J., and Hall, P.F., "The Influence Of Cytochalasin D On The Response Of Adrenal Tumor Cells To ACTH And Cyclic AMP," *Bioch. Biophys. Res Commun.*, Vol. 64, pp. 891-896 (1975).

10. Mrotek, J.J., and Hall, P.F., "Response Of Adrenal Tumor Cells To Adrenocorticotropin: Site Of Inhibition By Cytochalasin B," *Biochemistry*, Vol. 16, pp. 3177-3181 (1977).

11. Mrotek, J.J., Rainey, W., Lynch, R., Mattson, M., and Lacko, I., "A Scanning And Transmission Electron Microscope Examination Of ACTH-induced 'Rounding Up' In Triton X-100 Cytoskeletal Residues Of Cultured Adrenal Cells," Current Topics In Muscle And Non-muscle Motility (Plenum Press, New York, 1982), Vol. 2, pp. 45-52.

12. Lee, H.S., and Mrotek, J.J., "The Effect Of Intermediate Filament Inhibitors On Steroidogenesis And Cytoskeleton In Y- 1 Mouse Adrenal Tumor Cells," Cell Biology International Reports, Vol. 8, pp. 463-482 (1984).

13. Morris, P. D., "Cigarette Residues Affect Steroidogenesis In Cultured Y-1 Mouse Adrenal Tumor Cells," M.S. Thesis, Department of Biological Sciences, North Texas State University, Denton, Texas, pp.1-32 (1979).

14. Mattson, M.P., "Effects Of Exogenous Steroid On The Adrenal Plasma Membranes: Alteration Of Steroidogenesis" to be submitted to Steroids (1984).

15. Grant, P., "Neoplasia, an Abnormal Cell Phenotype", Biology of Developing Systems, (Holt, Rinehart and Winston, Dallas, Texas), pp. 670-681 (1978).

16. Stanwick, T.L., Anderson, R.W., and Nahmias, A.J., "Interaction Between Cyclic Nucleotides and Herpes Simplex Viruses: Productive Infection", Infect. Immun., Vol. 18, pp. 342-247 (1977).

17. Zaliubovkaia, N.P., and Kiselev, R.I., "[Biological Oxidation in Cells Exposed to Microwaves in the Millimeter Range]", Tsitol. Genet., Vol. 12, pp. 1232-1236 (1978).

18. Yu, T., and Srivastava, U., "Raman Spectroscopy of Ferrocytochromes and Carotenoids", J. Raman Spectroscopy, Vol. 9, pp. 166-175 (1980).

19. Willmer, J.S., and Laughland, D.H., "The Distribution of Radioactive Carbon in the Rat After the Administration of Randomly Labeled C14-beta Carotine", Cand. J. Biochem. Physiol., Vol. 35, pp. 819-826 (1957).

20. Popper, H., and Greenberg, R., "Visualization of Vitamin A in Rat Organs by Fluorescence Microscopy" Arch. Path., Vol. 32, pp.11-32 (1941).

21. Wallace, D.L., Plopper, C.G., Bucci, T.J., and Sauberlich, H.E., "Autoradiogrphic Localization of Vitamin A in the Adrenal Gland of Rats. Life Sci-

ences, Vol. 17, pp. 1693-1698 (1975).

22. Lowe, J.S., Morton, R.A., and Harrison, R.G., "Aspects of Vitamin A Deficiency in Rats", Nature, Vol. 172, pp. 716-719 (1953).

23. Johnson, B.C., and Wolf, G., "The Function of Vitamin A in Carbohydrate Metabolism; Its Role in Adrenocorticoid Production", Vitamins and Hormones, Vol. 18, pp. 457-483 (1968).

24. Cooper, D.Y., Levin, S., Narasimhulu, S., Rosenthal, O., and Estabrook, R.W., "Mechanism of C-21 Hydroxylation of Steroid", Functions of the Adrenal Cortex, Vol. 2, pp. 897-941 (1968).

25. Purvis. J.L., Battu, R.G., and Peron, F.G., "Generation and Utilization of Reducing Power in the Conversion of 11-Deoxycorticosterone to Corticosterone in Rat Adrenal Mitochondria", Functions of the Adrenal Cortex, Vol. 2, pp. 1007-1055 (1968).

26. Hall, P. F., "Part IV. Mixed-function Oxidases Of The Adrenal Cortex. Properties Of Soluble Cytochrome P-450 From Bovine Adrenocortical Mitochondria," Annals Of The New York Academy Of Sciences, Vol. 212, pp. 195-207 (1973).

27. Maynard, L.A., and Loosli, J.K., "Protein Metabolism", Animal Nutrition, 5th Edition, pp. 85-112 (1962).

28. Selye, H., "The Diseases Of Adaptation," Recent Progress In Hormone Research, Vol. 8, pp. 117-142 (1953).

29. "The Effects of Microwave on Populations Living Near Radiation Sources", Science News, August (1984).

1984 USAF-SCEEE SUMMER FACULTY RESEARCH PROGRAM

Sponsored by the

AIR FORCE OFFICE OF SCIENTIFIC RESEARCH

Conducted by the

SOUTHEASTERN CENTER FOR ELECTRICAL ENGINEERING EDUCATION

FINAL REPORT

PRELIMINARY MONTE CARLO STUDIES OF THE STRUCTURE OF MOLTEN SALTS

Prepared by: R. D. Murphy

Academic Rank: Professor

Department and   Department of Physics
University: University of Missouri-Kansas City

Research Location: Frank J. Seiler Research Laboratory
                            U.S. Air Force Academy, Colorado

USAF Research: Dr. John S. Wilkes

Date: August 10, 1984

Contract No.:   F49620-82-C-0035

PRELIMINARY MONTE CARLO STUDIES OF THE STRUCTURE OF MOLTEN SALTS

by

R. D. Murphy

ABSTRACT

The Monte Carlo method of statistical mechanics has been applied to
the study of the structure of a model of molten methylethylimidazolium
chloride, which is one constituent of a class of room-temperature molten
salts which are being studied as possible electrolytes for battery
applications. The Monte Carlo studies tend to confirm the view of the
structure of these ionic melts which has emerged from other data and
cast some light upon clustering phenomena in molten salts. Suggestions
for extension of the present work, both theoretically and
experimentally, are offered.

I. INTRODUCTION

During the past several years, a substantial amount of work has been done in the Chemical Sciences Directorate of the Frank J. Seiler Research Laboratory on the development of low-temperature electrolytes for battery applications. Work at the Seiler Laboratory has identified a very interesting class of room-temperature molten salts which appear to be most promising; in addition, these salts have possible applications in electroplating. The salts which have been identified[1] and studied are mixtures of aluminum chloride and methylethylimidazolium chloride, which at least in some concentration ranges are liquid at temperatures well below room temperature.

The substantial promise shown by these liquids has prompted a great deal of effort to determine and understand their chemical and physical properties. Careful studies of their phase diagram, conductivity, and viscosity[2], as well as of their nuclear magnetic resonance[3] properties, have recently been published. The NMR studies have provided information about the structure of the melts, and a systematic analysis of the concentration dependence of the chemical shifts has strongly suggested the existence in the melts of structure, i.e. a tendency of the ions in solution to form clusters. Specifically, Fannin et al.[3] have proposed that the anions and cations tend to form "chains" of ions of alternating sign. In order to see what light computer simulation techniques could

/ 9

shed on this problem, it was decided that the author would adapt his
Monte Carlo codes to perform a preliminary study of the problem at
hand.

II. OBJECTIVES

The objectives of this project were to: rewrite the existing Monte
Carlo code, which has been used to study a number of liquid systems
including molten salts, to study theoretically one of the melts which
has been studied experimentally at the Seiler Laboratory; to construct
potential functions as realistic as time and computer resources would
permit to describe the melt; and to compute the distribution functions
of these systems using the Monte Carlo code and to draw whatever
conclusions proved to be possible about the extent of the structure,
i.e. the molecular clustering, in these melts.

III. COMPUTER SIMULATION TECHNIQUES

The two principal large-scale machine simulation methods, each of
which has some variants, are the Monte Carlo and the molecular dynamics
methods. These methods have been discussed in detail elsewhere[4], and
here it will be noted only that the molecular dynamics method has the
advantage that transport properties, as well as equilibrium
thermodynamic properties, can be calculated. On the other hand, the
Monte Carlo method is simpler to implement, and it was chosen because of

the lack of knowledge about the intermolecular interactions. It was felt that until the intermolecular interactions are sufficiently well characterized that equilibrium thermodynamic properties can be reasonably accurately calculated, there would be little point in attempting to calculate the (considerably more difficult) transport properties. Furthermore, since the angular correlations which were used as a measure of molecular clustering are equilibrium properties, the simpler Monte Carlo method was sufficient and was deemed preferable.

The salt that was studied, pure imidazolium chloride, is molten at temperatures above about 90° C. The cation, imidazolium, is a heterocyclic planar molecule. The author's Monte Carlo codes had been written to treat only spherically symmetric intermolecular interactions. Because the imidazolium ring cannot be regarded in any reasonable approximation as being spherically symmetric, the (massive) job of converting the code to handle nonspherical interactions had to be undertaken. This job was completed, and the imidazolium cation was treated as a positive point charge surrounded by a soft-core repulsive potential whose equipotential surfaces were ellipsoids, the elongation of which was treated as a variable parameter. Then the standard Monte Carlo algorithm was used to generate configurations of a system of 128 particles in a box of volume V at a temperature T with probability proportional to the Boltzmann factor. The temperature, density, molecular sizes and elongation were chosen to approximate the corresponding parameters for imidazolium chloride at a temperature

104-5

elevated somewhat above its melting point because of the well-documented

tendency of molten salts not to "melt" during computer simulations close

to their melting point. In addition, some computer runs were done on a

model of sodium chloride, for comparison.

IV. RESULTS

The purpose of the computer experiments was to look at two-body and

three-body correlations among molecules. The results for the two-body

correlations are expressed in terms of the three radial distribution

functions which determine all the equilibrium thermodynamic properties

of such a system. These functions were examined for consistency, for

convergence, and for overall reasonableness; they appeared to be what

one would expect, although the absence of experimental information

precludes a direct comparison with experiment (see "Recommendations",

below). In particular, the calculations for imidazolium choride (as

well of course as those for sodium chloride) displayed the tendency

always seen[5] in molten salt calculations (and in those experiments which

have been done) to be "out of phase," indicating that the positive and

negative charges have a definite positional correlation: positive

charges are surrounded by a small number of negative charges (a

coordination number in the range of four to six).

The most interesting new results which emerged from the computer

studies were calculations of the three-particle correlations, somewhat

similar to calculations[6] recently done on other chloroaluminate melts. The thermal average of a "bond" angle, namely the anion-cation-anion angle for all triplets where two anions lie within one coordination distance of a cation were obtained, both for a model of molten sodium chloride and for a model of molten imidazolium chloride. For the case of sodium chloride, relatively few of these angles were $180°$, with a far larger number of angles at or near $90°$ and $120°$. For the model of imidazolium chloride, however, a very large preponderance of these anion-cation-anion angles were close to $180°$, with smaller secondary peaks in the distribution function around $67°$ and $109°$. This clearly implies the existence of the "stacking" or "chainlike" behavior postulated[3] in order to explain the NMR structural data.

A relatively simple physical picture emerges. In the case of simple molten salts like sodium chloride, it has been shown[5] that even in the molten phase the ions, presumably in order to minimize their electrostatic energy, form a liquid with short-range order much like the sodium chloride (NaCl) lattice, which is cubic. The author would propose that the major difference in the case of imidazolium chloride is the fact that the imidazolium cation, rather than being spherical like the sodium cation, is flat ("pancake shaped"). Thus, a chlorine anion would find it more energetically favorable to be above or below the center of the imidazolium ring, thereby producing precisely the structure predicted[3].

V. RECOMMENDATIONS

Although these results can be regarded as only preliminary, partly because of the lack of more definite knowledge about the intermolecular interactions, it can be stated that they are physically quite reasonable and most encouraging. In order to make further progress in understanding the structural properties of the molten salts of interest to the Seiler Laboratory, it would seem best to undertake a joint theoretical and experimental program to study the structure of the melts that are of interest and under consideration as possible electrolytes. Specifically, the following steps seem to be the most reasonable:

1. The current theoretical efforts to model the imidazolium chloride system, using all data available (including MNDO calculations) to prepare the best intermolecular potential, should be continued. In addition, study of other angular correlations among triplets by the Monte Carlo method, using the present potential functions, should be pursued in order to make clearer the nature of the structure of the system.

2. An experimental study by X-ray diffraction of molten imidazolium chloride should be performed in order to provide an experimental test of the assumed potentials and of the radial distribution functions computed from them. Only when they yield satisfactory agreement with experimental data can the intermolecular

potentials be regarded as reliable, and only when the intermolecular potentials are reliable can the conclusions regarding clustering be regarded as anything but preliminary.

3. In the longer run, it would be desirable to do neutron diffraction studies of imidazoliumn chloride, since this technique yields information complementary to that obtained by X-ray diffraction.

4. Because of the intended application of these molten salts as electrolytes in batteries, the question of their transport properties, e.g. their viscosity, electrical conductivity, and mobility, is crucial. As soon as reasonably accurate intermolecular potentials are determined, the molecular dynamics method should be applied to study these transport properties.

5. Finally, of course, it must be noted that the actual melts of greatest interest include aluminum chloride in varying proportions. All of the above steps (computer studies of the structure accompanied by X-ray and if possible neutron diffraction experiments and calculation of the transport properties) should be taken in the case of these melts. Although this is a rather large task, it is felt that it is feasible and that the preliminary steps reported here represent a very good start on this project.

Acknowledgements

The author would like to express his appreciation to the Air Force Systems Command, the Air Force Office of Scientific Research, and the Southeastern Center for Electrical Engineering Education for making possible his stay at the Frank J. Seiler Research Laboratory. He would like to thank the Laboratory for its most gracious hospitality and for making available the substantial computer resources that were required for this research project. Finally, he would like to acknowledge with sincere thanks a number of very helpful discussions with Dr. John Wilkes, who suggested this summer research problem.

REFERENCES

1. J. S. Wilkes, J. A. Levisky, R. A. Wilson, and C. L. Hussey, Inorg. Chem. $\underline{21}$, 1263 (1982).

2. A. A. Fannin, Jr., D. A. Floreani, L. A. King, J. S. Landers, B. J. Piersma, D. J. Stech, R. L. Vaughn, J. S. Wilkes, and J. L. Williams, J. Phys. Chem. $\underline{88}$, 2614 (1984).

3. A. A. Fannin, Jr., L. A. King, J. A. Levisky, and J. S. Wilkes, J. Phys. Chem. $\underline{88}$, 2609 (1984).

4. R. O. Watts and I. J. McGee, Liquid State Chemical Physics, (John Wiley and Sons, New York, 1976), pp. 80-87.

5. J. P. Hansen and I. R. McDonald, Phys. Rev. A $\underline{11}$, 2111 (1975).

6. M. L. Sabougni, A. Rahman and M. Blander, J. Chem. Phys. $\underline{80}$, 2141 (1984).

1984 USAF-SCEEE SUMMER FACULTY RESEARCH PROGRAM

Sponsored by the

AIR FORCE OFFICE OF SCIENTIFIC RESEARCH

Conducted by the

SOUTHEASTERN CENTER FOR ELECTRICAL ENGINEERING EDUCATION

FINAL REPORT

MILITARY FAMILY STRESS

Prepared by: Dr. Lena Wright Myers

Academic Rank: Professor

Department and   Department of Sociology
    University: Jackson State University

Research Location: Neuropsychiatry Branch, Clinical
Beam   Sciences Division, USAF School of
                                Aerospace Medicine, Brooks Air Force
                                Base, TX

USAF Research   Drs. Bryce Hartman, John Patterson,
    Colleagues: and David R. Jones

Date: August 10, 1984

Contract No: FR9620-82-C-0035

MILITARY FAMILY STRESS

by

Lena Wright Myers

ABSTRACT

This research pursuit derived from an indepth review of related
literature in an effort to discover and delineate the incidences of
stress and the techniques employed to resolve stress within military
families. It offers four broad questions to guide a projected explora-
tory study. The exploratory study should focus on the possible influ-
ence of family stress on occupational commitment or job involvement—
by comparing stress among dual-career and non-dual-career families.
A conceptual framework complemented by a theoretical orientation for
future implementation of the exploratory research is provided.

ACKNOWLEDGEMENTS

The author would like to express her appreciation to the Air Force

Systems Command, The Air Force Office of Scientific Research, and the

Southeastern Center for Electrical Engineering Education for the

sponsorship of this research effort.

She also expresses her gratefulness to the Air Force Personnel at

the Neuropsychiatry Branch, Clinical Sciences Division for the warm

receptivity that she experienced.

She is especially grateful to her USAF Research Colleagues:

Drs. Bryce Hartman, John Patterson, and David Jones for their untiring

interest and insightful suggestions offered this research endeavor.

I. INTRODUCTION

The primary objective of the initially proposed research effort for the SCEEE Fellow was to discover and delineate the stress resolution techniques used by middle age (40-45 years) United States Air Force Aviators. This objective was subsumed under the heading of Stress Resolution Among Middle Age United States Air Force Aviators. However, as a result of dialogue with her USAF Research Colleagues during her pre-summer visit, the decision to pursue research on Military Family Stress, including the same objective was made. This decision was based on knowledge of the limitations in securing an adequate sample of aviators for the research initially proposed. In addition, she and her colleagues concluded that research on military family stress would provide a more broadly based set of data than that previously proposed. Being knowledgeable of the fact that a period of ten weeks would not permit the effective implementation of an empirical research project, she and her USAF Colleagues decided that a logical point of departure would be that of an indepth search of related literature.

II. OBJECTIVES

The indepth search of related literature was accompanied by the primary preparatory objective of developing a research proposal for an exploratory study to be pursued in the future. From this primary preparatory objective, the following objectives for a research design were developed:

1. To explore a set of relationships that have been inadequately studied in part, in order to identify promising leads for future research; and

2. To assess the reliability and validity of measures that could be used in subsequent research dealing with work and family relations in the military.

III. APPROACH

In order to accomplish the preceding objectives, an indepth review of literature was conducted by using various indexing services. These sources included: Air University Libraries (Specifically, Maxwell AFB, AL), Strughold Aeromedical, Human Resources Laboratory, University campus libraries, and the Researcher's personal library.

IV. THE POSSIBILITY OF A NEW PARADIGM

During the last century, the U.S. military structure has experienced a demographic transformation. The military has shifted from an institution in which the majority of the personnel were unmarried to one in which the majority are married. As a result of this demographic transformation the internal structure of the military has shifted from individuals of families of origin to conjugal families. In other words, there seems to exist a more pronounced trend toward familistic institutions today than in previous years.

While military and non-military families may have some common experiences, there must exist some differences. Family separation and parental role changing may be two primary factors that create some forms of stress for these families. Separation and geographical disruption are generally the results of reassignment of the active duty member who, in most instances, is the husband/father. When these husbands/fathers are assigned to tactical or combat-ready units and are on call

most of the time, they may be unable to establish regular family rou-
tine. On the other hand, wives may experience particular stress in an
effort to assume both parental roles (if there are children within the
home), and in some instances, the occupational role.

An effort to discover and delineate the incidences of stress and
the techniques employed to resolve stress within military families is
of primary importance to the researcher. Therefore, the following four
basic questions to guide the research are provided:

1. Do men and women of military families experience the same
   incidence of stress?

2. Do military family members provide a supportive environment
   which may enhance stress tolerance or do they exacerbate
   stress?

3. To what extent is commitment to the military occupational role
   affected by family related stress? and

4. Has the rapidly increasing number of dual career families in
   the military created stress that affects military occupational
   role performance?

Even though the preceding are broad questions, the researcher is cast-
ing a broad net in pursuit of an exploratory study in order to identify
interesting relationships that could be studied more intensely in
follow-up research. In addition, there is an emphasis in the proposed
future research that differentiates it from most of the previous
research. That emphasis is upon the effects of family stress on work
attitudes and behavior. Most of the previous research has been of
effects in the opposite direction, i.e., the influence of being in the
military upon the family.

A. Review of a Relevant Study

The following study is discussed in more detail than others due to the fact that it produces evidence regarding the importance of the military family. It is especially relevant because it is a study of Air Force personnel and it points to many unanswered questions including some to be studied in the follow-up proposed research.

In May, 1984, two scholars conducted an investigation of occupational and domestic sources of pilot mental health and performance (1). The primary objective was to determine the effects of occupational and domestic sources of stress on pilot health, job satisfaction, and performance. Mailed specifically designed and pre-designed questionnaires generated responses from (N = 523) pilots with a 52.3% response rate, through the British Airline Pilots Association (BALPA) based in London. The Civil Aviation Authority Medic for Manchester Airport also served as a contact for additional subjects. A sample of 280 pilots' wives with a response rate of 56% was also used.

There were eleven trends in terms of stressors experienced by pilots identified in the research. These included: control scheduling, rostering, anxiety of courses and checks, home/work interface, career and achievement, insufficient flying responsibility and decision making, interpersonal problems, management and organizational issues, domestic status, fatigue and flying patterns. The three concerns relative to life events were emotional losses, pilot characteristics, and emotional gains. Subsumed under coping strategies were: stability of relationship and home life, social support, and wives' involvement.

The results of the study included the following:

—The investigation of domestic stress involved the identification and testing of twenty-nine issues.

—Responses indicate idiosyncracies of pilots' home life.

—The pilots were generally worried about problem identification and achievement.

—Factors relating to control, achievement, careers, and domestic health emerged; many of which contributed to occupationally oriented trends.

—There was a clear indication that domestic issues related to occupational oriented trends.

—With reference to the stressors at home that may affect work, the greatest impacts were related to unresolved and ongoing situations.

—When all items were loaded onto one single factor (stability), the items all related to the same issue (i.e., relationship between home and work). This factor was a significant negative predictor of depression.

—Stressful experiences from home to work were uniformally summarized in terms of a home/work relationship.

—Domestic stresses at work tend to be cognitive rather than behavioral.

—The four factors of coping strategies among the pilots were: stability of relationship and home life, reason and logic, social support and wife's involvement. Home life was found to play a major role in coping.

—The overall theme for ill health was centered around achievement and success. and

—The sources of stress identified by pilots' wives were: adopting domestic roles, job loss threats to marital relations, and the lack of an active role in the husband's career progression and social problems. Other interesting findings were that the wives perceived pilot job stress as being related to work pattern fatigue, anxiety of courses and checks; job stress on pilots relating to irritability, tension, and decreased performance.

B. Review of Other Related Literature

According to some scholars, problems of the army family have received relatively little attention in past research on the military (2). They offer as a possible reason for the lack of research on the army family as due to the very small percentage of married army personnel in the past years. Providing supportive data on the increase in the percentage of married army personnel, they state, "The fact that many soldiers now have family responsibilities, in addition to their army responsibilities, suggests that promotion and maintenance of family harmony should act to promote job satisfaction and high levels of job performance among soldiers from these families." However, Woelfel and Sevell's study showed no relationship between job satisfaction and marital satisfaction.

Hunter and Nice suggest that military duty presents a dangerous threat to the person in the military and the other members of his/her

family. They state that even though families are identified as being
of importance to military life, military planners and leaders, analysts,
and civilian leaders focus on hardware-oriented capabilities of military
personnel rather than on how families affect mission accomplishments.
The editors noted that in recent years, however, the military organiza-
tion has changed rapidly and more attention is given to family factors
than in previous years (3).

Reinerth states that the presence of the service family is,
further, a relatively new phenomenon arising from the need, since World
War II, for a large standing armed force as an aspect of national policy.
She suggests that the military family can be viewed as an asset or a
liability to the person's traditional performance of military duty.
Yet she identifies it as being unique and different in structure and
attitude as compared to civilian life in general (4). She notes that
frequent long-term separation of family members and, chronic mobility
that require adjustment and readjustment to different environments can
produce stress that may be disruptive to interpersonal family relations
and to the performance of military duty. What can society do to make
the stress a little more bearable for military family members? She
suggests that in some cases, society can prepare the family members for
the stress of separation by providing roles and norms of behavior before
the separation occurs. The preceding statement may be interpreted that
some degree of chronic stress may be advantageous in preparing for
crises as a result of predefined roles or pre-planned forms of behav-
ioral adjustment. Considering the fact that it is not necessarily a

common practice for a predefinition to occur, and regardless to the reason or length of the male absenteeism, it becomes very important for the wife to assume certain roles as the remaining spouse. This implies that it is the wife's role that may require the most readjustment.

A number of authors have discussed how military life has loosened ties between military men's conjugal families and their extended families and communities. They surmised that should the trend level off, there are few indications that the military will follow suit and place families close to their homes of origin (5, 6, 7).

One writer asks the question: what happens to families during the separation from the other family members? Then he attempts to answer that question by saying that the families are required to move off post and relinquish ties to the military community when these ties are most needed, especially if relatives are not close by to provide support. He goes on to say that should such relatives be available, excessive dependency on those relatives may develop (8).

To what extent are military wives involved in their husbands' careers? Existing social scientific literature usually categorizes responses to this question into three major orientations. The first of these is referred to as the housewife which is characterized by complete isolation from her husband's work. This type is not programmed by the occupational conditions of the husband, but is a result of her lack of personal interest or the non-interference policy that may be exhibited by her husband. The second type is referred to as the Corporate Executive's Wife. This type is characterized by isolation or involvement in the husband's career. Thus, involvement or lack of involvement

is regulated by her husband's employer. The third type consists of wives of diplomatic career officials, some clergymen, and other professionals. This type is the recipient of prescriptive behavior of full participation in the duties and activities that surround her husband's formal appointment or occupation. Her involvement is not regarded as a potential interference with her husband's career. In other words, she is complementary to her husband's career successes (9). The primary objective of research that was done by Stoddard and Cabanillas was to clarify the role of the Army Officer's wife and the changes that occur within it. They hypothesized that role stresses experienced by the officers' wives would increase directly with the number of years of the husbands' service and their attainment of higher rank and the duration of his military career. However, this hypothesis was validated only during the first half of the officers' career. Thereafter, depending upon perceived opportunities which might result from continued subjugation of personal and family needs to the requirements of an officer's wife, the decision to retire at the end of a 20-year career was accompanied by a rapid decrease in role stresses.

One author examines the changing role and perspectives of Air Force wives in terms of American societal trends (10). The following questions were raised: Are Air Force wives still oriented to their traditional roles, or have other pursuits become more important? What do they want? What are their points of view? Should they have a role? Should they be required or expected to participate in Air Force activities? What do they want from life? Does the Air Force complement or conflict with their personal lives, jobs, families, husbands, or sense

105-12

of selves? A survey relative to the preceding questions was conducted from a sample of wives of students and faculty members at the Senior Noncommissioned Officer Academy, Squadron Officer School, Air Command and Staff College, and wives of noncommissioned officers serving in the Headquarters Squadron at Maxwell Air Force Base. From the (N = 242) who responded to the survey, the results were as follows: (1) If given the opportunity to voluntarily choose preferred Air Force Activities, wives do not object to participation; (2) Traditional roles for the respondents have changed, allowing them more freedom to pursue their own interests with support from their husbands, simultaneously; and (3) Most wives are happy with the Air Force in cases where it does not interfere with their jobs, families, or personal lives.

At the Conference on Current Trends and Directions of Military Family Research in San Diego, California in 1977, the words of Dr. Benjamin Schlesinger of the University of Toronto suggest the need for the proposed research and are as follows:

> I am optimistic about the family; I believe
> it will survive. Let us look and do some
> research on what allows thousands of military
> families to manage. What makes these families
> tick? Percentage-wise, there are more military
> families who manage despite tremendous pressures,
> despite the moving, and we can learn from those
> who are surviving and help those who are not.
> Let us not forget that families have tremendous
> strength; let us build on them... (11).

C. The Theoretical Orientation

According to Commander Call, March-April, 1984:

> Stress is no stranger to the military, since
> our purpose in being is to respond to exactly
> the threat that our ancestors had to confront,
> but with small differences—it must be an
> organized, integrated effort of highly cohe-
> sive individuals confronting a known enemy.
> However, the less conspicious counterpart of
> this stress, equally destructive is the stress
> that impacts upon us on a daily basis, at work
> and at home (12).

The concept of stress may be viewed from a number of perspec-
tives. One author suggests that previous definitions of stress derived
from three primary points of departure: (1) the physical sciences (a
farce that distorts a body); (2) the physiological concept of homeostasis
(the disruption of the homeostatic conditions of the organism); and
(3) psychological (a factor or situation which poses some threat to the
physical and social well-being of the individual, frustrates the achieve-
ment of some desired goal, or elicits avoidance reactions) (13). Chiles
states that man is a psychological system that learns, strives, tires,
and fears. He suggests that "in evaluating a given situation that we
may suspect to be stressful, we should first consider the nature of the
forces acting upon the individual and the relationship those forces
have to the psychological systems."

105-14

According to McGrath,

> Social-psychological stress can arise from
> situational conditions which lead to subjec-
> tive or cognitive appraisal of threat. The
> threat can involve actual or anticipated harms
> to the physical self, the psychological self
> and/or interpersonal relations. The threat
> may also derive from conditions of the physi-
> cal and/or social environment which deprives
> the individual of opportunities to satisfy
> physical, psychological, and/or interpersonal
> needs (14).

The author concludes that the occurrence of stress and its effects can
be measured at physiological, psychological, behavioral (task and inter-
personal performances), and at the organizational level.

A medical sociologist identifies stress as a discrepancy be-
tween the demands impinging upon an individual—whether the demands are
external or internal challenges or goals, and the individual's responses
to these demands (15). However, in his discussion of stress and work,
another scholar simplifies the medical sociologist's concept of stress,
to which he refers as "the failure of routine methods for managing
threats." Gross perceived a form of slow stress that may be the result
of a career in an organization; stress in the occupational role (diffi-
culty in doing what is expected of the individual); and organizational
structure stress.

As noted by Hovath, the primary problem in compiling the literature on stress is that the concept of stress ha. been used with so many different meanings that there no longer seems to be one thing called "stress" which can be the subject of an overall review (16). According to this author, the concept of stress appears frequently in articles without any mention of what the author (writer) means by the term. Therefore, such confusion in the lack of a workable definition of stress, leaves two choices to the reviewer. These may be: (1) to consider all experiments that are referred to as investigations of stress or (2) consider only the experiments that fit the reviewer's definition of stress.

V.   RECOMMENDATION: A CONCEPTUAL FRAMEWORK

Much has been said about military families in general with some redundancy. But, what about dual career families? The number of such families has increased in the military at a rate even higher than among civilians. Dual careers must contain special potential for creating stress in the military. For example, if one spouse is transferred to another post, does the other give up a career and start over in the new setting? On the other hand, temporary duty separations might be more easily dealt with if the spouse left behind is busily employed. However, what happens in these circumstances to procedures for child care if they involve both spouses? This has relevance to question number 1 which the researchers raised in the Introduction to the proposal. This could be looked at in terms of differences in how employment for men and women is traditionally defined, and how trends are changing in the

military. One approach could be to compare stress among dual career families and non-dual career families.

The dramatic increase in the labor force participation rate of women over the past two decades has produced a much higher proportion of dual career families. Because of rising prices, low military pay, and diminished benefits, this pattern has occurred even more rapidly among armed services wives than among their civilian counterparts (17).

In a review of literature on military families, Hunter, et al, note that among the major changes that have occurred since the shift to an all volunteer force in 1973 are more dual career families and all military families, a greater number of active duty mothers and more single parent families within the military system (18). These changes are not only a consequence of the increasing labor force activity of women, but also of the rapid increase in the number of military personnel who are married. Members of the Air Force with families now comprise more than two thirds of the total force (19).

Most of the research that has been conducted on dual career families has emphasized the stress which this pattern creates. Sources of stress include problems in the division of household chores, child care, career disruptions occasioned by the transfer of one spouse to another location, and problems in the relative commitment of each spouse to career and family (20).

Several recent studies suggest that these stresses for working couples may be even more acute in the military because of the amount of geographic mobility than these positions entail (21). Williams for

example, found an increased amount of anxiety among dual career military families as the time for new duty assignments approached.

Suter also found that transfers were the most often stated problems by military working couples and that both military members and their working spouses showed a high level of frustration in attempting to manage a two career lifestyle (22).

There is some evidence that there may be a greater problem for women in the military than for men. The major conclusion reached by Woefel was that at least among persons in the enlisted ranks, family life had more impact upon the job performance and job satisfaction of women soldiers than men soldiers (23). One reason for expecting differences between men and women in the extent to which family life influences occupational role performance is the effect of what has been termed "asymmetrical permeable boundaries between work and family roles." The work role is traditionally more vulnerable to family demands for women than for men and this has been identified as a major source of stress for women on the job (24).

While there have been some studies of dual-career military families, this research has raised more questions than it has answered and among the questions that have been raised are those listed earlier as the guiding questions for the proposal in process. The proposal in process should help to answer the questions such as whether dual career produce more stress for women than for men, whether there are particular family patterns and characteristics that either enhance stress tolerance or exacerbate stress, and whether stress generated by dual careers affect military occupational role performance and reduces commitment to a military career.

It has been only during the past few decades that any concentrated research attention has been given to the military family. McCubbin and Dahl have documented the fact that the sociological study of the military family is an especially neglected research area (25). Of the research that has been done, there has been much more attention to effects of the military career upon the family than to ways in which family stress may affect work attitudes and behavior. Kanter, however, has argued convincingly that there are important effects of family life on work as well as the more frequently studied effects of work on the family (26).

One potentially important effect that does not appear to have been studied at all is the possible influence of family stress on occupational commitment or job involvement. An extensive review of both the family literature and job involvement literature shows no research on this relationship. There is a large and rapidly growing number of studies dealing with job involvement, work as a central life interest, perceived importance of work, and occupational commitment (27, 28). Work, and family are typically not separate and isolated arenas. It seems reasonable to expect that marital stress would influence level of commitment to work and as a result, would affect occupational role performance and even the decision to stay on the job. The latter effect should be of special interest to the military because of its concern with retention of personnel.

Occupational commitment has been conceptualized by Faunce as "self-investment in work." Self-investment is defined as a commitment

to work based on the relevance of work related values to self-esteem
(29, 30, 31). The research evidence indicates that work is the major
source of gains or losses in self-esteem for some people, while for
others, work has almost no bearing upon how they feel about themselves.
This variation clearly has an important influence upon work attitudes
and behavior. Research from which it is possible to infer differences
in self-investment in work have been done in a large number of occupa-
tions, but there do not appear to be any studies of the military.
Analysis of factors that affect the self-investment in work of Air
Force personnel, including family related stress, should produce new and
potentially useful information.

The efforts included in this final report will result in a research
proposal for an exploratory study that will respond to the four basic
questions to guide the research listed earlier.

REFERENCES

1. Cooper, C.L., and S.J. Sloan, <u>Job and Family Stress as Predictors of Pilot Health, Job Satisfaction and Performance</u>, USAF Grand No. AFOSR-83-0148, Department of Management Science, UMIST, Manchester, England, 1984.

2. Woelfel, J.C., and J.M. Savell, "Marital Satisfaction, Job Satisfaction, and Retention in the Army," in <u>Military Families: Adaptation to Change</u>, E.J. Hunter and D.S. Nice (Eds.), New York: Praeger Publishers, 1978, p. 17.

3. Hunter, E.J., and D. S. Nice, <u>Military Families: Adaptation to Change</u>, New York: Praeger Publishers, 1978.

4. Reinerth, J.B., "Separation and Female Centeredness in the Military Family," in <u>Military Families: Adaptation to Change</u>, E.J. Hunter and D.S. Nice, New York: Praeger Publishers, 1978, p. 169.

5. Janowitz, M., <u>The Professional Soldier: A Social and Political Portrait</u>, New York: Free Press, 1960.

6. Little, R.W., "The Military Family," in <u>Handbook of Military Institutions</u>, R.W. Little (Ed.), Beverly Hills, California: Sage Publications, pp. 247-270.

7. Dickerson, W.J., and R.J. Arthur, "Navy Families in Distress," <u>Military Medicine</u>, Vol. 130, pp. 894-898.

8. Stanton, M.D., "The Soldier," in <u>Outsiders, USA</u>, D. Spiegel and P.K. Spiegel, San Francisco: Rinehart, 1973, Chapter 21.

9. Stoddard, E.R., "The Military Intelligence Agent: Structural Strain in an Occupational Role," in <u>Social Dimensions of Work</u>, C.D. Bryant, Englewood Cliffs, NJ: Prentice Hall, Inc., 1954, pp. 570-582.

10. Warner, M.M.M., "The Air Force Wife-Her Perspective," *Air University Review*, May-June, 1984, pp. 47-53

11. Hunter, E.J., "Epilogue: Adapt or Opt Out," in *Military Family: Adaptation to Changes*, E.J. Hunter and D.S. Nice (Eds.), New York: Praeger Publishers, 1978, p. 243.

12. "The Darker Side of Stress." Adapted from an article in *Commanders Call*, Distribution is made by the U.S. Army AG Publications Center, 2800 Eastern Blvd, Baltimore, MD in accordance with DA Form 12-4 requirements, March-April 1984.

13. Chiles, W.D., *Assessment of the Performance Effects of the Stresses of Space Flight*, Aerospace Medical Research Laboratories, Aerospace Medical Division, Air Force Systems Command, Wright-Patterson Air Force Base, Ohio: December, 1966.

14. McGrath, J.E., *Social and Psychological Factors in Stress*, New York: Holt, Rinehart, and Winston, Inc., 1970.

15. Mechanic, D., "Social Structure and Personal Adaptation: Some Neglected Dimensions," in *Coping and Adaptation*, G.U. Coelho, et al (Eds.), New York: Basic Books, pp. 32-44.

16. Hovath, F.E., "Psychological Stress: A Review of Definitions and Experimental Research," *General Systems Yearbook*, Vol. 4, 1959.

17. Grossman, A., "The Employment Situation for Military Wives," *Monthly Labor Review*, February 1981, 104, 2, pp. 60-64.

18. Hunter, E.J., D. den Dulk, and J.W. Williams, *The Literature on Military Families, 1980: An Annotated Bibliography*, Technical Report USAFS-TR-80-11, DTIC Report No. AD-A093811, Colorado: United Stated Air Force Academy, August, 1980.

19. Orthner, D.K., *Families in Blue: A Study of Married and Single Parents of Families in the U.S. Air Force*, Greensboro, NC: Family Research and Analysis, 1980.

20. Rapaport, R., and R. Rapaport, *Dual Career Families*, London: Penguin, 1971; Kanter, R.M., *Work and Family in the United States*, New York: Russell Sage, 1977.

21. Williams, T., "Dual Career Families," in *Military Families: Adaptation to Change*, E. Hunter and D. Nice (Eds.), New York: Praeger, 1978.

22. Suter, D.J., *The Two-Career Family in the Navy*, Unpublished thesis, Naval Postgraduate School, Monterey, CA: 1979.

23. Woelfel, J.C., "Family Life and Job Performance in the U.S. Army," The Western Regional Meeting of the Inter University Seminar on Armed Forces and Society, Monterey, CA: May, 1979.

24. Pleck, J.H., in Kaha-Hut, R. and A.K. Daniels, *Women and Work*, New York: Oxford University Press, 1982, pp. 101-110.

25. McCubbin, H.I., and B.B. Dahl, "Research on the Military Family: An Enigma of Family Sociology," Paper Presented at the Western Sociological Association, White Water, WI: October 1975.

26. Kanter, R.M., *Work and Family in the United States: A Critical Review and Agenda for Research and Policy*, New York: Russell Sage Foundation, 1977.

27. Maurer, J.C., et al, "An Examination of the Central Life Interest Scale," *Academy of Management Journal*, 1981, 24, pp. 174-182.

28. Robinowitz, S., and D.T. Hall, "Organizational Research on Job Involvement," Psychological Bulletin, 1977. 84. pp. 265-288.

29. Faunce, W.A., and R. Dubin, "Individual Investment in Working and Living," in The Quality of Working Life Vol I, New York: Free Press, 1975, pp. 299-316; Faunce, W.A., "The Relation of Status to Self-Esteem," Sociological Focus, 1982, Vol 15, pp. 163-177.

30. _____, Problems in an Industrial Society, New York: McGraw Hill, 1981, pp. 130-181.

31. Myers, L.W., Black Women: Do they Cope Better?, Englewood Cliffs, New Jersey: Prentice-Hall, Inc., 1980.

1984 USAF-SCEEE SUMMER FACULTY RESEARCH PROGRAM

Sponsored by the

AIR FORCE OFFICE OF SCIENTIFIC RESEARCH

Conducted by the

SOUTHEASTERN CENTER FOR ELECTRICAL ENGINEERING EDUCATION

FINAL REPORT

AIR OXIDATION OF HYDRAZINE - A KINETIC STUDY

Prepared by: Dr. Datta V. Naik

Academic Rank: Associate Professor

Department and   Department of Chemistry
    University: Monmouth College, New Jersey

Research Location: Environics Division
                        Air Force Engineering and Services
                        Center, Tyndall Air Force Base, FL.

USAF Research: Dr. Daniel A. Stone

Date: July 30, 1984

Contract No.   F49620-82-C-0035

AIR OXIDATION OF HYDRAZINE - A KINETIC STUDY

by

Datta V. Naik

ABSTRACT

The oxidation of hydrazine in air has been studied in a 350-liter chamber made of Teflon® film using long-path Fourier transform infrared spectroscopy (FTIR). Among the chamber characteristics, its leak rate is found to be negligible, and the complete purging is shown to require a volume of fresh, dry air six times the volume of the chamber.

In the chamber, the rate of hydrazine air oxidation is strongly dependent on air humidity. With dry, purified air the half-life of hydrazine in the chamber is reproducible and has an average value of 12.6 $\pm$ 0.6 hours. The reaction rate is found to increase with increase in Teflon® surface (increase in surface to volume ratio) in the chamber. The reaction rate is also strongly influenced by the type and area of other surfaces placed in the chamber. Among the surfaces studied, copper increases the reaction rate the most followed by painted surfaces, aluminum, and stainless steel (Type 302), in that order. Suggestions for further research in this area are offered.

ACKNOWLEDGEMENT

I.   INTRODUCTION:

Hydrazine (N_2H_4) is an important member of the family
of high energy fuels widely used by the United States Air
Force and Space Transportation System. For example, hydra-
zine as a 70% solution in water is used as a propellant for
the emergency power unit (EPU) of the F-16 fighter plane.
A 50-50 blend of N_2H_4 and unsymmetrical dimethylhydrazine
(UDMH), known as Aerozine-50, is used as a fuel for the
Titan missile. Hydrazine and monomethylhydrazine (MMH) are
used in the Space Shuttles as propellants for the thrusters
and for the auxillary power units.

Hydrazine and its derivatives are highly toxic. The
recommended maximum exposure to hydrazine propellants is
extremely low. NIOSH recommends 30 ppb for hydrazine. The
widespread usage of hydrazine with its documented toxicity[1,2]
to humans and other organisms makes it necessary to charac-
terize the processes which control the fate of hydrazine in
the environment. In view of the problems associated with
spills and vapor releases which occur during handling, storage
and transport of hydrazine, this study was undertaken to
characterize the kinetics of air oxidation of hydrazine.

Previous work in this area by Stone[3] using glass reaction
chambers (30 ml - 55 l) had established that the hydrazine
oxidation in air proceeds by the main reaction:

$$N_2H_4(g) + O_2(g) \longrightarrow N_2(g) + 2H_2O(g) \tag{1}$$
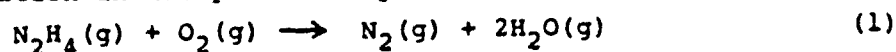
The production of small amounts of ammonia during the oxida-
tion was also reported and was attributed to heterogeneous
side reactions. The rate of hydrazine air oxidation was
found to be strongly dependent upon the reaction cell geometry,
surface composition of the cell, and its surface to volume
ratio.

Stone's experiments involved small glass reaction cham-

106-4

bers with high surface to volume ratios (minimum 0.3 cm^{-1}).
Actual air oxidation of hydrazine in ambient atmosphere is
expected to encounter a surface to volume ratio of 9×10^{-6} cm^{-1}[4].
Stone's kinetic study has been extended by Pitts and co-
workers[5,6] at the Statewide Air Pollution Research Center
(SAPRC) of the University of California at Riverside using
experimental conditions approaching those of the ambient at-
mosphere.

The SAPRC experiments were conducted using 3800-1 and
6400-1 Teflon[®] reaction chambers with significantly lower
surface to volume ratios. Teflon was chosen because of its
expected inertness in these processes. Unfortunately, only
a limited number of kinetic runs were made and the reported
values for the half-life (T) of the hydrazine decay in air
showed considerable scatter (Table 1). Nevertheless, the
data still agrees with the trends in the rates of hydrazine
air oxidation reported earlier. The half-life obtained with
the 6400-1 reaction chamber was longer than that obtained in
the 3800-1 chamber. The half-life obtained with wet air was
lower than that with dry air. The accelerated decay of the
hydrazines in wet air had been observed before by Stone[7].

The purpose of the present study was to obtain reliable
kinetic data for the air oxidation of hydrazine by using ex-
perimental conditions similar to those used at the SAPRC.

II. OBJECTIVES:

This project had two sequential goals. The first goal
was the determination of the characteristics of a newly-con-
structed reaction chamber made of Teflon[®] film for the air
oxidation of hydrazine. The characterization involved the
physical properties of the chamber (leak rate, purging time
etc.) and the effects of the chamber (surface, surface/volume
ratio, etc.) on the stability of hydrazine fuel vapors at
selected parts-per-million concentration levels. The second

TABLE 1. DECAY OF HYDRAZINE IN AIR IN TEFLON® CHAMBERS.[a]

Chamber Size (liters)	Relative Humidity of air	Length of Experiment (hrs)	Half-Life (hrs)
6400	13 %	6	16.4
3800	12 %	4	6.8
3800	12 %	6	10.8
3800	55 %	3.5	4.9

[a]Data from reference 6; Temperature: 22-24°C.
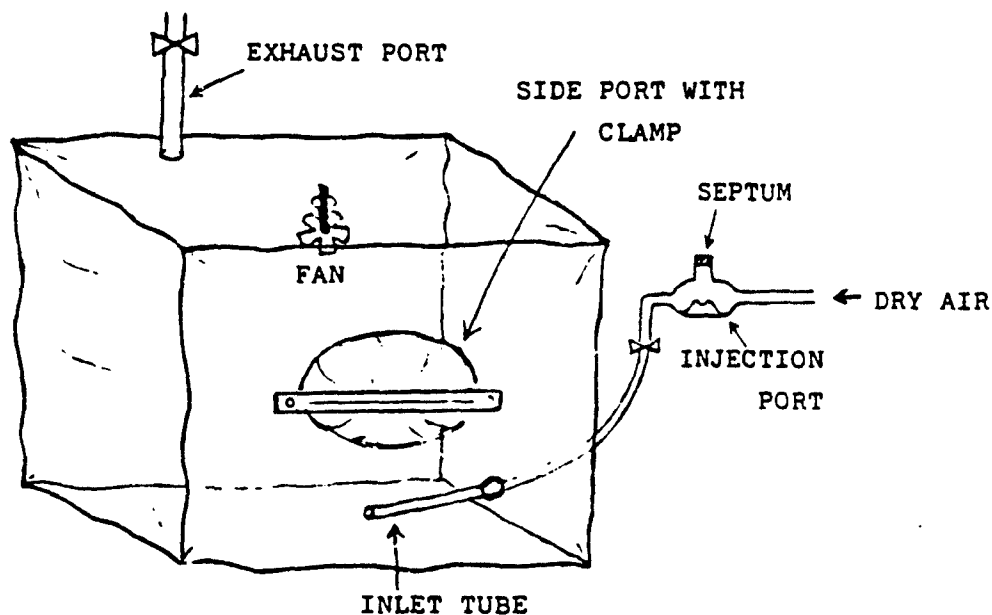
Figure 1. Teflon® Reaction Chamber. (Aluminum-Plexiglass Enclosure and the Multiple-Reflection Optics are not shown for clarity)

goal was to investigate the kinetics of the hydrazine air
oxidation as a function of different surfaces of known area
placed inside the chamber.

III. EXPERIMENTAL

III. 1. Reaction Chamber

The reaction chamber (Figure 1) was basically a bag
(0.9 m x 0.6 m x 0.7 m) constructed from DuPont FEP (50 μm
thick) Teflon® film. The bag was held semi-rigidly inside
a cage made of aluminum framing and plexiglass walls. A
valved exhaust of more than 30 l per minute was connected to
the top of the chamber. For vapor mixing purposes, a Teflon®
coated five-bladed fan was installed near the top of the
chamber and was driven by an external motor.

Introduction of hydrazine vapor and air to the chamber
was achieved through an inlet port consisting of Teflon®
tubing (7 mm i.d.) with one end extending inside the chamber.
The other end of the tubing was connected via a Teflon valve
to a small glass injection bulb equipped with a septum and
wrapped with a heating tape. The injection bulb in turn was
connected to an air purification unit through a glass man-
ifold with Teflon® valves.

The reaction chamber also contained a tubular port,
30 cm in diameter, on one of its sides for placement of
materials such as metal plates etc. in the chamber. This
port was closed by folding and was sealed with a wooden clamp
during kinetic runs. In addition, the plexiglass enclosure
was connected to a continuous hood-exhaust for safety reasons.

III. 2. Long Path-length Optics and FT-IR Spectrometer

The reaction chamber was equipped with the White-type[8]
multiple-reflection optics (Figure 2) which consisted of an
in-focus (nesting) mirror and two collecting mirrors, all

with a common radius of curvature of 80.0 cm. The multiple of the basepath (80.0 cm) attained, and thus the total pathlength was determined by counting the number of spots from a He-Ne laser as seen on the nesting mirror. The laser beam was kept in coincidence with the infrared source beam. The optics which were normally operated at 46 passes (pathlength of 3680 cm) was interfaced to the Nicolet 7199 Fourier Transform Infrared (FT-IR) Spectrometer and an HgCdTe detector (cooled with liquid nitrogen) through IRTRAN windows on the reaction chamber.

III. 3. Materials

Anhydrous hydrazine (fuel grade, 98+ percent purity) was obtained from Rocky Mountain Arsenal and was used as received. Pure methane gas was obtained from Fisher Scientific Co., and sulfur hexafluoride was supplied by Air Products and Chemicals, Inc.

The metal plates (copper, aluminum, and stainless steel #302) cut from stock metal (0.04-0.16 mm thick) were supplied by the Engineering Support Facility, Tyndall AFB. The plates were cleaned with soap and water and finally with acetone.

III. 4. Air Purification System

The dry, purified air was obtained from the air purification system that included compressed air (90-120 psi) from an Ingersoll-Rand compressor (7.5 HP), Zeks-Therm Dryer (Zeks Air Dryer Corp., Malvern, PA), Aadco 737 Pure Air Generator (Aadco Inc., Rockville, MD) and in the final stage, Pure Gas Heatless Dryer (General Cable, Apparatus Division, Westminster, CO). The air generated by this system was very dry and had a relative humidity of about 1-2 percent (determined with a General Eastern Model 1500 Hygrocomputer).
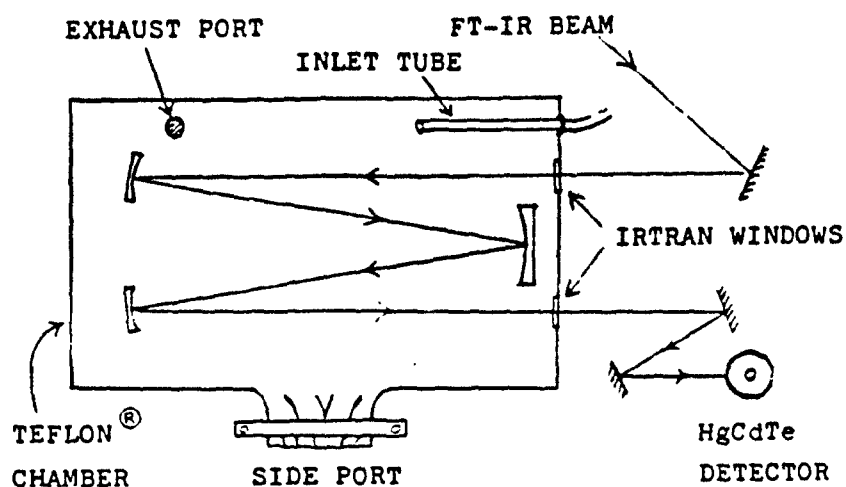
Figure 2.   Diagram of Multiple-Reflection Optics
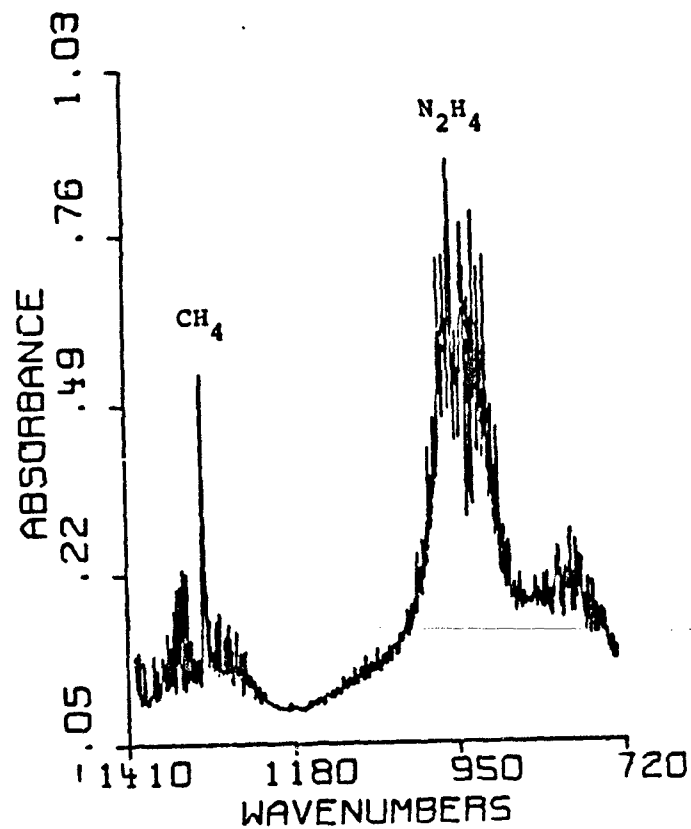
Figure 3.   Typical FT-IR Spectrum of the Chamber Contents

IV. **PROCEDURE:**

For each kinetic experiment, the reaction chamber was flushed with at least 6 volumes of dry air from the air purification system. The background spectrum of the dry air in the chamber was obtained before introduction of any hydrazine.

The hydrazine sample was introduced into the chamber by first removing some of the chamber air followed by the injection of the desired volume (usually 50 μl) of N_2H_4 into the injection bulb (pre-warmed to 60°-70°C). The hydrazine vapors were then flushed into the chamber by using dry air until the chamber was inflated to its normal size. The chamber contents were mixed with the fan during this operation.

V. **DATA COLLECTION AND PROCESSING:**

The concentration-time profile of hydrazine was monitored by FT-IR spectroscopy using 3680 cm pathlength (except where noted) and 1 cm^{-1} spectral resolution. The infrared spectra in the region 4000-700 cm^{-1} were recorded using 256 co-added interferograms for the background (dry air) spectrum and using 128 co-added interferograms for each sample spectrum. In the kinetic runs in the presence of metal surfaces, only 32 co-added interferograms per spectrum were used because of the observed faster reaction rates.

The concentration of hydrazine in the reaction chamber was calculated from its absorbance at 958 cm^{-1}. The absorbance coefficient of hydrazine at 958 cm^{-1} was determined in this laboratory to be 4.65 cm^{-1} atm^{-1} (base e). An FT-IR spectrum of hydrazine in the 1400-700 cm^{-1} region is shown in Figure 3. The peak at 1306 cm^{-1} is due to CH_4 which was routinely used with hydrazine to monitor chamber leakage (see Discussion).

106-10

VI. TREATMENT OF KINETIC DATA

Previous studies[3,9] have shown that the reaction between N_2H_4 and O_2 is first order in hydrazine and first order in oxygen. In the present study of the oxidation of hydrazine at parts-per-million concentration levels in air, the oxygen concentration will be in large excess. Therefore, the reaction should follow a pseudo-first order rate law, viz:

$$-\frac{d}{dt} [N_2H_4] = k [N_2H_4] \tag{2}$$

$$\text{or} \quad \ln [N_2H_4]_t = -kt + [N_2H_4]_i \tag{3}$$

where k = rate constant, and subscripts i and t represent hydrazine concentrations at time zero and at time t, respectively.

Therefore, a plot of $\ln [N_2H_4]_t$ vs time should be a straight line with the slope equal to -k. The half-life (τ) can be calculated from k by the relationship: $\tau = \frac{\ln 2}{k}$ (4)

A typical first order plot obtained for the air oxidation of hydrazine in the Teflon® reaction chamber is illustrated in Figure 4. All the kinetic plots yielded a correlation factor in the range of 0.996-1.000 except in the case of the kinetic data obtained with a painted aluminum surface (r^2 = 0.986-0.994).

VII. RESULTS AND DISCUSSION:

VII. 1. Chamber Characterization

A. Chamber Leak Rate: To determine the leak rate of the chamber, 5 torr of sulfur hexafluoride (SF_6) from a 48.5 ml pyrex bulb was flushed into the chamber with the dry air. The concentration of SF_6 in the chamber was followed as a function of time by measuring its absorbance at 947 cm^{-1}. The absorbance coefficient of SF_6 at 947 cm^{-1} was determined in this laboratory to be 495 cm^{-1} atm^{-1} (base e). Sulfur hexafluoride, which has the well defined infrared absorption, was chosen for the leak study because Teflon® film is not
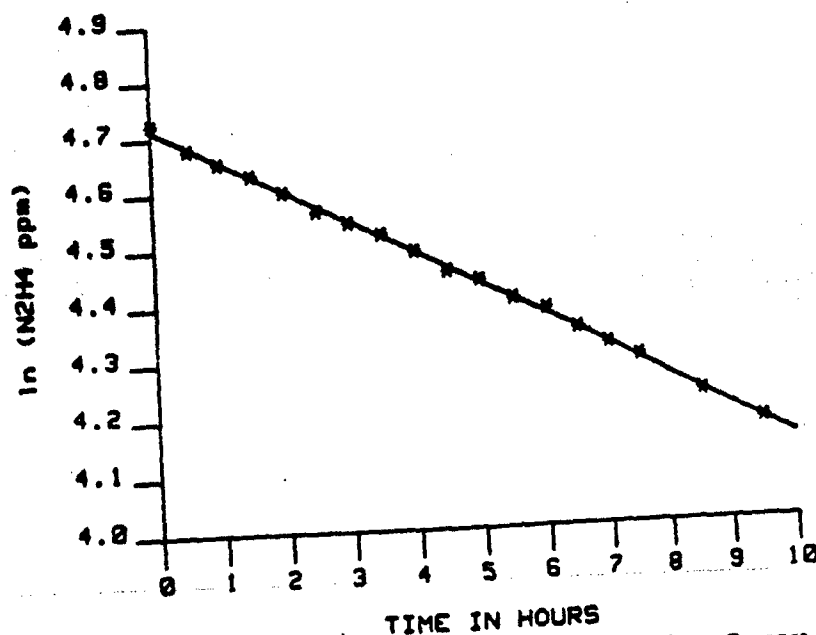
Figure 4. Typical Kinetic Plot for Hydrazine Decay in Air in the Teflon® Reaction Chamber: $\ln(N_2H_4$ ppm) versus Time. Correlation Factor, $r^2 = 0.999$
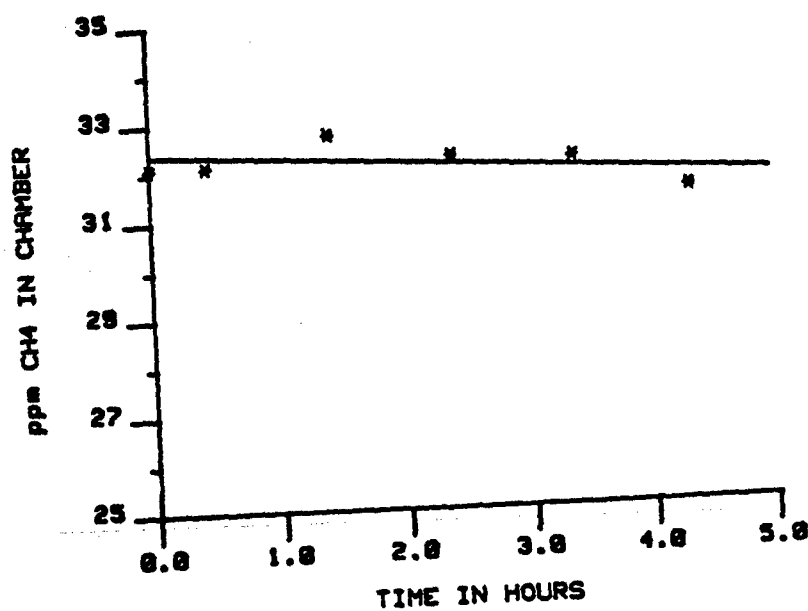
Figure 5. Plot of CH_4 Concentration (ppm) versus Time During a Kinetic Run

permeable to a molecule this large. Over a time period of 5 hours, the SF_6 concentration changed from 0.79 ppm to 0.78 ppm corresponding to a leak rate of less than 0.3% per hour. Thus the chamber appeared to be virtually leak-proof under the experimental conditions.

Since the side port of the chamber had to be opened and closed each time objects were placed inside or removed from the chamber, it became necessary to ascertain that the side port was airtight after such operations. Moreover, a leak could develop any time if the chamber was punctured or its seals broken. Therefore, leak integrity of the chamber had to be monitored during each of the N_2H_4 kinetic runs. Unfortunately, SF_6 could not be used for this purpose as its absorbance is in the same region (947 cm^{-1}) as that of N_2H_4 (958 cm^{-1}). Methane gas was found to be a satisfactory substitute for SF_6 for leak monitoring. Methane has a strong absorbance at 1306 cm^{-1} (absorbance coefficient = 11 cm^{-1} atm^{-1} (base e)[10]) and it does not interfere with N_2H_4 absorbance.

In practice, about 20 torr of CH_4 from a 500-ml pyrex bulb was introduced into the chamber along with the N_2H_4 sample to yield a concentration of about 32 ppm CH_4 in the chamber. The methane concentration was determined each time the N_2H_4 concentration was measured. A typical concentration-time profile of CH_4 during a N_2H_4 kinetic run is shown in Figure 5. The kinetic runs in which the methane concentration decreased significantly in the first 4 hours, were terminated at this point and the chamber was inspected for leaks.

B. Chamber Purge Characteristics

For each of the kinetic experiments, the chamber was flushed with the dry air (at a rate of about 30 liters per minute) prior to the final fill. The air inflow was balanced
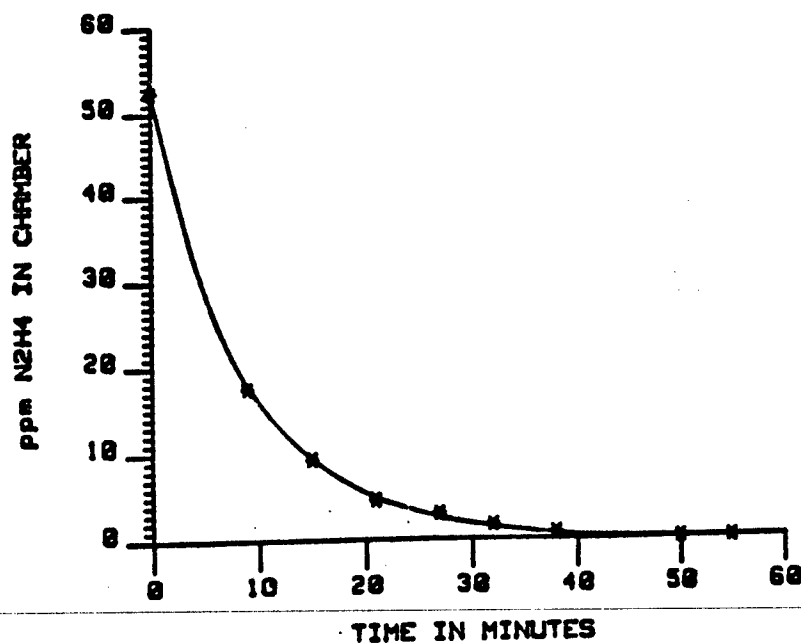
Figure 6. Chamber Purge Kinetics: Plot of Hydrazine Concentration (ppm) versus Time
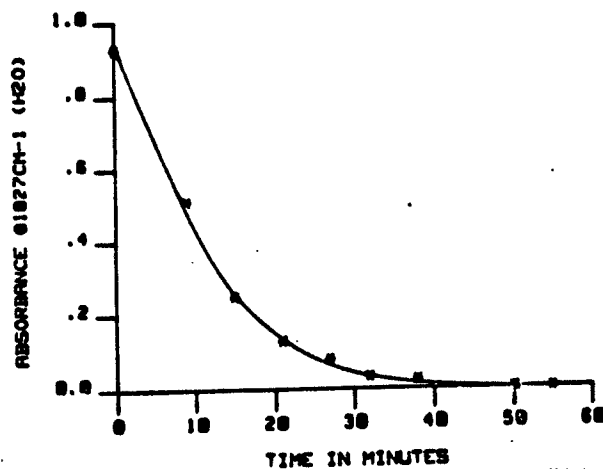
Figure 7. Chamber Purge Kinetics: Plot of Water Absorbance at 1827 cm^{-1} versus Time

by opening the chamber exhaust valve to maintain an equilibrium as noted by constant chamber volume. The mixing fan was kept running during this operation to ensure rapid purging. The time necessary for complete replacement of the chamber contents with fresh dry air was determined by following the decrease of N_2H_4 (left over from a previous kinetic run) concentration with time (Figure 6), and also by observing the decrease in water absorbance at 1827 cm^{-1} (Figure 7). Both measurements indicated that the purging was complete after about 45 minutes. Therefore, the routine flushing of the system was done for at least an hour, which corresponded to the use of a volume of fresh, dry air 6 times the volume of the chamber.

VII. 2. Rate of the Air Oxidation of Hydrazine in the Chamber

Initial kinetic experiments using room air and N_2H_4 in the chamber followed a first order rate law. However, the reaction rates obtained were not reproducible (Table 2). The wide scatter of the results was attributed to the varying moisture content of the room air. Consequently, subsequent experiments were conducted using only dry air from the air purification system.

The results obtained from kinetic runs with hydrazine and dry air in the chamber are summarized in Table 3. The first set of three experiments (#1-3) were conducted without any mixing of the chamber contents (chamber fan off), and showed poor reproducibility. Programmed mixing was used in the second set of three experiments (#4-6), and involved a t..aer which turned on the chamber fan for 2 minutes every half-hour during a run. The data revealed that mixing was essential to obtain reproducible kinetic data.

The average half-life obtained, with programmed mixing was 12.6 ± 0.6 hours. This value was considered to be the

106-15

TABLE 2. DECAY OF HYDRAZINE IN ROOM AIR.[a]

Exp. #	Length of Kinetic Run[b] (hrs)	# Data Points	k (hr^{-1})	τ (hrs)
1	6	10	0.146	4.8
2	6	11	0.085	8.2
3	6	11	0.183	3.8

[a]Initial concentrations: 97 - 112 ppm N_2H_4.

[b]Chamber contents were not mixed during these experiments.

TABLE 3. DECAY OF HYDRAZINE IN DRY, PURIFIED AIR.[a]

Exp. #	Initial N_2H_4 Concentration (ppm)	Program- med Mixing	# Data Points[b]	k (hr^{-1})	τ (hrs)
1	113	NO	18	0.0566	12.2
2	104	NO	17	0.0475	14.6
3	112	NO	14	0.0416	16.6
4	109	YES	9	0.0537	12.9
5	112	YES	9	0.0553	12.5
6	364[c]	YES	8	0.0562	12.3

[a]These and all other kinetic experiments were conducted at ambient laboratory temperature (23°-28° C).

[b]Length of the kinetic runs ranged from 9.5-12 hrs.

[c]FT-IR pathlength was 1760 cm for this kinetic run.

characteristic base-line half-life for the air oxidation of hydrazine in the chamber with its surface and inherent surface to volume ratio.

Kinetic runs #4-6 also reveal that the rate of air oxidation of hydrazine was independent of initial N_2H_4 concentration, as expected for a first order kinetics.

VII. 3. Effect of Surface to Volume Ratio

The effect of increased Teflon® surface to volume ratio (s/v) on the rate of air oxidation of hydrazine was studied by hanging several rectangular (45.0 cm x 30.5 cm) pieces of Teflon® film (50 μm) from the chamber ceiling using tiny pieces of Mylar® tape. The results of this study, summarized in Table 4, indicate a strong dependence of the reaction rate on the surface to volume ratio. The decrease in half-life with increase in s/v reveals the significant role of heterogeneous surface reaction between hydrazine and oxygen.

VII. 4. Effect of Metal Surfaces

The hydrazine-air reaction was studied in the presence of different metal surfaces (copper, aluminum, painted aluminum and stainless steel) in the chamber to determine the effect of each type of surface on the reaction rate. Metal plates (usually 10 cm x 60 cm) were held in place by two grooved Teflon® cylinders (diam. = 2.54 cm) with the long edge of the plates placed in the grooves. The cylinders could hold up to 15 plates with a groove separation no less than 3 cm.

The increase in Teflon® surface area due to the two Teflon® racks was estimated at 0.2 m². The half-life for the hydrazine decay in the presence of these racks (empty) was determined to be 12.2 hrs (average of four determinations). This value is comparable to the average half-life (12.6 hrs) in the absence of the racks. Therefore, the effect of the racks on the reaction rate was considered negligible.

106-17

TABLE 4. EFFECT OF TEFLON®-SURFACE TO VOLUME RATIO ON HYDRAZINE DECAY

Exp. #	Teflon® Area S, (m²)	S/V (m⁻¹)	# Kinetic Runs	Avg. k (hr⁻¹)	Avg. τ [b] (hrs)
1	3.5	10.9	3	0 0551	12.6±0.6
2	5.1	15.9	3	0.0726	9.5±0.8
3	6.2	19.4	4	0.0916	7.6±0.8

[a]Chamber volume: 320 liters; Chamber surface: 3.5 m².

[b]Errors given correspond to two standard deviations.

TABLE 5. EFFECT OF METAL SURFACES ON HYDRAZINE DECAY

Type of surface	Area (m²)	# Kinetic Runs	Avg. k (hr⁻¹)	Avg. τ [a] (hrs)
Copper	0.12	5	0.263	2.6±0.7
Aluminum	1.25	3	0.0801	8.6±0.6
Aluminum Foil	0.60	2	0.0548	12.6±0.3
Stainless Steel (Type 302)	0.80	3	0.0626	11± 1
Painted Aluminum (F-16 Type Paint)	30	3	0.249	2.8±0.8

[a]Errors given correspond to two standard deviations.

The reaction rates obtained in the presence of various metal surfaces are summarized in Table 5. Also listed in the Table are the surface areas of each metal used in the experiments. Among the surfaces studied, copper showed the most effect on the rate of the air oxidation of hydrazine. A copper surface of only $0.12 \, m^2$ yielded an average half-life for the reaction of only 2.6 hours. Aluminum foil ($0.60 \, m^2$) had no apparent effect on the reaction rate. Aluminum plates ($1.25 \, m^2$) cut from the stock metal increased the reaction rate substantially ($T = 8.7$ hrs). Stainless steel (Type 302) had only a slight effect on the reaction rate ($T = 11$ hrs with $0.80 \, m^2$). In addition to the metal surfaces, even a painted surface (Al plates coated with a paint used on U.S. fighter planes) accelerated the reaction ($T = 2.8 \, hrs/1.30 \, m^2$). This painted surface was more effective than all the metals studied except for copper.

X-ray photoelectron spectroscopy (XPS) studies have shown that at room temperature hydrazine is adsorbed molecularly on a copper surface[11] while the adsorption of hydrazine on aluminum[12] and iron[13] results in cleavage of the N-N bond and production of $NH_2 \cdot$, $NH \cdot$, N and H ad-atoms. It also has been noted that the H ad-atoms formed on Al and Fe remain adsorbed and inhibit subsequent adsorption of N_2H_4. These XPS results and the present study suggest that a surface exhibiting molecular adsorption of hydrazine will be more effective in accelerating the air oxidation of hydrazine than a surface which generates H ad-atoms on decomposition of adsorbed N_2H_4.

Table 6 lists some of the trends observed in the kinetic data obtained with the various surfaces. For all the surfaces except aluminum foil, the half-life obtained for the first kinetic run for each of the surfaces was shorter than for the subsequent runs. This pattern may be partly due to the poisoning of surface activity by accumulation of unidentified products on the surface. The small T values obtained for the

TABLE 6. TRENDS IN N_2H_4 KINETIC DATA WITH METAL SURFACES

Kinetic Run #	τ (hrs)				
	Copper	Aluminum	Al Foil	St. Steel	Painted Al
1	2.1	4.6[a]	12.7	10.0	1.5[a]
2	2.8	9.0	12.6	11.6	2.2
3	2.8	8.3[b]		11.8	3.2
4	3.2	8.4[b]			3.1
5	2.5[b]				

[a] Metal plates were cleaned before this kinetic run.

[b] These results were not used in calculation of average values listed in Table 5.

first kinetic runs with Cu, Al and stainless steel could not be duplicated by cleaning (soap-water/acetone) of the metal plates. A more rigorous cleaning or use of fresh metal plates is probably needed to duplicate the short half-lives.

VIII. RECOMMENDATIONS:

The results of the present study suggest a need for additional research efforts to investigate in detail the systematic effects of the following factors on the kinetics of air oxidation of hydrazine so as to understand better the atmospheric fate of hydrazine vapors.

1) Humidity
2) Temperature
3) Various surfaces - effects of surface type and surface area for typical contact materials (metals, concrete, asphalt, painted surfaces, soils, vegetation etc.)

In addition, since the maximum half-life cf N_2H_4 in air with negligible surface to volume ratio will be governed only by the rate of the homogeneous gas phase reaction of hydrazine in air, it is important to know the homogeneous rate constant. An effort should be made to determine this fundamental rate constant.

The present study has shown that the Teflon® surface is not totally inert to the N_2H_4-air system. Therefore, even with larger Teflon® reaction chambers (with smaller s/v), the heterogeneous surface reaction will continue to play a significant role in the overall reaction rate. One way to minimize the surface reaction is to use a reaction chamber made up of material completely inert to the N_2H_4-air system. Because this may be impractical, an alternate approach using an extrapolative study with Teflon® reaction chambers should be explored. It is suggested that the extrapolative study include measurements of overall rate constants for the reaction

with systematic variation in s/v of the chamber without changing any other chamber characteristics. The homogeneous rate constant could then be estimated by extrapolating the observed overall rate constants to zero surface to volume ratio.

REFERENCES

1. Aerospace Medical Research Laboratory. _Proceedings of the Fourth Annual Conference on Environmental Toxicology_, NTIS AD-781, Paper Laboratory, December 1973.

2. International Agency for Research on Cancer. _Evaluation of Carcinogenic Risk of Chemicals to Man._, Lyon, Vol. 4. International Agency for Research on Cancer, 1974.

3. Stone, D.A., _The Autoxidation of Hydrazine Vapor._ Report No. CEEDO-TR-78-17, Tyndall AFB, Florida: Air Force Syst. Command, Civ. Environ. Eng. Dev. Off., January 1978.

4. The National Research Council, _Ozone and other Photochemical Oxidants_, National Academy of Sciences, Washington DC, 1977, p. 66.

5. Pitts, J.N. Jr., Tuazon, E.C., Carter, W.P.L., Winer, A.M., Harris, G.W., Atkinson, R., and Graham, R.A., _Atomospheric Chemistry of Hydrazines: Gas Phase Kinetics and Mechanistic Studies._ Final Report ESL-TR-80-39. Tyndall AFB, Florida: Air Force Eng. Services Ctr., August 1980.

6. Tuazon, E.C., Carter, W.P., Brown, R.V., Atkinson, R., Winer, A.M., and Pitts, J.N.Jr., _Atomspheric Reaction Mechanisms of Amine Fuels._ Final Report ESL-TR-82-17. Tyndall AFB, Florida: Air Force Eng. Services Ctr., March 1934.

7. Stone, D.A., _The Vapor Phase Autoxidation of Unsymmetrical Dimethylhydrazine and 50-Percent Unsymmetrical Dimethylhydrazine-50-Percent Hydrazine Mixtures._ Report No. ESL-TR-80-21. Tyndall AFB, Florida: Air Force Eng. Services Ctr., April 1980.

8. White, J.L., "Long Optical Paths at Large Aperture", _Journal of the Optical Society of America_, Vol. 32, pp. 285-288, 1942.

9. Bowen, E.J. and Birley, A.W., "The Vapor Phase Reaction between Hydrazine and Oxygen", _Transactions of the Faraday Society_, Vol. 47, pp. 580-583, 1951.

10. Hanst, P.L., Wilson, W.E., Patterson, R.K., Gay, B.W. Jr., Chaney, W.W., and Burton, C.S., _A Spectroscopic Study of California Smog_, EPA Report No. 650/4-75-006, Feb. 1975, p. 12.

11. Matloob, M.H., and Roberts, M.W., "Electron Spectroscopic Study of Nitrogen Species Adsorbed on Copper", _Journal of the Chemical Society, Faraday Trans. 1_, Vol. 73, pp. 1393-1405, 1977.

12. Johnson, D.W., and Roberts, M.W., "Adsorption of Hydrazine and Ammonia on Aluminum", _Journal of Electron. Spectrosc. Relat. Phenom._, Vol. 19, pp. 185-195, 1980.

13. Matloob, M.H., and Roberts, M.W., "Adsorption of Hydrazine on Iron Studied by X-Ray Photoelectron Spectroscopy." *Journal of Chem. Res.* *(S)*, Vol. 1977, pp. 336-337, 1977.

1984 USAF-SCEEE SUMMER FACULTY RESEARCH PROGRAM

Sponsored by the

AIR FORCE OFFICE OF SCIENTIFIC RESEARCH

Conducted by the

SOUTHEASTERN CENTER FOR ELECTRICAL ENGINEERING EDUCATION

FINAL REPORT

CONCEPTUAL DESIGN OF THE USAF

INSTALLATION RESTORATION PROGRAM INFORMATION MANAGEMENT SYSTEM

Prepared by: Dr. Stephan J. Nix

Academic Rank: Assistant Professor

Department and   Department of Civil Engineering
  University: Syracuse University

Research Location: Occupational and Environmental Health Laboratory,
                        Office of Technical Operations

USAF Research: Major George R. New, USAF, BSC

Date: July 20, 1984

Contract No: F49620-82-C-0035

CONCEPTUAL DESIGN OF THE USAF

INSTALLATION RESTORATION PROGRAM INFORMATION MANAGEMENT SYSTEM

by

Stephan J. Nix

ABSTRACT

The conceptual design of a computerized information management system for the Air Force Installation Restoration Program (IRP) is outlined. The purpose of the IRP is to identify, quantify, and correct environmental problems associated with inactive hazardous waste disposal sites located on Air Force installations. There is a need to store the data collected in this program and provide the means through which information can be extracted from this data base. The conceptual design of the system evolves from an analysis of the demands on the system and the information needed to meet these demands. This analysis is followed by the development of the basic system structure. Implementation plans are also discussed.

ACKNOWLEDGEMENTS

The author is most appreciative of the opportunity provided by the Air Force Systems Command, the Air Force Office of Scientific Research, and the Southeastern Center for Electrical Engineering Education. The time spent at the Occupational and Environmental Health Laboratory, Brooks Air Force Base, Texas was productive and professionally enlightening. The personnel at OEHL provided an excellent working environment and were always supportive.

More specifically, I would like to thank Major George R. New for his important contributions and review of this manuscript. I would also like to thank Lt. Colonel Dennis F. Naugle for his overall guidance and efforts in making my stay as enjoyable and productive as possible.

I. INTRODUCTION

The environmental impact of hazardous material disposal sites, especially on the nation's water resources, has come to the forefront of public concern. Although the extent of this impact is largely unknown, there is considerable evidence to suggest significant contamination and a response by priviate industry and government is warranted.[1] The Department of Defense (DoD) initiated the Installation Restoration Program (IRP) in 1975 to address problems associated with past disposal practices at defense installations. Current IRP policy, delineated in Defense Environmental Quality Program Policy Memorandum 81-5[2], is "to identify and fully evaluate suspected problems associated with past hazardous material disposal sites on DoD facilities, control hazards to health or welfare that resulted from those past operations." The IRP also forms the basis for remedial actions required by the Comprehensive Environmental Response, Compensation, and Liability Act of 1980. The U.S. Air Force, because of its mission, has long been involved in operations that generate varying amounts of hazardous waste and, therefore, the potential for environmental contamination is present. This paper focuses on the Air Force role in the IRP and, more specifically, the conceptual design of an information management system to manage and effectively use the data that will be collected during this program.

The Installation Restoration Program is to be implemented in four phases. Each phase is briefly described below:[2,3]

Phase I — Installation Assessment. The purpose of this phase is to identify the sites at Air Force installations that have a potential for contaminant migration. Installations were selected for evaluation based

on a list of subjective criteria. At each selected base, records are reviewed and interviews conducted with personnel knowledgeable of past and present operations. Given this information, a procedure known as the Hazardous Assessment Rating Methodology (HARM) is used to rate the sites within an installation with respect to their potential environmental impacts. The Phase I studies are to be completed by the end of fiscal 1985.

Phase II — Confirmation and Quantification. The purpose of this phase is to confirm contamination at each site identified in Phase I and, if necessary, quantify the problem with respect to magnitude, extent, direction, and rate of movement. This is accomplished by analyzing samples from gouund water monitoring wells and, to a lesser degree, surface water bodies. Phase II studies will produce the major portion of the total IRP data base. This phase is discussed in more detail in a later section.

Phase III — Technology Base Development. This phase is concerned with the development of containment and decontamination technologies and contamination levels believed acceptable for public health and welfare where no officially established standards exist. Also included in this phase are benefit/cost analyses for the various control technologies.

Phase IV — Operation. This final phase formulates and executes a remedial action plan to abate the identified hazardous conditions. This also includes monitoring to ensure that standards and criteria are met and that public welfare is protected for present and future generations.

The monitoring data gathered in the Phase II studies and other accociated information will guide subsequent Phase II work, provide the basis for Phases III and IV, and help establish research and development priorities. These activities will require an information management system to (1) archive, retrieve, and analyze the data, (2) produce management and scientific summaries, and (3) provide the information needed by various deterministic models (primarily ground water mcdels). Such a system must be flexible enough to meet these and future needs without becoming unnecessarily complex and unwieldy. It is also important that the system be designed so that modifications and maintenance can be handled by Air Force personnel without undue external consultation. Overall, the system should not prove to be so costly as to overwhelm the benefits is provides. Higher levels of responsiveness, flexibility, security, accuracy, and reliability are directly related to higher costs, but not always to justifiable increases in benefits. While benefits are difficult, if not impossible, to quantify, it is important to justify system capabilities with identifiable, worthwhile returns. The focus of the remainder of this paper is the development of such a system, hereafter referred to as the Installation Restoration Program Information Management System or simply IRPIMS.

II. OBJECTIVES

The principal objectives of this study are to identify the demands on the IRPIMS, the information needed to satisfy these demands, and the basic components and structure of the system. A secondary aim is to sketch an implementation plan to insure that the most urgent needs are

addressed in a timely manner. What is presented here will be used to guide the detailed design and actual construction of the system. This phase will be handled by an external contractor familiar with information management systems and environmental sciences. In addition to these salient objectives, it is hoped that the approach used in this study will help other private and public organizations in establishing similar environmental information management systems.

III. INSTALLATION RESTORATION PROGRAM, PHASE II

Phase II of the IRP is a multistaged effort to quantify the magnitude, extent, direction, and rate of movement of contaminants from past hazardous waste disposal sites having the potential for contamination (as determined in Phase I). As mentioned previously, these data are essential to the later phases of the IRP. Responsibility for the technical management of all Phase II studies rests with the USAF Occupational and Environmental Health Laboratory (OEHL).

A Phase II study is conducted for each installation identified in Phase I in a staged or staged and tailored manner, depending upon the availability of resources. The staged approach divides the study into independent chronological tasks or stages under the assumption that resources are available to begin work on all sites demonstrating a significant contamination potential. The staged and tailored approach obligates funds to the higher priority sites when resources are limited.

Prior to each Phase II study, a survey is conducted to define the scope of work and costs of the initial stage, i.e., Stage 1. Stage 1 addresses the confirmation of contamination at each site on the

installation. This survey is guided by Phase I recommendations, the

concerns of Air Force officials, and the technical experience of OEHL

technical personnel. If necessary, subsequent stages quantify the problem

with respect to direction, rate, and extent of movement.

Phase II will provide the bulk of the environmental data necessary

to achieve the goals of the IRP, but data collected in Phase I studies and

other monitoring efforts are also important. The specific types of data

to be stored and managed by the IRPIMS are discussed in the next section.

IV. DEVELOPMENT OF A CONCEPTUAL DESIGN

The conceptual design of the IRPIMS was developed in three steps.

The first step involved the indentification of the demands the system.

The second step determined the information needed to satisfy these

demands. The third step involved the delineation of the basic system

structure and components. The reader is referred to two excellent works

in the area of environmental information management systems. One, the

work of Haseman et al. , describes a general approach for designing an

information management system. The other, a comprehensive treatise by

Everett, provides a discussion directed toward ground water information

management systems. Both guided the conceptual design of the IRPIMS.

At this point it is useful to define and contrast some terms used

throughout the remainder of this paper. The obvious place to start is

with the term "data". Data are the basic building blocks of information.

Data provide little information without some form of analysis. Even the

simple visual scanning of a set of data is a form of analysis in which

information is gleaned by noting trends, identifying ranges of values,

estimating averages, etc. For the purpose herein, a data base is defined

as a collection of data stored to serve the information needs of a specific application or group of applications. A data base management system organizes the data base, prepares data for application processing, and isolates the data base from application algorithms (i.e., maintains the independence of the data). An information management system is an integrated collection of components designed to verify and input data to the data base, manage the data base, and extract useful information from the data base.

Demands on the System

The successful design of an information management system begins by enumerating the demands on the system. This essentially involves identifying the system users and uses. The principal demands on the IRPIMS are listed below:

(1) The system will play an important role in guiding later Phase II studies. Information derived from earlier studies can be used to better direct a later effort by allowing more comprehensive study at an earlier stage.

(2) Similarly, information extracted from the IRPIMS will provide guidance for the ongoing operation, maintenance, and design of solid and hazardous waste disposal facilities under the Resource Conservation and Recovery Act (RCRA) of 1976.

(3) The technology assessment and standards/criteria development slated for Phase III and the remedial actions of Phase IV require detailed and accurate assessments of the extent of contamination at all affected sites. Obviously, information extracted from the IRPIMS is crucial to these efforts.

(4) The IRPIMS will be used to help structure and prioritize future USAF research and development work as well as provide a source of data.

(5) Deterministic computer models (especially ground water models) will be used in the later stages of some Phase II studies as well as several Phase III and Phase IV studies. Monitoring data and other information amassed in this sytem will be needed to verify and calibrate these models.

(6) Regulatory agencies may require site characterization in selected cases. The system should be able to provide information for this purpose.

(7) Beyond the activities envisioned for Phase III, the IRPIMS will provide information to help develop appropriate health and environmental standards, criteria, and guidelines.

(8) Other efforts within the Air Force, not directly related to the IRP, have produced or will be producing data similar to those generated by Phase II studies. The system should be able to accommodate these data while maintaining their identity.

(9) The information contained in IRPIMS will have significant research value to external agencies and other interested parties. The system should provide some amount of access to these groups.

While the items listed above are very general they do define the basic character of system. Obviously, the system must be broad in scope and possess considerable capabilities. This list is an important

precursor to the determination of the types of information that must be extracted from the data base and, of course, the composition of the data base.

Information Requirements

An excellent model of how data and information flow through an environmental planning organization or program such as the IRP, has been prepared by Haseman et al. A slight modification of their model was applied to the IRP. The result is shown in Figure 1. This model gives an excellent way to place the IRPIMS within the overall IRP structure.

There are three basic stages in this information flow model. The first stage involves data collection, encoding, verification, and storage. In other words, the raw data are processed and stored in a manner suitable for the identified information needs. Within this stage there are four distinct actions. The first involves the collection of data from IRP field work and related studies. The second involves encoding the data into a form readable by the computer and the third verifies the data. Finally, the data are stored in the data base through the data base management system.

The second stage of the model involves the extraction of information from the data base. This stage is the vital link between the data base and the demands for information. The user, by querying the system, is the point through which information demands are met. Each query is addressed through a process that begins with the data base
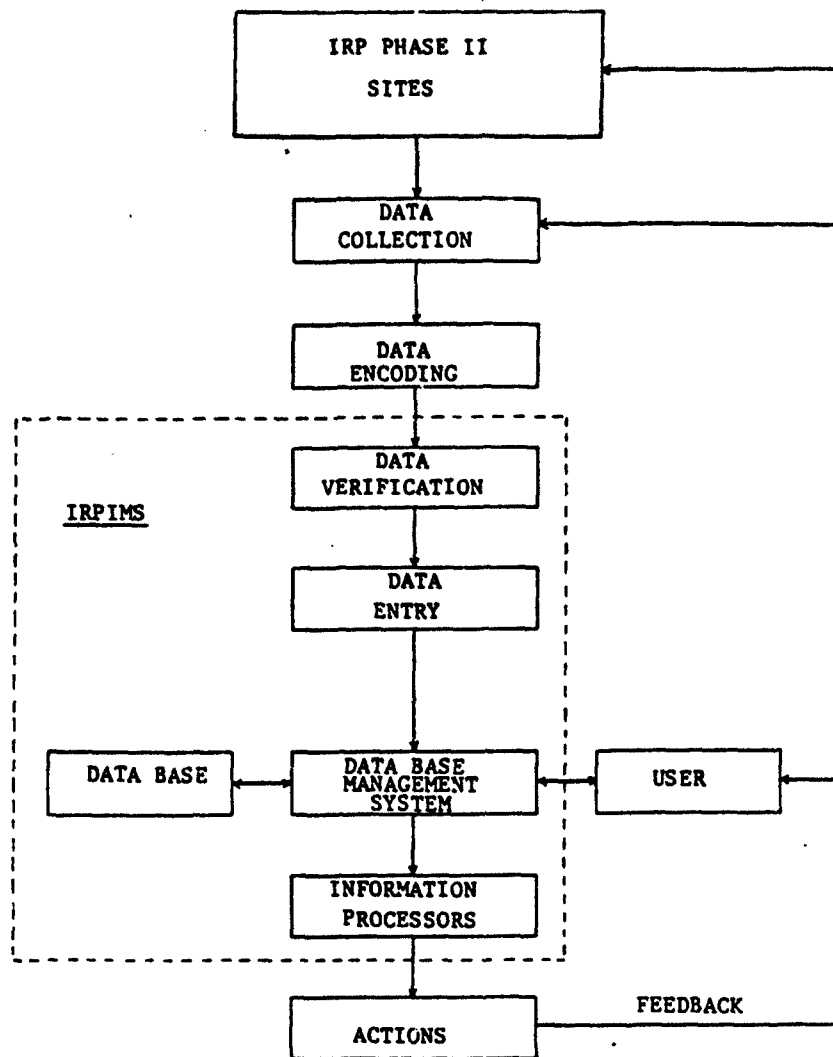
Figure 1. IRP Information Flow Model (after Haseman et al.[5])

mangement system preparing the appropriate data. These data are then
routed through the appropriate algorithms to extract the desired
information.

The third stage is concerned with the uses of the information
extracted from the data base. These uses were outlined earlier; the
purpose of evoking them at this point is to complete the information flow
model. Aside from the more obvious uses of information there are
important feedback mechanisms within the IRP. These feedback paths
suggest further action at the waste site, modify the types of data
collected, and affect the types of information requested of the system
through the user.

The model described above gives an abstract view of how data and
information flow through the IRP. The IRPIMS overlaps this model in the
last two steps of the first stage and the entire second stage (see Figure
1). However, to complete the model two important questions must be
addressed:

(1) What types of data should be collected and stored
in the data base?

(2) What types of information are to be extractable from the
data base?
These questions were answered through an analysis of the expected
information needs of the users and uses identified earlier. The proposed
contents of the data base are displayed in Table 1. The proposed types of
extractable information are shown in Table 2. Of course, these two tables

Table 1. Proposed Data Base Contents.

Data Category	Specific Data Requirements		
	Regional	Installation and Environs	IRP Waste Disposal Site
Identification	• Identification code • Name	• Identification code • Name	• Identification code
Location	• States • Counties • Townships, sections	• State • Counties • Township, sections • Municipalities • Geographic coordinates (benchmark)	• Installation • Geographic coordinates • Installation grid location
Maps		• Installation grid map (may be extended beyond installation boundary)	• Site grid map (may have greater resolution than installation grid map)
Waste Generators	• Location and description of major waste discharge sites*	• For each generation site: – location on installation grid map – composition of waste – amount of waste generated – disposal method	• For each IRP disposal site – which generators have deposited waste there – quantity of waste – waste disposal time line
Waste Disposal Sites	• Location and description of major waste disposal sites.*	• For each non-IRP waste disposal site: – location on installation grid map – identification code – design features (linings, impervious layers, drainage, structure, etc.) – chronology of disposal and waste types	• For each IRP waste disposal site: – location on site grid map – identification code – design features (linings, impervious layers, drainage, structure, etc.) – chronology of disposal and waste types – action classifications I – no further action II – further study III – remedial action
Topography	• Major topographic features*	• Elevation contours on installation grid map	• Elevation contours on site grid map

*Narrative

Table 1. Proposed Data Base Contents (continued).

Data Category	Specific Data Requirements		
	Regional	Installation and Environs	IRP Waste Disposal Site

Monitoring Locations	• General description of any pertinent monitoring locations*	• For each monitoring location not associated with a waste site:
		  – identification code
		  – geographic coordinates
		  – grid location
		  – type (surface water, monitoring well, supply well, observation well, etc.)
		  – construction date
		  – materials used in construction
		  – elevation of ground surface
		  – vertical location of the well bottom and screens
		  – sampling apparatus
		  – aquifers tapped
		  – pumping rate
			• For each monitoring location associated with a waste site:
			  – identification code
			  – geographic coordinates
			  – grid location
			  – type (surface water, monitoring well, supply well, observation well, etc.)
			  – construction date
			  – materials used in construction
			  – elevation of ground surface
			  – vertical location of the well bottom and screens
			  – sampling apparatus
			  – aquifers tapped
			  – pumping rate

Geology	• Principal systems, series, groups, formations, members and their characteristics (i.e., thickness, character of rocks, topographic expression, general waste bearing properties) • Soil associations, their characteristics (i.e., texture, permeability, shrink/swell potential, erosion factor, depth to bedrock, depth to high water table) and areal extent	• Location of systems, series, groups, formations members on installation grid map • Stratigraphy of each well (monitoring, supply, or observation) not associated with an IRP waste site	• Stratigraphy of each well (monitoring, supply or observation) associated with an IRP waste site

*Narrative

Table 1. Proposed Data Base Contents (continued).

Data Category	Regional	Specific Data Requirements	
		Installation and Environs	IRP Waste Disposal Site

Hydrology	• Description of surface water resources including major water bodies, drainage patterns, major uses, etc.*
	
	• Description of subsurface water resources including: aquifers and their areal extent, recharge/discharge zones, confining layers, major supply/recharge wells, piezometric surfaces, perched water zones, etc.*
		• For each surface water body:
		  – identification code
		  – type (river, stream, lakes, pond, channel, ditch, etc.)
		  – mean and extreme daily water elevation or flow
		  – location on installation grid map
		• Surface drainage patterns on installation grid map
		• For each aquifer:
		  – identification code on installation grid map
		  – areal and vertical location
		  – mean and extreme piezometric surfaces
		  – location of supply wells and their pumping rates
		  – location of recharge and discharge zones
		  – location of confining layers (areal and vertical)
		• For each monitoring location not associated with a waste site:
		  for each aquifer tapped:
		  – transmissivity
		  – storage coefficient
		  – hydraulic gradient
		  – permeability
		  – effective porosity
		  – dispersivity
		  – vertical conductivities of confining layers
			• For each surface water body:
			  – identification code
			  – type (river, stream, lake, pond, channel, ditch, etc.)
			  – mean and extreme daily water elevations or flows
			  – location on site grid map
			• Surface drainage patterns on site grid map
			• For each aquifer:
			  – identification code on site grid map
			  – areal and vertical location
			  – mean and extreme piezometric surfaces
			  – location of supply wells and their pumping rates
			  – location of recharge and discharge zones
			  – areal and vertical location of confining layers
			• For each monitoring location not associated with a waste site:
			  for each aquifer tapped:
			  – transmissivity
			  – storage coefficient
			  – hydraulic gradient
			  – permeability
			  – effective porosity
			  – dispersivity
			  – vertical conductivities of confining layers

*Narrative

Table 1. Proposed Data Base Contents (continued).

Data Category	Specific Data Requirements		
	Regional	Installation and Environs	IRP Waste Disposal Site
Water Quality and Sampling Results	• General water quality (surface and subsurface)*	• Records for each individual monitoring location not associated with an IRP site: for each sample; – sampling date – pumping duration – sampling depth – water table elevation – physical/chemical/biological analyses (STORET codes, concentrations, etc.) • All applicable water quality standards, criteria, guidelines, etc.	• Records for each individual monitoring location associated with an IRP waste site: for each sample; – sampling date – pumping duration – sampling depth – water table elevation – physical/chemical/biological analyses (STORET codes, concentrations, etc.)
History		• History of installation* • Chronology of installation missions	
References	• Applicable publications, reports, etc.*	• Applicable publications, reports, etc.*	• Applicable publications, reports, etc.*

*Narrative

Table 2. General Information Requirements.

Information Category	Components
Status Summaries	• Number of data entries for each item • Sampling dates • Sampling locations

Management Summaries	• Graphical representations
	   – histograms
	   – cumulative frequency
	• Appearance of items
	  (e.g., list of contaminants appearing on an installation)
	• Violations of standards, criteria, etc.
	• Recommended actions
	• Narratives

Statistical Summaries	• Maximums and minimums
	• Arithmetic means
	• Standard deviations
	• Regression coefficients
	• Correlation coefficients
	• Confidence intervals
	• Analysis of variance
	• Appropriate test statistics
	• Graphical representations
	   – histograms
	   – cumulative frequency

Data Reports	• Listings
	• Graphical representations
	   – variations with time
	   – variations in two and three dimensions

Formatted Model Input	• Model 1 (Not determined
	            as of
	• Model 2 this writing
	        •
	        •
	        •

are inseparable, but the distinction is important to the structure of the overall system. Each is a preliminary list that will probably change as the IRP effort matures and gains experience.

Each request for a summary or listing will call for specific subsets of the data base. These subsets should be defined by one or more of the categories and types of data listed in Table 1. For example, the user should be able to request the mean concentration for a particular contaminant detected at all sites within, say, the state of Florida or the correlation coefficient between two contaminants.

Basic System Structure

The identification of the demands on the IRPIMS and the associated information requirements is essential to the design of a successful system. The final task was to build upon these items and develop the basic system structure. However, care was taken not to "overspecify" the system structure. There are many excellent software packages on the market for data management and information processing. Therefore, only the level of specificity to insure that the IRPIMS does what is necessary is described here. The details will be left to those charged with the task of constructing the system. By creating this basic structure, environmental professionals in the Air Force are more likely to receive a system tailored to the job at hand. In general, it is essential that the users closely oversee (and if possible, participate in) the construction of an information management system. A system that performs the tasks required of it but is somewhat inefficiently designed is probably more costeffective than a highly efficient system capable of a vast array of amazing, but useless or marginally useful, capabilities.

Ideally, a cost-benefit analysis should be performed to "optimize" system capabilities. However, in this case, a qualitative sense of what is justified, and what is not, was applied. A good measure of common sense and judgement is probably all that is required in cases similar to this. A very large system, having a significant impact on the organizaiton it serves, would probably require more serious study. The reader is referred to a paper by King and Schrems [7] for a tutorial discussion of cost-benefit analysis and its application to information system design and operation.

The design of an information management system should include an analysis of the hardware best suited to the task. However, in this case, the hardware configuration is mostly fixed. The hardware available to the OEHL is probably typical of that found within larger environmental science and/or engineering firms and it represents a fairly substantial investment that performs admirably for a wide variety of applications. It is doubtful that the cost of a new or significantly modified configuration could be justified by the additional benefits attributable to the IRP alone. Significant changes would have to be justified in a laboratory-wide study of computing needs.

The natural question arising from this situation is "Why not use the hardware of an external vendor?" It was felt that the IRPIMS should be an "in-house" system. A dynamic program such as the IRP needs to be adaptable to changing needs and, thus, so does the IRPIMS. It should be readily accessible for data entry or modification and software additions or alterations. Additionally, the changing nature of relationships

between the Air Force and external contractors and the normal problems of day-to-day interactions suggest that the IRPIMS should be under the control of Air Force personnel.

The IRPIMS will contain five major components: (1) data entry, (2) the data base management system, (3) data base, (4) information extraction or processing, and (5) output production. Each component is briefly discussed below and their interrelationships are shown in Figure 2. There is some overlap between some of these components but this breakdown provides a good basic structure.

Data entry involves the acceptance and verification of data from the various IRP studies and other sources. There should be enough flexibility to allow entry from a variety of machine-readable sources including punch cards, magnetic tape, or by terminal keyboard. The verification procedures should, as a minimum, check for syntax errors, compatibility and consistency with other data, and for adherence to acceptable bounds.[5,8] The physical entry of the data into the data base will be handled by the data base management system as will any modifications to the data already within the system.

A good data base management system is essential to any information management system. Perhaps its most important function is to isolate the data base from the other portions of the system.[9,10,11,13] In other words, the data base is made independent of the data entry, information extraction, and output production software programs. This allows these components to be modified without affecting the data base.

A data base management system is classified by the manner in which it structures the data base.[10] These structures are generally classified
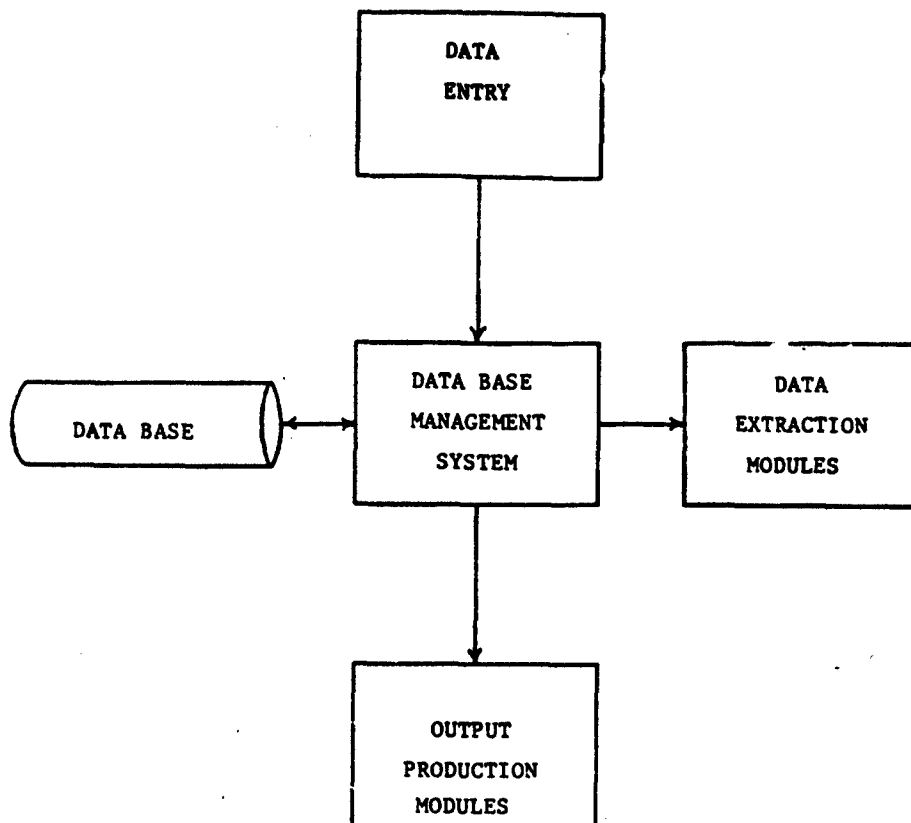
```
            ┌──────────────┐
            │    DATA      │
            │    ENTRY     │
            └──────┬───────┘
                   │
                   ▼
┌───────────┐  ┌──────────────┐  ┌──────────────┐
│           │  │  DATA BASE   │  │    DATA      │
│ DATA BASE │◄─┤  MANAGEMENT  ├─►│  EXTRACTION  │
│           │  │   SYSTEM     │  │   MODULES    │
└───────────┘  └──────┬───────┘  └──────────────┘
                      │
                      ▼
               ┌──────────────┐
               │   OUTPUT     │
               │ PRODUCTION   │
               │  MODULES     │
               └──────────────┘
```

Figure 2. Basic structure of the IRPIMS.

as hierarchic, network, relational, or semantic. Combined structures (e.g., hierarchic/relational) are also possible. A detailed discussion of these techniques is well beyond the scope of this paper. Most data base management systems used in environmental applications are hierarchical and/or relational.[6,9,8,13,16] Briefly, a hierarchic structure is one in which data are arranged such that any particular data item may have a number of related descendants, but no item may have more than one parent. Relational structures, as the name implies, rely on associations between data items. In a very simplistic sense, the structure can be likened to that of a table with each column representing a specific attribute and each row corresponding to an association. The table entries represent the data items. The interesting feature of all structures is that they really just attempt to model the world from which the data are collected.[20] There are a number of excellent data base management systems on the market.[6,9,16,13] The only restriction imposed by this study is that the one selected meet the overall needs of the IRPIMS at a reasonable cost.

The data base will be physically divided into several files in a way that will facilitate the updating and retrieval of data. The contents of these files are strongly suggested by the classification shown in Table 1. However, this will be influenced by the selection of the data base management system.

The data base management system also serves as the link between the data base and the information processing, data entry, and output production algorithms. More generally, it allows the user to retrieve, update, insert, and delete data from the data base.[13] At a more basic

level, the data base management system maps the data as stored in the computer to a form more familiar to the user or his application programs.

Information processing involves analyzing user queries and formulating and manipulating the data to meet these queries. The important requirement here is that the procedures be as modularized as possible. In other words, closely related types of information should be produced by specific, independent software modules. The modular approach facilitates the debugging, modification, and creation of processing software and allows the system to be readily tailored to the needs at hand. This approach also makes it much easier to effectively use "off-the-shelf" software. All software should be written in a familiar language (e.g., FORTRAN, BASIC, PL/1, etc.) in order to ease maintenance and modification. The types of information desired of the IRPIMS were outlined in Table 2.

Output production is involved with the visual display of information. The information required by the IRP (see Table 2) is not terribly sophisticated. Many of the requirements can probably be met with currently available software. Again, modularization is important if modifications and additions are to be readily accomplished. In addition to ordinary sequential and tabular forms of output, a moderate level of graphical capability is indicated by the needs outlined in Table 2.

One topic that cuts across the basic structure is the question of responsiveness. Faster response times to user queries require a more sophisticated and, thus more costly system. The IRP is not generally dealing with situations that require immediate information needs. Rapid response is desirable for a system used in environmental crisis management (e.g., toxic material spills) but not in a program designed to correct the

deleterious effects of past disposal practices. Therefore, the IRPIMS
should possess both real-time (or interactive) and batch processing
capabilities for making information queries or requests, producing status
summary reports (see Table 2), and entering and revising data in the data
base. However, all other user-system communications can probably be
handled in a batch mode. This is not intended to place firm restrictions
on the final system design but to again emphasize the need to justify
system capabilities in terms of the benefits delivered.

V. IMPLEMENTATION

The conceptual design that was outlined in the last section will
guide the detailed design, construction, and implementation of the IRP
Information Management System. The current plan is to have an experienced
external contractor perform these tasks. However, it will be necessary to
deliver items in a particular order. Phase II efforts have already begun
at a few installations. Therfore, in order to minimize encoding costs,
the most pressing need is for the data input formats and associated codes
(i.e., identification codes, parameter codes, etc.) to be developed and
disseminated to the various Phase II efforts.

Concurrently, the system software packages will be developed and
tested with the early Phase II results serving as excellent test data.
The first step will involve will be the selection and testing of a data
base management system. Because there are many excellent packages already
available this effort will probably involve matching one to the needs
outlined earlier; no significant software development is expected. The
various data entry, information processing, and output packages follow the
selection of the data base management system. Encouragement will be given

to the use of standard software routines available in the marketplace. A
complete set of documentation will also be developed so that Air Force
personnel can effectively use and maintain the entire system.

The expected completion date is mid-1985, barring any unforeseen
problems. The data input formats and codes should be in place by the end
of 1984. This schedule will allow most Phase II data to be transmitted in
the required format and provide the tools necessary to proceed with the
Phase III and IV activities in a timely manner.

VI. SUMMARY AND RECOMMENDATIONS

The IRP Information Management System will provide personnel at
the Occupational and Environmental Health Laboratory, and other groups in
and out of the Air Force, with a valuable tool for evaluating data gained
in an important and comprehensive environmental monitoring program. The
purpose of this study was to identify the demands that will be placed on
the system, the information needed to satisfy those demands, and the basic
system structure. In so doing, a set of guidelines have been established
for the construction and implementation of the system. This helps to
insure that the system will meet the needs of the IRP in a cost-effective
manner. The author hopes that this paper will aid other groups developing
similar information management systems by outlining one approach to the
problem.

The true value of a system such as this is, of course, the infor-
mation it contains. The IRPIMS will not only meet immediate needs but
also provide a valuable source of information for future research in the
fields of hazardous waste management, pollutant transport, and ground
water modeling.

REFERENCES

1. Pye, V.I. and Patrick, R., "Ground Water Contamination in the United States," <u>Science</u>, Vol. 221, August 19, 1983, pp. 713-718.

2. "DoD Installation Restoration Program," Defense Environmental Quality Program Policy Memorandum (DEQPPM) 81-5, December 11, 1981.

3. Lindenberg, B, "Air Force Installation Restoration Program: Making a Good Faith Effort," <u>Engineering and Services Quarterly</u>, Air Force Engineering Services Center, Winter 1982-1983.

4. "Installation Restoration Program Phase II Management Concept," presented at the Bioenvironmental Engineering Symposium, May 1984.

5. Haseman, W.D., Lieberman, A.Z., and Whinston, A.B., "Water Quality Management and Information Systems," <u>Journal of the Hydraulic Divisions</u>, ASCE, Vol. 101, No. HY3, March, 1975, pp. 447-493.

6. Everett, L.G., <u>Groundwater Monitoring</u>, General Electric Company, Schenectady, New York, 1980.

7. King, J.L. and Schrems, E.L., "Cost-Benefit Analysis in Information Systems Development and Operation," <u>Computing Surveys</u>, Vol. 10, March, 1978, pp. 19-34.

8. Mercer, M.W. and Morgan, C.O., "Storage and Retrieval of Ground-Water Data at the U.S. Geological Survey," Geological Survey Circular 856, U.S. Geological Survey, 1982.

9. Ross, R.G., <u>Data Base Systems: Design, Implementation, and Management</u>, AMACOM, New York, New York, 1978.

10. McGee, W.C., "Data Base Technology," <u>IBM Journal of Research and Development</u>, Vol. 25, No. 5, September, 1981, pp. 505-519.

11. Scheuermann, P., "On the Design and Evaluation of Data Bases," <u>Computer</u>, Vol. II, February 1978, pp. 46-55.

12. Blasgen, M.W., "Database Systems," <u>Science</u>, Vol. 215, February 12, 1982, pp. 869-872.

13. Mann, C.O., "Development of a Source Emission Data Base Design for the Aerometric Information Reporting System," <u>Journal of the Air Pollution Control Association</u>, Vol. 32, No. 10, October, 1982, pp. 1021-1024.

14. Larson, D.W. and Bingham, T., "Conversational Water Quality Data Retrieval System," <u>Journal of the Water Resources Planning and Management Division</u>, ASCE, Vol. 107, No. WR1, March, 1981, pp. 239-243.

1984 USAF-SCEE SUMMER FACULTY RESEARCH PROGRAM

Sponsored by the

AIR FORCE OFFICE OF SCIENTIFIC RESEARCH

Conducted by the

SOUTHEASTERN CENTER FOR ELECTRICAL ENGINEERING EDUCATION

FINAL REPORT

THE CYTOTOXIC EFFECTS OF TRIMETHYLPENTANE ON RAT RENAL TISSUE

Prepared by:	Dr. William N. Norton
Academic Rank:	Associate Professor
Department and University:	Department of Biological Sciences Southeastern Louisiana University
Research Location:	Aerospace Medical Research Laboratory Toxic Hazards Division, Pathology Branch
USAF Research:	Dr. David R. Mattie
Date:	August 10, 1984
Contract No.:	F49620-82-C-0035

THE CYTOTOXIC EFFECTS OF TRIMETHYLPENTANE

ON RAT RENAL TISSUE

by

William N. Norton

ABSTRACT

The aliphatic hydrocarbon 2,3,4 trimethylpentane induced
cytopathological renal lesions of the proximal convoluted tubule of the
adult male rat. No discernable cellular alterations were noted among the
hepatocytes examined. Three groups of 9 experimental organisms each
received the hydrocarbon by gavage administration twice weekly at a
concentration of 1.5 ml/kg body weight. The concentration proved to be
non-lethal. At each of the respective periods of 1, 2 and 4 weeks
subsequent to the initial exposure, 9 experimental and 5 control animals
were sacrificed. The kidneys and liver were excised and processed for
electron microscopy. The manifestations of toxicity were evident among
all organisms analyzed with the severity and extent of cellular
alterations a function of the duration of exposure. There were no
noticable aberrations among the cellular components of the glomeruli
examined from experimental organisms. The most prominent feature of
altered cells among the proximal convoluted tubules was the presence of
large membrane-bound granules. The structures were angular in contour
with the interior charcterized by a periodicity of parallel repeating
units. Focal sites of cellular degradation along the length of the
proximal tubule appeared to result in the release of cytoplasmic
organelles, nuclei and granules. In addition, whole cells were detached
from the basal lamina and presumably passed into the tubular lumen.

ACKNOWLEDGEMENT

I. INTRODUCTION

My research endeavors during periods as a graduate student, National Institute of Health Postdoctoral Fellow and University Professor have dealt with cellular biology. I was selected as an Air Force Summer Faculty Research Associate primarily because of my experience in the disciplines of cytopathology and electron microscopy. I am familiar with and have utilized a multiplicity of techniques related to both transmission and scanning electron microscopy.

With regard to my previous accomplishments, I have received national research awards and research grants pertaining to cytopathological and cytological studies from the National Science Foundation and the Air Force Office of Scientific Research. My research efforts have resulted in over 20 publications in national and international journals. Presently I am President of the Louisiana-Mississippi Society for Electron Microscopy and Director of the Research Center for the College of Science and Technology at Southeastern Louisiana University.

The Pathology Branch of the Toxic Hazards Division of the Air Force Aerospace Medical Research Laboratory (AMRL) investigates the potential pathological properties of a variety of chemicals and solutions which ar sed by the Air Force. The Branch employs several animal model systems and a diversity of administrative techniques to determine the specific sites of lesions both at the gross and cellular levels. A chemical of particular interest to the Toxic Hazards Division is trimethylpentane because of its ability to induce renal lesions which are similar pathologically to those obtained as a result of exposure to

several hydrocarbons present in both aviation fuels and conventional gasoline. The Toxicology, Pathology and Biochemistry Branches of the Toxic Hazards Division of AMRL for the past several years have been attempting to ellucidate the various toxicological consequences of exposure to hydrocarbons.

A diversity of branch chain hydrocarbons induce renal lesions among pre-mature male rats.[1] The lesions are characterized by an accentuated accumulation of hyaline droplets in the cytoplasm of proximal tubular epithelial cells.[1] Relatively low concentrations of hyaline droplets have been reported in cells of the proximal tubule of sexually mature rats.[2] The incidence of droplets has been correlated with the level of proteinuria, which in the adult male rat, has been recognized as a sexual characteristic feature since 1933.[3] The primary protein associated with urine of the adult male rat has been characterized as having a molecular weight of 26,400 Daltons[4], and has been described as $\alpha 2\mu$ globulin in the immunoelectrophoretic nomenclature.[5]

II. OBJECTIVES

The primary objective of the proposed investigation is to determine the cytopathological effects of trimethylpentane on rat hepatocytes and renal proximal tubules. Specifically, the study is designed to analyze:

(1) Cellular organelles for evidence of degradation or alteration.

(2) The fine structure of cytoplasmic granules induced by the hydrocarbon.

108-5

(3) The corticomedullary junction which represents the site of the renal lesion.

(4) The organelle content of hepatocytes to monitor for evidence of cytopathology.

III. PROCEDURE

Adult male Fischer rats were divided into experimental and control groups of 27 and 14 animals respectively. Three groups of 9 experimental organisms each received 2,3,4 trimethylpentane by gavage administration twice weekly at a concentration of 1.5 ml/kg body weight. The control animals received an equivalent dose of tap water.

Nine experimental and 5 control animals were sacrificed at each of the respective periods of 1, 2 and 4 weeks subsequent to the initial exposure. The kidneys were chemically fixed by means of perfusion via the aorta with a 2% glutaraldehyde solution buffered with 0.1M sodium cacodylate (pH 7.4). The liver was excised prior to perfusion, minced and fixed in a 6% glutaraldehyde solution buffered with 0.1M sodium cacodylate (pH 7.4). All tissues were post fixed in buffered 2% osmium tetroxide. The specimens were dehydrated in a graded series of ethanol and embedded in Epon 812. The tissues were sectioned with a Richert ultramicrotome and examined on a JEOL 100B transmission electron microscope.

IV. CONTROL TISSUE

The primary functional cell of the proximal convoluted tubule was rectangular to cuboidal in configuration with distal microvilli which projected into a central lumen. Proximally, the plasma membrane

invaginated to form narrow channels which contained cylindrical mitochondria. Within the cytoplasm were arrays of rough endoplasmic reticulum and polysomes. Spherical membrane-bound lysosomes were sparsely distributed. Desmosomes were evident at the proximal and distal regions of adjacent cells. The spherical nuclei were characterized by regions of peripherally-bound heterochromatin and dispersed euchromatin. The nucleoli were compact structures consisting of fibrillar and granular components. The basal lamina was comprised of a relatively thin amorphous layer of material covering the proximal surface of the cells.

V. EXPERIMENTAL TISSUE

There were no discernable alterations among the cellular components of the glomeruli observed from the experimental organisms. The basal lamina did not appear to be altered in thickness. Multivesiculated blebs protruded from both the fenestrated endothelial lining and the podocytes. However, blebs of a similar nature also were evident in control kidneys.

Epithelial cells forming the boundary of the Bowman's capsule appeared normal. The cytopathological effects of trimethylpentane on cells of the proximal convoluted tubule appeared to be a function of the length of exposure. In essence, the manifestations of toxicity were evident at the earliest period analyzed with severity and extent of cellular alterations increasing as the duration of exposure progressed. The most pronounced feature of exposed cells was the presence of large, angular, pleomorphic electron-dense granules which were membrane-bound.

The inner contents displayed a high degree of order with a parallel system of units indicating periodicity. The concentration, size and position of the granules varied among the cells.

The cytoplasm of cells forming the proximal tubule displayed a gradation of electron density. Micropinocytotic vesicles containing electron-dense material formed along the distal plasma membrane at the base of microvilli. Vacuoles of various diameters were evident, and focal sites of mitochondrial degradation were noted. There were no observable alterations of the nuclei or nucleolar constituents. The basal lamina encompassing the tubules appeared swollen with no evidence of dissociation or fragmentation. At various sites the basal lamina invaginated and followed the contour of the convoluted plasma membrane.

Focal sites of cellular degradation were noted along the length of the convoluted tubule. The affected cells were characterized by a progressive loss of microvilli, autolysis of mitochondria and various degrees of fragmentation of the distal plasma membrane. Regions were noted where cells appeared to detach from the basal lamina. Regions of plasma membrane fragmentation were evident among cells still bound to the basal lamina. Extensive degradation of mitochondria was observed in the detaching cells. Cellular fragments, isolated nuclei, membrane-bound granules and intact cells were present along the length of the proximal tubule lumen. Lesions at the corticomedullary junction were manifested in the form of distended tubules which appeared to result from the sequestering of cellular debris.

In comparison to control hepatocytes, no discernable cellular lesions or alterations resulted from exposure to the hydrocarbon. There appeared

to be some change in the smooth endoplasmic reticulum system; however, definitive results would be possible only if a morphometric analysis was conducted on the system.

VI. RECOMMENDATIONS

A number of investigators have suggested that the cytopathological effects of trimethylpentane and/or its metabolites may be related to the metabolism of the protein $\alpha 2\mu$ globulin. The biosynthesis of $\alpha 2\mu$ globulin occurs in the liver. Although the precise site of trimethylpentane metabolism has not yet been determined, in all probability the chemical is initially oxidized in the liver. Morphometric determinations at the electron microscopy level enables the investigator to conduct a statistical analysis of precise membrane bound systems. A morphometric analysis of both the rough and smooth endoplasmic reticulum systems may indicate whether significant increases in the biosynthetic and oxidative processes nave resulted from exposure to trimethylpentane.

Tritiated trimethylpentane may be administered to adult male rats to determine the initial and subsequent sites of accumulation within the experimental organism. Of particular interest would be the determination of whether trimethylpentane is associated with renal granules or hyaline droplets which proliferate as a result of exposure to various hydrocarbons. The tissues would be analyzed by electron microscopy to ellucidate the particular organelle associated with trimethylpentane or its metabolites.

An analysis of the acid phosphatase activity normally associated with lysosomes of the proximal convoluted tubule may indicate whether

trimethylpentane impacts on the degradative capabilities of the kidney. If such a phenomenon transpires, the proximal tubule may be incapable of metabolizing $\alpha 2\mu$ globulin, and as a result the latter may accumulate within secondary lysosomes until cytological damage ensues.

Considering the three recommendations it is my contention that the monitoring of tritiated trimethylpentane as a function of time would provide the most meaningful and supportive information. With this thought in mind I intend to apply for a Research Initiation grant, and submit as the primary objective the determination of tritiated trimethylpentane deposition in the adult male rat.

REFERENCES

1. R.H. Bruner, "Histopathologic Findings in F-344 Rats Exposed Intermittently For One Year to JP-10 Vapors and Held For Long-Term Oncogenic Studies," U.S. Air Force Technical Report No. 470-471. Aerospace Medical Research Laboratory, Wright-Patterson Air Force Base, Ohio, 1982.

2. J. Logothetopoulos and K. Weinbren, "Naturally Occurring Protein Droplets in the Proximal Tubules of the Rat's Kidney," Brit. J. Exper. Path., Vol. 36; pp. 402-406, 1955.

3. M.E. Bell, "The Natural Occurrance of Proteinuria in the Male Rat," J. Physiol., Vol. 79, pp. 191-196, 1933.

4. A.K. Roy, O.W. Neuhaus and C.R. Harmison, "Preparation and Characterization of a Sex-Dependent Rat Urinary Protein," Biochem. Biophys. Acta., Vol. 127, pp. 72-81, 1966.

5. A.K. Roy and O.W. Neuhaus, "Identification of Rat Urinary Proteins by Zone and Immunoelectrophoresis," Proc. Soc. Exp. Biol. Med., Vol. 121, pp. 894-899, 1966.

1984 USAF-SCEEE SUMMER FACULTY-GRADUATE STUDENT SUMMER
SUPPORT PROGRAM

Sponsored by the

AIR FORCE OFFICE OF SCIENTIFIC RESEARCH

Conducted by the

SOUTHEASTERN CENTER FOR ELECTRICAL ENGINEERING EDUCATION

Final Report

Computer-Based Optimization Algorithm
for LOGAIR Cargo Allocation

Prepared by: Dr. Kendall E. Nygard, Associate Professor
                                       and Director of Operations Research
                                    Timothy R. Downes, Graduate Student
                                       Researcher

Department and
    University: Division of Mathematical Sciences,
                                    North Dakota State University.

Research Location: Air Force Logistics Command, Directorate
                                     of Management Sciences (XRS)
                                    Wright-Patterson AFB, Ohio

USAF Research
    Contact: Mr John Madden

Date: August 10, 1984

Contract No.:   F49620-82-C-0035

Computer-Based Optimization Algorithms
for LOGAIR Cargo Allocation

by

Dr. Kendall E. Nygard
Timothy R. Downes

Abstract

This report describes a mathematical formulation for modeling the LOGAIR
system. It also discusses other contributions made during the summer
research program.

The LOGAIR system is a privately contracted airlift system prcviding
daily air cargo service to 56 bases in the continental United States
(CONUS). The Air Force manages and controls the operation which uses 16
separate routes. Allocation of cargo to system capacity is presently
handled manually by controllers stationed at WPAFB and various Air
Logistics Centers located elsewhere.

Because of the limited efficiency of manually allocating cargo, and the
great potential for human error, a way of mathematically modeling the
allocation process and incorporating this model into a computer-based
allocation system is investigated. The discussion centers on how certain
aspects of the allocation process can be modeled as a multi-period
generalized assignment problem, while other aspects could be modeled as a
multicommodity capacitated transshipment problem.

Although the above formulations are difficult combinatorial optimization
problems, recent studies suggest that the allocation models could be
solved daily on a microcomputer. The mathematical models developed to
date are presented and suggestions made for further research in
development of the model and for implementing this model as the basis of
a computer-based allocation system.

Acknowledgements

I. INTRODUCTION

Many problems of both practical and theoretical importance involve finding combinations of variables which provide optimal or near optimal solutions given an objective function and a specific set of constraints. For the Air Force in particular, one such problem is the daily task of allocating cargo to available airlift capacity in the LOGAIR (Logistics Airlift) system.

LOGAIR exists to provide fast transportation of high priority cargo among 56 Air Force bases in the Continental United States (CONUS). As shown in Figure 1, five Air Logistics Centers (ALC's) located at the Kelly, Tinker, Hill, McClellan and Warner-Robbins Air Force Bases as well as Wright-Patterson AFB (WPAFB) serve as cargo interchange points with feeder routes emanating from each location. Trunk routes connect the ALCs, WPAFB and points of embarkation at McGuire, Dover and Travis Air Force Bases. Allocation to these routes is made manually by controllers at WPAFB and some of the ALCs.

As Figure 1 suggests, allocation of cargo to the LOGAIR system is a complex task due to the enormous number of ways that pallets can be assigned to aircraft. The problem is complicated by multiple types and priorites of cargo pallets and types of aircraft. In addition, all bases must be adequately serviced and transit times must meet Air Force requirements. The complexity of the problem limits the efficiency of a manual allocation system, but lends itself to some degree of mathematical modeling and automation.

In an effort to model the more complex combinatorial characteristics of the cargo allocation problem, the authors have spent 10 weeks learning much of the operation of the LOGAIR system and developing preliminary models which reflect particular aspects of the allocation process. This paper describes these preliminary models, their use in a computer-based allocation system and the potential benefits of such a system. In addition, other contributions made to the AFLC during the same 10 week period are briefly discussed.

UNITED STATES AIR FORCE LOGISTIC AIRLIFT
ROUTE STRUCTURE
EFFECTIVE 1 OCTOBER 1983
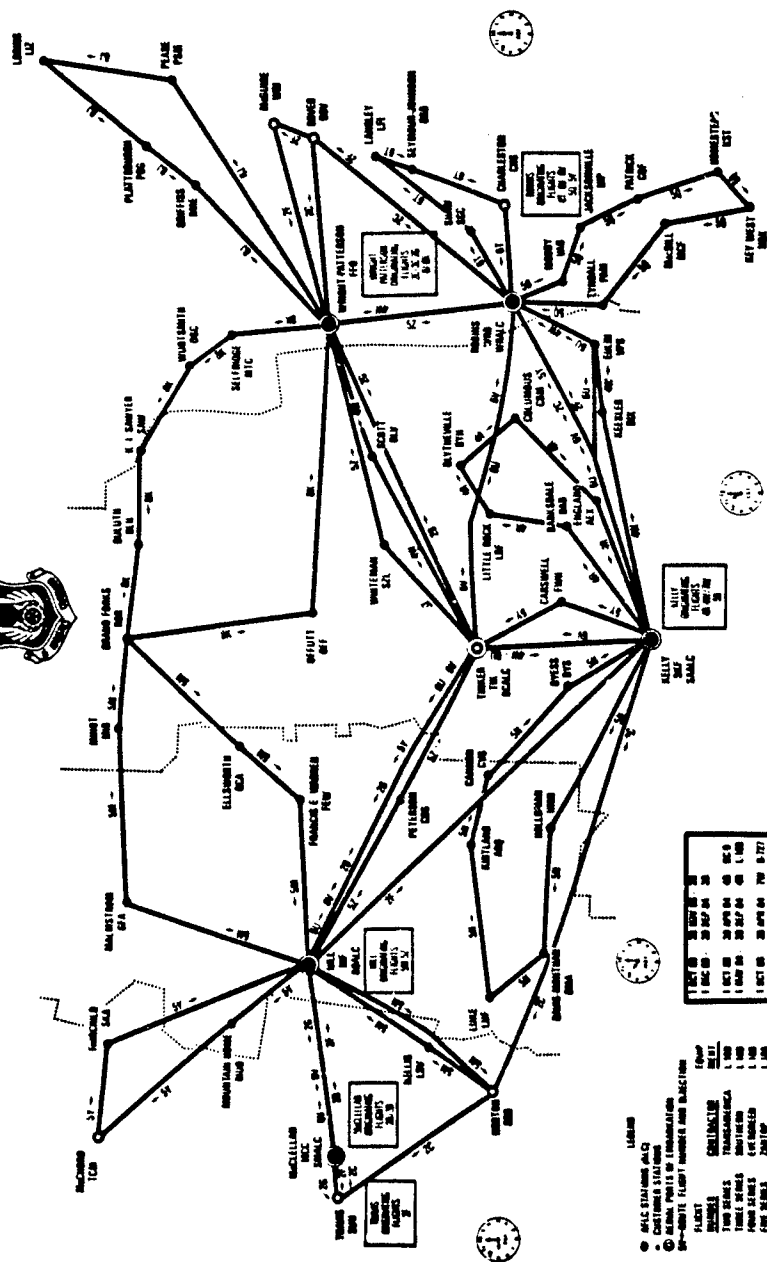
FIGURE 1

II. OBJECTIVES

The objective of this study was to develop a mathematical model for the LOGAIR cargo allocaton process. This model would be the basis for a computer-based on-line allocation system.

III. EVALUATION of PRESENT MANUAL ALLOCATION PROCESS

Because of the complexity of the cargo allocation process, the efficiency of a manual allocation system is limited. There are three basic reasons for this.

First, even the most experienced human controllers cannot simultaneously consider the enormous number of ways that the pallets could be assigned on a given day. As a result, it is frequently the case that allocations which move more cargo exist, but are overlooked by the controller. An underlying mathematical model could identify allocations which improve aircraft utilization and move more cargo.

Second, under the present entirely human allocation process, arithmetic errors tend to occur, necessitating backtracking and double checking at times when their human skills need to be more creatively used. A computer-based system would eliminate much of this error.

Finally, the ten LOGAIR controllers tend to use personalized allocation schemes, which produce a variety of final allocations. A mathematical model would add consistency to the process, making all persons involved more comfortable with the allocations, making it easier for supervisors to revie allocations and to train new controllers.

IV. THE MATHEMATICAL MODEL

During the Summer of 1984, preliminary work on the mathematical model was carried out by the authors. Several characteristics of the problem appear in models which have been recently described in the literature by the author of this proposal and other researchers. These include the multi-period and multiple-choice knapsack problems (Faaland, 1981; Sinha and Zoltners, 1979), the generalized assignment problem (Nygard et al, 1984; Nygard and Nelson, 1983; Fisher and Jaikumar, 1981); and the multicommodity network flow problem (Kennington and Helgason, 1980, Rosenthal,1983). We now present some of our progress on the mathematical model. The following notation is adopted:

Indices and Index Sets

i = index of a base served by LOGAIR. i = 1, 2, ...,n, where n is the total number of bases in the entire LOGAIR System. For a particular flight f, n_f is the index set of bases served by flight f.

p = index of a priority class for airlift available cargo.

$p \in P = \{s,1,2\}$, where s is special high priority (MICAP and 999 cargo), 1 and 2 are military standard transportation priorities 1 and 2.

f = index of a LOGAIR route. $f \in F$, where F is the set of all routes.

k = pallet index. $k \in K_{ij}^p$, where K_{ij}^p is the set of priority p pallets at base i destined for base j.

Constants

NUM_{ij}^p = Number of priority p pallets at base i destined for base j.

CAP_f = Pallet capacity of the aircraft type which flies route f.

d_{ij} = Distance from base i to base j.

W_{ij}^{pk} = Weight of the kth pallet of priority p at base i destined for base j.

PR_p = Mathematical "weight" associated with priority p (chosen so that higher priority cargo is allocated first)

$C_{ij}^{pk} = d_{ij} * W_{ij}^{pk} * PR_p$ = Benefit of Shipping the kth pallet of priority p from base i to base j.

Variables

$$X_{ij}^{fkp} = \begin{cases} 1, & \text{if the } k^{th} \text{ pallet of priority p at base i destined for base j is allocated to flight f} \\ 0, & \text{Otherwise} \end{cases}$$

For a particular fixed route index f, consider the following mathematical model:

$$\text{Max} \quad \sum_{i=1}^{n} \sum_{j=1}^{n} \sum_{p \in P} \sum_{k \in K_{ij}^{p}} c_{ij}^{pk} * x_{ij}^{pkf}$$

Subject to:

$$\sum_{j=2}^{n} \sum_{p \in P} \sum_{k \in K_{1j}^{p}} x_{1j}^{pkf} \leq CAP_f$$

$$\sum_{j=3}^{n} \sum_{p \in P} \sum_{k \in K_{1j}^{p}} x_{1j}^{pkf} + \sum_{j=3}^{n} \sum_{p \in P} \sum_{k \in K_{2j}^{p}} x_{2j}^{pkf} \leq CAP_f \quad (1)$$

$$\vdots \qquad\qquad \vdots \qquad\qquad \vdots$$

$$\sum_{j=n} \sum_{p \in P} \sum_{k \in K_{1j}} x_{1j}^{pkf} + \sum_{j=n} \sum_{p \in P} \sum_{k \in K_{2j}^{p}} x_{2j}^{pkf} +$$

$$+ \ldots + \sum_{j=n} \sum_{p \in P} \sum_{k \in K_{n-1,j}^{p}} x_{n-1,j}^{pkf} \leq CAP_f$$

$$\sum_{k \in K_{ij}^{p}} x_{ij}^{pkf} \leq NUM_{ij}^{p} \qquad\qquad\qquad (2)$$

$$i,j = 1,2, \ldots, n_f ; p \in P$$

Each constraint in set (1) represents a leg of the flight, and ensures that aircraft pallet capacity is not exceeded. Note that the constraints model off-loading along the route as appropriate, so that the constraints are not fully cumulative as they are in a multi-period knapsack problem (Faaland, 1981). An additional constraint set similar to (1) is needed to ensure that the total weight the aircraft is allowed to carry is not exceeded.

Constraint set (2) ensures that the model allocates only pallets which are actually available for shipment. In practice, this model must be expanded to accommodate the two different sizes of pallets in use, and the regularly occuring need to link two or more pallets together in a train. Constraint set (2) can be modified and written with equations by adding a dummy flight which can absorb all excess pallets from each leg at an artifically high cost. The new constraints would be:

$$X_{ij}^{pkd} + X_{ij}^{pkf} = 1 \qquad i,j = 1,2,\cdots,n_f \, ; \, k \in K_{ij}^r \, ; \, p \in P$$

where d is the index of the dummy flight. The resultant model might then be called a multi-period generalized assignment model. The model extends the generalized assignment model because the pallet allocations use aircraft capacity on flight legs beyond the leg on which they are first allocated. The author of this proposal has implemented two state-of-the-art generalized assignment codes for use in vehicle routing (Nygard et al, 1984; Nygard and Nelson, 1983).

The above model could only handle a few of the existing LOGAIR routes, since most of the routes have flight legs in common and tradeoffs among flights need to be accomodated. An extension of the above model could simultaneously allocate a collection of flights with common legs.

To accomplish the extension, a network can be defined, with a node for each base, and arcs for the flight legs. Assume that common flight legs are coalesced into a single arc, with a capacity equal to the sum of all the component flight leg capacities. The cargo allocation problem can then be modeled as an integer multi-commodity capacitated transshipment problem on this network. In this formulation, adopt the following notation:

b_{iq} = Supply of pallets of type q at base i, where $q \in Q$, an index set of all pallet types. In this model, there is a pallet type for each origin-destination pair (i,j) and priority p. Negative supply values are used for demands at destination bases.

U_h = Joint capacity over all commodities of network arc h, where $h \in H$, an index set of arcs in the network.

F_i = Forward star of node i (Collection of all arcs which originate at node i).

R_i = Reverse star of node i (Collection of all arcs which terminate at node i).

D_{hq} = Disutility associated with a pallet of type q being transported over arc h (This is the negative of the aircraft utilization measure used in the first model).

With this notation, the following optimization problem can be
written:

$$\text{Min} \quad \sum_{h \in H} \sum_{q \in Q} c_{hq} x_{hq}$$

Subject to:

$$\sum_{h \in F_i} x_{hq} \quad - \quad \sum_{h \in R_i} x_{hq} \doteq b_{iq} \qquad h \in H, q \in Q$$

$$\sum_{q \in Q} x_{hq} \leq U_h \qquad h \in H$$

$$x_{hq} \geq 0 \text{ and integer} \qquad h \in H, q \in Q$$

The solution to this optimization problem yields a set of integer
cargo movements (flows) which maximize aircraft utilization. If
there is surplus capacity on a common flight leg, the existing
LOGAIR preferred flight list would be used to choose among the
aircraft. A dummy node and dummy arcs leading to it from supply
nodes would absorb excess supply and ensure feasible allocations
when aircraft capacity cannot handle all cargo waiting to be moved.
Like the first model, this formulation requires refinement to handle
weight as well as pallet count capacity, and additional variables to
model alternative pallet sizes and trains.

Both of the above formulations are difficult combinatorial
optimization problems. However, very recent progress on the
generalized assignment problem carried out by the author (Vygard et
al 1984, Vygard and Nelson, 1983) and on the continuous version of
the multi-commodity capacitated transshipment problem by others
(Rosenthal, 1985) suggest that this cargo allocation problem can be
solved to optimality on a microcomputer on a daily basis. Under
this proposal, the basic research needed to fully develop these
models would be carried out. The study will be complete with actual
coding and experiments carried out.

V. RECOMMENDATIONS

Both of the above formulations are difficult combinatorial optimization problems. However, very recent progress on the generalized assignment problem carried out by one of the authors (Nygard et al 1984, Nygard and Nelson, 1983) and on the continuous version of the multi-commodity capacitated transshipment problem by others (Rosenthal, 1983) suggest that this cargo allocation problem can be solved to optimality on a microcomputer on a daily basis.

The authors have submitted a proposal to conduct the research that is needed to fully develop these models and to implement them as part of a computer-based allocation system. We feel that, aside from benefits realized from standardizing allocation procedures, expediting the allocation process and reducing arithmetic errors, the proposed system could result in the following three basic types of benefits:

1. Decreased Need to Invest in Spares. Lower Order and Ship Times (OST) and retrograde time (DRT) can allow a reduction in the investment for spares needed to maintain the same level of readiness. A recent study carried out by Gambill of AFLC/XRS (Gambill, 1984) calculated potential cost savings in inventory investment for a range of OST and DRT values and an 80% availability level. This study indicates that a decrease of one day in OST and DRT corresponds to a cost decrease of about $34.9 million, or about 2.3 percent.

2. Increased Readiness. Assuming system costs are held constant, reductions in OST and DRT can help increase readiness. Even though readiness is a function of many factors and MICAP items are typically shipped within DoD standards for transit time (Van Valkenburgh, 1980; Wasem, 1983), some calculations which relate to readiness improvement are still possible. One part of the Gambill Study (Gambill, 1984) assumed constant costs and calculated increases in the availability of weapon systems which result from OST and DRT decreases. For example, with a one day decrease in OST and DRT, weighted total availability over all weapon systems increased from a baseline of 80% to a new level of 81.95%.

3. Decreased Direct Costs. When major cargo backlogs occur, additional flights called extra sections are employed to move the cargo. Use of the proposed mathematical model may occassionally eliminate the need for extra sections, saving the direct costs of fuel, contractor payments, and landing fees. These annual operating costs for the entire LOGAIR system are presently about $100 million per year. Eliminating, for example, a 2000 mile flight which costs $7.5/mi to operate would save $15,000 in operating costs.

VI. OTHER CONTRIBUTIONS

In addition to researching a cargo allocation model formulation, the authors also presented several technical reports discussing alternative approach to problems of immediate concern for AFLC personnel.

One report suggests improvements to the Logistics Management Institute (LMI) Aircraft Availability Model used by AFLC/XRS. This report recommends several computational techniques which can potentially decrease run-times of the model by taking advantage of structure occurring naturally in the data and by replacing a sequential search by a binary search.

A second report discusses a program designed and coded this summer. The purpose of the program was to compare two files created by the same model on two separate computer systems to see if both files contain identical data. A copy of the program along with appropriate documentation was submitted to AFLC personnel for review.

A third report proposed a generalized network model to simulate how aircraft availability relates to maintenance, distribution and procurement systems. A scaled-down model was presented to appropriate AFLC personnel along with a description of how this approach might be applied on a larger scale.

A final report addressed the Air Force Program Objective Memorandum (POM) assessment. The POM involves the need to relate the funding of different categories of support to warfare capability of specific weapons systems. The approach suggested in this report modeled, in a macro way, how various support activities result in levels of weapons systems, and the way levels of weapon systems combine to result in general wartime capability. The technique used was the analytic hierarchy process developed primarily by Thomas Saaty (Saaty, 1982).

The suggestions made in the first two reports will likely be implemented. The latter two reports were presented to help AFLC personnel maintain an awareness of techniques in the forefront of current research. Copies of these reports may be obtained from HQ AFLC/XRS.

REFERENCES

(1) Faaland, B., "The Multiperiod Knapsack Problem," Operations Research 29(3), 1981 pp 612-616.

(2) Fisher, M., "The Lagrangion Relaxation Method for Solving Integer Programming Problems," Management Science 27(1), 1981.

(3) Fisher, M., R. Jaikumar, and L. Van Wassenhove, "A Multiplier Adjustment Method for the Generalized Assignment Problem," preprint to appear in Management Science, 1984.

(4) Gambill, J. "Study for LOGAIR Hub Return on Investment" AFLC/XRS document, June, 1984.

(5) Kennington, J. and R. Helgason, Algorithms for Network Programming New York: Wiley, 1980

(6) Nelson, M., K. Nygard, J. Griffin and W. Shreve, "Implementation Techniques for the Vehicle Routing Problem," Computers and Operations Research, in press, 1984.

(7) Nygard, K., R. Walker and P. Greenberg, "Computational Experience with a Generalized Assignment-based Algorithm for Vehicle Routing," technical report presented at the TIMS/CRSA National Meeting, San Francisco, May, 1984.

(8) Rosenthal, R. "Resource Directive Multicommodity Flows Algorithms," talk presented at North Dakota State University under the Operations research visiting scholar series, November, 1983.

(9) Saaty, T. and L. Vargas, The Logic of Priorities , Boston: Kluwer-Nijhuff, 1982.

(10) Sinha, P. and Z. Zoltners, "The Multiple Choice Knapsack Problem," Operations Research 27(3), 1983 pp 503-515.

(11) Van Valkenburg, N. "LOGAIR Mark 2: An Alternative Logistics Airlift System," Air Force Journal of Logistics, Spring, 1980, pp 25-29.

(12) Wasem, V., LOGAIR: A Study to Determine the Feasibility of Implementing a Hub and Spoke Distribtuion Network for LOGAIR AFLC document, October, 1983.

1984 USAF-SCEEE SUMMER FACULTY RESEARCH PROGRAM

Sponsored by the

AIR FORCE OFFICE OF SCIENTIFIC RESEARCH

Conducted by the

SOUTHEASTERN CENTER FOR ELECTRICAL ENGINEERING EDUCATION

FINAL REPORT

LASER DAMAGE STUDIES IN PURIFIED AND PLASTICIZED POLYAKYLMETHACRYLATES

Prepared by: Dr. Robert M. O'Connell

Academic Rank: Assistant Professor

Department and   Department of Electrical and Computer Engineering
    University: University of Missouri-Columbia

Research Location: Frank J. Seiler Research Laboratory
                      Directorate of Aerospace Mechanics Sciences
                      Laser Effects Branch

USAF Research: Major Terrence F. Deaton

Date: September 20, 1984

Contract No: F49620-82-C-0035

LASER DAMAGE STUDIES IN PURIFIED AND PLASTICIZED POLYAKYLMETHACRYLATES

by

Robert M. O'Connell

ABSTRACT

Experimental studies were made of the effects of monomer filtration and plasticization on the laser damage properties of polymethylmethacrylate and related transparent polymers. The results show that both processes can significantly improve single-shot damage thresholds. The multiple-shot damage measurements were insufficient to draw any similar conclusions. A simple technique that uses scattered, depolarized helium-neon laser light to estimate the concentration of micron-sized impurities in liquids or solids was developed and found to be a reliable predictor of single-shot damage resistance.

I.   INTRODUCTION

The lightweight, low-cost, and dye-impregnable properties of transparent polymeric glasses (plastics) make them attractrive for use in high-power military laser systems, both as passive elements such as lenses, windows, and Q-switches, and as active dye laser hosts.[1] Until recently, however, the relatively low resistance that plastics have to damage by high power laser light had prevented their use in these applications. Now, work performed recently in the Soviet Union suggests that the laser damage resistance of plastics can be greated improved,[2] and that long-lived plastic-host dye lasers are now possible.[3]

In light of the Soviet work, a plastics laser damage program was begun in late 1982 at the Frank J. Seiler Research Laboratory (FJSRL). This SCEEE Fellow participated in the program during a one year leave-of-absence from the University of Missouri under the University Resident Research Program (URRP). During that time the FJSRL laser damage facility was designed, assembled and characterized, and used to study the laser damage properties of various commercially available plastics, including polymethylmethacrylate,[4] bisphenol-A polycarbonate,[5] and cellulose acetate butyrate.[5] These measurements revealed that commercially available plastics have significantly lower laser damage resistance than commerciallly available optical qualilty glasses.

Ways of improving the damage resistance of plastics have been studied by several Soviet groups, but as reported in a review of that work,[1] there is a good deal of disagreement among the published Soviet reports, as well as many omissions which both preclude duplication of their measurements and make it impossible to interpret their results unambiguously. What can be gleaned from the Soviet reports is that monomer purification to remove micron and sub-micron sized absorbing inclusions, and plasticization to lower the material's induced elastic limit can improve it's laser damage resistance. However, the precise role of each process in improving either single and/or multiple-shot damage behavior, and the related problem of the physics of the damage process are not yet well-established. Thus, follow-on work to the leave-of-absence has consisted of plastics synthesis at the University of Missouri and laser damage testing at FJSRL.

In light of two years' experience in plastics damage work both at FJSRL and at the University of Missouri, and in order to expedite work on the project, the SCEEE fellow was assigned to FJSRL.

II. OBJECTIVES

Plastic synthesis work at the University of Missouri began with a study of the effects of various purification schemes on the laser damage resistance of polymethylmethacrylate (PMMA). These schemes included careful repeated distillations and filtration with membranes of different pore size. This work was conducted by a student and continued through the summer with the intention that samples would be sent to FJSRL for damage testing late in the summer. The results of these measurements would enable a determination of the effects of monomer filtration after distillation on the damage properties of PMMA and provide some insight into the role that impurities of different size play in the laser damage process. This study constituted one objective of the SCEEE fellowship.

Since the effects of the other material improvement process, plasticization, on the laser damage properties of plastics had not yet been studied in the U.S., it was stipulated as a second objective of the fellowship.

Whether plasticized or not, the laser damage properties of plastics are related to the concentration of absorbing inclusions, i.e., dust, in the material. An estimate of the dust content of a monomer or polymer sample would thus enable both an evalution of the effects of our efforts to remove dust and allow conclusions to be drawn concerning dust content and laser damage properties of the polymerized, damage tested materials. Thus finding and implementing a scheme to estimate the dust content of a monomer or polymer sample become a third objective of the fellowship.

In summary, the objectives of the SCEEE fellowship were as follows:

(1) Determine the effects of monomer filtration on the laser damage properties of PMMA.

(2) Determine the effects of plasticization on the laser damage properties of various transparent polyalkylmethacrylates.

(3) Design and implement a simple scheme to estimate the dust content of monomer and polymer samples.

III. SCATTERED DEPOLARIZED LASER LIGHT FOR DUST CONTENT ESTIMATION

The need for a way to quickly and easily estimate the dust content in our monomer and polymer samples evolved as the summer's work progressed, and eventually become the third objective listed above. However, since the product of the work on that objective, a helium-neon laser probe, was used to characterize the materials studied during work on the other two objectives and must be mentioned frequently in discussing them, the approach and results to Objective 3 are discussed first.

In a theoretical study of the role of absorbing inclusions in laser damage,[6] it was estimated that particles with diameters ranging from 0.1-1.0 μm are the ones most likely to absorb enough energy from a laser pulse to cause catastrophic heating of the surrounding transparent dielectric matrix and damage it. Thus the problem was to derive a scheme to detect and count particles in this size range that are embedded in a matrix of much smaller molecular matter.

It is well-known[7] that polarized light of a given wavelength will Rayleigh scatter from particles very small compared to the wavelength of the light. This means that the original polarization will be retained by the scattered light and that, therefore, no light will Rayleigh scatter in the polarization direction, i.e., the direction of the electric field vector. It is also well-known[7] that particles with dimensions of the order of the light's wavelength will depolarize the light and scatter it in all directions, including that of the original electric field vector.

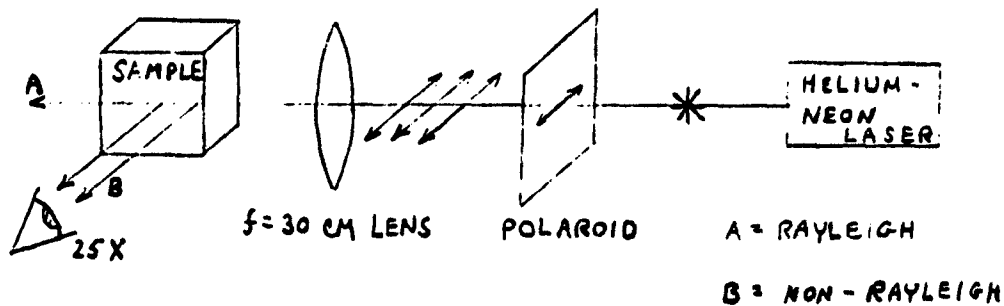These ideas were exploited with the arrangement shown in Figure 1.

$f = 30$ CM LENS   POLAROID   A = RAYLEIGH

B = NON - RAYLEIGH

Figure 1. Experimental arrangement for observing scattered depolarized helium-neon laser light

Helium-neon laser light was used because it's wavelength, 0.6328 μm, is "of the order" of the 0.1-1.0 μm sized particles to be detected and counted, and because it's red color permits simple visual observation of the particles. The beam was polarized with a sheet of polaroid, focused into the sample witn a 30 cm focal length lens to somewhat concentrate the beam, and observed with a 25X microscope mounted with it's observtion axis perpendicular to the scatter track and parallel to the electric field vector of the polarized light. This arrangement allowed observation of depolarized light from the micron-sized particles of interest against a minimized background of Rayleigh-scattered light from molecular matter and particles much smaller than those of interest. Thus the dust content of a sample could be estimated simply by counting the relatively bright scattering centers seen with the 25X microscope in the approximately 0.35 mm^3 volume occupied by a 5 mm length of scatter track.

This scheme proved to be most useful when it was used to estimate the relative dust content of two or more samples. For example, in a study of the effects of simple monomer purification (i.e., drying and single distillation) on the laser damage properties of PMMA[8], it was found that the purified sample had significantly greater resistance to laser damage than the unpurified sample. To confirm that the purification effort had actually been successful and could thereby be given credit for the improved damage resistance, the depolarized, scattered light scheme was used to estimate the relative dust content of the two samples. The unpurified material was found to contain approximately six times as many dust particles as the purified material, thereby establishing a direct correlation between dust content and susceptibility to laser damage. Similar results were obtained with the materials used in the work on Objectives 2 and 3. Details can be found in sections IV and V.

IV. THE EFFECTS OF MONOMER FILTRATION ON THE LASER DAMAGE PROPERTIES OF PMMA

In the above-mentioned study of the effects of simple monomer drying and distillation on the laser damage properties of PMMA[8], it was found that both the single- and multiple-shot behaviour could be significantly improved. The next step, and the subject of this objective, was to determine whether micropore filtration of the monomer prior to polymerization

would produce further improvement over distillation. Interestingly, researchers in another field have claimed that micropore filtration of distilled water actually leaves more particles of dimensions similar to that of the filter pore than it removes.[9] This would suggest that monomer filtration would not improve laser damage resistance.

To study this, three PMMA samples were synthesized at the University of Missouri and laser damage tested at FJSRL as part of the SCEEE fellowship. All three samples were made from carefully distilled monomer, a step which is necessary to remove hydroquinone inhibitor, but also eliminates a great deal of dust, as shown by the depolarized scattered light scheme with the samples used in the drying/distillation study[8] (see section III). Samples of the distilled monomer were then passed through a filter apparatus containing either no filter, a 0.40 μm filter, or a 0.22 μm filter, respectively. Polymerization was by ultraviolet initiation without any free-radical initiator. This method was found to be safer, cleaner, easier and faster than the thermal method used in Ref. 8, which required the use of a free radical initiator (a source of impurities).

Laser damage measurements were performed at FJSRL with the facility that has been described thoroughly in Ref. 4. Briefly, it consists of a 1.06 μm wavelength Q-switched Nd:YAG laser that provides 8 ± 2 nsec FWHM pulses with up to 300 mj/pulse at a pulse repetition frequency (PRF) of up to 10 pulses per second (pps). A 25 cm focal length lens focuses the beam into the test sample, and a collinear helium-neon laser beam is used to monitor damage. Careful knife-edge measurements of the focused 1.06 μm beam showed that its spatial profile is reasonably Gaussian in and near the focal plane with a $1/e^2$ radius (spot size) of 33 ± 1.7 μm and an associated focal volume (in PMMA) of approximately 0.01 mm^3. The spot size was determined by least-squares fitting a Gaussian profile to the numerically differentiated knife-edge data. The peak fluence level (J/cm^2) for each pulse was obtained by normalizing the measured spatial profile to the total pulse energy, which was measured calorimetrically. Based upon uncertainties in the spot size and the power meter used to monitor pulse energy, a standard deviation of 15% was obtained for these values.

For this work, laser damage was defined as a large enough permanent change in the material to be detected with the collinear helium-neon laser probe, which was found to be reliable in detecting damage sites as small as

5-10 μm in diameter. In addition to the laser probe, which suffers from high sensitivity to slight misalignment, the occurrence of damage was indicated by either a spark or flash, or by the appearance of one or more bright scattering centers in the beam path after irradiation.

To measure single-shot damage thresholds, defined as laser fluence levels (J/cm^2) with a 50% probability of causing damage in one pulse, approximately 10 sites in each test sample were irradiated with one pulse each at a given fluence level and evaluated, as discussed above, for the occurrence of damage. This process was repeated at several fluence levels. A plot of the resultant damage statistics is shown in Fig. 2 along with the
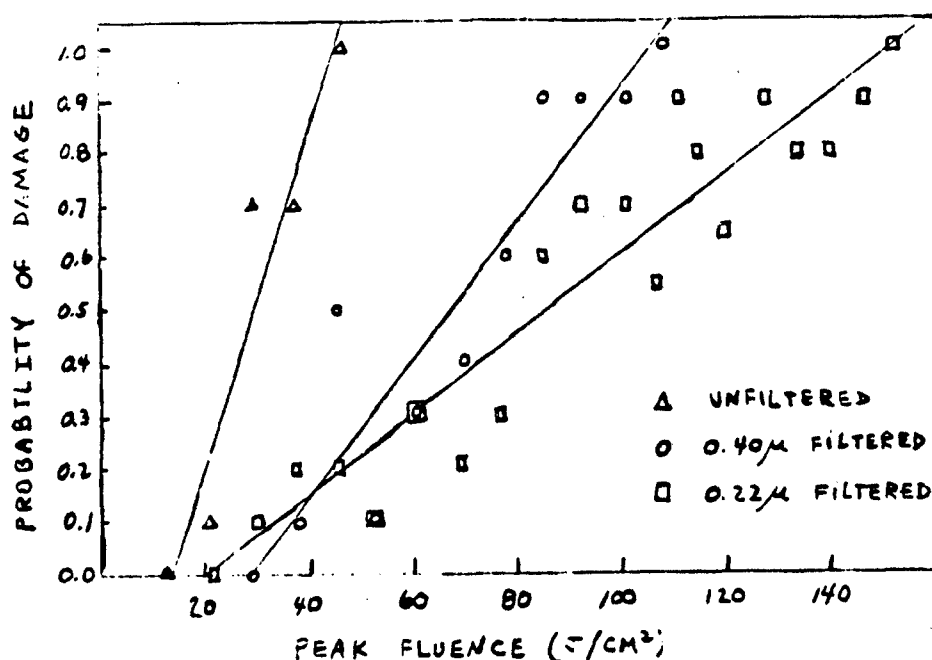

Figure 2. Single-shot damage statistics in the monomer-filtration study

results of least-squares-fitting (LSF) straight lines to the data. The statistical nature of the data is caused by the above-mentioned 15% standard deviation in the peak fluence values; by the subjectivity inherent in deciding whether damage occurred in marginal cases, which introduces no more than a 5% error in the damage probabilities; and by site-to-site variations in the material, as discussed in Ref. 8. The damage thresholds, obtained from the midpoints of the LSF lines, are given in Table 1 along

with the dust content of each sample, as determined with the depolarized scattered light scheme. Each dust content number in the table is the average of six readings taken with the scattered light probe.

TABLE 1. Dust Content and Single-shot Damage Thresholds of PMMA in the Monomer Filtration Study

Sample	Monomer Description	Dust Content (Particles/mm^3)	Single-shot Damage Threshold (J/cm^3)
E20	distill only	7.1	29
E22	distill and 0.4 μm filter	0.5	67
E24	distill and 0.22 μm filter	0.0	86

The data show a clear correlation between decreasing filter pore-size, significantly decresed dust content, and significantly increased single-shot damage thresholds. If these results are combined with that of reference 8, it can be concluded that micropore filtration can significantly reduce dust and improve single shot damage thresholds beyond, i.e., in addition to, the levels c improvement possible with distillation alone.[8]

It was not possible, in the time available, to extensively measure the multiple-shot damage behavior of all three of the samples listed in Table 1; only E-24, the cleanest and most single-shot damage-resistant one was tested and compared with the purified sample studied in Ref. 3.

Multiple-shot damage is that which occurs when a material is irradiated repetitively at laser fluence levels well below the single-shot threshold. To study the multiple-shot behavior of sample E-24, six sites were irradiated at one of several sub-threshold fluence levels and the number of pulses required to produce damage equivalent to single-shot damage

was recorded. The results of measurements made at laser PRFs of 1 and 10 pps are given in Table 2. For convenience, fluence levels are given both in absolute values (F) and as a fraction (F/F_{TH}) of the single-shot damage threshold (F_{TH}). As discussed elsewhere,[4] multiple-shot damage in PMMA is cumulative and grows slowly, especially at relatively low subthreshold fluence levels; thus there is some subjectivity in deciding when multiple-shot damage equivalent to single-shot damage has occurred. By comparing several single- and multiple-shot damage sites with 100x bright-field microscopy, it was determined that the helium-neon laser damage probe is a reliable damage indicator and greatly reduces the subjectivity in decision making. Thus, the numbers in Table 2 are accurate to within one or two shots at 1 pps and to within 10 to 20 shots at 10 pps.

TABLE 2. Site-to-site Results of Multiple-shot Damage Measurements in Sample E-24

Absolute Laser Fluence (J/cm^2)	Fractional Subthreshold Fluence(F/F_{TH})	No. of Pulses to Damage Each Site at 1 pps	Non-damaging Shots at 1 pps	No. of Pulses to Damage Each Site at 10 pps	Non-damaging Shots at 10 pps
32	0.36	91,50	250(4 sites)	13,50,35,30,40	1000(1 site)
16	0.18	80,50	250(4 sites)	100,130,60	1000(3 sites)
9	0.10	29,40	250(3 sites) 1000(1 site)	100,120	1000(4 sites)
4	0.04	70,160	250(4 sites)		1000(6 sites)

In Ref. 8, the 1 pps multiple-shot damage resistance of the material made from purified monomer was significantly greater than that of the material made from unpurified monomer. For example, whereas the unpurified sample damaged consistently within 30 shots at F/F_{TH} levels at or below 0.27, the purified sample always survived hundreds of shots without damage at comparable fluence levels. One useful way of describing a material's

multiple-shot damage resistance is in terms of the fractional subthreshold fluence level (F/F_{TH}) below which the cumulative damage process will not occur and the material will not damage. Since the unpurified material damaged so quickly at F/F_{TH} = 0.14, it's subthreshold "asymptote" must be well below this level. On the other hand, the purified material appeared to have an asymptote in the neighborhood of F/F_{TH} = 0.19 to 0.25.

The 1 pps data in Table 2 show that sample E-24 had no asymptote for F/F_{TH} levels as low as 0.04, a disappointing result. In fact, the material damaged in two of six indicated sites at each subthreshold fluence level, thereby giving very little indication of even approaching an asymptote. At 10 pps, the sample showed improved damage resistance with decreasing fluence levels, and an apparent asymptote at F/F_{TH} = 0.04. This behavior is more typical, but in light of the 1 pps results, it is somewhat comfusing because the PRF dependence seen in other studies[4,5,8] is not seen here. If the material has a 10 pps asymptote at F/F_{TH} = 0.04, it should have a 1 pps asymptote at an equal or greater F/F_{TH} level. The most plausible explanation for the discrepancy seen here is that an insufficient number of sites were irradiated to obtain a true statistical picture of the multiple-shot behavior of the sample. As explained in Ref. 8, a cleaner material will appear less uniform to a narrowly focused laser beam than a material that is not so clean because the probability of focusing on identical impurity/matrix environments from site-to-site is decreased in the cleaner material. Thus, a greater number of irradiated sites are needed in order to sample over the purity range of the material with the same uncertainty as in the more uniform, dirtier material.

V. THE EFFECTS OF PLASTICIZATION ON THE LASER DAMAGE PROPERTIES OF VARIOUS TRANSPARENT POLYALKYLMETHACRYLATES

As stated in the introduction, some of the Russian articles reviewed in Ref. 1 assert that plasticization should improve a material's laser damage resistance by allowing the relief of thermoelastic stresses. Supposedly, plasticization should be especially useful in the case of low fluence level, multiple-shot damage, which is very important from an applications point of view. Since no domestic research in this area had been reported to date, the initiation of such was established as an objective of the fellowship.

The first task was to decide which combinations of plastic/plasticizer to study. Plasticization can be accomplished either internally by copolymerization or externally by non-volatile, high molecular weight additives. In either case, the effect of the plasticizer is to soften the material and lower its glass transition temperature by reducing its density. Since some efforts at internal plasticization were already on-going at FJSRL, external plasticization was emphasized during the fellowship.

Because PMMA had been the subject of the purification studies (Ref. 8 and Section IV of this report), it was chosen as the primary host material in the plasticization study. In researching the matter, however, it was found that several other polyalkylmethacylates also had promise and should be studied if time were available. They are listed in Table III along with PMMA.

Table III. Promising Polyalkylmethacrylate Host Materials for Plasticization Study

Material/Abbreviation	Glass Transition Temperature Tg in ^{0}C	Solubility Parameter in $(cal/cm^3)^{1/2}$
Poly-methyl-methacrylate/PMMA	105	9.3
Poly-ethyl-methacrylate/PEMA	66	9.1
Poly-isopropyl-methacrylate/PiPMA	81	8.5
Poly-secbutyl-methacrylate/PsBMA	60	8.2
Poly-tertbutyl-methacrylate/PtBMA	105	8.3
Poly-cyclohexyl-methacrylate/PcHMA	66	9.2

Like PMMA, their monomers are commercially available and can be polymerized at room temperature[10] with ultraviolet (UV) initiation into clear, transparent amorphous solids. Furthermore, their glass transition temperatures (also called softening points) are well above room temperature (see Table III); thus, at and near room temperature the materials should be thermally stable and hard enough to polish easily, resist scratching, and maintain good optical figure, i.e., dimensional stability.

The plasticizers chosen for the study had to be transparent liquids at room temperature and be compatible with their plastic hosts.[11] The compatibility of two liquids can be quickly estimated by comparing their so-called solubility parameters.[11,12] Experience has shown that if the solubility parameters of a plastic host and a prospective plasticizer are within a cgs unit of each other, the material will be compatible in most proportions. After considering data on several phthalates, sebacates and adipates, it was decided that the four materials listed in Table IV could be used for this study with the host materials in Table III.

Table IV. Plasticizers Compatible with the Host Materials in Table III

Materials/Abbreviation	Solubility parameter in $(cal/cm^2)^{1/2}$
Dibutyl Phthalate/DBP	9.3
Dibutyl Sebacate/DBS	8.0
Di-2-Ethylhexyl Plathalate/DEHP	8.8
Dioctyl Adipate DOA	8.7

Since dibutyl phthalate (DBP) is a well-known plasticizer of PMMA[12] it was chosen as the primary plasticizer in the study. The others in Table IV would be studied if time permitted it (it did not).

Time did permit synthesis of several samples of each of the host materials PMMA, PEMA, and PcHMA from Table III. Individual samples of each host material were plasticized with 0, 5, and 10 weight percent of DBP, respectively. Also, one sample of PMMA was copolymerized with five weight percent CHMA. The maximum plasticizer content was limited to ten weight percent because plasticizers are known to reduce glass transition temperatures rather sharply,[13] and a material whose glass transition temperature is near room temperature would not have the desirable thermal and mechanical properties discussed above. The three monomers in question and the DBP were purified by distillation approximately as described in Ref. 8, with some minor practical differences. Thus, whereas PMMA could be fractionally distilled at atmospheric pressure in a nitrogen atmosphere, CHMA and DBP had to be vacuum distilled, and EMA had to be dried with calcium hydride as described in Ref. 8, then distilled in a nitrogen atmosphere. For polymerization, the monomer/plasticizer solutions were sealed in clean 6 cm x 17 mm diameter glass ampoules at atmospheric pressure and placed eight inches from a UV mercury lamp for five days.

The PMMA and PEMA produced this way were hard, odorless, bubble-free, crystal clear and transparent, i.e., of excellent optical quality and eligible for laser damage testing. All three PcHMA samples, however, while hard, odorless and bubble-free, turned slightly cloudy after two to three days in front of the mercury lamp. The sample with ten weight percent DBP took the longest time to turn cloudy, which suggests that the cloudiness was caused by a small degree of crystallization, which the plasticizer could delay, but not prevent. Time did not allow further investigation of this, and because of the cloudiness, the PcHMA samples were not laser damage tested. In final preparation for such testing, the PMMA and PEMA samples were cut and ground into one-half inch disks, then polished successively with 1.0, 0.3, and 0.05 μm alumina abrasives.

Damage tests on the PMMA and PEMA samples were performed exactly as described in the filtration study of Section IV. LSF straight lines were fit to single-shot damage statistics, as in Fig. 2, and the single-shot damage thresholds were obtained from the midpoints of the LSF lines. Table V lists the seven samples tested, their single-shot damage thresholds, and their respective dust contents as determined with the depolarized scattered light scheme, described in section III.

110-14

Table V. Dust Content and Single-Shot Damage Thresholds of PMMA and PEMA in the Plasticization Study

Sample	Description	Dust Content (Particles/mm^3)	Single-Shot Damage (Threshold J/cm^2)
R1	PMMA	20.0	32
R2	PMMA + 5% DBP	37.1	29
R3	PMMA + 10% DBP	31.4	32
R4	PMMA + 5% CHMA	51.2	26
R8	PEMA	72.9	19
R9	PEMA + 5% DBP	96.6	17
R10	PEMA + 10% DBP	97.7	17

Compared to the samples studied in Section IV (see Table 1) those listed in Table V unfortunately had more dust and, as expected, lower damage thresholds. Evidently, the procedures used in preparing the samples of Table V were not as successful in eliminating dust as those used in preparing the samples of Table I. Despite the high dust contents, the data in Table V allow an interesting observation to be made. Whereas the plasticized materials all had significantly higher dust contents than their unplasticized counterparts, their thresholds were not significantly lower. For example, sample R3 was more than 50% dirtier than R1, but their single-shot damage thresholds were identical. Combining this result with those of Ref. 8 and Section IV where damage thresholds are always inversely correlated with dust content, it can be concluded here that plasticiation can significantly increase single-shot damage thresholds. Because the dust contents

and damage thresholds of unplasticized PMMA and PEMA were so different, no valid comparison of the single-shot behaviour of the two materials can be made with the data of Table V.

Multiple-shot damage measurements were made on the seven samples listed in Table V also, but because of the limited time available, it was only possible to make a small number of measurements. Whereas the PMMA samples showed virtually no plasticizer-dependent multiple-shot behavior, the plasticized PEMA was somewhat more damage resistant than it's unplasticized counterpart. No valid conclusion can be made, however, because of the differences in dust content. To study the effects of plasticizer alone, both the unplasticized and plasticized samples would have to have identical, or at least similar, dust contents. Table V shows that such was not the case here.

VI. RECOMMENDATIONS

The scattered depolarized laser light scheme proved to be very successful in quickly estimating the dust content of a liquid or polymer sample and in illustrating the direct correlation between dust content and single-shot damage thresholds. As the next step in understanding the actual mechanism of damage, the scattered light scheme should be improved to electronically measure the size distribution of the dust particles.

Samples E20, E22, and E24 allowed firm conclusions to be drawn concerning the effect of monomer filtration on dust content and its concomitant relation to single-shot damage. Completion of the multiple-shot damage measurements begun here will allow similar conclusions to be drawn concerning the important multiple-shot damage problem.

The plasticization study was extensive enough to conclude only that it appears to have a significant effect on single-shot damage. This result was not firmly established and the multiple-shot measurements were even less conclusive. The work begun here with PMMA and PEMA should be completed, and studies of the other four materials in Table III should be begun. The polyalkylmethacrylates are easy to work with, relatively inexpensive, and laser damage studies with them as a family will provide new needed information about the damage mechanism.

ACKNOWLEDGEMENT

REFERENCES

1. R.M. O'Connell and T.T. Saito, "Plastics for High-Power Laser Applications: A Review," Opt. Eng., Vol. 22, p. 393, 1983.

2. K.M. Dyumaev, A.A. Manenkov, A.P. Maslyukov, G.A. Matyushin, V.S. Nechitailo, and A.M. Prokhorov, "Transparent Polymers: A New Class of Optical Materials for Lasers," Sov. J. Quantum Electron, Vol. 13, p. 503, 1983.

3. D.A. Gromov, K.M. Dyumaev, A.A. Manekov, A.P. Maslyukov, G.A. Matyushin, V.S. Nechitailo, and A.M. Prokhorov, "Efficient Plastic-Host Dye Lasers," paper MBB4, Proc. 13th International Quantum Electron Conf. Anaheim, Ca., June 18-21, 1984.

4. R.M. O'Connell, T.F. Deaton, and T.T. Saito, "Single- and Multiple-Shot Laser-Damage Properties of Commercial Grade PMMA," Appl. Opt., Vol. 25, p. 682, 1984.

5. R.M. O'Connell, T.T. Saito, T.F. Deaton, K.E. Seigenthaler, J.J. McNally, and A.A. Shaffer, "Laser Damage in Plastics at the Frank J. Seiler Research Laboratory," Proc. 15th Annual Symposium on Optical Materials for High Power Lasers, Boulder, Co., Nov. 14-16, 1983.

6. N. Bloembergen, "Role of Cracks, Pores, and Adsorbing Inculsions on Laser Induced Damage Threshold at Surfaces of Transparent Dielectrics," Appl. Opt., Vol. 12, p. 661, 1973.

7. H.C. Van de Hulst, Light Scattering by Small Particles, John Wiley and Sons, New York, 1957.

8. R.M. O'Connell, A.B. Romberger, A.A. Shaffer, T.T. Saito, T.F. Deaton, and K.E. Siegenthaler, "Improved Laser-Damage-Resistant Polymethlmethacrylate," J. Opt. Soc. Am. B, Vol. 1, December 1984.

9. C.J. Decedue and W.P. Unrih, "Detection and Measurement of Particles in Water Prepared for HPLC," Biotechniques, p. 78, March/April 1984.

10. W.D. Roff and J.R. Scott, Handbook of Common Polymers, CRC Press, Cleveland, Ohio, 1971.

11. P.D. Ritchie, Plasticizers, Stabilizers, and Fillers, Iliffe Books, Ltd., London, 1972.

12. J.A. Brydson, Plastics Materials, Fourth Edition, Butterworth Scientific, London, 1982.

13. P.F. Bruins, Plasticizer Technology, Reinhold, New York, 1965.

1984 USAF-SCEEE SUMMER FACULTY RESEARCH PROGRAM

Sponsored by the

AIR FORCE OFFICE OF SCIENTIFIC RESEARCH

Conducted by the

SOUTHEASTERN CENTER FOR ELECTRICAL ENGINEERING EDUCATION

FINAL REPORT

EXPERIMENTAL PHYSICS ASPECTS OF THE AFATL RAILGUN EFFORT

Prepared by:	Dr. William B. Pardo
Academic Rank:	Associate Professor
Department and	Department of Physics
University:	University of Miami
	Coral Gables, Florida 33155
Research Location:	Air Force Armament Laboratory (AFSC)
	AFATL/DLJG
	Eglin AFB, Florida 32542
USAF Research Colleague:	Mr. Kenneth K. Cobb
Date:	17 August 1984
Contract No:	F49620-32-C-0035

EXPERIMENTAL PHYSICS ASPECTS OF THE AFATL RAILGUN EFFORT

by

William B. Pardo

ABSTRACT

Techniques of data acquisition and analysis and their
relationship to system performance evaluation and modelling are
presented. The physics of the phenomena of muzzle flash and rail damage
is discussed. Recommendations for future experimental research are
given.

ACKNOWLEDGMENTS

I. INTRODUCTION:

The AFATL electromagnetic launcher's mission is the study of " a number of technology issues affecting ultimate development of an EML weapon. These include developing a ballistically stable projectile, improving reliability and optimizing the energy efficiency of the EML and power source."[1] Improving the reliability of the system will require a better understanding of the physical processes responsible for rail damage. The feasibility of optimizing the energy efficiency of the EML and power source depends on the validity of the electrical and thermal modelling of the system.

To this end K. Cobb et al.[2] have written a computer simulation of this multiple modular electromagnetic launcher. This model includes the effect of skin depth on rail resistance. The plasma armature is treated as an additional circuit component with its own electrical properties. The user can vary all module branch circuit parameters as well as rail resistance and inductance gradient. Numerical solutions executed on a Cyber 175 computer produce values for system parameters as function of time and position. Tabular and graphical display of the results are available as output.

In general, agreement between experimental results and the AFATL model predictions was good. Differences between ideal case predictions and experimental results provide a tool for significant improvement in the understanding of real system behavior and in the validity of the computer model.

II. OBJECTIVES OF THE RESEARCH EFFORT

The objective of this effort was improvement of the electrical and thermal modeling of the AFATL electromagnetic launcher system.

III. DATA ACQUISITION

The system diagnostics were designed to measure breech voltage, muzzle voltage, breech (rail) current, gas pressure at the preaccelerator, and projectile speed at the breech and muzzle. The rail current is measured at the rail breech with an actively integrated Rogowski-loop pick up at the rail breech. Voltage measurements are made between the rails at the breech and muzzle. Voltage and current signals are transmitted to the control console via optically isolated differential amplifiers and twisted shielded-pair cables. Breech and muzzle speeds were to be determined by measuring the time interval between the interruption of two collimated light beams 10 cm apart.

During many of the test firings at AFATL the breech voltage, muzzle voltage and rail current signals were recorded by Nicolet 4094 digital oscilloscopes set to sample every 2 nanoseconds. The 4096 events recorded by each channel were stored by the oscilloscopes in its own format on 5 1/4" floppy disks. The data arrays were transferred to 8" disks in a format compatible with the DLJG Tektronix 4054A graphics computer system by M.Sgt. D. Burkhett.

When the muzzle speed measurement system failed to perform as

expected a ballistic pendulum and a break paper time-of-flight system was installed. Two of the data acquisition channels had to be dedicated to the break paper system. Preliminary testing of optical diagnostics also required oscilloscope channels. The number of promising proposals for additional diagnostics soon overwhelmed the limited number of channels available. Assignment of priorities became a painful necessity with the inevitable result that until planned additional data acquisition capability is in place all potentially useful data can not be obtained simultaneously.

IV. DATA ANALYSIS

This summer the Tektronix graphics computer system became the primary tool in the analysis of data. It also served as a terminal for the Cyber 175 allowing graphics display through Plot 10 commands from the Cyber to the Tektronix system. Software was developed and is being used for transfer of data arrays to the Cyber memory as ASCII strings. Thus it is now possible to use the computing power of the Cyber together with the graphics capabilities of the Tektronix's system to develop a model whi h can incorporate empirical data.

Figure 1 shows the recorded muzzle voltage, breech voltage and rail current vs time as well as computed values of rail current squared from two test shots. The data analysis program used to generate the graphs also evaluates and displays the initial value of the observables, the time at which rail current began (start time), the
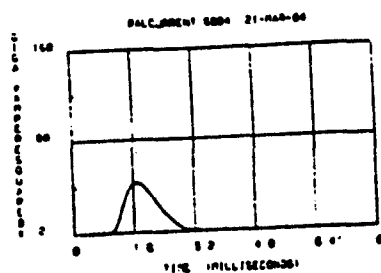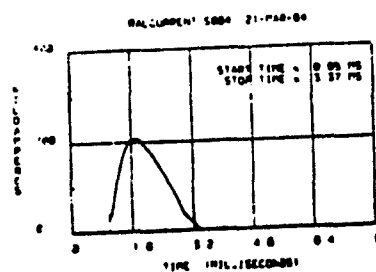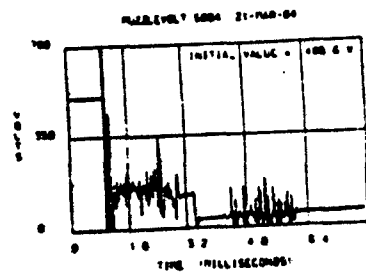
Figure 1a   Shot 004   21-MAR-84
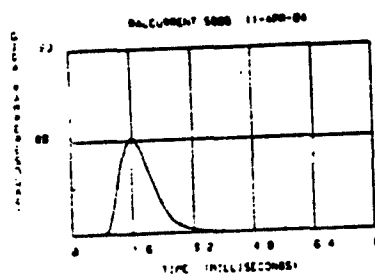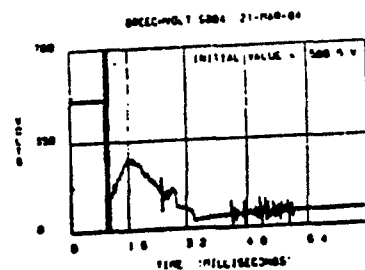
Figure 1b   Shot 005   11-APR-84

111-7

time at which the rail current became undetectable (stop time), the
duration of current and the r.m.s. value of the rail current.

An overlay of rail current and breech voltage obtained 17-JAN-84
is shown in Figure 2. The rail current and breech voltage traces have
similar shapes until about 3 ms after triggering. If the noise in the
muzzle voltage trace is filtered its shape is similar to the breech
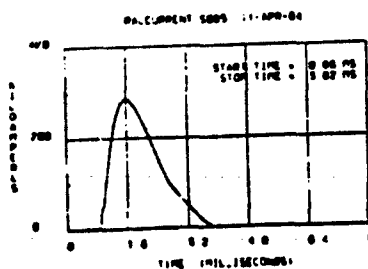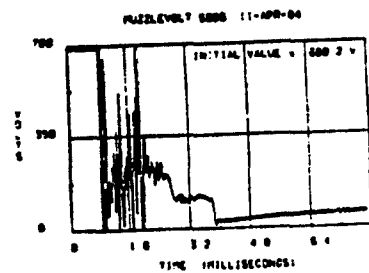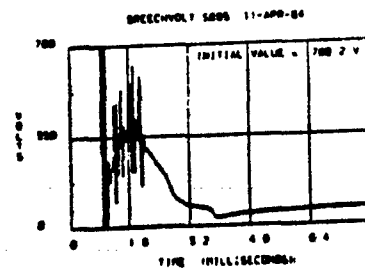voltage. When the current ceases, about 3.85 ms after triggering, the
muzzle voltage and breech voltage indicate that the capacitor banks
have not yet fully discharged. The slight rise in voltage after the
cessation of current is characteristic of the electrolytic capacitors
used to construct the power modules.

Since rail current is not present in the part of the rails
connecting the muzzle to the armature the muzzle voltage should give
the best indication of conditions across the plasma armature.

Attempts to analyze the voltage and current traces to obtain
plasma and rail properties were quickly frustrated by the presence of
"noise" of roughly 10 kHz frequency which appeared consistently in the
muzzle voltage traces. In records of the 11-APR-84 shot (Fig. 1b) the
"noise" is present in both voltage traces during rail current flow.
During the 21-MAR-84 shot (Fig. 1a) "noise" appeared in both voltage
traces after the current had ceased. Since the time resolution
capability of the system permits the recording of significant detailed
structure in the time dependence of the data, this "noise" component in
the voltage traces was the source of much concern and speculation. Fine
structure in the current distribution, periodic instability of the

thermal processes at the rail-plasma interface, cathode spot oscillations, instabilities in the plasma armature, periodic "blow-by" of plasma past the projectile, feedback resonances in the isolation amplifiers, mechanical resonances in the rail structure and balloting of the projectile were all considered as possible causal mechanisms.

Figure 3 shows the scale of the phenomenon. If the "noise" represents a real system effect, positive and negative voltages of almost ten times the magnitude of the largest voltage applied to the rails are present at the breech and muzzle. The fact that diodes are connected across the electrolytic capacitors in the power supplies to prevent reverse voltages increases the difficulty of understanding the effect. The simplest explanation might be that the "noise" is an artifact triggered by transients. If it is within the system it is of fundamental concern and future experiments should be designed to localize the source. If the cause is a characteristic of the instrumentation it should be corrected. In either case further analysis of existing voltage data should include numerical filtering. The rail current data has already been subjected to smoothing by the active integration that occurs before it reaches the recording oscilloscope.

V. PERFORMANCE EVALUATION

The acceleration of the projectile in the AFATL electromagnetic launcher is caused by the pressure exerted on its base by the plasma armature due to the interaction of the magnetic field within the armature, produced by the current in the rails, exerting a Lorentz
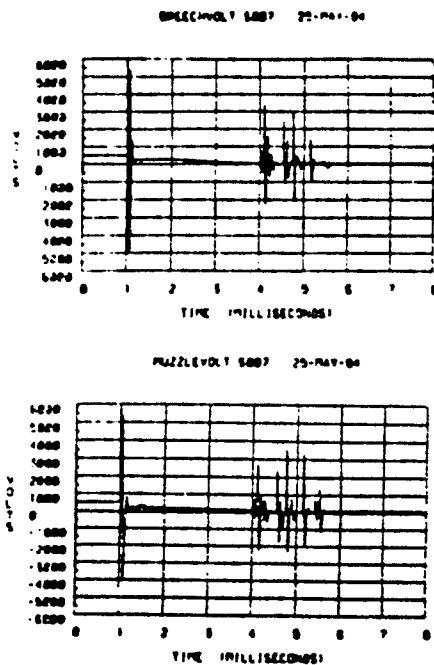
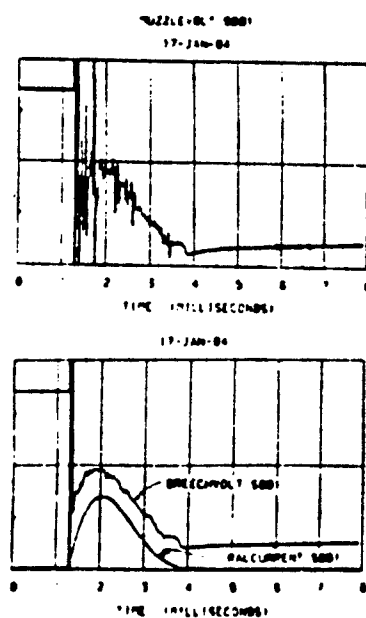Figure 3   Shot 007   23-MAY-84

Figure 2   Shot 001   17-JAN-84
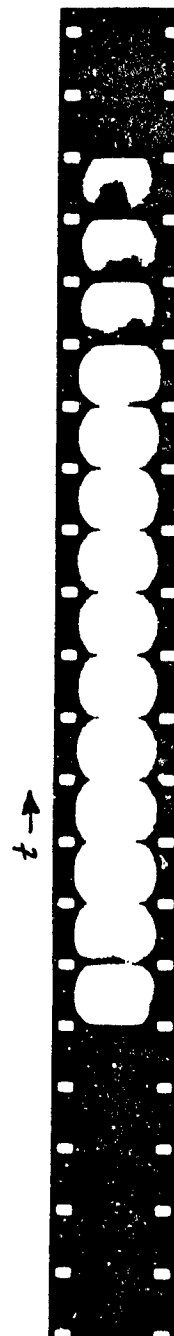
Figure 7   Shot 008   9-JUL-84

111-10

force on the current in the armature.

Many derivations of the equation for projectile acceleration in railguns assume ideal geometry , neglect friction and ignore "lost" current. With these assumptions the projectile acceleration

$$a_x = \ddot{X} = (L_x'/ 2M) \; I(t)^2 \tag{1}$$

where L_x' times the distance from the armature to the breech is equal to the inductance of rail-armature-rail system, M is the projectile mass. The subscripts b and m label values at the breech and muzzle respectively.

If we assume that $(L_x'/ 2M)$ does not vary appreciable during the shot the plot of $I(t)^2$ vs time has the same time dependence as the pressure curve of a conventional gun.

In any case the muzzle speed of the projectile can be calculated from the relation

$$\dot{X}_m - \dot{X}_b \; = \; \int_{t_b}^{t_m} a_x \; dt \; = \; \int_{t_b}^{t_m} (L_x'/ 2M) \; I(t)^2 \; dt \tag{2}$$

If the propulsion parameter $(a_x / I(t)^2) = (L_x'/ 2m)$ is treated as a constant the projectile muzzle speed

$$\dot{X}_m \; = \; \dot{X}_b \; + \; (L_x'/2m) \; (I_{rms}^2) \; (t_m - t_b) \tag{3}$$

and

$$(L_x'/2m) \; = \; (\dot{X}_m - \dot{X}_b) \; / \; (I_{rms}^2) \; (t_m - t_b) \tag{4}$$

where

$$I_{rms}^2 \equiv \left. \int_{t_b}^{t_m} I(t)^2 \, dt \middle/ (t_m - t_b) \right.$$

(5)

Equation (4) assumes that rail current present after the projectile leaves the rails ($t > t_m$) does not contribute to projectile propulsion.

If muzzle speed, breech speed, duration of shot and time dependence of rail current are recorded; the average propulsion parameter can be evaluated experimentally using equation (4) . Comparison with the value predicted using measured projectile mass M and apriori estimates of inductive gradient L_x' gives a good measure of the validity of the assumptions upon which equation (1) is based and provides a quantitative measure of performance.

Attempts at more realistic modeling have treated the armature as a magneto-fluid including the forces on the current distribution within the plasma armature due to local magnetic fields.[3] The effects of friction and non-ideal plasma geometry have been considered by Richardson.[4] Marshall[5] has noted that knowledge of the current distribution within the rails is essential. Mechanisms, such as plasma leakage from the armature past the projectile ("blow-by") or conducting insulators[6], by which current can flow from one rail to the other without passing through the armature drastically affect the validity of equation (1).

111-12

VI. MUZZLE FLASH

Figure 4 illustrates the presence of a discontinuity in the time derivative of the rail current. In all shots to date this effect has occurred 0.4 to 1.1 ms before the current became undetectable. This change could be accounted for by a rapid variation in the inductance of the system caused by the altered current distribution that occurs as the projectile leaves the rails. In Figure 4 t_1 is the time at which the projectile leaves the rails and t_2 is the time at which the current is interrupted. When $t > t_1$ the current become non-propellant since after the projectile leaves the muzzle the interaction of the plasma and projectile is drastically reduced. The behavior of the system undergoes a transition from conventional rail gun behavior to that of a plasma accelerator [7]. Although the plasma is still in electrical contact with the rails and can conduct appreciable current it is no longer confined by the projectile-sealed barrel. The plasma expands rapidly into the region in front of the muzzle causing a flash of light lasting several milliseconds. Figure 5 (9-JUL-84) indicates that the plasma arrives at the first break paper 4.7 ms after the passage of the projectile has caused a loss of conduction. Attributing the reestablishment of conduction to the arrival of the plasma is consistent with the extensive deposit of copper observed on surfaces through which the projectile passes after leaving the rails. This was especially obvious after the 9-JUL-84 shot where the break paper was the first surface beyond the muzzle.

Figure 7 was recorded during the 9-JUL-84 by a framing camera
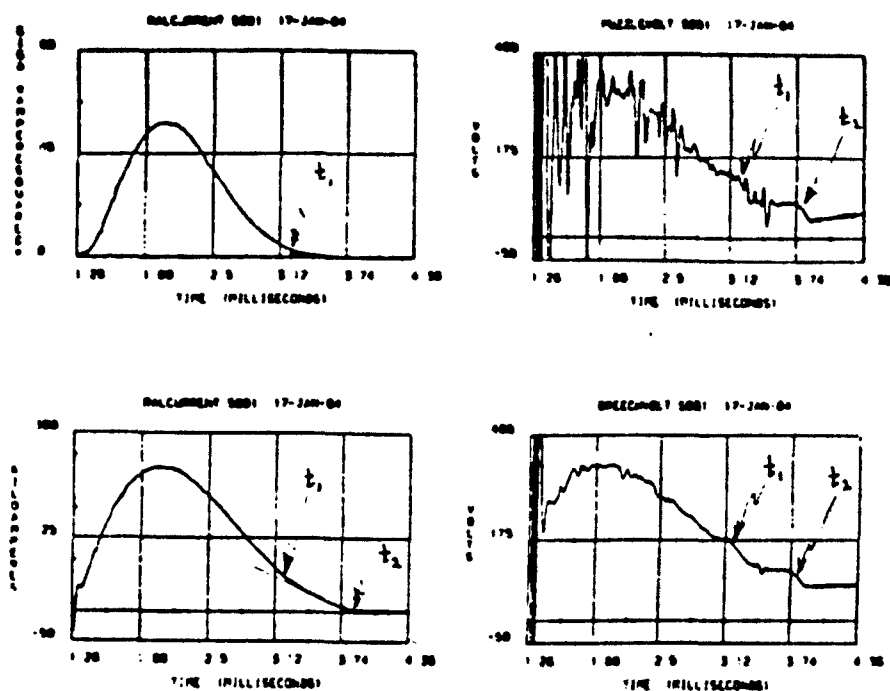
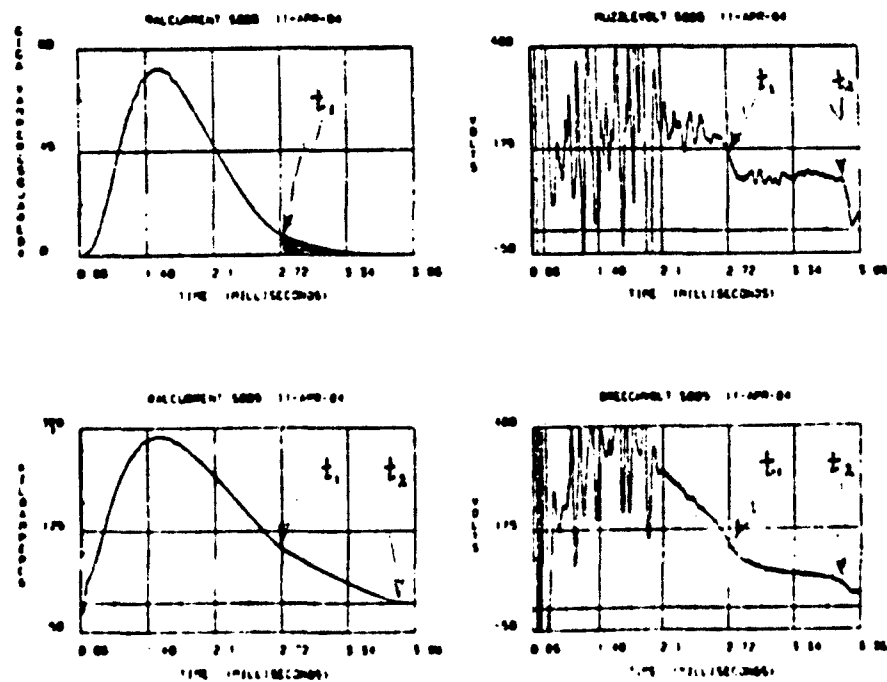Figure 4A   Shot 001   17-JAN-84

Figure 4B   Shot 005   11-APR-84

111-14

with a time interval between frames of about .29 ms. The camera was focused on a mirror arranged so that, until the projectile left the barrel and shattered the mirror (the first 3 frames) , only light coming from within the barrel could be detected. After the mirror was destroyed (the next 14 frames) the camera's focus was on the region between the muzzle and the first break paper. The film frames appear to be almost completely saturated by the muzzle flash which lasted more than 4 ms.

Photo cells were set to detect light emitted at the muzzle perpendicular to the direction of projectile flight. The time between the first detection of light by a photo cell and the restoration of break paper conduction was about 5.5 ms. Although the time of flight of the projectile down the rails appears to have been about 2.3 ms the rail current record does not show the current to have reduced to an undetectable level until about 3.2 ms after the arc was struck. By then the projectile had already destroyed the mirrors and penetrated the first break paper. The muzzle is open; thus the bore in front of the projectile is filled with air. It is possible that the light detected coming from the muzzle could be emission from a luminescent shock front preceding the projectile or, since the projectile was translucent to visible light, it could be coming from the plasma armature itself. Both photo detector records show a time during which the detected light signal either plateaus or decreases slightly. The duration of this effect is 0.1 ms on both traces. If a precursor shock front exists the shape of the time traces (Figure 6) could be accounted for by
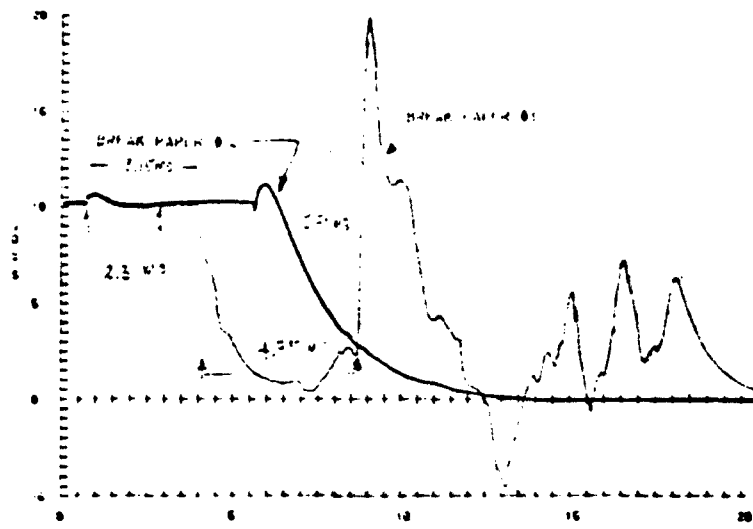
Figure 5   Shot 008   9-JUL-84
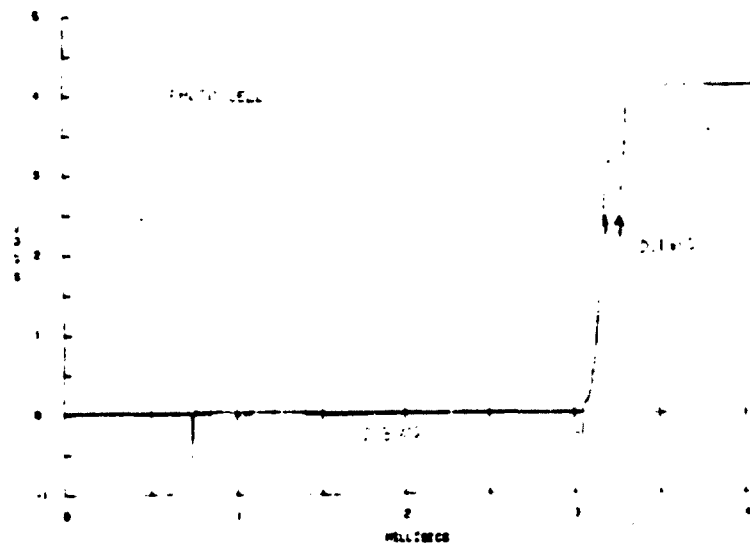
Figure 6   Shot 008   9-JUL-84

111-16

attributing the initial rise in signal to its exit from the bore and
the subsequent decrease in signal to the passage of an opaque object,
possibly the projectile. The saturation signal is probably due to the
expansion of the plasma armature beyond the muzzle and transition to a
non-propellant muzzle flash.

VII. RAIL DAMAGE

Thermal rail damage, where ohmic heating within the rail simply
evaporates material from the surface, is often accompanied or dominated
by destructive arc phenomena which tend to appear when high current
densities are present at the interface between the rail and the plasma
armature. In general the greatest damage occurs where the armature
current is high and the projectile's speed along the rails is low.
These conditions are most likely near the breech where thermal and arc
effects are both contributing to surface erosion. As the armature
speeds up arc effects dominate and discrete arc tracks are often
observed. These tracks are similar to the classical damage due to
arcing at electrical contacts.[8] .

Damage due to interactions of plasmas with fusion reactor walls
includes blistering, melting, cracking and embrittlement.[9] Material
is removed from the metal walls by plasma bombardment of the surface,
especially when large sheath potentials are present. The sheath between
the plasma edge and the metal surfaces plays an important role in the
arcing and sputtering (charge exchange neutral) effects allowing

replenishment of the plasma through a series of processes by which the plasma ions leave the plasma region, interact with the surface and return to the plasma. Evaporation, sputtering and arcing all play a role but unipolar arcing and ion (or charge exchange neutral) sputtering are thought to be the major mechanisms for metal erosion in fusion plasma experiments.[10] Vapor jets can also occur in many metal arcs.[11] These jets are ejected from the electrodes of any discharge if sufficient energy for vapor production is transferred to the surface by the charged particles accelerated by the anode or cathode fall.

Under a standardized set of test conditions rail materials vary greatly in capacity to resist arc damage. A 75% Cu - 25% W sintered rail appears to show the least damage .[12] The lifetime of these rails appeared limited primarily by the transport of copper through the sinter to the surface.[13]

Perhaps thermal rail damage could be reduced by using of a composite "sandwich" type rail, manufactured like our contemporary coinage, using a material with good high temperature characteristics, such as tungsten, at the rail-plasma surface with copper providing the remainder of the rail with a low resistance path. Its effect on the plasma armature may require additional copper at the base of the projectile to maintain the copper plasma as a suitable conductive path between the rails.

VIII. RECOMMENDATIONS

An extensive list of suggestions for expanding the experimental capabilities of the AFATL rail gun was prepared in collaboraton with K. Cobb who has written an informal test plan in which some of the suggestions have been incorporated.

At present the demands imposed by the AFATL railgun's mission exceed the system's capabilities. A facility dedicated to experimental studies of an electromagnetic launcher similar to the AFATL railgun would relieve the present system. With every advancement in the understanding of the technology of railguns new questions arise. Answering these questions will require major system modifications. Many technical issues will be resolved when the next generation of railguns are available but fundamental questions will continue to remain unanswered.

A railgun specifically designed to conduct physics experiments could permit easy modification of basic components. Provision could be made for state of art diagnostics and for the development of new techniques as required. Interaction between experimentalists and theorists is especially important for an effective operation that can support an active AFATL test program by providing increased understanding of the basic mechanisms and new diagnostic resources. Traditionally this kind of experimental facility functions well in a University environment.

REFERENCES

1. J. D'Aoust, K. Cobb, R. Creedon, L. Franklin, B. Lucas, P. Miller, and A. Peuron, *IEEE Transactions on Magnetics*, 20, 291 (March 1984)

2. Kenneth K. Cobb, Billy Lucas, and Lin Sellers, "Simulation of a Modular EM Rail gun", AFATL Report No. AFATL-84-16, Feb.- Sep. 1983.

3. J.D. Powell, "Two-dimensional Model for Arc Dynamics in the Railgun", ARDACOM Tech. Report. ARBRL-TR-02423.

4. D.D.Richardson, V.Kowalenko, *IEEE Transactions on Magnetics*, 20, 280 (March 1984)

5. Richard A. Marshall, *IEEE Transactions on Magnetics*, 20, 243 (March 1984)

6. Jerald V.Parker, W. Mark Parsons, "Arc Damage to Railgun Insulators", LA-UR 84-1934, May 1984.

7. Jad H. Batteh, "Analysis of a Rail Gun Plasma Accelerator", U.S. Army Ballistic Research Laboratory Technical Report. DAAK11-80-c-0102, December 1981.

8. A.J. Bedford, *IEEE Transactions on Magnetics*, 20, 348 (March 1984)

9. R.A. Gross, N Jensen, J.K. Tien, and N. Panayotou, in *Plasma-Wall Interactions* (Pergamon Press, New York, 1977), 481.

10. N.S. Brickhouse, "Experimental Studies of Impurity Production in the Tokapole II Tokamak", DOE/ET/53051-62, January 1984

11. W. Finkelburg, *Phys. Rev.*, 74, 1475 (1948)

12. A.J. Bedford, *IEEE Transactions on Magnetics*, 20,352 (March 1984)

13. D.D. Richardson (private communication)

1984 USAF-SCEEE SUMMER FACULTY RESEARCH PROGRAM

Sponsored by the

AIR FORCE OFFICE OF SCIENTIFIC RESEARCH

Conducted by the

SOUTHEASTERN CENTER FOR ELECTRICAL ENGINEERING EDUCATION

FINAL REPORT

ANALYSIS OF THE VALIDITY OF BARNES TRANSMISSOMETER DATA

Prepared by:	Prof. Martin A. Patt
Academic Rank:	Associate Professor
Department and University:	Department of Electrical Engineering University of Lowell
Research Location:	Air Force Geophysics Laboratory Optical Physics Division
USAF Research	Dr. Eric P. Shettle
Date:	July 31, 1984
Contract No:	F49620-82-C-0035

ANALYSIS OF THE VALIDITY OF BARNES TRANSMISSOMETER DATA

by

Prof. Martin A. Patt

ABSTRACT

Under NATO Project OPAQUE, large data files
were collected for subsequent processing by
the Air Force Geophysics Laboratory. The
validity of some of the supplemental 1400-
meter Barnes transmissometer data stored in
processed hourly-files was suspect. The data
has been carefully studied and a determination
has been made that the 1400-meter Barnes data
was not valid. The processing error which
resulted in the the bad data was found, and
the hourly data files were subsequently
reprocessed.

Acknowledgement

The author would like to thank the Air Force Systems Command, the Air Force Office of Scientific Research and the Southeastern Center for Electrical Engineering Education for providing the opportunity to spend a worthwhile and productive summer at the Air Force Geophysics Laboratory, Hanscom Air Force Base, Mass. The laboratory, and in particular the Optical Physics Division is hereby acknowledged for its hospitality and excellent working conditions. Very special thanks go to Mr. Eric P. Shettle for suggesting this area of research and for his collaboration and guidance.

The author acknowledges his debt to Prof. James E. Powers and Prof. Robert J. Dirkman who have spent so much of their time and energy developing both the hardware and software foundations upon which this work is based.

Finally, a good deal of appreciation is extended to Mr. Barry Lemieux for his perseverance in the face of many frustrations during this summer project.

I. INTRODUCTION

The OPAQUE program was a joint NATO program designed to make measurements of the optical and infrared properties of the atmosphere over a period of years at a number of locations in Europe. AFGL was responsible for the measurements at one of these sites in Northern Germany. The reduced data (on an hourly basis) from this station was put into one-month data files for subsequent analysis, and written to magnetic tape for exchange with the other national groups responsible for the measurements at the other sites.

The OPAQUE hourly-file is a one-month file containing 31 records, one for each day of the month. For months containing less than 31 days, the extra records are merely disregraded. Each daily record contains an array dimensioned 85 x 24. There are 85 entries for each hour of the day, the entries being derived from a ten minute period during the hour. The data entries reported for each hour are defined in Table 1. The 85 entries are initialized as follows:

1. (station number) 71
2. (date) year,month,day, packed into the six rightmost digits
3. (time) hour (0,1,2,...,23)
4. (duration of the measurement cycle) 10
5-10. (comments and scattering-filter-humidity) 0
11-57. (measurement values) $-1 \times 10^{+30}$
58-77. (weather data) $-1 \times 10^{+30}$
78-84. (data quality) appropriate number of 9's
85. (rain data) $-1 \times 10^{+30}$

With the exceptions of entries 76 and 85, entries 58 through 85 are not recorded by the measurement system data logger.

The processing of measurement values are of several types:

1. The AEG Point Vis. Meter, Eltro, Horizontal Luxmeter, Night Path Luminance, and the east direction VPFM require the beginning value, end value, maximum value, minimum value, and number of samples obtained in the ten minute period.

2. The vertical Luxmeter requires one value from each of the four compass points.

3. The VPFM samples in the south, west, and north compass points are required in addition to the five values above for the east direction.

4. The direct Epply and Barnes instrument require values entered, depending on the filter being used for the measurement.

All data values are entered into the daily arrays except if the value was not physically present, or the data could not be interpreted, or the data was out of range, and then a distinguishable flag value is entered in its place. Hence, if a scientific value is not entered for one of these reasons, one of the following values will be entered in its place:

$-1 \times 10^{+30}$ raw data for that time does not exist

$-9 \times 10^{+99}$ raw data exists, but it is impossible to interpret

$+8 \times 10^{+88}$ the calibrated scientific value is over-range

$-8 \times 10^{+88}$ the calibrated scientific value is under-range.

II. OBJECTIVES OF THE RESEARCH EFFORT

The validity of some of the 1400-meter Barnes transmissometer data stored in words 64, 65, and 28, 29 (from 7/1/80) of the processed hourly files was suspect because of apparent continuing erratic

fluctuations. The objective of the research effort centers around a thorough analysis of the processed minute-file data together with station-logs and supplemental information to determine whether or not the data stored in the minute-files truly reflects the scientific measurements of the Barnes transmissometer, and if valid to further determine why this validity is not reflected in the hourly-files.

III. OVERVIEW OF THE HOURLY-FILE GENERATING PROCESS

An overview of the programs used to generate and examine the hourly-files is shown in Figure 1. The boxes show the permanent files involved, and the directed lines show the procedures necessary to accomplish the task.

Before values can be placed in the hourly-file, it must be initialized with the INERIK procedure. The initial values have been listed previously.

The hourly-file is generated from the three stripped data files: the Stripped Minute Channel File, the Stripped Luxmeter File, and the Stripped Vislab File. The three corresponding procedures used to accomplish this are ERIK, LUXERIK, and VISERIK. These procedures generally depend on the time periods of the data.

Before the ERIK file generation is done, it is necessary to modify the Stripped Minute Channel File with the procedure CLEANLX. This is done to remove invalid data resulting from the time constant associated with range-changes in the non-rotating luxmeter.

Sometimes it is desirable to change a few entries in the hourly-
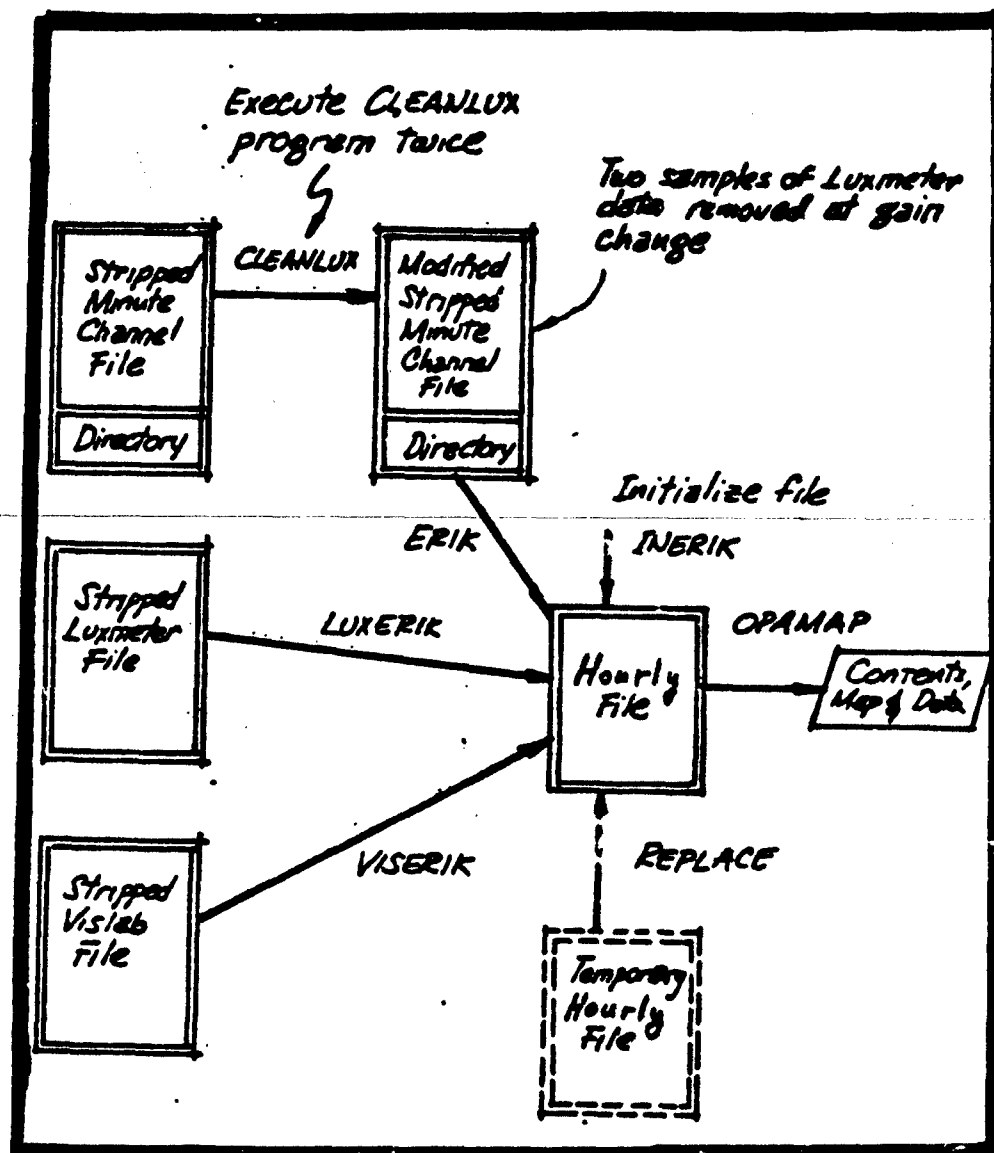
Figure 1. Overall View of Hourly-File Generating Program

file while leaving the others intact. This can be accomplished with the REPLACE procedure. A temporary hourly-file containing the required new values is.generated exactly as the hourly-file. Values in this temporary file can then replace corresponding values in the hourly-file. In general, one or more words (1 to 85) can be changed between any two times in the month.

The contents of the hourly-file can be examined with the OPAMAP procedure. Outputs that can be generated include daily maps (either for individual days or for a complete month) and numerical data in various forms.

IV. DESCRIPTION OF THE REVISED HOURLY OPAQUE DATA BANK FILE

The instrumentation for the atmospheric optical measurements at the Meppen OPAQUE site was changed significantly in the Fall, 1980. The reconfiguration of the instruments and the additional measurements added to the data set required a redefinition of the contents of the data words in the post-OPAQUE data bank files. These changes are reflected in Table 1. Format of the Revised Hourly OPAQUE Data Bank File.

V. REPROCESSING TO INCLUDE THE CORRECTED BARNES 1400 METER INSTRUMENT

An intensive investigation was launched in May and June of 1984 to ascertain the validity of the 1400 meter Barnes instrument data stored in hourly-file data-words 64,65,28, and 29.

The investigation showed that both the sparsity of data in these data-words, and the seeming inconsistency of the data were a result of a software problem in reading the 1400 meter Barnes filter-wheel position. Improvements were made in the software, and results were verified by comparison with station log entries. Reprocessing of the data was undertaken and completed prior to the end of July, 1984. The "corrections" were handled as "replacements" to the already existing hourly files which had been produced by (or for) A.F.G.L. and subsequently further processed at A.F.G.L. The following minute-data was incorporated in the hourly-files:

Word	Description
64	Beginning April, 1978, 1400 meter Barnes 3-5 micron filter (position 1) Analog Chan. 22
65	Beginning April, 1978, 1400 meter Barnes 8-12 micron filter (position 3) Analog Chan. 22
28	Beginning July, 1980, 1400 meter Barnes 8-13 micron filter (position 2) Analog Chan. 22
29	Beginning July, 1980, 1400 meter Barnes 4 micron or open (positon 0) Analog Chan. 22

VI. DIRECTORY OF HOURLY-FILES BEFORE REPLACEMENTS

The hourly-files to which "replacements" have been made were taken from magnetic tapes issued, cataloged, and housed at the A.F.G.L. Computer Center, as well as hourly-files already on the AFGL computer system as permanent files. The following tape directory documents

the replacement process.

	JAN	FEB	MAR	APR	MAY	JUN	JUL	AUG	SEP	OCT	NOV	DEC
1977	a	a	a	a	a	a	a	a	a	a	a	a
1978	a	a	a	1784	1784	1784	1784	1784	1784	1784	1784	b
1979	b	b	b	b	b	b	b	b	b	b	b	b
1980	b	b	b	4894	4894	4894	4894	4894	4894	4894	c	c
1981	c	c	c	c	c	c	c	c	c	c	c	c
1982	c	c	c	c	c	c	c	c	c	c	c	c
1983	c	c	c									

Notes: a - Replacement not applicable because 1400m Burnes
               measurements began April, 1978.

         b - Replacements were made to hourly-files already on the
               AFGL Cyber computer system as permanent files.

         c - Replacement process was not used. New hourly-files
               were generated.

VII. DIRECTORY OF HOURLY-FILES AFTER "REPLACEMENTS"

	JAN	FEB	MAR	APR	MAY	JUN	JUL	AUG	SEP	OCT	NOV	DEC
1977	2460	2460	2460	2460	2460	2460	2460	2460	2460	2460	2460	2460
1978	1784	1784	1784	4822	4822	4822	4822	4822	4822	4822	4822	4822
1979	4822	4822	4822	4822	4822	4822	4822	4822	4822	4822	4822	4822
1980	4822	4822	4822	4876	4876	4876	4876	4876	4876	4876	4876	4876
1981	4876	4876	4876	4876	4876	4876	4876	4876	4876	4876	4876	4876
1982	4876	4876	4876	4876	4876	4876	4876	4876	4876	4876	4876	4876
1983	4876	4876	4876									

Notes: Hourly-files stored on tape CC4876 do not contain MET data.

        Backup tapes of the hourly-files were made as follows:

112-10

NOS/BE TAPE	NOS/BE BACKUP	NOS BACKUP
CC4822	CC4825	CC4946
CC4876 •	CC4825	none

VIII. INCIDENTAL MAGNETIC TAPES GENERATED

CC48??	NOS/BE	Backup of Honohan's System of 1983
CC4839	?/BE	Backup of Patt daily, Summer 1984
CC4875	NOSBE	(continuation of CC4839)
CC4899	-NOS-	Sources, NOS-compilations, and procedures
PAT401	-NOS-	(same as CC4899)

IX. RECOMMENDATIONS

1. It is recommended that further processing of the hourly-files begin at once to exploit the large OPAQUE data base. Additional software should be created as soon as possible to automate the review of the instrument data contained therein with the view toward the development of an authentic atmospheric model.

2. It is strongly recommended that the procedures used under operating system NOS/BE be updated to run under the more modern NOS operating system currently being installed on the CYBER computer at A.F.G.L.

Table 1. Hourly-File Word Allocation

Word No.	Data Item	
1	Station No.	= 71
2	Date - Year,Month,Day	
3	Time	
4	Duration of Measurement cycle	010
5	Comment Numbers	
6	Comment Numbers	
7	Comment Numbers	
8	Comment Numbers	
9	Comment Numbers	
10	Scattering x 100 + Filter x 10 + Humidity	
11	S_s BEG	AEG Point
12	S_s FIN	Visibility Meter
13	S_s MAX	
14	S_s MIN	
15	NV	Number of Measurements
16	E_g BEG	
17	E_g FIN	Eltro
18	E_g MAX	Transmissometer
19	E_g MIN	
20	NV	
21	E_L BEG	
22	E_L FIN	Horizontal
23	E_L MAX	Luxmeter
24	E_L MIN	
25	NV	
26	E_v^N (North)	Vertical Luxmeter
27	E_v^E (East)	Off after 6/30/80

28	B_{15-2}	Barnes	8-13 mm (1500 m)
29	B_{15-4}	(eff. 7/1/80)	Open (1500 m)
30	L_p	BEG	
31	L_p	FIN	
32	L_p	MAX	Night Path Luminance
33	Lp	MIN	
34	NV		
35	F_p	BEG	Variable Path Function Meter
36	F_p	FIN	
37	A2	BEG	AEG, 2 meter
38	A2	FIN	(eff. 11/1/80)
39	A8	BEG	AEG, 8 meter
40	A8	FIN	(eff. 11/1/80)
41	A16	BEG	AEG, 16 meter
42	A16	FIN	(eff. 11/1/80)
43	A48	BEG	AEG, 48 meter
44	A48	FIN	(eff. 11/1/80)
45	A80	BEG	AEG, 80 meter
46	A80	FIN	
47	A80	MAX (10')	(eff. 11/1/80)
48	A80	MIN (10')	
49	SEL	BEG	Slant ELTRO
50	SEL	FIN	
51	SEL	MAX (10')	(eff. 11/1/80)
52	SEL	MIN (10')	

53	T_1	3-5μm BES
54	T_2	8-12μm Barnes Transmissometer (500m)
55	T_3	8-13μm
56	T_x	Open or 4μm
57	T_8	3-5m FIN
58	X	
59	A	
60	B	Aerosol Data
61	C	
62	D	
63	E	
64	B_{15-1}	3-5μm Barnes Transmissometer (1500m)
65	B_{15-3}	8-12μm (1500)
66	H	
67	I	Turbulence Data
68	N	Cloud Cover
69	dd	Wind Direction at 10 m
70	ff	Wind Speed at 10 m
71	d_2d_2	Wind Direction at 2 m
72	f_2f_2	Wind Speed at 2 m
73	ppp	Pressure
74	TTT	Temperature
75	$T_dT_dT_d$	Dew Point Temperature
76	r_fr_r	Rain Rate
77	E	General Ground State
78	QQQQ	Packed MR1 Data
79	QQQQ	Packed Eltro Data
80	QQQQQQQ	Packed Luxmeter
81	QQQQ	Packed Night Path
82	QQQQQQQ	Packed Vis Lab
83	QQQQQQQQQ	Packed Eppley Data
84	QQQQQ	Packed Barnes Data
85	RRR	Total Rain

112-14

References

1. F. Baer and P.J. Sheu, "Optimal Spatial Representations For Numerical Weather Prediction Models Based On Normal Mode Analyses", Optical Physics Division, A.F.G.L., Air Force Systems Command, USAF, Hanscom AFB, Mass, 1982. AFGL-TR-82-0028

2. J.E. Powers, R.J. Dirkman, and M.A. Patt, "The Processing And Analysis Of The Data From An Air Force Geophysics Laboratory Atmospheric Optical Measurement Station And Maintenance Of The Central Data Logger System", Optical Physics Division, A.F.G.L., Air Force Systems Command, USAF, Hanscom AFB, Mass, 1984. AFGL-TR-84-0081

3. J.E. Powers and R.J. Dirkman, "The Reduction and Analysis of Raw Data Tapes from the AFGL Project OPAQUE Data Processor", Optical Physics Division, A.F.G.L., Air Force Systems Command, USAF, Hanscom AFB, Mass, 1981. AFGL-TR-81-0130

4. J.E. Powers and R.J. Dirkman, "The Development and Support of the NATO Project OPAQUE U.S.A.F. System Control Programs", Optical Physics Division, A.F.G.L., Air Force Systems Command, USAF, Hanscom AFB, Mass, 1978. AFGL-TR-78-0176

1984 USAF-SCEEE FACULTY RESEARCH PROGRAM

Sponsored by the

AIR FORCE OFFICE OF SCIENTIFIC RESEARCH

Conducted by the

SOUTHEASTERN CENTER FOR ELECTRICAL ENGINEERING EDUCATION

FINAL REPORT

<u>PERMANENT PERIODIC MAGNETS</u>

<u>AND THE</u>

<u>REPRODUCIBILITY OF TRAVELING WAVE TUBES</u>

Prepared by:	Dr. James D. Patterson
Academic Rank:	Professor
Department and University	Department of Physics and Space Sciences Florida Institute of Technology (Prior to 1984 - S. Dakota School of Mines/Tech.)
Research Location:	Wright-Patterson AFB, Avionics Laboratory Microwave Technology Branch
USAF Research:	Richard L. Remski
Date:	24 August 84
Contract No:	F49620-82-C-0035

PERMANENT PERIODIC MAGNETS AND THE

REPRODUCIBILITY OF TRAVELING WAVE TUBES

by

James D. Patterson

ABSTRACT

The question of characterizing permanent periodic magnets (PPM), so that they will be relatively uniform and produce consistently satisfactory fields from traveling wave tube (TWT) to TWT is investigated. Two parts of this large problem were considered. First, the results of the investigation led to a short summary and list of references for magnet properties relevant to TWTs. Second, a calculation of field strengths from non-homogeneous ring magnets was made. The purpose of the calculation was to gain insight into the effect of inhomogeneities on measured field strengths at appropriate locations just outside the magnets. It is suggested that a quantitive study of how the pole pieces modulate the inhomogeneities would be very useful.

ACKNOWLEDGEMENTS

I. INTRODUCTION

Traveling wave tubes (TWTs) are used as high gain amplifiers over a broad frequency at microwave frequencies. This device utilizes the interaction of an electron beam with an electromagnetic wave.[1]

The TWT was invented by Dr. R. Kompfner in 1943. Further development of this concept soon followed. In 1953, Pierce made a major advance with the invention of periodic permanent magnet focusing, to control the electron beam whereby a major reduction in weight was achieved.[2]

TWTs have found wide application in communications (including satellite communication), radar and electronic countermeasures. The design of TWTs is continually being optimized but the transition from optimum design to production is still not without problems.[3]

Starting from fundamental work of Strnat, Becker, and others in 1966[4], the very powerful samarium cobalt magnets have been developed. Because of their high coercivity, saturation magnetization and energy product they have been ideal magnets to use in TWTs. This report focuses on magnetic materials as related to TWTs.

II. OBJECTIVES

The objective of this report is to make recommendations for producing the focusing magnets in TWTs so that the TWTs will behave properly with only minimal adjustments in the magnetic fields. The emphasis is on better ways of characterizing magnets so that the necessary uniformity can be built in without costly "shimming" of the magnets.

This is a relatively old problem and it has several aspects. One aspect concerns the material properties of magnets made and tested in a scientific laboratory versus those made commercially. It is probably easier to control the quality of a small batch of customized magnets than a large batch of mass produced ones. Several questions arise. Is each magnet homogeneous? Are there significant differences from magnet to magnet? When the ring magnets

are cut in half in order to place on the tube do significant perturbations remain after they are reassembled?

A related aspect is the stability of the magnets. Given a desired set of properties, can we be sure they will stay that way? Will these properties change while the magnets wait on the shelf? Will they change after the magnet is subjected to ambient working conditions? Here we might be concerned with temperature cycling as well as high temperatures. We also might be concerned with chemical changes and surface contamination. Although it is outside the scope of this report, electron beam control is also significantly affected by changes in cathode emission.

Another aspect is the effect of the pole pieces. Is it true that as long as the pole's pieces are not saturated, they tend to smooth out inhomogeneities in the magnets?[5] One might also wonder about optimizing the design of the pole pieces.[6]

As suggested by the above, at least two approaches can be considered. One approach is to look for magnets which are more uniform and stable. The other approach is to look for modifications in the design of traveling wave tubes which will make the TWTs more tolerant to deviations in magnetic properties.

The former approach will be emphasized in this report. In particular, the report will:

    a. Review the properties of some magnets which are being considered in the laboratory as well as those which are commercially available. Samarium cobalt magnets will be given special attention.

    b. Discuss a preliminary calculation that helps give a feeling for how variations in properties of the ring magnets will result in variations in the external fields they produce.

III. TRAVELING WAVE TUBES

The TWT makes use of a fast moving electron confined along the axis of a helical coil which carries an electromagnetic wave. The apparatus is

adjusted so the electron beam and the electromagnetic wave travel at almost the same speed (both measured in terms of net axial motion along the helix). The electromagnetic wave acts to bunch the electrons and the bunches of electrons in turn act to amplify the electromagnetic wave. According to J. R. Pierce[7], you can think of the situation as analogous to a breeze blowing over water and amplifying the waves on it.

In order for the TWT to work properly, the electron beam needs to be constrained near the axis of the helix. Nowadays, periodic permanent magnets (PPMs) are used for this purpose because they are small, lightweight, don't need electrical power and have little or no stray magnetic fields for the geometries currently employed.

The PPM structure is a collection of ring magnets separated by magnetic shims. The shims, also called magnetic pole pieces, should have high permeability. A typical structure is schematically shown in the Fig. 1. The parameters defining the TWT are not all independent. Some idea of their interconnectedness can be learned from the two equations below.

A magnetically shielded cathode is assumed. If L is the period of the magnetic field, V the beam voltage and B is the maximum value of the magnetic field, then it can be shown that[8]

$$L = c_1 \frac{\sqrt{V}}{B} \qquad (1)$$

for stable focussing where C_1 is an appropriate constant.

The diameter of the electron beam varies along the beam. The effect is called scalloping. For fixed L the effect is reduced if[9]

$$B = \frac{c_2 \sqrt{I}}{\bar{r} \sqrt[4]{V}} \qquad (2)$$

where C_2 is a constant, I is the beam current, V the beam voltage and $\bar{r}$ is the average radius of the electron beam. A detailed and analytical discussion of TWTs is given in the book by Gittins[9].

IV. MATERIAL PROPERTIES OF PERIODIC PERMANENT MAGNETS

Because of their large coercivity, saturation magnetization, energy product and relative stability, samarium cobalt magnets are being used for electron beam focusing in TWTs.[10-15] $SmCo_5$ is presently the most used, but other chemical compositions such as Sm_2Co_{17} are being considered.

The steps for making the samarium cobalt magnets include[14]:

1. Grinding the alloy into a powder. In order to prevent oxidation, this will probably be done in an inert atmosphere.

2. The powder is pressed and compacted and the magnetization of the particles is oriented by a strong magnetic field.

3. The material is then sintered and it may be annealed.

A study of these magnets has yielded the following comments.[14]

1. The magnitude of the magnetic field applied to orient the particles, described above, has an important effect on the coercive force.

2. The coercive force also depends on the particle size.

3. The coercivity depends on the nature of the surface and it increases when damaged layers are removed.

4. The coercivity also is strongly affected by the annealing temperature. Heating in air may also affect the coercivity.

Although values differ, depending on the method of preparation and on alloying, Strnat in 1978[11] listed the following as possible for the sintered "$SmCo_5$" type of magnets:

$(BH)_{max}$	24 MGOe or 191 $\frac{kJ}{m^3}$
$_mH_c$	12 kOe or 9.6×10^5 A/m
$\alpha = \frac{1}{B_r}\frac{dM}{dT} = 100$ from -50 to 100°c	$\sim -.04$

When we start to think about new materials for TWT PPM magnets we need to consider the properties which are most desirable. These include[13,16]:

1. Large remanence
2. High coercive force
3. Large energy product
4. Low α (temperature coefficient)
5. Good stability at high temperature
6. Small aging effects

One way to classify the rare earth permanent magnets is by the mechanisms that govern their magnetization versus field characteristics.[17] Their high coercivity is, in the end, strongly influenced by their large crystalline anistropy. In samarium cobalt "1-5" materials, apparently the dominant mechanism for magnetization changing with field is the nucleation of reverse domains while in the "2-17" materials it appears to be the motion of domain walls. Fine grain structures should make "1-5" materials have larger coercivity because it would be necessary to nucleate walls in several grains to have an appreciable effect. Various techniques, such as precipitation hardening, for pinning the walls should be most effective for "2-17" materials. It is possible to distinguish between these two cases by the shape of the virgin curve.[18] The nucleation mechanism shows a much steeper increase of magnetization with field near the origin. It should be mentioned, however, that some actual samarium cobalt magnets have become too complicated to easily fit this classification.[19] The reasons for high coercive force are many and various and a complete theory will not be soon in coming.

Sintered SmCo$_5$ magnets are still the most common commercial rare earth permanent magnets, but Sm$_2$CO$_{17}$ type permanent magnets are also showing promise.[16] They show smaller coercivities but larger energy products than SmCo$_5$ (over 30 MGOe has been reported for Sm$_2$Co$_{17}$ type magnets). Temperature compensation has been achieved through alloying with heavy rare earths. This reduces the temperature coefficient α. Alloying with Cr or Mn has been found to increase the coercivity[20]. Temperature compensated high-coercivity

"2-17" magnets have been discussed by Strnat et al[16]. It should be also mentioned that the magnets now may contain phases of both "1-5" and "2-17"[19], so a classification into one or the other is not always useful.

Two other rather nebulous topics need to be mentioned. One is the effect of aging and the other is the effect of structure. It has been strongly recommended by Strnat[13] that the relationship between microstructure[21] and magnetic hardness continue to be studied. In some cases, large changes in magnetic properties have been reported without a corresponding observable change in microstructure.[19]

There have been several aging studies [22-26]. Adler and Marick[26] feel $SmCo_5$ is adequately stable below 150°C but not above 250°C. They feel Sm_2CO_{17} is more stable. Das et al[25] relate the stability to several factors including the amount of Sm_2CO_7 that is present. Ervens[24] feels that some Sm_2CO_{17} type alloys have a coercivity that competes with $SmCo_5$ and that they exceed $SmCo_5$ in other ways including long term stability. Hong-Zu[23] et al feels that the question of aging involves many different processes dependent on temperature. Strnat and Luo[22] find significant initial flux decreases in $SmCo_5$ at 120°C but then the magnets seem to be relatively stable.

One must keep in mind that the kinds of magnets available in the laboratory will not necessarily also be available commercially. Mildrum[27] et al have summarized the properties of sintered rare earth-cobalt permanent magnets which are available commercially. An earlier summary of the properties of commercially available $SmCo_5$ magnets has been given in a review of Strnat[10]. Some typical numbers for commercial magnets from a review by Polk[28] follow.

	Intrinsic Coercivity (kOe)	(BH)max (MGOe)
Sm Co$_5$	16	18
Sm$_2$Co$_{17}$ type alloys with (e.g. Cu, Fe)	7	~22
Two phase microstructure with "1-5" and "2-17"	13.3	~30

Newer types of magnets are also being considered[29], among them the Nd$_2$Fe$_{14}$B type. This magnet seems to hold promise for an energy product of 43 MGOe but at the expense of a Curie temperature of about 585°K versus over 1000°K for SmCo$_5$. Of course, work proceeds to try to improve the high temperature properties. Other work on amorphous materials has produced sizeable coercivities by annealing amorphous materials[28].

V. RESULTS

It was decided that the general problem of producing traveling wave tubes with consistently satisfactory fields from tube to tube needed to be broken down into several problems. The general problem involves at least: (1) Studying non uniformities in the magnetic fields of available magnets. (2) Studying the effects of the pole pieces and seeing how they control variations from ideal field behavior in the region of the electron beam. (3) Calculating the trajectory of the electron beam in the actual near axis field.

In order to keep the size of the project manageable it was decided to concentrate on (1) above. Here two things have been done. One was to collect together a list of references describing samarium cobalt and related magnets which are useful in TWTs. These references have been mentioned in IV above. The other way of attacking (1) was to do a calculation of magnetic fields arising from inhomogeneous magnets. The calculation was suggested by measurements which have been used to try to define the inhomogeneity of the magnet.[17]

The geometry of the ring magnets is defined by Fig. 2. We calculated the three components of the field H_r, H_θ, H_z as a function of θ for $r = (OD + ID)/2$ and z small, i.e. near the flat surface of the magnet. Notation: inner diameter = ID and the outer diameter = OD.

We assume the magnetization of the ring can be approximated by a uniform magnetization which is perpendicular to the flat surface and parallel to the axis of the ring. We also assume that we have a magnet like samarium cobalt for which the demagnetization field is never sufficiently strong to reduce its magnetization a significant amount.

It is well known that for purposes of calculating the field we can replace the uniform magnetization with surface pole densities determined by the discontinuity in the magnetization. In order to be able to treat the case of inhomogeneities we replace the surface pole densities with a discrete set of "bar" magnets with north and south poles. We would then vary the strength of the poles from "bar" magnet to "bar" magnet to model the inhomogeneities.

The "bar" magnets were arranged uniformly on a square grid and their number increased until, to plotting accuracy, H_r, H_θ and H_z did not vary significantly with θ.

For "north" poles with pole strength P_{ij} at $(X_i, Y_j, 0)$ and "south" poles at $(X_i, Y_j, -B)$ where $(ID/2)^2 \leq X_i^2 + Y_j^2 \leq (OD/2)^2$, the fields at X, Y, Z are given by

$$H_z = K \sum_{i,j} P_{i,j} \left[Z\, F_{i,j}(z) - (z+B)\, F_{i,j}(z+B) \right] \tag{3}$$

$$H_Y = K \sum_{i,j} P_{i,j} \left[F_{i,j}(z) - F_{i,j}(z+B) \right] GX\,(X-X_i)$$
$$+ K \sum_{i,j} P_{i,j} \left[F_{i,j}(z) - F_{i,j}(z+B) \right] GY\,(Y-Y_j) \tag{4}$$

$$R H_\theta = K \sum_{i,j} P_{i,j} \left[F_{i,j}(z) - F_{i,j}(z+B) \right] (-Y)(X-X_i)$$
$$+ K \sum_{i,j} P_{i,j} \left[F_{i,j}(z) - F_{i,j}(z+B) \right] (X)(Y-Y_j) \tag{5}$$

where

$$F_{i,j}(z) = \left[(X-X_i)^2 + (Y-Y_j)^2 + Z^2 \right]^{-3/2} \tag{6}$$

$$G = R^{-1} = \left[X^2 + Y^2 \right]^{-1/2}. \tag{7}$$

All distances are expressed in terms of (OD/2) i.e. X = 2x/OD etc. The constant K was set equal to 1 for convenience of calculation, so only the relative sizes of the fields are meaningful.

We show two plots with relative dimensions appropriate to a real traveling wave tube. Fig. 3 shows two things. First in a uniform magnet H_z dominates H_r and H_θ is negligible (identically zero for a perfectly uniform magnet). A way of assembling the TWT magnets is to cut them in half and then place them over the cylindrical region through which the electron beam will pass. In the plots below, we assume this process leaves a gap between the half rings of width (.04) times the OD. Gaps of this size can cause more field fluctuation than sizeable random swings in the pole strength. We also notice that a gap can cause quite a noticeable H_θ. This should not have a large effect on electron motion down the axis, however. In Fig. 4, we assumed the two half rings were put together in a non matching way so one had a ±20% fluctuation in the amplitude and the other had a ±40% fluctuation. The major effect is still the gap and the non-negligible H_θ across the gap. It is easy to modify the computer program to handle a variety of cases. Some cases (not shown) of systematic variation in the pole strength were modeled with expected resulting systematic variation in the fields. See the appendix for the computer program.

Randomness in the pole strength didn't appear to be as effective in inducing field fluctuation as might have been expected. The grid we used had many hundreds of points so the random fluctuations tended to average out. More systematic variations can, of course, be important.

VI RECOMMENDATIONS.

There seems to be no clear criterion for how much the field can vary without seriously eroding the performance of the tube. There are many calculations of electron trajectories in which some phenomenological or semi-phenomenological assumptions are made about the field.[6,8] What seems to be needed is an accurate assessment of how much actual fluctuations in the

12. Strnat, K.J., "Rare-Earth Permanent Magnets: Development Trends and Their Implications for the Industry," _The Rare Earths in Modern Science and Technology_ Vol. 2 (Edited by G. J.McCarthy, J. J. Rhyne, and H.B. Silber) Plenum Publ. Co., 1980, pp. 505-510.

13. Strnat, K.J., "Recent Developments in the Field of Rare Earth Magnets and Their Uses in the USA," _Proc. 6th Intl. Workshop Rare Earth-C~ Perm. Mag._ (Ed. J. Fidler), Tech. U. of Vienna, 1982, pp. 479-484.

14. Nesbitt, E.A., and Wernick, J.H., _Rare Earth Permanent Magnets._ Academic Press, New York, 1973, pp. 148-178, 183.

15. Becker, J.J., "Permanent Magnets and Magnetic Fluids,", _J. Appl. Phys.,_ Vol. 41(3), pp.1055-1064 (1970).

16. Strnat, K. J., Mildrum, H.F., Ray, A.E., "Samarium-Transition Metal "2-17" Magnets Temperature Compensated with Erbium," _Proc. 7th Intl. Workshop Rare Earth-Co Perm. Mag._ (Edited by P. Xiaoshuo, H. Wenwang, and Y. Chengzhou, Y.), China Academic Publishers, 1983, pp. 409-419.

17. Gnehm, Ch., G. and Haberer, J. P., "Homogeneity of Rare Earth-Cobalt Magnets," _Proc. 6th Intl. Workshop on Rare Earth-Co Perm. Mag._ (Edited by J. Fidler), Tech. U. of Vienna, 1982, pp. 329-339.

18. Velicescu, M. "Development and Production of Rare Earth-Cobalt Permanent Magnet Alloys", _Proc. 6th Intl. Workshop Rare Earth-Perm. Mag._ (Edited by J. Fidler), Tech. U. of Vienna, 1982, pp. 341-347.

19. Liu, S., Strnat, K. J., and Mildrum, H.F., "Sintered "$SmCo_5$" Magnets - Relations Between Coercivity and the Anisotropy of Major and Minor Phases," _Proc. 6th Intl. Workshop Rare Earth-Co. Perm. Mag._ (Edited by J. Fidler), Tech. U. of Vienna, 1982, pp. 631-642.

20. Bergner, R. L., Leupold, H. A., Breslin, J. T., Rothwarf, F., and ...., A., "Temperature Dependence of the Magnetic Parameters in the $Sm_{2-x}Gd_xCo_{17-y}Mr_y$ Compounds," _J. Appl. Phys._ Vol. 50, 2352 (1979).

21. King, C.E., Harris, I.R., Murphy, D.W.A. and Kennedy, D., "Microstructural Aspects of Some Samarium - Cobalt Alloys," <u>Proc. 6th Intl. Workshop Rare Earth-Co Perm. Mag.</u> (Ed. J. Fidler), 1982, Tech. U. of Vienna, pp. 411-419 and Fidler, J., "Coercivity and Microstructure of REPM," <u>Proc. 5th Intl. Workshop Rare Earth-Co Perm. Mag.</u> (Ed. K. J. Strnat), U. of Dayton, 1981 pp. 407-442.

22. Strnat, R. M. W. and Luo, H.-L., "Oxidation Behavior of Rare-Earth Magnet Alloys," <u>Proc. 6th Intl. Workshop Rare Earth-Co Perm. Mag.</u> (Ed. by J. Fidler), Tech. U. of Vienna, 1982, pp. 457-468.

23. Hong-Zu, X, Min-jie, C., Shang-lan, L., Yuan-jin, H., Wei-thung, Y. and Jia-jiong, X., "The Aging Phenomena of $SmCo_5$ Permanent Magnets at 20°-740°C," <u>Proc. 6th Intl. Workshop Rare/Earth-Co Perm. Mag.</u> (Ed. by J. Fidler), Tech. U. of Vienna, 1982, pp. 677-692.

24. Ervens, W., "Some Properties of High-Coercivity 2:17 Magnets", <u>Proc. 6th Intl. Workshop Rare Earth-Co Perm. Mag.</u> (Ed by J. Fidler), Tech. U. of Vienna, 1982, pp. 319-327.

25. Das, D., Kumar, K., and Dauwalter, C.R., "Mechanism of Flux Decay in $SmCo_5$ Magnets," <u>IEEE Trans. on Magnetics</u>, Vol. <u>MAG-19</u>(5), pp. 2050-2052 (1983).

26. Adler, E. and Marik, H. J., "Stability of Samarium-Cobalt Magnets," <u>Proc. 5th Intl. Workshop on Rare Earth-Co Perm. Mag.</u> (Ed. by K. J. Strnat), U. of Dayton, 1981, pp. 335-356.

27. Mildrum, H. F., Graves, G. A. and Abdelnour, Z.A., "Engineering Properties of High Energy Product Sintered Rare Earth-Cobalt Permanent Magnets", <u>Proc. 5th Intl. Workshop on Rare Earth-Co Perm. Mag.</u> (Edited by K.J. Strnat), U. of Dayton, 1981, pp. 313-333.

28. Polk, D. E., "Permanent Magnet Material: an Opportunity to Reduce Cobalt Consumption," <u>Naval Research Reviews</u>, Vol. <u>34</u>, Four, pp. 24-34, (1982).

29. Robinson, A.L., "Powerful New Magnet Material Found," _Science_ Vol. 223, pp. 920-922 (1984) and Sellmyer, D.J., Ahmed, A., Mueach, G. and Hadjipanayis, G., "Magnetic hardening in rapidly quenched Fe - Pr and Fe - Nd alloys," _J. Appl. Phys._ Vol. $55_1(6)$, pp. 2088-2090 (1984).

30. Mendell, J. T., Quate, C. F. and Yocum, W.H., "Electron Beam Focussing with Periodic Permanent Magnetic Fields," _Proc. IRE_ Vol 42, pp. 800-810, May 1954.

31. Harman, W.A., Hollister, R.S. and Tillery, J.O., "Permanent Magnet Study for High Average Power TWTs", RADC-TR-78-288, Feb 1979 (AD-A067 319/4), Rome Air Development Center, Griffiss Air Force Base, New York, 13441.
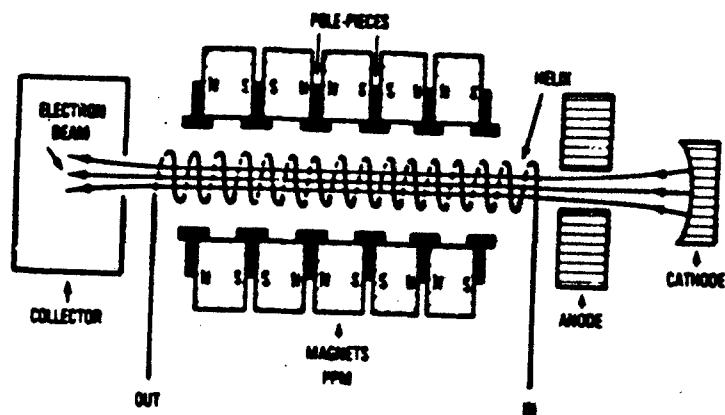
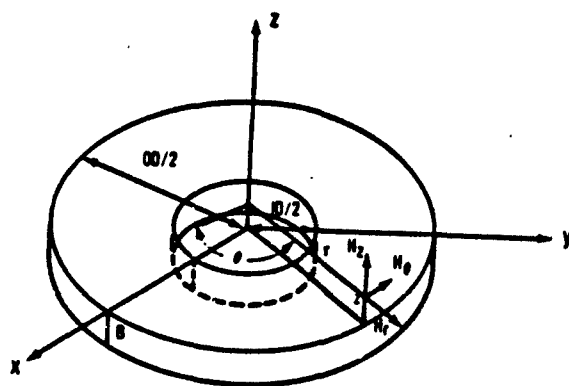**Fig. 1. Schematic of simplified TWT showing PPM focusing.**

Fig. 2. Geometry for ring magnets. Gaps are assumed to be cut along a diameter parallel to x-axis.
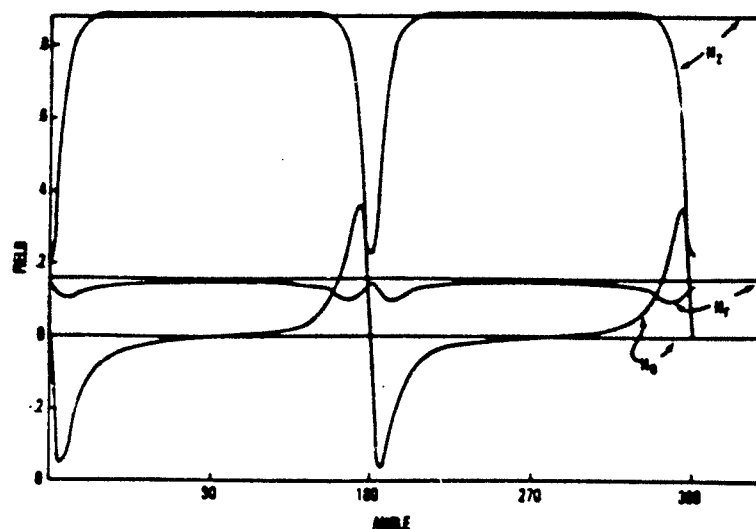
Fig. 3. Magnetic fields at mid radius as a function of θ. Straight lines = field of uniform magnet without gap. The curves show the effect of the gap. Here ID/OD = .55, 2Z/OD = .0743, 2B/OD = .525 and Gap Width/OD = .04.
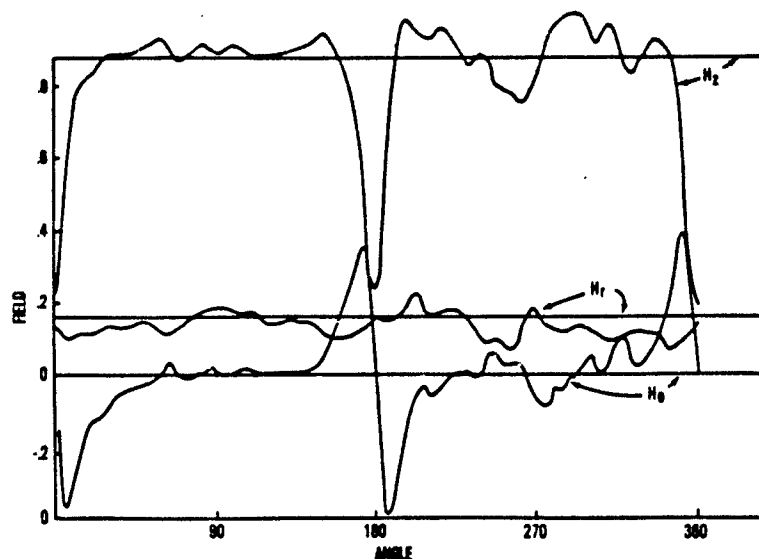

Fig. 4. Magnetic fields at mid radius as a function of θ. Straight lines = field of uniform magnet without gap. The curves represent the effect of the gap plus a random ±20% variation in pole strength for half of the ring on one side of the gap and a ±40% pole strength variation on the other side of the gap. Here ID/OD = .55, 2Z/OD = .0743, 2B/OD = .525 and the Gap Width/OD = .04.

113-19

```
5   REM   MAGNETIC FIELD PROBLEM          290  IF JJ >  = DP THEN 310
6   REM   FOR TWT RING MAGNETS            300  GOTO 420
7   REM   HZ,HR,HTHETA                    310  IJ = I1 * I1 + J1 * J1
8   REM   AS FUNCTION OF THETA            320  IF IJ < FF THEN 420
9   REM   FOR SPECIFIED Z,R               330  IF IJ > 1 THEN 420
10   INPUT "EVEN N GRID FACTOR=  "        340  AP = (X - I1) * (X - I1) + (Y
     ;N                                        - J1) * (Y - J1)
20   DIM RR(N,N)                          342  T1 = (AP + AA)
24  MM = N * N                            344  PT =   SQR (T1)
26  NP = (N + 1) / N                      350  TA = T1 * PT
28  EP = 2 / N                            352  T2 = (AP + BB)
30   INPUT "ANGLE FACTOR M=  ";M          354  QT =  SQR (T2)
32  PI = 3.14159254                       360  TB = T2 * QT
34  DT = 2 * PI / M                       363  GA = 1 / TA
40   INPUT "RANDOM AMPLITUDE FOR U        368  GB = 1 / TB
     PPER C=  ";AU                        370  GF = GB * (A + B)
45   INPUT "RANDOM AMPLITUDE FOR L        372  GG = A * GA
     OWER C=  ";AL                        374  GC = GG - GF
50   INPUT "ID/OD RATIO=  ";F             376  TC = GA - GB
60  FF = F * F                            382  IF JJ < NP GOTO 388
70  OO = (F + 1) / 2                      384  AM = AU
72   PRINT " (ID+OD)/(2OD)=  ";OO         386  GOTO 390
74   INPUT " 2R/OD FOR CALCULATION        388  AM = AL
     =  ";RA                              390  P = 1 + AM * RR(I,J)
80   INPUT "2Z/OD=  ";A                   392  H = H + P * GC
90  AA = A * A                            393  XR = XF * (X - I1)
100   INPUT "2(WIDTH OF RING)/OD=         395  YR = YF * (Y - J1)
      ";B                                 397  HP = XR * TC * P
110  BP = A + B                           399  HQ = YR * TC * P
120  BB = BP * BP                         401  H1 = H1 + HP
130   INPUT " GAP/OD=  ";D                403  H2 = H2 + HQ
140  DP = NP + D                          405  XT = ( - Y) * (X - I1)
150  DM = NP - D                          407  YT = X * (Y - J1)
160   FOR I = 1 TO N                      408  XT = XT / RA:YT = YT / RA
170   FOR J = 1 TO N                      409  HU = XT * TC * P
180  RR(I,J) = 2 *  RND (1) - 1           411  HW = YT * TC * P
190   NEXT J                              413  H3 = H3 + HU
195   NEXT I                              415  H4 = H4 + HW
200   FOR K = 1 TO M                      420   NEXT J
202  H = 0                                421   NEXT I
206  H1 = 0                               422  HR = (H1 + H2) / MM
207  H2 = 0                               423  HT = (H3 + H4) / MM
208  H3 = 0                               425  HZ = H / MM
209  H4 = 0                               427  TQ = (180 / PI) * TH
210  TH = DT * K                          428   PRINT
215  XF =   COS (TH)                      430   PRINT "THETA=  ";TQ
220  YF =   SIN (TH)                      440   PRINT "HZ=  ";HZ;"  HR=  ";H
225  X = RA * XF                               R;"  HT=  ";HT
230  Y = RA * YF                          442  TF = HZ * HZ + HR * HR + HT *
240   FOR I = 1 TO N                           HT
250  I1 = (I - (N + 1) / 2) * EP          444  TF =  SQR (TF)
260   FOR J = 1 TO N                      448  PRINT "TOTAL FIELD=  ";TF
270  J1 = (J - (N + 1) / 2) * EP          449  PRINT : PRINT
280  JJ = J * EP                          450  NEXT K
285  IF JJ < DM THEN 310                  460  END
```

1984 USAF-SCEEE SUMMER FACULTY RESEARCH PROGRAM
Sponsored by the
AIR FORCE OFFICE OF SCIENTIFIC RESEARCH
Conducted by the
SOUTHEASTERN CENTER FOR ELECTRICAL ENGINEERING EDUCATION
FINAL REPORT
OPERATOR ACTIVITIES IN WIND TUNNEL PWT 4T

Prepared by: Dr. M. Carr Payne, Jr.

Academic Rank: Professor

Department and   School of Psychology
University: Georgia Institute of Technology

Research Location: Arnold Engineering Development Center

USAF Research: Mr. Marshall Kingery

Date: August 15, 1984

Contract No: F49620-82-C-0035

<u>OPERATOR ACTIVITIES IN WIND TUNNEL 4T</u>

by

M. Carr Payne, Jr.

<u>ABSTRACT</u>

By observation and a task analysis, a research team determined
activities of Tunnel Operators, Instrument Technicians, Test/Operations
Coordinators, and Project Engineers as they performed testing in Wind
Tunnel 4T. Based on this data, recommendations are made which should
improve operations in the Control Room of Tunnel 4T.

Acknowledgement

I. INTRODUCTION

Wind tunnels have been developed as aerodynamic testing facilities in order to detect flaws and/or errors early in the design sequence. Such a tunnel simulates a moving object in the air by employing a fixed precise scale model which is placed in a moving air stream of known characteristics. Various measures are taken from the model as well as from the tunnel itself. This information is displayed in a control room where the entire operation of the tunnel is monitored and controlled.

As technology has evolved, new devices have become available. From time to time such devices have been added for tunnel operation, and information from them displayed in the control room. However, there has been no systematic examination of what information operators need to operate a tunnel or what form that information appropriately should take. Displays have been added on a piecemeal basis.

In recent years, costs of electrical power to operate a tunnel have been increasing until today power costs for a given test can easily exceed personnel costs. For this reason, there is a need to minimize the time needed for a human to make decisions about operation of a tunnel or about data being obtained from a model. This suggested the desirability of systematically examining the activities of personnel in the control room. In consultation with personnel at Arnold Engineering Development Center (AEDC), Tunnel 4T was selected for this study, as this tunnel was scheduled for use throughout the summer. By studying Tunnel 4T operations, procedures could be developed which could be used to study other test facilities.

II. OBJECTIVES OF THE RESEARCH REPORT:

This research effort involved a team composed of Drs. Gregory M. Corso and M. Carr Payne, Jr., and Mr. Michael J. Patterson, a graduate student on the SCEEE program. The objective was to carry out a task analysis of what operators do who work with Propulsion Wind Tunnel 4T. This analysis includes the nature of information needed to perform each task in tunnel operations. From this analysis recommendations can be made about displaying this information.

III. DESCRIPTION OF WIND TUNNEL 4T*:

Tunnel 4T is an aerodynamic wind tunnel for transonic studies, i.e. studies in which airflow velocity can be maintained at values up to 1.3 times the speed of sound (Mach 1). The tunnel constitutes a closed loop in which air continuously flows. Airflow is supplied by Plenum Evacuation System (PES) compressors which are also part of the systems of two other continuous propulsion wind tunnels, 16T and 16S. By compressing air, this system provides parallel streamlines with a uniform velocity profile at the entry to the tunnel's test section. A desired Mach number of the airflow is produced by regulating the PES compressors and controlling the pressure ratio across the nozzle of the tunnel. Tunnel 4T can be operated over a Mach number range from 0.20 to 1.30. By installing two removable supersonic nozzles nominal Mach numbers of 1.60 and 2.00 can also be obtained.

After passing through the nozzle, airflow passes through the test section, a rectangular volume 4 feet square in cross section and 12.5 feet long. This section is equipped with four porous walls, with porosity continuously variable from 0.0 to 10.0 percent open. Top and bottom walls can be diverged $\angle \frac{1}{2}$ degree from parallel, but side walls are fixed. The entire chamber is enclosed by a plenum chamber which allows part of the main tunnel airflow to be removed through the test section walls to alleviate interference and generate ⩗ when the tunnel is operated above Mach 1.0. This system produced airflow at controllable, known Mach numbers, known stagnation pressure and dynamic pressure, and stagnation temperatures from 90 to 135 degrees Fahrenheit (usually 100 degrees Fahrenheit). The corresponding Reynolds number of the airflow can be inferred from the combination of Mach number and pressure.

A scale model is placed in the test section where the airflow can pass over it. The model is small enough that it blocks less than 1% of the airflow when testing in the transonic range. It is usually mounted on a slender support referred to as a sting. The sting in turn is mounted to a movable boom. By this system, pitch and/or roll of the model may be changed either continuously or discretely during a

---

*For a more detailed description, see Reference 1.

test. Strain-gage balances are installed in the model to measure static aerodynamic forces and moments acting on the model. Balances to measure dynamic aerodynamic forces may also be used.

IV. TYPES OF TESTS CONDUCTED IN TUNNEL 4T:

Approximately 1300 air-on hours of testing are conducted in 4T each year. It is probably the busiest wind tunnel in the world. Although each test carried out in the tunnel is unique in that a particular model configuration and set of conditions are utilized, tests may be grouped into several types. Each of these types of test utilizes different information from the model and/or attachments, necessitating different instrumentation configurations in the control room. Each test is carried out under specified Mach number and pressure conditions. Control of these flow parameters is similar among different types of test.

Captive Trajectory Systems CTS) - An object attached to an aircraft is
    erred to as a store. In CTS tests the aircraft and store models
are mounted upside down in the tunnel. Each model is mounted on its own sting. CTS tests measure the aerodynamic characteristics of a store in various positions, either attached to the model or as it is separated from the model. Positions are computer-controlled with six degrees of freedom. A large amount of data is collected about store loads and motions in a short time period, as data is taken at closely-spaced points in a simulated trajectory. In the past year, approximately 60% of the work carried out in Tunnel 4T was CTS testing.

Free Drop Testing-
Some problems of store separation require greater flexibility in pitch and yaw motions than can be obtained with CTS test techniques. For these problems Free Drop Testing may be used. The store is attached to the model. When the desired conditions of the airflow are reached, the store is dropped from the model. It is photographed as it drops. Trajectory position data are obtained by analyzing these photographs. Approximately 5% of the work in Tunnel 4T in the last year was Free Drop Testing.

114-6

Force Testing -

Force and pressure characteristics of aerodynamic models can be obtained by mounting the model on a sting within the tunnel. Because of the wide variety of stings and balances available, Tunnel 4T is particularly suited for this test. Data is taken from different positions of model pitch and roll under varying combinations of tunnel conditions. Approximately 30% of the work in Tunnel 4T is force testing.

Others -

Other tests are carried out in Tunnel 4T on an occasional basis. For example, dynamic stability tests can be conducted. Magnus force and moments may be measured. This category of testing represents approximately 5% of the work in Tunnel 4T last year.

V.   PERSONNEL POSITIONS WITHIN WIND TUNNEL 4T:

Overall responsibility for testing is an Air Force function. Air Force personnel participate in planning each test program, and Air Force staff communicate with 4T control room personnel during testing. However, Air Force personnel do not operate the tunnel. Those functions are performed by contractor personnel. For this reason, Air Force personnel's role in testing is not described further in this paper.

Personnel involved in a test in Tunnel 4T can be divided into three groups according to activities performed:

(1) Definers of what data is needed from a test,

(2) Designers and planners of how to get this data,

(3) Operators of the tunnel and related sub-systems who carry out the plans and gather the data.

Persons involved with these different functions each has a role in testing.

User and Sponsor - The Sponsor is the originating party who has overall responsibility for test planning, programming, and funding. The Sponsor defines what data is needed from the test. Typically, the Sponsor has a contract with a User who has developed the hardware under test. The Sponsor's representatives and the User's representative(s) work together with personnel of AEDC and the Air Force to plan the

test. The User specifies conditions for the test program and supplies
the model. A User may also provide personnel who work on User-
supplied elements (e.g. a User may provide proprietary balances), along
with AEDC contractor personnel who ordinarily install a model in the
tunnel. Representatives of the User and the Sponsor have a work area
in the control room where they can evaluate data on-line. If there are
any changes that need to be made in the test requirements, they must
be approved by the Sponsor who funds the test program.

Project Engineer -

The Project Engineer is a professional engineer assigned to coordinate
all testing activities associated with a particular test program.
He/she works closely with the User and the Sponsor to plan and define
the test scope. During testing he/she specifies test conditions and
requests the Test/Operations Coordinator to interact with the tunnel
operator in establishing them. If the User or Sponsor wishes to make
any changes while a test is underway, the Project Engineer makes the
necessary calculations to specify appropriate tunnel conditions and
gives this information to the Test/Operations Coordinator.

Test/Operations Coordinator-

The Test/Operations Coordinator, sometimes referred to as Test
Engineer/Coordinator or Project Coordinator, works with Tunnel
Operators and Instrument Technicians to gather data according to
conditions specified by the Project Engineer. This person literally
co-ordinates activities in the control room. A log is kept of
everything that happens in tunnel 4T as indicated in the control room.
The Coordinator is responsible for ordering electrical power every
half hour when the tunnel is operating, and also monitoring power
usage. He monitors model installation and test conditions. He sees to
it that data-presenting devices such as line printers or graphics
terminals work properly. When the tunnel is not operating, he
oversees maintenance of various system used in testing.

Instrument Technician-

The Instrument Technician's primary responsibility is to install,
calibrate, and maintain equipment. An Instrument Technician runs
maintenance checks on computer programs displayed in the control room.
These programs control configurations of the model as well as

conversions of raw data from analog to digital form. When a CTS test
is run in the tunnel, an Instrument Technician monitors displays and
operates controls to insure that the store and/or model move to the
desired positions for a trajectory test. In Free Drop testing the
Instrument Technician, on signal from the Test/Operations Coordinator,
operates the mechanism (a "burn box"), which releases the store.

Tunnel Operator-

The Tunnel Operator opens and closes valves, which in turn, control
the pressure ratio and Mach number of air in the tunnel. The Project
Engineer specifies conditions of each, and the Tunnel Operator, who is
monitored by the Test/Operations Coordinator, opens and closes valves
to produce these conditions in the tunnel. When proper conditions are
met, data is gathered. The Tunnel Operator also places an order for
electrical power as requested by the Test/Operations Coordinator.

VI. TASK ANALYSIS:

In order to get to know personnel in the control room and to
become familiar with procedures, the research team made extensive
visits during each of the types of test conducted in the tunnel. The
tunnel is operated for three 8-hour shifts a day, so the team observed
during each shift. From these observations, questions were prepared
for use in an extensive interview conducted individually. Each person
interviewed was assured that his responses would be labeled only by
job title with nothing to identify him as an individual. During each
interview at least two members of the research team took detailed
notes of each person's responses as a check on reliability.

Each person interviewed was selected by the manager of his
particular position (e.g. tunnel operator), on the basis of experience
in operating Tunnel 4T. Each man was interviewed during his regular
shift at a time when he was not gathering data. All of the three
Test/Operations Coordinators assigned to 4T were interviewed. One
Tunnel Operator from each shift was interviewed in addition to a Craft
Supervisor for that position. Five Instrument Technicians and six
Project Engineers were interviewed. Among the Project Engineers, both
the Aerodynamics Section and the External Stores Section were
represented.

The interview was divided into two phases: (1) a specific description of what each person does, and (2) each person's concept of how his work station could be improved.

(1) Each interviewee was asked: "After pre-ops and system check-out have been completed what is the first activity that you do? Then, he was asked what information is needed for this activity and where that information is obtained. After that, the same questions were asked about the next activity that he performs. This procedure was continued until the interviewee had given a detailed description of his activities. Any differences in these activities with different types of tests were determined. How a person responded to any unusual situations and where he got the information that told him it was unusual, were checked. Finally, he was asked if there was anything else either in the way of information or of a device that would help him do his job. In addition, Test/Operations Coordinators were asked who they talk with on an inter-com or telephone during a test run. Project Engineers and Instrument Technicians were asked how they determine that data they have collected is valid, and their opinion of the trustworthiness of the systems used to collect the data.

(2) Each individual was shown a photograph of his work station. He was asked to indicate the more important displays and controls. He was also asked which he used more frequently. These photographs had been cut apart in such a way that the different displays and controls could be rearranged. Each person was asked to rearrange them to make a lay-out that he felt was better than the present arrangement. He was advised to make the lay-out without worrying about whether or not it was feasible to carry out his recommended changes. That is, he was to present a preferred lay-out, whether it involved modification of the present control room or whether it involved constructing a new control room.

Data from the Task Analysis-

Tunnel Operators - During a test run, a Tunnel Operator has four major activities: (1) he orders electric power every half hour as instructed by the Test/Operations Coordinator, (2) he calls the Plenum Evacuation System (PES) operators in a remote location to give tunnel conditions for the test, (3) he manipulates valves to bring tunnel conditions to the appropriate pressure and Mach number and to maintain them there as specified by the Project Engineer, and (4) he monitors all tunnel conditions. He relies on a mimic board to tell him which PES compressors are on-line. These provide the basic conditions within the tunnel which the Tunnel Operator fine-tunes to meet test conditions. He relies on the Status Annunciator panel to show that control parameters within the tunnel are satisfactory within tolerance. To set pressure, he uses Valve 65, which admits dry air. Valve 65 is manually controlled, as its operation by computer does not work properly. It is faster to set this valve manually than by computer. If test conditions permit use of atmospheric air (Mach number less than .6, pressure less than 1200 P_t) Valve 8Q can be used. If test conditions involve Mach numbers less than about .8, Valves 92 and 92A are used to set the Mach number. These are put on a computer which is better for fine tuning. If a higher Mach number is required, Valves 93 and 93A are used. In each case, Valves labeled A are "fine-tuning" valves, and are computer-controlled. However, Valve 93 must be adjusted continually because at these high Mach numbers, models may be moved by the airflow which causes conditions within the tunnel to change.

Tunnel Operators differ in their use of displays. Some consider the Real Time Data Display to be the most important display, as power usage can be estimated from it, and it shows Mach number and pressure. Others rely on a redundant LED display for information about Mach number and pressure and rarely use the Real Time Data Display for this purpose. Most operators rely on the TV monitors, as these make it possible for an operator to estimate in advance changes that he will have to make to keep tunnel conditions steady when a model moves.

Panel Layout Suggestions- Those Tunnel Operators, who made suggestions, agreed that displays which are frequently used, such as the TV monitors or the 4T Status panel, should be at the center of the work station at about eye level. Valves which are used more frequently, such as Valves 65, 92, 92A, 93 and 93A, should be mounted towards the bottom of the panel in the center. Valves should be functionally grouped. Valves 65 and 92 should be mounted beside each other, lower on the panel. LED-type pressure indicators should be mounted beneath each other rather than side by side between two valves as at present. Displays and controls which are not used frequently should be placed on the periphery of the Tunnel Operator's work station, as they are at present. These include displays for wall porosity, wall angles, diffuser walls, porosity walls, personnel interlock, ETF Make-up Duct Pressure, Valve control, and Remote loader.

Instrument Technicians- The Instrument Technician's work station is concerned with devices for gathering data. Relative usage depends on the particular test. Most of these devices are controlled by computer. For this reason, most of his responsibilities during a test run are primarily monitoring of displays and assisting with any changes in the model or stores. He monitors paper usage by line printers. During Free Drop Tests he is in charge of monitoring the amount of photographic film used. He also releases the store upon signal from the Test/Operations Coordinator. Before a test run is started, the Instrument Technician enters constants into the Data Acquisition Panel, and during CTS testing into the CTS Control Constant Boxes as instructed by the Project Engineer, who has calculated the constants. During CTS testing, an Instrument Technician mans the CTS Room next to the tunnel test section.

The Instrument Technicians consider the Data Acquisition Panel (DAPS) most important. He uses it, the TV monitors, and the CRT displays from 1160, DEC-10, and DDAS computers most frequently during a test run. The CRT display from computer 808C contains more detail than is needed, as all that is needed is to show that the system is running. This display is rarely used.

114-12

Panel Layout Suggestions-   Instrument Technicians generally seem
satisfied with the work station. However, it was suggested that E
Meter Relay and O'Graph Remote Control panels, the Test Article Status
Panel, as well as Servo-amplifier, Pos. feedback, and Tachometer plugs
be removed, as they are never used during the testing phase. The
single panel controlling pitch and roll, the LED displays of pitch and
roll and the pitch and roll meters should be combined, and preferably
placed close to the center of the work station. Otherwise, there were
no suggestions for major changes of panel positions.

Test/Operations Coordinator- As the person in charge of the
control room the Test/Operations Coordinator is responsible for seeing
to it that data is gathered under specified conditions as planned. He
personally inspects each model change to insure that the correct
configuration is mounted in the tunnel. He orders power every half
hour. He listens as a computer takes a data point. If the machine
sound is unusual ne checks to see if it is off-condition. He helps
the CTS operator if a bad store-ground occurs which can damage a
balance.

Because of the extent of his responsibilities, the
Test/Operations Coordinator makes extensive use of the TV monitors,
the Real Time Data Display, and the CRT display of computer 1160. The
CRt display of the DEC-10 computer is used, but not as often as the
others.

Panel Layout Suggestions- Test/Operations Coordinators are
pleased with the lay-out of the work station, and had no suggestions
for a change in what is displayed. If the work station were moved so
as to face the Tunnel Operator's and Instrument Technician's panels,
then the monitors should be moved to be in a line at eye level.

Project Engineer- The Project Engineer does most of his work in
advance in preparation for a test run. During the run, he verifies
that the correct constants are being used by checking a line printer
where they are tabulated. When data is coming, he checks data trends
by examining graphs of certain data on a GT-42 computer display. If
any change is required in the test plan, he makes the necessary
calculations and gives them to the Test/Operations Coordinator.

114-13

Because his task is one of checking rather than monitoring, the Project Engineer is less concerned with display of specific conditions than other personnel in the control room. He uses the tabulated and graphical data to observe trends. Having this in real-time would be a help to him.

VII. PROBLEM AREAS IDENTIFIED IN INTERVIEWS:

During the interviews several common problems were mentioned. These are tabulated in Table 1 according to how many people in each position mentioned that item.

1. Telephone and/or Intercom- Almost everyone who has visited Tunnel 4T has commented on the poor communications system. The telephone is a party line and often is hard to hear. The intercom between the control room and the remote CTS room often does not work.

2. Glare on instrument panels- Glare on these panels is bad enough that often operators turn off the room lights. This is less of a problem at the Test/Operations Coordinator's work station than at the Tunnel Operator's and Instrument Technician's stations.

3. Some controls are inconvenient to reach at the work station, or an improperly-designed control is being used.

4. Similarly, operators feel that some displays should be in a different location than is presently the case.

5. Extraneous people in the control room- At the beginning of a shift, numerous visitors drop by the control room. These people add to the noise level and general confusion in the control room.

6. Displays are not comprehensible or readable, or another display is needed. These display problems are not a major problem for Tunnel Operators but are for Instrument Technicians and Test/Operations Coordinators.

7. The Control Room should be closer to the tunnel- Instrument Technicians and Test/Operations Coordinators must make frequent trips

to the tunnel. This is especially true during Free Drop tests when there are frequent model changes which must be checked. The distance involved is a time-waster, not to mention a hazard during bad weather.

Other problems identified were mentioned by fewer people.

VIII. RECOMMENDATIONS:

The approach followed in the present study may be used to study other wind tunnels in which electrical power costs are greater than in Tunnel 4T, e.g. Tunnel 16T or the von Karman Facility tunnels. As these tunnels are less automated than 4T, and thus require more operators, greater savings may result from such a study.

Based on observation and the task analysis, the following items are recommended. Some of these apply to the entire control room, while others are for specific work stations.

Control Room-

1. Telephone and intercoms- A common complaint is that the telephone system is inadequate. It is a "party-line" in which too many stations are on the phone line. Sometimes, reception is poor. It is recommended that a new phone system be installed, preferably a "memory phone" with which a Test/Operations Coordinator can press a single button which would automatically connect with persons whom he calls frequently. We understand that the entire telephone system for AEDC is to be changed. This may take care of the problem, but at present the telephone is a real "choke point" in the Control Room.

The intercoms between the Control Room and the Computer Room and the Control Room and the CTS Room are old. Both need replacing with up-to-date equipment.

2. Glare - Glare from the surfaces of the work stations is sufficient to cause discomfort to operators. They often turn off overhead lights because of this. The glare could easily be reduced by placing diffusers over fluorescent bulbs above the work stations. Appropriate values of luminance of the glare source are presented in Reference 2 (p. 52).

3. **Noise and extraneous people-** A number of people drop by the first shift. This adds to the noise level in the Control Room. Personnel other than Air Force representatives, User, Sponsors, Project Engineers, Test/Operations Coordinators, Tunnel Operators, and Instrument Technicians needed for a test run should not be in the control Room during a test run unless they have a specific task to perform.

4. **Line printer-** One of the major contributors to noise in the Control Room is one line printer. One is used to monitor real-time data and another to print final copy of the data for the User. Real-time data can be monitored more rapidly from a CRT display in which data can be called up. As there is often a lag in print-outs from the printer, use of this CRT should save decision time for the Test/Operations Coordinator. As a User does not have printed data during a run, there is no need for this printer to be in the Control Room. It can be moved to another location where its noise is less of a problem.

5. **Complexity of information displayed-** Some displays are used solely to identify when tunnel conditions are met, or to monitor conditions. Use of digital information in such displays is overly complex. A bar diagram or a status indicator (such as a light which is on when conditions are satisfactory) is all that is required.

6. **Spare parts-** A few spare parts, such as fuses or light bulbs, should be available in the Control Room area. There has been a delay in replacing such parts when a report has been made to do so, lowering the quality of the display and control panels. For example, some light bulbs at the work stations are burned out. Ready availability of such bulbs, as well as agreement about who is allowed to change them would improve the displays.

7. **Separate work space for the User and Sponsor-** Both control room personnel and Users themselves would like for the User to have a work area outside of the Control Room. A User needs a TEKPLOT-like graphics display, but Users and Sponsors do not need the specific data available in the Control Room. Users and Sponsors need access to the Control Room and the Project Engineer, but noise present in the Control Room is disturbing to their work. A work place for Users and Sponsors

114-16

outside of the Control Room where they can discuss test data and where there is a real-time graphics display is needed.

8. <u>Location of a new Control Room-</u> If a new control room is built it should be closer to the tunnel. The present arrangement in which Test/Operations Coordinators and Instrument Technicians have to make frequent trips to the tunnel (some 72 steps) in all sorts of weather is not only hazardous but also is a time-waster. There is sufficient appropriate space available if a decision were made to build a new control room.

<u>Tunnel Operators-</u>

1. <u>Panel removal-</u> Remove from the Tunnel Operator's panel two unidentified counters and Remote Readout Power Supply #1, 2, and 5 panels. These are not used. The Tunnel Indicator is not needed by the Tunnel Operator, although other personnel may use it.

2. <u>Repair-</u> Valve 65 should be functionally computerized. The computer system for this valve does not work at present, which requires an operator to set it manually. Computerization should save time in the valve's operation in getting the tunnel on test conditions with a resulting saving in power.

4. <u>Design of controls-</u> When a valve is used to fine-tune test conditions, the control should be a knob rather than a push button. A person can make a more sensitive adjustment with a knob.

5. <u>Audible signal-</u> The audible signal when tunnel conditions have been met should be made slightly louder. This signal comes from a loudspeaker mounted on the Tunnel Operator's work station. However, it sounds as if it comes from behind him, so he sometimes does not hear it.

<u>Instrument Technicians-</u>

1. <u>Removal of panels</u> - Remove from the work station E meter Relay and O'Graph Remote Control panels and Test Article Status Panel in addition to Servo-amplifier, Pos. feedback and Tachometer plugs.

2. <u>Change in display-</u> Remove the CRT display for computer 8080 and replace it with an indicator light which shows when the computer 8080 system is running.

3. <u>Need display in CTS Room-</u> An indicator of Mach number should be installed in the CTS Room. At present, the Instrument

Technician there has no way of knowing when the tunnel is on conditions and the system is ready to gather data.

4. <u>Moving a panel</u>- The single panel controlling pitch and roll should be moved closer to the center of the work station.

5. <u>Instructions for new equipment</u>- When new equipment is installed, written instructions should be provided. At present, an Instrument Technician must learn its operation pretty much on his own.

<u>Test/Operations Coordinator</u>-

1. <u>TV display</u>- Higher contrast is needed in the TV display. This may not be possible because of the parameters for mounting the TV camera in the tunnel, but the availability of higher contrast equipment should be investigated. It is sometimes difficult to see changes in model position with the present TV monitor.

2. <u>Desk space</u> - The Test/Operations Coordinator needs more desk space. His responsibilities require him to do considerable writing. At present the space at his work station is cramped.

3. <u>Forms for Free Drop Test</u>- During a Free Drop Test the Test/Operations Coordinator must complete a number of forms, one each time the tunnel is opened. With all of his other activities this sometimes gets him behind. The form for this test should be redesigned to make it easier and faster to fill out.

4. <u>Location of work station</u>- If a new room were built the Test/Operations Coordinator's work station should be closer to the Tunnel Operators and Instrument Technician's panels, preferably facing them. This would allow more desk space. The Test/Operations Coordinator must interact with the Project Engineer and sometimes the User, so the Project Engineer's work station should continue to be nearby.

REFERENCES

1. "Test Facilities Handbook (Eleventh Edition)." Arnold Engineering Development Center, April 1981.

2. "Human Factors of Workstations with Visual Displays." International Business Machines Corporation, 1984.

TABLE 1
PROBLEM AREAS IDENTIFIED IN INTERVIEWS:
FREQUENCY OF COMMENTS MADE BY TUNNEL PERSONNEL

	Tunnel Operators N = 4	Instrument Technicians N = 5	Test/Operations Coordinators N = 3
Telephone and/or intercom	3	4	3
Glare on instrument panels	3	5	2
Controls out of reach or improper	4	3	0
Location of displays	4	3	1
Extraneous people in Control Room	0	5	2
Displays not comprehensible or readable or need another display	0	4	3
Control room closer to tunnel	0	3	3
Noise in Control Room	0	3	2
Availability of spare parts	1	3	0
Additional groups should be with operations, e.g. optical group	0	3	0
Controls not ordered	1	2	0
User workspace should be outside of the Control Room	0	1	2
Amount of working space	0	0	2
Problems of transfer to another tunnel	0	2	0
Air conditioning	0	1	1

114-20

1984 USAF-SCEEE SUMMER FACULTY RESEARCH PROGRAM

Sponsored by the

AIR FORCE OFFICE OF SCIENTIFIC RESEARCH

Conducted by the

SOUTHEASTERN CENTER FOR ELECTRICAL ENGINEERING EDUCATION

FINAL REPORT

FUTURE TACTICAL AIR CONTROL SYSTEM DATABASE DESIGN

Prepared by: William Perrizo
Academic rank: Associate Professor of Computer Science
Academic Department: Computer Science
University: North Dakota State University
Research Location: Hanscom AFB, MA, Mitre location
USAF Research Contact: Lt. Col. Paul Rainville
Date: August 29, 1984
Contract No: F49620-82-C-0035

FUTURE TACTICAL AIR CONTROL SYSTEM DATABASE DESIGN
by
William Perrizo and Donald A. Varvel

ABSTRACT

Tactical command and control systems in the era of TACS-2000 and beyond will be distributed in order to maintain a sufficient degree of survivability. The underlying database system will also be distributed. It must respond quickly to both updates and requests for information, and must contain enough redundancy to sustain simultaneous losses of several elements. Few production distributed databases exist, and none appears suited to this application. This report details our work on designing a suitable database system. Our major work to date has been the areas of data replication, backup, and concurrency control. Suggestions for further research in this area are offered.

Acknowledgement

I. INTRODUCTION

Future tactical command and control systems must be made mobile and capable of surviving enemy attacks. Since mobility precludes much hardening, such a system will have to be distributed so that no single element makes a very attractive target[19].

The underlying database system must respond quickly to both updates and requests for information, and must contain enough redundancy to sustain simultaneous losses of several elements. That means a distributed database must be used, and information sent where needed as soon as possible. Few production distributed databases exist, and none is suited to this application. A suitable database system must be designed.

Nearly all work on distributed databases[5,10,15,16] assumes the use of the relational model of data[7]. Older models, such as the hierarchical and network, assume that access to the data is a record at a time; such access is not reasonable in a distributed setting. For that reason we have assumed that the relational model will be used, but nothing in our work to date precludes the use of another model.

Database systems presently in use have in general been designed for a commercial environment, where occasional breaks in service and slow response may be tolerated but inconsistent or inaccurate results cannot. In a tactical system, slow response and unexpected breaks in service cannot be tolerated, but where information is approximate to start with some inconsistencies may be acceptable. We have therefore given considerable attention to maintaining the highest possible level of continuous service and to reducing or eliminating those factors which degrade responsiveness.

Our consideration of these problems may be divided into six topic areas: data modeling, data replication, site initialization and recovery, concurrency control, commitment and query processing. Others have done some work in several of these areas; our main work has been in the areas of replication, system recovery, and concurrency control.

II. OBJECTIVES

Future Tactical Air Control Systems must involve innovative concepts for tactical command and control during a high-intensity conflict of the future. Large easily-recognizable centers must be augmented or replaced by small elements which can perform a number of functions and are not easily identifiable. In short, most experts are

proposing distributing C^2 operations in the theater[19,16]. Preliminary studies support this assertion[13].

The following principles and constraints define the context for the future TACS database design. These principles were formulated based on many useful conversations with Air Force and civilian personnel.

1. As soon as possible after entering the system, data should be sent to each site with a need or potential need for it.
2. Automated systems within the overall information system must in no way limit the options available to commanders in the Air Force command hierarchy.
3. A reliable self-organizing communications network capable of handling large volumes of data is assumed to be available. Communication network issues are not treated in this study.
4. In Tactical Air Control Systems of the future, the data replication and distribution issue will be much more sensitive than it is in commercial systems, while the need for elaborate distributed query processing capabilities may not be as critical.
5. The methods for handling reconfiguration, initialization, and recovery must take into account the possibility that portions of the database may become unavailable, either by being in a state of relocation or through wartime attrition.

The following concepts should be considered in this design:
Data modeling
Data replication and distribution
Initialization and recovery
Concurrency control
Commitment
Query processing

Data Modeling:

Data modeling is a process for representing data, data relationships, and data manipulation operations in a systematic (often graphic) language. There are three widely accepted data models: hierarchical (data is structured in outline form), network (data is linked to form interlocking rings), and relational (data is structured into simple flat tables).

The data makeup and data requirements of a future tactical air control system are only partially known at this time. Therefore much of the data modeling effort must be postponed [2,3,9,11]. Where data modeling can be done, the relational data model[7] will be used because of its superior flexibility and clarity. This choice does not preclude using another model for the implemented system.

Structuring database records by considering data item usage can yield substantial efficiencies in the database system. Physical data modeling techniques such as mathematical clustering, iterative grouping,

and hierarchical aggregation will need to be used to determine efficient access paths and record, segment, file, and data set structuring[15].

Replication and Distribution:

Future tactical C^2 databases will serve well-structured functions. Replication methods must be formulated which will efficiently distribute data to all sites with a potential use for the information. This potential use may include new responsibilities taken on by backup sites when primary sites are lost. This part of the database design will be very important in the future TACS setting. New algorithms will need to be formulated, tested and evaluated, since the subject has not been extensively treated in the literature.

There will always be data transfer limitations on the network. Scheduling algorithms will be considered to prioritize the transfer of data. The transfer of data will be done according to a priority scheme based on urgency of the need at the various sites. (Sites with primary responsibility for a function have the most urgent need for data required by that function. Backup sites have less urgent needs.) In this way network idle time would be put to good use providing full or near full replication of data without jeopardizing high priority message traffic. This approach would give the commanders great flexibility in designating and shifting command and control responsibilities.

Different priority schemes will be suggested for different functions. For example, data destined for elements with area-based responsibility (e.g., present day Command and Reporting Centers) might best be prioritized based on proximity to the primary area of responsibility, whereas data destined for elements with global responsibilities (e.g., present day Tactical Air Control Centers) might best be prioritized in terms of the resolution of the data itself (details assigned low priorities, summary information high priority).

We assume that all required archival backups would be transmitted to sanctuaries outside the theater via a long haul network.

Initialization and Recovery:

A "drive up and plug in" C^2 element will undergo initial connection to the distributed database followed by one or more subsequent separations from it. For both initialization and recovery, algorithms are needed to bring the resident database up to date while avoiding unnecessary data transmissions and rewrites.

Concurrency Control:

The object of traditional concurrency control is to give each user

the illusion of being the sole user of the system. Lacking concurrency
control, write-write conflicts lead to lost updates and read-write
conflicts lead to inconsistent views of the data. Concurrency control
in a future TACS database system must provide protection from lost
updates and inconsistencies without degrading system performance.

Query Processing:

Query processors are the software modules which respond to user
requests (queries) for data or information. The required data may
reside at the query site (local query) or it may be distributed over one
or more other sites in the network (remote query). In light of design
constraint 1, as stated on page 2, local queries are expected to be for
more common than remote queries. The initialization and recovery
systems will require the ability to query other local databases and
remote querying will be necessary to ensure data consistency and
completeness. Thus, some capability for remote querying is necessary,
for initialization, recovery, consistency and for the occasional
user-issued ad-hoc remote query[12,17]. The query processor must be able
to answer the users request in a transparent fashion whether the data is
local or remote. That is, the user must not be required to know where
the data is located in order to query that data.

Commitment:

The fundamental function of a database management system is to
carry out transactions. Transactions are atomic units of work in the
sense that they are the smallest independent units of activity making up
database applications. Transactions are all-or-nothing propositions.
Their effect on the system should be as if they executed either in total
or else not at all. Transactions involving more than one resource
manager (such as high-command information dissemination) require two
phase commitment procedures. In the first phase each resource manager
must report a "ready to commit" message to the transaction coordinator.
If all resource managers report "yes", then in the second phase, the
coordinator issues a "commit" command; otherwise the coordinator issues
a "rollback" command. Due to the stringent time constraints on much of
the TACS data, commitment procedures will need to be very efficient.

III. REPLICATION AND DISTRIBUTION

Efficient methods for replicating and distributing data are needed
in a distributed information system serving well-structured military
command and control (c^2) functions where the loss of elements must be
anticipated.   The class of replication methods below contains all

methods consistent with the principles stated on page 2 of this proposal. Principle 1 and 2, restated below, are the most pertinent to the data replication issue.

PRINCIPLE 1
> All data needed by a site to perform its C^2 function (or any future functional assignment) should be sent to that site as soon as possible after it enters the system (full data replication).

PRINCIPLE 2
> The automated data replication method should in no way limit the commander's flexibility with respect to C^2-function assignments. The data replication site issue and the C^2-element backup site issue will be kept separate.

These two requirements were postulated as a setting for this analysis based on many discussions with knowledgeable Air Force personnel.

The phrase replication configuration will be used for a choice of data backup sites (primary, secondary, ...) for each site in the system. Following the first principle stated above, the data backup chain for each given site will be defined to consists of an ordering or chaining of all other sites in the system, where the first site in the chain is designated as the primary data backup site, the second is designated as the secondary backup site, etc.

A priority assignment method will be used to assist the network in queueing the data for transport. The details of this priority method will not be treated here, except to say that data being replicated to primary data backup sites is high priority, while data being replicated to lower level data backup sites is somewhat lower priority and high priority data is pre-emptive in communication network queues. Also, priorities will depend on the nature of the data as well as the destination. This priority method will allow the data backup process to use network idle time to advantage in extending data backup chains without adversely affecting the transmission time of high priority data. It still may be deemed unnecessary in some instances to have a complete chain of data backup sites. In such instances the full chain can be truncated at the appropriate depth.

It may be desirable to assign the same priority to more than one site (particularly in light of principle 2 above). That is, several sites could be designated as co-primary data backups (co-secondary data backups, etc.). To allow for this generality, we consider the chain of data backups for a site, a, in a system with sites, $N=\{a,b,...\}$ to be a sequence of subsets $N_{1,a}$, $N_{2,a}$,.... , where $N_{1,a}$ is the set of primary

data backups for a, $N_{2,a}$ is the set of secondary data backups for a, etc.

The following is a more formal treatment of the replication issue in which replication configurations are characterized using product functions.

Given sets N and M, the notation N*M will be used to represent the subset of the Cartesian product with the diagonal removed. For instance if N = {a,b} and M = {a,c}, then N*M = { (a,c) (b,a) (b,c) }. A replication configuration for a system with sites N={a,b,...} can be represented as a function, f, from N*N to the positive real numbers, R^+, in the following sense.

A function $f: N*N \longrightarrow R^+$ <u>represents</u> a replication configuration if for each site, a,

$$N_{1,a}, \; N_{2,a}, \; N_{3,a}, \; \ldots$$

is the data backup chain for a, where $N_{1,a} = \{b \text{ in } N \mid f(a,b) = \min(f(\{a\}*N)) \}$, $N_{2,a} = \{b \text{ in } N \mid f(a,b) = \min(f(\{a\}*(N-N_{1,a})) \}$, ...
The function f <u>canonically represents</u> the replication configuration if f assigns the value 1 to all primary backups, the number 2 to all secondary backups, etc.

It can be shown that these canonical functions characterize all replication configurations in the sense that every replication configuration is represented by one canonical function and each canonical function represents a unique replication configuration. (Recall that replication configurations with depths of 1 or 2 etc, can be derived from these by truncation.)

This fact 1 follows from the consideration that, given a replication configuration, the function which assigns 1 to all primary data backup sites, 2 to all secondary data backup sites, 3 to all third level data backup sites, etc., is canonical and that any canonical function, f, prescribes a replication configuration where the chain for site, a, is

$$N_{1,a}, \; N_{2,a}, \; N_{3,a}, \; \ldots \ldots , \; N_{max(f),a}$$

(the sets $N_{i,a}$ are defined above).

Non-canonical functions can be used to define configurations just as well as canonical functions; however the correspondence is no longer one-to-one. This fact is used below to define configurations from standard functions (such as distance).

PHYSICAL DISTANCE METHOD: Physical distance can be used to generate a replication configuration, as shown in figure 1. The function is

$f(a,b)=SQRT((a_1-b_1)^2 + (a_2-b_2)^2)$, where the position of site <u>a</u> is (a_1,a_2) in some Cartesian coordinate system. This configuration provides a separate data backup chain for each site.
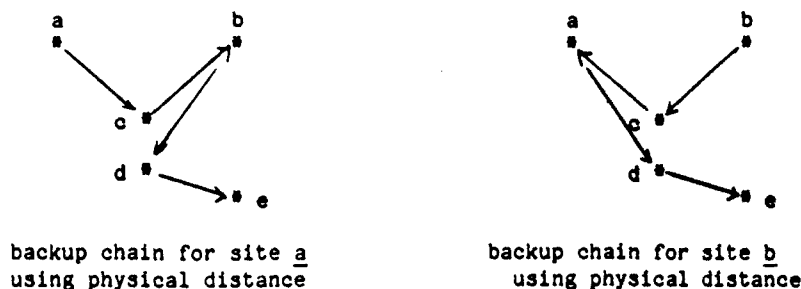

backup chain for site <u>a</u>   backup chain for site <u>b</u>
using physical distance   using physical distance

Figure 1

The question of data backup load was studied using analytic and statistical techniques. From analytic considerations, one can conclude that the expected number of sites for which a given site will be primary data backup is 1 and the maximum number of sites for which a given site will be primary data backup is 5. Using Monte Carlo techniques, the distribution of primary data backup loads was simulated. A graph of the results of this study is shown in Appendix A.

ADVANTAGES OF THE PHYSICAL DISTANCE METHOD:

1. Data backup sites are close to the backed up site itself. Therefore, for sites with area based responsibilities, the backup data could be expected to extend and enhance the resident data. In that sense it will tend to enhance the information content of the resident data.
2. The method will be robust under C^2-element moves over short distances, since such moves will only slightly alter the physical distance basis.
3. Backup loads are quite evenly distributed among the sites. Figure 4 shows the expected percentages of sites serving as primary backup for zero other sites, one other site, etc. The study was done using a Monte Carlo simulation.

DISADVANTAGES OF THE PHYSICAL DISTANCE METHOD:

1. The data backup capability is vulnerable to corridor attacks, due to physical proximity.

RECIPROCAL OF DISTANCE METHOD: Reciprocal of distance may be used, as in Figure 2. In this method, the function is $f(a,b) = 1$/physical distance.

backup chain for site a
using reciprocal of distance

backup chain for site b
using reciprocal of distance

Figure 2

ADVANTAGES OF THE RECIPROCAL OF DISTANCE METHOD:

1. The data backup capability is immune to corridor attacks, since data
    backups are far removed from the site which is being backed up.
2. The method will be robust under C^2-element moves over short
    distances, since such moves will only slightly alter physical
    distance and therefore change the reciprocal distance basis function
    only slightly.

DISADVANTAGES OF THE RECIPROCAL OF DISTANCE METHOD:

1. Data backup sites are chosen in inverse relationship to proximity.
    Thus, the replication process will require more communication
    resources.

CIRCULAR CHAIN METHOD: A circular chain may be used to designate backup
sites. This method involves an enumeration of the sites $N = \{a_1, a_2, .
. . \}$ according to an appropriate scheme (distance from a fixed point or
random enumeration, etc.). A closed chain is defined using that
enumeration. Technically, the function is $f(a_i, a_j) = (j-i) \bmod(n)$.

backup chain for site a
using enumeration a,c,b,d,e

backup chain for site b
using enumeration a,c,b,d,e

Figure 3

ADVANTAGES OF CIRCULAR CHAIN METHOD:

1. The configuration is easily tuneable via the enumeration choice.
2. The class of configurations provide maximum distribution of backup
    loads, in the sense that each site is primary data backup for
    exactly one other site, each is secondary data backup for exactly

one, etc.

3. The data transport priority scheme can be much simpler under this replication configuration method, since each site could send data to the next site on the chain as it receives the data itself, without the necessity of considering other issues. Thus, the priority scheme might depend only upon the nature of the data itself.

4. In the event of site loss, the reconfiguration is automated and immediate (the chain closes).

DISADVANTAGES OF CIRCULAR CHAIN METHOD:

1. It may prove too simplistic for future needs.

RANDOM METHOD: Backup selection may be done at random. The function, f(a,b), would involve random generation of a positive number for each pair, (a,b). This could be done allowing or disallowing two pairs to have the same number.

ADVANTAGES OF RANDOM METHOD:

1. The method would be difficult for the enemy to decipher.

DISADVANTAGES OF RANDOM METHOD:

1. There would be no control over such issues as backup loads, corridor immunity, etc.

TRUNCATED METHODS: Primary-only and primary-secondary backups are generated using each of the functions above. These methods are included in this study for comparison purposes.

A systematic evaluation of these and other alternatives is needed. There are many characteristics which need to be evaluated. One of the most critical is survivability.

IV. INITIALIZATION AND RECOVERY

At least one view of a future TACS[19] involves the following concepts:

1. The C^2 elements are mobile.
2. Each element contains part of the distributed database.
3. The communication network is separate; the C^2 element drives up and plugs in to a communication node.

In this view, at least, parts of the database will be separated from the whole while the C^2 element drives to its location. Those parts of the database will miss updates in the interim. Upon plugging in, they must be treated as candidates for either site initialization or recovery. Wartime attrition will lead to other situations where recovery is necessary; for example, the communication node into which the element is plugged might be lost, forcing the element to move to another.

A method for handling database site initialization and recovery has

been described by others[1]. The necessary information is transferred as a very large database transaction, under the system's usual method of concurrency control. This tidy solution can probably be used for all but the most perishable data, provided the concurrency control method is carefully designed to maximize responsiveness (see next section).

The problems implicit in handling very perishable data should be addressed. Such information as air surveillance may be worthless several minutes after it is generated. A tactical air control system must deal with some information that has an expected useful lifetime of a few seconds. Normal distributed database methods may or may not be sufficiently responsive. If not, alternative approaches should be investigated.

V. CONCURRENCY CONTROL

Concurrency control consist of a set of rules and procedures which, in a multiuser system (such as a TACS database), guarantee a given user non-interference by other concurrent users. Most database systems use some form of "locking" for concurrency control. A lock on a data unit is a "pass" granted one transaction that renders the unit "off limits" to other concurrent transactions that might interfere. Within the system each user transaction is handled by a transaction manager (TM). A lock is requested by a transaction manager from a lock manager. A requesting transaction manager is either granted or denied the lock by the lock manager. A TM owning a lock, releases it when finished with the unit. A common method for synchronizing this activity within a transaction is two phase locking[10]. Two phase locking (2PL) requires that all locks be acquired before any are released.

When conflicting lock requests are made on behalf of concurrent transactions, a protocol within the system must arbitrate in such a way that each transactions in turn gets the lockable unit (deadlocks in which both wait forever must be avoided or resolved). Many concurrency control methods exist to handle this arbitration (for a survey, see [8]).

A common application in a future TACS database system would involve the generation of composite or summary information using many items of raw data. Such a transaction would require locks on a set of lockable units but in no particular order (set of requests rather than a sequence). Much time can be lost if a lock is requested for a unit which is not available, forcing the transaction to become blocked (execution suspended) waiting for that lock while other needed locks are available. Since much of the TACS data is very perishable, these delays

would be intolerable.

New methods for handling set lock requests were formulated and tested during the second half of the SFRP effort. The rest of this section contains a description of this work. First, the methods are described. Next, the Concurrency Control Simulation evaluator is described. Finally, simulator results are presented.

NEW LOCK MANAGERS

The system is assumed to employ locks for concurrency control and a deadlock detection method which will eventually allow a transaction to complete, even in the face of repeated deadlocks. The following lock managers (LMs) were defined:

LM0 accepts lock requests from transaction managers (TMs), queues requests to locked units, responds to the request only when lock becomes available to the requesting TM. Thus, with LM0, TMs are blocked (from further processing) while waiting for LM0 to respond and the lock comes with the response. This is the standard method of lock management[8].

LM1 is a new lock management technique which has two lock request entry points: one blocking and one non-blocking. The blocking request is as in LM0. The non-blocking request returns True or False, depending on whether the lock is presently available.

```
Function LM1(Lockable_unit_ID, Lock_level, Transaction_ID): Boolean;
Begin
    If Lockable_unit_ID is available at Lock_level then begin;
        Record lock for Transaction_ID;
        LM1 := True
    End
    Else LM1 := False
End;
```

LM2 goes one step further. If the lock is not available, the transaction is entered into its queue.

```
Function LM2(Lockable_unit_ID, Lock_level, Transaction_ID): Boolean;
Begin
    If Lockable_unit_ID already locked by Transaction_ID
        or is available at Lock_level then begin
        Record lock for Transaction_ID;
        LM2 := True
    End
    Else Begin
        If Transaction_ID not in Lockable_unit_ID queue then
        place Transaction_ID in Lockable_unit_ID queue;
        LM2 := False
End;
```

LM3 is constructed so that it can be given a list of requests and instructed to unblock the transaction and return the lockable unit's ID

when any of the lockable units become available.

LM3 has three entry points: LM3I for nonblocking requests, LM3W for multiple blocking requests, and LM3R for releasing locks (the release portions of LM0, LM1 and LM2 were omitted due to simplicity). LM3 generates a blocking request list as it receives unsuccessful nonblocking requests.

```
Function LM3(Lockable_unit_ID, Lock_level, Transaction_ID): Boolean;
Begin
    If Lockable_unit_ID is locked by Transaction_ID
        or is available at Lock_level then begin;
        Record lock for Transaction_ID;
        LM3 := True
    End
    Else Begin
        If Transaction_ID is not in Lockable_unit_ID queue then
        place Transaction_ID in Lockable_unit_ID queue;
        If or-list for Transaction_ID doesn't exist then
            create an or-list for Transaction_ID;
        Insert Lockable_unit_ID in or-list;
        LM2 := False
    End
End;

Function LM3W(Transaction_ID): Lockable_unit_ID_type;
Begin
    If or-list is empty or non-existent then LM3W := error
    Else If no lock in the or-list is available then begin
        Block Transaction_ID;
        Dispatch another transaction
    End
    Else begin
        Select an awarded lock;
        Remove that lock from the or-list;
        LM3W := Lockable_unit_ID
    End
End;

Procedure LM3R(Lockable_unit_ID);
Begin
    If Lockable_unit_ID's queue is nonempty then begin
    Award the lock to a transaction from the queue;
        If transaction is waiting then begin
            Remove that lock from the or-list;
            Place the Lockable_unit_ID where the transaction
                expects a return value from LM3R;
            Unblock the transaction
        End
    End
End;
```

TRANSACTION MANAGERS

A transaction manager (TM) is an entity that interprets high-level queries by issuing lower-level requests, including negotiations with the

lock manager. Transaction manager 0 (TM0) below show the usual way a
transaction manager deals with a set request:

```
Begin
    For i := 0 to n do begin
        LM0(D_i, Lock_level, Trans_ID);
        Process D_i
    End
End;
```

It is possible to propose many TMs that use LM1 and LM2. One
approach would be to make no blocking requests at all, but to make
non-blocking requests for each unprocessed unit in turn until all have
been processed. This would involve busy waiting: it never blocks but
sometimes will find no locks available; the wait involves successive
unsuccessful calls on the lock manager. A busy deadlock is also
possible: T_1 holds a lock on D_1 and requests one on D_2; T_2 holds a lock
on D_2 and requests one on D_1; each pesters the lock manager.

There is no guarantee of successful completion with unlimited
non-blocking requests. There must be an upper limit on the number of
non-blocking requests made between blocking requests. TM1 makes
blocking requests only when an entire pass through the lockable units
with non-blocking requests finds none available.

```
TM1:
Begin
    While unprocessed units remain do begin
        Repeat process list using non-blocking requests
        Until a pass through the list finds all units locked;
        If at least one unprocessed unit remains then
            pick an unprocessed unit and make a blocking request for it
    End
End;
```

TM2 below makes one pass through the list of lockable units (LUs)
using non-blocking requests and then arbitrarily selects an unprocessed
LU to wait for. These two processes are alternated until no LUs remain
unprocessed. It differs from TM1 in that it never makes multiple
consecutive non-blocking passes through the list before making a
blocking request.

```
TM2:
Begin
    While unprocessed LUs remain do begin
        process list of LUs using non-blocking requests;
        If at least one unprocessed LU remains then
            pick an unprocessed LU and make blocking request
    End
End;
```

As the simulation data shows, cutting down on the number of non-blocking requests relative to the blocking requests seems to hurt performance. TM3 is proposed to improve that ratio:

```
TM3:
Begin
   Process list of LUs using non-blocking requests;
   Process list of LUs using blocking requests
End;
```

LM3 would be used with a simple transaction manager, TM4:

```
Begin
   Make pass through list using LM3I;
   While at least one unprocessed unit remains do
       Process (LM3W(Transaction_ID))
End
```

CONCURRENCY CONTROL METHOD EVALUATOR

A program was written in Pascal to simulate a small part of the database system in order to obtain a comparison of the new transaction and lock managers. The new transaction and lock managers do not improve the correctness of the database management system, only the performance. Estimates of that performance will help determine the relative worth of the various methods. The simulation employs Monte Carlo techniques in order to produce reasonable answers in reasonable time.

Performance evalution involved system performance (speed) and did not attempt to include considerations of survivability and robustness under external changes. This seems justified in light of the assumption that concurrency control is applied as locally as possible. Thus, the concurrency control method choice can be made to have little or no effect on the survivability and robustness of the system.

The simulation assumes a transaction exists which needs locks on a number of lockable units (LUs). Each LU has associated with it a delay time, the amount of time it will take the transaction to process the unit once it gets a lock. The time required to acquire an available lock is taken as the time unit. The transaction will find certain LUs available at certain times but not at others. For each LU, the program randomly generates intervals in the future during which the LU would be unavailable (locked by another TM) in the absence of the transaction under consideration. Queues of fairly stable length tend to form waiting for high activity LUs. Such queues are randomly generated as well.

Thus, the input to the simulation consists of a column of lockable

unit numbers (1,2,...,n); a column of LU processing delay numbers (3 to 15 time units); zero or more randomly generated intervals of unavailability listed under the Activity columns; and randomly placed fixed length queues listed under the Activity columns (# - 65 indicates a queue of fixed length 65 will always exist for this LU).

The program simulates the actual execution of a transaction in the activity environment described above and calculates the total time that the transaction will have to be active under the various combinations of Lock Managers and Transaction Managers. In addition to the Time Active column, there is a column indicating the total number of lock requests that were made. A lock request takes system time which affects the overall system performance, but is not reflected in the Time Active column. Therefore a column labeled Evaluation, which shows the Time active multiplied by $1 + \text{(number of additional lock requests)}^2$ is included to give a composite evaluation of performance.

The first row of the output table is labeled "Optimal". A carefully pruned tree search of all possibilities was used to produce a crystal-ball calculation of the minimun time active, given full knowledge of the unavailability intervals and queues. Since the unavailability intervals were known, no additioual lock requests were made. Thus, the Evaluation of Optimal equals the minimum time active. The final column expresses the Evaluation in ratio with the optimal Evaluation.

Appendix B contains the average results of several runs of the simulation for several sizes of transactions at a moderate activity density.

No combination of transaction and lock managers has enough information to achieve optimal performance. It was possible to simulate optimality only because all conflicts were known in advance. TM4/LM3 achieved the best performance in the simulation, but might prove difficult to implement. TM3/LM2 performed almost as well as TM4/LM3 and might constitute a good practical choice.

The TACS Database System might be designed to use different transaction managers in different circumstances. TM0 might be used to reduce the CPU time consumed in lock requests when there is little database activity, and a different manager used to improve response time when activity is heavier.

V. RECOMMENDATIONS

Evaluation of design alternatives in all six if the areas detailed

in Section II should be a major part of a future research effort. Programs similar in nature to the Distributed Operations Survivability Evaluator[13] and Concurrency Control Simulation (described above) should be designed to compare alternatives with respect to:

1. Survivability under attack
2. Robustness under external changes
3. Efficiency and processing speed
4. Appropriateness for future TACS databases (adherence to the principles listed in section II)

For example, a Data Backup Survivability Evaluator should be designed to estimate surviving Mission-Operational-Capacity following a series of simulated attacks. The method of data replication would be varied from one run of the simulation to another. The results of the series of simulations would provide a basis for preliminary evaluation of the theoretical advantages and disadvantages listed in section III.

The special problems of perishable data should be addressed early. We recognize the possibility of the emergence of a system that cannot be made to perform adequately. Again, simulations should help.

REFERENCES

1. Attar, R., Bernstein, P.A. & Goodman, N.; "Site Initialization, Recovery and Backup in a DDBS"; RADC-TR-83-226, Oct. 1983.

2. Black, M.D.; "Future TACS Deployment Configuration and Information Flow Requirements"; Mitre Working Paper, WP25004; September 1983.

3. Black, M.D.; "TACS Assured Information Flow Capping Architecture"; Mitre Working Paper, WP25525; July, 1984.

4. Carlis, J.V. & March, S.T.; "Computer-aided physical database design methodology"; Design Techniques 4:4; Dec. 1983; pp. 198-213.

5. Ceri, S. & Pelagatti, G.; Distributed Databases, Principles and Systems; McGraw-Hill, 1984.

6. Chen, P. P.; "The Entity-Relationship Model: Toward a Unified View of Data"; ACM Transactions on Database Systems; 1:1; pp. 9-36.

7. Codd, E. F.; "A Relational Model for Large, Shared Data Banks"; Communications of the ACM; Vol. 13, No. 6, pp. 377-387.

8. Date, C. J.; An Introduction to Database Systems; Addison-Wesley, 1983.

9. "ESD Tactical C^3I systems interface notebook"; draft; 1980.

10. Eswaran, J.N. et al; "The notion of consistency and predicate locks in a database system"; Comm. of ACM; 19 No. 11; Nov. 1976.

11. Hegerle, Col. M.J.; "System specification for Tactical Air Control Center Automation"; ESD #5500148A; Vol. II; Dec. 1971.

12. Hevner, A. R.; "Data Allocation and Retrieval in Distributed Database Systems"; Advances in Database Management, Vol. 2, P. Fisher, ed.; Heyden and Sons, 1983.

13. Kasputys, J.; "TACS-2000 survivability evaluator description"; MTR8790; Mitre Working Paper; Nov. 1982.

14. Lynch, N. A.; "Multilevel Atomicity — A New Correctness Criterion for Database Concurrency Control"; ACM Transactions on Database Systems; Vol. 8, No. 4, pp. 484-502.

15. March, S. T.; "Techniques for Structuring Database Records"; ACM Computing Surveys; Vol. 15, No. 1 (March 1983), pp. 45-79.

16. Morris, Maj. J.K.; "Assessment of TACS-2000 concepts and technology"; ESD Working Paper, ESD-TR-81-140; July 1981.

17. Perrizo, W.K.; "A Method for Processing Distributed Database Queries"; IEEE Transactions on Software Engineering; (To appear).

18. Ullman, J.D.; Principles of Database Systems, 2nd Ed.; Computer Science Press, 1982.

19. Wech, O.; "Sound Track for Animated Motion Picture TACS-2000".

APPENDIX A
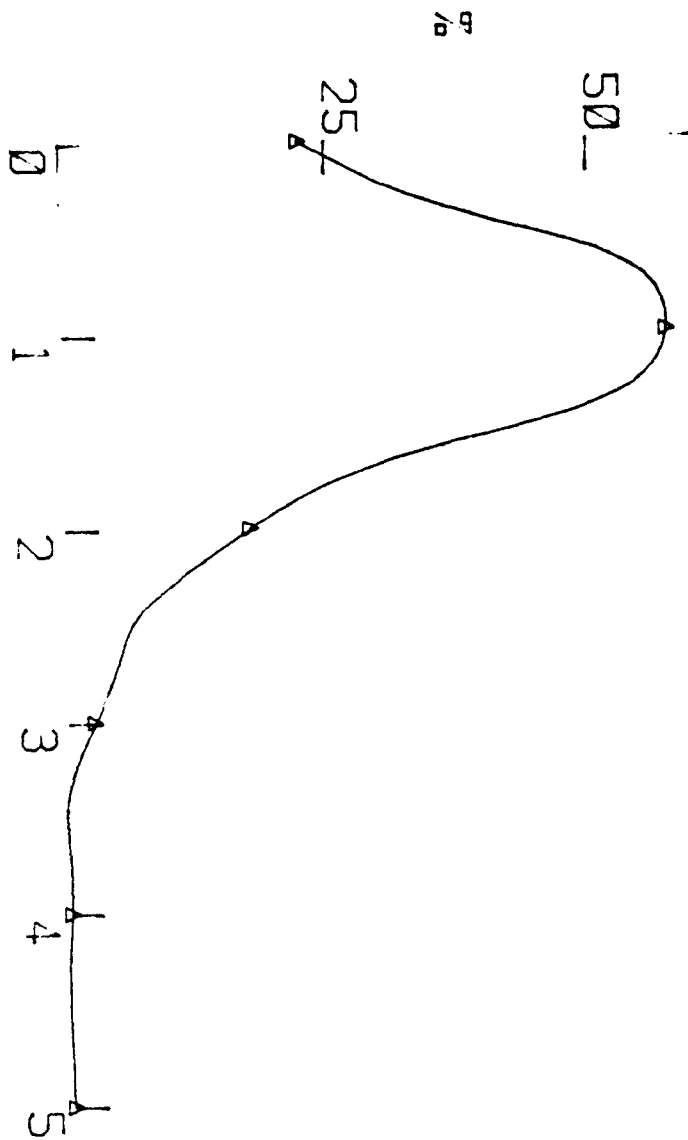
CLOSEST NEIGHBOR LOAD SIMULATION FOR 40 POINTS

AVERAGE RESULTS OF CONCURRENCY CONTROL SIMULATION WITH MEDIUM ACTIVITY

Parameters	Probability	Mean	Std. Dev.
Potential conflicts	0.010	150	50
Queues	0.100	250	80

Averages for 5 lockable units:

TM	LM	Time Active	Lock Requests	Evaluation	Eval/OptEval
Optimal		183.5	5.0	183.50	1.000
0	0	259.0	5.0	259.00	1.411
1	1	254.0	8.3	361.32	1.969
1	2	192.9	8.1	264.61	1.442
2	1	253.4	6.9	291.88	1.591
2	2	192.9	6.8	217.84	1.187
3	1	252.8	6.3	269.84	1.470
3	2	192.9	6.3	205.89	1.122
4	3	190.8	6.3	203.70	1.110

Averages for 10 lockable units:

TM	LM	Time Active	Lock Requests	Evaluation	Eval/OptEval
Optimal		207.6	10.0	207.55	1.000
0	0	427.3	10.0	427.25	2.059
1	1	382.5	15.5	498.21	2.400
1	2	243.2	15.1	305.22	1.471
2	1	381.0	13.1	418.86	2.018
2	2	244.9	12.8	263.42	1.269
3	1	381.0	12.3	401.10	1.933
3	2	245.9	12.3	258.91	1.247
4	3	236.1	12.3	248.54	1.197

Averages for 15 lockable units:

TM	LM	Time Active	Lock Requests	Evaluation	Eval/OptEval
Optimal		257.1	15.0	257.10	1.000
0	0	586.2	15.0	586.20	2.280
1	1	486.4	22.3	599.97	2.334
1	2	303.1	21.7	363.57	1.414
2	1	484.0	19.3	52?.91	2.034
2	2	305.0	18.9	325.04	1.264
3	1	491.0	17.6	506.32	1.969
3	2	306.3	17.6	315.81	1.228
4	3	298.0	17.6	307.30	1.195

Averages for 20 lockable units:

TM	LM	Time Active	Lock Requests	Evaluation	Eval/OptEval
Optimal		299.0	20.0	299.00	1.000
0	0	845.0	20.0	845.05	2.826
1	1	663.0	29.7	819.02	2.739
1	2	383.8	28.4	451.50	1.510
2	1	660.8	26.3	725.39	2.426
2	2	385.5	25.5	415.13	1.388
3	1	661.2	24.0	686.99	2.298
3	2	390.4	24.0	405.58	1.356
4	3	380.5	24.0	395.29	1.322

1984 USAF-SCEEE SUMMER FACULTY RESEARCH PROGRAM

Sponsored by the

AIR FORCE OFFICE OF SCIENTIFIC RESEARCH

Conducted by the

SOUTHEASTERN CENTER FOR ELECTRICAL ENGINEERING EDUCATION

FINAL REPORT

RAMAN SPECTROSCOPY OF GLYCOSAMINOGLYCANS FROM BOVINE CORNEA

Prepared by: Dr. Boake L. Plessy

Academic Rank: Professor

Department and   Division of the Natural Sciences
  University: Dillard   University

Research Location: School of Aerospace Medicine, Brooks
                       Air Force Base

USAF Research: Dr. John Taboada

Date: September 12, 1984

Contract No: F49620-82-C-0035

RAMAN SPECTROSCOPY OF GLYCOSAMINOGLYCANS FROM BOVINE CORNEA

by

Boake L. Plessy

ABSTRACT

Structural changes which may occur in the glycosaminoglycans of cornea with development, maturation, and senescence were investigated using laser Raman spectroscopy. Keratan sulfate and chondroitin sulfate were extracted from bovine cornea after proteolytic digestion and fractionated on a ECTEOLA cellulose column. After characterization of the isolated fractions, spectra were obtained on a modified commercial Raman spectrophotometer using the 514.5 nm, 488.0 nm, and 476.1 nm lines of an argon laser. Spectra were obtained with parallel and perpendicular polarization and on the Stoke's and anti-Stoke's lines. Suggestions are made for changes in sample handling and instrumentation to improve the quality of the spectra obtained.

I. INTRODUCTION

We have begun investigation into the structure of corneal stroma by Laser Raman Spectroscopy in order to develop a non-invasive probe to monitor both physiological changes and changes which occur on development, maturation, and senescence as a result of structural changes in constituent glycosaminoglycans.

Among the biological macromolecules, the proteoglycans, and particularly their polysaccharide sidechains, are of special interest because of their apparent physiological role. The primary role of these extracellular materials is structural in that they bind together cells and organs However, since all substances passing from cell to cell pass through this connective tissue, the composition and physical state, particularly of the hydrated matrix, is believed to be an important influence in the metabolism of cells. The matrix of the proteoglycan has been associated with physiological processes such as control of electrolytes and water in extracellular fluids, lubrication, calcification, and wound healing.

In general, the proteoglycans consist of a protein-core whose corneal macromolecular structure is little known. Glycosaminoglycan sidechains, either keratan sulfate or pure or sulfated chondroitin, are attached to this protein-core through O-glycosidic or N-glycosidic bonds.

The disaccharide repeating units of keratan sulfate and chondroitin-4-sulfate are shown in Figures 1 and 2 respectively.
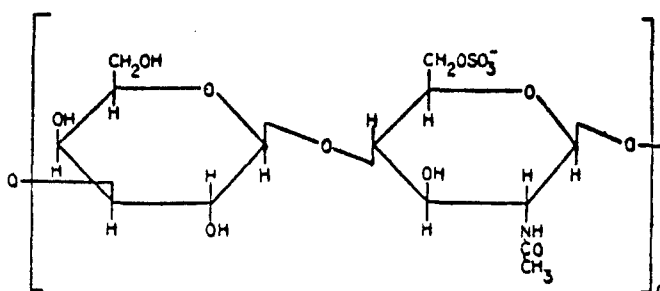
Figure 1. Keratan Sulfate
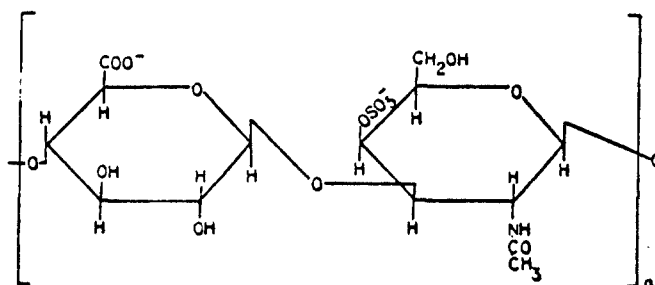
Figure 2. Chondroitin-4-sulfate

The repeating unit of keratan sulfate is N-acetylglucosamine and galactose polymerized through 1-3 β-glycosidic linkages with the glucosamine moiety sulfated in the C-6 position. The repeating unit of chondroitin-4-sulfate is composed of glucuronic acid bound to N-acetylgalactosamine through 1-3 β-glycosidic bonds and polymerized through 1-4 β-glycosidic bonds. The galactosamine moiety in cornea is either non-sulfated or

sulfated in the C-4 position as shown. Keratan sulfate constitutes about 67% of corneal glycosaminoglycans with pure or sulfated chondroitin constituting the remainder in corneal stroma.

Recent studies have demonstrated the feasibility of using laser Raman spectroscopy as a structural probe in biophysical aspects of eye research (1,2). The success achieved in the determination of sulfhydryl concentration changes along the optical axis during aging suggests its use in determining structural changes in corneal glycosaminoglycans . No precedent for this study exists in the biochemical literature although spectra of intact feline cornea collagen have been reported (3).

Biological applications of Raman spectroscopy have increased with the advent of reliable instrumentation, in particular, laser sources. Raman spectroscopy offers several advantages over traditional methods in determining structural characteristics of biomolecules. Spectra are amenable to molecular-level interpretation with accessible low-frequency modes sensitive to conformational changes in the molecule. Sample size requirements are small and spectra can be obtained in the liquid or solid phase or in solution. There is minimal interference by water in the spectral region from 2000-200 cm^{-1} and hence aqueous solutions of biological systems may be studied. The primary disadvantage encountered

in biological systems is the interference from fluorescent or luminescent background which accompanies irradiation of biological systems with intense laser sources (4,5).

II. OBJECTIVES

The proteoglycans of corneal tissue play an important role in the structural organization of the cornea and ultimately in its entire hydration characteristics and transparency. These biological macromolecules are of significance in the determination of the overall architecture of the extracellular matrix and there is evidence of variation of concentration of keratan sulfate-like components of tissue with development, maturation, and senescence. This study focused attention on the structure of proteoglycans and their age related changes. Specifically, the objectives were:

1. To obtain the laser Raman spectra of extracted proteoglycans and determine the groups responsible for the spectral lines observed.

2. To develop techniques for the determination of spectra for the intact cornea.

3. To use Raman spectroscopy as a non-invasive structural probe to elucidate changes in proteoglycan nature and concentration in cornea as a function of age.

    This study began with extensive literature searches on

the age related changes in corneal proteoglycans and on the Raman spectroscopy of proteoglycans or glycosaminoglycans. Neither problem had been previously reported in the literature. Therefore, extraction and characterization of glycosaminoglycans from cornea proceeded. It was anticipated that upon successful determination of Raman spectra and assignment of the spectral lines, the expertise of the laboratory in determining laser Raman spectra on intact animal lens would be used to develop similar techniques on bovine cornea, the ultimate goal being to develop laser Raman spectroscopy as a probe for studying age-related changes in corneal proteoglycans.

III. Materials and Methods

The glycosaminoglycans were isolated and measured using methods which have been previously described in detail in earlier papers (6,7). In brief bovine cornea were excised at the slaughterhouse less than one hour post-mortem. After removing any residual sclera, the cornea were stored at -70°C until use. Fifty-one thawed cornea were cut into small pieces and suspended in 200 ml of 0.1M phosphate buffer with EDTA and l-cysteine HCl added to a final concentration of 0.005M and adjusted to pH 6.5. The material was proteolytically digested with 360 mg of papain at 65°C for four hours with stirring. A small amount of insoluble residue was removed by

centrifugation at 7000 x g for 30 minutes and discarded. The clear supernatant was adjusted to 5% in sodium acetate and the glycosaminoglycans precipitated by the addition of 5 volumes of 95% ethanol. The precipitate was harvested by centrifugation and redissolved in 125 ml of water.

ECTEOLA cellulose (Sigma Chemical Co.) was prepared by washing with 1N sodium hydroxide, 1N hydrochloric acid, and water. A column 2 cm x 30 cm was gravity packed with an aqueous suspension of the prepared ECTEOLA.

The solution containing the corneal extract was applied directly to this column and washed in with one bed volume of water. The column was eluted with two bed volumes 0.02M hydrochloric acid, 0.3M hydrochloric acid and 2M sodium chloride at a flow rate of 1.5 ml/minute in sequence at room temperature. The appearance of glycosaminoglycans was monitored by layering 95% ethanol on the eluate. A precipitate at the interface indicated the presence of the desired material. The water and 0.02 M hydrochloric acid eluates were subsequently rechromatographed with a similar procedure with 2M ammonium formate replacing the 0.3M hydrochloric acid in the elution.

Glycosaminoglycans were obtained from solution by alcohol precipitation. The column eluates were adjusted to 2.5% in sodium acetate and 5 volumes of 95% ethanol was added. After standing overnight at room temperature, the

precipitate was harvested by centrifugation, washed with 95% alcohol and air dried.

The hexose content of the extracted glycosaminoglycans was determined by anthrone (8). Glucose served as the standard. Uronic acid content was determined by a modified carbazole reaction (9) with D-glucuronic acid lactone serving as standard. Total hexosamine content was obtained by a modified Elson-Morgon test after hydrolysis of the sample in 6N hydrochloric acid in sealed tubes at 95°C for six hours (10).

Spectra were recorded on a Varian Model 82 Laser Raman Spectrophotometer equipped with a triple grating monochromator. The excitation source was a Spectra Physics Model 164 Argon laser equipped with a Spectra Physics Model 265 Exciter. Wavelengths available were 514.5 nm, 488.0 nm, and 476.5 nm. The Raman lines were detected by photon counting using a Thorn Emi Gencom Model Fact-50 MKIII photomultiplier cooled to -25.5°C and powered with a Emi Gencom Model 3000R power supply. The analog output from a C-10 photon counter (Thorn Emi Gencom) was recorded on a Hewlett-Packard x-y recorder. The x input was obtained from a 5k precision potentiometer mechanically coupled to the monochromator and powered by a variable DC voltage supply with 0-5V covering a 2000 cm^{-1} range, selectable from 0-2000 cm^{-1} or 2000 - 4000 cm^{-1}. Spectra were recorded with reduced

ambient room light to reduce dark current count. The spectrophotometer was equipped for parallel or perpendicular polarization with an optical polarization scrambler available. Samples were run in either a 1cm x 2cm x 4cm rectangular cell or in a cylindrical cell of approximately 2.7 mm I.D. x 3 cm.

IV. DISCUSSION

The ECTEOLA chromatography of the glycosaminoglycans from corneal tissue resulted in two fractions. The analytical data on each is given in Table 1.

Table 1.

Eluate	2M Formate	2M Chloride
Hexose, %	10.8	29.1
Hexuronic acid, %	26.8	<1
Hexosamine, %	27.5	26.8
Hexose/Hexosamine*	0.38	1.07
Hexuronic acid/Hexosamine*	0.90	-
Hexose/Hexuronic acid*	0.43	-
Yield, mg	163	140

* Molar ratio

The ECTEOLA technique does not give complete separation of glucosaminoglycans from galactosaminoglycans. However, over 80% of the total glucosaminoglycans is recovered in the

2M sodium chloride fraction. Since only two eluting solutions were used, the 2.0M ammonium formate eluted carbazole positive chondroitin-4-sulfate and mixed chondroitin and keratan sulfates in the earlier stages of the chromatography while the 2.0M sodium chloride solution yielded essentially pure keratan sulfate in the latter stages as expected. This is indicated by the molar ratio of hexose to hexosamine of unity and the absence of significant carbazole positive material in the fraction.

The major changes expected in the structure in the corneal proteoglycan during development and aging are in the size and glycosaminoglycan composition. Although the information on age related changes in corneal keratan sulfate is limited, there is ample evidence from other tissues to warrant a detailed study on this species. Moreover, recent studies on rabbit cornea indicate that there are changes in the relative distribution of the glycosaminoglycan components as a function of age. The ratio of non-uronic acid containing glycosaminoglycans (keratan sulfate) to the uronic acid containing glycosaminoglycans decreased with age (11). Based on studies on human articular cartilage (12), the following types of changes in glycosaminoglycans can be anticipated with increasing age: increases or decreases in content of the proteoglycan coupled with increases or decreases in size; changes in the relative amounts of keratan

and chondroitin sulfates; increases or decreases in the protein concentration relative to the glycosaminoglycan content; change in the protein core with respect to amino acid profile.

Raman spectra were initially attempted on aqueous solutions of the formate fraction and chloride fraction at the 25 mM and 12.5 mM level respectively. In both cases, strong background fluorescence was observed. Ultraviolet spectra on each sample indicated intense UV absorption bands at 260 nm and 220 nm. The bands are not characteristic of the polysaccharide structure attributed to the glycosaminoglycans. Although fluorescent species have been reported in cornea (13,14), it was concluded that the source of the UV absorption and fluorescence was residual amino acid remaining with the glycosaminoglycan subsequent to incomplete proteolytic digestion. Much of the remaining spectroscopy was devoted to attempts to reduce this background interference.

Sample concentration was increased to the 0.1M level in order to overcome the effects of the fluorescent background. A cylindrical cell which would accommodate 0.5 ml of solution was constructed and an eightfold increase in intensity was anticipated. The improvement in the spectra were minimal. Additionally, laser excitation wavelengths were varied in order to move away from the excitation wavelength

for fluorescence. The wavelengths available other than than 514.5 nm were 488.0 nm and 476.5 nm. In both cases, there was only minimal improvement in the quality of the spectra obtained. Several other techniques were incorporated with varying degrees of success. Samples were run under conditions of both parallel and perpendicular polarization. Polarization reduced the level of fluorescence background but the low signal to noise ratio made interpretation of the spectra difficult. Several runs were made at increased laser power (25 amps current) with a corresponding reduction in slit width (2 cm^{-1}). Anti-stokes Raman spectra, which are unaffected by the intense luminescent background, were also run. The best spectra were obtained under the following conditions: The excitation wavelength was 488.0 nm and the spectra were obtained with parallel polarization. The spectra were obtained with a laser current of 25 amps and the slit width was 2 cm^{-1}. The spectral region scanned was 2000 cm^{-1} to 4000 cm^{-1}. Under these conditions, a distinct Raman line could be observed at 2940 cm^{-1}. Preliminary assignment would attribute this band to either C-H or N-H vibrations, both of which are part of the glycosaminog'ycan structure.

V. RECOMMENDATIONS

Although the original objectives of the project were not completely met, hindsight indicates that these objectives

were ambitious and would be better served in a project of longer duration. It has become clear that the ideas advanced have sound scientific basis and serve an area of interest for Air Force research. There are several areas which should be explored as a follow-on to this work. First, although it is desirable to obtain spectra on the isolated glycosaminoglycans, this approach is not necessarily a prerequisite to determination of proteoglycan changes in intact cornea and since it has been demonstrated that spectra can be obtained on these cornea, work in that area should proceed. Secondly, it has been documented that the extraction of glycosaminoglycans can be achieved without significant residual amino acids. These methods should be explored so as to minimize interference from luminescent materials. The argon laser source should be replaced by a krypton laser source as the 647.1 nm line does not excite the intense fluorescence associated with the 514.5 nm line. Third, since the glycosaminoglycans form transparent films or pellets when dried in vacuo, solid sampling should be explored as an alternative to produce optimal sample concentration and reduce any interference from water.

Finally, since a study will begin at the author's laboratory on age related changes in rat cornea, I recommend continued colloboration between the School of Aerospace Medicine and the investigator.

Acknowledgement

The author would like to acknowledge and thank the Air Force Systems Command, the Air Force Office for Scientific Research, and the Southeastern Center for Electrical Engineering Education for providing the opportunity for him to spend the summer engaged in meaningful and interesting research at the School of Aerospace Medicine, Brooks Air Force Base, San Antonio, Texas. He would like to thank the Epidemiology Division for its hospitality and loan of equipment and facilities.

The author owes a special debt of gratitude to Dr. John Taboada of the School of Aerospace Medicine for colloboration in choosing the area of research, guidance, and sponsorship in the program. He would also like to acknowledge the help of Dr. Otis McDuff, Dr. R. Krishnan and Dr. Jim Mrotek.

REFERENCES

1. Askren, C. C., Yu, N. T., and Kuck, J. F. R., "Variation of the Concentration of Sulfhydryl along the Visual Axis of Aging Lenses by Laser Raman Optical Dissection Technique ", Exp. Eye Res., Vol.29, pp.647-654, 1979.

2. Kuck, J. F. R., Yu, N. T., and Askren, C. C., "Total Sulfhydryl by Raman Spectroscopy in the Intact Lens of Several Species: Variations in the Nucleus and Along the Optical Axis During Aging," Exp. Eye Res., Vol. 34, pp. 23-37, 1982.

3. Goheen, S. C., Lis, L.J., and Kauffman, J. W., "Raman Spectroscopy of Intact Feline Corneal Collagen," Biochim. et Biophys. Acta, Vol. 536, pp. 197-204, 1978.

4. Gaber, B. P., "Biological Applications of Laser Raman Spectroscopy," American Laboratory, Vol. 8, pp. 15-24, 1977.

5. Koenig, J. L., Introduction to the Spectroscopy of Biological Polymers, edited by D. W. Jones, (Academic Press, Inc., New York), 1976.

6. Fransson, L, A. and Anseth, A., "Studies on Corneal Polysaccharides: IV. Chromatography of Corneal Glycosaminoglycans on ECTEOLA Cellulose using Formate Buffers as Eluting Solvents," Exp. Eye Res., Vol.6, pp.107-119, 1967.

7. Plessy, B. L., and Bettelheim, F. A., "Water Vapor Sorption of Keratan Sulfate," Mol. and Cell. Biochem., Vol.6, pp.85-91, 1975.

8. Dische, Z., in Methods of Biochemical Analysis, (Interscience Publishers, New York, 1955), Vol. 2, pp.36.

9. Bitter, T., and Muir, H. M., "A Modified Uronic Acid Carbazole Reaction," Anal. Biochem., Vol. 4, pp.330-334, 1962.

10. Antonopoulos, C. A., "Separation of Glucosamine and Galactosamine on the Microgram Scale and Their Quantitative Determination," Arkiv. F. Kemi. Vol.25, pp.243-247, 1966.

11. Knepper, P. A., Breen, M., Weinstein, H. G., and Black, L., "Intraocular Pressure and Glycosaminoglycen Distribution in the Rabbit Eye: Effect of Age and Dexamethasone," Exp. Eye Res., Vol.27, pp.567-575, 1978.

12. Roughley, P. J., and White, R. J., "Age-related Changes in the Structure of Proteoglycans Subunits from Human Articular Cartilage," J. Biol. Chem., Vol. 255, pp.217-224, 1980.

13. Laing, R. A., Fischbarg, J., and Chance, B., "Noninvasive Measurements of Pyridine Nucleotide Fluorescence from the Cornea," Invest. Ophthalmol. Vis. Sci., Vol. 19, pp.96-102, 1980.

14. Ringvold, A., "Cornea and Ultraviolet Radiation," Acta Ophthalmol., Vol.58, pp.63-68, 1980.

1984 USAF-SCEEE SUMMER FACULTY RESEARCH PROGRAM

Sponsored by the

AIR FORCE OFFICE OF SCIENTIFIC RESEARCH

Conducted by the

SOUTHEASTERN CENTER FOR ELECTRICAL ENGINEERING EDUCATION

FINAL REPORT

STUDY OF CONTROL MIXER CONCEPT

FOR RECONFIGURABLE FLIGHT CONTROL SYSTEM

Prepared by: Kuldip S. Rattan

Academic Rank: Associate Professor

Department and   Department of Electrical Systems Engineering,
   University: Wright State University

Research Location: Air Force Wright Aeronautical Laboratories
                    Flight Dynamics Lab
                    Flight Control Division
                    Control Systems Development Branch

USAF Research
   Colleague: Thomas J. Molnar

Date: Sept. 21, 1984

Contract: F49620-82-C-0035

STUDY OF CONTROL MIXER CONCEPT
FOR RECONFIGURABLE FLIGHT CONTROL SYSTEM

by

Kuldip S. Rattan

ABSTRACT

Reconfiguration of flight control law after effector failure is studied in this effort. The objective of this research is to evaluate the control mixer concept which utilizes generalized inverse to distribute control authority among the remaining effectors after failure. The unmanned research vehicle (URV) was selected as a test bed for evaluating this concept. A mathematical model containing split surfaces and linearized equations of motion for coupled longitudinal and lateral-direction axes is developed. Control mixer gain matrices were obtained for failed surfaces. Comparison of the unimpaired and reconfigured aircraft were performed using the Continuous System Modeling Program (CSMP) Difficulties encountered with the generalized inverse based control mixer concept are discussed and recommendations for further research in the area are given.

ACKNOWLEDGEMENTS

I. INTRODUCTION:

Present aircrafts which employ fly-by-wire (FBW) closed-loop flight control systems (FCS) are primarily designed with control laws that require each element of the control loop to perform properly. The control laws will cope with some failures, but with a reduced level of performance. These control laws are not very efficient to exploit the resulting control power if a primary surface becomes inoperative due to combat damage or mechanical failure. Stringent safety-of-flight reliability standards imposed on FCS's have resulted in the addition of extensive redundant hardware in aircrafts. The extra hardware results in considerable additional cost and reduces the mean time between maintenance actions. Most aircrafts have redundant control effectors and excess control power (present for performance reasons) which provide an alternative to adding redundant hardware through distributing the forces and moments of the failed surface to the remaining healthy control surfaces. Reconfiguration utilizes the existing redundancy in producing the generalized forces and moments acting on the aircraft, rather than the brute force approach of adding redundancy in actuator and servo hardware to ensure the operation of the effectors after failure and damage. This approach significantly increases the FCS survivability, while simultaneously reducing support requirements.

Reconfiguration of flight control law after effector failure is studied in this effort. The objective of this research is to evaluate the control mixer concept[1] which utilizes the generalized inverse to distribute control authority among the remaining effectors after failure. The unmanned research vehicle (URV) was selected as a test bed for evaluating this concept. The URV,XBQM-106, is an experimental aircraft developed by AFWAL/FIGL to study flight control concepts. The URV, as opposed to a manned full scale effort provide a low risk low cost test bed for research in reconfigurable flight control concepts.

The available mathematical model of the URV consisted of decoupled longitudinal and lateral-directional linearized equations. This model did not include split surfaces. Only differential ailerons, collective elavator, and rudder were available. In order to apply the control mixer concept to the URV, the existing model was modified for coupled longitudinal and lateral-directional linearized equations of motion. The

modified model included split elevator and ailerons surface effectors. Using the control effectiveness matrix of the URV and the control mixing concept, new gain matrices were obtained for failed surfaces. Comparison of the unimpaired and reconfigured aircraft were performed using the Continuous System Modeling Program (CSMP).

II. OBJECTIVES

The main objective of this research is to evaluate the control mixer concept which utilizes the existing redundancy of control surfaces in distributing the forces and moments of the failed surfaces to the remaining healthy surfaces. The specific objectives are

(1) To develop an algorithm for determining the control mixer gain matrix when number of outputs are greater than number of control surfaces.

(2) To develop a mathematical model of the URV in state variable form. The model should contain coupling between the longitudinal and lateral-directional axis and include split surface effects.

(3) Computer simulation of the impaired and reconfigured aircraft for failed surfaces.

(4) To identify problems and to find directions for future research.

III. CONTROL RECONFIGURATION ALGORITHM DESIGN

The block diagram of the existing and reconfigurable flight control systems are shown in Figs. 3.1 and 3.2. The objective of this section is to investigate the control reconfiguration algorithm proposed by General Electric,[1] and to obtain the control mixer gain matrix for the impaired URV. The GE algorithm utilizes the impaired and unimpaired control effectiveness matrices of the aircraft to produce the new gain matrix through the generalized inverse. In this study it is assumed that when the failure occurs, the surface is locked to the center position, i.e., the input to the aircraft from the failed surface is zero. Based on the above information, the control reconfiguration algorithm computes a new control mixer gain matrix which distributes the forces and moments of the
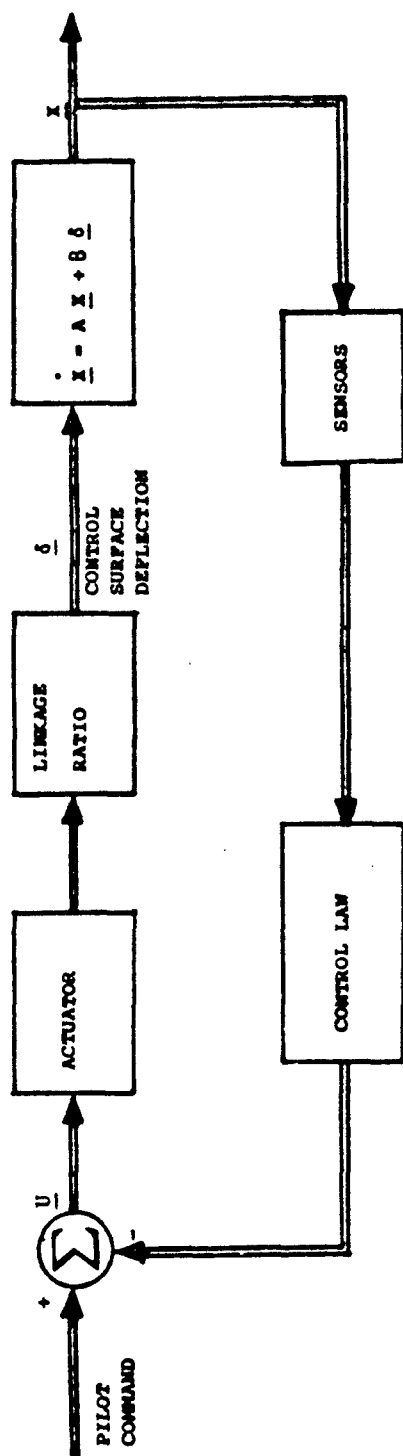
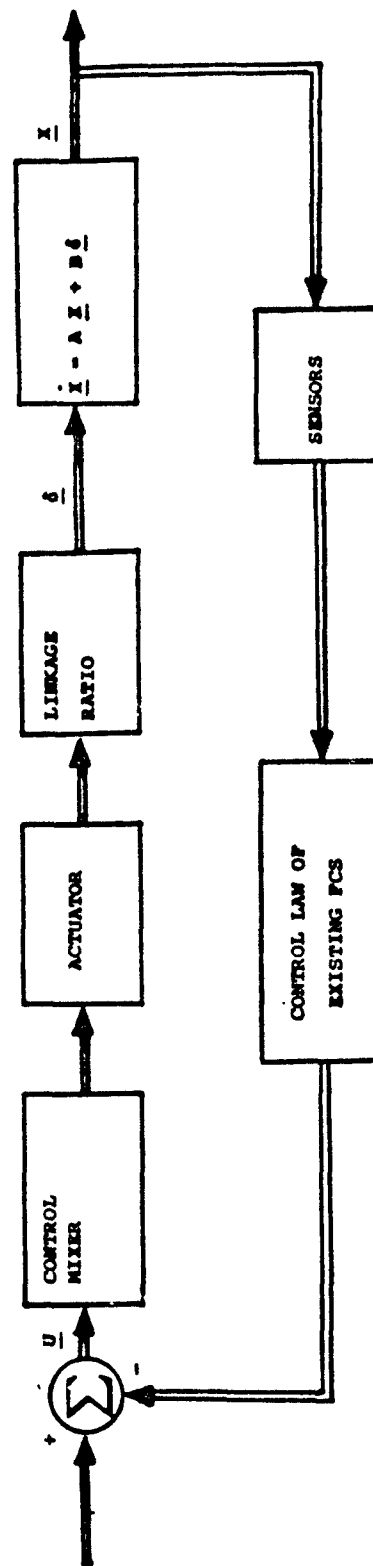Fig. 3.1. Existing flight control system

Fig. 3.2. Reconfigurable flight control system

failed surface to the remaining healthy surfaces. Reconfiguration is implemented as a gain-schedule algorithm. In the absence of control surface failure, the servo commands are set equal to the commands of the unimpaired aircraft.

3.1 Control Mixer Gains

The linearized continuous aircraft state equatons of the unimpaired aircraft are given by

$$\dot{\underline{x}}(t) = A \underline{x}(t) + B \underline{\delta}(t) \tag{3.1}$$

where $\underline{x}(t)$ is the aircraft state vector, $\underline{\delta}(t)$ is the aircraft control surface deflection vector and B is the control effectiveness matrix. Let us suppose that there are m states and n control surfaces. Therefore A is a nxn matrix and B is a mxn matrix. If the actuator dynamics are ignored, as in the GE report,[1] the control surface deflection vector, $\underline{\delta}$ is given by

$$\underline{\delta}(t) = K \underline{u}(t) \tag{3.2}$$

where $\underline{u}(t)$ is a pilot-plus FCS command vector. Assuming that the aircraft dynamics remain the same, the component of $\dot{\underline{x}}(t)$ due to control inputs is given by

$$\dot{\underline{x}}_u(t) = BK \underline{u}(t) \tag{3.3}$$

where K is a control mixer gain matrix. For the unimpaired aircraft, eqn. (3.3) can be written as

$$\dot{\underline{x}}_{uo}(t) = B_o K_o \underline{u}(t) \tag{3.4}$$

where B_o is the control effectiveness matrix and K_o is the control mixer gain matrix for the unimpaired aircraft. When the aircrfat becomes impaired, the control mixer gains must be altered and the state equatons become,

$$\dot{x}_{uI}(t) = B_I K_I \underline{u}(t) \tag{3.5}$$

where B_I is the control effectiveness matrix and K_I is the mixer gain matrix for the impaired aircraft. It is desired that the rate of change of aircraft states, $\dot{\underline{x}}$, for any input be unaffected by the impairment. Therefore

$$B_I K_I = B_o K_o \tag{3.6}$$

Equation (3.6) provides a design algorithm to determine the unknown gain matrix K_I. Solving eqn. (3.6)

$$K_I = B_I^+ B_o K_o \tag{3.7}$$

where B_I^+ is the pseudcinverse of the matrix B_I and depends on:

Theorem 3.1:

If B_I is a nonsingular matrix (no. of state equations equal to no. of control variables), the solution of eqn. (3.7) is given by

$$K_I = B_I^{-1} B_o K_o \tag{3.8}$$

Theorem 3.2:

If B_I is an $m \times n$ matrix ($m > n$, i.e., no. of state equations is greater than no. of control surfaces) of rank n, then the solution of eqn. (3.6) that minimizes the sum of squares of error $S = r^T r$, where $r = B_o K_o - B_I K_I$, is given by[2]

$$K_I = (B_I^T B_I)^{-1} B_I^T B_o K_o \tag{3.9}$$

Theorem 3.3:

If B_I is an $m \times n$ matrix ($m<n$, no. of state equations are less than number of control surfaces), then the solution of eqn. (3.6) that minimizes the norm of the deflection vector is given by

$$K_I = B_I^T (B_I B_I^T)^{-1} B_o K_o \qquad (3.10)$$

Since the matrix $B_I^T B_I$ or $B_I B_I^T$ is singular,[2] its inverse exists. Although eqns. (3.8)-(3.10) provide the solution for the unknown gain matrix, they do not address the important issue of control limits. An inherent property of pseudoinverse is to exploit excess degrees of freedom to minimize the sum of squares of error or norm of the deflection vector. Weighted least square error or normalization of the deflection by the physical limits provides a convenient method to addressing this problem. The burden of desired control input is distributed among the remaining healthy surfaces, taking into account the actual authority of each. This is done by modifying eqn. (3.7) as follows:

If B_I is an $m \times n$ matrix ($m>n$) of rank n, then the solution of eqn. $wB_I K_I = wB_o K_o$ in the least square error sense is given by

$$K_I = (wB_I)^+ wB_o K_o \qquad (3.11)$$

where w is a weighting matrix. Using the result of Theorem 3.2, eqn. (3.11) can be written as

$$K_I = (B_I^T H_1 B_I)^{-1} B_I^T H_1 B_o K_o \qquad (3.12)$$

where $H_1 = w^T w$. But if B_I is an $m \times n$ matrix ($m<n$) of rank n, the solution of eqn. (3.7) which distributes the control input, taking into consideration the control limit, can be obtained by pre-normalizing B_I with a matrix, AUTH,

$$K_I = AUTH(B_I . AUTH)^+ B_o K_o \qquad (3.13)$$

117-9

The AUTH matrix is a diagonal matrix and the diagonal elements represent the physical control surface deflection limits. Using the results of Theorem 3.3, we can write eqn. (3.13) as

$$K_I = H_2 B_I^T (B_I H_2 B_I)^T B_o K_o \qquad (3.14)$$

where $H_2 = AUTH \cdot AUTH^T$.

It should be pointed out here that the control mixer approach does not change the control structure that computes the deflection vector δ. The advantage of this approach is its simplicity and seperation of function. Hence controller design with no thought given to actuator failure can be combined with control mixer design discussed above.

IV. Aircraft Model for URV

The original model of the URV developed by KBG Corporation[3] contained linearized equations decoupled along the longitudinal and lateral-directional axes. The model did not split surfaces. In order to apply the control mixer concept to the URV, the model had to be modified to contain split surfaces and coupled longitudinal and lateral-directional equations. The modified model can achieve lateral-direction control using longitudinal control surfaces and longitudinal control using lateral-directional control surfaces. For example, using the left and right elevators differentially can produce a rolling moment. Also, aileron deflections in the same direction can produce a pitching moment. The ability to conrol the aircraft in this way is essential if the design of effective reconfigured control laws is to be achieved. The aircraft is modelled using five inputs and six outputs:

Inputs	Outputs

Inputs

Right Elevator (δ_{eR})

Left Elevator (δ_{eL})

Right Aileron (δ_{aR})

Left Aileron (δ_{aL})

  Rudder (δ_r)

Outputs

Angle of Attack (α)

Pitch Angle (θ)

Pitch Rate (q)

Sideslip Angle (β)

Roll Angle (ϕ)

Roll Rate (p)

Yaw Rate (r)

The linear perturbation equations used for this study were obtained by linearizing the nonlinear equations about a nominal operating point. The flight condition studied in this report is

CRUISE-MACH = 0.118 at 1500 ft

Tables 4-1, 4-2 and 4-3 provide some pertinent data of the URV aircraft

TABLE 4-1
URV AIRCRAFT DATA

Fuselage Length	122 in
Wing Area	19.66 ft^2
Mean Aerodynamic Chord	1.66 ft
Weight	177.1 lb
Actual C.G.	9.3 in
Reference C.G. (mean aerodynamic chord)	8.99 in

TABLE 4-2
URV AERODYNAMIC DATA

Alitude	1500 ft
M(Mach)	0.118
U_1(velocity)	131.27 ft/sec
I_{XX}(Roll mass moment of inertia)	11.18 slug-ft^2
I_{XY}(Pitch mass moment of inertia)	23.27 slug-ft^2
I_{ZZ}(yaw mass moment of inertia)	31.30 slug-ft^2
I_{XZ}(vertical plane mass cross product of inertia)	-1.66 slug-ft^2
b (wing span)	11.92 ft
c̄ (wing mean aerodynamic chord)	1.66 ft
$\bar{q}$ (dynamic pressure)	19.5943 abs/ft^2
s (wing reference arls)	19.66 ft^2

TABLE 4-3
AIRCRAFT AERODYNAMIC COEFFICIENTS IN THE STABILITY AXIS

α(deg) = 2.05		
C_L = 0.32	C_m = -.069	C_D = 0.0642
$C_{L_\alpha}(\frac{1}{deg})$ = 0.08	$C_{m_\alpha}(\frac{1}{deg})$ = -.027	$C_{D_\alpha}(\frac{1}{deg})$ = 0.18
$C_{L_{\delta e}}(\frac{1}{deg})$ = 0.0126	$C_{m_{\delta e}}(\frac{1}{deg})$ = -.0423	$C_{D_{\delta e}}(\frac{1}{deg})$ = 0.077
$C_{L_q}(\frac{1}{rad})$ = 6.25	$C_{m_q}(\frac{1}{rad})$ = -15.1	
$C_{L_\alpha}(\frac{1}{rad})$ = 1.22	$C_{m_\alpha}(\frac{1}{rad})$ = -4.1	
Side Force	**Yawing Moment**	**Rolling Moment**
$C_{y_\beta}(\frac{1}{deg})$ = -.0244	$C_{n_\beta}(\frac{1}{deg})$ = 0.0026	$C_{l_\beta}(\frac{1}{deg})$ = -.00095
$C_{y_p}(\frac{1}{rad})$ = 0.04	$C_{n_p}(\frac{1}{rad})$ = -.060	$C_{l_p}(\frac{1}{rad})$ = -.469
$C_{y_r}(\frac{1}{rad})$ = 0.63	$C_{n_r}(\frac{1}{rad})$ = -0.283	$C_{l_r}(\frac{1}{rad})$ = 0.129
$C_{y_{\delta_a}}(\frac{1}{deg})$ = 0.00205	$C_{n_{\delta_a}}(\frac{1}{deg})$ = -.00012	$C_{l_{\delta_a}}(\frac{1}{deg})$ = 0.00323
$C_{y_{\delta_r}}(\frac{1}{deg})$ = 0.003	$C_{n_{\delta_r}}(\frac{1}{deg})$ = -.0012	$C_{l_{\delta_r}}(\frac{1}{deg})$ = 0.00007

Using the aerodynamic coefficients shown in Table 4-3, additional stability derivatives were calculated to add split surface effects and couple the longitudinal and lateral direction equations. These are shown in Table 4-4.

TABLE 4-4
ADDITIONAL AERODYNAMIC COEFFICIENTS NEEDED FOR COUPLED EQUATIONS

$$
\begin{array}{ll}
C_{l_{\delta aL}}(\frac{1}{deg}) & = .00175 \\[4pt]
C_{l_{\delta aR}}(\frac{1}{deg}) & = -.00175 \\[4pt]
C_{n_{\delta aL}}(\frac{1}{deg}) & = -.00005 \\[4pt]
C_{n_{\delta aR}}(\frac{1}{deg}) & = 0.00005 \\[4pt]
C_{l_{\delta eL}}(\frac{1}{deg}) & = .000593 \\[4pt]
C_{l_{\delta eR}}(\frac{1}{deg}) & = -.000593 \\[4pt]
C_{n_{\delta eL}}(\frac{1}{deg}) & = 0 \\[4pt]
C_{n_{\delta eR}}(\frac{1}{deg}) & = 0 \\[4pt]
C_{m_{\delta aL}}(\frac{1}{deg})\ C_{m_{\delta aR}}(\frac{1}{deg}) & = -.00175 \\[4pt]
C_{m_{\delta eL}}(\frac{1}{deg})\ C_{m_{\delta eR}}(\frac{1}{deg}) & = -.0185
\end{array}
$$

The data of Tables 4-1 to 4-4, were used to obtain a model of the URV in the state variable form which is given by

$$\dot{\underline{x}}(t) = A\,\underline{x}(t) + B_0\underline{\delta}(t) \qquad (4.1)$$

where

$$\underline{x}(t) = [\alpha\ \theta\ q\ \beta\ \phi\ p\ r]^T$$

$$\underline{\delta}(t) = [\delta_{eL}\ \delta_{eR}\ \delta_{aL}\ \delta_{aR}\ \delta_r]^T$$

$$A = \begin{bmatrix} -2.632 & 0 & 1 & 0 & 0 & 0 & 0 \\ 0 & 0 & 1 & 0 & 0 & 0 & 0 \\ -39.63 & 0 & -3.382 & 0 & 0 & 0 & 0 \\ -0 & 0 & 0 & -.7399 & .2442 & .00096 & -.9849 \\ 0 & 0 & 0 & 0 & 0 & 1 & 0 \\ 0 & 0 & 0 & -17.6 & 0 & -8.94 & 3.16 \\ 0 & 0 & 0 & 22.09 & 0 & .137 & -2.05 \end{bmatrix} \qquad (4.2)$$

$$B_0 = \begin{bmatrix} .0073 & .0073 & -.01 & -.01 & 0 \\ 0 & 0 & 0 & 0 & 0 \\ .5118 & .5118 & -.0697 & -.0697 & 0 \\ 0 & 0 & .00055 & -.00055 & -.00159 \\ 0 & 0 & 0 & 0 & 0 \\ -.2489 & .2489 & .7356 & -.7356 & -.0685 \\ .0132 & -.0132 & -.0464 & .0464 & .1809 \end{bmatrix} \qquad (4.3)$$

V. SIMULATION RESULTS

The block diagram of the existing control law for the URV is shown in Fig. 5.1. The transfer functions of the servo and rate sensor are given by

$$servo = \frac{324}{s^2+25.4s+324} \qquad (5.1)$$

$$Rate\ sensor = \frac{50}{s+50} \qquad (5.2)$$

The gains of the rate sensors and the vertical gyro, and the linkage ratios are given in Table 5.1.

TABLE 5.1

Rate Sensor Gain	
Yaw:	0.05
Pitch:	0.05
Roll:	0.025
Vertical Gyro Gain	
Pitch:	.0416 v/°sec
Roll:	.0278 v/°sec
Linkage Ratio	
Rudder:	1.8
Elevator:	5.63
Aileron:	3.60
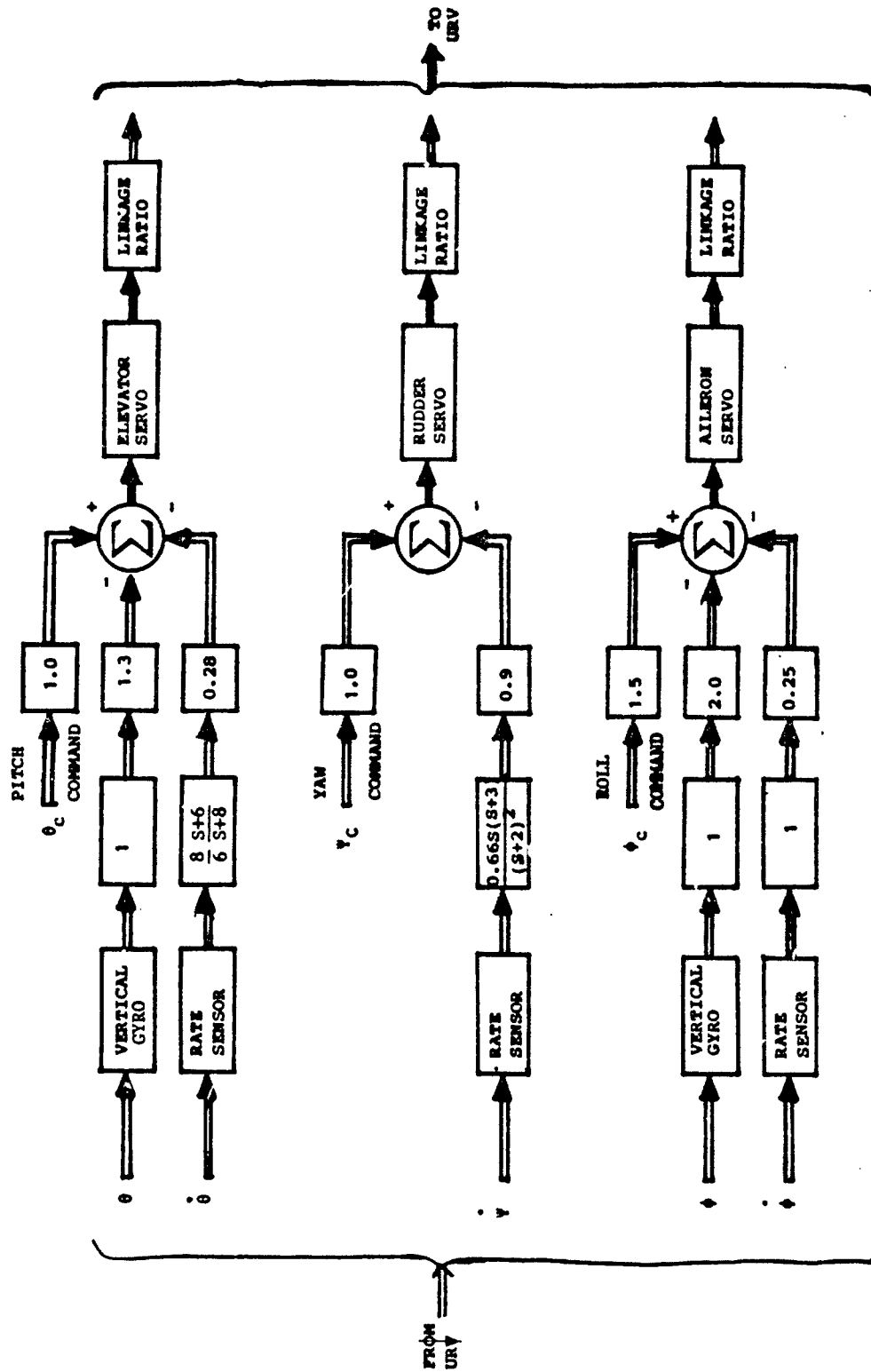
Fig. 5.1. Block Diagram of the Existing Control Law for the URV

The model of the URV developed in Chapter IV is verified before adding the control mixer reconfiguration algorithm. Fig. 5.2 shows the step response of the URV model (eqn. (4.1)) and FCS (Fig. 5.1). The control system is designed to be an uncoupled attitude controller and the responses reflect elevator to pitch angle, aileron to roll angle and rudder to yaw rate. The step responses of the existing system were also obtained and are also shown in Fig. 5.2. It can be seen from these plots that the two responses match very closely.

The control mixer algorithm derived in chapter III was then used to develop mixer gain matrices when the control surfaces are failed. The gain matrix for the unimpaired URV given by eqn. (5.3) reflects the highly uncoupled nature of the original control law design.

$$K_0 = \begin{bmatrix} 1 & 0 & 0 \\ 1 & 0 & 0 \\ 0 & 1 & 0 \\ 0 & -1 & 0 \\ 0 & 0 & 1 \end{bmatrix} \qquad (5.3)$$

B_0 and K_0 given by eqns (4.3) and (5.3) are used to derive new gain matrix K_I for various failure conditions.

5.1 Right Elevator Failed (Center and Locked)

The gain matrix for this failure was obtained using eqn. (3.9) and is given by

$$K_I = \begin{bmatrix} 2.0 & 0 & 0 \\ 0 & 0 & 0 \\ 0.3396 & 1 & 0 \\ -.3397 & -1 & 0 \\ 0.0283 & 0 & 1 \end{bmatrix} \qquad (5.4)$$
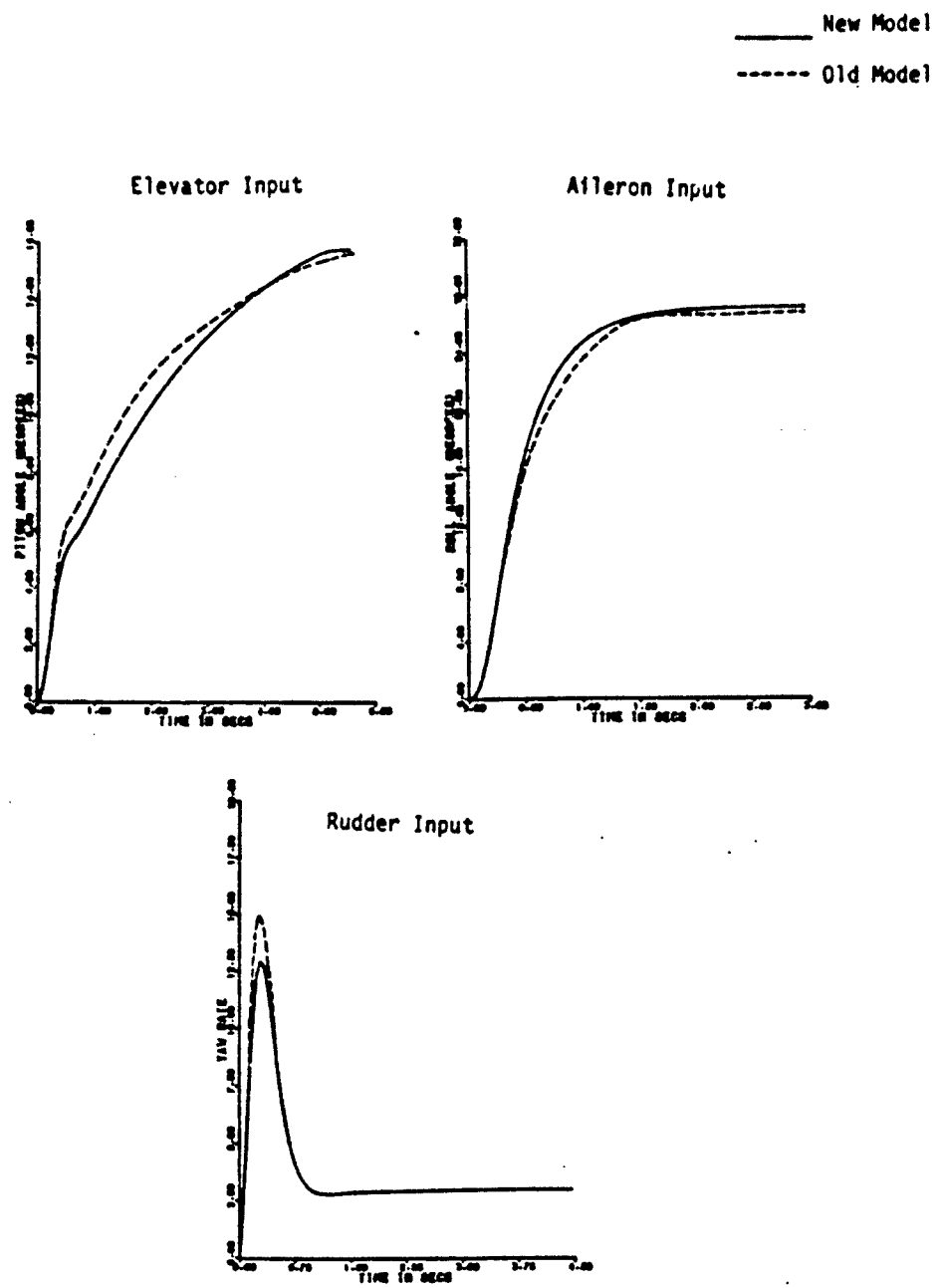
117-17

New Model

------- Old Model

Elevator Input

Aileron Input

Rudder Input

Fig. 5.2. Step Response of the Old and New URV Model

117-18

Fig. 5.3 shows the simulation results of the flight path of an impaired aircraft while the reconfiguration algorithm is activated. The impairment takes place at 4.5 secs. The results are compared with the flight path of the unimpaired aircraft. It can be seen from these figures that the effect of the loss in control is not seen until a time of approximately 6 seconds. This is due to the fact that a significant change in pitch rate is not required until 6 seconds. At 6 seconds the aircraft is commanded to pitch through an angle of 36 degrees. As shown in Fig. 5.3, the reconfiguration module compensates for the loss in control and makes it possible for the aircraft to follow this command. After this command is carried out the pitch rate settles quickly to the pitch rate value of the unimpaired aircraft and the aircraft is stable. Roll rate, roll angle, side slip and yaw rate responses of the unimpaired aircraft is zero whereas for the reconfigured aircraft, these responses are not zero because of the contribution of elevator input to ailerons and rudder as shown in eqn. (5.4).

5.2 Left Elevator Failed (Centered and Locked)

The gain matrix for this failure obtained using eqn. (3.9) is given by

$$K_I = \begin{bmatrix} 0.0 & 0 & 0 \\ 2.0 & 0 & 0 \\ -.3397 & 1 & 0 \\ .3396 & -1 & 0 \\ -.0283 & 0 & 1 \end{bmatrix} \qquad (5.5)$$

The simulation results of the impaired aircraft with this failure are similiar to the results shown in Figs. 5.3.
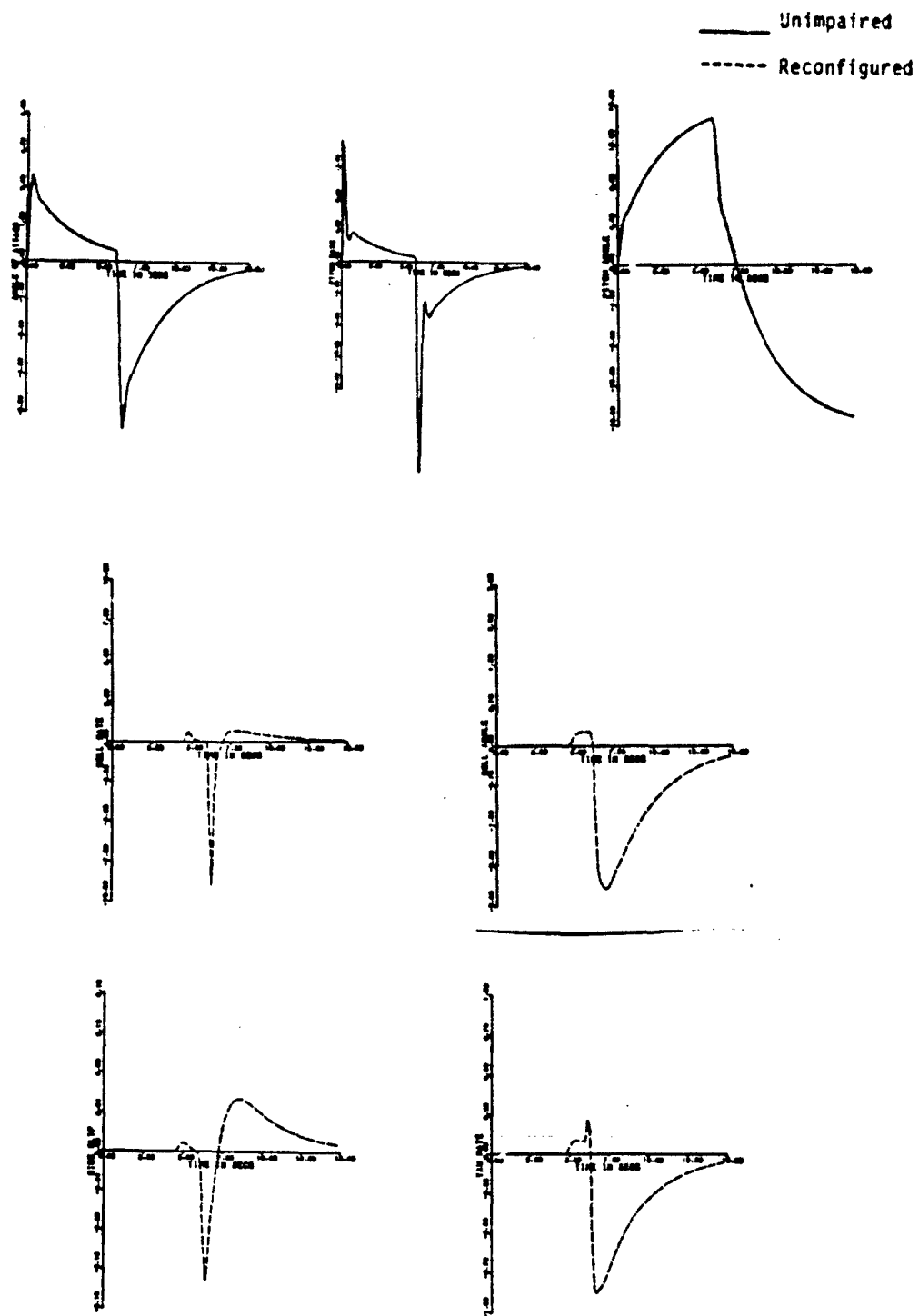
Fig. 5.3. Computer Simulation of Unimpaired and Reconfigured
           Aircraft - Pitch Command

5.3 Left Aileron Failed (Centered and Locked)

The gain matrix obtained using eqn. (3.9) for this failure is given by

$$K_I = \begin{bmatrix} 1.0 & -2.9358 & 0 \\ 1.0 & 2.9351 & 0 \\ 0 & 0 & 0 \\ 0 & -0.0058 & 0 \\ 0 & -.0832 & 1 \end{bmatrix} \qquad (5.6)$$

Fig. 5.4 shows the simulation results of the unimpaired and reconfigured aircraft. The impairment takes place at 4 seconds and a roll angle of 36 degrees is commanded at 5 seconds. It can be seen from Fig. 5.4 that the reconfiguration module compensates for the loss in control and makes it possible for the aircraft to follow the command with overshoot in the roll rate. After the command is carried out the roll attitude reaches the steady state value of the unimpaired aircraft and the aircraft is stable.

5.4 Right Aileron Failed (Locked and Centered)

The gain matrix K_I is given by

$$K_I = \begin{bmatrix} 1.0 & -2.9351 & 0 \\ 1.0 & 2.9351 & 0 \\ 0 & 0.0058 & 0 \\ 0 & 0 & 0 \\ 0 & -0.0832 & 1 \end{bmatrix} \qquad (5.7)$$

Simulation results of the unimpaired and reconfigured aircraft are similiar to the results shown in Fig. 5.4.
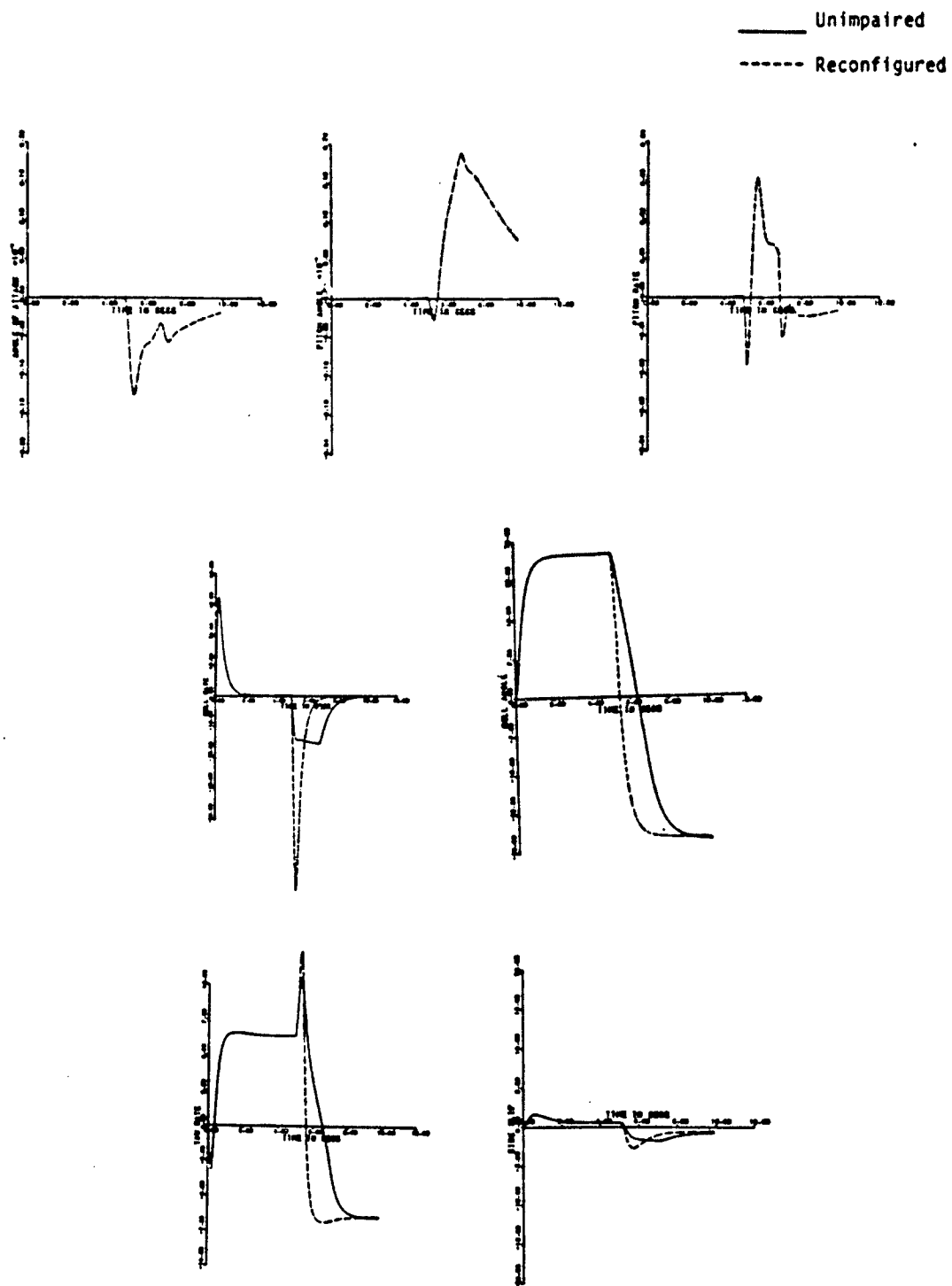
Fig. 5.4. Computer Simulation of Unimpaired and Reconfigured
Aircraft - Roll Command

117-22

5.5. Rudder Failed (Centered and Locked)

The gain matrix K_I obtained using eqn. (3.9) for this failure is given by

$$K_I = \begin{bmatrix} 1 & -0 & -35.1426 \\ 1 & 0 & 35.1426 \\ 0 & 1 & 11.94 \\ 0 & -1 & -11.94 \\ 0 & 0 & 0 \end{bmatrix} \qquad (5.8)$$

Fig. 5.5 shows the simulation results of the unimpaired and reconfigured aircraft commanded to yaw an angle of 18 degrees initially and impairment occuring at 4 seconds. It can be seen from this figure that the aircraft becomes unstable after the aircraft is commanded to yaw through an angle of 36 degrees at 5 seconds. This is due to the fact that other healthy surfaces do not have enough authority to compensate for this failure. K_I matrix given by eqn. (5.8) shows that excessive gain is needed for the other four healthy surfaces. Because of this, these surfaces saturate and the aircraft becomes unstable.
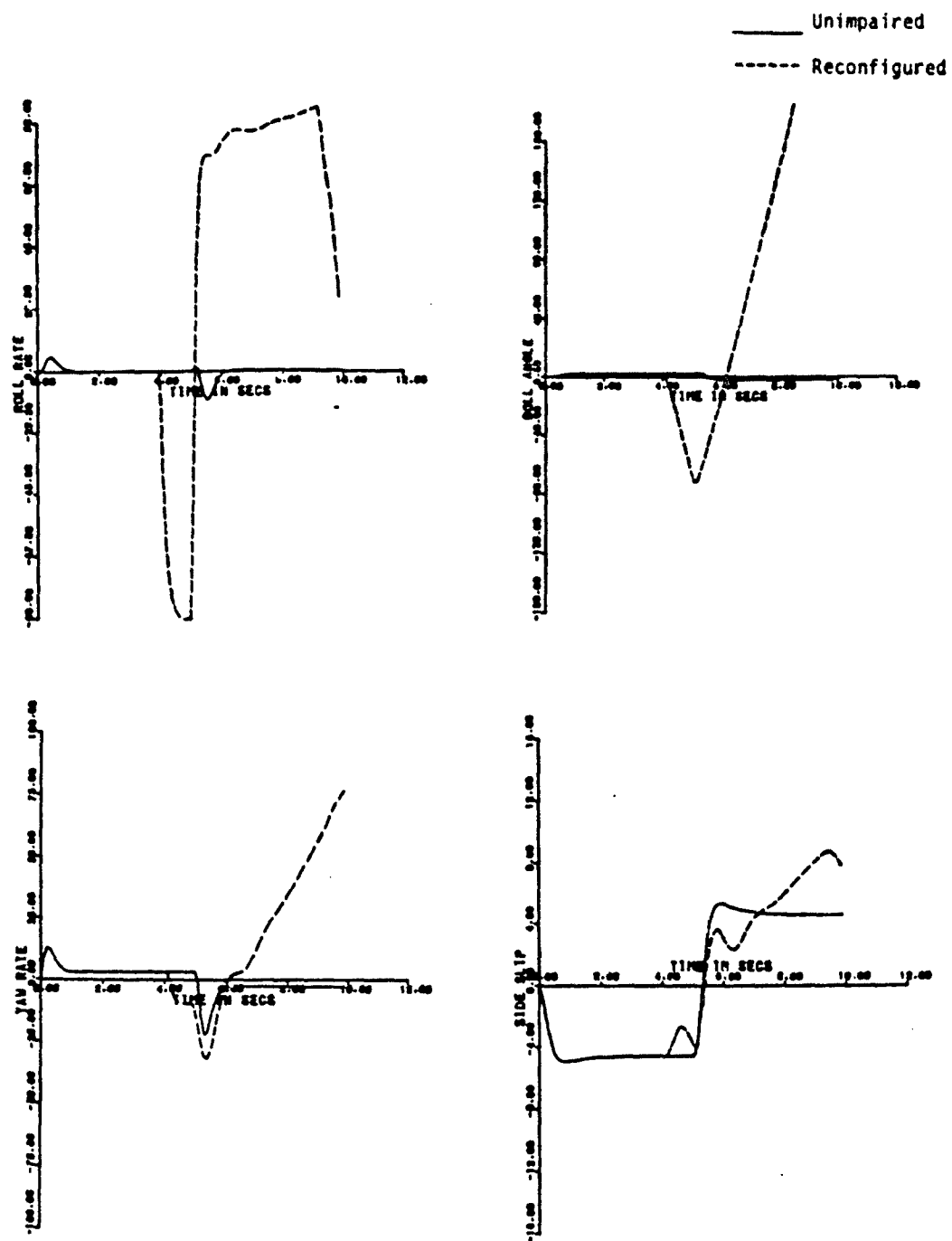
Fig. 5.5. Computer Simulation of Unimpaired and Reconfigured
Aircraft - Yaw Command

VI RECOMMENDATIONS

This research has focused upon the study of flight control law reconfiguration after effector failure. The control mixer concept which utilizes generalized inverse to distribute control authority among the remaining surfaces after failure was evaluated. In comparing output time histories, it is apparent that the reconfigured aircraft was able to track the unimpaired aircraft as long as there was another primary surface to provide the control power of the failed surface. For example, for a pitch command, one of the two elevator surfaces must be healthy for the aircraft to be able to track the unimpaired response. Results of Chapter V reveals that if the rudder is locked at the center position and there is a yaw command, the aircraft became unstable. These results suggest that the URV should be modified to provide additional control power redundancy in the yaw axis for reconfiguration studies. A more complete model of the URV that includes the aero changes should be developed. Ideally this should be a nonlinear model for higher fidelity and include the stability effects of missing and partially missing surfaces.

In determining the control mixer gain matrices, the failed surfaces were considered to be locked at the center position, i.e., the input from the failed surfaces was considered to be zero. No attempt was made to determine the gain matrices if the surface is locked at some other position or simply floating. In the future work, additional failure modes should be considered and the computer simulation obtained.

The present method of determining the gain matrices utilizes the generalized inverse as an optimization technique to distribute the forces and moments of the failed surface to the remaining healthy surfaces. This optimization technique is dependent on the relationship between the number of outputs and control surfaces. It exploits the excess degree of freedom without consideration of control surface physical limits. The burden of desired control inputs can be distributed among the remaining healthy surfaces by taking into account the actual authority of each. This can be done by multiplying the control effectiveness matrix of impaired aircraft by a diagonal matrix, [AUTH], which represents the physical control surface deflection limit. This is true only if number of outputs are less than number of control surfaces. But on the other

hand, if number of outputs are greater than number of surfaces, [AUTH]
matrix has no effect on minimization. This is because we are minimizing
the sum of square of error instead of norm of the deflection vector. One
way of distributing the control authority to other surfaces for the case
when number of outputs are greater than number of surfaces, is to
minimize the weighted sum of squares of error premultiplying the control
effectiveness matrix by a weighting matrix. Full rank factorization can
also be used as a technique for minimization. Study of both these should
be carried out in future work. Other optimization techniques available
should also be studied to find the best solution for control mixer gain
matrix.

For successful application of the control mixer concept to control
system reconfiguration, robustness of the FCS is an essential consi-
deration. This is necessary to compensate for unmodeled aerodynamics
effects caused by control surface failure and to compensate for inac-
curacies in estimating control derivatives for partially missing control
surface. Robustness of the existing control law of the URV should be
studied and recommendations on new control laws considering robustness
should be made.

REFERENCES

1. J.W. Davison, "Self-Repairing Digital Flight Control System Study," Final Report (Draft) - Parrt I, AFFDL-TR-.

2. Ben Noble, _Applied Linear Algebra_, Prentice Hall, Inc. Englewood Cliffs, New Jersey, 1969.

3. L.J. Linder, "Design, Development, Simulation, And Flight Test of A Low-Cost Digital Autopilot," Technical Report, KBG Corporation, AFFDL.

4. K.R. Lemble, "Dispersed and Reconfigurable Digital Flight Control Systems," Vol. I, Technical Report, AFFDL-TR-79-3125.

5. D.E. Russ, "Reconfigurable Digital Control Laws for the A-7D DIGITAC II Aircraft With Failed Primary Control Surfaces," Proceeding of the Workshop on Multivariable Control Systems, Sept. 1983, Technical Report, AFWAL-TR-83-3098.

6. J. Roskam, _Airplane Flight Dynamics and Automatic Flight Controls_, Part I, Roskam Aviation and Engineering Corporation, 1979.

7. _System/360 Continuous Systems Modeling Program_, User's Manual, IBM Program No. 360 A-CX-16X.

1984 USAF-SCEEE SUMMER FACULTY RESEARCH PROGRAM

Sponsored by the

AIR FORCE OFFICE OF SCIENTIFIC RESEARCH

Conducted by the

SOUTHEASTERN CENTER FOR ELECTRICAL ENGINEERING EDUCATION

FINAL REPORT

ANALYSIS OF ARMOR BRACKETRY

Prepared By: Hemen Ray

Academic Rank: Assistant Professor

Department and University: Department of Mechanical Engineering
                                    North Carolina A&T State University

Research Location: Flight Dynamics Laboratory
                                    Wright-Patterson AFB

USAF Research: James Hodges

Date: 16 July 1984

Contract No: F49620-82-C-C035

ANALYSIS OF ARMOR BRACKETRY

by

HEMEN RAY

ABSTRACT

The concept of rotating armor is introduced. The rotation of the armor in its plane is effected by using specially designed either inclined bracketry or bracketry fabricated with composites. By allowing the armor to rotate in its plane, the impact energy is absorbed in the rotational direction in addition to the normal to the plane of the armor, thereby reducing the force transmitted to the bracketry. Aircraft stiffness has also significant influence on the force transmitted to the bracketry. Application of these type of bracketry could increase the ballistic limit, or decrease the weight of the armor system. Suggestions for further research on armor bracketry are offered.

Acknowledgement

I. INTRODUCTION

The high-performance aircraft could be vulnerable to attack by missles, aircraft, heavy small arms, and conventional anti-aircraft fire. Addition of armor improves the survivability of these aircraft. Basically there are two types of armor systems for aircraft applications: integral structural armor and conventional armor. The integral armor is an integral load-carrying part of the aircraft. It serves the dual function of providing structural strength and ballistic protection. The conventional armor primarily provides ballistic protection [1]. Weight saving and combat effectivness are achieved by using integral armor [1, 2]. In certain applications, for example, existing aircraft, it is necessary to attach conventional armor. The conventional armor is attached to the aircraft by appropriate bracketry [3].

It is reported that there is excessive conservatism in the design data for the armor bracketry [4]. Use of heavier bracketry than necessary adds weight penalty. Considerable reduction in the weight of bracketry can be realized if the impact force transmitted to the bracketry is reduced. This can be achieved by using bracketry of proper stiffness such that the natural frequency of the bracketry and armor system is relatively low [5].

Armor bracketry with appropriate low stiffness will absorb appreciable amount of impact energy. But this requires some space for deflection when the armor is subjected to projectile impact. In certain situations there is not enough space for the armor to move normal to the plane of the armor. By using special bracketry the armor can be allowed to rotate in the plane of the armor so that less space is required normal to the armor plane. In this report the concept of rotating armor is introduced. The rotation of the armor in its plane is effected by using specially designed either inclined bracketry or bracketry fabricated from composites. By allowing the armor to rotate in its plane, the impact energy is absorbed in the rotational direction in addition to the usual normal to the plane of the armor. Application of these special type of armor bracketry could increase the ballistic limit, and thus improving the survivability of the high-performance aircraft for the Air Force.

II. OBJECTIVES

The objectives of the research effort is to develop optimum bracketry
for the conventional armor so as to obtain armor system of minimum weight
for the high-performance aircraft. Specifically, considering a single-
degree-of-freedom model, and central normal impact of a projectile, develop
and analyze bracketry to absorb energy in rotational direction in addition
to the normal to the plane of the armor. Introducing the concept of rotat-
ing armor, analyze inclined bracketry and bracketry fabricated from
composites. Investigate the influence of aircraft stiffness on armor
system as well.

III. INCLINED BRACKETRY

In this section a brief description of the inclined bracketry is
given followed by the equation of motion for the armor system and its
solution. Finally the force transmitted to the inclined bracketry is
compared with that on the straight bracketry and conclusions are drawn.

A square armor of size a x a is supported at the four corners by
four inclined supports as shown in Figures 1 and 2. The longitudinal axis
of each inclined support makes an angle θ with the plane of the armor.
The vertical plane containing the longitudinal axis of an inclined support
is at an angle of 45° with an edge of the armor. This type of bracketry
will allow the armor to rotate clockwise in addition to its downward
motion (viewed from top) when the armor is subjected to a central normal
impact of a projectile. By allowing the armor to rotate in its plane, a
part of the impact energy is absorbed in the rotational direction in
addition to the normal to the plane of the armor. When the armor is
supported by straight bracketry, as shown in Figure 3, it only moves down-
ward and does not rotate in its plane. Bracketry with different geometry
other than the inclined supports can also be used to obtain the desired
rotational motion as shown in Figure 4, where bracketry in the shape of
quarter circles are used.

The equation of motion of the armor is obtained by employing
Lagrange's equation. The armor is assumed to be rigid and is subjected
to a central normal impact of a projectile. The inclined supports are
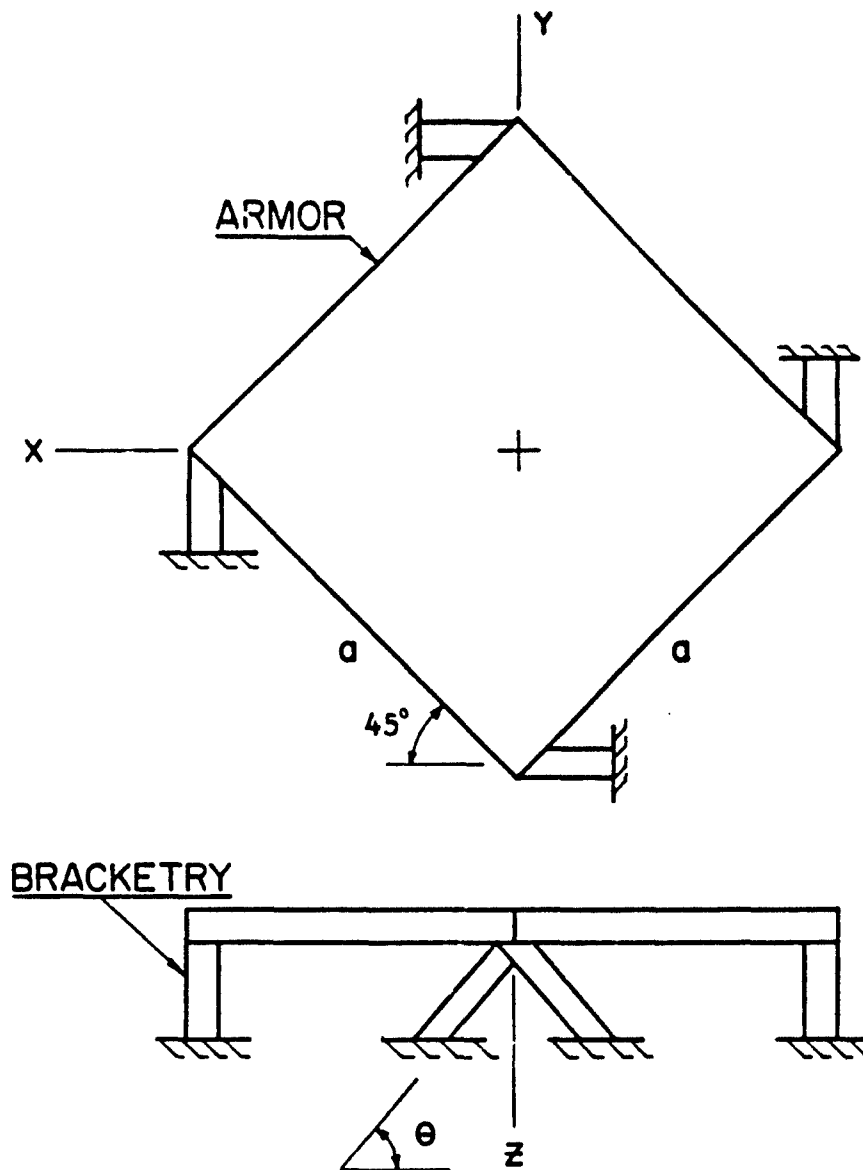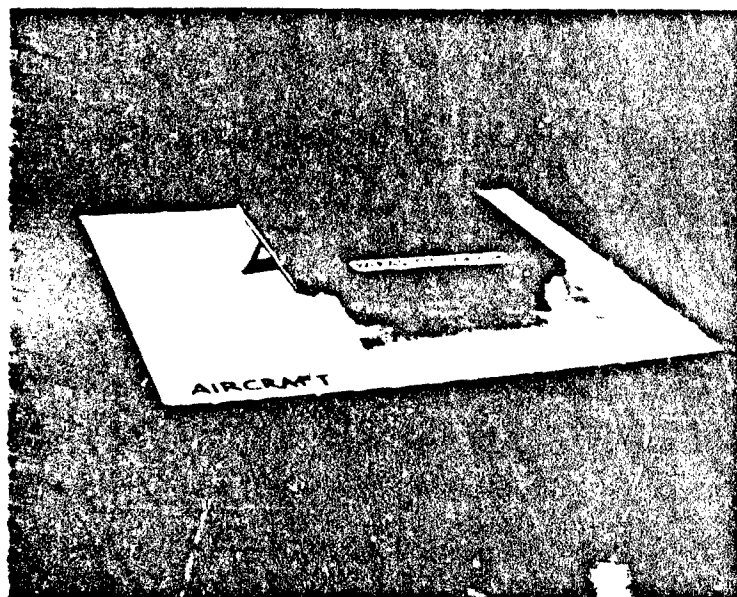
Figure 1. Inclined Bracketry
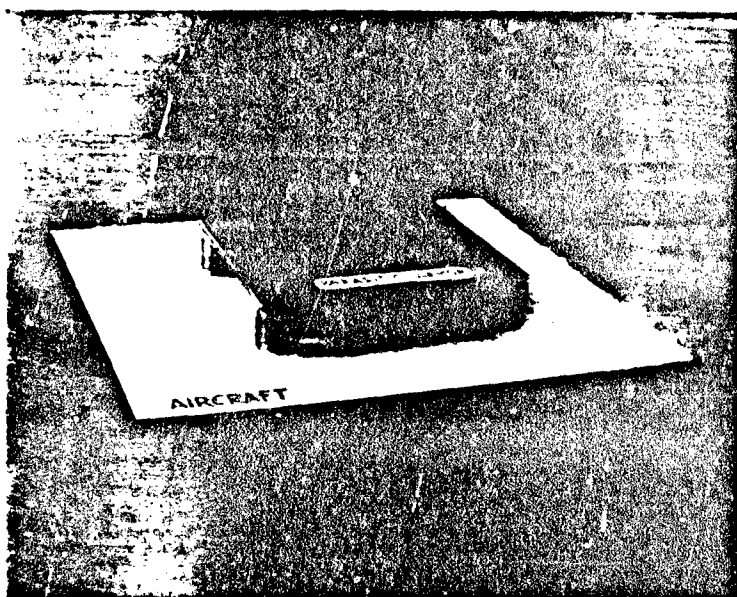
Figure 2. Inclined Bracketry

Figure 3. Straight Bracketry
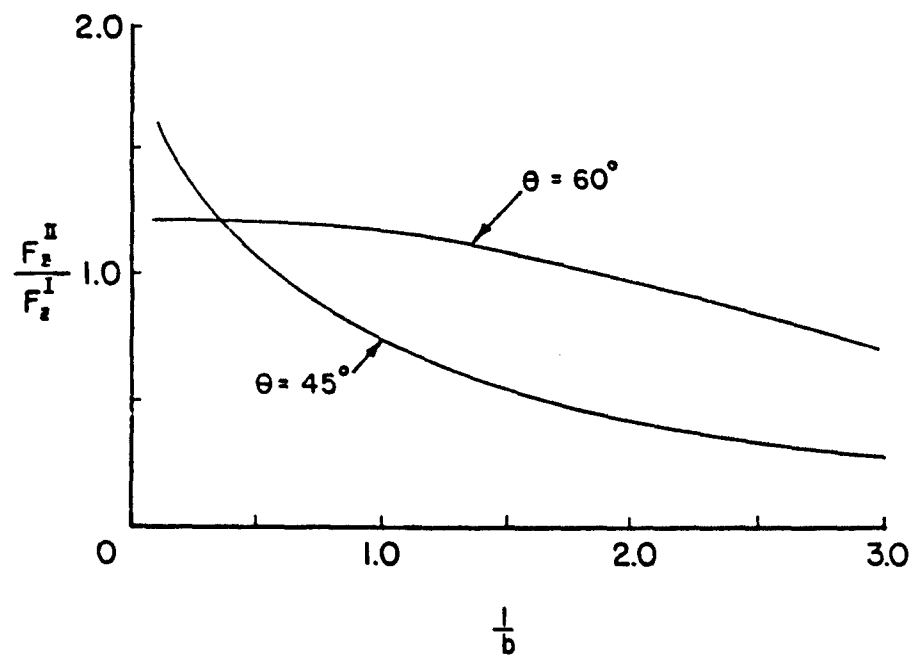
Figure 4. Bracketry With Quarter Circles

Figure 5. Ratio of the force on the inclined bracketry to that on the straight bracketry, as a function of the aspect ratio l/b.

113-8

considered to be attached to the armor by smooth ball joints. Under these idealized conditions, the potential energy V of the system is given by

$$V = 4 \left(\tfrac{1}{2} k_{z}^{\mathbb{I}} z^{2} \right) \tag{1}$$

where z is the displacement of the mass center of the armor in the z direction (see Fig. 1), and $k_{z}^{\mathbb{I}}$ is the stiffness of each inclined support in the z direction, and it is derived as

$$k_{z}^{\mathbb{I}} = \left[(l/AE)\sin^{2}\theta + (l^{3}/3EI)\cos^{2}\theta \right]^{-1} . \tag{2}$$

Here θ is the angle of inclination (see Fig. 1), l is the length, and A is the cross sectional area, E is the modulus of elasticity of the material, and I is the area moment of inertia about the bending axis of an inclined support.

The kinetic energy T of the system is

$$T = \tfrac{1}{2} m_{z} \dot{z}^{2} + \tfrac{1}{2} I_{G} \dot{\alpha}^{2} \tag{3}$$

where m_{2} is the mass of the armor, α is the angular displacement of the armor in its plane (xy plane), and I_{G} is the centroidal polar mass moment of inertia of the armor. A dot (˙) denotes derivative with respect to time t .

Substituting for α $(= \sqrt{2}\, c\, z/a)$ and I_{G} $(= m_{2}\, a^{2}/6)$, the kinetic energy (3) reduces to

$$T = \frac{1}{2} \left(1 + \frac{1}{3} c^{2} \right) m_{2}\, \dot{z}^{\,2} \tag{4}$$

where c is the ratio of the horizontal displacement of the end of an inclined support (the end that is attached to the armor) to the vertical displacement of the same end when a vertical load (in z direction) is applied to this end. Considering the axial and flexural deformation only, the approximate value of c is given by

$$c = \frac{1 + \dfrac{4 l^{2}}{b^{2}}}{\tan\theta \left(1 + \dfrac{4 l^{2}}{b^{2}\tan^{2}\theta} \right)} \tag{5}$$

where b is the dimension of each side of the cross section of an inclined support.

Applying Lagrange's equation and using (1) and (4), the equation of motion of the armor is

$$\ddot{z} + \omega_{z}^{2}\, z = 0 \tag{6}$$

where ω_{z} is the natural frequency of the system, and is given by

$$\omega_{z}^{2} = \frac{4 k_{z}^{\mathbb{I}}}{\left(1 + \tfrac{1}{3} c^{2} \right) m_{2}} \tag{7}$$

118-9

If the duration of impact is relatively short, and the projectile remains embedded in the armor, then the initial conditions for the armor motion, by considering the conservation of momentum, are

$$\text{at} \quad t=0, \quad z=0, \quad \dot{z} = \frac{mv}{m+m_2} \simeq \frac{mv}{m_2} \tag{8}$$

where m is the mass, and v is the speed of the projectile.

With the initial conditions (8), the solution to (6) is

$$z = \bar{Z} \sin \omega_2 t \tag{9}$$

where

$$\bar{Z} = (mv)/(m_2 \omega_2) \tag{10}$$

The value of the maximum total vertical force on the inclined bracketry is

$$F_z^{II} = 4 k_{q_2}^{II} \bar{Z} = mv \left[(4 k_{q_2}^{II}/m_2)(1 + \tfrac{1}{3}c^2) \right]^{1/2} \tag{11}$$

For the armor supported by straight bracketry (as shown in Fig. 3, or in Figs. 1, 2 with $\theta = 90°$), the value of the maximum total vertical force on the straight bracketry can be found as

$$F_z^{I} = mv \left(\frac{4 k_{q_2}^{I}}{m_2} \right)^{1/2} \tag{12}$$

where $k_{q_2}^{I}$ is the stiffness of each straight support in the vertical direction, and is given by

$$k_{q_2}^{I} = \frac{AE}{\ell}. \tag{13}$$

Here ℓ is the length, A is the cross sectional area, and E is the elastic modulus of the material of a straight support.

The ratio of the maximum total vertical force on the inclined bracketry to that on the straight bracketry is found from (11) and 12),

$$F_z^{II} / F_z^{I} = \left[(k_{q_2}^{II}/k_{q_2}^{I})(1 + \tfrac{1}{3}c^2) \right]^{1/2} \tag{14}$$

which reduces to, by using (2) and (13),

$$F_z^{II} / F_z^{I} = \left[(1 + \tfrac{1}{3}c^2)/(\sin^2\theta + \frac{4\ell^2}{3b^2}\cos^2\theta) \right]^{1/2} \tag{15}$$

This force ratio is plotted against the aspect ratio ℓ/b for $\theta = 45°$, 60° (Figure 5). From Figure 5 it is seen that the force on the inclined bracketry is less compared to that on the straight bracketry for larger values of ℓ/b. It is considerably less when $\theta = 45°$. For larger values of θ, the inclined bracketry approaches straight bracketry, and thus showing no significant reduction in force. The physical reason for this reduction of force is that part of the impact energy is used in rotating the armor

when the inclined bracketry is used. Also with increasing values of l/b, the natural frequency of the armor system with inclined bracketry reduces at a faster rate than that of armor with straight bracketry. This reduction in natural frequency causes less force to be transmitted to the bracketry. Therefore, by using the inclined bracketry the ballistic limit could be increased or for the same ballistic limit the weight of the bracketry can be decreased, and thus reducing the weight of the armor system.

IV. COMPOSITE BRACKETRY

In this section a brief description of the bracketry fabricated with composites is given followed by comparison of the force transmitted to the composite bracketry with that to the isotropic bracketry, and conclusion.

Figures 6 and 7 show the composite bracketry. Here the horizontal edges of a composite support are at angles of 45° with the edges of a square armor. The principal material axis of the composite makes a certain angle with the longitudinal axis (z = axis) of the bracketry. For this arrangement the armor will rotate clockwise (viewed from top) in addition to its downward motion when it is subjected to a central normal impact of a projectile. The mechanical behavior of orthotropic materials is used to effect rotation. When an orthotropic material is subjected to axial load directing not in the principal material direction, it undergoes shear deformation in addition to axial deformation. This shear deformation allows each corner of the armor to move in a horizontal plane, and thus effecting rotation of the armor.

For illustration the principal material axis of the composite is taken as 45° with the vertical axis (z - axis). With this material orientation, the stiffness of each composite support in the vertical direction (z - direction) can be found as

$$k_3^{\mathbb{I}} = A/(l\,\bar{S}_{22}) \tag{16}$$

where l is the length, A is the cross sectional area of a composite support, and the transformed reduced compliance $\bar{S}_{22}$ is given by [6]

$$\bar{S}_{22} = \frac{1}{4E_1}\left(1 - 2\nu_{12} + \frac{E_1}{E_2} + \frac{E_1}{G_{12}}\right) \tag{17}$$

where E_1, E_2 are Young's modulii in 1, 2 directions (1, 2 are the principal material directions), G_{12} is the shear modulus in 1-2 plane, and ν_{12} is Poisson's ratio for transverse strain in the 2-direction when stressed in the 1-direction.
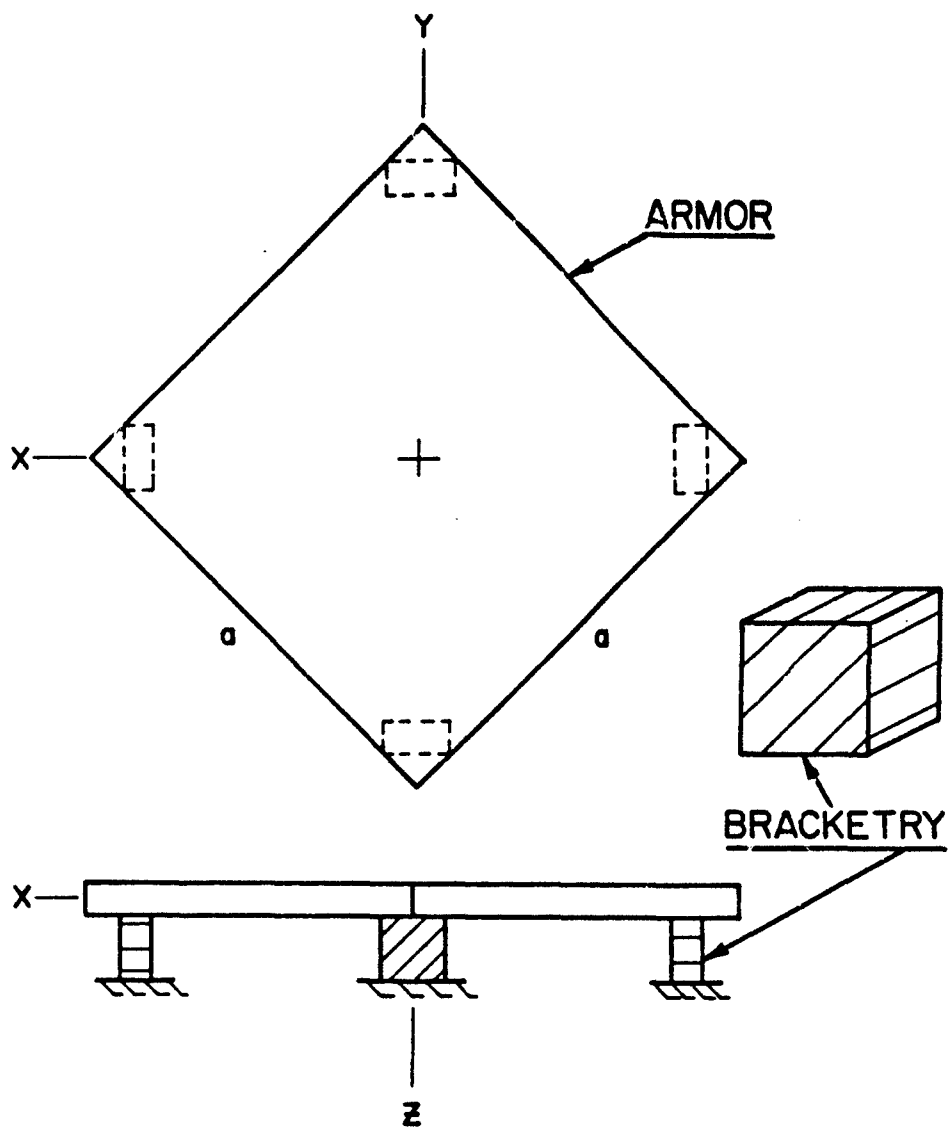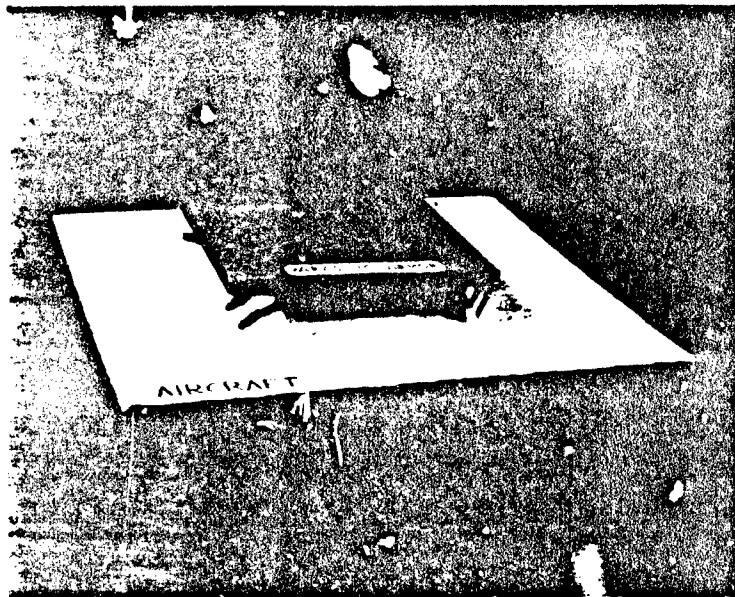
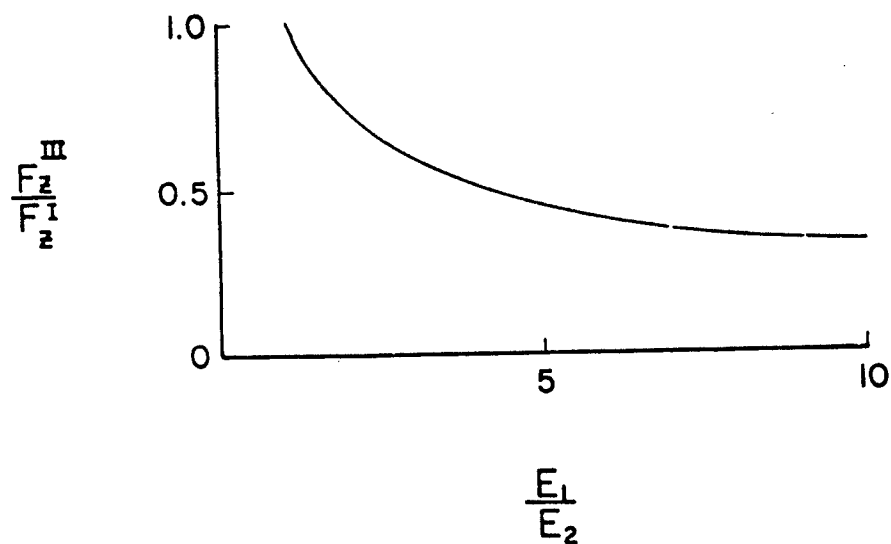Figure 6. Composite Bracketry

Figure 7. Composite Bracketry

Figure 8. Ratio of the force on the composite bracketry to that on
the isotropic bracketry, as a function of the modulii
ratio E_1/E_2.

The ratio of the horizontal displacement of the top of the composite support to the vertical displacement of the same end when a vertical load (in z-direction) is applied can be derived as

$$c = \bar{S}_{26} / \bar{S}_{22} \qquad (18)$$

where the transformed reduced compliance $\bar{S}_{26}$ is given by [6]

$$\bar{S}_{26} = \frac{1}{2E_1}\left[1 - \frac{E_1}{E_2}\right] \qquad (19)$$

Similar to the development of equation (14), the ratio of the maximum total vertical force F_z^{II} on the composite bracketry to that $\left(F_z^{I}\right)$ on the isotropic bracketry can be obtained as

$$F_z^{II} / F_z^{I} = \left[\,(k_z^{II}/k_z^{I})\,(1 + \tfrac{1}{3}c^2)\,\right] \qquad (20)$$

which reduces to, by using (13) and (16),

$$F_z^{II}/F_z^{I} = \left[\frac{1}{E\,\bar{S}_{22}}\left(1 + \tfrac{1}{3}\frac{\bar{S}_{26}}{\bar{S}_{22}}\right)\right]^{1/2}. \qquad (21)$$

Assuming that

$$E = E_1, \quad \nu_{12} = 0.5, \quad E_1 = 3G_{12},$$

the equation (21) reduces to

$$F_z^{II}/F_z^{I} = \left[\frac{E_2}{E_1}\left\{1 + \frac{1}{48}\left(\frac{E_2}{E_1}-1\right)^2\right\}\right]^{1/2} \qquad (22)$$

This force ratio is plotted against the modulii ratio E_1/E_2 (Figure 8). Figure 8 shows that the force transmitted to the composite bracketry is less compared to that transmitted to the isotropic bracketry. Significant reduction of force occurs for larger values of E_1/E_2. Similar to inclined bracketry the composite bracketry allows the armor to rotate in its plane in addition to its vertical motion, thereby transmitting less force to the bracketry.

V. INFLUENCE OF AIRCRAFT STIFFNESS ON ARMOR SYSTEM

In the foregoing analysis it is assumed that the armor is attached to a rigid surface by bracketry. But certain area of the aircraft where the armor is attached to may not be stiff enough to be considered rigid for the analysis. In this section the influence of aircraft stiffness on the armor system is shown.

A rigid armor of mass m_2 is attached to a rigid mass m_1 by bracketry of stiffness k_2. The mass m_1 is attached to a rigid surface by a spring of stiffness k_1. This mass-spring system m_1-k_1 represents the flexible area of the aircraft where the armor is attached to. It is assumed that the mass m_1 and m_2 are not of the same order of magnitude, and they are allowed to move in a vertical plane. The mass m_2 is subjected to a

projectile impact (normal impact) of relatively short duration. Under these idealized conditions the motion of m_2 can be considered to be independent of m_1, and the equations of motion for the system are given by

$$\ddot{z}_2 + \omega_2^2 z_2 = 0,$$
$$\ddot{\delta} + \omega_1^2 (1 + \tfrac{k_2}{k_1})\delta = \ddot{z}_2 + \omega_1^2 z_2 \tag{23}$$

where z_1, z_2 are displacements of mass m_1, m_2 (positive downward), and

$$\delta = z_2 - z_1, \qquad (24) \qquad\qquad \omega_1^2 = k_1/m_1, \quad \omega_2^2 = k_2/m_2 \tag{25}$$

Considering the conservation of momentum the initial conditions for the mass m_2 is

$$t = 0, \quad z_2 = 0, \quad \dot{z}_2 \simeq mv/m_2 \tag{26}$$

With the initial conditions (26), the solution to (23a) is given by

$$z_1 = (mv/m_2 \omega_2) \sin \omega_2 t \tag{27}$$

Since the bracketry stiffness k_2 is considerably less than the stiffness k_1 of the aircraft area, the term in the bracket in (23b) can be taken as 1. Initially the mass m_1, is assumed to have zero displacement and velocity, and accordingly using the initial conditions

$$t = 0, \quad \delta = 0, \quad \dot{\delta} = \dot{z}_2 - \dot{z}_1 = (mv)/m_2 \tag{28}$$

the solution to (23b) is given by

$$\delta = (mv/m_2 \omega_1) \sin \omega_1 t + (mv \omega_2 / m_2 \omega_2^2) \sin \omega_2 t \tag{29}$$

The maximum force on the bracketry i.e. the force between mass m_1 and m_2 is

$$F_z^{\overline{\text{II}}} = k_2 \delta_{max} = mv \omega_2 \left(1 + \tfrac{\omega_2}{\omega_1}\right). \tag{30}$$

In the absence of mass-spring m_1-k_1 , the maximum force F_z^I on the bracketry is (similar to eq. 12)

$$F_z^I = k_2 z_{2\,max} = mv \omega_2 \tag{31}$$

The rat > of the maximum force on the bracketry including the stiffness of the aircraft area to that on the bracketry excluding the aircraft stiffness is obtained from (30) and (31)

$$F_z^{\overline{\text{II}}} / F_z^I = 1 + \tfrac{\omega_2}{\omega_1} = 1 + \left[(k_2/k_1)(m_1/m_2) \right]^{1/2} \tag{32}$$

This force ratio is shown graphically in Figure 9 for two values of mass ratio. It shows when the armor mass is considerably less than the mass of the aircraft area, the force on the bracketry increases with the increase of the stiffness of the armor bracketry. Therefore, the stiffness of the armor bracketry should be considerably less than that of the aircraft area in order to reduce the force transmitted to the bracketry.

VI. RECOMMENDATIONS

Since the inclined and composite bracketry show promise in reducing the force transmitted to the bracketry, thereby decreasing the weight of
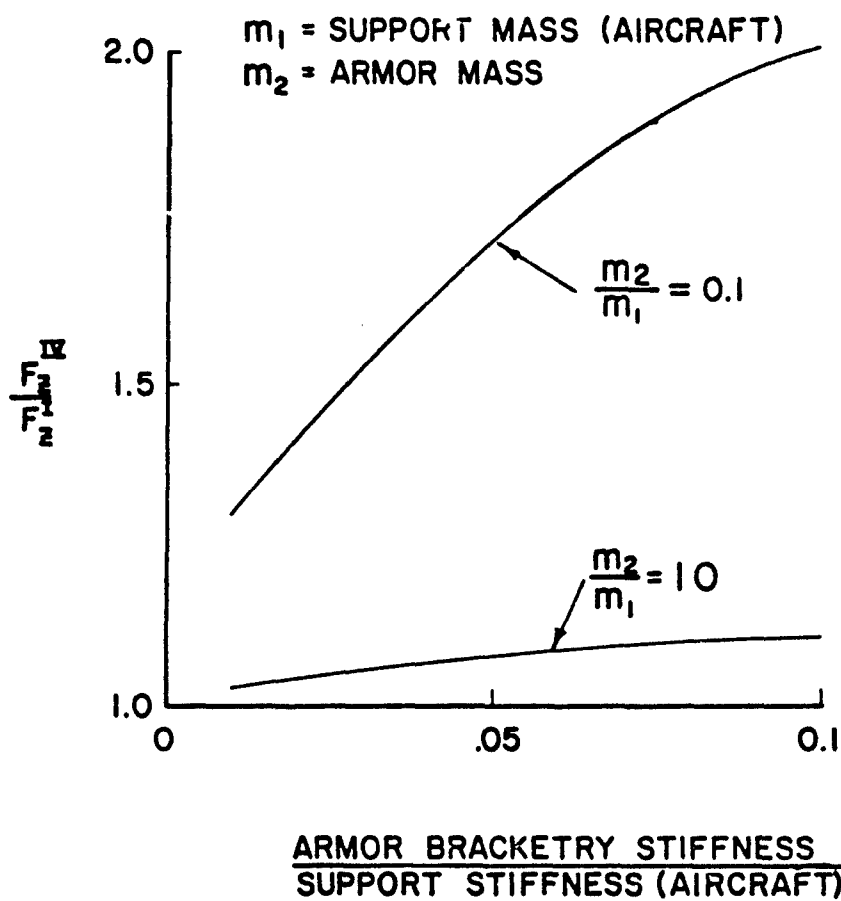
Figure 9. Ratio of the force on the bracketry including the stiffness of the aircraft area to that on the bracketry excluding the aircraft stiffness.

armor system and increasing the ballisting limit, further research should be directed to investigate their potential application:

* Include the more realistic data and information from the Penetration Equations Handbook [7] in the analysis of inclined and composite bracketry. For example, use the estimated impact force and pulse duration from [7] to obtain more realistic and accurate levels of force transmitted to the armor bracketry.

* Since the shear deformation is utilized to develop composite bracketry, rigorous analysis should be done on delamination of the composite bracketry.

* Perform analysis of 'inclined composite bracketry' to include the benefit of both the inclined bracketry and composite bracketry.

* Include the support motion (aircraft motion and g-levels) in the analysis of composite bracketry.

* Since the weight of the armor system could be further reduced by adhesively bonding the armor-bracketry system (suggested by Mover [8]), perform dynamic stress analysis of the bonded joints for representative armor-bracketry system.

REFERENCES

1. Buxton, R., and Verette, R., "Analytical and Experimental Development of Design Techniques for the Installation of Parasitic Armor," AFFDL-TR-68-26, Vol. I, Air Force Flight Dynamics Laboratory, Wright-Patterson Air Force Base, Ohio, March 1968.

2. Hodges, J., and Pendersen, A. H., "The Design and Test of an Integrally Armored Cockpit," MCAIR 71-019, McDonnell Aircraft Co., St. Louis, Mo, 3rd Aircraft Design and Operations Meeting of AIAA, 1971.

3. Hodges, J., "Design Techniques for Installing Parasitic Armor," AFFDL-TR-68-5, Air Force Flight Dynamics Laboratory, Wright-Patterson Air Force Base, Ohio, February 1968.

4. Laughlin, M. J., "Supplimental Discussion of Conservatism in the Development of Design Loads as Presented in the Final Report AFFDL-TR-68-26," Air Force Flight Dynamics Laboratory, Wright-Patterson Air Force Base, Ohio, June 1968.

5. Crede, C.E., Vibration and Shock Isolation, Wiley, 1951.

6. Jones, R. M., Mechanics of Composite Materials, McGraw-Hill, 1975, p 51.

7. Penetration Equations Handbook for Kinetic-Energy Penetrations, 61 JTCG/ME-77-16, November 1977.

8. Mayer, A. H., Meeting and Discussion on Armor System, Air Force Flight Dynamics Laboratory, Wright-Patterson Air Force Base, Ohio, 6 July 1984.

1984 USAF-SCEEE SUMMER FACULTY RESEARCH PROGRAM

Sponsored by the

AIR FORCE OFFICE OF SCIENTIFIC RESEARCH

Conducted by the

SOUTHEASTERN CENTER FOR ELECTRICAL ENGINEERING EDUCATION

FINAL REPORT

ARTIFICIAL INTELLIGENCE AND COMPUTATIONAL LINGUISTICS RESEARCH

Prepared by:	Dr. Larry H. Reeker
Academic Rank:	Professor
Department and University:	Department of Computer Science Tulane University
Research Location:	Air Force Human Resources Laboratory Training Systems Division Lowry Air Force Base, Colorado
USAF Research:	Maj. Hugh Burns, Ph.D.
Date:	August 1, 1984
Contract No.:	F49620-82-C-0035

ARTIFICIAL INTELLIGENCE AND
COMPUTATIONAL LINGUISTICS RESEARCH

by

Larry H. Reeker

ABSTRACT

Work in Artificial Intelligence and Computational
Linguistics was done at the Air Force Human Resources
Laboratory, Training Systems Division, in three dif-
ferent areas. The first area was "expert systems",
and the result was a demonstration system for use by
personnel at the laboratory. Secondly, a study was
undertaken of applications of computational linguis-
tics in the work of the laboratory, resulting in a
follow-up proposal. The third research area was an
investigation of the possibility of providing tools
for artificial intelligence in the Ada programming
language, and resulted in some programs for that pur-
pose. Suggestions are given for a follow-up project
investigating the provision of an adaptive natural
language interface for expert systems. Further
research in Ada implementation of artificial intelli-
gence tools is also suggested.

ACKNOWLEDGMENTS

I. INTRODUCTION

The field of computer science whose subject matter is the development of computer programs which perform activities that would be characterized as "intelligent" in humans is called artificial intelligence (AI). Among intelligent human activities is the use of natural languages, such as English, and the sub-field dealing with the use of computers in this area is called computational linguistics (CL). Although efforts in both fields date back to the time of the earliest digital computers, practical applications of AI and CL have gained wide notice only in the last few years, due largely to the availability of computing equipment with which the complex information processing required in AI and CL applications can be done efficiently.

Another reason that practical applications of AI and CL have become possible is the tendency of researchers in the field to move away from very general intelligent activities (such as general problem solvers), which were interesting theoretically but impossible to implement at today's state of knowledge, and to concentrate on specialized domains where known techniques are more adequate. It is possible, for instance, to design interesting and useful computer software that contains enough knowledge to draw conclusions that we associate in humans with expertise in some area (such as medical diagnosis or maintenance troubleshooting). These systems are popularly called expert systems.

Within computational linguistics, it has also been possible to narrow the domain enough to facilitate useful systems. Where it is desired to obtain a limited range of information from specialized and stylized natural language text, systems have been created for "specialized information extraction". It is possible to provide limited natural language interfaces for various computer-based systems (including expert systems), as well.

Summer work in this program was concerned with the investigation of various facets of AI and CL in the setting provided by the concerns of the Air Force Human Resources Laboratory, Training Systems Division.

II. OBJECTIVES

The Air Force Human Resources Laboratory, Training Systems Division, has undertaken to investigate the use of techniques from artificial intelligence and computational linguistics in the provision of training, particularly in the maintenance area. This effort is multifaceted, as outlined in [2] and implicit in the suggestions of [6].

The objectives of this project were to aid in the AFHRL efforts in three ways:

1) Provide a simple demonstration expert system, which personnel could use to examine how such systems work and demonstrate to others.

2) Provide some background in areas of computational linguistics that will be necessary or useful in these efforts, through discussion, lectures, and the implementation of computational tools, and hopefully lead to follow-on work in the area.

3) Investigate the feasibility of using the new common DOD language Ada for applications in computational linguistics and artificial intelligence.

The research component of this project included the work toward objective (3) and an investigation of the feasibility of an adaptive natural language interface for expert systems, combining work toward objectives (1) and (2) above. The approach was to study the problems carefully in light of available methodology and to analyze alternative solutions, then to write programs to investigate ideas for practical systems. Objective (3) was accomplished in conjunction with two graduate students from Tulane, whose work is discussed below and reported in more detail in their own final reports.

The initial work plan for the ten-week period included some effort in developing computational linguistics tools in the SNO-BOL4 programming language and a lecture on SNOBOL4 programming. This was replaced with a more extensive effort in Ada and LISP, both because of the direction in which our interests moved and because of the availability of Ada software and lack of SNOBOL4 systems.

III. IMPLEMENTATION OF A DEMONSTRATION EXPERT SYSTEM

The "Knowledge Base Developer", or KBD [7], is a system designed and implemented by Barry Schiff as an honors project at Tulane University. It has the capability to run as an expert system given a codified domain-specific knowledge base as input. The knowledge base is constructed through the KBD system, which provides a menu-oriented interface for making assertions and specifying inferences. Though written in LISP, the user interface is free of the syntactic conventions that make LISP formidable to the uninitiated. The inference machine and rule representation are relatively efficient, so that reasonable response is obtained on a VAX 11/780 with moderate-sized knowledge bases. The inference machine in KBD uses a weight system and a greedy approach to traverse a search tree looking for a conclusion.

A demonstration expert system for AFHRL was implemented in KBD. The knowledge base contain information on insects, and the system is able to identify the order of an insect based upon assertions (or answers to questions) regarding the physical description of a specimen (relative size and appearance of wings, shape of body, etc.). It asks for more information if the information that it has been given is insufficient. (Actually, only winged insect information was entered, since that was deemed sufficient for the demonstration.)

Some difficulties were experienced in the initial implementation of the system. Initially, no LISP system was available on the VAX 11/780 at AFHRL. A LISP implementation called TULISP was ported to the system to provide the proper environment, and some slight modification was made to the code to prevent problems that were encountered.

A lecture was given to interested personnel at the lab on LISP programming. There was considerable interest in LISP because it is currently the principal language for artificial intelligence research and is being used by General Dynamics in a system for maintenance aiding being written under contract to AFHRL. The demonstration system can be used as a further aid to staff in understanding LISP programming, since the code is accessible.

IV. COMPUTATIONAL LINGUISTICS EFFORTS

A number of discussions on the use of techniques from computational linguistics in the work of the Laboratory were held with Maj. Burns, leading to the production of a joint report by this author and Maj. Burns, which is being written this fall. In addition, a series of two talks was given at AFHRL on perspectives in the field, and on the investigator's work in specialized information extraction from natural language texts. Another talk was given on the possibility of developing individualized natural language interfaces for the types of expert systems being developed for

AFHRL. This latter topic is the subject of a proposal for follow-on research, which will be described briefly.

In any computerized system that requires natural language commands, it is common to use synonyms which the system cannot process. For example, people will use "output" or "write" instead of "print", or vice-versa. With the use of natural language assertions in an expert system, the problem becomes greater, since it is likely that there will be a variety of phrases that are synonymous from the user's standpoint, to only one of which the system can respond correctly. One solution to this problem might be a general natural language interface, but even then, the user may stray outside the bounds of the language accepted (since no such interface is going to contain all of English, at today's state of the art). Furthermore, a natural language interface of even moderate generality is likely to place heavy demands on computational resources and to slow the response of the system to all inputs.

A better solution to the synonymy problem is to continue using natural language assertions in the expert system, but to add to the system an ability to adapt to each user's particular modes of expression. Some of the variations found may be easily anticipated transformations of the assertions already contained in the system. Others may be misspellings and abbreviations. Others will be peculiar to individual users. It appears most practical, therefore, to develop a system that uses three levels of interpretation for assertions that it cannot handle directly.

The first level will contain facilities for dealing with misspellings and abbreviations, along with a file of the particular user's previously-used transformations, which the system will use in an attempt to transform novel inputs to known assertions. If none of these transformations works, a second stage will be invoked, in which a file is consulted that contains all of the transformations known to the system. If one of these is applicable, the system will query the user to see if it has transformed the sentence to the correct assertion, and if so, the transformation will be added to the user's file. If the second level is unsuccessful, a third level, which allows learning, will be entered. This level will be based upon the author's previous work in language acquisition modelling [5], and is described in more detail in the forthcoming proposal.

V. PATTERN-DIRECTED PROCESSING IN ADA

Ada is the new standard programming language developed for the United States Department of Defense. Concepts in it are based to a large extent on the languages SIMULA and Pascal. Most AI and CL research, on the other hand, is done in the language LISP, with some done in PROLOG, SNOBOL4, and a variety of other languages. If Ada is to become the common DoD language and if various "intelligent" applications are to be interfaced to programs written in Ada, then it would be convenient to be able to program AI and CL applications in Ada. With the aid of two graduate students from Tulane University, two projects were undertaken toward this end.

The language SNOBOL4 is based on a distinguished line of
programming languages which are "pattern-directed" in nature.
That is, they operate on data by searching for a pattern in the
data and then taking specified actions when the pattern is found.
The experimental language Post-X [1] was designed to build on
this notion, while extending it and providing a more convenient
control structure than SNOBOL4. Some of the notions embodied in
Post-X and some notions from LISP can be added to Ada, using Ada
"packages". Kenneth Wauchope [7], under the supervision of the
author and under the support of the AFOSR/SCEEE summer student
program, did exactly that. The result is a programming language
that is pattern-directed and that operates over data structures
other than strings, and that is compatible with other programs
written in Ada. In other words, the extension is more handy than
LISP for many tasks in artificial intelligence and computational
linguistics, and will also allow such applications to be embedded
in Ada programs quite easily. Although a working system was pro-
duced in the summer, further work is needed to make the system
easy to use, and is being done by Mr. Wauchope as a thesis pro-
ject.

Even in the area of string pattern matching, there are vari-
ous algorithms, and some are more convenient or more efficient
than others. With n Ada, the most elegant method of string pat-
tern matching is to use the tasking feature to implement corou-
tine pattern matching. This could not be done in the present Ada

system available at AFHRL because tasking was not implemented. The most straightforward method remaining was to write a backtracking algorithm. But backtracking (which is also what coroutines would do, covertly) is very costly, in terms of processing time, and moderately so in terms of storage. A possibly more time-efficient alternative was to use the well-known Earley parsing algorithm [3] - which can take a good deal of space, however. John Kreuter [4], as his AFOSR/SCEEE summer project under supervision of the author, undertook to compare various approaches, first implementing Earley's algorithm for SNOBOL4 patterns in Ada, with a provision for treating the results of the match in the manner of Post-X. Having completed this, he will continue to compare alternative implementations as a thesis project.

VI. RECOMMENDATIONS

Four follow-on efforts have been discussed in the text: continued study of computational linguistics applications in maintenance training and aiding, which is being undertaken by this author and Maj. Burns; investigation of adaptive natural language interfaces for expert systems, which is the subject of a follow-on proposal to AFOSR, further work on pattern-directed processing for general data structures, which is being undertaken as a thesis project by Mr. Wauchope; and comparison of string pattern matching algorithms with Earley's algorithm for use in implementing string processing in Ada, which is being undertaken as a thesis project by Mr. Kreuter.

REFERENCES

[1]   Bailes, Paul, and Larry Reeker, "An Experimental Applicative Programming Language for Linguistics and String Processing," Proceedings, 8th Intl. Conf. on Computational Linguistics , Tokyo, 1980, 520-525.

[2]   Dallman, Brian, "AFHRL Program for Artificial Intelligence Applications to Maintenance and Training," Artificial Intelligence in Maintenance: Proceedings of the Joint Services Workshop , Air Force Human Resources Laboratory, 1984.

[3]   Earley, Jay, "An Efficient Context-Free Parsing Algorithm," Communications of the Assoc. for Comput. Machinery , 13, 94-102, 1970.

[4]   Kreuter, John, "Pattern-Matching Algorithms in Ads," Final Report, 1984 USAF-SCEEE Graduate Student Summer Support Program, July 1984.

[5]   Reeker, Larry, "the Computational Study of Language Acquisition," Advances in Computers , vol. 15 (Yovits and Rubinoff, eds.), 181-237, Academic Press, New York, 1976.

[6]   Richardson, J. Jeffrey, "Artificial Intelligence: An Analysis of Potential Applications to Training, Performance Measurement and Job Performance Aiding," Report AFHRL-TP-83-28, Air Force Human Resources Laboratory, Training Systems Division, 1983.

[7]   Schiff, Barry, "KBD: A Tool for Knowledge Acquisition and Expert System Development," Honors Thesis, Tulane University Department of Computer Science, 1984.

[8]   Wauchope, Kenneth, "Pattern-Directed List Processing in Ada," Final Report, 1984 USAF-SCEEE Graduate Student Summer Support Program, July 1984.

1984 USAF-SCEEE SUMMER FACULTY RESEARCH PROGRAM

Sponsored by the

AIR FORCE OFFICE OF SCIENTIFIC RESEARCH

Conducted by the

SOUTHEASTERN CENTER FOR ELECTRICAL ENGINEERING EDUCATION

FINAL REPORT

MATHEMATICAL MODELING OF THE HUMAN CARDIOPULMONARY SYSTEM

<table>
<tr><td>Prepared by:</td><td>Dr. David B. Reynolds</td></tr>
<tr><td>Academic Rank:</td><td>Assistant Professor</td></tr>
<tr><td>Department and
University:</td><td>Department of Biomedical Engineering
Wright State University</td></tr>
<tr><td>Research Location:</td><td>Air Force Aerospace Medical Research Laboratory
Biodynamics and Bioengineering Division
Modeling and Analysis Branch</td></tr>
<tr><td>USAF Research
Colleague:</td><td>Dr. Ints Kaleps</td></tr>
<tr><td>Date:</td><td>24 August 1984</td></tr>
<tr><td>Contract No:</td><td>F49620-82-C-0035b</td></tr>
</table>

MATHEMATICAL MODELING OF THE HUMAN CARDIOPULMONARY SYSTEM

by

David B. Reynolds

ABSTRACT

The cardiopulmonary computer model developed by researchers at the University of Texas at Austin under contract with AFOSR is reviewed for its analytical soundness and appropriateness of application to problems of interest to the Air Force, especially the physiological effects of acceleration. From an analytical point of view, the biggest weakness of the model is in its treatment of flow in collapsible tubes. The accepted theory has been developed within the last ten years and has not been incorporated in the model. Another aspect needing attention is feedback control, at least in the circulation portion of the model. Although the original authors addressed this need, they had not incorporated feedback into the program by the end of the funding period. Other revisions of the analysis are addressed in the report. From a practical standpoint of use, the model should also be made more user-friendly and include computer graphics.

ACKNOWLEDGMENTS

I. INTRODUCTION:

A mathematical model of the human cardiopulmonary system was developed under AFOSR contract 79-0123 by investigators at the University of Texas, hereafter referred to as "originators" of the model. The model was actually constructed in two separate pieces, a pulmonary model and a cardiovascular model, with the eventual intent to integrate them. The models were numerically implemented on a digital computer and used to examine the effects of whole-body acceleration (WBA) and body position on respiratory mechanics, ventilation distribution, blood flow and blood volume distribution in the pulmonary and systemic circulations and the resulting gas exchange in the lung and tissues.

It is generally recognized now that the aviator is the limiting factor in the performance of the highest performance aircraft of today. Acceleration tolerance to blackout depends on onset rate, body position, body type, and other physiological and psychological variables and is several g's below the capability of the aircraft. Thus a small advantage in tolerance would probably mean a large advantage in combat engagement. Due to the high cost, limited number and noninvasive nature of experiments in the human centrifuge, development of a good cardiopulmonary model to direct and augment these studies is desirable.

II. OBJECTIVES:

The objectives of the summer support period are: (1) get the pulmonary model running on the Perkin-Elmer computer at AFAMRL/BBM; (2) review the pulmonary model for its merits, deficiencies and applicability to the goals of AFAMRL; (3) list improvements, modifications and suggest specialized areas of application of the pulmonary model; (4) get the circulatory model from the originators and have it compiled and running on the Perkin-Elmer computer; (5) perform steps (2) and (3) for the circulatory model; (6) integrate the two models into a combined cardiopulmonary model; (7) plan continuation studies involving the use and/or further development of the model.

III. PULMONARY MODEL:

A. Brief Description. The pulmonary model attempts to simulate
lung mechanics and regional ventilation in normal and abnormal
situations. Normal situations include prediction of many of the
pulmonary function tests including maximal expiratory flow-volume (MEFV)
curves, dynamic compliance, and washout of a test gas from the lungs.
Examples of abnormal conditions would be any mode of WBA and various
disease states.

In the model, the muscles of respiration (diaphragm, abdomen
and chest wall) are simulated by two driving pistons having mass and
orientation with respect to other elements of the model. The conducting
zone (upper airway and tracheobronchial tree down to the respiratory
bronchioles) is simulated by a five-chambered bifurcating system of air
passages. Finally, the gas exchange zone (alveoli) is simulated by six
alveolar chambers. Gravitational forces on the chest, diaphragm and
abdomen and resulting effects on pleural and abdominal pressures are
simulated. The gradient of pleural pressure and its effects on regional
alveolar chamber volumes are included in the model.

B. Critique. Due to lack of space in this report, the reader is
referred to the originators' progress reports for figures describing the
models. The pulmonary model is most completely described in Section C of
the December 1979 Progress Report for AFOSR contract 79-0123 by R.E.
Collins, R.E. Calvert and H.H. Hardy[1]. Unless otherwise mentioned, all
references to figures, equations and discussions of the pulmonary model
by the originators come from that report.

The functional schematic diagram of the pulmonary model is
shown in Fig. 1. The diaphragm/abdomen muscle complex is modeled as a
single, horizontal piston situated below the lowest alveolar
compartments. Although modeled as a single piston due to the
reciprocating action of these muscles, their mass distribution is taken
as orthogonal with diaphragm in the horizontal and abdomen in the
vertical plane. The lung itself has a conductive zone consisting of five
bifurcating air chambers labeled A_1 through A_5 and a six chambered

respiratory zone labeled ALV_1 through ALV_6. Chamber A_1 simulates nasal/oral cavities, larynx, trachea and primary bronchi. Chambers A_2 and A_3 simulate secondary and some tertiary bronchi and all lower order bronchi supplying the upper third of the lung, i.e. alveolar chambers ALV_1 and ALV_2. Conductive chambers A_4 and A_5 correspond to all lower order bronchi and supply the lower two-thirds of the lung, i.e. alveolar chambers ALV_3 through ALV_6.

Although the pulmonary model does not have as many branches as the real bronchial tree, which has over 100,000 bronchial segments before reaching the beginning of the gas exchange zone, it does have five conducting chambers and six alveolar compartments rather than the customary one of each. Thus, intercompartmental gradients of pressure, volume and their rates of change during breathing can be simulated, which cannot be done in a single compartment. Also, the conductive chambers have some of the inherent asymmetry of the real bronchial tree in that pathways to alveolar regions are shorter to the upper lobes and longer to the lower lobes. One of the gradients modeled is the gradient of pleural pressure, i.e. pressure at the surface of the lung. Forces arising from contraction of diaphragm and chest wall muscles are transmitted to the pleural surface, causing lung volume to change by the change in applied pressure.

The originators assume a hydrostatic-like gradient in pleural pressure, somewhat as if the lung tissue behaves like a liquid[2]. However, even the referenced authors stated that agreement between lung tissue density and measured pleural pressure gradient in dogs could have been coincidental. In man in both the head-up and lateral (lying on the side) position at functional residual capacity (FRC), the average pleural pressure gradient is slightly more than 0.2 cm H_2O per cm vertical distance down the lung[3]. Lung tissue density is about 0.22 gm/ml. In rabbits and dogs, the pleural pressure gradient varies with body position and in some positions is not constant, and similar results are indirectly found in man[3]. However, for a given species and posture, pleural pressure is uniquely related to percentage of lung height[4]. The reasons for the gradient are probably more complex than the fluid-like model and are discussed at length by Agostoni[3]. However, Glaister[5] contends that

the fluid-like model appears to adequately represent the underlying mechanics during acceleration. Thus, the originators' equation, while possibly not based on sound physical grounds, may empirically describe the situation. More research is needed in this area to verify this simple relation.

The chamber leading to the exterior of the airways in the originators' Fig. 1 corresponds to the volume measuring device or spirometer. However, this device measures only volume changes and not absolute volume. This part of the model could be extended to include an active device rather than a purely passive one. For example, a mechanical ventilator could be simulated given appropriate driving functions. This would be an interesting spinoff of the model since mechanical ventilator design just recently received more engineering input. Also, due to the interest in defensive measures to chemical warfare, the services may be interested in compact ventilators for field use. The originators specify that source/sink relations for individual gases are included in the spirometer chamber so that life support systems (e.g., pilot's cockpit) can be modeled, but as far as we are aware, no ventilator functions have been included.

The originators also assume that conductive and alveolar chambers have ideal mixing, i.e., incoming and resident gas mix instantly. For numerical methods, this means within one integration step (0.01-0.001 s). They argue that because chamber volumes are small and flow rates high, the assumption is valid. This argument is true in the upper conducting airways where velocities are relatively high, volumes small and tubes nonuniform, factors which all result in increased mixing. The assumption is probably valid in the alveolar compartments where diffusion over the very small distances involved is effective in gas species distribution. In the region in between, the assumption may not be valid. In the bronchioles, the gas velocities are low (creeping flow) but distances are still too large for diffusion to be effective in mixing. This region has been postulated as having the highest resistance to gas transport in the bronchial tree[6]. Consequently, the effects of adding more conductive compartments needs further study.

The mathematical development of the model starts with a volume

conversion equation for the thoracic cavity, which is equated to lung air
volume plus a constant volume comprised of pleural fluid and lung tissue.
Though not explicitly stated, the tissue volume must include blood
volume. Whether blood volume should be treated as constant is
questionable, particularly if the model is to be integrated with a
circulatory model (containing a pulmonary circulation) and used to study
blood redistribution with hypergravity. In support of this criticism,
Guyton[7] states that while the lungs contain only 450 ml of blood normally
(9% of total blood volume), their capacity for change ranges from about
50% to 200% of that volume. For example, Guyton[7] states that during
"bugle" blowing (or Valsalva maneuver with a slow leak or "grunting,"
often used by individuals to increase their tolerance to $+G_z$), the high
pressures in lungs, thorax, and abdomen can cause as much as 250 ml of
blood to be shifted out of the pulmonary circulation and into the
systemic circulation. In addition, blood flow in thoracic and abdominal
vena cava may be shut off until microcirculation pressure becomes greater
than thoracic and abdominal pressures. Thus lung blood volume must be
considered variable if realistic predictions of what happens to blood
volume during "grunting" are to be obtained.

The next set of equations described are the equilibrium
equations of forces across the muscles (pistons) and alveolar chambers.
Since all pressures act on nearly equal (or assumed equal) surface areas,
force balance becomes a pressure balance. Inertial terms are considered
negligible. Modeling the alveolar chambers as thin-walled elastic
elements with a volume dependence of elastic "recoil" pressure is
generally acceptable. The additional element in the muscle model is a
force or pressure generator term which is a driving function.
Considering the complexity of the entire model, a simple model for the
actuators is probably reasonable. Mechanical properties of alveolar
compartments are nonlinear but uniform, thus due to the pleural pressure
gradient, intercompartmental differences in the distribution of inspired
volume are predicted.

The modeling of the diaphragm-abdomen is less than clear. The action of these two muscle groups has been lumped together, but they are treated separately in terms of mass distribution. Their action is lumped since the diaphragm is predominantly active during inspiration and the abdomen during expiration. Thus a single force balance equation simulates the reciprocating action of the two groups. Masses of the two are treated separately since the diaphragm is mainly horizontal while the abdomen is vertical in the head-up position. Presumably, values for elastic recoil and driving pressures together with mass and its geometric distribution must be supplied. Other than a general statement, no values are given for geometry and mass distribution. Presumably abdomen and diaphragm are treated as thin muscle sheets oriented perpendicular to each other as shown in the originators figure.

This lack of information is but one example of a common occurrence in the originators pulmonary model: verbal descriptions are provided but actual data/equations are not, as least in the written documentation. If these data/equations are in the computer program only, they would be extremely difficult to decipher and find. In fact, a general listing of symbology for all relevant, non-dummy computer program variables is not available, which makes deciphering even more difficult.

The originators then state the need for four more sets of equations. The ideal gas equation can be written for each alveolar compartment. Secondly, water vapor is treated separately from the other gases since it is assumed saturated and must also have a source. Also, mass balance equations can be written for each chamber and pressure-flow equations can be written for transport between chambers. For some unknown reason, the pressure-flow equations are deferred to a later section by the originators, yet in the ensuing paragraphs they lead one to believe that by differentiating and algebraically manipulating the volume, force balance, ideal gas and mass balance equations for the gases involved plus accounting separately for saturated water vapor, one obtains the complete set of differential equations describing the dynamics of the pulmonary gas system. The pressure-flow relations for the conducting airways have been ignored for some reason and thus for this reason alone the dynamics cannot have been totally accounted for.

motion is identical for gas flow in a rigid tube, liquid flow in a uniform, horizontal open channel, or incompressible fluid flow in a collapsible tube:

$$\frac{\partial u}{\partial t} + u\frac{\partial u}{\partial x} = -\frac{1}{\rho}\frac{\partial p}{\partial x} \qquad (2)$$

Where u is velocity, t is time, x is distance along the tube, ρ is mass density of the fluid and p is pressure. The continuity equations are

$$\frac{\partial A}{\partial t} + \frac{\partial}{\partial x}(Au) = 0 \qquad \text{for a collapsible tube} \qquad (3a)$$

$$\frac{\partial \rho}{\partial t} + \frac{\partial}{\partial x}(\rho u) = 0 \qquad \text{for gas flow in a rigid uniform tube} \qquad (3b)$$

$$\frac{\partial h}{\partial t} + \frac{\partial}{\partial x}(hu) = 0 \qquad \text{for horizontal, uniform open channel flow} \qquad (3c)$$

In these equations, A is cross-sectional area and h is free surface height. Note that A, ρ, and h play analogous roles in their respective equations. The propagation velocity of small disturbances is related to the rate of change of pressure with A, ρ, and h, respectively for the three cases (see Eq. (1) for the collapsible tube case).

Consequently, the originators' model may be valid only in the range of breathing flow rates such that velocity in any given bronchus is much less than the local wave speed. Their simulation of maximal expiration, which gave them trouble and understandably so, is not consistent with the currently accepted theory of flow limitation in collapsible tubes. Thus, their maximal flow predictions are not acceptable to this reviewer, even though they claim to adequately describe experimental data. Since submaximal breathing has bronchial velocities which may be much smaller than wave speed, these predictions may be acceptable, although some reservations about the handling of airway resistance are to follow.

Treatment of airway resistance by the originators initially was semitheoretical. Rohrer's equation for bronchial flow resistance was cited and its terms explained. Rohrer's equation is a quadratic pressure-flow relation of the airways in which the flow squared term accounts for turbulent pressure losses and the linear term for pressure losses in laminar flow. Other investigators have disputed this claim[9], but we have shown its validity in rigid tracheobronchial models[10,11] and in excised human lungs during steady submaximal expirations over a wide range of physiological flow rates[12]. In these studies we propose a dimensionless form of the equation which correlates air and other gas mixtures on a single curve. This equation has also been incorporated into a model of maximal expiratory flow in which airways were allowed to be collapsible[13]. Good agreement with experimental data for subjects maximally expiring different gas mixtures of widely varying properties was obtained from the model. The latter model incorporates the theory of flow limitation at wave speed presented above and also includes frictional effects via the Rohrer equation inserted in the equation of motion.

At this point, due to difficulties in applying the Ro'rer equation to high expiratory flows, the originators abandon it in favor of a purely empirical curve fitting of airway resistance data at several lung volumes obtained from the literature. Submaximal pressure-flow predictions they deemed adequate. We contend in this report that the failure to predict maximum expiratory flow-volume (MEFV) curves is not due to the inadequacy of the Rohrer and/or lung compliance equations as is stated in the originators' report, but arises from failure to consider the mechanism of flow limitation in collapsible tubes. This is demonstrated by the adequacy of predictions made by the model referred to in the last paragraph which did consider flow limitation. The originators' "predictions" seem to be not much more than a curve fitting of clinical data and not an analytical model based on airway mechanics.

A few additional comments on some of the assumptions listed in
the originators' chapter on airway resistance are appropriate. They
state that resistance to flow through the upper airway (exterior to the
lungs) is not a function of lung volume. Stanescu et al.[14] have shown
that upper airway resistance is a function of lung volume, flow magnitude
and direction, and breathing frequency. The primary site for the
resistance and its variation with the above parameters seems to be the
glottis (the opening between the vocal cords), which can change
cross-section greatly--from zero to maximally open. The variable
resistance of the upper airway can greatly confuse the interpretation of
overall airway resistance. It is for this reason that resistance is
usually measured while subjects pant shallowly since this causes the
glottis to stay maximally open, thus stabilizing and minimizing the
contribution of the upper airway. The variability of upper airway
geometry may be one cause of the recent findings in man showing that
dimensionless plotting of airway resistance vs. characteristic Reynolds
number do not consolidate data obtained with different gases on the same
curve[15,16]. These findings are in direct contradiction to our findings
for steady flow in rigid tracheobronchial models and excised lungs.
Since Stanescu et al. do not give actual glottal areas but only relative
changes, it is not possible to estimate glottal resistance and its
variation. However, the direction of the glottal changes with flow rate
and frequency are in the correct direction to qualitatively explain the
discontinuous dimensionless resistance curves. Unsteady flow, as occurs
during panting, has been shown to cause discontinuous dimensionless
resistance--Reynolds number curves on rigid tracheobronchial models[17].
These problems are just some of the reasons why airway resistance is so
poorly understood, thus less frequently used as a pulmonary function
test. Some accounting for the variability of upper airway geometry and
unsteady flow effects on airway resistance should be topics for future
research and revisions of the pulmonary model. More immediate, however,
would be the incorporation of flow limitation in collapsible tubes.

IV. CIRCULATORY MODEL

A. Brief Description.

The originators' circulatory model was first described in their December 1979 progress report and subsequently published paper[18]. The model includes systemic and pulmonary circulation elements. The basic assumption for the blood vessels is that many branching vessels can be treated as a single uniform vessel. However, systemic and pulmonary arteries, veins and capillaries are separate elements. In addition, small veins, leg veins, and large veins are differentiated. The systemic circulation includes a four-chambered pumping heart, systemic arteries, tissue compartments representing head, upper torso, lower torso, legs, and return of blood to the heart through small and large veins. The pulmonary circulation has blood compartments paralleling the ventilation compartments discussed in the pulmonary model above. A model element includes a capacitive element or model chamber and a resistive element or model segment. Three types of chambers are included which simulate lung capillaries, tissue capillaries, and vessels with no gas exchange capability. Heart and leg vein valves are also included. Flow through the leg, mitral and tricuspid valves is controlled by pressure differential only, whereas aortic and pulmonary valves are modeled to include inertial closing.

The equations of the model are divided into four areas: axial blood flow, transverse vessel wall motion, pressure-volume relationships for elements, and gas transport. These will be discussed more in detail below.

The circulatory model has apparently undergone revision since its initial formulation in 1979. The originators' November 1980 progress report[19] outlined two problem areas: (1) pooling of blood even under normal gravity in the head-up sitting position and (2) numerical instability of the integration routine when pooling occurs. Whether these problems were corrected in their published work is uncertain, but in the latter, they stress the need for modifying the handling of the pressure-volume (P-V) relationships of circulatory elements as well as

incorporating feedback control. The latter is an essential part of a complete circulatory model and the primary physiological deficiency in the originators' circulatory model. The P-V relationships are associated with numerical instabilities (or so the originators state) due to the form of the P-V equation at large pressures, at which volumes approach asymptotic values. They suggest that handling the equations in a "slightly more complex numerical manner" will alleviate the problem, which arises when large, sustained whole-body accelerations are imposed. Whether these changes in numerical methods had been accomplished by the end of the funding period is not clear, since no mention of them is made in the final report. Based on recent personal communications with the originators, feedback control equations were not fully implemented in the computer program available at the time of the final report.

B. Critique.

The equations for axial motion of the blood through the segments are derived from conservation of linear momentum and mass for a deformable control volume. Segment length is assumed constant in all segments of the model. Cross-sectional area is assumed constant in the aorta and pulmonary artery. Cross-sectional area is assumed uniform in peripheral segments, but must vary as segment volume varies. Segment volume in turn is a function of transmural pressure. The assumption of segment uniformity appears to be violated, since the axial motion equation predicts a decrease in internal pressure, which for constant external pressure would mean decreasing transmural pressure along the vessel length and thus, decrease in volume. Presumably, this is handled by the Windkessel-type model[20], in which each model element is considered to be a distensible chamber in series with a rigid tube. However, the model is an extension of the single element Windkessel model in that inertial terms in the flow equation are included (at least in the larger vessels) and several elements representing different body tissues are connected together. The force terms in the momentum equation include pressure, weight, and frictional forces. The latter are modeled by Rohrer's equation discussed previously in the pulmonary section of this

report. Also, no accounting for the phenomena of flow limitation in collapsible tubes is made. Flow limitation is likely to occur at the entrance of small venules of the pulmonary circulation and in the vena cava of the systemic circulation[8]. In addition, it may occur in thoracic arteries during maneuvers which increase intrathoracic pressure[8]. This problem could be at least partially remedied by comparing flow speed with wave speed in the various segments of the model and adjusting the calculation procedure depending upon how close flow speed is to wave speed.

Also, no mention is made of the non-Newtonian behavior of blood flow. This is especially true in the smaller vessels where lower shear rates exist and the non-Newtonian behavior is more pronounced[20]. In this case, the Poiseuille-Hagen equation should at least be modified by an appropriate factor.

The gas transport equations for a compartment at present include those for O_2 and CO_2 only. Molar conservation equations for the latter are written, with terms accounting for flow transport in and out, diffusion, and volume change of a compartment. Perfect mixing in each element and instantaneous equilibrium between gases in solution in plasma and bound to hemoglobin are assumed. A uniform diffusion gradient within vessel walls is also assumed. Equations for moles of O_2 dissolved in plasma and bound to hemoglobin are written. The CO_2 content of blood was not separated into plasma and hemoglobin content, but a single equation relating the moles of CO_2 in a chamber to the product of partial pressure, whole blood volume, and a saturation function was written. The saturation function was taken from the work of other investigators. All in all, the gas transport equations appear satisfactory in form. Some of the parameters such as the diffusion coefficients and metabolic rates of O_2 and CO_2 disappearance and appearance are probably varied to obtain a good simulation of normal data. In fact, parameter studies should be the first investigations of a model with so many values left to the investigator's choosing. The possible nonuniqueness of solutions where so many parameter values are left as inputs to the model is a definite drawback to multicompartment models.

Although the originators present feedback control equations in their final report, these were never fully incorporated into the computer program. Thus, the program currently available has no feedback control. Since the model was designed to study short-term effects, the physiologic controls simulated are the baroreceptor and chemoreceptor reflexes. These reflexes are mediated by their action on heart rate, heart contractility, and vascular compliance/resistance. These additions are currently part of the Ph.D. dissertation research of David Martin at the University of Texas. His expectation for finishing this is by summer 1985. Consequently, to have a reliable working computer model of the cardiopulmonary system which includes feedback control, we must either wait for Martin's results or make an effort on our own. In Martin's opinion, the cardiopulmonary model without feedback control is not helpful in modeling the short-term physiological effects of acceleration.

V. RECOMMENDATIONS:

The framework upon which the cardiopulmonary model is built appears to be acceptable. The multicompartments allow regional variation which has not been simulated in previous models. However, the lumped nature of its many compartments allows for integration with respect to time but does not consider spatial variation within a compartment. For example, coupled effects such as pressure drop in a vessel or airway causing nonuniform narrowing are not accounted for. Consequently, the following modifications/additions are recommended for future study.

1. Incorporate the theory of flow limitation in collapsible tubes in both the pulmonary and circulation parts of the model.

2. Revise the pressure-area equations for vessels to simulate data for negative as well as positive transmural pressures. Currently, only the latter are modeled. This is important since some of the most interesting collapsible tube flow phenomena occur around zero transmural pressure.

3. Investigate the need for more complex modeling of the pleural pressure gradient.

4. Replace the empirical resistance formulas in the pulmonary model with the experimentally proven Rohrer's resistance equation. This equation written in dimensionless variables is also appropriate for flow of gases other than air. Rohrer's equation has also been included in a previous model of maximal expiration[13] which uses the theory in 1. and Rohrer's equation is also currently used in the circulatory model.

5. Include feedback control in the circulatory part of the model. Investigate the need for feedback control in the ventilatory model as well. The version recently received at AFAMRL has no feedback control in either portion. Control is probably more important in the short-term cardiovascular function, but the possibility of impaired gas exchange may lead to breathing changes mediated mainly through the effects of CO_2 on respiratory centers.

6. Clean up the coding of the program and make the input/output more user friendly. In this regard, investigate the possibility of writing the model in a simulation language, such as ACSL (Advanced

Continuous Simulation Language). Documentation of computer variables and explanation of the flow of the program is poor and should be improved. Adding user-friendly input/output graphics is also desirable, which is part of the package of ACSL.

7. Correct other problems as detailed in the body of this report. In some cases this may require experimental data on some aspect of lung or circulation function in addition to that available in the literature. For example, the effect of unsteady flow on resistance in lung airways has not been quantified completely. Pressure-flow behavior of the upper airways also needs quantification with respect to the appropriate parameters. In vivo pressure-area behavior of the smaller vessels and bronchi is difficult to obtain and may have to be approximated.

REFERENCES

1. Collins, R. E., R. E. Calvert, and H. H. Hardy, "Mathematical Simulation of the Cardiopulmonary System," Progress Report, AFOSR 79-0123, December 1979.

2. Kreuger, J. J., T. Bain, and J. L. Patterson, Jr., "Elevation gradient of intrathoracic pressure," _J. Appl. Physiol._, 16, 1961, pp. 465-468.

3. Agostoni, E., "Transpulmonary Pressure," Ch. 6 in _Regional Differences in the Lung_, Ed. J. B. West, New York, Academic Press, 1977, pp. 245-280.

4. D'Angelo, E., M. V. Bonanni, S. Michelini, and E. Agostoni, "Topography of the pleural surface pressure in rabbits and dogs," _Resp. Physiol_. 8, 1970, pp. 204-229.

5. Glaister, D. H., "Effect of Acceleration," Ch. 8 in _Regional Differences in the Lung_, Ed. J. B. West, New York, Academic Press, 1977, pp. 323-379.

6. Scherer, P. W., Personal communication.

7. Guyton, A. C., _Basic Human Physiology: Normal Function and Mechanisms of Disease_, Philadelphia, W. B. Saunders, 1977.

8. Fung, Y. C., _Biodynamics: Circulation_, New York, Springer-Verlag, 1984.

9. Pedley, T. J., R. C. Schroter, and M. F. Sudlow, "Gas Flow and Mixing in the Airways," In _Bioengineering Aspects of the Lung_, Ed. J. B. West, New York, Dekker, 1977, Vol. 3, pp. 163-265.

10. Reynolds, D. B. and J. S. Lee, "Steady Pressure-Flow Relationship of a Model of the Canine Bronchial Tree," _J. Appl. Physiol_.: _Respirat. Environ. Excercise Physiol_. 51:1072-1079, 1981.

11. Reynolds, D. B., "Steady Expiratory Flow-Pressure Relationship in a Model of the Human Bronchial Tree," _J. Biomech. Engr. Trans_. ASME 104:153-158, 1982.

12. Reynolds, D. B., "Model Studies of Expiratory Pressure-Flow Relations in Man," _Proc. 35th Ann. Conf. Engr. Med. Biol_., Vol. 24, Philadelphia, 1982, P. 92.

13. Lambert, R. K., T. A. Wilson, R. E. Hyatt, and J. R. Rodarte, "A Computational Model for Expiratory Flow," J. Appl. Physiol.: Respirat. Environ. Exercise Physiol. 52:44-56, 1982.

14. Stanescu, D. C., J. Pattijn, J. Clement, and K. P. Van de Woestijne, "Glottis Opening and Airway Resistance," J. Appl. Physiol. 32:460-466, 1972.

15. Lisboa, C., L. D. H. Wood, J. Jardim, and P. T. Macklem, "Relationship Between Flow, Curvilinearity, and Density Dependence of Pulmonary Pressure-Flow Curves," J. Appl. Physiol.: Respirat. Environ. Exercise Physiol. 48:878-885, 1980.

16. Slutsky, A. S., J. M. Drazen, C. F. O'Cain, and R. H. Ingram, Jr., "Alveolar Pressure-Airflow Characteristics in Humans Breathing Air, He-O_2, and SF_6-O_2," J. Appl. Physiol.: Respirat. Environ. Exercise Physiol. 51:1033-1037, 1981.

17. Isabey, D. and H. K. Chang, "Steady and Unsteady Pressure-Flow Relationships in Central Airways," J. Appl. Physiol.: Respirat. Environ. Exercise Physiol. 51:1338-1348, 1981.

18. Hardy, H. H., R. E. Collins, and R. E. Calvert, "A Digital Computer Model of the Human Circulatory System," Med. Biol. Eng. Comput. 20:550-564, 1982.

19. Collins, R. E., R. E. Calvert, D. Martin, and L. Carmack, "Mathematical Simulation of the Cardiopulmonary System," Progress Report, AFOSR 79-0123, November 1980.

20. Fung, Y. C., Biomechanics: Mechanical Properties of Biological Materials, New York, Springer-Verlag, 1981.

1984 USAF-SCEEE SUMMER FACULTY RESEARCH PROGRAM

Sponsored by the

AIR FORCE OFFICE OF SCIENTIFIC RESEARCH

Conducted by the

SOUTHEASTERN CENTER FOR ELECTRICAL ENGINEERING EDUCATION

FINAL REPORT

MODELING OF NONLINEAR SEAT CUSHIONS

Prepared by: Dr Joseph E. Saliba

Academic Rank: Assistant Professor

Department and   Department of Civil Engineering
University: University of Dayton

Research Location: Aerospace Medical Research Laboratory
Biodynamics & Bioengineering Division
Biomechanical Protection Branch

USAF Research: Mr James W. Brinkley

Date: 10 July 1984

Contract No.:   F49620-82-0035

NONLINEAR MODELING OF

SEAT CUSHIONS

by

Joseph E. Saliba

ABSTRACT

A brief review of the history of seat cushions, modeling and
analysis, in addition to a qualitative description of their influence
on occupants during ejection or impact is first presented. Next, two
nonlinear modeling approaches are described. The first is based on
the mathematical theory of nonlinear viscoelasticity where the consti-
tutive equations, relating stresses and strains, are written as a
hereditary integral. This theory makes use of expressing the stress
by a polynomial expansion in linear functionals of strain history. A
minimum of two different levels of stress are needed in single-step
creep tests to determine the mechanical properties of the nonlinear
material. The second approach is based on the step-by-step integra-
tion method where the nonlinear behavior is approximated by a sequence
of successively changing linear systems. The damping and stiffness
properties are based on the current deformed state at the beginning of
each time increment and hold constant during that increment. These
mechanical properties are computed from the damping force versus
velocity and the stiffness versus displacement curves. Finally, the
seated man model, in series with the seat cushion model, is recom-
mended for investigating qualitatively the influence of the seat
cushions on spinal injuries during ejection.

ACKNOWLEDGEMENTS

I. INTRODUCTION

As inflight refueling is becoming a routine operation, the aircraft mission durations are on a constant increase, making comfort very critical for aircrew effectiveness. This is changing the criterion upon which seat cushions are being designed. In addition to this, the ever-increasing need of faster aircraft with higher performance capabilities leads more to the likelihood of escape during supersonic flight and a higher probability of escape during violent aircraft motions.[1] This is increasing the difficulties of ejecting crew members fast enough to clear the vertical fin at high dynamic pressure and to reach a safe height from low-altitude escapes. Therefore, there is understandable pressure and a need to increase the impulse of rocket/ catapult accelerators to levels never perceived before. This urge to increase the impulse and the need to also increase the seat cushion thickness for comfort is escalating the likelihood of vertebral injury due to the possible magnification of the acceleration forces acting on the occupant of the seat during ejection or impact.

During a seat ejection a large headward force is suddenly applied to the aircraft seat. This force is then transferred through the seat cushion to the seat occupant. The mechanical properties of the seat cushion, such as stiffness, damping and thickness can influence the magnitude and duration of this transferred force. The most desirable seat cushion is the one that can act as an efficient shock absorber, thus decreasing the force acting on the seat occupant. This ideal situation can be accomplished by transmitting gradually the force from the seat to the occupant while the cushion is being deformed slowly, thus causing the occupant's acceleration to be smaller or lower than the seat, but over a longer time period so that final velocities of both the seat and occupant are the same.[2] With a thick cushion of low damping resistance, the force acting on the seat consumes an appreciable time interval, compressing the cushion and with very small force

being transferred during that time. Thus, for a short time the occupant is lagging in movement behind the seat which is picking up velocity. After bottoming occurs, the occupant is impacted by the seat, and the occupant, for an instant, is accelerated more rapidly than the seat. The relative lag in the movement of the occupant, relative to the seat, causes surplus kinetic energy to be stored by the seat. Later, during the ejection (during the bottoming) this excess kinetic energy is shared between the occupant mass and the mass of the seat. This excess kinetic energy can produce an overshoot of acceleration acting on the occupant body. This problem can be solved by using a high damping material in addition to decreasing the cushion thickness such that under normal weight it is almost fully compressed, thus significantly lowering the kinetic energy stored during the movement lag, which in turn reduces the potential of overshoot of acceleration.

Latham[3] and Bondurant[4] were the first to investigate the effect of cushions on ejection seat performance. Hodgson et al[5] conducted cadaver tests investigating the increased spinal loads due to cushions in comparison to non-cushion conditions. Then based on a study by Whittenberg[6], urethane foams were found to be acceptable as seat cushion materials. Similar studies by Glaister[7] resulted in recommending polyurethane foam as a desirable material. After the development of lumped parameter dynamic models independently by von Gierke, Kornhauser[8] and Payne,[9] additional work on the analysis of seat cushion dynamics was performed by Payne[10] showing analytically rough estimates of the effect of the seat cushion on the response of the human body to acceleration input.

In describing natural phenomena, one can represent the physical laws that are applicable in terms of rather complex equations. To reduce the complexity of the equations, certain assumptions more or less consistent with the physical situation can be made. The seemingly most popular assumption is that of linearization of the physical phenomena

which in turn leads to simpler equations for the idealized problem. This idealization is in many instances inadequate to describe or predict the behavior of physical systems. In fact, nonlinear analysis usually leads to new phenomena that cannot be predicted by the linear theory. On the other hand, many observed phenomena are unexplainable or unjustifiable except by considering the nonlinearities present in the system.

Unfortunately, this linearization process has almost always been assumed in describing the behavior of seat cushions.[11]   In 1968 Shaffer,[12] using analog computer and the nonlinear experimental cushion force-deflection curves in conjunction with the spinal man-model, analyzed the effect of cushions on the dynamic response index. A year later, Payne[13] tried a similar model and tried to correlate his results with those of Shaffer. Both investigators realized the need for more sophisticated study in which a lower "pelvic mass" is included in the model of the man. Thus, we can see the need to explore with more depth and better experiments the optimum nonlinear constitutive equations that best describe the nonlinear behavior of seat cushions.

II. OBJECTIVES

The main objective of this study is to develop a systematic procedure or method to explore the formulation of the governing equations that best describe the nonlinear behavior of seat cushions. In summary, the main objectives are:

A. To find the best possible constitutive stress-strain equation that best predicts the behavior of seat cushion under impact loads.

B. To investigate experimental means of determining the mechanical properties which enter the constitutive relations of nonlinear viscoelasticity theory.

A secondary objective of this study is to determine the feasibility
and the degree of difficulty introduced in determining the material
properties of the seat cushions from the single-level creep or stress-
relaxation tests.

III. NONLINEAR VISCOELASTICITY

The nonlinear viscoelastic theory similar to the linear one is based
on the memory hypothesis. This simply means that the current value of
stress or strain is determined by the complete past history of strain
or stress, respectively. The development of the nonlinear
viscoelastic theories follows in many aspects the lines suggested by
the well-established theories of nonlinear elasticity. Because of the
memory for past events and many other complications, the application
of the viscoelastic theories has not achieved the popularity that
nonlinear elasticity has attained.

A good review of the development of the nonlinear theory of visco-
elasticity up to 1952 was given by Truesdell[14]. Between 1952 and
1959, Green and Rivlin[15] and later Green, Rivlin and Spencer[16]
developed an isothermal theory of viscoelasticity based on the
approximation of stress or load functional by an expansion of poly-
nomial in terms of linear functionals. The Green and Rivlin theory
is primarily based on the Rivlin and Ericksen[17] one which states that
the component of stress at time t depends only on the gradients of
displacement such as velocity, acceleration, second acceleration up to
$(n-1)^{th}$ acceleration at time t. The Green and Rivlin theory states
that stress at time t depends on the displacement gradients at time t
and at N previous instants of time in the interval 0 to t. In 1964
Coleman[18] developed his general thermodynamic theory for material with
memory based on the fading-memory principle developed by Coleman and
Noll.[19] The most recent proposed theory is that of Laws[20] which is
an alternative thermodynamic theory that could have many applications
in fluid-type problems.

IV. DERIVATION OF CONSTITUTIVE RELATIONS FOR SOLIDS

Calling X_k the coordinates of a typical particle in the reference configuration with reference to fixed rectangular Cartesian axes. If we define x_i the deformed configuration coordinates of the same particle at any time and refer to the same fixed axes as those used for X_k, then the entire deformation history can be written as

$$x_i(\tau) = x_i(X_K, \tau) \tag{1}$$

The deformation gradient can then be written as the partial derivatives with respect to reference coordinates

$$x_{i,L}(X_K, \tau) = \frac{\partial x_i(X_K, \tau)}{\partial X_L} \tag{2}$$

As stated previously, the theory of "simple materials" is founded upon the condition that the current value of the field variables depends upon the past history of the deformation gradient. Thus, the constitutive relation can be written as

$$\sigma_{ij} = \overset{\infty}{\underset{s=0}{X_{ij}}} \left[x_{j,L}(X_K, t-s), \; x_{j,L}(X_K, t) \right] \tag{3}$$

where X_{ij} is a functional that does not vary or change with respect to time and which satisfies time translation invariance. Such restrictions automatically exclude yielding behavior due to the changes of the constitutive relations before and after yielding occurs. The theory of simple material described below is due to Noll[21], and some of its applications shall be made to solids where the reference axes are those of the undeformed configuration. Defining the strain as

$$2E_{KL}(X_K, \tau) = x_{k,K} \cdot x_{k,L} - \delta_{KL} \tag{4}$$

where δ_{kl} is the Kronecker symbol. Note that in (4) the lower indices designate tensor components with respect to the deformed configuration coordinates while upper case indices designate tensor components with respect to the reference configuration coordinates. Thus, E_{kl} represents the strain with respect to the undeformed configuration.

Combining the local entropy production inequality with the local energy balance yields the following inequality

$$-\rho \dot{A} + \sigma_{ij}d_{ij} \geqslant 0 \tag{5}$$

where ρ is the mass density, A the specific stored energy (per unit mass), σ_{ij} the Cauchy stress tensor defined with respect to the deformed configuration, and d_{ij} is expressed in terms of the velocity gradient as

$$2d_{ij} = v_{i,j} + v_{j,i} \tag{6}$$

where

$$v_i(\cdot) = \dot{x}_i(\tau, X_K) \quad \text{or} \quad v_i = v_i(t) \tag{7}$$

The superimposed dot designates partial differentiation with respect to time. Based on the memory hypothesis, the stored energy can be rewritten as a functional of the past history of the deformation

$$A = \mathop{\overset{\infty}{\underset{s=0}{\Psi}}}(E_{KL}(t-s), E_{KL}(t)) \tag{8}$$

where the dependence of the strain upon the X_k coordinates is implied. No discontinuity of the functional with respect to strain is allowed.

To differentiate (8) with respect to time, first we define

$$\| E \| = \left[\int_0^\infty E_{KL}(t-s)E_{KL}(t-s)h^2(s)\,ds \right]^{\frac{1}{2}} \tag{9}$$

where h(s) is a monotonically decreasing function called an influence function of order r such that

$$\lim_{s \to \infty} s^r h(s) = 0 \tag{10}$$

This collection of histories with a finite norm forms a Hilbert space. Also note that the energy functional $\overset{\infty}{\underset{s=0}{\Psi}}(\ )$ is taken to be a Frechet differentiable in that Hilbert space thus

$$\overset{\infty}{\underset{s=0}{\Psi}}(E_{KL}(t-s) + \delta E_{KL}, E_{KL}(t)) = \overset{\infty}{\underset{s=0}{\Psi}}(E_{KL}(t-s), E_{KL}(t))$$
$$+ \overset{\infty}{\underset{s=0}{\delta\Psi}}(E_{KL}(t+s), E_{KL}(t)/\delta E_{KL}(t-s) \tag{11}$$
$$+ 0\|\delta E_{KL}(t-s)\|$$

where $\overset{\infty}{\underset{s=0}{\delta\Psi}}(\ )$ is the first order Frechet differential which is linear in $\delta E_{kl}(t-s)$, and continuous in all variables. This functional expansion is similar to a Taylor series expansion for functions. Using the Frechet differential in (8) which can then be substituted into (5) yields

$$\sigma_{ij}d_{ij} - \rho\frac{\partial}{\partial E_{KL}(t)}\overset{\infty}{\underset{s=0}{\Psi}}(E_{KL}(t-s), E_{KL}(t)\dot{E}_{KL} + \rho\overset{\infty}{\underset{s=0}{\Lambda}}(\ ) \geqslant 0 \tag{12}$$

where

$$\overset{\infty}{\underset{s=0}{\Lambda}}(\ ) = \overset{\infty}{\underset{s=0}{\delta\Psi}}(E_{KL}(t-s), E_{KL}(t)\frac{dE_{KL}(t-s)}{dt}) \tag{13}$$

substituting for $\dot{E}_{kl} = d_{ij}x_{i,L}$ in (12) we then get:

$$\left[\sigma_{ij} - \rho\frac{\partial}{\partial E_{KL}(t)}\overset{\infty}{\underset{s=0}{\Psi}}(E_{KL}(t-s), E_{KL}(t))x_{i,K}x_{j,L}\right]d_{ij} + \rho\overset{\infty}{\underset{s=0}{\Lambda}}(\ ) \geqslant 0 \tag{14}$$

For (14) to vanish for a given deformation history implies that

$$\sigma_{ij} = \rho\frac{\partial}{\partial E_{KL}(t)}\overset{\infty}{\underset{s=0}{\Psi}}(E_{KL}(t-s), E_{KL}(t)) x_{i,K}x_{j,L} \tag{15}$$

and

$$\rho\overset{\infty}{\underset{s=0}{\Lambda}}(\ ) \geqslant 0 \tag{16}$$

which implies that the rate of dissipation of energy must be positive or zero. Thus, the constitutive relation written in a more symbolic form is

$$\sigma_{ij} = \rho \frac{\partial A}{\partial E_{KL}} x_{i,K} x_{j,L} \tag{17}$$

If the material is isotropic, some simplification can then be made in rewriting the stored energy as a functional of invariants of the history of the strain function.

Let us now represent the stored energy A by using the approximation theorem outlined below and which was first suggested by Chacon and Rivlin.[22] Based on the Stone-Weierstrass theorem, let $f_{(i)}$ designate the linear functionals

$$f_{(i)} = \mathop{T}_{s=0}^{\infty}(i) \ (E_{KL}(t-s), E_{KL}(t)) \qquad i = 1, 2, \dots, N \tag{18}$$

Thus the stored energy functional can be approximated by the expansion

$$A = \sum_{i=1}^{N} f_{(i)} + \sum_{i=1}^{N} \sum_{j=1}^{N} f_{(i)} f_{(j)} + \dots \tag{19}$$

where the polynomial expansion is truncated at the level involving N products. Using the Riesz representation, the linear functionals can be represented as a Steiltjes integral such as:

$$f_{(i)} = \int_0^{\infty} E_{KL}(t-s) \, dg_{KL}^{(i)}(s) \, ds \tag{20}$$

where

$$g^{(i)}(\tau) = 0 \qquad \tau < 0 \tag{21}$$

and where $g^{(i)}(\tau)$ and their first derivatives are assumed to be continuous for $\tau > 0$. Integrating by parts equation (20) we then get

$$f_{(i)} = \int_{-\infty}^{t} g_{KL}^{(i)}(t-\tau) \frac{\partial E_{KL}(\tau)}{\partial \tau} d\tau \tag{22}$$

Inserting (22) into (19) we then get:

$$A = \int_{-\infty}^{t} g_{KL}(t-\tau_1) \frac{\partial E_{KL}(\tau)}{\partial \tau} d\tau \tag{23}$$

$$+ \int_{-\infty}^{t}\int_{-\infty}^{t} g_{KLMN}(t-\tau_1, t-\tau_2) \frac{\partial E_{KL}(\tau_1)}{\partial \tau_1} \frac{\partial E_{MN}(\tau_2)}{\partial \tau_2} d\tau_1 d\tau_2 + \ldots$$

where the functions $g_{KL}(\tau)$, $g_{KLMN}(\tau_1,\tau_2)$ etc. are determined to model the behavior of the material and must not contradict the fading memory hypothesis. For isotropic material, symmetry requirements must be achieved and the stored energy functional is written as

$$A = \int_{-\infty}^{t} g(t-\tau) \frac{\partial E_{KK}(\tau)}{\partial \tau} d\tau + \int_{-\infty}^{t}\int_{-\infty}^{t} \gamma(t-\tau_1,t-\tau_2) \frac{\partial E_{KK}(\tau_1)}{\partial \tau_1} \frac{\partial E_{LL}}{\partial \tau_2} d\tau_1 d\tau_2 \tag{24}$$

$$+ \int_{-\infty}^{t}\int_{-\infty}^{t} \Delta(t-\tau_1,t-\tau_2) \frac{\partial E_{KL}(\tau_1)}{\partial \tau_1} \frac{\partial E_{KL}(\tau_2)}{\partial \tau_2} d\tau_1 d\tau_2 + \ldots$$

V. DETERMINATION OF MECHANICAL PROPERTIES FOR NONLINEAR MATERIAL

The Green-Rivlin theory, which is very similar to the one prescribed in the previous section, is the most popular theory so far to be used in determining the mechanical properties of nonlinear material with memory. This theory makes use of expressing the stress by a polynomial expansion in linear functionals of strain history. Most of the mechanical properties which have been determined are of the one-dimensional specialization of the theory.

In 1965 Lockett[23] suggested a rather involved series of experiments of the creep or stress relaxation type which can characterize the mechanical properties of simple materials. These tests involved a number of steps performed sequentially with complex combinations of variable input amplitudes and time of initiation. Neis and Sackman[24] proposed an optimization procedure to which a good agreement can be shown in predicting the response to constant stress rate inputs. The most recent approach was proposed by Gottenberg et al[25] which renders the procedure of determining material properties for nonlinear material similar to that propsed by the linear theory of viscoelasticity.

The popular one-dimensional constitutive equation obtained from the Green-Rivlin theory, and which can also be obtained from the previous section, has the form

$$\sigma(t) = \int_{-\infty}^{t} G_1(t-\tau) \frac{dE(\tau)}{d\tau} d\tau + \int_{-\infty}^{t}\int_{-\infty}^{t}\int_{-\infty}^{t} G_3(t-\tau_1, t-\tau_2, t-\tau_3) \qquad (25)$$

$$\times \quad \frac{dE(\tau_1)}{d\tau_1} \frac{dE(\tau_2)}{d\tau_2} \frac{dE(\tau_3)}{d\tau_3} d\tau_1 d\tau_2 d\tau_3 + \cdots$$

The absence of even-ordered terms in the above equation is due to the absence of odd-ordered terms in writing the stored energy form to satisfy its non-negative condition. To obtain the creep integral, the same expansion procedure that leads to (25) can be used with the stress and strain interchanged.

$$E(t) = \int_{-\infty}^{t} J_1(t-\tau) \frac{d\sigma(\tau)}{d\tau} d\tau + \int_{-\infty}^{t}\int_{-\infty}^{t}\int_{-\infty}^{t} J_3(t-\tau_1, t-\tau_2, t-\tau_3) \frac{d\sigma(\tau_1)}{d\tau_1} \frac{d\sigma(\tau_2)}{d\tau_2} \frac{d\sigma(\tau_3)}{d\tau_3}$$

$$\times \quad d\tau_1 d\tau_2 d\tau_3 + \cdots \qquad (26)$$

with $J_i(\ )$ being the creep-type properties which characterize the material. The reasons creep tests are favored over stress relaxation ones is due to many experimental difficulties encountered in a relaxation test. A typical example is the stress relaxation function of a Newtonian fluid which is indeed a Dirac function which could not be measured. In fact, if the material has special dependencies on the current time derivatives of the strain, then the stress relaxation experiments are not suitable for determining the mechanical behavior of those materials.

If single-step creep tests are to be used, then equation (26) reduces to

$$E(t) = J_1(t)\sigma_0 + J_3(t,t,t,)\sigma_0^3 \qquad (27)$$

where

$$\sigma(t) = 0 \qquad \text{for } t < 0$$
$$\sigma(t) = \sigma_0 \qquad \text{for } t \geqslant 0$$

A minimum of two different levels of stress are needed in single-step creep tests to determine the functions $J_1(t)$ and $J_3(t,t,t)$.

Because two terms are kept in the constitutive relation, test data can be fit exactly only at two separate levels of stress, thus limiting the degree of nonlinearity which can be treated if only two terms of the expansion are considered. Theoretically, many levels of stress can be considered by increasing the number of terms in the expansion. But the process becomes very cumbersome and complex, thus unpractical if not impossible to use.

VI. THE STEP-BY-STEP INTEGRATION APPROACH

A step-by-step integration approach is next attempted to analyze this problem. Using this procedure, the response is determined for a series of short time increments. By estabishing dynamic equilibrium at the beginning and end of each interval, and by assuming a response mechanism, the motion is then determined during that interval. To account for the nonlinear nature of the seat cushion, new properties are computed based on the current deformed state at the beginning of each time increment. Thus, the displacement and velocities computed at the end of one interval are used as the initial conditions for the next computational interval. This procedure is then continued step-by-step approximating the nonlinear behavior by a sequence of successively changing linear systems.

Due to equilibrium the forces acting on the the seat cushion mass at any instant of time t require that:

$$F_I(t) + F_D(t) + F_S(t) = P(t) \tag{28}$$

where F_I, F_D, F_S, and P are the inertia, damping, stiffness and the external forces respectively. A short time later the equation would be:

$$F_I(t + \Delta t) + F_D(t + \Delta t) + F_S(t + \Delta t) = P(t + \Delta t) \tag{29}$$

121-14

Subtracting (29) from (28) and rewriting it in incremental form we get:

$$\Delta F_I(t) + \Delta F_D(t) + \Delta F_S(t) = \Delta P(t) \tag{30}$$

where
$$\begin{aligned}
\Delta F_I(t) &= F_I(t + \Delta t) - F_I(t) \\
\Delta F_D(t) &= F_D(t + \Delta t) - F_D(t) \\
\Delta F_S(t) &= F_S(t + \Delta t) - F_S(t) \\
\Delta P(t) &= P(t + \Delta t) - P(t)
\end{aligned} \tag{31}$$

Expressing the incremental forces in this form

$$\begin{aligned}
\Delta F_I(t) &= m \ddot{U}(t) \\
\Delta F_D(t) &= C(t) \Delta \dot{U}(t) \\
\Delta F_S(t) &= k(t)\Delta U(t)
\end{aligned} \tag{32}$$

where m, C(t) and k(t) represent the mass, damping and stiffness properties during that time invertal. The damping properties can be obtained from the slope of the damping force versus velocity curve while the stiffness from the stiffness force versus the displacement graph. Thus

$$C(t) \approx \left[\frac{dF_D}{dU}\right]_t \qquad\qquad k(t) \approx \left[\frac{dF_S}{dU}\right]_t \tag{33}$$

Any kind or form of nonlinearity can be included in this type of analysis. Thus, nonlinear hysteretic material in which the force depends on the past history of deformation as well as the current values can be analyzed by this approach.

$$m\ddot{U}(t) + C(t)\Delta\dot{U}(t) + k(t)\Delta U(t) = \Delta P(t) \tag{34}$$

To numerically integrate equation (34) we shall assume that the acceleration varies linearly during each time increment while the

properties of the system remain constant during the interval. Thus, we can write

$$\ddot{U}(\tau) = \Delta\ddot{U}(t) + \frac{\Delta\ddot{U}}{\Delta t}\tau \qquad (35)$$

where τ is the time variable between time t and $t + \Delta t$ and $\Delta\ddot{U}$ is the change in acceleration during that same time interval. Integrating, we then can write the velocity and displacement as follows:

$$\dot{U}(\tau) = \dot{U}(t) + \ddot{U}(t)\tau + \frac{\Delta\ddot{U}}{\Delta t}\frac{\tau^2}{2} \qquad (36)$$

$$U(\tau) = U(t) + \dot{U}(t)\tau + \ddot{U}(t)\frac{\tau^2}{2} + \frac{\Delta\ddot{U}}{\Delta t}\frac{\tau^3}{6} \qquad (37)$$

Using the above equations, the incremental velocity and acceleration can then be expressed as function of the incremental displacement substituting these incremental velocity and acceleration into (34) yields the following equation

$$K(t) \Delta U(t) = \Delta P_T(t) \qquad (38)$$

where

$$K(t) = k(t) + \frac{6}{\Delta t^2}m + \frac{3}{\Delta t}C(t) \qquad (39)$$

$$\Delta P_T(t) = \Delta P(t) + m\left[\frac{6}{\Delta t}\dot{U}(t) + 3\ddot{U}(t)\right] + c(t)\left[3\dot{U}(t) + \frac{\Delta t}{2}\ddot{U}(t)\right] \qquad (40)$$

Due to many approximations, error will arise in the incremental-equilibrium relationship which might tend to accumulate from step to step. To avoid this, the accelerations can be computed by imposing the total equilibrium condition at the beginning of each step of the analysis.

For any given time increment, the analysis will consist of the following operations:

1. Initial velocity and displacement values are known (either from values at the end of the preceding increment or as initial conditions of the problem).

2. The nonlinear properties $C(t)$ and $k(t)$ as well as $F_D(t)$ and $F_S(t)$ forces are computed based on the current values of U and $\dot{U}$.

3. The initial acceleration is then computed as

$$\ddot{U}(t) = \frac{1}{m}\left[P(t) - F_D(t) - F_S(t)\right]$$

4. $\Delta P_T(t)$ and $K(t)$ are computed from (40) and (39).

5. The displacement increment is computed from (38).

6. The velocity increment is computed from

$$\Delta\dot{U}(t) = \frac{3}{\Delta t}\,\Delta U(t) + 3\dot{U}(t) - \frac{\Delta t\ddot{U}(t)}{2}$$

7. Finally, the velocity and displacement at the end of the increment are obtained from

$$\dot{U}(t + \Delta t) = \dot{U}(t) + \Delta\dot{U}(t)$$
$$U(t + \Delta t) = U(t) + \Delta U(t)$$

when the last step has been completed, the entire process may be repeated for the next time interval until the analysis is finished.

The damping force versus velocity curve can be obtained by the initial slope of the creep test for different stress levels or, if

instrumentation is available from vibrational tests, by adjusting the input frequency until the response is 90 degrees out of phase with the applied loading. Then the applied load is exactly balanced by the damping force, which can then be plotted versus the velocity for one loading cycle. The stiffness force versus the displacement graph can also be plotted from the steady-state solution of the creep tests or from vibration by simply vibrating the system very slowly at essentially static conditions.

VII. RECOMMENDATIONS

Now that we can model and analyze nonlinear seat cushions theoretically, the next logical step is to verify it experimentally. A test plan should be proposed and implemented to accomplish this objective. This test plan should verify the feasibility of the experimental means of determining the mechanical properties which enter into the constitutive relations. This test plan should be designed to verify the degree of confidence and the accuracy of predicting responses using these constitutive equations. Once the theoretical constititutive relations are verified, the seated man model should be interphased with the cushion mode. With this combined model the conditions of actual experiments can be reproduced, and the theoretical and experimental results can be compared for these low amplitude impact forces. Once we are able to match the existing data, the combined model can be subjected to much larger impulsive forces and the response can be predicted theoretically. Thus, we can then investigate the influence of the seat cushion on the spinal injuries of the seat occupant without actualy subjecting him to these large impulsive forces. This combined model can also be used as a design tool to determine the optimum thickness, for example, for a given seat cushion.

REFERENCES

1. James W. Brinkley, "Personnel Protection Concepts for Advanced Escape System Design," Wright-Patterson Air Force Base, Ohio, 1984.

2. Stuart Bondurant, "Optimal Elastic Characteristics of Ejection Seat Cushions for Safety and Comfort," WADC Technical Note 58-260, Wright Air Development Center, Wright-Patterson Air Force Base, Ohio, 1958; AD 203 384.

3. F. Latham, "A Study in Body Ballistics," Proceedings of the Royal Society B, Vol 147, pp. 121-139.

4. Stuart Bondurant, "Optimal Elastic Characteristics of Ejection Seat Cushion for Safety and Comfort, " WADC Technical Note 58-260, Wright Air Development Center, Wright-Patterson Air Force Base, Ohio; 1958, AD 203 384.

5. V. R. Hodgson, H. R. Lissner, and L. M. Patrick, "Response of the Seated Human Cadaver to Acceleration and Jerk With and Without Seat Cushions," Human Factors, Vol 5, pp 505-523; October 1963.

6. R. K. Whittenberg, "Improved Seat and Back Cushions," WADC TR 59-376, Aerospace Medical Laboratory, Wright-Patterson Air Force Base, Ohio; 1959.

7. D. H. Glaister, "Properties of Polyurethane Foams in Relation to Their Use as Ejection Seat Cushion Materials," Flying Personnel Research Committee, Report 1184, Air Ministry, 1961.

8. M. Kornhauser and A. Gold, "Application of the Impact Sensitivity Method of Animate Structures," presented at National Academy of Sciences Symposium on Impact Acceleration Stress, Brooks Air Force Base, San Antonio, Texas, November 1961.

9. P. R. Payne, "An Analog Computer Which Determines Human Tolerance to Acceleration," presented at National Academy of Sciences Symposium on Impact Acceleration Stress, Brooks Air Force Base, San Antonio, Texas November 1961.

10. Peter R. Payne, "A General Cushion Theory," Working Paper No. 149-2, Revision A, June 1968, Payne Division, Wyle Laboratories, Rockville, Maryland.

11. F. Latham, "A Study in Body Ballistics," Proceedings of the Royal Society B., Vol 147, pp 121-139.

12. D. A. Sha...er, "Analog Results of Acceleration Inputs to a Simple Man Model in Series with 19 Different Cushion Models," Working Paper 149-4, May 1968, Payne Division, Wyle Laboratories.

13. Peter R. Payne, "Injury Potential of Ejection Seat Cushions," _J. Aircraft_, Vol 6, No. 3, pp 273-278, May-June 1969.

14. C. Truesdell, "Corrections and Additions to the Mechanical Foundations of Elasticity and Fluid Dynamics," _J. Rat. Mech. Anal._ 2, 593-616, 1953.

15. A. E. Green and R. S. Rivlin, "The Mechanics of Nonlinear Materials with Memory, Part I," _Arch. Rat. Mech. Anal._ Vol 1, pp 1-21, 1958.

16. A. E. Green, R. S. Rivlin, and A. J. M. Spencer, "The Mechanics of Non-Linear Materials with Memory, Part II," _Arch. Rat. Mech. Anal._, Vol 3, pp 82-90, 1959.

17. R. S. Rivlin and J. L. Ericksen, "Stress-Deformation Relations for Isotropic Materials," _J. Rat. Mech. Anal._, Vol 4, pp 323-425, 1955.

18. B. D. Coleman, "On Thermodynamics, Strain Impulses, and Visco-elasticity," _Arch. Rat. Mech. Anal._, Vol 17, 230, 1964.

19. B. D. Coleman and W. Noll, "An Approximation Theorem for Functionals with Applications in Continuum Mechanics," _Arch. Rat. Mech. Anal._, Vol 6, pp 355-370, 1960.

20. N. Laws, "On the Thermodynamics of Certain Materials With Memory," _Int. J. Eng. Sci._, Vol 5, pp 427-434, 1967.

21. W. Noll, "A Mathematical Theory of the Mechanical Behavior of Continuous Media," _Arch. Rat. Mech. Anal._ Vol 2, 197 (1958).

22. R. V. S. Chacon and R. S. Rivlin, "Representation Theorems in the Mechanics of Materials with Memory," _Z. Angew. Math. Phys._ Vol 15, 444, 1964.

23. F. J. Lockett, "Creep and Stress-Relaxation Experiments for Nonlinear Materials," _Int. J. Eng. Sci._, Vol 3, p. 59, 1965.

24. V. V. Neis and J. L. Sackman, "An Experimental Study of a 27 Nonlinear Material with Memory," _Trans. Soc. of Rheo._, Vol 11, p. 307, 1967.

25. W. G. Gottenberg, J. O. Bird, and G. L. Agrawal, "An Experimental Study of a Nonlinear Viscoelastic Solid in Uniaxial Tension," _J. Appl. Mech._, 36, 558, 1969.

1984 USAF-SCEEE SUMMER FACULTY RESEARCH PROGRAM

Sponsored by the

AIR FORCE OFFICE OF SCIENTIFIC RESEARCH

Conducted by the

SOUTHEASTERN CENTER FOR ELECTRICAL ENGINEERING EDUCATION

FINAL REPORT

THE RELATIONSHIP OF FIBRINOGEN AND PLASMA LIPIDS TO
BUBBLE FORMATION AT THE AIR INTERFACE DURING DECOMPRESSION SICKNESS

Prepared by: Walter L. Salters, Ph.D.

Academic Rank: Associate Professor of Biology

Department and   Natural Sciences Department
University: South Carolina State College

Research Location: Clinical Pathology Branch
                       Clinical Sciences Division
                       United States Air Force School of Aerospace
                         Medicine
                       Brooks Air Force Base, Texas   78235

USAF Research   Christopher E. Jones, Captain, USAF, BSC
Colleague: Chief, Clinical Pathology Laboratory Function

Date: August   1984

Contract No: F49620-82-0035

THE RELATIONSHIP OF FIBRINOGEN AND PLASMA LIPIDS TO

BUBBLE FORMATION AT THE AIR INTERFACE DURING DECOMPRESSION SICKNESS

by

Walter L. Salters, Ph.D.

ABSTRACT

Fibrinogen and plasma lipids have been implicated as being etiolog-ically significant in decompression sickness (DCS) during blood-bubble formation at the air-surface interface. When fibrinogen is deposited on the bubble's surface, it becomes possible for the adhesion and aggregation of intravascular lipids and other blood components (i.e., platelets) at its surface. Determination of the concentration of these serological constituents in plasma and serum from experimental subjects before and after hypobaric flights in the altitude chamber will perhaps make it possible to assess their role in DCS. This study reveals that, through quantitative determination of plasma concentrations of cholesterol, high-density lipoprotein-associated cholesterol, triglycerides and fibrinogen, it may eventually become possible to determine subjects who are less prone to experience DCS during simulated compression/decompression exercises, and to better understand some of the hazardous effects of experimental aviation studies on flight personnel.

Acknowledgement

The author would like to thank the United States Air Force School of Aerospace Medicine, the Air Force Office of Scientific Research, and the Southeastern Center for Electrical Engineering Education for the privilege of spending a very educationally rewarding and worthwhile summer with the Clinical Pathology Laboratory Function (NGPC), Brooks AFB, Texas. He would also like to acknowledge the staff of the Clinical Pathology Branch for their excellent hospitality and for making the laboratory working environment a most pleasant one.

Finally, he would like to thank Captain Christopher E. Jones, Ph.D., USAF, BSC, Chief of the Clinical Laboratory Function, for his sponsorship, helpful suggestions and guidance during the course of this study.

I. INTRODUCTION

Decompression sickness (DCS) has variously been referred to throughout its history as the bends, caisson's disease (in tunnel workers), compressed air illness, and dysbarism. In reality, it is a syndrome which results when people are subjected to an overly abrupt and extensive reduction in environmental barometric pressure. As the various names imply, it has been encountered not only by deep-sea divers, but also by high-altitude aviators and men employed in underground engineering projects in which compressed air is used to hold back ground water. It also constitutes a potential hazard for astronauts and even for commercial air passengers should an accidental rapid loss of cabin pressure occur. The condition appears to be the result of the formation of bubbles of inert gas (chiefly nitrogen, when air is the breathing gas) in fluids and tissues of the body. Inert gases like nitrogen are dissolved in body tissues and fluids and, with sufficient time, reach a state of concentration equilibrium with the environment. If the reduction in barometric pressure exceeds the rate at which dissolved nitrogen can diffuse across the various membrane barriers of the body and be eliminated in the expired air, a state of supersaturation occurs and bubbles may form (1). The advent of the Doppler ultrasonic probe appears to have yielded convincing evidence that intravascular bubbles are associated with decompression and DCS, even in the absence of overt signs of the bends (2).

In DCS, the symptoms and signs are varied, ranging in severity from skin rash and joint pain to central nervous system disturbances, respiratory difficulties, paralysis, and acute circulatory shock, depending upon the extent and location of the offending bubbles. Treatment classically has revolved around the principle of recompression of the victim with a view of driving the bubbles back into solution, with moderate, controlled decompression to allow the harmless diffusion and elimination of inert gas.

Warren et al. (3) developed a method for in situ fixation of
tissues which permitted the examination of blood and bubbles by electron
microscopy. Using explosively decompressed rats with massive intravas-
cular bubble formation, it was shown that bubbles acquired a coating
approximately 200 Å in thickness, which appeared to consist primarily
of fibrinogen. Lipid micelles also became entrapped at the air-blood
interface, and platelets appeared to be selectively attracted to the
interface, with platelet adhesion progressing to platelet aggregation.
Jacobs and Stewart (4) may have been the first to observe the effects
of bubble formation and platelet aggregation. Upon severing the tips
of the tails of decompressed rats, they saw bloody froths issuing from
the vessels, and upon microscopic examination, found that the bubbles
were surrounded by platelet aggregates. They speculated that such
aggregates might occlude fine blood vessels, resulting in microemboli.

Based upon these observations, it would appear that compression-
decompression may be associated with the development of a hypercoaguable
state at the air-liquid interface during bubble formation. Evidence
suggest that this phenomenon may be detected in the absence of overt
signs of DCS. Using various models of decompression sickness, several
investigators have detected evidence of increased clotting activity,
including clotting factors (5). Philip et al. (6) used a rat decom-
pression model that produced a wide spectrum of severity of signs of
DCS and found a strong association between the severity of DCS and the
degree of disturbance in the clotting times in dogs and rabbits before
and during decompression from 6-11 ATA. Accelerated clotting was found
in 12 animals, but in four animals that showed signs of DCS, the
clotting time was prolonged. Many early experiments suggested that
the hypobaric environment itself might set the stage for hyperactivity
of the clotting system which is triggered by a too-rapid decompression.
Even experiments with air-injected rabbits have indicated the presence
of an air-blood interface alone will activate the hemostatic mechanism (1).

These observations of altered clotting activity after DCS suggest a very significant role of fibrinogen at the bubble-air interface.

After the observation in 1907 by Vernon (7) that gaseous nitrogen was 5.3 times more soluble in fats than in water, considerable attention has been given to the possible influence of body lipids in the etiology of DCS. It was not until 1945 that Berg et al. (8) recognized the possible significance of plasma lipids in DCS. During in vitro experiments, they showed that hydrophobic surfaces such as lanolin and paraffin retained minute air films which acted as nuclei for bubble growth. It was concluded that similar phenomenon might also occur in vivo. Interest in plasma lipids became even more profound when it was found that fat embolism was a not-uncommon post-mortem finding in human fatalities from DCS following decompression at high altitudes. Haymaker et al. (9) reported two fatalities after high-altitude flying. The victims had histopathological evidence of fat embolism and both had patent foramen ovales. The researchers noted intense generalized lipemia and pointed out that the patent foramen ovale permitted the entry of gas bubbles, which otherwise would be filtered out by the lungs, into the left side of the heart, and hence reached the brain and other vital organs. The same also would be true of lipid emboli. Subsequently, laboratory experiments confirmed the presence of fat emboli in various organs and tissues in animals with severe DCS (10).

It has also been postulated by some investigators that intravascular bubbles triggered the aggregation of platelets and that coalesced plasma lipids become incorporated into such aggregates. Pauley and Crockett (11) reported that the coalescence of plasma lipids was the most likely source of fat emboli, and that there was electron microscopic evidence that lipid particles became incorporated at the gas-liquid interface of intravascular bubbles produced in rats by rapid decompression. Therefore, it appears that the trapping of such thrombi composed of bubbles, platelets, and lipids would explain the disappearance of plasma lipids from the circu-

lating blood, as had been observed in rats severely affected by DCS.
Elevated plasma lipids have been shown experimentally to accelerate blood
clotting, favor experimental thrombogenesis, increase the platelet adhe-
siveness, reduce the circulating platelet count and aggregate platelets
in vitro. In light of these observations, it is reasonable to conclude
that elevated lipid levels could increase the incidence and severity of
experimental DCS, and that it would seem reasonable to assume that plasma
lipids play a significant role in the etiology of clinical DCS. Based
upon these observations, this investigation was undertaken to further
elucidate the role of fibrinogen and plasma lipids in bubble formation
at the air-liquid interface during DCS.

II. OBJECTIVES

The primary objective of this research project was to determine the
concentration of fibrinogen and plasma lipids in the serum and/or plasma
of Air Force hypobaric subjects before and after exposure to simulated
altitude changes in the hypobaric chambers of the Crew Technology Divi-
sion at the School of Aerospace Medicine, Brooks AFB. These analytical
determinations would thereby allow the evaluation and elucidation of
their role in bubble formation during DCS.

The approach of this investigation was to correlate fibrinogen and
plasma lipids to DCS in the following ways:

(1) Assess and determine the serological concentration of fibrinogen and
    circulating plasma lipids following varying simulated altitude expo-
    sures.

(2) Correlate the concentrations of fibrinogen and lipids vs the tendency
    toward bubble formation and the degree of DCS.

(3) Determine the relationship of fibrinogen and plasma lipids to plate-
    let adhesion and aggregation at the air-liquid interface of the gas
    bubble during DCS.

It perhaps should be noted at this point that the goals and objectives of this research effort could not be assessed to the degree desired by the investigator due to circumstances beyond his control. He was unfortunately informed on June 29, 1984 (midway in the research period), that the facility from which donor subjects' blood samples were being obtained to carry out this investigation was being closed for technical reasons until July 31, 1984. Nonetheless, and in spite of the fact that the number of plasma and serum samples obtained was minimal, the researcher did analyze and assess those samples that he was able to obtain. Due to the difficulties encountered and noted above, this research effort should be extended and a more detailed study pursued with a much larger population of hypobaric flight subjects.

III. METHODS AND RESULTS

A. Collection of blood samples

Blood samples were obtained from normal healthy USAF hypobaric subjects by venipuncture into 7 ml vacutainer tubes containing no coagulant. The samples were allowed to clot at room temperature for one hr, centrifuged at 2000 rpm for 10 min, the serum decanted into clear 5 ml sterile polystyrene tubes and stored at -20° C until used for assay of plasma lipids: cholesterol (Chol), high-density lipoproteins-associated cholesterol (HDL-Chol) and triglycerides (Trig) concentrations. The collection of plasma samples for fibrinogen concentration determinations were obtained, centrifuged, decanted and stored under the same conditions, except that they were drawn into 5 ml vacutainer tubes containing the anticoagulant sodium citrate. One pre-flight sample of blood was drawn from all hypobaric subjects in each category described above. An additional sodium citrate sample of blood was drawn from subjects who experienced DCS.

B. Bends screening index protocol

The bends screening index protocol profile used by the Hypobaric Branch for volunteer subjects was as follows:

1. One hour of pre-breathing 100% pure O_2.

2. Subjects were to be exposed to at least six randomly
selected flights in the altitude chambers.

  a. One at 25,000 ft or 5.45 psi (281.8 mmHg).

  b. Three at 27,500 ft or 4.88 psi (252.4 mmHg).

  c. Two at 30,000 ft or 4.36 psi (225.6 mmHg).

3. The duration of each flight was for 8 hr unless grade II
DCS symptoms occurred, at which time the subject was immediately removed
from the chamber.

4. Intervals for successive flights were to be never less than
two days apart for subjects who completed the experimental hypobaric
procedures.

C. Assay for fibrinogen concentration determinations

The quantitative determination of fibrinogen in all plasma samples
was conducted using a Fibrometer. The fibrinogen test procedures were
conducted according to those specified by the Sigma Chemical Company,
St Louis, Missouri, from which the fibrinogen test kits (No. 880) were
obtained. All plasma samples were assayed in duplicate with an average
of the two clotting times subsequently determined and recorded (Table 1).

Based on the following general principle:

$$\text{Fibrinogen} \xrightarrow{\quad\text{Thrombin}\quad} \text{Fibrin} \qquad (1)$$

When plasma is diluted with barbital buffer (with albumin) and then
allowed to clot with excess thrombin, the fibrinogen concentration
becomes rate limiting and inversely proportional to the clotting time,
yielding a linear relationship when plotted on log-log two cycle graph
paper (Figure 1). The calibration curve prepared by use of a fibrinogen
reference supplied in the kit is used to determine the fibrinogen concen-
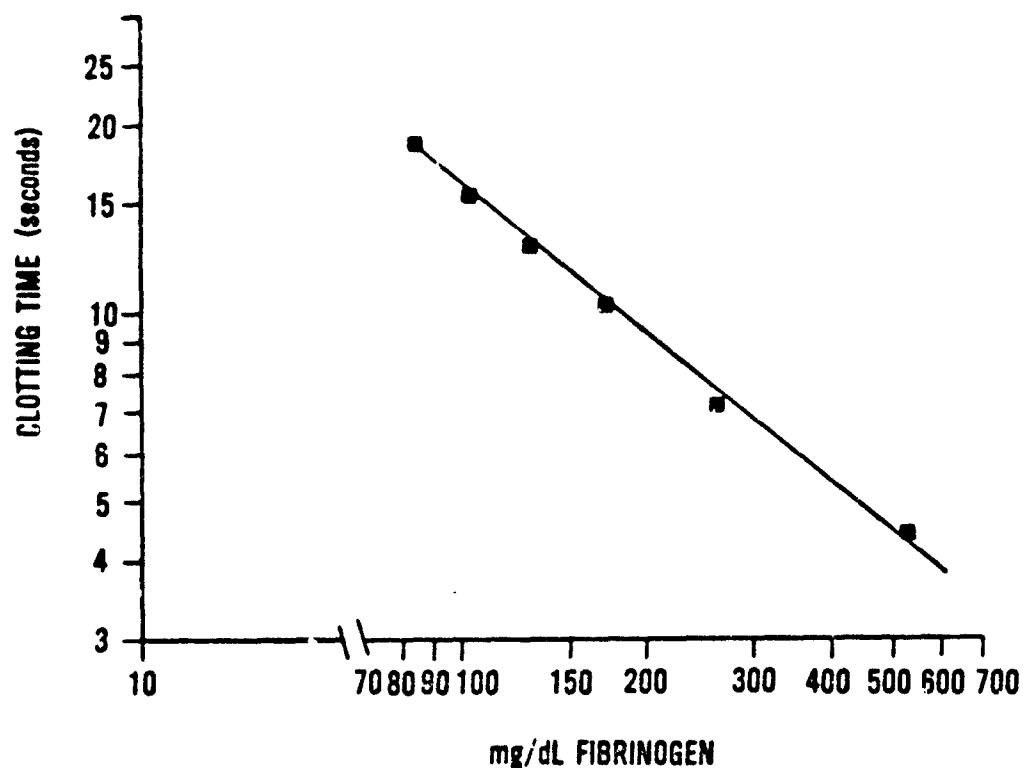trations in the subjects' plasma samples (12), which is shown in Table 1.

Figure 1. Fibrinogen calibration curve.

FIBRINOGEN CONCENTRATIONS (mg/dl)				
Subject	Dilution Factor	Fibrinogen Concentration	Clotting Time (sec.)	Average Clot. Time
1*				
2	1:10	88#	17.7/18.2	17.9
3*				
4	1:10	240	7.2/6.9	7.0
5	1:10	145	12.1/11.7	11.9
6	1:10	127	13.3/13.3	13.3

Table 1. Fibrinogen concentrations for hypobaric subjects.

Note: Normal range, Adults: 180-310 mg/dl

*Sodium citrate plasma was not available for assay.
#Fibrinogen concentration after subject was removed from chamber.

D. Assay for plasma lipids

The samples used for the determination of plasma lipids (Chol, HDL-Chol and Trig) concentrations were assayed using an Abbott VP Bichromatic Analyzer. A bichromatic filter with a wavelength of 500/600 nm was used to quantitate the concentrations of Chol and HDL-Chol respectively. A 340/380 nm filter was used for the Trig assays. All assays were conducted according to the protocol specified by Abbott Diagnostic Division Laboratories for use with the Abbott VP Bichromatic Analyzer. The quantitative concentrations of Chol, HDL-Chol and Trig (expressed in mg/dl) found in the serum of the six hypobaric subjects are shown in Table 2. The calculated concentrations of low-density lipoprotein cholesterol (LDL-Chol) and Chol to HDL-Chol ratio is also shown in Table 2.

| CONCENTRATIONS (mg/dl)					
Subject	Chol	HDL-Chol	LDL-Chol	Chol:HDL-Chol	Trig
1	158	32	126	4.9	111
2*	189	54	135	3.5	150
3	130	46	84	2.8	118
4*	141	32	109	4.4	78
5*	219	45	174	4.9	126
6	220	41	179	5.4	89

Table 2. Plasma lipids concentrations.

Notes: 1. Normal Ranges.　Cholesterol　　　100-250

HDL-Cholesterol　25-75

Triglycerides　　0-150

2. *Subjects who showed signs of bubble formation.

The chemical principles of the procedures used in the analyses to quantitate the concentration of Chol, HDL-Chol and Trig shown in Table 2 are based upon the following generalizations:
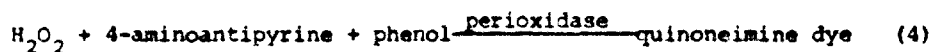
(1) Cholesterol

Cholesterol esters in serum are hydrolyzed to free cholesterol by cholesterol ester hydroylase;

$$\text{cholesterol esters} \xrightarrow[\text{esterase}]{\text{cholesterol}} \text{cholesterol} \qquad (2)$$
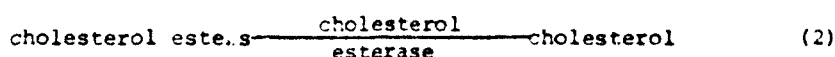
The free cholesterol produced is oxidized to cholest-4-en-3-one with simultaneous production of hydrogen peroxide;

$$\text{cholesterol} + O_2 \xrightarrow[\text{oxidase}]{\text{cholesterol}} \Delta^4\text{-cholestenone} + H_2O_2 \qquad (3)$$
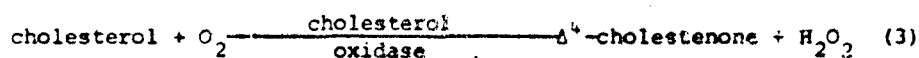
The H_2O_2 oxidatively couples with 4-aminoantipyrine and phenol in the presence of peroxidase to yield a quinoneimine dye;

$$H_2O_2 + \text{4-aminoantipyrine} + \text{phenol} \xrightarrow{\text{perioxidase}} \text{quinoneimine dye} \qquad (4)$$

The quinoneimine dye has an absorption maximum of 500 nm. The amount of color measured by the Abbott Analyzer is directly proportional to the total cholesterol content of the subject's sample (13,14) given in Table 2.

(2) HDL-Cholesterol

At neutral pH, sulfated polysaccharides will form insoluble complexes with serum low-density lipoproteins (LDL) and very low-density lipo-proteins (VLDL) in the presence of divalent cations. Under such conditions, insoluble lipoproteins-polyanion-cation complexes are formed. The insoluble complexes form more readily when the protein-to-lipid ratio is low. Consequently, VLDL precipitates more readily
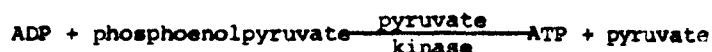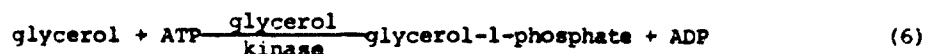
than LDL, and LDL more readily than HDL. The proper concentration
of polyanion and cation allows the selective precipitation of lipo-
protein fractions. Dextran sulfate and Mg^{++} in predetermined con-
centrations selectively precipitate VLDL and LDL. The cholesterol
in the HDL fraction is then quantitated using the Abbott analyzer
by determining the cholesterol in the supernatant following centri-
fugation (15). The results are shown in Table 2.

(3) Triglycerides

Triglycerides are completely hydrolyzed to free glycerol and free
fatty acids by a microbial lipase;

$$\text{triglycerides} \xrightarrow{\text{lipase}} \text{glycerol + free fatty acids} \tag{5}$$

The liberated free glycerol is then reduced enzymatically by the
following sequential reactions:

$$\text{glycerol + ATP} \xrightarrow[\text{kinase}]{\text{glycerol}} \text{glycerol-1-phosphate + ADP} \tag{6}$$

$$\text{ADP + phosphoenolpyruvate} \xrightarrow[\text{kinase}]{\text{pyruvate}} \text{ATP + pyruvate}$$

$$\text{pyruvate + NADH + H}^+ \xrightarrow[\text{dehydrogenase}]{\text{lactate}} \text{lactate + NAD}$$

The disappearance of NADH observed at 340 nm is a stoichiometric
measure of the glycerol present, which in turn is related to the
triglyceride content of the subjects' samples (16) shown in Table 2.

IV. DISCUSSION

The methods used in this investigation for the determination of fibrin-
ogen and plasma lipid concentration are presently routine laboratory
procedures for obtaining data that is of relevance in the diagnosis of

cardiovascular disorders. However, they may be of equal value in the search for serological conditions that may be of relevance in determining the susceptibility of subjects to experience DCS due to bubble formation under experimental hypobaric conditions.

From the data obtained and reported in Table 2, many parameters pertaining to cholesterol concentrations can be calculated (i.e., LDL-Chol and VLDL) once the analytical determinations of Chol, HDL-Chol and Trig have been made. Based on methods reported by Friedewald et al. (17), LDL-Chol can be calculated by use of the following formula:

$$C_{LDL} = C_{plasma} - C_{HDL} - Trig/5 \qquad (7)$$

Through correlations of the many variables that can be obtained and calculated from these data, there appears to be many serological characteristics pertaining to plasma lipids that can be evaluated.

Even though the subject population was small in this study, and some of the values observed were within the normal expected ranges, parameters such as those reported above and elsewhere in this report (Tables 1 and 2) may be of paramount importance in the prediction of subjects to experience DCS from those that are less prone to experience DCS and bubble formation. Such serological parameters may also be essential in assessing the extent of the adhesion and aggregation of blood platelets and plasma lipids at the blood-bubble interface in DCS. Moreover, the validity of these serological differences would be even more meaningful if all parameters are determined both before and after the hypobaric exposure in all subjects.

In spite of the small number of subjects evaluated in this investigation, it may be of importance at this point to report that subjects Nos. 2, 4 and 5 did develop venous bubbles detectable by Doppler, and subject No. 1, who had no signs of bubble formation during the exposure,

had to be removed from the hypobaric chamber prior to the completion of the 8-hr flight period due to development of DCS symptoms. Since the only "down" sample of plasma that was analyzed for fibrinogen concentration was that obtained from subject No. 2 (88 mg/dl) upon being taken out of the chamber after a 2-hr flight period, it is possible that low fibrinogen concentration might have been detected in the plasma of all subjects who showed signs of bubbling. The low concentration of fibrinogen observed in this case may have been due to the fact that much of the fibrinogen from the blood had already been coated on the surface of the bubbles formed. This assumption is in agreement with other investigators who reported the adhesion and aggregation of plasma lipids at the bubble surface interface due to the deposition of fibrinogen (1,18).

In regard to plasma lipid concentrations, it is possible that some relative characteristics of significant value might have been detected if all parameters noted herein had been analyzed and correlated before and after the hypobaric flight procedures. Philip (1) reported from studies using the rat treadmill decompression test that susceptibility to DCS was increased following alimentary lipemia, and that severity was related to plasma lipid levels. Therefore, since the subject's diet prior to the experimental flights was not known, consideration of these parameters might also have been of paramount importance in this research investigation.

Finally, in the light of these observations, it would seem reasonable as well as advantageous to further elucidate and pursue the role of fibrinogen and plasma lipids in the etiology of DCS at the blood-bubble surface interface. Preliminary results revealed in this investigation indicate that further study of bubble surface interaction with these serological components of the blood warrants further consideration with a larger population of subjects and a longer period of time for pursuing the study.

V. RECOMMENDATIONS

It is strongly recommended that extensive studies and observation in reference to fibrinogen and plasma lipids at the bubble surface interface during DCS be investigated. These studies are feasible at the USAF School of Aerospace Medicine in cooperation with the Hypobaric Research Division and the Clinical Pathology Laboratory Function. Since the preliminary groundwork has been laid to pursue these studies that are of value in hypobaric research, it is suggested that another summer be allowed this researcher to further investigate these phenomena. It is further suggested that, due to the type of equipment and the facilities required to pursue this investigation, the research effort be conducted at this specific research location.

Finally, in spite of the obstacles which resulted in the problems encountered and reported elsewhere in this report, another research effort of significant interest has surfaced which this researcher intends to pursue at his home institution. The problem is of relevance to the United States Air Force experimental hypobaric research effort and can conceivably be pursued within the guidelines and specifications of the Air Force Office of Scientific Research Initiation Program. It has been strongly suggested and recommended that this effort be pursued.

REFERENCES

1. R. B. Philip. "A Review of Blood Changes Associated With Compression-Decompression: Relationship to Decompression Sickness," Undersea Biomed. Res., vol. 1(2), pp 117-150, 1974.

2. K. H. Smith and M.P. Spencer. "Doppler Indices of Decompression sickness: Their Evaluation and Use," Aerosp. Med., vol. 41(12), pp 1396-1400, 1970.

3. B. A. Warren, R. B. Philip and M. J. Inwood. "The Ultrastructural Morphology of Air Embolism: Platelet Adhesion to the Interface and Endothelial Damage," Br. J. Exp. Pathol., vol. 54(2), pp 249-259, 1973.

4. M. H. Jacobs and D. R. Stewart. "Observations on the Blood of Albino Rats Following Rapid Decompression," U.S. National Research Council, Comm. Aviat. Med. Report, Washington D.C., pp 1-5, 1942.

5. R. B. Philip, P. Schacham and C. W. Gowdey. "Involvement of Platelets and Microthrombi in Experimental Decompression Sickness: Similarities with Disseminated Intravascular Coagulation," Aerosp. Med., vol. 42(5), pp 494-502, 1971.

6. R. B. Philip, M. J. Inwood and B. A. Warren. "Interactions Between Gas Bubbles and Components of the Blood. Implications in Decompression Sickness," Aerosp. Med., vol. 43(9), pp 946-953, 1972.

7. H. M. Vernon. "The Solubility of Air in Fats, and Its Relation to Cassion Disease," Proc. Roy. Soc., vol. 79, pp 366-371, 1907.

8. W. E. Berg, M. Harris, D. M. Whittaker and C. W. Twitty. "Additional Mechanisms for the Origin of Bubbles in Animals Decompressed to Simulated Altitudes," J. Gen. Physiol., vol. 28(3), pp 253-258, 1945.

9. W. Haymaker, A. D. Johnson and V. M. Downey. "Fatal Decompression Sickness During Jet Aircraft Flight," J. Aviat. Med., vol. 27(1), pp 2-17, 1956.

10. J. R. Clay. "Histopathology of Experimental Decompression Sickness," Aerosp. Med., vol 34(12), pp 1107-1110, 1963.

11. S. M. Pauley and A. T. K. Crockett. "Role of Lipids in Decompression Sickness," Aerosp. Med., vol. 41(1), pp 56-60, 1970.

12. Sigma Technical Bulletin No. 88u. The Quantitative Determination
     of Fibrinogen in Plasma. Sigma Chemical Company, St Louis MO, 1982.

13. C. C. Allain, L. Poon, S. G. Richmond and P. Fu. "Enzymatic deter-
     mination of Total Serum Cholesterol," Clinical Chem, vol. 20(1),
     pp 470-475, 1974.

14. A-Gent Cholesterol Test Guide No. 95-8841-FD. Abbott Laboratories,
     Diagnostic Division, South Pasadena CA, 1981.

15. A-Gent High-Density Lipoprotein Test Guide No. 95-8806-F2. Abbott
     Laboratories, Diagnostic Division, South Pasadena CA, 1979.

16. A-Gent Triglyceride Test Guide No. 95-8847-FD. Abbott Laboratories,
     Diagnostic Division, South Pasadena CA, 1982.

17. W. T. Friedewald, R. I. Levy and D. S. Fredrickson. "Estimation of
     the Concentration of Low-Density Lipoprotein Cholesterol in Plasma,
     Without Use of the Preparative Ultracentrifuge," Clinical Chem.,
     vol. 18(6), pp 499-502, 1972.

18. L. Vroman, A. L. Adams and M. Klings. "Interactions Among Human
     Blood Proteins at Interfaces," Fed. Proc., vol. 31(2), pp 1494-
     1502, 1971.

IN MEMORY OF

Dr. Lowell Schipper

who died during his appointment on the
1984 Summer Faculty Research Program

1984 USAF-SCEEE SUMMER FACULTY RESEARCH PROGRAM

Sponsored by the

AIR FORCE OFFICE OF SCIENTIFIC RESEARCH

Conducted by the

SOUTHEASTERN CENTER FOR ELECTRICAL ENGINEERING EDUCATION

FINAL REPORT

EVALUATION OF TRAINING PERFORMANCE FOR

THE USAF CRITERION TASK SET (CTS)

Prepared by: Dr. Robert E. Schlegel
                    David W. Patterson

Academic Rank: Assistant Professor
                    Graduate Assistant

Department and   School of Industrial Engineering
   University: University of Oklahoma

Research   USAF Aerospace Medical Research Laboratory,
   Location: Human Engineering Division,
                    Workload and Ergonomics Branch

USAF Research   Dr. Clark A. Shingledecker
   Colleague:

Date: September 10, 1984

Contract No: F49620-82-C-0035

EVALUATION OF TRAINING PERFORMANCE FOR

THE USAF CRITERION TASK SET (CTS)

by

Dr. Robert E. Schlegel

David W. Patterson

ABSTRACT

A study was conducted to determine the required number of
training sessions for subjects to achieve asymptotic perfor-
mance on the Criterion Task Set (CTS) information processing
performance battery. The CTS is composed of nine tasks which
measure independent information processing resources. One
task measures perceptual input, six tasks measure central pro-
cessing and two tasks measure motor output.

Twenty subjects were divided into four groups. One group
trained on all nine tasks. The other three groups trained on
different three-task subsets. All subjects trained for two
hours per day on five consecutive days.

Performance measures for the majority of tasks included
response time and accuracy. Subjective workload measures were
also obtained. Preliminary analysis of the data indicates
similar learning patterns for the nine-task and three-task
groups with all groups demonstrating rapid improvement on most
tasks. Recommendations for further data analysis and research
extensions are also provided.

ACKNOWLEDGEMENTS

1.0 INTRODUCTION

Recent trends in workload research have concentrated on two areas. The first area has been the development of workload theory, that is, models which can predict human information processing/performance capability. The second area of concentration has been the development of specific measurement techniques. Unfortunately, there have been very few attempts to coalesce these theory and task developments into unified workload assessments. The Air Force Criterion Task Set (Shingledecker et al., 1982, 1983) was designed for this purpose.

1.1 Air Force Criterion Task Set (CTS)

The Criterion Task Set (CTS) is based on a synthesis of current human performance models (Wickens, 1981; Sternberg, 1969) which hypothesize that human performance is dependent on a number of information processing resources, stages and specific functions. The three major divisions are perceptual input, central processing and motor output.

The elements of the combined model were operationally defined in terms of the characteristics of tasks which would place predominant demands on them. These definitions were then used to select candidate tasks for the CTS. Each of the tasks was subjected to parametric study to establish prescribed testing conditions and loading levels. The result was a group of standardized primary tasks designed to assess a range of func-

tional determinants of human performance. Of primary importance is the fact that not only was the battery developed with concern for the fundamental characteristics of operational environments but it also integrates existing information processing theory.

The battery is presented on a CRT display while the subject responds using a keypad and other controls designed to allow full response capability to the various tasks. In most tasks, individual stimuli are presented sequentially and response time and accuracy scores are collected. Each task, except Interval Production, may be conducted at three distinguishable workload levels: low, medium and high. Individual trials for each task are of three minutes duration.

Table 1. CTS Version 1.0 Tasks Listed by
Information Processing System Division.

STAGE	TASK	CODE
Input/Perceptual	Probability Monitoring	PM
Central Processing	Memory Search	MS
	Continuous Recall	CR
	Spatial Processing	SP
	Mathematical Processing	MP
	Linguistic Processing	LP
	Grammatical Reasoning	GR
Output/Motor	Unstable Tracking	UT
	Interval Production	IP

The nine tasks within CTS Version 1.0 are listed in Table 1 according to their hypothesized relationship to the information processing divisions. A brief description of each task

follows.

Visual Probability Monitoring (PM). The subject is required to monitor 1, 3 or 4 simulated meters and determine whether a bias condition is present. This occurs when a pointer stays on one side of the meter center line a higher percentage of time than on the other. The percentages for the 1-, 3- and 4-dial conditions are 95%, 85% and 75% respectively.

Memory Search (MS). An initial set of 1, 4 or 6 letters is presented to the subject for memorization. Following this, the subject must identify whether a randomly generated letter is a member of that set.

Continuous Recall (CR). The subject is presented with pairs of 1-, 2- or 4-digit numbers, one below the other, and must compare the top number with a previous display as well as memorize the bottom number for later comparison.

Spatial Processing (SP). The subject compares an initial histogram of 2, 4 or 6 bars with a second histogram that has been rotated 0, 90, 180 or 270 degrees.

Grammatical Reasoning (GR). Sentences describing the positioning of symbols are presented with the symbols below. The subject must determine whether the sentences correctly describe the positioning of the symbols.

Mathematical Processing (MP). The subject is required to decide whether the result of a mathematical expression involving

124

1, 2 or 3 operators (+ or -) is greater than or less than the value 5.

Linguistic Processing (LP). At the low level, the subject decides whether presented pairs of letters are physically identical. For the medium level, the subject decides whether both letters are vowels or consonants. At the high level, the subject is required to identify antonyms.

Unstable Tracking (UT). The subject attempts to maintain the position of an object, representative of an airplane, in the middle of the screen using a rotating control knob. The dynamics of the task magnify the control error to prevent stable control of the object.

Interval Production (IP). The subject attempts to create regular timing intervals using a tapping paddle at a rate between 1 and 3 taps per second.

While additional members of the CTS are still under development, extensive research has been conducted on the nine tasks included in CTS Version 1.0. The purpose of these parametric studies has been to determine training requirements for each task on an individual basis, to fix stimulus pacing rates and to select three standard loading levels based on statistically reliable performance differences and subjective estimates of task complexity.

A primary application of the CTS is as a test instrument to

124-7

evaluate the relative sensitivity, reliability and intrusiveness of a variety of available workload measures. Preliminary workload metric evaluation studies (Shingledecker et al., 1983) have been initiated to demonstrate the experimental procedures and to illustrate the potential variation in diagnosticity that exists among workload measures.

In addition to the original design intention stated above, the CTS forms an independent Performance Assessment Battery which may be used to assess the effects of various stressors on individual components of the human information processing system. This property may lead to eventual adoption of the CTS for the Tri-Service Drug Screening Program (1983).

To further the use of the CTS in both basic and applied research programs, it is essential to develop a comprehensive performance data base, including a multivariate analysis to investigate the interrelatedness of the subtests, i.e., the internal structure of the task set. A preliminary requirement for the development of this comprehensive data base is to establish a task administration methodology including an optimal training protocol.

2.3   OBJECTIVES

During the development of the CTS, human subjects were trained and tested on each task separately. The data reflect the learning characteristics of each task on an individual task basis often involving subjects with prior experience on the

124-4

same or related tasks. Little information has previously been available on the crossover learning that may exist or the training characteristics for the three final workload levels of each task. Until the current study, no comprehensive administration of the entire test battery has been made to a group of naive subjects.

The development of an optimal training protocol is even more crucial, in light of the amount of time required to administer the entire battery. A single subject may require up to two hours for an administration involving the performance of each task once at each workload level. This emphasizes the importance of optimally allocating a limited amount of training time to each of the tasks. It has been observed that some tasks require few training trials while others require extensive training for stabilized performance.

The specific objectives for the current research were:

1. determine the required number of sessions to achieve asymptotic performance on each task when naive subjects are trained on all tasks or a subset of tasks concurrently,

(2) compare the performance of subjects concurrently trained on all nine tasks with the performance of subjects trained on various three-task subsets,

(3) examine the inter-subject variability and inter-task performance relationships,

(4) develop the structure of a training protocol model to

allocate and sequence task training trials within a limited
training period, and

(5) relate task performance to a subjective workload as-
sessment measure.

3.0   RESEARCH METHODOLOGY

3.1   General Approach

Four different subject groups were established to compare the
performance of subjects trained on all nine tasks vs. indivi-
dual three-task subsets. In assigning tasks to groups, an at-
tempt was made to balance the category of information process-
ing, type of visual stimuli, task difficulty and other charac-
teristics (Table 2).

Table 2.   Basis for Task Assignment.

GROUP	TASK	Type I/P/O	CHARACTERISTICS	VISUAL STIMULI
A	------------all nine tasks------------			
B	MS	P	memory	alpha
	PM	I	visual, probability assessment	graphic
	GR	P	logic, spatial, grammar	symbol/alpha
C	MP	P	math, logic	numeric
	UT	I/O	visual/motor	graphic
	SP	P	spatial, visual, memory	graphic
D	LP	P	matching, grammar, visual	alpha
	IP	O	timing, motor	--------
	CR	P	memory, spatial	numeric

Each task was assigned to the overall set and one subset. A comparison of learning patterns would determine performance differences between subjects trained on a large set of tasks vs. a smaller subset. Due to training time limitations, five trials of each workload level of each task were performed for Group A tasks and fifteen trials were performed for Group B, C and D tasks.

3.2 Subjects

Twenty male subjects, age 18 to 25 years, were recruited from the Wright State University Campus. All subjects were enrolled in Air Force ROTC and were naive with respect to the CTS battery and other research efforts at AFAMRL/HE. The subjects attended an orientation session to become acquainted with the CTS and the goals of the study, and to perform a "SWAT sort" related to the subjective workload measure. The voluntary informed consent of each subject was obtained at this time in accordance with AFR 169-3.

Subjects were randomly assigned to Groups A, B, C and D, five subjects per group. Each subject trained on the appropriate CTS tasks for two hours per day on five consecutive days. Groups B and D trained during the first week of data collection, Groups A and C during the second week.

3.3 Equipment and Software

The CTS is implemented on a Commodore 64 microcomputer system.

Two such systems were used, each consisting of the following units: Commodore 64 microcomputer, Commodore 1541 disk drive, Commodore 1526 printer, monochrome Panasonic experimenter's monitor, color Commodore 1702 subject's monitor and three subject response devices.

Modifications were made to the CTS software to provide automatic sequencing through the task levels and automatic filename construction for data storage. A coding scheme was devised which included Group, Subject, Task, Level and Trial identifiers. CTS tasks and data were all stored on floppy disk with a separate diskette for each task group and each subject. On the average, two 5-1/4" data diskettes were required per subject with a total of 2500 trials (data files) for the entire study.

3.4   Subjective Workload Assessment Technique (SWAT)

To relate task performance to a subjective workload measure, the SWAT Scale was used. The SWAT Scale (Reid, 1982; Reid, Eggemeier, and Nygren, 1982) is a psychometric instrument subjectively measuring three major dimensions of workload: Time, Effort, and Stress. Given the demands of any specified workload period, subjects rate each dimension on a 1 to 3 Likert-type scale.

The unique aspect of this scale is that it not only provides a means for obtaining an individual subject's workload ratings, but also a method for establishing across-subject comparabili-

124-12

ty. This is accomplished by having each subject complete a SWAT Sort, i.e., each subject sorts a card deck of all 27 combinations of the three rating levels for all three workload dimensions. The sorting order is then subjected to conjoint scaling yielding a standardized rating metric which can be used for comparisons across subjects (Nygren, 1982).

Subjects performed the initial SWAT card sort during the orientation session. Following each trial, the subject provided his SWAT ratings on a data collection form for later incorporation into the performance data base.

3.5   Procedure

Subjects were trained on their assigned tasks during the same two hour time block on five consecutive days. Subjects in Group A sequenced through the set of tasks in the following order: MS, PM, GR, MP, UT, SP, LP, IP, CR. All tasks have three levels except IP, thus yielding 25 trials per subject during the two-hour period. Within each task, subjects sequenced through the levels from low to high in order.

All other subjects performed three trials at each level of each task. The sequence for Group B was MS, PM, GR with a total of 27 trials per day. Group C followed the sequence MP, UT, SP with 27 trials per day and Group D followed the sequence LP, IP, CR with a total of 21 trials due to the single level of the IP task. One trial at each level of each task was completed before repeating the task sequence. As in

124-13

Group A, subjects sequenced through the levelr from low to
high in order.

Two subjects were tested simultaneously by the experimenter,
one subject from each group on each Commodore system. All
data was permanently saved on floppy disk for later data
reduction and analysis.

3.6   Analysis

Performance measures for the majority of tasks included
response time and accuracy. These measures were obtained for
each stimulus presentation and could be summarized by select-
ing the statistics option in the CTS software. Using these
statistics, patterns of performance improvement over time
could be obtained based on estimates of learning curve parame-
ters for the various subject groups.

In addition, further analysis of the correlation between the
various tasks and the SWAT ratings can give a better indica-
tion of task structure and the relationship to a subjective
workload measure. These techniques and others are discussed
in more detail in Section 5.1.

4.0   PRELIMINARY RESULTS

Summary statistics (i.e., reaction time) were obtained for all
trials. Overall averages as a function of trial number were
plotted for each task at each workload level. An example us-
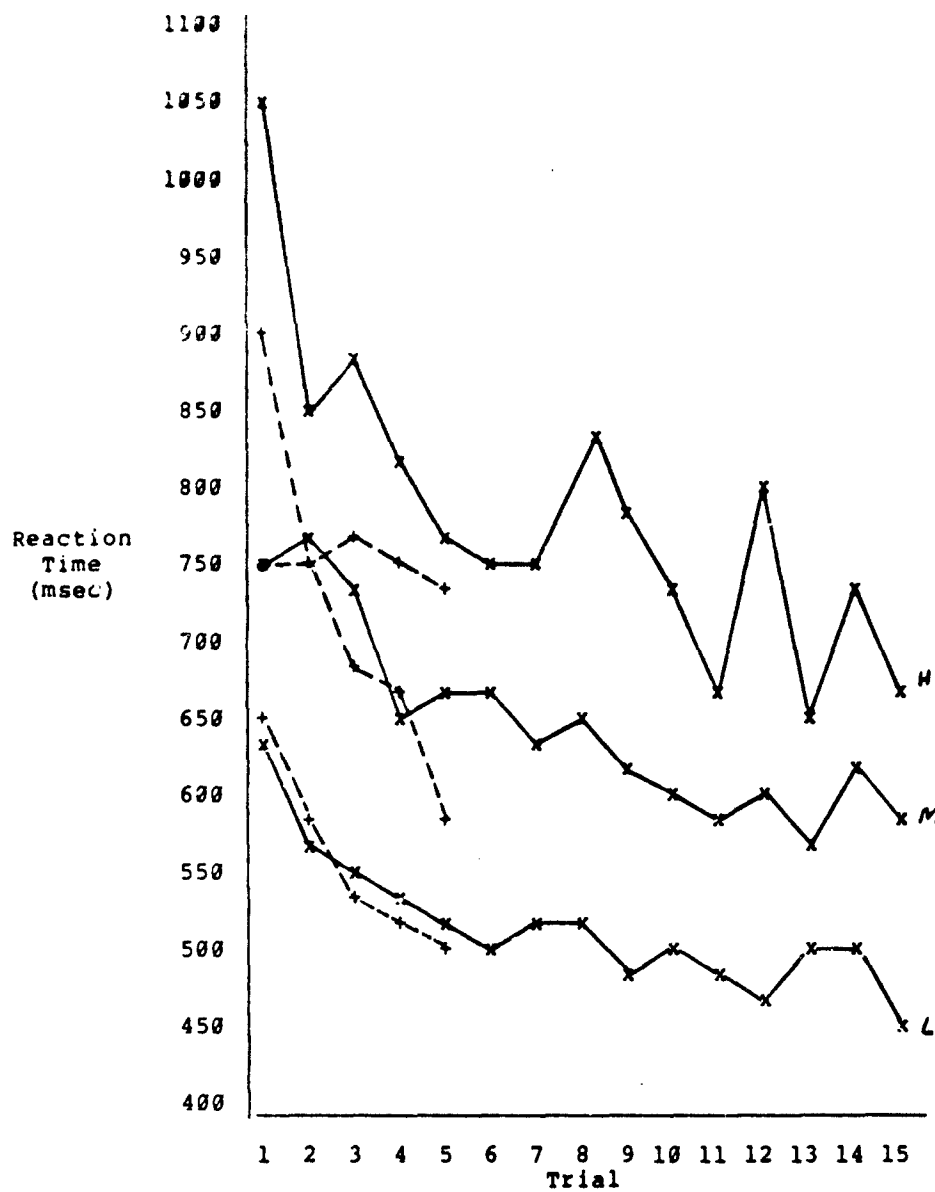ing the Memory Search (MS) task is given in Figure 1.

Figure 1. Reaction Time vs. Trial Number
for Memory Search Task.

With the exception of the Continuous Recall (CR) and Interval

Production (IP) tasks, the pattern of improvement was at least as good as that demonstrated in Figure 1 with minimal variability during the later trials. However, high variability did exist with Probability Monitoring (PM) due to the structure of the task which does not appear to provide sufficient stimuli per trial to yield a stable measure, especially at the medium and high workload levels.

The SWAT ratings showed consistent ordered differences between workload levels for all tasks. Examination of the ratings also provides a comparison of the relative difficulty across tasks. A ranking of tasks based on SWAT ratings is given in Table 3. Of the tasks with three distinct workload levels, Mathematical Processing (MP) had the lowest rating ("easiest") and Continuous Recall (CR) the highest ("most difficult").

Table 3. Subjective Task Difficulty Based on SWAT.

Workload Rank	Task
Low 1	Interval Production
2	Mathematical Processing
3	Spatial Processing
4	Memory Search
5	Probability Monitoring
6	Linguistic Processing
7	Grammatical Reasoning
8	Unstable Tracking
High 9	Continuous Recall

5.0   RECOMMENDATIONS

Several recommendations exist for future analysis of the data and extension of the research activity.

124-16

5.1 Guidelines for Data Analysis and Implementation

First, descriptive statistics for all tasks must be compiled to form the basis of norms and parameter estimates. This includes a breakdown by trial number, group and individual subject. Following this, analyses of variance should be conducted for each task to isolate differences between groups, subjects, trials and workload levels.

Second, learning curves need to be constructed to examine individual learning rates for tasks, groups and subjects. In addition, tests for stable task performance should be performed to determine the number of trials required for asymptotic performance. This will provide the answers to the major research questions of the study, including a comparison of the learning characteristics of subjects trained on the full battery vs. a subset of tasks.

Third, exploratory and confirmatory factor analyses should be performed to determine the factor structure of the CTS battery (e.g., LISREL IV Program-Joreskog, 1978, 1980). This includes computing the correlations between performance on all tasks within Group A with performance on corresponding tasks in Groups B, C and D.

Additional factor analyses and other multivariate procedures should be performed to assess the degree to which CTS performance is related to SWAT ratings for each task and workload level.

Final implementation of the research results involves construction of the optimal training protocol model. This might be accomplished through the use of a mathematical optimization procedure (e.g., linear programming) to achieve the greatest degree of training on all tasks within limited time constraints.

5.2   Suggestions for Future Research

In terms of extending the research activity, the current study forms the basis for developing a comprehensive data base for the CTS workload performance test battery including a multivariate investigation of the inter-relationships of the CTS tasks.

Additionally, data should be collected on the relationship between the CTS tasks and context variables in the categories of (1) Local Environment (e.g., time, temperature, noise, obscurants to perception, protective clothing); (2) Individual Status (e.g., fatigue, sleep loss, emotional stressors, disease, nutrition, drug use); and (3) Long-Term Individual History (e.g., training, prior experience, gender, age and important individual differences in such variables as intelligence level, arousal and task/cognitive ability).

A target application of the results of these follow-on studies is the development of Performance Assessment Batteries for the second phase of the Tri-Service Drug Screening Program (1983). Numerous additional applications of the CTS battery have been

124-18

outlined in previous reports (Shingledecker et al., 1982, 1983).

REFERENCES

Joreskog, K.G., "Structural Analysis of Covariance and Correlation Matrices," Psychometrika, 43, 443-477. 1978.

Joreskog, K.G., "Basic Issues in the Application of LISREL," Data, 1, 1-6, 1980.

Metzler, T.R. and Shingledecker, C.A., Register of Research in Progress on Mental Workload, Technical Report, AFAMRL-TR-82-42, Air Force Aerospace Medical Research Laboratory, Wright-Patterson Air Force Base, Ohio, July 1982.

Nygren, T.E., Conjoint Measurement and Conjoint Scaling: A Users Guide, Technical Report, AFAMRL-TR-82-22, Air Force Aerospace Medical Research Laboratory, Wright-Patterson Air Force Base, Ohio, April 1982.

Reid, G.B., Subjective Workload Assessment: A Conjoint Scaling Approach, Aerospace Medical Association Annual Scientific Meeting, Bal Harbor, Florida, 153-154, May 10-13, 1982.

Reid, G.B., Eggemeier, F.T. and Nygren, T.E., "An Individual Differences Approach to SWAT Scale Development", Proceedings of the Human Factors Society 26th Annual Meeting, 639-642, October 1982.

Shingledecker, C.A., Crabtree, M.S. and Acton, W.H., "Standardized Tests for the Evaluation and Classification of Workload Metrics," Proceedings of the Human Factors Society 26th Annual Meeting, 648-651, October 1982.

Shingledecker, C.A., Acton, W.H. and Crabtree, M.S., "Development and Application of a Criterion Task Set for Workload Metric Evaluation," SAE Technical Paper 831419, Aerospace Congress & Exposition, Long Beach, California, October 1983.

Sternberg, S., "The Discovery of Processing Stages: Extension of Donders' Method," Acta Psychologica, 30, 276-315, 1969.

Tri-Service Drug Screening Program, The Effect of Chemical Warfare Treatment Drugs on Military Performance, prepared by the Military Performance Working Group, Research Area V, U.S. Army Research and Development Command, Fort Detrick, Maryland, October 1983.

Wickens, C.D., Processing Resources in Attention, Dual Task Performance, and Workload Assessment, Engineering Psychology Research Laboratory Technical Report EPL-81-3, University of Illinois, 1981.

1984 USAF-SCEEE FACULTY RESEARCH PROGRAM

Sponsored by the

AIR FORCE OFFICE OF SCIENTIFIC RESEARCH

Conducted by the

SOUTHEASTERN CENTER FOR
ENGINEERING EDUCATION

FINAL REPORT

Regenerative Heat Transfer in an
LSSCDS Engine

Prepared by:	Howard Schleier
Academic Rank:	Associate Professor
Department and University:	Dept. Chemical Engineering Technology
	Norwalk State Technical College

Research Location:	AFRPL/LKDB
	Edwards AFB, CA 93523

Under the Direction of:	Darwin G. Moon

Date:	7 Aug 84

Contract No.:	F49620-82-C-0035

REGENERATIVE HEAT TRANSFER
IN AN LSSCDS ENGINE

BY

Howard Schleier

ABSTRACT

TDK/BLM analyses of the Large Space System Cryogenic Deployment System (LSSCDS) were modified to correct the incoming enthalpy of the H_2 fuel. The geometry of the combustion chamber was included in the rocket contour and some interations were made to reasonable convergence. Radiation upstream of the throat was estimated. The acceleration parameter was checked to see whether any relaminarisation occurred. Velocity profiles were checked for the possibility of any BL separation.

It was determined on the basis of the above assumptions that the cooling load was approximately $414^{Btu}/_s$ as compared with Rocketdyne's estimate of $670^{Btu}/_s$. The $414^{Btu}/_s$ is $399 + 15^{Btu}/_s$ for radiation.

INTRODUCTION

In the development of the LSSCDS engine, a low thrust (500 lb) high expansion ($\epsilon = 1230$) design, the question of the heat load for regeneration was investigated. TDK/BLM was modified to include the combustion chamber. Computer runs were modified to account for hotter H_2 entering and possible effects of radiation were evaluated upstream of the throat.

Acceleration parameters and velocity profiles were sampled at various points along the axis to check for the possibility of relaminarization and separation, and our postulates indicated a discrepancy between the Air Force Rocket Propulsion Laboratory (AFRPL) and Rocketdyne predictions.

PROCEDURE

TDK/BLM runs were done on the LSSCDS rocket with regeneration. The inlet temperature of the fuel was adjusted for the regeneration until reasonable convergence was achieved (3 iterations). Radiation (Appendix A) was estimated upstream of the throat. The velocity profile was examined throughout the nozzle to see whether any indications of separation were apparent. Acceleration parameters were calculated at varying positions to check for any indications of relaminarization of the boundary layer. The Reynolds number based on momentum thickness was calculated as an indicator of transition from laminar to turbulent and this transition was postulated.

The LSSCDS engine was run at a 6:1 O:F ratio at the rate of a total of 1.05 lbm/s. Other specifications are in Appendix F.

RESULTS

The TDK/BLM program was corrected through trial and error such that the inlet hydrogen temperature conformed with the regenerative cooling load. This correction reduced the convective cooling load from $670^{Btu}/_s$ to $410^{Btu}/_s$ to $399^{Btu}/_s$. Specific Impulse to Vacuum (IVAC), based on equilibrium conditions, was reduced from 524s to 514s, and on frozen conditions from 472s to 467s (Appendix B). Radiation losses upstream of the throat were approximated at $13^{Btu}/_s$, and were ignored downstream (Appendix A). The final input to the TDK/BLM run is indexed in Appendix F.

Manual calculation of the acceleration parameter is documented in Appendix C. One easily sees that this criteria is well below the 2E-6 to 3E-6 required for relaminarization past the point where the expansion ratio is 2. Though there is a possibility of the K reaching a critical value from the throat to the point where epsilon equals 2, the area for heat transfer is so small that it does not merit investigation. One can reasonably conclude that no relaminarization takes place that would noticeably affect heat transfer estimates.

The velocity profiles as shown in Appendix E show positive velocities except at the wall. However, at the wall, where the velocity is zero, the slopes of the velocity profiles are strongly positive, thus eliminating the possibility of separation.

The TDK/BLM run per Appendix D assumed a laminar BL upstream of the throat and a turbulent BL downstream.

It was also noted that IVAC was reduced by 5-10s by correcting for hydrogen inlet conditions.

$5\ 4$

CONCLUSIONS

1. It is unlikely from our assumptions that the regenerative load of $670^{Btu}/_s$ can be met with these specifications. Provisions should be made for alternative means of driving the compressors in the event that the $670^{Btu}/_s$ specification is not met.

2. Corrections in the inlet temperature of the hydrogen reduced IVAC by 5-10 s.

3. Examination of the acceleration parameter indicates that no relaminarization occurs.

4. The conditions necessary for separation of the BL are not indicated in the velocity profiles.

RECOMMENDATIONS

1. The assumption made indicated that $670^{Btu}/_s$ is highly unlikely and that alternative methods of supplying or supplementing the energy necessary to drive the compressors be considered.

2. Repeat the investigation on the newest version of TDK/BLM.

3. Update TDK/BLM to include radiation effects.

4. Update TDK/BLM to include matching the regenerative load with the inlet conditions.

5. Update TDK/BLM to to include a serious model of the combustion chamber.

6. Gather experimental data be gathered to reinforce or reject these conclusions.

REFERENCES

1. Lauduay, L. D. and Lifchitz, E. M., _Fluid Mechanics_, Pergamon, Vol 6, New York, 1959.

2. Evans, Harry L., _Laminar Boundary Layer Theory_, Addison-Wesley Publishing Co., Reading, MA, 1968.

3. Weibelt, John A., _Engineering Radiation Heat Transfer_, Holt, Rinehart & Winston, New York, 1966.

4. Welty, James R., et al, _Fundamentals of Momentum Heat and Mass Transfer_, John Wiley and Sons, New York, 1976.

5. Wolf, Helmut, _Heat Transfer_, Harper & Row, New York, 1983.

6. _The Dynamics and Thermodynamics of Compresible Fluid Flow_, Shapiro, Ascher H., Vol 1, John Wiley & Sons, New York, 1953.

7. Bird, R. Byron, et al, _Transport Phenomena_, John Wiley and Sons, New York, 1960.

8. Schlichling, Hermann, _Boundary Layer Theory_, McGraw-Hill, New York, 1968.

9. "Laminarization of a Turbulent Boundary Layer," Bach, et al, _Journal of Heat Transfer_, Vol. 92, , Aug 1970, pp 333-344.

10. Rohsenow, Warren M., _Handbook of Heat Transfer_, McGraw-Hill, New York, pp 7-150 to 7-167.

NOMENCLATURE

Symbol	Definition	Units
A	area	ft^2
C_p	average heat capacity	Btu/lbm-R
K	acceleration parameter	none
$\dot{m}$	mass flow	lbm/s
Pe	edge pressure	lbm/ft^2
q	heat transfer rate	Btu/S
R	radius	ft
R	gas constant	$\frac{ft-lbf}{lbm-R}$
Re	Reynolds number based on	none
IVAC	specific impulse to vacuum	lbf-s/lbm
Re θ	Reynolds number based on θ	
S	distance along surface	ft
Te, T	edge temperature	degR, degK
TAD	adiabatic	deg-K
U2	final edge velocity	ft/s
U1	initial edge velocity	ft/s
Ue	edge velocity	ft/s
X	axial distance	ft
ϵ	expansion ratio	none
Ve	Edge velocity	lbm/ft-s
ρe	edge density	lbm/ft^3
μ	viscosity	lbm/ft-s

ACKNOWLEDGEMENTS

APPENDIX A

Estimate of Radiation Losses (Ref. 3)

(Consider 6:1 O:F all O_2 Vanishing On Combustion. Basis 1.05 lbm/s)

Comp	Before		After	
	lbm/s	mol/s	lbm/s	mol/s
O_2	0.90	0.0281	0.0000	.00000
H_2	0.15	0.0750	0.1375	.01975
H_2O	0.00	0.0000	1.0125	.07500
Total	1.05	0.1031	1.1500	.07600

Re_p

X H_2O	= 5625/7500		= 0.75
Pw	= 75 x 510 psia/14.7 psia/atm		= 26 atm
H/D (cyl)	= 3.5"/1.898"		= 1.84 say 2
L	= 0.76 D = .76 x 1.898"/12" ft		= 0.12 ft
PwL	= 0.120 ft x 2.60 atm		= 3.12 atm ft say 2 ft-atm
T	= 3575 D x 1.8 R/K		= 6435 R

Extrapolation of $\varepsilon'w$:

$\varepsilon'w$	T (R)
.2	3500
.15	4350

$$\frac{\ln .2 - \ln .15}{3500 - 4350} = \frac{\ln .2 - \ln \varepsilon'w}{3500 - T}$$

or $\varepsilon'w = \exp - (.426 = 3.38 \, E - 4 \, T)$

or $\varepsilon's = \exp - (.426 = 3.38 \, E - 4 \, T)$

for T $= 6435$, we get $\varepsilon'w$ $= 0.0742$

P $= 510 \text{ psia}/14.7 \text{ psia/atm}$ $= 34.7$ atm

$(P + Pw)/2 = (34.7 + 26.0)/2$ $= 30.0$ am

Cw $= 1.5, \varepsilon = 1.5 \times 0.074$ $= 0.111$

εs $= $ say 0.8

Ts $= 1420$ R

$PwL \, \dfrac{Ts}{Tg}$ $= 3 \times 1420/6435$ $= 0.662$

$\varepsilon's$ $= 0.22$

Cw $= 1.50$

Eg $= 0.33$

α $= (\dfrac{6435}{420})^{.45} \times 0.33 = 0.651$

Then (q/A) rad

$= 0.8 \times 0.1714\epsilon{-}8 \ (0.111 \times 6435^4 - .65 \times 1420^4)$

$= 2.57 \ \epsilon 5 \ \text{Btu}/_{\text{ft}}{}^2 - h$

$= 0.496 \ \text{Btu}/_{\text{in}}{}^2{}_{-s}$

The upstream area for heat transfer is then $\pi \times 1.898'' \times 3.5''$ for the cylinder plus $\pi S = (1.898'' + .792'')/2$ for the frustum where

$$S \qquad = \ 2^2 + (\frac{1.898 - .792}{2})^2 \ {}^{0.5} = 2.08 \ \text{in}$$

or $\quad A \qquad = 20.9 + 8.79 = 29.7 \ \text{in}^2$

and $\quad q$ rad $= 14.7 \ \text{Btu}/_s$

APPENDIX B

Correction for Inlet Temperature of H_2 into Combustion Chamber.

732K corresponds to 670 Btu/s while the computer calculates the load to be 410 Btu/s. An estimate of 463K produces 399 Btu/s. If the inlet temperature of the fuel is assumed to be 451K, a q very close to 399 Btu/s results, and convergence is assumed.

APPENDIX C

Calculation of K.

ε	R	Te	μH1	PE
2	4.67 E-02	3939	4.42 E-05	2.27341 E3
10	1.04 E-01	3332	3.85 E-05	8.05225 E2
100	3.30 E-01	2238	2.86 E-05	9.58130 E1
250	5.22 E-01	1865	2.45 E-05	3.97277
300	5.72 E-01	1811	2.45 E-05	3.47452
350	6.17 E-01	1726	2.24 E-05	2.78905
400	6.60 E-01	1672	2.24 E-05	2.41312
450	7.00 E-01	1612	2.02 E-05	2.04791
1230	1.16 E-00	1121	1.58 E-05	4.38345 E0

ε	U2	U1	S2	S1	R	ρ
2	1.15404 E4	1.15022 E4	4.48318 E1	4.46855 E1	1.19 E2	4.85 E3
10	1.26801	1.26288	5.24529	5.21014	1.11	2.18
100	1.42733	1.41631	9.00995	8.68223	1.10	3.89 E4
250	1.47253	1.46700	1.34343 E00	1.27068 E00	1.10	1.94
300	1.47862	1.47253	1.42398	1.34343	1.10	1.74
350	1.48816	1.48295	1.61288	1.51332	1.10	1.47
400	1.49417	1.48816	1.72417	1.61288	1.10	1.31
450	1.50072	1.49417	1.84913	1.72417	1.10	1.15
1230	1.55074	1.54942	4.02611	3.94268	1.10	3.55 E5

APPENDIX C (Cont.)

$\underline{A_e}$	$\underline{K}$
2	1.79 E-6
10	1.60 E-6
100	1.21 E-6
250	4.43 E-7
300	4.87 E-7
350	3.60 E-7
400	4.14 E-7
450	4.09 E-7
1230	2.93 E-7

Sample Calculation For K @ ϵ = 250

U2	= 1.47253 E4	U1	= 1.46700 E4
S2	= 1.34343	S1	= 1.27068
Pe	= 3.97277	Te	= 1865
(from Te)	= 2.45 E-5	R	= 1.10 E2
(from gas law)	= 1.94 E-4		

and $K \approx \dfrac{\mu}{\rho U_2^2} \dfrac{\left(U^2 - U_1\right)}{S_2 - S_1}$ = 4.43 E-7

125-16

APPENDIX D

Sample Calculation for Re Θ.

$$Re\ \Theta = Re\ w^* \times \frac{R}{c^*}$$

@ x $= -\ .25294$

$$Re\ \Theta = \frac{1.0612\ E-1}{-7.8394\ E-4} \times (-2.9625\ E-2)$$
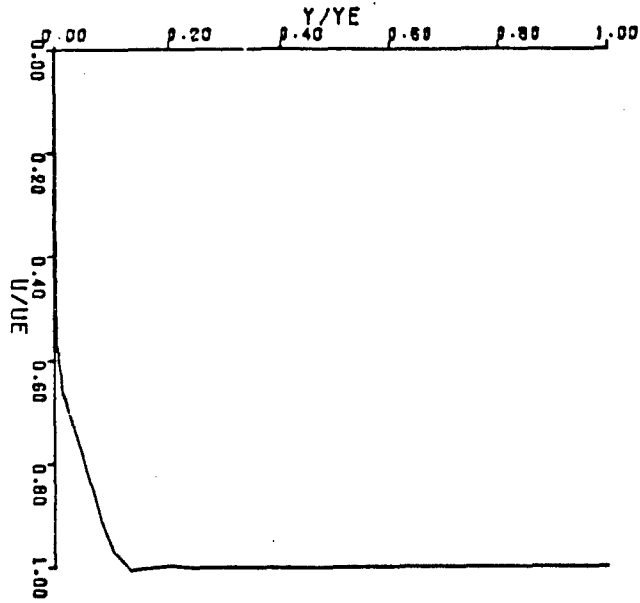
$$= 401$$

APPENDIX III (Cont.)

t_e K

t_e	K
2	1.79 E-6
10	1.60 E-6
100	1.21 E-6
250	4.43 E-7
300	4.87 E-7
350	3.60 E-7
400	4.14 E-7
450	4.09 E-7
1230	2.93 E-7

Sample Calculation For K @ ε = 250

U2 = 1.47253 E4	U1 = 1.46700 E4
S2 = 1.34343	S1 = 1.27068
Pe = 3.97277	Te = 1865
(from Te) = 2.45 E-5	R = 1.10 E2
(from gas luw) = 1.94 E-4	

and $K \approx \dfrac{\mu}{\rho \, U_2^2} \left(\dfrac{U^2 - U_1}{S_2 - S_1} \right) = 4.43$ E-7
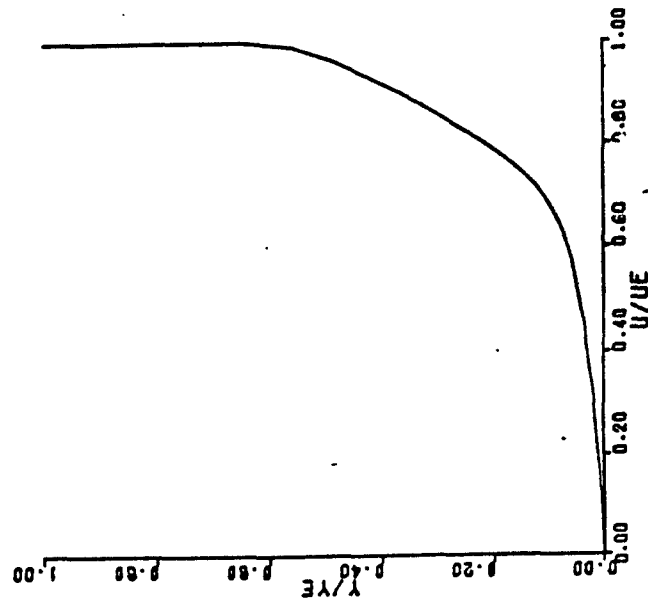
125-18

APPENDIX E.
VELOCITY PROFILES

VELOCITY PROFILE
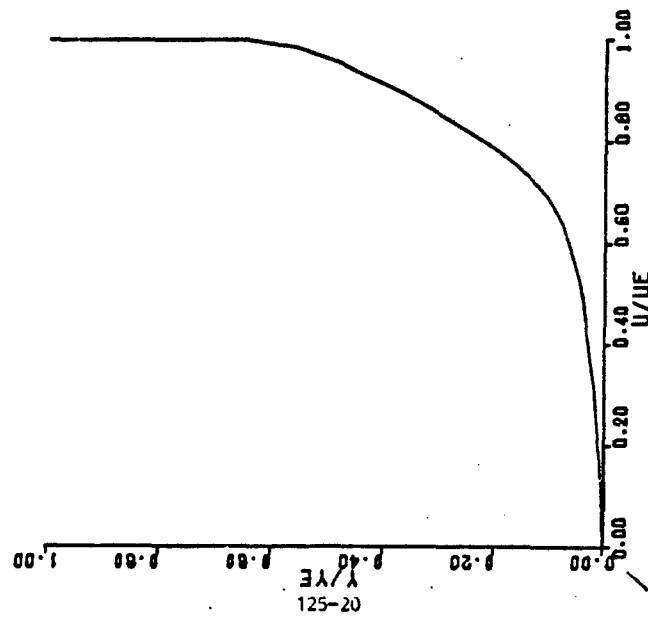EPS = 1.00
R = 0.099
Z = 0.008
UE = 5677.6
YE = 0.0278040

VELOCITY PROFILE
EPS = 200.00
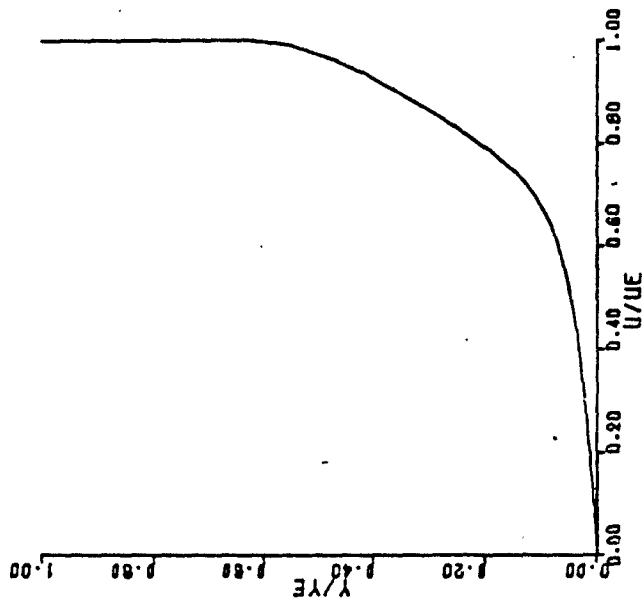R = 0.467
Z = 0.592
UE = 14571.1
YE = 0.0076000

125-19
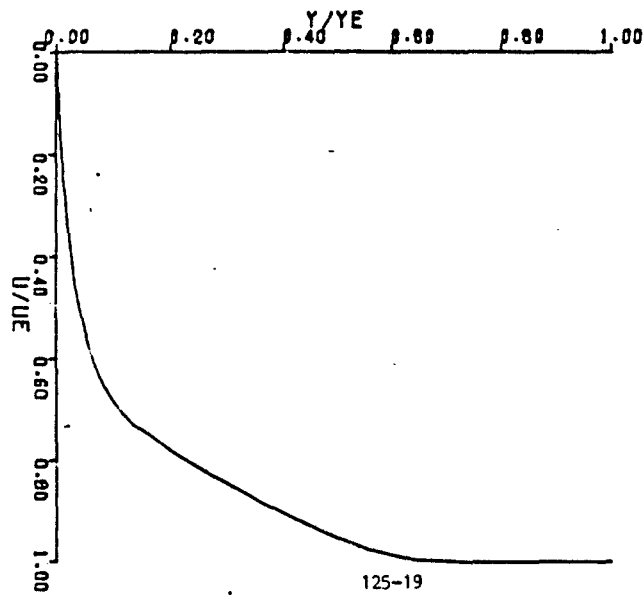
VELOCITY PROFILE
EPS = 350.00
R = 8.617
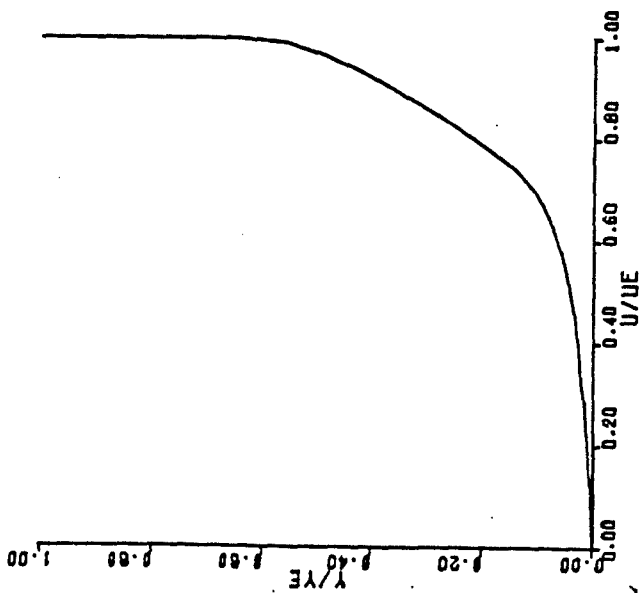Z = 0.944
UE = 14847.4
YE = 0.091872S

VELOCITY PROFILE
EPS = 900.00
R = 8.572
Z = 0.826
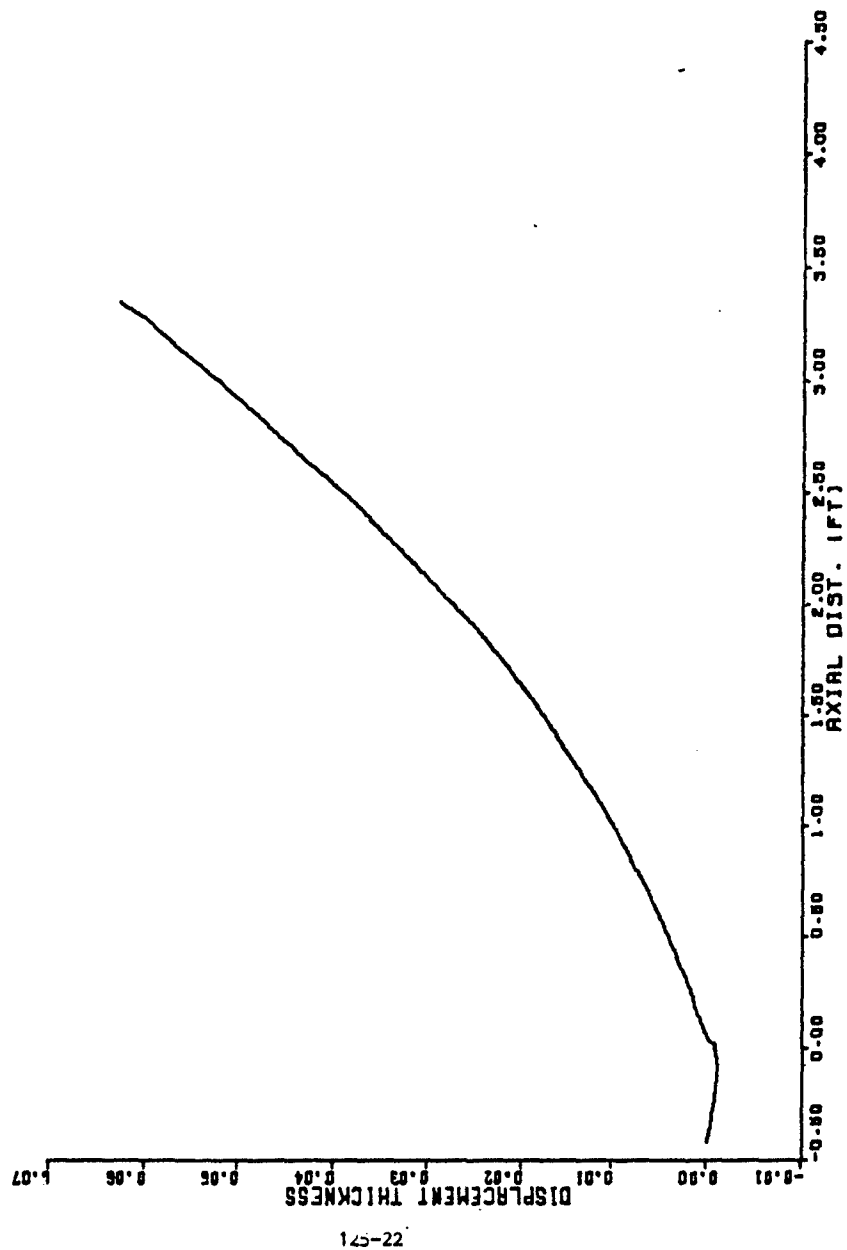UE = 14784.1
YE = 0.0805084

125-20

VELOCITY PROFILE
EPS = 1229.00
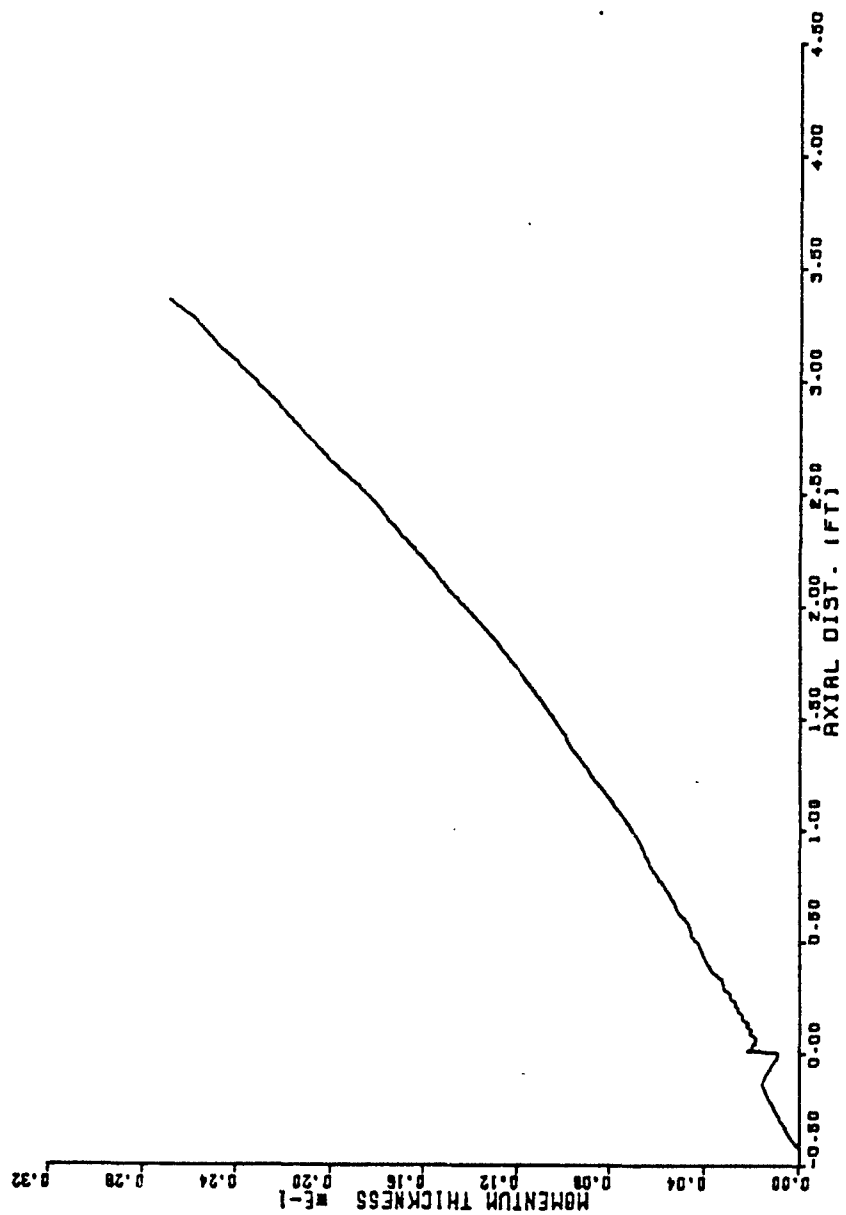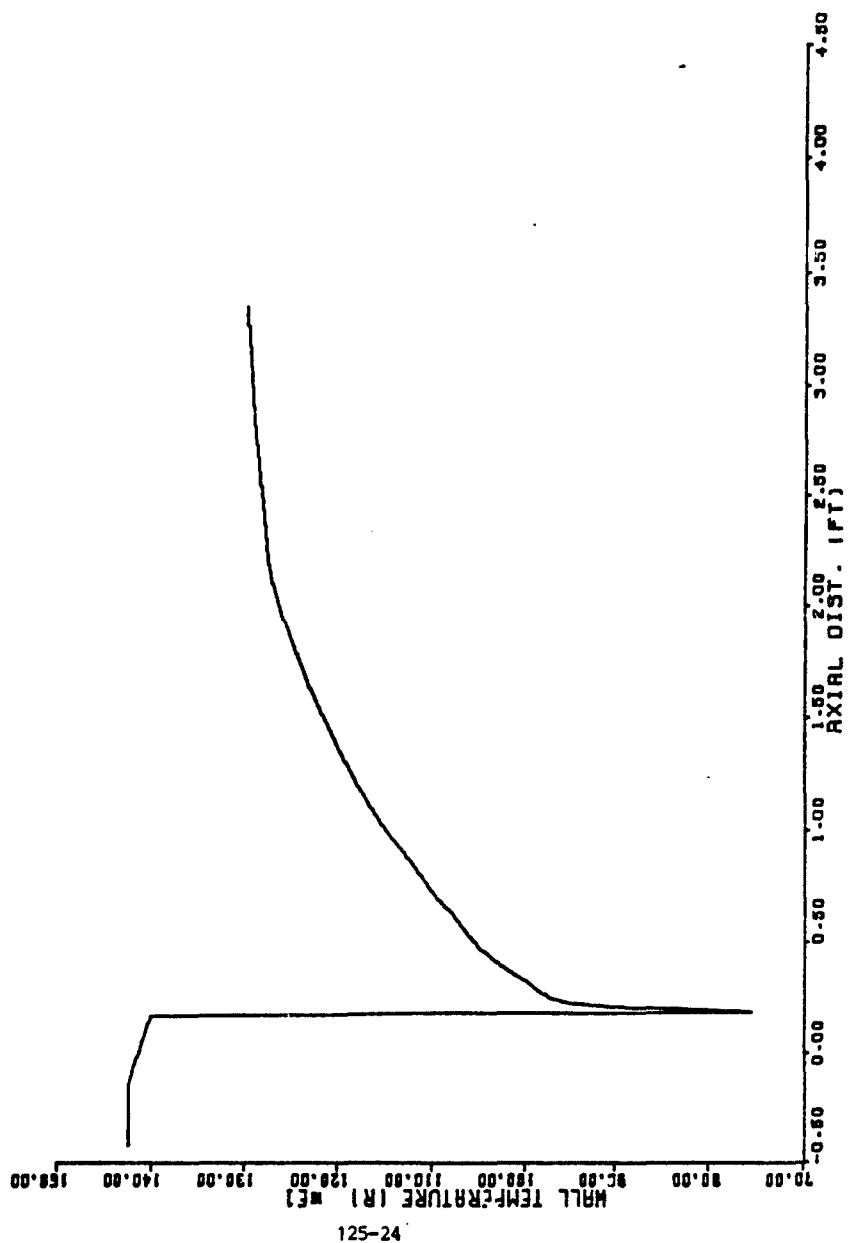R = 1.157
Z = 5.355
UE = 15500.9
YE = 0.4378344

VELOCITY PROFILE
EPS = 490.00
R = 0.660
Z = 1.062
UE = 14914.0
YE = 0.1040207

125-21

AXIAL DIST. (FT)

DISPLACEMENT THICKNESS

125-22

MOMENTUM THICKNESS ⨯E-1

AXIAL DIST. (FT)

125-23

125-24

```
U=1A
$DATA
 ODE=1, ODK=1, NZONES=1, TDK=1, BLM=1, IRPEAT=0,
 ECRAT=5.74,
 IDFF = 1,
 ASUB=5.74,
 NASUB=1,
 ASUP = 2.,10.,100.,250.,300,350,400.,450.,1230.,
 NASUP=9,
 RSI=.396,RWTU=1.5,RWTO=.4,THETAI=19.6,RI=2.2570092,
 IWALL=4, THE=7.5, THETA=52.,
 NWS=18,
 RS(2) = 4.525521,7.118348,10.17437,12.74705,15.62130,
         17.70160,19.93531,22.32207,23.55274,24.90623,
         26.25730,27.64676,29.08603,30.57244,32.09558,33.66819,35.07151,
 ZS(2) = 3.393143,6.412590,10.77932,15.20709,21.06752,
         25.98110,31.96279,39.25118,43.53655,48.36374,
         53.70052,59.64015,66.33606,73.89566,82.41176,92.14554,101.7669,
 RZNORM=1.,
 EPS=1230.,
 $END
REACTANTS
 H 2.                                    00        130.       3124.06    451.06
 O 2.                                              100.      -1422.1     90.890

NAMELISTS
 $ODE
 RKT=.TRUE.,
 P(1)=509.96,PSIA=.TRUE.,XP=1.,
 QFSKED(1)=0.0,JF=.TRUE.,
 $END
REACTIONS    O-H     MAY 3-4 1972   JANNAF PSWG
 H + OH = H2O   , A=7.5E23 , N=2.6  , B=0.,                    HOMER,HURLE
 O + H  = OH    , A=4.0E18 , N=1.   , B=0.,                    BAULCH
 O + O  = O2    , A=1.2E17 , N=1.   , B=0.,                    BAULCH
 H + H  = H2    , A=6.4E17 , N=1.   , B=C.,                    BAULCH
END TBR REAX
 H2 + OH = H + H2O , A=2.19E13, N=0.00, B=3.13,                BAULCH
 OH + OH = O + H2O , A=5.75E12, N=0.00, B= 0.78,               BAULCH
 H + OH = O + H2 , A=7.33E12, N=0.  , B=7.3,                   BAULCH
 O + OH = H + O2 , A=1.3E13 , N=0.  , B=0.,                    BAULCH
LAST REAX
THIRD BODY REAX RATE RATIOS
SPECIES H2,5.,5.,5.,4.,
SPECIES H2O,20.,5.,5.,20.,
SPECIES O2,5.,5.,4.,1.5,
SPECIES H,12.5,12.5,12.5,25.,
SPECIES O,12.5,12.5,12.5,25.,
SPECIES OH,12.5,12.5,12.5,25.,
LAST CARD
 $ODK
 MAVISP=1,JPRNT=-2,EP=1230.0,JPFLAG=0,PI=509.96,XP(1)=1,
 $END
 $TRANS
 MP=150, PMCRIT = 0.,
 $END
 $MOC
 NC=0,
 $END
 $BLM
 IHFLAG = 0,
 KSEGS = 10,
 NTR = 3,
 NTQW = 39,
 XINO(1) = -12.626,
 NTSPS = 10*101,
 RINO(1) = 2.395E2,
 PEO(1) = 506.813,
 TEO(1) = 6434.,
 UEO(1) = 553.159,
 XTQW(1) = -12.626,-11.6,-10.5,-9.5,-8.5,-7.5,-6.5,5.5,-4.5,
           -3.7653,-3.3684,-2.5843,-2.2737,-1.2315,-.93790,-.45273,
           -.29598,0.,.066563,2.5363,4.6458,5.7230,7.3647,6.3513,
           9.8297,10.877,12.065,13.419,14.958,19.499,21.013,26.692,
           31.495,39.026,46.839,58.921,64.424,83.450,101.77,
 XSEG = -12.626,-9.5,-4.5345,0.,2.,15.1653,25.,44.,66.,85.,101.77,
 TQW(1) = 1425.,1430.,1435.,1440.,1450.,1440.,1430.,1400.,1320.,
          1230.,1195.,1123.,1097.,1155.,1210.,1250.,1392.,1433.,
          1235.,585.,550.,946.,967.,984.,998.,1013.,1027.,1041.,
          1055.,1092.,1098.,1125.,1152.,1192.,1232.,1262.,1275.,
          1270.,1300.,
 APROF=1,200,300,350,400,1229, NPROF=5,
 KOTPLT=1,KMTPLT=1,KTWPLT=1,
 $END
TITLE CASE=1 H2/O2
DATA
```

1984 USAF-SCEE SUMMER FACULTY RESEARCH PROGRAM

Sponsored by the

AIR FORCE OFFICE OF SCIENTIFIC RESEARCH

Conducted by the

SOUTHEASTERN CENTER FOR ELECTRICAL ENGINEERING EDUCATION

FINAL REPORT

RAMAN SPECTROSCOPY STUDIES OF EXTRINSIC P-TYPE SILICON

Prepared by: Dr. James Schneider   and   Michael Wager

Academic Rank: Professor   Graduate Student

Department and   Physics Department
    University: University of Dayton

Research Location: Air Force Wright Aeronautical Laboratories
                      Materials Laboratory
                      Electromagnetic Materials Division
                      Laser and Optical Materials Branch

ASAF Research
    Colleague: Dr. Patrick M. Hemenger AFWAL/LMPO

Date: August 25,1984

Contract No: F49620-82-C-0035

RAMAN SPECTROSCOPY STUDIES OF EXTRINSIC P-TYPE SILICON

by

James Schneider
and
Michael Wager

ABSTRACT

Raman spectroscopic studies of extrinsic p-type silicon samples were undertaken at temperatures of 300 K, 77 K, and near 4 K. These samples were conventionally doped with group IIIA elements. Using both incident light of a pulsed, frequency-doubled, Nd:YAG laser at 532nm and near IR laser pulses at 1064 nm, Raman scattering was investigated under several scattering geometries. With 532 nm light, the frequency shift of the LO phonon peak near 520 cm^{-1} in the Raman spectra of strained thin films of silicon on zirconia substrates was investigated by back scattering geometry. The weak Raman spectra from the doped impurities in bulk silicon samples was not observed with the visible incident radiation which is too strongly absorbed to penetrate the bulk of the sample. A study of the effect of a surface depletion layer on silicon samples of various thicknesses when used in Hall measurements to determine carrier concentration was conducted.

Acknowledgement

I. INTRODUCTION

The research and development of high quality extrinsic silicon material for fabrication of infrared detectors for use in operational systems is of continuing importance to the Air Force. The optical and electrical characterization of these materials is necessary for the scientific understanding of the mechanisms and properties that are to be employed in useful devices. Hall effect studies continue to be in the mainstream of techniques that yield interesting and useful details concerning the electrical transport properties of semiconducting materials. Visible and infrared absorption and emission spectroscopies are among the spectral characterization techniques that yield a great deal of information about the electronic excitations in semiconductors. Raman scattering spectroscopy is a useful tool for studying electronic transitions which may be forbidden by selection rules or which occur in experimentally inconvenient spectral regions for infrared spectroscopy.

In this study we consider the application of Raman scattering specroscopic techniques to silicon samples conventionally doped with one of the group IIIA elements such as boron, aluminum, gallium, indium, or thallium. Silicon is a much studied, technologically important, material. The quality and purity of these crystals has been driven by their frequent use as the base materials for sophisticated device fabrication. Among the open questions in silicon that could yield under the continued improvement in state-of-the-art experimental techniques and the availability of higher quality crystals is a better understanding of shallow p-type acceptor impurities such as the group IIIA elements. Raman spectroscopy has been used extensively to study phonon spectra and phonon interactions in pure and doped silicon,[1-7] but comparatively few researchers[8-11] have reported studies of electronic transitions in this semiconductor. In their now classic paper, Wright and Mooradian[8,9] reported on Raman scattering from phosphorus donor and from boron acceptor impurities in silicon. They observed a rather weak, sharp line at 23.4 meV which was attributed to the boron acceptors. Jain, Lai and Klein[11] produced an extensive Raman scattering study of phosphorus-doped silicon which included some observations concerning

antimony and arsenic donor impurities in silicon. Their paper also contained a section concerning their observations on p-type acceptors in silicon. They reported a sharp line at 184 cm^{-1} (22.8 meV) in the Raman spectra of boron-doped silicon which was attributed to an electronic transition associated with the boron acceptor state. In addition, they reported unsuccessful attempts to observe similar transitions in aluminum-doped and gallium-doped silicon samples, and commented on not understanding this absence in their spectra.

Due to the extreme similarity of Group IIIA acceptor absorption spectra, it would seem reasonable to expect transitions similar to the reported boron electronic transition to occur in aluminum, gallium, indium, and thallium-doped silicon. To the best of our knowledge, attempts have only been made in aluminum and gallium-doped samples and these previous negative results were reported some years ago when silicon sample quality was less developed. As was pointed out by Klein[12] in a review on elecronic scattering in semiconductors, it is generally felt that additional theoretical and experimental work is necessary for better understanding of acceptor states in silicon.

It is, however, not an easy experiment to undertake due to a combination of facts. Firstly, while the ratio of Raman to Raleigh scattering intensities is generally in the order of 10^{-8} to 10^{-12}, with incident high power lasers a Raman scattered intensity is, in general, readily detectable. However, Raman interactions in silicon, other than with the LO phonon, are known to be very weak. Signal levels are therefore very low and even small electronic noise such as dark current in the photomultipler detector is a big problem. Secondly, since silicon is not transparent to visible light, lasers operating at near infrared wavelengths must be employed in order to probe the volume of the silicon samples. Detector sensitivity becomes a problem at these IR wavelengths because the only photocathode that even has any sensitivity in that region is the S-1 cathode and its quantum efficiency for the production of photoelectrons is very poor.

II. OBJECTIVES

The research was directed at the spectral properties of acceptor
impurities in silicon crystals doped with various group IIIA elements
(boron, aluminum, gallium, indium, or thallium). The general goal is
to make some contribution to the enhanced understanding of the role of
these dopants in silicon. Raman spectroscopy, which has provided a
great deal of information about electronic transitions in other
semiconductors, was the principal experimental technique that was used
in an attempt to improve and expand the current understanding of the
role of the acceptor levels resulting from these dopants in high quality
silicon semiconductor samples that are now available. Experimental data
was sought over the temperature range from room temperature to cryogenic
temperatures obtained from use of liquid nitrogen and liquid helium
cooling fluids. Information obtained from the Raman scattering data
should compliment the ongoing experimental work in infrared absorption
in these materials at the WPAFB Materials Laboratory.

The first objective was to get a Raman scattering system into
operation and to repeat and verify previously reported results. Since
the LO phonon interaction is the strongest peak observed from both pure
and doped silicon, we sought first to detect and observe this well known
phonon spectra. An existing laser-Raman experimental set-up using a
SPEX triple-monochrometer and a visible 532 nm wavelength pulsed laser
was available for use in this investigation. With a change of output
mirrors this same laser, which provides a an output beam at the 1064 nm
wavelength of the Nd:YAG crystal when the frequency-doubling LiI crystal
is removed, could be used in the eventual desired infrared mode. We
chose to use this laser in the more convenient visible, frequency-
doubled mode in the preliminary phases of the project. For probing the
volume of the samples it was known that the laser would have to be
changed to pulse in the infrared region of the spectrum where the
absorption coeficient of silicon is low. Nevertheless, it was thought
worthwhile to seek some preliminary data from boron-doped silicon with
the experimentally more convenient visible incident laser light probing
near the surface. We sought first to gain experience and confidence with

126-6

this experimental system and its operation. Since there was quite a bit of power available from this laser at 532 nm, we thought it possible, at least, that even weak signals from electronic Raman levels in the Si:B crystals might be detectable using the visible incident light even though it would not penetrate very far into the samples due to the very high absorpion in silicon at this wavelength.

First the optical elements required to effectively get the incident laser light to the sample and to direct the scattered light on the entrance slit of the triple spectrometer were redesigned to be appropriate for this experiment geometry. Then an existing sample holder, capable of temperature dependent studies between room and near 4K, was modified and adapted to this experimental arrangement. The signal detection electronics had to been slightly modified and tested for gated, digital signal processing and recording. Gating the detection electronics to process signals only during time that the laser is providing in input pulse is an effective technique to reduce dark count noise from the photomultiplier detector. The digital signals were recorded on magnetic tape as well as converted to analog signals for observation on chart paper. A microcomputer was used to take the recorded digital data from the magnetic tape and to process this data for presentation and display.

The second stage of the project was to convert to operation with the 1064 nm wavelength of the pulsed Nd:YAG laser. Using the same gated electronic digital signal processing system, a full experimental study of all group IIIA acceptor dopants was planned in available high quality silicon. The study was undertaken in an attempt obtain new data and to advance an understanding of the role of acceptors in silicon.

Two side objectives were considered for possible inclusion in our research program. The first related effort was to use the strongest and more easily observed Raman scattering line attributed to the LO phonon interaction in silicon to investigate the condition of strain in thin samples of single crystal silicon on saphire (SOS) and/or silicon on zirconia (SOZ) insulating substrates. The Raman line from the LO phonon interaction is reported be a rather strong function of the crystal strain and thus it is considered to be a convenient indicator of the

126-7

condition of strain in these thin-film crystals. If time and conditions dictated, a second side objective was to devote some effort to experimental Hall effect measurements. Since Hall measurements are rather routinely undertaken in this branch of the Materials Laboratory at Wright Patterson Air Force Base and the equipment is functional and operating, it was planned that when and if equipment failures or other delays in the laser Raman scattering experiments made the time available, that time would be devoted to Hall effect studies on silicon.

III. RAMAN SCATTERING SYSTEM; EXPERIMENTAL TECHNIQUES

The laser Raman experimental set-up is based on a pulsed Nd:YAG laser, a SPEX triple monochrometer, photon counting detection, and a gated digital signal processing system. Figure 1 shows a schematic representation of this pulsed laser Raman spectroscopy system[13]. The laser is capable of operating in the burst, Q-switched mode which generates about 10 output pulses of approximately 200 nanosecond duration during each 150 to 200 microsecond long bursts. Burst rates are normally set at about 50 per second and the average power delivered is in the order of hundreds of milliwatts with peak power during each of the Q-switched pulses in the kilowatt range.

The basic idea is to reduce unwanted detection of background signals due to stray light and photomultiplier dark current by gating the digital signal detection electronics ON only when there is temporal coincidence with an input laser pulse. A small portion of the incident laser light pulse is reflected onto a PIN diode. The output of this diode unit serves both as a timing pulse and as a means to sample, monitor, and record the incident laser power. A Time Pickoff Unit (Ortec 260) feeds this pulse from the diode to an integrator and sample/hold unit that yields an analog signal representative of input laser power. This analog output is both digitized for digital recording and used as the denominator in a divider (PAR 230 Multiplier Unit) to give a normalized output for analog recording used to visually monitor scans.
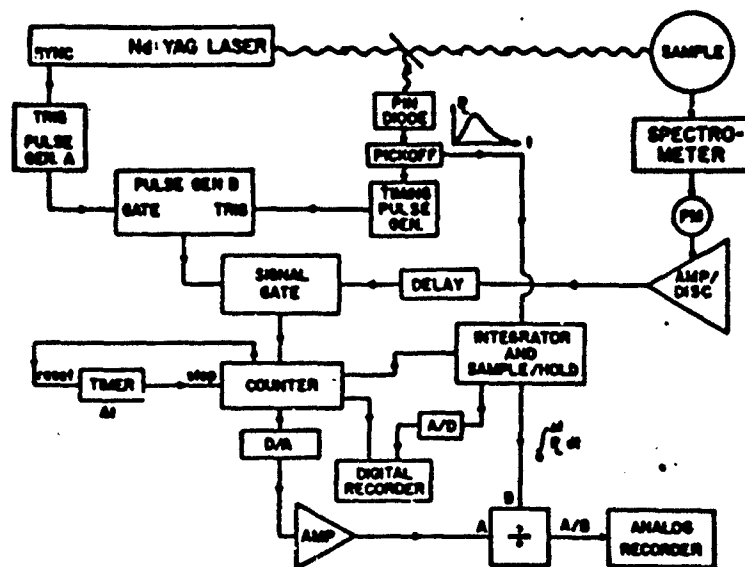
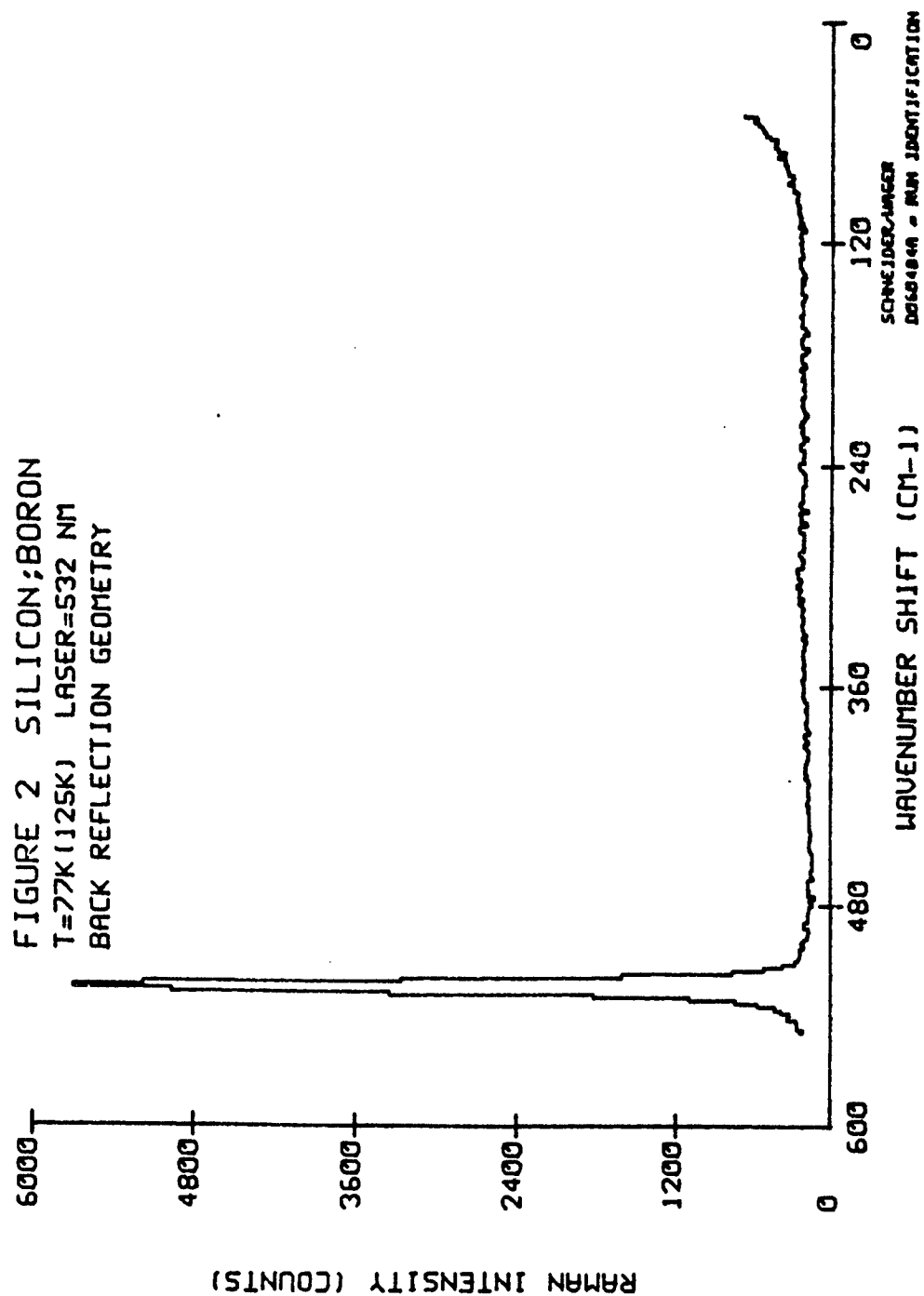Figure 1. Schematic of Pulsed Laser Raman spectroscopy System

This same output from the PIN diode provides a timing pulse (Ortec 403) to trigger a pulse generator (pulse generator B in figure 1; Systron-Donner 100A Pulse Generator). Additionally, the synchronized output from the Chromatix laser lamp flash circuit is used to trigger another pulse generator (pulse generator A in figure 1; portion of PAR CW-1 Boxcar Integrator) that is used to feed the enable gate of pulse generator B in figure 1. In this configuration, pulse generator B provides an output pulse to open a gate to the digital counter (SSR 1120 Photon Counter) only during the time duration of each pulse of the laser, and spurious firing of pulse generator B is virtually eliminated. Since scattered photons detected by the photomultiplier on the exit slit of the spectrometer are counted by the digital counter only during the short time (100-200 ns) that the laser is active, background signal from photomultiplier dark current, fluorescence, ambient light, etc., are essentially reduced to near zero and weak signals are observable. Typical operation is to hold at a spectrometer setting for a fixed number of input laser pulses, with signal to noise ratio improved at larger numbers of input pulses.

Three digital signals are recorded for each setting of the spectrometer, the scattered photon count from the counter, the digitized output from the integrator and sample/hold circuit that is proportional to the incident laser power, and a digitized signal from the spectrometer setting that gives the wavenumber shift measured from the incident laser wavelength. These three signals are processed through a PAR Series 260 multiplexer unit and recorded on magnetic tape (Texas Instruments Silent 700 ASR data terminal) for subsequent processing. The digital output of the photon counter is also converted to an analog signal for analog recording on an x-y plotter used primarily as an operator monitor

IV. RAMAN SCATTERING SPECTRUM OF Si WITH VISIBLE LIGHT

Samples are mounted on a cold finger of an Air Products Heli-Tran using either liquid nitrogen or liquid helium cryogenic fluids. Figure 2 show a typical spectrum from a silicon sample with boron concentration of 10^{17} in the back reflection geometry. The cold finger was at 77K and the sample was under 125K. The spectrometer was held at a fixed wavelength counting scattered photons for an interval determined by 4000 incident laser pulses. The only strong feature is the silicon LO phonon interaction at 523 cm^{-1} shift below the energy of the 532 nm incident laser wavelength. No features associated with a boron acceptor impurity is discernable.

Figure 3 shows two scans on the same crystal taken with the sample on the 4K cold finger, but with different scattering geometries. The scale is amplified to look for features in the spectrum (LO phonon counts at the 524 cm^{-1} peak were near 8000). In back reflection, the background count is several hundred counts per 4000 laser pulses, due either to weak Raman signals or stray laser light reflecting its way through the spectrometer to the detector as noise. The lower curve is for a geometry with the incident laser light directed nearly parallel to the surface and the collected scattered light at 90 degrees to this incident beam. Note the background reduced to only several per 4000

FIGURE 2 SILICON;BORON
T=77K(125K) LASER=532 NM
BACK REFLECTION GEOMETRY

WAVENUMBER SHIFT (CM-1)

RAMAN INTENSITY (COUNTS)

SCHNEIDER/AMGER
D060894 - RUN IDENTIFICATION

126-11

FIGURE 3 SI;B #1152
T=4K(35K) LASER =532 NM
BACK REFLECTION   GLANCING (90°)

RAMAN INTENSITY (COUNTS)

WAVENUMBER SHIFT (CM-1)

SCHNEIDER/UNGER
D860884 = RUN IDENTIFICATION

126-12
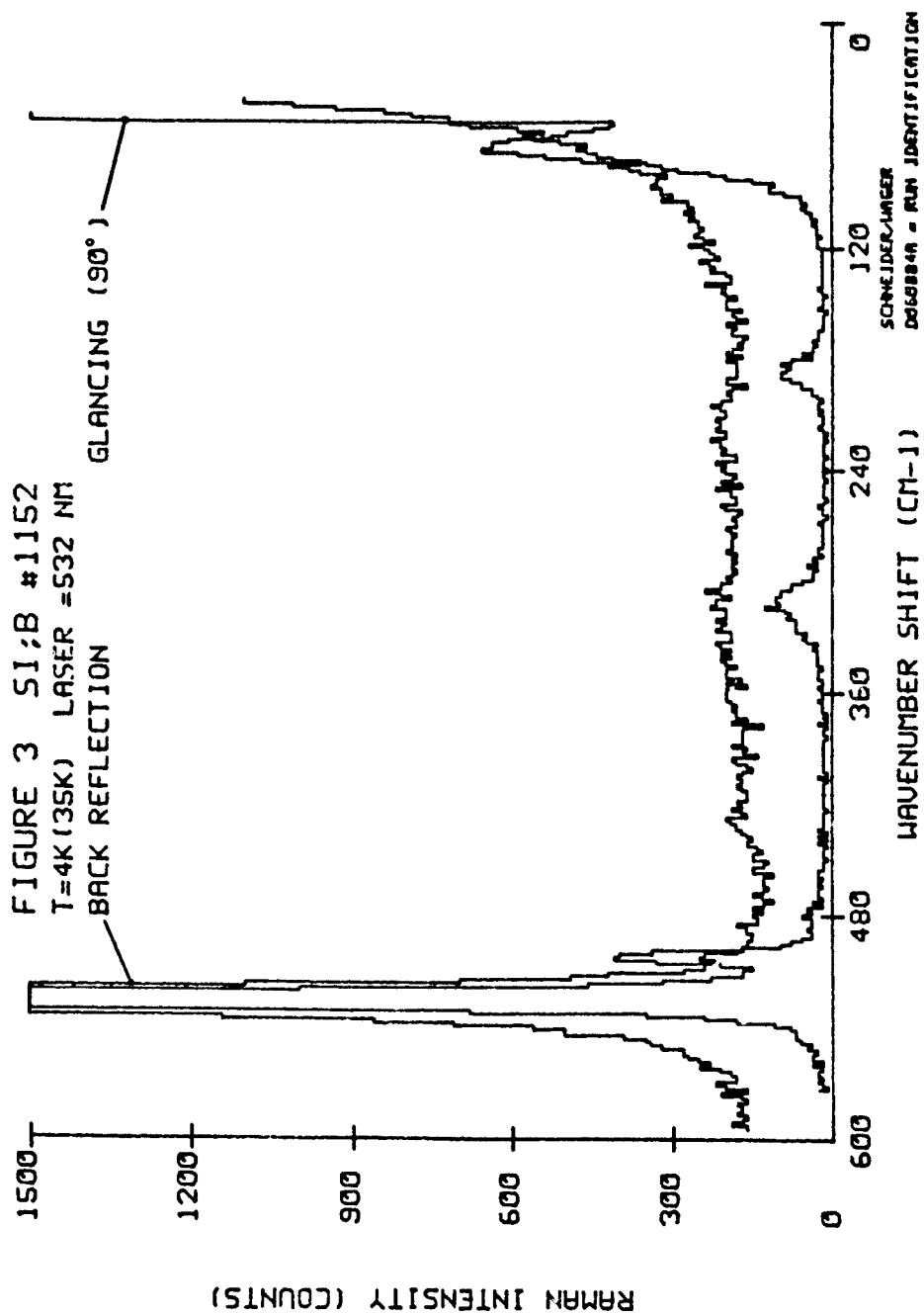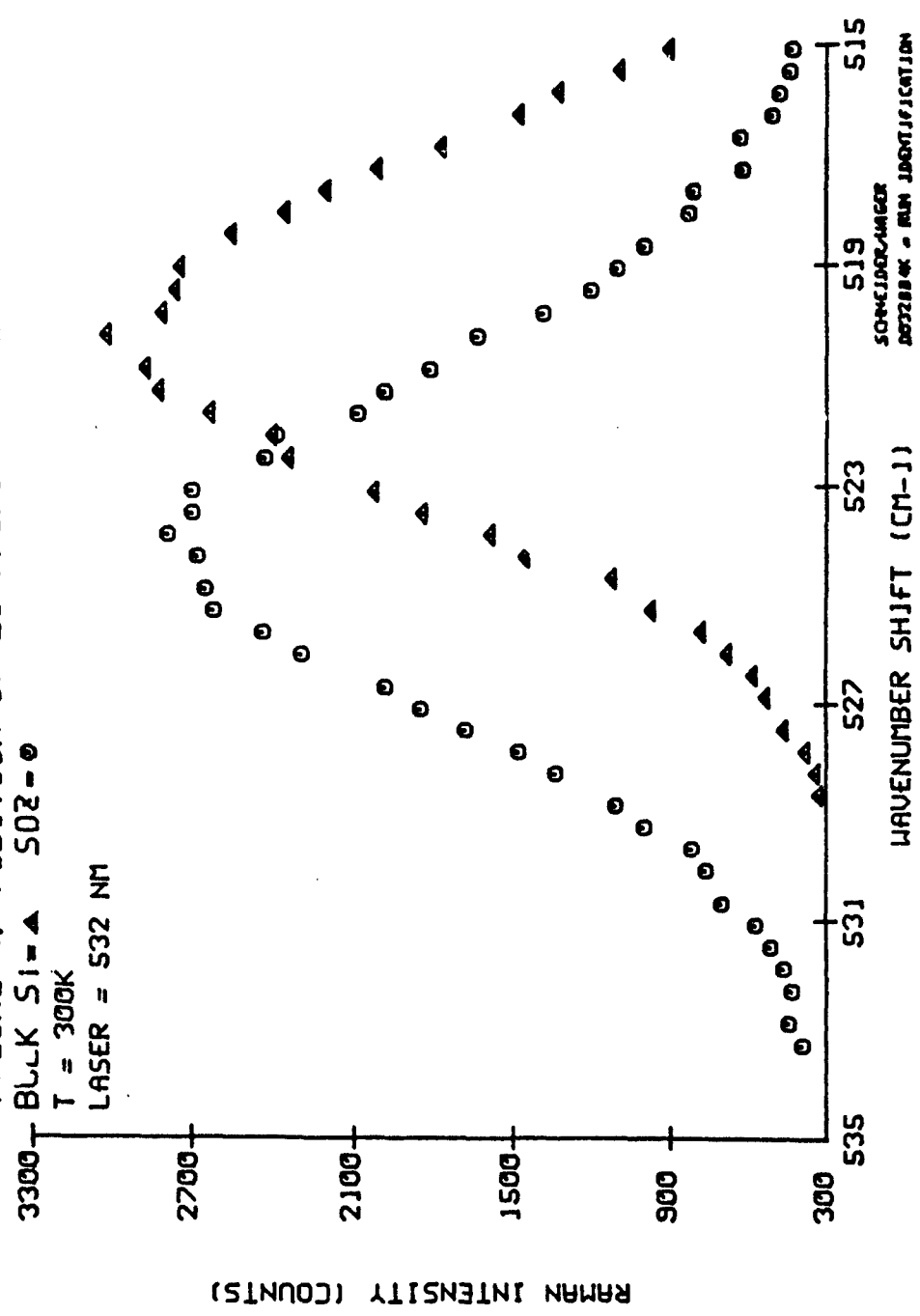
FIGURE 4. POSITION OF LO PHONON PEAKS
BULK SI = ▲   SO2 = ⊕
T = 300K
LASER = 532 NM

126-13

laser pulses with this geometry the less specularly reflected light scatters into the spectrometer slit than with back reflection geometry. The two "peaks" in this Raman spectrum were at first thought to be the previously reported[8,11] boron electronic Raman line at 184 cm^{-1} (23 meV) and weak lattice phonon lines near 306 cm^{-1} (37.9 meV). Attempts to repeat this data on the same sample revealed that the "peaks" were actually artifacts that resulted from an increase in the specularly reflected light from the sample that occurred when we were actually burning pit holes in the sample periodically, and it just happened to occur on the run shown at the time when the spectrometer was at 184 cm^{-1} the position. It became obvious that highly absorbed visible light was not going to permit the observation of electronic Raman features.

Visible laser light at 532 nm was useful only for the strong LO phonon peak determination. A side project to use the position of this phonon peak to determine strain conditions in thin silicon films on zirconia (SOZ) and on saphire (SOS) substrates was very successful. A sample of the observed several wavenumber shifts to higher energy in strained silicon films is shown in figure 4. The strain calculated from such shifts correlated well with x-ray measurements, and were much more convenient.

V. RAMAN SCATTERING SPECTRUM OF Si WITH IR LASER LIGHT

It was obvious in hindsight that the 1064 nm line from the YAG laser should be used to investigate silicon. At low temperatures, this corresponds to a region of low absorption and the volume of the sample can be probed. Several experimental snags were however encountered in short order. First, the existing spectrometer with a pair of 1200 g/mm gratings could not mechanically be turned past 1.0 micron position, and we needed to work in the 1064 to 1130 nm range. Gratings with 600 g/mm were needed, but not available for months. An attempt to borrow 600 g/mm gratings from other groups at the lab was partially successful in that two were found from different researchers, but both were blazed at angles that were inefficient for 1100 nm light (one blazed at 600 nm
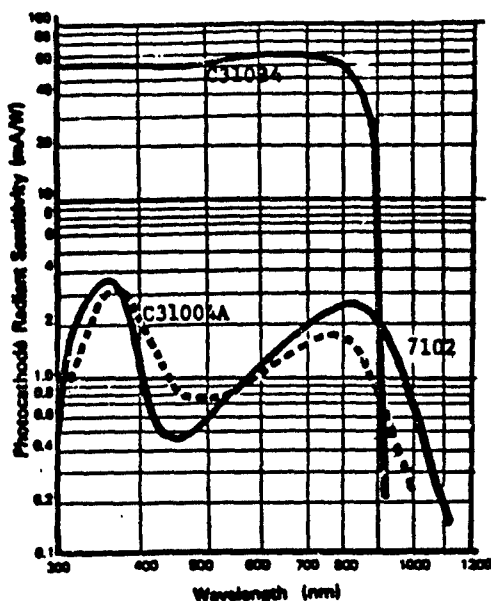
Figure 5. Spectral Response

wasn't too bad, but the one blazed at 1850 nm gave only a few percent transmission at 1100 nm as expected from grating efficiency curves). Next, the existing (very efficient in the visible) C31034 end window photomultiplier had to be replaced by one with S1 response. The only tube available with S1 response was a C31004A side window tube that did not fit in the existing cooled housing. PM tubes with S1 photocathodes must be cooled to reduce dark current noise. Dark emission is reduced by an order of magnitude for every 20 degrees cooling (Dark emission from 10^7 electrons per sec per cm^2 at +20C to 10^4 e s^{-1} cm^{-2} at -40C). Two cooled PM housings were designed and built for the side window C31004 tube, one using liquid nitrogen and the other using thermoelectric coolers. They worked well to reduce dark current, but detected signals near 1100 nm and beyond in that spectrometer with inefficiently blazed gratings and the cooled C31004A PM tube were extreemly weak. Essentially no Raman signal was detectable, even from the stronger phonon interactions in silicon. A closer investigation of tube response revealed that the C31004 tube is a reflective photocathode type. While it has a Ag-0-Cs photocathode like other S1 Class tubes, its extended IR sensitivity is not good compared with the transmisive photocathode types like the 7102 end window tube. It became obvious what was necessary to do this experiment, but it was not going to be possible to accomplish the task during the tenure of the SCEEE Fellowships. A pair of 600 g/mm gratings blazed for efficiency at 1.0 or 1.2 microns and a super-cooled photomultiplier housing with an end window, transmissive, photocathode photomultiplier tube selected for extended IR range sensitivity were necessary. All are available for reasonable costs, but not in a reasonable time frame.

126-15

VI. HALL EFFECT STUDIES

The Hall effect is a valuable tool for studying semiconductor material. From Hall measurements the type of electronic carrier, the number of carriers per unit volume, and their mobility can be obtained. By taking Hall data over a wide range of temperatures, the carrier concentration information can yield the identity of and the concentration of the electrically active impurites. Since an experimental Hall measurements apparatus was available in the Materials Laboratory along with high quality "pure" bulk samples of silicon, attention was directed for the balance of the research period was directed at a study of the possible effect of surface depletion layers on carrier concentration determinations.

In a piece of high purity silicon, a quadravalent substance, the surface of the material will have many "unbonded sites." The electrons from these bonds can move into the bulk of the material and leave the surface of the material with a positive charge. Samples are normally prepared by treating the silicon material with acid solutions which removes the outer layer of oxidized and damaged silicon. A new oxide layer is carefully grown on the surface by immersing the sample in boiling distilled water. With a "perfect" oxide present, the surface is electically neutral but for any realistic situation there may be a small positive charge left at the surface. This gives rise to a small region of depleted carriers called the depletion region. Depending on the quality of the oxide grown, this region is estimated to have a thickness from 1-100 microns. The question posed is whether or not the depletion region significantly affects the measured carrier concentration. The depletion region is an insulating region in the sample. Current equations used for calculating carrier concentration include the thickness, t, of the sample used but they do not account for the

```
xxxxxxxxxxxxxxxxxxx d  T        d = thickness of depletion region
  :               :    |  t     t = measured thickness
  :               :    |        t-2d = true(effective) thickness
xxxxxxxxxxxxxxxxxxx d  ⊥
```

$$P_{measured} = P_{true} \left(1 - 2d/t \right)$$

126-16

possible presence of the depletion region. For thick samples the effect is negligible but for thin samples with true or effective thickness of t-2d the effect on hole concentration, p , could be quite significant.

In order to study the effects of the thickness of the depletion region, Hall measurements using the Van der Pauw technique were planned on a set of high quality silicon samples. We elected to make a series of measurements, beginning with three identically prepared samples each having a thickness of about 2 millimeters. Standard laboratory procedures were followed and Hall runs were undertaken on the three samples. These same three samples were then thinned to about 1 millimeter, repolished, and processed for a second set of Hall measurements. Subsequent thinning and polishing to smaller and smaller thicknesses of about 0.5 millimeters, 0.25 millimeters, etc., were anticipated. Before the Hall measurements were taken, the three sample set was cleaned in a boiling soution of alcohol followed by a boiling solution of diluted hydrochloric acid and rinsed in distilled water. The physical thickness of each sample was then measured. The oxidized silicon layer was etched off in a room temperature solution of hydrofluoric acid and then a new oxide layer was grown on the silicon samples in a twenty minute bath of boiling distilled water. The process was intended to ensure that the surface of each of the samples was treated identically.

The data generated by the Hall apparatus was then processed through computer programs to yield plots of carrier concentration, resistivity, Hall mobility, and Hall coefficient against temperature. Measurements have been completed on all three samples at the first two thicknesses. All three samples survived and have been turned back to the lab's crystal polishing technician for continued thinning. Since we a located physically close to the Materials Laboratory at Wright Patterson Air Force Base, it is anticipated that we will maintain contact and continue to be involved in this series of experiments after our official tenure as SCEEE fellows has terminated. Shown in figure 6 is a representitive comparison plot of carrier concentration against temperature on one of the three samples. The two curves result from different sample thickness of the same sample. The top curve (using +
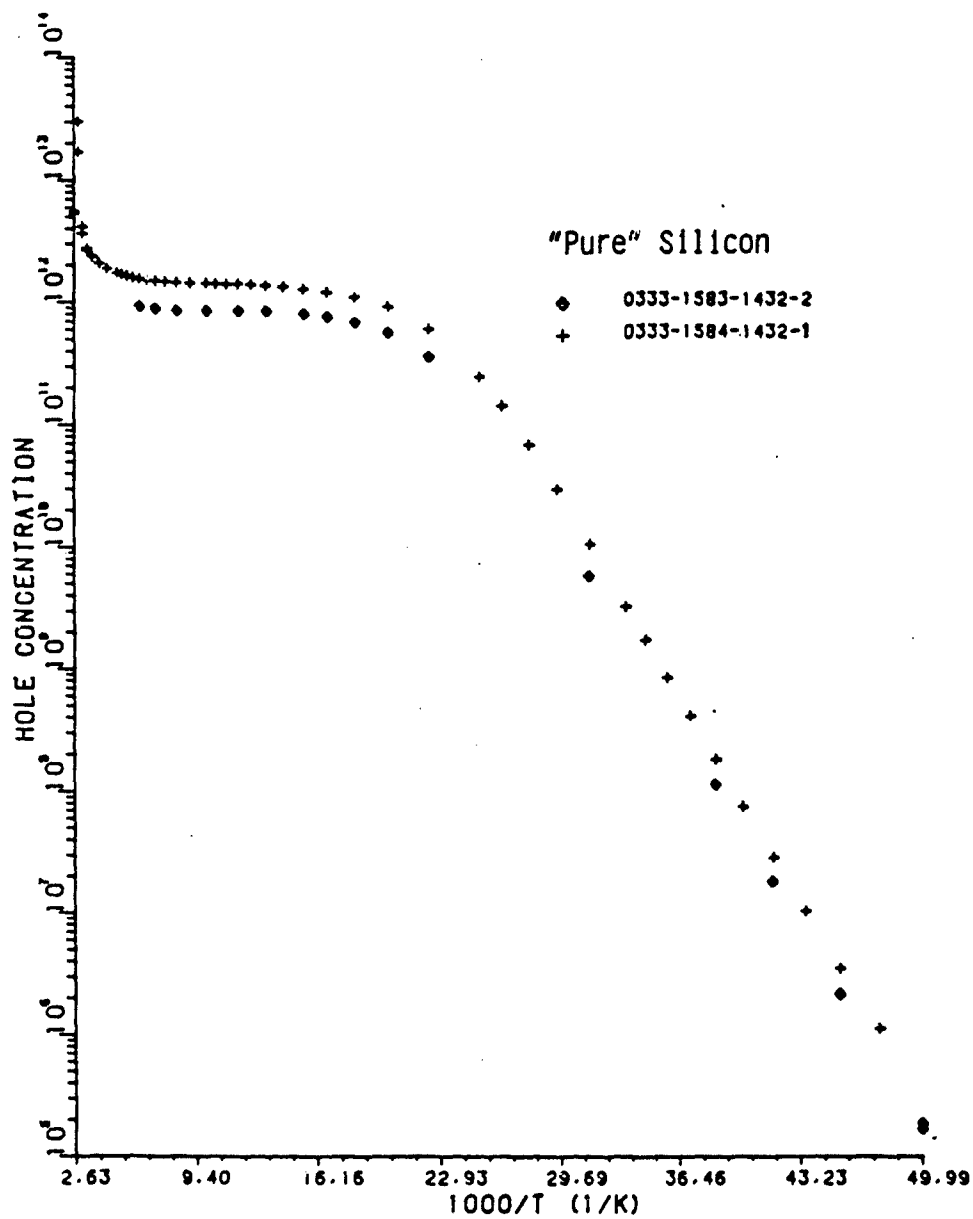
Figure 6. Hole concentration as a function of temperature for two
thicknesses of the same sample. + = 2 mm , ◆ = 1 mm

symbols) is for the sample at a thickness of two millimeters; the lower curve (using symbols of a point in a box) is for a thickness one millimeter. Each of the three samples exhibited this same phenomenon. The slope of the straight line portion gives the activation energy of the carrier. The carrier is boron which is always present in "pure" silicon. The leveling off of the curve represents the fact that the temperature is high enough that all the carriers of that type have been activated. At this time it is not clear as to whether the hopefully identical depletion regions in samples of different total thickness has affected the carrier concentration determination significantly. Obviously additional runs at smaller thicknesses are necessary before any firm conclusions are drawn from this data.

VII. RECOMMENDATIONS

Three additional pieces of equipment are needed to do a Raman study of silicon doped with group IIIA elements on the Raman apparatus used in this study. A pair of gratings with 600 g/mm that are blazed for high reflectance in the 1100 nm range, a super-cool photomultiplier housing to reduce dark current in the S1 type photocathode of the photomultiplier, and a selected, extended infrared range, photomultiplier with transmissive front window photocathode. The area of the photomultiplier's photocathode should be small since that will also reduce the dark current in the tube, and the image of the spectrometer slit at the photocathode is not large. A Hamamatsu R632A tube selected for a high red to total response ratio would be a good choice.

Additional studies of these impurities in silicon seem to be warranted at this time due to the availability of high grade silicon materials and the questions that remain concerning the existence of electronic Raman scattering from acceptors in this material. It's a difficult experiment in this infrared range, but has a good chance of some success with an efficient Raman detection system at these wavelengths.

126-19

REFERENCES

1. J. P. Russel, Appl. Phys. Lett. 6, 223 (1965)

2. J. H. Parker, Jr., D. W. Feldman and M. Ashkin, Phys. Rev., 155 (3) 712 (1967)

3. R. K. Chang, J. M. Ralston and D. E. Keating, Light Scattering Spectra of Solids, Edited by G. B. Wright (Springer-Verlag 1968)

4. Paul A. Temple and C. E. Hathaway, Phys. Rev. B 7 (8), 3685 (1973)

5. B. A. Weinstein and Manuel Cardona, Solid State Com., 10, 961 (1972)

6. K. Uchinokura, T Sekine and E. Matsuura, Solid State Com., 11, 47 (1972)

7. K. Uchinokura, T Sekine and E. Matsuura, J. Phys. Chem. Solids, 35, 171 (1974)

8. G. B. Wright and A. Mooradian, Phys. Rev. Lett., 18 (15), 608 (1967)

9. G. B. Wright and A. Mooradian, Proc. 9th Intern. Conf. Physics of Semiconductors, Moscow, 1067 (1968)

10. J. M. Cherlow, R. L. Aggarwal and B. Lax, Phys. Rev. B, 7 (10), 4547 (1973)

11. Kanti Jain, Shui Lai and M.V. Klein, Phys. Rev. B, 13 (12), 5449 (1976)

12. M. V. Klein, Light Scattering in Solids, Ed. M. Cardona, (Springer-Verlag, 1975, 1983-2nd)

13. P.P. Yaney, J. Raman Spectry., 5, 219, (1976)

1984 USAF-SCEEE SUMMER FACULTY RESEARCH PROGRAM

Sponsored by the

AIR FORCE OFFICE OF SCIENTIFIC RESEARCH

Conducted by the

SOUTHEASTERN CENTER FOR ELECTRICAL ENGINEERING EDUCATION

FINAL REPORT

BACTERIOLOGIC TECHNIQUES FOR THE ISOLATION AND IDENTIFICATION
OF LEGIONELLAE

Prepared by: Gordon D. Schrank

Academic Rank: Associate Professor

Department and University: Department of Biological Sciences

                                     St. Cloud State University

Research Location: Epidemiology Division

                                     School of Aerospace Medicine

                                     Brooks AFB, Texas 78213-5000

USAF Research: Dr. Jerome P. Schmidt

Date: August 17, 1984

Contract No.:   F49620-82-C-0035

BACTERIOLOGIC TECHNIQUES FOR THE ISOLATION AND IDENTIFICATION

OF LEGIONELLAE

by

Gordon D. Schrank

ABSTRACT

Efforts were directed at providing methods for the tentative
identification of Legionellae submitted for characterization and
determining if routine isolation of Legionellae from environmental samples
is feasible without the use of laboratory animals or embryonated eggs.
The three major groups of Legionellaceae can be differentiated using dye
containing media; these groups include the genus Legionella and proposed
genera Tatlockia and Fluoribacter. Other tests useful for tentative
separation of species include brown pigment production on media containing
aromatic substrates, growth in the presence of 1% NaCl, the results of
a modified hippurate test, and the oxidase reaction. Further research
is needed to insure that these organisms can be isolated from environmental
samples. Current pretreatment and plating media were found to be
inadequate for the routine recovery of Legionellae when present in low
numbers. Suggestions for further research are included.

I. INTRODUCTION:

Members of the family _Legionellaceae_ are somewhat unusual Gram negative
rods that are found in numerous aquatic environments and may be the cause
of respiratory illness in humans. The term "Legionnaires' Disease" refers
to illness caused by _Legionella pneumophila_. However, it is now clear
that similar infections have occurred throughout the United States and
other parts of the world and that _L. pneumophila_ and related organisms
in the family _Legionellaceae_ are responsible for these illnesses.

Members of the family _Legionellaceae_ are rods which measure about
0.3 to 0.9 μm in width and may be 2 to 20 μm in length (Brenner, et al.
1984). The longer filamentous forms are more common in laboratory
cultures; short rods are most commonly seen in infected tissues. They
are Gram-negative but stain poorly by the conventional Gram stain. This
reaction may be enhanced by substituting carbol fuchsin for safranin in
the Gram staining procedure. The organisms are flagellated and require
L-cysteine-HCl and iron salts (ferric pyrophosphate or ferric nitrate)
for growth. These organisms are best cultured in the laboratory on a complex
medium containing yeast extract, activated charcoal, alpha-ketoglutarate,
potassium hydroxide, and agar as well as the cysteine and iron salt.
The addition of ACES buffer (N-2-acetamido-2-aminoethane-sulfonic acid)
enhances growth by buffering the pH of the medium between 6.85 to 7.0.
The organisms do not grow on conventional blood agar or numerous other
media. A defined medium has also been described for the organisms (Warren
and Miller, 1979).

Other characteristics of Legionellae include a positive catalase test
and a negative or weakly positive oxidase reaction. The organisms liquefy

gelatin and are negative for urease and nitrate reduction. They do not
ferment carbohydrates. Therefore, growth of the organisms in the
laboratory requires specialized media and identification of species is
based on a few characteristics. Final identification requires direct
fluorescent antibody testing, gas liquid chromatography, and
deoxyribonucleic acid (DNA) hybridization (Weaver and Feeley, 1979).

The Microbiology Section of the Epidemiology Division is a reference
center for Air Force clinical laboratories throughout the world. The
personnel at this lab have received requests for confirmation and
identification of Legionellae. Because these organisms are relatively
new to the clinical laboratory experience, laboratory personnel have not
set up procedures for isolation and identification of Legionellae. These
organisms may be a part of the flora of cooling towers and institutional
hot water systems. Therefore, in addition to the need for information
on tests for confirming a clinical isolation of Legionellae, laboratory
personnel wished to investigate the feasibility of isolating the organisms
from environmental sources without the use of laboratory animals.

My experience in microbiology includes work in a clinical laboratory
as well as a contract involving Brucella sp. Therefore, I had experience
with clinical microbiology as well as fastidious bacteria which require
special isolation techniques. In addition, the Brucella are organisms
with considerable pathogenic potential for laboratory workers. Experience
in working with such organisms provides an increased sense of laboratory
safety necessary for working with bacteria which may be transmitted to
personnel by the aerosol route.

II. OBJECTIVES:

The objectives of this project are listed below:

Major Objective:

The major objective of this research is to prepare working protocols for the isolation and identification of Legionella pneumophila and other organisms in the family Legionellaceae.

Detailed Objectives:

1) Research all previously described commercial or in-house prepared media used for growing Legionellae.

2) Determine what media and reagents should be purchased commercially and those which should be made in-house.

3) Determine biochemical tests required for the identification and differentiation of Legionellae. Such tests include staining, colonial morphology and pigmentation, dye sensitivity, catalase and oxidase determinations, fluorescent staining and others as determined by literature review.

4) Develop a simple, rapid protocol to isolate such organisms from both clinical and environmental specimens.

5) Develop flow charts that may be used for processing specimens and for characterizing Legionellae isolates. These flow charts must be detailed for the purpose of standardizing laboratory procedures with changes in laboratory personnel.

6) Once the above objectives have been completed, determine if Legionellae may be recovered from aquatic organisms such as protozoa and insect larvae.

Because of the growth rate and difficulty of isolating Legionellae from mixed cultures, it was agreed that these objectives were reasonable for the ten week research period. A complicating factor involves the

recent isolation of numerous new species of Legionellae which must be differentiated from known strains. This aspect of the project clearly demonstrates the need for future research relating to specific isolation and differentiation within this group of organisms particularly when final identification is based on techniques not routinely used in most clinical laboratory settings (i.e., fatty acid extraction and analysis and DNA hybridization).

II. NOMENCLATURE:

The nomenclature of Legionellae is rather complex because this group of organisms has only recently been described. The organisms used in this study are described in Table 1. Both the original and proposed names are shown along with spelling variations (Brenner, et al. 1984; Vickers and Yu, 1984).

III. CULTURE MEDIA:

Culture medium bases, from commercial sources and or prepared in-house, were compared for usefulness in culturing the eight test organisms. Historically, Legionellae have been cultured both in vitro and in vivo. In vivo methods include the use of guinea pigs and embryonated chicken eggs. In vitro culture has been accomplished using a number of media including Mueller-Hinton Agar enriched with ferric pyrophosphate and L-cysteine. Charcoal yeast extract (CYE) agar replaced this medium. Further research led to the modification of CYE agar to include apha-keotglutarate and ACES buffer (BCYE agar; Feeley, et al. 1979). Difco Laboratories has recently made the BCYE agar base available commercially. The Mueller-Hinton agar was tested and found to be suitable only for the cultivation of L. pneumophila. The other Legionellae did

127-6

not grow on this medium. Another medium tested contained a commercial supplement prepared by Oxoid Laboratories. This medium supported the growth of L. pneumophila, L. micdadei, and L. bozemanii. Both L. micdadei and L. bozemanii grew poorly on this medium. Oxoid also previously supplied an antibiotic supplement containing colisitin, vancomycin, trimethoprim, and amphotericin B that may be added to the basal medium. This supplement inhibited the growth of all the Legionellae except L. pneumophila. Addition of this antibiotic supplement to the Difco BCYE agar inhibited the growth of L. dumoffii, L. bozemanii, L. longbeachae, L. jordanis, and L. gormanii. Only L. pneumophila grew well on the medium while L. micdadei and L. wadsworthii grew poorly. It is clear that the BCYE agar is superior for the growth of the Legionellae tested. The medium may be prepared from components or from the commercial Difco base to which the Difco supplement containing ferric pyrophosphate and L-cysteine is added. The commercial medium as prepared is quite satisfactory and provides for excellent growth of all strains tested. The commercial preparation usually gives the optimum pH without adjustment. The in-house version of this medium appears more granular due to the size of the charcoal particles.

IV. CULTURE CONDITIONS AND PRESERVATION OF STOCK CULTURES:

All Legionellae tested grew well when incubated at 35°C in the presence of 2.5% CO_2. Although we found no difficulty in growing the organisms in the presence of 6% CO_2, numerous references in the literature would indicate that this concentration of gas may be toxic to fresh isolates (Balows, et al. 1981). Therefore, it seems that all culture work should be done in a candle extinction jar incubated at 35°C. We found that all

eight Legionellae grew more slowly at 25°C.

Stock cultures may be maintained on BCYE agar slants at room temperature for at least two weeks. Refrigeration reduces viability. Most strains tested at CDC survive for at least 16 weeks on these slants. We also found that the organisms could be frozen in tryptic soy broth or CYE broth containing 10% glycerol. The BCYE glycerol mixture seems to be somewhat better for maintaining the viability of L. wadsworthii and L. longbeachae.

It is noteworthy that several authors have found that reconstituting Legionellae with saline decreases viability (Balows, et al. 1981). All transferring of organisms where sterile 0.85% saline would be used should be done with sterile water.

V. STAINING AND OTHER TESTING:

Legionellae may be stained by the conventional Gram stain. However, these Gram negative organisms stain poorly with safranin even with prolonged contact with the dye. Therefore, other staining methods are advisable and several were tested including a modified Gram stain procedure which employs carbol fuchsin as a counterstain. This staining procedure gives excellent results. The Gimenez method may be used to stain organisms which hav. been grown in yolk sacs. Although the stain may be used with conventional cultures, the organisms do not stain as intensely as with the modified Gram stain.

Staining with Sua·n black B solution may be used to demonstrate blue-black or blue-gray droplets in the cytoplasm of the organisms. There is some variability among species with regard to the abundance of lipid. However, a.. eight organisms were positive for lipid inclusions.

Direct fluorescent antibody staining was performed using conjugates prepared at the Centers for Disease Control. It is suggested that this test be performed on isolated cultures as well as environmental or patient isolates. We used a polyvalent conjugate to test for the presence of L. pneumophila in environmental samples. The conjugate, as prepared, gave some cross reactivity with environmental organisms which morphologically did not fit the description of Legionellae. However, this test is necessary to determine the relative numbers of organisms which may be present in a sample. Newer monoclonal antibody preparations should be tested when they become commercially available (Antibodies, Inc.).

VI. TESTING OF KNOWN LEGIONELLAE:

The organisms all require L-cysteine-HCl and none grow on conventional blood agar. None produce acid from carbohydrates and carbohydrate testing requires a special basal medium (Weaver and Feeley, 1979). All strains are positive for catalase. This test may be performed on a slant using 2-3 ml of 3% hydrogen peroxide or by placing a loop of inoculum in a drop of hydrogen peroxide. It should be noted that the growth needs to be broken up slightly so that the organisms and the peroxide mix well. This may be accomplished with a capillary pipet or by other appropriate methods. Gelatinase activity may be demonstrated using a strip of black and white film that is placed in a 0.5 ml turbid suspension (McFarland standard No. 1) of organisms in a 13 x 100 mm test tube. The tube should be incubated in 2.5% CO_2 for 48-72 hours at 35°C. We noted that a conventional gelatinase test is usually positive in 72 hours but requires a very heavy inoculum.

The oxidase test is performed using a 0.5% solution of tetramethyl-p-phenylenediamine dihydrochloride which is used to wet a piece of filter paper. Transfer growth using an iridium loop and rub the inoculum into the wet area. A dark blue color should appear in 10 sec. We found variability in using the oxidase test. Two organisms (L. pneumophila and L. micdadei) gave inconsistent results; they were often negative while L. jordanis gave a positive reaction. Finally, L. longbeachae consistently gave a weak oxidase test. One factor in the test appeared to be the age of the plate from which the test material was obtained. For most consistent results, we found that cultures no more than 72 hours old should be used.

In general, Legionellae show variability in their sensitivity to sodium chloride. Buffered yeast extract broth (Ristroph, et al. 1980) containing 1% NaCl may be used to differentiate L. pneumophila and L. longbeachae from the other six organisms (See Table 2). This test was performed by inoculating the broth with two drops of a suspension of organisms equivalent to a McFarland standard No. 1. The tubes are incubated for 72-96 hours at $35^{\circ}C$ in the presence of 2.5% CO_2.

The standard nitrate test is negative for all known Legionellae. They are also negative for a modified nitrate test where 0.2% potassium nitrate is incorporated into agar slants which contain Fildes' enrichment (Weaver and Feeley, 1979). These slants should be incubated for seven days. Likewise, the urease test using Christensen's urea agar slants is negative at 24 hours. The slant should be inoculated using a very heavy inoculum since the organisms do not grow on this medium and testing requires the large inoculum to insure that the enzyme is present in

sufficient amounts to give a positive test (Weaver and Feeley, 1979).

Neither the standard or rapid hippurate hydrolysis test may be used with Legionellae (Hebert, 1981). A modified hippurate test has been described whereby 0.4 ml of a 1% sodium hippurate test is inoculated with organisms grown on BCYE agar for 48-72 hours (approximate tubidity - McFarland standard No. 1). The caps are tightened and the culture incubated at 35°C for 18-20 hours. After incubation, 0.2 ml of ninhydrin reagent is added to each tube, the caps are tightened, and the mixture is incubated at 35°C for 10 minutes. The tubes are removed and observed for 20 minutes and any shade of purple is recorded as positive. Controls include uninoculated sodium hippurate, suspensions of Legionellae in water and, if available, Campylobacter fetus, subspecies jejuni and C. fetus, subspecies intestinalis are used as positive and negative controls, respectively. Most strains of L. pneumophila are positive while other Legionellae have been reported to be negative.

In our experience neither standard motility medium nor BYE broth containing 0.3% agar are useful in testing for motility of these organisms although electron microscopy would indicate that most, if not all, strains have flagella. We inoculated both types of media with a very heavy inoculum and observed for 1 week. Growth into the medium is not adequate for use although the organisms did grow well in the soft BYE agar.

VII. AUTOFLUORESCENCE, GROWTH ON DYE CONTAINING MEDIA, AND SUBSTRATE REACTIONS:

Growth of Legionellae was tested on dye-containing media including BCYE supplemented with brom cresol purple (BCP) and brom thymol blue (BTB) in combination or BCP alone. The color of Legionellae on these media

when viewed with room light and long wave ultraviolet (UV) light is useful
in differentiation of Fluoribacter and Tatlockia sp. from Legionella sp.
(Vickers and Yu, 1984). Three Legionella species fluoresce on either
medium; this fluorescence is part of the basis for the proposed genus name
change from Legionella to Fluoribacter for L. bozemanii, L. dumoffii,
and L. gormanii. All three organisms show a bright white autofluorescence
when viewed using long wave UV light. The dye media can be useful in
differentiating L. micdadei. This organism gives a red fluorescence when
grown on BCYE containing BCP and viewed using long wave UV. After 72-96
hours of incubation, the colonies appear deep blue in color when viewed
with room light. When grown on media containing BCP and BTB and viewed
with long wave UV, colonies of both L. pneumophila and L. wadsworthii
appear dull green while L. jordanis colonies appear green-yellow. Finally,
L. longbeachae produces an extracellular green fluorescence pigment when
grown on BCYE containing both BCP and BTB. Our findings would indicate
that the medium containing only BCP should be used to assist in
differentiating L. micdadei from the other species. The combination of
BCP and BTB should be used to judge autofluorescence and pigment production.

Several substrates may be added to the basal medium from which charcoal
has been omitted (BYE agar). Four of the organisms produce brown pigment
in the presence of tyrosine and cystine; these include L. pneumophila,
L. bozemanii, L. gormanii, L. jordanis, and L. longbeachae. Some of these
reactions are in variance with those reported in the literature. This
substrate reaction along with other substrates including
3,5-diaminobenzoic acid (3,5-DABA), 3,4-diaminobenzoic acid (3,4-DABA)
and 3-aminotyrosine should be tested at a future date. The latter three

compounds were unavailable for testing during the research period. Fluorescence of colonies can be viewed on this agar as well as the dye-containing BCYE agar.

VIII. ISOLATION OF ORGANISMS FROM ENVIRONMENTAL SAMPLES:

Attempts were made to screen water samples for Legionellae. These samples were taken from areas as far as 200 miles west of San Antonio. The samples were concentrated by filtration and screened using polyvalent fluorescent antibody. Although some samples appeared to have very low numbers of suspect organisms present, we were unable to isolate any Legionellae from natural sources. Potable water was tested from the hot water system of the laboratory (shower heads and sediment from the hot water holding tank). The cooling tower for the same building was also tested. We were able to recover Legionellae that had been seeded into some of these samples. A major problem that exists with environmental samples is finding a method of reducing the growth of contaminating organisms while allowing for the growth of Legionellae. The seeded samples were treated with heat (56°C for 30 minutes), acid (pH 2.2 buffer or acid solution), or heat followed by acid. Although several reports would indicate that acid treatment is superior, our results would indicate that the nature of the specimen may influence the effectiveness of the treatment. Heat treatment appeared to better reduce the contaminating organisms and Legionellae could be recovered as long as the seeding inoculum was fairly high (approximately 10^{6} to 10^{8} organisms/ml). No attempts were made to isolate organisms using embryonated eggs or guinea pigs. In general, isolation of organisms in vitro appears unlikely unless Legionellae are present in high numbers and the number of contaminants

127-13

can be reduced.

Various antibiotic-containing media have limited usefulness. The Oxoid antibiotic supplement certainly was effective in reducing contaminants although among the Legionellae, only L. pneumophila would grow on the medium. Media supplemented with glycine, vancomycin and polymyxin (GVP) or polymyxin, anisomycin, and vancomycin (PAV) may be useful. However, pretreatment of the sample is necessary and the concentration of Legionellae is also a factor.

Finally, it was hoped that insect larvae and free-living protozoa could be tested for their potential role as carriers of Legionellae. The goal was not realized due to time limitations and difficulties in obtaining larvae.

IX. PROTOCOL FOR PRELIMINARY IDENTIFICATION OF LEGIONELLAE:

The suggested identification protocol for Legionellae is shown in Figure 1 and Table 2. We do not recommend routine attempts at isolation of the organism from environmental samples without the availability of guinea pigs. Therefore, the protocol assumes that a pure or relatively pure sample has been submitted to the reference laboratory for identification.

X. RECOMMENDATIONS:

The recommendations regarding the protocol for characterization of Legionellae are contained in Figure 1. A clear need exists for continued research in at least two major areas. First, continued efforts need to be directed at improving differentiation of the various species of Legionellae. Ultimate identification requires sophisticated procedures that are not routinely performed in many clinical laboratories. Continued

effort in this area should assist laboratories in making a presumptive identification of these various organisms.

Our experience with environmental samples would indicate that no medium provides for complete inhibition of contaminants while allowing for the growth of Legionellae. It is unlikely that such a medium can be designed. However, it seems clear that a number of media formulations may be necessary to provide for optimal recovery of Legionellae. The incorporation of different combinations of antibiotics and natural inhibitory dyes into media that support the growth of Legionellae is proposed as a continuation of this project. Preliminary testing during the research period would indicate that individual dyes and dye combinations should be included in BCYE. Another important aspect of media development relates to the incorporation of chemotherapeutic agents into media. It is clear that a single antibiotic supplement that allows for the growth of all known Legionellae may not be found. However, various antibiotic supplements may be needed to insure recovery of suspected organisms. This approach may assist not only in recovery of Legionellae but in the differentiation of species.

TABLE 1. Nomenclature of the _Legionellaceae_ for the research project.

ORIGINAL DESIGNATION	SPELLING VARIATION	PROPOSED NAME	SEROGROUP	STRAIN
Legionella pneumophila	---	_Legionella pneumophila_	Serogroup 1	Philadelphia 1
Legionella bozemanii	_Legionella bozemanae_	_Fluoribacter bozemanae_	Serogroup 1	WIGA
Legionella micdadei	---	_Tatlockia micdadei_	Serogroup 1	TATLOCK
Legionella dumoffii	---	_Fluoribacter dumoffii_	Serogroup 1	NY-23
Legionella gormanii	---	_Fluoribacter gormanii_	Serogroup 1	LS-13
Legionella jordanis	---	_Legionella jordanis_	Serogroup 1	BL-540
Legionella wadsworthii	---	_Legionella wadsworthii_	Serogroup 1	81-716A
Legionella longbeachae	---	_Legionella longbeachae_	Serogroup 1	Long Beach 4

FIGURE 1. Protocol for tentative identification of Legionellae.

```
┌─────────────────────────────────────────────────────────┐
│        Catalase Positive, Gram Negative Bacilli         │
│   No Growth on Blood Agar, Require Cysteine for Growth   │
│   Negative Slide Agglutination for Francisella tularensis│
└─────────────────────────────────────────────────────────┘
                            │
        ┌───────────────────────────────────────────────┐
        │  Appearance of Colonies on BCYE Medium Containing BCP │
        └───────────────────────────────────────────────┘
              ┌─────────────────────────────┐
┌──────────────────────────────────────────┐   ┌────────┐
│ Deep Blue Coloration at 72 Hours-Room Light│   │ Others │
│ Red Appearance Under Long Wave Ultraviolet Light│ └────────┘
│     Legionella (Tatlockia) micdadei        │
└──────────────────────────────────────────┘
                            │
        ┌───────────────────────────────────────────┐
        │ Fluorescence Under Long Wave Ultraviolet Light│
        │    (BCYE Medium Containing BCP and BTB)       │
        └───────────────────────────────────────────────┘
        ┌──────────────────────────┐   ┌──────────────────────────┐
        │ Blue-White or White-Green Fluorescence│ │ Yellow or Yellow-Green   │
        │   Legionella (Fluoribacter) bozemanii │ │  Extracellular Fluorescence│
        │   Legionella (Fluoribacter) dumoffii  │ │   Legionella lor;beachae  │
        │   Legionella (Fluoribacter) gormanii  │ └──────────────────────────┘
        └──────────────────────────┘
                ┌──────────────────────────┐
                │ Dull Green or Yellow Colonies│
                │    Legionella pneumophila    │
                │    Legionella jordanis       │
                │    Legionella wadsworthii    │
                └──────────────────────────┘
```
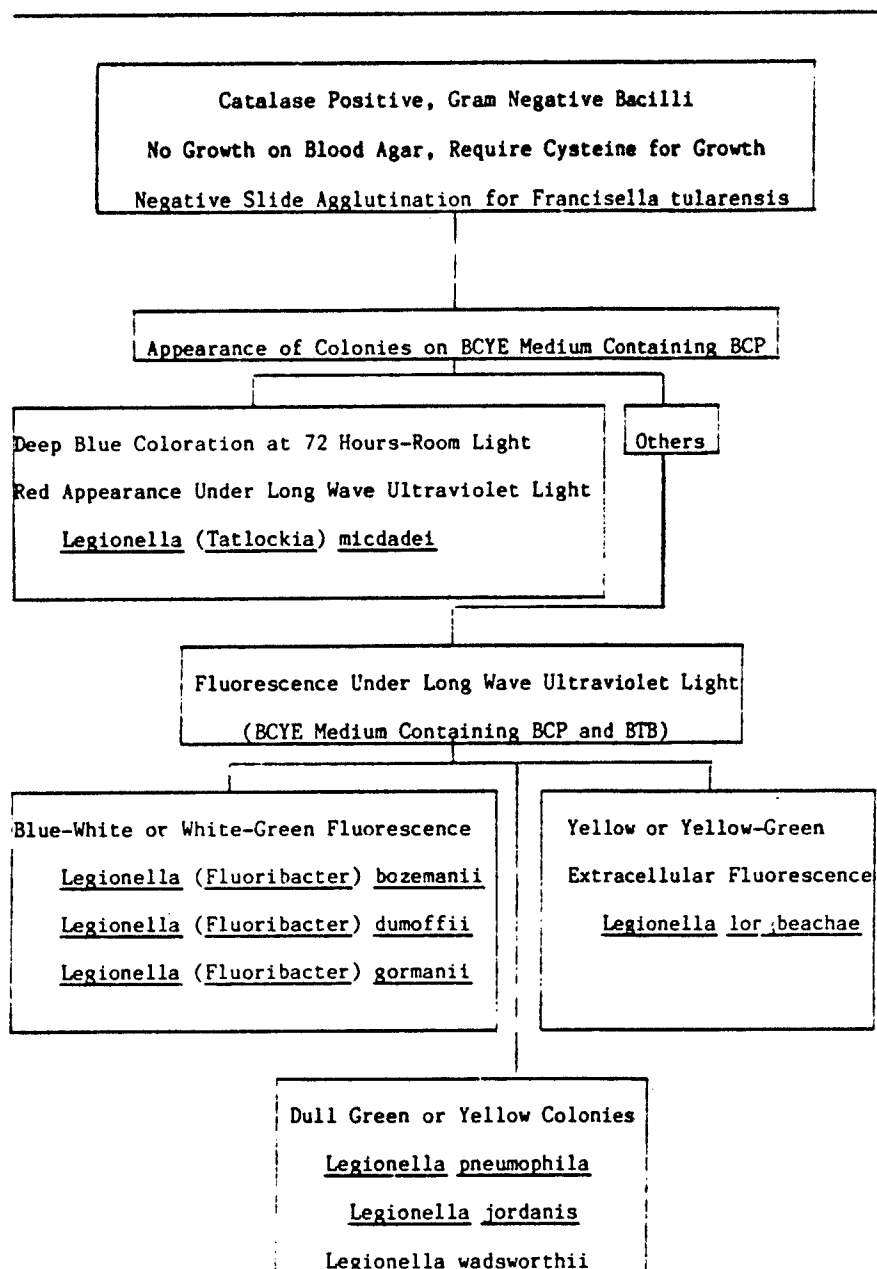
TABLE 2. Continued characterization of Legionellae.

Legionella (Tatlockia) micdadei
Browning on BYE Agar containing Cystine and Tyrosine   - Negative
Growth in BYE Broth + 1% NaCl   - Negative
Modified Hippurate Test   - Negative
Oxidase Reaction   - Variable

Legionella (Fluoribacter) bozemanii
Browning on BYE Agar containing Cystine and Tyrosine   - Positive
Growth in BYE Broth + 1% NaCl   - Negative
Modified Hippurate Test   - Negative
Oxidase Reaction   - Negative

Legionella (Fluoribacter) dumoffii
Browning on BYE Agar containing Cystine and Tyrosine   - Variable
Growth in BYE Broth + 1% NaCl   - Negative
Modified Hippurate Test   - Negative
Oxidase Reaction   - Negative

Legionella (Fluoribacter) gormanii
Browning on BYE Agar containing Cystine and Tyrosine   - Positive
                                            (Extracellular Browning)
Growth in BYE Broth + 1% NaCl   - Negative
Modified Hippurate Test   - Negative
Oxidase Reaction   - Negative

Legionella pneumophila
Browning on BYE Agar containing Cystine and Tyrosine   - Positive
                                            (Extracellular Browning)
Growth in BYE Broth + 1% NaCl   - Positive
Modified Hippurate Test   - Positive
Oxidase Reaction   - Variable

Legionella jordanis
Browning on BYE Agar containing Cystine and Tyrosine   - Positive
Growth in BYE Broth + 1% NaCl   - Negative
Modified Hippurate Test   - Negative
Oxidase Reaction   - Variable

Legionella wadsworthii
Browning on BYE Agar containing Cystine and Tyrosine   - Variable
Growth in BYE Broth + 1% NaCl   - Negative
Modified Hippurate Test   - Negative
Oxidase Reaction   - Negative

Legionella longbeachae
Browning on BYE Agar containing Cystine and Tyrosine   - Positive
Growth in BYE Broth + 1% NaCl   - Positive
Modified Hippurate Test   - Negative
Oxidase Test   - Weak Positive

ACKNOWLEDGMENTS

REFERENCES

Balows, A., E.D. Renner, C.M. Helms, and W. Johnson. 1981. Legionelloris (Legionnaires' Disease). In Balows, A. and W.J. Hausler (Eds.). Bacterial, Mycotic, and Parasitic Infection, American Public Health Association.

Brenner, D.J., J.C. Feeley, and R.E. Weaver. 1984. Family VII. Legionellaceae. In Krieg, N.R. and J.G. Holt (Eds.). Bergy's Manual of Systematic Bacteriology, Williams & Wilkins.

Feeley, J.C., R.J. Gibson, G.W. Gorman, N.C. Langford, J.K. Rasheed, D.C. Mackel and W.B. Baine. Charcoal-Yeast Extract Agar: Primary Isolation Medium for Legionella pneumophila. J. Clin. Microbiol. 10:437-441.

Herbert, G.A. 1981. Hippurate Hydrolysis by Legionella pneumophila. J. Clin. Microbiol. 13:240-242.

Ristroph, J.D., K.W. Hedlund, and R.G. Allen. Liquid Medium for Growth of Legionella pneumophila. J. Clin. Microbiol. 11:19-21.

Vickers, R.M. and V.L. Yu. 1984. Clinical Laboratory Differentiation of Legionellaceae Family Members. J. Clin. Microbiol. 19:583-587.

Warren, W.J. and R.D. Miller. 1979. Growth of Legionnaires' Disease Bacterium (Legionella pneumophila) in Chemically Defined Medium. J. Clin. Microbiol. 10:50-55.

Weaver, R.E. and J.C. Feeley. 1979. Cultural and Biochemical Characterization of the Legionnaires' Disease Bacterium. In Jones, G.L. and G.A. Hebert (Eds.). "Legionnaires'" The Disease, The Bacterium and Methodology, U.S. Dept. of Health, Education, and Welfare Publ. No. CDC 79-8375.

1984 USAF-SCEEE SUMMER FACULTY RESEARCH PROGRAM

Sponsored by the

AIR FORCE OFFICE OF SCIENTIFIC RESEARCH

Conducted by the

SOUTHEASTERN CENTER FOR ELECTRICAL ENGINEERING EDUCATION

FINAL REPORT

A THREE-DIMENSIONAL RADIATION BOUNDARY CONDITION

FOR MESOSCALE NUMERICAL MODELS

Prepared by: Dr. Keith L. Seitter

Academic Rank: Assistant Professor

Department and   Department of Earth Sciences
  University: University of Lowell

Research Location: Air Force Geophysics Laboratory
                      Meteorology Division
                      Atmospheric Prediction Branch

USAF Research: Donald A. Chisholm

Date: August 1, 1984

Contract No: F49620-82-C-0035

A THREE-DIMENSIONAL RADIATION BOUNDARY CONDITION

FOR MESOSCALE NUMERICAL MODELS

by

Dr. Keith L. Seitter

ABSTRACT

The response of the lateral boundary conditions to waves generated during the geostrophic adjustment process is investigated in a three-dimensional meso-beta numerical model of the atmosphere. It is shown that the reflective nature of specified boundary conditions leads to significant errors even when strong damping is used to remove wave energy. The multi-dimensional radiation condition of Raymond and Kuo (1984) is implemented in the model and shown to allow outward propagation of the waves without reflection. The development of several routines to produce computer generated graphics of the model output are also outlined.

I. INTRODUCTION

The Atmospheric Prediction Branch (LYP) of the Air Force Geophysics Laboratory (AFGL) has recently received a version of the NOAA-ERL three-dimensional meso-beta cloud and precipitation model developed by Nickerson[1]. (In this report, the version of this model being used at AFGL will be referred to as WARM5.) The Air Force has plans to use this operationally as a mesoscale model which may be nested within a larger scale meso-alpha or global model. This requires the improvement of the boundary conditions on the side (lateral) boundaries of the model.

Since these lateral boundaries do not exist in nature, the goal of the boundary condition is to have the boundary appear as "open" as possible, with disturbances being able to propagate out of the model domain with little or no reflection by the artificial boundary. Orlanski[2] proposed a Sommerfeld radiation condition which was shown to be superior to other formulations[3]. Raymond and Kuo[4] developed a multi-dimensional radiation condition. This radiation condition was shown to be more accurate than the Sommerfeld condition for large scale and meso-beta two-dimensional models[4], and Seitter[5,6] used it successfully in a two-dimensional meso-gamma model. While the mathematical framework of the condition was extended to three dimensions, it had not been implemented in a three-dimensional model. The need for a good lateral boundary condition in WARM5 and the apparent superiority of the Raymond and Kuo radiation condition made the testing of this condition in the AFGL model an attractive project for a summer faculty research appointment.

II. OBJECTIVES

Prior to actual testing of the radiation condition, several preliminary objectives required completion. They were:

(1) Creation of a new version of the model called WARM5KSn (where "n" indicates the subversion) which has all moist processes removed.

(2) Development of software to allow direct graphical output of the model variable fields.

(3) A simulation using the dry model with the original boundary conditions to investigate the production and behavior of waves generated during the geostrophic adjustment process.

The following objectives relate directly to the implementation and testing of the radiation condition:

   (4) Development of the numerical code for the radiation condition which is consistent with the finite difference and time schemes of the model.

   (5) Implementation of the debugged code in the dry version of the model and a simulation using the same initial conditions as the run with the original boundary conditions.

   (6) Analysis of the results of the simulations to determine the ability of the radiation condition to allow outward propagation of waves through the boundary.

During the appointment it became clear that a further objective was desirable:

   (7) The investigation of the geostrophic adjustment process itself in the numerical model and how the space discretization and time schemes used in the model affect the adjustment process.

III. COMPUTER GENERATED GRAPHICS OF MODEL OUTPUT

In order to aid in the interpretation of the model output, several software packages were developed to make use of the NCAR Graphics Library. The first package plots a skew-T log-p diagram to display a sounding and also plots the vertical profiles of u and v component winds. The geopotential heights of the mandatory pressure levels are plotted on the wind profile. An example of the output from this routine is shown in Figure 1.

In order to view changes in variables with time or differences between model predicted variables and observation, a routine which constructs difference (or error) profiles was written. Figure 2 shows a typical frame from this routine, which allows the user to plot one to three profiles on each frame for each of six different verification variables.

Figure 3 shows the output of a routine to produce three-dimensional perspective views of complex terrain. A fourth routine was written by adapting an existing program for use with the NCAR graphics library. This program produces contours plots of the model variables or vector plots of the horizontal winds on horizontal model or constant pressure
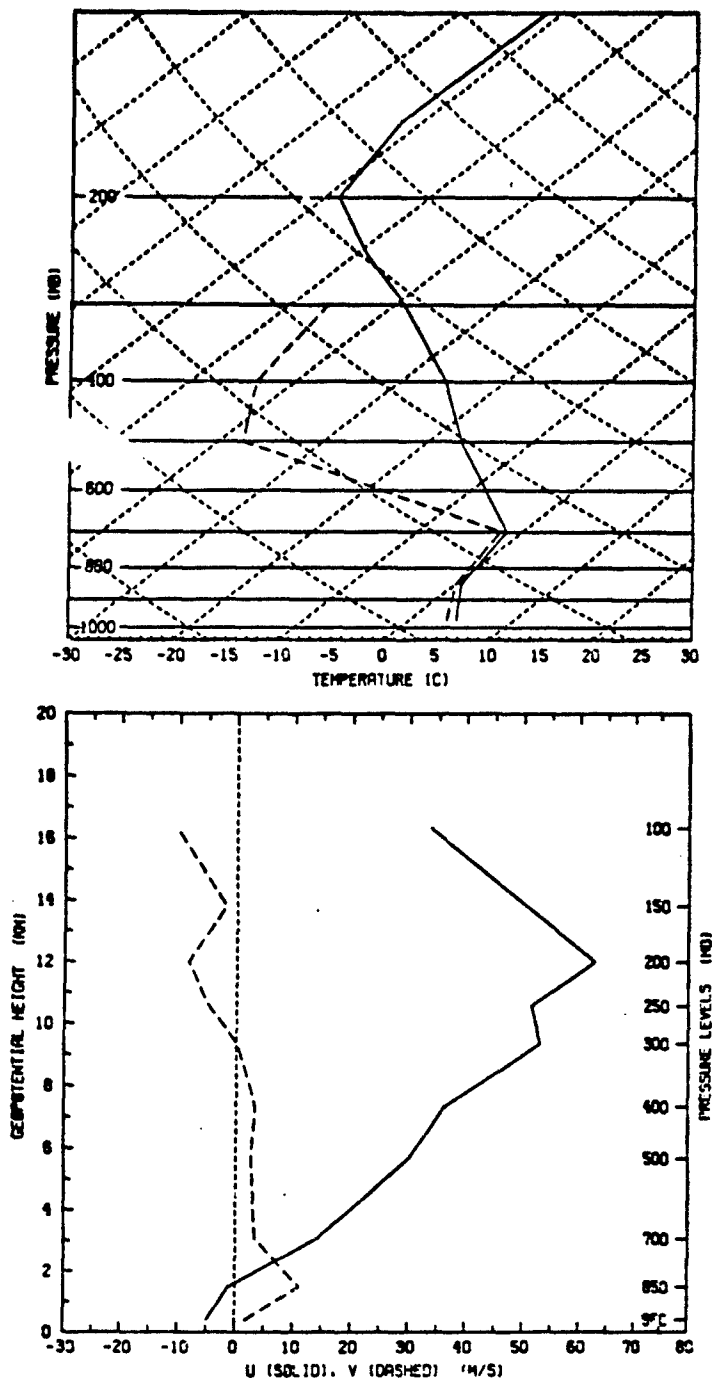
Figure 1. (a) Temperature (solid) and dewpoint temperature
sounding plotted on skew-T log p diagram.

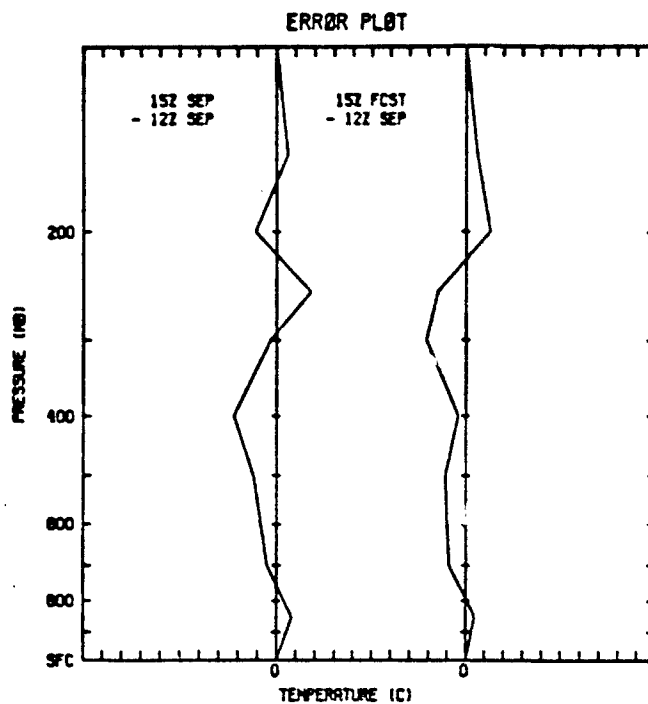(b) Profiles of u and v component winds and mandatory
lev l heights.

128-5

ERRØR PLØT

Figure 2. Example of one frame from the routine to plot difference profiles.
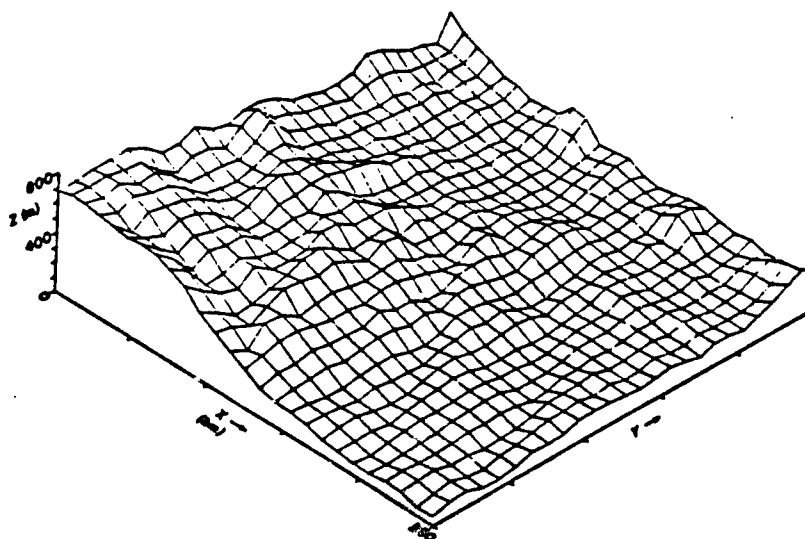

Figure 3. Example of perspective plot of complex terrain field.

levels. An example of a contour plot using this routine is shown in Figure 5.

IV. THE MODEL

a. WARM5 and WARM5KS2

The basic equations and method of solution of the WARM5 model are described in detail by Nickerson[1], so only the aspects of the model of immediate interest to this project will be presented in this section.

The WARM5 model is a three-dimensional primitive equation hydrostatic model which is written in a modified sigma-coordinate system. The horizontal domain is 500 km X 500 km with a grid spacing of 20 km in both directions. In the vertical, the model uses 16 levels to cover the region from the surface to zero pressure with the modified sigma-coordinate packing several layers in the surface boundary layer. The variables are distributed on a staggered grid as described by Anthes and Warner[7].

Time integration is accomplished by the leapfrog scheme with a Time-and-Space-Uncentered (TASU) Matsunno scheme applied every eighth and ninth time step. The TASU Matsunno scheme accomplishes several tasks in the model. It prohibits the time-splitting instability associated with the leapfrog scheme, helps eliminate $2\Delta X$ noise associated with centered-only differences, and is highly damping of high frequency waves generated during the initial geostrophic adjustment. One negative aspect of the TASU Matsunno scheme is that it is a two-step scheme, so each time step requires twice the computation time of the leapfrog scheme. A Shapiro filter is applied on the horizontal velocity variables after each time step to eliminate $2\Delta X$ noise in the wind field[1]. It can be shown that this is equivalent to using an explicit diffusion with an eddy viscosity of $K = 1.67 \times 10^6$ m^2/s, so this filter will act to damp waves of all frequencies.

The boundary conditions currently in WARM5 are specified values of temperature, mixing ratio, pressure, and precipitation variables on all boundaries and specified values of u and v winds on inflow lateral boundaries with extrapolation on outflow. On the top and bottom boundary u = v = 0. The specified boundary values are set during the initialization

process which simply uses an input sounding to construct a horizontally homogeneous atmosphere.

The modification of WARMS, called WARMSKS2, has all the moist processes removed from WARMS. This was done to improve computation speed (by about 30%) and because the testing of the lateral boundary conditions is more straightforward (with no loss of generality) in a dry model.

b. WARMSKS3

In WARMSKS3, the original lateral boundary conditions of WARMSKS2 are replaced with the multi-dimensional radiation condition. The details of the derivation of this condition are given by Raymond and Kuo[4]. The condition may be written

$$\frac{\partial \psi}{\partial t} + C_x \frac{\partial \psi}{\partial x} + C_y \frac{\partial \psi}{\partial y} + C_z \frac{\partial \psi}{\partial z} = 0 \qquad (1)$$

where ψ is the value of one of the variables on the boundary. The component phasespeeds, C_x, C_y, C_z, are computed by inverting this equation and evaluating the derivatives at the previous timestep, one grid point interior to the boundary[4].

In the current study, only the dynamic variables are treated with this condition while the thermodynamics variables are specified. This is motivated by the work of Clark[8] and the observations of Anthes and Warner[7] concerning interior velocity errors resulting from geostrophically adjusted thermodynamic boundary value errors. The actual prognostic variables used in the model which correspond to the dynamic variables are πu, πv, and π, where π is the time and space dependant surface pressure. For π, which is a two-dimensional quantity, (1) is used without the z-component. Also, for the π condition the inversion of (1) is accomplished at the current timestep rather than the previous one. For πu and πv the vertical derivative $\partial \psi / \partial z$ is evaluated as $g \partial \psi / \partial \phi$ where ϕ is the geopotential calculated in the model.

In all cases the phase speeds calculated are forced to satisfy the Courant-Friedrichs-Levy condition[8]. For the component perpendicular to the boundary, C is set to zero if the calculated value of phasespeed indicates inflow. Note that because the C's are phase speeds, the condition allows the outward propagation of a disturbance through a boundary with inflow winds.

The numerical code is written to be consistent with the TASU Matsunno scheme on those timesteps in which it is used and leap-frog on the other timesteps. The code was written in an easily modifiable form for this testing procedure with the knowledge that it could be made more computationally efficient.

V. THE GEOSTROPHIC ADJUSTMENT PROCESS

The radiative boundary condition is formulated to allow wave motions generated in the model to exit the domain with little or no reflection. This motivates some discussion of the mechanism which generates these waves. The atmosphere tends to maintain itself in a state of geostrophic (or more correctly gradient) balance. If a perturbation disrupts this balanced state, the atmosphere returns to balance via a mechanism referred to as geostrophic adjustment. The means of accomplishing this depends on the scale of the disturbance. For the smaller scales of motion of concern here, the adjustment process proceeds by the generation of high frequency external inertial-gravity waves (which will be called external waves) and low frequency internal inertial-gravity waves (which will be called gravity waves). These waves propagate away from the disturbance leaving a balanced state behind[8].

The WARM5 model is initialized with horizontally homogeneous conditions which are in balance only if the winds are identically zero and the terrain is flat. This is the trivial case since there would be no evolution in time except by vertical diffusion. For all other cases, the model will immediately generate waves at the start of the integration which will act to bring the model into balance.

The specified boundary conditions used in WARM5 are, however, purely reflective to the waves. Therefore, without some mechanism of removing wave energy, the model would "slosh" around without ever obtaining a balanced state. The TASU Matsunno time scheme is used in WARM5 because it damps the external wave and is meant to remove it quickly. The Shapiro filter tends to damp the meteorologically important gravity waves as well as the external wave so that the model can approach geostrophic balance. This is a serious drawback of the Shapiro filter because several mesoscale phenomena are a result of gravity waves

(such as mountain lee waves and wave initiated clouds) and this filter
prohibits the proper evolution and propagation of these waves.

The attractive feature of the radiative boundary condition is that
it allows the waves generated during the adjustment process to exit the
domain, leaving the balanced state behind, without requiring strong damp-
ing characteristics. This should result in a more natural adjustment pro-
cess and allow the removal of the Shapiro filter and the replacement of
the TASU Matsunno scheme with one which is more computationally efficient.

VI. RESULTS OF THE BOUNDARY CONDITION TESTS

a. Initial Conditions

For the boundary condition tests, the model was run with a flat
surface terrain located at sea-level. The initial temperature structure
was the U.S. Standard Atmosphere sounding shown in Figure 4. The initial
atmosphere was horizontally homogeneous and the winds were identically
zero in the domain. Thus, the initial conditions were in perfect geo-
strophic balance.

In order to generate a distrubance, an oblate ellipsoid temperature
perturbation was added gradually during the first 20 min. This warm
bubble was 200 km in diameter horizontally and about 5 km deep, centered
at about 700 mb. The maximum temperature at the center reached about
3.0°C above the environment. During the growth of the bubble, the pressure
was modified hydrostatically to a maximum pressure perturbation of about
-2.0 mb, as shown in Figure 5, and vertical velocities and horizontal
winds were generated. At 20 min, the warm bubble was instantaneously
removed, leaving the fields out of balance and initiating the geostrophic
adjustment process.

b. Results with the Original Boundary Conditions (WARM5KS2)

A 4 hr simulation was made with the initial perturbation located
in the center of the domain as shown in Figure 5. The high frequency
external wave generated during the adjustment process is most easily
identified in the surface perturbation pressure. Figure 6 shows the
wave at T = 40 min propagating radially outward from the center.
Theoretically, the external wave should have a phase speed of about
300 m/s, but in the model its speed is about 100 m/s due to the phase
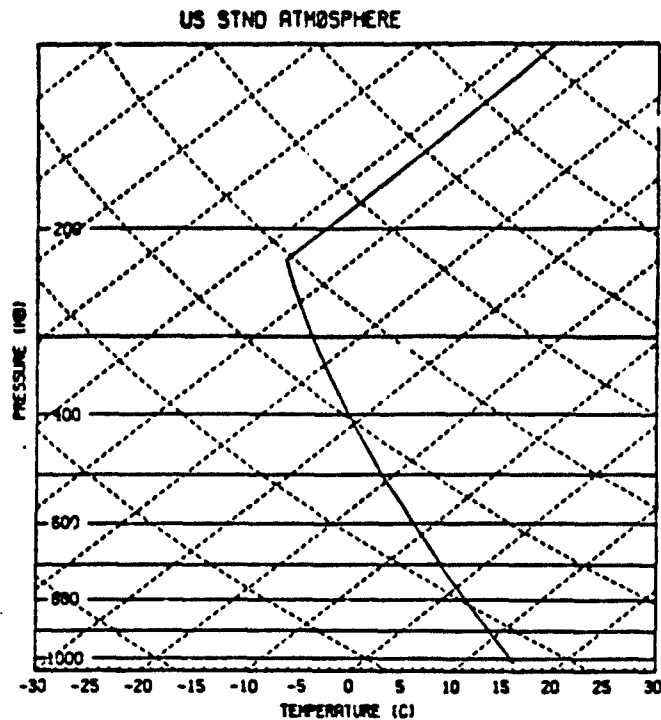
US STND ATMOSPHERE

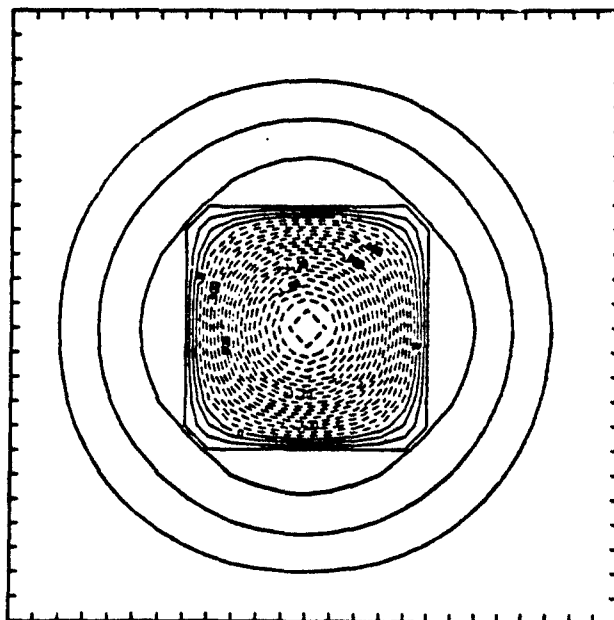Figure 4. U.S. Standard Atmosphere sounding used as initial conditions in the model.

Figure 5. Surface pressure perturbation at T = 20 min for WARM5KS2. The entire model domain is shown with North toward the top and tick marks at 20 km intervals. The contour interval is 0.1 mb.
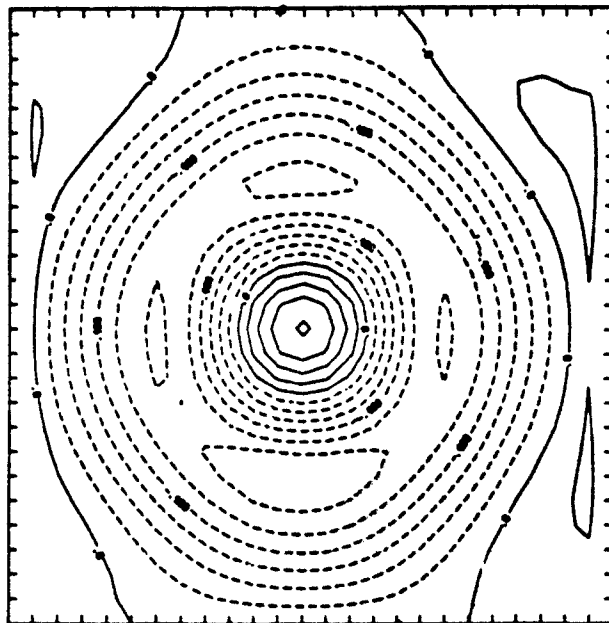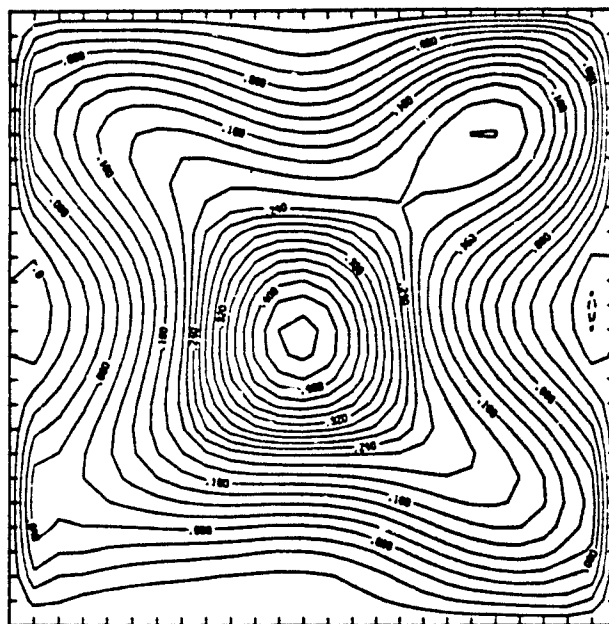
Figure 6.   As in Figure 5 at T = 40 min.

Figure 7.   Surface perturbation pressure at T = 80 min for WARM5KS2.
            Note that the contour interval is now 0.02 mb.

error associated with the leapfrog scheme[8]. As anticipated, the wave
experiences multiple reflections off the boundary which interfere to
produce complicated pressure patterns during the integration. Figure 7
shows the pressure field at T = 80 min.

Even though the TASU Matsunno scheme damps the waves, constructive
interference can produce a substantial perturbation pressure at times.
For instance, at T = 80 min the maximum perturbation pressure is 0.44 mb.
By T = 160 min it has been reduced to 0.10 mb, but at T = 180 min the
waves interfere to give a maximum perturbation pressure of 0.28 mb. This
indicates that significant errors, perhaps 15% to 20% of the initial
error, could be present in an operational forecast well beyond 2 hr of
simulated time.

The slow moving internal gravity wave is most easily traced in the
model level 9(~ 730 mb) vertical velocity. At T = 20 min, the vertical
velocity is 5.9 cm/s at the center of the warm bubble. This wave propa-
gates outward with an initial speed of about 27 m/s, but slows as it
approaches the boundary. Significant damping occurs with the vertical
velocity in the crest being reduced to 0.26 cm/s by T = 120 min. The
small amplitude of the wave in the later stages of the integration makes
analysis of possible boundary reflection difficult.

In order to investigate the damping caused by the Shapiro filter,
the root-mean-square horizontal and vertical velocities were calculated
every 5 min. A plot of these quantities versus time is shown in Figure 8.
As can be seen, they decay exponentially after the initial buildup of the
perturbation. An exponential curve was fit by least squares to the r.m.s.
horizontal velocity from T = 25 min to T = 2 hr, and the decay rate was
calculated. This can be related to the equivalent diffusion of the
Shapiro filter by assuming the diffusion is linear and that the dominant
wave is the first normal mode of the domain (L = 500 km). Then the decay
rate corresponds to an eddy viscosity of $K = 1.66 \times 10^6$ m^2/s, which is
almost exactly the value corresponding to the Shapiro filter.

Another 4 hr simulation was conducted with the perturbation located
100 km west of the center. The surface perturbation pressure at T = 80 min
is shown in Figure 9. Comparison with Figure 7 shows that the off-center
location on the initial disturbance resulted in a less symmetric wave
pattern and a very different interference pattern. This simulation shows
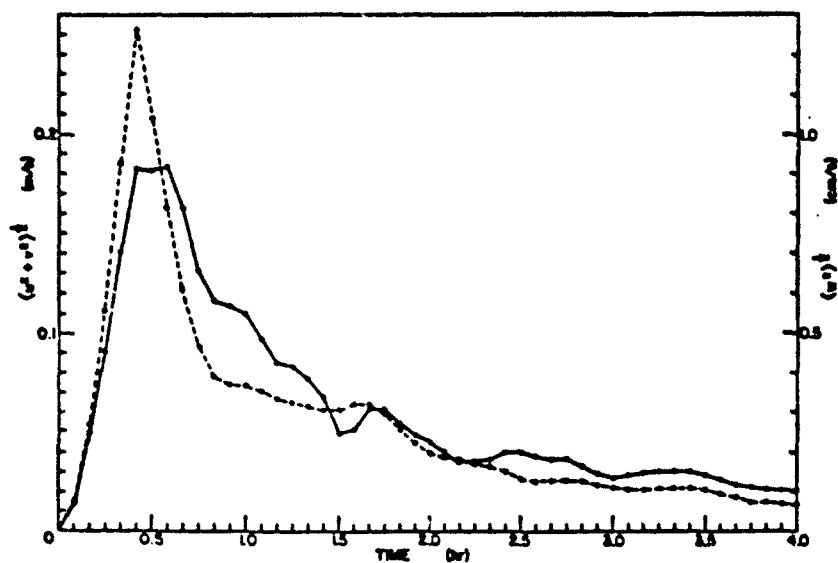
Figure 8. Root-mean-square horizontal velocity (solid) and vertical velocity (dashed).
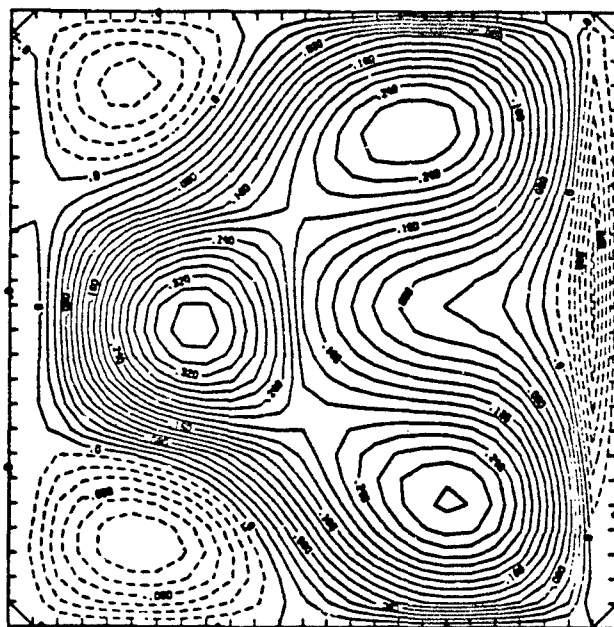

Figure 9. As in Figure 7 but for the WARM5KS2 simulation which used the off-center disturbance.

128-14

that the error distribution is determined by the position of the disturbance relative to the boundaries. This is purely a result of the reflective nature of the boundary conditions. Another point concerning this simulation is that the phase speed of the gravity wave propagating toward the east boundary is not retarded as quickly as in the previous simulation. This suggests that the boundary, which is further from the disturbance in this case, may play a role in altering the phase speed.

c. Results with the Multi-dimensional Radiation Condition (WARM5KS3)

Time constraints permitted only one 4 hr simulation using the model with the radiation boundary condition. The initial conditions were identical to those used for the centered disturbance case of WARM5KS2. Hence, the T = 20 min surface perturbation pressure was identical to Figure 5.

Unfortunately, a coding error which could not be detected in the 10 min debugging runs resulted in an instability in the surface pressure at the northeast and northwest corner points. This instability did not result in noticeable errors until about T = 60 min and did not significantly influence the surrounding points until after T = 80 min. It did, however, influence the horizontal velocities enough to make the r.m.s. velocity calculations useless.

The first 80 min of this simulation can be used to show the properties of the radiation condition for the fast external wave. The slower internal wave does not reach the boundary before the corner instability destroys the solution. Figure 10 shows the surface perturbation pressure at T = 40 min. We would expect a nearly circular wave for this symmetric disturbance and comparison with Figure 6 shows that the wave is more circular when the radiation condition is used. The north and south boundaries appear to be more noisy than the east and west boundaries. This may be because the model treats east-west slabs individually, and a more complicated formula is required to calculate the needed differences across slabs. There may still be some inconsistencies in the numerical code on these boundaries.

Figure 11 shows the pressure field at T = 80 min. Comparison with Figure 7 shows that the boundary allowed the wave to exit the domain without reflection. This is especially evident if we concentrate on the east and west boundaries. In Figure 11, the NE and NW corner points are artificially zeroed in order to allow the plot to use the same contour
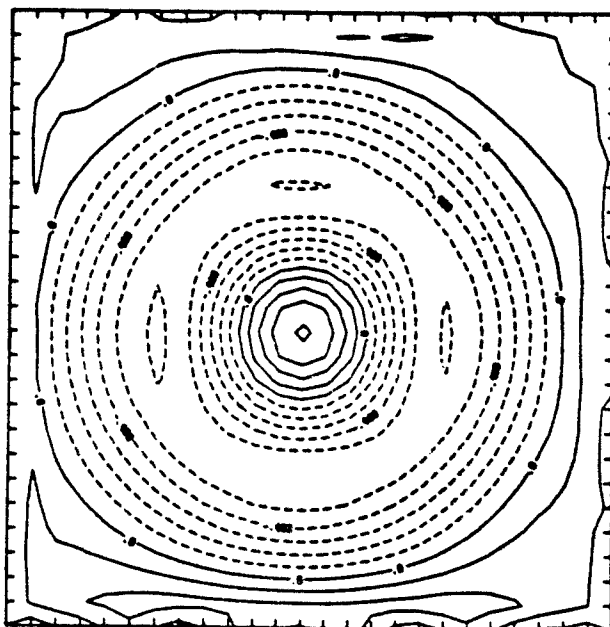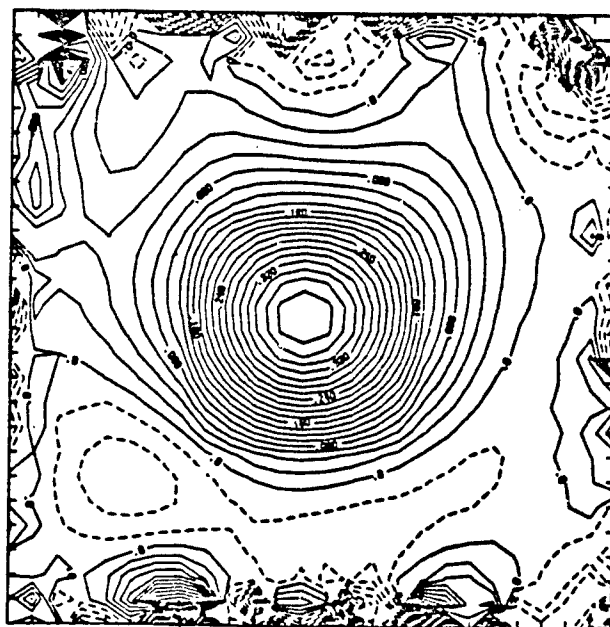
Figure 10. As in Figure 5 for WARM5KS3 at T = 40 min.

Figure 11. As in Figure 7 for WARM5KS3 at T = 80 min.

interval as in Figure 7. The errors on these points at this time are about 0.8 mb.

The boundary noise evident in Figure 11, even on the east and west boundaries, could be caused by several factors. A very likely candidate is the switch from leapfrog to TASU Matsunno time stepping schemes every eighth and ninth timesteps. The boundary condition uses information from preceding timesteps in the calculation of the phasespeeds and there is a problem in this calculation when the time scheme changes. Printouts of the calculated phasespeeds show a discontinuity every tenth time step (on the first leapfrog step after the two TASU Matsunno steps).

VII. CONCLUSIONS

Despite numerical problems with the WARM5KS3 simulation, the ability of the multi-dimensional radiation condition to allow waves to exit the domain without reflection has been demonstrated. The length of the appointment and the turn-around time required for simulations longer than 10 min prohibited carrying this project to a more fruitful completion. There are, however, several other points which are clear:

(1) The current boundary conditions are inadequate if the initial imbalance is not very small or if any rapid changes occur during the model integration.

(2) A study of the geostrophic adjustment process in the model is necessary to determine the ability of the model to balance a more realistic initial state and the time required for this balance. Useful predictive information is available only after the balance is complete, so an understanding of this process is essential for operational use of the model.

(3) The Shapiro filter results in excessive diffusion of the horizontal velocities. The strong damping may be necessary to reach balance using the current boundary conditions since it removes wave energy, but it prohibits proper evolution of the meteorologically important internal inertial-gravity waves and may cause unrealistic smoothing of the wind fields.

128-17

VIII. RECOMMENDATIONS

Given the conclusions which may be drawn from the results of this study, the following recommendations can be made:

(1) Continue work with the radiation condition to produce a useful boundary condition free from the numerical problems evident in this study. Remove the Shapiro filter and TASU Matsunno time scheme since these should not be needed when the radiation condition is used. To control time splitting, incorporate a time filter such as the Asselin filter[8]. To control noise, use an explicit eddy diffusion with a reasonable value for the eddy viscosity (the code for this diffusion is already in the model with the viscosity set to zero).

(2) Study further the geostrophic adjustment process in the model. One part of this study should use the current model to investigate the adjustment through the removal of wave energy by damping. Another should use the improved radiation condition model of recommendation (1) to study the adjustment through the removal of wave energy by outward radiation. Theoretical work should also be carried out on the effect of the finite difference and time schemes on the adjustment process. This study should strive to determine how long the adjustment process takes in the model and at what time useful predictive information can be obtained.

ACKNOWLEDGMENTS

REFERENCES

1. Nickerson, E.C., "On the Simulation of Airflow and Clouds Over Mountainous Terrain," Beit. Phys. Atmos., 52, pp. 161-177, 1979.

2. Orlanski, I., "A Simple Boundary Condition of Unbounded Hyperbolic Flows," J. Comp. Phys., 21, pp. 251-269, 1976.

3. Clark, T.L., "Numerical Simulations with a Three-dimensional Cloud Model: Lateral Boundary Condition Experiments and Multicellular Severe Storm Simulations," J. Atmos. Sci., 36, pp. 2191-2215, 1979.

4. Raymond, W.M., and H.-L. Kuo, "A Radiation Boundary Condition for Multi-dimensional Flow," Quart. J.R. Met. Soc., 110, pp. 535-551, 1984.

5. Seitter, K.L., "Numerical Simulation of Thunderstorm Gust Fronts," AFGL Tech. Report, AFGL-TR-83-0329, 34 pp., 1984.

6. Seitter, K.L., and H.-L. Kuo, "The Dynamical Structure of Squall-line Type Thunderstorms," J. Atmos. Sci., 40, pp. 2831-2854, 1983.

7. Anthes, R.A., and T.T. Warner, "Development of Hydrodynamic Models Suitable for Air Pollution and Other Mesometeorological Studies," Mon. Wea. Rev., 106, pp. 1045-1078, 1978.

8. Haltiner, G.J., and R.T. Williams, Numerical Prediction and Dynamic Meteorology, 2nd Ed., John Wiley & Sons, New York 1980.

1984 USAF-SCEEE SUMMER FACULTY RESEARCH PROGRAM

Sponsored b, the

AIR FORCE OFFICE OF SCIENTIFIC RESEARCH

Conducted by the

SOUTHEASTERN CENTER FOR ELECTRICAL ENGINEERING EDUCATION

FINAL REPORT

CALCULATION OF ENHANCED HEATING IN TURBULENT BOUNDARY LAYERS INFLUENCED BY FREE STREAM TURBULENCE

Prepared by:	Dr. Paavo Sepri
	and Mr. Jon L. Ebert
Academic Ranks:	Associate Professor
	and Graduate Student
Department and University:	School of A.M.N.E.
	University of Oklahoma
Research Location:	Air Force Wright Aeronautical Laboratories
	Aero-Propulsion Laboratory
	Turbine Engine Division
	Components Branch
USAF Research Contact:	Mr. Charles D. MacArthur
Date:	27 August 1984
Contract No.:	F49620-82-C-0035

4 4~

CALCULATION OF ENHANCED HEATING IN TURBULENT

BOUNDARY LAYERS INFLUENCED BY FREE STREAM TURBULENCE

by

Paavo Sepri and Jon L. Ebert

ABSTRACT

A preliminary phenomenological computational model has been formulated
and implemented for the purpose of predicting increased heating in boundary
layer environments which are influenced by free stream turbulence. The
model has been constructed primarily by scrutiny of recently published
extensive flow measurements over heated flat plates, and it is also
supported partially by analytical considerations. The mixing length model
existing in the code STANCOOL has been modified to incorporate these free
stream turbulence effects. The comparisons between measurements and
calculations generally show improvement, but certain discrepancies are
noted which require further investigation. An apparently novel
observation is made concerning the structure of much of the outer region of
a turbulent boundary layer in the presence of higher levels of free stream
turbulence. Several variables follow a simple exponential character which
may be of fundamental importance. This observation is used to lend
credence to the computational model, but it also raises an apparent dilemma
involving the energy equation. A central role in these calculations is
played by the turbulent Prandtl number profile, the modeling of which
determines quantitatively the heating of a surface. Comments are offered
in connection with possible channel flow effects on measurements of Pr_t
which indicate large decreases towards the free stream.

ACKNOWLEDGEMENTS

I. INTRODUCTION

In the design of modern turbines it is becoming increasingly important to have a computational tool which can predict blade heating environments accurately and cost-effectively. The subject is sensitive owing to conflicting requirements; namely, improved engine performance is connected with increased gas temperature, whereas increased blade lifetime requires a lowered blade temperature. Since a blade typically operates near its structural limit, it is estimated that a decrease of only 30° F could double its lifetime[1]. Current methods of blade cooling, such as transpiration and/or internal flow, are also limited by their adverse effects on overall engine efficiency. Coolant flow rates are essentially limited by the allowable pressure differential along the passages. In view of these restrictions in design, it is important to have accurate means of calculating the associated blade heat transfers.

Any attempt to calculate the flow environment around the blades is hindered by the compounded complexity of the actual case, and also by the fact that turbulence remains an unsolved problem in general. Therefore, for this short investigation, an attempt is made to focus on a simplified problem, which retains some of the essential phenomena of the actual problem. The investigation is thus restricted to turbulent flow over a 2D flat plate which is heated so as to yield heat flux information. This restriction is particularly relevant from the computational viewpoint, owing to the recent publication of extensive experimental results for this case by Blair[2-8].

One of the important effects, which influence heat transfer to a surface, is the presence of free stream turbulence (FST) external to the boundary layer. Although this subject has received considerable attention

in the past[9-15], there appear to be conflicting claims[11] and an incomplete understanding, especially for the regime of higher FST levels encountered by turbine blades. It has been one of the goals of the recent investigations by Blair[2], Bradshaw[11], and Hancock[16] to clarify experimentally the extent of augmented heating in the presence of increased FST.

In an investigation prior to the present one, MacArthur[1] has applied a recent version of the widely used code STAN5[17] to assess the extent of predictability of FST effects in turbulent heating, as compared with the measurements of Blair. The results were mixed: although some cases agreed well, and several trends were generally followed, it was apparent that the code neither reliably nor accurately predicted the location and extent of transition nor the observed increase in heating in a fully turbulent boundary layer modified by increased FST levels. This code, named STANCOOL, has several model options for calculating transition and also the structure of a turbulent boundary layer. Although one might have expected the inclusion of a turbulence kinetic energy equation into the model to have produced better results than the simpler mixing length model, both calculations agreed with each other better than with the data in several cases. These results have pointed to the need for improved computational capability.

The present investigation is meant to be in continuation of the effort by MacArthur, with the overall aim of understanding the effect of FST in the augmentation of turbulent heat transfer. This investigation focuses on the case of turbulent flow over a flat plate and the method of modifying STANCOOL so as to produce better agreement with the recent measurements by Blair.

II. OBJECTIVES

It is appropriate to make a distinction between two types of objectives: long range and immediate. Clearly, the long range objectives are beyond the scope of the present investigation because the actual problems of interest are exceedingly complex, with various aspects having been subjected to considerable attention for several decades. Nevertheless for the sake of perspective, one might nominate two long range objectives. The practical objective involves the attainment of a computational capability which predicts heating and flow conditions in the real turbine blade environment both accurately and cost-effectively. An objective from the more philosophical viewpoint, but with practical consequences, is the increased understanding of the mechanisms and structure of turbulent shear flows.

For the present investigation the immediate objectives are restricted to the following:

(1) To achieve a working understanding of the existing code, STANCOOL, which is meant to calculate boundary layer development and heating in flow situations similar to those in turbine blade environments.

(2) To become familiar with literature pertaining to the effects of free stream turbulence on heating augmentation, in particular the recent extensive experimental works by Blair.

(3) To formulate a preliminary turbulence model which incorporates the effects of FST into STANCOOL in an improved fashion.

(4) To compare results of the modified code with Blair's data.

(5) To recommend continued investigations in light of the present findings.

By means of these fundamental investigations, it is anticipated that

more accurate and reliable codes will eventually be at hand.

III. PROBLEM DESCRIPTION

In order to meet the objectives listed in the previous section, the method of attack has consisted of four phases. First, Blair's data have been logged into computer storage for the purposes of plotting, scrutiny, and eventual comparison with computations. Second, detailed profile data have been compared with corresponding profiles obtained from STANCOOL, utilizing the mixing length model for computations. These comparisons have revealed possible causes for the earlier discrepancies[1] noted for Stanton number, which may be viewed as an integrated effect. Third, a modification of the turbulence model is being proposed on the basis of these comparisons and on the basis of earlier observations by Miyazaki and Sparrow[9] and Belov et al.[10]. Last, a comparison is made between Blair's data and the results of the new model.

A full description of the configuration and the physical parameters is given in Blair's reports[2-8], and earlier computations using STANCOOL have been described by MacArthur[1]. The latest documentation available for the use of STANCOOL is given in Reference 17. Briefly, the measurements were made in a recirculating wind tunnel over a heated flat plate with a mean external velocity of 100 ft/sec. Typical mean temperature differences between the wall and the free stream were in the range 10°F to 40°F. The free stream turbulence level was varied by means of insertion of 5 different grid configurations upstream of the tunnel contraction section. The streamwise decay of FST intensity was in accord with those of previous grid generated experiments, and the intensity ranged approximately from 0.25% to 7%. Measurements included wall temperature distributions, wall heat fluxes, profiles of mean velocity and mean temperature, and profiles

of various turbulence correlations at selected downstream locations.

In Figure 1 are illustrated the variations of Stanton number and skin friction coefficient with changes in Reynolds number and FST parametrically. FST is seen to influence the results in two ways: (1) the location of transition moves upstream dramatically with increasing FST, and (2) both S_t and C_f increase in the fully turbulent boundary layer as FST increases. In fact, the results have shown[4] that the Reynolds analogy factor, $2S_t/C_f$, increases with FST, indicating that the heating is proportionately more sensitive to FST than is the skin friction coefficient. This observation is particularly important for turbine blade cases because these may occur at higher levels of FST (perhaps 20%) than have been measured in simulations. Blair's data for S_t are more extensive and exhibit less scatter than those for C_f. Therefore, the S_t data provide a better basis for comparison with computations. The solid lines in Figure 1 represent results from STANCOOL utilizing the pre-existing mixing length model. The predictions of transition location are not adequate, although it is important to note[4] that the experimental transition for grid configuration 0 (least FST) was prematurely effected owing to 3D corner flow effects, and that the extreme mismatch with calculations in this case should be discounted. Since the pre-existing mixing length model provides no mechanism for FST effects, the increase of S_t and C_f in the fully turbulent region is clearly not followed by the computations. During the ten week summer period of investigation, the focus has been restricted to the structure of the fully turbulent boundary layer.

Since S_t and C_f are evaluated at the solid boundary only, they possibly represent symptoms of more pervasive phenomena occuring throughout the
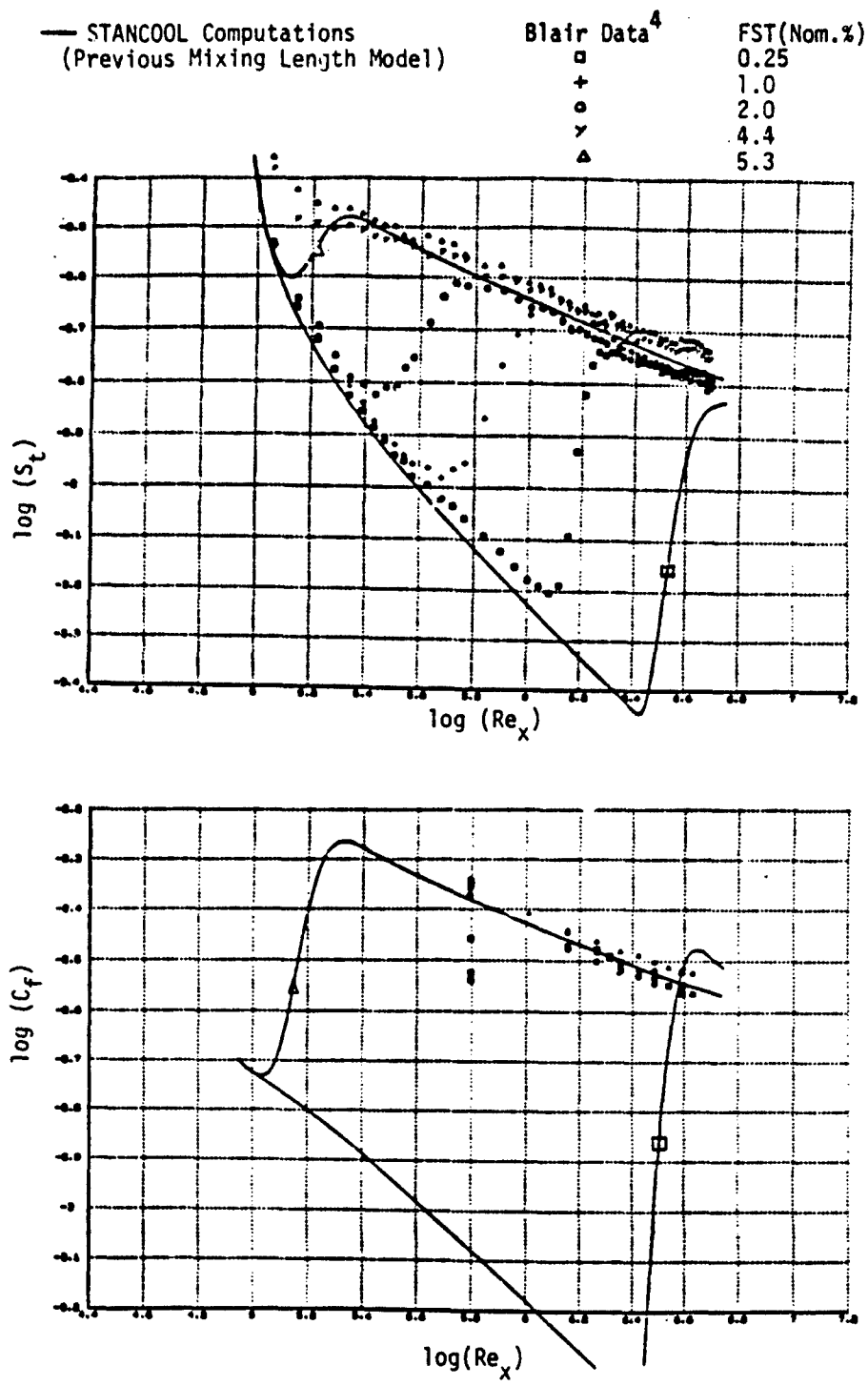
Figure 1: Comparisons of log (S_t) and log (C_f) vs. log (Re_x) for various levels of FST.

boundary layer structure. In an effort to improve the understanding of underlying causes, a comparison of mea ⌐rofiles was made. In Figure 2 are sample comparisons between computed and measured mean profiles at downstream location x = 84 in. with grid configuration 4 (greatest FST). For this extreme case it is evident that the existing mixing length model does not match the $\bar{u}$ profile in the center of the boundary layer, although the match near the wall appers to be better. However, the wall region is better shown in a logarithmic format since the variations there are extremely rapid. Similar comparisons of $\bar{u}$ in cases of weaker FST show much better agreement, indicating that FST has a marked effect on boundary layer structure.

Lastly, in the comparison of profiles, it is important to illustrate the effect of FST on the Reynolos stress term $\overline{u'v'}$, and on the turbulent heat transfer term, $\overline{v'T'}$. These terms need to be modeled correctly, so that the ensuing computations of $\bar{u}$ and $\bar{T}$ produce the correct results for skin friction and wall heating respectively. In Figure 2 it is seen that the mixing length hypothesis does not produce an adequate characterization of the Reynolds stress profile. In fact, the mismatch becomes worse as the FST increases. The experiments clearly indicate that values for $\overline{u'v'}$ and $\overline{v'T'}$ are increased towards the boundary layer edge and are decreased towards the wall in comparison to the model. Later results herein will show that the characteristics of turbulence decay into the free stream are severely altered by the presence of FST.

The avenue for an improved computation scheme then becomes more apparent. FST effects need to be accurately incorporated into the $\overline{u'v'}$ and $\overline{v'T'}$ descriptions. Subsequent computations of $\bar{u}$, $\bar{T}$, S_t and C_f should then reflect better matches with the corresponding data. This point should
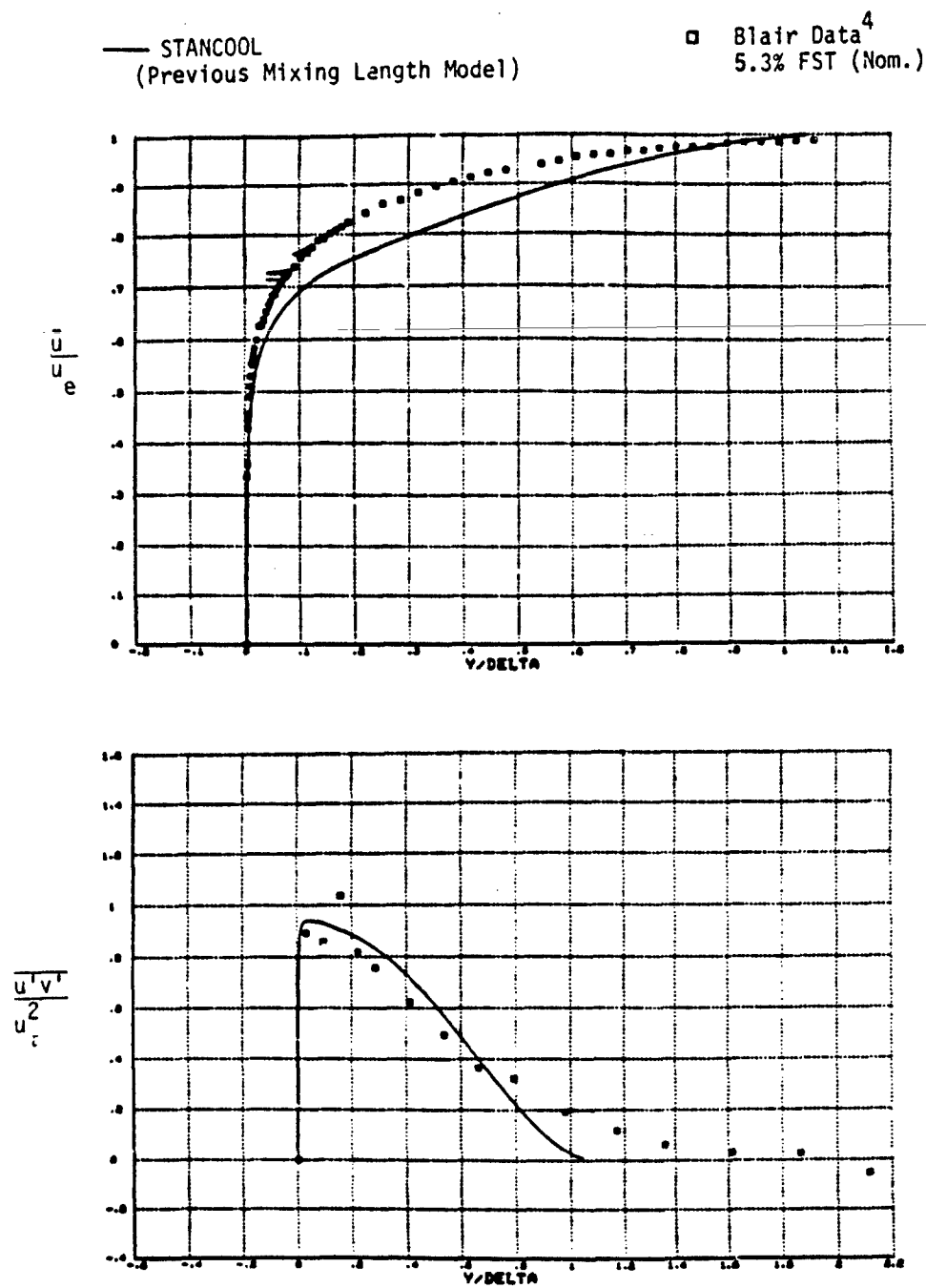
Figure 2: Mean velocity and Reynolds stress profiles.

be valid regardless of the complexity of the computational method, such as inclusion of higher order turbulence equations. An improvement in terms of a modified mixing length model is attempted in the next section.

IV. MODELING OF FREE STREAM TURBULENCE

A rational and consistent model for $\overline{u'v'}$ and $\overline{v'T'}$ is difficult to construct. Every model based on the equations of motion, regardless of complexity, requires a set of closure assumptions. In past investigations it has occurred that even the most refined and time consuming approaches have lead to results that have failed to produce improved predictions. The approach taken here has been to scrutinize Blair's data in order to appreciate the actual effects of FST, and then to formulate a simple model which contains the observed effects. By variations of the model parameters, important interplays in the equations of motion are highlighted, thereby indicating directions for continued and more accurate modeling.

The initial observation has been that the mixing length model fails to capture the essence of Coles' wake region[18] as the FST increases. Furthermore, as is evident from Figure 2, the turbulence structure extends into the free stream far beyond the usual definition of the boundary layer edge, δ. This observation has also been made in References 19-22. However the extent to which the outer structure influences the wall region is not clear, and needs to be assessed. In studying the effect of FST on heating at the stagnation point of a cylinder, Miyazaki and Sparrow[9] proposed the following extention to the mixing length model:

$$-\overline{u'v'} = \ell^2 \left|\frac{\partial \bar{u}}{\partial y}\right|\frac{\partial \bar{u}}{\partial y} + A\ell u_e I_e (\frac{y}{\delta})\frac{\partial \bar{u}}{\partial y} - \overline{u'_e v'_e} (y/\delta)^2 \qquad (1)$$

where the first term on the right is the usual mixing length model[9] and the second two terms represent the additional effects of FST. Here, I_e is the turbulence intensity external to the boundary layer. The coefficient, A, is the sole parameter that may be adjusted to match data. Miyazaki and Sparrow claim that the inspiration for their model originated from the experimental work of Belov et al.[10], who observed that the r.m.s. fluctuation profile in the absence of FST was augumented in a linear fashion by the presence of FST.

Equation (1) appeared to be a reasonable starting point for the present investigation, especially since the measurements of Belov et al. were conducted over a flat plate, and also because the modification of STANCOOL would be particularly simple. The mixing length model was changed to:

$$-\overline{u'v'} = \epsilon_M \frac{\partial \bar{u}}{\partial y} \tag{2}$$

where $\epsilon_M = \ell^2 \left|\frac{\partial \bar{u}}{\partial y}\right| + A\ell u_e I_e (y/\delta)$

This change in the code produced a significant, but limited, improvement. Now, several correct trends were introduced which were absent earlier: S_t and C_f increased with I_e; the $\bar{u}$ and $\bar{T}$ profiles became fuller and matched Blair's data better; and the $\overline{u'v'}$ and $\overline{v'T'}$ profiles extended into the free stream at an improved rate. However, inconsistencies also appeared. With only one free parameter, A, it was not possible to match the variety of comparisons simultaneously. In particular:

(1) With a good $\overline{u'v'}$ match, the $\bar{u}$ comparison with data was noticeably inadequate, although improved over the previous model; and vice-versa.

129-13

(2) The S_t and C_f predictions required different values for A than did the mean profiles.

(3) The slope of S_t and C_f vs. Re_x did not agree with the data for a constant value for A.

In an attempt to improve the Miyazaki and Sparrow model, Blair's data were replotted in several variations, one of which was a semilogarithmic version of the velocity defect, as exemplified in Figure 3. It is striking that the mean velocity defect appears to be well characterized by an exponential behavior for approximately the outer 80% of the boundary layer. Since this observation appears to be new in the literature, and since profound deductions might be connected with it, the issue was pursued further. The present conclusions are summarized as follows:

(1) The exponential character does not occur for lower levels of FST (<3%) as seen from Blair's data, in which cases the free stream levels are approached more rapidly.

(2) It is suspected that the exponential character is approached as a limiting form for sufficiently high FST (>4% here), and that this form may hold for all higher levels of FST.

(3) The mean temperature behavior has an exponential character which appears identical to that of the mean velocity.

(4) A short distance downstream of the leading edge (~2 ft), the velocity and temperature profiles become self-preserving to an excellent degree, as described by the subsequent equations.

(5) The $\overline{v'T'}$ profile also has a limiting exponential character as seen in Figure 3. However, the corresponding $\overline{u'v'}$ profile appears not to have such a form, either owing to experimental scatter or to a fundamental
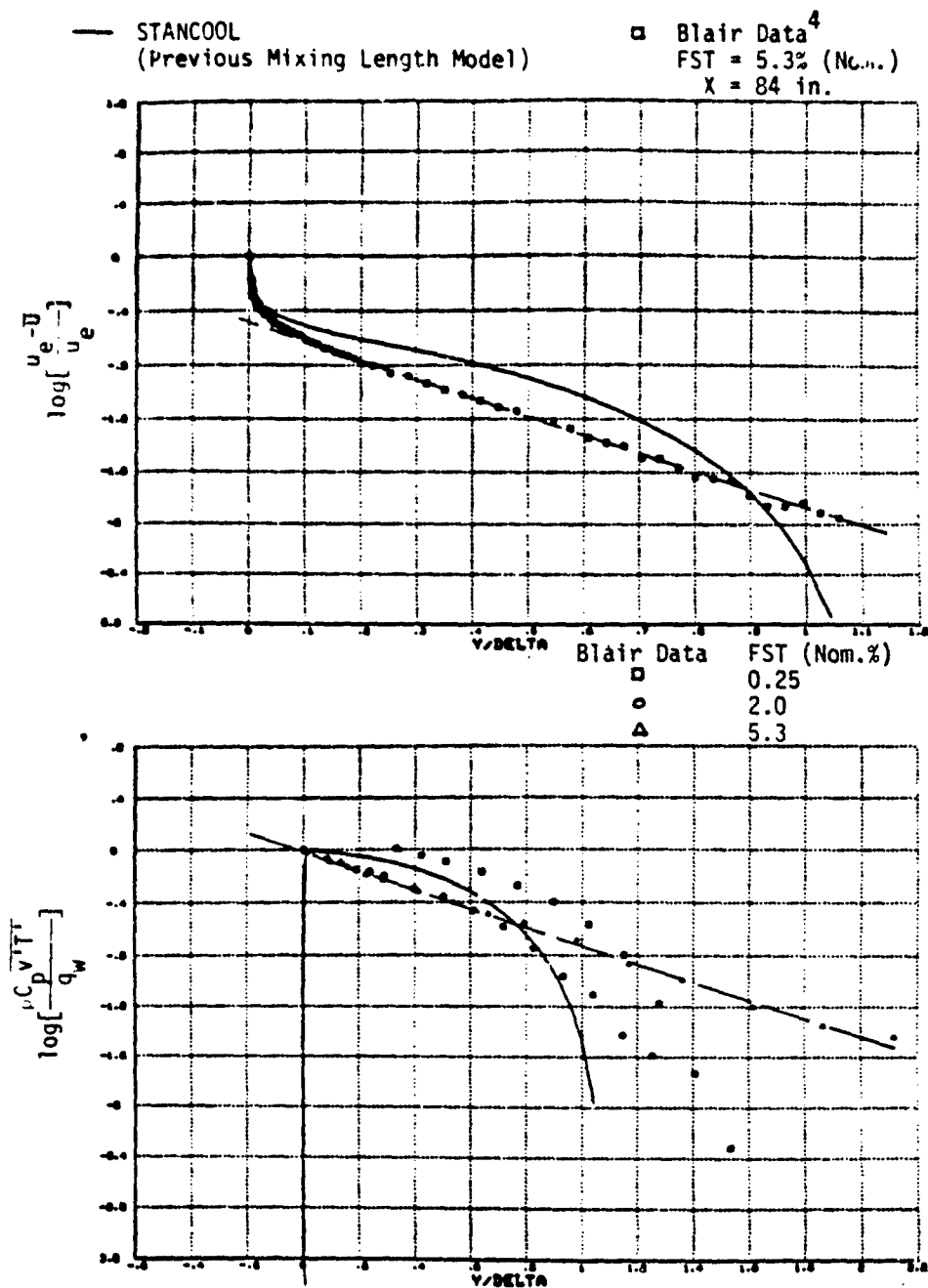
129-14

Figure 3: Boundary layer wake region characterized by exponential decay for cases of high FST levels.

difference in its nature. It is extremely interesting to note that the exponential decay rate of $\overline{v'T'}$ appears to be exactly one half of the corresponding rates for $\overline{T}$ and $\overline{u}$. This point will resurface in what follows.

Given the observed exponential character of the outer region, it is possible to utilize the mean fluids equations to deduce explicit functional forms for $\overline{u'v'}$ and $\overline{v'T'}$ as applicable. The argument is summarized as follows:

(1) From experimental observation:

$$\frac{\overline{u}}{u_e} = 1 - \frac{1}{\beta} \exp[-\alpha \frac{y}{\delta}] \quad ; \quad \frac{\overline{T}-T_e}{T_w-T_e} = \frac{1}{\beta} \exp[-\alpha \, y/\delta] \tag{3}$$

where $\alpha, \beta \cong \sqrt{10}$

(2) From the ideal gas equation ($\overline{p} \cong$ constant):

$$\frac{\rho_e}{\overline{\rho}} = 1 + [\frac{T_w}{T_e} - 1] \frac{\exp}{\sqrt{10}} [-\sqrt{10} \, y/\delta] \tag{4}$$

(3) By integration of the conservation of mass equation:

$$\frac{\overline{\rho}\,\overline{v}}{\rho_e u_e} = - [\frac{1}{T_e} \frac{dT_w}{dx} + \frac{T_w}{T_e} \frac{1}{\delta} \frac{d\delta}{dx} (1 + \sqrt{10} \, \frac{y}{\delta})] \frac{\delta \exp[-\sqrt{10}y/\delta]}{10} \tag{5}$$

(4) By integration of the momentum equation:

$$-(\frac{\overline{\rho}}{\rho_e}) \frac{\overline{u'v'}}{u_e^2} = \{c(x) \frac{\partial\overline{u}/u_e}{\partial y/\delta} + [\frac{1}{R_{e\delta}} + \frac{1}{10} \frac{d\delta}{dx} (1+\sqrt{10} \, \frac{y}{\delta})]\} \frac{\partial u/u_e}{\partial y/\delta} \tag{6}$$

(5) By integration of the energy equation:

$$-(\frac{\overline{\rho}}{\rho_e}) \frac{\overline{v'T'}}{u_e^3} = \{A_T(x)+yB_T(x)\}\exp[-\sqrt{10} \, y/\delta] \tag{7}$$

+ higher order exponentials

Several observations are made concerning these equations. First, the form obtained for $\overline{u'v'}$ in Equation (6) is strikingly similar to the Miyazaki and Sparrow model given in Equation (2), and therefore this model appears to have further support. It should be emphasized that Equation (6) is not meant to be applicable in the wall region in which the exponential behavior is not observed. However, the term which includes the coefficient, $c(x)$, is very similar in form to the usual mixing length hypothesis. This leads to the speculation that FST may influence the wall region directly through this non-linear term. Second, there are two additional terms appearing in Equation (6) which do not appear in the earlier model. In comparison to the other terms, $R_{e\delta}^{-1}$ is negligible for the fully turbulent boundary layer, and it is therefore discarded below. The constant term is comparable to the y/δ term and is therefore retained below. Third, the coefficient of the y/δ term explicitly depends on x, whereas in the initial model based on Equation (2) the factor, A, was considered to be constant.

The deduction following from the energy equation leads to a note-worthy dilemma. For the high FST cases the experimental results for $\overline{v'T'}$ consistently follow the form shown in Figure 3, in which the decay rate is one half that of the mean velocity and mean temperture. However, these assumptions lead to Equation (7), which indicates that the slowest decay is identical to that of $\bar{u}$ and $\bar{T}$, not the half power. Furthermore, the appearance of the y/δ factor in Equation (7) suggests that the semilogarithmic plot should not yield a straight line, in contradiction to experimental observation. Such a mismatch in form cannot be reconciled by adjusting the magnitudes of the coefficients; and therefore, there appears to be a fundamental inconsistency, which may have profound consequences. It is

necessary to reconsider the assumptions leading to Equation (7). Such an effort is beyond the present scope and is recommended for continued investigation. In brief, however, the mean energy equation leading to Equation (7) is the one utilized in STANCOOL, and it is commonly assumed to apply[17] in these cases. By cursory inspection and by an order of magnitude analysis, it appears that certain correlation functions involving density fluctuations ought not be neglected, and inclusion of these may resolve the dilemma.

In light of the previous discussion, the turbulence model formulated for the present study has evolved to the following:

Eddy viscosity:

$$\epsilon_M = \ell^2 \left|\frac{\partial \bar{u}}{\partial y}\right| + Au_e I_e(x)\ell\delta^m(x)D^n u_\tau^2(x)[1 + B(y/\delta)] \tag{8}$$

Turbulent Prandtl number:

$$Pr_t = \frac{\epsilon_M}{\epsilon_H} = \frac{\ell^2\left|\frac{\partial \bar{u}}{\partial y}\right| + [C_1 I_e + C_2]u_e\ell\delta^m D^n u_\tau^2 [1 + 3\frac{y}{\delta}]}{a\ell^2\left|\frac{\partial \bar{u}}{\partial y}\right| + C_3 u_e\ell\delta^m D^n u_\tau^2[1 + B\frac{y}{\delta}]\exp[\frac{B}{4}\frac{y}{\delta}]} \tag{9}$$

where

   D is the van Driest damping factor[17].

and

$$u_\tau^2 \sim \tau_w(x) \sim \frac{d\delta}{dx}$$

In Equation (8) the damping factor is included so that the FST addition vanishes in the wall region in comparison to the mixing length model. Furthermore, the streamwise dependence of the FST effect may be adjusted via the power of $\delta(x)$. The form chosen for Pr_t requires further comment, as it is clearly a compromise utilized soley for the sake of computation in

STANCOOL. In STANCOOL the turbulence effect on heating is modeled directly through Pr_t, and use of any other method would require extensive alterations of the code. In the spirit of the Reynolds analogy, it is assumed that the forms of $\overline{u'v'}$ and $\overline{v'T'}$ are similar, and this leads to the ratio expressed in Equation (9). The added modifications are introduced primarily in an effort to fit Blair's measurements of Pr_t. The exponential factor is added in compensation for the observed decay rate of $\overline{v'T'}$ and also to produce the large decrease of Pr_t with increasing y that has been observed by several investigators [4, 9]. The constant, a, is included in an effort to vary Pr_t in the near wall region, and the constants C_1, C_2, C_3 are chosen to match the observed increase of Pr_t with increasing I_e.

V. RESULTS

It 's shown in this section that typical computations utilizing the model described by Equations (8) and (9) can produce results which are in better agreement with Blair's data than was the case with the original STANCOOL options. However, it is not claimed that the new model is free of inconsistencies, nor that it may be used with confidence in extrapolation to other flow regimes. The model is intended to highlight some of the new observations concerning te effects of FST, and also to be a vehicle for continued improvements.

Figures 4, 5, and 6 are intended to parallel the earlier discussions, with the inclusion of the results of the latest computations. In Figure 4 the computed boundary layer has been forced to undergo transition near the experimentally observed locations, with the objective of removing this added uncertainty from the comparisons. In contrast to Figure 1, the Stanton number now increases in the turbulent boundary layer as the FST
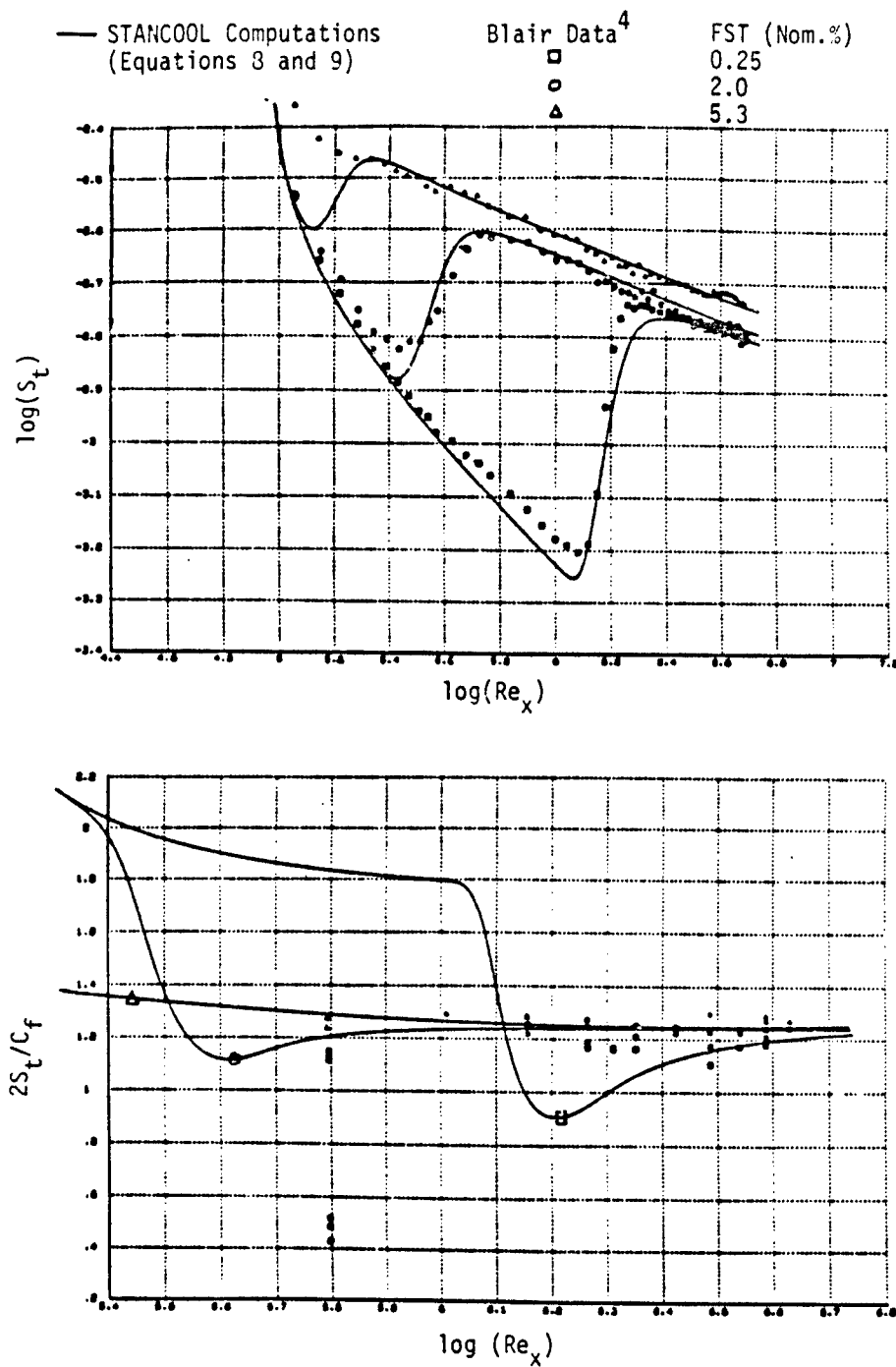
Figure 4: New mixing length model. Comparisons of Stanton number and Reynolds analogy factor with Blair's data.

level increases, and the comparison is good. In order to achieve these computations, the parametric values chosen in the model are as follows:

$$
\begin{aligned}
A &= 0.013 \\
m &= 1 \\
n &= 4 \\
B &= \sqrt{10} \\
C_1 &= 3 \\
C_2 &= 0.2 \\
C_3 &= 0.2 \\
a &= 1.18, \ 1.20, \ 1.50 \qquad \text{(as FST increases)}
\end{aligned} \tag{10}
$$

In addition, the exponential coefficient in the van Driest damping factor[17] was chosen to be: $A^+ = 35$. During the search for these values, several other observations emerged. As might have been anticipated, significant changes in the outer portions of the $\overline{u'v'}$ and Pr_t modeling had minor effects on C_f and S_t, unless the exponent of the damping factor, n, was chosen small enough so that the usual mixing length did not dominate the wall region. Although it has been claimed[11] that the wall region is rather insensitive to external changes, it is evident from Figure 3 that FST influences not only the wake but also that the law of the wall region is greatly reduced in size, perhaps disappears totally for high FST levels. It is vitally important to have measurements to small values of $y^+(\sim 5)$, because the character of the damping factor cannot be inferred from the logaritnmic region. In the present computations, the FST influence on C_f and S_t required an independent adjustment of A^+ in order to effect correct trends. In addition, the near wall region of Pr_t required adjustment via the parameter, a, in order to model FST effects on S_t.

Although the arguments leading to Eqution (6) prescribe a specific x dependence for the turbulence model, this dependence had to be slightly altered by the exponent, m, in Equation (8) in order to match the observed x variation of C_f and S_t.

In the lower half of Figure 4 are shown the variations of the Reynolds

analogy factor, $2S_t/C_f$, with changes in R_{ex} and FST. At several downstream stations the scatter in the data provides an indication of three dimensional flow effects, since these differences arise from variations in spanwise location.[4] Nevertheless, as the FST increases from 0.25% to 5%, it appears that $2S_t/C_f$ increases from 1.15 to 1.25 approximately. The present Pr_t model is seen to yield a computational result that is similar qualitatively. It should be noted that the laminar computation of the Reynolds analogy factor is high owing to the experimental staggering of heating onset with respect to the leading edge[4].

In Figure 5 is exhibited an improved overall calculation of $\bar{u}$ as compared with Figure 2. By further adjustment of the parameters it is possible to decrease the mismatch near the wall. A similar improvement occurs for $\bar{T}$. However acceptable this plot may seem in the wake region, a detailed scrutiny in semilogarithmic form reveals that the measured exponential decay of the corresponding deficits (cf. Figure 3) is not reproduced by the computations. Therefore, a fundamentally correct nature is absent from the modeling. However, this difference may be important only in principle. Further comparisons of velocity profiles are shown in law of the wall coordinates in the lower half of Figure 5. There is an important mismatch in the logarithmic region between the computations and the data, and this corresponds to the mismatch in the upper half of the figure. Although further adjustments of the parameters could decrease the mismatch, it is clear that further investigation is required. It is seen that an increase of FST has a pronounced effect in decreasing Coles' wake region[18].

Another deficiency is revealed in Figure 6 in regard to the $\overline{v'T'}$ comparison. In spite of the fact that S_t and $\bar{T}$ have been well calculated

STANCOOL Computations   □ Blair Data[4]
(Equations 8 and 9)   FST = 5.3% (Nom.)
                            X = 84 in.

$\frac{\bar{u}}{u_e}$

Y/DELTA

Blair Data	FST
□	0.25
○	2.0
△	5.3

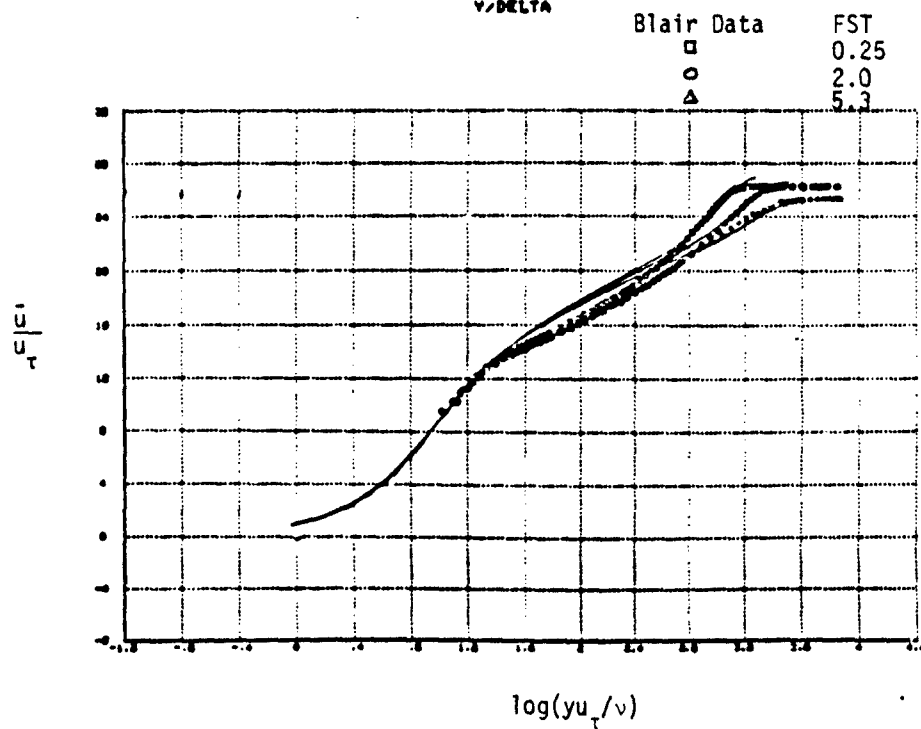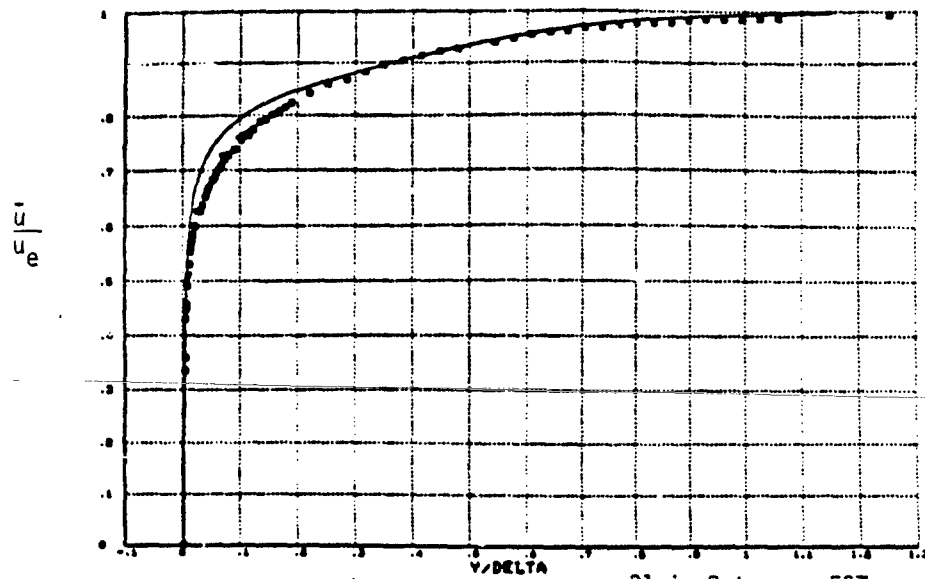$\frac{\bar{u}}{u_\tau}$

$\log(yu_\tau/\nu)$

Figure 5: Velocity profile comparisons with new mixing length
           model.

129-23

(in comparison), the corresponding calculation for $\overline{v'T'}$ has not matched the data, although a correct trend has been established with increasing FST. None of the parametric variations in the modeling seem to have produced the exponential character of the measured $\overline{v'T'}$, and this issue remains perplexing.

Lastly, in Figure 6, the comparisons of Pr_t are shown. The main observations are that the near wall modeling influences S_t, whereas the bulk of the Pr_t shape influences the T profile only slightly in the wake region. During scrutiny of Blair's data, it was noticed that outside of the boundary layer Pr_t passed through zero and became negative in some cases. Since the downward trends were too consistent to be attributed to experimental scatter, an explanation was sought. It was already noted earlier that the turbulence clearly extends beyond the usual boundary layer edge. In fact, towards the most downstream stations of measurement, the data indicate that the structure is still non-uniform even at the channel centerline, whereas the boundary layer thickness is roughly of half that length. Therefore, it is very likely that channel flow effects have influenced the Pr_t measurements. Since only the upper wall is heated, the $\overline{v'T'}$ profile has the same sign throughout the channel height, while $\overline{u'v'}$ must change sign near the tunnel centerline by symmetry. Since the upper and lower boundary layers are not matched in thickness, it is probable that $\overline{u'v'}$ and $\frac{\partial u}{\partial y}$ have zero crossings at different y locations, thereby invalidating the usual mixing length approach. Such circumstances could lead to negative values for Pr_t. It is therefore conjectured that true boundary layer measurements, uncontaminated by channel effects, would not contain such large decreases in Pr_t in the wake region as were observed here. It would be of interest to reconsider previous Pr_t measurements (and the wide
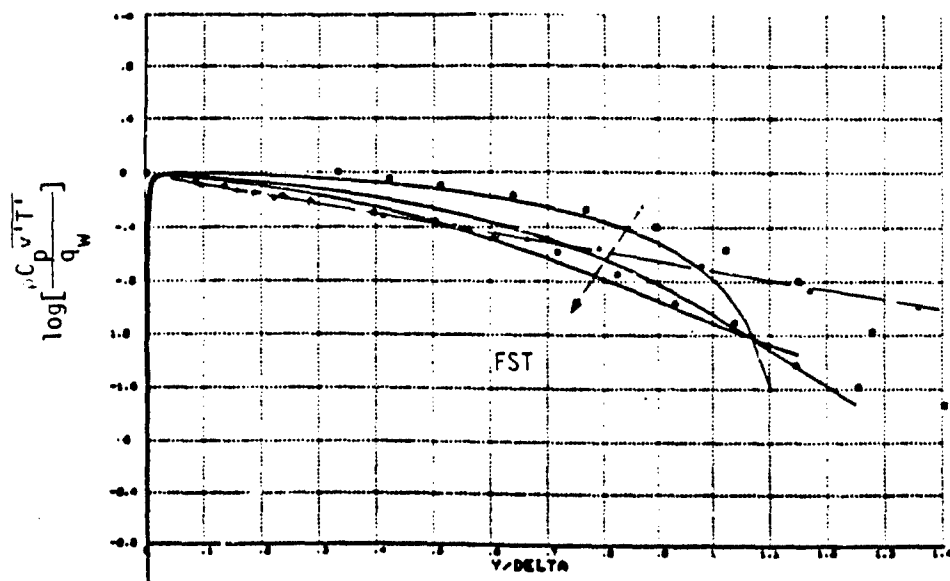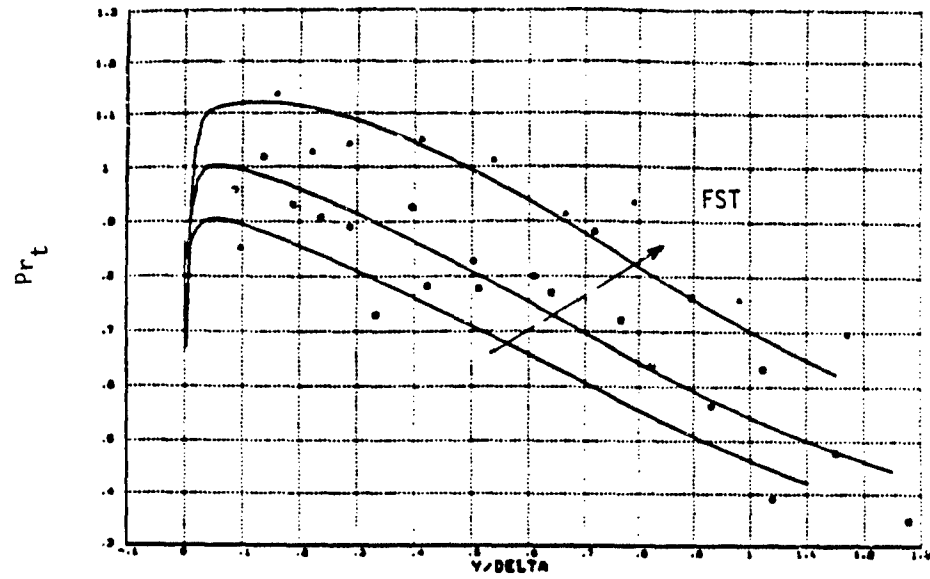
Figure 6: Comparisons of Pr_t and $\log \left[\dfrac{\rho C_p \overline{v'T'}}{q_w}\right]$ models with Blair's data.

scatter in results) more systematically in light of this channel flow observation. A further question arises as to which case is closer to the actual turbine blade situation. These issues remain for continued investigation.

VI. SUMMARY OF ACCOMPLISHMENTS

(1) A working knowledge of the code STANCOOL has been attained.

(2) An extension of the Miyazaki and Sparrow model for FST effects has been incorporated into STANCOOL.

(3) The extensive measurements of Blair have been studied and compared with sample calculations using the modified code. Results have shown a significant improvement, but several discrepancies have been identified.

(4) A fundamental exponential behavior in the wake region of a turbulent boundary layer for cases of high FST has been noted, apparently for the first time.

(5) An explanation is proposed for the observed large drop in Pr_t in the wake region. It is conjectured that this behavior is symptomatic of channel flow effects in such experiments.

(6) Deductions from the observed exponential behavior reveal a logical dilemma concerning the energy equation. This dilemma may be of fundamental importance and requires further investigation.

VII. RECOMMENDATIONS:

Several issues require further investigation experimentally, theoretically and computationally. In order of increasing difficulty in each category these are:

Experimental

(1) Exploration of the outer boundary layer with hot wires for cases of higher FST to determine the extent of the exponential character noted for the first time herein.

(2) Measurements of Pr_t designed to assess the extent of channel flow influence on this variable.

(3) Variation of FST scale size.

(4) Measurements in thicker boundary layers to determine heat transfer and the damping factor very close to the surface.

(5) Experiments to include measured density fluctuations in environments of higher levels of FST.

Theoretical

(1) Further deductions concerning the exponential wake region.

(2) Formulation of an FST model which includes the influence of scale sizes and phase lags throughout the boundary layer.

(3) Further refinements to the theory of transition onset and extent in the presence of FST.

(4) Resolution of the observed heat transfer dilemma involving the energy equation. Assessment and inclusion of additional correlation terms involving density and perhaps pressure fluctuations.

Computational

(1) Continuation of the present modeling. Inclusion of further data comparisons.

(2) Extension of the current modeling to include the TKE equation and higher order equations.

(3) Further modeling of FST effects on transition.

(4) Calculations including pressure gradient and non-equilibrium cases.
     Extensions to higher FST calculations.

VIII. <u>REFERENCES</u>:

1. MacArthur, C. D., "Prediction of Free-Stream Turbulence Effects on Boundary Layer Heat Transfer - An Evaluation of the Heat Transfer Code STAN5", <u>1983 USAF-SCEEE Graduate Student Summer Support Program</u>, Contact No: F49620-82-0035, 16 September 1983.

2. Blair, M. F., "Influence of Free-Stream Turbulence on Turbulent Boundary Layer Heat Transfer and Mean Profile Development, Parts I & II", <u>ASME Journal of Heat Transfer</u>, Vol. 105, February 1983, pp. 33-47.

3. Blair, M. F., "Influence of Free-Stream Turbulence on Boundary Layer Transition in Favorable Pressure Gradients", <u>ASME Journal of Engineering for Power</u>, Vol. 104, October 1982, pp. 743-750.

4. Blair, M. F., "The Effect of Free-Stream Turbulence on the Turbulence Structure and Heat Transfer in Zero Pressure Gradient Boundary Layers", <u>United Technologies Research Center Report</u>: R82-915634-2, East Hartford, Conn., November 1982.

5. Blair, M. F., "Final Data Report-Vol. I-Velocity and Temperature Profile Data for Zero Pressure Gradient, Fully Turbulent Boundary Layers", <u>UTRC Report</u> R81-914388-15, E. Hartford, Conn., January 1981.

6. Blair, M. F., "Final Data Report-Vol. II-Velocity and Temperature Profile Data for Accelerating. Transitional Boundary Layers", <u>UTRC Report</u> R81-914388-16, E. Hartford, Conn., January 1981.

7. Blair, M. F., "Combined Influence of Free-Stream Turbulence and Favorable Pressure Gradients on Boundary Layer Transition and Heat Transfer", <u>UTRC Report</u> R81-914388-17, E. Hartford, Conn., March 1981.

8. Blair, M. F., "The Influence of Free-Stream Turbulence on the Zero Pressure Gradient Fully Turbulent Boundary Layer", <u>UTRC Report</u> R80-914388-12, E. Hartford, Conn. September 1980.

9. Miyazaki, H. and E. M. Sparrow, "Analysis of Effects of Free-Stream Turbulence on Heat Transfer and Skin Friction", <u>ASME Journal of Heat Transfer</u>, Vol. 99, November 1977, pp. 614-619.

10. Belov, I. A., Gorshkov, G. F., Komarov, V. S., and V. S. Terpigor'ev, "Influence of Jet Turbulence on Flow in the Boundary Layer Near the Wall", Translated from <u>Zhurnal Prikladnoi Mekhaniki i Tekhnicheskoi Fiziki</u>, No. 6, November-December 1982, pp. 77-82.

11. Simonich, J. C., and P. Bradshaw, "Effect of Free-Stream Turbulence on Heat Transfer through a Turbulent Boundary Layer", <u>ASME Journal of Heat Transfer</u>, Vol. 100, November 1978, pp. 671-677.

12. Bayley, F. J. and W. J. Priddy, "Effects of Free-Stream Turbulence Intensity and Frequency on Heat Transfer to Turbine Blading", <u>ASME Journal of Engineering for Power</u>, Vol. 103, January 1981, pp. 60-64.

13. McDonald, H., and J. P. Kreskcvsky, "Effect of Free Steam Turbulence on the Boundary Layer", _Int. J. Heat Mass Transfer_, Vol. 17, 1974, pp. 705-716.

14. Junkhan, G. H., and G. K. Serovy, "Effects of Free-Stream Turbulence and Pressure Gradient on Flat-Plate Boundary-Layer Velocity Profiles and on Heat Transfer," _ASME Journal of Heat Transfer_, Vol. 89, May 1967, pp. 169-176.

15. Hall, D. J., and J. C. Gibbings, "Influence of Stream Turbulence and Pressure Gradient upon Boundary Layer Transition", _Journal of Mechanical Engineering Science_, Vol. 14, No. 2, 1972, pp. 134-146.

16. Hancock, P. E., and P. Bradshaw, "The Effect of Free-Stream Turbulence on Turbulent Boundary Layers", Dept. of Aeronautics, Imperial College, London, England, Report in Progress - Private Communication.

17. Crawford, M. E., and W. M. Kays, "STAN5 - A Program for Numerical Computation of Two-Dimensional Internal and External Boundary Layer Flows", _NASA CR-2742_, November 1976.

18. Coles, D. E., "Turbulent Boundary Layers in Pressure Gradients: A Survey Lecture Prepared for the 1968 AFOSR-IFP-Stanford Conference on Computation of Turbulent Boundary Layers", _Rand Corp. Memorandum_ RM-6142-PK, October 1969.

19. Charnay, G., G. Comte-Bellot, and J. Mathieu, "Development of a Turbulent Boundary Layer on a Flat Plate in an External Turbulent Flow", _AGARD_ CP93, Paper No. 27, 1971.

20. Huffman, F. D., D. R. Zimmerman, and W. A. Bennet, "The Effect of Free-Stream Turbulence Level in Turbulent Boundary Layer Behavior", _AGARD_ AG164, 1972, pp. 91-115.

21. Hancock, P. D., "Effect of Free-Stream Turbulence in Turbulent Boundary Layers", Ph.D. Thesis, Imperial College, London Univ., 1980.

22. Evans, R. L., "Free-Stream Turbulence Effects on the Turbulent Boundary Layer," _A.R.C._ C.P. 1282, 1974.

1984 USAF-SCEEE SUMMER FACULTY RESEARCH PROGRAM

Sponsored by the
AIR FORCE OFFICE OF SCIENTIFIC RESEARCH
Conducted by the
SOUTHEASTERN CENTER FOR ELECTRICAL ENGINEERING EDUCATION

FINAL REPORT

AN ADJOINT SYSTEMS APPROACH
TO LEARNING AND TRANSFER OF TRAINING

Prepared by: Dr. Robert E. Shaw

Academic Rank: Professor

Department and   Department of Psychology
    University: University of Connecticut

Research Location: Air Force Aerospace Medical Research Laboratory
                    Human Engineering Division

USAF Research   Dr. Rik Warren

Date: September 7, 1984

Contract No: F49620-82-C-0035

AN ADJOINT SYSTEMS APPROACH
TO LEARNING AND TRANSFER OF TRAINING

by

Robert E. Shaw

ABSTRACT

The primary motivation of ground-based flight simulator training is the belief that this will provide a safe, relatively inexpensive, and effective way to train pilots. It is assumed, of course, that such training will transfer positively and significantly to the flying of real aircraft. However no conclusive experimental evidence currently exists to support this claim. One reason for the lack of such evidence is overdependence of the current research on the Optimal Control Model which is ill-suited for either motivating the appropriate experiments or predicting and explaining learning and transfer of training effects. Reasons for these conclusions are reviewed and recommendations for the development of adaptive models within the more promising field of adjoint systems theory are given. A mathematical overview of this new approach is provided that should be empirically tested. Recommendations are made for doing so.

Acknowledgements

I. INTRODUCTION

An important goal of the AFAMRL/HEF is to increase crew effectiveness through ground-based simulator training. Unfortunately, no current mathematical model predicts learning and transfer effects in manual control tracking tasks, as candidly acknowledged by one of the authors of the highly popular optimal control model for human performance, or OCM approach.[1] The OCM approach provides no such model because it assumes that subjects perform optimally, thus leaving no room for improvement through learning.[2]

As a remedy, Levison[1] proposed including in the OCM an "internal model" to represent the subject's understanding of task-demands, and to provide parameters that might be "tweaked" for each change in initial conditions over trials or tasks. Thus it was hoped that adaptive effects could be modelled. But the addition of ad hoc parameters to a model fails as a general solution, and causes additional problems. For instance, it increases the need for brute force tweaking of parameters. This is an undesirable feature of a model because it limits its usefulness to post hoc curve fitting of data in lieu of genuine prediction over distinct task situations (e.g., different simulators, or from simulator tasks to real flight).

Indeed the OCM model is already liable to the charge of over-parametrization, that is, of having too many parameters to tweak. This results in excessive predictive power. The only models of explanatory value in science are those whose number of degrees of freedom do not exceed the number of constraints required to describe the phenomenon in question. Too few parameters to manipulate, then not all aspects of the phenomenon will be predictable, and thus the model is formally incomplete. Too many parameters, then aspects not belonging to the phenomenon will be falsely predicted, and thus the model is formally inconsistent.

The problem when developing a model is to hold the number of parameters to a minimum so as to avoid inconsistency and yet to have sufficient parameters to be complete. Models that achieve this balance are said to be in reduced form -- a property required if models are to possess both observability and controllability.[3]

130-4

Furthermore the use of describing functions * by the OCM approach only exacerbates the problem of over-parametrization. Describing functions typically have five parameters, perhaps as many as nine; thus, making this approximation technique liable to the charge of possessing excessive power for curve fitting human behavior.* Because of this large number of degrees of freedom, such functions can fit a wide variety of human behavior. Unfortunately, the flexibility of the describing function makes it incapable of precise prediction.*

An equally serious problem with the use of describing functions for modelling learning curves is that this technique can be misleading. The transmission time lag of the describing function is not the transmission time of the human from whose transfer function the describing function parameters are derived.

Another problem of the OCM approach has been its exclusive use of artificial compensatory tasks rather than the more natural pursuit tracking tasks. Apparently, the primary justification for the adoption of compensatory rather than pursuit task paradigms is that it makes modelling of tracking task data by the OCM more convenient. This is an artificial restriction, and one that renders the model unrealistic for making predictions about real world manual tracking tasks because they invariably involve matching output to input (pursuit) rather than merely reducing error (compensatory).

Finally, because transfer of training is ultimately the goal of ground-based simulator training, it should be pointed out that there is evidence of asymmetry of transfer between compensatory and pursuit tracking. This means that practice with the pursuit display benefits subsequent performance with the compensatory display more than does practice throughout with the compensatory display alone.*

For all of the above reasons , a strong case can be made for the need for an alternative approach to modelling adaptive systems in manual tracking tasks

II. OBJECTIVES

The main objectives of this project was to assess the potential of the OCM approach for modelling learning and transfer effects in flight simulation tracking tasks, and if necessary, to

suggest a more viable approach to the problem. In previous work,[7] the author had determined the generic form of learning equations that any minimally adequate adaptive system must satisfy if it is to be a realistic model for psychological learning theory. Figure 1 shows, in operator notation, the form that such an adaptive system assumes, while Table 1 exhibits the equations themselves. For the reasons given above, the OCM approach is not a likely candidate. Using the depicted system of integrodifferential equations as a presription of the job an adaptive system must do to learn, we set out to determine if such a system could be found.

III. LEARNING AS MODELLED BY A SYSTEM OF ORTHOGONALLY ADJOINT EQUATIONS

We begin with a brief summary of the Shaw & Alley paper[7] that treats learning as a functional governed by the system of four dual integrodifferential equations depicted in Table 1. Here it is argued that learning takes two forms:

First, action learning tunes the learner toward minimum energy expenditures in both orienting its sensory systems and controlling the motor system along an optimal path through task-demands to the task-goal. And second, there is perceptual learning which tunes the learner toward maximum information processing needed to orient and steer the motor systems along the optimal path. The optimization of both energy and information processing by the learner in task-specific ways requires modelling by functional equations that are temporally dual (Table 1 viewed row-wise), and satisfies the controllability criterion.[3]

On the one hand, learning is hereditary, being an accumulation of experiences over time that alters the initial conditions, or state of "readiness", of the action/perception systems toward optimal energy expenditures in responding to subsequent, recurring task-demands. But such "past-pending" control processes are goal "blind", being causal rather than intentional. On the other hand, learning is anticipatory as well, being an accumulation of expectancies over time that alters the final conditions, or the state of sensitivity, of the action/perception systems toward optimal information detection of the relevant task parameters (direction, distance, effort) needed

to steer a careful course toward the task-goal. By contrast, such "future-tending" processes have goal "acuity", being acausal, or intentional, and satisfy the observability criterion.[3]

In addition, the learning problem can be viewed from two perspectives: From the internal perspective of the learner as a system of degrees of freedom (state-variables) to be controlled and accomodated to a context of potentially non-linear, time-varying constraints -- the demands of the task-environnment, or from the external perspective of the task-environment as a dual system of such constraints (dual state-variables) that define the task for the learner. Thus the functional equations for modelling learning are not only temporal duals (Table 1 viewed row-wise) but perspective duals as well (Table 1 viewed column-wise).

These four functional equations define what can be called an orthogonally adjoint system. The system is orthogonally adjoint because, in one direction (designated the temporal duals), it consists of two pairs of dual equations to model hereditary (reinforcement) influences, on the one hand, and anticipatory (expectancy) influences, on the other. In the other direction (designated the perspective duals), two pairs of dual equations are defined over conjugate (information and energy) variables of the actor/perceiver control system, coupled in a mutual but reciprocal relationship with the task-environment.

Two mathematical questions were raised -- one general and the other specific. The general question was whether this system of learning equations could be satisfied by some kind of optimal control system with time lag. The answer was affirmative. The specific question was how to model the fact that whenever an action is successfully controlled and the goal attained, then it must result from the accurate perception of environmental constraints. This proved to be tantamount to the claim that when learning occurs, then an inner product operator[4] must exist whereby perceptual information is scaled invariantly over time to the energy requirements of control. Again the answer was affirmative.

Let us consider the form that these dual equations for information and control take within the mathematical theory of adjoint systems theory. It should be pointed out that the field

130-7

of adjoint systems is not well known, and, therefore, to make clear its use for modelling the problems at hand, we present a graded development of this approach. We begin with the simplest case, the _scalar_ one, and then develop the equations for the intermediate _matrix_ case, and, finally, arrive at the most involved equations for the _time lag_, or hereditary/anticipatory case.

IV. MATHEMATICAL FORMULATION OF THE LEARNING EQUATIONS AS AN ADJOINT IFORMATION/CONTROL SYSTEM WITH TIME LAG

For the reasons given in the previous section, the best model for adaptive systems is one which combines reinforcement and expectancy theories of learning into a single theory by means of the orthogonally adjoint system of equations.[7] Here action, as a control variable, is dual to perception, as an observation variable, in the sense understood in modern control theory.[3] Interestingly enough, in modern control theory, there exists several sets of dual, or adjoint equations, which might be used to explain the process of learning as described.

What follows is a summary of the relevant equations from modern control theory that might be used in learning theory to model the duality of perception, formally construed as observation, and action, formally construed as control.[7] Next, these equations are then expanded by considering a special class of control problems, the adjoint system, to accomodate the mutual and reciprocal relationship between the actor/perceiver and the task-environment.[7,10,11,12]

Finally, equations are proposed for a time delay system which exhibits hereditary effects, and whose adjoint system exhibits anticipatory effects -- on the analogy of reinforcement and expectancy theories, respectively. Thus, the time delay equations define adjoint systems with memory and anticipation. In addition, these systems exhibit the sequential, possibly nonlinear effects of trials, and other variables, such as "learning-to-learn", that may significantly affect learning and transfer effects.

We begin with a simple scalar differential equation process and investigate its adjoint system.

V. THE ADJOINT SYSTEM: SCALAR CASE

The scalar form of the adjoint system is the simplest case of a system defined by temporally dual equations. Recall that this : fundamental duality defines the relationship between perceptual information and action control. Consider the scalar first order differential equation

$$\dot{x}(t) = (d/dt)\, x(t) = a(t), \text{ with } x(t_o) \qquad (1)$$

being given as denoting the system of interest. Here $a(t)$ is generally described as a continuous function of time t. Eq. (1) is integrated forward in time from $t = t_o$, the initial time, until $t = t_f$, the final time. Associated with the function $x(t)$ is the adjoint system $\alpha(t)$, which satisfies

$$\dot{\alpha}(t) = -\,\alpha(t)\, a(t) \qquad (2)$$

where $\alpha(t_f)$ is specified at the terminal time. What is noteworthy is that $\alpha(t)$ is integrated <u>backwards</u> in time from $t = t_f$ to $t = t_o$, and also differs from the right hand side of Eq. (1) by a change in sign. If constant $a > 0$, then Figure (2a) illustrates the pole-zero diagram of the original system. Their adjointness, or duality, is manifested in them appearing as mirror images about the complex $(j\omega)$ axis. All adjoint systems, including the vector/matrix cases and the time lag (hereditary) cases, exhibit this involutive character when plotted against their original system. Figure (2b) illustrates how each equation is integrated <u>forward</u> or <u>backward</u> in time, respectively.

It is also possible for $a(t)$ in Eq. (1) to vary with time; the adjoint system can be defined accordingly. An important quantity in analyzing the solutions to these equations is the fundamental, or state transition, matrix which is defined for the system Eq. (1) as follows:

$$\dot{\phi}(t,t_o) = a(t)\,\phi(t,t_o), \quad \phi(t_o,t_o) = I \qquad (3)$$

where I indicates 1 for the scalar case and a unit diagonal matrix for the matrix case. This reduces to

$$\phi(t,t_o) = e^{a(t-t_o)} \qquad (4)$$

if a is constant. The solution $x(t)$ of Eq. (1) can be written as

$$x(t) = \phi(t,t_o)\, x(t_o) \qquad (5)$$

For the adjoint sytem, the state transition matrix satisfies

$$\dot{\phi}(t,t_o) = -\,a(t)\,\phi_a(t,t_f) \qquad (6)$$

$$\phi_a(t_f,t_f) = I \qquad (7)$$

which, for $a = $ constant, reduces to

$$\phi_a(t,t_\bullet) = e^{a(t_\bullet -t)} \tag{8}$$

From this it follows that

$$\phi_a[t_o ,t] = \phi[t, t_o] \tag{9}$$

or

$$[\phi_a]^{-1} = \phi \tag{10}$$

Thus the adjoint system acts like an inverse system, but proceeds _backwards_ in time. The most interesting relationship between the original system and the adjoint system occurs when we observe the inner product operator. For two scalars $x(t)$ and $\alpha(t)$, we define the _inner product_ operator as the scalar product of the components. This turns out to be equal to a constant for all time, i.e.

$$\langle \alpha(t), x(t)\rangle = \alpha(t) x(t) = \text{constant (independent of time)} \tag{11}$$

If we use the simple example illustrated thus far, then we see for a = constant

$$\langle x(t), \alpha(t)\rangle = x(t_o) e^{a(t-t_\bullet)} \quad (t_\bullet) e^{a(t_\bullet -t)} \tag{12}$$

$$= x(t_o) \alpha(t_\bullet) e^{a[t_\bullet -t_\ell]} \tag{13}$$

$$= \text{constant (independent of time)} \tag{14}$$

To better illustrate what happens if a(t) depends on time, we present a time varying example [13] to demonstrate more explicitly these calculations.

Example 1: Given the system

$$\dot{x}(t) = - t\, x(t), \quad \text{with } x(t_o) \text{ specified,} \tag{15}$$

then the solution is

$$x(t) = x(t_o) e^{(t_o^2 -t^2)/2} \tag{16}$$

and

$$\phi(t,t_o) = e^{(t_o^2 -t^2)/2} \qquad \text{for } t \geq t_o \tag{17}$$

while

$$\phi(t,t_o) = 0 \qquad \text{for } t < t_o \tag{18}$$

The adjoint system satisfies

$$\dot{\alpha}(t) = + t\, \alpha(t), \quad \text{with } \alpha(t_\bullet) \text{ specified} \tag{19}$$

The solution is

$$\alpha(t) = \alpha(t_\bullet) e^{(t^2 -t_\bullet^2)/2} \tag{20}$$

and

$$\phi_a(t,t_\bullet) = e^{(t^2 -t_\bullet^2)/2} \tag{21}$$

Note:

$$\phi_a[t,t_\bullet]\, \phi[t,t_o] = e^{(t_o^2 -t_\bullet^2)/2} \tag{22}$$

$$= \text{constant (independent of time)} \tag{23}$$

also

$$\langle x(t), \alpha(t)\rangle = x(t_o) e^{(t_o^2 -t^2)/2}\, \alpha(t_\bullet) e^{(t^2 -t_\bullet^2)/2} \tag{24}$$

or

$$\langle x(t), \alpha(t)\rangle = x(t_o) \alpha(t_\bullet) e^{(t_o^2 -t_\bullet^2)/2} \tag{25}$$

$$= \text{constant (independent of time)} \tag{26}$$

VI. THE ADJOINT SYSTEM: MATRIX CASE

The results presented here for the scalar case easily generalize to a matrix case. We can now define the dual

properties of _controllability_ and _observability_ by which the role of action and perception in the learning process can be modelled. In addition, we can also define the _inner product operator_, the means by which perceptual information can be scaled to the control of action. We follow Kalman[3] and define the original system equations as an n component column vector x(t) as follows:

$$(d/dt)\ \bar{x}(t) = A(t)\ \bar{x}(t) + B(t)\ u(t),\ \text{with } x(t_o) \text{ specified} \quad (27)$$

where A(t) is an n x n matrix, B(t) is an n x n matrix, and u(t) is a p x 1 state transition matrix $\phi(t,t_o)$ which satisfies

$$\dot{\phi}(t,t_o) = A(t)\ \phi(t,t_o) \quad (28)$$

$$\phi(t_o,t_o) = I \quad (29)$$

Aossciated with the system depicted by Eq.(27) is an observation vector y(t), an m component column vector, which satisfies

$$y(t) = H(t)\ \bar{x}(t) \quad (30)$$

where H(t) is an m x n matrix relating the observation in the vector y(t) from $\bar{x}(t)$. The adjoint system associated with Eqs.(27, 30) is given by

$$(d/dt)\ \bar{\alpha}(t) = -A^T(t)\ \bar{\alpha}(t) + H^T(t)\ u(t) \quad (31)$$

$$z(t) = B^T(t)\ \bar{x}(t) \quad (32)$$

$\bar{\alpha}(t_\diamond)$ is specified and Eqs.(31, 32) are integrated backwards in time. The superscript T indicates matrix transpose. With this matrix notation, it is now possible to define some properties of the original system Eqs.(27, 30), such as, _complete_ controllabilty and _complete_ oservability. It is also possible to generalize the definition of the inner product operator. We do so in the next section.

VII. _PROPERTIES OF THE ORIGINAL SYSTEM (COMPLETE CONTROLLABILITY AND COMPLETE OBSERVABILITY) AND THE INNER PRODUCT OPERATOR_

The system Eqs.(27, 30) is _completely controllable_ if there exists some input u(t) which takes the system initially at rest $\bar{x}(t_o) = 0$ to any arbitrary state $\bar{x}(t_\diamond) = \bar{x}_\diamond$ in a finite length of time t = $t_\diamond$. This property holds if the following matrix is positive definite for some $t_o > t_o$:

$$W(t_o,t_\diamond) = \int_{t_o}^{t_\diamond} \phi(t_\diamond,t)\ B(t)\ B^T(t)\ \phi^T(t_\diamond,t)\ dt \quad (33)$$

The measure of complete controllability is related to the minimum amount of control energy u(t) necessary to transfer $\bar{x}(t_o) = 0$ to $\bar{x}(t_\diamond) = \bar{x}_\diamond$ in $t_\diamond$ seconds.

Of interest to determining the optimality of the control is

the degree to which the amount of work done approaches the minimum. For this we need an equation defining __minimum energy__:

$$\text{Min } E = \|\tilde{x}(t_*)\|^2 W^{-1}(t_o,t_*) = \tilde{x}^T(t_*) \ W^{-1}(t_o,t_*) \ \tilde{x}(t_*) \qquad (34)$$

Thus small values of $W(t_o,t_*)$ imply little controllability, for this means that large amounts of energy are required to transfer $\tilde{x}(t_o) = 0$ to $\tilde{x}(t_*) = \tilde{x}_*$, and conversely.

As mentioned earlier, since perceptual information guides action, there must exist a duality between the energy required for control and the information that provides the measure of control. Such a measure is guaranteed by the duality of complete controllability to complete observability. We define this condition next.

A system is said to be __completely observable__ if it is possible to determine the exact value of $\tilde{x}(t_o)$ given the values of $y(t)$ in a finite interval (t_o,t_*), where $t_o < t_*$. The original system Eqs.(27,30) is completely observable if the following matrix is positive definite for some $t_* > t_o$:

$$M(t_o,t_*) = \int_{t_o}^{t_*} \tilde{\phi}^T(t,t_*) \ H^T(t) \ H(t) \ \tilde{\phi}(t,t_*) \ dt \qquad (35)$$

We come now to an important lemma:

__Lemma 1:__ A system is completely controllable if and only if its dual (adjoint) is completely observable, and conversely.   •

The proof of this lemma follows directly from the dual relationships

$$\tilde{\phi}(t_*,t) = \tilde{\phi}_a^T(t,t_*) \qquad (36)$$

$$B(t) = H_a^T(t) \qquad (37)$$

and by substituting into Eqs.(33,35) the relationships specified by Eqs.(36,37).

Analogous to the case of minimum energy, we can ask what happens to information when the system successsfully achieves control of action with respect to some goal? Given the duality of complete observability with complete controllability, then whenever energy is minimized information must be maximized. Thus the measure of complete observability is related to the maximum amount of perceptual information as follows:

$$\text{Max Info} = \|\tilde{y}(t_*)\|^2 M^{-1}(t_o,t_*) = \tilde{y}^T(t_*) \ M^{-1}(t_o,t_*) \ \tilde{y}(t_*) \qquad (38)$$

The last item of interest for the matrix case involves the inner product of the original system with its dual, for it

provides the measure of control (energy) against perception
(information). The definition of the inner product operator for
the matrix case can also be given:

Definition: Inner Product operator

Let $\|\bar{x}\|^2 = [\bar{x}^T\bar{x}]$ and $<\bar{x},\bar{x}> = [\bar{x}^T\bar{x}]$. where $\bar{x}$ is an
n x 1 column vector.

Using the above definition, we can now construct a lemma to show
in the matrix case, as in scalar case, that the inner product
between the original system and its adjoint is a temporal
invariant.

Lemma 2: If u(t) = 0 in Eq.(27), then $<\bar{x}(t),$ (t)> = $\bar{x}^T\alpha$ =
constant (independent of time). This may
alternatively occur if u(t) is in feedback form:

$$u(t) = - K(t) \bar{x}(t) \tag{39}$$

and Eq.(39) is substituted into Eq.(27).

These results can now be extended to systems with
hereditary influences, sometimes called systems with retardation,
or still more commonly, with time lag. Such systems are minimal
for modelling adaptive changes in control due to learning through
reward. We can also extend these results to the adjoint system
which exhibits dual anticipatory influences characteristic of
learning as a function of change in expectancies.

VIII. THE ADJOINT SYSTEM: TIME LAG CASE

The results of adjoint systems theory extend naturally to
systems with time lag. [13,14] In this case the plant (vector
equation) satisfies

$$\dot{\bar{x}}(t) = A_1\bar{x}(t) + B_1\bar{x}(t - T) + B_2\bar{u}(t) \tag{40}$$

$$\bar{y}(t) = \bar{H}(t) \bar{x}(t) \tag{41}$$

An important change is now introduced into the matrix case as
described by Eqs.(40,41). Where the simpler matrix case of
control systems requires independent evaluation of the initial
conditions of its differential equations, the time lag case of
adjoint systems does not. Instead these systems now require an
initial function to express any influence that builds up over
time as a result of learning, transfer of training, learning-to -
learn, or fatigue. The initial function, also called a
"hereditary functional", is an operator that, in a sense,
"automatically" updates the initial conditions of the

130-13

differential equations of the matrix case system. It is this capability which renders the time lag system truly adaptive so that the "tweaking" of individual parameters over trials or tasks is unnecessary.

The hereditary functional for the time lag system can be stated as

$$\bar{x}(t) = \bar{\phi}(t) \quad \text{for } t \in [t_0 - \mathcal{T}, t_0] \tag{42}$$

Also associated with system Eqs.(40,41) is the state transition matrix

$$(d/dt) \; \Psi(t,t_0) = A_1\Psi(t,t_0) + B_1\Psi(t - \mathcal{T},t_0) \tag{43}$$

for $t \in [t_0, t_+ - \mathcal{T}]$

$$(d/dt) \; \Psi(t,t_0) = A_1\Psi(t,t_0) \quad \text{for } t \in [t - \mathcal{T},t_+] \tag{44}$$

$$\Psi(t,t_0) = I \quad \text{for } t \in [t - \mathcal{T},t_0] \tag{45}$$

Associated with the system Eqs.(40,41) is the adjoint system $\lambda(t)$ which satisfies

$$\dot{\lambda}(t) = -\lambda(t)A_1(t) - \lambda(t + \mathcal{T})B_1(t + \mathcal{T}) \quad \text{for } t \in [t_0, t_+ - \mathcal{T}] \tag{46}$$

$$\dot{\lambda}(t) = -\lambda(t)A_1(t) \quad \text{for } t \in [t_+ - \mathcal{T}, t_v] \tag{47}$$

$$\lambda(t_+) = I \tag{48}$$

There are also equivalent definitions of controllability, observability, and an inner product operator for these systems.[15,16,17]

Definition: Completely Controllabilty

The system Eqs.(40,41) is <u>completely controllable</u> if (sufficient condition) the following matrix is of full rank:

$$G_1(t_0,t_+) = \int_{t_0}^{t_+} \Psi(t_+,s) \; B(s) \; B^T(s)\Psi^T(t_+,s) \; ds \tag{49}$$

for $t_+ > t$

Definition: Complete Observability

The system is likewise <u>completely observable</u> if the following matrix is of full rank:

$$G_2(t_0,t_+) = \int_{t_0}^{t_+} \Psi(s,t_+) \; H^T(s) \; \Psi^T(s,t_+) \; ds \tag{50}$$

The inner product definition now extends to the following[14]:

$$\langle x(t), \lambda(t) \rangle = x^T(t) \lambda(t) + \int_{\mathcal{T}}^{0} x^T(t + s) \; \lambda(t + s) \; ds \tag{51}$$

It is useful to study the time lag system and its adjoint system in the complex plane. Figure (3) illustrates the pole-zero diagram for the original system $x(t)$ and its adjoint system $\lambda(t)$ for the scalar time lag example. System $x(t)$ can be classified as an infinite dimensional system, with its poles having a particular pattern. The mirror image about the $j\omega$ axis of this pattern is the diagram for $\lambda(t)$, the adjoint system. Because the

poles of $x(t)$ and $\lambda(t)$ are both _ordered_, then the time delay system $\bar{x}(t)$ is considered a _hybrid_ between a finite dimensional system (a finite number of poles), as shown in Figure (2a), and a true infinite dimensional system (such as a partial differential equation system). For a true infinite dimensional system, the pole-zero pattern would be scattered throughout the complex plane with many different curves extending to infinity in various directions (Figure 4).

IX. FORMULATION OF AN OPTIMAL CONTROL PROBLEM

The adjoint system arises naturally in optimal control problems. [18] Here the system equation can be described by an ordinary matrix differential equation acting forward in time of the form

$$\dot{x}(t) = F(t)\, \underline{x}(t) + G(t)\, \underline{u}(t), \quad \text{with } \underline{x}(t_0) \text{ specified} \qquad (52)$$

We wish to find the control action $u(t)$ to minimize a scalar objective functional given by

$$J = (1/2)[x^T(t_*)\, S_* x(t_*)] + (1/2)\int_{t_0}^{t_*}(\underline{x}^T A \underline{x} + \underline{u}^T B \underline{u})\, dt \qquad (53)$$

which is called, "the linear quadratic problem". The optimal control law is specified by

$$u* = - K\, \underline{x}(t) \qquad (54)$$

where K satisfies a Riccati type equation which has been studied extensively, and for which types of solutions are known. [19,20,21]

Let $\bar{\lambda}(t)$ satisfy the adjoint equation

$$\bar{\lambda}(t\ ) = S_* \qquad (55)$$

$$\dot{\bar{\lambda}}(t) = - F^T \bar{\lambda}(t) - A\, x(t) \qquad (56)$$

With this formulation, the $\bar{\lambda}$ is the adjoint, or dual system, to the original system $x(t)$. Eq.(56) is integrated backwards from $t = t_*$ to produce the desired result at $t = t_0$. The optimal control condition can be written $u* = - B^{-1}G^T\bar{\lambda}(t)$, indicating the relationship between the forward control action and the backwards acting, goal-specific, perceptual information. We turn next to realization of the dual equations of Table 1.

X. A FINAL FORMULATION OF THE LEARNING MODEL

From the numerous equations presented in the earlier sections, we wish to find a set of equations to fit those postulated in Section I. We need a time-forward system to model control action and a time-backward system to model perception. The inner product operator demonstrates the existence of an

invariance which should hold over the learning process. Furthermore, since learning appears to evolve by sequential trials, and we wish to have a formulation that relates one trial to another, then the time lag system with an initial function representation seems quite plausible. Here the time lag variable τ would separate different trials. Let us see how this time lag variable works.

As argued above, the most general form for the learning model would be a time lag system directed forward in time to represent the action (control) variable. For instance,

$$x(t) = \phi(t) \text{ for } t \in [t_o - \tau, t_o] \tag{57}$$

$$\dot{x}(t) = A_1(t) x(t) + B_1 x(t - \tau) + C(t) u(t), \text{ for } t \geq t_o \tag{58}$$

where = the trial number and the initial function and the initial function $\phi(t)$ represents hereditary changes due to experience. Each trial is separated by τ units, thus allowing discontinuities to occur at $t = t_o + n\tau$ where n is an integer. The dual or adjoint variable required to measure perceptual learning could be modelled by $\lambda(t)$, which is directed backwards in time. The equations for $\lambda(t)$ are as follows:

$$\dot{\lambda}(t) = -\lambda(t)A_1 - \lambda(t + \tau) B_1(t + \tau), \text{ for } t \in [t_o, t_* - \tau] \tag{59}$$

$$\dot{\lambda}(t) = -\lambda(t)A_1, \text{ for } t \in [t_* - \tau, t_*] \tag{60}$$

$$\lambda(t_*) = I \tag{61}$$

The state transition matrices $\psi(t,s)$ satisfy Eqs. (43 - 45). Thus, by the earlier definitions, the system is completely controllable if $G_1(t_o, t_*)$ of Eq. (49) is of full rank, and completely observable if $G_2(t_o, t_*)$ of Eq. (50) is also of full rank. Since the adjoint system proceeds backward in time, this seems to be a viable model.

The invariant rule determined by the inner product suggests a measure of the system's innate capacity for learning-to-learn, or for fatigue, that is,

$$Q = \langle \lambda(t), x(t) \rangle = \text{constant (independent of time)} \tag{62}$$

$$= x^T(t) \lambda(t) + \int_{-\tau}^{0} x^T(t + s) \lambda(t + s) ds \tag{63}$$

Notice that large values of Q indicate high values of coordination between action and perception, which implies a large capacity for learning-to-learn. By contrast, when Q is small in value, this indicates a low capacity for "learning-to-learn", or may be related to subject fatigue.

130-16

XI. ARGUMENTS SUPPORTING THIS LEARNING MODEL

Learning may be best characterized by a (possibly nonlinear) hereditary/anticipatory functional in lieu of more simplified models. Considerable evidence also suggests that action and perceptual processes must be duals and reciprocal to one another. A number of arguments support the model introduced in the last section. These arguments are based on the characteristics of the equations presented in the last section and well known results from research on learning.

(1) The effects of learning are cummlative such that experience carries over to facilitate later performance. The differential equation system Eqs.57-58 and 59-61 have this property in the forward and backward integration of $x(t)$ and $\lambda(t)$. These values determine anticipatory and hereditary influences of expectancies and experiences on learning that accumulate forward and backward in time, respectively.

(2) In learning experiments, successive trials may not appear to belong to the same set. Learning often is discontinuous (Thorndike's "belongingness" problem). The system Eqs.57-61 with possible discontinutites at $t = t_i + n\mathcal{T}$ at each time lag interval $\mathcal{T}$, where $\mathcal{T}$ separates each trial, provides for this effect.

(3) Learning, in the most general case, may need to be characterized by a non-linear function. This nonlinearity may result from the mutual constraining of action and perception, a "closed loop "model, as predicted from the Principle of Mutuality -- the basic principle of ecological psychology. The set of Eqs.(57-61) has this effect where $x(t)$ supports the past-pending (action) viewpoint and $\lambda(t)$ supports the future-tending (perception) viewpoint.

(4) Although not yet depicted, from the symmetry of the system of equations defined over the temporal (informatiom/energy) duals, the perspective duals, defined by the reciprocal constraints of the environment and organism, can be easily generalized from Eqs.(57-61).

Thus, from points (3) and (4), we see that the total formulation, Eqs.(57-61), provides a mathematically coherent model of an adaptive ecosystem, and thus provides both the motive

130-17

and means for incorporating learning theory into ecological psychology.

(5) There are two types of learning: action learning characterized here by x(t)) and perception learning characterized here by λ(t)). They give rise to two sets of data points and each changes as the trial numbers increase. Recall that $\langle x, \lambda \rangle$ = a constant, hence large changes occur in $\lambda = \Delta\lambda$ produce large changes in x = Δx. Thus as large perceptual changes occur, they induce large changes in the processes controlling action. Also ✓ small changes in λ induce small changes in x. This is because of the reciprocal nature of these systems.

(6) We also need to characterize "learning to learn" or fatigue effects within this adjoint systems context. If $Q_1 = \langle x, \lambda \rangle$ was one experimental condition and $Q_2 = \langle x, \lambda \rangle$ is another experimental condition, and if $Q_1 \gg Q_2$, then a greater disposition for learning is represented by the first experimental condition. Q_2 may indicate more fatigue to the subject than the condition Q_1.

(7) Learning theorists know that the behavior of a system depends on more than initial conditions. It also depends on the entire cumulative effect of experience. The _initial_ _function_ representation for x(t) and λ(t) in Eqs.(57-61) allows for this.

(8) The integrodifferential equations suggested by Shaw & Alley[7] for learning, as depicted in Table 1, are now seen to apply to the response variable [y(t)] in terms of the trial to trial variables [x(t)] and take the form:

$$[Y(t)] = K [X(t)] + \int_a^b K(t,s) [X(s)]\, ds$$

This is satisfied by Eqs.(57-61) as can easily be shown.

(9) The ecological approach to psychology argues that there should be a duality between action and perception. The equations for x(t) and λ(t) given here, indeed, are duals in a strict mathematical sense. If x(t) is completely controllable, then λ(t) is completely observable. If x(t) is completely observable, then λ(t) is completely controllable. Thus orthogonally adjoint systems provide a rigorous mathematical formulation for the most fundamental assumptions of the ecological approach.

(10) Because action response measurements tend to stabilize with time (e.g. error scores on the same task with repeated trials), then, conversely, one would expect the processing of perceptual information, the dual of the action variable, to exhibit unstable

response characteristics. Figures (5a-c) illustrate the form of the relationships these variables take. From figure (2a) we see that if $x(t)$ is stable (left half plane pole), then $\lambda(t)$ should show unstable characteristics (right half plane pole). Thus if $x(t)$ is asymptotic stable in time, $\lambda(t)$ should show an unstable solution. This may help to explain goal-gradient effects, that is, why uncertainty decreases as energy expenditure increases as the organism approaches its goal. Figure (5c) illustrates how this effect of perceiving and action being inversely proportional is an invariant quantity determined by the inner product operator Q operating on $x(t)$ and $\lambda(t)$. Notice that Q, the measure of the disposition to learn, is illustrated for both high Q values and also for a low value of Q.

XII. Recommendations

From the review of the shortcomings of the OCM approach and the promise of the new approach, the following recommendations seem reasonable: The orthogonally adjoint systems model for learning, transfer-of-training, and learning-to-learn should be theoretically developed and empirically tested on pursuit rather than compensatory displays alone.

Furthermore, in order to assess any advantage the adjoint systems approach might enjoy over the OCM approach, it would be useful to let the two approaches compete directly in predicting and modelling data obtained from the same experimental project to see how they compare and contrast. However given the decade or so overwhich the OCM model has been allowed to be developed, refined, and tested, it would be both unfair and unrealistic to attempt a hasty evaluation of the adjoint systems approach. Serious application of these new mathematical techniques will require that the model be programmed. The programming effort in all likelihood will require a few years of research and development to achieve satisfactory results before definitive tests can be completed.

Thus it is recommended that this new approach be developed and tested in phases of moderate duration in order to determine its theoretical validity and practical feasibility. This would require the collaborative efforts of experts in adaptive systems theory and ecological psychology.

REFERENCES

1. W. H. Levison, "Development of a Model for Human Operator Learning in Continuous Estimation and Control Tasks "AFAMRL-TR-83-088, Air Force Aerospace Medical Research Laboratory, Wright-Patterson Air Force Base, December 1983.

2. D. L. Kleinman, S. Baron, W. H. Levison, "An Optimal Control Model of Human Response Part I: Theory and Validation", Automatica, Vol. 6, pp. 357-369, 1970.

3. R. E. Kalman et al., "Fundamental Study of Adaptive Control Systems", ASD-TR-61-27, Vol. 1, April 1962.

4. D. T. McRuer and H. R. Jex, "A Review of Quasi-Linear Pilot Models", IEEE Trans. on Human Factors in Electronics, Vol. HFE-8, No. 3, pp. 231-249, September 1967.

5. E. C. Poulton, Tracking Skill and Manual Control, Academic Press, New York, 1974.

6. Poulton & Freeman, 1966 (See above for reference).

7. R. E. Shaw & T. R. Alley, "How to Draw Learning Curves: Their Use and Justification", in T. Johnston & A. Pietrewicz (Eds.), Issues in the Ecological Study of Learning, Lawrence Erlabaum & Associates, Publishers, Hillsdale, New Jersey (in press).

8. D. W. Repperger, "A Model for a Learning Theory Based on Adjoint (Dual) Systems with Retardation", unpublished memo to R. E. Shaw, AFAMRL, Wright-Patterson Air Force Base, July 1984.

9. R. E. Shaw & E. Mingolla, "Ecologizing World Graphs", Behavioral and Brain Sciences, Vol. 5, pp. 648-50, 1982.

10. R. E. Shaw & J. Todd, "Abstract Machine Theory and Direct Perception", Behavioral and Brain Science, Vol. 3, pp. 400-401, 1980.

11. R. E. Shaw & M. T. Turvey, "Coalitions as Models for Ecosystems: A Realist Perspective on Perceptual Organization", in M. Kubovy & J. Pomerantz (Eds.), Perceptual Organization, Lawrence Erlbaum Associates, Pub. Hillsdale, New Jersey, 1981.

12. R. E. Shaw, M. T. Turvey, & W. M. Mace, "Ecological Psychology: The Consequence of a Commitment to Realsim", in W. Weimer & D. S. Palermo (Eds.), Cognition and the Symbolic Processes II, Lawrence Erlbaum & Associates, Publishers, Hillsdale, New Jersey, 1982.

13. R. Bellman, Differential-Difference Equations, Academic Press, 1973.

14. D. H. Eller, J. K. Aggarwal, & H. T. Banks, "Optimal Control of Linear Time Delay Systems", IEEE Transactions on Automatic Control, Vol. AC-14, No. 6, pp. 678-687, December 1969.

15. D. W. Repperger & A. J. Koivo, "On Stable Forward Filtering and Fixed-Lag Smoothing in a Class of Systems with Time Delay", IEEE Transactions on Automatic Control, June 1974.

16. D. W. Repperger, "An Algorithm for the Computation of the Minimum Energy Solution of Systems with Retardation", The International Journal of Control, August 1974.

17. L. Weiss, Time Delay Systems: Controllability; Algebraic Criterion", IEEE Transactions on Automatic Control, pp.443-444, August 1970.

18. A. E. Bryson & Y. C. Ho, Applied Optimal Control, Ginn & Company, 1969.

19. D. W. Repperger, "On Covariance Propagation Using Matrix Continued Fractions", The International Journal of Systems Science, Vol. 10, No. 18, pp.913-925, 1979.

20. D. W. Repperger, "A Doubling Approach for Determining the Solution of Riccati-Type Equations Utilizing Matrix Continued Fractions", The International Journal on Systems Science, Vol. 14, No. 2, pp. 209-221, 1983.

21. D. W. Repperger, "An Implementation Method for the Discrete Kalman Filter with Application to Large Scale Systems", The International Journal of Control (in press).

22. P. M. DeRusso, R. J. Roy, & C. M. Close, State Variables for Engineers, John Wiley & Sons, Inc., 1965.

Table 1

Table of Duals

PERSPECTIVE DUALS

	Organism-Perspective (Action)	Environment-Perspective (Perception)
Energy (Control)	$y(t) = \int_o^t K_0(t,s)\, x(s)ds$ (Equation I)	$x(t) = \int_s^t K_E(t,s)\, y(s)ds$ (Equation II)
Information (Observation)	$x(t) = \int_s^t K_0^*(s,t)\, y(s)ds$ (Equation III)	$y(t) = \int_s^t K_E^*(s,t)\, x(s)ds$ (Equation IV)

(TEMPORAL DUALS — left margin label)

Note. The transforms whose kernels take the form $K(t,s)$ designate "past pending" integrals which sum energy interactions from some past state (s) to some future state (t). By contrast, those with kernels of the form $K^*(s,t)$ designate "future tending" integrals that sum information transactions from some potential future goal state (t) "backwards" in time to some current state (s).
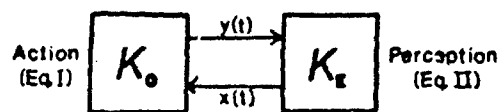
I ENERGY (CONTROL) DUALS
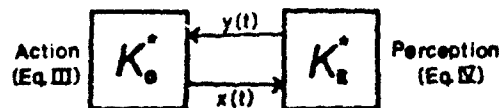
II INFORMATION (OBSERVATION) DUALS

Fig. 2: Diagram of the energy (control) and information (observation) duals shown in operator notation. The corresponding equations (denoted in parentheses) for perception and action are given in Table 1.

complex $(j\omega)$ axis

real(σ)axis

$-a$ 0 $+a$

pole of x(t)-system   pole of α(t)-system
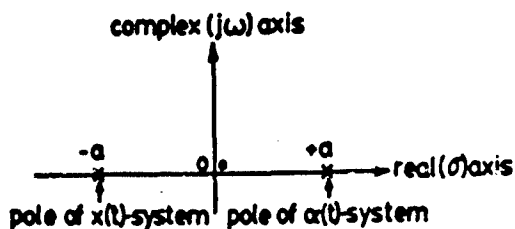
FIGURE 1a: The pole-zero pattern of the original system x(t) and its adjoint system α(t) for a scalar, first order ordinary differential equation.

x(t)

time axis

α(t
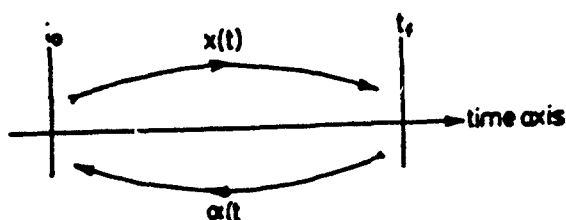
FIGURE 1b: Original system x(t) integrates forward in time, from initial time t_o to final time t_f, whereas the adjoint system α(t) integrates backward in time, from final time t_f to initial time t_o.

$j\omega$

$\bar{x}(t)$ $\lambda(t)$
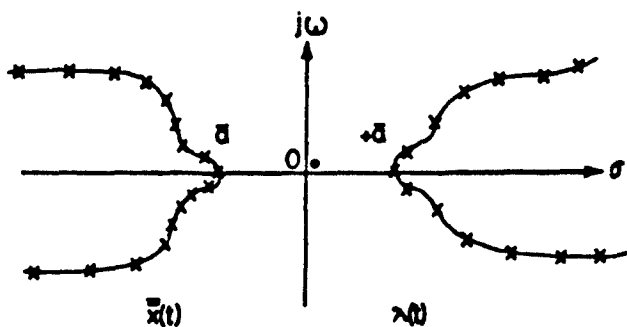
FIGURE 2: The pole-zero pattern for the time lag system and its adjoint system. The pole pattern for the original system $\bar{x}(t)$ is on the left whereas that for the adjoint system λ(t) is on the right.

FIGURE 3: The pole-zero pattern for a true infinite dimensional system — a partial differential equation.

x(t)=action variable

(a)

t_o t_1 t_2 t_3 trials t_f

λ(t)=perception variable

(b)

t_o t_1 $2t_1$ $3t_1$ trials t_f-2t

(c)

Q=constant=Q_1 t_f

Q=constant=Q_2 t_f

t_o trials t_f
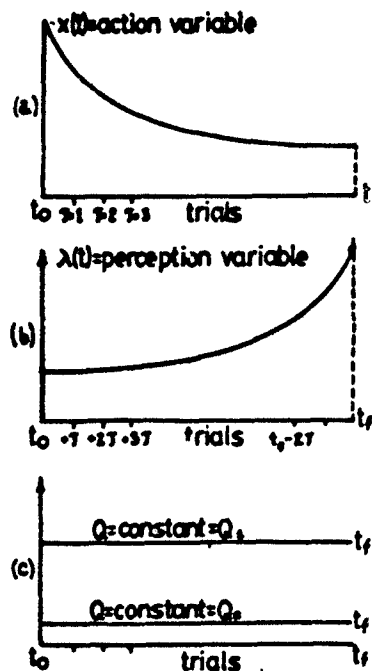
FIGURE 4: (a) depicts the asymptotic learning curve derived from measurement of change in the action (energy) variable x(t) over trials =T (b) depicts the corresponding dual learning curve derived from measurement of the adjoint perception (information) variable (t) over trials = t_o -T. (c) shows the curves resulting from the inner product operator = <x(t), λ(t)> = Q, a constant for all time. Relatively high Q values (Q_1) represent "learning-to-learn" whereas relatively low values (Q_2) represent fatigue or low capacity for learning.
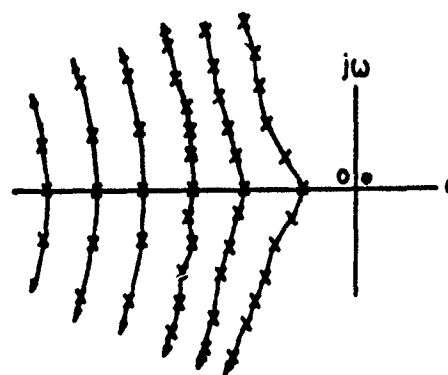
$j\omega$

σ

130-23

1984 USAF-SCEEE SUMMER FACULTY RESEARCH PROGRAM

Sponsored by the

AIR FORCE OFFICE OF SCIENTIFIC RESEARCH

Conducted by the

SOUTHEASTERN CENTER FOR ELECTRICAL ENGINEERING EDUCATION

Final Report

THE THEORY OF SELF-HEATING PHENOMENA IN EXPLOSIVES WITH APPLICATIONS TO EAK

Prepared by: Dr. John W. Sheldon

Academic Rank: Professor

Department: Physics Department

University: Florida International University

Research Location: Eglin AFB, High Explosive Research and Development

                     Explosives Dynamics Laboratory

USAF Research: Thomas G. Floyd

Date: 20 June 1984

Contract No: F49620-82-C-0035

The Theory of Self-Heating Phenomena in Explosives with Applications to EAK

by

John W. Sheldon

ABSTRACT

Pertubation theory is used to obtain the steady state temperature distribution in a subcritical spherical self-heating explosive. The theory is also used to obtain the time constant for supercritical self-heating to explosion. The effects of melting with self heating in the liquid state are analyzed in slab geometry, an approximate theory is developed and a numerical program described. Conditions are obtained for significant self-heating before melting is complete and it is shown that the melt front approaches a constant velocity as it proceeds through the solid.

Acknowledgement

I. INTRODUCTION

Materials that undergo exothermic chemical decomposition reactions can exhibit self-heating phenomena. At steady state the heat lost by conduction and or convection is just balanced by the heat generated; however, above a certain critical temperature more heat will be generated than can be removed by these means and the temperature will increase to ignition or explosion. The phenomena has been studied in connection with the spontaneous ignition of haystacks,[1] coal piles[2] and wool,[3] as well as high explosives.[4-8] When the primary heat loss mechanism is conduction the treatment of Frank-Kamenetzky is most often quoted, and when the major heat loss is by convection the pioneering work of Semenoff[10] applies.

In the present work the heat is generated by a first order chemical reaction and the conditions for existence of a steady state temperature distribution were determined. The highest wall temperature for which a steady state exists is the critical temperature for the explosive. The goal of the present analysis is to obtain steady state temperature profiles for subcritical conditions and investigate the thermal transient response of an explosive to conditions in excess of critical. It is well-known that for supercritical conditions in an explosive there is an induction time delay to explosion. Numerical calculations of this induction time were carried out some time ago[11] for slab, cylindrical and spherical geometries. Here, in Section III, the calculation for spherical geometry is performed using perturbation theory. The advantage of this approach is that it yields an expression for the induction time so that its dependence on the thermochemical parameters is clear.

The theory of melting with self-heating in the liquid is presented in Section IV and an approximate solution obtained. In Section V a numerical solution to the problem of melting during self-heating is described.

131-4

II. OBJECTIVES OF THE RESEARCH EFFORT

Among the many tests required to qualify an explosive as an IHE (insensitive high explosive) are the thermal tests to determine the relative safety of the material under conditions of self-heating.[12] In support of these tests procedures for calculating critical temperature and induction time must be developed and experimentally checked. The present work is an effort to broaden the theoretical background in which these experimental tests on EAK (45.68% ethylenediamine dinitrate, 46.17% ammonium nitrate and 8.15% potassium nitrate) are conducted. The specific goals are:

1. Obtain a theoretical estimate of the thermal time constant and estimates of the temperature profile during the induction period prior to explosion.

2. Incorporate into the theory of self-heating the simultaneous melting process. This is important since EAK melts well above ambient temperature (103 C) and self-heating is only significant in the liquid state.

III. PERTURBATION THEORY OF SELF-HEATING IN A SPHERE

The thermal energy equation can be written for heat loss by conduction and heat generated by a first order chemical reaction in dimensionless form as

$$\frac{\partial \theta}{\partial t} = \nabla^2 \theta + e^{-1/\theta} \tag{1}$$

where $\theta = RT/E$, time is in units of $\frac{CE}{QZR}$ and length in units of $\left(\frac{E\lambda}{\rho QRZ}\right)^{\frac{1}{2}}$. E is the activation energy of the reaction, Z is the frequency factor in the Arrhenius first order rate law, Q the heat per unit mass released by the reaction, ρ the mass density, C the heat capacity, λ the thermal conductivity and R the gas constant. Using $\theta(\vec{r},t) = \theta_s(\vec{r}) + \delta(\vec{r},t)$ and expanding about the steady state, eq (1) becomes

$$\frac{\partial \delta}{\partial t} = \nabla^2 \delta + f(\vec{r})\delta \tag{2}$$

where

$$f(\vec{r}) = \frac{e^{-1/\theta_s(\vec{r})}}{\theta_s^2(\vec{r})}$$

and

$$\nabla^2\theta_s + e^{-1/\theta_s} = 0 \qquad\qquad (3)$$

The conditions which lead to a solution of eq (3) have been extensively investigated[4-9] and exact solutions are available for slab, cylindrical and spherical geometry in terms of known functions. For simplicity and consistency the approximate solution to eq (3) obtained for $\frac{\theta-\theta_w}{\theta_w} \ll 1$ is used here. It is expressed in spherical geometry by

$$\theta_s(r) = \theta_w + \theta_w^2\left(\frac{j_o(Br)}{j_o(BL)} - 1\right) \qquad\qquad (4)$$

where j_o is the spherical Bessel function of the first kind, $B = \frac{e^{-\theta_w/2}}{\theta_w}$ and θ_w is the dimensionless wall temperature at $r = L$. The temperature difference ΔT between the center and outside (wall) radius of a one liter sphere of EAK is obtained from eq (4) and presented in Table I.

Table I

Temperature difference ΔT in a self-heating 1 liter sphere of EAK

$T_w(°C)$	$T(°C)$
150	1.2
155	2.4
160	5.4
165	15.0
166	31.0
167	45.0
168	81.0
169	256.0
170	∞

The solution to the time dependent eq (2) for spherical geometry is obtained by using $f(r)=f(L) = B^2$ and separating variables. The result is

$$\theta(r,t) = \theta_s(r) + \sum_{n=1}^{\infty} A_n j_o(\gamma_n \frac{r}{L}) \exp\left(-\left(\frac{\gamma_n^2}{L} - B^2\right)t\right)$$ (5)

where A_n's are determined from initial conditions and the γ_n's are the zeros of the Bessel functions $\left(j_o(\gamma_n) = 0\right)$. Considering only the 1st term in the series and taking $B_c = \frac{\gamma_1}{L}$, then the time constant τ, for the self-heating leading to explosion is given by

$$\tau = \frac{1}{B^2-B_c^2}\left(\frac{CE}{QZR}\right)$$ (6)

This time constant is presented as a function of temperature in Table II for a one liter sphere of EAK.

Table II

Time Constant, for a 1-liter sphere of EAK

$T_w(°C)$	$\tau(s)$
170	61,366
175	7,314
180	2,905
185	1,390
190	753
195	427
200	250
205	149
210	91
215	56
220	35
225	22
230	14

IV. MELTING WITH A SELF-HEATING LIQUID; APPROXIMATE THEORY

The melting process is considered in a one dimensional semi-infinite system. The solid surface is initially located at $x=0$ with solid material in the range $0 \leq \ <\infty$. It is assumed that the solid is uniformly at the melting temperature T_p. At $t=0$ the temperature of the $x=0$ boundary is raised and fixed at $T_w > T_p$.

As heat flows into the solid melting begins and the liquid formed begins to self-heat. The transient heat conduction equation for the liquid with heat generation by a first order chemical reaction can be put in the form

$$\frac{\partial n}{\partial t} = \alpha \frac{\partial^2 n}{\partial x^2} + \beta e^n \tag{7}$$

where

$$n(x,t) = \frac{E}{RT_w^2}\left(T(x,t) - T_p\right),$$

the thermal diffusivity $\alpha = \lambda/\rho c$ and $\beta = \left(\frac{QZ}{C}\right)\left(\frac{E}{RT_w^2}\right)\exp\left(-\frac{E}{RT_w} - n_w\right)$. The heat balance at the solid-liquid interface located at $Xp(t)$ can be expressed by

$$-\frac{\partial n}{\partial x}\bigg)_{Xp} = S \frac{dX_p}{dt} \tag{8}$$

where $S = \frac{\Delta H_f E}{\alpha CRT_w^2}$ with $\Delta H_f =$ latent heat of fusion. The approximate form for $n(x,t)$ used by Goodman[13] for similar problem is used here in the form

$$n(x,t) = A(t)[X - X_p(t)] + B(t)[X - X_p(t)]^2 \tag{9}$$

using $dn(X_p(t),t) = 0$

$$\frac{\partial n}{\partial X}\bigg)_{X_p} \frac{dX_p}{dt} + \left(\frac{\partial n}{\partial t}\right)_{X_p} = 0 \tag{10}$$

Inserting eq (7) and (8) into (10) yields

$$\left(\frac{\partial \eta}{\partial X}\right)^2 = S\alpha \frac{\partial^2 \eta}{\partial X^2} + S\beta e^{\eta} \tag{11}$$

at $X_p(t)$. Eqs (9) and (11) and the wall condition $\eta_w = AX_p + BX_p^2$ yields the following expressions for A and B

$$A = \frac{S\alpha}{X_p} \left[1 - \sqrt{1 + \frac{2\eta_w}{S\alpha} + \frac{X_p^2}{S\alpha^2}\beta} \right] \tag{12a}$$

$$B = \frac{A}{X_p} + \frac{\eta_w}{X_p^2} \tag{12b}$$

Substituting eqs (9) and (12) in (8) gives $X_p \frac{dX_p}{dt} = \alpha \left[\sqrt{1 + \frac{2\eta_w}{S\alpha} + \frac{X_p^2}{S\alpha^2}\beta} - 1 \right]$ which can be integrated to give

$$\sqrt{1 + \mu + y} - \sqrt{1 + \mu} + \ln\left(\frac{\sqrt{1 + \mu + y} - 1}{\sqrt{1 + \mu} - 1}\right) = \frac{\beta}{S\alpha} t = t' \tag{13}$$

where $\mu = \frac{2\eta_w}{S\alpha}$, $y = \frac{\beta}{S\alpha^2} X_p^2$, t' are dimensionless. Eq (13) is plotted in Figure 1 for five values of μ.

The condition for a maximum temperature T_m, in the liquid _above_ the wall temperature, that is when there is significant self-heating, can be expressed as $\left(\frac{\partial \eta}{\partial X}\right)_{X=0} > 0$ which leads to the condition $y > \mu(1 + \mu)$. The location of this maximim temperature is then given by

$$y_m = \frac{\sqrt{1 + \mu + y} - (1 + \mu)}{2\sqrt{1 + \mu + y} - 2 - \mu} \tag{14}$$

131-9
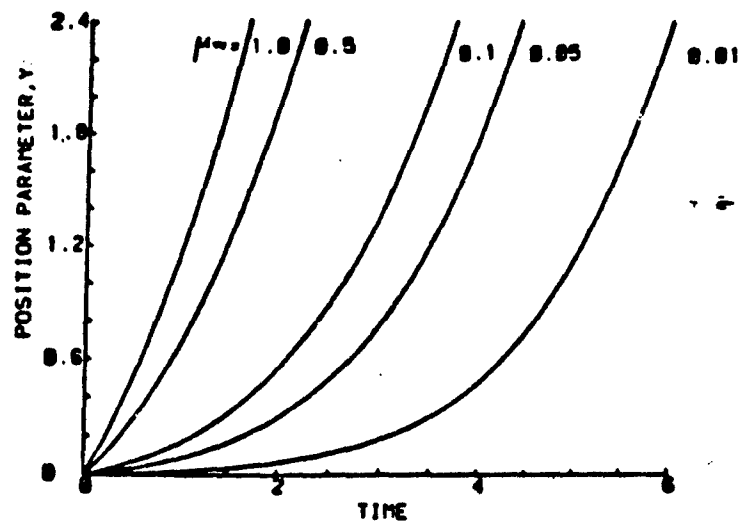
FIGURE 1. DIMENSIONLESS PLOT OF THE MELTING FRONT
POSITION AS A FUCTION OF TIME FOR A RANGE
OF WALL TEMPERATURE PARAMETER, μ_w.

FIGURE2. DIMENSIONLESS PLOT OF THE LOCATION OF THE
MAXIMUM TEMPERATURE AS A FUCTION OF TIME
FOR A RANGE OF WALL TEMPERATURE PARAMETER, μ_w.

131-10

and its value by

$$\mu_m = \frac{\left(\sqrt{1 + \mu + y} - 1\right)^2}{2\left(\sqrt{1 + \mu + y} - 1\right) - \mu} \tag{15}$$

where $\mu_m = \frac{2C}{\Delta H_f} (T_m - T_p)$. Figures 2 and 3 display y_m/y and μ_m respectively. The velocity of the melting front v_p, obtained by differentation of eq(13) is given by

$$v_p = \frac{dX_p}{dt} = \frac{\alpha}{X_p} \left[\sqrt{1 + \mu + y} - 1\right] \tag{16}$$

Then in the limit as $X_p \longrightarrow \infty$, $v_p \equiv \left[\left(\frac{QZ\alpha}{\Delta H_f}\right) \exp\left(-\frac{2E}{RT_w} + \frac{ET_p}{RT_w^2}\right)\right]^{\frac{1}{2}}$ the limiting velocity of the melting front with heat generation.

V. MELTING WITH SELF-HEATING IN A LIQUID: NUMERICAL CALCULATION

The two phase system is considered in slab geometry with slab ½-width L. Initially the slab is all solid with ambient temperature T_o. At $t = 0$ the wall temperature is raised to $T_w > T_p$ where T_p is the melting point. The conduction equation with heat generation in the liquid phase is

$$-\alpha_1 \frac{\partial^2 T_1}{\partial X^2} + \frac{\partial T_1}{\partial t} = \left(\frac{QZ}{C}\right) \exp\left(-\frac{E}{RT}\right) \tag{17}$$

and in the solid phase where no heat is generated

$$-\alpha_2 \frac{\partial^2 T_2}{\partial X^2} + \frac{\partial T_2}{\partial t} = 0 \tag{18}$$

The heat balance at the interface is given by

$$\alpha_1 \frac{\partial T_1}{\partial X} - \alpha_2 \frac{\partial T_2}{\partial X} = \left(\frac{\Delta H_f}{C}\right) \frac{dX_p}{dt} \tag{19}$$

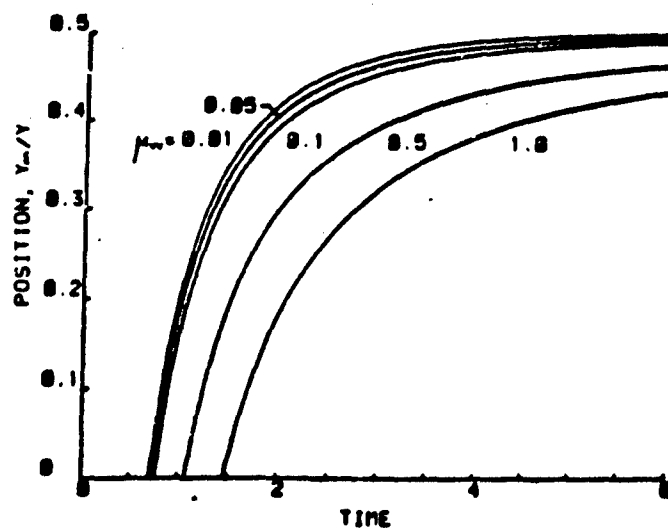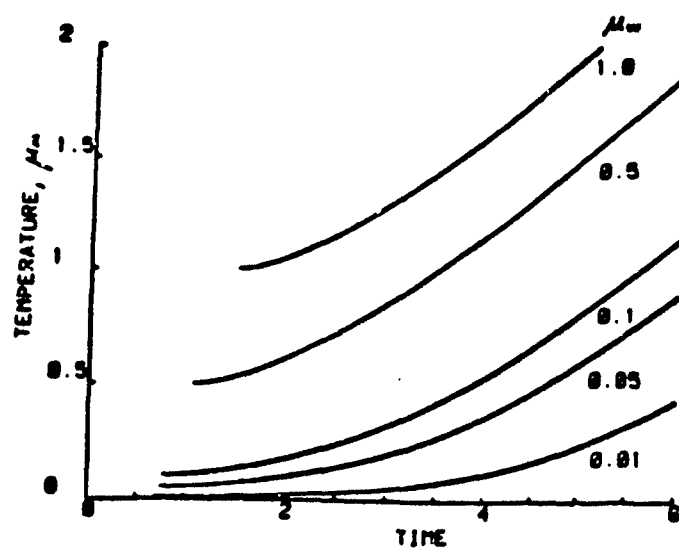FIGURE 3. DIMENSIONLESS PLOT OF THE MAXIMUM TEMPERATURE
AS A FUNTION OF TIME FOR A RANGE OF WALL
TEMPERATURE PARAMETER, μ_w

where $X_p(t)$ is the location of the melt line (see sketch in Figure 4).
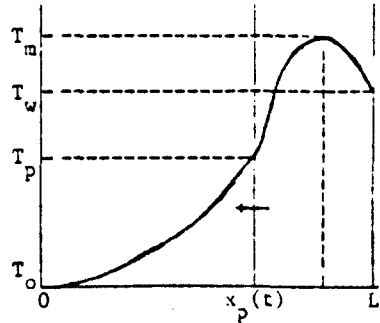
FIGURE 4. THE COORDINATE FRAME FOR A MELTING FINITE SLAB
WITH SELF-HEATING

The numerical procedure is as follows. For a fixed X_p and considering the liquid inert ($Z = 0$ in eq (17)), the boundary conditions are $T_1(L,t) = T_w$, $T_1(X_p,t) = T_2(X_p,t) = T_p$ and $\left(\dfrac{\partial T_2}{\partial X}\right)_{X=0} = 0$. For an initial temperature distribution $T_1(x,0) = f_1(x)$ and $T_2(x,0) = f_2(x)$ the temperature distribution after an assumed time interval Δt can be calculated from the exact expressions for the above boundary conditions, [14]

$$T_2(x,t) = T_p + \frac{2}{x_p} \sum_{j=0}^{\infty} \exp\left(-\alpha_2 (2j+1)^2 \pi^2 t / 4 x_p^2\right) \cos\left(\frac{(2j+1)\pi x}{2x_p}\right)$$

and

$$\cdot \left[\frac{2x_p (-1)^{j+1} T_p}{(2j+1)\pi} + \int_0^{x_p} f_2(x') \cos\left(\frac{(2j+1)\pi x'}{2x_p}\right) dx'\right] \quad (20)$$

$$T_1(x,t) = T_p + (T_w - T_p)\left(\frac{x - x_p}{L - x_p}\right) + \frac{2}{\pi} \sum_{j=1}^{\infty} \frac{T_w \cos(j\pi) - T_p}{j} \sin\left(\frac{j\pi(x - x_p)}{L - x_p}\right) \cdot$$

$$\cdot \exp\left(-\frac{\alpha_1 j^2 \pi^2 t}{(L - x_p)^2}\right) + \frac{2}{(L - x_p)} \sum_{j=1}^{\infty} \sin\left(\frac{j\pi(x - x_p)}{(L - x_p)}\right) \exp\left(-\frac{\alpha_1 j^2 \pi^2 t}{(L - x_p)^2}\right) \cdot$$

$$\cdot \int_{x_p}^{L} f_1(x') \sin\left(\frac{j\pi(x' - x_p)}{L - x_p}\right) dx' \quad (21)$$

The temperatures at each spacial station are then increased by an amount ΔT_Q where

$$\Delta T_Q = \left(\frac{QZ\Delta t}{C}\right) \exp\left(-\frac{E}{RT_1(x,\Delta t)}\right) \tag{22}$$

which accounts for the heat generated by the chemical reaction. The temperature distribution is then used to compute the temperature gradients at the solid-liquid boundary and through the use of eq (19) determine $\frac{dX_p}{dt}$. For the melt line to advance a spacial step ΔX, requires a time $\Delta t' = \Delta X/(dX_p/dt)$. If $\Delta t' \neq \Delta t$ then a new value of Δt is assumed and the calculation of $\Delta t'$ repeated until $\Delta t' = \Delta t$ to within 1%. Then X_p is advanced into the solid by ΔX and using the temperature distribution from the last step as the initial distribution, the process is re-peated. In the sample calculation shown in Figure 5 some self-heating prior to complete melting is evident. The physical constants and parameters used in this calculation are typical values and do not represent any particular explosive. Only 20 spacial steps were used in the sample calculations. The position of the melting front as a function of time is shown in Figure 6 and Figure 7 shows the velocity of the melting front as a function of time. Note that this velocity rapidly approaches a constant as the melt line proceeds, just as was found in Section IV for the case of the solid intially at the melting temperature.
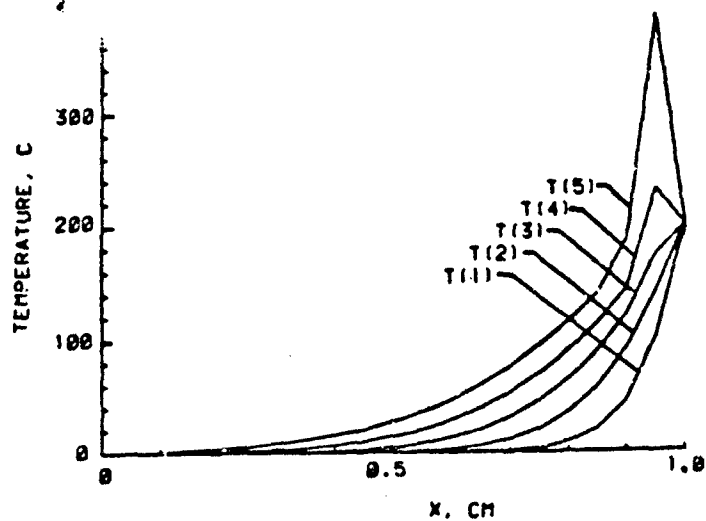
FIGURE 5. TRANSIENT TEMPERATURE PROFILES; L=1 CM.
$\Delta H/c$ =10.0Z/C=4×10†20 1/S, E=18 KCAL, α_s=
α_L= 8.81 (CM†2)/S, T_∞=200°C, T_F=20°C,
T_0 =0°C, T(1)=8.11 S, T(2)=8.55 S, T(3)=1.34 S,
T(4)=2.47 S, T(5)=3.93 S. 20 SPACIAL STEPS
WERE USED WITH 20 TERMS IN THE SUMS IN
EQS. (20) AND (21).
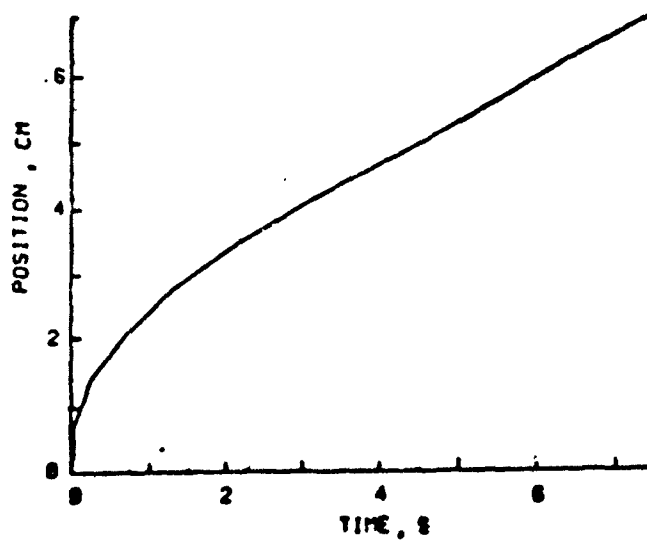
FIGURE 6. THE POSITION OF THE MELTING FRONT AS A
FUNCTION OF TIME.

131-15
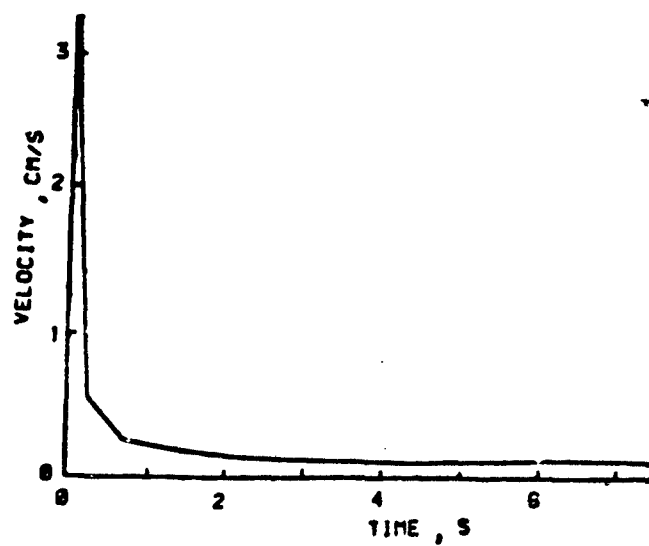
FIGURE 7. THE VELOCITY OF THE MELTING FRONT AS A
FUCTION OF TIME.

VI.   RESULTS AND DISCUSSION

The pertubation theory presented in Section III indicates that substantial temperature increases due to self-heating occur only when the critical temperature is closely approached.   In the EAK example presented in Table I, it is shown that just 5°C below critical temperature the temperature rise due to self-heating is only 15°C, yet at 1°C below critical it rises 256°C.   The same theory demonstrates the sensitivity of the induction time constant to the wall temperature.   From Table II, raising the wall temperature from 1 to 20°C above critical lowers the induction time from 17 hours to 4 minutes.

The approximate theoretical analysis of the melting process with self-heating results in dimensionless plots of the melting front position, the maximum temperature and its location as functions of time.   The curves of melting front position vrs, time plotted in Figure 1 would all be linear if there was no self-heating, the case treated by Goodman.[13]   It is also noted that the slope of all the the curves in Figure 1 approach a constant value indicating a limiting constant velocity for the advance of the melting front.   This is in contrast to the monatonic decrease of the melting front velocity with increasing X_p when there is no self-heating.[13]   A limiting velocity was also observed for the numerical example as shown in Figure 7.

The assumptions made throughout this work are that heat loss is by conduction and heat generation is by a first order chemical rate process.   Preliminary observations of a one-liter EAK sphere raised to 180°C ($\sim$20°C above critical temperature) indicate that gaseous reaction products generate strong convection currents in the liquid while generating little heat.   These results case doubt on the validity of both assumptions.   In future work, a more sophisticated rate expression, even including reactant consumption such as was done by Boddington et al,[15] could be incorporated into the numerical theory.

VIII. RECOMMENDATIONS

The two major assumptions in all of the work presented here are:

1. All heat removal is by conduction.

2. The chemical reaction in the explosive is a simple first order reaction.

The first assumption will always give a lower critical temperature than the observed value. For most applications, this provides a safety factor. However, the errors due to assumption 2 are unpredictable and could be very large. Much work needs to be done on a more realistic chemical kinetic model for the specific explosive under consideration. For EAK laboratory chemical kinetic studies are needed. Once this done, a more realistic theory could be developed following the procedures of Section IV or a more accurate numerical calculation could be carried out following Section V with the only modification being in the form of eq (22).

References

1. H.P. Rothbaum, _J. Appl. Chem. 13_, 291 (1963).

2. W.H. Roll, _Mechanization 27_, 27 (1963).

3. I.K. Walker, W.J. Harrison and A.J. Read, _New Zealand J. Sci, 12_, 302 (1969).

4. P.L. Chambre, _J. Chem. Phys. 20_, 1795 (1952).

5. A.R. Shouman, A.B. Donaldson and H.Y. Tsao, _Combustion and Flame 23_, 17 (1974).

6. A.R. Shouman and A.B. Donaldson, _Combustion and Flame 29_, 213 (1977).

7. W. Kordylewski, _Combustion and Flame 34_, 109 (1979).

8. T. Boddington, C. Feng and P. Gray, _J. Chem. Soc. Faraday II_, 79, 1499 (1983).

9. D.A. Frank-Kamenetzky, _Acta Phyisicochimica U.R.S.S. 10_, 365 (1939).

10. N. Semenoff, _Z. Physk 48_, 571 (1928).

11. J. Zinn and C.L. Mader, _J. Appl. Phys. 31_, 323 (1960).

12. _Safety and Performance Tests for Qualification of Explosives_, NAVORD OD 44811 Vol 1, Jan 1972.

13. T.R. Goodman, _Trans. ASME 8_, 505 (1959).

14. H.S. Carslaw and J.C. Jaeger, _Conduction of Heat in Solids_, Claredon Press (1959).

15. T. Boddington, C. Feng and P. Gray, _J. Chem. Soc. Faraday Trans II, 79_ 1481 (1983).

FINAL REPORT

THE DEVELOPMENT OF COMPUTATIONAL EFFICIENCIES IN

CONTINUUM FINITE ELEMENT CODES USING MATRIX DIFFERENCE EQUATIONS

Prepared by: Dr. Harold C. Sorensen

Academic Rank: Associate Professor

Department and University: Civil and Environmental Engineering
                                 Washington State University

Research Location: Air Force Weapons Laboratory
                                 Civil Engineering Research Division
                                 Kirtland AFB, Albuquerque, New Mexico

USAF Research: Dr. Timothy J. Ross

Date: August 24, 1984

Contract No.:   F49620-82-C-0035

THE DEVELOPMENT OF COMPUTATIONAL EFFICIENCIES IN

CONTINUUM FINITE ELEMENT CODES USING MATRIX DIFFERENCE EQUATIONS

by

Harold C. Sorensen

ABSTRACT

The feasibility of using the Matrix Difference Equation (MDE) theory to obtain computational efficiencies in continuum finite element codes is investigated in this research. The study centered around the SAMSON2 code, which is a state-of-the-art 2-D code for dynamic structural analysis undergoing development within AFWL/NTE. The SAMSON2 code was studied in detail. From this study it was learned that solutions obtained with the use of the higher order elements are in error and that the slideline concept is not being used as it was originally intended. Correcting these algorithms in the code would make the code more efficient and accurate. A brief summary of the theory associated with the SAMSON2 code is presented.

A study of the MDE method was begun. The method has been shown to reduce the computational effort for a certain class of elastic structures. Extension to the non-linear case appears feasible. A brief summary of the MDE method is given. A section on recommendations for further research in these areas is also included.

ACKNOWLEDGEMENTS

I. INTRODUCTION

The Matrix Difference Equation (MDE) method is a state-of-the-art technique which has been used in the free and forced vibration analyses of spatially periodic structures, where a spatially periodic linear elastic structure is a linear array, either longitudinally or circumferentially, of identical substructures. The method takes advantage of the repetitive nature of the structure so that the order of the matrices involved in the solution is approximately equal to the number of degrees of freedom on one substructure boundary. Therefore, significant cost savings in computing can be expected compared to analysis by conventional finite element techniques. This method was pioneered by Mr. Paul Denke, who is an employee of the Douglas Aircraft Corporation (DAC).

Dr. Timothy J. Ross, who is an employee of the Air Force Weapons Laboratory (AFWL), became aware of the MDE method through informational brochures published by DAC which circulated through AFWL. He obtained more information on MDE from DAC and concluded that the method might be used to reduce the computing costs associated with SAMSON2 which is a nonlinear, inelastic finite element code used by AFWL personnel to solve problems involving dynamic analyses of above ground and buried structures, i.e., soil-structure interaction problems. Hence, a feasibility study of the use of the MDE method became apparent.

My formal educational training is in Civil Engineering (B.S.) and Engineering Mechanics (M.S. and Ph.D.). I have taught university courses in structural analysis and design, computer methods in structural analysis, design of foundation elements and structural dynamics for the past eighteen years. When my application for the AFOSR-SFRP was circulated in AFWL, it was decided that my expertise matched that required for the

feasibility study of the MDE method. As a result I was awarded a SFRP fellowship for summer '84 to initiate the study.

II. OBJECTIVES OF THE RESEARCH EFFORT

The goal of this research effort is to effect computational efficiencies in the numerical algorithms of continuum finite element computer codes used in dynamic soil-structure interaction analyses. As a means of accomplishing this goal during the summer appointment period, the SAMSON2 code will be used. This code is a state-of-the-art research tool undergoing development within AFWL/NTE.

Although the research effort will be centered around the SAMSON2 code, the general theory should be adaptable to other continuum finite element codes.

Progress in the development of the efficient numerical algorithms will be documented in a final report covering the summer research period. The final report will contain suggestions for further computational efficiencies and will contain a discussion on any techniques found to be less efficient than the current SAMSON2 algorithms.

III. APPROACH TO ACCOMPLISH RESEARCH OBJECTIVES

The objectives stated above are accomplished by investigating three research task areas. These task areas are all independent and the accumulated sum of the independent task efforts should satisfy the overall objectives of the research. These three task areas are:

Task 1. Use the MDE method to reduce the size of the algebraic solution matrix.

a. Review the procedures which pertain to linear elastic structures which are spatially periodic.

132-5

b. Investigate adaptations of this symmetry restriction to geometries of continuum elements which have more than one plane of symmetry. This step will deal with many substructures within an extended spatial field in which each substructure will be assumed spatially periodic within its boundary.

c. Develop a procedure to combine the individual substructure characteristics into the total model solution matrix.

Task 2. Begin the development of a soil-structure interaction element which is both compatible with the MDE theory and the current numerical integration schemes of the SAMSON2 code.

a. Become familiar with the parameters which have been used to characterize structure-medium interaction modeling.

b. Formulate an element which takes these parameters into consideration for use in the SAMSON2 code.

c. Implement the new element into the SAMSON2 code and run test solutions.

Task 3. Investigate the impact of the MDE method on the higher ordered finite elements presently available in the SAMSON2 code.

a. Become familiar with the operation and use of the SAMSON2 code.

b. Investigate the code definition of the finite elements beginning with the lowest order element and progressing

to the highest order element.

    c.   Incorporate the MDE theory into the existing code element definitions is appropriate.

IV. NARRATIVE OF THE RESULTS OF EACH APPROACH

This narrative will include all three approaches and will give the accomplishments achieved in each task. The order in which the tasks were stated is not the order in which the tasks were performed. This narrative will present the tasks in the order they were performed.

The first and probably the most important aspect of having a successful summer was to become familiar with the operation and use of the SAMSON2 code (Task 3a)[*]. Two graduate students (GSSSP students accompanying me) were directed to learn the CRAY computer syntax and JCLs in order to learn how to run a problem solution using SAMSON2, including how to input data, run the program and interpret the output. While the students were performing this task, I was studying the two manuals[1,2] for the SAMSON2 code learning how to develop an appropriate set of input data. I chose to develop the input data for a simple cantilever beam with a concentrated load at the free end. I used 16-4 node continuum elements for the finite element model. The input for a solution of the same cantilever beam using 64 rectangular continuum elements was available in the users manual and served as a gui for the input for my sample solution. This simple example was chosen because the mathematical solution by basic mechanics principles was also easily obtained and used as a check on the output of the computer solution for ease of interpretation and understanding.

---

[*] The information in the parentheses refers to the Task list stated in Section III - APPROACH TO ACCOMPLISH RESEARCH OBJECTIVES.

[1,2] Superscript numbers refer to references given in the bibliography.

When the input data were completed, the students were asked to run the problem using SAMSON2. Much dialogue took place between us and our AFWL colleagues as we struggled to obtain a successful computer run for this problem. We were eventually successful and the results of the computer solution compared favorably to the theoretical calculations. To reinforce the students' learning process, they were asked to obtain complete solutions including development of the input data to the same beam five other ways using different elements and different loads. At the completion of this task, a good proficiency level was reached with respect to the operation and use of the SAMSON2 code. As a test of this proficiency, the two students were asked to obtain the computer solution for a "real" problem which had been previously obtained by personnel at AFWL. This proved to be a very educational experience for the students as they became aware of the trials and tribulations associated with real world problems.

After this very beneficial initial learning period, attention was now directed to understanding some of the finite elements concepts and principles. Steve Miller (G.S.) was assigned to investigate the code definition of the various elements in the code and to obtain an IBM compatible version of the SAMSON2 code (Task 3b). Bob Bigelis (G.S.) was assigned to begin the development of a soil-structure interaction element (Task 2a) and to become familiar with another powerful finite element code available at AFWL called ANSYS.[23] I began a study of the finite element theory in order to guide the students and to be able to understand the MDE method theory (Task 1a).

Each of the two graduate students will summarize their research activities in an individual final report. I will give only a brief summary of each student's activities here.

Steve Miller worked for two weeks in attempting to obtain an IBM compatible version of SAMSON2. He eliminated all of the diagnostics generated by the IBM compiler. Then in attempting to run a sample problem, underflow problems in the solution were encountered. Steve did not have the time or the computer programming background to correct this problem, so the task was transferred to AFWL personnel. During the remainder of the ten week period, he made a very thorough study, including references to finite element theory, of the program statements in SAMSON2 as they relate to a solution using a constant strain triangle continuum finite element. Steve is now very familiar with the code and associated finite element theory and should be able to accomplish some of the tasks (Task 3b and Task 3c) which we hope to continue in regard to the impact of the MDE theory on the higher order finite elements in SAMSON2.

Bob Bigelis worked several weeks learning ANSYS. He is now fairly proficient in the use of this code as he has run computer solutions of several very practical problems using shell elements. During the remainder of his ten week period, he studied the slideline formulation in the SAMSON2 code, including the soil-structure interaction concepts and the various failure criteria. He has developed a good background in this topic, which should allow him to accomplish some of the tasks (Task 2b and Task 2c) which we hope to continue in regard to development of a soil-structure interaction element which is both compatible with the MDE theory and the current numerical integration schemes in the SAMSON2 code.

I have never had a formal course in finite element theory. Although I have attended several short courses on the subject and am

familiar with many of the concepts from teaching and use of the stiff-
ness matrix method, I needed some remedial work on the subject. Therefore
I spent several weeks studying finite element theory [3,4,5,6] in conjunc-
tion with a more indepth study of SAMSON2. This lead to brief studies
of other topics such as substructuring, static condensation of matrices,
fast Fourier transforms and soil-structure interaction. These studies
also provided backgound information for my later study of the MDE method.

I also reviewed finite difference techniques[7] because one of the
main algorithms in SAMSON2 is based on these techniques.

After these initial activities, I spent the remainder of my eight
week summer period learning as much as possible about the MDE method.
This was done by studying a report[8] on the method written by P. Denke,
Douglas Aircraft Corporation (DAC) and other references from the scien-
tific literature.[9,10,11,12] I worked through a simple example problem,
which helped immensely to understand the concepts of the method and, to
gain further insight into the method, visited with Mr. P. Denke in his
office of Douglas Aircraft Corporation in Long Beach, California. I
believe that I have learned enough about the MDE method to be able to
accomplish some of the tasks (Task 1b, Task 2c and Task 3c) which I hope
to continue in regard to the use of the Matrix Difference Equation
theory to reduce the size of the algebraic solution matrix.

V. SUMMARY OF THE SAMSON2 CODE[1] (Task 3a)

The SAMSON2 computer program is a two-dimensional code for the
dynamic structural analyses of plane and axisymmetric solids. The
program uses explicit time integration and is particularly suited to the
analyses of large displacement, large strain problems involving non-
linear material behavior and structure-media interface (SMI) problems.

It has been specifically developed for the dynamic response analyses of buried structures subjected to shock loading. It can also be used to analyze above ground structures.

The finite element library in the code includes:

* bar element

* straight and curved beam elements

* axisymmetric shell element

* triangular continuum element using either three, five or six nodes

* quadrilateral continuum element using either four or eight nodes

These elements can be combined in any consistent manner to model plane or axisymmetric SMI problems.

The code contains provisions for multiple integration time steps (subcycling) and has a structure-media interface modeling feature that permits sliding, separation and impact between two materials and also accurately treats large relative tangential displacements at the interface.

The program is restricted to lumped mass solutions and uses an explicit central difference method in the time domain for which the acceleration is assumed constant over the time step, the velocity is evaluated at the half time step and the displacement is evaluated at the end of the time step. The explicit central difference method does not require the solution of any equations in advancing a time step. Consequently, the program does not evaluate a stiffness matrix. However, the program requires a relatively small time step for stability of the solution. There are also provisions for maintaining an energy balance and for accounting for the "hour glass effect". The program calculates the accelerations, velocities, displacements, strains and stresses in the finite elements at each time step.

The basic equations used in the code are as follows.

The governing equations of motion for the finite element mesh in explicit form are

$$[M]\{\ddot{u}\} + [C]\{\dot{u}\} + \{f\}^{int.} = \{f\}^{ext.} \qquad (1)$$

where $\{u\}$ is the matrix of nodal displacements, $[M]$ the mass matrix, $[C]$ the damping matrix, $\{f\}^{int.}$ the nodal forces which are obtained from the resistance of the finite elements to deformation and $\{f\}^{ext.}$ the nodal forces arising from external loads. The superposed dots denote time derivatives, so $\{\dot{u}\}$ are the nodal velocities and $\{\ddot{u}\}$ are the nodal accelerations.

The nodal accelerations at any time step are obtained from the equations of motion, Eq. 1, as

$$\{\ddot{u}\}^n = [M]^{-1}\left(\{f\}^{ext.} - \{f\}^{int.} - [C]\{\dot{u}\}^{n-\frac{1}{2}}\right) \qquad (2)$$

where n denotes any particular time step and $n-\frac{1}{2}$ indicates the previous half time step. The new nodal velocities and nodal displacements are determined from the central difference formulas

$$\{\dot{u}\}^{n+\frac{1}{2}} = \{\dot{u}\}^{n-\frac{1}{2}} + \Delta t\{\ddot{u}\}^n \qquad (3)$$

$$\{u\}^{n+1} = \{u\}^n + \Delta t\{\dot{u}\}^{n+\frac{1}{2}} \qquad (4)$$

where fractional superscripts denote midstep values.

With initial conditions for u^o and $\dot{u}^o$ known, the program calculates $\ddot{u}^1$ from Eq. 2, then calculates $\dot{u}^{o+\frac{1}{2}}$ from Eq. 3 and u^1 from Eq. 4. Then from appropriate material laws, etc., strains and stresses are calculated and one cycle is complete. All parameter values are updated and the procedure is repeated. This process continues through the time domain desired for the solution. Large problems can require large amounts of computer time. Hence, there is a need for finding and implementing techniques which will result in reduced computing time.

VI. SUMMARY OF THE MDE METHOD[8,9] (Task 1a)

The MDE method has been incorporated into a finite element computer program which has been used successfully by Douglas Aircraft Corporation to solve problems involving bounded vibrating spatially periodic structures. The order of the matrices to be solved is approximately equal to the number of degrees of freedom of one substructure boundary. This concept can be demonstrated through the use of a simple example problem as follows.

Consider a simply supported beam modeled by six identical beam elements as shown in Figure 1. For each beam element, there exist four degrees of freedom, one translation and one rotation at each end. Thus the beam has twelve degrees of freedom since two displacements are constrained to be zero at the beam supports. The standard procedure for this problem would require the solution of a set of twelve simultaneous equations (or appropriate numerical techniques) to obtain the eigenvalues. By contrast the MDE method would require the solution of only two simultaneous equations (this is the number of degrees of freedom of one element boundary, i.e., one translation and one rotation) into which different parameters would be substituted seven different times. Two of
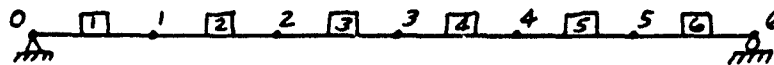
a) Entire beam

Note: The numbers in the boxes indicate element numbers.
The other numbers designate the nodes.

b) One element
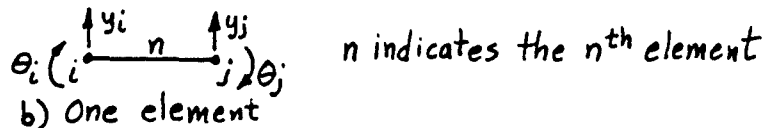
n indicates the nth element

Figure 1. Finite element model of a simple beam.

the seven different calculations, which are associated with the end ele-
ments, yield modes which give zero displacements everywhere and are,
therefore, discarded to give the required twelve eigensolutions. The
computer solution for the MDE method would be much faster than that for
a standard solution.

The objective of the MDE approach is to develop methods of analysis
for free and forced vibrations of spatially periodic structures that
take advantage of the periodicity. The method, at present, has been
applied only to periodic elastic structures which have simply supported
or guided ends. It is dependent upon the substructure being symmetric
about a median axis, and damping is a linear combination of assembled
mass and stiffness matrices for which a modal transformation decouples
the degrees of freedom.

The MDE approach is based on a finite element model of a single
substructure. Writing the equations of dynamic equilibrium and com-
patibility of displacements between adjacent substructures leads to a
matrix difference equation. The solution of this difference equation
and satisfaction of the end conditions yield the displacement and inter-
nal force responses of the structure.

The method is analogous to the differential equation analysis of a
uniform vibrating beam in which an infinitesimal element is considered.
Differential equations expressing dynamic equilibrium of the element and
compatibility of displacements are written. Solutions to these
equations satisfying the boundary conditions are found. A key point in
this analogy is that only one differential element requires considera-
tion, since all of the other infinitely many elements are identical. By
comparison, in MDE theory the difference equation is analogous to the

differential equation and only one substructure (differential element) requires consideration.

The finite element method is applied to the substructure in order to obtain a mechanical impedance matrix, based upon conditions of equilibrium and compatibility at substructure boundaries. The order of the difference equation is reduced by eliminating force variables and introducing substructure displacement modes. A solution is found by calculating eigenvalues and eigenvectors of a related characteristic equation. The result is a closed form expression in the longitudinal direction. The method is general and applicable to complex structures, because of the finite element basis. All forcing functions are sinusoidal functions of time of a single frequency ω. Hence, the problem is solved in the frequency domain.

The basic equations used in the method are of the following form. The linear equations of motion for a substructure in harmonic motion are

$$\underset{\sim}{A}\,\underset{\sim}{\Delta} = \underset{\sim}{P}_u \tag{5}$$

where $\underset{\sim}{A}$ is the mechanical impedance matrix, $\underset{\sim}{\Delta}$ is a column matrix of complex displacement amplitudes and $\underset{\sim}{P}_u$ is a column matrix of complex external load amplitudes in the unconstrained degrees of freedom. The impedance matrix is given by

$$\underset{\sim}{A} = \underset{\sim}{K} - \omega^2 \underset{\sim}{M} + i\omega \underset{\sim}{C} \tag{6}$$

where ω = frequency, $i = \sqrt{-1}$ and $\underset{\sim}{K}$, $\underset{\sim}{M}$ and $\underset{\sim}{C}$ = square stiffness, mass and damping matrices for the substructure as derived by standard finite element procedures. By a suitable transformation, Eq. 5 can be written for a substructure boundary as

$$\underset{\sim}{\hat{A}}_B\,\underset{\sim}{\hat{\Delta}}_B = \underset{\sim}{\hat{P}}_{u_B} \tag{7}$$

132-15

The impedance, displacement and load matrices can be partitioned as follows:

$$\left[\begin{array}{c|c} \hat{A}_{B\ell\ell} & \hat{A}_{B\ell r} \\ \hline \hat{A}_{Br\ell} & \hat{A}_{Brr} \end{array}\right] \left\{\begin{array}{c} \hat{\Delta}_{B\ell} \\ \hat{\Delta}_{Br} \end{array}\right\} = \left\{\begin{array}{c} \hat{P}_{u_{B\ell}} \\ \hat{P}_{u_{Br}} \end{array}\right\} \tag{8}$$

where the subscripts ℓ and r refer to the left and right boundaries of the substructure. Equation 8 with force variables retained can be put into the following matrix difference form:

$$\hat{Y}^{i+1} - \hat{N}\,\hat{Y}^{i} = 0 \tag{9}$$

where

$$\hat{N} = \left[\begin{array}{c|c} -\hat{A}_{Brr}\hat{A}_{B\ell r}^{-1} & \hat{A}_{Br\ell} - \hat{A}_{Brr}\hat{A}_{B\ell r}^{-1}\hat{A}_{B\ell\ell} \\ \hline -\hat{A}_{B\ell r}^{-1} & -\hat{A}_{B\ell r}^{-1}\hat{A}_{B\ell\ell} \end{array}\right] \xi\, \hat{Y}^{i} = \left\{\begin{array}{c} \hat{P}_{u_{Br}} \\ \hat{\Delta}_{Br}^{i} \end{array}\right\} \tag{10}$$

and subscript i indicates the equations apply to the ith substructure.

A solution of Eq. 9 is

$$\hat{Y}_{k}^{i} = \hat{G}_{k}\,\hat{\lambda}_{k}^{i} \tag{11}$$

where $\hat{G}_{k}$ is a column matrix and $\hat{\lambda}_{k}^{i}$ is a scalar. Substituting $\hat{Y}_{k}^{i}$ from Eq. 11 into Eq. 9 gives

$$\left(\hat{N} - \hat{\lambda}_{k}\,\hat{I}\right)\hat{G}_{k} = 0 \tag{12}$$

Equation 12 is the characteristic equation of the substructure with force variables retained which can be solved for the eigenvalues $\hat{\lambda}_{k}$ and the eigenvectors $\hat{G}_{k}$.

Equation 8 can be rearranged in a similar manner but with the force variables eliminated to give

$$\left[\hat{A}_{B\ell r}\hat{\lambda}^{2} + \left(\hat{A}_{B\ell\ell} + \hat{A}_{Brr}\right)\hat{\lambda} + \hat{A}_{Br\ell}\right]\hat{G}_{\Delta} = 0 \tag{13}$$

132-16

Equation 13 is the characteristic equation of the substructure with force variables eliminated. Unfortunately, Eq. 13 is quadratic in λ, but the matrices in the equation are only half as large as those in Eq. 12. This feature is important because the computational effort required to solve a characteristic equation increases rapidly with the order of the equation.

Another feature of the MDE approach is the introduction of a modal technique that further reduces the order of the characteristic equation, thereby further reducing computational time. Once all substructure eigensolutions are found, a complete modal solution of the entire structure is available, which completes a linear elastic solution.

VII. RECOMMENDATIONS

Personnel at AFWL who use the SAMSON2 code state that solutions obtained wih the use of the higher order elements (5 and 6 node triangles and 8 node quadrilateral) are not correct. They also state that computational efficiencies would result if the higher order elements could be used. Therefore, it is recommended that a complete study of the higher order elements (Task 3b) be performed and used to check the logic statements in the code in order to correct the procedure for these higher order elements. This study is preliminary but essential in order to obtain the understanding of finite elements and the SAMSON2 code to be able to determine how and where the MDE method can be effectively incorporated into the existing code element definitions (Task 3c).

Users of SAMSON2 also state that the slideline formulation in the code is not used effectively because of lack of understanding of the formulation criteria. Hence, it is recommended that a study (Task 2a) be made to develop a new friction law for the slideline in the SAMSON2

code so that real world problems can be modeled effectively. It is also
recommended that a study be initiated to develop a new SMI element which
will model the soil-structure interaction (Task 2b). These studies are
preliminary but essential in order to obtain the understanding required
to develop a SMI element compatible with the MDE theory and the SAMSON2
algorithms (Task 2c).

My study of the MDE method has been relatively superficial.
However, I have learned enough to believe that the method does have
definite possibilities toward reducing computational time associated
with finite element computer codes. Hence, it is recommended that
further study be made concerning the MDE method (Task 1a). This study
should include a more indepth analysis of the MDE method and the initial
development of non-linear solutions (Task 1b).

This study is essential in order to ascertain the feasibility of
the MDE approach as it may be used to reduce the size of the algebraic
solution matrix in codes used by AFWL personnel. Discussions with Mr.
P. Denke, DAC, confirm that extension to the non-linear case would be
difficult but possible and would result in computational efficiencies in
non-linear solutions.

I intend to apply for a Research Initiation Program grant which
will include each of these recommendations.

<u>REFERENCES</u>

1. Belytschko, T. and Robinson, R.R., "SAMSON2: A Nonlinear Two-Dimensional Structure/Media Interaction Computer Code," AFWL Final Report No. AFWL-TR-81-109, January 1982.

2. Schreyer, H.L., Richards, C.G., Bean, J.E. and Durka, G.R., "SAMSON2, A Nonlinear Two-Dimensional Structure-Media Interaction Computer Code: Users Manual," AFWL Report No. AFWL-TN-82-, September 1982.

3. Martin, H.C. and Carey, G.F., <u>Introduction to Finite Element Analysis</u>, McGraw-Hill Book Company, 1973.

4. Cook, R.D., <u>Concepts and Applications of Finite Element Analysis</u>, John Wiley and Sons, 1974.

5. Desai, C.S. and Abel, J.F., <u>Introduction to the Finite Element Method</u>, Van Nostrand Reinhold Company, 1972.

6. Zienkiewicz, O.C., <u>The Finite Element Method in Engineering Science</u>, McGraw-Hill Book Company, London, 1971.

7. James, M.L., Smith, G.M. and Wolford, J.C., <u>Applied Numerical Methods for Digital Computation</u>, 2nd Edition, Harper and Row Publishers, 1977.

8. Denke, P.H., "Matrix Difference Equation Analysis of Bounded Vibrating Spatially Periodic Structures," McDonnell Douglas Corporation Report No. MDC J7414, March 1982.

9. Denke, P.H., Eide, G.R. and Pickard, J., "Matrix Difference Equation Analysis of Vibrating Periodic Structures," AIAA Journal, Volume 13, No. 2, 1975, pp. 160-166.

10. Denke, P.H., "Aircraft Windshield Bird Impact Math Model, Part I Theory and Applications," Air Force Flight Dynamics Laboratory Report No. AFFDL-TR-77-99, December 1977.

11. Denke, P.H. and Eide, G.R., "Aircraft Transparent Closure Bird Impact Math Model," Proceedings of the Conference on Aerospace Transparent Materials and Enclosures, Long Beach, CA, April 1978.

12. Sengupta, G., "Vibration of Periodic Structures," <u>The Shock and Vibration Digest</u>, Volume 12, No. 3, March 1980.

13. Clough, R.W. and Penzien, J., <u>Dynamics of Structures</u>, McGraw-Hill Book Company, 1975.

14. Downey, G.L. and Smith, G.M., <u>Advanced Dynamics</u>, International Textbook Company, 1960.

15. Harrison, H.D., Computer Methods in Structural Analysis, Prentice-Hall, Inc., 1973.

16. Hughes, T.J.R. and Belytschko, T., "A Precis of Developments in Computational Methods for Transient Analysis," Journal of Applied Mechanics, Volume 50, December 1983, pp. 1033-1041.

17. Newland, D.E., Random Vibrations and Spectral Analysis, Longman, 1975.

18. Fertis, D.G., Dynamics and Vibration of Structures, John Wiley and Sons, 1973.

19. Bowles, J.E., Foundation Analysis and Design, Third Edition, McGraw-Hill Book Company, 1982.

20. Streeter, V.L., Fluid Dynamics, McGraw-Hill Book Company, 1948.

21. Chen, W.F., Plasticity in Reinforced Concrete, McGraw-Hill Book Company, 1982.

22. Burden, R.L., Faires, D.J. and Reynolds, A.C., Numerical Analysis, Second Edition, Prindle, Weber & Schmidt Publishers, Boston, Massachusetts, 1978.

23. DeSalvo, G.J. and Swanson, J.A., ANSYS ENGINEERING ANALYSIS SYSTEM USER'S MANUAL, Vol I & Vol II, February 1982, Swanson Analysis Systems, Inc., P.O. Box 65, Houston, Pennsylvania 15342.

1984 USAF-SCEEE SUMMER FACULTY RESEARCH PROGRAM

Sponsored by the

AIR FORCE OFFICE OF SCIENTIFIC RESEARCH

Conducted by the

SOUTHEASTERN CENTER FOR ELECTRICAL ENGINEERING EDUCATION

FINAL REPORT

BASE COMMUNICATIONS ARCHITECTURE SECURITY ISSUES

Prepared by: Charles J. Spiteri, P.E.

Academic Rank: Associate Professor

Department and University: Dept. of Electrical and
                                      Computer Technology
                                      Queensborough Community
                                      College of the City
                                      University of New York

Research Location: Hanscom A.F.B., ESD/XRC

U.S.A.F. Research   Mr. Sidney Sternick

Date: August 17, 1984

Contract No: F49620-82-C-0035

BASE COMMUNICATIONS ARCHITECTURE SECURITY ISSUES

by

Charles J. Spiteri

ABSTRACT

The problem of applying DoD and 1974 Privacy Act mandated
security to Air Force Base Local Area Networks is addressed. Both
existing and future techniques and devices used to protect classified
and privacy traffic on computer networks were researched. A plan for
implementing security measures on base LANs is proposed in a three
phase plan. The proposal utilizes today's technology for networks
currently being installed. Data segregation by frequency, time or
physical means, coupled with available encryption is recommended.
Single and multilevel trusted interface units and gateways are proposed
as they become available. End to end encryption is also proposed,
either as a companion or alternative technique, depending on base and
technology parameters. Suggestions are made to continue research in
this vital area.

ACKNOWLEDGEMENT

The author gratefully acknowledges the Air Force Systems Command, the Air Force Office of Scientific Research, and the Southeastern Center for Electrical Engineering Education for making the Summer Faculty Fellowship Program possible.

Special thanks are extended to all those whose assistance and encouragement made this report possible. Civilian and military personnel at ESD, MITRE staff members, and my wife, Nancy, have all played a part towards making this a successful and enjoyable summer.

BASE COMMUNICATIONS ARCHITECTURE SECURITY ISSUES

I.   INTRODUCTION:

In order to modernize and improve intrabase and interbase com-
munications, ESD/XRC is developing a Base Communications Architecture
which will evolve over the coming years. All modes of communications
including telephone, radio, video and computer communications are
being studied. One aspect of the study involves the use of Local
Area Networks (LANs). These networks will be used to accommodate
the proliferation of office automation equipment and provide impor-
tant services such as electronic mail, teleconferencing and data
transfer.

The Privacy Act of 1974 and the DoD requirements for the treat-
ment of classified information place security constraints on these
networks. This paper focuses on the many security problems that
impact the implementation and utilization of Local Area Networks on
Air Force bases.

II. OBJECTIVES:

There are two objectives of this project. First, in order to
provide a sound foundation, existing security techniques were iden-
tified. Also, developing and proposed measures were researched and
evaluated.

Next, a combination of existing and future techniques were
integrated into a proposal for secure LANs that could be put into
place now and evolve with emerging technology. Since the require-
ments for individual bases may vary, no one approach can be proposed
for all bases. Also, future technological trends will determine the
final course chosen. The proposal provides a sound security system
which may be implemented in phases. Alternative choices are given
to accommodate individual needs and possible technological develop-
ments.

III. EXISTING SECURITY TECHNIQUES:

There is a set of security measures which will be implemented
on all bases. These techniques, both general and applicable to
LANs, are identified in this section of the report.

Administration- Security is an area that all levels of civilian and military administrators must concern themselves with. The upper levels must recognize, analyze and form directives to address the needs and problems which are presented to them. They must enforce accountability for actions and establish policies which will be communicated to all personnel.

Middle management acts as the interface between higher and lower levels of management. They will pass down guidance and directives from the upper levels, while at the same time act as a means of recognizing and reporting problems. deficiencies, and suggestions.

Lower management, and individual security officers are responsible for the strict enforcement of mandated rules and procedures. In addition, they are obligated to report problems, deficiencies and violations.

Finally, no security system is workable without the cooperation of all personnel involved. Each and every system user is responsible for both implementing and improving the overall security of the system.

Physical- The two main areas of physical security concern the facilities and the LAN communications medium. It is assumed that judicious practices to protect the facilities against natural and man-made disasters will be in effect. In additon, classified hardware and software will require physical protection. Each element is to be protected to at least the level of information it handles, commensurate with DoD practices. Equipment which handles data protected by the 1974 Privacy of Information Act may also require physical segregation.

The most popular medium for LANs to date is coaxial or triaxal cable. A rapidly emerging competitive medium is the various classes of fiber optic cable. In some instances, it may be necessary to use radio waves to provide links to mobile or physically isolated parts of a network, or where satellite links are used.

All of the above media are subject to passive and/or active wiretapping. In the passive case, emanations from the medium or terminal devices are intercepted by unauthorized receivers. In the case of radio waves, the cost of a suitable antenna is the only prerequisite to tapping. Cables, connectors and terminal equipment radiate various levels of energy which may be received by suitable

equipment. If any medium is physically accessed, a passive tap may
be made using compatible technology. This includes fiber optic cable.

Active wiretapping involves accessing the medium also. However,
as opposed to listening only, the intruder injects unauthorized
traffic. This may provide erroneous information or could cause a
denial of service to some or all users.

If a medium may be physically accessed, it may be captured and
severed. In this case all authorized users will be denied sercvice.

In the case of fiber optic cable, topological limitations may
also exist. Due to the losses and reflections of TEE couplers, fiber
optic cable may be best suited to STAR and LOOP topologies as
opposed to BUS TREES.

The traditional means of medium protection are sealing and
encryption. In sealing, the medium is enclosed in a welded conduit
while in a building. Outside, it would be buried to a suffici at
depth so as to protect it, or be sealed in concrete, or pressurized
conduit, and guarded.

If the medium cannot be isolated as described, or if there are
TEMPEST problems, encryption is the only alternative. Although
under development, there are currently no encrypting devices for LANs.

Sealing the medium makes maintainance difficult at best.
Encryption, which will be discussed in detail later, is expensive
and complex to implement. The choices of whether to employ one or
both techniques must be made on an individual basis. The decision
will be based on geographic parameters such as the size and layout
of the base, and other factors such as the number of users to be
served and the severity of the perceived threat. In the case of any
broadcast of data, however, encryption is mandated.

Personnel Access Control- Personnel Access Control is sometimes
referred to as user authentication. The users of base LANs are
expected to possess a variety of clearances, as does the multilevel
traffic on the net. There must exist a means to verify the access
level of the users and provide access to data for which they are
cleared. At the same time care must be taken so as to insure that
these measures do not present a "denial of service" problem to
authorized personnel by their complexity. Prospects exist for
having multiple levels of classified data available at a single net-
work interface device.

Traditionally, access control has been accomplished by using
user passwords. If done in a non-encrypted system in an open
environment, this technique may prove unreliable at best. At the
other end of the spectrum are the relatively costly techniques
involving electronic voice and fingerprint recognition.

Among the measures which appear cost effective are the use of
magnetically encoded i.d. cards and so called "smart cards", which
contain embedded microprocessor chips. A correlation can be
established between the specific card and the terminal to which it
is presented. Unauthorized users can, therefore, be easily iden-
tified. It may further be required that the card remain inserted in
the reader while the session is in progress, and that the session be
terminated upon withdrawal of the card. Another option is the use
of magnetic encoders to alter the coded information at the end of
each session. This would deter fraudulent cards. Additional pro-
cedural and physical options could be added to reduce the risk of
system compromise to an acceptable level.

Other issues which must be explored concern the choice between
distributed and central authentication. The possibility exists for
a central access control center at some facilities. In a distri-
buted controlled system, the source and/or the destination nodes may
provide the authentication service. These issues must be addressed
on a base by base perspective to allow for a wide variety of
requirements and available resources.

Data Access Control- A closely related topic to authentication is
data access control. There are two sets of issues in this area.
One pertains to access control of ADP central data bases. This
control would be applied during sessions between a user and a host
computer. The second set involves communications and the exchange
of data between nodes within a LAN or on interconnected LANs.

Since most Air Force bases have central data bases contained on
a mini or mainframe, and these resources may be accessed via a LAN,
host to user interactions must be addressed. The data base must be
protected against unauthorized access, modification and denial of
authorized access. The problem involves user authentication, but
transcends it. The requirement is for the implementation of the
"simple security principle" (no read up), and the "star principle"
(no write down), in a multi-level environment. These principles

133-7

evolved from the Bell-Lapadula security model.

The realization of such controls becomes part of the host's overall operating system, specifically a memory access controller which mediates all main storage access. The controller would intermediate in all interactions between subjects (users) and objects (data files). It has also been called a Reference Monitor.

Such a monitor is the subject of many research and development projects involving software, hardware and firmware. These projects generally involve the design of a kernelized secure operating system (KSOS) which would perform the monitor functions and, at the same time, emulate an existing operating system such as UNIX. Among the players are: MITRE, UCLA, Honeywell and others. Needless to say, if a multi-level secure data base is to be accessed by a multi-level secure community, some form of memory access control will be required. This control must also address the threat posed by "trojan horse programs." These are user generated programs, which although appearing innocuous, actually contain embedded code to subjugate the data base.

The second set of issues concern data access and exchange as applied to LANs only. Similar problems to those previously described will exist if devices and users of a variety of clearances wish to communicate. The same security principles apply as before except that a central mini or mainframe computer cannot be assumed.

This set of problems, and their tentative solutions will be addressed in other sections of this report. The solutions involve the use of one or more of the following:

1. Encryption
   a. end to end
   b. link to link
2. Mediation by LAN devices such as:
   a. single and multilevel interface units
   b. trusted bridges or guards
   c. internet gateways

IV. NEW AND EMERGING TECHNOLOGIES:

In researching the two developing technologies, encryption and data mediation, two facts become clear. First, the techniques may be used separately or in conjunction with each other. Secondly,

their state-of-the-art nature and costs warrant special treatment of these topics. Because of these characteristics, a more detailed view of these topics is presented.

Encryption- The use of encryption in data storage and transmission is an important and viable measure. It can also add significant system costs and impede the free flow of data. The techniques should, therefore, be used judiciously and only where necessary.

There are two basic considerations which mandate the use of encryption. In the first case, there may be a need to restrict access to data at terminal devices. This may be due to the fact that some personnel may not be cleared to the level of some of the traffic, or that the physical security of the terminal is such that access by uncleared personnel is likely.

Second, and moreover, the medium of the LAN must be physically protected to the highest security level of the data on it. Unless the medium is physically secure (contained in welded pipes, etc.) and protected from attacks to it, encryption is needed. An excellent example is the use of various microwave and other "free space" links used in communications where hard wiring is impractical. Without encryption the cost of a suitable antenna is the only deterrent to passive (eavesdropping) wiretapping. In the case of coaxial and fiber optic cable, physical access to the medium is tantamount to having a broadcast transmission. In conjunction with passive wire-tapping there also exists the possibility for active (intruder) wiretapping which may provide a more severe threat. In addition, close physical proximity is not always required. R.F. emissions and leakages present their own set of problems.

Various encryption techniques have been developed to address these problems. All of the transformations performed by the various algorithms involve either substitution or transposition of the cleartext data to arrive at a ciphertext version of it. If both techniques are used, the algorithm performs what is called product transformations.

In the case of substitution transformations, the characters or groups of characters of the plaintext are replaced with characters or groups of characters from a ciphertext character set. Single character substitution is referred to as monographic substitution, where multiple character substitution is called polygraphic. In

74

addition, there are monoalphabetic and polyalphabetic substitutions. In the monoalphabetic case, the cipher alphabet is usually derived from the plaintext alphabet, with a clear mapping existing from one set to the other. In the polyalphabetic case, there are many cipher alphabet sources which are used on a rotating basis. This discourages a statistical analysis on the ciphertext based on language characteristics.

The data to be transmitted may also be rearranged or transposed without actually changing the individual characters. Most modern encryption algorithms involve product transformations, however, in which the data is both transposed and substituted for.

The two methods of performing cryptographic transformations are stream and block transformations. In the stream method, which is usually applied to voice transmissions, the algorithm continually encodes data as it becomes available, independent of any other data. The encoded data can then be transmitted immediately. There are no limits as to the length of the data stream which may be processed. In the block method, which seems better suited to LANs, a fixed data block length, N bits or bytes, are encrypted at a time, with the resultant block sometimes dependent on all the data contained within it.

In 1977, the National Bureau of Standards approved the Data Encryption Standard (DES), which was developed by IBM, as a federal standard. DES was made mandatory for any civilian agency of the federal government which required encryption to protect privacy data. The technique resulted from the 1974 Privacy of Information Act. The DES algorithm, which is described in FIPS 46, consists of an iterative number of product transformations on a 64 bit data block using a 64 bit (56 bit key plus 8 parity bits) key. In addition, DES may operate in a variety of modes of varying complexity. Implementation costs run in the thousands of dollars for a stand alone unit to hundreds for a DES chip. Almost all government agencies utilize DES to encrypt privacy data.

Unfortunately DES has not been, nor does it appear that it will be, certified by NSA for classified data. Any encryption of classified data must be done by NSA approved devices. These include the various KG devices now in use, as well as other classified product lines currently under development. The development and certification

of new NSA approved encryption devices generally involves a large investment in time and money.

The use of encryption brings forth a number of associated issues. One involves the nature of the encryption keys. In general, the keys may be thought of as closed (or private) or open (public keys). In a public key system, the key used to encrypt the data is a matter of public record. The decryption key, which is distinct from the encryption key, is protected. In a private key system, there is generally only a single secret key used to encrypt and decrypt the data, and it must be protected. In a private key system, there is generally only a single secret key used to encrypt and decrypt the data, and it must be protected. Military encryption usually utilizes private key systems, whereas public key systems appear to be commercially oriented. The private key system has choices and constraints associated with it.

First, there must be different keys for individuals or groups of users, or as a minimum each security level. Next, the distribution of those keys involves the following. Should a central "key distribution center" be responsible for generating and distributing the keys, or should it be done by the session users? Should the keys be transferred physically (by courier) or automatically using the old or a unique key? Should the keys be used for a specific period of time, or for a session only? Factors involved in deciding these issues include costs, complexities, and the survivability based on presumed threats.

As for implementing encryption on LANs is concerned, there are two techniques which may be employed. They are: link encryption and end to end encrytion (E3). The devices currently in use in non LAN applications involve link to link encryption. In this technique, each node at the end of a link decrypts arriving data and encrypts data to be transmitted over the next link. This is done to determine the routing, because the interfaces at the nodes are not capable of handling encrypted data. The encrypting and decryption takes place in devices on the receiving or sending ports of a node. The node itself must be physically protected, because the classified plaintext exists in it. This process is somewhat time consuming, because the entire data packet must be completely decrypted and encrypted at every node. The process is usually implemented in the

133-11

Data Link Layer of protocol.

End to end encryption would be implemented in a higher layer such as the Presentation Layer. Using E3 the sender encrypts the message, and it remains encrypted while being transmitted through the network, until it reaches its intended destination.

In link systems, then, keys need only be exchanged between adjacent nodes, where in E3 the key distribution problems previously stated must be dealt with.

As mentioned, the cryptographic devices currently used by NSA are link encryptors. Various development programs for E3 devices for long haul and local nets may produce certifiable devices for LANs by the 1990's. The current expectations are for an E3 Secure Communications Controller (SCCL) to evolve from a similar long haul net device being developed by Motorola. NSA has other classified projects under investigation.

A technique related to encryption should be mentioned here. It involves the use of unique, coded, digital signatures for authentication. This technique is used by banking systems to prevent intruders from encroaching upon the system. It involves appending a message or packet dependent signature onto a transmitted packet. If the packet were altered along the way, the old signature would be determined to be invalid at the destination. It is similar to parity or CRC error detection in its implementation, but its purpose is authentication.

Transmission security could be further enhanced by sending dummy messages on a net. This will discourage traffic analysis and key determination on encrypted lines.

Data Separation by Mediation- In addition to encryption, there is a developing technique for separation of data by mediation. In this technique, the device which interfaces the user to the LAN is aware of the security classification of the data and the user, and mediates data exchanges to enforce security.

The network interface unit (NIU) is a microprocessor based device that interfaces the user devices to the network medium. Among its functions are:

1. Accepts data from attached devices.
2. Buffers data until the medium can be accessed.
3. Transmits data in addressed packets.

133-12

4. Receives all packets and accepts those with its own address.

5. Buffers incoming data.

6. Passes data to attached devices at the proper rate.

7. Performs error correcting if applicable.

NIUs vary in complexity depending on the protocols implemented in them.

In a secure LAN the interface may be called upon to perform security functions. A trusted interface unit (TIU) performs all the above NIU functions with the following additional tasks.

A single level TIU operates at a single assigned security level. It labels each frame it transmits with its' security level. In addition, it will accept only frames that are labeled with its' own or a lesser security level. The additional functions are generally implemented in the Data Link Protocol Layer.

A refinement of the single level TIU is the variable level TIU. This device would contain a manual or host controlled switch which would allow it to operate at different security levels at different times.

Again, variable and multilevel TIUs have been the subject of many papers, but they will not exist for several years. The most promising candidate appears to be interfaces being developed by SDC for the DIA. These interface devices have network front ends (NFEs) which interface to the DoDIIS, and will process TOP SECRET compartmentalized data. They will screen the traffic with regard to compartment, as a multilevel TIU would do for security levels. It is believed that with minor modifications, the screening could be done by security level. Since these devices are meant to operate in a physically protected environment, a problem may arise in their multilevel certification. Again, liaison must be established with the sponsoring agency to further explore the prospects.

In many LANs, several smaller but compatible subnets are established, and interconnected with devices called bridges. The bridge consists of at least two NIUs linked together. In a homogeneous network, the bridge passes packets back and forth between the subnets. It must be aware of all addresses on each subnet to do this. In the event that each subnet operated at a different security level, the bridge would be required to act as a guard, performing the security functions described for a multilevel TIU.

133-13

The next possibility is that the subnets on a base will not be compatible, which is possible if various groups do not coordinate purchasing. In this case, separate, incompatible nets exist as opposed to subnets. The bridging device, then, must support the protocols of any and all connected nets, increasing its complexity significantly. These devices are called gates or internet gateways, and generally serve to interface a LAN to a long haul net.

A multilevel secure gateway is being developed by R.A.D.C. under contract. Units are expected to be tested within a year. Although practical and necessary for LAN to haul net interfacing, it is hoped that intrabase LANs will not have to be interconnected by anything as complex or expensive as an internet gateway. As it appears now, it is a distinct possibility.

Until the various enumerated devices become certified and available, there is only one acceptable means of handling multilevel classified data. That is to separate each level of data on its own subnet. Interface units of a single security level would be connected to each net, with no means of bridging the subnets. This represents a simple topological albeit restrictive means of implementing multilevel security.

Related techniques involve separation by frequency or time allocation. Each of these methods has its own associated drawbacks, but may be easier to implement than some of the more sophisticated proposals. The final choices must be made on the techniques which are realistically expected to be available, and their associated costs.

Finally, it should be reemphasized that the Air Force base environment, as opposed to an underground command center, poses additional security problems. If the physical security of the medium and terminal hardware cannot be assured, or if RF emanations may be intercepted by unauthorized listeners, encryption will be required.

V. PROPOSALS FOR LAN SECURITY

In an attempt to discern the security requirements for A.F. base LANs now and for the future, it will be found that there is no clear consensus. A number of factors are responsible for this.

There exists a wide disparity in the type and size of bases,

both in the U.S. and overseas. Some bases support wing operational units, others provide logistics support, while still others are command and control centers. In the U.S. bases tend to be larger and multipurpose. Overseas bases are smaller and more unifunctional. They also perceive more of an immediate tactical and subversive threat. It is safe to assume, however, that all bases will acquire LANs over the coming years, and that multilevel security will eventually be implemented on them. The networks will probably develop over a number of years. Each group on a base (finance, logistics, personnel, etc.) will probably acquire their own network as funds become available. The security measures, therefore, must also be somewhat evolutionary, encompassing a variety of possible topologies, from a single LAN to multiple interconnected LANs.

Phase I- As mentioned, it is anticipated that single or independent networks will exist on a particular base. If there is privacy or classified data that will be transmitted on such a net, there appear to be two choices for implementing security. The privacy and classified data must be separated by means of: (1) frequency, channel, or time partitioning and/or (2) encryption.

Time partitioning requires that classified and privacy data be transmitted only during certain allowed periods. It requires physical control at all terminals and interface units. Frequency and channel separation are somewhat less restrictive, but tests must be performed to insure that sidebands are sufficiently suppressed so as to insure there will be no interfrequency leakages.

Encryption appears to be a satisfactory candidate, particularly for baseband (single channel) systems. However, only DES, which is not approved for classified data will probably be available in the near future.

In an attempt to avoid the absolute requirement for encryption, or restrictive time allocating, it is recommended that broadband networks be considered for initial base LANs where security will be required. The options for implementing security are more plentiful.

The security of the transmission medium and interface units must still be addressed. If unauthorized access to the medium and the interface units is possible, encryption will be mandated. DES will suffice for privacy data, but not for classified data. In this case one of two choices exists. Either certify DES temporarily or

adapt an existing link encryption device to the LAN. Given the past
doctrine, the latter seems more probable.

If frequency or channel separation are used, separate bus
interface units will be required for each level of classified data.
The same is true if link encryption is used, unless each user is
cleared system high.

If the base remains with a single LAN on it, two alternatives
for the future exist. Trusted interface units (TIUs), first single
then multiple level, implemented at the Data Link Protocol Layer
will remove the separation requirement. These devices will probably
exist first but are more risky, being subject to tampering and
failures. Also, of course, physical and personnel security must be
insured.

Link encryption used in conjunction with TIUs, or end to end
encryption represents the other alternative. As a minimum, separate
keys will be required for each security level in the case of end to
end encryption.

Phase II- As time passes, most bases will acquire multiple LANs.
With some amount of planning and the application of standards, a
degree of compatibility can be achieved. If not, the gateways which
interconnect heterogeneous LANs will have to support each of the
different protocol structures, as well as perform the other gateway
functions. This will embody additional complexity an   .ur the
associated expense into the gateways.

The requirement may remain for separation of the different
classes of data until suitable procedure and devices emerge for
multilevel data handling. Two strategies exist.

First, there may be factors which allow the different classes
of data to be put on separate LANs. One situation which would allow
this is a natural geographic separation on the bases which already
exists or could be easily provided. Each net would then operate at
its own system high level, with encryption provided where it is
required by physical and personnel security. Another parameter
which would justify this strategy is traffic flow. Some bases may
have enough classified or privacy traffic to warrant a separate LAN
for it. If the amount of high level security traffic is sufficient,
a classified net could operate at that system high level.

The alternative plan calls for multiple Phase I type nets,

133-16

using frequency allocations and separate BIUs. The use of encryption should be made on a base by base basis.

The existence of these parallel communities of LANs will require gateways or guards to interconnect them. A number of companies are doing research and development in this area. The interconnection will provide redundancy, easier maintainability, and a greater chance for survivability. Mediation of data will also have to be provided for. The choice between these two methods depends on the characteristics of the particular base.

For overseas bases at least, there appears to be a dire need for LAN encryption devices. This is due to an increased unfriendly personnel threat, coupled with the fact that medium security is more difficult to guarantee. In the U.S., many bases are physically situated in areas where R.F. emanations from terminal equipment and connections becomes tantamount to broadcasting data to unfriendly but appreciative listeners. These sorely needed devices will emerge, hopefully within the coming years. NSA is currently preparing a timeframe for the development of LAN encryption devices. Phase III- In the event of rapid technological progress, the Phase II techniques may not need to be implemented. This depends on the development of the following Phase III alternatives.

The first initially consists of single, then multiple level Trusted Interface Units (TIUs) to provide security mediation. If single level devices emerge first, a separate interface will be required for each class of data. Multilevel TIUs would be preferred over variable TIUs, in that a central operator would not be required for a color change. The technical risk in implementation is low if the devices themselves are physically protected. Otherwise, the certification process would bring the risk to medium.

The second alternative, E3, may have to be implemented anyway depending on the physical and personnel security issues already mentioned. The certification not only of the process, but the key distribution techniques is a concern, as is the cost and complexity of such a system. If the given constraints of a base mandate encryption, there is no choice. Interfacing, as soon as possible, with the appropriate agencies becomes imperative.

Gateways or guards will be required in any case. In the case of the interconnection of LANs with incompatible packets sizes, a

133-17

gate may have to fragment packets. If these packets were block encrypted, they would have to be reassembled at the destination before decryption. This further points out the need for compatibility and planning.

Trusted operating systems would be required for multilevel data bases. The expense in developing these systems for each manufacturer's operating system may be prohibitive at worst, wasteful at best. Research and development in the area must be monitored.

The writer would like to reiterate a bias against a dependency on the traditional password techniques. The bias may have developed by watching too many hightech movies, but more likely from current events. Smart i.d. cards, which could be used to operate addressable wall taps as well as allow physical access, is an alternate suggestion.

Any LAN installed on an AF base must be designed for crisis/threat survivability, priority transmissions, and maintainability. Multiple interconnected LANs using E3 for physical security vice welded conduit and hardware "cast in concrete" address most of these factors.

It is hoped that the overall planning effort will proceed with all due speed. The installation of incompatible nets, without sufficient traffic capabilities for the future, only makes the final effort more difficult and expensive.

VI. RECOMMENDATIONS:

Given the spate of needs involved in establishing secure LANs and the dearth of presently available devices, it immediately becomes clear that a team effort is required. Several steps should be taken, keeping in mind that security is only one aspect of the Base Communications Architecture.

First, communications must be established with the groups and organizations that are doing the research and development in the fields of multilevel mediation devices and encryption, as well as the certifying agency.

Second, the resources of the Air Force must be integrated and directed towards the planning for secure LANs. Representation from ESD, AFCC MITRE (Basecomm and Bus Networking groups), the AFLANSPO, and the users groups is needed. The specific needs and acquisitions

of each group on each base must be monitored and influenced so as to insure the development of secure, compatible networks.

Lastly, but most important, it is hoped that a set of Air Force LAN standards is generated, which include security. Homogeneous network performance can be achieved only if uniform standards are applied.

References

Textbooks:

1. Rullo, Thomas A., _Advances in Computer Security Management, Volume I_, Philadelphia, Pa., Heyden and Son Inc., 1980.

2. Stallings, William, _Local Networks, An Introduction_, New York, New York, Macmillan Inc., 1984.

3. Tanenbaum, Andrew S., _Computer Networks_, Englewood Cliffs, New Jersey, Prentice Hall Inc., 1981.

4. Wofsey, Marvin M., _Advances in Computer Security Management, Volume II_, Chichester, England, Wiley Heyden Inc., 1983.

Papers:

5. Cheheyl, M.H., "Security Guards", MITRE WP-24472, October 1982.

6. Fam, Bahaa W., "A Survey of Internet Gateways", MTR 9111, September 1983.

7. Kent, Stephen T., "Security in Computer Networks", _Protocols and Techniques for Data Communications Networks_, Prentice Hall, 1981.

8. LaPadula, Leonard J., "DoDIIS LANs, Issues and Answers", M83 55, December 1983.

9. Marsden, Russ F., "An Overview of Five Operating System Security Kernels", MTR 9034, September 1984.

10. Neugent, William, "WIS ADP Security Implementation Analysis", MTR 83W00147, September 1983.

11. Shelton, James, S., "ASIMS Local Area Network Security Report", MTR 8862, January 1983.

12. Shirey, Robert W., "Computer Network Access Control", MTR 83W00154, November 1983.

13. Shirey, Robert W., "Security Architectures for Local Area Networks in Command Centers", MTR 83W0162, December 1983.

14. Shirey, Robert W., "Local Area Network Security", MITRE WP 82W00587, October 1982.

15. Shirey, Robert W., "Security Architectures for Local Area, Packet Switched Networks", MITRE WP 83W00288, March 1983.

16. Shirey, Robert W., "Security Architectures for Long Haul Packet Switching Networks", MTR 83W00163, December 1983.

17. Sidhu, Deepinder, "Design for Secure Local Area Network", MTR 8702, March 1982.

18. Van Slyke, Richard, "Internal Communciations for the Osan HTACC", RADC-TR-83-227, October, 1983.

1984 USAF-SCEEE GRADUATE STUDENT SUMMER SUPPORT PROGRAM

Sponsored by the

AIR FORCE OFFICE OF SCIENTIFIC RESEARCH

Conducted by the

SOUTHEASTERN CENTER FOR ELECTRICAL ENGINEERING EDUCATION

FINAL REPORT

CARDIOVASCULAR RESPONSES OF HIGH- AND LOW-FIT MEN TO HEAD-DOWN REST

FOLLOWED BY ORTHOSTASIS AND EXERCISE

Prepared by: Dr. William G. Squires

                                Debra K. Rotto

                                Diane M. Rotto

Academic Department: Physiology

University: Texas Lutheran College and Graduate

                                School of Biomedical Sciences, University

                                of Texas Health Science Center at San

                                Antonio

Research Location: Aerospace Physiology Laboratory, Biomedical

                                Division. Chemical Defense Branch

USAF Research Contact: Dr. Sarah Nunneley

SFRP Supervising

  Faculty Member: Dr. William G. Squires

Date: August 7, 1984

Contract No.:   7930-14-04

CARDIOVASCULAR RESPONSES OF HIGH- AND LOW-FIT MEN TO HEAD-DOWN REST

FOLLOWED BY ORTHOSTASIS AND EXERCISE

by

Debra K. Rotto

Diane M. Rotto

William G. Squires

ABSTRACT

Head-down rest (HDR), a ground-based simulation of weightlessness, minimizes the hydrostatic intra- and extravascular pressure gradients that are normally present in the upright position causing a headward fluid shift. As a result, adaptive changes in other body systems occur producing signs of orthostatic intolerance upon reexposure to normal gravitational forces. These adaptive changes seem to differ between the levels of aerobic fitness. With this in mind, a preliminary study was conducted in which a similar protocol to this human study was followed except dog models were used. However, the dogs were instrumented acutely and thus were under the influences of anesthesia and positive pressure ventilation so this must be taken into account when considering the results. The results indicate that a difference does exist between trained and untrained dogs in response to head-down rest (HDR). In view of the different parameters measured and the data collected, the trained dogs responded with a lesser degree of variation. In other works, the trained dogs displayed a more stable system enabling them to better contend with any perturbation they might encounter. The trained dogs seemed to be able to compensate physiologically for the disturbances they confronted, thus minimizing the physiological stress and maximizing the homeostatic state. On the other hand, the untrained dogs lacked this physiological stability causing a pronounced response to the HDR. Consequently, the training effect seems to allow one to respond to change (HDR or weightlessness) with minimal physiological stress. However, this may be detrimental to orthostatc tolerance. It becomes important then to take into account the aerobic fitness of an individual when dealing with the weightless environment.

I. INTRODUCTION:

The major focus of the experiment will be to compare responses to zero gravity and orthostatic tolerance post-tilt between individuals with different fitness levels. Understanding the mechanisms involved requires elucidation of changes in plasma renin-angiotensin levels, plasma catecholamine levels, body fluid shifts, and segmental volume changes. As a result, further significance could be drawn from this study regarding the use of the head-down tilt method as a means of pre-flight preparation for the pilot.

During normal erect posture most blood volume is usually maintained below the level of the heart. Under zero gravity or head-down rest there is a headward shift of body fluids from the lower portions of the body. Therefore, blood tends to pool in the thoracic cavity. This massive fluid shift induces adaptive changes in other body systems. These changes are referred to in Figure 1 below.
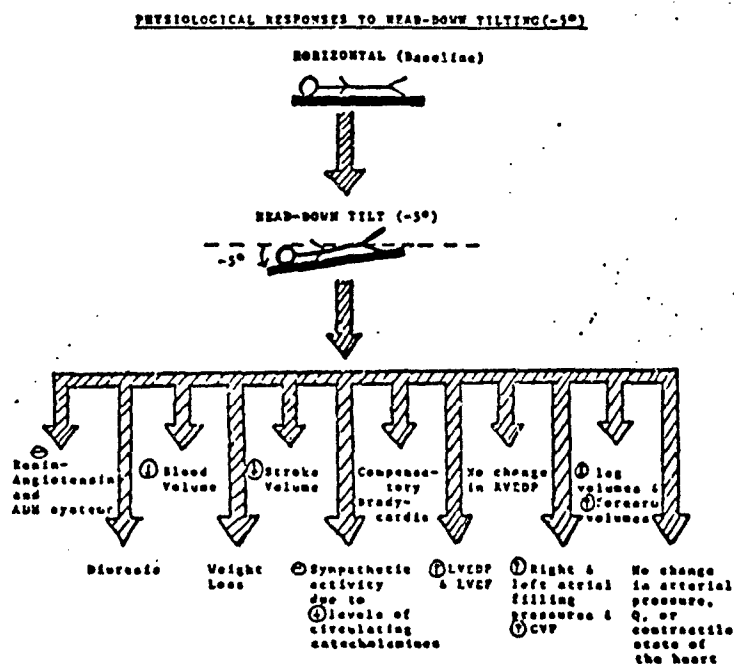

FIGURE 1

134-3

Due to the ambitious nature of this project, time limitations and necessary approval of th.' rotocol from the Surgeon General's Committee, this study was not carrie. out this summer, but will be done sometime in the future under the sponsorship of the Air Force Office of Scientific Research. However, a study similar to the one outlined here using trained and untrained dogs instead of human subjects as the experimental models was conducted during the fall and winter of 1983 and the spring of 1984 under an AFOSR mini-grant. The results from this experiment are discussed in another section of this report.What follows is the proposed protocol for this experiment.

II. OBJECTIVES:

The objectives of this experiment are to determine if individuals of different working capacities respond differently to head-down rest and to elucidate the time course of volume changes in the right and left heart, so that a correlation between these changes with other biochemical and physiological changes may be made. In this way a clearer understanding of the mechanisms involved with volume regulation might be brought forth.

III. PROCEDURES:

A.) HUMAN STUDY

1.) Data Collection: During the week before the experiment the subject will visit the laboratory for familiarization with all equipment and procedures. He will perform an orthostatic tolerance test and a maximal exercise stress test (bicycle ergometer) in the afternoon at about the same time as the post-HDR test. On the day of the experiment, the subject will report to the laboratory at 0730 and will be instrumented with electrodes for ECG and IPG, venous canula, BP cuff and echo probe. He will then rest in the horizontal and head-down positions until 1430, following which he will undergo orthostatic tolerance and maximal exercise stress tests, as before. He should be finished at 1500.

2.) Conditions: All observations will be made at an ambient temperature of 18 to 22 degrees C. During the resting portions of the experiment, every effort will be made to eliminate sudden noise, bright light, and other vasoactive stimuli.

3.) Blood Volume and Fluid Balance: The subject will be weighed nude to an accuracy of 10 g before and after the experiment, and all intervening intake and output will be measured. His blood volume will be determined by the carboxyhemoglobin method at the beginning of horizontal rest: The level of COHb involved is far below the clinically significant value. Shifts in plasma volume will be estimated using Hct and Hb.

4.) Heart Rate: All subjects will be instrumented with a standard ECG for monitoring heart rate and rhythm.

5.) Blood Pressure: Brachial systolic and diastolic pressures will be taken with a conventional manometric system during each test sequence.

6.) Segmental Fluid Shifts: Measurement of segmental fluid shifts will employ impedence plethysmography, a technique based on changes in the electrical properties of tissue, with changes in fluid content. Data will be collected for six body segments: The upper and lower extremities will each be divided into proximal and distal segments and the torso will be divided into splanchnic and thoracic segments. This configuration requires a total of nine standard ECG electrodes on each subject. This electrical impedence measurement is a clinically approved, non-occlusive method that may be used to obtain the data required for this experiment.(3)

7.) Echocardiography: Echocardiographs will be obtained using a series ultrasonoscope with its transducer placed in the third, fourth. or fifth intercostal space, depending on the size of the subject. Endocardial echoes of the left side of the interventricular septum and the posterior left ventricular wall will be identified as suggested by Popp et al. (4). Left ventricular volumes and stroke volumes will be calculated according to the method of Teichholz et al. (5).

8.) Blood Analysis: Blood will be drawn through a venous cannula with heparin lock. Carbon monoxide determination of blood volume involves inhalation of a tiny, safe dose of CO and taking of two 7-ml blood samples. Every fifteen minutes the first two hours and every hour thereafter, 8-10 ml of blood will be drawn from an arm vein for determination of HCT, hemoglobin, sodium and potassium, catecholamines, plasma renin activity, plasma aldosterone and plasma antidiuretic hormone. The volume of blood withdrawn will be replaced with an equal volume of plasma substitute. The Hct, Hb, Na+ and K+ will be determined by conventional methods. Plasma renin activity, catecholamines, aldosterone and ADH will be measured by radioimmuno-assay methods (1,2).

9.) Urine Analysis: Urine will be analyzed for Na+ and K+ using flame photometry.

TIMELINE

ONE WEEK PRIOR: Record physical measurements:
Weight and height (nude)
Body composition determination by
underwater weighing
Orthostatic (standing) tolerance test
Max exercise stress test on bicycle ergometer
(Balke protocol)

TIME	ACTIVITY
0730-0900	Report to the laboratory; weighing, briefing and instrumentation with electrodes, venous line, blood pressure cuff, and echocardiogram.
0900-1000	Horizontal rest (0 degrees). Blood volume measurement. Data collection every fifteen minutes (ECG, IPG, blood pressure, and blood sample). Urine collected as necessary and at 1000.
1000-1400	Head-down rest (-6 degrees). Data collected every 15 minutes during the first hour and hourly thereafter. Light lunch(soup through a straw, 1200-1300). Urine collected as necessary, bladder emptied at 1400.
1400-1415	Horizontal rest.
1415-1430	Horizontal measurements.
1430-1530	Orthostasis and maximal exercise stress test on bicycle ergometer.
1530-1600	Debriefing and dismissal.

134-6

B.) DOG STUDY: Six healthy mongrel dogs (15-25 kg) were used
as experimental animals. The animals were anesthetized with thiamyl-
sodium (4ml/5 lb i.v.) followed by a chloralose/urethane (15 ml/5 lb
i.v.) and ventilated under positive pressure through a cuffed
endotracheal tube with a standard volume animal respirator (Havard
Apparatus, Waltham. MA). The animal was positioned on the right side
and an incision made on the left hindleg to expose the saphenous vein
into which a catheter was inserted. The catheter was connected to a
3-way stop-cock so that drugs could be administered and venous blood
samples withdrawn. The dog was then placed on his left side and a
small neck incision was made. The right common carotid was exposed and
a pulsed Doppler flow probe tied into place. Careful attention was
paid to assure normal carotid artery flow velocity with no constriction.
The pulsed Doppler flow probe was calibrated in terms of Doppler
frequency shift. A baseline zero can be established and a linear
relationship between flow and frequency shift has been established in
vivo (6). A Doppler flow probe was also placed on the iliac
artery under direct vision. Precaution was taken to prevent arterial
constriction. The dog was again positioned on the right side and a
left flank incision made through which the left renal artery was
identified and encircled with a pulsed Doppler flow probe. As with
the other flow probes, careful attention was taken to avoid constriction
of the artery. A catheter was inserted into the dog's urinary bladder
in order to measure urine output. A catheter was inserted into the
left femoral artery and threaded up into the aorta for measurement of
the systemic arterial pressure (Statham p230 Db pressure transducer).
Central venous pressure (CVP) was obtained by inserting a catheter into
the jugular vein and attaching it to a Statham p230 Db pressure
transducer.
Electrocardiographic (ECG) lead AVF was established through needle
leads in all four limbs. Next, a left thoracotomy was performed
through the fifth intercostal space and the heart was suspended in
a pericardial cradle. With the aid of a purse string suture, a solid
state pressure transducer (Koingsberg P-7, Pasadena, CA) was inserted
through a stab wound into the left ventricular apex. A Koingsberg
pressure transducer was also inserted through a stab wound into the
right atrium.
     The instrumentation allowed for measurement of left ventricular
pressure (LVP), right atrial pressure (RAP), left ventricular end
diastolic pressure (LVEDP), systemic arterial systolic pressure (SP),
and diastolic pressure (DP), central venous pressure (CVP), heart
rate (HR), renal. carotid and iliac artery blood flow (RF,CF,IF),
urine output, and calculation of the first derivation of left vent-
ricular pressure (LV dP/dt). Recordings were made on an eight
channel recorder (Gould brush mark 200).
     Following instrumentation, control baseline measurements were
made for 5 minutes of LVP, RAP, LVEDP, SP, DP, CVP, HR, RF, CF, IF
while LV dP/dt and mean arterial were calculated. A 5 ml sample
of blood was drawn from the catheter in the saphenous vein for
measurement of catecholamines (norepinephrine, epinephrine), plasma
renin and aldostrone After initial measurements were taken, the dog
was tilted to a 6 degree declination. Measurements were taken every
15 minutes for two hours, then the dog was tilted back to horizontal
position. After the last measurements were made, the flow probes
were calibrated in vivo, then the dog was euthanized with a saturated

solution of KCL.

IV. RESULTS: What we can conclude from this study is that when
head-down tilt is used as a model to simulate weightlessness, the
aerobic fitness of the subjects has to be taken into consideration.
We found significant differences between the two groups of trained
and untrained (cage-confined) dogs in CVP, arterial pressure, LVP,
contractility of the heart (as measured by the first derivitive of
change in pressure over change in time) and RF, CF, and IF. It seems
that the cardiovascular system in the trained dogs was more stable
and less susceptible to the perturbations introduced by head-down
tilt while the untrained dogs showed much more variation and changes
of greater magnitude in the cardiovascular parameters measured.

V. RECOMMENDATIONS: Despite the many studies on man's adaptation
to simulated zero gravity, no conclusive evidence exists as to the
effect of physical fitness on this response to zero gravity. Although
objective comparisons of athletes and non-athletes give variable
results, it has been suggested that the more physically fit person
(high VO2) is less tolerant to orthostatic stress when volume depleted
as a result of diuresis during head-down rest. This loss of blood
volume is analogous to heat-related volume loss.
     The investigators in this study would eventually like to find
out if, in fact, there are relative physiological and biochemical
changes between trained and untrained subjects, dog and human,
and if so, to what degree these parameters vary when the subjects
go from the horizontal position to a 6 degree head-down position.
Understanding the mechanisms involved requires elucidation of
changes in plasma renin-angiotensin levels, plasma catecholamine
levels and body fluid shifts. As a result, further significance
could be drawn from this study regarding the use of the head-down
tilt method as a means of pre-flight preparation for the pilot.
     Studies have shown that increased activity of the carotid sinus
nerve due to hypervolemia or manual stimulation with electrodes
results in a reflex decrease in the force of atrial systole by a
decrease in sympathetic activity to the heart. A suggestion for
follow-up research would be to isolate the carotid sinus nerve in
an animal model. A small neck incision could be made to expose the
left internal carotid artery at its origin where there is a bulbous
enlargement, the carotid sinus, which is about 3 mm in diameter and
4 mm in length It contains an afferent fiber called either the
carotid sinus nerve or the Hering nerve which is a branch of the
glossopharyngeal nerve (IX). A microelectrode could then be placed
on the carotid sinus nerve to measure its electrical activity.
Then one could determine if it was stimulation of the carotid sinus
nerve or the reduction in circulating catecholamines that decreases
sympathetic activity to the heart resulting in an attenuation of the
force of atrial systole.

Mean "CVP" Values — Trained vs Untrained Dogs
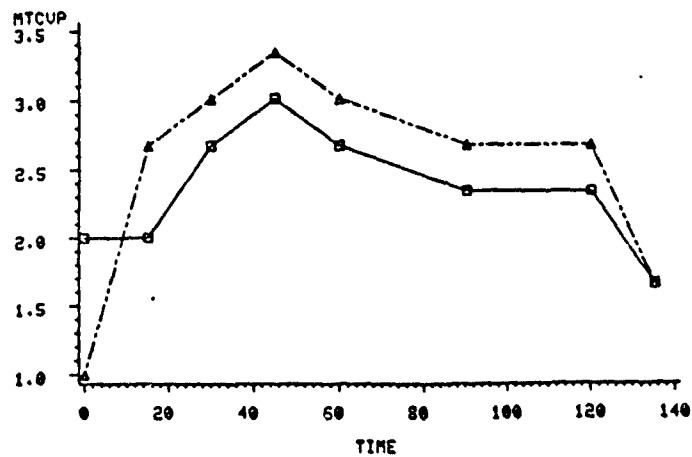
Mean values for Trained dogs are represented by solid line —
Untrained dogs by broken line

FIGURE 2 - Central Venous Pressure

Mean "A" Values — Trained vs Untrained Dogs

Mean values for Trained dogs are represented by solid line —
Untrained dogs by broken line

FIGURE 3 - Mean Arterial Pressure

134-9

Mean "AS" Values -- Trained vs Untrained Dogs

Mean values for Trained dogs are represented by solid line --
Untrained dogs by broken line

FIGURE 4 - Arterial Systolic

Mean "AD" Values — Trained vs Untrained Dogs

Mean values for Trained dogs are represented by solid line --
Untrained dogs by broken line
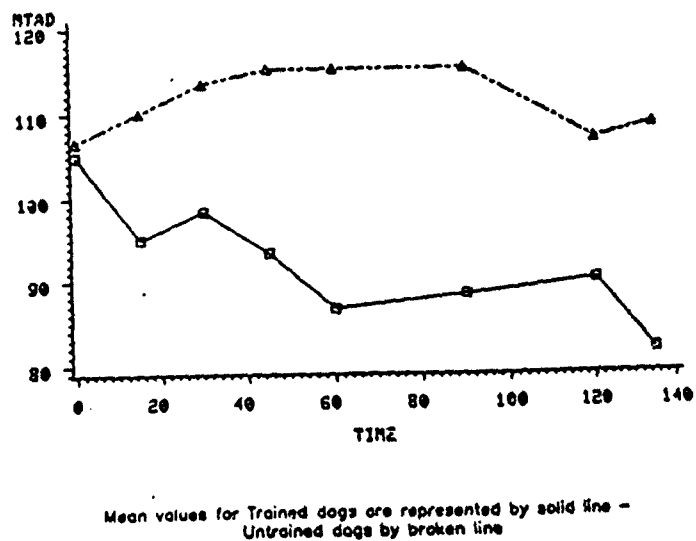
FIGURE 5 - Arterial Diastolic

134-10

Mean "LVP" Values — Trained vs Untrained Dogs

Mean values for Trained dogs are represented by solid line —
Untrained dogs by broken line
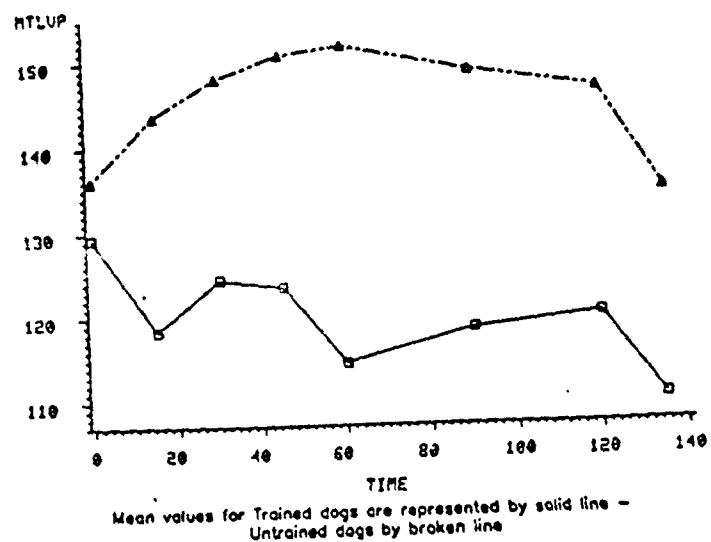
FIGURE 6 - Left Ventricular Pressure

Mean "Pdpdt" Values — Trained vs Untrained Dogs

Mean values for Trained dogs are represented by solid line —
Untrained dogs by broken line
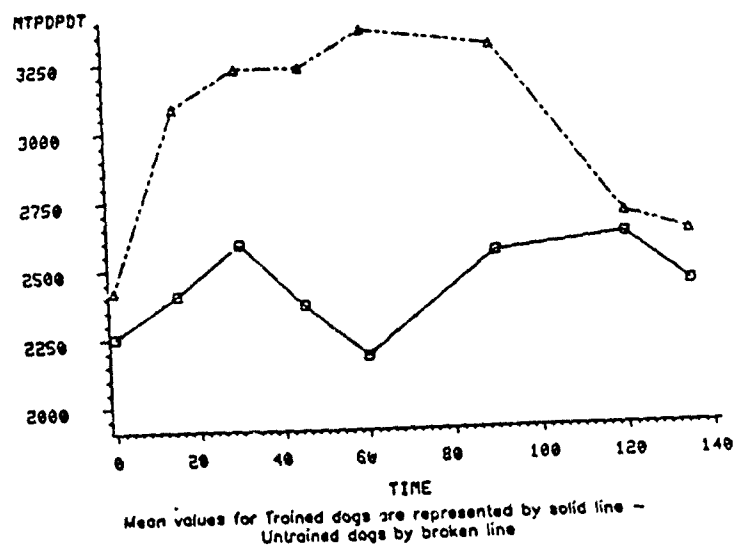
FIGURE 7 - Positive dp/dt

134-11

Mean "CF" Values — Trained vs Untrained Dogs

Mean values for Trained dogs are represented by solid line —
Untrained dogs by broken line
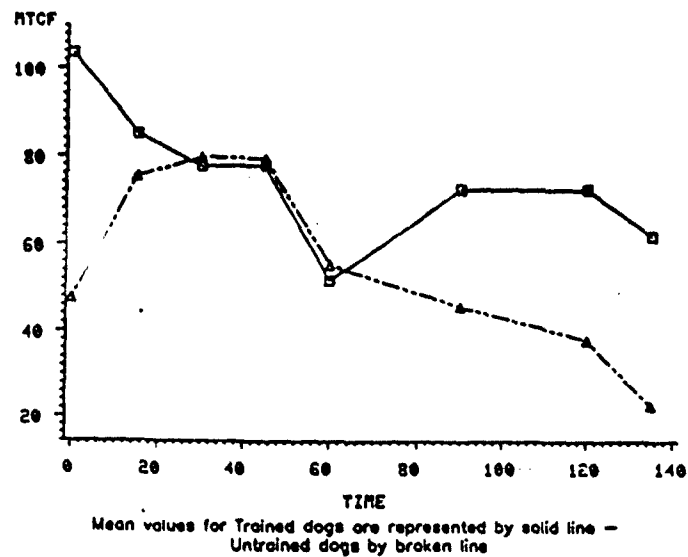
FIGURE 8 - Carotid Flow

Mean "RF" Values — Trained vs Untrained Dogs

Mean values for Trained dogs are represented by solid line —
Untrained dogs by broken line
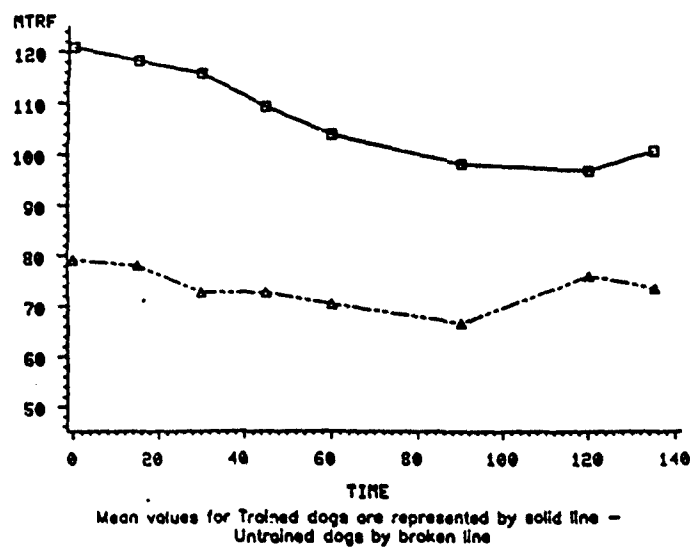
FIGURE 9 - Renal Flow
134-12

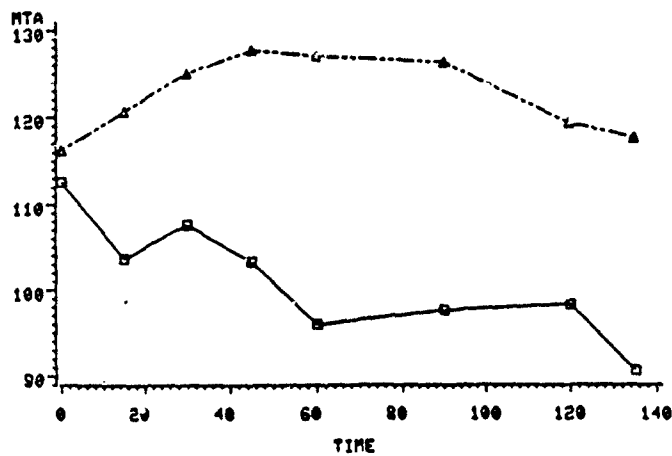## Mean "IF" Values -- Trained vs Untrained Dogs

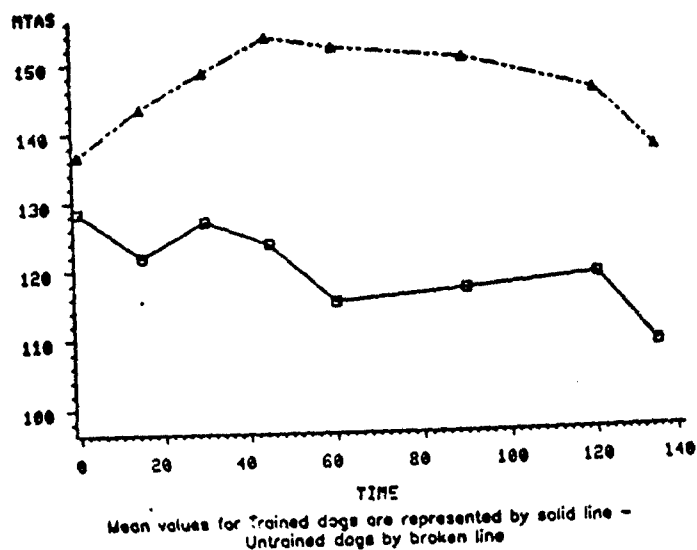Mean values for Trained dogs are represented by solid line --
Untrained dogs by broken line
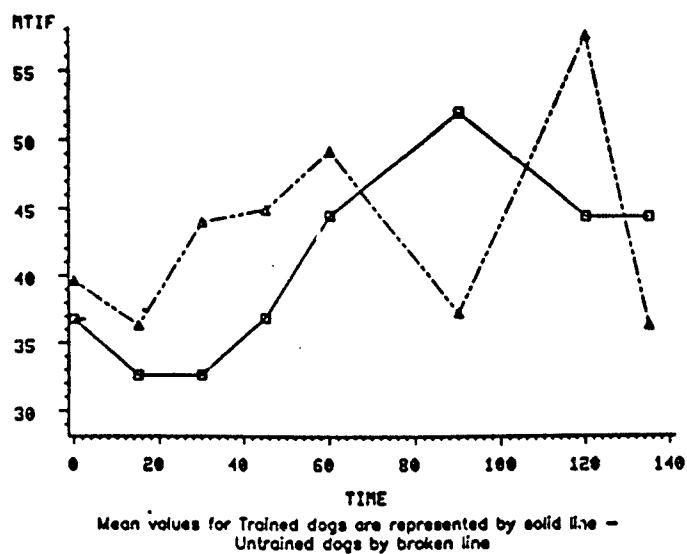
FIGURE 10 - Iliac Flow

REFERENCES

1.) Gomez-Sanchez, C., D.C. Kim, N.M. Kaplan, "A radioimmuno-
assay for plasma aldosterone by immunologic purification,"
J. Clin. Endocrin. Metab. Vol. 36, pp. 795-798, 1973.

2.) Haber, E., T. Koerner, L.B. Page, B. Klenian, A. Purnode,
"Application of a radioimmunoassay for angiotensin I to the
physiological measurements of plasma renin activity in normal
human subjects," J. Clin. Endocrin. Metab. Vol. 29, pp. 1349-
1355, 1969.

3.) Nyboer, J., Electrical Impedence Plethysmography, Second edition,
Springfield, Illinois, Charles C. Thomas, 1979.

4.) Popp, R.L., S.B. Wolfe, R. Hirata, H. Feigenbaum,"Estimation
of right and left ventricular size ultrasound," Am. J. Cardiol.
Vol. 24, pp. 523, 1969.

5.) Teichholz, L.E., T. Kreulen, M.V. Herman, R. Gorlin,"Problems
in echocardiographic volume determinations: echocardiographic-
angiographic correlations in the presence or absence of asynergy,"
Am. J. Cardio. Vol. 37, pp. 7, 1976.

6.) Hartley, C.J., H.G. Hanley, R.M. Lewis, F.S. Cole,"Synchronized
pulsed Doppler blood flow and ultrasonic dimension measurement
in concious dogs," Ultrasound in Med. and Biol. pp.99-110, 1978.

ACKNOWLEDGEMENT

1984 USAF-SCEEE SUMMER FACULTY RESEARCH PROGRAM

sponsored by the

AIR FORCE OFFICE OF SCIENTIFIC RESEARCH

conducted by the

SOUTHEASTERN CENTER FOR ELECTRICAL ENGINEERING EDUCATION

FINAL REPORT

RECOMMENDATIONS ON COMBUSTION RESEARCH AT

TYNDALL AIR FORCE BASE, FLORIDA

Prepared by: Dr. Arthur M. Sterling

Academic Rank: Professor

Department and   Department of Chemical Engineering
University: Louisiana State University

Research Location: Engineering and Services Center
                            Tyndall Air Force Base, FL

USAF Research: Capt. Paul Kerch

Date: September 25, 1984

Contract No: F49620-82-C-0035

RECOMMENDATIONS ON COMBUSTION RESEARCH AT TYNDALL AIR FORCE BASE, FLORIDA

by

Dr. Arthur M. Sterling

ABSTRACT

With a view toward long-term research objectives, the current program on soot-abatement research being supported by the Environics Division of the Engineering and Services Center at Tyndall Air Force Base has been reviewed. It is argued that the environmental consequences of soot emission from aircraft engines for Air Force operations warrent an expanded research program, and recommendations on the objectives, the direction, and the scope of an expanded program are given.

ACKNOWLEDGMENT

The author would like to thank the Air Force Systems Command, the Air Force Office of Scientific Research and the Southeastern Center for Electrical Engineering Education for the opportunity to work with the Engineering and Services Center at Tyndall Air Force Base, Florida. The efforts extended by Colonel Boyer and Major Brocato made the experience personally as well as professionally rewarding.

The staff of the Environics Division was extremely helpful and cooperative, and the resources and support provided by Lieutenant Colonel Fulford and Major Padgett were greatly appreciated. In particular, special thanks are due Captain Paul Kerch for the enormous time and effort he extended on my behalf.

I. INTRODUCTION

The Environics Division of the Engineering and Services Center at Tyndall Air Force Base, Florida, is responsible for dealing with environmental problems associated with Air Force operations. Included in these problems are the adverse consequences of soot formation in gas-turbine combustors.

Several factors tend to reduce the effectiveness of the research on soot formation conducted and supported by the Environics Division. But the most important factor is the absence of a long-range research plan to provide direction and continuity of effort. The main objective of this work was to formulate such a plan.

Determining the status and direction of relevant research in the field was the most time-consuming phase of this assignment. This involved an extensive review of reports, technical articles, and similar documents. The opportunity to meet with current contractors, and to attend the AFOSR/ONR Contractors Meeting on Airbreathing Combustion Research was generously provided. The Twentieth Symposium (International) on Combustion, attended separately from this assignment, also provided substantial background.

The concepts and philosophy of combustion research that were culled from this review are presented in this report instead of a conventional literature view. The intent is to focus attention on appropriate research strategies rather than on the minutia of individual research programs.

After a statement of the goals and objectives of this work, the practical environmental problems of soot emission are identified. The fundamental problem, and strategies to deal with the fundamental problem are then discussed. These discussions provide the basis for a review of current soot-abatement research at Tyndall and a recommended plan for future research. Finally, suggestions for follow-on research are given.

II. GOALS AND OBJECTIVES

The goal of this work was to improve the effectiveness of the research conducted and supported by the Environics Division of the Air Force Engineering and Service Center at Tyndall Air Force Base.

The specific objectives were to:

1. Specify the current and anticipated practical environmental problems associated with soot formation in gas-turbine combustors.

2. Identify the fundamental physical phenomena underlying these problems and relate these phenomena to similar practical environmental problems that must be dealt with by the Environics Division.

3. Review the current and anticipated research efforts of the Environmental Sciences Branch with respect to these problems.

4. Survey, through available literature and personal contacts, related research efforts in other military, governmental, industrial, and university laboratories.

5. Formulate a comprehensive plan for soot-abatement research that will help to eliminate duplication of research efforts, improve technology transfer, and optimize research efforts and expenditures.

III. GLOBAL PROBLEM

Soot formation in gas-turbine combustors is of increasing concern to the U.S. Air Force. Traditionally, combustor design has focussed on achieving maximum power and reliable performance at all operating speeds and altitudes; the sooting tendency of these combustors was accepted as an undesirable, but tolerable, characteristic. This is no longer the case -- Air Force operations are now hindered by soot emission from aircraft engines. Furthermore, as fuel specifications are broadened to allow higher aromatic content, and as new engines (designed to operate at higher compression ratios) are developed, the propensity for sooting will increase.

From the viewpoint of jet engine design and maintenance, soot formation is undesirable because it limits operating temperatures and decreases engine lifetime. At combustion temperatures, soot provides a source for radiative heat transfer to the combustor liner. This effect can lead to structural damage or failure. Also, when soot impacts on combustor surfaces, such as turbine blades, it may deposit on or erode these surfaces causing failure or severe maintenance problems.

The emission of soot from jet engines is also undesirable for both tactical and environmental reasons. Soot increases plume visibility and thus reduces the tactical effectiveness of aircraft. But it is the environmental consequences of soot emission that are critical. The real or perceived reduction in air quality during routine aircraft training and readiness operations is impeding these missions. For example, engine test cell operations in California have been severely curtailed because of a failure to meet EPA standards for particulate emissions.

The involvement of the Engineering and Service Center at Tyndall Air Force Base with the sooting problem follows from the environmental concerns. Specifically, the Environmental Sciences Branch of the Environics Division is responsible for dealing with soot emission from jet aircraft engines. Although it is generally recognized that the ultimate solution to soot formation lies in improved engine design, the cost of retrofitting existing engines with design modifications is prohibitive. Thus the effort of the Environmental Sciences Branch has been directed toward fuel additives. What is needed is a plan to focus and coordinate this effort.

135-6

IV. FUNDAMENTAL PROBLEM

A. OVERVIEW

The mechanisms of soot formation are deeply embedded in the complex process of combustion, a process that involves very rapid chemical reactions and high rates of physical transport at elevated temperatures. Although combustion science has not yet developed the comprehensive understanding needed to solve the problem of sooting in combustors, its fundamental, axiomatic approach is beginning to develop fragments of the picture, and the direction of future research is being focussed.

Some general combustion conditions that lead to soot formation are well known. For example, it is known that rich fuel mixtures and low combustion temperatures promote sooting. It is also known that an increase in fuel aromatic content and an elevation of pressure (conditions anticipated for future aircraft engines) increase soot yield. This information has been used to correlate empirically the effect of variations of fuel properties on the durability and performance of a given combustor.

It is a much more difficult task, however, to predict how the performance of a given fuel, or the effects of changes in fuel properties, will vary from one combustor to another. Because of the complexity of the underlying phenorena, empirical methods will have little value. Rather, a comprehensive understanding of the mechanisms of soot formation will be required.

It is the second, more difficult task that must be addressed if the global problem of soot emission is to be solved. Thus the effort of the Environics Division should be directed toward elucidating the basic mechanisms of soot formation, with a strong focus on the effect of fuel additives. Although there have been numerous empirical studies of the effect of fuel additives on full scale combustors, i.e. the first task discussed above, the effect of fuel additives on basic mechanisms has received relatively little attention. But combustion science has developed to the stage where fundamental studies are now feasible, and support of these fundamental studies by the Air Force will provide the information necessary to deal with the global problem of soot emission.

B. MECHANISMS FOR SOOT FORMATION

The prevailing concept for the mechanisms of soot formation can be summarized by a pathway of series and parallel rate processes as shown below.

FUEL AND OXYGEN
↓
PYROLYSIS (SOOT PRECURSORS)
(Chemical)
↓
NUCLEATION
(Chemical and Physical)

SURFACE GROWTH (Chemical) ↗ ↘ COAGULATION (Physical)
↘ ↗
SOOT
↙ ↘
BURNOUT (Chemical)   EMISSION (Physical)
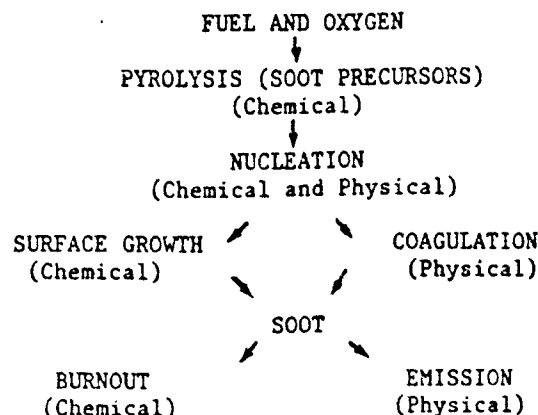
Although this concept is quite simple, the details along the pathway are extremely complex. Each of the rate processes are strongly coupled to the local temperature, pressure, and species concentration, which in turn are coupled to the local rates of heat and mass transport (i.e. aerodynamics and radiation). The process is further complicated by the very large number of chemical species that take part in an even larger number of chemical reactions.

The difficulty of predicting the effect of a fuel additive on soot formation is evident when one recognizes that the added species may have an effect at each stage in this pathway, and the effect may be to either promote or supress the rate process, depending on local conditions. It should not be surprising, therefore, that a given additive may supress soot formation in one type of combustor (or flame) while it may promote soot formation in another.

To understand the processes of soot formation one needs to understand the processes of combustion, and an elucidation of these processes will provide an understanding of the formation and emission of other chemical species. The implications are clear. A comprehensive program on soot formation in combustors will provide the knowledge to deal with the environmental consequences of related combustion processes, such as hazardous waste incineration, and will have comprehensive application to a variety of environmental problems faced by the Air Force.

C.   DIRECTIONS OF CURRENT COMBUSTION RESEARCH

Despite the complexity of the combustion process, modern laboratory and computation techniques have made possible a progressively better understanding of its basic subunits -- flames. Intensive research is underway on shock flames, pre-mixed flames, laminar diffusion flames, turbulent diffusion flames, and spray flames. Each successive flame in the above list adds one or more complicating factor.

For example, the simplest flame (from a mechanistic viewpoint) is developed in a shock tube, where a shock wave rapidly compresses and heats a dilute fuel mixture to a precise and predetermined pressure and temperature. Because the fuel is dilute, the ensuing chemical reactions do not alter the reaction temperature over the period of observation. Furthermore, the reacting mixture is uniform and therefore unaffected by transport processes. Thus the chemical reactions are decoupled from other mechanisms, and they can be studied in detail to provide important kinetic data in the early stages of fuel pyrolysis and soot formation.

A more common flame, the pre-mixed flame, is relatively well understood. When fuel and oxygen are combined and mixed before burning, the need for diffusional transport of the reactants is eliminated. But there are significant variations in temperature, concentration, and velocity in the direction of gas flow. Thus the chemical reactions become coupled with the temperature, and the ignition, propagation, and extinction of the flame are dominated by the chemical kinetics and the prevailing temperature field, which in turn depends on reaction rates, heat-release, and heat conduction and radiation. Despite the increased complexity, accurate models for the kinetics of pre-mixed flames with simple fuels, such as methane, are now available.

Our understanding of more complex flames is less complete. In a laminar diffusion flame, the flame of a candle for example, oxygen and fuel must be brought into contact by molecular and convective diffusion. This requirement leads to fuel-rich regions of the flame, a condition well known to promote the formation of soot, which gives the flame its luminescence. Furthermore, the coupling of chemical kinetics with convective and molecular transport make the analytical modeling of laminar diffusion flames much more difficult. Nevertheless, laminar diffusion flames provide a well-controlled experimental model by which

fundamental combustion mechanisms and the effects of alterations in flame conditions on combustion products can be studied.

Turbulent diffusion flames are one step closer to practical fires. Because turbulence enhances the mixing of fuel and oxygen, combustion is more efficient. The interpretation of laboratory data on turbulent diffusion flames, however, is more difficult because of our inability to model turbulence accurately. Empirical eddy-diffusion models, which are adequate to describe flows like those in boundary layers, are inadequate to describe complex turbulent reacting flows. Although the modeling of turbulent reacting flows is a current area of intense theoretical research, models sufficiently detailed for a mechanistic interpretation of data from turbulent diffusion flame seem remote. Thus investigations of turbulent diffusion flames, in the near future will be limited to phenomenological descriptions and empirical results. Nevertheless, such studies are extremely important because they serve as a bridge between simpler laboratory flames and practical combustors, and they provide experimental observations against which models of turbulent reacting flows can be tested.

A still more complicated laboratory model, and one characteristic of many practical combustors including gas turbine engines, is a spray flame. When liquid fuel droplets are injected into a turbulent flame, they must be heated and the fuel vaporized before it can burn. Thus two additional physical processes must be accounted for, and these processes are strongly coupled to the velocity and temperature fields. At present, only the global features of spray flames are known. The detailed combustion mechanisms that determine combustion efficiency, soot formation, and the like are still to be elucidated. Ultimately, the improved design of fuel injection nozzles and gas turbine combustors will depend on how well we understand these details.

To develop a predictive capability for the effect of fuel additives in gas turbine combustors, we need to develop a firm understanding of additive effects in flames -- from the very simplest to the most complex. These studies must build one upon the other, and they must be closely coordinated. Shock tube studies can separate out the temperature and concentration effects from the aerodynamics. Studies with pre-mixed flames can reveal the effects of one-dimensional

temperature and concentration fields. Diffusion flames can provide information of the effects of the relative rates of chemical reaction and mass and heat transport, and the like. Although there is no lack of interest or effort in flame research, there is a surprising and unfortunate lack of coordination and interaction.

D. IMPLICATIONS FOR RESEARCH PLANNING

What approaches can be taken to develop the comprehensive understanding needed to solve the problem of soot formation in combustors? Let's consider two extremes.

One could, for example, initiate programs in say ten different laboratories to study the sooting behavior of ten different fuel-additive systems in pre-mixed flames. Such a program would have a uniformity of approach, and upon collecting and analyzing the results of these studies, one might develop a good understanding of fuel additive effects in pre-mixed flames. But one could not predict from these results the effect of the additives in any given combustor.

In contrast, one could establish a large research team in a single, well-equipped laboratory. Experimental measurements with shock tubes, pre-mixed flames, laminar diffusion flames, turbulent diffusion flames and spray flames could be carried out on identical fuel-additive systems. The hypothesis of soot formation developed and tested for each experimental system could be continuously tested against comparable hypotheses developed for the other experimental systems in order to develop a global hypothesis valid for all systems. In other words, the study would be designed not for uniformity of approach but for convergence to the solution. As with any study of such breadth, the keys to convergence would be the continual coordination of, and interaction between, various parts of the study.

A third and more practical intermediate approach would be to establish programs in different centers, each center studying soot formation in a different type flame, but each using the same fuel-additive systems. Clearly, the coordination and interaction needed for a successful solution would be more difficult, but the program would provide convergence. The key would be for the coordinating center to be actively involved in at least one part of the experimental program.

The third, intermediate approach seems suitable as a model for the Environics Division to use in planning future research: there is a niche in current combustion research for fuel additive effects on soot formation; this research is relevant to the environmental problem; and a substantial portion of a broad-based experimental program is already in place. What is left to develop is an extension of the experimental program to other flames and a means to provide the coordination.

V. STATUS OF COMBUSTION RESEARCH AT TYNDALL AFB

The past combustion research supported by the Environics Division of the Engineering and Services Center at Tyndall Air Force Base has been concerned with additive effects on soot formation. This effort has been underway for approximately six years. In 1978, the Engineering and Services Center requested a review of soot control by fuel additives that was undertaken by Professor J.B. Howard and Professor W.J. Kausch, Jr. at MIT. The major conclusion was that metal additives, particularly those of Mn, Fe, and Ba, can reduce the soot content in the exhaust of practical flames. It was noted, however, that the understanding of the role of additives was qualitative, and it was recommended that the mechanisms of additive action be investigated in well-controlled laboratory flames. In 1979, a contract was initiated with Professor G.S. Samuelson at the University of California, Irvine, to develop methods by which additive effects on soot formation in a laboratory scale combustor could be studied (see below). As part of this contract, a laboratory scale combustor and a laser diagnostic system for particle size measurements were constructed and installed at Tyndall. Also in 1979, a study was initiated at the Mobile Energy Division of Southwest Research Institute, under the direction of D.W. Naeyeli, G.E. Fodor, and C.D. Moses, to investigate the use of fuel microemulsions for soot reduction. Tests were run in a T-63 combustor. The major conclusions were that fuel-alcohol emulsions reduced soot formation, and that when ferrocene was added to the emulsion, its effect was to catalyze the oxidation of soot rather than to suppress its formation.

In-house research on sooting was carried out at Tyndall from 1980 through 1982. This work involved developing techniques for collecting combustion aerosols with an isokinetic probe and analyzing the samples with an electrical aerosol analyzer. Measurements were made on the laboratory-scale combustor. Since that time, the combustor has been modified and the laser-based particle size analyzer has been installed, but few systematic studies have been carried out by Tyndall personnel.

The current involvement of the Environics Branch with combustion research (soot formation in particular) is exclusively through contracts. Three research programs are currently being supported. Two

of these are research contracts, one dealing with measurements on laminar diffusion flames, the other with highly turbulent recirculating flames. The third is a task-order contract dealing with specific problems in the Tyndall combustion laboratory.

A brief overview of the goals and status of these contracts is given below. This is followed by an evaluation of the status and potential of the Tyndall combustion laboratory.

A. CURRENT CONTRACT RESEARCH

1. Laminar Diffusion Flames

Studies on laminar diffusion flames are being carried out by Dr. Paul Bonczyk at United Technology Research Center, East Hartford, Connecticut. The objective is to clarify the mechanisms responsible for fuel-additive suppression of soot.

Laser diagnostics (Mie scattering, extinction, laser-induced fluorescence, and coherent anti-Stokes Raman spectroscopy) will be used to provide in-situ and spatially precise measurements of soot particle size, species concentrations, additive chemical status, and temperature throughout the flame zone. These data will provide the basis for a coherent, quantitative explanation of the action of organic and inorganic compounds of Ba, Fe, K, and Mn on soot formation and burnout.

Although this program is well-conceived, and is being conducted in a setting with access to expertise in related areas (especially laser diagnostics), it would benefit greatly from access to kinetic data obtained independently for the same system of fuels and additives. Thus the collaboration of this program with related programs using shock tubes to obtain kinetic data, as well as with programs using pre-mixed and turbulent flames should be encouraged.

2. Turbulent Flames

Professor G.S. Samuelson is investigating soot production in complex turbulent diffusion flames at the University of California, Irvine. A model laboratory combustor is used to simulate two important features of practical combustors -- swirl and highly-turbulent recirculation. The objective is to provide quantitative information

about the effects of fuel properties, fuel-additive properties, and combustor operating conditions on soot formation and burnout. Both prevaporized and liquid fuels are being tested.

Laser-diagnostic.techniques are used to provide spatially-resolved, non-invasive measurements of mean velocity, soot number density, and size distributions of soot particles and fuel droplets. These techniques include laser-doppler velocimetry, intensity ratioing, and laser interferometry. Comparisons of these non-invasive measurements with results from conventional sampling probes have also provided a measure of probe effects, an important consideration for recirculating flows.

The interpretation of soot measurements obtained from this combustor, in terms of fundamental mechanisms for soot formation and burnout, is extremely difficult in the absense of estimates for local unmixedness. Such estimates could be obtained from non-invasive measurements of local species concentration. Thus the addition of laser-based diagnostics for concentration measurements (CARS) would substantially enhance the contribution of this program to the overall understanding of soot formation and abatement.

3.   Task-Order Contracts

The Environics Branch has established a task-order contract with the University of Florida. Of several projects handled under this contract by Dr. Charles Proctor, one deals specifically with the operation of the experimental combustion facility in the Tyndall laboratory. The objectives are to verify the intensity ratio technique for particle size analysis and to characterize the effect of modifications to the Dilute-Swirl Combustor on soot formation.

Particles of known size will be used to calibrate the intensity-ratio processor. Of specific interest is the accuracy of the method and the sensitivity of measurements to system parameters and particle properties (such as refractive index). Also of interest is the continuity of measured size distributions over variations in the angle ratios.

The DSC will be modified to simulate a bluff-body combustor. The aerodynamics of this configuration will be characterized at the

University of Florida, and the concomitent sooting behavior will be characterized at Tyndall.

B.   IN-HOUSE RESEARCH

1.   Overview
A substantial effort has been extended to establish and equip a combustion research laboratory at Tyndall Air Force Base. But it has been difficult to maintain the level of research effort because the staff members in the Environics Division have relatively short tours of duty. As new personnel frequently move into and out of staff positions, they carry with them their own interests and their own backgrounds. It is not surprising, therefore, that continuity of research effort and focus is often lacking. And this lack of continuity affects not only the ability to conduct in-house research, but also the ability to monitor and to coordinate effectively contract research on a problem as complex as soot formation in combustors. It is clear that in-house research is a necessary component for an effective, comprehensive research program.

2.   Potential
The potential for significant in-house research is excellent. The laboratory has facilities that duplicate the basic equipment being used by Professor Samuelson at UCI, i.e. a Dilute Swirl Combustor (DSC) and an Integrated Particle Sizing System (IPSS). There are also available a variety of aerosol generators and aerosol sizing instruments. In addition, the Environics Chemistry Laboratory is equipped to provide substantial support in analytical chemistry.

Of even greater importance is the commitment by the Engineering and Service Center to deal with the problem of soot formation on a fundamental level. The combustion laboratory has been identified as an important component for a technology thrust within the Environics Division, i.e. there is administrative support to move toward technology development (basic research) in combustion.

Thus the basic elements for effective in-house research -- a well-equipped laboratory and administrative support -- are present.

135-16

VI. RECOMMENDATIONS

It is recommended that a viable combustion laboratory be re-established within the Engineering and Services Center at Tyndall Air Force Base, and that this laboratory be fully operational in three years.

The responsibilities of the laboratory should be to:

- Develop an expertise in basic combustion science.

- Carry out substantial portions of a comprehensive, fundamental research program on soot formation and abatement, with a strong focus on the effects of fuel additives.

- Establish and coordinate related contract research with other private, university, and government laboratories.

- Act as a central clearing house for pertinent technology transfer.

A. BASIS FOR RECOMMENDATION

This recommendation is based on the following hypotheses, summarized from the preceeding sections:

1) The understanding and control of combustion, and the resolution of its environmental consequencies are, and will continue to be, significant areas of concern for Air Force operations.

2) The understanding and control of soot formation and abatement can be achieved only through a comprehensive, coordinated investigation of its fundamental mechanisms and processes.

3) The current approach of the Engineering and Services Center to environmental problems associated with soot formation will neither lead to a timely resolution of current problems nor provide a technological base for the resolution of future combustion problems in other related areas, such as hazardous waste incineration.

4) The Engineering and Services Center is committed to develop and support a quality thrust in combustion science.

B. RECOMMENDED PROCEDURES

To make the Combustion Laboratory operational in three years, immediate steps need to be taken to

1) Define the direction and scope of the laboratory.

2) Determine manpower needs and initiate a search for personnel.

3) Provide suitable facilities and adequate ancillary services.

In addition, the interim research program needs to be tailored to the anticipated direction and scope of the laboratory. Recommendations on these steps are given below.

1. Direction and Scope

As the centralized and coordinating laboratory in a comprehensive research program, the Tyndall Combustion Laboratory should develop the in-house expertise and facilities to

- Critically evaluate instrumentation and techniques for combustion measurements including, but not limited to, laser diagnostics. For example, the analytical instrumentation in the Environics Chemistry Laboratory should be fully utilized. Instrument development, however, should not be a topic for in-house research.

- Establish a fundamental program for measurements of the fate and effect of fuel additives in premixed flames. As well as providing fundamental information crucial to the coordination of contract research, pre-mixed flames will provide a well-controlled environment for instrument evaluation.

- Extend to new additives and modified combustor configurations, measurements of sooting characteristics in the Dilute Swirl Combustor.

- Coordinate related contract research on shock tubes, laminar diffusion flames, and laboratory-scale combustors. When appropriate, contract research should be expanded to include spray flames.

- Maintain state-of-the-art knowledge of fundamental combustion science.

135-18

2. Personnel

A combustion laboratory with the direction and scope proposed above will require a staff with expertise, continuity and dedication. It is proposed that the staff include, as a minimum,

- one permanent senior scientist
- two temporary junior scientists
- one permanent full-time technician
- one permanent half-time secretary.

The senior scientist will be the key to developing a viable combustion laboratory and providing the continuity of research. Clearly, this position will require an individual with proven expertise in the field of combustion, a keen interest in experimental investigations of fundamental combustion mechanisms, and experience in the administration of multi-disciplinary research programs. A minimum five year commitment should be required of the initial appointee.

The junior scientists should be temporary in the sense that their commitment to the laboratory would be from one to three years. One of the positions should be staffed by military personnel with a three-year term appointment. The second position should be used for one to two year "visiting" appointments of university faculty (under the University Resident Research Program, for example), post-doctoral associates, and the like.

The technician, whether military or civilian, should be permanent. The individual should have a working knowledge of digital electronics, and experience with optical systems would be desirable. Given the outstanding technical training programs offered by the Air Force, it should not be too difficult to find a suitable candidate. The importance of this position, however, should not be underestimated. The success of the combustion laboratory will depend, in large part, on staffing the position with a competent and dedicated individual.

The secretary should be half-time in the sense that either part-time work or shared responsibilities with other programs within the Environics Division would be acceptable.

135-19

3. Facilities and Support

A modern research laboratory with the goals, scope, and personnel proposed above will require modern research facilities and adequate ancillary support. Thus assurances should be made now for adequate laboratory space in the new Research Center. The selection and purchase of major pieces of laboratory equipment, however, should be at the discretion of the Senior Scientist and be in keeping with the specific objectives of the Combustion Laboratory.

Two other problem areas require an early resolution. First, steps should be taken to assure access to a large, high-speed digital computer, since the modeling of fundamental combustion phenomena will be an integral part of the research program. Second, the telephone system needs to be vastly improved. The present system is inconvenient, time consuming, and totally inadequate to meet the needs of a modern laboratory. If my experience is typical, the number of man-hours expended by the use of the present Autovon system must be enormous. To achieve the goals proposed above, laboratory staff will need frequent and rapid telephone access, and they will need to expend their time on more productive activities than dealing with the present telephone system.

C. INTERIM PROGRAMS

To provide the proposed combustion laboratory with strong foundation, due consideration needs to be given to the program over the next three years. These considerations need to include both contract and in-house research.

1. Contract Research

The present contract research should be continued and adequately supported. The programs being carried out by Dr. Bonczyk and Dr. Samuelson are responsive to the problem, well-conceived, and productive. If these programs are continued and encouraged to develop, they will provide an exceptionally strong base for the proposed comprehensive research program. Thus any tendency to put these programs on a "back burner" during the interim period should be avoided.

Contract research should be initiated to provide crucial kinetic data from shock-tube measurements. As discussed above, this work will be a vital part of the comprehensive program, and it should be initiated at the earliest opportunity.

Finally, the contract research needs to be much more closely co-ordinated. Travel funds should be made available to the contractors for yearly one- to two-day workshops at Tyndall to evaluate and compare current results, identify specific problem areas, and coordinate future work. Also, copies of progress reports should be routinely distributed among the contractors. The initial step to improve coordination has been taken through an informal meeting of the contractors at the Twentieth Symposium on Combustion in Ann Arbor, where it was uniformly agreed that coordination is desirable and necessary, and that informal coordination would be established. But this coordination needs to be formalized by Tyndall personnel.

The proposed coordination in the interim period should not be con-strued as a means to exclude others from participation in the future research program. Rather it should be regarded as the most efficient way to build the foundation. Once the combustion laboratory is established, the continued participation of the present contractors will rest on their indivdual merits.

2.   In-house Research

During the next three years, the in-house research needs to focus on the operation of current experimental equipment, i.e. the Integrated Particle Sizing System (IPSS) and the Dilute Swirl Combustor (DSC). The present condition of this equipment precludes the collection of meaningful data. A recommended sequence for in-house research, together with a time-table (to coordinate with a move to the new AFESC laboratories in 1985) is given in Table I.

This work could be accomplished in several ways. First, it could be the prime responsibility for the recently approved, but as yet unfilled, position for a mechanical engineer in the Environmental Sciences Branch. Second, it could be handled as a task order under the contract with the University of Florida. Third, a new contract for all or part of this work could be established.* Whichever option, or combination of options, is selected, the work must be initiated as quickly as possible. It has to be done, whether or not the other recommendations given here are favorably received. The unacceptable alternative is to abandon in-house research activities completely.

---

* A RISE proposal to perform portions of the recommended work for 1984-85 has been submitted by the author.

Table I. Recommended Tasks for In-house Research 1984-87

Year	Tasks
1984-85	• Identify and correct problems with the IPSS Ratio Processor electronics.
	• Identify and correct problems with the IPSS Ratio Processor software.
	• Correct and extend the IPSS Ratio Processor software tables (cross-section, probe volume correction, etc.).
	• Initiate critical analysis of IPSS Visibility Processor electronics and software.
	• Purchase minor equipment for laboratory[a]
	• Establish, in consultation with current contractors, a program of DSC measurements for next two years.
1985-86	• Move to new Research Laboratory (install DSC, IPSS, and other particle sizing equipment).
	• Allign optical system of IPSS.
	• Evaluate Ratio Processor Data (calibration and interpretation).
	• Evaluate Visibility Processor Data (calibration and interpretation).
	• Duplicate selected portions of Irvine data.
	• Initiate DSC measurements.
	• Review in-house program in consultation with contractors.
1986-87	• Complete initial DSC measurements program.
	• Prepare for laboratory additions.
	• Review in-house program in consultation with contractors.

[a] A list of recommended minor equipment has been transmitted to the Environmental Sciences Branch separately from this report.

135-22

VII. SUGGESTIONS FOR FOLLOW-ON RESEARCH

The objectives of the suggested follow-on research are to:

1) Provide assistance to the Environics Division in solving some
    immediate instrumental problems, and

2) Establish a basis for assitance in meeting future research
    objectives.

The immediate problem deals with the Integrated Particle Sizing
System software. It is suggested that the correction of software
problems recommended in Section VI is an appropriate first-year task for
a new Ph.D. student in chemical engineering at LSU. This work can be
done at LSU, and a RISE proposal to support this effort has been
submitted.

The future work would, ideally, involve the same Ph.D. student.
The intention is to seek Air Force support for this student to conduct
full-time dissertation research in the Tyndall combustion laboratory.
It is anticipated that this appointment would be from two to three
years. The topic of the research can be determined at a later time, but
it should be in keeping with the long-range objectives of the
laboratory.

1984 USAF-SCEEE SUMMER FACULTY RESEARCH PROGRAM

Sponsored by the

AIR FORCE OFFICE OF SCIENTIFIC RESEARCH

Conducted by the

SOUTHEASTERN CENTER FOR ELECTRICAL ENGINEERING EDUCATION

FINAL REPORT

ELECTROMAGNETIC LENS DESIGN TECHNIQUES

Prepared by: Dr. Alexander P. Stone

Academic Rank: Professor

Department and   Department of Mathematics and Statistics
    University: University of New Mexico

Research Location: Air Force Weapons Laboratory
                                      NTATT
                                      Kirtland Air Force Base
                                      Albuquerque, New Mexico 87117

USAF Research Colleague: Dr. Carl E. Baum

Date: July 23, 1984

Contract No: F49620-82-C-0035

ELECTROMAGNETIC LENS DESIGN TECHNIQUES

By

Alexander P. Stone

ABSTRACT

A lens design technique developed by Baum for transitioning TEM waves, ideally with no reflection or distortion, between cylindrical and conical transmission lines uses a differential geometric approach combined with Maxwell's equations and the constitutive parameters ϵ and μ in an orthogonal curvilinear coordinate system. Isotropic but inhomogeneous media are considered. An alternative approach, which has been used in the design of an anisotropic lens, uses differential impedance and transit-time matching. These two approaches are shown to be equivalent under certain assumptions. Recommendations are made for further research on these methods.

ACKNOWLEDGEMENT

I. **INTRODUCTION**

The problems to be investigated under the 1984 Summer Faculty Research Program arose in earlier research on electromagnetic lens design. This research was started during the 1982 SFR Program and continued under a 1983 AFOSR minigrant. This research was concerned with a differential geometric scaling technique developed by C.E. Baum for EM lens design. The basic idea in this approach is the creation of a class of electromagnetic problems, each having a complicated geometry and medium, which are equivalent to an electromagnetic problem having a simple geometry and medium. Solutions to Maxwell's equations can then be used in specifying certain types of EM lenses for transitioning TEM waves, without distortion or reflection, between certain types of transmission lines.

An important alternative to this differential geometric method in lens design is an impedance matching approach. If a lens is to be inserted between two transmission lines it is clear that not only do impedances have to be matched but that the travel time for waves following different paths have to be equal if we want no reflection and no distortion of the propagated wave front. This impedance matching approach has been described by Baum in a problem in which a lens is to be inserted between two cylindrical coaxial waveguides of different size. In this problem only the geometry and medium were considered, and the matching obtained by Baum matched a reflectionless and distortionless TEM wave between certain transmission lines as verified by an analysis using a fields approach. This approach is reviewed in section 3. The method was also utilized by Baum and Stone in a design problem involving an anisotropic lens for launching TEM waves on a conducting circular conical system.

Thus in considering these two approaches to EM lens design it is natural to ask such questions as (a) will similar results be obtained in a particular design application by each method, (b) are the two methods equivalent in any sense, and (c) is it possible to develop a set of axioms

which will unify these two approaches. In the summer research an effort was made to address some of these issues. In this report the two approaches to EM lens design are reviewed in sections 3 and 4, and results obtained and recommendations for follow up research appear in sections 5 and 6.

II. OBJECTIVES

The main objective in this report is to show that the differential geometric scaling and impedance matching approaches in EM lens design are essentially equivalent under certain geometrical and physical assumptions. Each of these approaches has been used successfully in certain applications by Baum (in [1]), and Stone in ([2]), and finally by Baum and Stone (in [5]). The more general issue of obtaining a set of axioms to unify these approaches is left for future research. This main objective was carried out by studying the special cases where each of the two methods was used, and investigating the underlying assumptions in each application.

III. IMPEDANCE MATCHING APPROACH

An excellent illustration of the use of the impedance matching approach to a lens design problem appears in [4]. In this reference the authors consider two cylindrical coaxial waveguides of different size as illustrated in figure 3.1. The waveguide section of the left, which is region I, has inner and outer cylindrical radii denoted by $\rho = A$ and $\rho = B \equiv \lambda_t A$ respectively, while the waveguide section on the right, which is region III has its respective inner and outer radii given by $\rho = A'$ and $\rho = B' \equiv \lambda_t' B'$ with $A' > A$. Both waveguides are filled with the same simple uniform medium of constant ϵ and μ, and $\sigma \equiv 0$. Physical considerations will require that the transverse ratios λ_t, λ'_t be equal. The problem considered in [4] was that of finding a perfect matching section II between regions I and III such
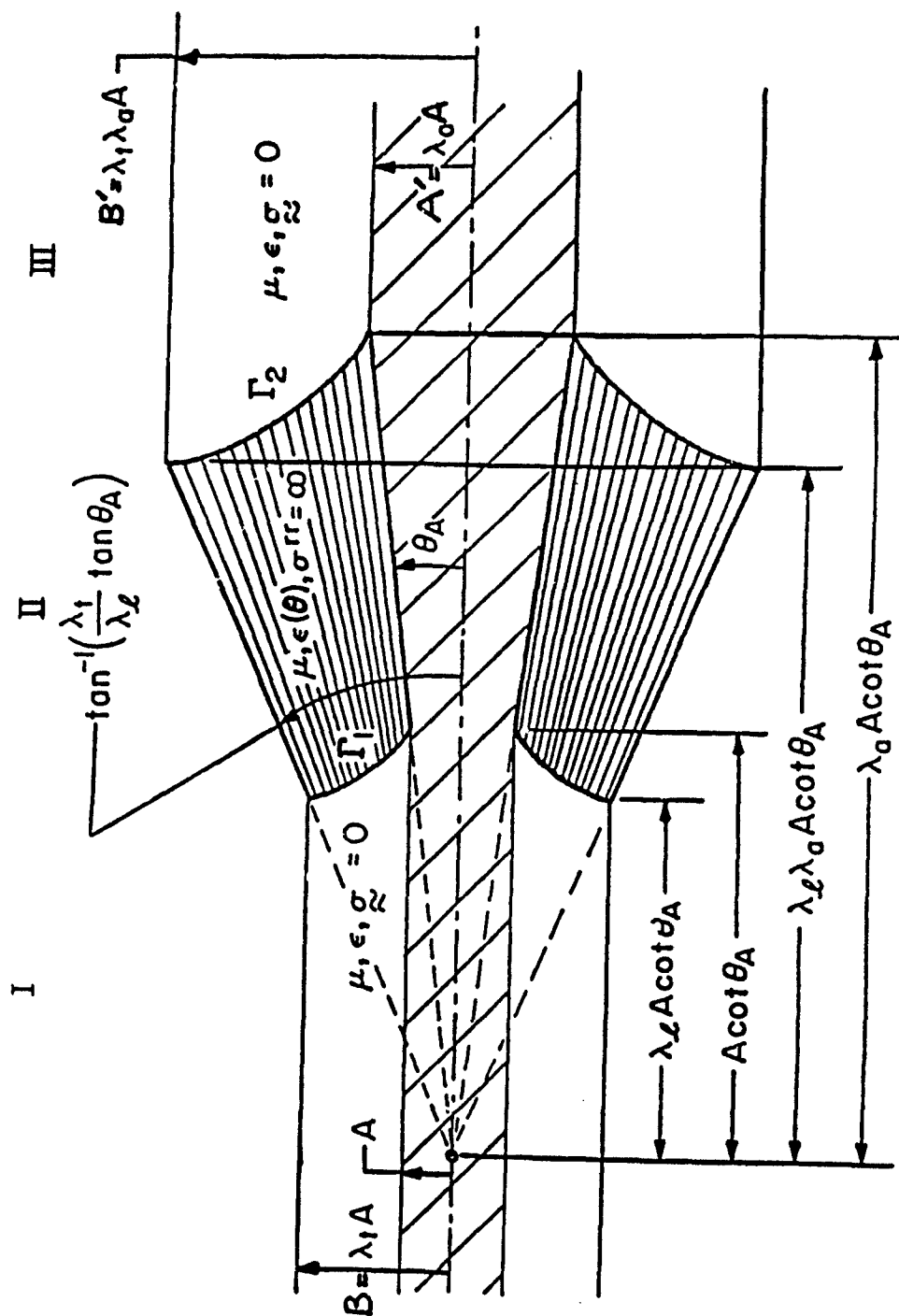
Figure 3.1: Coaxial Waveguide Geometry (SSN #169)

136-6

that a TEM wave incident from the left side could propagate into a TEM wave in region III without reflection and without distortion. In the lens region II a variable $\epsilon(\theta)$ and anisotropic conductivity σ was permitted, but the lens was to have the same fixed μ as in the cylindrical regions. One way of obtaining a perfect matching for regions I, II, and III is to insert coaxial conducting layers in all the regions with spacing d and thickness Δ of each sheath satisfying $\Delta << d$ (for negligible reduction of impedance by conductor thickness) and also satisfying $d << \lambda$ (for propagation of only TEM mode), where λ is the wavelength of the TEM wave. This condition is needed if there is to be no distortion. Moreover, for negligible loss to be introduced by the conductors one would also need

$$\sqrt{\frac{\omega\epsilon}{\sigma}}\, L << d \quad \text{if} \quad \frac{1}{\sqrt{\omega\mu\sigma}} << \Delta \tag{3.1}$$

and

$$\frac{L}{\sigma\Delta}\, \sqrt{\frac{\epsilon}{\mu}} << d \quad \text{if} \quad \Delta << \frac{1}{\sqrt{\omega\mu\sigma}} \tag{3.2}$$

where L is the longitudinal dimension in region II. Finally, for a TEM wave to propagate from I, through II, and into III without distortion a plane wave front in I should appear as a plane wave front in III: that is, the traveling time of waves along paths of different radii should be equal. Thus, (see figure 3.2) we require the travel times along $MM'\, M''$ and its infinitesimally changed version $OO'\, O''$ to be equal, and so we obtain

$$\sqrt{\mu\epsilon(\theta)}\, [r_2(\theta)-r_1(\theta)] + \sqrt{\mu\epsilon}\, \Delta_1 \tag{3.3}$$

$$= [r_2(\theta+d\theta) - r_1(\theta+d\theta)]\sqrt{\mu\epsilon(\theta+d\theta)} \quad \sqrt{\mu\epsilon}\, \Delta_2$$

where

136-7
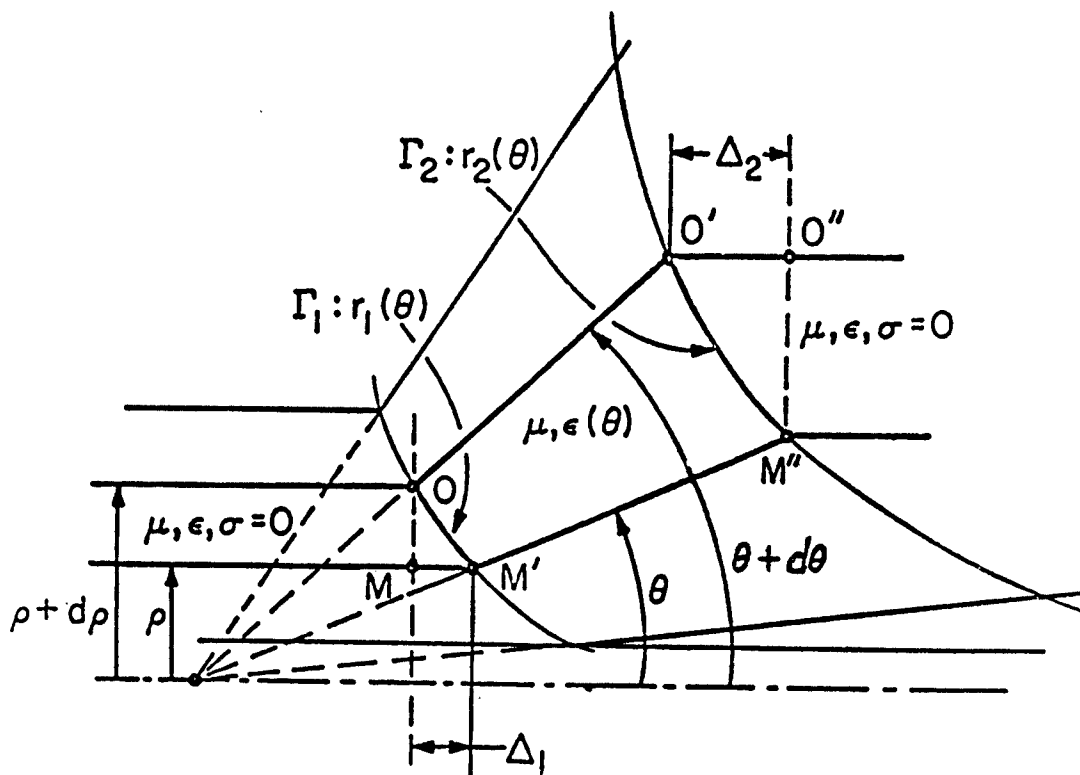
Figure 3.2: Travel Time Geometry (SSN #169)

$$\Delta_1 = r_1(\theta)\cos(\theta) - r_1(\theta + d\theta)\cos(\theta + d\theta)$$

(3.4)

$$\Delta_2 = r_2(\theta)\cos(\theta) - r_2(\theta + d\theta)\cos(\theta + d\theta) .$$

Some elementary calculus coupled with the fact that the $r_1(\theta)$ which describes the boundary between region I and II, and the $r_2(\theta)$ which describes the boundary between regions II and III, are related by a constant factor, leads to a differential equation given by

$$r'(\theta)[\cos(\theta) - \sqrt{\epsilon(\theta)/\epsilon}] - r(\theta)[\sin(\theta) + \frac{(\epsilon(\theta)/\epsilon)'}{2\sqrt{\epsilon(\theta)/\epsilon}}] = 0 .$$

(3.5)

Similarly if we require impedances to be matched on the appropriate boundaries, then we are led to another differential equation through the infinitesimal matching on the boundaries between regions I and II and between regions II and III. Thus since the impedance for the TEM wave of a cylindrical coaxial waveguide is

$$Z_{cyl.} = \frac{V}{I} = \sqrt{\frac{\mu}{\epsilon}} \frac{ln(\rho_{outer}/\rho_{inner})}{2\pi}$$

(3.6)

and that for a conical coaxial waveguide is

$$Z_{con.} = \frac{V}{I} = \frac{\sqrt{\frac{\mu}{\epsilon}}}{2\pi} ln|\frac{\tan(\theta_{outer}/2)}{\tan(\theta_{inner}/2)}|$$

(3.7)

one obtains for the infinitesimal matching on the boundary between regions I and II

$$\sqrt{\frac{\mu}{\epsilon}} ln(\frac{\rho + d\rho}{\rho}) = \sqrt{\frac{\mu}{\epsilon(\theta)}} ln\left| \frac{\tan(\frac{\theta + d\theta}{2})}{\tan(\frac{\theta}{2})} \right| .$$

(3.8)

136–9

Thus equation (3.8) leads to a differential equation

$$\frac{r'(\theta)}{r(\theta)} + \frac{1}{\sin(\theta)}[\cos(\theta) - \frac{1}{\sqrt{\epsilon(\theta)/\epsilon}}] = 0 \tag{3.9}$$

which is obtained by expanding the preceding equation and using $\rho = r\sin(\theta)$. Both $r_1(\theta)$ which describes the boundary between regions I and II and $r_2(\theta)$ which describes the boundary between regions II and III will satisfy (3.9) since the ratio $r_2(\theta)/r_1(\theta)$ is a positive constant greater than 1. We thus have a system of first order ordinary differential equations given by (3.5) and (3.9). We note that the choice in region II of $\epsilon(\theta)$ as a function of θ only is made because the TEM propagation is independent of ϕ and any dependence on r would give rise to a reflection. Solutions to the preceding system are obtained in [4] and have the form

$$r(\theta)\sin(\theta) = c_2\exp\left[\frac{-r(\theta)\cos(\theta)}{c_1}\right] \tag{3.10}$$

and

$$\epsilon(\theta) = \epsilon\left[\frac{c_1 + r(\theta)\cos(\theta)}{r(\theta)}\right]^2 \tag{3.11}$$

where c_1 and c_2 are determined by the geometry. Detailed plots of the boundary surfaces and $\epsilon(\theta)$ are included in [4]. In all of the above analysis only the geometry and medium were considered in the impedance matching approach. That this matching obtained indeed matches a reflectionless and distortionless TEM wave from region I to III can be verified by a fields approach. One may consider, for example, TEM solutions to Maxwell's equations in regions I and II with appropriate boundary conditions and find an $\epsilon(\theta)$ which is consistent with that given by (3.11). A similar result is obtained by considering regions II and III, and hence the solutions to the system (3.5) and (3.9) do indeed give yield to perfect matchings. We note that

136-10

this particular matching problem was also solved in [4] by the more general procedure of differential geometric scaling.

Another application of this approach appears in [5], where an exact solution to an anisotropic lens design problem is given. Just as in the application previously described, impedance matching and transit time conservation give rise to a system of ordinary differential equations describing the lens geometry and medium.

IV. DIFFERENTIAL GEOMETRIC SCALING APPROACH

We first consider a Cartesian coordinate system (x,y,z) and an orthogonal curvilinear coordinate system (u_1,u_2,u_3) with line element

$$(ds)^2 = h_1^2(du_1)^2 + h_2^2(du_2)^2 + h_3^2(du_3)^2 \tag{4.1}$$

with the scale factors h_i , $i = 1,2,3$, given by

$$h_i^2 = (\frac{\partial x}{\partial u_i})^2 + (\frac{\partial y}{\partial u_i})^2 + (\frac{\partial z}{\partial u_i})^2 \tag{4.2}$$

If certain combinations of the h_i , assumed positive, are defined as

$$(\alpha_{ij}) = \begin{bmatrix} h_1 & 0 & 0 \\ 0 & h_2 & 0 \\ 0 & 0 & h_3 \end{bmatrix} \quad (\beta_{ij}) = \begin{bmatrix} h_2h_3 & 0 & 0 \\ 0 & h_1h_3 & 0 \\ 0 & 0 & h_1h_2 \end{bmatrix}$$

$$(\gamma_{ij}) = \begin{bmatrix} h_2h_3/h_1 & 0 & 0 \\ 0 & h_1h_3/h_2 & 0 \\ 0 & 0 & h_1h_2/h_3 \end{bmatrix} \tag{4.3}$$

then one can write out the usual expressions for $\nabla \Phi$, $\nabla \times \vec{E}$, and $\nabla \cdot \vec{E}$ in the u_i coordinate system in terms of physical components of the vector $\vec{E}$. Another set of vectors and operators (formal vectors and formal operators) may be written out in terms of tensor components. For example, if $\vec{E}$ has components E_1, E_2, E_3 referred to the u_i coordinates, then $\vec{E}'$, the formal vector, has components E_1', E_2', E_3' and we write

$$\vec{E}' = (\alpha_{ij}) \cdot \vec{E} \tag{4.4}$$

while

$$\nabla \Phi = (\alpha_{ij})^{-1} \cdot \nabla \Phi' \quad , \text{ where } \quad \Phi = \Phi' \quad , \tag{4.5}$$

and

$$\nabla \times \vec{E} = (\beta_{ij})^{-1} \cdot \nabla' \times E' \quad . \tag{4.6}$$

The result one obtains is that Maxwell's equations

$$\nabla \times \vec{E} = -\frac{\partial \vec{B}}{\partial t} \qquad \nabla \cdot \vec{D} = \rho$$

$$\nabla \times \vec{H} = \vec{J} + \frac{\partial \vec{D}}{\partial t} \qquad \nabla \cdot \vec{B} = 0 \tag{4.7}$$

together with the constitutive relations

$$\vec{D} = (\epsilon_{ij}) \cdot \vec{E}$$

$$\vec{B} = (\mu_{ij}) \cdot \vec{H} \tag{4.8}$$

and the equation of continuity

$$\nabla \cdot \vec{J} = -\frac{\partial \rho}{\partial t}$$

can be rewritten in the form

$$\nabla' \times \vec{E}' = -\frac{\partial \vec{B}'}{\partial t} \qquad \nabla' \cdot \vec{D}' = \rho'$$

$$\nabla' \times \vec{H}' = \vec{J}' + \frac{\partial \vec{D}'}{\partial t} \qquad \nabla' \cdot \vec{B}' = 0$$

with

$$\vec{D}' = (\epsilon_{ij}') \cdot \vec{E}' \qquad (4.9)$$

$$\vec{B}' = (\mu_{ij}') \cdot \vec{H}'$$

$$\nabla' \cdot \vec{J}' = -\frac{\partial \rho'}{\partial t}$$

where

$$(\epsilon_{ij}') = (\gamma_{ij}) \cdot (\epsilon_{ij}) \ , \ (\mu_{ij}') = (\gamma_{ij}) \cdot (\mu_{ij}) \ , \ (\alpha_{ij}') = (\gamma_{ij}) \cdot (\alpha_{ij}) \qquad (4.10)$$

and where it is assumed that (ϵ_{ij}) , (μ_{ij}) , (α_{ij}) are real constant diagonal matrices which are independent of frequency, though possibly functions of position. Note that the primed equations (4.9) are of the same form as equations (4.7) and (4.8), and so if we think the u_i as a Cartesian coordinate system, a known solution of Maxwell's equations referred to Cartesian coordinates can be taken and if primed quantities are substituted for unprimed quantities, solutions to (4.9) can be found. The result turns out to be that we have a solution to Maxwell's equations for which (ϵ_{ij}) , (μ_{ij}) and (α_{ij}) may be anisotropic and/or inhomogeneous. The basic idea is then to pick (ϵ_{ij}') , (μ_{ij}') , and (α_{ij}') and boundary surfaces of convenient

forms in the u_i coordinate system so that a solution can be obtained in terms of the formal quantities. If some particular relationship between the u_i coordinates and the x, y, z coordinates is chosen, then the parameters (ϵ_{ij}), (μ_{ij}) and the geometry of the boundary surfaces are determined and the solution can be applied to the case under study.

In problems related to inhomogeneous isotropic media, the constitutive parameter matrices are diagonal matrices of the form

$$(\epsilon_{ij}) = \epsilon(\delta_{ij}) \ , \ (\mu_{ij}) = \mu(\delta_{ij}) \tag{4.11}$$

where ϵ and μ are scalar functions of position. The formal quantities then look like

$$(\epsilon_{ij}') = \epsilon(\gamma_{ij}) \ , \ (\mu_{ij}') = \mu(\gamma_{ij}) \ . \tag{4.12}$$

If we impose the restriction that $\sigma = 0$, then the conductivity matrix is the zero matrix. Note that an inhomogeneous TEM wave with subscripts 1 and 2 only has no interaction with ϵ_{33}' or μ_{33}' in which case each of the matrices (ϵ_{ij}') and (μ_{ij}') has constant and equal diagonal entries in the first two diagonal positions. Hence such TEM solutions may be used to define lenses to match waves onto cylindrical and/or conical transmission lines.

We now consider inhomogeneous TEM plane waves which propagate on ideal cylindrical transmission lines and assume the wave to be propagating in the positive u_3 direction with formal constitutive parameters given as

$$(\epsilon_{ij}') = \begin{pmatrix} \epsilon' & 0 & 0 \\ 0 & \epsilon' & 0 \\ 0 & 0 & \epsilon_3' \end{pmatrix} \quad (\mu_{ij}') = \begin{pmatrix} \mu' & 0 & 0 \\ 0 & \mu' & 0 \\ 0 & 0 & \mu_3' \end{pmatrix} \tag{4.13}$$

where ϵ' and μ' are positive constants, and ϵ_3' and μ_3' are not specified. Since only waves with no field components parallel to the u_3 direction will be considered, then ϵ_3' and

136-14

μ_3' do not enter into the formal constitutive relations given in equations (4.9). Hence, since only ϵ' and μ' are significant, we may assume the medium to be formally isotropic and homogeneous. We also note that by a direct application of known results for cylindrical transmission lines to the formal setting we have, for $i = 1,2$

$$E_i' = E_{i_0}'(u_1, u_2) f(t - u_3/c')$$

$$H_i' = H_{i_0}'(u_1, u_2) f(t - u_3/c') \tag{4.14}$$

and

$$E_3' = 0, \ H_3' = 0$$

where $c' \equiv (\mu'\epsilon')^{-1/2}$ and $c \equiv (\mu_0\epsilon_0)^{-1/2}$ and $f(t - u_3/c')$ can be chosen to specify the waveform. These formal fields are related by

$$E_1' = Z_0' H_2' \quad and \quad E_2' = -Z_0' H_1' \tag{4.15}$$

where $Z_0' = (\mu'/\epsilon')^{1/2}$ is the formal wave impedance. These results all require that the conducting boundaries be represented in terms of only their u_1 and u_2 coordinates and lead us to the conclusion that it is only necessary to restrict the first two diagonal components of the formal matrices given in equations (4.13). The constitutive parameter matrices given in equations (4.11) still correspond to isotropic inhomogeneous media and so the formal constitutive parameter matrices have the form (4.12). If equations (4.11) and (4.13) are combined, we obtain

$$(\gamma_{ij}) = \begin{pmatrix} h_2 h_3/h_1 & 0 & 0 \\ 0 & h_3 h_1/h_2 & 0 \\ 0 & 0 & h_1 h_2/h_3 \end{pmatrix} = \frac{1}{\epsilon}(\epsilon_{ij}') = \frac{1}{\mu}(\mu_{ij}'). \tag{4.16}$$

Since equations (4.16) imply

$$\frac{h_2 h_3}{h_1} = \frac{h_3 h_1}{h_2} = \frac{\epsilon'}{\epsilon} = \frac{\mu'}{\mu} \qquad (4.17)$$

$$\frac{h_1 h_2}{h_3} = \frac{\epsilon_3'}{\epsilon} = \frac{\mu_3'}{\mu}$$

we obtain the result that

$$h_1 = h_2 \qquad (4.18)$$

and also that ϵ and μ are given by

$$\epsilon = \epsilon' / h_3 \quad and \quad \mu = \mu' / h_3 . \qquad (4.19)$$

Clearly ϵh_3 and μh_3 are constants and the formal wave impedance is equal to the physical wave impedance since

$$Z_0' = (\frac{\mu'}{\epsilon'})^{1/2} = (\frac{\mu h_3}{\epsilon h_3})^{1/2} = (\frac{\mu}{\epsilon})^{1/2} = Z_0 . \qquad (4.20)$$

Finally, since ϵ_3' and μ_3' are arbitrary, we look for orthogonal curvilinear coordinate systems for which the scale factors h_1 and h_2 are equal. For these systems the scale factor h_3 determines ϵ and μ in view of equations (4.19). Examples of this technique appear in references [1] and [4]. We also note that it is possible, as noted in the next section, to replace the delay term in (4.14) by an expression of the form $f(t-g(u_3))$.

v. EQUIVALENCE OF APPROACHES TO EM LENS DESIGN

We assume that we have a lens geometry with orthogonal coordinates (u_1, u_2, u_3) and that a TEM wave propagates in the u_3 direction. Thus u_3 in particular applications can

represent, for example, the z , r , η or ς of cylindrical, spherical, bispherical, or toroidal coordinates. Surfaces of constant u_3 are spheres or planes and these generalized coordinates are constructible from rotational coordinates (v_1,ϕ,v_3) as in [1].

In the differential geometric scaling approach we have a line element,

$$(ds)^2 = h_1^2(du_1)^2 + h_2^2(du_2)^2 + h_3^2(du_3)^2 \qquad (5.1)$$

where the u_i coordinates are constructed from orthogonal coordinates (v_1,ϕ,v_3) by the formulas

$$u_1 = \lambda(v_1)\cos(\phi)$$

$$u_2 = \lambda(v_1)\sin(\phi) \qquad (5.2)$$

$$u_3 = F(v_3) ,$$

which result in an orthogonal system (u_1,u_2,u_3) in which surfaces of constant u_3 (or v_3) are spheres or planes. The functional form $F(v_3)$ gives some flexibility in choosing h_3 which defines the properties of the lens medium (i.e., the ϵ and μ). The assumption that our medium is formally homogeneous and isotropic, and that (v_1,ϕ,v_3) is a rotational system leads to the result that $h_1 = h_2$, and $h_3 = h_{v_3}|\dfrac{dv_3}{du_3}|$, and since ϵ_r , the relative permittivity, is given by $\epsilon_r = 1/h_3$, we have

$$\epsilon_r = f(v_1,v_3) = g(u_1,u_2,u_3) . \qquad (5.3)$$

In the differential impedance matching and local transit time conservation approach the following conditions should hold for the (u_1,u_2,u_3) coordinate system in the lens:

(a) $\dfrac{\Delta u_2}{\Delta u_1} \sqrt{\dfrac{\mu}{\epsilon}}$ is not a function of u_3

136-17

(b) $\sqrt{\mu\epsilon}$ is not a function of u_1 or u_2

between ending boundaries of the lens. Condition (a) results from considering an impedance expression of the form

$$\int_{u_2}^{u_2+\triangle u_2} E_2 \, dl \Big/ \int_{u_1}^{u_1+\triangle u_1} H_1 \, dl$$

on surfaces $u_3 = $ constant, and E_2 is evaluated along curves with $u_1 = $ constant, while H_1 is evaluated along curves with $u_2 = $ constant. Condition (a) also implies impedances are matched at lens boundaries which are given by equations of the form $f(u_1, u_2) = 0$, and so the quantities V and I are conserved (i.e., no reflections). Condition (b) says that differential transit times for waves following different paths are conserved.

A differential geometric scaling given by equation (5.1) clearly implies condition (a), (impedance matching), since μ/ϵ is a constant for our medium. Condition (b) is also satisfied because of the physical assumptions made. Thus differential impedance matching and transit time is implied by the scaling introduced.

Conversely, let us assume ϵ and μ are scalar functions of position and that we have $\vec{E}$ and $\vec{H}$ only in the u_1 and u_2 directions. Our wave propagates in the u_3 direction, and we assume that it has no dependence on u_3 except for a delay. Thus $E_3 = H_3 = 0$ and if the quantities $E_i\triangle_i$ and $H_i\triangle_i$, $i = 1,2$, with $\triangle_i$ the change in arc length in the u_i direction, are all of the form $f(t - g(u_3))$, then E_1/E_2 and H_1/H_2 are constants, (i.e., constant polarization), surfaces of constant u_3 are constant phase surfaces, and voltage and current are conserved differentially. We will also have

$$\frac{\triangle_1}{\triangle_2}\left(\frac{E_1}{H_2}\right) = \frac{-\triangle_2}{\triangle_1}\left(\frac{E_2}{H_1}\right) = constant \qquad (5.4)$$

and if the constant in (5.4) is evaluated by solving Maxwell's equations, then h_1/h_2 and μ/ϵ are constants. Thus Conditions (a) and (b) will be satisfied differentially and we will have macroscopic transit time matching at the lens boundaries. We are, of course, in this analysis assuming that we have a "differential cube" as shown below.
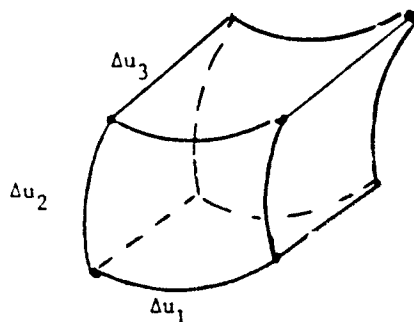
VI. **RECOMMENDATIONS**

The techniques of scaling and impedance matching as applied to EM lens design have been described and shown to be equivalent under certain geometrical and physical assumptions in the previous section. There are, however, several remaining questions which need to be answered, and the research to accomplish this will be proposed in my application for a Research Initiation Grant (RISE). Among these questions are:

(a) Which physical and geometrical conditions can be eliminated or amended so that the approaches remain equivalent in some sense? In particular, can the conditions on the $E_i \Delta_i$ and $H_i \Delta_i$ imposed in section 5 be relaxed? For example, suppose we assume that these quantities have a u_1 dependence in addition to a time delay. Then the quantities which appear in (5.4) will still be constants on surfaces of constant u_1 and this should imply electric boundaries on u_1 surfaces if $E_1 = 0$ and magnetic boundaries iff $H_1 = 0$. Thus conditions on the scale factors h_i and ϵ and μ should then

result.

(b) Are the two approaches discussed in this report amenable to an axiomatic treatment?

Answers to these questions would be helpful in unifying procedures for EM lens design.

A separate issue, related to the impedance matching approach, is the study of a certain non-linear, first order, ordinary differential equation which seems to be typical of conical systems, such as that described in section 4. One may obtain such an ordinary differential equation (ODE) in the form

$$\frac{d\epsilon_r}{d\theta} = \frac{2}{\sin(\theta)}[(1+\epsilon_r)\cos(\theta) - 2\sqrt{\epsilon_r}]$$

where ϵ_r and θ are the relative permittivity and conical angle. It is possible to obtain an explicit solution in the form

$$\epsilon_r = \left(\frac{\cos(\theta)}{u}\right)^2$$

where u satisfies an Abel ODE (see [6]). With appropriate initial conditions the ϵ_r obtained agrees precisely with the result obtained in [4]. It would be interesting to study such equations in general and investigate their symmetry groups. Moreover one might also wish to investigate ODES which describe the media for other lens geometries.

It is the author's view that a unification of the various approaches to EM lens design would prove to be quite useful in studying EM phenomena. The results of the earlier investigations have found applications in EMP theory, which is an area of interest to both the Air Force and the EM community.

REFERENCES

1. C.E. Baum, "A scaling technique for the design of idealized electromagnetic lens", Sensor and Simulation Note 64, August 1968, Kirtland AFB, AF Weapons Laboratory, Albuquerque, NM 87117.

2. A.P. Stone, "A differential geometric approach to electromagnetic lens design", Sensor and Simulation Note 282, April 1983, Kirtland AFB, AF Weapons Laboratory, Albuquerque, NM 87117. (Also to appear in revised form under same title in Electromagnetics, Vol. 4, #1).

3. C.E. Baum, "EMP simulators for various types of nuclear EMP environments: An interim categorization", Sensor and Simulation Note 240 (also in IEEE Transactions on Antennas and Propagation, Vol. AP-26, No. 1, Jan. 1978, pp. 35-53, and in IEEE Transactions on EM Compatibility, Feb. 1978).

4. T.C. Mo,. C.H. Papas, and C.E. Baum, "Differential geometry scaling method for electromagnetic field and its applications to coaxial waveguide functions", Sensor and Simulation Note 169, March 1973 (also as a paper by the same authors under the title of "General scaling method for electromagnetic field with application to a matching problem", J. Math. Physics, Vol. 14, pp. 479-483, April 1973.)

5. A.P. Stone and C.E. Baum, "An anisotropic lens for launching TEM waves on a conducting circular conical system", Sensor and Simulation Note 285, June 1984, Kirtland AFB, AF Weapons Laboratory, Albuquerque, NM 87117.

6. G.M. Murphy, *Ordinary Differential Equations and Their Solutions*, (D. Van Nostrand Co., N.Y., 1960), pp. 23-27.

1984 USAF-SCEEE SUMMER FACULTY RESEARCH PROGRAM

Sponsored by the

AIR FORCE OFFICE OF SCIENTIFIC RESEARCH

SOUTHEASTERN CENTER FOR ELECTRICAL ENGINEERING EDUCATION

FINAL REPORT

THE ROLE OF ANTIOXIDANT NUTRIENTS IN PREVENTING HYPERBARIC
OXYGEN DAMAGE TO THE RETINA

Prepared by :   William L. Stone, Ph.D.
                     and George Howard, Jr.

Academic Rank: Assistant Professor

Department and
   University: Department of Biomedical Sciences
                     Meharry Medical College

Research Location: Brooks Air Force Base, School of Aerospace
                     Medicine, Division of Hyperbaric Medicine.

USAF Research: Col. Richard Henderson, M.D., Chief of Clinical
                     Investigations and Acting Director, Division
                     of Hyperbaric Medicine

Date: September 6, 1984

Contract No.   F49620-82-C-0035

THE ROLE OF ANTIOXIDANT NUTRIENTS IN PREVENTING HYPERBARIC OXYGEN DAMAGE TO THE RETINA

by

William L. Stone

ABSTRACT.

Hyperbaric oxygen was found to affect adversely the electrophysiological response of the retina to light in rats fed a diet deficinet in both vitamin E and selenium. Both vitamin E and selenium are micronutrients thought to play essential roles in preventing in vivo lipid peroxidation. Rats fed diets supplemented with vitamin E and/or selenium and treated with 2.0 ATA (atmospheres absolute) of 100 percent oxygen for 1.5 hours per day for 4 weeks did not show any decrease in electroretinogram response. The retina is known to be particularly susceptible to oxidative damage caused by in vivo lipid peroxidation. Dietary antioxidants appear to provide protection from hyperbaric oxygen damage to the rat retina.

I. INTRODUCTION:

Hyperbaric oxygen treatment is currently being used by the School of Aerospace Medicine to treat a variety of clinical disorders. These clinical disorders include gas gangrene, gas embolism, decompression sickness, carbon monoxide poisoning and wound healing enhancement. The therapeutic benefits of long term hyperbaric oxygen treatment are potentially limited by the adverse clinical and pathological effects of high oxygen concentration upon the retina and lung. In addition, many drugs and toxins are known to directly promote oxidative damage or to interfere with enzymatic antioxidant mechanisms. This raises the possibility of adverse drug-hyperbaric oxygen interactions in patients undergoing long-term hyperbaric oxygen therapy.

Gable and Townsend (1) have observed pulmonary lesions in victims of fatal military aircraft accidents "possibly attributable to prolonged intermittent supplemental oxygen, stressing the potential hazard of oxygen toxicity for aviators" (2). Oxygen toxicity to retinal and pulmonary tissues most likely involves free radical damage to biological membranes. Vitamin E and selenium are nutrients that play a central role in physiological antioxidant mechanisms. Vitamin E effectively quenches free radicals generated by lipid peroxidation. Selenium is a cofactor for glutathione peroxidase which detoxifies lipid hydroperoxides. Humans deficient in vitamin E and/or selenium may be particularly susceptible to the pathophysiological consequences of hyperbaric oxygen. Conversely, dietary supplements of these micronutrients may offer considerable protection against oxygen toxicity.

The retina is more sensitive to toxic and environmental disorders than most tissues. The retina is particularly predisposed to the

toxic effects of lipid peroxidation initiated by oxy-radicals. This
is because the retina has: a) a very high content of polyunsaturated
fatty acids (about 30% 22:6n3) which are very susceptible to lipid
peroxidation (6); b) a very high consumption of oxygen, about seven
times more per g of tissue than the brain and ; c) the presence of
pigments (e.g. retinal) capable of inducing photosensitized oxidation
reactions (7). Retinal lipid peroxidation is likely to be accelerated
under conditions of hyperbaric oxygen stress.

In animal models hyperbaric oxygen causes severe retinal pathology
and, in humans, causes loss of visual fields and visual definition
(8). The ability of the retina to resist oxidative damage is very
dependent upon the functioning of both enzymatic and chemical
antioxidant mechanisms (3). A number of important antioxidant
mechanisms are very dependent upon micronutrient intake. We have
previously shown that rat retinas have significant levels of vitamin
E, glutathione-S-transferase, and the selenoenzyme glutathione
peroxidase (3,4). Retinal vitamin E and glutathione peroxidase are
decreased to very low levels by nutritional deficiency of vitamin E
and selenium, respectively (7,9). Retinal glutathione-S-transferase
activity is induced in the absence of dietary vitamin E and selenium
(4).

Rats deficient in vitamin E and selenium (the B dietary group) show
a decreased a- and b-wave electroretinogram (ERG) amplitude (9).
Recent in vitro studies of Armstrong, et al. (10), have shown that
intravitrael injections of synthetic lipid hydroperoxides into rabbit
eyes causes a marked decrease in the amplitude of the a-, b-, and
c-waves of the ERG. The retinal pigment epithelium of rats fed the
diet deficient in both vitamin E and selenium also show a large

accumulation of lipofuscin pigment (9) as well as major
ultrastructural alterations (11). Lipofuscin pigment is thought to be
a by-product of in vivo lipid peroxidation and can be measured by
fluorescent microscopy.

The information presented above suggests that hyperbaric oxygen
damage to the retina would be greatly accelerated in cases of
antioxidant nutrient deficiences and inhibited by dietary
supplementation with antioxidant nutrients.

II   ~CTIVES OF THE RESEARCH EFFORT:

The primary goal of this project was to determine if hyperbaric
oxygen damage to the retina and lung is accelerated in organisms
deficient in dietary antioxidant nutrients and inhibited in organisms
supplemented with antioxidant nutrients. Rats will be used as an
experimental model in this work. Damage to the retina will be
determined noninvasively by measurement of electroretinograms (ERGs).
When ERGs show evidence of retinal damage the rats will be sacrificed
and the retinas and pulmonary tissues examined by fluorescent
microscopy, as well as light and electron microscopy. Lung tissue
samples will also be collected and biochemically characterized as
described below.

III. EXPERIMENTAL DESIGN:

Rats were fed diets deficient in antioxidant nutrients. The
antioxidant nutrients tested in this initial study were vitamin E and
selenium. A factorial design was utilized in which the dietary groups
were:

1) a basal diet deficient in both vitamin E and selenium but

   adequate in all other nutrients (the basal or B diet)

2) a basal diet plus vitamin E (the B+E diet)

3) a basal plus selenia diet (the B+Se diet)

4) a basal plus vitamin E plus selenium diet (the B+E+Se diet)

The detailed composition of the basal diet is given in Table IV. Enough feed has been mixed to continue the nutritional experiments to the end of October, 1984 ; i.e. for a total of 16 weeks or 8 weeks beyond the end of the SFRP tenure.

Male, 30 g, inbred Fischer-344 (CDF) rats were obtained from Charles River Breeding Laboratory. The P.I. has utilized this rat strain in nutritional experiments analogous to those proposed here. The time course for development of nutritional deficiencies in vitamin E and selenium is well characterized in this strain. We have also performed extensive histopathology studies on Fischer-344 rats fed diets identical to those used in this study. It takes about 5 weeks for 50 g rats to lose half of their blood selenium and half of their plasma vitamin E content when fed the basal diet. After 10 weeks, the rats have only about 10% of their initial blood vitamin E and selenium. After 20 weeks, rats are almost totally depleted of both micronutrients and suffer retinal damage under nonstress conditions.

The animals were housed in suspended stainless steel, wire-bottomed cages and maintained at 25±2 C and 50% relative humidity. Lighting was on a 6:00 AM to 6:00 PM light period and a 6:00 PM to 6:00 AM dark

period. Upon arrival at Brooks AFB, the rats were fed a normal Purina laboratory chow (Rodent Laboratory Chow 5001, Ralston Purina Co., St. Louis, MO) and water ad libitum for 1 week. The rats were randomly divided into the four dietary groups designated above. Eight animals were used per dietary group (32 rats in total). The basal group was fed a Torula yeast-based diet having very low levels of vitamin E and Se but adequate levels of all other nutrients as proposed by the National Research Council for the Laboratory Rat. The basal+vit E+Se group was fed an indentical diet but supplemented with 50 mg vitamin E per kg of diet (1.1 IU per mg of DL-alpha-tocopherol) and 0.4 ppm Se (added as sodium selenite). All dietary supplies were purchased from U.S. Biochemical Co, Cleveland, OH. The Torula-based diets were prepared in small batches by slowly mixing the constituents to avoid heating, and stored at 4 C. The glass and stainless steel feeders, obtained from Hazelton Systems, Aberdeen, MD, were filled every 2 days and any uneaten food discarded to einimize rancidity. The glass and stainless steel feeders as well as a small (2 kg capacity) Hobart food mixer were shipped to Brooks AFB from the P.I.'s laboratory at Meharry Medical College. Rats in all the dietary groups were provided with deionized water to which 3 ppm chromium (as CrCl3) was added. Both diet and drinking water were provided ad libitum. Half the rats from each dietary group were treated with 2.0 ATA of pure oxygen for 1.5 hr per day. This treatment began 2 weeks after the start of the dietary regimens. The other half of the rats provide a nonHBO control groups to monitor retinal damage that might be due to antioxidant deficiency alone.

At weeks 2, 4, and 6 and 8, electroretinograms (ERGs) of rats in each dietary group were recorded. ERG measurements were made using an

137-7

aluminized mylar plastic positive electrode placed on the cornea of
each rat. This electrode effectively eliminates the possibility of
corneal damage. The ground electrode was attached to the rat ear
lobe. A negative pin electrode was inserted under the scalp. We used
a ganzfeld (whole field) flash, a Grass photostimulator and a Tektonix
model 6512 recording oscilloscope with a 5A22N differential amplifier
and a 5B10N time base amplifier. The animals were placed in a dark
room for 1 hr before measuring ERGs. About 10 min before recording an
ERG, each rat was anesthetized (IM injection) with 0.1 ml of ketamine
(50 mg/ml). At least six's a- and b-wave amplitude measurements were
made for each eye and the results (at least 12 measurements per rat)
averaged. The P.I. and Mr. George Howard were responsible for these
measurements.

Rats from each dietary group have been evaluated for plasma vitamin
E, plasma glutathione peroxidase (GSHPX), and red blood cell
glutathione peroxidase at week 3. Plasma and RBC samples were
collected at week 7 and will be analyzed on the P.I.'s return to
Meharry Medical College. Glutathione peroxidase is a selenoenzyme and
its activity in plasma and red blood cells (RBCs) is a good measure of
selenium status. Blood is obtained from each rat after cutting (under
methoxyfluorane anesthetization) off a small section from the end of
the tail. This process is relatively untraumatic and can easily be
done on the same rat on a biweekly basis. Blood is separated into
plasma and washed RBCs. The glutathione peroxidase assays on plasma,
and RBCs as well as plasma vitamin E assays will be done at Meharry
Medical College by the P.I. and Mr. George Howard, a summer graduate
student SCEEE fellow.

When the rats exposed to hyperbaric oxygen and deficient in vitamin
E and/or selenium showed signs of retinal damage (such as diminished
ERG a- and b-wave amplitudes), they were sacrificed (by overdose of
methoxyfluorane) for detailed biochemical and cytopathology studies.
Control animals, not exposed to hyperbaric oxygen were also
sacrificed.   Rats fed the diet deficient in both vitamin E and
selenium and treated with HBO (the B+HBO group) have already shown
decreased ERG a-wave amplitudes compared with the nonHBO B group.
Rats from the B and B+HBO group have therefore been sacrificed for
future biochemical and cytopathology studies.

IV.   THE EFFECTS OF HYPERBARIC OXYGEN ON ELECTRORETINOGRAMS:

At weeks 2 and 4, hyperbaric oxygen treatment had no apparent
effect on ERGs recorded from rats on any of the dietary regimens. As
shown in Table I, rats exposed to hyperbaric oxygen treatemnt for 4
weeks, and fed a basal diet (B diet) deficient in vitamin E and
selenium for 6 weeks, have decreased ERG a-wave amplitudes (P<0.05)
and b-wave amplitudes compared to age-matched rats fed an identical
diet but not treated with hyperbaric oxygen. Rats fed diets deficient
in vitamin E (B+Se diet) or selenium alone (B+E diet) did not show any
decline in ERG a- or b-wave amplitudes when exposed to hyperbaric
oxygen at this time (see Table I). We anticipate, however, that rats
deficient in vitamin E or selenium will eventually show decreased
retinal function as they become progressively more deficient in these
micronutrients. Acute deficiency of vitamin E and selenium takes no
longer than 15 weeks on the dietary regimens.

V.   THE EFFECT OF HYPERBARIC OXYGEN ON WEIGHT AND WEIGHT GAIN:

Rats fed the B diet deficient in both vitamin E and selenium for 5
weeks, and treated with hyperbaric oxygen (HBO) for 3 weeks show a
decreased weight and weight gain compared with age-matched rats fed an
identical diet but not receiving HBO treatment (see Table II).
Similarly, rats fed the vitamin E deficient diet and treated with HBO
(B+Se+HBO) are also beginning to demonstrate a reduced weight and
weight gain which might indicate the onset of chronic HBO toxicity and
retinal damage. HBO treatment does not appear to be adversely
affecting the weight or weight gain of rats fed the vitamin E and
selenium supplemented diet (the B+E+Se diet) or the diet supplemented
with vitamin E alone (the B+E diet).

VI. ANTIOXIDANT STATUS OF RATS:

Plasma vitamin E, red blood cell and plasma Se-glutathione
peroxidase activities we- measured in rats, in all dietary groups, 3
weeks after the start of the nutritional regimens. As expected, rats
fed the B diet have significantly lower plasma vitamin E as well as
plasma and RBC Se-glutathione peroxidase activities compared to rats
fed the B+E+Se diet (see Table III). We have recently obtained plasma
and RBC samples at week 7 and plan to measure plasma vitamin E, plasma
and RBC glutathione peroxidase and RBC glutathione levels in these
samples. This work will be done at Meharry Medical College in the
P.I.'s laboratory.

VII. RECOMMENDATIONS:

Dietary deficiences of both vitamin E and selenium were found to
adversely effect the electrophysiological response of the retina to
light. Rats are generally considered a species very resistant to

oxidative damage. Our preliminary results suggest that nutritional
supplementation of patients with antioxidant nutrients could diminish
the oxygen toxicity problems associated with HBO therapy. We do not
yet know if deficiency of vitamin E or selenium alone will be
associated with hyperbaric oxygen damage to the rat retina. We
recommended that the nutritional experiments be continued for an
additional 4 to 6 weeks so that ERG measurements can be made on rats
treated with hyperbaric oxygen and acutely deficient in vitamin E
(B+Se group) or selenium (B+E group).

It is also recommended that the follow-on biochemical studies of
lung tissue, and light/electron microscopy studies of lung and retinal
tissues, be pursued as detailed in the RESEARCH INITIATION PROPOSAL.

Animals in the B and B+HBO groups were euthanized at week 6 and
samples of lung tissue stored at -70 C for biochemical analyses (see
below). The rats were perfused with Karnofsky's fixative. Retinal
and lung tissues were embedded in Epon for future analyses by
fluorescent microscopy, phase contrast microscopy, and electron
microscopy.

Rats have enzymatic antioxidant mechanisms that can be induced in
response to oxidative stress (3,4,5). The degree to which a organism
can induce these enzymatic antioxidant mechanisms may be an important
parameter in determining an organism's susceptibility to oxygen
toxicity. These potential physiological responses must be
characterized before the relevancy of our results to humans can be
understood. Glutathione-S-transferase activity in the rat lung
increases in response to hyperoxia (5). A number of
glutathione-S-transferase isozymes have a "nonselenium glutathione
peroxidase" activity that may protect against damaging in vivo lipid

peroxidation reactions. We therefore recommend that the
glutathione-S-transferase isozyme profiles in the lungs of antioxidant
deficient and supplemented rats be measured and characterized. Mr.
George Howard, Jr. and the P.I. have developed high pressure liquid
chromatographic procedures for the rapid separation and purification
of glutathione-S-transferase isozymes. These biochemical
determinations should be done on rats treated with hyperbaric oxygen
(HBO) and on control nonHBO rats raised under normal conditions.

The results of the light/electron microscopy studies of lung and
retinal tissues would certainly benefit by quantitative computer-image
analysis.

9. REFERENCES:

1) Gable, W.D., Townsend, F.M. (1962) Aerospace Med. 33,
   1344.

2) Balentine, J.D. in Oxygen and Physiological Function,
   ed. by F.F Jobsis, Professional Information Library,
   Dallas, TX (1976).

3) Stone, W.L. and Dratz, E.A. (1982) Exp. Eye Res.,
   35, 405-412.

4) Stone, W.L., and Dratz, E.A. (1980) Biochim. Biophys. Acta,
   631, 503-506.

5) Jenkinson, S.G., Lawrence, R.A., Burk, R.F. and Gregory, P.E.

(1983) Toxicol. and Applied Pharmacol., 68, 399-404

6) Farnsworth, C.C., Stone, W.L., and Dratz, E.A. (1978)
Biochim. Biophys. Acta, 552, 281-293.

7) Stone, W.L., Katz, M.L., Lurie, M., Marmor, M.F. and
Dratz, E.A. (1979) Photochem. Photobiol., 29, 725-730.

8) Nichols, C.W. and Lambertson, C.J. (1969)
New Engl. J. Med., 281, 25-30.

9) Katz, M.L., Stone, W.L., and Dratz, E.A. (1978) Invest.
Ophthalmol., 17, 1049-1058.

10) Armstrong, D., Hiramitsu, T., Butterridge, J.,
and Nilsson, S.E. (1982) Exp. Eye Res., 35, 157-171.

11) Katz, M.L., Parker, K.R., Handelman, G.J., Bramel, T.L.
Dratz, E.A. (1982) Exp. Eye Res., 34, 339-369.

ACKNOWLEDGEMENTS

Table I. The effect of hyperbaric oxygen (HBO) on a- and b-wave electroretinogram amplitudes (mean±SEM) in rats fed diets deficient or supplemented with vitamin E and/or selenium.

Dietary group 1	a-wave	b-wave
	microvolts	
B+HBO(3)	88±9*	251±41
B(4)	139±13	351±37
B+E+HBO(4)	153±8	315±37
B+E(4)	166±7	312±13
B+Se+HBO(4)	140±16	306±54
B+Se(4)	141±6	266±16
B+E+Se+HBO(4)	143±18	294±37
B+E+Se(4)	147±11	281±37

1 Pure oxygen at 2.0 ATA for 1.5 hr per day was given for 5 days per week for 4 weeks prior to measurement of ERGs. Rats were fed the indicated diets for 6 weeks prior to the measurement of ERGs. Selenium and vitamin E supplementation was 0.4 ppm and 50 mg/kg diet, respectively. The number of rats used in determining a data entry is given in parentheses.

* P<0.05

Table II. Weights and weight gains (mean±SEM) of rats fed diets deficient or supplemented with vitamin E and/or selenium and with or without hyperbaric oxygen treatment.

Dietary group 1	weight gain	weight
	g/100 g/week	g
B++HBO	7.2	170±3
B	10.9	188±2
B+E+HBO	12.5	204±7
B+E	12.5	198±4
B+Se+HBO	9.3	180±3
B+Se	14.4	199±5
B+E+Se+HBO	13.9	190±4
B+E+Se	11.1	187±3
LC	9.7	199±5

1 Hyperbaric oxygen was provided as in Table I but for 3 weeks prior to weight measurements. Rats were on the indicated diets for 5 weeks prior to weight measurements. Dietary supplementation was as described in Table 1.

Table III. Antioxidant levels (mean±SEM) in rats fed diets supplemented or deficient in vitamin E and/or selenium and with or without hyperbaric oxygen (HBO) treatment.

Dietary group 1	plasma vitamin E ug/ml of plasma	glutathione peroxidase	
		plasma milli e.u./ul	RBC milli e.u./mg Hb
B+HBO	1.6±0.2	0.5±0.2	219±55
B	1.9±0.2	0.5±0.2	244±42
B+E+HBO	4.9±0.3	NM	NM
B+E	5.7±0.3	NM	NM
B+Se+HBO	1.5±0.3	3.4±0.4	637±147
B+Se	1.5±0.3	2.2±0.2	658±217
B+E+Se+HBO	5.0±0.8	3.0±0.4	984±180
B+E+Se	5.4±0.4	2.6±0.5	1417±110

1 Hyperbaric oxygen was provided as in Table I but for 1 week prior to measurement of antioxidant levels. Rats were on the indicated diets for 3 weeks prior to measurement of antioxidant levels. Eight rats were in each dietary group and half were treated with HBO. Milli e.u. for glutathione peroxidase activity is nanomoles of NADPH oxidized per min. NM indicates not measured at this time point.

. Table IV. Composition of basal diet.

Ingredient	g/100g
Tourla yeast	36.00
Sucrose	43.05
Corn oil, tocopherol stripped	14.50
Vitamin mix 1	2.20
Mineral mix Draper 2	4.00
L-Methionine	0.25

1. The vitamin mixture provided: (in mg/100 g of diet) ascorbic acid, 99; inositol, 11; choline chloride, 16.5; p-aminobenzoic acid, 11; niacin, 9.9; riboflavin, 2.2; pyridoxine-HCl, 2.2; thiamin HCl, 2.2; calcium pantothenate, 6.6; biotin, 0.05; folic acid, 0.2; vitamin B-12, 0.003. In addition the vitamin mixture contains: (in units /100 g of diet) vitamin A acetate, 1980; calciferol(D3), 220.

2. The salt mix provided (in mg/100 g of diet): $CaCO_3$, 654; $CuSO_4.5H_2O$, 0.72; $Ca_3(PO_4)_2$, 1422; Ferric citrate.$3H_2O$, 64; $MnSO_4.H_2O$, 5.5; potassium citrate.H_2O, 946; KI, 0.16; K_2HPO_4, 309; NaCl, 432; $ZnCO_3$, 1.8; and $MgCO_3$, 164.

1984 USAF-SCEEE SUMMER FACULTY RESEARCH PROGRAM

Sponsored by the

AIR FORCE OFFICE OF SCIENTIFIC RESEARCH

Conducted by the

SOUTHEASTERN CENTER FOR ELECTRICAL ENGINEERING EDUCATION

FINAL REPORT

NAPHTHALENE ADSORPTION BY FLORIDA SOILS

Prepared by: Dr. Jimmy J. Street

Academic Rank: Associate Professor

Department and   Soil Science Department
    University: University of Florida

Research Location: Tyndall Air Force Base
                          Environics Laboratory
                          Tyndall AFB, Florida 32403

USAF Research   Mr. Thomas Stauffer

Date: September 17, 1984

Contract No: F49620-82-C-0035

NAPHTHALENE ADSORPTION BY FLORIDA SOILS

by

Jimmy J. Street

ABSTRACT

.Fifteen Florida soils and a synthetic Al and Fe hydroxide and a
natural humic acid were evaluated for naphthalene adsorption via a
batch equilibrium experiment. Use of the Langmuir and Freundlich
adsorption equations were only moderately successful in describing
the adsorption process. Evaluation of several soil chemical properties
and their relationship to the adsorption of naphthalene indicated that
only soil organic carbon was important, while pH, mineralogy, "active"
Al and Fe content were not important.

It appears from this study that adsorption of naphthalene, a
non-ionic, non-polar organic constituent of Air Force jet fuels, can
be adsorbed by soils and thus this process will play an important role
in the environmental fate of this compound in the soil/water system.
The nature of the chemical interaction of naphthalene and soil organic
matter was not elucidated, but base line data on the importance of soil
organic matter was accumulated.

Acknowledgement

I. INTRODUCTION:

The release of aircraft fuels to the environment and the subsequent impact on the environment is of great concern to the United States Air Force. Distillate fuels are complex mixtures of aliphatic and aromatic hydrocarbons. Several of these organic constituents are highly toxic and their fate in the environment is a high priority research for the Air Force.

The primary pathways for dissipation of jet fuel hydrocarbons in the environment include volatilization, abiotic and biotic sorption, and degradation. The primary pathway for loss of a particular hydrocarbon depends on its solubility, volatility, molecular size and configuration, polarity, and functional group chemistry. In conjunction with the chemistry of the organic compound, the physical and chemical properties of soils, sediments and waters receiving these organic compounds must also be considered. The soil is often the receiving medium for many of the organic compounds dispersed into the environment. There is potential danger that some toxic organic compounds may penetrate the soil and contaminate the groundwater and thus cause a monumental health problem.

The migration and/or transformation of organic compounds in soils is influenced by a myriad of factors in the soil environment. However, the most influential of these factors is the adsorption of the compounds by soil constituents. The adsorption of organic compounds by soils has been shown to be related to a number of soil properties including pH, CEC, clay content and type, organic matter content and hydrous metal oxide content(Means et al., 1979; Osgerby, 1970; Karickhoff et al., 1979; Means et al., 1980).

The majority of research dealing with organic compounds and ad-
sorption on to soil and soil constituents has dealt with ionic or polar
organic molecules such as insecticides, herbicides, and toxic contaminants.
Two classes of non-ionic organic pollutants are currently being investi-
gated by the Air Force. They are those typically found in cleaning
solvents and degreasers such as trichloroethylene(TCE) and those found
in jet fuels such as toluene and naphthalene. The adsorption of non-
ionic organic compounds such as naphthalene has been referred to as
hydrophobic adsorption. Hydrophobic adsorption increases as compounds
become less polar; that is, as molecular weights, molecular volumes,
or carbon numbers increase and as water solubilities decrease(Gustafson
et al., 1968; Gustafson and Paleos, 1971).

Hydrophobic adsorption of certain organic compounds has been highly
correlated with the organic carbon content of soils and sediments
(Karickhoff et al., 1979; Khan et al., 1979; Hassett et al., 1980).

II. OBJECTIVES

The objectives of this summer research period were to determine
the amount of naphthalene adsorbed on different Florida soils and the
type of adsorption isotherm equation that best describes the adsorption.
Secondary objectives were to relate certain soil chemical properties with
the intensity and magnitude of naphthalene adsorption. The types of
adsorption equations investigated were the Langmuir and Freundlich
equations and the soil chemical properties including mineralogy, soil
organic carbon, pH, E_4/E_6 ratio of the humic material, and "active" Fe
and Al content.

III. MATERIALS AND METHODS

Experimental soils

Fifteen soils were collected from the State of Florida based upon their diversity in mineralogy, clay content, and organic matter content. Soils were classified according to the SCS system and the characterization data obtained from the Soil Science Department at the University of Florida. Soils were air-dried and screened to pass a 2 mm stainless steel sieve and stored until needed. The chemical and physical characteristics are shown in Table 1.

Total soil carbon (i.e., organic matter content) was determined at Tyndall Air Force Environics Laboratory using the wet combustion technique described by Nelson and Summers(1982). A titrimetric procedure for CO_2 determination using KOH was employed for quantitation of soil organic carbon. Soil organic matter characterization was done using the extraction scheme described by Schnitzer(1982). Humic and Fulvic acids from all 15 soils were isolated and dried using a rotary evaporator and stored for later analysis. The E_4/E_6 ratio of the isolated humic materials were measured on a Cary model 219 uv spectrophotometer using the method described by Schnitzer(1982).

Naphthalene analysis was performed using a Water's Associates HPLC unit using a model 450 variable wavelength uv detector at 220 nm wavelength, 1 cm cell path, μ-Bondapak C_{18} column, and a 75%/25% acetonitrile/water elutent. Known naphthalene standards were prepared in decane and used to quantitate the saturated aqueous solution of naphthalene and the various dilutions used in the adsorption study.

Table 1. Selected Soil Chemical Properties of Experimental Soils

Soil	$\frac{Al[1]}{\%}$	$\frac{Fe[1]}{\%}$	$\frac{Organic\ C}{\%}$	E_4/E_6	pH
Orangeburg B22tg	0.15	1.50	0.15		3.9
Bethera B21tg	0.01	0.36	0.22		3.7
Hornsville B21t	0.39	2.40	0.27		3.8
Myakka Ap			0.32	3.91	
Arredondo Ap			0.37	4.90	5.8
Duplin B2t	0.83	2.80	0.47		3.7
Orangeburg Ap	0.03	0.23	0.51	4.72	4.4
Cander Ap			0.60	3.57	
Greenville Ap	0.29	2.30	0.71	4.81	4.9
Bethera A1	0.02	0.27	0.83	4.74	4.0
Duplin A1	0.10	0.83	0.87	4.45	3.9
Oktibbeha Ap	0.44	4.20	0.97		5.3
Hornsville A1	0.49	0.32	1.04	4.58	4.5
Appalachee Ap	0.23	2.90	1.41	5.53	4.1
Terra Ceia Muck			13.62	6.39	5.8

[1] "Active" Al and Fe extracted by cit.-dith. method

Soil Components

Synthetic Al and Fe hydroxides were prepared by titrating $Al_2(SO_4)_3$ and $FeCl_3$ with NaOH to a metal/hydroxide ratio of 1:3. The metal hydroxides were washed repeatedly with deionized water until a negative Cl test with $AgNO_3$ was obtained. Metal hydroxides were freeze-dried and stored at 5°C until needed. Humic acid was extracted from a Terra Ceia muck by the method of Schnitzer(1982). The humic acid was then freeze-dried and stored at room temperature until used.

Adsorption Experiments

Adsorption studies were performed in acid-washed 40 ml polyethylene centrifuge tubes sealed with teflon septums and screw-type caps. Five grams of soil, 200 mg of $Al(OH)_3$ and $Fe(OH)_3$, and 100 mg of humic acid were placed in the tubes and the appropriate amount of saturated naphthalene solution added and the tubes brought to maximum volume with 0.1 $\underline{N}$ $CaCl_2$ solution to minimize head space and subsequent naphthalene volatilization loss. Tubes were placed on a rotary tumbler and mixed for 24 hours. Samples were then centrifuged for 20 minutes at 9000 rpm in a Sorvall refrigerated centrifuge. One hundred μl of supernatent was withdrawn and analyzed for naphthalene as previously described. Known standards were included on each run to account for adsorption on to container walls. Initial naphthalene concentrations were approximately 2.7, 5.4 13.0, 20.3, and 26.0 μg/ml. The mass of naphthalene adsorbed was calculated as the difference in initial and final concentration minus the amount absorbed by the container walls.

IV. RESULTS AND DISCUSSION

The naphthalene adsorption isotherms were obtained by equilibrating 5.00 g portions of air-dried soil with 40 mls of 0.01 $\underline{M}$ $CaCl_2$ solutions containing 0, 2.7, 5.4, 13.0, 20.3, and 26 μg naphthalene per ml of solution in 40 ml septum-capped polyethylene centrifuge tubes. The equilibrium naphthalene concentration in μg/ml was plotted versus the μg of naphthalene adsorbed per g of soil or sorbate. All adsorption data for all 15 soils and the synthetic Al and Fe hydroxides and the natural humic acid were plotted according to the Langmuir and Freundlich equations. The form of the Langmuir equation used was

$$C/S = \frac{1}{kS_{max}} + \frac{C}{S_{max}} \tag{1}$$

where C, S, S_{max}, and k are the equilibrium solution concentration of the adsorbate, the amount of adsorbate adsorbed at C, the maximum adsorption, and a constant, respectively. If the adsorption fits the Langmuir equation, a plot of $1/S$ versus $1/C$ should yield a straight line with a slope of $1/S_{max}$ and an intercept of $1/kS_{max}$.

The second type of adsorption equation investigated was the Freundlich equation

$$S_o = kC_o^{1/n} \tag{2}$$

where S_o, C_o, k, and $1/n$ are the amount of adsorbate adsorbed, the equilibrium solution concentration of adsorbate, a constant, and a constant, respectively. The logarithm form yields

$$\log S_o = \log k + 1/n \log C_o \tag{3}$$

138-9

A plot of log S_o versus log C_o yields a straight line with a slope of $1/n$ and an intercept of log k. Data fitting either of these adsorption models does not imply information regarding the chemical nature of nor the mechanism of adsorption, but rather allows an empirical description of the overall adsorption process. However, in the case of the Langmuir equation, the parameters S_{max} and k are of predictive value because they are the adsorption maximum at which naphthalene forms a monolayer on the solid surface and a constant related to the bonding energy of the naphthalene on the solid surface, respectively.

There was not a consistent trend for either adsorption equation on all fifteen soils. In some cases the Langmuir equation better described naphthalene adsorption, and in other cases the Freundlich equation was better suited. There was not a significant statistical relationship between any of the soil chemical properties listed in Table 1 and the adsorption equation parameters S_{max}, Langmuir k, $1/n$, or the Freundlich k. However, there was a strong relationship between soil organic C and increased naphthalene adsorption. In general, increasing soil organic C increased naphthalene adsorption across all soils. It appears that adsorption on to Al and Fe oxides is of little or no significance as evident by evaluating the subsoil horizons of 4 of the experimental soils in addition to the synthetic Al and Fe hydroxides.

The relationship between soil organic C and naphthalene adsorption is not clear because of the variability in soil organic matter. In order to better characterize the soil organic matter, the humic material was extracted from several soils and characterized by the E_4/E_6 ratio to determine certain properties of the humic fraction. The ratio of optical densities or adsorbances of silute, aqueous humic and fulvic acid solutions

at 465 and 665 nm (E_4/E_6) has been shown to: (1) indicate particle size; (2) be correlated with free radical concentration, contents of O, C, CO_2H and total acidity; (3) not be related to the concentration of condensed aromatic rings.

In general, the soil organic C content decreases with depth in most soil profiles and thus comparisons of adsorption data from the top soil and the subsoil of the same profile indicate the contribution of soil organic C to the adsorption process. Although all fifteen soils were evaluated, only the data from the following soils will be discussed: Orangeburg Ap, Orangeburg B22tg, Terra Ceia muck, and Bethera B21tg. The adsorption of naphthalene on the Orangeburg Ap and B22tg (subsoil) are shown in Figures 4a and 8a. It can be seen in these figures that the Ap horizon significantly adsorbs more naphthalene than the subsoil horizon (B22tg).

Evaluation of the Langmuir and Freundlich equations for the two Orangeburg soils indicates that either equations describes naphthalene adsorption for the Ap sample, but neither appear to describe the adsorption on the subsoil (B22tg)(Figures 4b, 4c, 8b, 8c). The two soils that exhibited the maximum and minimum naphthalene adsorption were the Terra Ceia muck and the Arredondo fine sand (Figures 9a and 11a). The Langmuir or the Freundlich equation describes naphthalene adsorption on the Terra Ceia muck, but neither produce a good fit for the Arredondo sand. All experimental soils exhibited some capacity for naphthalene adsorption with increasing adsorption related to increasing organic carbon, but not related to mineralogy, pH, or "active" Al and Fe oxides and hydroxides.
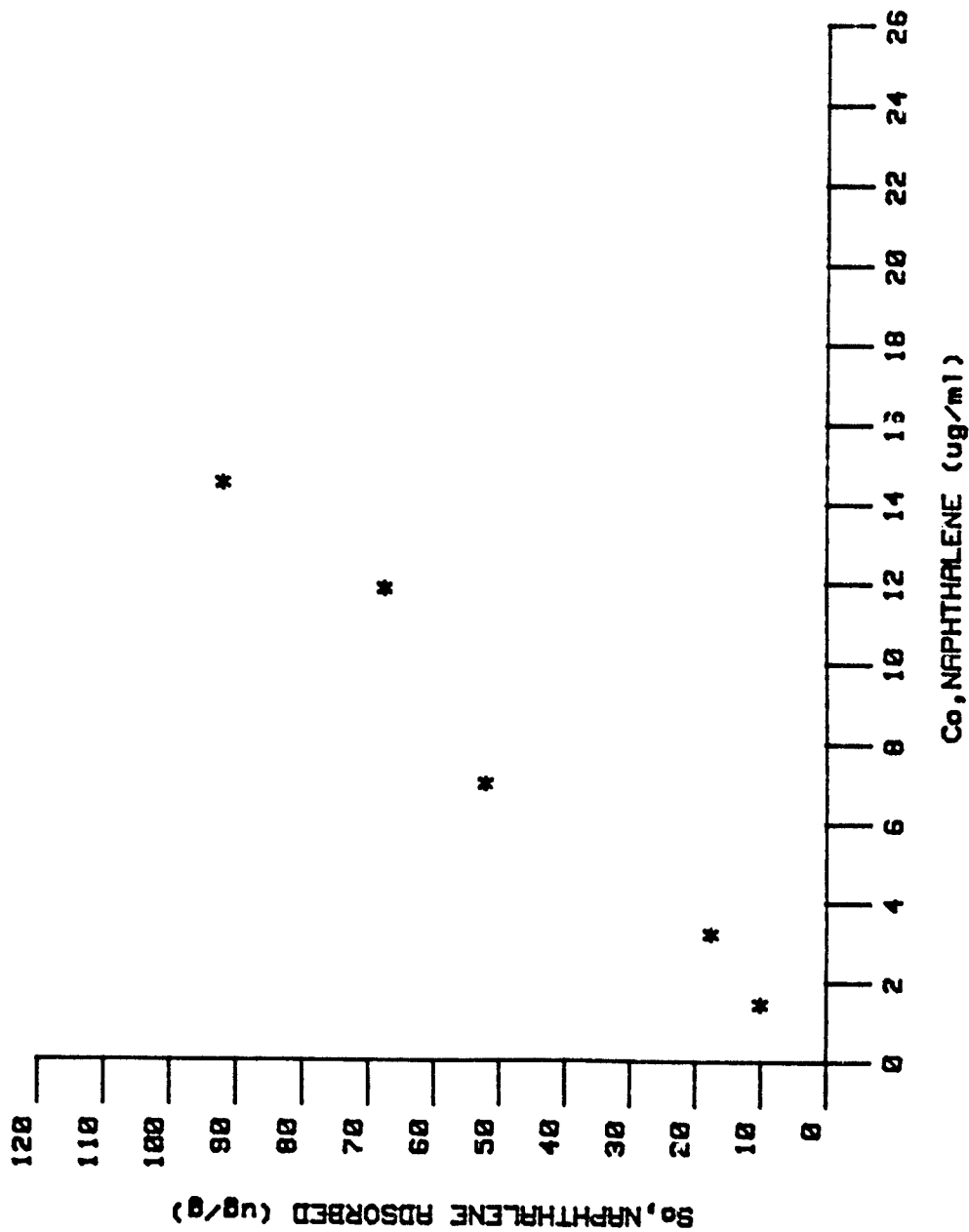
FIG.4a : NAPHTHALENE ADSORPTION ON ORANGEBURG Ap SOIL
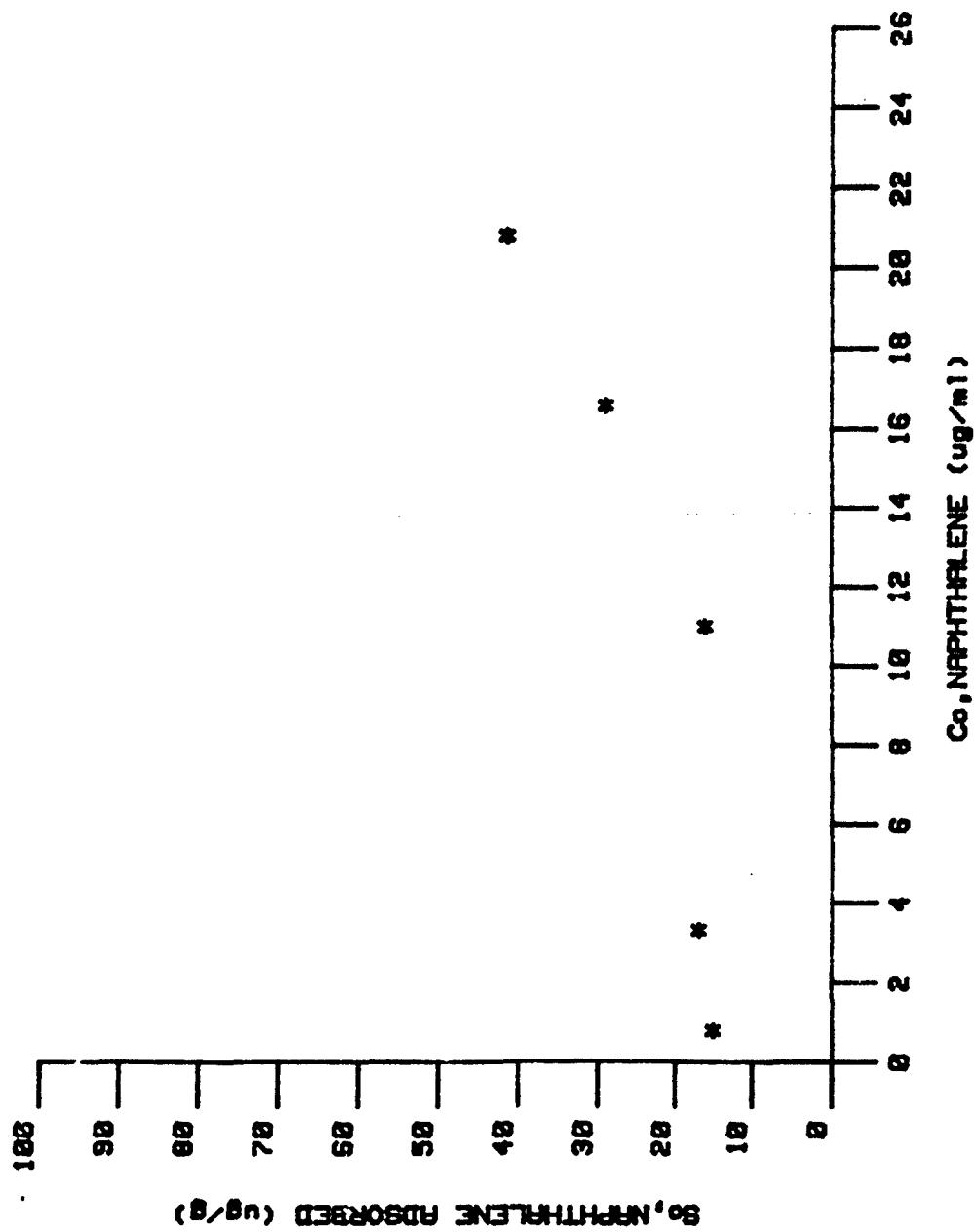
FIG.8a : NAPHTHALENE ASORPTION ON ORANGEBURG B22tg SOIL

138-13
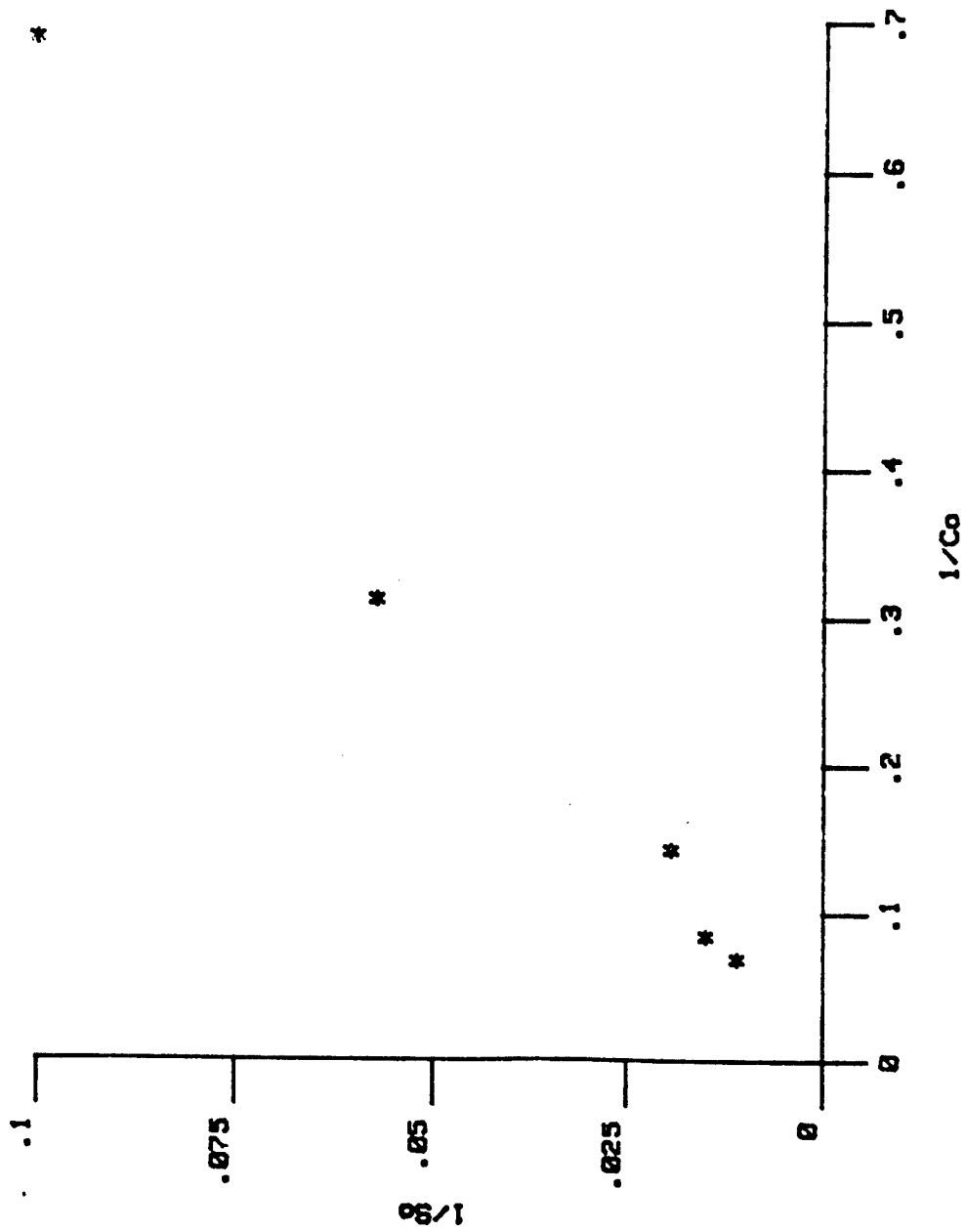
FIG.4b : LANGMUIR PLOT FOR ORANGEBURG Ap SOIL

138-14
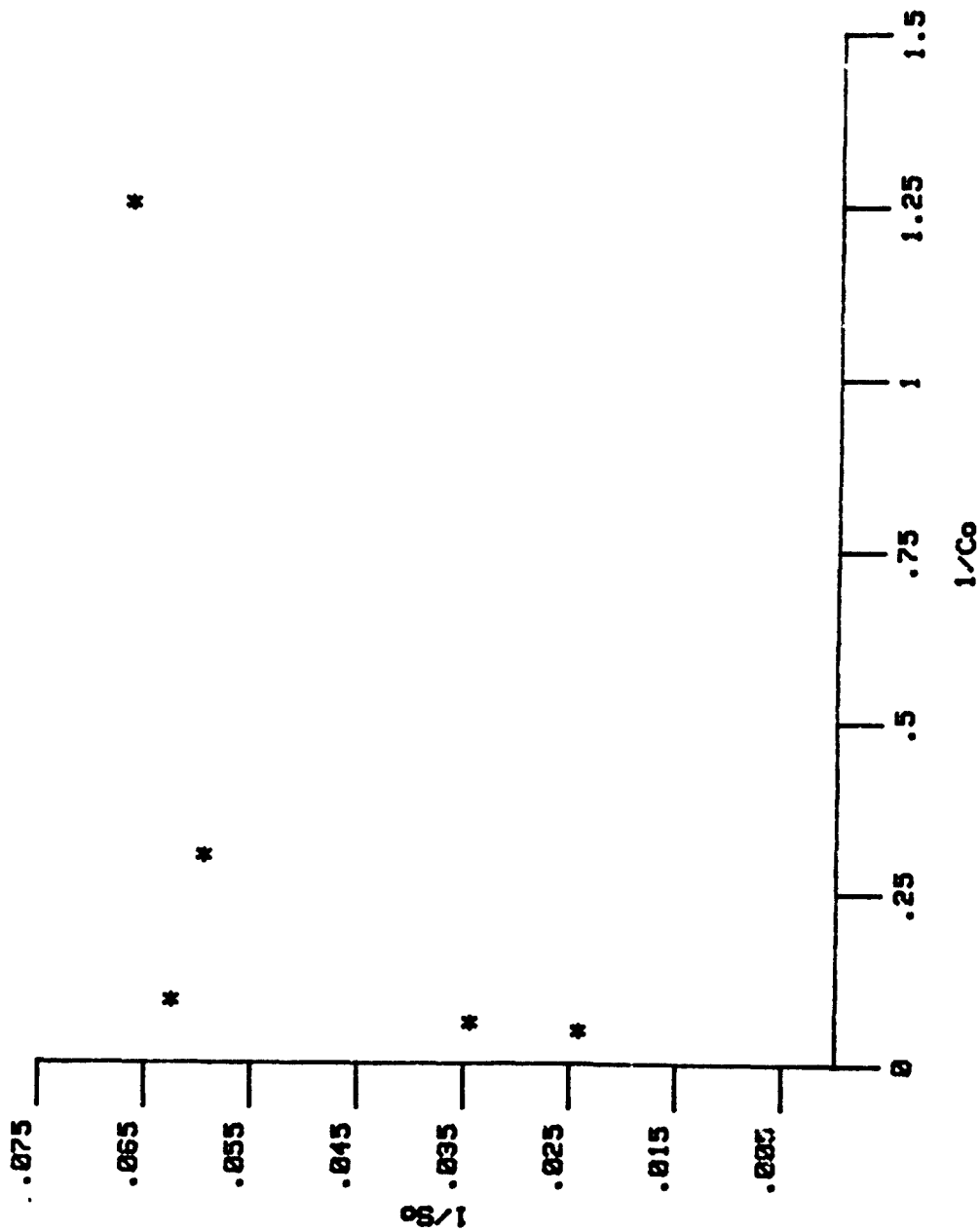
FIG.8b : LANGMUIR PLOT FOR ORANGEBURG B22tg SOIL
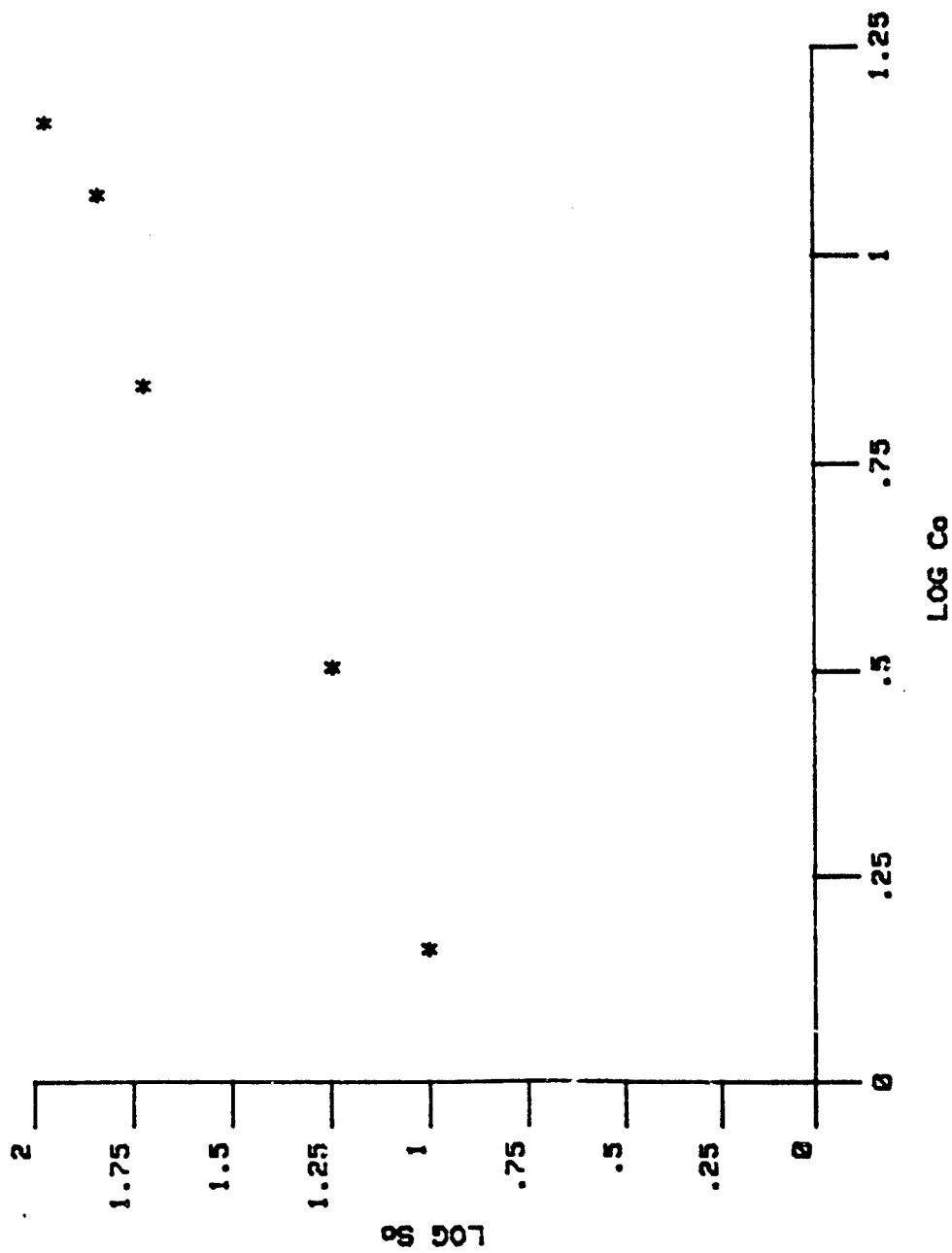
FIG.4a : FREUNDLICH PLOT FOR ORANGEBURG Ap SOIL

FIG.8a : FREUNDLICH PLOT FOR ORANGEBURG B22tg SOIL

LOG Co

LOG Qe
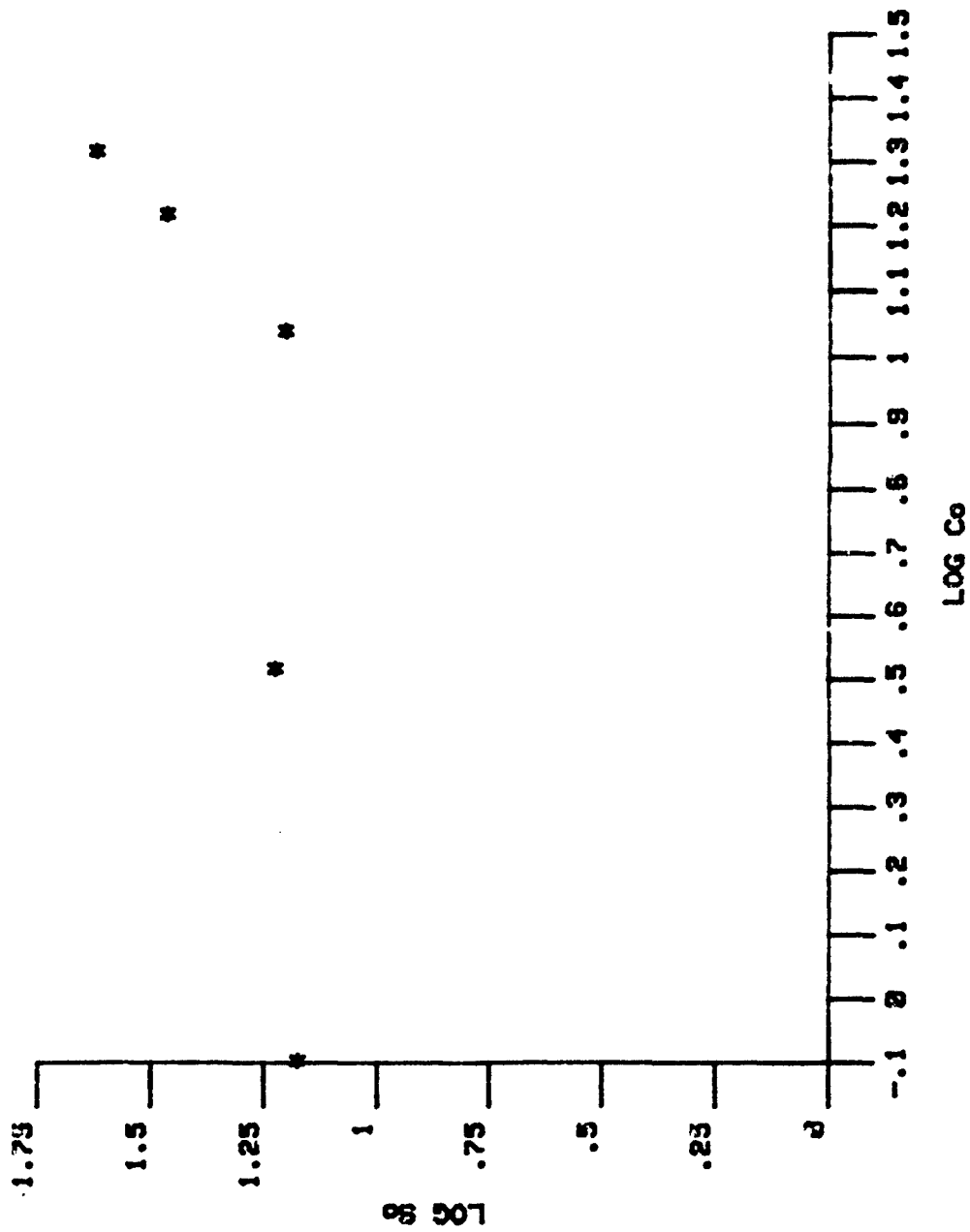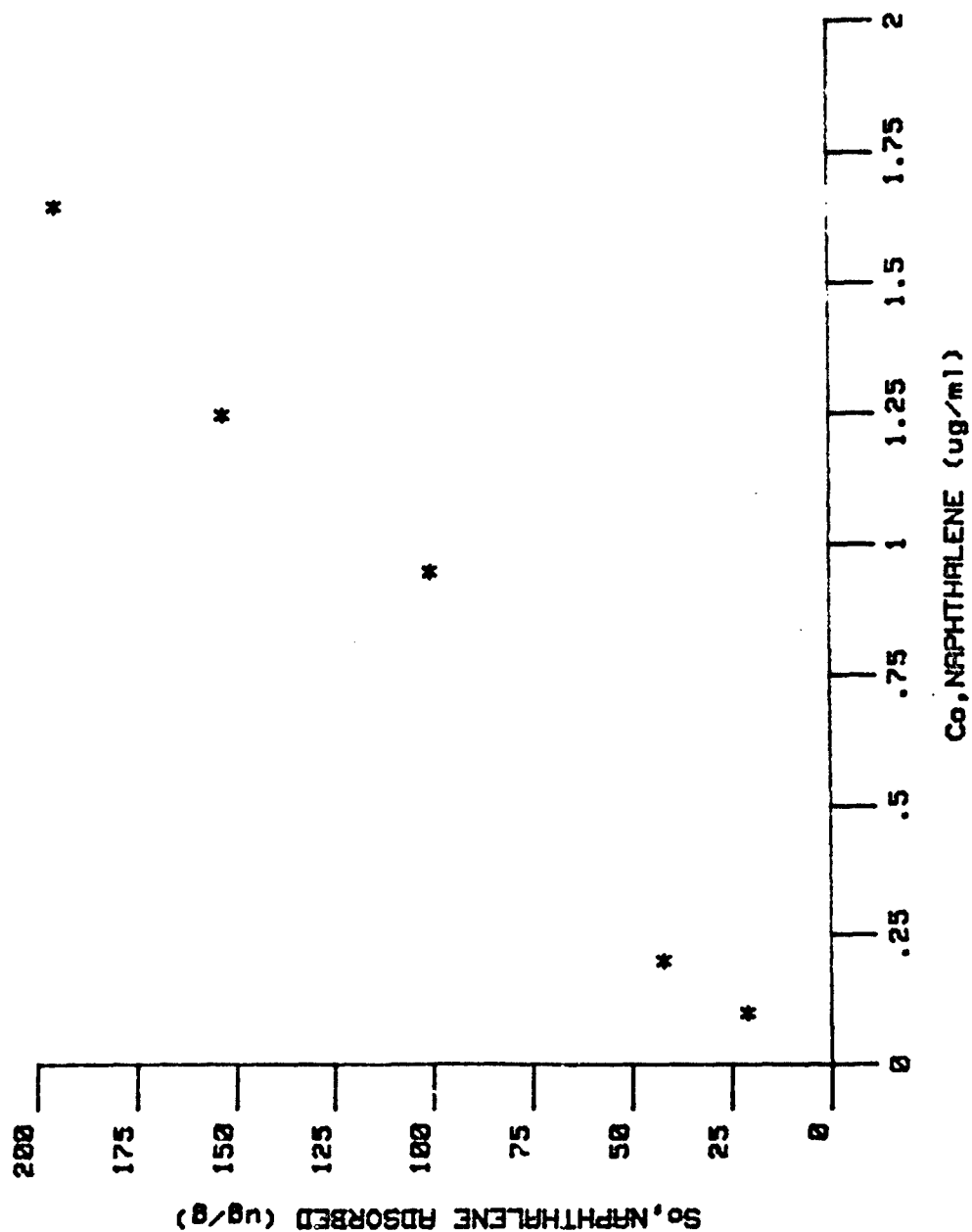
FIG.9a : NAPHTHALENE ADSORPTION ON TERRA CEIA MUCK

138-18
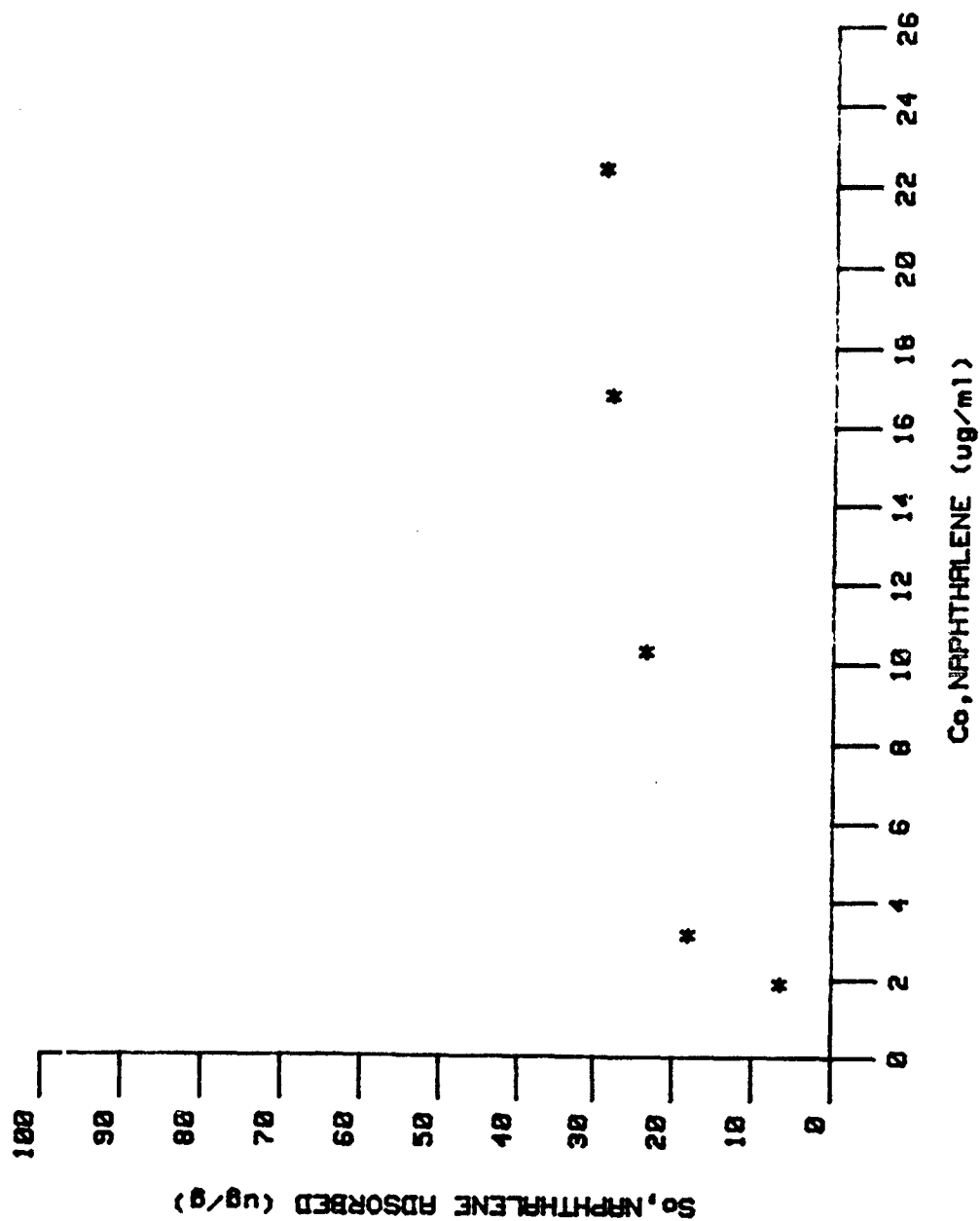
FIG.11a : NAPHTHALENE ADSORPTION ON ARREDONDO SOIL

VI. RECOMMENDATIONS

Results from the experiments conducted this summer at the Environics Laboratory at Tyndall AFB, Florida, indicate the importance of soil organic matter in the adsorption of naphthalene by soils. However, to better manage the fate of this Air Force fuel constituent, the following information or experiments are needed:

(1) The nature of the chemical interaction of a non-ionic, non-polar compound such as naphthalene and soil organic matter needs to be elucidated via more basic research at a molecular level.

(2) The reversibility of the adsorption process and the kinetics of this process needs to be investigated to assure a mass balance approach to the fate of naphthalene in the soil/water system.

(3) Adsorption of naphthalene from more complex (i.e., multiple solvent system) solutions that closely simulate jet fuels needs evaluation.

(4) Development of a model that includes volatization, biotic degradation, adsorption/desorption processes and transport components that will assist in the evaluation of the overall impact of naphthalene in the environment.

REFERENCES

1. Gustafson, R.L., R.L. Albright, J. Heisler, J.A. Lirio, and O.T. Reid, Jr. 1968. Adsorption of Organic Species by High Surface Area Styrene-Divinyl-Benzene Copolymers. Ind. Eng. Chem. Prod. Res. Dev. 7:107-115.

2. Gustafson, R. and J. Paleos. 1971. Interactions Responsible for the Selective Adsorption of Organics on Organic Surfaces. pp. 213-237. In S. D. Faust and J.V. Hunter (Ed.) Organic Compounds in Aquatic Environments. Marcel Dekker, Inc., New York.

3. Karickhoff, S.W., D.S. Brown, and T.A. Scott. 1979. Sorption of Hydrophobic Pollutants on Natural Sediments. Water Res. 13:241-248.

4. Khan, A., J.J. Hassett, W.L. Banwart, J.C. Means, and S.G. Wood. 1979. Sorption of Acetophenone by Sediments and Soils. Soil Sci. 128:297-302.

5. Hassett, J.J., J.C. Means, W.L. Banwart, and S.G. Wood. 1980. Sorption Properties of Sediments and Energy-related Pollutants. Ecological Research Series EPA-600/3-80-041, Athens, Georgia.

6. Schnitzer, M. 1982. Chapter 30-Organic Matter Characterization. In Methods of Soil Analysis, Part 2 - Chemical and Microbiological Properties. 2nd Edition. Edited by A.L. Page, R.H. Miller and D.R. Keeney. Madison, Wisconsin.

7. Nelson, D.W. and L.E. Sommers. 1982. Chapter 29-Total Carbon, Organic Carbon and Organic Matter. In Methods of Soil Analysis, Part 2-Chemical and Microbiological Properties. 2nd Edition. Edited by A.L. Page, R. H. Miller and D. R. Keeney. Madison, Wisconsin.

8. MacIntyre, W.G., C.L. Smith, P.O. deFur and C.W. Su. 1982. Hydrocarbon Fuel Chemistry; Sediment Water Interaction. Final Report on USAF/AFESC, Contract No. F08635-81-C-0019.

1984 USAF-SCEE SUMMER FACULTY RESEARCH PROGRAM

Sponsored by the

AIR FORCE OFFICE OF SCIENTIFIC RESEARCH

SOUTHEASTERN CENTER FOR ELECTRICAL ENGINEERING EDUCATION

FINAL REPORT

AN OPTIMAL TRAJECTORY PROBLEM

Prepared by: Dr. John J. Swetits

Academic Rank: Professor

Department and   Department of Mathematical Sciences
    University: Old Dominion University

Research Location: Wright-Patterson Air Force Base
                      Avionics Laboratory, Surface Strike Group

USAF Research: R. Bryan

Date: September 18, 1984

Contract No: F49620-82-C-0035

AN OPTIMAL TRAJECTORY PROBLEM

by

John J. Swetits

ABSTRACT

A least cost model for determining an optimal trajectory for attacking multiple targets on a single pass of the attacking aircraft is investigated. A Quasi-Newton procedure and a Levinberg-Marquardt procedure for solving an unconstrained model are compared. A penalty-multiplier method for solving a constrained model is investigated.

I. INTRODUCTION

One of the most demanding tasks forcing the Air Force is countering the massed armor attack. The problem for the Air Force is to destroy enough targets, fast enough, with an acceptable aircraft survival rate. Present day weapon delivery and fire control systems are oriented primarily toward attacking a single target per pass. A means for attacking multiple targets on a single pass is needed, not only to increase the target kill rate, but also as a way of reducing aircraft attrition.

In the intermediate range of target spacing, there presently exists no fire control guidance, either to the pilot or to an automatic control system, for either aircraft trajectory or targeting sensor control. For a pilot to sequence present day fire control systems for each target, simultaneously choosing an aircraft trajectory that maintains survivability as well as accurate weapon pointing, would be a virtually impossible task. An algorithm that generates near-optimal trajectory guidance would solve these problems.

In the feasibility study described in [8], a trajectory model was developed that resulted in an unconstrained cost function which is to be minimized to obtain an optimal attack trajectory. The cost was expressed as a sum of squares of a set of residuals. For the model that was considered, twenty four independent variables and one hundred and ninety-two residuals were involved. A Levenberg-Marquardt [6] algorithm was used in [8] for the minimization of the cost function. Since the cost function was unconstrained, a number of difficulties were noted. Some of the optimal trajectories contained undesirable or unrealistic features. Mathematical conditioning problems were also noted, and there were some questions about the efficiency of the Levenberg-Marquardt algorithm.

II. OBJECTIVES

The main objective of the project was to investigate a constrained version of the optimization problem described in I. In order to gain some insight into the unconstrained cost function, the unconstrained problem was investigated through a Quasi-Newton [4,5] optimization algorithm. The objective here was to obtain a comparison with the Levenberg-Marquardt algorithm. A penalty-multiplier technique [2] was used to investigate a constrained version of the problem wherein the aircraft altitude was constrained.

III. QUASI-NEWTON METHODS

Let F be a real valued function of n real variables. Then it's well known [4] that $\bar{x}$ is a local minimum of F if F is sufficiently smooth, $\nabla F(\bar{x}) = 0$, where ∇F is the gradient of F, and $\nabla^2 F(\bar{x})$ is positive definite, where $\nabla^2 F$ denotes the Hessian of F. A popular technique for locating $\bar{x}$ is Newton's method. Let x_k be an estimate of $\bar{x}$. Then the next estimate, x_{k+1}, is chosen to satisfy

$$x_{k+1} = x_k - (\nabla^2 F(x_k))^{-1} \nabla F(x_k) . \qquad (1)$$

Newton's method works very well with rapid convergence if the initial estimate of $\bar{x}$ is sufficiently close to $\bar{x}$. However the difficulties with the method are well known and are detailed, for example, in [4].

The difficulties mentioned above motivated the development of a class of optimization techniques known as Quasi-Newton methods. The methods are designed to be globally convergent and to behave like Newton's method when one is sufficiently close to a minimum of the objective function. A convenient summary of the technique is given in [5], while

detailed convergence results can be found in [4].

Here we briefly describe the procedure and the specific method used in the project. Let x_k be an estimate of $\bar{x}$, a local minimum of F. Let H_k be a positive definite matrix. Generate a search direction, S_k, by

$$S_k = -H_k \nabla F(x_k) . \qquad (2)$$

Locate α_k so that

$$F(x_k + \alpha_k S_k) = \min_{\alpha > 0} F(x_k + \alpha S_k) . \qquad (3)$$

The next estimate, x_{k+1}, of $\bar{x}$ is given by

$$x_{k+1} = x_k + \alpha_k S_k . \qquad (4)$$

Revise H_k to obtain H_{k+1} and repeat (2), (3), (4) until convergence to $\bar{x}$ is obtained. H_{k+1} is required to be positive definite and to satisfy

$$x_{k+1} - x_k = H_{k+1}(\nabla F(x_{k+1}) - \nabla F(x_k)) . \qquad (5)$$

(5) is known as the Quasi-Newton condition.

For this project, H_{k+1} was obtained from H_k by means of the Broyden-Fletcher-Goldfarb-Shanno updating procedure: with $\delta_k = x_{k+1} - x_k$ and $\gamma_k = \nabla F(x_{k+1}) - \nabla F(x_k)$

$$H_{k+1} = H_k + (1 + \frac{\gamma_k^T H_k \gamma_k}{\delta_k^T \gamma_k}) \frac{\delta_k \delta_k^T}{\delta_k^T \gamma_k} - (\frac{\delta_k \gamma_k^T H_k + H_k \gamma_k \delta_k^T}{\delta_k^T \gamma_k}) . \qquad (6)$$

The efficiency of the above scheme depends on the initial estimate of $\bar{x}$, the initial choice of H_1, and how well (3) can be accomplished. In practice (3) is not accomplished exactly, but α_k is only chosen so that $F(x_k + \alpha_k S_k)$ is sufficiently smaller than $F(x_k)$. For the present

implementation, an Armijo-type procedure [1] was used to achieve the
reduction. In addition it was required that x_{k+1} satisfy

$$S_k^T \nabla F(x_{k+1}) \geq \rho S_k^T \nabla F(x_k) \qquad (7)$$

where ρ was fixed between 0 and 1.

(7) insures that H_{k+1}, given by (6), is positive definite.

The Quasi-Newton method, as described above, tested very well. The
efficiency of the procedure compared with that reported in the
literature on a variety of test problems. However, when the method was
used on the multiple target trajectory problem, it was consistently
inferior to the Levenberg-Marquardt algorithm. Since the updating
procedure given by (6) is generally acknowledged to be the best of the
Quasi-Newton methods [4,5], it seems reasonable to conclude that one
will not be able to improve on the Levenberg-Marquardt algorithm for
the unconstrained optimization problem considered in the project.

IV. PENALTY-MULTIPLIER METHODS

We now consider the constrained optimization problem

$$\text{minimize } F(x)$$

subject to

$$g_i(x) \leq 0, \; i = 1,\ldots,j$$

where each of F, g_i, $i = 1,\ldots,j$, is a real valued function of n real
variables.

One type of penalty-multiplier method for solving the constrained
problem is as follows. Select scalars λ_i^k, $i = 1,\ldots,j$ and c_k. Form

$$L_k = F + \sum_{i=1}^{j} \lambda_i^k g_i^+ + \frac{1}{2} c_k \sum_{i=1}^{j} (g_i^+)^2$$

where

$$g_i^+ = \max\{g_i, -\lambda_i^k/c_k\} .$$

Locate an unconstrained minimum of L_k, say $\bar{x}_k$. Update λ_i^k, $i = 1,\ldots,j$, and c_k to obtain λ_i^{k+1}, $i = 1,\ldots,j$, and c_{k+1}. Use $\bar{x}_k$ as a starting guess for locating an unconstrained minimum of L_{k+1}, where L_{k+1} is obtained from L_k by replacing c_k by c_{k+1} and λ_i^k, $i = 1,\ldots,j$, by λ_i^{k+1}, $i = 1,\ldots,j$. The procedure used for updating λ_i^{k+1}, $i = 1,\ldots,j$, and c_k was

$$\lambda_i^{k+1} = \lambda_i^k + c_k g_i^+(\bar{x}_k), \quad i = 1,\ldots,j$$

and

$$c_{k+1} = \begin{cases} \beta c_k & \text{if } \sum_{i=1}^{j} (g_i^+(\bar{x}_k))^2 > \gamma \sum_{i=1}^{j} (g_i^+(\bar{x}_{k-1}))^2 \\ c_k & \text{if } \sum_{i=1}^{j} (g_i^+(\bar{x}_k))^2 \le \gamma \sum_{i=1}^{j} (g_i^+(\bar{x}_{k-1}))^2 \end{cases}$$

where $\beta > 1$ and $0 < \gamma < 1$ were fixed. A detailed and exhaustive treatment of penalty multiplier methods may be found in [2].

This procedure was chosen in order to obtain baseline information about the trajectory attack problem when aircraft altitude is constrained. It is relatively easy to program and can use existing unconstrained optimization softward. When used with the Levenberg-Marquardt unconstrained optimization algorithm, the procedure produced acceptable attack trajectories. However, the method is slow. Optimal trajectories were obtained but with an unacceptably high number of function evaluations.

VI. RECOMMENDATIONS

Clearly, considerably more work needs to be done to obtain a better understanding of the behavior of the trajectory cost function and to solve the constrained minimization problem in an efficient way. Regarding the latter, there are a number of alternative procedures - feasible directions, penalty methods, dual methods and recursive quadratic programming methods. Of these, the last mentioned appears to offer the best chance of solving the constrained problem in a reasonable amount of time. The basic idea of the method is to solve a sequence of quadratic programming problems wherein the objective function is a quadratic approximation to the Lagrangian of the constrained problem, and the constraints in the quadratic problem are linear approximations to the full constraints. A survey of such methods is given in ⌐3]. Of these, a recent algorithm of Powell ⌐7] appears to offer promise and is well worth investigating.

ACKNOWLEDGEMENT

REFERENCES

1. Armijo, L., "Minimization of Functions Having Lipschitz Continuous First Partial Derivatives", Pacific J. Math., Vol. 16, pp. 1-3, 1966.

2. Bertsekas, D.P., Constrained Optimization and Augmented Lograngian Methods (Academic Press, New York, 1982).

3. Biggs, M.C., "Recursive Quadratic Programming Methods for Non-Linear Constraints", in Nonlinear Optimization 1981, M.J.D. Powell, ed., (Academic Press, London, 1982), pp. 213-221.

4. Dennis, J.E. and More, J., "Quasi-Newton Methods, Motivation and Theory", S.I.A.M. Review, Vol. 19, pp. 46-89, 1977.

5. Fletcher, R., Practical Methods of Cptimization, Vol. 1, Unconstrained Optimization, (John Wiley, Chichester, 1980).

6. Marquardt, D.W., "An Algorithm for Least Squares Estimation", S.I.A.M. J. Applied Math., Vol. 11, pp. 431-441, 1963.

7. Powell, M.J.D., "A Fast Algorithm for Nonlinearly Constrained Optimization Calculations", in Numerical Analysis, Dundee 1977, G.A. Watson, ed., (Lecture Notes in Mathematics, 630, Springer-Verlag, Berlin, 1978).

8. Wild, T.J., Bryan, R.S. and Wicker, D.W., "Sequential Target Attack-Interim Report", Wright Aeronautical Laboratories, August, 1983.

1984 USAF-SCEEE SUMMER FACULTY RESEARCH PROGRAM

Sponsored by the

AIR FORCE OFFICE OF SCIENTIFIC RESEARCH

Conducted by the

SOUTHEASTERN CENTER FOR ELECTRICAL ENGINEERING EDUCATION

FINAL REPORT

THE ROLE OF VORTEX SHEDDING IN A BLUFF-BODY COMBUSTOR

Prepared by: Dr. Richard S. Tankin

Academic Rank: Professor

Department and   Department of Mechanical and Nuclear Engineering
     University: Northwestern University

USAF Research: Dr. W. M. Roquemore

Date: September 1, 1984

Contract No.:   F49620-82-C-0035

THE ROLE OF VORTEX SHEDDING IN A BLUFF-BODY COMBUSTOR

by

Richard S. Tankin

ABSTRACT

The results from visual observations and studies of high speed cine
pictures of reacting flows with and without heat release in an axisymmetric,
unducted, and vertically mounted bluff-body combustor are presented. For the
reacting experiment without heat release, the fuel, a small concentration of
$TiCl_4$ vapor added to dry air, is ejected from a jet located at the center of
the bluff body. Turbulent mixing of the $TiCl_4$ and H_2O vapor contained in the
annulus air, results in the formation of micron size particles of TiO_2 and
with sheets of light directed both vertically and horizontally, provide a
remarkably detailed visualization of the dynamic structures in the central jet
and the recirculation zone behind the bluff body. The results from similar
experiments with heat release are presented where $TiCl_4$ vapor is added to the
gaseous propane and burned. Vortex shedding from the bluff-body is clearly
evident in the experiments without heat release. However, vortex shedding did
not occur in the combustion propane experiments because the recirculating flow
became laminar as a result of the increase in kinematic viscosity due to the
increase in temperature. Oscillations in the shear layer, observed in all the
combusting experiments, grow in amplitude with increasing annulus air
velocity. However, the flame lifted from the bluff body face before these
oscillations reached sufficient amplitude to produce vortex shedding.

140-2

Acknowledgement

The author would like to thank the Air Force Systems Command, the Air Force Office of Scientific Research and the Southeastern Center for Electrical Engineering Education for providing him with an opportunity to spend a very worthwhile and productive summer at the Aero Proplusion Laboratory, Wright Patterson Air Force Base, Ohio. He would like to acknowledge the laboratory, in particular the Fuels and Lubrication Division, for its cooperation and hospitality.

Finally, he would like to thank Mr. R. L. Britton and M. C. M. Reeves for helping in the initial stages of the experiments and the computations. Special thanks is extended to Dr. W. M. Roquemore for suggesting the research topic and collaborating closely with the author.

I. INTRODUCTION

The Aero Propulsion Laboratory (APL) has developed a bluff body research combustor for the purposes of: (1) evaluating the performance of conventional probes and advanced laser techniques and (2) for conducting experiments to aid in evaluating and developing combustion models. Numerous experiments and theoretical analyses have yielded a detailed understanding of many of the characteristics of the combustor.[1] High speed movies have proven to be the most useful technique for understanding the turbulent combusting flow field. They revealed the existence of large scale vortices shed from the bluff body which plays an important role in the mixing processes in the near and far wake regions. The interpretation of single point laser Doppler anemometer (LDA) and coherent anti-Stokes Raman spectroscopy (CARS) measurements in terms of the large scale structures has been greatly enhanced by the use of high speed cine pictures. Flow visualization coupled with simultaneous single or multiple point measurements is believed to be essential for understanding the details of flows containing large scale structures.

Sheet-lighting has been used in recent years to provide quantitative two-dimensional (2-D) visualization of flow fields. Long, et al., used a Lorenz/Mie scattering technique in an aerosol seeded jet to study the entrainment and mixing processes.[2] Escoda and Long, in a similar study, used Rayleigh scattering to study a freon jet.[3] Crosley[4] and Kychakoff, et al.[5] used fluorescence scattering to record the 2-D view of the OH formed in a flame. Johnson and Bennett studied turbulent mixing processes of coaxial jets discharging into an expanded duct using a fluorescent tracer in a water tunnel experiment.[6] Koochesfahani, et al.[7] and Dimotakis, et al.[8] also used a fluorescent dye in water tunnel experiments to study the mixing in chemically reacting shear layers and jets, respectively. These studies have demonstrated the value of different sheet-lighting techniques for studying flows containing large scale structures.

The objective of this paper is to introduce a two-dimensional (2-D) sheet-lighting technique coupled with a fast chemically reacting system that can provide detailed visualization of turbulent mixing processes without heat release. This technique also offers the potential for making simultaneous velocity and relative product concentration measurements. Visualization results obtained in a small unducted bluff-body combustor, of similar design

to that used in Reference 1, are presented as a demonstration of the technique. Micron size TiO_2 particles are used as the scattering mdeia. These particles are formed as a product of the reaction of $TiCl_4$ and H_2O. This reaction has been used by several investigators to provide seed particles for LDA measurements.[9,10] To our knowledge, however, the potential use of this reactive system as a tool for studying turbulent mixing processes has not been explored. The TiO_2 particle size has been reported to be fairly uniform and is generally in the 0.2 to 1 micron range with only a small fraction in the 2 to 3 micron range.[10] Particles in this size range can follow the flow and also provide good Mie scattering centers. Normally, large concentrations of TiO_2 particles are formed so that the prospects of obtaining unbiased LDA results by uniformly sampling, as demonstrated in Reference 10, appear good. The scattered light intensity from a measurement volume might also be directly proportional to the TiO_2 concentration; however, this point needs to be carefully examined before such a claim can be made. The reaction seems to be nearly instantaneous since TiO_2 particles begin to form just at the exit of a high speed jet in which a uniform mixture of $TiCl_4$ and dry air is injected into humid air. This indicates that the reaction is mixing limited and can be effectively used to study turbulent mixing processes. The corrosive nature of $TiCl_4$ and HCl may have discouraged its use in the past but with proper handling procedures and good ventilation and exhaust systems, this does not appear to be a serious problem.

II. OBJECTIVES OF RESEARCH EFFORT

The objective of this research was to study, by sheet-lighting, the reaction zone using $TiCl_4$ vapor and dry air as fuel and room air as the oxidizer. The water vapor in the room air reacts with the $TiCl_4$ to form TiO_2 particles. High speed motion pictures and 35 mm still pictures were taken. The Mie scattering from the TiO_2 particles gives an insight into the complicated fluid flow in the reaction zone as well as the vortex shedding.

III. EXPERIMENTAL SET-UP

A schematic diagram of the experimental set-up is shown in Figure 1. The bluff body combustor was symmetrically mounted in a small vertical combustion tunnel. The fuel nozzle located at the center of the 60 mm diameter bluff

body is 4.78 mm in diameter. This nozzle has a short-tapered contour as recommended by ASME for providing a flow with a flat velocity profile and low tubulence intensity at the exit. The combustion tunnel was also designed to provide air with a flat velocity profile and low turbulent level to a test section. The tunnel, with an 80 mm diameter, can be operated either ducted or unducted. For the experiments reported in this paper, it was unducted and thus subject to room air currents. During the experiments, the only ventilation system operating was the exhaust hood which was placed about 50 cm directly above the tunnel. Though precautions were taken to still the room air, disturbances in the combustor flow field attributed to room air currents were occasionally observed, especially when the combustor was operated at annulus velocities of 2 m/s or less.

The 60 mm diameter bluff body has also been operated in the 254 mm diameter, ducted combustion tunnel at APL. Although the results from these experiments will not be presented in this paper, several observations are noteworthy. In the large ducted tunnel, the flame was attached to the bluff body face at annulus velocities in excess of 20 m/s; whereas in the small unducted tunnel, the flame lifted from the face when the velocity exceeded about 4 m/s. If the small tunnel was operated long enough for a layer of soot about 2 mm thick to form on the bluff body face, the flame would remain attached for velocities up to 8 m/s. The combusting experiments reported in this paper at high annulus velocities used the soot layer to stabilize the flame. About a ± 2.5% variation in the annulus velocity at different spatial locations was noted in the small tunnel. This variation did cause some asymmetry in the flow field and could have contributed to the flame detachment problem. Vortex shedding from the bluff body was observed in the large tunnel with an annulus velocity of about 18 m/s but not in the small tunnel where the velocity was about 8 m/s.

The flow rate in the central jet at the nozzle exit is measured with calibrated rotameters. A pressure regulator is used to set and maintain a given flow rate of air to the annular region of the nozzle. A pitot tube and precision monometer are used to determine the velocity at the annular exit. This determination was made prior to each test run.

Experiments were conducted with building air flowing in the annular region and either dry air or propane containing small amounts of $TiCl_4$ vapor

140-6

flowing through the central jet. Some experiments were conducted to show the differences in the flow field with and without heat release. In these experiments, $TiCl_4$ vapor was added to the propane but not ignited. In some combusting experiments, $TiCl_4$ vapor was added to the propane to increase the particle concentration so that cine pictures could be made.

The optical set-up consists of a 4-watt Argon Ion Laser, which is operated at the 5145 A Argon Ion line. The laser beam strikes a quartz rod whose diameter is 8 mm. This rod acts as a cylindrical lens. The light beam fans out in a plane perpendicular to the axis of the quartz rod. The angle of divergence depends on the rod diameter (greater for small diameters). The thickness of the sheet-light is approximately equal to the diameter of the laser beam exiting from the laser (1.25 mm). To increase the intensity of sheet-lighting of the test section, a plane front-surfaced mirror was placed behind the test section. The position of this mirror was adjusted so that the sheet-light is reflected back on itself. In this manner, the light intensity at the test section is increased nearly twofold. Tests were also conducted with horizontal and vertical sheets of light simultaneously appearing in the test section. To accomplish this, a beam splitter, another cylindrical rod, and a mirror were added to the optical set-up. A variable speed chopper was installed at the laser output to allow strobing of the light sheets and make possible observations of dominant frequencies and vortex shedding.

Because of the continuum radiation from hot carbon particles in the propane flames, the laser light scattered by the cooler carbon and TiO_2 particles within certain sections of the flame zone was difficult to observe. This difficulty was overcome by using a narrow, band-pass optical filter. The filter used was centered at 5145 A and had a half-width of 90 A. The light intensity at 5145 A is reduced 40%. With this filter in place, the yellow continuum radiation from the carbon in the reaction zone is nearly eliminated; thus, allowing one to observe the sheet-lit plane within the propane flame.

Still pictures (35 mm) and high speed motion pictures were taken of the sheet-lighted reacting flow. At the beginning of each reel (or roll) of film a target (10 mm grid) was mounted over the center of the nozzle, where the laser sheet is located. The target was used to focus the camera as well as provide a grid for making measurements from the photographs. The sheet-light

140-7

intensity was sufficient to allow still picture, in most instances, to be taken at f 4.0 1/2000 second. Motion pictures were taken, in most instances, at f 2.8 and 1000 frames per second. The shutter speed of the motion pictures is approximately 1/2600 sec. To take pictures when the sheet-light is horizontal, a mirror was installed at about 60 cm above the nozzle. Thus, it was possible to make photographs directly above the nozzle with the optical axis of the camera perpendicular to the horizontal sheet-light. When the optical filter was in place, it was necessary to increase the exposure time one stop.

Tests were conducted over a wide range of operating conditions. For example, in the cold flow experiments, the Reynolds number of the annular flow was varied from 1250 to 22,500, the central jet from 290 to 5,000. For the propane experiments, the Reynolds number of the annular flow varied from 2500 to 10,000; the central jet from 500 to 11,000, calculated based on inlet conditions.

IV. RESULTS AND DISCUSSIONS

This section is organized into two subsections: Reacting Cold Flow and Combusting Flow. The results obtained from ejecting a mixture of $TiCl_4$ vapor and dry air from the central jet and mixing this with moist air from the annulus are presented in the reacting cold flow subsection along with the locations of the forward and aft stagnation points for a wide range of annulus velocities. Descriptions of the flow field that result for different fuel velocities and a trace of the time history of shed vortices are also presented. The combusting flow fields are described in the combusting flow subsection. $TiCl_4$ vapor was added to the central propane jet to aid in visualizing the flow field through the flame. Also, some photographs of the non-combusting propane and $TiCl_4$ mixture are presented.

IVa. Reacting Cold Flow

Location of Forward and Aft Stagnation Points. The bluff body combustor can be thought of as two widely spaced jets: an annular jet and a central fuel jet. A recirculation zone is established as a result of the expansion and entrainment of the annular jet. The reverse flowing air in the recirculation zone is in direct opposition to the flow of the central jet.

For flow conditions at which the momentum of the reverse flowing air is larger than the momentum of the central jet, the central jet flow will be turned back towards the bluff body. The axial velocity of the central jet is zero at the point where this occurs. The centerline location, where the central jet is turned, is called the forward stagnation point. The maximum centerline length of the recirculation zone is called the aft stagnation point. When the momentum of the central jet is larger than that of the reverse flowing air, the central jet will penetrate the recirculating zone, and hence no stagnation points exist along the centerline.

The forward and aft stagnation points were measured over a wide range of annular and central jet velocities. These measurements were made by simply mounting an L-shaped tube on a vertical traversing mechanism and using it as a positioning probe that could be readily moved in and out of the test section. Some judgement is required on the mean location of the stagnation points because of fluctuations, but by visually averaging, the results appear to repeat fairly well. (A typical set of sheet lighted photographs are shown in Figure 2.)

The procedure is as follows: The annular air flow is set at a prescribed flow (determined by pitot measurements) and the central fuel jet (TiCL$_4$ vapor and air) is varied incrementally until the jet penetrates. At each incremental change, the position of the forward stagnation point is measure. Two sets of data were collected on different days. Figure 3 shows a typical set of data points. Except for the lowest annular flow rates (1 to 3 m/s) the variation between the data points was generally less than 10%. A total of approximately 500 measurements were made. The data for each annulus velocity were averaged and a smooth curve was drawn through the points. The data collected were to be plotted as dimensionless variables with the fundamental variables being L (forward stagnation point), L$_p$ (aft stagnation point), V$_A$ (annular velocity), V$_j$ (central jet velocity), d$_o$ (outer diameter of annulus), d$_i$ (inner diameter of annulus), d$_j$ (diameter of central jet) and ν, the following relation is obtained:

$$\frac{L}{L_p} = f_1 \left(\frac{V_j}{V_A}, \ V_A \frac{(d_o - d_i)}{\nu}, \ \frac{V_j d_j}{\nu}, \ \frac{d_o}{d_i}, \ \frac{d_j}{d_o} \right)$$

Since the geometry in these experiments is fixed,

$$\frac{L}{L_p} = f_2\left(\frac{V_j}{V_A}, V_A \frac{(d_o - d_i)}{\nu}, \frac{V_j d_i}{\nu}\right)$$

it was found that the data (L/L_p) collapsed to a single curve when plotted against V_j/V_A (see Figure 4).

The data points were obtained from smooth curve fits of the averaged data as previously explained. The aft stagnation point was found to have a constant value of 49 mm for annulus velocities greater than 4 m/s. The equation for the curve is given on the graph. The observation that penetration occurs at a velocity ratio of one should not be generalized since a different size bluff body or central jet would very likely give a different result. These data suggest that the time average flow fields are similar for conditions where the ratio of annular velocity (V_A) to central jet velocity (V_j) is a constant.

Let us define at onset of penetration a friction factor, $\bar{f}$, as

$$\bar{f} = \frac{V_j^2 D_i}{2 L_p (V_A + V_j)^2} \quad .$$

The following table of $\bar{f}$ versus R_A is computed from the data.

Table I. Values of $\bar{f}$ versus R_A

R_A	$\bar{f}$
1,250	.0111
2,500	.0135
3,750	.00940
5,000	.01053
7,500	.0133
10,000	.0130
12,500	.0127
15,000	.0140
17,500	.0141
20,000	.0136
22,500	.0120

For turbulent flow in the annulus $(R_A < 10,000)$, $\bar{f} = .0132 \pm 9\%$. It would be interesting to determine how geometrical changes in the nozzle effect $\bar{f}$. If it is truly a constant (0.0132) for turbulent flow over a wide range of geometries, it would be significant. One could then compute the aft stagnation point (L_p) knowing the entrance conditions and the central jet

140-10

diameter.

Flow Field Descriptions. Of necessity, turbulent recirculating flows are usually described in terms of time averaged flow fields. Visual observations of the sheet-lit reacting cold flow field of the bluff body tend to provide a time averaged view. Viewed in this way, flow conditions with the same velocity ratio (V_j/V_A) appear similar to the eye. In general, one observes a large recirculation zone (a toroidal vortex) which is bound to the bluff body and is driven by the annular jet. The central jet flow extends into the center of the recirculation zone. A second recirculation zone, which is driven by the central jet as it entrains fluid, appears narrow and stretched along the stem of the central jet. In an attempt to characterize the visually observed flow fields, three general flow conditions might be identified. The first condition is characterized by the domination of the annular jet. The second is where neither jet dominates and the third is where the central jet dominates. Each of these will be discussed in the following paragraphs.

The annular jet appears to dominate the flow field for small velocity ratios (V_j/V_A) up to a value of about 0.4. For these conditions, the momentum of the reverse flow is sufficiently large to turn the central jet flow before it reaches the height of the time averaged center of the large recirculation zone. The vortex center is approximately 25 mm above the bluff body. In this case, the central jet is very unstable and moves from side to side in an erratic way. Figure 20 shows a snapshot of the flow field with the annular jet dominant. Although the snapshot does not represent the time averaged view of the flow, it does clearly show the asymmetry of the flow field produced by the central jet being pushed to the left at the instance the picture was taken.

Neither jet appears to dominate the flow field for velocity ratios between 0.4 and about 1.5. When the momentum of the central jet is sufficient to move the forward stagnation point above the axial height of the large vortex center, the stem of the jet does not move. However, the tip of the jet does fluctuate a distance of a few millimeters in all directions. As the velocity ratio approaches one, the central jet penetrates about 50% of the time and at a ratio of about 1.5, it penetrates 100% of the time.

140-11

The central jet appears to dominate the flow field for velocity ratios greater than 1.5. The central jet appears to entrain a large quantity of annulus air. The annulus air is pulled in around the shear layer of the annular jet and back along the shear layer of the central jet. The central jet entrainment can also reduce the size of the recirculation zone.

Although the velocity ratio is a good parameter to characterize the time average flow field, it is not sufficient. Flow fields at low and high velocities, but with a constant velocity ratio, appear very different when the laser sheet is chopped. Large spiral vortices are apparent in the shear layer of the annular jet and other vortices are observed in the central jet. Some of these vortices are captured in the photographs in Figure 2. These vortices can interact in numerous ways depending on the Reynolds numbers of the two jets. For annulus velocities below 1 m/s $\left(Re = V_A \dfrac{(d_o + d_i)}{\nu} = 1250\right)$ the recirculation zone appears to be laminar. At velocities between 1 and 8 m/s (Re > 10,000), quasi periodic spiral vortices are formed in the shear layer of the annular jet. The size of the spiral vortices is reduced as the velocity is increased. At 8 m/s (Re = 10,000) a notable change in the noise level occurs and frequency random vortex shedding is apparent. We believe the flow transitions to fully developed turbulence at this point. A similar transition from laminar to turbulent flow was noted in the central jet. It appeared laminar for velocities below 1 m/s and transitioned to turbulent flow at about 8 m/s. Figure 5 shows the dynamic events occurring in a horizontal plane 37 mm above the nozzle face.

IVb. Combusting Flow

Flow Field Description. The first photograph in Figure 6 shows a flame stabilized on the bluff body face where the annulus velocity is 1 m/s and the central jet propane velocity is 0.5 m/s. The second photograph shows a laser sheet-lit view of the same flame taken with an optical filter to eliminate light from sources other than the laser. The Mie scattered light from the soot and TiO_2 particles clearly show the laminar structure of the flame. The central jet is identified by a bright jet boundary surface. Surrounding the jet is a bound toroidal vortex. The vortex center is located approximately 20% of the bluff body diameter above the base. The bright converging downstream structure is a flame zone which is observed in the laboratory to extend very near to the base of the bluff body. The dark region

on the right-hand side between jet surface and vortex ring shows an air entrainment pathway into the recirculation zone. In high speed movies, such entrainment pathways are observed to exist for extended periods of time compared to the period of rotation of the vortex.

The third photograph in Figure 6 shows a sheet-lit view of non-combusting flow with propane and $TiCl_4$ in the central jet and the same inlet conditions as the combusting case. In contrast to the exothermic flow, the cold flow is in a transition state with active vortex shedding from the bluff body. Comparison of the cold flow structure with that of the hot flow confirms that the latter flow is strongly affected by combustion laminarization due to the large increase in kinematic viscosity at higher temperature (approximately a factor of 10).

Figure 7 shows a propane flame with a central jet velocity of 4 m/s and an annulus air velocity of 1 m/s. With this increase in velocities, the flame exhibits a tower-like structure created by a train of large amplitude interfacial waves developed in the mixing layer between the recirculation zone and the annulus air. These waves are prematurely terminated at the tip of the recirculating wake before they mature into spiral vortices. The center photograph in Figure 7 is a laser sheet-lit view which reveals the interior structure of this flame. The irregular arrangement of structures in the wake and upper portion of the central jet indicate that both the wake and jet are in a transition state. The third photograph shows the non-combusting case with the propane and $TiCl_4$ in the central jet. Comparison between combusting and noncombusting cases again demonstrates the strong laminarization effect induced by combustion.

V. RECOMMENDATIONS AND CONCLUSIONS

Laser sheet-lighting the product of a chemical reaction combined with photography, especially high-speed movies, is shown to be a very valuable tool in the study of a bluff body combustor. In contrast to seeding the upstream flow with particles for visualization, sheet-lighting the product of a fast chemical reaction in the flow field provides a view of the mixing processes and how the product and air species are transported. The $TiCl_4$ water vapor reaction proved to be an excellent choice for use in this new program.

In this study, three primary modes of operation of the combustor with their characteristic flow structures are identified. These modes are a highly dominant annular jet mode, a highly dominant central jet mode, and an intermediate mode where the central jet penetrates the recirculation zone of the bluff body intermittenly. Measurements of the central jet stagnation point normalized by the aft stagnation point of the recirculation zone are found to correlate with the ratio of central jet to annular jet velocity for the cold flow cases. Thus, the jet velocity ratio is found to be one of the parameters which can be used to characterize the time average flow field of an operating mode.

The dynamics of large vortex structures appears to play a governing role in mass transport and mixing in all of the flows studied. Vortex shedding from the bluff body appears to be a primary mechanism of mass exchange between the recirculation zone, annuluar jet, and downstream region for the cold flow cases. The high speed movies reveal that the flow fields are not axisymmetric and steady, but rather, highly three-dimensional and unsteady in terms of the dynamic evolution of large scale vortical structures. In combusting flows, a strong laminarization effect due to heat release with consequent increase in kinematic viscosity was observed. This effect appears to prevent vortex shedding from the bluff body for the flow rate range of this study.

The success of this sheet-lighting visualization technique combined with high speed cine photography in this study opens up a wide range of possibilities for future studies. A few of these possibilities include: the study of the effect of blockage ratio on combustor operating modes and flow field dynamics, the study of ducted versus unducted flows, and a study correlating the visualization of vortex dynamics recorded in high speed movies with the results of simultaneous measurements made with advanced diagnostic techniques such as laser Doppler anemometer and coherent anti-Stokes Raman spectroscopy. The prospects of acoustically driving the flow and using a sheet-lit laser strobe for conditional sampling seems another attractive possibility.

REFERENCES

1. W. M. Roquemore, et al., "Utilization of Laser Diagnostics to Evaluate Combustor Models," AGARD No. 353, Combustion Problems in Turbine Engines, Vol. 19, pp. 1151-1157, 1981.

2. M. B. Long, B. T. Chu and R. K. Chang, "Instantaneous Two-Dimensional Gas Concentration Measurements by Light Scattering," AIAA Journal, Vol. 19, pp. 1151-1157, 1981.

3. M. Carla Escoda and Marshall Long, "Rayleigh Scattering Measurements of the Gas Concentrtion Field in Turbulent Jets," AIAA Journal, Vol. 21, No. 1, pp. 81-84, 1983.

4. M. J. Dyer and D. R. Crosley, Optics Letters, Vol. 7, p. 382, 1982.

5. George Kychakoff, et al., "Quantitative Visualization of Combustion Species in a Plane," Applied Optics, Vol. 21, No. 18, pp. 3225-3229, 1982.

6. B. V. Johnson and J. C. Bennett, "Mass and Momentum Turbulent Transport Experiments with Confined Coaxial Jets," NASA CR-165574, Nov. 1981.

7. M. M. Koochesfahani, P. E. Dimolakis and J. E. Broadwell, "Chemically Reacting Turbulent Shear Layers," AIAA-83-0475, Jan. 1983.

8. P. E. Dimotakis, J. E. Broadwell and R. D. Howard, "Chemically Reacting Turbulent Jets," AIAA-83-0474, Jan. 1983.

9. J. B. Moss, "Simultaneous Measurements of Concentration and Velocity in an Open Premixed Turbulent Flame," Combustion Science and Technology, Vol. 22, pp. 119-129, 1980.

10. R. R. Craig, et. al., "A General Approach for Obtaining Unbiased LDV Data in Highly Turbulent Non-Reacting and Reacting Flows," AIAA-84-0366, Jan. 1984.
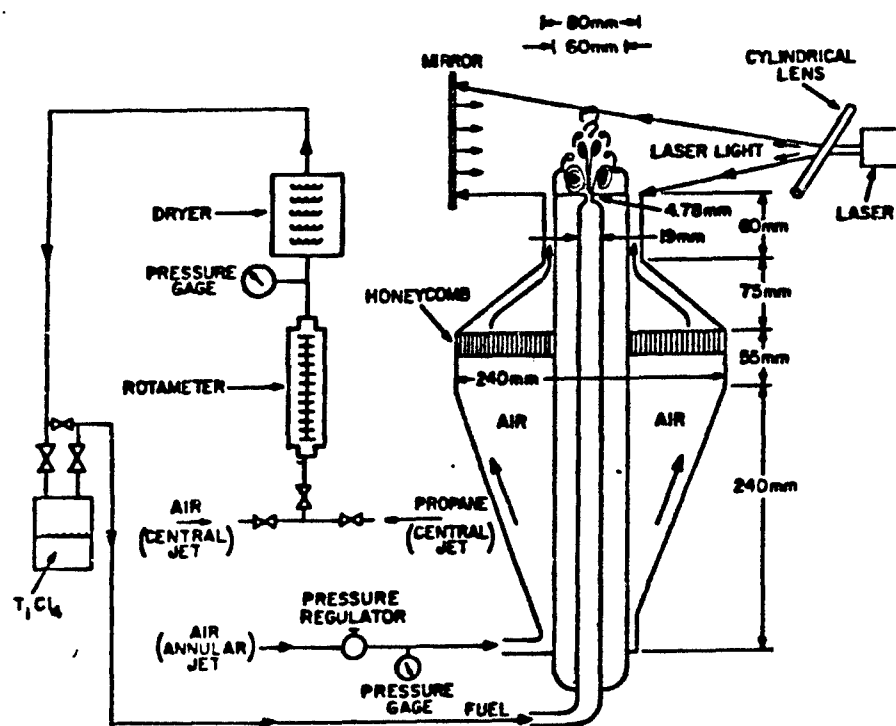
Figure 1. Illustration of the experimental set-up.
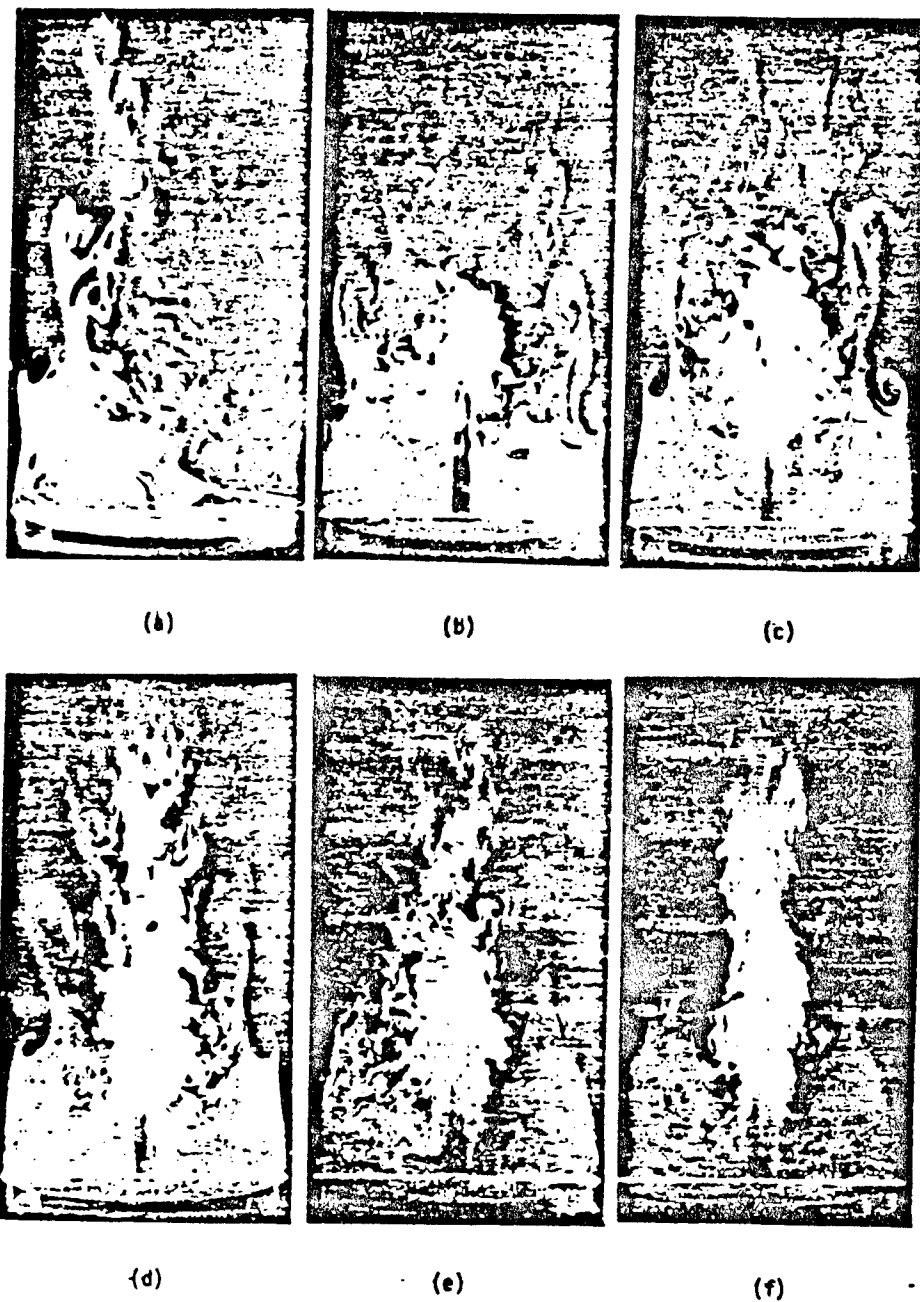
Figure 2 Photographs for a fixed annulus velocity of 4 m/s and central jet (TiCl$_4$ vapor and dry air) velocities of (a)1, (b)3, (c)6, (d)8, (e)12, and (f) 15 m/s.
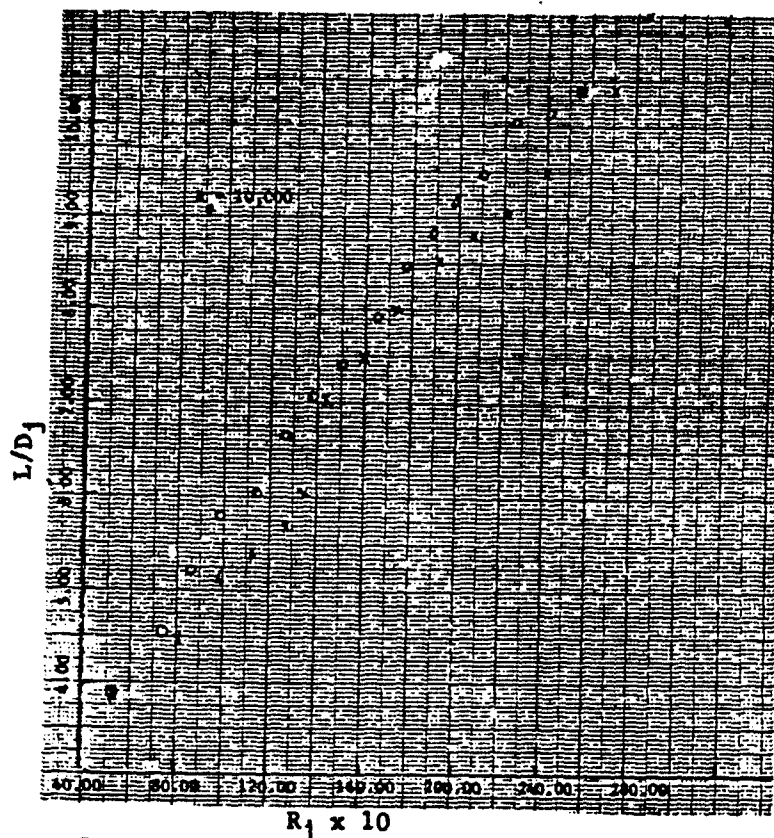
Figure 3. Comparison between data taken on different days.

$$Y = 1 - 1.2 * (1-X)**1.8$$
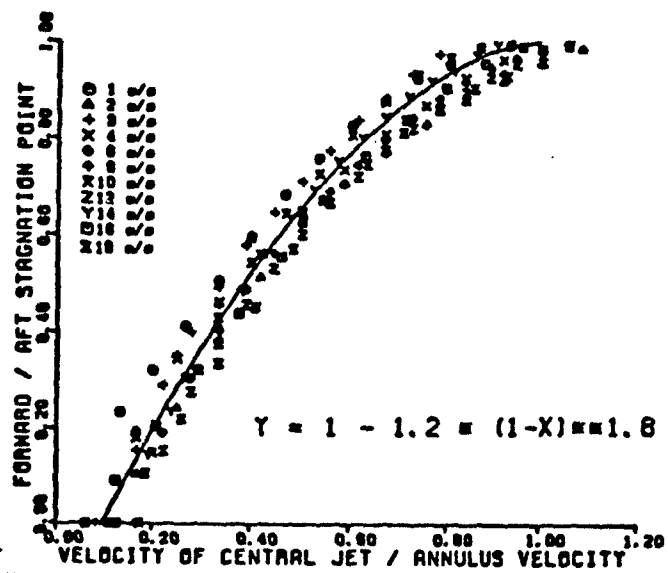
Figure 4 Location of the forward stagnation point for different velocity ratios.
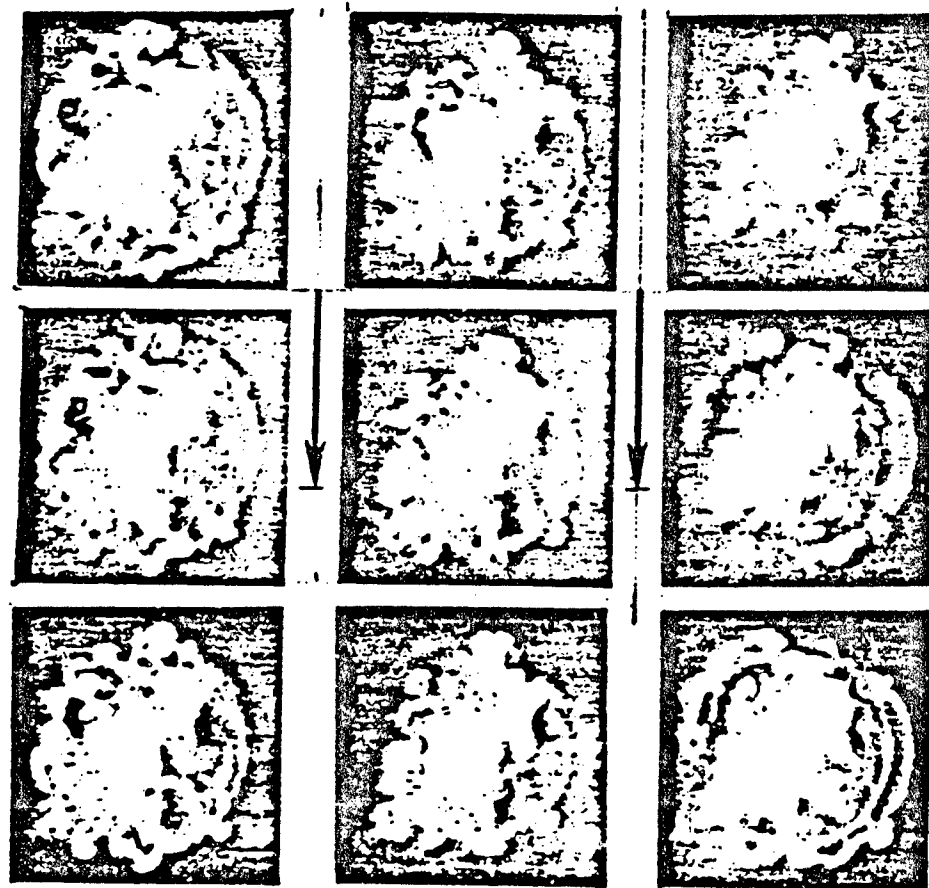
Figure 5. High speed cine pictures (1000 frames/s) of a sheet lit horizontal plane located 37 mm above the bluff body for an annulus velocity of 4 m/s and a central jet (TiCl₄ vapor and dry air) velocity of 4 m/s.
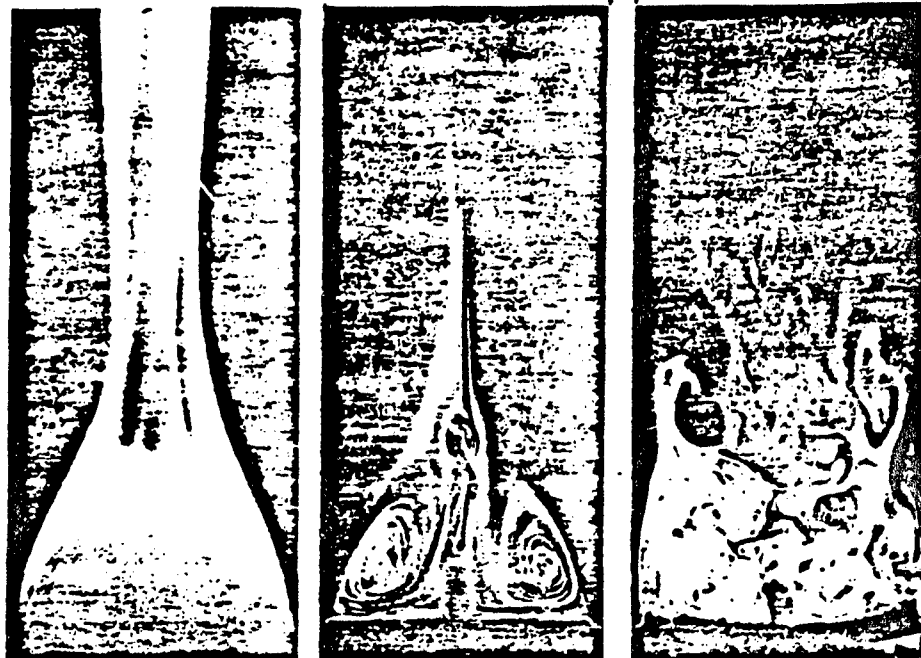
Figure 6. Photographs for an annulus velocity of 2 m/s and a central jet (propane + TiCl$_4$ vapor) velocity of 0.5 m/s of; left to right: the flame, sheet lit flame, sheet lit non-combusting flow.
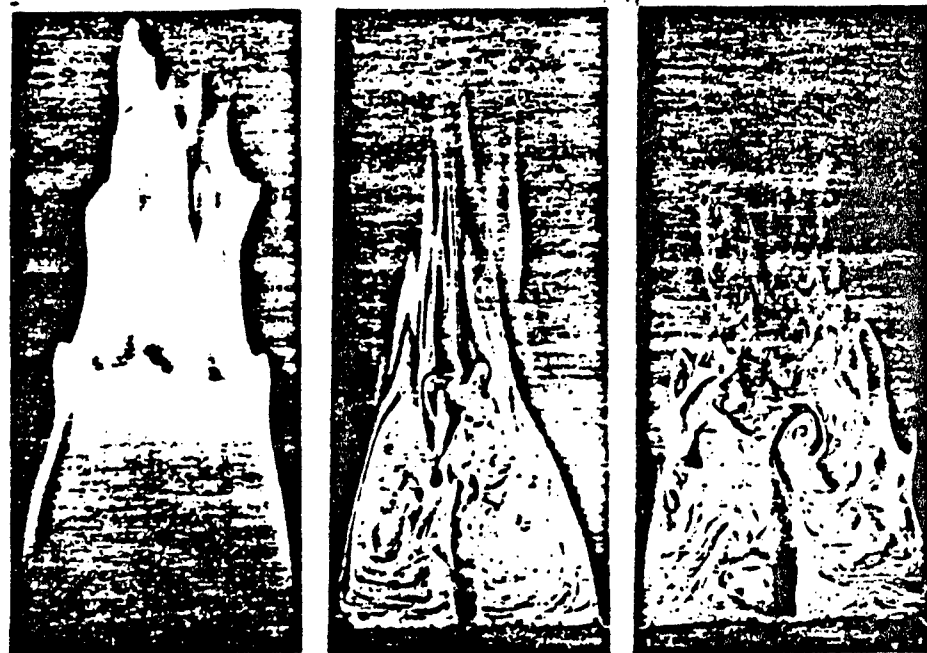
Figure 7 Photographs for an annulus velocity of 4 m/s and a central jet (propane mixed with TiCl$_4$ vapor) velocity of 1 m/s of; left to right: the flame, sheet lit flame, sheet lit non-combusting flow.

1984 USAF-SCEEE SUMMER FACULTY RESEARCH PROGRAM

Sponsored by the

AIR FORCE OFFICE OF SCIENTIFIC RESEARCH

Conducted by the

SOUTHEASTERN CENTER FOR ELECTRICAL ENGINEERING EDUCATION

FINAL REPORT

AN INVESTIGATION OF ACETYLCHOLINE AS A NEUROTRANSMITTER OF CEREBELLAR

MOSSY FIBERS

Prepared by:	Dr. William E. Thomas
Academic Rank:	Assistant Professor
Department and Uinversity:	Physiology Department Meharry Medical College
Research Location:	SAM/Brooks AFB, Clinical Sciences Division, Neuropsychiatry Branch
USAF Research:	Dr. David Terrian, Dr. Bryce Hartman
Date:	September 15, 1984
Contract No:	F49620-82-C-0035

AN INVESTIGATION OF ACETYLCHOLINE AS A

NEUROTRANSMITTER OF CEREBELLAR MOSSY

FIBERS

by

William E. Thomas

ABSTRACT

The function of acetylcholine as a neurotransmitter of cerebellar mossy fibers was investigated using a subcellular fractionation procedure. The synthetic and degradative enzymes for acetylcholine were present in a purified fraction of mossy fiber terminals or glomeruli; however, no enrichment was found. Studies of choline uptake revealed the presence of a high-affinity transport system in the glomerular fraction. This choline uptake system exhibited a K_t of 1.1 µM and a V_{max} of 5.46 pmol/min/mg protein. Uptake was Na^+ dependent, inhibited by hemicholinium-3, and could be distinguished from homoexchange. On the basis of the presence of CAT, AChE, and especially high-affinity choline uptake in the purified glomerular preparation, it was concluded that some fraction of the mossy fibers is cholinergic.

141-2

ACKNOWLEDGMENTS

I. Introduction

The function of acetylcholine (ACh) as a neurotransmitter of mossy fibers in the cerebellum is an unresolved issue. The mossy fibers are one of the two sources of afferent input to this tissue and terminate in a large glomerular synaptic structure. In some early studies, histochemical staining for acetylcholinesterase (AChE) showed this enzyme to be localized in a subpopulation of mossy fiber terminals [1,2]. However, concurrent physiological studies indicated that it was unlikely that ACh was a transmitter of the mossy fibers [3]. Still other physiological investigations supported ACh as a potential mossy fiber transmitter [4]. Using biochemical techniques, choline acetyltransferase (CAT) activity was shown to be localized in the granular layer of the cerebellum [5], the layer containing the mossy fiber terminals. Further biochemical studies have shown that CAT co-localizes with AChE and that both enzymes are significantly reduced by deafferentation [6].

A favored technique in investigating mossy fiber neurochemistry has been subcellular fractionation. The large size of the mossy fiber terminal enhances the ability to isolate the synaptic glomerulus by differential centrifugation. In initial subcellular fractionations of cerebellum, ACh [7] and CAT [8] were enriched in fractions containing the mossy fiber glomeruli. However, subsequent reports of more extensive fractionations, yielding purer fractions of mossy fiber terminals, indicated no enrichment of CAT activity in these fractions [9,10,11,12]. In contrast to this finding, Kan et al. [13] reported the immunohistochemical localization of CAT in mossy fibers. Thus, while there is some evidence to suggest that ACh may be a transmitter of the mossy

fibers, there are conflicting reports which render the issue unclear.

The cerebellum plays a pivotal role in motor control and coordination. An enhancement of cerebellar function may produce a direct enhancement of motor activity. In this light, the U.S. Air Force has a continuing interest in understanding cerebellar function. The pilot-cockpit interphase is highly dependent upon motor coordination. An understanding of cerebellar function may lead to ways to improve this function and result in an enhancement of motor coordination and pilot performance.

The author of this report has nine years of neurochemical research experience. Much of the work performed during this period involved cholinergic mechanisms in the CNS. My continuing interests have been the identification of cholinergic cells in the CNS, particularly the cortex, and an investigation of the properties of ACh metabolism by these cells. These interests proved very compatible with the Air Force's interest in understanding cerebellar function and resulted in the research project described herein.

II. Objectives

The overall objective of this research project was to evaluate the role of ACh as a neurotransmitter of cerebellar mossy fibers. Identification of the transmitter compounds used by individual neurons is basic to an understanding of the function of any area of the CNS. The cerebellar cortex offers some advantage in this regard because of the relatively small number of cell types it contains. The identification of the transmitters used by various neurons in the cerebellum would clearly contribute to a better understanding of cerebellum operation. Furthermore, knowledge of the transmitter

141-5

compounds may lead to a mechanism for improving cerebellar function. Toward this end, the present study was undertaken in an effort to resolve the question of whether ACh is a transmitter of one class of afferent processes to the cerebellum, the mossy fibers.

III. Approach

A critical aspect of the approach implemented in this investigation was the utilization of a highly purified preparation of mossy fiber glomeruli. Dr. David Terrian of Brooks AFB has developed a sub-cellular fractionation procedure for the preparation of a fraction of mossy fiber glomeruli. The details of this subcellular frac-tionation procedure will not be discussed here; however, greater than 95% of the material in the final fraction is glomerulus parti-cles. Dr. Terrian kindly provided the subcellular fractions of cerebellar tissue (bovine) used in this project and was a valuable collaborator in the performance of this work.

The approach utilized in this study was to determine the level of cholinergic marker enzymes, CAT and AChE, in cerebellar subfrac-tions. The activity of both enzymes was assayed according to pre-viously published radiometric procedures[14,15]. In this way, the co-enrichment of cholinergic markers with the mossy fiber glomeruli was investigated. In addition, the high-affinity uptake of choline was investigated in the purified glomerular fraction. Choline up-take experiments were performed essentially as described by Maleque et al.[16] using tritiated choline. High-affinity choline uptake has been indicated as a specific marker of cholinergic nerve terminals. Thus, choline uptake by the glomerular fraction, in conjunction with the subcellular distribution of CAT and AChE, was used to assess

the potential cholinergic nature of cerebellar mossy fibers.

IV. Results

A. Subcellular distribution of CAT and AChE

The subcellular fractionation procedure used resulted in the
production of seven major subcellular fractions. The initial
homogenate of bovine cerebellar tissue was filtered several times
to obtain a filtrate fraction. A pellet corresponding to the
nuclear fraction, and containing the mossy fiber glomeruli, was
obtained by centrifugation of the filtrate. Subsequent differen-
tial centrifugation of the nuclear fraction in Ficoll resulted
in the production of a crude mitochondrial pellet and a super-
natant fraction which contained the glomerulus particles. The
supernatant fraction was washed and pelleted to yield the crude
gomerular fraction. The crude glomerular fraction was sub-
fractionated on sucrose gradients to yield a fraction of
medullated fibers and the purified glomerular fraction.

The activities of CAT and AChE in the initial homogenate
of cerebellum and the subcellular fractions are presented in
Table I. The level of both enzymes in the homogenate is con-
sistent with established values for cerebellar tissue. The
enzyme CAT, which is considered a highly specific marker of
cholinergic terminals, showed no enrichment in the purified
glomerular fraction in comparison to the initial homogenate.
Also, none of the intermediate fractions containing the glomerulus
particles (filtrate, nuclear, supernatant and crude glomerular)
showed any enrichment of CAT. The enzyme AChE is a less specific
marker of cholinergic terminals than CAT. The purified glomerular

141-7

Table I. Distribution of CAT and AChE in Subcellular Fractions of Cerebellum

Fraction	CAT (pmol/min/mg)	AChE (nmol/min/mg)
homogenate	19.65 ± 5.96	10.18 ± 3.37
filtrate	13.14 ± 2.67	8.83 ± 2.07
nuclear	17.19 ± 1.41	18.01 ± 3.68
crude mitochondrial	14.82 ± 3.66	21.55 ± 5.02
supernatant	12.21 ± 0.74	7.92 ± 1.82
crude gomerular	9.23 ± 1.98	9.76 ± 2.58
medullated fibers	7.12 ± 0.39	13.68 ± 2.11
purified glomerular	12.79 ± 1.19	17.81 ± 4.92

141-8

fraction exhibited only a slight enrichment of AChE, and the intermediate fractions containing the glomerulus particles showed no consistent pattern of AChE enrichment. These findings for both enzymes are in agreement with previously published results[10,12].

The previous interpretation given to the lack of enrichment of CAT and AChE in purified glomerular preparations was that this eliminated the possiblity of ACh as a transmitter of the mossy fibers. However, while CAT and AChE are not enriched in the glomerular fraction, both enzymes are certainly present. Possible neurochemical heterogeneity of glomerulus particles in combination with the level of recovery and even the possibility of differential recovery of various neurochemical types must be considered. These considerations appear to warrant a different interpretation. Thus, a more accurate conclusion from the present findings would be that they do not provide strong support for ACh as a neurotransmitter of the mossy fiber; however, the findings are not completely negative.

B. Uptake of choline by the purified glomerular fraction

High-affinity choline uptake was investigated in the purified glomerular fraction as another means of assessing the presence of cholinergic terminals. As shown in Fig. 1, the glomerular fraction accumulated ^{3}H-choline and the level of uptake was dependent on protein concentration (the lines in all figures were determined by linear regression). This uptake was determined at a choline concentration (0.1 µM) which is well within the range of high-affinity choline uptake reported for other cholinergic preparations. At the same concentration of

141-9
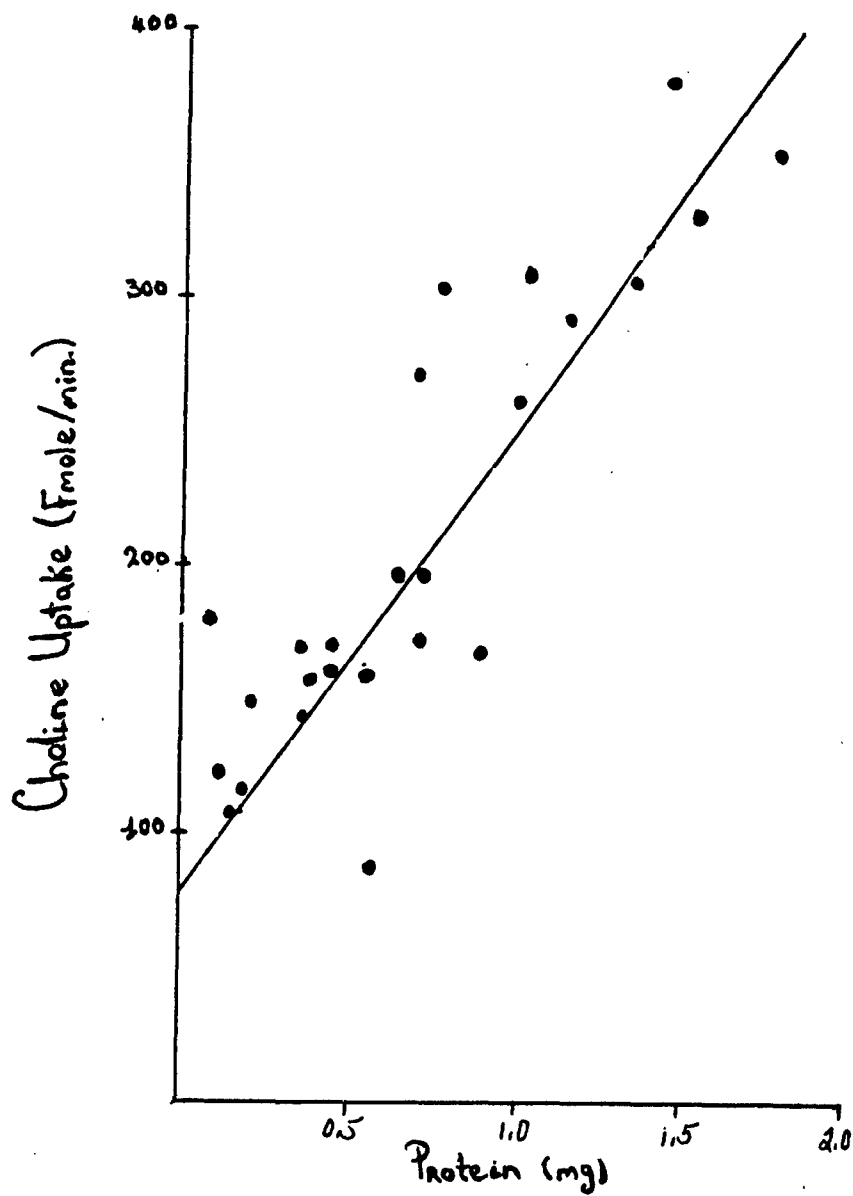
Fig. 1. Dependence of choline uptake on glomerular fraction protein concentration. The indicated protein concentrations of purified glomerular fraction were incubated with 0.1 µM ^{3}H-choline for 5 min.

141-10

labelled choline, uptake remained linear for at least 30 min (Fig.2). Thus, the glomerular fraction exhibited choline uptake at low concentrations of choline, uptake was dependent on glomerular fraction protein concentration and was linear with time.

The level of choline uptake was determined at different choline concentrations. Uptake increased as the concentration of labelled choline increased (Table II). The data presented in Table II was analyzed via a Lineweaver-Burke double reciprocal plot to determine the kinetic constants of uptake. As shown in Fig. 3, choline uptake by the purified glomerular fraction had a K_t of 1.1 μM and a V_{max} of 5.46 pmol/min/mg protein. These values correspond well with the kinetic constants of high-affinity choline uptake determined in various cholinergic systems.

While the above mentioned features of choline uptake by the glomerular fraction support the existence of a specific high-affinity choline transport system in this preparation, other properties of neurotransmitter-related high-affinity choline transport in nervous tissue have been characterized. These include a dependence on Na^+ ions and select inhibiton by the compound hemicholinium-3. Hence, the effects of reduced Na^+ concentration and hemicholinium-3 on choline uptake by the purified glomerular fraction was investigated. Uptake was significantly inhibited by hemicholinium-3 (Table III). A 5 μM concentration of this compound reduced uptake by 79%, and a higher concentration produced further inhibition. In experiment II (Table III), the Na^+ concentration was reduced from the normal value of 118 mM to 32

141-11
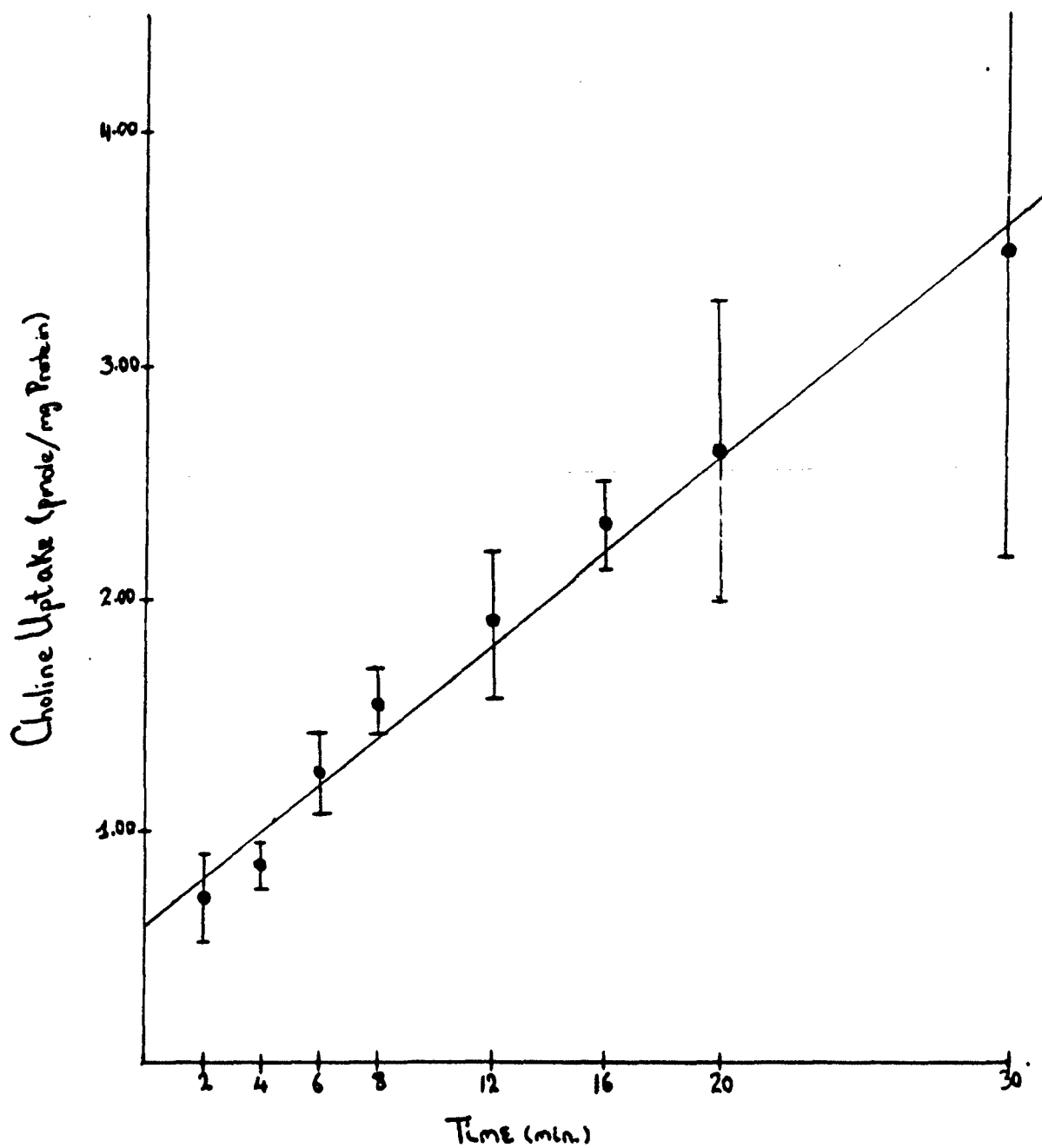
Fig. 2. Time dependence of choline uptake by the purified glomerular fraction. 0.35-0.77 mg of glomerular fraction protein was incubated with 0.1 uM ^{3}H-choline for the indicated time periods.

141-12

Table II. Kinetics of Choline Uptake by
the Purified Glomerular Fraction

choline concentration (μM)	choline uptake (pmol/min/mg)
0.05	0.24 + 0.04
0.10	0.45 + 0.06
0.50	1.67 + 0.34
1.00	2.80 + 0.31
5.00	7.50 + 1.40
25.00	23.17 + 5.20

$K_t = 1.1 \, \mu M$

$V_{max} = 5.46 \, pmol/min/mg$
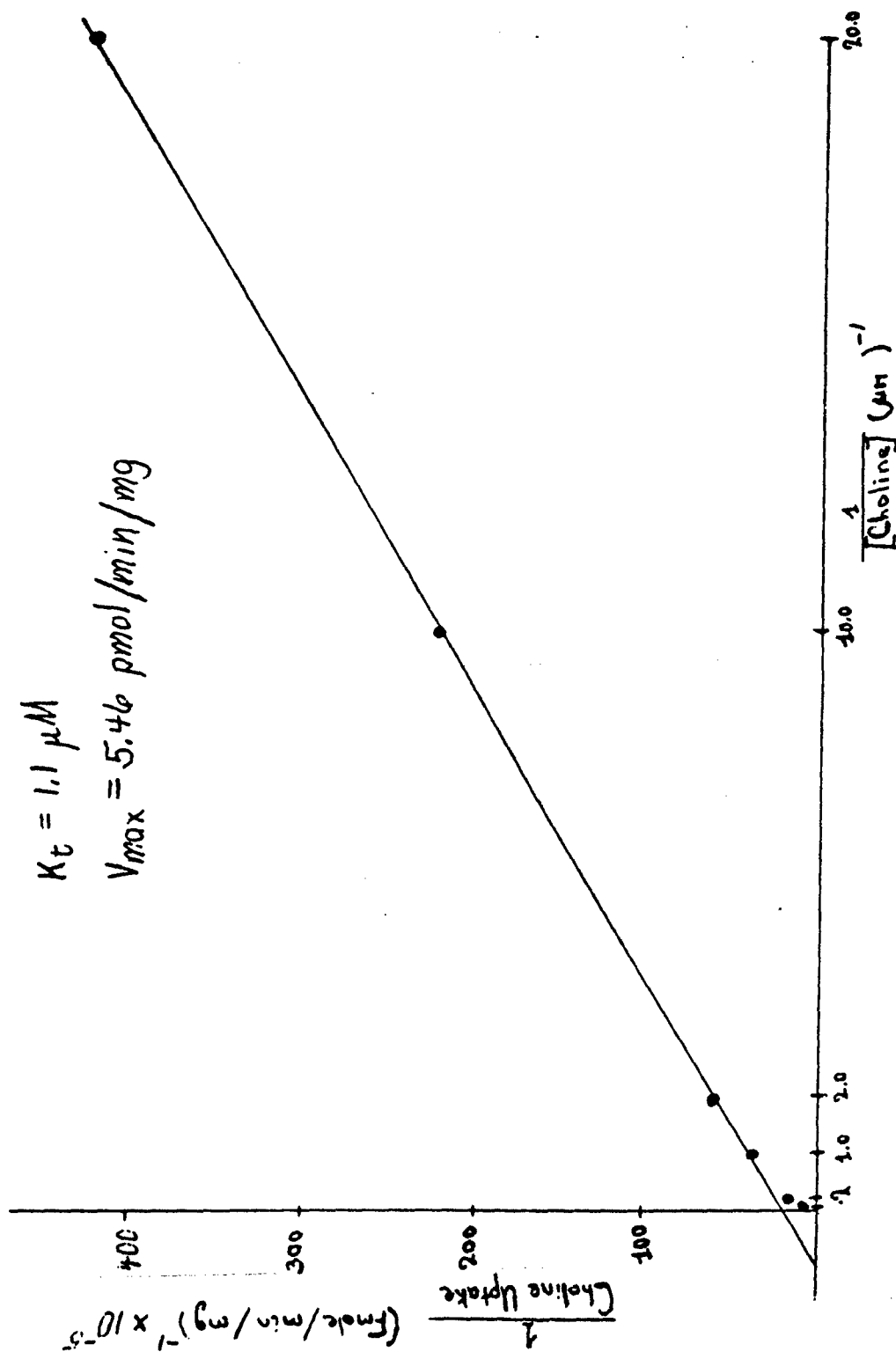
Fig. 3. Double reciprocal plot of choline uptake kinetics of the purified glomerular fraction.

141-14

Table III. Properties of Choline Uptake by the Purified Glomerular Fraction

condition	concentration	choline uptake (fmol/min/mg)	%inhibition
I. control[a]		357.2	
hemicholinium-3[b]	5 μM	73.3	79.5
	50 μM	36.1	89.9
II. control		255.4	
reduced Na[+][c]	32 mM	187.0	26.8
	0 mM	124.3	51.3
III. control		225.2	
Unlabelled choline[d]	250 μM	94.9	57.9
	1 mM	92.6	58.9

a All samples were incubated with 0.1 μM ^{3}H-choline for 5 min.
b Purified glomerular fraction was preincubated with hemicholinium-3.
c Purified glomerular fraction was preincubated with reduced Na$^+$.
d Purified glomerular fraction was postincubated with unlabelled choline.

and 0 mM by replacement with equimolar amounts of sucrose. At 32 mM Na^+, a significant reduction in choline uptake was observed. Greater than 50% of the uptake was inhibited in Na^+-free medium.

A complicating factor in the characterization of high-affinity choline uptake in other areas of nervous tissue has been the presence of a homoexchange mechanism. Homoexchange is clearly distinct from high-affinity uptake in that it results in no intracellular accumulation of choline, it is a direct exchange of intracellular choline for extracellular choline. Choline entering the cell via homoexchange is thought to reside in a different pool from that entering via high-affinity uptake. Choline in the homoexchange pool can be flushed or turned over by replacement with extracellularly derived choline. The contribution of homoexchange to the total choline uptake in the purified glomerular fraction was investigated. Aliquots of the glomerular fraction were incubated with ^{3}H-choline to load them with label. These aliquots were then postincubated with excess unlabelled choline to turnover or flush exchangeable intracellular label. As shown in Table III (experiment III), a significant portion of the choline contained by the glomerulus particles was exchangeable. However, with postincubation in increasing amounts of unlabelled choline, the amount of labelled choline exchanged plateaued. This was reached at a level of approximately 59% of the total ^{3}H-choline content. Thus, a significant fraction was also not exchangeable and remained within the glomerulus particles. This fraction, greater than 40%, appears to correspond to accumulation via a high-affinity choline transport system.

141-16

On the basis of these results, the purified glomerulus particles contain a high-affinity uptake system for choline. This uptake system has a K_t of 1.1 µM and a V_{max} of 5.46 pmol/min/mg. The uptake system is inhibited by hemicholinium-3 and dependent on Na^+ ions. A choline homoexchange system also exists in the glomerulus particles. Choline uptake by the high-affinity transport system can be distinguished from homoexchange. Greater than 40% of the total choline uptake corresponded to specific high-affinity transport.

V. Recommendations

The overall conclusion from this project is that it is highly likely that ACh is a transmitter of some mossy fibers in bovine cerebellum. Even though no enrichment of CAT or AChE was found in the purified glomerular fraction, significant amounts of both enzymes, comparable to the crude homogenate, were present. This emphasizes the possibility that the mossy fibers may have heterogeneous transmitter chemistry and that some fraction is cholinergic. While the result from the subcellular distribution of CAT and AChE must be viewed simply as not eliminating the possibility of ACh as a transmitter of the mossy fibers, the identification of a high-affinity uptake system for choline provides strong, if not conclusive, evidence of cholinergic function. High-affinity choline uptake has been tauted as a highly specific marker for cholinergic terminals. Thus, on the basis of the presence of CAT, AChE, and especially high-affinity choline uptake in the purified glomerular fraction, it is concluded that some fraction of the mossy fibers is cholinergic.

While the described results strongly support the conclusion reached, this conclusion cannot yet be viewed as unequivocal. There are several additional experiments which would act to confirm the stated conclusion. These experiments are given as the following recommendations:

(1) Determine the distribution of ACh itself in cerebellar subcellular fractions.

(2) Investigate the releaseability of label under physiological conditions from purified glomerulus particles after ^{3}H-choline uptake.

(3) Verify the identity of releaseable label as being ACh.

These immediate recommendations, which would confirm the overall conclusion of this project, represent part of the basis for follow-on research in the form of a Research Initiation Grant. These experiments, as well as unfinished experiments from a second project described in the accompanying final report, will be proposed in a subsequent Research Initiation Grant.

In conclusion, the present results of this project provide strong support for ACh as a transmitter of cerebellar mossy fibers and the immediate recommendations would establish this unequivocally. As a long range recommendation, it is suggested that electron microscopic immunohistochemical localization of CAT in the purified glomerular fraction would allow a determination of the percentage of mossy fibers that are cholinergic.

REFERENCES

1. Csillik, B., F. Joo and P. Kasa, "Cholinesterase Activity of
   Archicerebellar Mossy Fibre Apparatuses," J. Histochem.
   Cytochem., Vol. 11, pp. 113-114, 1963.

2. Silver, A., "Cholinesterases of the Central Nervous System
   with Special Reference to the Cerebellum," Int. Rev. Neurobiol.,
   Vol. 10, pp. 57-109, 1967.

3. Crawford, J.M., D.R. Curtis, P.E. Voorhoeve and V.J. Wilson,
   "Acetylcholine Sensitivity cf Cerebellar Neurones in the Cat,"
   J. Physiol., Vol. 186, pp. 139-165, 1966.

4. McCance, I. and J.W. Phillis, "Cholinergic Mechanisms in the
   Cerebellar Cortex," Int. J. Neuropharmacol., Vol. 7, pp. 447-462,
   1968.

5. McCaman, R.E. and J.M. Hunt, "Microdetermination of Choline
   Acetylase in Nervous Tissue," J. Neurochem., Vol. 12, pp. 253-259,
   1965.

6. Kasa, P. and A. Silver, "The Correlation between Choline
   Acetyltransferase and acetylcholinesterase Activity in Different
   Areas of the Cerebellum of Rat and Guinea Pig," J. Neurochem.,
   Vol. 16, pp. 389-396, 1969.

7. Israel, M. and V.P. Whittaker, "The Isolation of Mossy Fibre
   Endings from the Granular Layer of the Cerebellar Cortex,"
   Experientia, Vol. 21, pp. 325-326, 1965.

8. Fonnum, F., "Application of Microchemical Analysis and Subcellular
   Fractionation Techniques to the Study of Neurotransmitters in Discrete

141-19

REFERENCES (cont'd)

Areas of Mammalian Brain," <u>Adv</u>. <u>Biochem</u>. <u>Pharmacol</u>., Vol. 6, pp. 75-88, 1972.

9. Balazs, R., F. Hajos, I.A. Michaelson, R. Tapia and G. Wilkin, "Isolation of a Fraction from Rat Cerebellum Enriched in nerve Terminals of One Single Type (Mossy-Fibre Terminals)," <u>Biochem</u>. <u>J</u>., Vol. 128, pp. 81-82P, 1972.

10. Hajos, F., R. Tapia, G. Wilkin, A.L. Johnson and R. Balazs, "Subcellular Fractionation of Rat Cerebellum: An Electron Microscopic and Biochemical Investigation. I. Preservation of Large Fragments of the Cerebellar Glomeruli," <u>Brain</u> <u>Res</u>., Vol. 70, pp. 261-279, 1974.

11. Tapia, R., F. Hajos, G. Wilkin, A.L. Johnson and R. Balazs, "Subcellular Fractionation of Rat Cerebellum: An Electron Microscopic and Biochemical Investigation. II. Resolution of Morphologically Characterised Fractions," <u>Brain</u> <u>Res</u>., Vol. 70, pp. 285-299, 1974.

12. Balazs, R., F. Hajos, A.L. Johnson, G.L.A. Reynierse, R. Tapia and G.P. Wilkin, "Subcellular Fractionation of Rat Cerebellum: An Electron Microscopic and Biochemical Investigation. III. Isolation of Large Fragments of the Cerebellar Glomeruli," <u>Brain</u> <u>Res</u>., Vol. 86, pp. 17-30, 1975.

13. Kan, K.-S., L.-P. Chao and L. F. Eng, "Immunohistochemical Localization of Choline Acetyltransferase in Rabbit Spinal Cord and Cerebellum," <u>Brain</u> <u>Res</u>., Vol. 146, pp. 221-229, 1978.

REFERENCES (cont'd)

14. Fonnum, F., "A Rapid Radiochemical Method for the Determination of Choline Acetyltransferase," _J. Neurochem._, Vol. 24, pp. 407-409, 1975.

15. Reed, D., K. Gotto and C. Wang, "A Direct Radioisotopic Assay for Acetylcholinesterase," _Analyt. Biochem._, Vol. 16, pp. 59-64, 1966.

16. Maleque, M.A., R.F. Newkirk and J.G. Townsel, "Kinetics of [^{3}H] Choline Uptake in Abdominal Ganglia of _Limulus polyphemus_," _Biochem. Pharmacol._, Vol. 28, pp. 985-990, 1979.

1984 USAF-SCEEE SUMMER FACULTY RESEARCH PROGRAM

Sponsored by the

AIR FORCE OFFICE OF SCIENTIFIC RESEARCH

Conducted by the

SOUTHEASTERN CENTER FOR ELECTRICAL ENGINEERING EDUCATION

FINAL REPORT

Unified Real Part of Susceptibility over

Millimeter through Infrared Region

Prepared by: Ken Tomiyama

Academic Rank: Assistant Professor

Department and   The Department of Electrical Engineering
   University: Pennsylvania State University

Research Location: Infrared Physics Branch
                      Optical Physics Division
                      Air force Geophysics Laboratory

USAF Research: Francis X. Kneizys

Date: July 31, 1984

Contract Number: F49620-82-C-0035

Unified Real Part of Susceptibility over

Millimeter through Infrared Region

by

Ken Tomiyama

ABSTRACT

The imaginary part of the complex susceptibility from millimeter
to infrared and beyond has been studied extensively because of
its association with the absorption spectra.   However, the recent
trend of computing the dispersion has developed the need for the
real part of the susceptibility as well.   This report partially
answers this need by proposing an approximate unified real part
expression with the line coupling term included for the use in
both millimeter and infrared regions.   The approach is to examine
the two limiting forms in the millimeter and infrared regions,
obtained through the Kramers-Kronig relationship, from the res-
pective approximate imaginary parts in those regions.   Then the
two profiles were bridged by observing the transition from one
range to the other.   The accuracy of the proposed function was
numerically checked using a newly obtained series expression for
the exact real part, and was shown to be excellent in the
vicinity of the line center where the real part is nontrivial.

142-2

I. Introduction:

The imaginary part of the complex susceptibility has been studied extensively in conjunction with the radiation and absorption spectra among other applications. There is a large accumulation of knowledge on functional forms of the imaginary part and their characteristics. Recent advances in spectral theory and measurement techniques prompted the need for the real part of the susceptibility, which is related to the dispersion in a similar manner as that of the imaginary part to the absorption. It is known that the real and imaginary parts of the complex susceptibility are related by the Kramers-Kronig relationship through the Hilbert transform (Van Vleck 1977). Simply, what we need to acomplish is to find a functional form of the real part that corresponds to the known imaginary part via this relationship. However, one point to be made is that previous studies dealt with this subject either from the millimeter (MM) wave or infrared (IR) wave perspective but not in the unified manner (for example, Kemp 1978, Marshall 1978, and Liebe 1981).

Our strategy will be to start with the MM wave case and then to move on to the IR case. We introduce several approximations for the IR case to simplify the computation. Then the two results will be bridged together by introducing a new real part function. The proposed function will be shown to reduce to the two extreme cases by taking proper limits.

We use the Van Vleck-Huber line shape function (Huber 1966, and Van Vleck 1977) with the line coupling (Rosenkrantz 1975) here. It is noted that it is important to incorporate the zero-sum rule of the line coupling terms (Balanger 1958). However, we

142-3

will show that as long as one keeps the complete expression, correct results can be obtaind even for a single line without using the zero-sum rule.

Ultimate justification of the proposed real part would be the numerical comparison with the exact expression. However, because the closed form of the exact real part is not available, we derived an infinite series representation. The obtained series expression was used successfully in the numerical validation of the proposed real part.

II. Objective:

The main objective of this project is to propose and validate a unified approximate real part of the complex susceptibility. For this end, we pose the following specific objectives;

  (1) To obtain an approximate real part for the MM wave region using the corresponding approximate imaginary part and the Hilbert transform as explained above.

  (2) To repeat (1) for the IR region.

  (3) To propose a unified real part for the entire frequency range using the results in (1) and (2).

  (4) To obtain an exact real part in an infinite series form.

  (5) To assess the accuracy of the proposed real part by numerically comparing it with the exact value.

III. Van Vleck-Huber without Line Coupling:

The negative of the imaginary part of the complex susceptibility $X''(v)$ in $1/(cm^{-1} \, mol/cm^2)$ at wave number v (1/cm) due to a

transition at v_i (1/cm) with strength $\widetilde{S}_i$ (1/(mol/cm^2)) and half-width a_i (1/cm) can be expressed as (Huber 1966)

$$X''(v) = \frac{1}{\pi} \tanh(\widetilde{b}v) \, [\widetilde{S}_i f(v) + \widetilde{S}_i f(-v.] \, , \qquad (3-1)$$

where $\widetilde{b} = hc/2kT$ (cm) with Plank's constant h (erg-sec), speed of light c (cm/sec), Boltzmann constant k (erg/K), and temperature T (K), and $f(v)$ is the Lorentz line shape function given by

$$f(v) = a_i \, / \, \{(v_i - v)^2 + a_i^2 \} \, . \qquad (3-2)$$

This expression will be refered to as the Van Vleck-Huber line shape here. First we consider the MM wave region for which the result has been known (Kemp 1978). Because $\widetilde{b}v$ is small in the MM region ($\widetilde{b} = 1/412$ at t = 296 K), we have,

$$\tanh(\widetilde{b}v) = \widetilde{b}v \, . \qquad (3-3)$$

Hence the approximate imaginary part becomes

$$X''(v)|_{MM} = (\widetilde{S}_i \widetilde{b}v/\pi) \, \{f(v) + f(-v)\} \, . \qquad (3-4)$$

The corresponding real part $X'(v)|_{MM}$ will be given by the Hilbert transform $H[.]$ defined as (Baranger 1958)

$$H[g(v)] = (1/\pi)\int_{-\infty}^{\infty} \{1/(u-v)\} \, g(u) \, du \, . \qquad (3-5)$$

Using this,

$$X'(v) = H[X''(v)|_{MM}]$$

$$= (\widetilde{S}_i \widetilde{b}/\pi) \, H[\{v \, f(v) - a_i \, g(v)\} - \{v \, f(-v) - a_i \, g(-v)\}] \, , \qquad (3-6)$$

where $g(v)$ is given by

142-5

$$g(v) = (v_i - v) / \{(v_i - v)^2 + a_i^2\} . \qquad (3\text{-}7)$$

The two types of Hilbert transforms needed in Eq. (3-6) are standard ones (Bateman 1954). Using those results, we arrive at the following expression.

$$X'(v)|_{MM} = (\tilde{S}_i \tilde{b} v_i / \pi) [\{(a_i / v_i) f(v) + g(v)\}$$

$$+ \{(a_i / v_i) f(-v) + g(-v)\}] . \qquad (3\text{-}8)$$

On the other hand, for the IR case $|\tanh(\tilde{b}v)|$ may be replaced by the unity since $\tilde{b}v$ can be assumed large. Hence,

$$\tanh(\tilde{b}v) = \text{sgn}(v) , \qquad (3\text{-}9)$$

where the signum function $\text{sgn}(v)$ takes the value $1(-1)$ if the argument v is positive(negative). Then $X''(v)$ becomes

$$X''(v)|_{IR} = (\tilde{S}_i / \pi) \, \text{sgn}(v) \{f(v) + f(-v)\} . \qquad (3\text{-}10)$$

For this, we have

$$X'(v)|_{IP} = H[X''(v)|_{IR}]$$

$$= (2\tilde{S}_i / \pi) \tan^{-1}(v / a_i) \{g(v) + g(-v)\}$$

$$+ (\tilde{S}_i / \pi) \log_e [(v^2 + a_i^2)/v_i^2] \{f(v) + f(-v)\} . \qquad (3\text{-}11)$$

Using the IR approximation $v_i / a_i \gg 1$, and if we assume $v \simeq v_i$, this equation may be simplified as

$$X'(v)|_{IR} = (\tilde{S}_i / \pi) \{g(v) + g(-v)\} . \qquad (3\text{-}12)$$

It is interesting to note that Eq. (3-12) can also be

obtained from the following approximation.

$$X''(v)\big|_{IR2} = (\widetilde{S}_i/\pi)\{f(v) - f(-v)\}. \tag{3-13}$$

The fact that this is a good approximation for $X''\big|_{IR}$ in Eq. (3-10) can be seen by recognizing the negligible contribution of $f(v)$ in negative v range and the same of $f(-v)$ in positive v range. The obvious advantage of this function is the non-existence of the discontinuity. The more significant issue here is that Eq. (3-13) would have been one of the equivalent forms of Eq. (10) if the Lorentz function $f(v)$ would have satisfied the fractuation dissipation theorem (Kubo 1966),

$$f(-v) = e^{-2\widetilde{b}v} f(v). \tag{3-14}$$

Examining two results, Eqs. (3-8) and (3-12), we now propose the following real part of the susceptibility for the use in both MM and IR region.

$$X'_p(v) = (\widetilde{S}_i/\pi)\tanh(\widetilde{b}v_i)[\{g(v) + (a_i/v_i)f(v)\}$$
$$+ \{g(-v) + (a_i/v_i)f(-v)\}]. \tag{3-15}$$

It can easily be shown that this result reduces to the MM result, Eq. (3-8), by letting $\widetilde{b}v_i$ small. Similarly the IR result, Eq. (3-12), can be obtained by taking $\widetilde{b}v_i$ large and a_i/v_i small. The consistency of the proposed function can also be shown by taking the inverse Hilbert transform and to compare the result with the original imaginary part. For this we compute

$$X''_p(v) = H^{-1}[X'_p(v)] = -H[X'_p(v)]$$

$$= (\widetilde{b}v/\widetilde{b}v_i) \tanh(\widetilde{b}v_i) \; (\widetilde{S}_i/\pi) \; \{f(v) + f(-v)\} \; . \qquad (3-16)$$

The MM case can trivially be obtained by using the approximation in Eq. (3-3). The IR case also be checked by using Eq. (3-9) and by setting $v/v_i \cong 1$ in Eq. (3-16).

IV. Van Vleck-Huber with Line Coupling:

In the MM region it has been recognized that the line coupling term is necessary in order to obtain accurate absorption spectra. This correction, translated to the imaginary part of the susceptibility, can be expressed as (Balanger 1958)

$$X''_c(v) = (\widetilde{S}_i/\pi) \tanh(\widetilde{b}v) \; \{f(v) + r_i \, g(v) + f(-v) + r_i \, g(-v)\} \; , \qquad (4-1)$$

where r_i is the line coupling coefficient which is subject to the following constraint called the zero-sum rule in this work.

$$\sum_i \widetilde{S}_i \, r_i = 0 \; . \qquad (4-2)$$

Again we start from the MM renge where Eq. (3-3) is valid. Hence

$$X''_c(v)|_{MM} = (\widetilde{S}_i \, \widetilde{b}v/\pi) \; \{f(v) + r_i \, g(v) + f(-v) + r_i \, g(-v)\} \; , \qquad (4-3)$$

and

$$\sum_i X'_c(v)|_{MM} = H[\sum_i X''_c(v)|_{MM}]$$

$$= (\widetilde{b}/\pi) \; H[-\sum_i \widetilde{S}_i \, r_i + \sum_i \{(v + r_i \, a_i)f(v) - (a_i - r_i \, v_i)g(v)\}$$

$$+ \sum_i \widetilde{S}_i \, r_i - \sum_i \{(v + r_i \, a_i)f(-v) - (a_i - r_i \, v_i)g(-v)\}] \; . \qquad (4-4)$$

Note that the summation is explicitly taken in this equation and that the Hilbert transform of the entire sum is taken for the

142-8

proper treatment of the zero-sum rule. We now can use the zero-sum rule to eliminate two terms $-\sum_i \tilde{S}_i r_i$ and $+\sum_i \tilde{S}_i r_i$ in this equation. However, one can immediately notice that those two terms cancel each other regardless of their values. This is significant because it indicates that we can drop the summation from Eq. (4-4) and consider the Hilbert transform of a sigle line, Eq. (4-1), at a time. In effect, we have shown that the line profile in Eq. (4-3) is equivalent to the following one.

$$X''_c(v)|_{MM} = (\tilde{S}_i \tilde{b}/\pi)\{[(v_i + r_i a_i)f(v) - (a_i - r_i v_i)g(v)]$$

$$- [(v_i + r_i a_i)f(-v) - (a_i - r_i v_i)g(-v)]\}. \quad (4-5)$$

Thus we drop the summation from Eq. (4-4) and proceed.

$$X'_c(v)|_{MM} = H[X''_c(v)|_{MM}]$$

$$= (\tilde{S}_i \tilde{b}/\pi)[\{(v_i + r_i a_i)f(v) - (a_i - r_i v_i)g(v)\}$$

$$- \{(v_i + r_i a_i)f(-v) - (a_i - r_i v_i)g(-v)\}]. \quad (4-6)$$

The validity of this result can be checked by taking the inverse Hilbert transform and seeing the agreement with Eq. (4-5).

Now for the IR region, we again use the approximation in Eq. (3-13) for the line-coupled imaginary part. Thus we have

$$X''_c(v)|_{IR} = (\tilde{S}_i/\pi)\{[f(v)+r_i g(v)] - [f(-v)+r_i g(-v)]\}. \quad (4-7)$$

The corresponding real part $X'_c(v)|_{IR} = H[X''_c(v)|_{IR}]$ can easily be evaluated as

$$X'_c(v)|_{IR} = (\tilde{S}_i/\pi)\{g(v)-r_i f(v) + g(-v)-r_i f(-v)\}. \quad (4-8)$$

142-9

The matching of Eqs. (4-6) and (4-8) with the corresponding cases without line coupling can be seen by setting $r_i = 0$ in the respective equations.

As in the last section, we propose the following real part for all frequencies through the examination of two limits.

$$X'_{cp}(v)$$
$$= (\widetilde{S}_i /\pi) \tanh(\widetilde{b}v_i) [(1 + r_i a_i /v_i)g(v) - (r_i - a_i /v_i)f(v)$$
$$+ (1 + r_i a_i /v_i)g(-v) - (r_i - a_i /v_i)f(-v)] . \qquad (4-9)$$

It is a trivial matter to show that this reduces to Eq. (4-6) as the MM limit is taken. The agreement of the IR limit can also be shown as before. Instead, we check the validity by taking the inverse Hilbert transform and comparing the result with the original imaginary part. For this end we use Eq. (4-9).

$$X''_{cp}(v) = H^{-1}[X'_{cp}(v)] = -H[X'_{cp}(v)]$$
$$= (\widetilde{S}_i / v_i) \tanh(\widetilde{b}v_i) [\{(a_i - r_i v_i)g(v) - (v_i + r_i a_i)\}$$
$$- \{(a_i - r_i v_i)g(-v) + (v_i + r_i a_i)f(-v)\}] . \qquad (4-10)$$

The MM limit can easily be checked using the approximation in Eq. (3-3). On the other hand, the IR approximation in Eq. (3-9), namely $\tanh(\widetilde{b}v_i) = 1$, and $a_i /v_i = 0$, again gives the right form.

V. Exact Real Part and Numerical Comparison:

First, we present an exact expression for $X'(v)$ in an infinite series form which can be obtained through the use of a

known Lorentz expansion of the tanh(.) function given by (National Bureau of Standards 1964),

$$\tanh(\pi x/2) = (4x/\pi) \sum_{k=1}^{\infty} 1/\{x^2 + (2k-1)^2\} . \qquad (5-1)$$

We use this in Eq. (4-1) to obtain the following

$$X''(v) = (2\tilde{S}_i /\pi\tilde{b}) \sum_{k=1}^{\infty} \{v/(v^2 +e(k)^2)\}$$

$$\{f(v) + r_i g(v) + f(-v) + r_i g(-v)\} , \qquad (5-2)$$

where

$$e = (2k - 1) / (2\tilde{b}) . \qquad (5-3)$$

The advantage of this expression is that it is straightforward to obtain the Hilbert transform of each term in the summation. In fact, the partial fraction expansion of the summand gives,

$$X''(v) = (2\tilde{S}_i /\pi\tilde{b}) \sum_{k=1}^{\infty} [\{2A(k)v/(v^2 +e(k)^2)\}$$

$$+ \{B(k)f(v) + A(k)g(v)\} - \{B(k)f(-v) + A(k)g(-v)\}] , \qquad (5-4)$$

with

$$A(k) = \{a_i(v_i^2 +a_i^2 -e(k)^2) + r_i v_i(v_i^2 +a_i^2 +e(k)^2)\} / D(k) ,$$

$$B(k) = \{v_i(v_i^2 +a_i^2 +e(k)^2) - r_i a_i(v_i^2 +a_i^2 -e(k)^2)\} / D(k) ,$$

$$D(k) = (v_i^2 +a_i^2 -e(k)^2)^2 + 4v_i^2 e(k)^2 . \qquad (5-5)$$

Because the summation converges absolutely, the Hilbert transform and the summation can be interchanged and we can obtain the following desired result.

$$X'(v) = H[X''(v)]$$

142-11

$$= (2\tilde{S}_i/\pi\tilde{b}) \sum_{k=1}^{\infty} [\{2A(k)e(k)/(v^2 + e(k)^2\}$$

$$+ \{B(k)g(v) - A(k)f(v)\} + \{B(k)g(-v) - A(k)f(-v)\}] \ . \qquad (5-6)$$

Although this series expression is not suitable for repeated use since it converges slowly at the rate of $1/k$, it may be used for verification of the proposed real part.

This series was coded together with the proposed one, Eq. (40), and they were compared numerically for three line locations of 10, 412, and 1500 (1/cm) which represent MM, inter-mediate, and IR regions, respectively. The choice of 412 (1/cm) was made because it gives $\tilde{b}v_i = 1$ for $T = 296$ (K), where neither approximations, Eq. (3-3) and Eq. (3-9) for tanh(.), are adequate. Therefore we can evaluate the performance of the proposed real part in the intermediate region. A typical result is given in Figure 1.

VI. Conclusons and Discussions:

A unified approximate real part of the susceptibility over the entire MM and IR regions which corresponds to the Van Vleck-Huber line shape with line coupling is proposed. The function was obtained through careful examination of two limiting cases of MM and IR wave regions where the real parts were explicitly computed from the respective limiting forms of the imaginary part using the Hilbert transform. The inverse Hilbert transform of the proposed real part was computed as well to demonstrate the consistency of the function.

In the process of deriving the expression for the real part
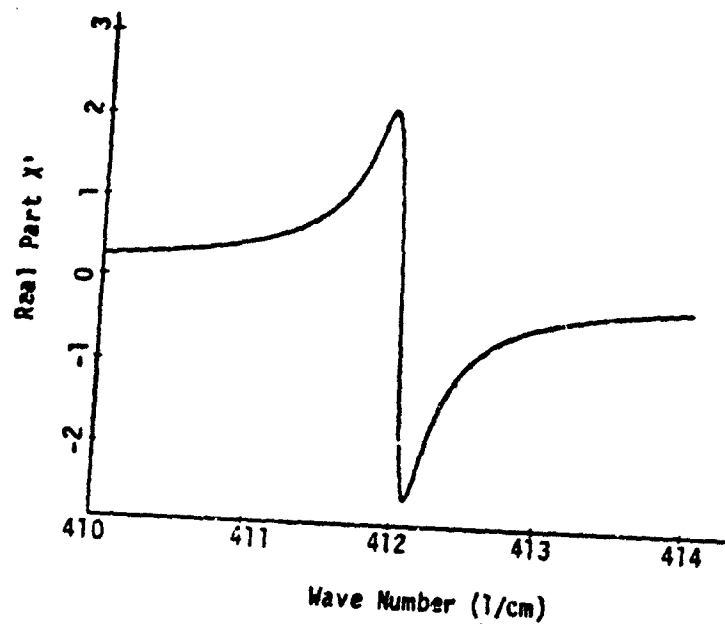
Figure 1-a.
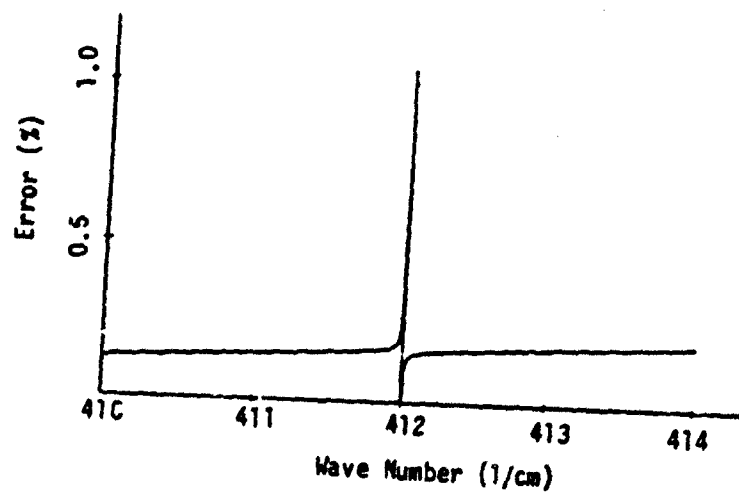
Figure 1-b.

Figure 1. Proposed real part of susceptibility with line-coupling for a single line at $v_i = 412$ (1/cm) with $S_i = 2.0$, $a_i = 0.1$ (1/cm), $r_i = 0.1$ and $\tilde{b} = 1/412$. A single point in Fig. 1-b at the zero crossing of the real part is eliminated from the plot due to the overflow caused by the division by very small real part. Figs. 1-a and 1-b are for the vicinity of the line center, and Figs. 1-c and 1-d are for the far wing.

142-13
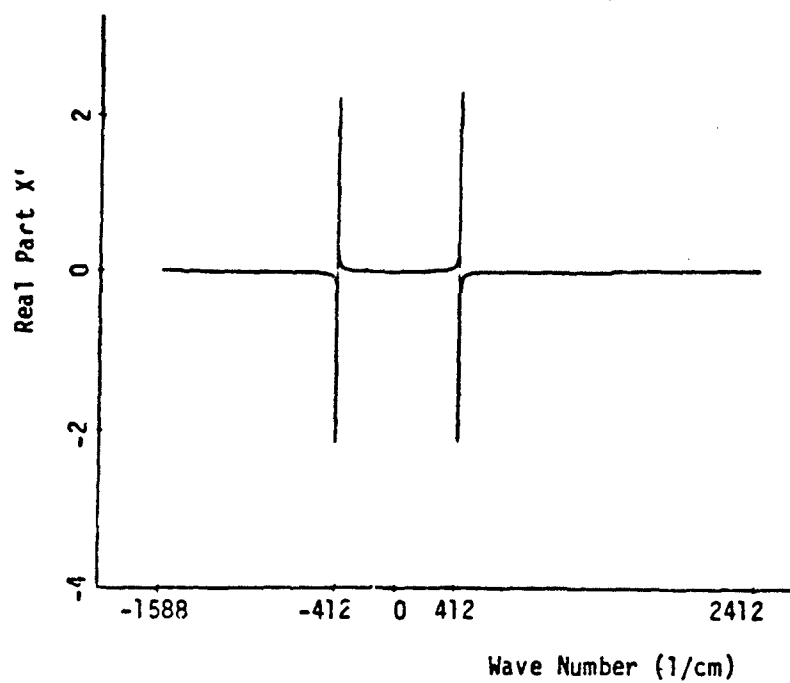
Figure 1-c.

Figure 1-d.

142-14
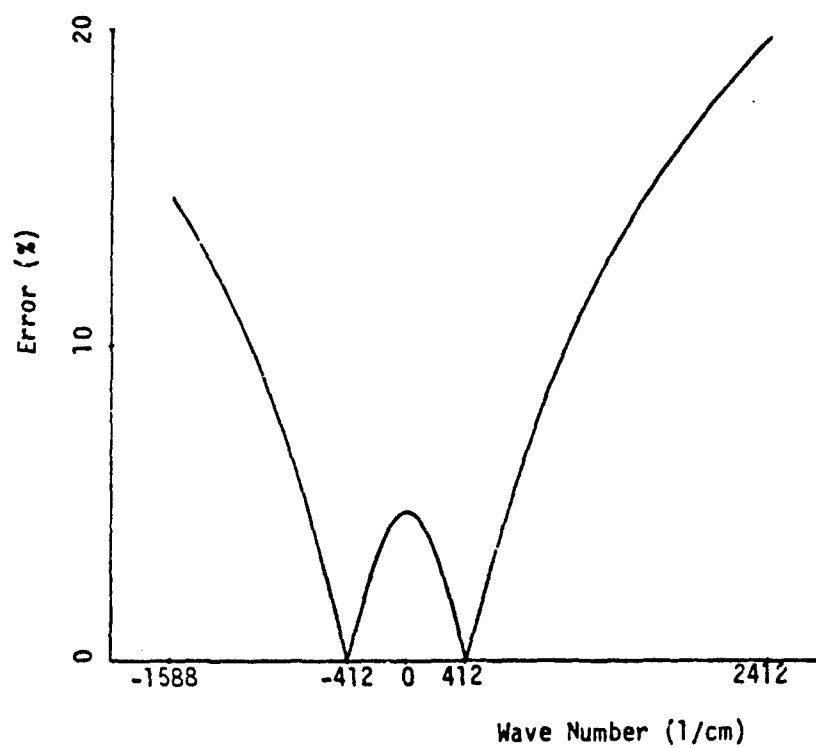
in the MM region, we recognized that a proper result can be
obtained for individual lines even if the line coupling term is
considered. The zero-sum rule, which is considered to be
essencial for the validity of Rozenkranz line coupled profile,
was found to be not essencial in obtaining consistent results.
Only requirement necessary to keep a proper consistency of the
real and imaginary parts was that a complete profile defined over
the entire real line be used. Therefore it is important to use
symmetric line shapes such as the Van Vleck-Huber profile.

The exact real part of the susceptibility was obtained in
the form of an infinite series by exploiting the Lorentz expan-
sion of the tanh(.) function and the known Hilbert transform of
the Lorentz function. The obtained series was successfully used
in numerical verification of the proposed approximate real part.
It was observed that good accuracies were obtained over the wide
range of ±1500 (1/cm) from the line center for the intermediate
and IR cases, and of ±100 (1/cm) for the MM case. The matchings
were found to be excellent in the vicinity of the line center, as
may be seen in Fig.1.

VII. Recommendations:

It is noted that the proposed real part can be used in
conjunction with the absorption line parameters in the entire
frequency range. Thus the vast data base such as the line
parameter compilation (Rothman 1983) can be used for the
evaluation of the real part spectra. It is an easy task to
incorporate the proposed real part into an absorption computation

code such as FASCODE (Clough 1981).

The proposed real part showed excellent agreement near the center of the line. However, the accuracy slowly deteriorates as the distance from the line center increases. The obvious reason for this is that the approximations for the tanh(.) function are valid only on limitted frequency ranges. Therefore, the corresponding approximate real parts also lose their accuracy for wider frequency range. A partial solution for this would be to use a line shape function which decreases to zero faster than the used Lorentz function. This would results in de-emphasizing the frequency region away from the center and hence would improve the accuracy of the resulting real part. An ultimate solution, however, is to find the closed form solution for the real part. The investigation for this requires such expertise as complex integration theory, special function theory and especially the broad applied mathematics which enables one to systematically attack the problem.

Acknowledgement

The auhter would like to express his appreciation to the Air Force Systems Command, the Air Force Office of Scientific Research and the Southeastern Center for Electrical Engineering Education for providing him with the opportunity to spend a very stimulating and productive summer at the Air Force Geophysics Laboratory, Hanscom AFB, Mass. He is indebted to the laboratory, in particular the Optical Physics Division, for its generosity and hospitality. He would like to thank Francis X. Kneizys and S. A. (Tony) Clough for leading him into this area of research which has turned out to be very fruitfull. Finally he would like to aknowledge many helpfull discussions and collaborations with staffs of Infrared Physics Branch, especially Gail P. Anderson, Eric P. Shettle and James H. Chetwynd.

REFERENCES

Baranger, M. "Problem of Overlapping Lines in the Theory of Pressure Broadening," Physical Review, Vol. 111, No. 2, July 1958, pp 494-504.

Bateman Manuscript Project. Tables of Integral Transforms, Vols. 1 and 2, McGraw-Hill, New York, NY, 1954.

Bolton, H. C. "Some Practical Properties of Kronig-Kramers Transform," The Philosophical Magazine, Vol.19, No. 159, March 1969, pp 487-499.

Bracewell, R. The Fourier Transform and Its Application, McGraw-Hill, New York, NY, 1965.

Campbell, G.A., and R.M. Foster. Fourier Integrals for Practical Applications. D. Van Nostrand, Princeton, NJ, 1948.

Clough, S.A., F.X. Kneizys, R. Davis, R. Gamache, and P. Tipping. "Theoretical Line Shape for H2O Vapor: Application to the Continuum," in Atmospheric Water Vapor, edited by A. Deepak, T.D. Wilkerson, and L.H. Ruhnke, Academic Press, New York, NY, 1980, pp 25-46.

Clough, S.A., F.X. Kneizys, L.S. Rothman, and W.O. Gallery. "Atmospheric Spectral Transmittance and Radiance: FASCODE1B," SPIE Vol.277-Atmospheric Transmission, 1981, pp 152-166.

Clough, S.A., R.W. Davis, and R.H. Tipping. "The Line Shape for Collisionally Broadened Molecular Transitions: A Quantum Theory Satisfying the Fluctuation Dissipation Theorem, in Spectral Line Shape Vol. 2, edited by K. Burnett, Walter de Gruyter, New York, NY, 1983, pp 553-568.

Fahrenfort, J. "The Methods and Results of Dispersion Studies," Chapter XI in Infra-red Spectroscopy and Molecular Structure, M. M. Davies ed., Elsevier, New York, NY, 1963.

Huber, D.L., and J.H. Van Vleck. "The Role of Boltzmann Factors in Line Shape," Reviews of Modern Physics, Vol. 38, No.1, January 1966, pp 187-204.

Kemp, A. J., J. R. Birch, and M. N. Afsar. "The Refractive Index of Water Vapor: A Comparison of Measurement and Theory," Infrared Physics, Vol. 18, 1978, pp 827-833.

Kubo, R. "The Fructuation-Dissipation Theorem," in Reports on Progress in Physics, Vol. XXIX Part 1, A. C. Stickland ed., The Institute of Physics and the Physical Society, London, 1966, pp 255-284.

Liebe, H. J. "Modeling Attenuation and Phase of Radio Waves in Air at Frequencies below 1000 GHz," Radio Science, Vol. 16, No. 6, November-December 1981, pp 1183-1199.

Marshall, A. G., and D. C. Roe. "Dispersion versus Absorption: Spectral Line Shape Analysis for Radiofrequency and Microwave Spectrometry," Analytical Chemistry, Vol. 50, No. 6, May 1978, pp 756-763.

Martine, P. C. "Sum Rules, Kramers-Kronig Relations, and Transport Coefficients in Charged Systems," Physics Review, Vol. 161, No.1, September 1967, pp161-155.

National Bureau of Standards. Handbook of Mathematical Functions with Formulas, Graphs, and Mathematical Tables, U.S. Department of Commerce, Washington, D.C., 1964.

Rosenkranz, P.W. "Shape of the 5 mm Oxigen Band in the Atmosphere," IEEE Transactions on Antennas and Propagation, Vol. AP-23, No. 4, July 1975, pp 498-505.

Rothman, L.S., et al. "AFGL Atmospheric Absorption line Parameters Compilation: 1982 Edition," Applied Optics, Vol. 22, No. 15, August 1983, pp 2247-2256.

Toll, J. S. "Causality and the Dispersion Relation: Logical Foundations," Physical Review, Vol. 104, No. 6, December 1956, pp 1760-1770.

Van Vleck, J.H., and D.L. Huber. "Absorption, Emission, and Linebreadths: A Semihistorical Perspective," Reviews of Modern Physics, Vol. 49, No. 4, October 1977, pp 939-959.

Van Vleck, J.H., and V.F. Weisskopf. "On the Shape of Collision-Broadened Lines," Reviews of Modern Physics, Vol. 17, Nos. 2 and 3, April-July 1945, pp 227-236.

1984 USAF-SCEEE SUMMER FACULTY RESEARCH PROGRAM

Sponsored by the

AIR FORCE OFFICE OF SCIENTIFIC RESEARCH

Conducted by the

SOUTHEASTERN CENTER FOR ELECTRICAL ENGINEERING EDUCATION

Final Report

NUMERICAL MODELING OF MULTIPHASE TURBULENT RECIRCULATING FLOWS IN SUDDEN-EXPANSION RAMJET GEOMETRY

Prepared by: Dr. Albert Y. Tong

Academic Rank: Assistant Professor

Department and   Department of Mechanical Engineering
    University: University of Texas at Arlington

Research Location: Aero Propulsion Lab
                       Wright-Patterson AFB
                       Dayton, Ohio

USAF Research: Dr. Roger R. Craig

Date: August 17, 1984

Contract No: F49620-82-C-0035

NUMERICAL MODELING OF MULTIPHASE TURBULENT RECIRCULATING FLOWS IN SUDDEN-EXPANSION RAMJET GEOMETRY

by

Albert Y. Tong

ABSTRACT

The numerical modeling of multiphase flow in a sudden-expansion ramjet combustor geometry has been studied. The objective is to develop a computer code which can be used for the systematic study of the flow characteristics. The possibility of adapting and modifying existing computer codes available at the Aero Propulsion laboratory has been examined. It has been found that it would be most efficient to develop a custom-made droplet spray code and incorporate it into the existing STARBC code for the multiphase flow calculations. The details of the droplet spray formulation and the overall solution scheme are presented. Finally, certain research problems which are related to the present research are suggested for future study.

Acknowledgement

I. INTRODUCTION:

In recent years there has been a reawakening interest in the use of ramjet propulsion systems for modern strategic and tactical missiles. The advantages of ramjet propulsion are the high specific impulse (resulting in enhanced range and/or speed capability) and a conceptually simple system requiring no moving parts other than those associated with the fuel system.

The basic ramjet combustor configuration is the so-called sudden expansion dump combustor as shown in Figure 1. In this type of combustor, liquid fuel is sprayed into the ram air upstream of the dump station, although it may also be injected directly into the chamber via side-wall inlets. Primary flame stabilization is provided by the flow recirculation regions, which may be supplemented, at the expense of total pressure loss, with mechanical flameholding devices at the air inlet/combustor interface and/or the presence of inlet air swirl, obtained by the use of tangential injection or swirl vanes.

The flow throughout is multiphase, subsonic, turbulent, and involves large-scale recirculation zones. With strong swirl in the inlet flow a central toroidal recirculation zone (a recirculation bubble in the middle of the chamber near the inlet) also presents itself. Even gross features of the flow are not known quantitatively with certainty: for example, factors affecting the existence, size, and shape of the recirculation zones.

Liquid sprays play an important role in combustion performance and emission of pollutants. Local values of air/fuel ratio are governed by trajectories of individual droplets, rates of vaporization and mixing of fuel vapor with air. Atomizers produce sprays with a wide range of droplet sizes, velocities and initial direction of flight. The droplets interact with gas streams, which can deflect the particles from their trajectories. Vapor is released in the wakes of the droplets and these trails of vapor mix by convection and diffusion with the airstreams. The rates of vaporization are governed by the temperature and vapor pressure concentrations of the environment through which the droplets traverse. Since combustion efficiency and temperature distributions are directly dependent upon air/fuel ratio distributions, an accurate prediction of composition of the fuel vapor evaporating at the droplet surface is important for spray combustion analysis. Also, changes in spray characteristics can result in important changes in combustor performance.

The present work is concerned with the computer modeling of the multi-phase flow fields in a sudden-expansion ramjet combustor. It is part of several concurrent research efforts undertaken at the Air Force Aero Propulsion Laboratory to gain further insights into the characteristics of these type of flow field.

II. OBJECTIVES:

The goal of the summer research is to investigate via numerical modeling, the flow characteristics in a sudden-expansion ramjet combustor described in the previous section. The particular problem is concerned with liquid fuel injections along with turbulent swirling flows at the combustor inlet. The study is restricted to steady flow in axisymmetric geometries under non-reacting conditions.

The objective is to develop a computer code which can be used for systematic study of flow characteristics in a ramjet dump combustor.

III. APPROACH ADOPTED IN THIS RESEARCH:

The possibility of adapting and modifying developed computer codes to the ramjet geometry and flow conditions has been considered. Several existing computer codes on fluid flow modeling available at the Aero Propulsion Laboratory have been examined. They are briefly outlined below:

1. STARPIC[1] (Swirling Turbulent Axisymmetric Recirculating flows in Practical Isothermal Combustor geometries)

   This code is based on the popular TEACH-X[2] code except that an equation for a swirl velocity component is included. The code is written essentially to model the flow in turbine combustors and the subroutine that specifies the initial conditions is somewhat more flexible than the TEACH code. The inlet conditions may include a sloping upstream boundary which is modelled within the calculation regime by a series of boundary steps.

   This code appears to be suitable for the flow field calculations. However, it is only for single-phase flows and droplet model has to be inserted in order to use it. Also, a diffusion equation and an energy equation would be needed.

2. STARRC[3] (Swirling Turbulent Axisymmetric Recirculating and Reacting Compressible Code)

This code uses the aforementioned STARPIC as a based code to which several features are added. The diffusion equation from TEACH-T code is added together with the enthalpy equation except that the enthalpy could be either the specific static or stagnation enthalpy as determined by a logic switch. The inclusion of the equation of state for calculation of density together with the stagnation enthalpy equation allows isentropic compressibility effects to be included. The boundary conditions allow the inclusion of a sloping upstream boundary and a downstream exit nozzle both of which are modelled by a series of finite steps. An expanding or an expanding-contracting grid can automatically be generated in the x-direction. The first approximation combustion of the TEACH-T code has been included and provision made for the planned addition of reaction kinetics. Again, this code which appears to be suitable for the present flow field calculation, is only for single-phase flows. A droplet model has to be inserted in order to use it.

3.   NASA-GARRETT 3-D[4]

This 3-D program is general and capable of predicting recirculating flows in three-dimensional geometries. The code's input and boundary conditions are specifically oriented towards gas turbine combustor geometries. Reacting or non-reacting, swirling or non-swirling, diffusion and/or premixed flames, and gaseous and/or liquid fuel combustion can be handled by the program. The code solves for all the quantities of STARRC in a three dimensional flowfield plus the mass fractions of unburned fuel, oxygen, carbon monoxide, C_xH_y, H_2, CO_2 and H_2O, three radiation flux vectors, soot and NO_x emissions and the fuel spray trajectory, droplet size distribution, and evaporation rate.

The adaptation of the code to the ramjet configuration appears to be useful. However, it has been found that the limitations in memory storage and speed capability of the computer system at the laboratory severely restrict, and practically prohibit the use of the code.

4.   ADD-PTRAK-VAPDIF[5]

This program calculates the operating characteristics of premix-

ing-prevaporizing fuel/air mixing passages. The calculation procedure utilizes three computer codes: The ADD code which calculates the axisymmetric or two-dimensional distributions of velocity, pressure and temperature of the air flow; the PTRAK code which calculates the nonequilibrium heat-up, vaporization, and trajectories of the liquid fuel droplets in a three-dimensional flow field; and the VAPDIF code which calculates the diffusion of fuel vapor into a moving air stream. The general approaches adopted in these codes are briefly described below:

ADD: First, an orthogonal coordinate system is constructed for the duct from the potential flow solution such that the stream function forms the coordinates normal to the wall and the velocity potential forms the coordinate tangent to the wall. By approximating the real streamlines by the potential flow streamlines, the governing viscous flow equations are reduced to a parabolic system of partial differ-ential equations which can be solved by a forward numerical integration procedure. The effects of fuel are neglected.

PTRAK: The analysis assumes lean equivalence ratios. Thus the air flow behavior can affect the fuel droplet behavior, but the fuel drop-let behavior does not affect the air flow behavior. The spray is divided into a number of classes. The code calculates the trajectory, vaporization rate, and temperature variation of each class of droplets. Large droplets may shatter into smaller droplets. Droplets from two classes may coalesce into larger entities. Droplets may collide with the duct walls and either rebound or undergo additional vaporization. A distribution of fuel vapor sources is calculated for use in the vapor diffusion computer program.

VAPDIF: With lean fuel assumption, the diffusion equations reduce to one equation for the mass fraction of fuel vapor diffusing into a known gas (air) flow field. The thermodynamics properties of the fuel vapor and air mixture are taken to be the thermodynamic properties properties of air. It is further assumed that the cloud of liquid fuel droplets does not interact with the fuel vapor other than to produce a source term in the diffusion equation. The diffusion equa-tion which is reduced to a linear second order partial differential

equation is solved by a forward marching integration technique.

Although the PTRAK code appears to have a rather detailed liquid fuel droplet model, both the ADD and the VAPDIF codes are parabolic in nature and therefore are not applicable to flows containing regions of separation.

It appears from this survey that none of the computer codes examined above (other than the NASA-GARRETT 3-D code which is limited by computer memory space) can be directly adapted for the two-phase recirculating flow calculations. One alternative is to combine the flow field calculation from the STARRC code with the PTRAK code which calculates the non-equilibrium heat-up, vaporization, and trajectories of the liquid fuel droplets in a decoupled flow field. However, this will be complicated by the fact that the PTRAK code utilizes an orthogonal streamline ordinate system used by the ADD code. While the streamline coordinate system obtained from the potential flow solution via the Schwarz-Christoffel transformation is quite elegant, it is not useful for the viscous flow situation.

Furthermore, the models used in the PTRAK code for elastic droplet collisions, droplet shattering, droplet coalescence and droplet wall interaction are untested. Their validities are quite questionable. On the other hand an oversimplified model is used for the droplet heating and vaporization.

Instead, it would be more efficient to develop a new droplet spray code custom-made for the STARRC code. This STARRC compatible droplet code will minimize the amount of modification effort required for the STARRC code. In addition, the recent developments in the droplet vaporization theory can also be incorporated. This approach is adopted in the present study. The details of the formulation of the droplet code and the overall solution scheme are given in the next section.

IV. FORMULATION AND SOLUTION SCHEME

The analysis of a two-dimensional gas-droplet flow field incorporating the effect of gas-droplet mass, momentum and energy coupling has been done by Crowe and co-workers[6,7]. The model was founded on the idea of regarding the condensed phase as a source of mass, momentum and energy to the continuum phase proposed by Migdal and Agosta[8]. Basically the calculation scheme utilized the cellular approach in which each computational cell was regarded as a control volume. Eulerian conservation equations were applied to the

143-8

gas phase and Lagrangian equations of droplet motion and thermal energy balance were applied to a finite member of droplet size ranges representing the size distribution within the spray. Recording the mass, momentum and energy of the droplets on crossing cell boundaries provide the droplet source terms for the gas flow equations.

The complete solution for a gas-droplet flow field is executed as illustrated in Figure 2. The calculation begins by solving the gas flow field assuming no droplets are present. Using this flow field, droplet trajectories together with size and temperature histories are calculated. The mass, momentum and energy source terms for each cell throughout the flow field are then determined. The gas flow field is solved again with these source terms incorporated. This iteration process continues until the flow field equations are satisfied to within a predetermined value and the solution which accounts for the mutual interaction of the droplet and gas is obtained.

This approach is used in the present study. Since the STARRC code also uses cellular approach, it can be used readily for the gas flow calculation. The only minor modification is the insertion of the droplet source terms into the conservation equations. The equations used for the droplet trajectories, size, temperature and source terms are outlined below.

Droplet Equations:

The equation of motion of a droplet is given by

$$\frac{d\vec{V}}{dt} = \frac{3}{8} \frac{\rho_g}{\rho_\ell} \frac{C_D}{R} (\vec{U} - \vec{V})|\vec{U} - \vec{V}| + \vec{g} \qquad (1)$$

$$\frac{d\vec{X}}{dt} = \vec{V} \qquad (2)$$

where $\vec{U}$ and $\vec{V}$ are the gas and droplet velocities respectively, C_D is the drag coefficient, R is the droplet radius, $\vec{g}$ is the gravity vector and $\vec{X}$ is the droplet location vector.

The drag coefficient for an evaporating liquid droplet depends primarily on the Reynolds number, Re, and the Spalding transfer number, B. Various relations for C_D have been proposed[9].

143-9

For the heat and mass transfer, if one assumes uniform droplet temperature and quasisteady gas phase along with spherical symmetry, the following equation for droplet vaporization can be obtained.

$$\frac{\dot{m}}{4\pi R \rho_g D} = \ell n \ (1 + B) \tag{3}$$

$$B = \frac{C_{pg}(T_g - T_\ell)}{H} = \frac{Y_{fs}}{1 - Y_{fs}} \tag{4}$$

$$H = L + \frac{1}{\dot{m}} \ \frac{4}{3} \pi \ R^3 \rho_\ell C_{p\ell} \ \frac{dT_\ell}{dt} \tag{5}$$

where $\dot{m}$ is the droplet mass vaporization rate, H is the effective latent heat of vaporization, D is the mass diffusivity, Y_{fs} is the fuel vapor mass fraction at the droplet surface, C_p, T and ρ represent specific heat, temperature and density respectively with subscripts g and ℓ denoting the gas phase and the liquid phase.

Combining Equations 3 to 5 yields

$$\frac{dR}{dt} = \frac{\rho_g}{\rho_\ell} \ \frac{D}{R} \ \ell n (1 + B) \tag{6}$$

$$\frac{dT_\ell}{dt} = \frac{\dot{m}}{\frac{4}{3}\pi \ R^3 \rho_\ell C_{p\ell}} \ [\frac{C_{pg}(T_g - T_\ell)}{B}] \tag{7}$$

Equations 1, 2, 6 and 7 form a system of coupled first order ordinary differential equations and they can be solved readily by using a Runge-Kutta scheme.

It should be noted that Equations 3-7 are based on spherical symmetry. Many investigators [10,11] suggested empirical correlations for vaporization rate in a convective field as a correction to the spherical symmetric case. The typical form of correlation is $m_{convection} = \dot{m} \ F(Re, Pr)$ where F(Re, Pr) is the correction factor. For example, the Ranz-Marshall[12] correlation is given by $F(Re, Pr) = 1 + 0.3 \ Re^{\frac{1}{2}} \ Pr^{1/3}$. Although this type of correlations is very simple, there is really very little theoretical justification for them.

Recently, Tong and Srignano[13,14,15] developed a simplified model for the problem of droplet vaporization. The model accounted for the

liquid-phase internal circulation and the axisymmetric gas-phase convection. The results were in close agreement with the results of a more detailed model. The model was also examined in a spray vaporization situation[16]. The feasibility of incorporating the model into a one-dimensional spray vaporization calculation was verified and the potential usefulness of the model in an overall spray situation was demonstrated.

This model, which is physically more realistic in a convective situation, will be incorporated in the droplet calculation. Since the overall solution scheme remains the same, the details of the simplified analysis is omitted here.

Droplet Source Terms

The entry of the droplets is represented by a finite number of entry ports. The mass of droplet radius, R_i, which enters per unit time at port j is given by

$$\dot{m}_{ij} = \dot{m}_T \, X_j \, Y_i \tag{8}$$

where $\dot{m}_T$ is the total droplet mass inflow rate, X_j is the fraction of droplet mass which enters at port j and Y_i is the fraction of droplet mass with initial radius R_i. The number flow rate of the droplets of radius R_i from port j is determined by

$$N_{ij} = \frac{3 \, \dot{m}_T \, X_j \, Y_i}{4\pi \, \rho_\ell \, R_i^3} \tag{9}$$

Droplet tracking allows the size, velocity temperature and position of the droplet to be determined in the calculation domain. Droplet source terms are obtained by calculating the loss or gain of the droplet mass, momemtum and energy within each cell. Summing up the respective source terms for droplets representing different size ranges gives the total droplet source terms.

From here onwards, trajectory "ij" denotes trajectory of droplets originated at port j with initial radius R_i. The net efflux rate of droplet mass from a computational cell due to trajectory ij is

$$\Delta\dot{m}_{ij} = \frac{4}{3} \, \pi\rho_\ell N_{ij} [R_{i,out}^3 - R_{i,in}^3] \tag{10}$$

143-11

where subscripts in and out denote quantities i..to and out of the computation cell respectively. The source term for mas 's given by summing over all droplet trajectories which traverse a given cell:

$$\Delta \dot{m} = \sum_{j} \sum_{i} \Delta \dot{m}_{ij} \tag{11}$$

The momentum source term and the energy source term are evaluated in the same fashion. The momentum source term for a given cell is given by

$$\Delta \vec{M} = \sum_{j} \sum_{i} \Delta \vec{M}_{ij} \tag{12}$$

where

$$\Delta \vec{M}_{ij} = \frac{4}{3} \pi \rho_{\ell} N_{ij} [(\vec{V}_i R_i^3)_{out} - (\vec{V}_i R_i^3)_{in}] \tag{13}$$

The energy source term is given by

$$\Delta E = \sum_{i} \sum_{j} \Delta E_{ij} \tag{14}$$

where

$$\Delta E_{ij} = \frac{4}{3} \pi \rho_{\ell} N_{ij} [(h_i R_i^3)_{out} - (h_i R_i^3)_{in}] \tag{15}$$

and h_i is enthalpy of the droplet.

V. PRESENT STATUS OF THE RESEARCH

The STARPIC and STARRC codes are both operational and flow field calculations for some test cases have been obtained. The droplet program presented in the previous section are being implemented into the STARRC code.

VI. RECOMMENDATIONS

At this point, it appears to be logical to recommend the completion of the implementation of the spray model presented in this report into the STARRC code. This task will be proposed for follow-on research work. Apparently, the numerical scheme is very promising and can be used readily for comparison with the on-going experiments being performed in the Aero Propulsion Laboratory.

In addition, the following related task, which the author considers to be important, deserves attention:

1. The numerical simulations of multiphase flow field are highly sensitive to the assumptions made for inlet boundary conditions. Much careful thought has to be devoted to providing these inlet conditions. Temptation to post-dict the experimental results by careful tailoring of the inlet conditions should be avoided.

2. The scheme which solves the steady state form of the gas phase equations in the STARRC code employs the "SIMPLE" method. Although this scheme has proven to be quite effective, its convergence rate can be improved. The "SIMPLER" algorithm, a revised version of "SIMPLE", provides a more accurate pressure field for each iteration through the momentum equations, thereby speeding convergence. In addition, operational improvements such as mesh imbedding, adaptive grids, dynamic variation of underrelaxation factors should be considered.

3. Although the widely used k-ε model of turbulence has been proven to be adequate in a variety of flows, it has been found that it performs poorly in confined vortex flows. Extreme caution in the use of the k-ε model in highly swirling flows is recommended.

4. The existing mathematical models for droplet shattering, droplet coalescence and droplet wall interaction are untested. Experimental investigation is needed.

The above are considered to be useful research problems and are recommended for future study.

REFERENCES

1. D. G. Lilley and D. L. Rhode, "A Computer Code for Swirling Turbulent Axisymmetric Recirculating Flows in Practical Isothermal Combustor Geometries." NASA CR-3442 (1982).

2. A. D. Gosman and F. J. K. Ideriah, "A General Computer Program for Two-Dimensional, Turbulent, Recirculating Flows," Report, Department of Mechanical Engineering, Imperial College, London (1976).

3. W. H. Harch, "Numerical Modelling of Ramjet Combustors," AFWAL-TR-82-2113 (1983).

4. T. W. Bruce, H.C. Mongia and R. S. Reynolds, "Combustor Design Criteria Validation," USARTL-TR-78-55(A,B,C) (1979) [Garrett Report 75-211682(38)].

5. O. L. Anderson, L. M. Chiapetta, D. E. Edwards and J. B. McVey, "Analytical Modeling of Operating Characteristics of Premixing-Prevaporizing Fuel-Air Mixing Passages," NASA CR-167990, R82-915362-40 (1982).

6. C. T. Crowe, "Gas-Droplet Flow Field in the Vicinity of an Atomizer," Eleventh JANNAF Combustion Meeting (1974).

7. C. T.Crowe, M. P. Sharma and D. E. Stock, "The Particle-Source-In. Cell (PSI-CELL) Model for Gas-Droplet Flows," Journal of Fluids Engineering, Vol. 99, pp. 325-332 (1977).

8. D. Migdal and V. D. Agosta, "A Source Flow Model for Continuous Gas-Particle Flow, "Journal of Applied Mechanics, vol. 35, No. 4, pp. 860-865 (1967).

9. M. C. Yuan an L. W. Chen, "On Drag of Evaporating Liquid Droplets," Combustion Science and Technology, Vol. 14, pp. 147 (1976).

10. A. Williams, "Combustion of Droplets of Liquid Fuels: A Review," Combustion and Flame, Vol. 21, pp. 1-31 (1973).

11. G. M. Faeth, "Current Status of droplet and Liquid Combustion," Progress in Energy and Combustion Science, Vol. 3, pp. 191-224 (1977).

12. W. E. Ranz and W. R. Marshall, "Evaporation from Drops," Chemical Engineering Progress, Vol. 48 pp. 141 (Part I); 173 (Part II) (1952).

13. A. Y. Tong and W. A. Sirignano, "Analysis of Vaporizing Droplet with Slip, Internal Circulation, and Unsteady Liquid-Phase and Quasi-steady Gas-Phase Heat Transfer," ASME-JSME Thermal Engineering Joint Conference, Honolulu, Hawaii (1983).

14. A. Y. Tong and W. A. Sirignano, "Analytical Solution of Diffusion and Circulation in a Vapor ~ing Droplet," Nineteenth Symposium (International) on Combustion, pp. 1007-1020 (1982).

15. A. Y. Tong and W. A. Sirignano, "Multicomponent Droplet Vaporization in a High Temperature Gas," Submitted to the ASME Winter Annual Meeting, New Orleans, (1984).

16. S. K. Aggarwal, A. Y. Tong and W. A. Sirignano, "A Comparison of Vaporization Models in Spray Calculations," accepted to AIAA Journal; see also AIAA 83-0152 (1983).
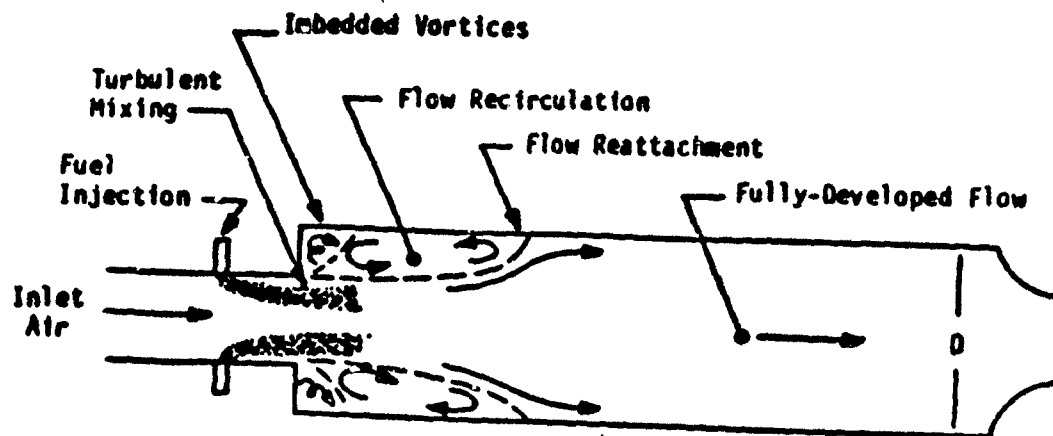
Figure 1. Ramjet Combustor Flowfield
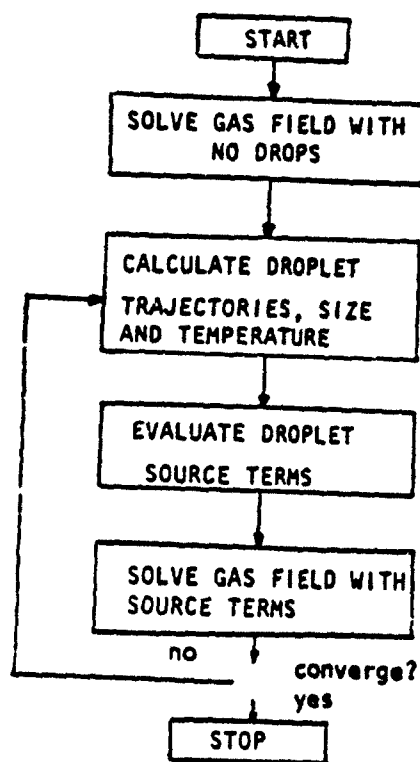
Figure 2. Computation Scheme

143-16

1984 USAF-SCEEE SUMMER FACULTY RESEARCH PROGRAM

Sponsored by the

AIR FORCE OFFICE OF SCIENTIFIC RESEARCH

Conducted by the

SOUTHEASTERN CENTER FOR ELECTRICAL ENGINEERING EDUCATION

FINAL REPORT

DEVELOPMENT OF THREE COVARIANCE STRUCTURE MODELS FOR
ANALYSIS OF PERFORMANCE MEASUREMENT PROJECT DATA

Prepared by: Robert J. Vance

Academic Rank: Assistant Professor

Department and University: Psychology Department, Ohio State University

Research Location: AFHRL/MODP

USAF Research Contact: Lt Col Rodger D. Ballentine

Date: 25 September 1984

Contract No: F49620-82-C-0035

DEVELOPMENT OF THREE COVARIANCE STRUCTURE MODELS
FOR ANALYSIS OF PERFORMANCE MEASUREMENT PROJECT DATA

by

Robert J. Vance

ABSTRACT

Three covariance structure models were developed to assess the construct validity of several job performance measures being developed for the Jet Engine Mechanic Specialty. The analyses are designed to clearly explicate the criterion space, that is, the criterion constructs and their interrelationships. Data will be collected during January-April, 1985, and analyses will be conducted shortly thereafter. Results of the analyses will contribute to an understanding of the job performance domain of the Jet Engine Mechanic Specialty. They will also provide information about the relative usefulness of the various measures employed, and about the validity of the ASVAB for predicting job success. It was recommended that future research focus on development of a method for assessing the costs and benefits associated with each of the performance measures, and with assessment of the utility (gain in productivity) of personnel management practices.

I. INTRODUCTION

The Performance Measurement Project being conducted by AFHRL/MODP is nearing final stages of development of an innovative and complex system for measuring the job performance of jet engine mechanics. The central measures of performance consist of two forms of a work sample test called Walk Through Performance Testing (WTPT). The WTPT-Hands On will require job incumbents to perform a series of job tasks according to instructions provided by a test administrator. The test administrators will be highly trained subject matter experts (i.e., former supervisors of jet engine mechanics), and test administrators will have the additional duties of observing, evaluating, and rating incumbents as they perform the WTPT-Hands On. The WTPT will also be administered in an interview format. Here, incumbents will be asked to describe in detail the steps they would perform in order to accomplish a task, without actually performing the task. Again, subject matter experts will administer the WTPT-Interview, and observe, evaluate, and rate the performance of incumbents.

Each of the approximately 360 jet engine mechanics to be tested will perform on both forms of the WTPT, for a total test time of approximately seven hours. In addition to the WTPT measures, performance will be assessed using four rating scales. These will include a Task Level Rating Form, a Dimensional Level Rating Form, a Global Level Rating Form, and an Air Force Wide Rating Form. Each rating form will be completed by the incumbent's supervisor, by the incumbent him- or herself, and by one or more of the incumbent's coworkers (peers). Thus, twelve sets of ratings will be obtained for each incumbent (four rating scales times three sources).

One of the stated purposes of The Performance Measurement Project is to develop sound measures of job performance in order to permit determination of valid cutting scores for the Armed Services Vocational Aptitude Battery (ASVAB), the test used to assist in the decision process for assigning recruits to specialties. ASVAB scores for each jet engine mechanic in the sample will be available, as will a Technical School score. Together these scores will be used to assess

144-3

recruit capability. Other variables thought to influence job performance will also be measured. These include task and job experience, motivation to perform one's job, and commitment to the Air Force. Other measures may eventually be included in the project as well.

The purpose of the summer research project was to develop a data analysis plan for The Performance Measurement Project, particularly with regard to investigating the construct validity of the job performance measures (WTPT and ratings). Incorporation of related measures such as ASVAB scores into the overall analysis plan was also desired. To these ends, three reports were written in which a number of analyses were proposed to address project needs. These will be described in more detail below. The present author was selected for the summer faculty position because of extensive past research experience in job performance measurement, and because of past experience with the data analytic techniques to be utilized.

II. OBJECTIVES

A variety of job performance measures will be utilized in the Performance Measurement Project. These are expected to vary in terms of fidelity of measurement and expense of administration. A clear understanding of the interrelationships of the measures is needed so that the project may proceed in the most efficient manner. The primary analysis technique to be employed will be covariance structure modeling, and a subset of this, confirmatory factor analysis. Both of these analysis techniques are quite complex, and require a preliminary model of the expected interrelationships of the variables. Formulating such a model requires a thorough understanding of the project goals and the measures to be obtained. The objectives of the summer research effort were:

1. to obtain a thorough understanding of project goals and measuring instruments through studying project materials and through discussions with project management;

2. to develop data analysis models (covariance structure and confirmatory factor analysis) for use on project data;

3. to document the proposed models and analyses in the form of. written reports.

The next three sections of this report are condensed from the original reports developed over the summer.

III. DESCRIPTION OF THE COVARIANCE STRUCTURE MODEL OF PERFORMANCE MEASUREMENT PROJECT VARIABLES

1. Assumptions

Proficiency will be measured by two components of Walk-Through Performance Testing (WTPT), Hands-on and Interview. There will be three measured variables associated with each component, percent of tasks correctly completed, percent of critical tasks correctly completed, and an average task proficiency rating. Task and job experience measures will be obtained for WTPT items, the former as the relative percent of time spent performing each task and the recency of experience, the latter as time in specialty. Ratings of job proficiency will be obtained from Task Level, Dimension Level, Global Level, and AF Level rating scales completed by supervisor, self, and peer sources. A summary rating will be derived from each scale and source combination for each incumbent. ASVAB component scores and training scores will also be available for each incumbent (the numbe of each type of score is yet to be determined).

2. Research Questions

The analyses described below will answer the following questions:

a. Do the data support a model which holds that the 25 observed variables are produced in part by 11 unobserved or latent variables? Are the observed variables adequate (i.e., statistically significant) measures of the latent variables?

144-5

b. Do the latent variables significantly influence one another as the model proposes? Are the WTPT latent variables central to the model as indicated? Are the rating variables "surrogates" to the WTPT variables? Does the "recruit capabilities" latent variable as measured by ASVAB and training scores account for substantial variance in WTPT performance?

c. If the proposed model does not fit the data, what model(s) can explain the relationships found in the data?

3. The Conceptual Model

Figure 1 presents the conceptual model of the anticipated relationships among the constructs assumed to be measured by the methods described above. Central to the model are the WTPT Hands-on and Interview constructs. These are regarded by project management as measures of performance with the greatest fidelity of all the measurement techniques used in the research. They are depicted as separate constructs because of the obvious differences in methods of data collection, and because they differ in specific task content. Although not included in Figure 1, it is assumed that there will be three measured variables for each WTPT construct.

The constructs of task experience and recruit capabilities are shown as having direct influences on both WTPT constructs. Incumbents with more experience on the job are expected to perform better on the WTPT than those with less experience. The arrows in the model indicate that one variable has an effect on another, or accounts for substantial variance in it. The technique is sometimes called "causal modeling," since the model is presumed to represent the true processes underlying the observed data. Recruit capability is also shown as having direct influences on both WTPT constructs. The individual's job proficiency as measured by the WTPT is thought to be determined in part by initial aptitude as measured by ASVAB and training scores.

The model also shows that the various ratings account for variance in the WTPT constructs. Each rating construct is a summary measure of

job performance as assessed by that particular scale by three sources. Although not formally included in the model, the more specific ratings (task and dimension level) are expected to explain more variance in WTPT constructs than are the more global ratings (global and AF level). The left side of Figure 1 contains the multitrait-multimethod (MTMM) model of sources of variance in ratings (see Section IV). The supervisor, self, and peer source constructs are not shown as directly influencing any of the other constructs in the model. Rather, they serve to explain variance in the measured rating variables. It may happen that analysis of the MTMM model will indicate that changes should be made in this model. For example, if analysis of the MTMM model reveals that supervisors and peers are not distinct sources of rating variance, but that they are encompassed in a source called "ratings by others," the models in Figures 1 and 2 will be altered to reflect this.

4. The Formal Model

Figure 2 presents a covariance structure model comprising 25 observed or measured variables and 11 unobserved or latent variables for the constructs discussed previously. Two types of latent variables are depicted, exogenous variables (ξ's) and endogenous variables (n's). Endogenous latent variables are shown as being caused or influenced by exogenous latent variables. No causes or direct influences on exogenous latent variables are shown, as these are assumed to lie outside the scope of the model. The arrows linking latent variables depict what is called the structural model. Also shown is the measurement model, the relationships of measured to unmeasured variables. The x's denote indicators of exogenous latent variables, the y's denote indicators of endogenous latent variables.

The covariance structure model contains all of the components of the confirmatory factor model (CFA; see Section IV), plus additional parameters (Long, 1983b). In essence, the covariance structure model contains two CFA models, one for the x variables and one for the y variables. The model includes observed exogenous variables (x_i's), exogenous common factors (ξ_j's), unique factors affecting x_i's

(δ_i's), and covariances among common factors (ϕ_{ij}'s) (not shown in Figure 2). The covariance structure model also contains observed endogenous variables (y_k's), endogenous common factors (η_i's), unique factors affecting y_k's (ϵ_k's), unique factors or disturbances affecting η_i's (ζ_i's), direct effects of exogenous latent variables ξ_j's on endogenous latent variables η_i's (γ_{ji}'s), and direct effects of endogenous latent variables η_i's on one another ($\beta_{ii'}$'s). No direct effects among the η's are included in Figure 2.

In matrix terms, the general forms of the factor equations for observed variables x and y are

$$x = \Lambda_x \xi + \delta \tag{1}$$

$$y = \Lambda_\eta \eta + \epsilon \tag{2}$$

These equations may be compared to equations 1 to 6 for specific observed variables.

The structural model specifies that endogenous latent variables are related to exogenous latent variables and other endogenous latent variables by equations of the general form

$$\eta = \beta \eta + \Gamma \xi + \zeta \tag{3}$$

or, alternatively (and equivalently),

$$\ddot{\beta} \eta = \Gamma \xi + \zeta \tag{4}$$

or, in reduced form (whereby endogenous latent variables are expressed only in terms of exogenous latent variables and errors in equations),

$$\eta = \ddot{\beta}^{-1} \Gamma \xi + \ddot{\beta}^{-1} \zeta \tag{5}$$

Since observed variables x and y can be expressed in terms of measurement model components (see equations 1 and 2), and structural

144-8

equations can be expressed in terms of components of factor equations (see equation 5), it follows that the covariance equation of observed variables can be expressed in terms of parameters of the structure and factor equations,

$$\Sigma = \left[\begin{array}{c|c} \Lambda_y \ddot{\beta}^{-1}\left(\Gamma\Phi\Gamma+\Psi\right)\ddot{\beta}'^{-1}\Lambda_y' + \Xi_\epsilon & \Lambda_y \ddot{\beta}^{-1}\Gamma\Phi\Lambda_x' \\ \hline \Lambda_x\Phi\Gamma'\ddot{\beta}'^{-1}\Lambda_y' & \Lambda_x\Phi\Lambda_x' + \Xi_\delta \end{array}\right] \qquad [6]$$

Thus, the variances and covariances of the observed matrix Σ are expressed in terms of the parameters of the eight matrices, $\Lambda_x, \Lambda_y, \Gamma, \beta,$ Φ, Ψ, Ξ_δ and Ξ_ϵ. Generally stated, specification of a model such as appears in Figure 2 determines which parameters of the eight matrices are to be estimated and which are constrained or fixed to zero.

Parameter estimation involves finding values for the parameters that will reproduce the matrix Σ as closely as possible (Long, 1983). Parameter estimation is accomplished by the computer program LISREL (Joreskog and Sorbom, 1984). Estimates are obtained according to the maximum likelihood (ML) criterion. The advantages of ML estimates are that they are approximately unbiased, have sampling distributions as small as any other possible estimates, are approximately normally distributed, and are scale invariant (Long, 1983a). Since these properties are asymptotic, it follows that the larger the sample size, the better.

Once the model has been estimated, it must be assessed for goodness of fit. Assessment of fit involves testing the statistical significance of individual parameters (with z statistics), and the overall fit of the model (with a chi-square test). Significance of a portion of the model, for example, that trait and method factors are correlated, is tested by comparing the X^2 of the first model to the X^2 of a second (nested) model in which trait and method correlations are constrained to equal zero.

5. Summary

The output of the LISREL program will include ML estimates of the parameters in the eight matrices, standardized estimates of these parameters, standard errors of the estimates of parameters, z values as tests of significance that each parameter is different from zero, and modification indices for parameters. The output also provides a chi-square test of the goodness of fit of the model, a correlation matrix of latent variables, and a variety of additional optional information. If the overall chi-square value is significant, it indicates that the data are significantly different from the model; thus, the hypothesis that the proposed model could have produced the data must be rejected. Generally, the next step is to test another model, one based on information gained from the first analysis.

IV. DESCRIPTION OF MULTITRAIT-MULTIMETHOD MODEL OF RATINGS

1. Assumptions

There will be four types of rating scales and three sources of ratings. Task Level, Dimension Level, Global Level, and AF Level ratings will be completed by Supervisor, Self, and Peer. One summary rating will be obtained from each scale type and source combination, yielding 12 scores per incumbent. In the event that more than one supervisor or peer completes the ratings for a given incumbent, scores will be averaged to derive a single value from that source. This will produce a 12x12 correlation matrix (4 scales by 3 sources), based on a sample of N incumbents. Method and trait effects are assumed to be additive and linear, and all other effects are essentially random (Alwin, 1974). For this discussion, sources will be assumed to be analogous to traits in MTMM terminology, and scales will correspond to methods.

2. Research Questions

The analyses described below will answer the following questions:

a. To what extent does variance in the 12 measured variables reflect the effects of latent scale and source variables? Are supervisor, self, and peer sources identifiable as distinct latent variables? Are task, dimension, global, and AF rating methods distinguishable as separate latent variables?

b. To what extent are the latent source variables intercorrelated (i.e., with other sources of variance removed)?

c. To what extent are the latent rating method variables intercorrelated (i.e., with other sources of variance removed)?

d. To what extent are source and method factors intercorrelated (i.e., with other sources of variance removed)?

In summary, the analyses will reveal the extent to which source and method factors contribute to observed scores, and the extent to which latent factors are related to one another. The results may also indicate that latent variables are not present as defined by the model. For instance, it may be determined that supervisors and peers are not distinctly different sources of variance, necessitating creation of a new latent variable in the model called "ratings by others."

3. The Model

Figure 3 presents a Multitrait-Multimethod (MTMM) Confirmatory Factor Analysis (CFA) model for the variance components of the observed scores from three rating sources on four types of rating scales. The model represents each observed scores (x_i) as comprising variance due to source, method, and unique or error variance.

The LISREL program used to test the model will:

a. provide standardized maximum likelihood estimates of model parameters;

b. provide tests of significance for each parameter;

c. provide a test of f'' of the overall model to the data;

d. provide a correlation matrix of the task and method factors.

These results will permit conclusions about the convergent and discriminant validity of the measurement of job performance.

V. DESCRIPTION OF MULTITRAIT-MULTIMETHOD MODEL OF FIVE "CORE" TASKS

1. Assumptions

There will be five "core" tasks that will be assessed by means of Walk-Through-Hands On, Walk-Through-Interview, Task Level Ratings by Supervisor, Task Level Ratings by Self, and Task Level Ratings by Peer. This will yield a 25x25 correlation matrix resulting from five traits (tasks) measured by five methods. For each task and method combination, a single summary score will be obtained or derived for each job incumbent. Method and trait effects are assumed to be additive and linear, and all other effects are essentially random (Alwin, 1974).

2. Research Questions

The analyses described below will answer the following questions:

a. Do the 25 measured variables (x_1 to x_{25}) adequately measure the five latent task variables? Stated another way, do the data support a model which holds that the 25 observed variables are produced in part by five unobserved task variables? Results which answer this question will indicate both convergent and discriminate validity.

b. Do the 25 measured variables reflect the effects of five latent method factors (i.e., WTPT-Hands On, WTPT-Interview, Supervisory Ratings, Self Ratings, Peer Ratings) as specified by the model?

144-12

c. To what extent are the latent task variables intercorrelated (i.e., with other sources of variance removed)?

d. To what extent are the latent methods factors intercorrelated (i.e., with other soures of variance removed)?

e. To what extent are task and method latent variables intercorrelated (i.e., with other sources of variance removed)?

In summary, the analyses will reveal the extent to which five tasks have actually been measured, the extent to which the techniques of measurement contribute variance to the observed scores, and the extent to which the task and method latent variables are interrelated.

3. The Model

Figure 4 presents a Multitrait-Multimethod (MTMM) confirmatory factor analysis (CFM) model for the variance components of the observed scores on five "core" tasks as measured by five methods. The model represents each observed score (x_i) as comprising variance due to task, method, and unique or error variance.

The LISREL program used to test the model will:

a. provide standardized maximum likelihood estimates of model parameters;

b. provide tests of significance for each parameter;

c. provide a test of fit of the overall model to the data;

d. provide a correlation matrix of the task and method factors.

These results will permit conclusions about the convergent and discriminant validity of the measurement of job performance.

VI. RECOMMENDATIONS

It is recommended, first of all, that the analyses described herein be the primary data analyses for the jet engine mechanic data set. Given the need to explicate the criterion space, covariance structure modeling is the only analysis technique capable of doing so for a project of this magnitude. The project and analyses represent potentially important contributions to our understanding of job performance measurement, and of covariance structure modeling as a means of exploring construct validity.

A second recommendation is that the AF Human Resources Laboratory acquire the LISREL computer program needed for covariance structure modeling. The program is essential to the Performance Measurement Project, and will undoubtedly serve many other HRL research projects in the years to come as well.

A third recommendation concerns assessment of the relative costs and benefits of the Performance Measurement Project components. Upon completion of work on the Jet Engine Mechanic Specialty, work will commence on performance measurement for seven additional specialties. It is important to know whether each of the performance measures is a good measure, and, perhaps more importantly, whether it is worth the cost of using it. The construct validity analyses described in this report will provide some of the information needed to assess the relative costs/benefits of each measure, but more information is needed for a complete analysis. Since the project will produce performance measures that will be subsequently used to validate other personnel management practices (e.g., placement via ASVAB scores), a larger question concerns the utility (i.e., gain in productivity) resulting from the use of these practices. This researcher will propose to survey the methods available for cost/benefits and utility analyses, and to adapt these techniques for use in this project. This proposal will be submitted to SCEEE for follow-up research monies through the RISE program.

ACKNOWLEDGEMENTS

REFERENCES

Alwin, D. F. (1974). Approaches to the interpretation of relationships in the multitrait-multimethod matrix. In H. Costner (Ed.), Sociological methodology 1973-1974. San Francisco, CA: Jossey-Bass. pp. 79-105.

Joreskog, K. G., & Sorbom, D. (1984). LISREL VI: Analysis of linear structural relationships by the method of maximum likelihood (3d ed). Mooresville, IN: Scientific Software, Inc.

Long, J. S. (1983a). Confirmatory factor analysis. Beverly Hills, CA: Sage Publications.

Long, J. S. (1983b). Covariance structure models: An introduction to LISREL. Beverly Hills, CA: Sage Publications.
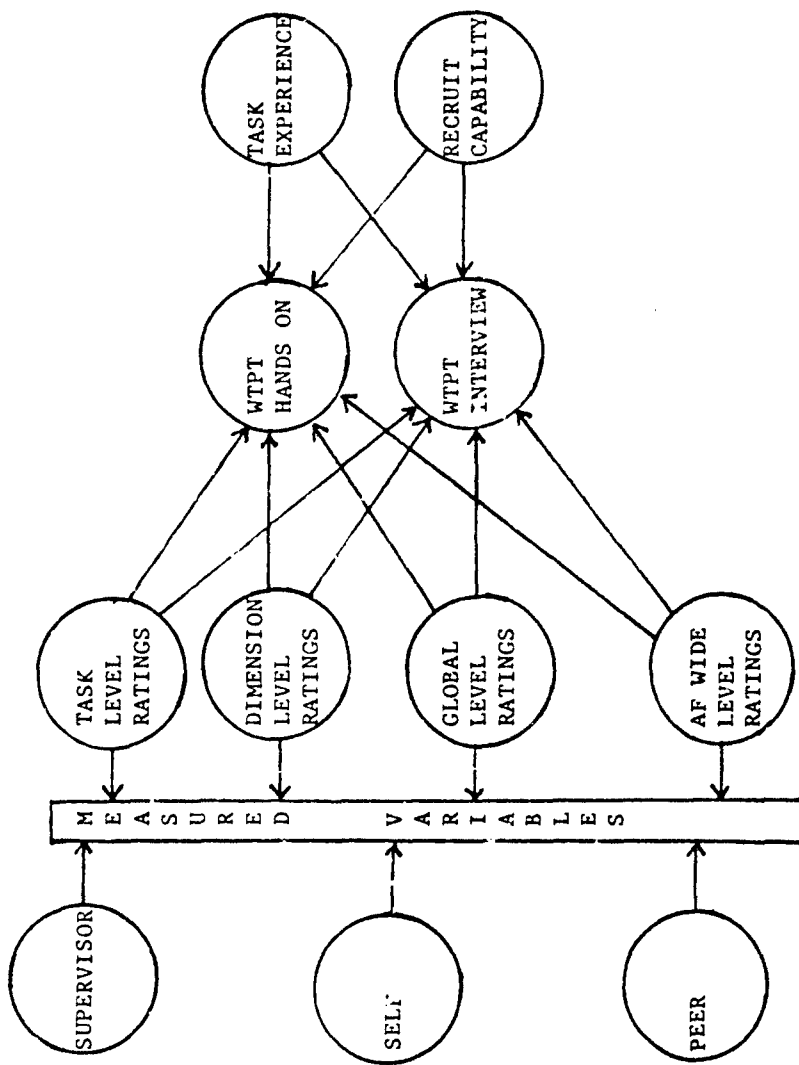
Figure 1. Conceptual Model of Relationships among Constructs
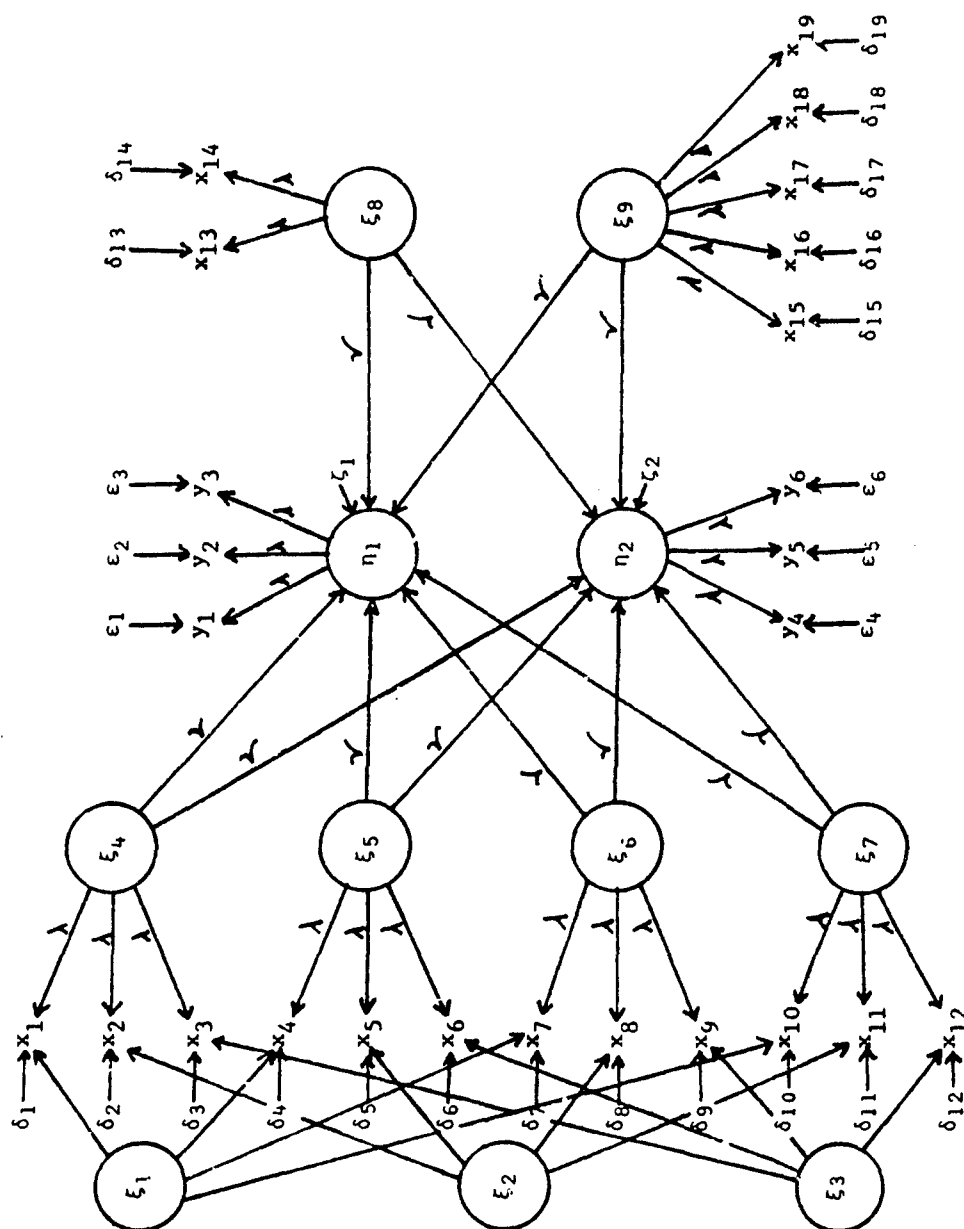
Figure 2. Covariance Structure Model for Performance Measurement Constructs
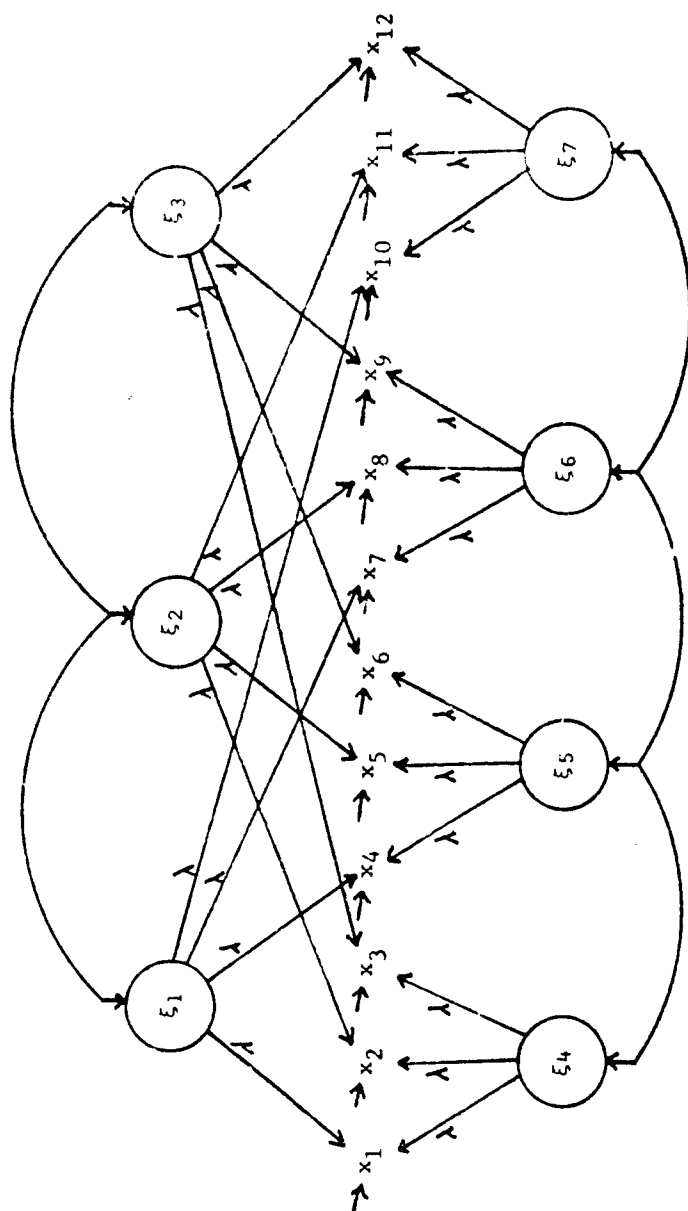
Figure 3. Multitrait-Multimethod Confirmatory Factor Analysis Model for Ratings
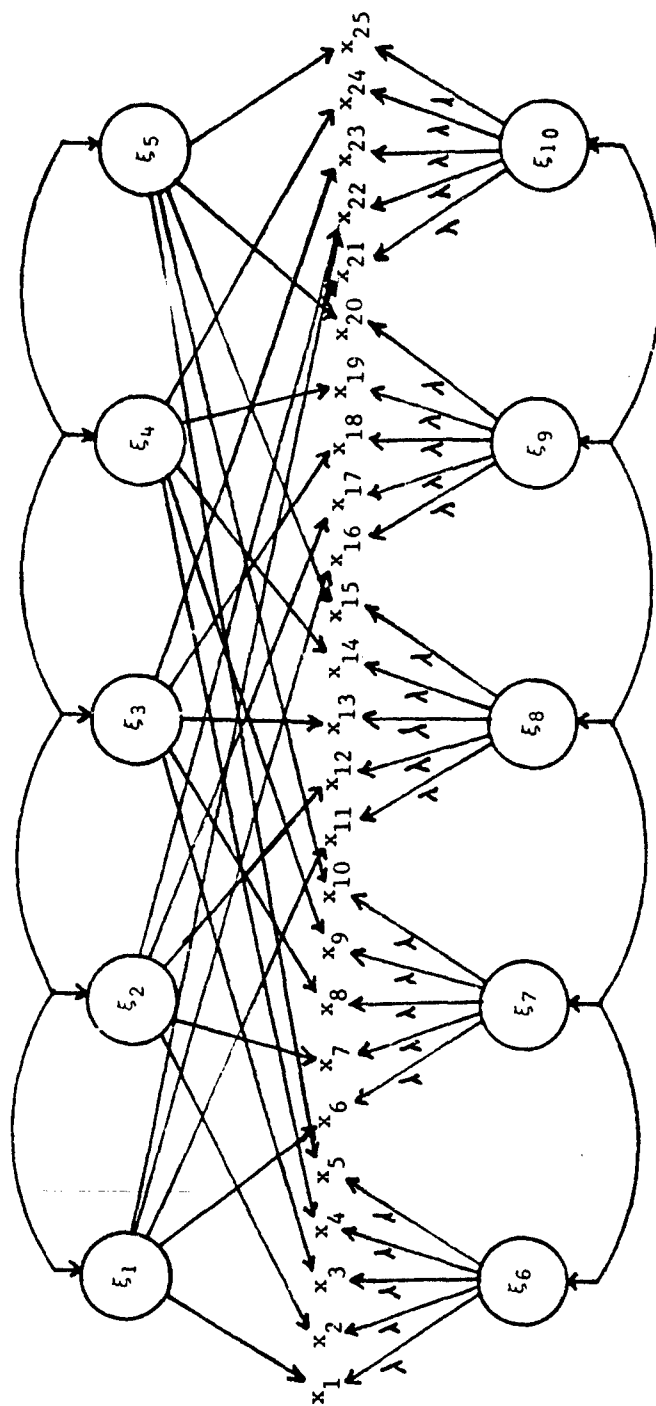
Figure 4. Multitrait-Multimethod Confirmatory Factor Analysis Model for Core Tasks

1984 USAF-SCEE SUMMER FACULTY RESEARCH PROGRAM

Sponsored by the

AIR FORCE OFFICE OF SCIENTIFIC RESEARCH

Conducted by the

SOUTHEASTERN CENTER FOR ELECTRICAL ENGINEERING EDUCATION

FINAL REPORT

LAMINARIZATION IN HIGHLY ACCELERATED FLOW

Prepared by: Dr. Brian Vick

Academic Rank: Assistant Professor

Department and   Mechanical Engineering Department
  University: Virginia Polytechnic Institute and State University

Research Location: Air Force Rocket Propulsion Lab
                    LKDB, Edwards AFB CA 93523

USAF Research: Darwin G. Moon

Date: August 31, 1984

Contract No: F49620-82-C-0035

LAMINARIZATION IN HIGHLY ACCELERATED FLOW

by

Brian Vick

ABSTRACT

In the presence of severe streamwise accelerations, such as encoun-
tered in rocket nozzles and in flow over turbine blades, initially
turbulent boundary layers can undergo a reverse transition towards a
laminar state. This phenomenon of flow laminarization has not been
adequately accounted for in the current schemes (TDK/BLM) used to pre-
dict rocket nozzle performance and thus forms the subject of this inves-
tigation. Despite the existance of important applications, basic infor-
mation on laminarization is scarce with only a very few experimental
results and some rather inconclusive theoretical studies available in
the literature. In the present investigation the existing state of
knowledge is examined and a plan of attack to bring the complex pheonom-
enon of flow laminarization onto a solid theoretical foundation is
outlined.

ACKNOWLEDGEMENT

The author would like to thank the Air Force Systems Command, the Air Force Office of Scientific Research and the Southeastern Center for Electrical Engineering Education for providing the opportunity to participate in the Summer Faculty Research Program and to work at the Rocket Propulsion Lab, Edwards AFB CA. The research experience with the Orbital Propulsion Section was very fruitful in terms of developing new and interesting areas for future research.

Particular appreciation is expressed to Darwin G. Moon for suggesting the research, to 2 Lt. Kevin R. Benson for support with the computer codes and to all the people in the Space Propulsion Branch who helped to make the summer a truly rewarding experience.

NOMENCLATURE

A   =   damping constant

$$C_f/2 = \frac{\tau_w}{\rho\, u_e^2} = \text{friction factor}$$

C_H =   Stanton number

H   =   total enthalpy

L   =   mixing length

$$k = \tfrac{1}{2}\overline{(u'^2 + v'^2 + w'^2)} = \text{turbulence kinetic energy}$$

$$K = \frac{\nu_e}{u_e^2}\frac{du_e}{dx} = \text{acceleration parameter}$$

N   =   parameter defined by eq. (8c)

P_r =   Prandtl number

r   =   radial coordinate

$\dot{q}$ =   heat transfer rate

T   =   temperature

u   =   mean x-velocity

v   =   mean y-velocity

x   =   axial coordinate

y   =   transverse coordinate

Greek Symbols

δ = boundary layer thickness

ϵ_m = eddy viscosity

ρ = density

μ = viscosity

ν = kinematic viscosity

τ = shear stress

γ = intermittency parameter

Subscripts

e = boundary layer edge conditions

t = turbulent quantity

w = wall condition

INTRODUCTION

This investigation concerns the behavior of turbulent boundary layers which experience reverse transition toward laminar flow under conditions such as strong streamwise pressure gradients. Such an effect could exist under conditions experienced in rocket nozzles, in flow over turbine blades, on external flow over surfaces of aerodynamic vehicles, in high temperature gas cooled nuclear reactors and in a variety of turbomachinery applications. Particular interest concerns cooled rocket nozzles, where laminarization could reduce both friction drag and heat transfer in regions of strong streamwise flow acceleration. In rocket nozzles such as the LSSCDS which is under consideration for use in orbital transport vehicles, the reduction in frictional drag in a laminarizing boundary layer is advantageous but probably accounts for only a small percent difference in specific thrust as compared to a fully turbulent boundary layer, however, the reduction in heat transfer could cause excessively high temperatures in the throat region and could lead to serious design difficulties.

The occurrence of laminarization involves a complex interrelationship among many parameters, however, any condition which tends to straighten out the flow field or reduce the turbulence will cause a turbulent flow to experience a reverse transition towards the laminar state. A strong favorable streamwise pressure gradient tends to reduce the turbulent fluctuations in the flow direction and is a commonly occurring cause of laminarization. However, other effects such as compressibility can also assist the laminarization process. For instance, in gas flow with wall cooling, the flow tends to accelerate in the

streamwise direction towards regions of denser fluid, thus reducing the turbulence. Also a cooled wall with curvature such as found in rocket nozzles will tend to stratify the cold, denser fluid against the walls and thus suppress the turbulence in the transverse direction; an effect analogous to a centrifugal separator. Centrifugal acceleration has a similar effect as gravitational acceleration with either effect capable of intensifying or reducing the level of turbulence. Indeed there are other physical effects which could cause laminarization, such as natural convection, wall heating, or wall injection or suction. This investigation will center around situations involving streamwise flow acceleration caused by strong pressure gradients since this is the dominant cause of flow laminarization for applications of interest, such as in rocket nozzles.

145-7

OBJECTIVES

This investigation focuses on flow laminarization as it effects boundary layer predictions. Motivation for the investigation originated from a need by the AFRPL to obtain better performance predictions in rocket nozzles. In particular, the large space system cryogenic development system (LSSCDS) engine, which is a high area ratio (1230 to 1) low thrust (500 lb_f) expander cycle engine, is currently being considered for use as an orbital transfer vehicle (OTV). This particular application has brought to light the interesting and little understood pheonomenon of reverse transition for which the modified mixing length turbulence model currently used in performance prediction codes (BLM) is unable to adequately deal with. As a result the objective of this investigation is to study the physical effects causing laminarization, to determine the parameters indicating the relative importance of reverse transition and to look at analytical models capable of accurately predicting this complex phenomenon.

LITERATURE REVIEW

Turning our attention to the literature, we find that an overwhelming and rapidly increasing amount of information can be found concerning fluid mechanics and convective heat transfer. However, basic information on turbulent flows that experience a severe flow acceleration and thermal environment leading to laminarization is scarce.

Evidence of transition from turbulent to laminar flow of gases in tubes due to wall heating was presented in references [1,2] while reverse transition due to fluid injection at the surface [3,4] has also been investigated. The nature and basic structure of a turbulent flow under the influence of strong favorable pressure gradients has been examined in references [5-8]. Results indicate that the longitudinal velocity fluctuations and skin friction decrease and that significant departures from the universal "law of the wall" occur in regions of strong favorable pressure gradients. An interesting set of experiments was performed by Moretti and Kays [9] where the effects of flow acceleration and wall temperature on the Stanton number was investigated. Here the acceleration parameter

$$K = \frac{v_e}{u_e^2} \frac{du_e}{dx} \qquad (1)$$

was introduced and found to be a useful indication of laminarization, although a correlation based on K alone was not possible. The results of [9] as well as the acceleration parameter will be elaborated on in later sections.

A series of experimental studies into flow phenomena and laminarization in nozzles were performed by Back, Massier, and Cuffel [10-15]. These works contain the most definitive data available for nozzles and the results of [14] will form the basis for comparisons with existing computer codes presently used for theoretical predictions, since this work involves boundary layer and heat transfer measurements in a convergent-divergent nozzle with high accelerations and wall cooling. Although a few other experiments have been performed [16,17], the available data is generally insufficient for any extensive theoretical comparison or for gaining a thorough understanding into the effects of laminarization for most applications of interest.

The literature contains several theoretical works [18-26] in which various approaches have been applied and comparisons with experiments have been made. Deissler [18] considers an incompressible boundary layer and uses simplified equations for the Reynolds shear stress and turbulent heat transfer leading to values which remain frozen as they are convected along streamlines. The results presented are in fair agreement with data from [9] but the results have acceptable accuracy only during the early or intermediate development of highly accelerated flow, since strong acceleration tends to diminish the Reynolds stress and turbulent heat transfer in a turbulent boundary layer. An asymptotic theory, constructed for large values of a pressure gradient parameter, has been attempted [19] but appears to have difficulty with the viscous sublayer, which limits the applicability of the approach when laminarization is in progress. Integral forms of the boundary layer equations are considered in [20] under restricted boundary

conditions which lend themselves to a convenient similarity analysis.
The results indicate that for accelerating turbulent boundary layers,
the thickness of the thermal layer may exceed that of the velocity layer
which causes the Stanton number to decrease. The case under
consideration, however, is too specialized to allow for general
conclusions or for an extension of the mathematical analysis to more
general problems.

The theoretical models presented in references [21-25] will be
examined in subsequent sections. Briefly they include a simplified
model using a completely laminar sublayer near the wall and turbulent
wake region [21], a model governed by the integral form of the turbu-
lence kinetic energy equation [22], a two-equation turbulence model [23-
24] and an analysis requiring the solution of approximated transport
equations for the turbulent shear stress, turbulent kinetic energy, and
energy dissipation rate [25]. The merits of the various approaches as
well as a critical examination of the current prediction methods will
now be examined.

BOUNDARY LAYER EQUATIONS

The boundary layer equations of a steady, compressible fluid for both laminar and turbulent axisymmetric flow are well known and can be written as

Continuity

$$\frac{\partial}{\partial x}(\rho u r^k) + \frac{\partial}{\partial y}(\overline{\rho v r^k}) = 0 \tag{2}$$

Momentum

$$\rho u \frac{\partial u}{\partial x} + \overline{\rho v}\frac{\partial u}{\partial y} = \rho_e u_e \frac{du_e}{dx} + \frac{1}{r^k}\frac{\partial}{\partial y}[r^k(\mu\frac{\partial u}{\partial y} - \overline{\rho u'v'})] \tag{3}$$

Energy

$$\rho u \frac{\partial H}{\partial x} + \overline{\rho v}\frac{\partial H}{\partial y} = \frac{1}{r^k}\frac{\partial}{\partial y}\{r^k(\frac{\mu}{Pr}\frac{\partial H}{\partial y} + \mu(1 - \frac{1}{Pr})\,u\,\frac{\partial u}{\partial y} - \overline{\rho H'v'})\} \tag{4}$$

where k = 1 for axisymmetric flows, k = 0 for two-dimensional flows and $r(x) = r_o(x) + y\,\cos\phi$. The edge velocity, u_e is determined from the external potential flow solution and is considered as a known input. Boundary layer equations (2-4) accurately model many flow situations encountered in practice, including rocket nozzles.

Equations (2-4) require an initial condition and boundary conditions which are taken as

$$u = 0\;,\;v = 0\;,\;y = 0$$

$$T = T_w(x)\;\text{or}\;\dot{q} = \dot{q}_w(x)\;,\;y = 0 \tag{5a}$$

$$u = u_e\;,\;H = H_e\;,\;y = \delta \tag{5b}$$

Equations (2-5) comprise a formidable set of non-linear coupled partial differential equations. The major difficulty is the fact that they do not form a closed set since we have no way of relating the

Reynolds stress, $\overline{\rho u'v'}$, and turbulent heat flux, $\overline{\rho H'v'}$, to the mean flow quantities through either first principles or universally valid postulates. Much work in turbulent modeling has been performed in order to remedy this situation but no model has been able to predict all situations of interest and at the present we are happy to have any model which is able to accurately predict even a limited class of flow situations. One particularly difficult situation involves flow under strong favorable pressure gradients which motivates the present investigation.

PRESENT TURBULENCE MODEL

Performance predictions in rocket nozzles presently consist of an inviscid core flow solution known as the Two-Dimensional Kinetics Computer Program (TDK, reference [26]) which is integrated with a boundary layer code known as the Boundary Layer Analysis Module (BLM, reference [27]). The procedure consists of running TDK with the desired geometry and chamber conditions and using the solution as the freestream conditions needed to run BLM. Once BLM has been run a displaced wall can be calculated in order to determine a more accurate inviscid shape with which to rerun TDK.

BLM models the flow field using eqs. (2-5) with the possibility of mass transfer at the wall included. After transformation of variables the Keller Box Method [28] is employed to solve the equations.

The key ingredient for accurate predictions in boundary layers is the choice of the turbulence model. BLM uses the concepts of eddy viscosity and turbulent Prandtl number given as

$$\overline{\rho u'v'} = \rho \varepsilon_m \frac{\partial u}{\partial y} , \qquad \overline{\rho H'v'} = \rho \frac{\varepsilon_m}{Pr_t} \frac{\partial H}{\partial y} \tag{6}$$

A constant value of $Pr_t = 0.9$ is used along with the eddy viscosity formulation due to Cebeci and Smith given by

$$\varepsilon_m^+ = \begin{cases} \dfrac{L^2}{\nu} \dfrac{\partial u}{\partial y} \gamma\gamma_{tr} & y < y_c \\[4mm] \dfrac{0.0168}{\nu} \displaystyle\int_0^\infty |(u_e - u)| dy \gamma\gamma_{tr} & y > y_c \end{cases} \tag{7}$$

where

$$L = 0.4y[1 - \exp(-y/A)] \qquad (8a)$$

$$A = 26(\frac{\rho}{\rho_w})^{1/2} \frac{\nu}{N} u_\tau^{-1} \qquad u_\tau = (\frac{\tau_w}{\rho_w})^{1/2} \qquad (8b)$$

$$N^2 = 1 - 11.8 \frac{\mu_w}{\mu_e} (\frac{\rho_e}{\rho_w})^2 p^+ \qquad (8c)$$

$$p^+ = \frac{\nu_e u_e}{u_\tau^3} \frac{du_e}{dx}, \qquad (8d)$$

The parameter γ is an intermittency term defined by

$$\gamma = \frac{1}{1 + 5.5(y/\delta)^6} \qquad (9)$$

and γ_{tr} is a parameter that accounts for the transition region which exists between laminar and turbulent flow and the value of y_c is determined by requiring continuity of the function ε_m^+.

The eddy viscosity model given by eq. (7) consists of an inner region defined by a modified mixing length expression and an outer region based on the velocity deficit. The mixing length expression (8a) is an extension of the well known Van Driest model which is obtained by replacing the damping parameter A of eq. (8b) by the expression

$$A = 26 \frac{\nu_e}{u_\tau} \qquad (10)$$

For incompressible, flat plate flow (dP/dx = 0) with no heat or mass transfer the Van Driest model has met with considerable success.

Encouraging results obtained from the Van Driest model motivated the extension to compressible flow with pressure gradients and heat transfer as described in eqs. (8a-8d). For the case of incompressible flow with zero pressure gradient, expression (8b) for the damping parameter A reduces to expression (10). However, since an eddy viscosity model using a mixing length concept as described by eqs. (8a-8d) has no rigorous physical justification (see reference [29], pp. 215-217), it remains to be seen how well it stands up against experimental data.

A thorough testing for a wide variety of situations is not possible since data under conditions of laminarization is quite limited. The most definitive experimental data seems to be that of Back, Cuffel and Massier [14] where boundary layer and heat transfer measurements for air flow in a convergent-divergent nozzle with wall cooling were performed.

In the description of BLM[27] a plot comparing Back's nozzle [14] with corresponding BLM predictions was presented and is reproduced as Fig. 1 in this work. The acceleration parameter, K, is shown in Fig. 2 for the conditions corresponding to Fig. 1 (P_t = 150.5 psia, T_t = 1500°R) along with plots for a number of lower pressures. Fig. 1 clearly shows appreciable error in the predicted values of the Stanton number which would in turn lead to significant errors in predicted values for heat flow rates and temperatures in the nozzle. In particular, the predicted values are significantly higher than the experimentally measured values, indicating that in a flow with strong streamwise accelerations, the turbulent boundary layer is indeed

reverting towards a laminar state and that a fully turbulent model cannot possibly follow such trends.

Since the conditions of Fig. 1 correspond to the pressure giving the lowest value of the acceleration parameter shown in Fig. 2, the logical question is whether even more deviation from experiment would be encountered at pressures corresponding to even higher values of the acceleration parameter, such as the curve for $P_t = 20$ psia in Fig. 2. This matter was brought up at the 5 week point of the author's 10 week appointment at the AFRPL. At the time of this writing the TDK/BLM code has still not been able to successfully produce results for the geometry and flow conditions of Back's nozzle. A succession of computer bombs have resulted as a result of such things as bad documentation and gas property tables which do not extend to low enough temperatures. Another error, however, has been encountered which deserves consideration since it relates directly to the eddy viscosity model used in BLM. This concerns situations where the flow acceleration is so high that the term P^+ of eq. (8d) becomes so large that the value of N^2 in eq. (8c) becomes negative and when the square root is attempted for use in eq. (8b), the computer code immediately grinds to a halt. The conclusion of these findings is that the eddy viscosity model of eqs. (8a-d) which has no rigorous physical justification, also produces severe error in regions of moderate flow acceleration as shown in Fig. 1, and produces mathematical nonsense (square roots of negative numbers) in regions of severe flow acceleration. Thus, improved models are needed if accurate predictions are to be made for boundary layers under high favorable streamwise pressure gradients.

In order to assess the relative degree of laminarization on a particular flow, we need to quanitfy a parameter or group of parameters which indicate this phenomenon. Reference [14] shows that the acceleration parameter, K, is a useful but not direct indication and proceeds to show that the combination $K/(C_f/2)^{3/2}$ may be a better direct indication of laminarization. Fig. 7 of reference [14] is included as Fig. 3 in the present work and shows that for values of $K/(C_f/2)^{3/2} > 0.40$, the velocity profiles resemble more closely a laminar as opposed to a turbulent flow, especially near the wall.

While the Reynolds number gives good indications of a laminar to turbulent transition, it seems to be a misleading indication of reverse transition since signs of laminarization can appear at surprisingly high Reynolds numbers. Parameters such as K, $K/(C_f/2)^{3/2}$ or $K/(C_f/2)$ appear to give better indications and further investigation needs to be conducted in order for engineers and designers to assess the importance of laminarization in terms of quatified parameters.

ALTERNATIVE MODELS

Since the eddy viscosity model described by eqs. (7-9) appears to give predictions which are significantly in error for situations involving reverse transition, alternative models are considered.

Laminar Sublayer Model

Since the mechanism by which turbulence is produced in the wall vicinity is apparently suppressed in accelerating flows, a turbulence model consisting of a completely laminar sublayer region near the wall and a turbulent wake region away from the wall is considered [21]. The mathematical description is

$$
\epsilon_m^+ = \begin{cases} 0 & , \quad 0 < y^+ < 20 \\ \dfrac{0.018}{\nu_e} \displaystyle\int_0^\infty (u_e - u)\, dy \ , & \quad y^+ > 20 \end{cases}
\tag{11}
$$

Although the model has appeal because of its simplicity and gives results which are in fair agreeemnt for incompressible flow, the main issue of concern is merely being avoided. A turbulent boundary layer under high acceleration does not suddenly revert to a laminar flow but instead goes through a gradual reverse transition where it begins to show the characteristics of a laminar flow. An eddy viscosity model as described in eq. (11) may be useful for some initial estimates because of its simplicity but cannot possibly incorporate the physical effects or give accurate predictions for complex flows. Therefore the model is not considered sufficient for obtaining accurate calculations required for applications such as high performance rocket nozzles.

Two-Equation Model

The two-equation turbulence model involves solving transport equations for two scalar properties, namely the turbulence energy and energy dissipation, from which characteristic velocity and length scales may be deduced. The technique retains the notion of eddy viscosity and turbulent Prandtl number given by eq. (6), but instead of directly postulating a form for ε_m^+ such as eq. (7), transport equations for the turbulence kinetic energy and energy dissipation are solved from which the eddy viscosity is formed. The form used by Jones and Launder [23,24] was developed for incompressible flow and is given as

Turbulent viscosity hypothesis

$$- \overline{\rho u'v'} = \mu_\tau \frac{\partial u}{\partial y} \equiv (c_\mu \rho k^2 / \varepsilon) \frac{\partial u}{\partial y} \tag{12}$$

Turbulence kinetic energy

$$\rho u \frac{\partial k}{\partial x} + \rho v \frac{\partial k}{\partial y} = \frac{\partial}{\partial y} \left[\left(\mu + \frac{\mu_\tau}{\sigma_k} \right) \frac{\partial k}{\partial y} \right]$$
$$+ \mu_\tau \left(\frac{\partial u}{\partial y} \right)^2 - \rho \varepsilon - 2 \mu \left(\frac{\partial k^{1/2}}{\partial y} \right)^2 \tag{13}$$

Turbulence "dissipation" rate

$$\rho u \frac{\partial \varepsilon}{\partial x} + \rho v \frac{\partial \varepsilon}{\partial y} = \frac{\partial}{\partial y} \left[\left(\mu + \frac{\mu_\tau}{\sigma_\varepsilon} \right) \frac{\partial \varepsilon}{\partial y} \right] \tag{14}$$
$$+ c_1 \frac{\varepsilon}{k} \mu_\tau \left(\frac{\partial u}{\partial y} \right)^2 - \frac{c_2 \rho \varepsilon^2}{k}$$
$$+ 2.0 \frac{\mu \mu_\tau}{\rho} \left(\frac{\partial^2 u}{\partial y^2} \right)^2$$

The c's and δ's in the above equations were assigned as constants and the f's were assigned as functions of k and ϵ. A sample of the results obtained with this model are presnted on Fig. 4 where a comparison with the data of Moretti and Kays [9] is shown. We see that the theoretical predictions using the two-equation model are able to follow the experimentally observed dip in the Stanton number in the regions of high flow acceleration while the mixing length model does not.

Although the mixing length concept has been employed to provide accurate predictions for a wide variety of boundary layer flows, it may plausibly be argued that for complex flows a mixing length hypothesis will never provide the degree of predictive accuracy a designer needs. However, one should interpret the encouraging looking results of Fig. 4 with cautior since the model described by eqs. (12)-(14) has been taylored specifically to treat high acceleration flows. This is an unavoidable difficulty with all turbulence models, however, since all must eventually rely on some degree of empiricism in order to close the equations. Nevertheless, the type of modeling presented here appears to have promise for extension to a variety of applications including compressible, high-speed flows in rocket nozzles.

Integral Equation Model

The only analysis available in the literature which is designed to handle compressible flow under strong favorable pressure gadients is the work of Kreskovsky et al. [22]. Here the concepts of eddy viscosity and turbulent Prandtl number (eqs. (6)) are retained but the analysis uses the turbulence kinetic energy equation along with an integral form of the turbulence kinetic energy and some empirically assigned parameters and correlations to arrive at a complete description of the turbulence.

The results in [22] were compared with the results of Moretti and Kays [9] as shown in Fig. 5 and clearly do not follow the data as closely as the Jones-Launder model [23,24] in regions of strong flow acceleration. The integral form adopted in reference [22] is computationally more convenient than the two-equation model but cannot be expected to give as accurate results and thus is not recommended over the analysis of the previous section.

SUMMARY AND CONCLUSIONS

A need for improved performance predictions in rocket nozzles brought up the question as to the influence of strong favorable pressure gradients leading to a reversion of initially turbulent flow towards laminar state. The investigation revealed the following:

Nature of Laminarization

Several effects including severe streamwise acceleration tend to break down a turbulent boundary layer, even at quite high Reynolds number. Boundary layer measurements, when viewed in conjunction with heat transfer measurements, reveal the complex nature of the flow and thermal behavior and their complicated interrelationship when laminarization occurs. Quite different considerations govern the onset of normal and reverse transition since the former depends on the nature of laminar flow and of any disturbance that may be present while the latter depends on the nature of fully developed turbulent flow. Thus any analysis on the difficult topic of normal transition becomes inappropriate when dealing with the doubly difficult subject of reverse transition. As a result the mechanism and basic nature of the laminarization process is still a controversial issue.

Parameters Indicating Laminarization

While normal transition is indicated quite well by the Reynolds number, it has been found to be a somewhat misleading quantity since reverse transition has been observed at relatively high Reynolds numbers. In fact, no experimental parameter has indicated exactly when laminarization will occur but a fair indication seems to be the acceleration parameter [9,14] where laminarization is observed for values of K

greater than 2 or 3 x 10^{-6}. However, the drop in Stanton number seems to lag the initiation of high values of K and a more direct indication of the reverse transition process may be the parameters $\frac{K}{(C_f/2)^{3/2}}$ or $\frac{K}{(C_f/2)}$. This issue is still unresolved and requires further investigation.

Turbulence Models

The present turbulence model used in TDK/BLM is a modified Van Driest mixing length hypothesis. It has no rigorous physical justification and as demonstrated in Fig. 1 gives inaccurate predictions in high acceleration flows. The most promising improvement seems to lie in a higher order turbulence model such as the two-equation turbulence model of Jones and Launder [23,24] which seems to produce good results (See Fig. 4 and 5.) when applied to imcompressible flow. It is believed that modeling of this type should be extended to compressible high speed flows since it has greater flexibility to include the dominant physical effects and produce more accurate results than a mixing length type model.

RECOMMENDATIONS

Results of the present investigation indicate a need for further study in the following areas.

Quantify Parameters Indicating Laminarization

Since the present turbulence model used in BLM produces reliable results under conditions of zero or modest pressure gradients, there exists a need to quantify the parameters indicating laminarization in order for designers to assess when the phenomenon should be considered. Thus, a thorough investigation into the importance of the acceleration parameter, K, and the quantities $\dfrac{K}{(c_f/2)^{3/2}}$ and $\dfrac{K}{c_f/2}$ should be undertaken as well as a search for a more significant parameter indicating the breakdown of fully turbulent boundary layers.

Develop Theoretical Model

Since the modified mixing length expression given by eqs. (8a-d) is unable to adequately match experimentally observed flow conditions under high favorable pressure gradients, a more rigorous theoretical model needs to be developed. The most promising model appears to be a two-equation model such as an extension of the Jones-Launder model [23,24] for compressible, high speed flows. Since a theory which gives good results for incompressible flow has no guarantee of success for compressible flows or for other conditions for which it was not developed and tested, an even higher order turbulence model such as that of reference [25] may be needed to obtain the degree of accuracy desired for high performance rocket engine predictions or other applications.

Obtain Experimental Data

The most philosophically appealing or physically rigorous turbulence model can be considered as nothing more than speculation until it has been scrutinized against reliable experimental data. Thus the lack of data, especially in high temperature, high speed compressible flow, is a major roadblock for performing a rigorous testing of any theoretical considerations and an effort should be made to obtain more data under a wider range of flow conditions.

Integrate Improved Theoretical Predictions with TDK/BLM

After developing and thoroughly testing a theoretical model which gives the degree of accuracy required for applications of interest, it should be integrated as a subroutine into the existing boundary layer code BLM. Since TDK/BLM gives accurate results under zero or modest pressure gradients, the parameters indicating laminarization should be tested by the code and a subroutine using an i proved turbulence model should be called upon for situations when reverse transition is significant.

In summary, the entire effort that needs to be undertaken is the gaining of insight into laminarization by searching for the underlying physical causes and quantifying the indicating parameters. Then a turbulence model capable of predicting the phenomenon should be developed, thoroughly tested against experiment and integrated as a subroutine into the existing TDK/BLM computer code. Finally it is noted that the nature of turbulence and its description continues to present a challenge to scientists and engineers who strive for a better understanding and improved capability to predict the world around us and the

present investigation hopefully has suggested a plan to add another
piece to this mysterious puzzle.

REFERENCES

1. Bankston, C. A., "The Transition from Turbulent to Laminar Gas Flow in a Heated Pipe," _Journal of Heat Transfer,_ Vol. 92, pp. 569-578, 1970.

2. Coon, C. W. and H. C. Perkins, "Transition from the Turbulent to the Laminar Regime for Internal Convective Flow with Large Property Variations," _Journal of Heat Transfer,_ Vol. 92, pp. 506-512, 1970.

3. Pennell, W. T., E. R. G. Eckert and E. M. Sparrow, "Laminarization of Turbulent Pipe Flow by Fluid Injection," _J. Fluid Mechanics,_ Vol. 52, part 3, pp. 451-464, 1972.

4. Baker, R. J. and B. E. Launder, "The Turbulent Boundary Layer with Foreign Gas Injection--II. Predict," _Internation Journal of Heat and Mass Transfer,_ Vol. 17, pp. 293-306, 1974.

5. Badri Narayanan, M. A. and V. Ramjee, "Reverse Transition from Turbulent to Laminar Boundary Layer in a Highly Accelerated Flow," _Journal of the Aeronautical Society of India,_ Vol. 20, No. 1, pp. 39-59, 1968.

6. Patel, V. C. and M. R. Head, "Reversion of Turbulent to Laminar Flow," _J. Fluid Mechanics,_ Vol. 34, pp. 371-392, 1968.

7. Blackwelder, R. F. and L. G. Kovasznay, "Large-Scale Motion of a Turbulent Boundary Layer during Relaminarization," _Journal of Fluid Mechanics,_ Vol. 53, pp. 61-83, 1972.

8. Leont'yev, A. I., YE. V. Shipov, V. N. Afans'yev, and V. P. Zabolotskiy, "Experimental Study of the Structure of Turbulent Thermal Boundary Layer in Laminarized Flows Developed in Strong Favorable Pressure Gradients," _Heat Transfer-Soviet Research,_ Vol. 13, pp. 43-53, 1981.

9. Moretti, P. M. and W. M. Kays, "Heat Trnasfer to a Turbulent Boundary Layer with Varying Free-Stream Velocity and Varying Surface Temeprature--An Experimental Study," _International Journal of Heat and Mass Transfer,_ Vol. 8, pp. 1187-1202, 1965.

10. Back, L. H., P. F. Massier, and R. F. Cuffel, "Some Observations on Reductions of Turbulent Boundary-Layer Heat Transfer in Nozzles," _AIAA Journal,_ Vol. 4, pp. 2226-2229, 1966.

11. Back, L. H., P. F. Massier and R. F. Cuffell, "Flow Phenomena and Convective Heat Transfer in a Conical Supersonic Nozzle," _Journal of Spacecraft and Rockets,_ Vol. 4, pp. 1040-1047, 1967.

12. Back, L. H., P. F. Massier, and R. F. Cuffel, "Effect of Inlet Boundary-Layer Thickness and Structure on Heat Transfer in a Supersonic Nozzle," *Journal of Spacecraft and Rockets*, Vol. 5, pp. 121-123, 1968.

13. Back, L. H., R. F. Cuffel and P. F. Massier, "Laminarization of a Turbulent Boundary Layer in Nozzle Flow," *AIAA Journal*, Vol. 7, No. 4, pp. 730-733, 1969.

14. Back, L. H., R. F. Cuffel and P. F. Massier, "Laminarization of a Turbulent Boundary Layer in Nozzle Flow-Boundary Layer and Heat Transfer Measurements with Wall Cooling," *Journal of Heat Transfer*, pp. 333-344, August 1970.

15. Back, L. H., R. F. Cuffel and P. F. Massier, "Influence of Contraction Section Shape and Inlet Flow Direction on Supersonic Nozzle Flow and Performance," *Journal of Spacecraft and Rockets*, Vol. 9, pp. 420-427, 1972.

16. Launder, B. E., "Laminarization of the Turbulent Boundary Layer in a Severe Accleration," *Journal of Applied Mathematics*, Vol. 31, pp. 707-708, 1964.

17. Shiina, Y., K. Fujimura, and H. Kawamura, "Measurement of Reverse Transition in Converging Duct Flow," *Journal of Nuclear Science and Technology*, Vol. 17, pp. 869-871, 1980.

18. Deissler, R. G., "Evolution of the Heat Transfer and Flow in Moderately Short Turbulent Boundary Layers in Severe Pressure Gradients," *Interation Journal of Heat and Mass Transfer*, Vol. 17, pp. 1079-1085, 1974.

19. Narasimha, R., and K. R. Sreenivasan, "Relaminarization in Highly Accelerated Turbulent Boundary Layers," *Journal of Fluid Mechanics*, Vol. 61, pp. 417-447, 1973.

20. Launder, B. E., and F. C. Lockwood, "An Aspect of Heat Transfer in Accelerating Turbulent Boundary Layers," *Journal of Heat Transfer*, Vol. 91, pp. 229-234, 1969.

21. Schmidt, J. F., D. R. Boldman, and C. Todd, "Laminarization Model for Turbulent Eddy Transport in Highly Accelerated Nozzle Turbulent Boundary Layers," NASA TMX-2501, February 1972.

22. Kreskovsky, J. P., S. J. Shamroth and H. McDonald, "Application of a General Boundary Layer Analysis to Turbulent Boundary Layers Subjected to Strong Favorable Pressure Gradients," *Journal of Fluids Engineering*, Vol.b 97, pp. 217-224, 1975.

23. Jones, W. P. and B. E. Launder, "The Calculation of Low-Reynolds-Number Phenomena with a Two-Equation Model of Turbulence," _International Journal of Heat and Mass Transfer_, Vol. 16, pp. 1119-1130, 1973.

24. Jones, W. P. and B. E. Launder, "The Prediction of Laminarization with a Two-Equation Model of Turbulence," _Int. J. Heat Mass Transfer_, Vol. 15, pp. 301-314, 1972.

25. Hanjalic, K. and B. E. Launder, "Contribution Towards a Reynolds-Stress Closure for Low-Reynolds-Number Turbulence," _Journal of Fluid Mechanics_, Vol. 74, pp. 593-610, 1976.

26. Nickerson, G. R., D. E. Coats, and J. L. Bartz, "The Two-Dimensional Kinetic (TDK) Reference Computer Program," Engineering and Programming Manual, Ultrasystems, Inc., prepared for Contract No. NAS9-12652, NASA JSC, Dec. 1973.

27. Cebeci, T., "Boundary Layer Analysis Module," prepared for Software and Engineering Associates, Inc., January 1982.

28. Kewller, H. B. and Tuncer Cebeci, "Accurate Numerical Methods for Boundary-Layer Flows. II: Two-Dimensional Turbulent Flows," _AIAA Journal_, Vol. 10, No. 9, pp. 1193-1199, 1972.

29. Cebeci, T. and A. M. O. Smith, "Analysis of Turbulent Boundary Layers," Academic Press, Inc., 1974.
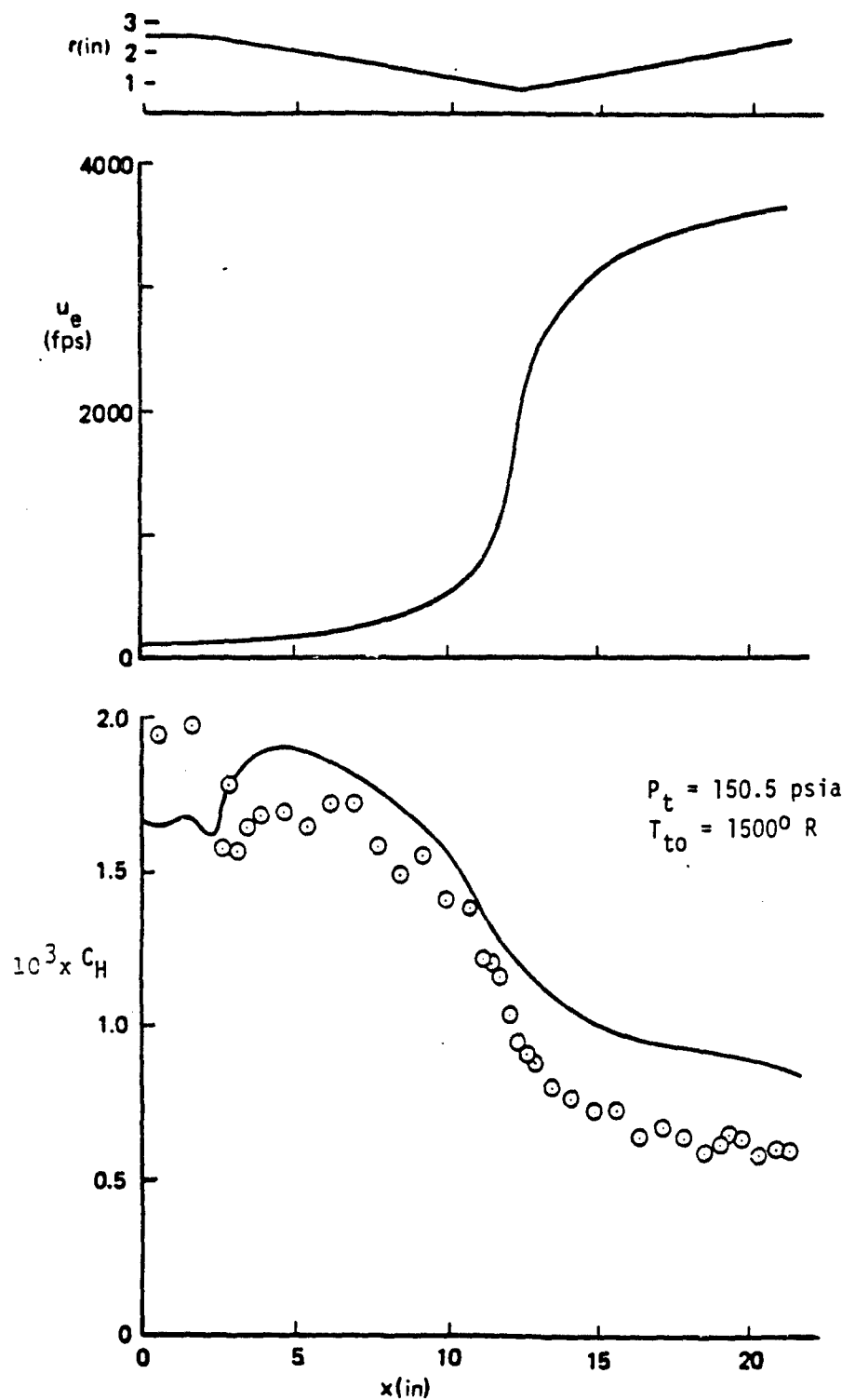
Fig. 1 Nozzle geometry, external velocity and Stanton number distributions for Back's nozzle.[14]
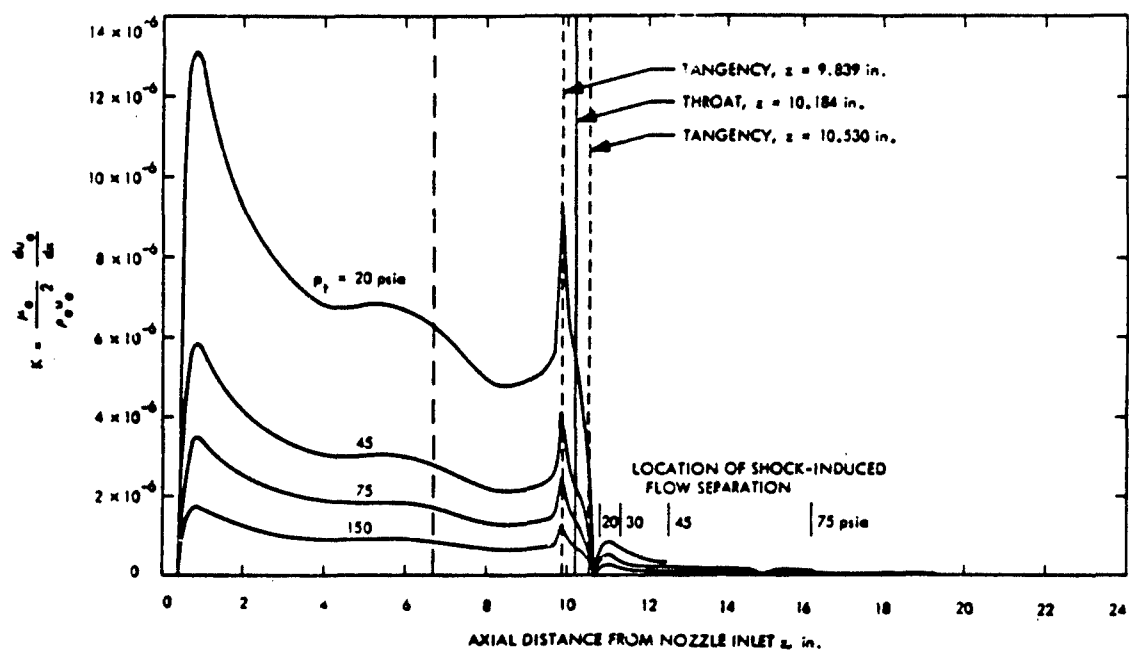
Fig. 2 Variation of the acceleration Parameter, K, for Back's
Nozzle. [14]
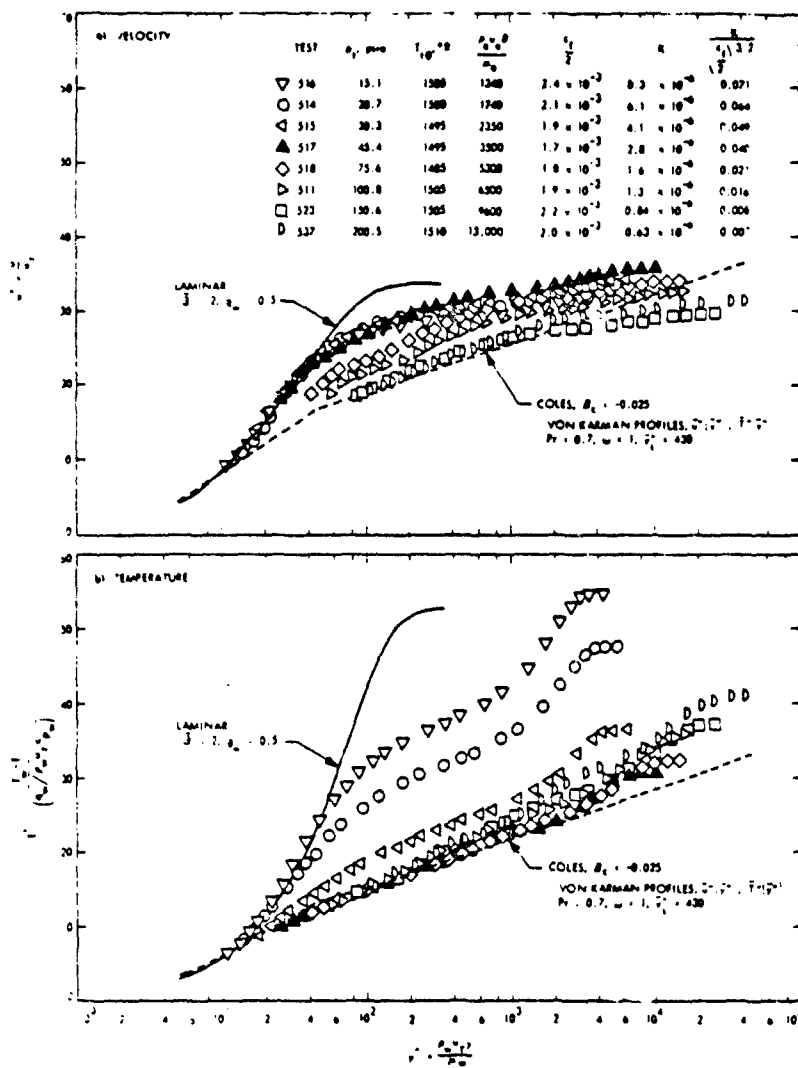
Fig. 3 Reverse transition velocity and temperature profiles in
Back's nozzle. [14]
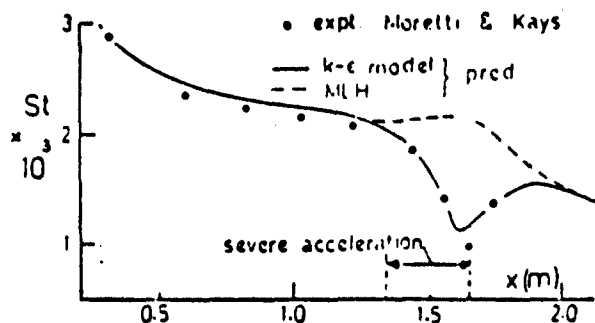
Fig. 4   Comparison between predicted and experimental
results for heat transfer in an accelerated flow

o Data of Moretti
and Kays Run 11
[9]

— Prediction of
Kreskovsky et al
[22]

--- Prediction of
Launder and Jones
[24]
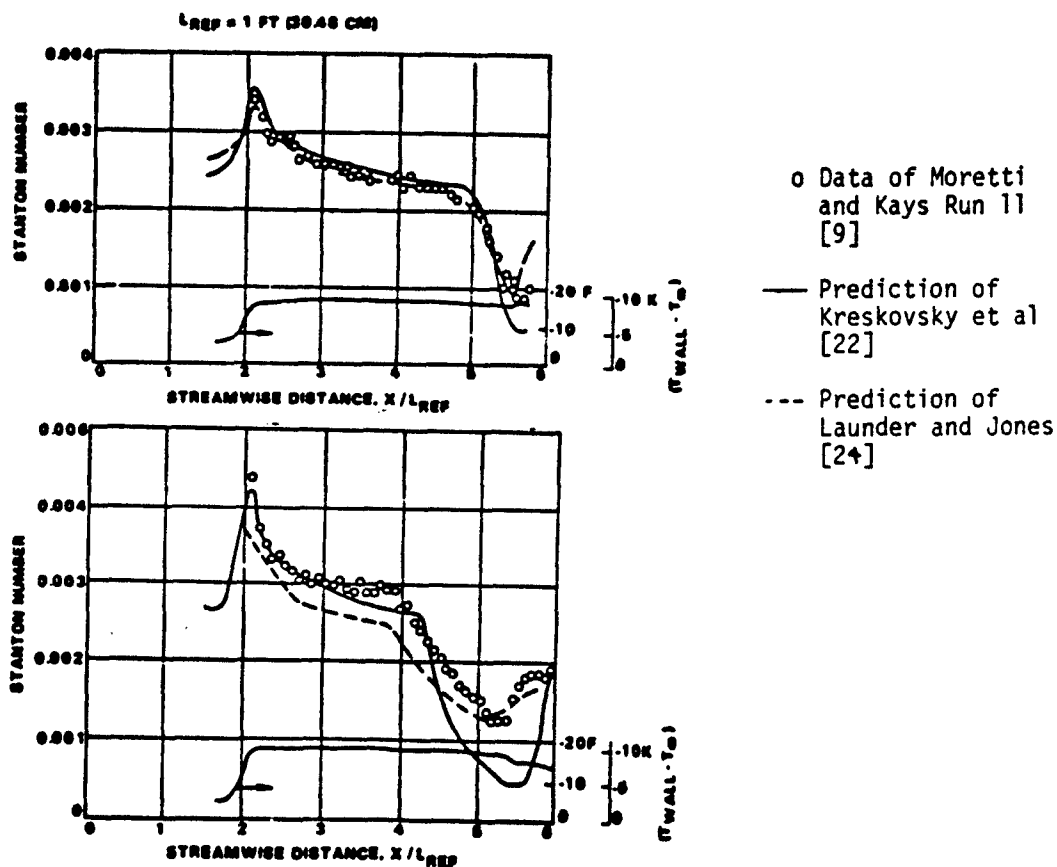
Fig. 5   Comparison between predicted and experimental
results for heat transfer in an accelerated flow

1984 USAF-SCEEE SUMMER FACULTY RESEARCH PROGRAM

Sponsored by the

AIR FORCE OFFICE OF SCIENTIFIC RESEARCH

Conducted by the

SOUTHEASTERN CENTER FOR ELECTRICAL ENGINEERING EDUCATION

FINAL REPORT

DEVELOPMENT OF COMPUTER-ASSISTED INSTRUCTION

IN

BASIC ELECTRONIC TROUBLE SHOOTING

Prepared by: Dr. Stephen A. Wallace

Academic Rank: Associate Professor

Department and   Institute of Cognitive Science
  University: University of Colorado-Boulder

Research Location: Air Force Human Resources Laboratory
                      Lowry Air Force Base

USAF Research: Dr. Roger Pennell

Date: July 19, 1984

Contract No: F49620-82-C-0035

DEVELOPMENT OF COMPUTER ASSISTED INSTRUCTION

IN

BASIC ELECTRONIC TROUBLE SHOOTING

by

Stephen A. Wallace

ABSTRACT

The paper outlines a proposal for the development of a computer-assisted instruction system in electronic troubleshooting. In Phase 1 of the project, a computer-simulated troubleshooting system will be developed. The system will be designed to teach naive students the principles of logic function operation, a major component of modern electronic circuits. In Phase 2, an initial experiment will be performed which will investigate the effects of various feedback schedules on the initial training and the long term retention of troubleshooting logic function circuits. Suggestions for future research in the transfer of training area are outlined.

Acknowledgement

The author would like to thank the Air Force Office of Scientific
Research and the Southeastern Center for Electrical Engineering Educa-
tion for providing me with the opportunity to partake in this project at
the Human Resources Laboratory, Lowry Air Force Base. I would like to
personally thank Dr. Roger Pennell, my effort contact person, for all his
support, and Drs. Gerry Deignan, Bob Summers, and Brian Dallman for their
helpful discussions. I very much appreciated the support I received from
all the personnel at the Laboratory.

I. INTRODUCTION

Today's Air Force operates largely in an electronic environment. Almost any task that one can think of, from the loading and storage of supplies through fire control to decisions of the field commander, depends for its success on the adequate functioning of electronic devices. Because competent electronics technicians are unlikely to enlist in the Air Force, the Air Force must develop competence in essentially naive recruits if it hopes to keep pace with increasing electronic functionality that modern engineering can provide. Thus, the Air Force invests considerable of its resources in selection and training programs designed to identify those among its recruits with greatest aptitude for electronics and efficient instructional capacity to produce knowledgeable and skilled technicians. In addition, military resources are used for the development of manuals intended to provide adequate information for both the assembly and maintenance of units of electronic equipment that may not have been covered during basic electronics courses.

Despite the best efforts of the Air Force (and in fact this seems to be true in civilian settings as well), common knowledge has it that trainees learn very little in basic electronics courses. In the best of circumstances, trainees come away with little more than a vocabulary for parts and some general rules for assembly. When they confront their first real assembly or troubleshooting problem, they are nearly as helpless as an untrained recruit. Thus, a major concern for the Air Force is not only how to train individuals on basic electronics, but also to understand the variables that can affect acquisition of maintenance and troubleshooting skills. In this regard, it is important for research to focus on the training of these skills, the ability to transfer to variations of the original skill or task, and the ability to retain these skills over time.

II. OBJECTIVES

The objective of this paper is to outline a two phase proposal for future research. In the first phase, a computer-assisted instruction system will be developed which will teach naive students the rules of logic function operation, important components in most modern electronic

circuits. The system will allow the student to troubleshoot computer-generated circuits consisting of various logic functions. The student will be able to test input and output lines, replace components, and request other types of feedback. In the second phase, an experiment is proposed which will examine how frequent strategy feedback should be given in initial training to promote the long-term retention of these types of troubleshooting skills.

III. THE BASIC TRAINING AND RETENTION ISSUE

The focus of the present proposal is on certain issues related to basic training of electronic principles. According to some experts (e.g. Halff, 1983; McGrath, 1983), the problem of basic training in the military is a severe one because the quality of the recruit pool is expected to remain low for several years. This problem is primarily a result of the decline of standards in the public schools during the 1970's. Also, the resource pool itself is declining. In 1978, the prime recruit population of 17 year olds numbered 4,25 million. By 1990, this number will reduce to less than 3.25 million. The problem is compounded by the fact that fewer and fewer quality recruits will face basic training on increasingly complex military equipment (McGrath, 1983). The technological advances in computers and electronic equipment have far outdistanced comparable improvements in basic training and instruction.

Thus, at one end of the continuum is the problem of basic training. However, at the other end is the problem of retention of technical maintenance and troubleshooting skills. Indeed, in a detailed study of some 300 vehicle repair tasks being performed by military mechanics, Hayes (1982) found that 71% contained errors that were judged to be serious by trained observers. Furthermore, the study indicated that the quality of the maintenance work did not improve with experience, but rather declined. This serious state of affairs points to the importance of investigation into alternative techniques in basic training and instruction of maintenance and troubleshooting skills.

IV. ISSUES IN COMPUTER-ASSISTED INSTRUCTION

Perhaps the most innovative mode of training to surface in both civilian and military settings in the last 15 years has been computer-assisted instruction (CAI). Most of the early CAI programs were stimulus-response oriented in which questions would be posed to the student and the student's solutions were compared to prestored answers for evaluation. Later, more sophisticated intelligent-computer-assisted instruction (dubbed ICAI) programs were developed and contained not only representations of the subject matter but carried on dialogue with the student and used the student's mistakes to diagnose errors and offer alternative solutions (Barr & Fiegenbaum, 1982). One of the first ICAI programs to be developed for military settings was SOPHIE (SOPHisticated Instructional Environment) by John Seely Brown, Richard Burton and their colleagues (Brown, Burton and Bell, 1974). SOPHIE was designed to teach electronic troubleshooting skills on a simulated power supply circuit. The system would insert a fault(s) into the circuit and the student, via elaborate interactions with the computer, would find the fault(s) by making measurements and by generating and testing hypotheses. SOPHIE could evaluate the student's hypotheses and tell the student the worth of each measurement.

Most of the ICAI systems, such as SOPHIE, SCHOLAR (see Carbonell, 1970) and WUMPUS (Carr and Goldstein, 1977), provide stimulating and entertaining environments which help keep the students interested in what they are trying to learn. But, of course, the critical questions are: (1) does the learning environment they create facilitate the long-term retention of the skill (2) do these environments promote optimal transfer to real tasks; (3) are ICAI environments as effective or perhaps more effective than other traditional modes of instruction? It is perhaps unfair to be too critical of many of the ICAI systems since many of them are still being evaluated as effective instructional environments (Psotka, 1983). In spite of the limited success of some ICAI systems such as SOPHIE (Brown, Rubinstein and Burton, 1976), many of them are designed around the questionable assumption that providing feedback to the student on every trial promotes the best learning

(e.g., Anderson, Boyle, Farrell and Resier, 1984). In the next section, arguments are made against this assumption.

V. THE FREQUENCY OF FEEDBACK ISSUE

Psychomotor research has determined that performance improvement is highly dependent on the frequency and precision of augmented KR, defined as information supplied to the trainee from an external source, such as an instructor, about the trainee's performance relative to the criterion or goal. Performance improvement is not optimal unless the quantity and quality of augmented KR is sufficient (e.g., Bilodeau et al., 1959; Newell, 1974; Rogers, 1974; Wallace et al., 1976).

There are, however, major limitations on this research which could have relevance to ICAI environments. First, the tasks that have been examined have been quite simple in the sense that the number of possible alternative strategies for achieving the criterion movement is small. In most real life tasks that are of particular importance to the Air Force, there are typically many ways or paths to completion. This is particularly true in the case of electronic troubleshooting tasks which are the focus of the present proposal. In multi-solution tasks such as these, the influence of KR on learning, transfer and retention is not known. Second, over the years it has been suggested that KR is the strongest and most important variable controlling performance and learning (Adams, 1971; Bilodeau & Bilodeau, 1961). However, augmented KR has been typically manipulated during initial training trials without performance evaluation on retention trials (see Salmoni, Schmidt and Walter, 1984, for detailed discussion). Thus, in general, it is unclear whether the benefits of augmented KR are short or long term.

For example, Bilodeau and Bilodeau (1958) concluded from their results several years ago that learning is determined by the absolute number of KR trials and not by the relative number of KR to no KR trials. Their design and the design of several other KR studies suffered a serious flaw in that KR manipulations were made only during initial acquisition trials without subsequent retention tests. Recently, Johnson et al., (1980) performed a similar experiment but included a retention test one week

after the original acquisition trials. In contrast to the earlier
Bilodeau and Bilodeau (1958) study, Johnson et al., found that learning
was best in the group receiving the most no KR trials. In other words,
people seemed to remember the task better if they were not always given
information concerning the outcome of their attempts. More specifically,
the relative frequency of KR to no KR trials determined learning, not
the absolute number of KR trials. These results are important because
they emphasize the necessity of including retention trials to determine
learning - a point also recently emphasized by Schmidt (1982).

Aside from methodological issues, the results of Johnson et al., beg
the question of why should learning be enhanced as a result of more no
KR experience? One answer, suggested by Schmidt (1982), is that more no
KR experience during initial training makes the task inherently more
difficult. The subject has to invest more effort (Kahneman, 1973) to
process the relevant task cues and to achieve the performance criterion.
As a result, these cues are processed "deeper" and more elaborately into
memory and are more resistant to forgetting (Craik & Lockhart, 1972;
Leight & Ellis, 1981). On a more practical side, it probably makes sense
for the trainee to practice under no KR conditions because on-the-job
performance is typically done in the absence of augmented KR. Certain-
ly this is true in most electronic troubleshooting tasks.

VI. RECOMMENDATIONS

The review of relevant literature has pointed out several areas of
concern which should be addressed by future research. Clearly, a major
problem for the Air Force, and indeed the military in general, is to
improve basic training in order to produce quality technicians who re-
tain their skills over long time periods. According to Hagman and Rose
(1983) there are three approaches to improving retention. One approach
is to modify the task or redesign the equipment to automate easily for-
gotten procedures. Another approach is to assign people to tasks which
match their abilities. The final approach is to improve basic training
with the view that better initial training should enhance learning and
promote retention (Schendel, Shields and Katz, 1980). It is argued
that this latter approach is probably the most cost-effective.

Efforts should be made at the entree level to improve instruction in technical skills. ICAI is one promising method which has been used to teach or improve a variety of basic skills such as geometry (Anderson et al., 1984) and electronics (Brown et al., 1978). However, it is argued that one important issue related to ICAI is how frequent feedback should be given to the student to promote long term retention of the skill or knowledge. The current proposal wishes to address these issues by 1) developing an ICAI system for the learning and retention of basic electronic principles in troubleshooting logic function circuits, and 2) by outlining basic experiments which examine the feedback frequency issue. Testing and experimentation will be primarily focused on final year high school and first year college students.

Proposed Methodology

The proposed methodology will consist of two phases, each phase requiring approximately 6 months to complete. In phase 1, an elementary ICAI system in troubleshooting electronic logic function circuits (tentatively called ELF) will be developed. The short term goal of this phase will be to develop ELF to the point where basic experiments can be performed on students naive in electronic principles. The long term goal is to develop ELF so that it can be regarded as a bonified teaching tool and to assist instructors in the teaching of basic electronics troubleshooting skills. It should be emphasized that ELF will assist the student in learning about the principles of logic functions - components in modern electronic circuitry not included in SOPHIE, for example. In phase 2, one experiment is planned which will investigate the frequency of feedback and its effects on long term retention of troubleshooting skills in the ELF environment. More detailed descriptions of these two phases now follow.

Phase 1. Once fully developed, the ELF system will 1) graphically represent electronic circuits of different complexities on a CRT screen; 2) be able to place fault(s) into the circuit; 3) recognize, test and replace commands and provide feedback to the student about the cost-effectiveness of these requests. To produce these features, ELF will contain five software components written in INTERLISP and will be

integrated by a knowledge program called LOOPS (Stefik, Bobrow, Mittal and Conway, 1983).

1. A low-level language processor will be required to facilitate communication between the user and the system.

2. A "blackboard" will be needed to parameterize the various circuits and to place faults in the circuits.

3. A knowledge base of logic function operations and problem solving rules will be required. For example the rule governing AND-gate operations is as follows:

If both inputs are "1"s, then output is "1";

If either input is "0", then output is "0".

Five logic functions will be initially incorporated into ELF computer simulated circuits: AND-, NAND-, OR-, NOR-, and XOR-gates.

4. A schedule will be used to control the order of rule processing and determining the cost-effectiveness of possible solutions.

5. A justifier will be needed to provide feedback to the student. In the early stages of ELF, feedback about the student's test and replace requests will be given. As the system develops, the student could also receive feedback about the cost-effectiveness of the request, and be given appropriate strategies if help is requested.

Phase 2. Following the completion of the ELF system in phase 1, at least one experiment is planned to investigate the frequency of feedback issue. Is the long term retention of basic electronic troubleshooting skill dependent on the frequency of feedback in initial training? The type of feedback referred to here is that which informs the student about the appropriateness of a particular test or replace request. For example, naive troubleshooters tend to perform many more tests which are redundant (i.e. do not reduce the uncertainty about the fault location) compared to experts. This type of feedback will be manipulated in the experiment. Also, following initial training in a particular feedback frequency condition, subjects will be required to return for a test of retention on different circuit configurations than that used in initial training. Retention tests will occur one day and one month after initial training.

Subjects - Sixty subjects, primarily recruited from the University of
Colorado and neighboring high schools, will participate. An equal
number of males and females will be used.

Apparatus - Simulations and troubleshooting will be done via a Digital
Equipment Corporation VT 105 graphics CRT terminal. The terminal is
interfaced with a VAX-11/780 main frame computer located in the Depart-
ment of Psychology. Testing and data collection will be done in a sound-
proof, air-conditioned chamber.

Procedures - The procedures in phase 2 require each subject to participate
in three types of sessions. In the preliminary training sessions, all
subjects will be taught the rules underlying the operation of five logic
functions: AND, NAND, OR, NOR, and XOR-gates. Instruction will be com-
puter-assisted. Following instruction on each logic function, the sub-
ject will be tested on the rules governing each. Two 1½ hour sessions
on separate days are anticipated for this purpose.

In the experimental training sessions, subjects will attempt to learn
how to troubleshoot simulated electronic circuits consisting of various
configurations of the five logic functions. The task of the subject will
be to locate and replace faulty logic functions within a circuit. The
configuration difficulty of the circuits and number of faults to be placed
in the circuits will be determined by pilot testing. Within a given trial,
the subject will be able to make three types of requests: test a given
input or output line and receive either a "0" or "1" as feedback; ask
whether the circuit has been corrected; and request to replace a logic
function. Each request will be assigned some cost factor and these
will accumulate within each trial and be stored in the computer for feed-
back purposes. The task of the subject will be to find and replace the
faulty logic function(s) in the shortest time at the lowest cost within
a trial.

Subjects will receive several trials of practice (the length of each
trial to be determined by pilot testing) within each day over five days
of practice. Subjects will be assigned to one of three experimental
groups. In the 100% condition, subjects will receive feedback about the
appropriateness of each troubleshooting request on all initial training

trials. In the 33% condition, subjects will receive feedback every third trial, and in the 0% condition feedback will not be given. Following the experimental practice trials, one half of the subjects in each condition will return one day later for a retention test. They will be required to troubleshoot a novel circuit in the absence of strategy feedback. One month later, the other half of the subjects in each condition will return for a retention test. This type of design allows for a more accurate estimate of long term retention unconfounded by previous practice on the immediate retention test.

Design and Analysis - A Feedback Condition X Trials ANOVA will be used to analyze the initial training trials. Retention data will be analyzed using a Feedback Condition X Retention Test X Trials ANCVA with the first two factors as between-subject. Dependent variables to be analyzed will be time to solution, cost of test and replace requests, and number of requests.

VII. EXPECTED OUTCOMES AND FUTURE DIRECTIONS

If the results of Johnson et al. (1980) are valid and generalizeable, we can make the following predictions. During initial training trials, those groups which receive more KR trials relative to no KR trials, will improve more rapidly in troubleshooting performance. However, on later retention tests, we would expect the groups which receive a lower ratio of KR to no KR trials to retain the troubleshooting abilities to a better degree. The implication of these results for training Air Force recruits is that to insure the long term retention of troubleshooting ability, trainees should not always receive KR from the instructor after all trials.

One issue in future experiments will be how best to organize the training experience such that the trainee will be able to transfer to deviations of the original criterion troubleshooting task. Past research on simple verbal (Battig, 1979), cognitive (Hiew, 1977) and motor skills (McCracken & Stelmach, 1977; Shea & Morgan, 1977) has shown that the amount of positive transfer to variations of the original task is a function of the variability of original training.

146-12

In the electronic troublshooting task considered in the present pro-
posal, there are several ways to structure the training regimen. At its
simplest level, the trainee needs to acquire knowledge of how each of the
five (or more) logic functions work. What is the best way to acquire
and retain this knowledge? Should the trainee be provided with a large
block of trials in which the malfunction is located only in the and-gate
function? Following this, another block of or-gate malfunctions would
be provided--and so on with the other logic functions. While this train-
ing procedure may facilitate the acquisition of knowledge about how each
function works, it could be argued that this type of training would not
effectively develop knowledge about how the logic functions work together
in an integrated circuit to control the external devices. Based on pre-
vious research, and we see no reason why it shouldn't apply to trouble-
shooting skills, a random presentation of malfunctions from trial to
trial across the various logic functions should develop a stronger in-
ternal representation and generally more applicable knowledge about how
the logic functions work together. This stronger system level knowledge
should facilitate transfer to deviations of the original circuit confi-
guration. The ability to transfer effectively to deviations of the ori-
ginal learning task is a major quality of an expert troublshooter. Thus,
in this line of research, subjects would transfer to either the same cir-
cuit with the malfunction located at random locations, to a circuit con-
taining the same logic functions but in a different configuration or to
a circuit containing logic functions never experienced before.

REFERENCES

1. Anderson, J.R., Boyle, C.F., Farrell, R. and Reiser, B. (1984). Cognitive principles in the design of computer tutors, *Proceedings of the Sixth Annual Conference of the Cognitive Science Society*, June 28-30, Boulder, Colorado, 2-9.

2. Adams, J.A. (1971). A closed-loop theory of motor learning. *Journal of Motor Behavior*, 3, 111-150.

3. Battig, W.F. (1979). The flexibility of human memory. In L. Cermack and F. Craik (Eds.), *Levels of processing in human memory*, Hillsdale, NJ: L. Erlbaum Assoc.

4. Barr, A. and Feigenbaum, E.A. (1982). The handbook of artificial intelligence. William Kaufmann, Inc.

5. Bilodeau, E.A. and Bilodau, I.M. (1958). Variable frequency knowledge of results and the learning of simple skills. *Journal of Experimental Psychology*, 55, 379-383.

6. Bilodeau, E.A. and Bilodeau, I.M. (1961). Motor skills learning. *Annual Review of Psychology*, 12, 243-280.

7. Bilodeau, E.A., Bilodeau, I.M. and Schumsky, D.A. (1959). Some effects of introducing and withdrawing knowledge of results early and late in practice. *Journal of Experimental Psychology*, 58, 142-144.

8. Brown, J.S., Burton, R.R. and Bell, A.G. (1974). SOPHIE: A sophisticated instructional environment for teaching electronic troubleshooting (an example of AI in CAI). BBN Rep. No. 2790, Bolt Beranek and Newman, Inc., Cambridge, Mass.

9. Brown, J.S., Rubinstein, R. and Burton, R. (1976). Reactive learning environment for computer assisted electronics instruction, BBN Rep. No. 3314, Bolt Beranek and Newman, Inc., Cambridge, Mass.

10. Carr, B. and Goldstein, I. (1977) Overlay: a theory of modeling for computer aided instruction. AI Memo 406, AI Laboratory, Massachusetts Institute of Technology.

11. Carbonell, J.R. (1970). AI in CAI: An artificial intelligence approach to computer aided instruction. *IEEE Transaction on Man-Machine Systems*, MMA-11 (4): 190-202.

12. Craik, F.I.M. and Lockhart, R.S. Levels of processing: A framework for memory research. *Journal of Verbal Learning and Verbal Behavior*, 1972, 11, 671-684.

13. Hagman, J.D. and Rose, A.M. (1983). Retention of military tasks: A review, _Human Factors_, _25_, 199-213.

14. Halff, H. (1983). Overview of training and aiding. _Artificial intelligence in maintenance, Vol. 1: Proceedings of the Joint Services Workshop_, October 4-6, Boulder, Colorado.

15. Hayes, F.J. (1982). _Maintenance performance research in the Army_. Proceedings, Psychology in the Department of Defense, 527-532, Eighth Annual Symposium, USATA-TR-82-10, April 21-23.

16. Hiew, C.C. (1973). Sequence effects in rule learning and conceptual generalization. _American Journal of Psychology_, _90_, 207-218.

17. Johnson, R.W., Wicks, G. and Ben Sira, D. (1980). Practice in the absence of knowledge of results: Skill acquisition and retention. Paper presented at North American Society for the Psychology of Sport and Physical Activity Conference, Boulder, Colorado.

18. Kahneman, D. (1973). _Attention and effort_. Englewood Cliffs, NJ: Prentice Hall.

19. Leight, K.A. and Ellis, H.C. (1981). Emotional mood states, strategies and state dependent memory. _Journal of Verbal Learning and Verbal Behavior_, _20_, 251-275.

20. McCracken, H.D. and Stelmach, G.E. (1977). A test of the schema theory of discrete motor learning. _Journal of Motor Behavior_, _9_, 193-201.

21. McGrath, M. (1983). The need for improvements in weapon systems maintenance: What can AI contribute? _Artificial intelligence in maintenance, Volume I: Proceedings of the Joint Services Workshop_, October 4-6, Boulder, Colorado.

22. Newell, K.M. (1974). Knowledge of results and motor learning. _Journal of Motor Behavior_, _6_, 235-244.

23. Psotka, J. (1983). Artificial intelligence contributions to training and maintenance. _Artificial intelligence in maintenance, Vol.I: Proceedings of the Joint Services Workshop_, October 4-6, Boulder, Colorado.

24. Salmoni, A., Schmidt, R.A. and Walter, C.B. (1984). Knowledge of results and motor learning: A review and critical reappraisal, _Psychological Bulletin_, _95_, 355-386.

25. Schendel, J.D., Shields, J.L. and Katz, M.S. (1980). Retention of motor skills: Review. JSAS _Catalog of Selected Documents in Psychology_, _10_, 21, (Ms. No. 2016).

26. Schmidt, R.A. (1982). *Motor control and learning: A behavioral emphasis*. Human Kinetics Publishers, Champaign, IL.

27. Shea, J.B. and Morgan, R.L. (1979). Contextual interference effects on the acquisition, retention, and transfer of motor skill. *Journal of Experimental Psychology: Human Learning and Memory*, 5, 179-187.

28. Stefik, M. Bobrow, D.G., Mittal, S. and Conway, L. (1983). Knowledge programming in LOOPS: Report on an experimental course, *The AI Magazine*, 4, 1-13.

29. Wallace, S.A., DeOreo, K.L. and Roberts, G.C. (1976). Memory and perceptual trace development in ballistic timing. *Journal of Motor Behavior*, 8, 133-137.

1984 USAF-SCEEE SUMMER FACULTY RESEARCH PROGRAM

Sponsored by the

AIR FORCE OFFICE OF SCIENTIFIC RESEARCH

Conducted by the

SOUTHEASTERRN CENTER FOR ELECTRICAL ENGINEERING EDUCATION

FINAL REPORT

THE DEVELOPMENT OF A COMPUTERIZED SYSTEM FOR MANAGEMENT
INFORMATION AND INTER-OFFICE COMMUNICATION

Prepared by: Dr. Yin-min Wei

Academic Rank: Professor

Department and   Department of Computer Science
    University: Ohio University

Research Location: Air Force Aerospace Medical Research
                        Laboratory, Technical Service Division,
                        Plans and Programs Branch

USAF Research: Mr. Robert F. Bachert

Date: August, 1984

Contract No: F49620-82-C-0035

THE DEVELOPMENT OF A COMPUTERIZED SYSTEM FOR MANAGEMENT
INFORMATION AND INTER-OFFICE COMMUNICATION

by

Yin-min Wei

ABSTRACT

This effort concentrates on the development of an overall system
configuration and capability requirements for distributed multi-computer
system for shared information storage and retrieval and data-
communication between offices. This system needs computers which have
enough large storage units to hold the files, abilities to understand
human's requests in natural language, and abilities to quickly deliver
requested information to the humans in easy-to-understand formats.

ACKNOWLEDGEMENT

The author would like to thank the Air Force Office of Scientific Research and the Southeastern Center for Electrical Engineering Education for providing him the opportunity to spend a very stimulating and fruitful summer at the Air Force Aerospace Medical Research Laboratory, Wright-Patterson AFB, Ohio. He would like to express his appreciation to the laboratory, in particular to the Plans and Programs Branch of the Technical Services Division, for its hospitality and good working environment.

Further, he would like to thank Mr. Robert Bachert for suggesting this area of research and for his collaboration and guidance. His appreciation goes to Mr. Dave Brungart and Mr. Richard Bennett for many of the helpful discussions, to Dr. Billy Crawford for his encouragement, and, in particular, to Dr. George C. Mohr, Commander of the Laboratory, for his discussion of the goals and objectives of the laboratory information system which is being developed.

His appreciation also goes to Col. Gary Adams, Col. Dan Johnson, Mrs. Sears, Mrs. Trnka, Mrs. Cross, and Mrs. Haskett. They together have made his summer assignment very pleasant.

C O N T E N T S

I. INTRODUCTION

Every organization, whether it is in research , manufacturing, or
service, can benefit from a good computerized system for information
storage and retrieval as well as for communication between all the
offices. As a teacher of information systems, my long range goal is to
design better information systems; and my short range goal is to
design a better user-to-system interface. This interface would assist
the on-line users to carry-on conversations with the system in order
to find the information they need.

During my pre-summer visit to Wright-Patterson AFB, Mr. Robert
Bachert invited me to participate in the planning of a computer-
network for management information and data communication for the
Aerospace Medical Research Laboratory (AMRL). I accepted the
invitation because the activity would help me : (1) to refine the
requirements for user-to-system interface, and (2) to refine the
directions for my future information system research.

II. OBJECTIVES OF EFFORT

This effort concentrates on the development of an overall system
configuration and capability requirements for a distributed
multi-computer system for shared information storage and retrieval and
data-communication between offices. This system needs computers which
have enough large storage units to hold the files, abilities to
understand human's requests in natural language , and abilities to
quickly deliver requested information to the humans in easy-to-
understand formats. Since this study is undertaken for the Air Force
Aerospace Medical Research Laboratory (AMRL), the proposed system will
be described with special reference to the AMRL laboratory. But the
proposed system could be implemented to meet the needs of any other
research organization.

147-5

III. OVERVIEW OF COMPUTERIZED/MANUAL INFORMATION SYSTEMS

At AMRL, computerized system will be used to support its internal activities , and its external communications with other units of the Air Force. The computerized system works in parallel with the present existing mechanisms (communication as well as information storage and retrieval) to enhance the AMRL activities.

Consider first the communication between all the offices and people in AMRL. At the present, there are three types of communication: telephone, face-to-face and written messages and documents through internal mail service. All of these 3 types of communication flow freely without any management restriction. This un-restrictive nature will be maintained for communications utilizing computer network. This means that people will have un-restrictive freedom to send/receive messages over the computer network.

The next to be considered are the information storage and retrieval, reporting and distribution over a computer network. This computerized information network is supposed to complement, not to immediately replace, the manual system being used today. The manual information system consists of all the file drawers in the offices, and the mail-service between the offices.

To complement the manual information system, and to work efficiently, the computer network will be structured to match the major information-flow patterns within AMRL.

IV. COMPUTER-NETWORK FOR INFORMATION AND COMMUNICATION

The proposed computer-network in Figure 1 is for messages between people as well as for data (information) communication between computers in the network. Each individual member of the laboratory would have access to a computer on or near his desk for his work.

In general, a computer at a higher level would have more capabilities in hardware and software. For example, the computer for the Laboratory Commander will have decision support software. The natural language interface is desirable for all computers. Its choice for a particular computer will depend upon cost/benefit analysis.

In Figure 1, the computers within a branch form a small cluster. The small clusters within a division make up a larger cluster. The communication paths between computers within a small cluster are shorter to make the communications within a branch quicker, thus to accomodate the frequent communication needs between members in the same branch. The communication paths between branches are longer, and the paths between divisions are even longer. However, one computer is able to reach every other computer in the network.

On the other hand, the computers for all division chiefs belong to the same small cluster, thus the communication between division heads are just as convenient as communication between members within a branch.
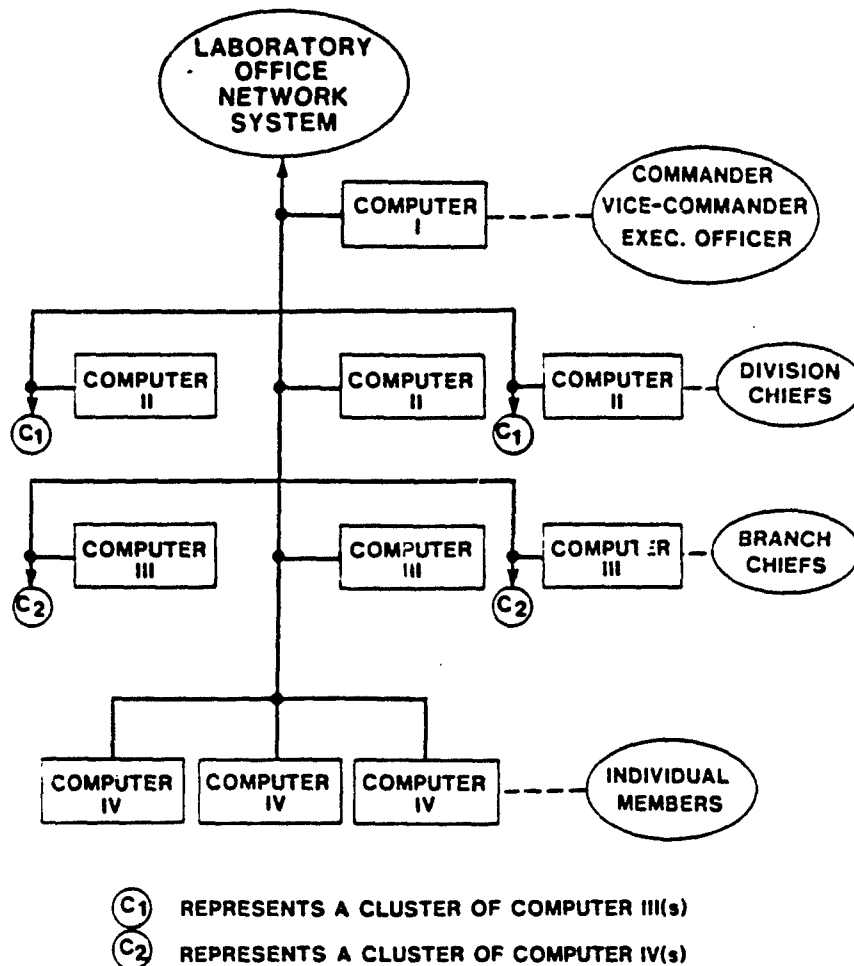
Figure 1   COMPUTER-NETWORK FOR INFORMATION
            AND COMMUNICATION.

V. DATABASE ORGANIZATION

1) The Guding Principles

At the 1982 National Conference of the American Society of Information Science, the president of a University stated that he has been receiving too much information (from his subordinates). Our feelings, after some soul-searching for interpretation, are that he had received too much information details. What he wanted was information summaries. This led us to the one guiding principle that computers at the upper-level store only summarized management information. The details are stored in the lower-levels.

Another guiding principle, as suggested by Dr. Mohr (Commander of AFAMRL), is that each person is responsible to maintain (i.e. add/delete/update) the portion of database related to his activity in a computer near him. (Note: HIS is used for brevity to represent HIS/HER, HE for HE/SHE and HIM for HIM/HER.) Only he or his alternate may modify his portion of the database, others can have authorized access by permission. By organizational logic, his boss would have authorized access.

However, there can be exceptions to this logic. The specifications for Laboratory Office Network System (LONS) released in April 1983 by Rome Air Development Center (RADC) allowed a sub-organization to lock up a part of its database to refuse access by anyone including its upper-level organization. [1]

2) Distributed Database

As a consequence of the guiding principle that each member of an organization maintains and guards the part of

the database related to his activities, the database is
divided into parts and stored into separate computers to be
maintained by separate individuals. Thus, each individual
will have electronic as well as physical control over his
part of the database.

VI. DATABASE ACCESS AND DATA DIRECTORY

Today's long distance telephone calls are connected
through local telephone exchanges, trunk lines, and
telephone exchanges at the other end. There are no direct
connections from each telephone to other telephones. The
computer to computer communications would be handled in a
similar fashion.

We consult telephone directory to locate the address
(i.e., telephone number) on the telephone network of an
organization or a person, before we can reach them by
telephone. In a computer-network, each computer consults a
directory which contains the data-file names and their
location in the computer-network, thus able to reach a
desired data file. Martin [2] claimed that the directory
for data-files together with data dictionary play a central
role in a database system. He illustrated that claim with
a diagram from Cullinane Corporation's advertisement
(Figure 2). At its center, you can see the integrated data
dictionary.

The data accesses between computers are by agreement.
And the accesses are limited to "Read Only". In principle,
a high-level computer is allowed to access most of the data
in its subordinate computers (i.e. at lower-level in its
cluster). Each computer's directory contains information

Report Generator

CULPRIT can be used to produce complex reports quickly, easily, and with a bare minimum of coding. It can access virtually any file structure including conventional files or data bases. CULPRIT is economical. It can produce up to 100 reports with a single pass. CULPRIT can be used as a powerful stand-alone facility or as part of a fully integrated data base management system. From Cullinane, EDP AUDITOR combines the capabilities of CULPRIT with a special Library of Audit Routines.

INTELLECT

This sophisticated English language inquiry system is designed for use by those in top management who have no background in computers, but have a need for timely information. Operating with a large, flexible dictionary, this new system has an outstanding ability to respond to conversational questions.

On-Line Query

On Line Query is an interactive information retrieval system. Fully integrated with IDMS, it requires no programming in order to be immediately useful upon installation. It provides managers and user departments with a powerful, easy to use set of English commands that allow instant access to selected information stored in the data base.

ESCAPE

ESCAPE is an interface that lets a DL/1 application program access an IDMS data base. Users with an investment in DL/1 applications can use IDMS without having to rewrite their DL/1 programs. And IDMS users can take advantage of the many useful DL/1 programs available from independent vendors.

Distributed Data Base

Cullinane's Distributed Database System allows multiple IBM computers to share a common IDMS data base. It supports applications programs at remote sites and allows them to access a central data base with complete user transparency and full data integrity.

Input Processor

IDMS Input allows programmers, as well as nontechnical end users, to develop application programs in an IDMS batch environment. This new product comes with its own simple language, making it easier and faster to program with IDMS input than with traditional programming language.

Data Communications

IDMS-DC is a data communications system designed specifically for use in the data base environment. Fully integrated with IDMS, IDMS/DC gives faster response time, more economical use of memory, and greater simplicity of use than a nonintegrated TP monitor can. IDMS/DC provides a powerful recovery facility, mapping support, storage protection, and other data integrity features.

Universal Communications Facility

Applications developed with IDMS UCF will run under any TP monitor without modification. With IDMS/UCF, programmers don't have to know the characteristics of the TP monitor they are using or may use. Applications will execute equally well through terminals connected to CICS, SHADOW II, Intercomm, Westi, Task/Master, and others.

On-Line Program Development

INTERACT is an on-line system for program development, remote job processing, text editing, and word processing. It offers a powerful command repertoire, fast terminal response time, and economical CPU requirements.

CULPRIT EDP AUDITOR · INTELLECT · ON LINE QUERY · IDMS DB/DC · UNIVERSAL COMMUNICATIONS FACILITY · APPLICATION DEVELOPMENT SYSTEM · INTERACT · INTEGRATED DATA DICTIONARY · ESCAPE CONVERSION AID · INPUT PROCESSOR · DISTRIBUTED DATA BASE SYSTEM

Figure 2. Diagram from Cullinane's advertisements which show the dictionary at the center, not the DBMS.

on how to reach those data-files, to which it has been allowed access, by automatic dialing. However, information request from a computer in one division may be sent to the computer in another division chief's office; and further contact to a computer in that division, based on information location from that response , will be necessary to reach the desired information.

Information request from a computer in one laboratory to a computer in another laboratory will be handled in the same manner.

VII. NATURAL LANGUAGE QUERY AND DECISION SUPPORT SYSTEM

It is our concept that the chief executives need not to learn the computer jargons or the artificial computer languages. They should be able to communicate with computer in our daily-use English language. With this in mind, we have been looking for natural English interface in the market-place.

The current expectations [3] are that the big computer manufacturers will all get into the natural language interface business. At the present time, there are only products from the start-up companies. Artificial Intelligence Corporation, Waltham, MA has the most successful natural language interface product -- INTELLECT, which runs on IBM mainframes. We can expect that similiar products from other companies will be available soon.

1) Natural Language Query System

After a natural language query has been interpreted by natural language interface into a formatted query, it is

sent to a decision-support system which will map-out a
strategy to arrive at the answers. The searches for data
are assisted by the DataBase Management System (DBMS).
Conceptually, the whole query-answer process can be
described by the diagram in Figure 3. In simple systems,
the Decision Support System (DSS) is most likely integrated
with the database managment system (DBMS). In general, the
DSS requests data from DBMS, and after having processed the
received data, issues requests for more data. This looping
operation continues until DSS is satisfied with the answers
or has decided that satisfactory answers can not be
obtained. In either case, answers are returned for the
query.

2)   INTELLECT Natural Language Package

At the present time, the INTELLECT Natural Language
Package by Artificial Intelligence Corp works the best.
It converses with you like a human being (of course there
are limitations). It works out a strategy to perform a
loop of data retrieval and processing until answers are
found to your query (see Figure 3). In analyzing your
query, it also is able to fill in what is implied but not
explicitly expressed in your query.

In order to achieve those listed above, the INTELLECT
[4] has been programmed to handle four key issues. These
are:

(a)   What is the proper density of language coverage?

(b)   How to resolve language ambiguity?

(c)   How to navigate through the database for the
       desired information?

NATURAL LANGUAGE QUERY

NATURAL LANGUAGE
INTERFACE

FORMATTED QUERY

DECISION SUPPORT
SYSTEM

ANSWERS

DATA

STRATEGY FOR
ARRIVING THE ANSWERS

DATABASE MANAGEMENT
SYSTEM
AND DATA
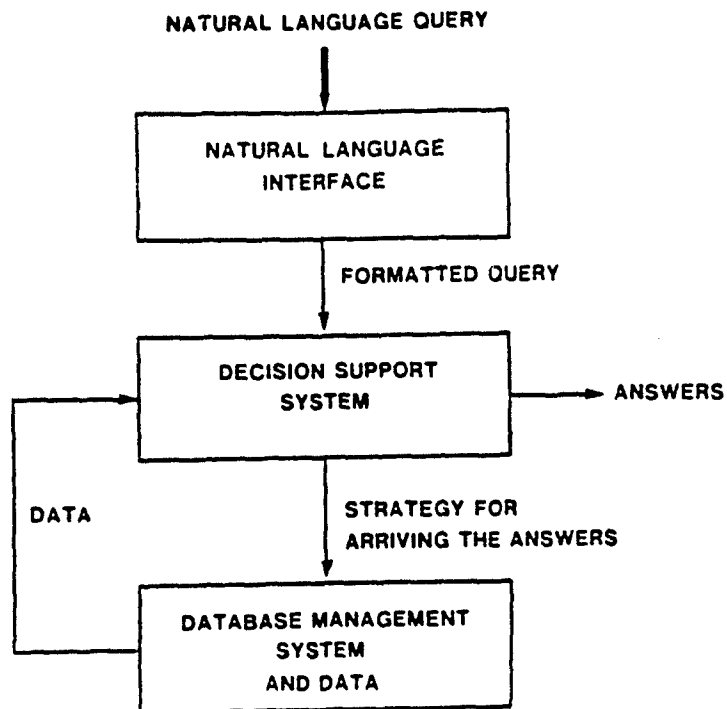
Figure 3. PROCESS FOR ANSWERING NATURAL
LANGUAGE QUERY.

(d)   How to fill in the implied (not explicitly
       expressed) information into the query?

The item (a) refers to the many allowed variations of
a given expression. Conceptually, in the linguistic space,
expressions which have identical meaning form a cluster.
More expressions in a cluster means higher density of
language coverage, which in turn means a more complex
program structure for the INTELLECT to recognize all the
variations.

The item (b) refers how to choose one meaning out of
several possible means for a term. The INTELLECT has
ability to recognize the multiple meanings for a word.
Consider the example:

        "FOR OHIO AND IOWA, PRINT THE NAME AND
        AGE OF ANYONE WHO EARNS BETWEEN $30,000 AND
        $50,000 AND IS MARRIED."

There are four AND in the above search statement. Each has
a different meaning. They imply respectively, a search for
both (Ohio and Iowa), a list of both fields to be retrieved
(name and age), a range specified by a pair of values
(between $30,000 and $50,000) as well as a search of
persons meeting both qualifications (and married). A good
system must be capable to recognize all these possible
meanings.

The item (c) refers how to go through a number of the
data files in the database in a step-by-step approach in
order to obtain the information requested. This means that

the INTELLECT must know the file structures in the database quite well.

The item (d) refers to memorizing the previous queries and the retrieved results for those queries in order to understand what are implied by the present query. For example, there are two queries in this order:

1) Who are the managers at ABC Corp?

2) How many of them are under 30?

The word "them" in the second query refers to the list of names retrieved for the first query.

The item (d) also refers to another situation. For example:

"What was the company total sale two years ago?"

Since this is the year of 1984, the INTELLECT would retrieve the company total sale in 1982. This means that INTELLECT keeps track of the time frame.

3) Decision Support System

The Decision Support System (DSS) has been characterized as interactive computer-based systems that help decision makers utilize data and models to solve unstructured problems [5]. The term "unstructured problems" has been used to mean not pre-defined problems. The Management Information Systems (MIS) are supposed to provide data to pre-defined types of manager's query. It is the predecessor to the development of DSS. However from a system analyst's view, MIS is a degenerated type of DSS;

and a degenerated MIS is the straight-forward data retrieval system. It is from this view that the diagram in Figure 3 represents a universal information system for natural language query.

VIII. PROCEDURE FOR SYSTEM IMPLEMENTATION

The basic strategy for system implementation is to grow the computerized system slowly in parallel with the existing manual system, and to phase out the manual system gradually at the same time. This approach seems to have the best chance to succeed. The validity of this approach has been confirmed by the statement, "parallel installation seems the most likely to succeed...," of Sprague and Carlson, in their book Building Effective Decision Support System [5]. One proposal for the system implementation consists of five steps. Those steps are detailed in a memo [6] to Mr. Robert Bachert, my effort-focal-point at AMRL.

IX. RECOMMENDATIONS FOR FUTURE RESEARCH

Our research goal is to extend our abilities for designing good information systems. Naturally, the question, "What is a good information system ?" would arise. With the understanding that an information system is used to provide information needs of humans, we know that a good information system should have all the capabilities of a human being. That means it should be made intelligent by some artificial methods. Thus, the study of all aspects of artificial intelligence are within the domain of information system research.

Sowa states in his book [7] that, " Artificial
Intelligence is the study of knowledge representations and
their use in language , reasoning, learning, and problem
solving." Thus there are five broad areas for our future
research. Among those five, knowledge representation is the
most fundamental element of them all. Since six years ago,
this writer has begun research on semantic network which is
a sub-area of knowledge representation. He plans to
continue that research, and use the ORACLE Relational
Database Management System in combination with programming
language to implement those new semantic networks for
demonstration purposes.

R E F E R E N C E S

1. Laboratory Office Network System (LCNS)
   Specification: Rome Air Development Center,
                    Grifiss Air Force Base,
                    New York, 1 April 1983

2. James Martin, Managing the Database Enviroment
   Prentice Hall, 1983, pp 127-129

3. Jan Johnson, "Easy Does It - Natural Language Query
   Systems" Datamaticn, June 1984, pp 48-59

4. Larry R. Harris, "Natural Language Simplifies Computer
   Access" Systems and Software, Jan 1984, pp 206-210

5. Ralph H. Sprague, Jr., Eric D. Carlson, Building
   Effective Decision Support System, Prentice-Hall,
   1982 p 4 and pp 155-7

6. The Development of a Computerized System for Management
   Information and Inter-office Communication , Memo
   to Mr. Robert Bachert, AFAMRL/TSZ, Wright-Patterson
   AFB; August 1984.

7. J.F. Sowa, CONCEPTUAL STRUCTURES , inforamtion
   processing in mind and machine, Addison-Wesley, 1984.

1984 USAF-SCEE SUMMER FACULTY RESEARCH PROGRAM

Sponsored by the

AIR FORCE OFFICE OF SCIENTIFIC RESEARCH

Conducted by the

SOUTHEASTERN CENTER FOR ELECTRICAL ENGINEERING EDUCATION

FINAL REPORT

THE "PROCESSING WINDOW" FOR THE NEAR BETA Ti-10V-2Fe-3Al ALLOY.

Prepared by: Dr. Isaac Weiss

Academic Rank: Associate Professor

Department and   School of Engineering
    University: Wright State University

Research Location: Materials Laboratories
                     Structural Metals
                     Wright-Patterson AFB, 45435

USAF Research   Dr. F. H. Froes
    Contact:

Date: September 21, 1984

Contract No.:   F49620-82-C-0035

THE "PROCESSING WINDOW FOR THE NEAR BETA

Ti-10V-2Fe-3Al ALLOY

by

Dr. Isaac Weiss

ABSTRACT

The control of grain size, grain shape and uniformity in order to avoid the formation of mixed grain size structure during processing from the ingot can be of great importance for further thermomechanical processing and for optimizing of final mechanical properties. It has ber . shown that this control can be achieved by processing through a certain temperature range termed the "processing window". The objective of the present work was to determine the "processing window" for the commercial Ti-10V-2Fe-3Al alloy. Test coupons taken from the ingot were forged to different total strain of 30% and 105% at temperatures ranging between 705°C (1300°F) and 1365°C (2500°F). Following deformation, the test pieces were annealed under vacuum at temperatures ranging from 815°C (1500°F) to 1337°C (2450°F) for 1 hour. Specimens were then oil quenched so that progress of static recrystallization could be followed. It was found that the appearance of the mixed grain size structure is associated with the recrystallization /grain growth behavior at high temperatures. The "processing window" for material forged to a 105% true strain was observed to extend to a higher processing temperature with minimum processing temperature of 1145°C (2100°F) and lower annealing temperature of 1050 C (1950 F) in comparison to the "processing window" for the material forged to a true strain of 30%.

Acknowledgement

I. INTRODUCTION:

Because of the interplay between recrystallization and grain growth, processing of beta titanium alloys can lead to the formation of a mixed grain size structure containing large and small grains (1). The mixed grain size structure is undesirable and contributes to poor high temperature flow, and inferior room temperature properties. Once introduced, it is impossible to remove the mixed grain size structure by heat treatment alone, so that processing is needed to uniformly refine the microstructure (1).

Mixed grain structures were found after either cold or warm working [below 855°C (1575°F)] the metastable beta titanium alloys, Ti-10Mo-6Cr-25Al and Ti-10Mo-8V-2.5Al and annealing at 980°C (1800 F). This microstructure is a result of selective recrystallization in the finer grains, with the driving force for grain growth rapidly decreasing because of the competition from recovery, resulting in a mixed grain size (1).

Studies of the austenite microstructure during hot rolling of steels reveals that under the conditions where partial recrystallization occurs in the transition temperature range from recrystallization to non-recrystallization, the mixed grain structure is produced by preferential recrystallization at austenite grain boundaries, the grain interior being left unrecrystallized (2). In addition, when coarse austenite grains are growing rapidly after recrystallization, as a result of light deformation passes, a mixed grain structure also develops (3,4).

II. OBJECTIVES OF THE RESEARCH EFFORT:

The purpose of the present study was to investigate the effect of:

1. Hot deformation,

2. Post deformation heat treatment,

III. MATERIALS AND EXPERIMENTAL PROCEDURE:

Forging blanks (50mm x 25mm x 25mm) were taken from a 305mm cast ingot with a nominal composition of Ti-10V-2Fe-3Al. These were hot die forged to true strain of 30% and 105% at temperatures between 1300°F and 2500°F as shown in table 1.

Table '

Serial Number	Forging Temperature (°F)	True Strain (%)	Annealing Temperature (°F)	Annealing Time (hr)	Cooling
A(30)	1300	30	1500-2400	1	Oil-Q
A(105)	1300	105	1500-2400	1	Oil-Q
B(30)	1700	30	1500-2400	1	Oil-Q
B(105)	1700	105	1500-2400	1	Oil-Q
C(30)	1900	30	1500-2400	1	Oil-Q
C(105)	1900	105	1500-2400	1	Oil-Q
D(30)	2300	30	1500-2400	1	Oil-Q
D(105)	2300	105	1500-2400	1	Oil-Q
E(30)	2500	30	1500-2400	1	Oil-Q
E(105)	2500	105	1500-2400	1	Oil-Q

A 50 ton hydraulic press was used at a ram speed of 5cm/min. (2in/min.). Deformed specimens were polished and macroetched in Kroll solution to groove the deformed grain boundaries. The etched specimens were then vacuum annealed for 1 hour at temperatures between 1500°F and 2450°F. Following oil quenching, the polished surface of the annealed specimen simultaneously shows

the prior deformed grain boundaries ("ghost boundaries") and the position of the newly recrystallized grains (thermally etched). This procedure was used to evaluate the progress of recrystallization during annealing (5).

IV. INITIAL MICROSTRUCTURE:

The initial microstructure of the forging blanks are shown in figure 1. These forging blanks were taken along the cast ingot. Samples A(105), B(105), C(105), D(105), and E(105) all contain columnar grain structure, while specimens B(30), C(30), A(30), D(30), and E(30) display an equiaxed grain morphology.

V. MICROSTRUCTURE OF DEFORMED SAMPLES:

The specimens forged to a true strain of 30% exhibiting the original as cast microstructure. Some elongated grains are found to exceed 50mm in length while most of the equiaxed grains are smaller than 25mm. Deformation to a true strain of 105% flattens both the equiaxed and elongated grains in a direction perpendicular to the forging axis.

VI. MICROSTRUCTURE OF DEFORMED AND ANNEALED MATERIAL:

The microstructures of specimens forged to true strain of 30% at 1700 °F [Specimens B(30)], 2000 °F [Specimen C(30)], 2500 °F [Specimen E(30)] and subsequent annealed at 1900°F for 1 hour are shown in Figure 2. Annealing samples with columnar and equiaxed structure at 1900 °F resulted in a mixed grain structure as shown in figures 2b, 2c, and 2e. Here, the recrystallized grains are superimposed on the "ghost boundaries" of the deformed grains. The volume fraction of the recrystallized grain is smaller than that of the recovered grains. The recrystallized grains exhibit a large radius of curvature indicating a very low driving force for

148-6

growth into the recovered region (1,6). A fully recrystallized microstructure (Fig. 3) is observed whenever specimens with columnar and equiaxed grains are forged at 1700°F, 2000°F, and 2500°F and annealed above 2300°F. This fully recrystallized microstructure apparently results from the high annealing temperatures and the high driving force for grain boundary migration. This microstructure still contains the "ghost boundaries" of the original grains, which appear to be smaller than the newly recrystallized grains. The large recrystallized grains are the result of recrystallization and rapid grain growth occuring during annealing after deformation of 30%. Finer recrystallized grains are produced in annealed samples forged to a total true strain of 105%. The smaller grains are the result of an increase in the nucleation density which occurs during the deformation and the subsequent anneal.

VII.   THE PROCESSING WINDOW:

Figure 4 and 5 show the effect of processing and annealing temperatures on the microstructure of specimens forged to a true strain of 30% and 105% respectively. Specimens forged 30% [(1700° F specimens B(30)] were found to require a lower anneal temperature of 2300°F to produce a fully recrystallized structure than samples processed at 2300°F and 2500°F. These observations can be rationalized in terms of the way these grains deform and the driving force for recrystallization and growth during annealing. The partially recrystallized microstructures observed at lower annealing temperatures (below 2300°F) are associated with sub-structure formation during the deformation as well as slow migration of the recrystallized grain boundaries during annealing.

148-7

During deformation of beta titanium (which has a high stacking fault energy) dynamic recovery occurs. This process is so rapid that dynamic recrystallization is suppressed (7). 'n subsequent annealing, nuclei for static recrystallization develop selectively along grain boundary regions where the localized strain is greater and more crystal deformation systems tend to operate as a result of plastic incompatibility. These nuclei rapidly produce new recrystallized grains with large radius of curvature. The well developed and homogeneously distributed recovered sub-structure present in the grain interior, especially in specimens deformed at 2500 °F, reduces the stored energy accumulated during deformation to such a low level that the driving force for growth of the recrystallized grains is very low (1). Under these conditions grain boundary migration of the recrystallized grains is extremely slow and a mixed grain size structure develops. A mixed grain size structure can also form during annealing when the deformation substructure tends to localize, as appears to occur during forging at 1700 °F, and subsequent annealing at 2200 °F between the regions in the processing diagram (Fig. 4 and 5) in which a mixed grain structure occurs a "processing window" exists for which a uniform recrystallized structure results. Similar results are obtained for material processed to 105% true strain. The "processing window" is observed to expend toward higher processing temperature, with a minimum processing temperature of 2100 °F, as well as to lower annealing temperature, with minimum annealing temperature of 1950 °F compared to the "processing window" for material forged 30% as shown in figure 5. The shift of the "processing window" may be attributed to a more uniform sub-structure which forms during forging above 1800 °F, as well as the increase in driving force for grain growth during annealing.

148-8

Recommendation

The "processing window" determined in this work was found to be a result of the non-homogeneous deformation below $1800°F$. However, initial grain shape and size and solute concentration both affect the magnitude of the "processing window" and should be investigated in future research work.

References

1. F. H. Fores, C. F. Yolton, J. P. Hirth, R. Ondercin and D. Moracz, "Proceedings of the Beta and Near-Beta Alloys Symposium,"· AIME/TMS, Atlanta, GA, March (1983).

2. J. D. Jones and A. B. Rothwell, "Deformation Under Hot Working Conditions," Iron and Steel Inst. Publication 108, Iron and Steel Inst., London (1968).

3. A. Le Bon and L. N. De Saint-Martin, "Microalloying 75," International Symposium on High-Strength, Low Alloy Steel, Union Carbide Corp., New York, N.Y., (1977).

4. L. J. Cuddy, Metall. Trans., 12A, (1981), p. 1313.

5. I. Weiss, F. H. Froes, and D. Eylon, Metall. Trans. 1984, in press.

6. H. P. Stuwe: Recrystallization of Metallic Material. F. Haessner, Ed. Dr. Reiderer, Verlag GMBH, Stuttgart, (1978), p. 13.

7. H. J. McQueen and J. J. Jonas, "Treatise on Materials Science and Technology", vol. 6, Plastic Deformation of Materials, Acad. Press, (1975).

FIG. 1   1 inch

DEF 1700°F, 30%
ANN 1900°F
6,000µm

DEF 2000°F, 30%
ANN 1900°F
6,000µm

DEF 2500°F, 30%
ANN 1900°F
6,000µm

FiG 2

DEF 1700°F, 30%
ANN 2300°F
6,000µm

DEF 2000°F, 30%
ANN 2300°F
6,000µm

DEF 2500°F, 30%
ANN 2300°F
6,000µm

FiG 3
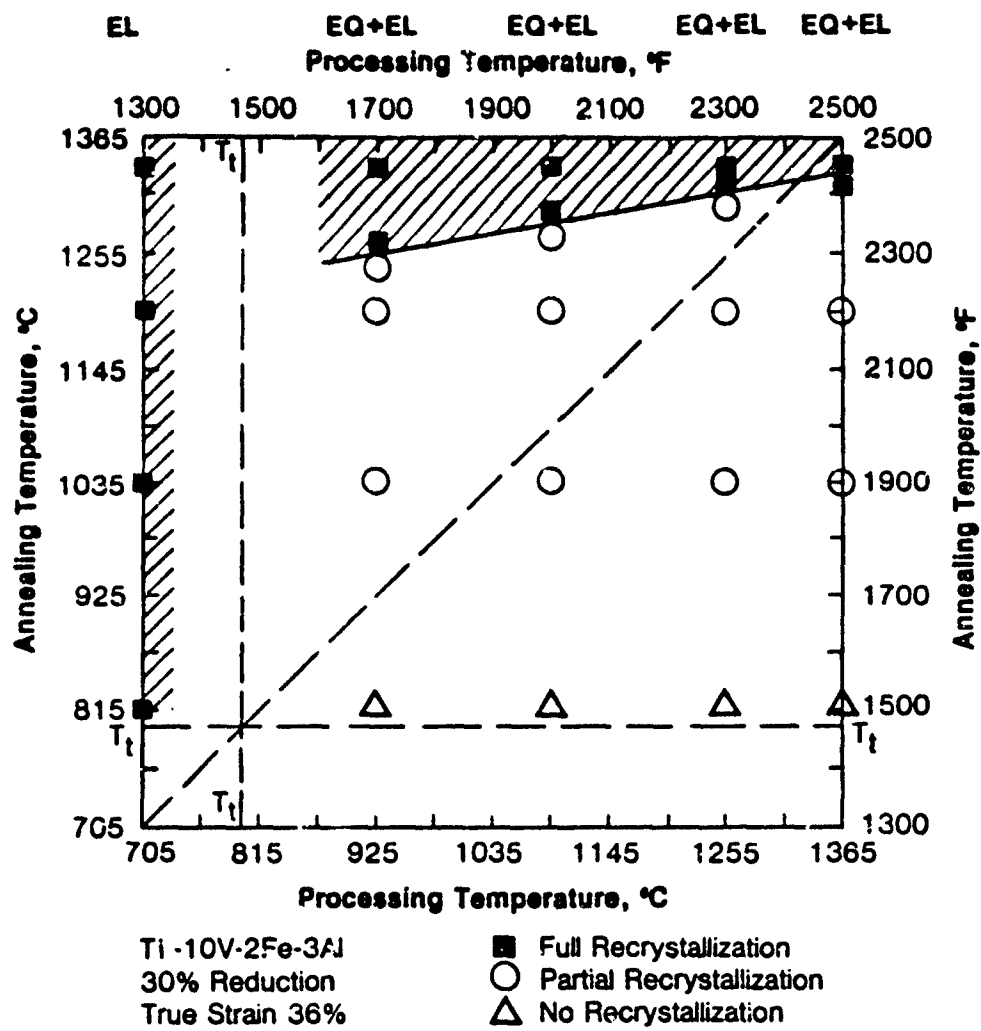
Fig. 4
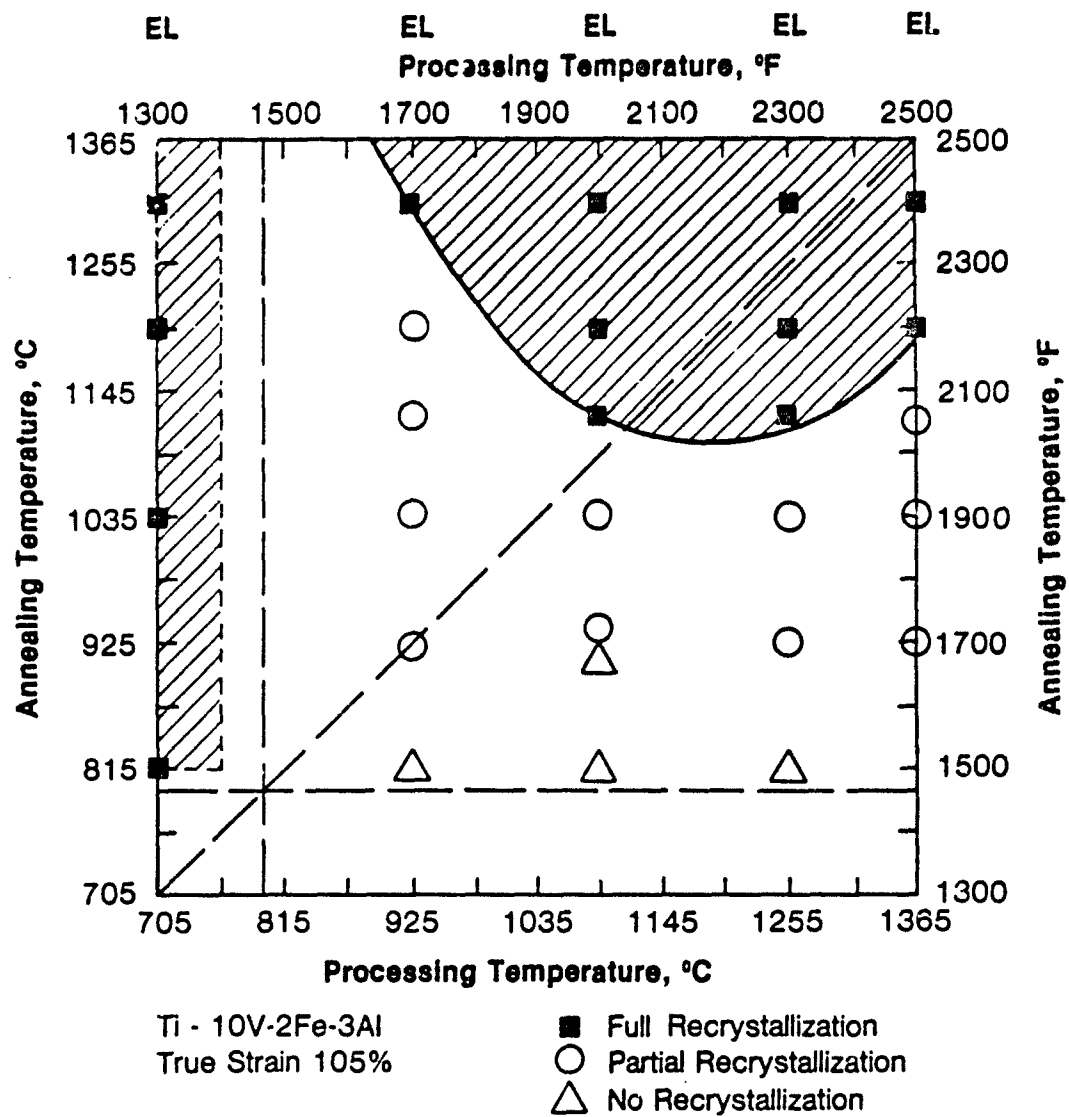
Fig. 5

1984 USAF-SCEEE SUMMER FACULTY RESEARCH PROGRAM

Sponsored by the

AIR FORCE OFFICE OF SCIENTIFIC RESEARCH

Conducted by the

SOUTHEASTERN CENTER FOR ELECTRICAL ENGINEERING EDUCATION

FINAL REPORT

EFFECTS OF HUMIDITY ON GASEOUS PHASE ADSORPTION OF

TRICHLOROETHYLENE BY ACTIVATED CARBON

Prepared by: Dr. Martin D. Werner

Academic Rank: Assistant Professor

Department and   School of Public Health
   University:
                        University of Texas

                        San Antonio, Tx

Research Location: Air Force Engineering and Services Center

                        Environics Division, Environmental

                        Engineering Branch

USAF Research: Captain Randy Gross

Date: 24 August 1984

Contract No: F49620-82-C-0035

EFFECTS OF HUMIDITY ON GASEOUS PHASE ADSORPTION OF
TRICHLOROETHYLENE BY ACTIVATED CARBON

by

Martin D. Werner

ABSTRACT

Theoretical models applied to the adsorption of four
concentrations of trichloroethylene (TCE) (300, 600, 1000, 1300
mg/m^3) from air at low relative humidity predicted the following:
adsorptive capacity of activated carbon (maximum error compared
to actual data < 17%), shape of the breakthrough curve (maximum
error < 4%), and time to contaminant breakthrough (maximum error
< 8%). These low humidity data were then compared to TCE
adsorption by the same carbon at four other relative humidities
(25%, 50%, 65%, 85%). The following observations were made.
Increasing levels of humidity had increasingly deleterious
effects on the adsorptive capacity of activated carbon at all TCE
concentrations tested. The adverse effect caused by the presence
of water vapor was more significant at the lower TCE concentra-
tions than at higher concentrations. The presence of water vapor
not only decreased the carbon's adsorptive capacity but also
reduced its efficiency by increasing the dispersion of the break-
through curve. Data at all humidity levels fit the Dubinin-
Polanyi isotherm equation equally well, indicating the impact of
water vapor on the adsorptive capacity of carbon for TCE is
predictable and could be accurately modeled.

ACKNOWLEDGEMENTS

I. INTRODUCTION

Air stripping of volatile organic contaminants (VOC) from water is emerging as an efficient treatment process. Additionally, air stripping has the advantage of being much less expensive than alternative control processes, such as aqueous phase activated carbon. For these reasons, it is an attractive alternative to the Air Force for their groundwater cleanup operations. However, several states consider the contaminants transferred to the gaseous phase during air stripping as a point source of air pollution which may require additional cleanup efforts. In anticipation of added control requirements, the Air Force has initiated research to investigate pollution control processes to remove VOC from the discharged air of a stripping operation.

Gaseous phase carbon adsorption is a process by which VOC in air could be removed. However, characteristics of the discharge air of a stripping operation are not optimal for efficient adsorption. Two major problems exist with the stripper discharge air. First, the VOC concentration in the air is likely to be low because of the advantage of a high air to water ratio during a typical stripping operation. Unfortunately, the capacity of activated carbon for an adsorbate decreases with decreasing adsorbate concentration. Most research on gaseous phase carbon adsorption has been performed at higher VOC concentrations than would be encountered from a stripping operation; thus, theoretical formulations to predict adsorption efficiency have been developed for, and verified by, adsorption at high VOC concentrations. It is necessary to determine whether these theoretical

models are valid predictors at VOC concentrations within the range produced during an air stripping operation. Second, the air streams containing the VOC would also have a high water vapor concentration. Numerous reports written on the subject of gaseous phase carbon adsorption mention the detrimental effect of humidity on the adsorption process (e.g., 1,2,3), but few studies exist which have quantified the magnitude of the impact. Furthermore, no study has been located which has systematically tested the effect of several levels of humidity on adsorptive efficiency at various concentrations of a VOC. If there is an interaction between the relative adsorption efficiency at different humidity levels and VOC concentration, it would be desirable to take measures to optimize adsorption effectiveness in an overall air stripping/carbon adsorption process. For example, if a given level of humidity has a greater deleterious effect at lower VOC concentration than at higher concentration, it may be desirable to reduce the air to water ratio in the stripping operation to increase the VOC concentration in the air and, thereby, increase the effectiveness of subsequent carbon adsorption.

The present study was designed to investigate the above mentioned problems pertaining to carbon adsorption of VOC from air stripping discharge, and to begin to determine whether VOC adsorption will be a viable option to the Air Force.

II. RESEARCH OBJECTIVES

The primary objective of the project was to assess the impact of water vapor concentration on the effectiveness of trichloroethylene (TCE) adsorption by activated carbon. To meet the objective, it was first necessary to assure that the experimental system was providing reliable results, based on existing published research and theoretical models. Thus, a secondary objective was to apply existing theory to the experimental data to assess agreement between theory predictions and the data for the following important factors: (1) the adsorptive capacity of the activated carbon, (2) shape of the breakthrough curve, and (3) time to a given level of contaminant breakthrough. The accurate body of theory based on sound assumptions will be recommended to the Air Force for potential use in additional research and full scale operation. The effect of humidity on each of the above mentioned fators will be assessed to further analyze the nature and extent of the impact of water vapor on TCE adsorption.

III. EXPERIMENTAL METHODS AND DESIGN

The experimental system employed for this research is illustrated in Figure 1. Dry (< 5 percent relative humidity) purified air entered the system through a pressure valve (2). The air was split immediately following the pressure valve into two streams. A small portion (0.2 to 0.5 percent) flowed through an air flow controller (3) to the TCE generating apparatus consisting of a 4.5 cm impinger tube partially filled with TCE

Figure 1. Diagram of the Experimental System
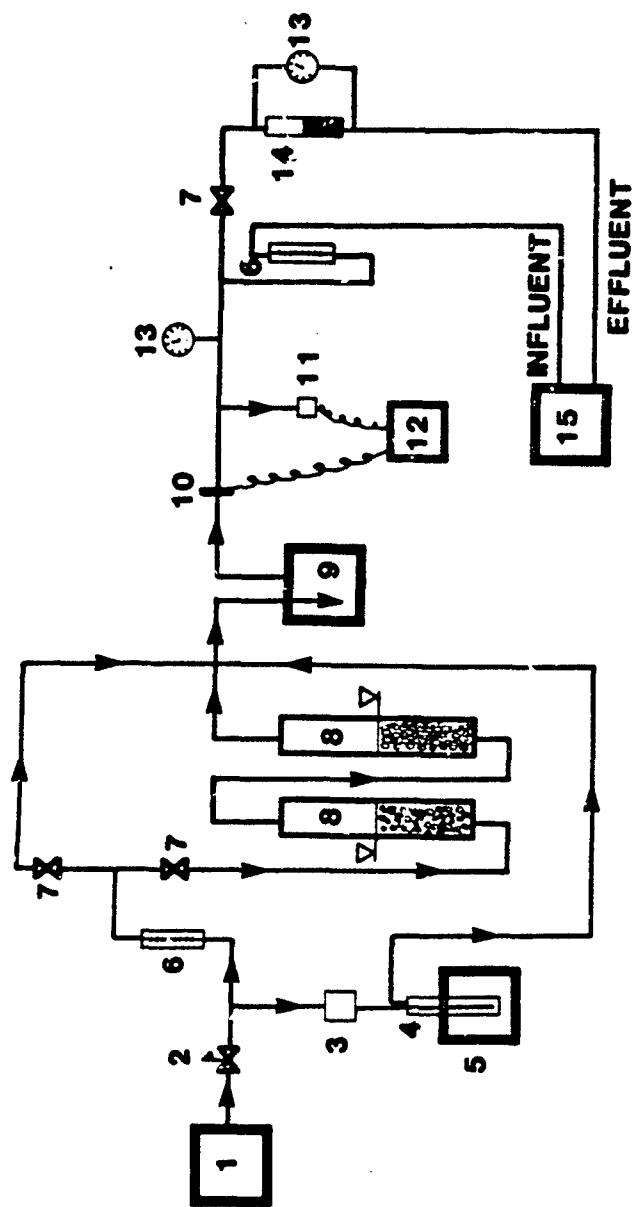
1. DRY, PURE AIR GENERATOR
2. PRESSURE VALVE
3. AIR FLOW CONTROLLER
4. IMPINGER TUBE FOR TCE
    GENERATION
5. CONSTANT TEMP BATH
6. ROTOMETER
7. FLOW VALVE

8. HUMIDITY GENERATOR
9. EQUALIZATION VESSEL
10. TEMP PROBE
11. DEWPOINT SENSOR
12. HYGROCOMPUTER
13. PRESSURE GAGE
14. ACTIVATED CARBON COLUMN
15. GAS CHROMATOGRAPH

149-7

(4) in a temperature controlled water bath (5). The bulk of the air (~10 l/min) flowed through a rotometer (6) and into the main portion of the system. That main air stream could also be split, a portion flowing through two 5 cm glass tubes (8) connected in series and partially filled with water to humidify the air. The tubes contained plastic Pall rings to distribute the air and increase air-water contact. The first tube in the series was wrapped with heating tape to warm the water and thereby increase its rate of transfer to the air stream. The other portion of the air flow was kept dry. The three portions of air (TCE laden, water vapor laden, and pure dry air) were united and directed through a 20 liter equalization vessel (9) to dampen short-term variation in TCE concentration and air humidity. The total air stream then passed over a temperature probe (10) and a small air volume (25 ml/min) entered a dew point sensor (11). Thus, air temperature and water vapor concentration were continuously monitored using a General Eastern Model Hygrocomputer (12). Air pressure was measured within the system using a pressure gage (13). A portion of the air stream (2.3 l/min) was then diverted to a gas chromatograph (15) for influent TCE concentration determination, while the remainder (7.7 l/min) was directed through the activated carbon column (14). Effluent from the column was also directed to the gas chromatograph for TCE concentration analysis. A second pressure gage (13) connected across the column measured pressure drop due to air flow through the carbon.

The 7.7 l/min air flow through the activated carbon column resulted in a linear velocity of 25 cm/s in the 2.54 cm column and an air retention time within the carbon of 0.5 s. TCE concentration in influent and effluent air was measured at 15 to 20 minute intervals throughout an experimental run. When the effluent TCE concentration stabilized at the influent concentration the experiment was terminated.

CECA GAC48C Carborundum® activated carbon was used for all trials. A weighed amount of carbon (37.5 g) which was distilled water washed and oven dried was placed over a thin layer of glass wool in the column to give a carbon bed depth of 13.5 cm. Experiments were performed at 4 TCE concentrations (roughly 300, 600, 900, and 1300 mg/m^3) each at 5 levels of relative humidity (<5, 25, 50, 65 and 85 percent).

IV. RESULTS AND DISCUSSION

A. Data Fit to Model Predictions

Most theoretical models developed to predict the various critical aspects of carbon adsorption have been developed for one adsorbate system under conditions of low humidity. Therefore, only the data collected under the lowest water vapor concentrations (<5% relative humidity) will be analyzed in this section. In the following section that data (considered to be the base-line data) will be compared to data collected under conditions of higher relative humidity to assess the impact of water vapor on carbon adsorption.

Traditionally, adsorption isotherms have been used to relate the adsorptive capacity of carbon to some equilibrium concentration of the adsorbate. Three commonly used isotherm equations are listed and described in Table 1. Although all of these isotherm equations are used to describe gaseous phase carbon adsorption, and all fit the data of this experiment well, only the Dubinin-Polanyi equation makes valid assumptions for this application (4). In addition, the Dubinin-Polanyi equation is much more powerful and useful as a prediction method than the other equations (4,5). For the above reasons, only the Dubinin-Polanyi equation will be utilized for subsequent theoretical formulation in this paper. Figure 2 shows the fit of the low humidity data to Dubinin-Polanyi equation.

The Dubinin-Polanyi equation can be used to predict an isotherm at any temperature and with any adsorbate based on the isotherm of a reference adsorbate. Values for parameters of the equation can be found in the literature or in chemistry handbooks. Figure 3 graphically depicts the experimental data, and includes a comparison with the equation's predictions. The the predictions represent maximum adsorptive capacity which is usually measured under static conditions, whereas the actual values were obtained by dynamic adsorption for which kinetic effects could reduce the adsorptive capacity. Even with that problem, the actual value of each point is within 17% of its predicted value. Wo, a parameter based on pore size distribution of the carbon, was not available from the manufacturer for the

TABLE 1. ISOTHERM EQUATIONS AND CORRELATION COEFFICIENTS
OBTAINED FROM EXPERIMENTAL DATA

<u>Langmuir Isotherm</u> ($r^2 = 0.952$)

$Q = Qm \ kCe/(1 + kCe)$

$1/Q = 1/Qm \ kCe + 1/Qm)$

    Q = Adsorbate sorbed per unit mass of adsorbent

    Ce = Equilibrium adsorbate concentration

    Qm = Limiting (maximum) sorptive capacity of adsorbent

    k = Coefficient of adsorbate/adsorbent system

<u>Freundlich Isotherm</u> ($r^2 = 0.986$)

$Q = k \ C^{1/n}$

$\log Q = \log k + 1/n \ \log C$

    k,n = coefficients of adsorbate/adsorbent system

<u>Dubinin-Polanyi Isotherm</u> ($r^2 = 0.983$)

$W = Wo \ e^{-Ks/B^2 (RT \ ln \ Po/P)^2}$

$\ln W = \ln Wo - Ks/B^2 \ (RT \ \ln \ Po/P)^2$

    W = Volume of adsorbate sorbed per unit adsorbent

    Wo = Limiting (maximum) sorptive capacity of adsorbent,
        (0.505 ml/g)

    K = Parameter dependent on adsorbent/adsorbate system,
        ($2.89 \times 10^{-9} \ mol^2/J^2$)

    B = Affinity coefficient of adsorbate, (1.14)

    R = Universal gas constant, (8.3143 J/Mol/K)

    T = Temperature in Kelvin, (296 K)

    P = Actual vapor pressure of adsorbate (mm Hg)

    Po = Saturated vapor pressure of adsorbate (60 mm Hg at 296K)
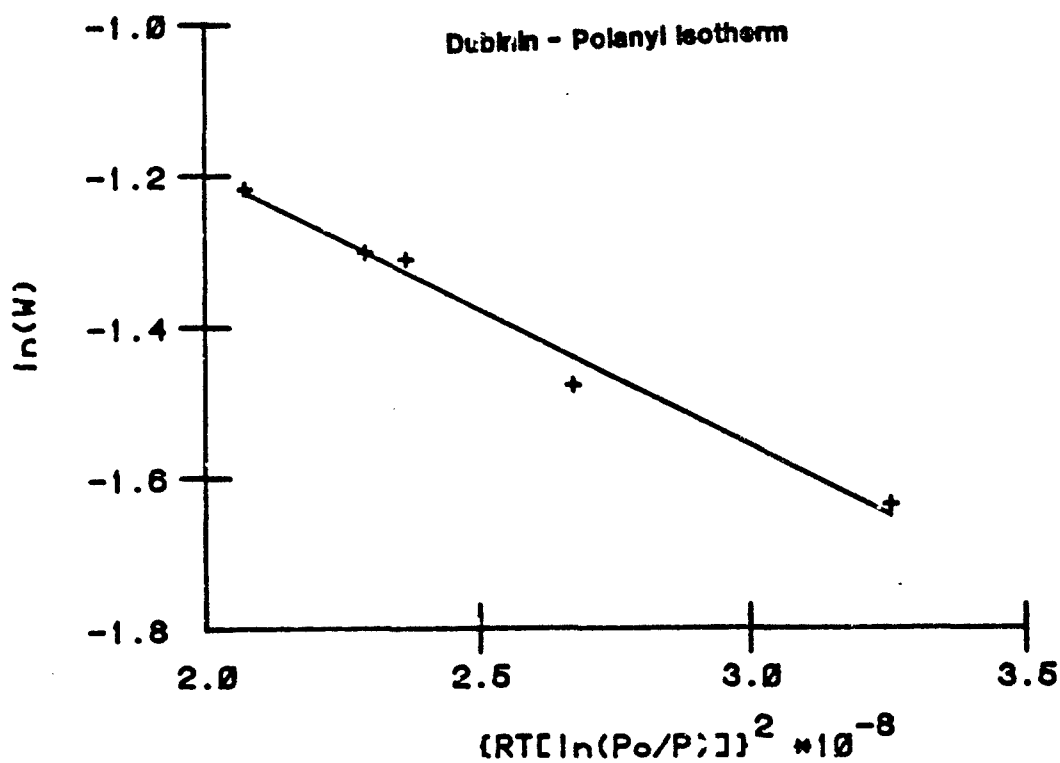
Figure 2. Low Humidity Data Fit to the Dubinin-Polanyi Isotherm Equation

149-12

carbon used for these experiments so the value for a closely related carbon (CECA 410) was substituted. Urano et al. (5) presents a complete explanation for the application of the Dubinin-Polanyi equation and for the conversions necessary to obtain the independent variable in units of concentration (g/m^3) and the dependent variable as mass adsorptive capacity (g/g).

Contaminant breakthrough curves from activated carbon beds typically follow a sigmoidal pattern, resulting from the normal distribution of velocities among the population of adsorbate molecules (6). Thus, according to Gruber and coworkers (6,7,8), the breakthrough curve can be described by a cumulative normal probability curve, and the dispersion of the curve for a given set of conditions can be calculated from as few as two points on the curve. If the degree of dispersion, or standard deviation (σ), for the curve is known along with a single point on the curve the remainder of the curve can be predicted. Furthermore, the relative standard deviation (defined as σ/T_{50}, where T_{50} is time to breakthrough of 50% of the influent concentration) should be the same for any concentration of a given adsorbate/adsorbent combination (6,7). Therefore, the potential exists for predicting an entire breakthrough curve by knowing only a single point on a curve and the relative standard deviation obtained at another adsorbate concentration. The obvious advantage of using this concept is that time to critical contaminant breakthrough can be estimated with few effluent samples.

149-13
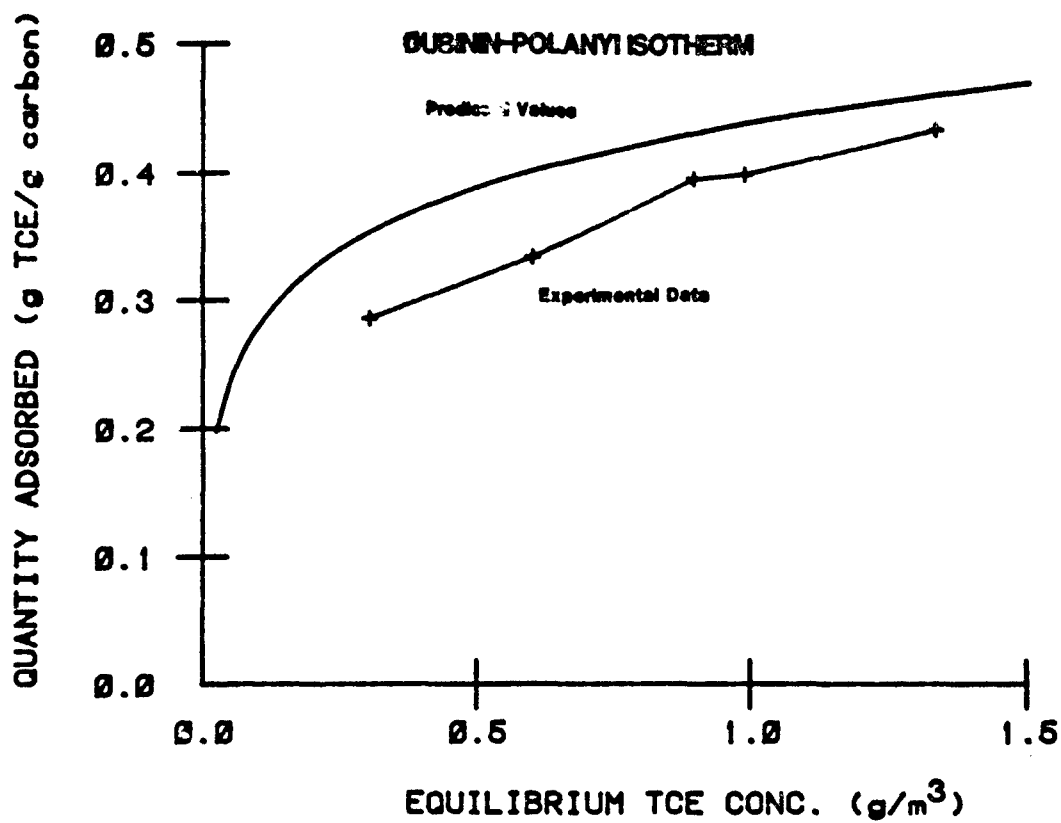
Figure 3. Adsorptive Capacity Predicted by the Dubinin-Polanyi
Isotherm Equation Compared to Actual Experimental Data

149-14

Experimental data were applied to the above concept. Overall adsorptive capacity was predicted within -3.5 to +3.7 percent (mean = 0.4%) of the actual measured capacity. The relative standard deviation ranged from 0.100 to 0.167 with a mean of 0.126. These results indicate a TCE breakthrough curve can be accurately predicted by an adjusted cumulative probability curve and the concept of the relative standard deviation.

Gruber and Burgess (7) present several equations to predict the time to a critical level of contaminant breakthrough from an activated carbon column. Using the assumption of a predictable shape for the breakthrough curve (as described above) and a generalized Dubinin-Polanyi isotherm presented by these authors, time to 50% breakthrough was predicted for the various TCE influent concentrations used in this study. Comparisons between predictions and actual breakthrough time are presented in Table 2. The maximum error for predicting breakthrough time was 7.4 percent.

Based on the above analyses two conclusions are made. First, the data generated by this research effort are reliable based on comparisons with predictions of existing theoretical models. Thus, the base-line data obtained at low humidity can be compared with confidence to higher humidity trials to assess effects of humidity on carbon adsorption. Second, the existing body of theory was very useful for predicting critical factors of contaminant adsorption by activated carbon. This body of theory might prove useful for full-scale operations.

149-15

TABLE 2. DEVIATION FROM PREDICTED TIME TO 50% BREAKTHROUGH
AT LOW RELATIVE HUMIDITY (<5%)

Influent Conc. (mg/m³)	Breakthrough Time (hour)		Percent Deviation
	Actual	Predicted	
303	76.5	71.2	+7.4
602	45.1	45.6	-1.1
895	35.9	34.6	+3.8
987	32.8	32.2	+1.9
1331	26.4	25.9	+1.9

B. Effects of Water Vapor on Adsorption

The quantity of TCE adsorbed per gram of activated carbon at each influent TCE concentration and level of relative humidity tested are presented in Figure 4. Excluding the trials with 25% humidity at 1000 and 1300 mg TCE/m^3, increasing concentrations of water vapor had an increasing deleterious effect on the carbon's adsorptive capacity for TCE. Actual values obtained during the study are listed in Table 3. Although numerical differences of adsorptive capacity between high and low humidity are generally less at lower TCE influent concentrations than for higher concentrations, the relative differences are greater for the former. An example will help to illustrate this. Subtracting values for the lowest relative humidity (<5%) from the highest (85%) at TCE influent concentrations of 300 mg/m^3 and 1300 mg/m^3 results in differences in adsorptive capacity of 0.259 g/g at the lower TCE concentration and 0.313 g/g at the higher concentration. However, the percent adsorptive capacity maintained was higher for the 1300 mg TCE/m^3 comparison (28%) than for the 300 mg/m^3 comparison (9%).

Loss of adsorptive capacity at various relative humidities was calculated for each humidity trial within an influent TCE concentration. These comparisons are presented in Table 4. In all cases, relative adsorptive capacities decreased faster with increasing relative humidity at low TCE concentrations than at higher TCE concentrations. Thus, there is an important interaction between relative humidity and TCE concentration which

149-17
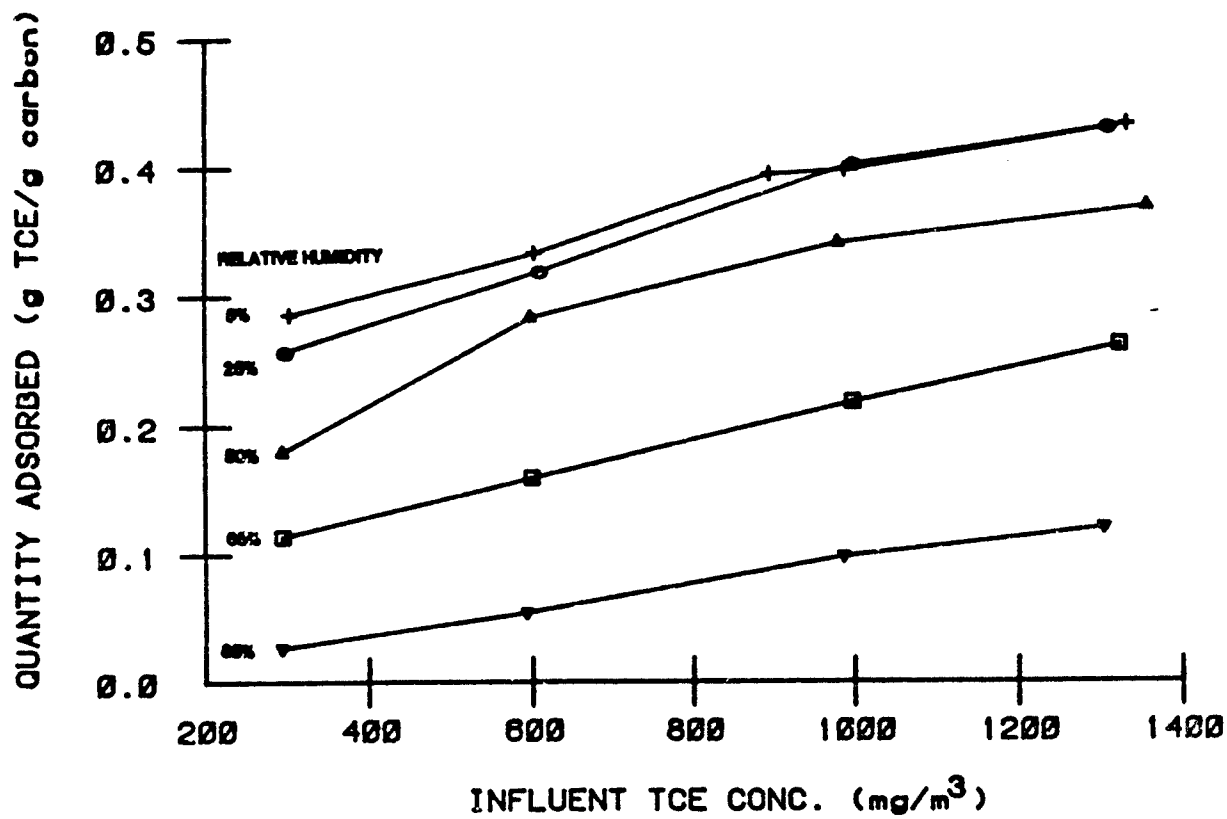
Figure 4. Measured Adsorptive Capacities at Various Influent
TCE Concentrations and Levels of Relative Humidity

TABLE 3.   TCE ADSORBED AT VARIOUS INFLUENT CONCENTRATIONS
AND LEVELS OF RELATIVE HUMIDITY

Relative Humidity (%)	TCE Influent Conc (mg/m^3)	TCE Adsorbed (gTCE/g carbon)
<5	303	0.286
25	295	0.257
50	293	0.180
65	295	0.114
85	293	0.027
<5	602	0.334
25	605	0.320
50	597	0.284
65	599	0.160
85	593	0.054
<5	895	0.395
<5	987	0.399
25	995	0.403
50	978	0.342
65	996	0.218
85	986	0.098
<5	1331	0.434
25	1306	0.431
50	1356	0.370
65	1322	0.262
85	1304	0.121

TABLE 4. TCE ADSORBED STANDARDIZED TO THAT ADSORBED AT LOW
          RELATIVE HUMIDITY (<5%)

TCE Influent	Relative Humidity (%)				
Conc. (mg/m³)	<5	25	50	65	85
	Relative Amount Adsorbed				
300	100	90	63	40	9
600	100	96	85	48	16
1000	100	101	87	55	25
1300	100	99	85	61	28

TABLE 5. TIME TO BREAKTHROUGH OF 10% OF THE INFLUENT TCE
          CONCENTRATION STANDARDIZED TO THAT VALUE AT LOW
          RELATIVE HUMIDITY (<5%)

TCE Influent	Relative Humidity (%)				
Conc. (mg/m³)	<5	25	50	65	85
	Relative Amount Adsorbed				
300	100	67	58	32	9
600	100	82	77	38	15
1000	100	93	80	48	24
1300	100	87	83	51	27

should be considered when designing an air stripping/gaseous phase carbon adsorption process. In some cases, it may be beneficial to reduce the air to water ratio of the stripping operation (even though that would reduce stripping efficiency) to obtain a higher concentration of VOC in the air and, thereby, reduce the negative impact of water vapor during the air adsorption portion of the operation.

The shape of the breakthrough curve is a factor, in addition to the overall adsorption capacity, which could influence the length of time a batch of activated carbon can be utilized. As discussed previously in this paper, dispersion associated with a breakthrough curve can be described by the relative standard deviation of the curve. The mean relative standard deviation was 0.126 (range = 0.100 to 0.167) for the low humidity trials; that same parameter's value was 0.210 (range 0.156 to 0.298) considering all trials above the minimum relative humidity. Thus, water vapor not only reduced the adsorptive capacity of the carbon in these experiments but also caused the breakthrough curve to be more dispersed over time. A result of widening the breakthrough curve is to reduce the carbon's efficiency since a critical breakthrough concentration (if less than 50% of the influent adsorbate concentration) will be reached sooner than it would be for a narrower breakthrough curve even if the carbon in both cases had the same overall adsorptive capacity. Table 5 contains the time to breakthrough of 10% of the influent TCE concentration standardized to the breakthrough time for the

lowest humidity (i.e., the humidity at which water vapor is assumed to have no effect). If water vapor had no effect on the carbon's efficiency due to changes in the shape of the breakthrough curve, values in Table 4 and Table 5 would be identical. Values in Table 5 are less than the corresponding values in Table 4, which reflects the effect of the increased dispersion of the breakthrough curves. Surprisingly, the breakthrough curves were not dispersed at highest relative humidity (85%). No conclusive explanation can be offered for that apparent anomalay at this time. Results of the analysis of data in Table 5 are of practical importance only when a single column is employed. If two or more columns are employed in series the entire adsorptive capacity of the first column could be exhausted, so the shape of the breakthrough curve would be of little significance.

Data from each humidity level were fit to the Dubinin-Polanyi Isotherm model. As demonstrated in Figure 5 results at all humidity levels fit the model equally well (r^2 greater than 0.92 for all cases). The changing slopes from one humidity level to another also clearly demonstrates the interaction between humidity levels and adsorbate concentrations. A given humidity level exerted a greater effect at low TCE concentrations than at higher concentrations, as discussed earlier in this paper.

Since the Dubinin-Polanyi Isotherm equation is followed so closely at all humidities it can be assumed that water vapor is exerting a predictable effect on the carbon's capacity to adsorb
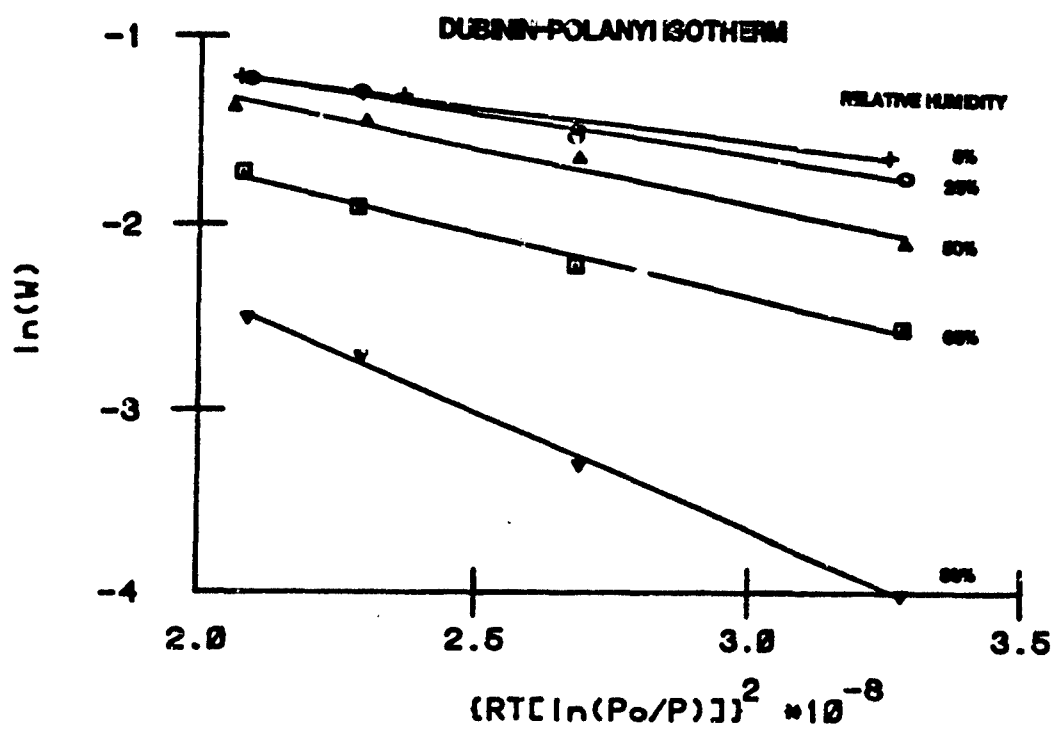
Figure 5. TCE Adsorption Results at Five Levels of Relative
Humidity Fit to the Dubinin-Polanyi Isotherm
Equation

149-23

TCE. The predictability suggests that the system could be accurately modeled to asses the impact of, or the interference caused by, water vapor on the adsorptive capacity of carbon at other levels of humidity.

V. SUMMARY AND CONCLUSIONS

A. Models exist which accurately predicted results of trichloroethylene (TCE) adsorption by activated carbon from air at low levels of humidity. The following important factors were predicted:

1. Adsorptive capacity of activated carbon.

2. Shape of the contaminant breakthrough curve.

3. Time to breakthrough of a given contaminant concentration.

B. Water vapor exerted a deleterious effect on activated carbon's adsorptive capacity. Increasing levels of relative humidity had increasing deleterious impacts. The effect of humidity was greater at low TCE concentrations than at the higher TCE concentrations tested. In general, water vapor also caused a greater degree of dispersion in the contaminant breakthrough curve which has the effect of reducing the efficiency of the carbon to an extent greater than suggested by the reduction caused to the carbon adsorptive capacity.

C. The Dubinin-Polanyi equation fit the data obtained at all levels of relative humidity equally well, indicating the effect of water vapor on TCE adsorption, and possibly other organic contaminants, could be accurately modeled.

VI. RECOMMENDATIONS

This research demonstrated (1) the accuracy of several models for predicting important aspects of gaseous phase carbon adsorption at low relative humidity and, (2) the predictable effect water vapor has on the effectiveness of the adsorption process. Both of these were demonstrated for a single adsorbate, TCE, under constant experimental conditions. It is recommended that these findings be applied to the design and operation of full-scale adsorption processes. To extend the usefulness of the results, three areas of additional research are recommended. First, adsorption models need to be tested on a variety of adsorbates in different classes of organic compounds under varying conditions of adsorption (e.g. different carbons, different air flow rates and different temperatures). The object of the testing would be to determine how robust existing models are. Existing adsorption studies which have been published could be used for this analysis. Second, a model should be developed to predict the effect of humidity on gaseous phase carbon adsorption for different adsorbates under various levels of relative humidity. Results of this research indicate the effect of water vapor on adsorption should be amenable to accurate modeling. Third, the interaction between adsorbates in a multi-adsorbate system (i.e., competitive adsorption) needs to be investigated. The approach to this problem could be similar to the one taken for the second research recommendation.

REFERENCES

1. Howard. A.G., and R. Pizzie, "Sampling of Chlorinated and Brominated Haliforms from Humid Atmospheres," Ann. Occup Hyg., 1981, 24: 167-173.

2. VIC Manufacturing Company, "Carbon Adsorption/Emission Control: Benefits and Limitations," VIC Manufacturing Co., Minneapolis, MN, 1979.

3. Musakin, G.A., T. G. Plachenov, Yu. M. Plokhov, and A G. Rybnikov, "Influence of the Parameters of Carbon Adsorbents on their Dynamic Adsorption Capacity for Organic Vapors," Zhurnal Prikladnoi Khimii, 1979, 52: 2569-2573.

4. Milan Smisek and Slavoj Cerny, Active Carbon: Manufacture, Properties and Application, Elsevier Publishing Company, New York, 1970.

5. Urano Kohei, Shigeaki Omori, and Eui Yamamoto, "Predictive Methods for Adsorption Capacities of Commercial Activated Carbons in Removal of Organic Vapors." Environ Sci. Technol., 1982, 16: 10-14.

6. Grubner. Otto and William Burgess, "Simplified Description of Adsorption Breakthrough Curves in Air Cleaning and Sampling Devices," Am. Ind. Hyg. Assoc. J., 1979, 40: 169-179.

7. Grubner, Otto and William Burgess, "Calculation of Adsorption Breakthrough Curves in Air Cleaning and Sampling Devices," Environ. Sci Technol., 1981. 15: 1346-1351.

8. Grubner. Otto and Dwight W. Underhill, "Calculation of Adsorption Bed Capacity by the Theory of Statistical Moments," Separation Science, 1970, 5: 555-582.

1984 USAF-SCEEE SUMMER FACULTY RESEARCH PROGRAM

sponsored by the

AIR FORCE OFFICE OF SCIENTIFIC RESEARCH

Conducted by the

SOUTHEASTERN CENTER FOR ELECTRICAL ENGINEERING EDUCATION

FINAL REPORT

A COMPARATIVE ANALYSIS OF WHISPERED AND NORMALLY
PHONATED SPEECH USING AN LPC-10 VOCODER

Prepared by:	Dr. Johnny R. Wilson
Academic Rank:	Associate Professor
Department and University:	Department of Speech and Hearing South Carolina State College
Research Location: Division:	Rome Air Development Center Intelligence, Reconnaissance and Analysis
USAF Research:	Dr. James Mosko
Date:	November 8, 1984
Contract No:	

A COMPARATIVE ANALYSIS OF WHISPERED AND NORMALLY PHONATED SPEECH USING AN LPC-10 VOCODER

by

Johnny R. Wilson

ABSTRACT

The determination of the performance of the LPC-10 Vocoder in the processing of adult male and female whispered and normally phonated connected speech was the focus of this study. It was found that the LPC-10 Vocoder's analysis of whispered speech compared quite favorably with similar studies which used sound spectrographic processing techniques. It was also found that shifting from phonated speech quality to whispered speech quality caused a substantial increase in the phonemic formant frequencies and formant bandwidths for both male and female speakers.

The data from this study showed no evidence that the LPC-10 Vocoder's ability to process voices with pitch extremes and quality extremes was limited in any significant manner. A comparison of the unprocessed natural vowel waveforms and qualities with the synthesized vowel waveforms and qualities revealed almost imperceptible differences.

It was recommended that an investigation of the LPC-10 Vocoder's ability to process linguistic and dialectical suprasegmental features such as intonation, rate and stress at low bit rates should be a critical issue of concern for future research.

Acknowledgement

I. INTRODUCTION

The determination of the most efficacious method of transmitting speech signals in narrowband form has been a major focus of speech researchers and communications engineers dating back as far as 1928 when Homer Dudley introduced a device called a "vocoder"[1]. The development of efficient speech coding methods continues to be an area of critical concern, especially for the Air Force, because the ability to manipulate speech signals over communications transmission channels through efficient and versatile coding procedures would greatly enhance air-to-air and air-to-ground reconnaissance and surveillance.

Significant advancements have been made in speech coding technology since Dudley's prototype vocoder. Moreover, the narrowband linear predictive coding (LPC) technique has become widely used in both civilian and military applications[2]. However, in spite of its recent widespread use, in spite of the many improvements made in it and in spite of its adoption as the military standard, the LPC vocoder still has not undergone a systematic and comprehensive evaluation for general and practical applications.

The present project was designed to test the LPC-10 Vocoder's performance during the processing of speakers whose voices represent vocal extremes in respect to pitch and quality. The impetus for this study emanated from the following general hypotheses and findings that were reported in recent signal and speech transmissions literature:

1. A speaker's voice quality has a clear effect on the subsequent LPC quality[3].

2. The efficacy of LPC analysis has been shown to be dependent on the fundamental frequency of the voiced signal[4].

3. Narrowband LPC notoriously lacks robustness[5].

4. LPC has difficulties with the voices of women and children[6].

5. The presence of whisper and nasality has a negative influence on intelligibility for both male and female LPC quality[7].

150-4

Although a few studies have examined the performance of
LPC vocoders for design purposes, their "robustness", i.e.
their ability to process a variety of voice types and speaking
styles during practical user applications is yet to be de-
termined. Information pertaining to the robustness of LPC
vocoders is of utmost importance to signal transmissions
personnel and to communications engineers becasue such in-
formation should aid in continued development and improvement
of speaker independent speech recognition technology.

II. OBJECTIVES

The overall objective of the present project was to
determine the robustness of the LPC-10 Vocoder by assessing
its ability to process voices with pitch and quality extremes.
The specific objectives were:

> 1. To evaluate the ability of the LPC-10 Vocoder
> to process phonated and whispered speech.
>
> 2. To evaluate the ability of the LPC-10 Vocoder
> to process voices representing different sexes,
> i.e. voices with fundamental frequency and for-
> mant frequency extremes.
>
> 3. To determine the acoustic characteristics, i.e.
> the formant frequencies, formant bandwidths and
> formant amplitudes of male and female phonated
> and whispered vowels during connected speech.

Whispered and phonated voice characteristics were selected
as the focus of this study because (1) they represent two
extremes of voice production or laryngeal activity[8], (2)one
of the concomitants of human fatigue is dysphonia which may
range from partial to complete loss of voice and (3) previous
research has indicated that the formant frequencies of whispered
isolated vowels are higher than those of phonated isolated
vowels[9]. Male and female voices were used because it is
commonly known that the habitual pitch for female voices
is almost twice the habitual pitch for male voices.

The LPC technique was of particular concern to this
study because, as pointed out earlier, it has been adopted
as the military standard. Purportedly, this technique is

especially attractive to military communications personnel because (1) only a short segment of speech is needed to yield accurate results, (2) it is suitable for analyzing high pitched voices, such as women and children, and (3) data rate can be reduced to approximately 2400 bits/sec. without producing degradation in speech quality[10].

III. METHOD

Subjects

Seven young adult males and four young adult females who demonstrated normal speech and hearing characteristics produced the speech samples for this study. Their ages ranged from 19-32 years and 17-24 years, respectively. The mean age for males was 23.6 years and the mean age for females was 21.3 years. All of the subjects grew up in the northeastern region of the United States and spoke primarily General American English dialect.

Speech Sample

Each of the 11 subjects was instructed to first normally phonate a list of five sentences and secondly to whisper the same list. Embedded in each of the five stimulus sentences was an "h_d" word in which were embedded the experimental vowels: /i/, /æ/, /u/, /ɑ/ and /ʌ/ (see Figure 1).

These particular vowels were selected because they represent essentially the cardinal or articulatory extremes for English vowel production (see Figure 3).

Instrumentation

The LPC-10 Vocoder was the speech processing device used in the present study. The LPC-10 is a time-domain device that analyzes and synthesizes speech using the principles of linear predictive coding. Linear predictive coding is a speech modeling technique which approximates a given speech signal as a linear combination of past samples of a hypothetical input to a system whose output is the given speech signal. The predictor coefficients which become the parameters of the digital analysis filter are determined by minimizing the squared differences between the actual

speech samples and the linearly predicted ones.

Since the vocoder analyzes a given speech sample before
it reconstructs it from the analysis data, it is possible
to remove information redundancy or to compress a speech
sample if desired.

It should be noted that device used in the present
study was computer simulation of the LPC-10 Vocoder. For
testing purposes, the computer simulated version of the
vocoder actually allowed more flexibility.

Recording Procedure

Each of the subject's speech samples was stored by
recording them on a Uher Model 4000 Report IC reel-to-reel
magnetic tape recorder while each subject was seated in
an IAC sound attenuating booth. Each subject was allowed
to practice the list of sentences under the whispered and
phonated conditions until he felt comfortable with his pro-
ductions. An Uher Model M518 Dynamic Microphone was positioned
5 inches in front of each subject's mouth, slightly below
the level of the lips during the recording of the samples.
Any samples that the investigator judged as faulty during
his monitoring of the recording sessions were repeated by
the subject until an acceptable sample was produced.

Analysis Procedure

Prior to analyzing the speech samples, each of the
vowel embedded words was isolated from the carrier sentences
by mechanical hand splicing. One foot of leader tape was
spliced onto each side of each of the vowel-embedded words
so that the vowel samples could be fed continuously into
the computer during analysis. During the splicing procedure,
the phonated and whispered productions of a given vowel
were paired so that they could be subsequently analyzed
and displayed together.

Thus each of the 11 subjects had a total of 5 pairs
of vowel-embedded words which were fed from the tape recorder
output directly into the analog-to-digital preprocessor
(see Figure 2). For example, a phonated /i/ and a whispered
/i/ were digitized and analyzed together, and so on.

The digitalization process consisted of low pass filtering each of the sample pairs at 5000 Hz with a sampling rate of 10000 Hz. Once the sample pairs were digitized, they were stored on a disk as a sampled data file or primary file.

At this point, the linear predictive coding analysis phase was initiated by giving the computer the API command which instructed the simulated vocoder to analyze and model the spectral characteristics of the input data (the digitized sample pair in the sampled data file) using the linear predictive coding method. In addition, the excitation or fundamental frequency status was determined using a modified cepstral processing technique.

Upon completion of the LPC analysis via the API execution, the analysis data was stored on a disk and designated as the secondary file or analysis file. From the analysis file, a variety of acoustic parameters could be extracted (see Figure 2) once the appropriate command was given.

The first data analysis output program was the speech spectrogram (SGM). This program computed a frequency spectrum at specified points in time of the speech samples by performing a Fast Fourier Transform (FFT) on the coefficients that were determined during the LPC analysis. When SGM was completed, the formant frequencies, formant bandwidths and formant amplitudes became available in the analysis file.

Following the SGM program, a Formant Tracking (FTR) program was executed which essentially provided a trace of the formant trajectories on the previously completed digital spectrogram (see Figure 5).

At this point, the fundamental frequency, formant frequency, formant amplitude and formant bandwidth data were printed out by activating the Interactive Editing (IAE) mode. Thus for each of the speech samples, the fundamental frequencies, formant frequencies, formant bandwidths, and formant amplitudes were printed out for 8 frames or points in time (duration of each frame=6.4 ms) from the center of each of the vowel samples.

From the analysis data file, three additional graphic displays of the phonated and whispered speech samples were

produced: SP1 (Spectral Plot), PPL (Frequency Plot), PDI
(Raw Spectral Plot) and VTR (Vocal Tract Plot). Examples
of these displays may be observed in Figures 6-10, respective-
ly. The SPL display is a three-dimensional plot of formant
frequency and amplitude as functions of time. The PPL display
is essentially the same as the SPL display with the exception
that the spectrum of each frame is displayed separately
which allows a more detailed observation of formant frequency
and amplitude variations over time. The PDI display is
a raw spectral display of the harmonics as well as the for-
mants for a selected segment of a given sample. A smoothing
curve (SSP) may be superimposed on the raw spectrum to show
actual formant peaks and peak amplitudes.

The VTR display shows the vocal tract configurations
that produced the various formant frequencies at specific
points in time.

V. RESULTS

Twenty (20) phonated and 20 whispered speech samples
were identified as meeting the target vowel productions
for the female subjects while 35 phonated and 35 whispered
samples were identified as meeting the target vowel produc-
tions for the male subjects. Thus 40 adult female vowels
and 70 adult male vowels taken from connected speech provided
the analysis data for this study. The mean values obtained
from the LPC acoustic analyses are tabulated in Tables 1-9.
Males

An observation of the data in Table 1 indicates that
Formant 1 is higher in frequency for all five vowels when
they are whispered than when they are phonated. Formant
1 for the whispered vowels was on the average 147 Hz higher
than Formant 1 for the phonated vowels.

Table 2 indicates that the Formant 1 bandwidths followed
a similar trend. The Formant 1 bandwidths for the whispered
vowels were on the average 59 Hz wider than the Formant
1 bandwidths for the phonated vowels.

The Formant 1 amplitudes followed a reverse trend as can be observed in Table 3. The Formant 1 amplitudes were on the average 9 dB greater in magnitude for the phonated vowels than for the whispered vowels. However, Table 3 also indicates that there was a shift in energy towards Formant 3 for the whispered vowels wherein most of the spectral energy was concentrated at Formants 1 and 2 for the phonated vowels. The Formant 3 amplitudes are on the average 2 dB greater in magnitude for the whispered vowels than Formant 3 for the phonated vowels. It may also be observed that Formants 1, 2 and 4 amplitudes were greater for the phonated vowels for the male speakers. One of the more salient differences between phonated and whispered vowels then was the shift of spectral energy towards Formant 3 for whispered vowels. Figures 6, 7 and 10 provide graphic examples of this trend.

The same trends that were reported for Formant 1 center frequencies for phonated and whispered vowels may be observed for Formants 2, 3 and 4. Formants 2, 3 and 4 for the vowel /i/, however, were higher in frequency for the phonated vowels than for the whispered vowels.

No discernible pattern of difference can be observed for Formants 2, 3 and 4 bandwidths, although the Formant 2 bandwidths were wider for all of the whispered vowels than for the corresponding phonated vowels with the exception of the vowel /u/ (see Table 2).

Table 3 indicates further that all of the formant amplitudes were greater for the phonated vowels except for the Formant 3 amplitudes. As was noted earlier, the majority of the spectral energy was concentrated at Formant 3 for the whispered vowels.

It can also be observed in Table 1 that the mean fundamental frequency (F_0) for the male phonated vowels was 126 Hz while the mean F_0 for the whispered vowels was 0 Hz. The 0 values for the whispered vowels verified that indeed the whispered vowels were not voiced or phonated (Whisper is defined as the production of normally phonated sounds without voice[11]). The 126 Hz mean F_0 is also very close

to the normative value given in the literature for adult
male habitual pitch.

Females

An examination of Table 4 indicates that the mean Formant
1 frequencies for females were on the average 167 Hz higher
for the whispered vowels than for the phonated vowels. The
same trend was observed earlier for the male subjects.

Table 5 indicates that the Formant 1 and 2 bandwidths
were wider for the whispered than for the phonated /i/,
/u/ and /ɑ/ while the opposite trend for the vowels /æ/
and /ʌ/ is indicated. The Formant 1 bandwidths were on
the average 57 Hz wider for the whispered vowels than for
the phonated vowels while the Formant 2 bandwidths were
on the average 96 Hz wider.

As was observed with the male speakers, Formant
2 center frequencies were higher for all of the whispered
vowels than for the phonated vowels with the exception of
the vowel /i/ (see Table 4). No discernible pattern of
difference was observed for Formants 3 and 4 center frequen-
cies, bandwidths and amplitudes.

Table 4 shows that the mean fundamental frequency for
the female phonated vowels was 217 Hz and the mean F_O for
the whispered vowels was 0. As was pointed out for the
males, the 0 Hz F_O for the female whispered vowels verified
by definition that the female whispered vowels lacked voice.

The 217 Hz mean F_O is almost identical with the 220
Hz normative habitual pitch that is commonly reported in
the literature for young adult females.

VI. DISCUSSION AND CONCLUSIONS

A comparison of the male and female phonated and whispered
vowel spectra as produced by the LPC-10 Vocoder indicated
that for all of the experimental vowels, Formant 1 center
frequencies were higher under the whispered condition than
under the phonated condition. The actual mean differences
were 147 Hz and 167 Hz for the males and females, respectively.
The identical finding was reported by Kallail and Emanuel

(1984). However, the present study used male and fer...e vowels in connected speech wherein the Kallail and Emanuel study used female vowels only spoken in isolation.

The increased Formant 1 center frequency for whispered vowels can probably be attributed to greater vertical tongue constriction that is used when producing whispered vowels. Figures 7 and 8 provide graphic evidence of greater tongue height and greater constriction in the pharyngeal area for whispered vowels than for phonated vowels. It is well known that vowel Formant 1 center frequency is associated with movements of the tongue within the vertical plane of the oral cavity. It is also well known that the frequency of Formant 1 is raised by constriction of the pharynx[12].

A comparison of the adult male phonated vowel formants with those reported by Peterson and Barney[13](P & B) and Fairbanks and Grubbs[14] indicates very close agreement (see Table 7). The mean differences between the Peterson and Barney male Formant 1, 2 and 3 frequencies and the LPC-10 male phonated Formant 1, 2 and 3 frequencies were 45 Hz, 116 Hz and 53 Hz, respectively.

Similarly, Table 8 shows that adult female phonated vowel formants compared quite favorably with the adult female formants reported by Peterson and Barney. The mean differences between the P & B adult female Formant 1 frequencies and the LPC adult female phonated Formant 1 frequencies were 71 Hz, 125 Hz and 220 Hz, respectively.

These results would suggest that the linear predictive coding fundamental frequency and formant frequency extraction techniques are quite adequate when compared with the data obtained from conventional sound spectrographic techniques. It should be pointed out however that the adult females' Formant 3 values as reported by the present study and those reported by Peterson and Barney are different enough to suggest some measurement disparity. The present data did not permit the specification of the direction of the disparity.

In an effort to assess the LPC vocoder's ability to process whispered speech, the LPC measured whispered vowel formants as produced by adult females were compared to the

female whispered vowel formants reported by Kallail and
Emanuel (K & E) which were measured with the sound spectro-
graph. These data are presented in Table 9. It can be
observed that the mean differences between LPC measured
whispered Formants 1,2 and 3 and the spectrographic whis-
pered Formants 1,2 and 3 were 89 Hz, 283 Hz and 311 Hz,
respectively. Although these results compare favorably,
all of the vowel Formant 3 values measured with the sound
spectrograph were higher than the Formant 3 values that
were obtained with the LPC vocoder. A similar result was
noticed earlier when the Peterson and Barney female Formant
3 values were compared with the LPC Formant 3 values.
This trend suggests that one of the two measurement tech-
niques understimated or over estimated Formant 3 center
frequency values. Additional research is needed to clarify
this issue more definitively.

In summary, the data obtained from this study suggests
the following:

1. The LPC-10 Vocoder's performance in pro-
cessing whispered and phonated speech when
compared with conventional sound spectro-
graphic techniques measured up quite favora-
bly for the first two formants in adult male
and female speakers. The LPC vocoder's abili-
ty to process the higher formants needs further
research.

2. The LPC-10 Vocoder processed voices with
pitch extremes quite well. Its fundamental
frequency tracking precision compared very
closely with previously reported spectrographic
data for male and female vowels.

3. The most salient acoustic difference between
phonated and whispered vowels in connected
speech was an increase in the frequency of
the first three formants, the greatest increase
occurring at Formant 1 for males and females.

4. Whispered vowels had wider formant bandwidths
than phonated vowels for male and female spoken
vowels.

5. For phonated vowels, most of the spectral
energy was concentrated at the first two formants
for males and females while the majority of
the spectral energy shifted from the lower two

150-13

formants to the Formant 3 area for male and female whispered vowels.

6. The LPC-10 Vocoder's synthesized phonated and whispered vowel waveforms and qualities and the unprocessed phonated and whispered vowel waveforms were barely discernible, although the difference between the synthesized and unprocessed whispered vowel waveforms and qualities were slightly more noticeable than the differences between the unprocessed and synthesized phonated vowel waveforms and qualities (see Figure 11).

VII. RECOMMENDATIONS

Although the results of the LPC-10 Vocoder's processing of phonated and whispered speech and the data obtained from previous spectrographic analysis compared rather well, there is still a need for further research which systematically tests the LPC vocoder's ability to process more intermediate qualities such as nasality, harshness, stridency, etc.

It would also be extremely important to determine the influence of dialectal differences (regional and foreign) on the processing ability of the LPC-10 Vocoder. There is a dearth of research relative to this issue.

Finally, there is a need for research to study the influence of various suprasegmental or prosodic speech features such as intonation, rate and duration on LPC vocoding at different bit rates, particularly at 2400 bits/second and lower.

PHONATED

1. The syllable <u>heed</u> is the word.

2. The syllable <u>had</u> is the word.

3. The syllable <u>who'd</u> is the word.

4. The syllable <u>hod</u> is the word.

5. The syllable <u>hud</u> is the word.

WHISPERED

1. The syllable <u>heed</u> is the word.

2. The syllable <u>had</u> is the word.

3. The syllable <u>who'd</u> is the word.

4. The syllable <u>hod</u> is the word.

5. The syllable <u>hud</u> is the word.

Figure 1. The stimulus material used by each of the 11 subjects to produce the experimental vowel samples. Each of the vowels were produced with the same consonantal environment while the vowel embedded words were contained in the same carrier sentences.
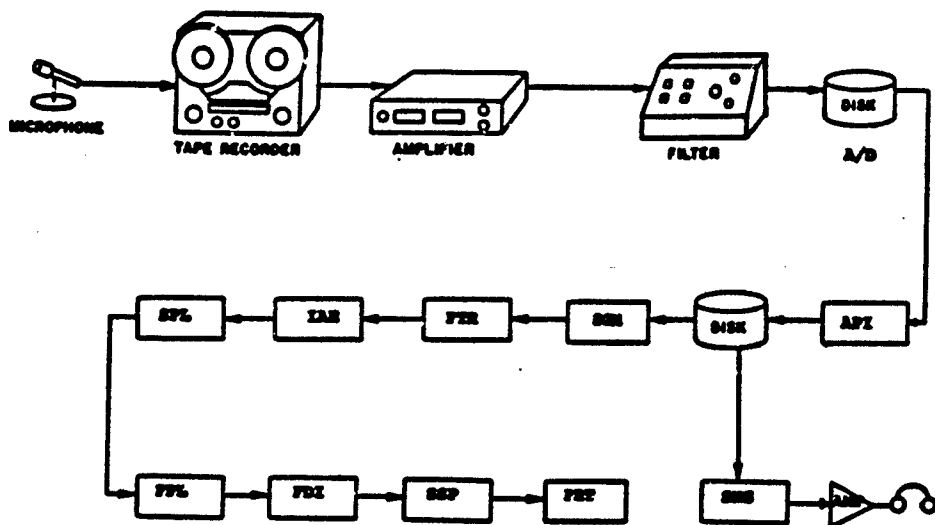
Figure 2. Block diagram of the computer simulation of the LPC-10 Vocoder used to analyze and synthesize the phonated and whispered speech samples.
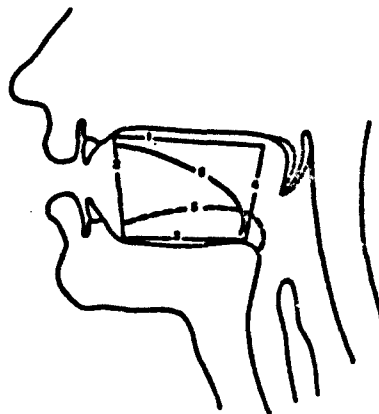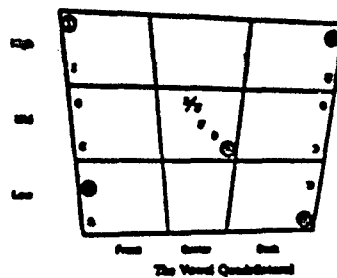
Figure 3. A diagram of the relative tongue positions in the oral cavity used in the General American English production of the five (5) experimental vowels: /i/,/æ/,/u/,/U/,/ʌ/.
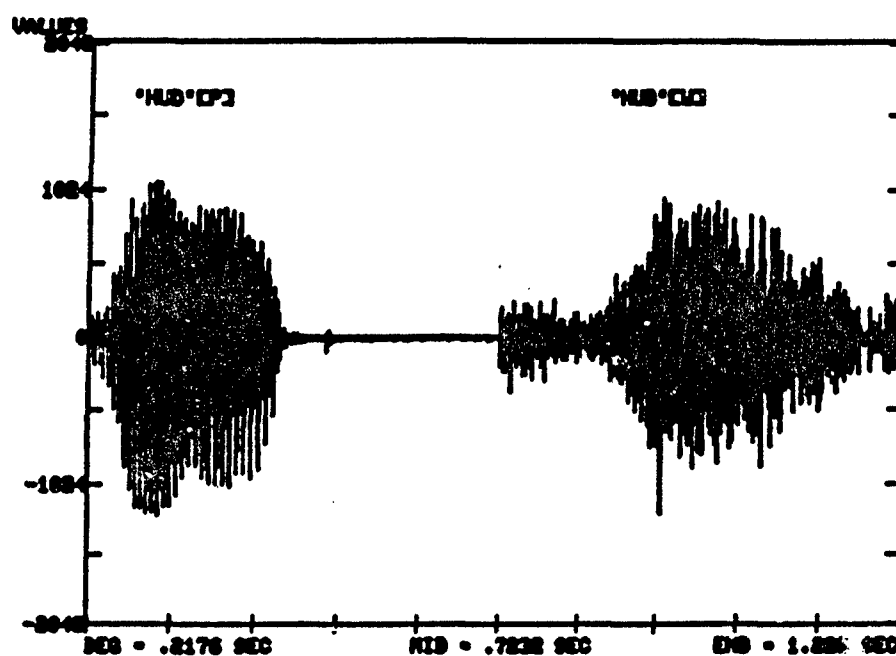
Figure 4. An oscillographic display of an adult male's production of a phonated [P] and whispered [W] vowel /ʌ/ prior to LPC processing. Note that the vowel is embedded in the word "Hud".
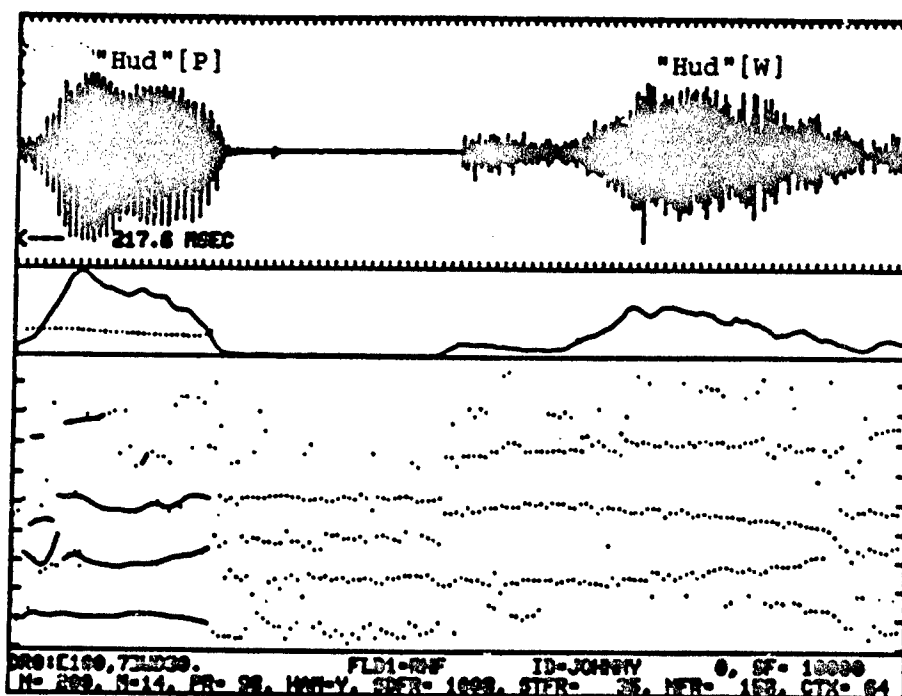
Figure 5. A digital spectrogram [SGM] with formant tracking [FTR] for an adult male speaker's production of a phonated [P] and whispered [W] vowel /ʌ/ embedded in the word "Hud".
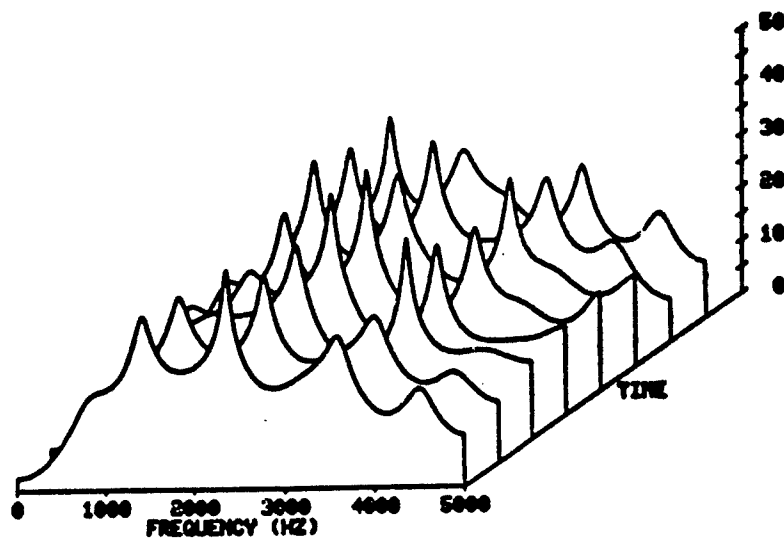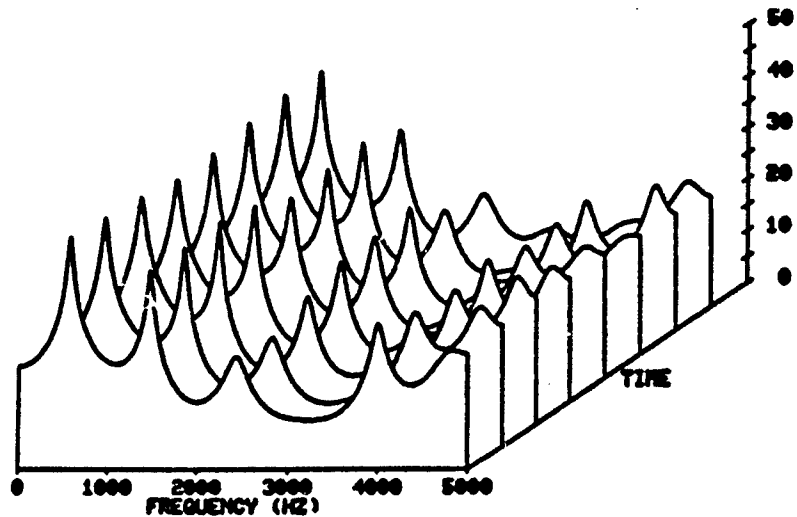
Figure 6. A 3-dimensional plot [SPL] of 8 frames of formant frequency and amplitude as a function of time for an adult male's (a)phonated and (b)whispered production of the vowel /ʌ/.
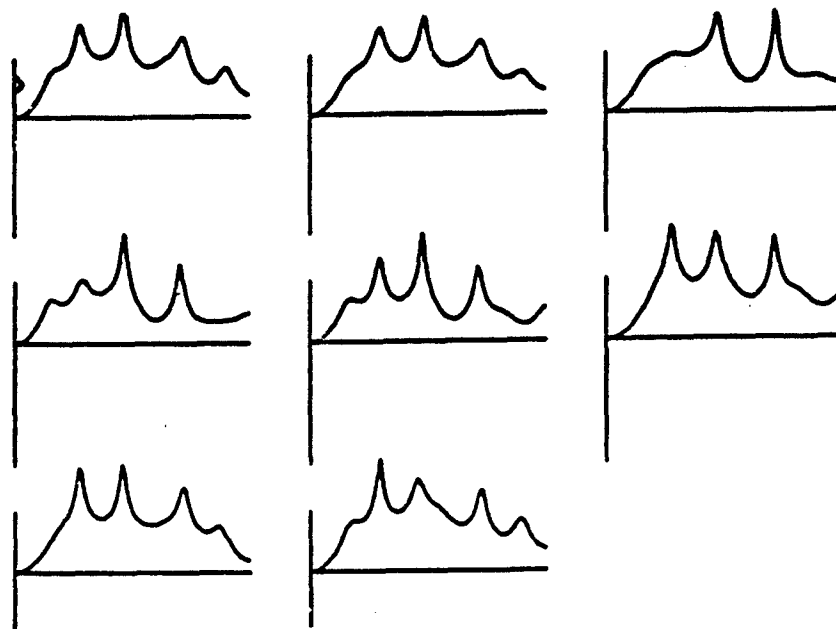
(b)
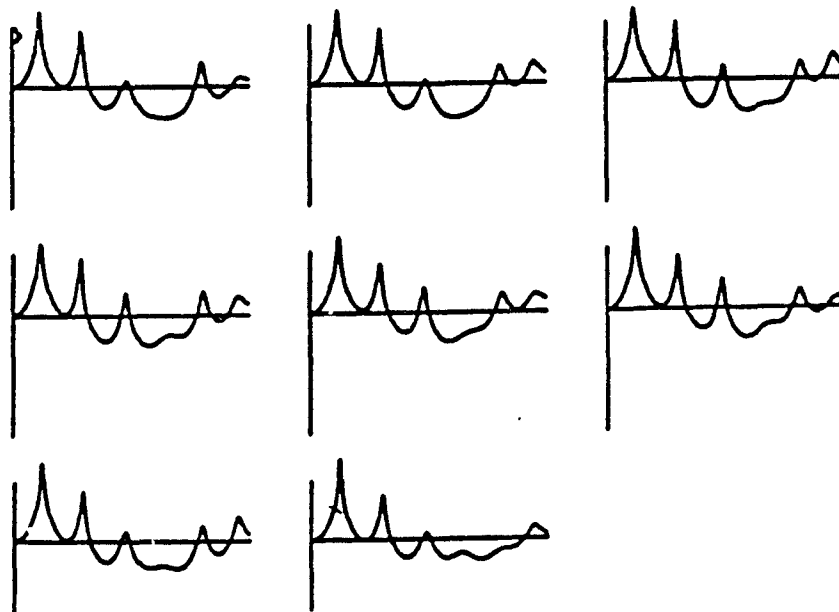
(a)

Figure 7. Frequency plot (FPL) of 8 frames of an adult male
speaker's spectral tilt variations during the production of
(a) phonated /ʌ/ and /b/ whispered /ʌ/.

150-21
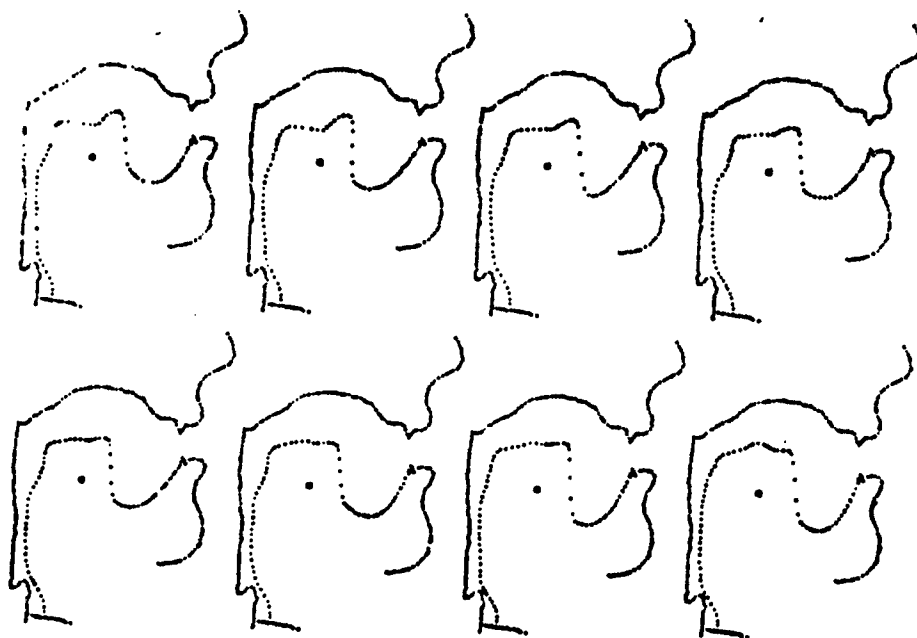
Figure 8. The vocal tract [VTR] configurations over 8 frames during an adult male's phonated production of the vowel /ʌ/.
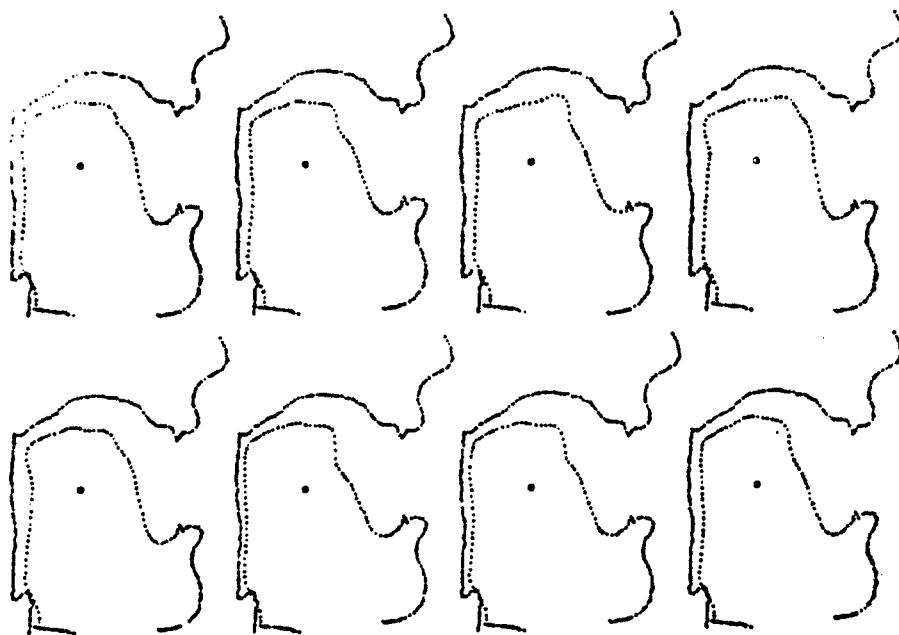
Figure 9. The vocal tract (VTR) configurations over eight frames during an adult male's whispered production of the vowel /ʌ/.
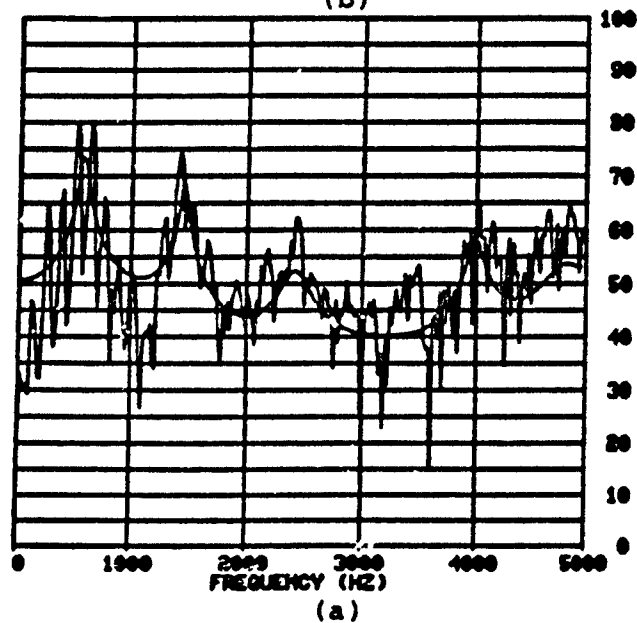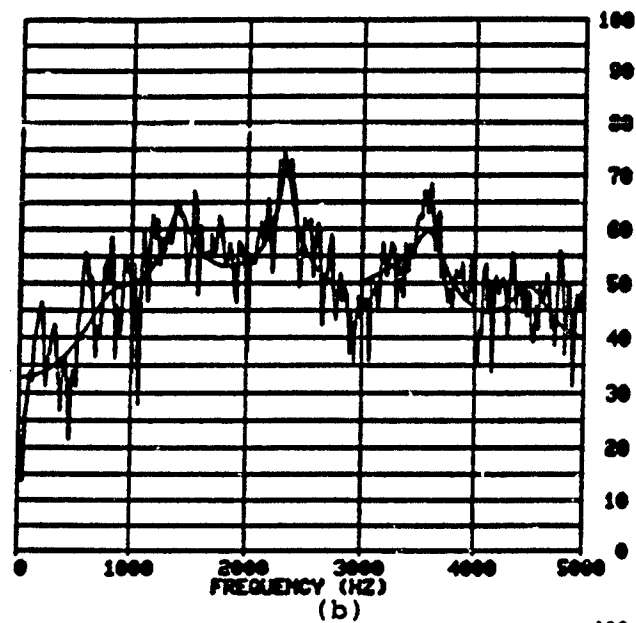
Figure 10. An FFT raw spectrum (FDI) and smooth spectrum (SSP) of an adult male's (a) phonated and (b) whispered production of the vowel /ʌ/.
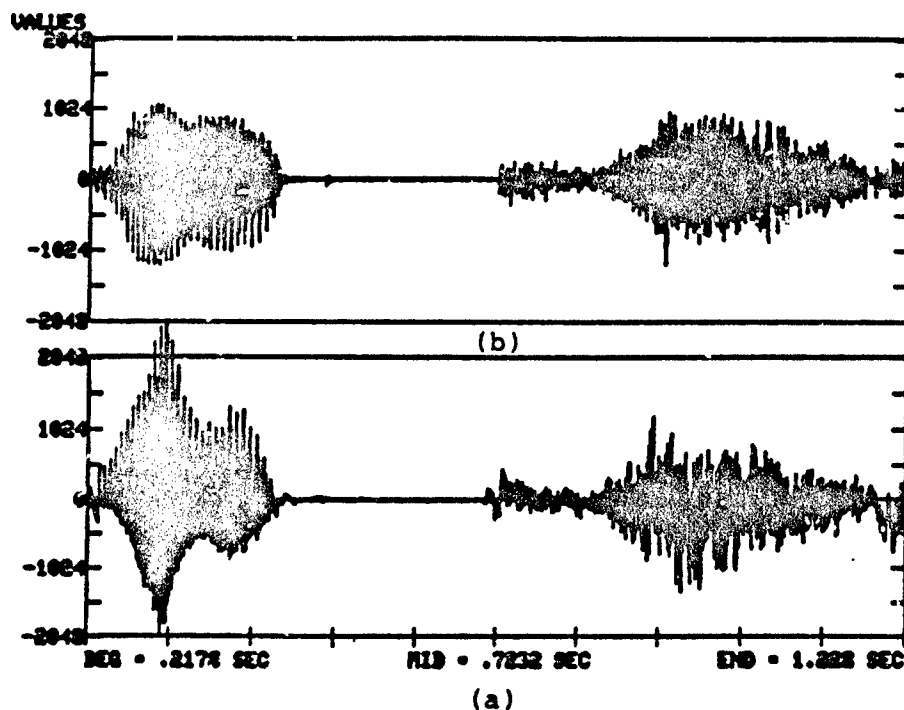
Figure 11. An oscillographic display of an adult male's
(a) natural production of the phonated and whispered vowel
/ʌ/ and (b) the synthesized waveform of the adult male's
production of the phonated and whispered vowel /ʌ/.

Table 1. Average formant frequency and fundamental frequency values for male phonated and whispered productions of the experimental vowels. Standard deviations are given in parentheses below each of the mean values. Negative differences indicate that the whispered values are larger than the phonated values.

n=7		*F1	F2	F3	F4	F₀	
PHONATED	X̄	337	2341	3045	3797	132	[1]
	S.D.	(34)	(153)	(285)	(369)	(18)	
WHISPERED	X̄	458	2061	2945	3585	0	
	S.D.	(98)	(392)	(230)	(227)		
DIFFERENCE		-121	280	100	212	132	

PHONATED	X̄	620	1753	2495	3613	123	[æ]
	S.D.	(41)	(262)	(209)	(213)	(13)	
WHISPERED	X̄	779	1869	2624	3655	0	
	S.D.	(108)	(208)	(272)	(431)		
DIFFERENCE		-159	-116	-129	-42	123	

PHONATED	X̄	359	983	2250	3366	135	[u]
	S.D.	(35)	(150)	(206)	(291)	(14)	
WHISPERED	X̄	419	1125	2478	3419	0	
	S.D.	(155)	(147)	(156)	(188)		
DIFFERENCE		-60	-142	-228	-53	135	

PHONATED	X̄	721	1325	2431	3517	116	[ɑ]
	S.D.	(78)	(190)	(147)	(335)	(10)	
WHISPERED	X̄	905	1518	2461	3610	0	
	S.D.	(76)	(141)	(169)	(186)		
DIFFERENCE		-184	-193	-30	-93	116	

PHONATED	X̄	588	1340	2517	3587	123	[ʌ]
	S.D.	(35)	(96)	(158)	(181)	(10)	
WHISPERED	X̄	799	1418	2565	3609	0	
	S.D.	(52)	(114)	(205)	(291)		
DIFFERENCE		-211	-78	-48	-22	123	

F1=Formant 1   F3=Formant 3
F2=Formant 2   F4=Formant 4
F₀=Fundamental Frequency

*All formant and fundamental frequency values are in Hertz (Hz).

150-26

Table 2. Average formant bandwidth values for male phonated and whispered productions of the experimental vowels. Standard deviations are given in parentheses below each of the mean values. Negative differences indicate that the whispered values are greater than the phonated values.

n=7		*B1	B2	B3	B4	
PHONATED	X̄	138	158	251	270	[i]
	S.D.	(19)	(22)	(57)	(111)	
WHISPERED	X̄	237	262	246	300	
	S.D.	(65)	(102)	(83)	(51)	
DIFFERENCE		-99	-104	5	-30	

		*B1	B2	B3	B4	
PHONATED	X̄	142	167	223	248	[æ]
	S.D.	(22)	(63)	(64)	(82)	
WHISPERED	X̄	170	232	235	292	
	S.D.	(43)	(107)	(68)	(67)	
DIFFERENCE		-28	-65	-12	-44	

		*B1	B2	B3	B4	
PHONATED	X̄	130	181	248	355	[u]
	S.D.	(15)	(39)	(108)	(183)	
WHISPERED	X̄	232	179	295	246	
	S.D.	(73)	(39)	(152)	(79)	
DIFFERENCE		-102	2	-47	109	

		*B1	B2	B3	B4	
PHONATED	X̄	144	190	226	347	[a]
	S.D.	(15)	(68)	(103)	(120)	
WHISPERED	X̄	171	193	207	294	
	S.D.	(24)	(28)	(58)	(73)	
DIFFERENCE		-27	-3	19	53	

		*B1	B2	B3	B4	
PHONATED	X̄	132	197	203	298	[ʌ]
	S.D.	(6)	(71)	(60)	(131)	
WHISPERED	X̄	171	210	187	238	
	S.D.	(19)	(40)	(45)	(69)	
DIFFERENCE		-39	-13	16	60	

B1=Bandwidth 1   B3=Bandwidth 3
B2=Bandwidth 2   B4=Bandwidth 4

*All bandwidth values are in Hertz (Hz).

150-27

Table 3. Average formant amplitude values for male phonated and whispered productions of the experimental vowels. Standard deviations are given in parentheses below each of the mean values. Negative differences indicate that the whispered values are greater than the phonated values.

n=7		*A1	A2	A3	A4	
PHONATED	X̄	18	14	11	11	
	S.D.	(5)	(2)	(4)	(4)	[1]
WHISPERED	X̄	10	13	12	10	
	S.D.	(4)	(3)	(6)	(3)	
DIFFERENCE		8	1	-1	1	

PHONATED	X̄	19	15	10	9	
	S.D.	(4)	(3)	(2)	(3)	[æ]
WHISPERED	X̄	11	14	13	6	
	S.D.	(3)	(2)	(3)	(2)	
DIFFERENCE		8	1	-3	2	

PHONATED	X̄	23	16	8	8	
	S.D.	(9)	(3)	(3)	(2)	[u]
WHISPERED	X̄	14	15	8	8	
	S.D.	(6)	(3)	(2)	(2)	
DIFFERENCE		9	1	0	0	

PHONATED	X̄	24	17	8	8	
	S.D.	(4)	(5)	(3)	(3)	[ɑ]
WHISPERED	X̄	13	16	11	7	
	S.D.	(5)	(4)	(5)	(2)	
DIFFERENCE		11	1	-3	1	

PHONATED	X̄	23	14	8	8	
	S.D.	(2)	(3)	(2)	(2)	[ʌ]
WHISPERED	X̄	12	12	10	7	
	S.D.	(3)	(2)	(3)	(3)	
DIFFERENCE		11	2	-2	1	

A1=Amplitude 1   A3=Amplitude 3
A2=Amplitude 2   A4=Amplitude 4

*A1, amplitude values are in decibels (dB).

150-28

Table 4. Average formant frequency and fundamental frequency values for female phonated and whispered productions of the experimental vowels. Standard deviations are given in parentheses below each of the mean values. Negative differences indicate that the whispered values are greater than the phonated values.

n=4		*F1	F2	F3	F4	F₀	
PHONATED	X̄	386	2787	3592	4020	226	[i]
	S.D.	(104)	(305)	(415)	(643)	(25)	
WHISPERED	X̄	570	1640	2789	3537	0	
	S.D.	(107)	(376)	(273)	(161)		
DIFFERENCE		-184	1147	803	483	226	

PHONATED	X̄	773	1936	2804	3681	209	[æ]
	S.D.	(70)	(209)	(114)	(427)	(18)	
WHISPERED	X̄	896	2034	2889	3702	0	
	S.D.	(87)	(334)	(345)	(319)		
DIFFERENCE		-123	-98	-85	-21	209	

PHONATED	X̄	432	1164	2434	3725	231	[u]
	S.D.	(46)	(319)	(187)	(243)	(23)	
WHISPERED	X̄	526	1294	2536	3597	0	
	S.D.	(155)	(215)	(240)	(194)		
DIFFERENCE		-94	-130	-102	128	231	

PHONATED	X̄	842	1442	2778	3864	201	[ɑ]
	S.D.	(43)	(232)	(209)	(206)	(16)	
WHISPERED	X̄	999	1557	2561	3541	0	
	S.D.	(62)	(76)	(76)	(255)		
DIFFERENCE		-157	-115	217	323	201	

PHONATED	X̄	662	1321	2276	3273	218	[ʌ]
	S.D.	(89)	(421)	(609)	(660)	(18)	
WHISPERED	X̄	941	1627	2676	3712	0	
	S.D.	(42)	(214)	(415)	(365)		
DIFFERENCE		-279	-306	-400	-439	218	

F1=Formant 1   F3=Formant 3
F2=Formant 2   F4=Formant 4
F₀=Fundamental Frequency

*All formant and fundamental frequency values are in Hertz (Hz).

150-29

Table 5. Average formant bandwidth values for female phonated and whispered productions of the experimental vowels. Standard deviations are given in parentheses below each of the mean values. Negative differences indicate that the whispered values are greater than the phonated values.

n=4		*B1	B2	B3	B4	
PHONATED	X̄	132	172	348	228	[i]
	S.D.	(15)	(70)	(205)	(91)	
WHISPERED	X̄	208	462	235	229	
	S.D.	(40)	(50)	(51)	(18)	
DIFFERENCE		-76	-290	113	-1	
PHONATED	X̄	174	237	191	351	[æ]
	S.D.	(46)	(109)	(44)	(56)	
WHISPERED	X̄	171	269	227	350	
	S.D.	(30)	(51)	(35)	(97)	
DIFFERENCE		3	-32	-36	1	
PHONATED	X̄	122	167	344	245	[u]
	S.D.	(7)	(20)	(142)	(110)	
WHISPERED	X̄	261	213	371	348	
	S.D.	(104)	(74)	(14)	(81)	
DIFFERENCE		-139	-46	-27	-103	
PHONATED	X̄	177	203	347	395	[a]
	S.D.	(34)	(71)	(128)	(196)	
WHISPERED	X̄	230	251	239	267	
	S.D.	(32)	(42)	(20)	(9)	
DIFFERENCE		-53	-48	108	128	
PHONATED	X̄	172	192	182	221	[ʌ]
	S.D.	(57)	(60)	(49)	(45)	
WHISPERED	X̄	159	256	256	240	
	S.D.	(21)	(17)	(29)	(28)	
DIFFERENCE		13	-64	-74	-19	

B1=Bandwidth 1   B3=Bandwidth 3
B2=Bandwidth 2   B4=Bandwidth 4

*All bandwidth values are in Hertz (Hz).

150-30

Table 6. Average formant amplitude values for female phonated and whispered productions of the experimental vowels. Standard deviations are given in parentheses below each of the mean values. Negative differences indicate that the whispered values are greater than the phonated values.

n=4		*A1	A2	A3	A4	
PHONATED	X̄	20	15	11	9	
	S.D.	(8)	(4)	(4)	(7)	[1]
WHISPERED	X̄	7	10	11	13	
	S.D.	(2)	(2)	(1)	(3)	
DIFFERENCE		13	5	0	-4	

PHONATED	X̄	18	13	8	7	
	S.D.	(4)	(6)	(2)	(4)	[æ]
WHISPERED	X̄	15	10	11	6	
	S.D.	(5)	(2)	(3)	(2)	
DIFFERENCE		3	3	-3	1	

PHONATED	X̄	27	14	9	9	
	S.D.	(7)	(5)	(1)	(2)	[u]
WHISPERED	X̄	14	16	6	9	
	S.D.	(5)	(4)	(1)	(1)	
DIFFERENCE		13	-2	3	0	

PHONATED	X̄	20	17	6	8	
	S.D.	(3)	(4)	(4)	(2)	[ɑ]
WHISPERED	X̄	12	14	10	6	
	S.D.	(5)	(2)	(2)	(2)	
DIFFERENCE		8	3	-4	2	

PHONATED	X̄	19	16	10	7	
	S.D.	(3)	(3)	(4)	(2)	[ʌ]
WHISPERED	X̄	18	13	8	5	
	S.D.	(5)	(5)	(3)	(2)	
DIFFERENCE		1	3	2	2	

A1=Amplitude 1 A3=Amplitude 3
A2=Amplitude 2 A4=Amplitude 4

*All amplitude values are in decibels (dB).

150-31

Table 7. The mean formant frequencies and fundamental frequencies for adult male phonated vowels as determined by the LPC vocoder and the mean formant frequencies and fundamental frequencies for adult male vowels reported by Peterson and Barney (P & B) as measured with a sound spectrograph.

		F1	F2	F3	F₀	
LPC	$\bar{X}$ n=7	337	2341	3045	132	
P & B	$\bar{X}$ n=33	270	2290	30..	136	[i]
Difference		67	51	35	-4	

LPC	$\bar{X}$ n=7	620	1753	2495	123	
P & B	$\bar{X}$ n=33	660	1720	2410	127	[æ]
Difference		-40	33	85	-4	

LPC	$\bar{X}$ n=7	359	983	2250	135	
P & B	$\bar{X}$ n=33	300	870	2240	141	[u]
Difference		59	113	10	-6	

LPC	$\bar{X}$ n=7	721	1325	2431	116	
P & B	$\bar{X}$ n=33	730	1090	2440	124	[ɑ]
Difference		-9	235	-9	-8	

LPC	$\bar{X}$ n=7	588	1340	2517	123	
P & B	$\bar{X}$ n=33	640	1190	2390	130	[ʌ]
Difference		-52	150	127	-7	

F1=Formant 1   F3=Formant 3
F2=Formant 2   F₀=Fundamental
                     Frequency

*All formant frequency values are in Hertz (Hz).

Table 8. The mean formant frequencies and fundamental frequencies for adult female phonated vowels as measured with the LPC vocoder and the mean formant frequencies and fundamental frequencies for adult female phonated vowels as reported by Peterson and Barney (P & B) as measured with a sound spectrograph.

		F1	F2	F3	Fo	
LPC	$\bar{X}$	386	2787	3592	226	[i]
P & B	$\bar{X}$	310	2790	3310	235	
Difference		76	-3	282	-9	

LPC	$\bar{X}$	773	1936	2804	209	
P & B	$\bar{X}$	660	2050	2850	210	[æ]
Difference		113	-114	-46	-1	

LPC	$\bar{X}$	432	1164	2434	231	
P & B	$\bar{X}$	370	950	2670	231	[u]
Difference		62	214	-236	0	

LPC	$\bar{X}$	842	1442	2778	201	
P & B	$\bar{X}$	850	1220	2810	212	[a]
Difference		-8	222	-32	-11	

LPC	$\bar{X}$	662	1321	2276	218	
P & B	$\bar{X}$	760	1400	2780	221	[^]
Difference		-98	-79	-504	-3	

F1=Formant 1   F3=Formant 3
F2=Formant 2   F4=Formant 4

*All formant frequency values are in Hertz (Hz).

Table 9. Mean formant frequencies for adult female whispered vowels reported by Kallail and Emanuel (K & E) and the mean formant frequencies for adult female whispered vowels as measured with the LPC vocoder. Negative differences indicate that the LPC values are greater than the K & E values.

		F1	F2	F3	
LPC	$\bar{X}$ n=20	570	1640	2789	
K & E	$\bar{X}$ n=4	423	2778	3232	[i]
Difference		147	-1138	-443	

LPC	$\bar{X}$ n=20	896	2034	2889	
K & E	$\bar{X}$ n=4	1057	2006	2989	[æ]
Difference		-161	28	-100	

LPC	$\bar{X}$ n=20	526	1294	2536	
K & E	$\bar{X}$ n=4	478	1393	2853	[u]
Difference		48	-99	-317	

LPC	$\bar{X}$ n=20	999	1557	2561	
K & E	$\bar{X}$ n=4	1073	1411	2959	[ɑ]
Difference		-74	146	-398	

LPC	$\bar{X}$ n=20	941	1627	2676	
K & E	$\bar{X}$ n=4	956	1624	2971	[ʌ]
Difference		-15	3	-295	

F1=Formant 1   F3=Formant 3
F2=Formant 2   F4=Formant 4

*All formant frequency values are
in Hertz (Hz).

150-34

REFERENCES

1. Schroeder, M. R., "Vocoders: Analysis and Synthesis," *Proc. IEEE*, Vol. 54, pp. 720-734, 1966.

2. Kang, G. S. and Everett, S., "Improvement of the LPC Analysis," *ICASSP*, Boston, pp. 89-92, 1983.

3. Kahn, M. and Garst, P., "The Effects of Five Voice Characteristics on LPC Quality," *ICASSP*, pp. 531-534, 1983.

4. Hermansky, H., H. Fujisak and Sato, Y., "Analysis and Synthesis of Speech Based on Spectral Transform Linear Predictive Method," *ICAASP*, pp. 777-780, 1983.

5. Kang, G. S. and Everett, S., "Improvement of the LPC Analysis," *ICASSP*, Boston, pp. 89-92, 1983.

6. Berney, C. L. and Harshman, C., "Voiceware Does It Differently," *Mini-Micro System*, pp. 1-6, 1982.

7. Kahn, M. and Garst, P., "The Effects of Five Voice Characteristics on LPC Quality," *ICASSP*, pp. 531-534, 1983.

8. Lashley, C. O. *Vibratory Action of the Vocal Folds During Whisper*. Unpublished Master's Thesis, University of Florida, 1984.

9. Kallail, K. J. and Emanuel, F. W. "Formant-Frequency Differences Between Isolated Whispered and Phonated Vowel Samples Produced by Adult Female Subjects," *J. Speech and Hearing Res.*, Vol. 27, pp. 245-251, 1984.

10. Atal, B. S. and Hanauer, S. L., "Speech Analysis and Synthesis by Linear Prediction of the Speech Wave," *J. Acous. Soc. Amer.*, Vol. 50, pp. 637-655, 1971.

11. Lashley, C. O. *Vibratory Action of the Vocal Folds During Whisper*. Unpublished Master's Thesis, University of Florida, 1984.

12. Pickett, J. M., The *Sounds of Speech Communication*. Baltimore, University Park Press, 1980.

13. Peterson, G. E. and Barney, H. L., "Control Methods Used in the Study of Vowels," *J. Acoust. Soc. Amer.*, Vol. 24, pp. 175-184, 1952.

14. Fairbanks, G. and Grubbs, P., "A Psychophysical Investigation of Vowel Formants," *J. Speech and Hearing Dis.*, Vol. 4, pp. 203-219, 1961.

15. Kallail, K. J. and Emanuel, F. W., "Formant-Frequency Differences Between Isolated Whispered and Phonated Vowel Samples Produced by Adult Female Subjects," *J. Speech and Hearing Dis.*, Vol. 27, pp. 245-251, 1984.

1984 USAF - SCEEE Summer Faculty Research Program

Sponsored by the

AIR FORCE OFFICE OF SCIENTIFIC RESEARCH

Conducted by the

SOUTHEASTERN CENTER FOR ELECTRICAL ENGINEERING EDUCATION

FINAL REPORT

COGNITIVE FACTORS IN COMPUTER-AIDED FAULT DIAGNOSIS

Prepared by: Dr. Krystine Batcho Yaworsky

Academic Rank: Associate Professor

Department and   Psychology Department
University: LeMoyne College, Syracuse, NY

Research Location: Air Force Human Resources Laboratory,
                    Logistics and Human Factors Division,
                    Combat Logistics Branch

USAF Research: Dr. William B. Askren

Date: August 10, 1984

Contract No: F49620-82-C-0035

COGNITIVE FACTORS IN COMPUTER-AIDED FAULT DIAGNOSIS

by

Krystine Batcho Yaworsky

ABSTRACT

This report addresses issues concerned with the task of
troubleshooting equipment failures in a context of increasingly more
complex technology and sophisticated computer aids. Based upon a
review of the literature on troubleshooting and human information
processing, principles are suggested as guidelines for the design of
computer aids for fault diagnosis. Such principles follow from an
analysis of the needs of problem solvers for means of coping with
short-term memory constraints, for the activation of a meaningful
context in which information can be understood and retained, and for
mechanisms for retrieving information and distinguishing
between the relevant and the irrelevant. In order to translate
principles of cognitive functioning into design characteristics,
empirical investigation is needed to ensure valid generalizability
from the traditional setting to the computer-aided environment.
Recommendations as to the types of questions which need to be
explored are provided along with examples of relevant research in
the literature. The primary concern underlying all the recommenda-
tions is that the usefulness of specific design features should be
evaluated empirically in experimental designs simulating essential
aspects of the troubleshooting task before considerable investments
in time, effort, and expense are committed to the development of
sophisticated computer aids.

151-2

ACKNOWLEDGEMENTS

The author wishes to thank the Air Force Systems Command, the Air Force Office of Scientific Research, and the Southeastern Center for Electrical Engineering Education for providing her with the opportunity to explore challenging research issues at the Air Force Human Resources Laboratory, Wright-Patterson AFB, Ohio. She would like to acknowledge the Laboratory, in particular the Combat Logistics Branch, for its facilitation of her summer work.

In particular, the author would like to recognize the assistance of Mr. Robert Johnson and Dr. William Askren. Finally, special thanks are extended to Mr. Terry Miller and Dr. William Kane for their encouragement, helpful comments, and productive discussions.

I. INTRODUCTION

As aircraft systems become increasingly more complex, the need for automated aids for maintenance on those systems also increases. However, the adoption of complex automated diagnostic aids will ultimately result in the existence of two complex technologies - the original equipment and the associated diagnostic system. The technician responsible for troubleshooting and repair will then be required to interact not only with the complex equipment, but also with the system designed to aid diagnosis and repair. The role of maintenance personnel will then be multifaceted, including tasks such as implementation of procedures in accordance with instructions from a computerized assistance system, fault diagnosis with computer assistance, diagnosis of faults not found by the system, and monitoring the automated diagnostic system itself for possible failures. Successful performance on all these tasks would require an understanding of both the equipment and the diagnostic system together with expertise in the general problem solving skills necessary for efficient troubleshooting. Given the scope of knowledge and skills relevant to this situation, it is reasonable to expect that responsibility for various aspects of the overall problem will be allocated to personnel with different areas of expertise. For example, the routine maintenance technician might not be expected to remedy less frequently encountered faults in the computerized diagnostic system.

151-4

Assuming that computerized fault isolation will become the rule and manual fault isolation the exception, the technician's task will be considerably different from what it has been. Rather than using troubleshooting skills, the technician's primary task will evolve into one of executing procedures according to instructions from the computer aid. Optimization of the technician's performance in the new situation requires efforts to design computer aids with attention to the abilities and limitations of the user. One difficulty, however, is that most of the available research in the area of human performance in troubleshooting was designed to apply to the traditional setting. With the major activities of the primary task altered, it is uncertain how much of the present literature can be generalized to the future context.

However, it is not yet clear how extensive and how reliable automated maintenance can become. It is anticipated that, given the current state of technology, there will remain faults that are not located automatically (Gunning, 1984; Smillie, 1984). The extent and reliability of automated diagnostics will affect the roles played by technicians and experts. Expectations of degrees of automation will influence the design of computer aids as well as personnel selection and training.

Within the context of incomplete and/or imperfect automation, a variety of problems might be anticipated. For example, if the automated system cannot localize a fault, the troubleshooter will be faced with a demanding problem solving task. Should

relevant portions of the computerized aids become unavailable, the troubleshooter would need to rely upon his own expertise. The ideal maintainer in such circumstances would need a high level of sophisticated knowledge of the equipment and an ability to interact with the computerized system to access data bases and utilize whatever diagnostic assistance is available, as well as expert problem solving skills.

Although it is not possible at present to determine with precision the likelihood of such circumstances occurring, it is essential to consider the consequences of such events. As the degree of automation of problem solving and decision making increases and the task of the technician becomes increasingly proceduralized, concern for generating and maintaining competence at levels appropriate to the demands of infrequently occurring circumstances should also increase. Expert problem solving skills are a function of experience; if they are used only infrequently, maintaining expertise is an important issue (Anderson, 1980; Bainbridge, 1983; Mayer, 1983).

From this perspective, it can be argued that research concerned with the cognitive skills involved in troubleshooting is at least as important as it has been in the past (Margulies and Zemanek, 1983). Since the simplest faults to localize will be covered by routine computerized procedures, the faults which will remain for the troubleshooter will be the most difficult ones. Research concerned with developing or maximizing such skills will remain

critical for problems not resolved by routine procedures. In addition, if the computer aids available to the expert are to enhance his abilities, they must be designed with attention to the strengths and weaknesses of human cognitive processes.

Concern has been expressed (e.g. Bainbridge, 1983) that the ultimate degree of automatization would lead to a logical paradox such that automated systems are developed to replace the less reliable human with a more reliable system, but the human must ultimately pass judgment on the system. This paradox can be resolved with a clearer understanding of the distinction between reliability and depth of understanding. Reliability refers to the consistency with which a skill is applied, not to the quality or accuracy of the skill. Research on expertise in a variety of settings (e.g. Brehmer, 1981; Goldberg, 1970) has suggested that although a person may have developed a highly accurate model for problem solving or decision making, he may not adhere to it consistently. By contrast, the computer can be expected to perform consistently, although the accuracy of its model is contingent upon that embodied in the programming done by men. Therefore, monitoring and modifying systems intended to aid the human depends upon the user's depth of understanding of both the equipment and the system designed to aid in troubleshooting it. Research is needed to clarify how such understanding can be facilitated.

One aspect of this issue is whether the computerized aiding system can be designed so that interaction with it facilitates the

development of useful mental representations of the equipment and computerized aiding system. This question follows from a prior concern with determining if such representations would enhance troubleshooting ability. It is reasonable to suppose that commonalities would exist across different modes of interacting with the system. The design and implementation of these different modes together with decisions as to allocation of personnel time and resources to them is not a trivial consideration. For example, a completely proceduralized mode would be optimal for the reliably known troubleshooting tasks. However, competency for non-routine tasks might be hindered by this strategy. This suggests the desirability of two additional modes of operation. One of these modes might be an enriched procedural system to facilitate the development of knowledge about the system while executing computer-specified instructions. The other mode might be useful solely for training. Decisions as to when and by whom these modes should be used must be guided by personnel needs within the context of the extent and dependability of automation. If the technician will need to perform active problem solving when the system is ineffective or unavailable, the educative features of computer aiding must be given greater weight. On the other hand, if experts will take over in such situations, it might be more efficient for the technician to employ proceduralized diagnosis only. In this latter case, an important concern will be the development of the experts for the system.

II. OBJECTIVES

In order for computer aids to achieve the goals outlined above, they must be designed with consideration of human cognitive abilities relevant to troubleshooting. One objective of this paper is to identify basic principles of cognitive processing which are likely to be applicable to problems encountered in the computer-aided troubleshooting environment. The following characteristics of basic cognitive processes are from the available troubleshooting literature.

This literature was reviewed with an effort to extrapolate to the automated aids. This analysis was facilitated by abstracting principles of cognitive functioning from the psychological literature on problem solving and from the growing literature on human-computer interaction. However, any generalizations must be empirically validated. The second goal of this paper, therefore, is to articulate the research questions to be addressed if computer aids are to be designed for optimal human-computer operation.

III. COMPLEXITY AND THE NEED FOR STRUCTURE

An obvious characteristic of advanced aircraft systems is the presence of ever increasing degrees of complexity. The available literature on troubleshooting abilities in the traditional situation is the product of studies conducted in the context of equipment developed by technology through the 1970's. Such equipment was designed by engineers who possessed normal cognitive limitations on dealing with complexity. As pointed out by Wohl (1983), electronics

technology is moving toward computer aided design (CAD), which could exceed such natural limitations. Although the implications of CAD for fault diagnosis are not yet known, there is evidence that human diagnostic performance declines disproportionately at high levels of complexity. Wohl (1982) developed a model of the human-machine interaction process in diagnosing electronic equipment malfunctions from repair time data from various types of electronics equipment. Wohl's model (1983) demonstrates that equipment complexity indexed by the degree of interconnectedness among components (the average number of items directly connected to any one item), is highly correlated with human diagnostic performance in electronic maintenance. The model predicts that if a piece of equipment exceeds an average interconnectivity upper limit of approximately seven or eight, some proportion of equipment failures will be virtually nondiagnosable. A legitimate concern, therefore, is whether CAD may result in designs which exceed human capability for dealing with complexity.

The upper limit on average interconnectivity of seven or eight suggests that the constraint on performance is related to the limited capacity of human short-term memory (Miller, 1956). The fact that a person can deal consciously with only about seven items at any one time can help explain many of the characteristics of human problem solving behaviors. Intuitively, however, it is clear that people manage situations containing far greater amounts of information. The apparent discrepancy is resolved by considering

the definition of an "item." Each of the approximately seven items may entail a great deal of information, just as seven 10-letter words may be viewed as containing 70 pieces of information. The critical concern in understanding human capacity, therefore, is with the constitution and development of "chunks" of information which can be processed in active working memory. The seven-words example illustrates that chunks can be acquired through experience and then be recognized as single units (at some level) in a process of pattern recognition. In this report, the label "pattern recognition" refers simply to problem solving by direct mapping from observations to solution based on prior experience (Rouse, 1983). The reliance on pattern recognition in place of a more analytic process can be viewed as a means of coping with the limited capacity of short-term memory which would otherwise restrict severely the ability to deal with complexity.

It would be expected, then, that the limits on performance studied by Wohl (1982, 1983) reflect processing in situations where pattern recognition is not dominant. As explained by Wohl, the characteristic shape of his cumulative frequency distributions (CFD) of active repair time suggests the presence of two different causal processes. One process accounts for the successful completion of 65 - 80 percent of all repairs within two hours. The high slope of the relevant portion of Wohl's functions implies an accelerating process in which the probability of locating the fault increases with time. Although it is not possible to determine the nature of the process

accounting for this performance, it is clear that these repairs are instances of fairly rapid solution methods, which may well include pattern recognition. The second process underlies a low - slope portion of the plots, reflecting a decelerating process in which the probability of fault localization decreases as time increases. It is this second portion of the graphs to which Wohl's model applies. Presumably, the methods used in these repair situations involve more analytic approaches. Using Rasmussen's (1981) taxonomy of search strategies, Wohl suggests that the early, accelerating portions of the CFD's reflect the operation of symptom or S-rules, which are system-determined associations which map symptoms directly onto system structure. When S-rules do not result in successful fault isolation, context-free topographic or T-rules are used to guide the search through networks of functional relationships. The use of T-rules might account for the later, decelerating portions of the CFD's.

The preference for simple methods over more demanding ones involving greater cognitive effort, referred to as following the path of least resistance, has been observed elsewhere. For example, Rasmussen and Jenson (1974) have studied the mental procedures used by skilled electronics repairmen in their working environment through analysis of verbal protocols. They found a strong preference for general search routines characterized by rapid, impulsive decisions based upon information at the moment with little carryover from prior observations. Even when the routine search

procedures were unsuccessful, the technicians did not consider it worthwhile to study and draw inferences from the internal functioning of the circuitry. The preference for pattern recognition is so robust a finding that Rouse (1983) has incorporated it into a general model of human problem solving. According to this model, the central mechanism for problem solving attempts to solve a problem first by recognizing a pattern. If a pattern is not recognized, more analytical modes of reasoning must be used.

The literature supports, therefore, the notion that pattern recognition is one mechanism used for overcoming the limitation on short-term memory which restricts man's ability to deal with complexity. One possible approach to improving performance in situations characterized by the later decelerating portions of Wohl's (1982) functions would be to consider whether patterns could be learned in order to deal with the complexity. This approach raises an important basic issue: how are patterns acquired and can pattern recognition processes be facilitated? Facilitation might be possible in two ways: the recognition of already acquired patterns; and the initial acquisition of pattern knowledge.

The literature on differences between experts and novices suggests that experts typically possess a greater number of meaningful chunks or patterns of related units. Although many such studies have been conducted in the area of game playing such as chess (Chase and Simon, 1973; Simon and Gilmartin, 1973) and Gomoku

(Eisenstadt and Kareev, 1975), evidence exists to suggest that such findings are characteristic of performance whenever the perception and recall of meaningful relationships are important. For example, Badre (1982) studied chunking in the processing of military scenarios and Egan and Schwartz (1979) obtained expert-novice differences in the chunking of electronic circuit diagrams into meaningful sub-circuits. Research is needed to determine whether such expert-novice differences in chunking exist also in the area of trouble-shooting. This question is currently under investigation by researchers at the Learning Research and Development Center, University of Pittsburg (Bond, Eastman, Gitomer, Glaser, and Lesgold, 1983), who are studying chunking of components of electronic circuit diagrams. It may be, however, that the patterns used by technicians are patterns of relationships among symptoms and structural units rather than patterns of circuit components. Identification of such patterns and clarification of their role in determining level of performance are issues in need of empirical research.

Even more important, perhaps, is the need cited above for research designed to clarify how patterns are acquired. Certainly one plausible hypothesis is that rote learning occurs as a function of repeated exposure. That this mechanism plays a role in pattern acquisition is quite likely given the simple observation that expertise is developed only with years of experience (Anderson, 1980). It might also be suggested, however, that attention to

meaningful relationships or rule-governed regularities is an
important process underlying pattern acquisition. For example, the
fact that words can be recognized more quickly than nonsense strings
can be described as an illustration of pattern recognition acquired
through repeated exposure. On the other hand, the observation that
pronounceable nonwords can be recognized more quickly than non-
pronounceable nonwords (McClelland and Johnston, 1977) suggests
that certain rule-governed regularities may facilitate pattern
recognition of relatively less familiar material. The effectiveness
of rule-governed relationships obviously depends upon knowledge of
the regularities. The interaction between such knowledge and features
of the stimulus was illustrated in a study by Eisenstadt and Kareev
(1977) in which reconstruction of a given game board configuration
was shown to vary with the subject's assumption that the configura-
tion was from one of two different games. Evidently, the arrangement
of pieces was encoded differently depending upon the rules of play
which were considered relevant to the display. From this perspec-
tive, it is reasonable to propose that efforts to facilitate pattern
recognition should include methods to encourage the acquisition of
knowledge of the structure of relationships.

An important concern in the design of systems intended to aid
troubleshooters would be to determine whether aspects of the display
might affect the ability to recognize relationships critical to
pattern identification. As expressed by Rouse and Rouse (1979), in
addition to problem solving complexity, which is related to various

attributes of problems, there exists perceptual complexity, which is related to aspects of the display. For example, in the game-playing context, Eisenstadt and Kareev (1977) found that detection of an important configuration was affected by features of the display in terms of the Gestalt principles of proximity and continuity. In the domain of troubleshooting, Brooke and Duncan (1983) found that reduction in perceptual complexity by changing the direction of signal flow in the format of displays of logic unit networks reduced the number of suboptimal tests made. In an earlier study using a similar paradigm, Brooke and Duncan (1981) had found an effect of the format of the connections among units on diagnostic efficiency. This minor change in display appeared to lose its effectiveness as practice increased. As pointed out by the authors, their paradigm allowed for a shift from problem solving towards pattern recognition. It seems likely, therefore, that display format can influence pattern recognition, and that complexity is a function of problem structure, display format, and degree of knowledge possessed by the problem solver. However, it is not clear what relationship exists between pattern recognition and problem solving.

When recourse to pattern recognition is unsuccessful, other methods for coping with the limited capacity of short-term memory are necessary to solve a complex problem. One obvious means of coping is to support memory with external aids for record keeping. It is natural that the computer would be envisioned as a means for expanding memory storage. At a very simple level, a computer aid

can serve this function by operating as a dynamic blackboard.
Active windowing, for example, can provide a space for the user to
make notes or update adjustments to a representation of changes in
state. At this level, however, the aid is not much superior to
paper and pencil. At a somewhat higher level, detailed graphics
which can be marked or modified by the user would constitute a
distinct advantage over hard-copy. One would expect that
porformance would be facilitated by having the computer narrow down
the amount of information with which the user must cope. For
example, Rouse and Hunt (1984) studied troubleshooting of computer
simulations of network representations of systems. Performance was
improved by a sophisticated bookkeeping aid that used the structure
of the network and known outputs to eliminate (by crossing off)
components that could not be the fault. The aid continued to
eliminate components as a result of tests selected by the user. By
helping the user to attend to only those components which still
remained in the feasible set, this type of aid effectively reduced
load on short-term memory and resulted in an improvement in
troubleshooting performance. The observation that subjects retained
their advantage when the aid was removed indicates that the aid also
facilitated the acquisition of effective problem solving skills. The
importance of attention to structure in problem solving was further
illustrated in Rouse and Hunt's finding that reinforcement which
informed the user of the degree to which his test choice was
consistent with an optimal strategy degraded performance and yielded

negative transfer to the unaided situation. By contrast, feedback which explained the nature of user errors in terms of the structural implications of prior tests resulted in improved performance and benefitted later performance with aiding removed.

These examples illustrate that in order for a limited capacity system to deal effectively with complex information it must reduce the amount of information in a meaningful way, either by capitalizing upon structure inherent in the situation or by actively imposing some structure upon the situation. For optimal improvement, therefore, computer aids must provide more than a simple space for record keeping. The user needs a way to organize information. Organization enables a problem solver to process more information simultaneously because many pieces of data have been collapsed into large chunks of related material. In many situations, the solution to a problem depends upon the recognition of a relationship which is perceived when critical problem components are processed simultaneously in working memory. Structure also guides the search for relevant information, thereby enabling the user to distinguish between useful and irrelevant information. Material which is organized is more easily comprehended and assimilated into long-term memory.

IV. MENTAL MODELS AND EXPLANATION

An important concern in designing computer aids for fault diagnosis is the identification of ways in which the advantages of organization might be realized by the troubleshooter. Simply making increasingly greater amounts of information available in computerized

151-18

data bases will not solve the problems encountered by technicians
dealing with increased technological complexity. Increases in
unstructured information would create an additional layer of
complexity between the technician and the equipment. The avail-
ability of potentially useful information is not productive unless
the technician is able to make effective use of it. One perspective
on providing structure which has been receiving attention recently
is the consideration of how a person understands a system in terms
of a mental representation or model. The major approaches in this
area are presented in a book by Gentner and Stevens (1983) and are
summarized in a report by Smith and Collins (1983).

Following the distinction used throughout this report between
pattern recognition and other problem solving modes, the literature
on mental models appears to be most relevant to situations requiring
the use of the more inferential techniques. For example, in de Kleer
and Brown's (1983) model, troubleshooting can be viewed as the
inverse of the envisioning process, because envisioning involves the
inference of function from structure, whereas troubleshooting
requires the determination of structure from function. The model
predicts the degree of similarity between the perturbed function and
the normal function will affect the difficulty of fault diagnosis,
assuming that the troubleshooter uses his understanding of the
functioning of the system to find the fault.

The notion that mental models may be helpful in problem solving
has been suggested in a variety of contexts. Larkin (1983) suggests

that differences in problem solving performance between novices and experts in physics are related to their use of different problem representations. Physics students who were taught to use physical representations of circuits using diagrams, analogies and visualization solved significantly more problems than did students without such training. Having analyzed protocols of attempts to understand and explain how a heat exchanger works, Williams, Hollan, and Stevens (1983) propose that mental models assist reasoning by facilitating prediction of the behavior of a system, generation of explanations, and recall. Clarifying the nature of the mechanism(s) by which mental models accomplish such benefits is important in order to be able ultimately to predict the degree of usefulness of a particular model in a given situation.

Gentner (1983) maintains that understanding of a new system develops through analogy with an already familiar system. According to Gentner, analogy involves a mapping of elements from the familiar system to the new one. Specific properties of the elements are not transferred, but the relationships among the elements are preserved. It is not clear how the process of differential transfer is determined or achieved. Within the problem domains of psychiatric diagnosis and dispute resolution, Kolodner and Simpson (1984) have proposed an organizational scheme of memory structures in an attempt to explain how relevant past experiences are retrieved for application to a new problem in a process they refer to as "similarity - triggered analogical reasoning." According to their

model, knowledge from experiences is organized in generalized
episodes in which individual experiences are indexed according to
their differences. The process of retrieving cases to apply to a
new experience entails a search for indices associated with features
which differentiate the new case from others in the same generalized
episode. However, before the process of analogical reasoning can be
fully understood, further research is needed to explore the nature of
the features used in determining the choice of episode or system to
be used in the analogy.

According to Kolodner and Simpson's (1984) observations, the
particular example selected for analogical comparison serves to
direct and focus decision making. Successful diagnosis can be
viewed, therefore, as somewhat dependent upon the choice of an
appropriate exemplar for comparison. The importance of the specifics
of the analogical base is also illustrated by the findings of Gentner
and Gentner (1983), who demonstrated that the nature of the
particular mental model taught to students in the form of different
analogies for electricity affected performance on problems which
pertained to circuits containing either two batteries or two
resistors connected in series or in parallel. Their results
illustrate that different models may have different types of
advantages for understanding various aspects of a system.

This idea that a single model or analogy may be inadequate for
complete understanding of a new system was also evident in the
protocols studied by Williams et al. (1983). Williams et al. point

out that subjects used more than one model in answering questions about how a heat exchanger works. The emphasize the importance of the ability to integrate incomplete models to achieve successful reasoning. There is a need for research to explore how such a process of integration takes place and how it relates to understanding a new system.

Although evidence exists to support the notion that employing a mental model is beneficial in learning about an unfamiliar device or system, the usefulness of a model can be expected to vary with several factors. As illustrated by the Gertner and Gentner (1983) findings cited above, specific features of a model transfer in different ways to learning different aspects of a new system. An even more basic concern, however, is the consideration of how the role of a model might change depending upon the nature of the task demands in a given situation. As pointed out by Kieras and Bovair (1983), an understanding of how a system works does not seem to be always necessary (e.g., as in our effective use of the telephone system despite an absence of an accurate model). They suggest that a mental model may be unnecessary if the device is very simple or if the procedures for using it are well known. Therefore, the knowledge of how a system is structured and how it functions would be most useful in situations requiring skills beyond the type of procedural knowledge acquired by rote (e.g., learning to operate a new device, troubleshooting). Using a device designed specifically for their research, Kieras and Bovair found that providing subjects with a

mental model facilitated their learning to operate the device by accelerating rate of acquisition of procedures and decreasing errors. Their findings from a second experiment supported their hypothesis that the model improved performance by enhancing the subjects' ability to infer the procedures. Kieras and Bovair concluded that it is not the conceptual depth of understanding, but the degree of relevance of the model to the actual task demands that determines the usefulness of the model.

From this perspective, an understanding of the task demands of troubleshooting with computer aids is essential in determining the appropriate level and type of information which should be provided . Assuming that the technician will engage in active troubleshooting in some situations would suggest that computer aids should be designed to encourage the development of mental models which will be useful when inferential skills become necessary. However, if the acquisition of useful models is a time consuming, effortful process and if the time spent in inferential activity is minimal, the cost-benefit tradeoff may argue against attempts at model formation. On the other hand, the findings of Kieras and Bovair (1983) suggest that models may even benefit the acquisition of procedural knowledge. Clearly, further research is needed to determine the relevance of mental models to troubleshooting, especially within the context of computer aided diagnosis.

One conception of the "routine" mode of computer assistance would anticipate that the technician would follow procedural instructions generated by the computer. It might be argued that in this

mode of operation, mechanisms designed to promote model formation would be superfluous and possibly costly in terms of distracting and time-consuming cognitive activities. However, data from experiments by Smith and Goodman (1982) suggested that supplementing procedural instructions with explanatory material benefitted certain aspects of performance in a task requiring assembly of an electrical circuit of the type found in a flashlight. In particular, explanatory material facilitated understanding of instructions as evidenced by faster reading times, fewer errors in execution, and enhanced recall. The explanatory statements were of two types, both of which provided higher-level information in an hierarchical arrangement in which instructions functioned as instantiations of higher level concepts. One type of explanation incorporated structural information concerning the components of the circuit and their inter-connections. The other type of explanation provided functional information by emphasizing the dynamics of current flow.

One aspect of Smith and Goodman's results which is particularly relevant to the troubleshooting task is their findings which suggest that functional explanations enhanced the ability to reason about the circuit and to troubleshoot faulty versions of the circuit. The fact that the evidence was marginal leaves this issue unresolved. If such a finding could be supported in further research, it would imply that the type of supplementation used by Smith and Goodman might serve different types of useful functions in various phases or modes of computer-aided troubleshooting. Identification of such

functions and their associated contexts would require empirical studies in which both the type of explanatory material and the nature of the task demands are varied.

Although the precise mechanisms by which mental models and analogy function to facilitate understanding, memory, and reasoning have not yet been clearly identified, the advantages of models and analogies as heuristics can be understood within the more general psychological framework of context effects. The process of comprehension requires that a new object, event, or utterance be interpreted within an existing knowledge base. Meaning comes from an integration of new material with relevant information acquired through experience (Haviland and Clark, 1974). Studies of linguistic comprehension have shown that understanding can be facilitated by the provision of a prior context in ways as simple as presenting a drawing containing relevant relations among elements or by heading a passage with an appropriate title (Bransford and Johnson, 1972, 1973).

The important point illustrated by such studies is that comprehension depends upon the availability of a meaningful context in which new information can be interpreted. This interpretive aspect of comprehension has been shown to involve active cognitive processes such as the use of knowledge about relations to make inferences and to generate hypotheses (Bransford and McCarrell, 1977). Viewing comprehension as such an active process and as contingent upon prior knowledge enables one to understand the variability in performance in tasks as related to differences in prior context. The type of

information a person brings to the task will influence his ability to understand what would objectively be seen as simple instructions. Because memory is strongly related to level of comprehension, poorly understood material tends not to be remembered. Consequently, initial difficulties in comprehension tend to perpetuate themselves as it is difficult to build the necessary knowledge base if each experience is not well remembered. The design of computer-based instructions and explanations, therefore, should include consideration of such context effects. Instructions will be understood more readily if an appropriate referent or concept has been preactivated. This preactivation can be achieved by careful wording and sequencing of statements. As described above, the use of explanatory statements to activate a concept in a hierarchial framework is an example of how such preactivation can benefit performance (Smith and Goodman, 1982).

However, it can readily be seen that the usefulness of such devices would fluctuate as the needs of the user change with experience. Ideally, computer aids should be designed with the capability to adapt to the user (Rouse, 1981; Smillie, 1984; Williges and Williges, 1983) and should be conceptualized as dynamic rather than as static entities. The application of artificial intelligence to such problems of adaptability has been primarily in the context of intelligent computer assisted instruction systems which develop user models to enable the aid to respond to differences in knowledge and understanding by the user (Smith and Collins, 1983). For example, within the domain of medical diagnosis, the expert system MYCIN was

developed to give advice in the diagnosis of infectious diseases.
GUIDON, an intelligent computer-aided instructional program, is being
developed to teach diagnostic problem-solving using the rules of
MYCIN as the material to be learned (Clancey, 1984a, 1984b). An
important facet of GUIDON is its use of student modelling to direct
flexible dialogue interaction in a mixed-initiative program.
Implementation of GUIDON has yielded observations of value to the
design of computer aids which will require human interaction. For
example, students found the MYCIN rules to be difficult to
understand, remember, and use in developing a problem-solving
approach. These difficulties have been related to the fact that
valuable information concerning the hierarchial structure of data
and hypotheses and the top-down nature of searching the problem
space was implicit in the rules, but not explicity available to the
user. Clancey points out the importance of having the user learn
strategies rather than learning problem-solving steps by rote. In
an effort to make such structural and strategic knowledge explicit,
MYCIN's rules are being reconfigured in NEOMYCIN. An important
feature of NEOMYCIN is the addition of the capacity for justification
of rules. Clancey argues that justifications promote understanding
which allow the problem solver to go beyond rote rules in unusual
situations.

The ability to go beyond the aid in unusual situations is an
important practical concern given the current state of automated
diagnostics. Automatic test equipment does not isolate all failures

and cannot isolate certain types of problems. Fault isolation is often ambiguous, resulting in a list of possible fault locations (Coppola, 1984). Developing the competency to deal with trouble-shooting situations not covered automatically can be approached in a variety of ways. One vehicle would be the development of intelligent computer-aided instructional programs such as GUIDON for trouble-shooting. For example, an expert system based on the Feed-Device-Ground inferencing strategy is being developed to train students in automotive electrical troubleshooting (Feurzeig, Frederiksen, White, and Horwitz, 1984).

Another approach, which can be complementary to the first, is to design the computer-aided diagnostic system in such a way that its use entails an educative dimension or mode. An illustration of such an effort is the Intelligent Maintenance Aid (IMA), which is currently in operation as a prototype dealing with diagnosis of faults in the microwave stimulus interface of the F-16 Avionics Intermediate Shop (Hinchman and Morgan, 1984). In addition to its diagnostic function, IMA serves an educative function by providing explanations of lines of reasoning and for recommended actions.

The possibility of designing computer aids for troubleshooting which will concurrently promote the growth of knowledge about the system as well as develop good problem solving skills raises many questions and issues for empirical investigation. How great a role should the educative dimension play in the computer-assisted environment? Should it operate in a separate mode or be integrated

into the normal working system? Should its adaptability to the changing needs of the technician be computer or user initiated? What role might mental models and/or analogy play in troubleshooting performance?

VI. INFORMATION DISPLAY AND DESIGN CHARACTERISTICS

The preceding discussion argues that structure is beneficial both in acquiring new information and in applying information during problem solving. Identification of structure involves the ability to attend selectively to those elements which are related in a meaningful way. In order to integrate the appropriate elements, those elements must be present in active memory at the same time (Ohlsson, 1984). Since short-term memory is limited in both capacity and duration, the display format and the order of presentation of information can affect problem solving performance. The need to have the right information in active memory at the right time suggests that the computer can play an important role in facilitating problem solving, but if used incorrectly can also interfere with performance. For example, the computer's tendency to be used for sequential display of information can potentially conflict with the problem solver's need for information displayed simultaneously. This sequential/simultaneous distinction is important because it is related to the differences between sequential and parallel processes in the human cognitive system. The extent to which each of these two types of processing is involved in troubleshooting has not been directly addressed by empirical investigation. It might be imagined

151-29

that the importance of structural knowledge implies a special aspect
to the task which would be best dealt with by parallel processing.
The associational aspects of relating symptoms to structures might
imply a pattern recognition mode which entails configural processing.
However, the use of functional information and serial testing
procedures would suggest more sequential and analytic types of
processes. Relevant to this processing distinction, two stages of
research would be desirable. First, research is needed to delineate
the roles played by each processing mode in troubleshooting.
Secondly, research could then be directed at determining how the
nature of display format and order of presentation of information
interact with each type of process.

On the basis of general principles of cognitive functioning,
guidelines can be suggested concerning the types of information
which should be displayed simultaneously.

(1) When one type of information is needed to operate upon
another. For example, when help is needed to facilite   election
from displayed material or to edit text, etc., the help information
should not erase the material to be used or manipulated.

(2) When two types of data or material are to be compared.

(3) When a pattern or a relationship among variables needs to
be identified.

An obvious limitation to the idea of simultaneous presentation
is the size of the screen. Given this constraint, attention should
be paid to providing easy ways to shift back and forth between

sources of information, data bases, alternate views, etc. Given the short duration of active memory, it is also important to consider the user's problem of remembering where he is in the computer aid system. Efficient movement within the computer system may depend upon what Young (1983) refers to as a mental model of an interactive device. According to Young, the user's model of an interactive device entails a mapping of correspondences between task structures and action sequences. There is a need for research to explore how acquiring such a model can be facilitated. On the basis of the literature on context effects reviewed above, one might predict that simple aids such as a diagram of the system components and their interrelationships might prove beneficial.

Accessing the appropriate information can be difficult also if the means for requesting information presumes more knowledge on the part of the user than he has available. This difficulty can arise when menus are used, for example, and the user is uncertain as to the structure represented by the menu. An example of one approach to alleviating such a difficulty is the implementation of a browser to allow the user to examine a complex system without prior knowledge of its exact structure (Fischer, 1983). Such an interface depends upon multiple windows for the selection and expansion of components to be scanned.

VI. MOTIVATIONAL VARIABLES

Although consideration of ways to make computer aids compatible with human cognitive strengths and limitations is essential, another

important concern has largely been ignored. Very little attention
has been given to design characteristics which will impact on
motivational variables. For example, it might be argued that success
in the design of effective educative features in a computer aid will
be irrelevant if there is no incentive for the technician to use or
to attend to such features. Because performance tends to follow a
path of least resistance, it could be that material perceived as
superfluous would be ignored. If the educative function is to be
realized in practice, research must explore means for providing an
effective incentive structure for its use. The problem of trying to
achieve a particular kind of use by the technician is also manifest
in design issues concerned with compatibility. If the system is too
difficult to use, the user may become frustrated and stressed
(Chapanis, 1982). Under stress, problem solving performance
decrements as cognitive narrowing and stereotyped thought increase
(Bainbridge, 1983; Mandler, 1979). However, if the computer aid
oversimplifies the task of the technician, little mental effort will
be engaged and consequently little learning will occur.

On a more general level, motivational effects of computer
assistance can be ancitipated depending upon the user's attitude
toward the device. Currently, novice users often feel ambivalent
toward the computer. While on one level, the computer can create an
illusion of power and control, on another it can invoke fear, resent-
ment, and a feeling of loss of control (Sheridan, Vamos, and Aida,
1983). These attitudes are important because ultimately they can

affect performance (Margulies and Zeranek, 1983). For example, a feeling of loss of control can lead to passivity and learned helplessness, a decreased ability to adapt to new situations and to acquire new knowledge (Seligman, 1975). The investment of too great a trust in the computer can also lead to a loss of the sense of personal accountability. To avoid a "diffusion of responsibility," it is important that the allocation of responsibility and control is made explicit. By virtue of its position between the man and the equipment he is to repair, the computer can also contribute to a sense of alienation due to increased psychological distance from the problem to be solved. It is possible that the problem of distance can be alleviated with the use of mental models, dynamic representations of the system, and informative feedback. Mental models might also be found useful in minimizing negative affective reactions. For example, Kieras and Bovair (1983) observed that subjects who did not have a mental model of a device were more likely to experience confusion and frustration. They made more statements describing the device as unreliable and arbitrary, and they engaged in more inefficient, trial-and-error strategies. It can be argued, therefore, that a person's model of a device can effect, to some extent, the way in which he interacts with the device.

VII. RECOMMENDATIONS

It is not possible to predict precisely how the nature of the task demands on the technician will change with increases in computer-assisted diagnostics. However, the available evidence

151-33

suggests that the decision to design aids which would ultimately transform the technician's task into a purely proceduralized one would entail the risk of losing competency not only necessary in situations requiring manual troubleshooting, but also desirable to facilitate performance in the proceduralized mode. A major recommendaticn which follows from this paper is that an effort should be made to explore ways in which computer aids can be designed not only to maximize performance in the proceduralized mode, but also to enhance understanding and skills important in active troubleshooting. Research questions which must be addressed in pursuit of such a goal have been delineated and justified throughout this paper. For convenience, the major issues recommended for empirical investigation are summarized in the list below, followed by a brief commentary on each.

1. The development of computer aids entails substantial investments in time and expense. Before such investments are made, the usefulness of design features in maximizing performance should be evaluated empirically in experimental designs which capture the essential elements of the task.

Recommendations two through eight represent ways of approaching this goal. Lines of research should be guided by the distinction between task demands in proceduralized and active troubleshooting. An important issue is whether the principles for design differ substantially for the two types of situations.

2. What level of understanding is needed by the technician in the computer-aided troubleshooting task?

Approaches to this question should include effort to determine whether the addition of explanatory material and statements of justification affect performance in the proceduralized mode and whether they facilitate performance in unusual circumstances.

3. Should an educative function be incorporated into the troubleshooting aid, and if so, how can this best be accomplished?

Closely related to the second recommendation, this issue expresses a concern for the cost-benefit tradeoff between potentially decreased efficiency and enhanced learning involved in supplementing an aid with an educative function. Misapplication of educative features could result in wasted effort or even decrements in performance due to distraction and mental overload.

4. What roles might mental models and the use of analogical reasoning play in troubleshooting?

Given the recency of interest in mental models, empirical investigations of this research area will need to cope with many unknowns. Among others, the following areas need to be explored: (a) the mechanisms by which mental models and analogies influence problem solving and memory, (b) the process by which exemplars are selected for comparison in analogical reasoning, (c) differential advantages of different models and analogies, and (d) the integration of multiple models to achieve successful reasoning.

5. What is the relationship between pattern recognition and inferential problem solving processes?

Answers to this question will be important in an environment in which faults not covered by automation will leave the troubleshooter with complex problems requiring sophisticated inferential skills. Evidence suggests that technicians usually engage in pattern recognition. How this tendency will affect performance as the growth in complexity escalates is an important concern.

6. To what extent does troubleshooting involve sequential and parallel processing? What is the relationship between processing mode and design features such as display format?

These concerns are related to modality differences, processing modes, and short-term memory constraints. Certain task demands may be handled most effectively by certain processing modes and different modes may be differentially affected by various aids to memory and organization. For example, visual/spatial display is important to parallel processing, whereas temporal factors may affect sequential processing. Preserving a concern with compatibility between modality of input/output devices and processing demands of the task (Fischer, 1983) will be important when other practical concerns in terms of physical constraints (Polson, 1984) are being considered (e.g. the need for auditory format when a technician is occupied visually and manually with the equipment). Better understanding is needed of the differential advantages of information processing modes. One might ask if the preference for visual over auditory display in certain

situations (Moray, 1981) reflects a general bias or if it depends upon task demands. For example, some evidence suggests that in tasks requiring comparison judgments, people have greater confidence in visual processing, but perceive acoustic processing to be less time consuming (Yaworsky, 1983). In such tasks, visual processing is preferred to a greater extent when accuracy is emphasized than when speed is stressed.

7. Design of computer aids should include consideration of the following:

(a) provision of prior context to facilitate comprehension, memory, and reasoning.

(b) assistance in coping with the limitations of short-term memory.

(c) capacity to display appropriate types of information simultaneously.

(d) mechanisms for examining contents of the system without prior detailed knowledge.

(e) ways for the user to develop an accurate mental model of the computer as an interactive device.

(f) adaptability to the changing needs of the user.

These design considerations are based upon current research findings in the cognitive psychology literature. The justification for each suggestion is provided at appropriate places in the text. The goal of such concerns is to make optimal use of human strengths and to maximize performance within the constraints of human limitations.

8. What is the impact of design characteristics on motivational variables which affect performance.

Recommendation of this research area is based upon findings which suggest that affective and motivational reactions affect performance. Research is needed to study such effects in the context of trouble-shooting tasks. In particular, attention needs to be devoted to: (a) incentives for the use of educative features, (b) retention of a sense of control and accountability by the technician, and (c) coping with increased psychological distance between the technician and the equipment.

VIII. CONCLUSION

As the increased complexity of sophisticated aircraft systems necessitates growth in computer systems to aid in troubleshooting, it is imperative that attention be devoted to design characteristics of the aids. Although it is not clear precisely how the task demands will be altered by the expansion of computerized aids, principles of cognitive functioning can guide the research necessary to develop aids which will be compatible with human abilities. Before substantial investments in time and expense be committed to the development of computer aids, the usefulness of specific features should be tested empirically in experimental designs simulating the critical elements of the task.

REFERENCES

1. Anderson, J. R., <u>Cognit   Psychology and its Implications</u>, San Francisco, W. H. Freeman, 1980.

2. Badre, A., "Selecting and Representing Information Structures for Visual Presentation," <u>IEEE Transactions on Systems, Man, and Cybernetics</u>, 1982, <u>SMC-12</u>, 495-504.

3. Bainbridge, L., "Ironies of Automation," <u>Automatica</u>, 1983, <u>19</u>, 775-559.

4. Bond, L., Eastman, R., Gitomer, D., Glaser, R., and A. Lesgold, "Cognitive Task Analyses of Technical Skills: Rationale and Approach," Report Draft, Learning Research and Development Center, University of Pittsburgh, December, 1983.

5. Bransford, J. D. and M. K. Johnson, "Contextual Prerequisites for Understanding: Some Investigations of Comprehension and Recall, "<u>Journal of Verbal Learning and Verbal Behavior</u>, 1972, <u>11</u>, 717-726.

6. Bransford, J. D. and M. K. Johnson, "Considerations of Some Problems of Comprehension," In Chase, W. G. (Ed.), <u>Visual Information Processing</u>, New York, Academic Press, 1973, 389-392.

7. Bransford, J. D. and N. S. McCarrell, "A Sketch of a Cognitive Approach to Comprehension: Some Thoughts about Understanding What it Means to Comprehend, " In Johnson-Laird, P. N. and P. C. Wason (Eds.), <u>Thinking: Readings in Cognitive Science</u>, Cambridge, Cambridge University Press, 1977, 377-399.

8. Brehmer, B., "Models of Diagnostic Judgement," In Rasmussen, J. and W. B. Rouse (Eds.), <u>Human Detection and Diagnosis of System Failures</u>, New York, Plenum Press, 1981, 231-239.

9. Brooke, J. B. and K. D. Duncan, "Effects of System Display Format on Performance in a Fault Location Task," <u>Ergonomics</u>, 1981, <u>24</u>, 175-189.

10. Brooke, J. B. and K. D. Duncan, "Effects of Prolonged Practice on Performance in a Fault-Location Task," <u>Ergonomics</u>, 1983, <u>26</u>, 379-393.

11. Chapanis, A., "Computers and the Common Man," In Kasschau, R. A., Lachman, R., and K. R. Laughery (Eds.), Houston Symposium 3, <u>Information Technology and Psychology: Prospects for the Future</u>, Praeger, 1982, 106-132.

12. Chase, W. G. and H. A. Simon, "Perception in Chess," <u>Cognitive Psychology</u>, 1973, <u>4</u>, 55-81.

13. Clancey, W. J., "GUIDON," In Artificial Intelligence in Maintenance: Proceedings of the Joint Services Workshop, Boulder, Colorado, 1984a, 181-188.

14. Clancey, W. J., "Teaching Classification Problem Solving," In Proceedings of the Sixth Annual Conference of the Cognitive Science Society, Boulder, Colorado, 1984b, 44-46.

15. Coppola, A., "Artificial Intelligence Applications to Maintenance," In Artificial Intelligence in Maintenance: Proceedings of the Joint Services Workshop, Boulder, Colorado, 1984, 23-43.

16. De Kleer, J. and J. S. Brown, "Assumptions and Ambiguities in Mechanistic Mental Models," In Gentner, D. and A. L. Stevens (Eds.), Mental Models, Hillsdale, New Jersey, Lawrence Erlbaum Associates, 1983, Chap. 8, 155-190.

17. Egan, D. E. and B. J. Schwartz, "Chunking in Recall of Symbolic Drawings," Memory and Cognition, 1979, 7, 149-158.

18. Eisenstadt, M. and Y. Kareev, "Aspects of Human Problem Solving: The Use of Internal Representations,: In Norman, D. A. and D. E. Rumelhart (Eds.), Explorations in Cognition, San Francisco, Freeman, 1975.

19. Eisenstadt, M. and Y. Kareev, "Perception in Game Playing: Internal Representation and Scanning of Board Positions," In Johnson-Laird, P. N. and P. C. Wason (Eds.), Thinking: Readings in Cognitive Science, Cambridge, Cambridge University Press, 1977, 548-564.

20. Feurzeig, W., Frederiksen, J., White, B., and P. Horwitz, "Designing an Expert System for Training Automotive Electrical Troubleshooting," In Artificial Intelligence In Maintenance: Proceedings of the Joint Services Workshop, Boulder, Colorado, 1984, 189-191.

21. Fischer, G., "Symbiotic, Knowledge-Based Computer Support Systems," Automatica, 1983, 19, 627-637.

22. Gentner, D., "Structure Mapping: A Theoretical Framework for Analogy," Cognitive Science, 1983, 7, 155-170.

23. Gentner, D. and D. R. Gentner, "Flowing Waters or Teeming Crowds: Mental Models of Electricity," In Gentner, D. and A. L. Stevens (Eds.), Mental Models, Hillsdale, New Jersey, Lawrence Erlbaum Associates, 1983, Chap. 6, 99-129.

24. Gentner, D. and A. L. Stevens (Eds.), Mental Models, Hillsdale, New Jersey, Lawrence Erlbaum Associates, 1983.

25. Goldberg, L. R., "Man versus Model of Man: A Rationale, Plus Some Evidence, for a Method of Improving on Clinical Inferences," Psychological Bulletin, 1970, 73, 422-432.

26. Gunning, D., "Integrated Maintenance Information System," Preliminary Draft, Air Force Human Resources Laboratory, Combat Logistics Branch, 1984.

27. Haviland, S. E. and H. H. Clark, "What's New? Acquiring New Information as a Process in Comprehension," Journal of Verbal Learning and Verbal Behavior, 1974, 13, 512-521.

28. Hinchman, J. H. and M. C. Morgan, "Application of Aritificial Intelligence to Equipment Maintenance," In Artificial Intelligence in Maintenance: Proceedings of the Joint Services Workshop, Boulder, Colorado, 1984, 363-378.

29. Kieras, D. E. and S. Bovair, "The Role of a Mental Model in Learning to Operate a Device," Technical Report No. 13 UARZ/DP/TR-83/ONR-13, University of Arizona, Department of Psychology, 1983.

30. Kolodner, J. L. and R. L. Simpson, "Experience and Problem Solving: A Framework," In Proceedings of the Sixth Annual Conference of the Cognitive Science Society, University of Colorado, Boulder, Colorado, 1984, 239-243.

31. Larkin, J. H., "The Role of Problem Representation in Physics," In Gentner, D. and A. L. Stevens (Eds.), Mental Models, Hillsdale, New Jersey, Lawrence Erlbaum Associates, 1983, Chap. 5, 75-98.

32. Mandler, G., "Thought Processes, Consciousness, and Stress," In Hamilton, V. and D. M. Warburton (Eds.), Human Stress and Cognition, New York, John Wiley & Sons, 1979, Chap. 6, 179-201.

33. Margulies, F. and H. Zemanek, "Men's Role in Man-Machine Systems," Automatica, 1983, 19, 677-683.

34. Mayer, R. E., Thinking, Problem Solving, Cognition, New York, W. H. Freeman, 1983, 320-325.

35. McClelland, J. and J. Johnston, "The Role of Familiar Units in Perception of Words and Non-Words," Perception & Psychophysics, 1977, 22, 249-261.

36. Miller, G., "The Magical Number Seven, Plus or Minus Two: Some Limits on Our Capacity for Processing Information," Psychological Review, 1956, 63, 81-97.

37. Moray, N., "The Role of Attention in the Detection of Errors and the Diagnosis of Failures in Man-Machine Systems" In Rasmussen, J. and W. B. Rouse (Eds.), Human Detection and Diagnosis of System Failures, New York, Plenum, 1981, 185-198.

38. Ohlsson, S., "Attentional Heuristics in Human Thinking," In Proceedings of the Sixth Annual Conference of the Cognitive Science Society, Boulder, Colorado, 1984, 273-276.

39. Polson, P. G., "The Psychology of Human-Machine Systems," In Richardson, J. J., Keller, R. A., Maxion, R. A., Polson, P. G., and K. A. DeJong, Artificial Intelligence In Maintenance, Vol. 2: Synthesis of Technical Issues and Framework for Research Development, and Application, Preliminary Draft, 1984, 29-46.

40. Rasmussen, J., "Models of Mental Strategies in Process Plant Diagnosis," In Rasmussen, J. and W. B. Rouse (Eds.), Human Detection and Diagnosis of System Failures, New York, Plenum, 1981, 241-258.

41. Rasmussen, J. and A. Jensen, "Mental Procedures in Real-Life Tasks: A Case Study of Electronic Troubleshooting, Ergonomics, 1974, 17, 293-307.

42. Rouse, W. B., "Human-Computer Interaction in the Control of Dynamics Systems," Computing Surveys, 1981, 13, 71-99.

43. Rouse, W. B., "Models of Human Problem Solving: Detection, Diagnosis, and Compensation for System Failures," Automatica, 1983, 19, 613-625.

44. Rouse, W. B., and R. M. Hunt, "Human Problem Solving in Fault Diagnosis Tasks," In Advances in Man-Machine Systems Research, Vol. 1, JAI Press Inc., 198⁄, 195-222.

45. Rouse, W. B. and S. H. Rouse, "Measures of Complexity of Fault Diagnosis Tasks," IEEE Transactions on Systems, Man, and Cybernetics, 1979, SMC-9, 720-727.

46. Seligman, M., Helplessness, San Francisco, W. H. Freeman, 1975.

47. Sheridan, T. B., Vamos, T., and S. Aida, "Adapting Automation to Man, Culture, and Society," Automatica, 1983, 19, 605-612.

48. Simon, H. A. and K. A. Gilmartin, "A Simulation of Memory for Chess Positions," Cognitive Psychology, 1973, 5, 29-46.

49. Smillie, R. J., "Implications of Artificial Intelligence for a User Defined Technical Information System," In Artificial Intelligence in Maintenance: Proceedings of the Joint Services Workshop, Boulder, Colorado, 1984, 353-358.

50. Smith, E. E. and A. Collins, "Applied Cognitive Science," Technical Report No. 2, Bolt Beranek and Newman Inc., Report No. 5499, 1983.

51. Smith, E. E. and L. Goodman, "The Role of Explanatory Material," Technical Report No. 1, Bolt Beranek and Newman, Inc., Report No. 5088, 1982.

52. Williams, M. D., Hollan, J. D. and A. L. Stevens, "Human Reasoning About a Simple Physical System" In Gentner, D. and A. L. Stevens (Eds.), Mental Models, Hillsdale, New Jersey, Lawrence Erlbaum Associates, 1983, Chap. 7, 131-153.

53. Williges, R. C. and B. H. Williges, "Human-Computer Dialogue Design Considerations," Automatica, 1983, 19, 767-773.

54. Wohl, J. G., "Maintainability Prediction Revisited: Diagnostic Behavior, System Complexity, and Repair Time," IEEE Transactions on Systems, Man, and Cybernetics, 1982, SMC-12, 241-250.

55. Wohl, J. G., "Cognitive Capability versus System Complexity in Electronic Maintenance," IEEE Transactions on Systems, Man, and Cybernetics, 1983, SMC-13, 624-626.

56. Yaworsky, K. B., "Visual and Acoustic Processing in Making Same-Different Judgments," Perceptual and Motor Skills, 1983, 56, 499-504.

57. Young, R. M., "Surrogates and Mappings: Two Kinds of Conceptual Models for Interactive Devices," In Gentner, D. and A. L. Stevens (Eds.), Mental Models, Hillsdale, New Jersey, Lawrence Erlbaum Associates, 1983, Chap. 3, 35-52.

1984 USAF-SCEEE SUMMER FACULTY RESEARCH PROGRAM

Sponsored by the

AIR FORCE OFFICE OF SCIENTIFIC RESEARCH

Conducted by the

SOUTHEASTERN CENTER FOR ELECTRICAL ENGINEERING EDUCATION

FINAL REPORT

CHARACTERIZATION OF CERAMIC-CERAMIC COMPOSITES

Prepared by: Dr. Chyang John Yu

Academic Rank: Assistant Professor

Department and   Department of Engineering
  University: Wilkes College

Research Location: Materials Laboratory (AFWAL/MLLM), Metals & Ceramics
                Division, Processing & High Temperature Materials Branch
                    Wright-Patterson Air Force Base

USAF Research   K. S. Mazdiyasni

Date: 25 September 1984

Contract No.:   F49620-82-C-0035

CHARACTERIZATION OF CERAMIC-CERAMIC COMPOSITES

by

Chyang John Yu

ABSTRACT

Nicalon SiC fiber reinforced magnesium aluminum silicate composites, which were fabricated from alkoxide derived hydroxide slurry and with different process parameters were analyzed with SEM, STEM, EDX and Electron Microprobe. It was found from these analyses that excessive residual carbon left in the matrix due to an incomplete binder burnout reacts with Al_2O_3 in the matrix. These reactions generate volatile species of AlO and/ or Al_2O and leave the matrix with a porous structure at 1250°C. It was also found that the residual carbon in the matrix reacts with niobium ions to form NbC precipitates for all the samples. The presence of NbC crystals along the fiber/matrix interface as a result of reaction between SiC fiber and niobium ions in the matrix apparently improves the flexural strengths of the composites. A prolonged organics burnout cycle provided a pore free sample at 1250°C and its flexural strength of 95 ksi is the highest among all the samples prepared so far.

I. INTRODUCTION:

The current use of Ni- and Co- containing superalloys to fabricate high temperature components of gas turbine engine has imposed significant limitations due to high material and fabrication costs, limited availabilities of strategic metals, high materials density and the need of using cooling air. The development of a substitution material has therefore attracted most of the attentions in the past decade. The high performance structural ceramics such as silicon carbide, silicon nitride, transformation-toughened zirconia and ceramic-matrix composites, for the most part, exhibit good stress-rupture performance and strength at both room temperature and high temperatures up to ∿ 1200°C (2200°F), and they are considered as the most promising candidates in this application.

The recent work of United Technology Research Center[1] by fabricating Nicalon fiber reinforced LAS matrix material demonstrates its good mechanical properties including flexural strengths and fracture toughness up to 900°C. The Nicalon® SiC fiber reinforced Magnesium .luminum Silicate (MAS) composite systems was studied by a number of investigators which include UTRC, T. Mah, and the Materials Laboratory of AFWAL in the past several years. The slurry of alkoxide derived hydroxide solution mixture of MAS compositions were processed to load the fibers. Vacuum hot pressing was then employed to densify the composites. The mechanical properties of the composites strongly depend on the densification and strength of the matrix material, fiber-matrix interactions and fiber-matrix bonding strength. Characterizations of the existing phases and their distribution, microstructural features and the phases present at the fiber/matrix interface would definitely provide foundations which unable us to understand the effects of processing parameters on the microstructural development of the composites.

II. OBJECTIVES:

The main objectives of this project were to characterize the Nicalon®
SiC fiber reinforced MAS composites and assess the effect of variations in
processing parameters, such as hot pressing temperatures and the heating
rates of binder burnout cycle, on microstructural development of the
composites.   The temperature of complete burnout of the organic materials
in composites was determined by thermogravimetric Analysis (TGA).   X-Ray
diffraction technique was used to identify the phases presented in the
composites. Microstructural distribution of different phases was charac-
terized with Scanning Electron Microscope (SEM), Energy Dispersive X-ray
(EDX) and Wavelength Dispersive X-ray (WDX). The qualitative chemical
compositions and phase distribution at the fiber/matrix interface were
analyzed with Scanning Transmission Electron Microscope (STEM) and EDX.
The results of these analyses unable us to understand the effects of
processing parameters on microstructural development, which in turn
determines the mechanical properties of the composites.

III. EXPERIMENTAL PROCEDURE:

1. Samples Preparation and Process Control

Nicalon® fiber reinforced composite samples were made by E. Hermes[2] for
microstructural analyzes. Four samples were prepared under four different
processing conditions. Temperatures and heating rates of the composites at
different stages of the manufacturing process are believed to be the most
important parameters in controlling the final density and percentage of
porosity of the composites, and also the degrees of reactions between
fibers and the matrix. A TGA run with a heating rate of 250°C/hr indicated
that no significant weight loss of the sample was measured for temperature
over 440°C, and it suggested that a peak temperature of 450°C for binder
burnout should be adequate. Two different binder burnout cycles were
therefore chosen as follows: 1) Fast cycle: with a heating rate of
20°C/min from room temperature to 450°C and hold at 450°C for 30 minutes;
2) Slow cycle: the samples were held at 100, 200, 300, 380, and 450°C

respectively during the heating cycle for 120 minutes with a constant heating rate of 20°C/min starting from room temperature. Three different hot pressing temperature, i.e., 1250, 1300 and 1380°C were chosen in preparing samples experienced a fast binder burnout cycle, and a hot pressing temperature of 1250°C was chosen for samples have gone through a slow binder burnout cycle.

2.   Characterization of Composites

In order to assess the effect of variations in processing parameters, such as hot pressing temperature and the heating rate of binder burnout cycle, on microstructural development of the composites, a series of experiments were conducted. Each sample, which corresponds to one set of processing parameter was analyzed with x-ray diffraction techniques by E. Hermes[2] to identify the phases being present. Microstructural feature of the samples was examined with Scanning Electron Microscope (SEM). Energy Dispersive x-ray (EDX) and Electron Microprobe were used to analyze the microstructural chemical compositions and phase distribution of the composites. Fiber/matrix interface composition and matrix precipitates composition were also analyzed by EDX and Electron Microprobe.

IV. RESULTS:

1. Mechanical Properties

The 4-point flexural strengths of composites prepared with different hot pressing temperatures or different binder burnout cycles were measured by Hermes[2] and are presented in Table I. Tension and compression modes fracture dominates for span/depth ratio greater than 20, while the mixtures of tension, compression and shear modes fracture prevail for smaller span/depth ratios. The important point to note from Table I are that with the same fast binder burnout cycle, a hot pressing temperature of 1300°C gives a higher flexural strengths then other two pressing temperatures; while using a slow binder burnout cycle and hot pressing temperature of 1250°C, the flexural strength is the best among all the samples processed.

2. Microstructural Characterizations

Micrograph of polished samples No. 1-4 taken by SEM are shown in Fig. 1(a) - 1(d). By comparing Fig. 1(a), (b), (c) and (d), it is obvious that sample No. 4 is nearly pore free while samples Nos. 1 and 3 both have huge pore regions. On the other hand, most of the fibers in sample No. 3 were reacted severly with the matrix material. It is also noted that sample No. 3 had a strong fiber-matrix interaction, and no clear fiber boundary can be defined.

X-ray diffraction patterns of sample Nos. 1-3 analyzed by Hermes[2] all show niobium carbide (NbC), zirconium oxide (ZrO_2) and high quartz structure of magnesium aluminum silicate ($MgO \cdot Al_2O_3 \cdot 3SiO_2$) phases. Sample No. 1 has also a stronger peak of high cordierite ($2MgO \cdot 2Al_2O_3 \cdot 5SiO_2$) phase than sample No. 2, while sample No. 3 has no high cordierite phase at all.

Fine precipitates in the matrix of sample No. 1 have high niobium and zirconium contents as analyzed by wavelength dispersive x-ray (WDX) mode of an electron microprobe. The intensity ratios of Nb or Zr peak to Al peak

are compared for precipitates and matrix region without precipitates. The
peak rations of Zr/Al and Nb/Al are 0.76 and 1.88 respectively on an
arbitrary scale for the precipitates as compared with 0.10 and 0.48 on the
same scale for other matrix region. Carbon detection unfortunately has not
been set up yet for the microprobe and no C analysis was done. However,
based on the evidence of presence of NbC and ZrO_2 phases as verified by
x-ray diffraction, and these precipitates are the only phase high in
niobium and zirconium contents in the matrix as analyzed by EDX, it is
believed that these precipitates are indeed the mixtures of niobium car-
bides and zirconium oxides. Wavelength dispersive x-ray analysis of the
fiber/matrix interfacial region of sample No. 1 was preformed in a stepwise
fashion, and the results are given in Table II. It indicates that no
diffusion of Mg, Al, Zr and Nb into the fiber occurred, and these elements
all stay in the matrix. The EDX spectrum of the precipitates in the matrix
of sample No. 3 are given in Fig. 2, and it showed a superposition peak of
Zr and Nb. It is concluded that these precipitates in sample No. 3 are the
mixtrues of NbC and ZrO_2 phases as confirmed by x-ray diffraction data.

A 3mm disc of smaple No. 2, which has a longitudinally oriented fiber
direction, was polished to a uniform thickness of 2.5 mil. Then a thin
foil was prepared by ion milling technique. The sample was bombarded with
argon gas at an angle of incidence of 15° for 37 hours, where the argon gas
was accelerated with a gun voltage of 6KV and a gun current of 1 mA. A
Scanning Transmission Electron Microscope (STEM) was used to analyze this
foil and a STEM image is shown in Fig. 3(a). It can be seen that some dark
particles precipitates along the fiber/matrix interface. Energy Dispersive
X-ray analysis of the overall interfacial region and the precipitates along
the interface are shown in Fig. 4(a) and (b) respectively, and Fig. 4(b)
shows a strong Nb peak as compared with Fig. 4(a). An EDX mapping micro-
graph of Nb is shown in Fig 3(b), and it verifies that the dark particles
along the interface are rich in niobium. Based on these results and the
x-ray diffraction data, it suggested that there are NbC crystals precipi-
tates along the fiber/matrix interface.

A higher magnification micrograph of the area as indicated by an arrow in Fig 1(a) are shown in Fig. 5(a). This area is in a porous region and an EDX analysis of the discontinuous phases shown are given in Fig. 5(b). This spectrum showed a strong silicon peak and a weak magnesium peak, and no aluminum peak was found at all.

V.   DISCUSSION AND CONCLUSIONS:

There are good correlations between the flexural strengths as given in Table I and micrographs as shown in Fig. 1(a)-(d) of the composites. Sample No. 4 has a nearly pore free microstructural feature and it also gives the best flexural strength. Sample No. 2 has a limited amount of pores and it has the second best flexural strength. Sample No. 1 and No. 3 both are very porous and they have the lowest flexural strengths as expected.

Sample No. 1 was processed at 1250°C with a fast binder burnout cycle. Figure 5 suggests that in some of the porous regions, the matrix has undetectable aluminum ions by EDX. Borom et al[3] verified that in reducing atmosphere with the presence of hydrogen gas and carbon, alumina reacts with carbon to form Al_2O and AlO gas species thru the following reactions:

$$Al_2O_3(s) + C(s) \underset{}{\overset{H_2}{\rightleftharpoons}} 2AlO(g) + CO(g)$$

$$Al_2O_3(s) + 2C(s) \underset{}{\overset{H_2}{\rightleftharpoons}} Al_2O(g) + 2CO(g)$$
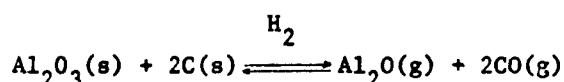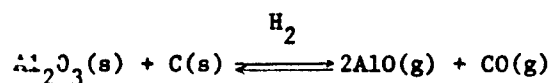
During the vacuum hot pressing cycle of the composites, hydroxides provide the needed hydrogen atmosphere and the residual carbons in the matrix are expected to react with alumina to form volatile AlO and Al_2O species leaving behind the matrix with porosities which is low in aluminum content. When the hot pressing temperature increases to 1300°C, the matrix material is less viscous and the rearrangement of the material in the matrix fills up the pores generated by volatizations of AlO and/or Al_2O. This explains the less porous structure of sample No. 2 as shown in Fig. 1(b). On the

other hand, when a slow organic burnout cycle was used, a far much less amount of carbon was left in the matrix and most of them reacted with niobium to form niobium carbide as will be discussed later. The chance for volatilization of gas species of aluminum oxides was reduced dramatically and a pore free composite was formed as shown in Fig. 1(d). Sample No. 3 was processed at 1380°C which was too high a hot pressing temperature and gave stronger reactions between fibers and matrix than those processed at lower temperatures. Figure 1(c) shows that the fiber/matrix reaction causes a degradation of fibers and creates some pores due to the volatilization of some matrix material. Further experiments will be carried out by using Mass Spectrograph to analyze the volatile species.

Niobium carbide crystal precipitates are found in the matrix for all of the samples. Based on thermodynamics calculation, with the presence of carbon at low oxygen partial pressures and in vacuum, formation of niobium carbide is much preferred than that of niobium oxide.[2] Carbon sources in the composites are coming from the SiC fibers themselves as well as carbon left in the matrix originated from organic solvent and binder. The reaction between fiber and niobium ions in the matrix form NbC crystals which are segregated along th fiber/matrix interfaces as shown in Fig. 3, while the reactions of niobium ion and the residual carbon in the matrix form fine NbC precipitates.

Sample No. 1 has no niobium carbide precipitates along the fiber/matrix interface as analyzed by electron microprobe, the brittle fracture of this sample indicates that there are good fiber/matrix bondings. Samples No. 2-4 all have niobium carbide precipitates along the fiber/matrix interface as shown in Figs. 1(d) and 3. It is expected that the presence of niobium carbide precipitates along the interface causes a weaker bonding between the fiber and matrix, and as a result the flexural strength of the composites is improved. A more continuous string of NbC crystals are expected for sample No. 4 since it was processed with a slow binder burnout cycle and a far much less residual carbon should be left in the matrix. This enhances the possibilities of niobium reaction with SiC fibers to form NbC along the interface. A thin foil of sample No. 4 will be analyzed with STEM in the future to verify this speculation.

VI. RECOMMENDATIONS:

This study demonstrates that microstructural characterization indeed unable us to understand more on how the composites changes their microstructural feature and phases distribution as a function of processing parameters. It also gives good correlations between the microstructure and mechanical properties of various samples processed somewhat differently. It is therefore recommended at this point to continue on this characterization study, and more specifically:

(1) To determine the chemical reaction temperatures, phase transformation temperatures and identify the volatile species of matrix material itself and composites with DTA/TGA/Mass spectrograph.

(2) Study the reaction of alkoxy derived niobium oxide and carbon to form niobium carbide with DTA and TGA.

(3) Develop a technique to semi-quantatively compare the relative NbC contents in matrix for different process parameters, and also determine NbC content of matrix material alone by processing them thru identical thermal cycles and hot pressing conditions as composites.

(4) Follow-on the STEM and EDX analysis on samples fabricated with different process parameters, such as sample No. 4.

(5) Analyze the chemical constituents and phase distribution at the fiber/matrix interface with Scanning Auger Spectrograph.

ACKNOWLEDGMENTS

REFERENCES

1. J. J. Brennan and K. M. Prewo, "Investigation of Lithium Aluminosilicate (LAS)/SiC Fiber Composites for Naval Gas Turbine Application," Final Report R83-9163232-4 on NASC Contract N00019-82-C-0438, 30 Oct 1983.

2. E. Hermes, K. S. Mazdiyasni, "Processing and Characterization of SiC Fiber Reinforced Magnesium Aluminum Silicate Composites," to be presented at the NASA/DoD meeting at Cocoa Beach, FL, Jan 85.

3. M. P. Borom, F. J. Klug, W. D. Pasco, I. C. Huseby, M. F. X. Gigliotti, and C. A. Bruch, "Development of Advanced Core and Model Materials for Directional Solidification of Eutectics," Final Report AFML-TR-77-211 on Air Force Contract 62102F 73500140, Oct 1977, pp. 142-149.

TABLE I Four-point flexural strengths of samples No. 1-4
where the test span(S) of 0.75 in. was used

Sample No.	Hot Pressing Temperature (°C)	Flexural Strength (ksi)	Sample Thickness t(in.)	S/t
1*	1250	13.2	.063	11.9
		18.0	.064	11.7
2	1300	68.7	.024	31.3
		69.6	.025	30.0
3	1380	43.6	.036	20.8
4	1250	94.9	.025	30.0
		47.9	.040	18.8

* Brittle fracture for both tests

TABLE II WDX intensities on Mg, Al, Zr, and Nb at the fiber/matrix
interface of sample No. 1, where the center of area B is
located at the fiber/matrix interface; the center of area A is
near the interface and within the fiber region; the center of
area C is near the interface and within the matrix region.

	Area A	Area B	Area C
Mg	0.6	1.2	2.2
Al	2.2	5.1	6.5
Zr	0.5	0.9	1.4
Nb	1.4	2.9	3.8

+ All the intensities are on relative scale

152-14
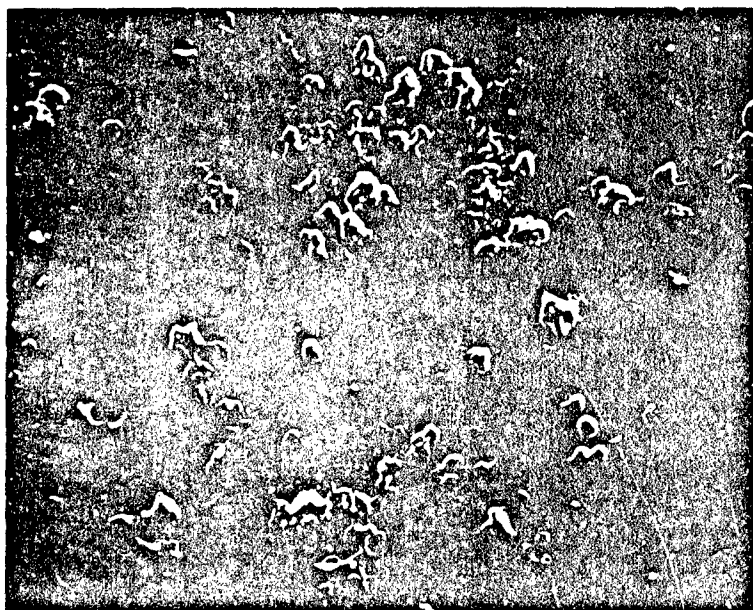
(a)

(b)

Fig. 1 Microstructures of samples hot pressed at (a) 1250°C (sample No. 1),
(b) 1300°C (sample No. 2), and (c) 1380°C (sample No. 3) all with fast
binder burnout cycles; (d) 1250°C (sample No. 4) with slow binder
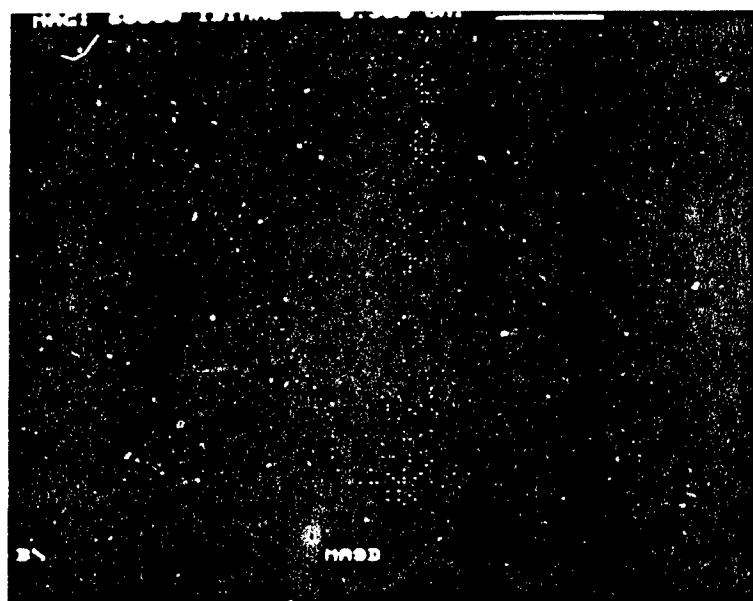burnout cycle (X 200 magnifications).
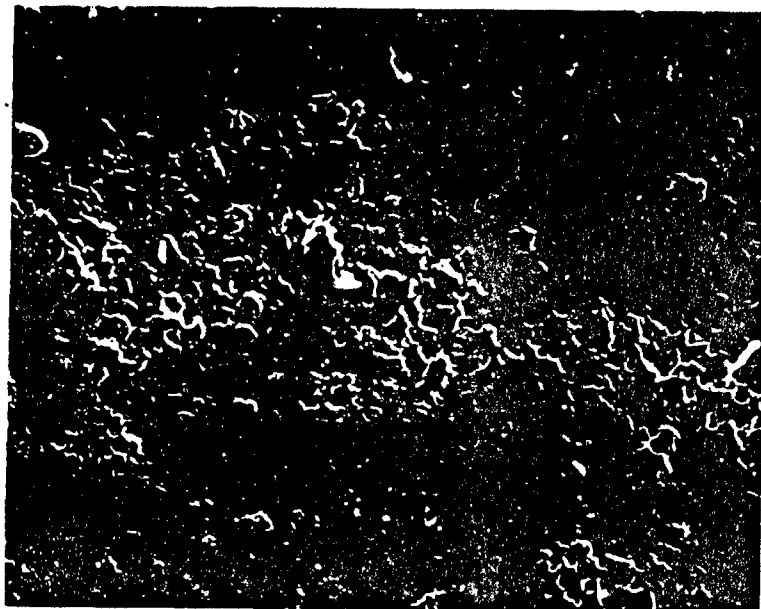
(c)
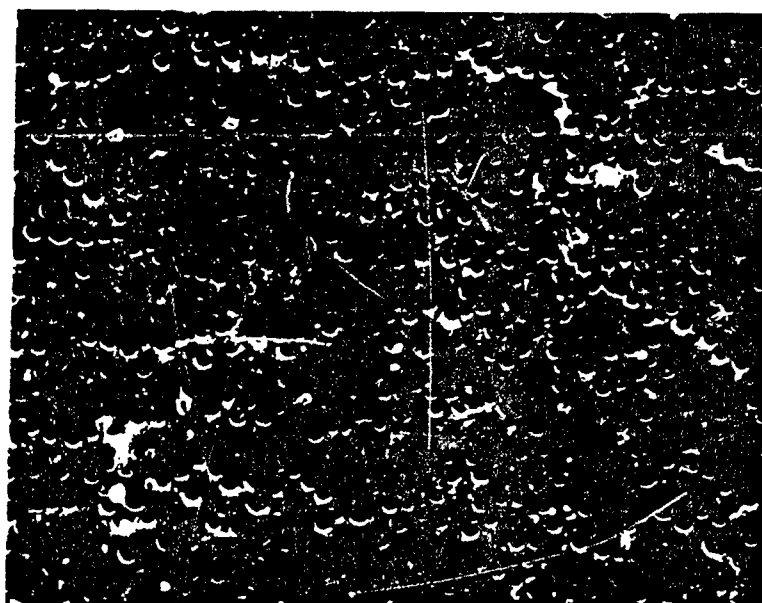
(d)

Fig. 1

152-16
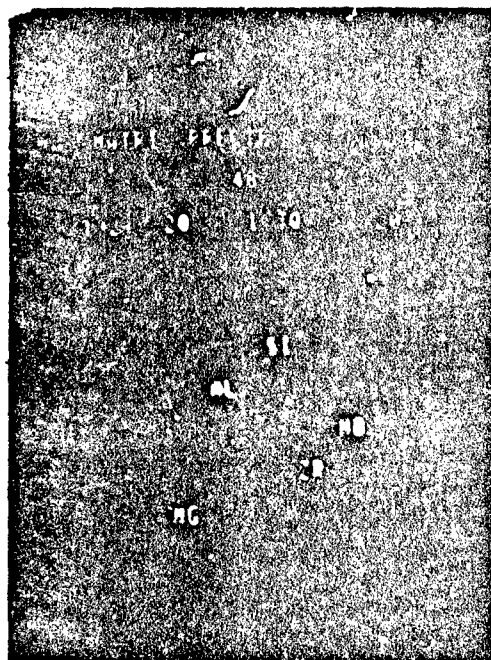
Fig. 2 Energy dispersive X-ray spectrum of the
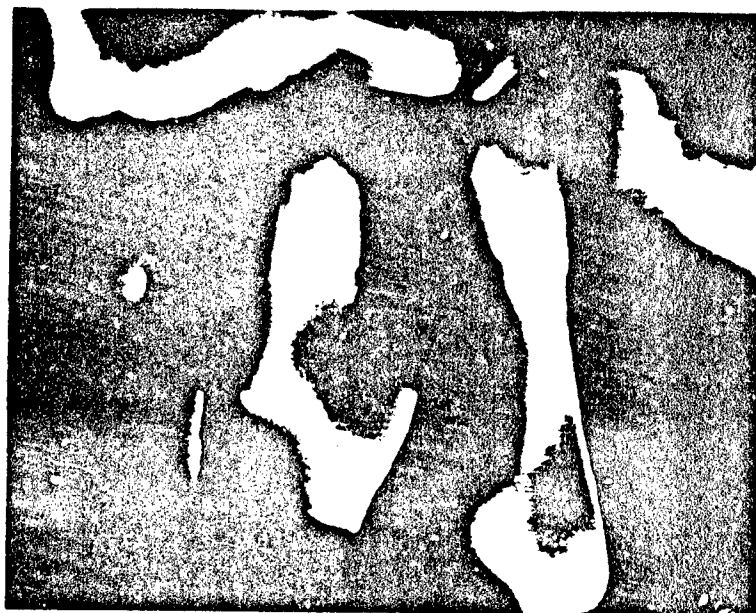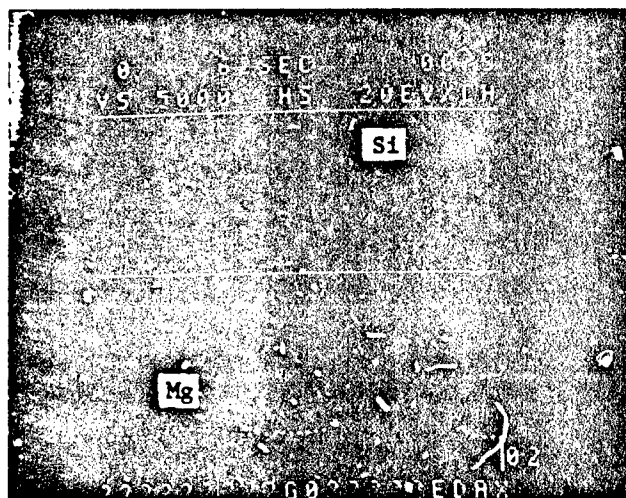precipitates in the matrix of sample No. 3

X60,000

(a)

(b)

Fig. 3 (a) STEM image of a fiber/matrix interface;
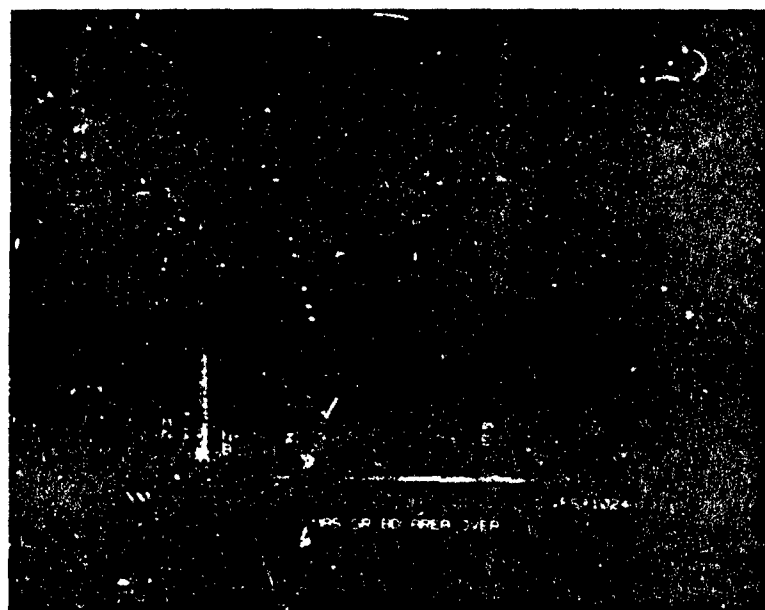   (b) EDX niobium element mapping of the same
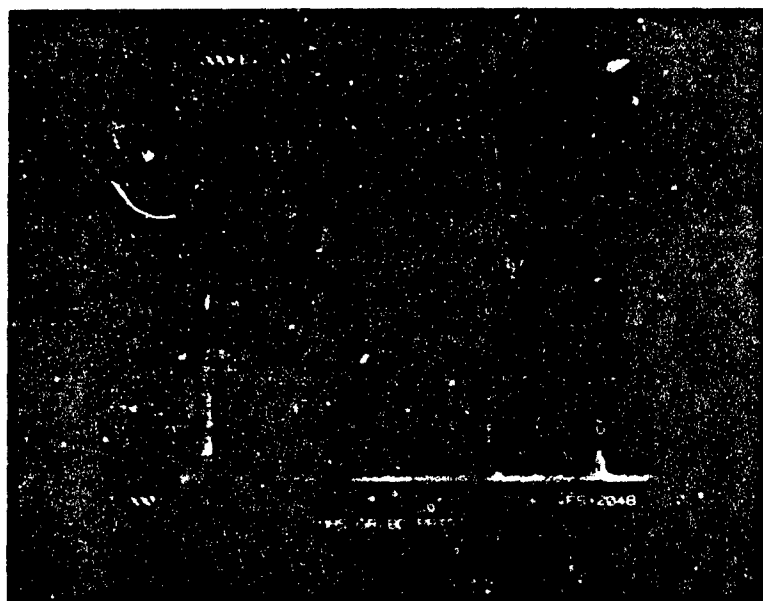   area.

X5,000

(a)

(b)

Fig. 5 (a) Matrix phase in the porous region of
         sample No. 1; (b) EDX analysis of these
         phases.

(a)

(b)

Fig. 4 EDX analysis of (a) the overall fiber/matrix
        interface region as shown in Fig. 3; (b) the
        precipitates along the interface.

152-18

END

FILMED

7-85

DTIC